VOLUME 26 / NUMBER 5
MARCH 8, 1988
ACC. NOS. N88-13215 TO N88-14063

# STAR

AN ABSTRACT JOURNAL

# Scientific and Technical Aerospace Reports

PRODUCED BY THE
SCIENTIFIC AND TECHNICAL
INFORMATION
DIVISION

NASA

NATIONAL AERONAUTICS AND SPACE ADMINISTRATION

## WHAT YOU CAN DO FOR *STAR*

All users of this abstract service are urged to forward reports to be considered for announcement in *STAR*. This will aid NASA in its efforts to provide the fullest possible coverage of all scientific and technical publications that might support aeronautics and space research and development. If you have prepared relevant reports (other than those that you will transmit to NASA, DoD, or DOE through the usual contract- or grant-reporting channels), please send them for consideration to the NASA Scientific and Technical Information Facility, P.O. Box 8757, B.W.I. Airport, Maryland 21240.

Reprints of journal articles, book chapters, and conference papers are also welcome. These will be considered for announcement in *STAR's* companion journal, *International Aerospace Abstracts*.

You may specify a particular source to be included in a report announcement if you wish; otherwise the report will be placed on public sale at the National Technical Information Service. Copyrighted publications will be announced but not distributed or sold.

## PURCHASE OF *STAR*

The semimonthly issues are available for sale by the Superintendent of Documents, U.S. Government Printing Office, Washington, D.C. 20402.

## PUBLISHED BY:

**UNITED STATES GOVERNMENT**
**NATIONAL AERONAUTICS AND SPACE ADMINISTRATION**
SCIENTIFIC AND TECHNICAL INFORMATION DIVISION
*Scientific and Technical Aerospace Reports*, Volume 26, is prepared by the NASA Scientific and Technical Information Facility operated for the National Aeronautics and Space Administration by RMS Associates.

The Administrator of the National Aeronautics and Space Administration has determined that the publication of this periodical is necessary in the transaction of the public business required by law of this Agency. Use of funds for printing this periodical has been approved by the Director of the Office of Management and Budget through March 22, 1988.

**US ISSN 0036-8741**

## INTRODUCTION

*Scientific and Technical Aerospace Reports (STAR)* is a major component of a comprehensive National Aeronautics and Space Administration information system covering aeronautics, space, and supporting disciplines. *STAR* is issued on the 8th and 23rd of each month and announces current publications of the following types:

- NASA, NASA contractor, and NASA grantee reports
- Reports issued by other U.S. Government Agencies, domestic and foreign institutions, universities, and private firms
- Translations in report form
- NASA-owned patents and patent applications
- Dissertations and theses

Journal, book, and conference literature, cover-to-cover journal translations, and certain foreign dissertations are announced in a companion journal, *International Aerospace Abstracts (IAA),* available on subscription from the American Institute of Aeronautics and Astronautics, Technical Information Service, 555 West 57th Street, 12th Floor, New York, New York 10019.

### SUBJECT SCOPE

Subject scope of *STAR,* and *IAA* includes all aspects of aeronautics and space research and development, supporting basic and applied research, and applications. Aerospace aspects of earth resources, energy development, conservation, oceanography, environmental protection, urban transportation, and other topics of high national priority are also covered.

### OTHER NASA PUBLICATIONS

Other NASA publications and information services are described in the publication, *The NASA Scientific and Technical Information System ... and How to Use It,* available without charge from the NASA Scientific and Technical Information Facility, P.O. Box 8757, B.W.I. Airport, Maryland 21240.

### HOW TO USE *STAR* SUBJECT CATEGORIES

*STAR* is categorized by 10 major subject divisions divided into 76 specific subject categories and one general category/division. The major subject divisions are listed in the Table of Contents, together with a note for each that defines its scope and provides any cross-references. For example:

**AERONAUTICS**

Includes aeronautics (general); aerodynamics; air transportation and safety; aircraft communications and navigation; aircraft design, testing and performance; aircraft instrumentation; aircraft propulsion and power; aircraft stability and control; and research and support facilities (air).

For related information see also *Astronautics.*

Each major division is further divided into as many as nine specific categories, which are identified by category numbers.

Abstracts in *STAR* are grouped by specific category, the categories appearing in sequential order. Category breaks in the abstract section are identified by the category number and title, and a scope note. Cross-references to other categories are provided as appropriate. For example:

**02 AERODYNAMICS**

Includes aerodynamics of bodies, combinations, wings, rotors, and control surfaces; and internal flow in ducts and turbomachinery.

For related information see also *34 Fluid Mechanics and Heat Transfer.*

## CROSS-REFERENCES

Individual *STAR* abstracts are not ordinarily cross-referenced, except for certain conference reports or book translations that have had separate abstracts written for their component papers or chapters. Citations and abstracts of the components follow immediately after those of the parent document. When the subject content of a component differs sufficiently from the general content of the parent, a cross-reference citation also is printed at the end of the category to which it normally would have been assigned if it were independent.

## DOCUMENTS ON MICROFICHE

Documents on microfiche(1) are designated by a pound sign (#) following the accession number. The pound sign is used without regard to the source or quality of the microfiche.

## AVAILABILITIES

One or more sources from which a document announced in *STAR* is available to the public is given in each citation. The most commonly indicated sources and their acronyms or abbreviations are listed below. If the publication is available from a source other than those listed, the publisher and his address will be displayed on the availability line or in combination with the corporate source line.

Avail: NTIS. Sold by the National Technical Information Service. Prices for hard copy (HC) and microfiche (MF) are indicated by a price code following the letters HC or MF in the *STAR* citation. Current values for the price codes are given in the tables on page vii.

Initially distributed microfiche under the NTIS SRIM (Selected Research in Microfiche) is available at greatly reduced unit prices. For this service and for information concerning subscription to NASA printed reports, consult the NTIS Subscription Section, Springfield, Va. 22161.

NOTE ON ORDERING DOCUMENTS: When ordering NASA publications (those followed by the * symbol), use the N accession number. NASA patent applications (only the specifications are offered) should be ordered by the US-Patent-Appl-SN number. Non-NASA publications (no asterisk) should be ordered by the AD, PB, or other *report number* shown on the last line of the citation, not by the N accession number. It is also advisable to cite the title and other bibliographic identification.

Avail: SOD (or GPO). Sold by the Superintendent of Documents, U.S. Government Printing Office, in hard copy. The current price and order number are given following the availability line. (NTIS will fill microfiche requests, as indicated above, for those documents identified by a # symbol.)

(1) A microfiche is a transparent sheet of film, 105 by 148 mm in size, containing as many as 60 to 98 pages of information reduced to micro images (not to exceed 26:1 reduction).

Avail: BLL (formerly NLL): British Library Lending Division, Boston Spa, Wetherby, Yorkshire, England. Photocopies available from this organization at the price shown. (If none is given, inquiry should be addressed to the BLL.)

Avail: DOE Depository Libraries. Organizations in U.S. cities and abroad that maintain collections of Department of Energy reports, usually in microfiche form, are listed in *Energy Research Abstracts*. Services available from the DOE and its depositories are described in a booklet, *DOE Technical Information Center - Its Functions and Services* (TID-4660), which may be obtained without charge from the DOE Technical Information Center.

Avail: ESDU. Pricing information on specific data, computer programs, and details on ESDU topic categories can be obtained from ESDU International Ltd. Requesters in North America should use the Virginia address while all other requesters should use the London address, both of which are on page vi.

Avail: Fachinformationszentrum, Karlsruhe. Sold by the Fachinformationszentrum Energie, Physik, Mathematik GMBH, Eggenstein Leopoldshafen, Federal Republic of Germany, at the price shown in deutschmarks (DM).

Avail: HMSO. Publications of Her Majesty's Stationery Office are sold in the U.S. by Pendragon House, Inc. (PHI), Redwood City, California. The U.S. price (including a service and mailing charge) is given, or a conversion table may be obtained from PHI.

Avail: NASA Public Document Rooms. Documents so indicated may be examined at or purchased from the National Aeronautics and Space Administration, Public Documents Room (Room 126), 600 Independence Ave., S.W., Washington, D.C. 20546, or public document rooms located at each of the NASA research centers, the NASA Space Technology Laboratories, and the NASA Pasadena Office at the Jet Propulsion Laboratory.

Avail: Univ. Microfilms. Documents so indicated are dissertations selected from *Dissertation Abstracts* and are sold by University Microfilms as xerographic copy (HC) and microfilm. All requests should cite the author and the Order Number as they appear in the citation.

Avail: US Patent and Trademark Office. Sold by Commissioner of Patents and Trademarks, U.S. Patent and Trademark Office, at the standard price of $1.50 each, postage free. (See discussion of NASA patents and patent applications below.)

Avail: (US Sales Only). These foreign documents are available to users within the United States from the National Technical Information Service (NTIS). They are available to users outside the United States through the International Nuclear Information Service (INIS) representative in their country, or by applying directly to the issuing organization.

Avail: USGS. Originals of many reports from the U.S. Geological Survey, which may contain color illustrations, or otherwise may not have the quality of illustrations preserved in the microfiche or facsimile reproduction, may be examined by the public at the libraries of the USGS field offices whose addresses are listed in this Introduction. The libraries may be queried concerning the availability of specific documents and the possible utilization of local copying services, such as color reproduction.

Avail: Issuing Activity, or Corporate Author, or no indication of availability. Inquiries as to the availability of these documents should be addressed to the organization shown in the citation as the corporate author of the document.

## NASA PATENTS AND PATENT APPLICATIONS

Patents and patent applications owned by NASA are announced in *STAR* under appropriate subject categories and are referenced in the *STAR* indexes. In the Report/Accession Number Index, patents are indexed by the NASA Case Number (which appears in lieu of the report number in other indexes), the U.S. Patent Number, the U.S. Patent Application Serial Number, and the U.S. Patent Class. Patent applications for which patents have not yet been issued are indexed by the NASA Case Number and the U.S. Patent Application Serial Number.

NASA *patent application specifications* are sold in paper copy by the National Technical Information Service at price code A02. Microfiche are sold at price code A01. The US-Patent-Appl-SN- number should be used in ordering either paper copy or microfiche from NTIS. Printed copies of *patents* (which are not microfiched) are available for purchase at $1.50 per copy from:

Commissioner of Patents and Trademarks
U.S. Patent and Trademark Office
Washington, D.C. 20231

When ordering patents, the U.S. Patent Number should be used, and payment must be remitted in advance, preferably by money order or check payable to the Commissioner of Patents and Trademarks. Prepaid purchase coupons for ordering are also available from the Patent and Trademark Office. The patents and patent applications announced in *STAR* are owned by NASA and are available for royalty-free licensing. Requests for licensing terms and further information should be addressed to:

Associate General Counsel for Intellectual Property/Code GP
National Aeronautics and Space Administration
Washington, D.C. 20546

## ELIGIBILITY AND REGISTRATION FOR NASA INFORMATION PRODUCTS AND SERVICES

A variety of services is available to organizations of the following types that have registered with NASA to receive specific services or products:

1. NASA offices, research centers, contractors, subcontractors, grantees, and consultants;
2. Other U.S. Government agencies and their contractors;
3. Libraries in the United States that have arrangements with NASA to maintain collections of NASA documents for public reference;
4. Other organizations in the United States having a need for NASA documents in work related to aeronautics and space research;
5. Organizations abroad that have established reciprocal document exchange arrangements with NASA.

Only the central service points or central points of document acquisition and control within qualified organizations are eligible to register for NASA products and services. Domestic organizations that may be eligible to receive various classes of NASA publications and services should address their requests for registration or for further information to:

NASA Scientific and Technical Information Facility
ATTN: Registration Activity
P.O. Box 8757
B.W.I. Airport, Maryland 21240

Organizations abroad should direct requests to the same address, but to the attention of: International Exchange Program.

## AVAILABILITY OF *STAR* ABSTRACTS ON MICROFICHE

Microfiche of the abstract sections of this issue and other issues of *STAR* are available on annual subscription from NTIS as PB88-911300, Attn: Subscriptions, 5285 Port Royal Road, Springfield, Virginia 22161. Annual subscription rates are $70.00 North America; $140.00 foreign. Abstract sections for previous years retroactive to 1964 are available at the current rates. Microfiche for individual *STAR* issue abstract sections are not available.

## PUBLIC COLLECTIONS OF NASA DOCUMENTS

**DOMESTIC:** NASA and NASA-sponsored documents and a large number of aerospace publications are available to the public for reference purposes at the library maintained by the American Institute of Aeronautics and Astronautics, Technical Information Service, 555 West 57th Street, 12th Floor, New York, New York 10019

**EUROPEAN:** An extensive collection of NASA and NASA-sponsored publications is maintained by the British Library Lending Division, Boston Spa, Wetherby, Yorkshire, England for public access. The British Library Lending Division also has available many of the non-NASA publications cited in *STAR*. European requesters may purchase facsimile copy or microfiche of NASA and NASA-sponsored documents, those identified by both the symbols # and * from ESA - Information Retrieval Service European Space Agency, 8-10 rue Mario-Nikis, 75738 Paris CEDEX 15, France.

## FEDERAL DEPOSITORY LIBRARY PROGRAM

In order to provide the general public with greater access to U.S. Government publications, Congress established the Federal Depository Library Program under the Government Printing Office (GPO), with 50 regional depositories responsible for permanent retention of material, inter-library loan, and reference services. At least one copy of nearly every NASA and NASA-sponsored publication, either in printed or microfiche format, is received and retained by the 50 regional depositories. A list of the regional GPO libraries, arranged alphabetically by state, appears on the inside back cover. These libraries are *not* sales outlets. A local library can contact a Regional Depository to help locate specific reports, or direct contact may be made by an individual.

## ADDRESSES OF ORGANIZATIONS

American Institute of Aeronautics and Astronautics
Technical Information Service
555 West 57th Street, 12th Floor
New York, New York 10019

British Library Lending Division,
Boston Spa, Wetherby, Yorkshire,
England

Commissioner of Patents and Trademarks
U.S. Patent and Trademark Office
Washington, D.C. 20231

Department of Energy
Technical Information Center
P.O. Box 62
Oak Ridge, Tennessee 37830

ESA-Information Retrieval Service
ESRIN
Via Galileo Galilei
00044 Frascati (Rome) Italy

ESDU International, Ltd.
1495 Chain Bridge Road
McLean, Virginia 22101

ESDU International, Ltd.
251-259 Regent Street
London, W1R 7AD, England

Fachinformationszentrum Energie, Physik, Mathematik GMBH
7514 Eggenstein Leopoldshafen
Federal Republic of Germany

Her Majesty's Stationery Office
P.O. Box 569, S.E. 1
London, England

NASA Scientific and Technical Information Facility
P.O. Box 8757
B.W.I. Airport, Maryland 21240

National Aeronautics and Space Administration
Scientific and Technical Information Division (NTT-1)
Washington, D.C. 20546

National Technical Information Service
5285 Port Royal Road
Springfield, Virginia 22161

Pendragon House, Inc.
899 Broadway Avenue
Redwood City, California 94063

Superintendent of Documents
U.S. Government Printing Office
Washington, D.C. 20402

University Microfilms
A Xerox Company
300 North Zeeb Road
Ann Arbor, Michigan 48106

University Microfilms, Ltd.
Tylers Green
London, England

U.S. Geological Survey Library
National Center - MS 950
12201 Sunrise Valley Drive
Reston, Virginia 22092

U.S. Geological Survey Library
2255 North Gemini Drive
Flagstaff, Arizona 86001

U.S. Geological Survey
345 Middlefield Road
Menlo Park, California 94025

U.S. Geological Survey Library
Box 25046
Denver Federal Center, MS914
Denver, Colorado 80225

# NTIS PRICE SCHEDULES

(Effective January 1, 1988)

## Schedule A
## STANDARD PRICE DOCUMENTS AND MICROFICHE

| PRICE CODE | PAGE RANGE | NORTH AMERICAN PRICE | FOREIGN PRICE |
|---|---|---|---|
| A01 | Microfiche | $ 6.95 | $13.90 |
| A02 | 001-010 | 9.95 | 19.90 |
| A03 | 011-050 | 12.95 | 25.90 |
| A04-A05 | 051-100 | 14.95 | 29.90 |
| A06-A09 | 101-200 | 19.95 | 39.90 |
| A10-A13 | 201-300 | 25.95 | 51.90 |
| A14-A17 | 301-400 | 32.95 | 65.90 |
| A18-A21 | 401-500 | 38.95 | 77.90 |
| A22-A25 | 501-600 | 44.95 | 89.90 |
| A99 | 601-up | * | * |
| NO1 | | 49.50 | 89.90 |
| NO2 | | 48.00 | 80.00 |

## Schedule E
## EXCEPTION PRICE DOCUMENTS AND MICROFICHE

| PRICE CODE | NORTH AMERICAN PRICE | FOREIGN PRICE |
|---|---|---|
| E01 | $ 8.50 | 17.00 |
| E02 | 11.00 | 22.00 |
| E03 | 12.00 | 24.00 |
| E04 | 14.50 | 29.00 |
| E05 | 16.50 | 33.00 |
| E06 | 19.00 | 38.00 |
| E07 | 21.50 | 43.00 |
| E08 | 24.00 | 48.00 |
| E09 | 26.50 | 53.00 |
| E10 | 29.00 | 58.00 |
| E11 | 31.50 | 63.00 |
| E12 | 34.00 | 68.00 |
| E13 | 36.50 | 73.00 |
| E14 | 39.50 | 79.00 |
| E15 | 43.00 | 86.00 |
| E16 | 47.00 | 94.00 |
| E17 | 51.00 | 102.00 |
| E18 | 55.00 | 110.00 |
| E19 | 61.00 | 122.00 |
| E20 | 71.00 | 142.00 |
| E99 | * | * |

*Contact NTIS for price quote.

## IMPORTANT NOTICE

NTIS Shipping and Handling Charges
U.S., Canada, Mexico — ADD $3.00 per TOTAL ORDER
All Other Countries — ADD $4.00 per TOTAL ORDER

Exceptions — Does NOT apply to:
ORDERS REQUESTING NTIS RUSH HANDLING
ORDERS FOR SUBSCRIPTION OR STANDING ORDER PRODUCTS *ONLY*

NOTE: Each additional delivery address on an order requires a separate shipping and handling charge.

VOLUME 26 NUMBER 5 / MARCH 8, 1988

# TABLE OF CONTENTS

## AERONAUTICS

Includes aeronautics (general); aerodynamics; air transportation and safety; aircraft communications and navigation; aircraft design, testing and performance; aircraft instrumentation; aircraft propulsion and power; aircraft stability and control; and research and support facilities (air).

For related information see also *Astronautics.*

**01 AERONAUTICS (GENERAL)** 529

**02 AERODYNAMICS** 529

Includes aerodynamics of bodies, combinations, wings, rotors, and control surfaces; and internal flow in ducts and turbomachinery.

For related information see also *34 Fluid Mechanics and Heat Transfer*

**03 AIR TRANSPORTATION AND SAFETY** 543

Includes passenger and cargo air transport operations; and aircraft accidents.

For related information see also *16 Space Transportation* and *85 Urban Technology and Transportation.*

**04 AIRCRAFT COMMUNICATIONS AND NAVIGATION** 544

Includes digital and voice communication with aircraft; air navigation systems (satellite and ground based); and air traffic control.

For related information see also *17 Space Communications, Spacecraft Communications, Command and Tracking* and *32 Communications and Radar.*

**05 AIRCRAFT DESIGN, TESTING AND PERFORMANCE** 544

Includes aircraft simulation technology.

For related information see also *18 Spacecraft Design, Testing and Performance* and *39 Structural Mechanics.* For land transportation vehicles see *85 Urban Technology and Transportation.*

**06 AIRCRAFT INSTRUMENTATION** 547

Includes cockpit and cabin display devices; and flight instruments.

For related information see also *19 Spacecraft Instrumentation* and *35 Instrumentation and Photography.*

**07 AIRCRAFT PROPULSION AND POWER** 548

Includes prime propulsion systems and systems components, e.g., gas turbine engines and compressors; and onboard auxiliary power plants for aircraft.

For related information see also *20 Spacecraft Propulsion and Power, 28 Propellants and Fuels,* and *44 Energy Production and Conversion.*

**08 AIRCRAFT STABILITY AND CONTROL** 550

Includes aircraft handling qualities; piloting; flight controls; and autopilots.

For related information see also *05 Aircraft Design, Testing and Performance.*

**09 RESEARCH AND SUPPORT FACILITIES (AIR)** 552

Includes airports, hangars and runways; aircraft repair and overhaul facilities; wind tunnels; shock tubes; and aircraft engine test stands.

For related information see also *14 Ground Support Systems and Facilities (Space).*

## ASTRONAUTICS

Includes astronautics (general); astrodynamics; ground support systems and facilities (space); launch vehicles and space vehicles; space transportation; space communications, spacecraft communications, command and tracking; spacecraft design, testing and performance; spacecraft instrumentation; and spacecraft propulsion and power.

For related information see also *Aeronautics*

**12 ASTRONAUTICS (GENERAL)** 553

For extraterrestrial exploration see *91 Lunar and Planetary Exploration.*

**13 ASTRODYNAMICS** N.A.

Includes powered and free-flight trajectories; and orbital and launching dynamics.

**14 GROUND SUPPORT SYSTEMS AND FACILITIES (SPACE)** N.A.

Includes launch complexes, research and production facilities; ground support equipment, e.g., mobile transporters; and simulators.

For related information see also *09 Research and Support Facilities (Air).*

**15 LAUNCH VEHICLES AND SPACE VEHICLES** 553

Includes boosters; operating problems of launch/space vehicle systems; and reusable vehicles.

For related information see also *20 Spacecraft Propulsion and Power.*

**16 SPACE TRANSPORTATION** N.A.

Includes passenger and cargo space transportation, e.g., shuttle operations; and space rescue techniques.

For related information see also *03 Air Transportation and Safety* and *18 Spacecraft Design, Testing and Performance.* For space suits see *54 Man/System Technology and Life Support.*

**17 SPACE COMMUNICATIONS, SPACECRAFT COMMUNICATIONS, COMMAND AND TRACKING** 554

Includes telemetry; space communications networks; astronavigation and guidance; and radio blackout.

For related information see also *04 Aircraft Communications and Navigation* and *32 Communications and Radar.*

**18 SPACECRAFT DESIGN, TESTING AND PERFORMANCE** 554

Includes satellites; space platforms; space stations; spacecraft systems and components such as thermal and environmental controls; and attitude controls.

For life support systems see *54 Man/System Technology and Life Support.* For related information see also *05 Aircraft Design, Testing and Performance, 39 Structural Mechanics,* and *16 Space Transportation.*

**19 SPACECRAFT INSTRUMENTATION** N.A.

For related information see also *06 Aircraft Instrumentation* and *35 Instrumentation and Photography.*

**20 SPACECRAFT PROPULSION AND POWER** 556

Includes main propulsion systems and components, e.g. rocket engines; and spacecraft auxiliary power sources.

For related information see also *07 Aircraft Propulsion and Power, 28 Propellants and Fuels, 44 Energy Production and Conversion,* and *15 Launch Vehicles and Space Vehicles.*

## CHEMISTRY AND MATERIALS

Includes chemistry and materials (general); composite materials; inorganic and physical chemistry; metallic materials; nonmetallic materials; propellants and fuels; and materials processing.

**23 CHEMISTRY AND MATERIALS (GENERAL)** 556

**24 COMPOSITE MATERIALS** 557

Includes physical, chemical, and mechanical properties of laminates and other composite materials.

For ceramic materials see *27 Nonmetallic Materials.*

**25 INORGANIC AND PHYSICAL CHEMISTRY** 560

Includes chemical analysis, e.g., chromatography; combustion theory; electrochemistry; and photochemistry.

For related information see also *77 Thermodynamics and Statistical Physics.*

**26 METALLIC MATERIALS** 563

Includes physical, chemical, and mechanical properties of metals, e.g., corrosion; and metallurgy.

**27 NONMETALLIC MATERIALS** 567

Includes physical, chemical, and mechanical properties of plastics, elastomers, lubricants, polymers, textiles, adhesives, and ceramic materials.

For composite materials see *24 Composite Materials.*

**28 PROPELLANTS AND FUELS** 570

Includes rocket propellants, igniters and oxidizers; their storage and handling procedures; and aircraft fuels.

For related information see also *07 Aircraft Propulsion and Power, 20 Spacecraft Propulsion and Power,* and *44 Energy Production and Conversion.*

**29 MATERIALS PROCESSING** 571

Includes space-based development of products and processes for commercial application.

For biological materials see *55 Space Biology.*

## ENGINEERING

Includes engineering (general); communications and radar; electronics and electrical engineering; fluid mechanics and heat transfer; instrumentation and photography; lasers and masers; mechanical engineering; quality assurance and reliability; and structural mechanics.

For related information see also *Physics.*

**31 ENGINEERING (GENERAL)** 571

Includes vacuum technology; control engineering; display engineering; cryogenics; and fire prevention.

**32 COMMUNICATIONS AND RADAR** 573

Includes radar; land and global communications; communications theory; and optical communications.

For related information see also *04 Aircraft Communications and Navigation* and *17 Space Communications, Spacecraft Communications, Command and Tracking.* For search and rescue see *03 Air Transportation and Safety,* and *16 Space Transportation.*

**33 ELECTRONICS AND ELECTRICAL ENGINEERING** 577

Includes test equipment and maintainability; components, e.g., tunnel diodes and transistors; microminiaturization; and integrated circuitry.

For related information see also *60 Computer Operations and Hardware* and *76 Solid-State Physics.*

**34 FLUID MECHANICS AND HEAT TRANSFER** 579

Includes boundary layers; hydrodynamics; fluidics; mass transfer and ablation cooling.

For related information see also *02 Aerodynamics* and *77 Thermodynamics and Statistical Physics.*

**35 INSTRUMENTATION AND PHOTOGRAPHY** 583

Includes remote sensors; measuring instruments and gages; detectors; cameras and photographic supplies; and holography.

For aerial photography see *43 Earth Resources and Remote Sensing.* For related information see also *06 Aircraft Instrumentation* and *19 Spacecraft Instrumentation.*

**36 LASERS AND MASERS** 586

Includes parametric amplifiers.

For related information see also *76 Solid-State Physics.*

**37 MECHANICAL ENGINEERING** 589

Includes auxiliary systems (nonpower); machine elements and processes; and mechanical equipment.

**38 QUALITY ASSURANCE AND RELIABILITY** N.A.

Includes product sampling procedures and techniques; and quality control.

**39 STRUCTURAL MECHANICS** 591

Includes structural element design and weight analysis; fatigue; and thermal stress.

For applications see *05 Aircraft Design, Testing and Performance* and *18 Spacecraft Design, Testing and Performance.*

## GEOSCIENCES

Includes geosciences (general); earth resources and remote sensing; energy production and conversion; environment pollution; geophysics; meteorology and climatology; and oceanography.

For related information see also *Space Sciences.*

**42 GEOSCIENCES (GENERAL)** **611**

**43 EARTH RESOURCES AND REMOTE SENSING** **619**

Includes remote sensing of earth resources by aircraft and spacecraft; photogrammetry; and aerial photography.

For instrumentation see *35 Instrumentation and Photography.*

**44 ENERGY PRODUCTION AND CONVERSION** **622**

Includes specific energy conversion systems, e.g., fuel cells; global sources of energy; geophysical conversion; and windpower.

For related information see also *07 Aircraft Propulsion and Power, 20 Spacecraft Propulsion and Power,* and *28 Propellants and Fuels.*

**45 ENVIRONMENT POLLUTION** **623**

Includes atmospheric, noise, thermal, and water pollution.

**46 GEOPHYSICS** **624**

Includes aeronomy; upper and lower atmosphere studies; ionospheric and magnetospheric physics; and geomagnetism.

For space radiation see *93 Space Radiation.*

**47 METEOROLOGY AND CLIMATOLOGY** **626**

Includes weather forecasting and modification.

**48 OCEANOGRAPHY** **629**

Includes biological, dynamic, and physical oceanography; and marine resources.

For related information see also *43 Earth Resources and Remote Sensing.*

## LIFE SCIENCES

Includes life sciences (general); aerospace medicine; behavioral sciences; man/system technology and life support; and space biology.

**51 LIFE SCIENCES (GENERAL)** **629**

**52 AEROSPACE MEDICINE** **629**

Includes physiological factors; biological effects of radiation; and effects of weightlessness on man and animals.

**53 BEHAVIORAL SCIENCES** **630**

Includes psychological factors; individual and group behavior; crew training and evaluation; and psychiatric research.

**54 MAN/SYSTEM TECHNOLOGY AND LIFE SUPPORT** **630**

Includes human engineering; biotechnology; and space suits and protective clothing.

For related information see also *16 Space Transportation.*

**55 SPACE BIOLOGY** **N.A.**

Includes exobiology; planetary biology; and extraterrestrial life.

## MATHEMATICAL AND COMPUTER SCIENCES

Includes mathematical and computer sciences (general); computer operations and hardware; computer programming and software; computer systems; cybernetics; numerical analysis; statistics and probability; systems analysis; and theoretical mathematics.

**59 MATHEMATICAL AND COMPUTER SCIENCES (GENERAL)** **N.A.**

**60 COMPUTER OPERATIONS AND HARDWARE** **631**

Includes hardware for computer graphics, firmware, and data processing.

For components see *33 Electronics and Electrical Engineering.*

**61 COMPUTER PROGRAMMING AND SOFTWARE** **631**

Includes computer programs, routines, algorithms, and specific applications, e.g., CAD/CAM.

**62 COMPUTER SYSTEMS** **637**

Includes computer networks and special application computer systems.

**63 CYBERNETICS** **638**

Includes feedback and control theory, artificial intelligence, robotics and expert systems.

For related information see also *54 Man/System Technology and Life Support.*

**64 NUMERICAL ANALYSIS** **639**

Includes iteration, difference equations, and numerical approximation.

**65 STATISTICS AND PROBABILITY** **643**

Includes data sampling and smoothing; Monte Carlo method; and stochastic processes.

**66 SYSTEMS ANALYSIS** **645**

Includes mathematical modeling; network analysis; and operations research.

**67 THEORETICAL MATHEMATICS** **645**

Includes topology and number theory.

## PHYSICS

Includes physics (general); acoustics; atomic and molecular physics; nuclear and high-energy physics; optics; plasma physics; solid-state physics; and thermodynamics and statistical physics.

For related information see also *Engineering.*

**70 PHYSICS (GENERAL)** **645**

For precision time and time interval (PTTI) see *35 Instrumentation and Photography;* for geophysics, astrophysics or solar physics see *46 Geophysics, 90 Astrophysics,* or *92 Solar Physics.*

**71 ACOUSTICS** 646
Includes sound generation, transmission, and attenuation.
For noise pollution see *45 Environment Pollution.*

**72 ATOMIC AND MOLECULAR PHYSICS** 647
Includes atomic structure, electron properties, and molecular spectra.

**73 NUCLEAR AND HIGH-ENERGY PHYSICS** 649
Includes elementary and nuclear particles; and reactor theory.
For space radiation see *93 Space Radiation.*

**74 OPTICS** 649
Includes light phenomena and optical devices.
For lasers see *36 Lasers and Masers.*

**75 PLASMA PHYSICS** 651
Includes magnetohydrodynamics and plasma fusion.
For ionospheric plasmas see *46 Geophysics.* For space plasmas see *90 Astrophysics.*

**76 SOLID-STATE PHYSICS** 654
Includes superconductivity.
For related information see also *33 Electronics and Electrical Engineering* and *36 Lasers and Masers.*

**77 THERMODYNAMICS AND STATISTICAL PHYSICS** 657
Includes quantum mechanics; theoretical physics; and Bose and Fermi statistics.
For related information see also *25 Inorganic and Physical Chemistry* and *34 Fluid Mechanics and Heat Transfer.*

## SOCIAL SCIENCES

Includes social sciences (general); administration and management; documentation and information science; economics and cost analysis; law, political science, and space policy; and urban technology and transportation.

**80 SOCIAL SCIENCES (GENERAL)** N.A.
Includes educational matters.

**81 ADMINISTRATION AND MANAGEMENT** 657
Includes management planning and research.

**82 DOCUMENTATION AND INFORMATION SCIENCE** 658
Includes information management; information storage and retrieval technology; technical writing; graphic arts; and micrography.
For computer documentation see *61 Computer Programming and Software.*

**83 ECONOMICS AND COST ANALYSIS** N.A.
Includes cost effectiveness studies.

**84 LAW, POLITICAL SCIENCE AND SPACE POLICY** 659
Includes NASA appropriation hearings; aviation law; space law and policy; international law; international cooperation; and patent policy.

**85 URBAN TECHNOLOGY AND TRANSPORTATION** 659
Includes applications of space technology to urban problems; technology transfer; technology assessment; and surface and mass transportation.
For related information see *03 Air Transportation and Safety, 16 Space Transportation,* and *44 Energy Production and Conversion.*

## SPACE SCIENCES

Includes space sciences (general); astronomy; astrophysics; lunar and planetary exploration; solar physics; and space radiation.
For related information see also *Geosciences.*

**88 SPACE SCIENCES (GENERAL)** 659

**89 ASTRONOMY** 660
Includes radio, gamma-ray, and infrared astronomy; and astrometry.

**90 ASTROPHYSICS** 660
Includes cosmology; celestial mechanics; space plasmas; and interstellar and interplanetary gases and dust.
For related information see also *75 Plasma Physics.*

**91 LUNAR AND PLANETARY EXPLORATION** 660
Includes planetology; and manned and unmanned flights.
For spacecraft design or space stations see *18 Spacecraft Design, Testing and Performance.*

**92 SOLAR PHYSICS** 661
Includes solar activity, solar flares, solar radiation and sunspots.
For related information see *93 Space Radiation.*

**93 SPACE RADIATION** 661
Includes cosmic radiation; and inner and outer earth's radiation belts.
For biological effects of radiation see *52 Aerospace Medicine.* For theory see *73 Nuclear and High-Energy Physics.*

## GENERAL

Includes aeronautical, astronautical, and space science related histories, biographies, and pertinent reports too broad for categorization; histories or broad overviews of NASA programs.

**99 GENERAL** 662

**Note: N.A. means that no abstracts were assigned to this category for this issue.**

**SUBJECT INDEX** ..... I-1
**PERSONAL AUTHOR INDEX** ..... I-53
**CORPORATE SOURCE INDEX** ..... I-61
**CONTRACT NUMBER INDEX** ..... I-73
**REPORT/ACCESSION NUMBER INDEX** ..... I-75

# TYPICAL CITATION AND ABSTRACT

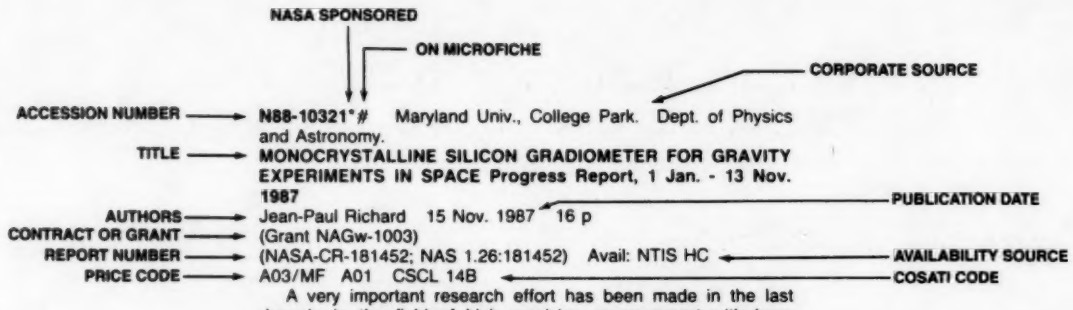


A very important research effort has been made in the last decade in the field of high precision measurement with laser instrumentation. The development of a space borne gradiometer operating at a high sensitivity level using laser measurement of the distance between proof mass over a short base line of order one meter is discussed. Two aspects of laser technology make it a promising tool for gradiometry measurements: quantum limited accuracy and absolute distance measurements. The quantum limit associated with laser instrumentation was formulated. The relevant quantum and classical sources of errors in laser measurements were reviewed and corresponding laser performance requirements for gradient measurements were evaluated. Some mechanical quality factor measurements were made on simple resonant monocrystalline silicon suspensions. It was discovered that the use of zero derivative restoring forces to position the gradiometer test masses will dramatically reduce the gradiometer temperature control requirements. A laser beam side injection scheme was discovered which permits rejection of common mode accelerations. These concepts are briefly discussed. Author

VOLUME 26 NUMBER 5 / MARCH 8, 1988

# Scientific and Technical Aerospace Reports

*A Semimonthly Publication of the National Aeronautics and Space Administration*

## 01 AERONAUTICS (GENERAL)

**N88-13215#** Societe Nationale Industrielle Aerospatiale, Toulouse (France). Div. Avions.
**THE A320 AIRBUS PROGRAM [LE PROGRAMME AIRBUS A320]**
Roger Bergoend 1987 8 p In FRENCH
(SNIAS-872-111-105; ETN-88-91187) Avail: NTIS HC A02/MF A01

The A320 program including aircraft characteristics, program time table, history, and financial aspects is described. ESA

**N88-13216#** Societe Nationale Industrielle Aerospatiale, Paris (France).
**A PROJECT OF AN INTELLIGENT SYSTEM TO HELP ON-LINE TROUBLE SHOOTING**
P. Chanet and J. P. Fournier 1987 15 p In FRENCH and ENGLISH
(SNIAS-872-111-106; ETN-88-91188) Avail: NTIS HC A03/MF A01

Aircraft maintenance problems and the possible applications of artificial intelligence to solve them are discussed. Artificial intelligence techniques seem able to help trouble shooting on commercial aircraft. The ideal system should be on board and able to dialog with the technician, providing intelligent reports, diagnoses, or action proposals. Such a system is being developed. ESA

**N88-13217#** Societe Nationale Industrielle Aerospatiale, Toulouse (France). Div. Avions.
**DESIGN AND CONTROL OF REPAIRS OF CARBON FIBER LIFT AUGMENTATION FLAPS IN THE ATR42 AIRCRAFT [LA CONCEPTION ET LE CONTROLE DES REPARATIONS DES VOLETS HYPERSUSTENTATEURS DE L'ATR42 EN CARBONE]**
Guy Hellard 1987 6 p In FRENCH
(SNIAS-872-111-112; ETN-88-91193) Avail: NTIS HC A02/MF A01

A simplified repair techniques was developed to solve the possibility of occurrences of maintenance problems due to lack of experience and equipment to deal with carbon fiber composites. Dry carbon fabric is used. The strength of the element after repair was tested, reproducing experimentally the most frequent damage cases. ESA

## 02 AERODYNAMICS

Includes aerodynamics of bodies, combinations, wings, rotors, and control surfaces; and internal flow in ducts and turbomachinery.

For related information see also *34 Fluid Mechanics and Heat Transfer.*

**N88-13218*#** Coe Engineering, Inc., Los Altos, Calif.
**PREDICTIONS OF F-111 TACT AIRCRAFT BUFFET RESPONSE AND CORRELATIONS OF FLUCTUATING PRESSURES MEASURED ON ALUMINUM AND STEEL MODELS AND THE AIRCRAFT**
Charles F. Coe and Atlee M. Cunningham, Jr. (General Dynamics Corp., Fort Worth, Tex.) 1987 152 p
(Contract NAS2-11420)
(NASA-CR-4069; NAS 1.26:4069) Avail: NTIS HC A08/MF A01 CSCL 01A

Results of buffet research that was conducted as part of the joint USAF/NASA F-111 TACT Research Program are presented. The correlation of wind tunnel and flight measurements of buffet excitation showed that there generally was good agreement between measurements of pressure fluctuations on the models and aircraft in regions of separated flow. At shock-wave boundaries of the separated flow, correlations of pressure fluctuations were not so good, due to Reynolds number and static elastic effects. The buffet prediction method, which applies a forcing function that is obtained by real-time integration of pressure time histories with the natural modes, is described. The generalized forces, including the effects of wing and tail, correlations of predicted and measured damping, and correlations of predicted and measured buffet response are presented. All presented data are for a Mach number of 0.8 with wing-sweep angles of 26 and 35 deg for a range of angles-of-attack that include buffet onset to high intensity buffeting. Generally, the buffet predictions were considered to be quite good particularly in light of past buffet-prediction experience. Author

**N88-13219#** Advisory Group for Aerospace Research and Development, Neuilly-Sur-Seine (France). Fluid Dynamics Panel.
**AERODYNAMICS OF HYPERSONIC LIFTING VEHICLES**
Nov. 1987 560 p In ENGLISH and FRENCH Symposium held in Bristol, United Kingdom, 6-9 Apr. 1987
(AGARD-CP-428; ISBN-92-835-0435-6) Copyright Avail: NTIS HC A24/MF A01

The Symposium was conducted at the outset of a new era in hypersonic aerodynamics. The Proceedings therefore present a valuable stock taking of the status of the field after a comparative lull in the last decade. A particular gap exists in the field of experimental facilities. At the same time, developments in computational fluid dynamics and experimental techniques provide possibilities that did not exist 10 years before. The papers presented were grouped in the fields: experimental facilities; experimental techniques and results; computational techniques; design methods; and projects. The most significant results of the symposium was a perspective of the need for special effort in the near future. For individual titles, see N88-13220 through N88-13252.

**N88-13220#** Calspan Corp., Buffalo, N. Y.
**A SURVEY OF EXISTING HYPERSONIC GROUND TEST FACILITIES: NORTH AMERICA** c09
C. E. Wittliff *In* AGARD, Aerodynamics of Hypersonic Lifting Vehicles Nov. 1987 17 p (For primary document see N88-13219 05-02)
Copyright Avail: NTIS HC A24/MF A01

In the past several years there was a significant increase in the number of programs involving hypersonic vehicles, resulting in a resurgance of interest in experimental testing in hypersonic wind tunnels. Unfortunately, there are far fewer such facilities operating now than there were 10 or 15 years ago. The primary purpose is to survey the current status of hypersonic wind tunnels in North America and to describe their performance characteristics. As a part of this survey a comparison is drawn to the number and type

of hypersonic wind tunnels that were active in the 1960's and 1970's relative to the current situation. Emphasis is placed on hypersonic aerodynamic and aerothermal testing and related areas. In surveying the hypersonic wind tunnels that are active in North America, all but one are located in the USA. There is a gun tunnel in Canada that will be reactivated this year. Author

**N88-13221#** Von Karman Inst. for Fluid Dynamics, Rhode-Saint-Genese (Belgium).
**EUROPEAN HYPERSONIC WIND TUNNELS c09**
J. F. Wendt *In* AGARD, Aerodynamics of Hypersonic Lifting Vehicles Nov. 1987 24 p (For primary document see N88-13219 05-02)
Copyright Avail: NTIS HC A24/MF A01

Although the hypersonic flow regime will probably be the first to be dominated by computational techniques due to serious experimental simulation problems, the next generation of lifting reentry vehicles will still rely on wind tunnels not only for design validation but also to verify computer codes through benchmark test cases. Evidence for this statement is the proposal to utilize European hypersonic tunnels for upwards of 2000 occupancy days from 1986 to 1993 on the HERMES project. Basic research in hypersonics required for the post-HERMES era will also rely heavily on wind tunnels and their associated instrumentation. Thus, it is appropriate to review the present statue of hypersonic tunnels. The requirements for flow simulation in the hypersonic regime are briefly discussed, and the present situation summarized. Gaps are identified and suggestions for improvements are put forward. Author

**N88-13222#** Office National d'Etudes et de Recherches Aerospatiales, Paris (France).
**PREPARATION OF QUALIFICATION TESTS OF A PLASMA GENERATOR FOR THE FEEDING OF A HYPERSONIC WIND TUNNEL [PREPARATION D'ESSAIS PROBATOIRES D'UN GENERATEUR DE PLASMA POUR L'ALIMENTATION D'UNE SOUFFLERIE HYPERSONIQUE] c75**
H. Consigny, C. Pacou, O. Papirnyk, Ph. Sagnier, and J. P. Chevallier *In* AGARD, Aerodynamics of Hypersonic Lifting Vehicles Nov. 1987 14 p In FRENCH Previously announced in IAA as A87-44341 (For primary document see N88-13219 05-02)
N88-13219 05-02)
Copyright Avail: NTIS HC A24/MF A01

Qualification tests have validated the use of a plasma generator as the feed for the R6 CH hypersonic wind tunnel that is to be employed for the Hermes project. In the first part of the study, a blast pipe using existing elements and fulfilling the conditions necessary for sounding (as determined by flow calculations), is developed. A gas flow rate of 0.26 kg/s and a gas power of 2,090,000 W are projected for an intake with a 1 sq cm cross section. Probe instrumentation for the measurement of dynamic pressure, local mass flow, and enthalpy were developed to verify the homogeneity of the flow. IAA

**N88-13223#** Queensland Univ., Brisbane (Australia). Dept. of Mechanical Engineering.
**SHOCK TUNNELS FOR REAL GAS HYPERSONICS c09**
R. J. Stalker *In* AGARD, Aerodynamics of Hypersonic Lifting Vehicles Nov. 1987 10 p (For primary document see N88-13219 05-02)
Copyright Avail: NTIS HC A24/MF A01

The application of free piston shock tunnels to the simulation of real gas effects in hypersonic flight is discussed. It is pointed out that the primary simulation variables for this purpose are the stagnation enthalpy and the binary scaling parameter. The free piston reflected shock tunnel is considered first, and it is shown how test time limitations play a major role in determining the limiting stagnation enthalpy for a given model size. Nevertheless, flight values of the two simulation variables, for vehicles similar to the Space Shuttle Orbiter, can be matched by an existing free piston shock tunnel up to speeds of 1 km/s. Experiments performed in this shock tunnel are used to demonstrate real gas effects in model flow. Radiative energy loss limits the maximum stagnation enthalpy available with reflected shock tunnels. Fortunately, operation in the nonreflected mode circumvents this limitation, and in addition, allows higher values of the binary scaling parameter; although it also leads to greatly reduced test times. The use of the prior steady flow technique to enable high enthalpy nonreflected shock tunnel operation is described, and examples of experiments performed in the facility are used to demonstrate that short test times do not preclude worthwhile experimentation. A variant of the free piston shock tunnel, which is intended for propulsion research at high velocities, also is briefly described. Author

**N88-13224#** Complere, Inc., Palo Alto, Calif.
**TURBULENCE MEASUREMENT IN HYPERSONIC FLOW**
F. K. Owen and W. Calarese (Air Force Wright Aeronautical Labs., Wright-Patterson AFB, Ohio.) *In* AGARD, Aerodynamics of Hypersonic Lifting Vehicles Nov. 1987 17 p Sponsored in part by Hunting Engineering, Ltd., Ampthill, United Kingdom (For primary document see N88-13219 05-02)
Copyright Avail: NTIS HC A24/MF A01

An assessment was made of the potential for hot wire and laser anemometer measurements of turbulent fluctuations in hypersonic flow fields. The results of experiments conducted in the AFWAL M=6 High Reynolds Number Wind Tunnel are reported and comparisons made with previous hot wire turbulence measurements. Author

**N88-13225#** Technische Univ., Brunswick (West Germany). Inst. fuer Stroemungsmechanik.
**EXPERIMENTAL INVESTIGATIONS ON BLUNT BODIES AND CORNER CONFIGURATIONS IN HYPERSONIC FLOW**
Dietrich Hummel *In* AGARD, Aerodynamics of Hypersonic Lifting Vehicles Nov. 1987 16 p (For primary document see N88-13219 05-02)
(Contracts Schl-5/82; Hu-254/2)
Copyright Avail: NTIS HC A24/MF A01

Within the framework of some theses hypersonic flows were investigated theoretically as well as by experiments in the hypersonic facility gun tunnel of the institute. Some of these activities during the last year are summarized. The first problem to be treated is that of a blunt body of revolution with subsonic blowing in the stagnation point region against the hypersonic main flow. Surface pressure and heat transfer measurements were carried out for two bodies at different free-stream Mach numbers and for various blowing rates. Remarkable agreement was obtained in comparison with a combination of Newtonian and potential theory. The second problem discussed is that of the hypersonic flow in corners formed by intersecting swept wedges. The corner angle and the leading-edge sweep angle were varied systematically. The flow field was analyzed by means of pitot pressure measurements in a characteristic cross section and the flow structure near the wall was determined from oilflow pictures as well as from wall pressure and heat transfer measurements. Strong vortical flows were detected underneath the corner shock system. Starting from a 90 degree corner of unswept wedges, the heat flux in the corner center can be reduced considerably by increasing the corner angle and by sweeping the leading-edges back. Author

**N88-13226*#** Texas Univ., Austin. Dept. of Aerospace Engineering.
**DRIVING MECHANISM OF UNSTEADY SEPARATION SHOCK MOTION IN HYPERSONIC INTERACTIVE FLOW**
D. S. Dolling and J. C. Narlo, II *In* AGARD, Aerodynamics of Hypersonic Lifting Vehicles Nov. 1987 12 p Sponsored in part by NASA, Washington, D.C. and ONR, Washington, D.C. (For primary document see N88-13219 05-02)
(Grant AF-AFOSR-0112-86)
Copyright Avail: NTIS HC A24/MF A01 CSCL 01A

Wall pressure fluctuations were measured under the steady separation shock waves in Mach 5 turbulent interactions induced by unswept circular cylinders on a flat plate. The wall temperature was adiabatic. A conditional sampling algorithm was developed to examine the statistics of the shock wave motion. The same

algorithm was used to examine data taken in earlier studies in the Princeton University Mach 3 blowdown tunnel. In these earlier studies, hemicylindrically blunted fins of different leading-edge diameters were tested in boundary layers which developed on the tunnel floor and on a flat plate. A description of the algorithm, the reasons why it was developed and the sensitivity of the results to the threshold settings, are discussed. The results from the algorithm, together with cross correlations and power spectral density estimates suggests that the shock motion is driven by the low-frequency unsteadiness of the downstream separated, vortical flow. Author

**N88-13227#** Cranfield Inst. of Tech., Bedford (England). Coll. of Aeronautics.

**THE EFFECTS OF SWEEP AND BLUNTNESS ON A GLANCING SHOCK WAVE TURBULENT BOUNDARY LAYER INTERACTION**

N. R. Fomison and J. L. Stollery *In* AGARD, Aerodynamics of Hypersonic Lifting Vehicles Nov. 1987 18 p Sponsored in part by Hunting Engineering, Ltd., Ampthill, United Kingdom (For primary document see N88-13219 05-02)

Copyright Avail: NTIS HC A24/MF A01

An experimental investigation was conducted into the effects of leading edge sweep and bluntness on the flow characteristics of a glancing shock wave turbulent boundary layer interaction generated by a fin-on-plate configuration. A series of sharp swept fins (covering angles of sweep from 0 to 75 deg) and a series of blunt unswept fins (ranging in leading edge diameter from 0 to 25.4 mm) were tested at incidences of up to 30 deg at a Mach number of 2.4 and a freestream Reynolds number of 2,600,000/m. Observations of the mean flow were made using oil flow visualization, static pressure measurements, schlieren photography, and vapor screen visualization techniques. In addition, some limited measurements of the unsteady static pressures beneath the interaction were taken. Flow field models are proposed to include the effects of sweep and bluntness and the governing parameters controlling the extent of the disturbed flow and the pressure levels beneath the interaction are examined. Author

**N88-13228#** Institut Franco-Allemand de Recherches, St. Louis (France). Dept. d'Aerodynamique.

**AN ULTRA-HIGH-SPEED CINEMATOGRAPHIC METHOD FOR THE STUDY OF WAKES IN HYPERSONIC BALLISTIC RANGES [UNE METHODE CINEMATOGRAPHIQUE ULTRA-RAPIDE POUR L'ETUDE DES SILLAGES EN TUNNEL DE TIR HYPERSONIQUE]** **c36**

Axel Koeneke, Bernard Charles Jaeggy, and Germain Koerber *In* AGARD, Aerodynamics of Hypersonic Lifting Vehicles Nov. 1987 13 p In FRENCH (For primary document see N88-13219 05-02)

Copyright Avail: NTIS HC A24/MF A01

Optical methods are among the only possibilities to study hypersonic wakes in ballistic ranges. Because of the flow velocities involved the methods employed must permit exposure time well below one microsecond. The ISL has used ultrahigh speed visualization techniques for the study of the transition of hypersonic wakes for quite some time, but the means available up to now did not permit investigation of the time-history of the instabilities in the wake. The use of a laser equipped with an acousto-optical modulator is proposed as a source of ultrashort, highly energetic pulses with high repetition rate to be used to record a certain number of images of the same experiment in order to study the time history of these instabilities. Advantages of the laser as a light source are not only the high energies available together with pulse duration down to 20 nanoseconds, but mostly the free choice of repetition rate independently of exposure time, and the possibility to synchronize the pulses with external events. The laser is a point source and as such can be used in a variety of different optical setups. The coherent nature of the laser light even permits holographic techniques. The reception system capable of recording the images at a sufficient rate is the basic problem in the development and use of the proposed setup. Author

**N88-13229#** Royal Aircraft Establishment, Farnborough (England). Aerodynamics Dept.

**THE DRAG OF SLENDER AXISYMMETRIC CONES IN RAREFIED HYPERSONIC FLOW**

T. J. Rhys-Jones *In* AGARD, Aerodynamics of Hypersonic Lifting Vehicles Nov. 1987 12 p (For primary document see N88-13219 05-02)

Copyright Avail: NTIS HC A24/MF A01

An experimental study performed in the RAE Low Density Tunnel to determine the aerodynamic characteristics of a range of slender axisymmetric bodies in rarefied hypersonic flow is described. The main purpose of this study was to assess the effects of cone angle, nose bluntness, and Reynolds number on the zero incidence drag of cones. In addition, some measurements of axial force, normal force, and pitching moment at incidence were made. The bodies tested at a nominal Mach number of 10 and at flow conditions which correspond to those in the transitional rarefied flow regime. These data were compared with correlations developed to represent the change in drag coefficient in this flow regime between continuum and free-molecular flow. Author

**N88-13230#** Deutsche Forschungs- und Versuchsanstalt fuer Luft- und Raumfahrt, Goettingen (West Germany). Inst. for Experimental Fluid Mechanics.

**LOW REYNOLDS NUMBER INFLUENCE ON AERODYNAMIC PERFORMANCE OF HYPERSONIC LIFTING VEHICLES**

Georg Koppenwallner *In* AGARD, Aerodynamics of Hypersonic Lifting Vehicles Nov. 1987 14 p (For primary document see N88-13219 05-02)

Copyright Avail: NTIS HC A24/MF A01

The aerodynamic performance of lifting reentry vehicles in the high Mach number (Ma is greater than 10) and high altitude (H is greater than 50 km) regime is analyzed. Due to the high flight velocity of chemical reactions, the low density viscous and rarefaction effects are of importance. Free flight data of the U.S. Shuttle and low density wind tunnel data of DFVLR are used. It is found that aerodynamic performance loss and a destabilizing pitching moment change can be explained by viscous-rarefaction effects. Author

**N88-13231#** Johns Hopkins Univ., Laurel, Md. Applied Physics Lab.

**HYPERSONIC AIRBREATHING PROPULSION: EVOLUTION AND OPPORTUNITIES** **c07**

P. J. Waltrup *In* AGARD, Aerodynamics of Hypersonic Lifting Vehicles Nov. 1987 29 p (For primary document see N88-13219 05-02)

Copyright Avail: NTIS HC A24/MF A01

A history of the evolution of airbreathing propulsion, with emphasis on the development of supersonic combustion ramjet (scramjet) engines, is presented. The current status of scramjet engines is discussed and deficiencies in fundamental and applied data and/or knowledge, which comprise opportunities for future work, are noted. Author

**N88-13232#** Naval Weapons Center, China Lake, Calif. Propulsion Research Branch.

**COMBUSTION RELATED SHEAR-FLOW DYNAMICS IN ELLIPTIC SUPERSONIC JETS**

K. C. Schadow, E. Gutmark, S. Koshigoe, and K. J. Wilson *In* AGARD, Aerodynamics of Hypersonic Lifting Vehicles Nov. 1987 13 p (For primary document see N88-13219 05-02)

Copyright Avail: NTIS HC A24/MF A01

An elliptic jet having an aspect ratio of 3:1 was studied and compared to a circular jet at three Mach numbers: M = 0.15, 1, and 1.3. Hot-wire measurements and Schlieren photography were employed. The superior mixing characteristics of an elliptic jet relative to a circular jet, which were found in previous works in subsonic jets, prevail in the sonic jet and are further augmented by the shock structures of the supersonic underexpanded jet. The major and minor axes switch at a distance of 3 diameters from the nozzle, and the spreading rate of the minor axis side is twice that of a subsonic jet. The experimental data are supported by

the results of the linear instability analysis of the supersonic elliptic jet which show that the initial vortices are bending at the major axis side in a similar way to the process which occurs in a subsonic elliptic jet. Author

**N88-13233*#** National Aeronautics and Space Administration. Langley Research Center, Hampton, Va.
**NUMERICAL ANALYSIS OF FLOW THROUGH SCRAMJET ENGINE INLETS**
Ajay Kumar *In* AGARD, Aerodynamics of Hypersonic Lifting Vehicles Nov. 1987 11 p (For primary document see N88-13219 05-02)
Copyright Avail: NTIS HC A24/MF A01 CSCL 01A

A set of computer programs was developed to analyze flow through supersonic combustion ramjet (scramjet) inlets. These programs solve either the two or three dimensional Euler/Navier-Stokes equations in full conservation form by MacCormack's explicit or explicit-implicit method. An algebraic two-layer eddy viscosity model is used for turbulent flow calculations. The programs are operational in Control Data CYBER-200 series vector-processing computer system and were optimized to take maximum advantage of the vector processing capability of the system. Since their development, the programs were extensively verified and used to analyze a number of very complex inlet configurations. Results are presented from two-dimensional, quasi-three-dimensional, and three-dimensional analyses of the inlet flow field to illustrate the use of the program. Author

**N88-13234*#** National Aeronautics and Space Administration. Ames Research Center, Moffett Field, Calif.
**NUMERICAL SIMULATION OF THE HYPERSONIC FLOW AROUND LIFTING VEHICLES**
Yehia Rizk (Sterling Federal Systems, Inc., Palo Alto, Calif.), Denny Chaussee, and Joseph Steger *In* AGARD, Aerodynamics of Hypersonic Lifting Vehicles Nov. 1987 11 p Previously announced as N87-22116 (For primary document see N88-13219 05-02)
Copyright Avail: NTIS HC A24/MF A01 CSCL 01A

A method of solving the viscous hypersonic flow field around realistic configurations is presented. The numerical procedure for generating the required finite difference grid and the two-factored implicit flow solver are described. Results are presented for the shuttle orbiter and a generic wing-body configuration at hypersonic Mach numbers. Author

**N88-13235#** Dornier-Werke G.m.b.H., Friedrichshafen (West Germany). Aerodynamics Dept.
**SOLUTION OF SOME 3-D VISCOUS AND INVISCID SUPERSONIC FLOW PROBLEMS BY FINITE-VOLUME SPACE-MARCHING SCHEMES**
H. Rieger *In* AGARD, Aerodynamics of Hypersonic Lifting Vehicles Nov. 1987 17 p (For primary document see N88-13219 05-02)
Copyright Avail: NTIS HC A24/MF A01

For prediction of steady supersonic flow fields two numerical methods for solution of the three-dimensional Euler and parabolized Navier-Stokes (PNS) equations are considered. Both are based on a Finite-Volume discretization (FVD) of the governing conservation laws and because of the special properties of steady supersonic flows cost-effective space-marching integration techniques can be applied. Both methods are described and results for inviscid and viscous flows are presented. In view of the upcoming European space transportation activities the simulation of hypersonic flows past complex blunted lifting vehicles requires also efficient methods for solution of the full, not-reduced Navier-Stokes equations. These are needed to provide solutions for supersonic and hypersonic flow fields with large subsonic regions and also to get accurate initial conditions for the space marching codes developed. A relaxation procedure for the steady form of the not-reduced Navier-Stokes and the Euler equations is described and some first results are presented. Author

**N88-13236#** Office National d'Etudes et de Recherches Aerospatiales, Toulouse (France).
**HYPERSONIC LAMINAR BOUNDARY LAYER: PARAMETRIC STUDY FOR THE REPRESENTATION OF REAL GAS EFFECTS [COUCHE LIMITE LAMINAIRE HYPERSONIQUE ETUDE PARAMETRIQUE DE LA REPRESENTATION DES EFFETS DE GAZ REEL]**
B. Aupoix, C. Eldem, and J. Cousteix *In* AGARD. Aerodynamics of Hypersonic Lifting Vehicles Nov. 1987 14 p
In FRENCH (For primary document see N88-13219 05-02)
Copyright Avail: NTIS HC A24/MF A01

A sensitivity study of the real gas model was performed in boundary layer computations on an hyperboloid equivalent to the Space Shuttle windward symmetry plane; for the STS 2 reentry. The real gas model is due to Straub and accounts for only five chemical species while assuming thermodynamic equilibrium. The study has brought into evidence the dependence of both wall heat flux and displacement thickness, not only upon the wall catalycity but also upon the selected reaction rates and the wall temperature. The skin friction coefficient is insensitive to the real gas model. Moreover, only a few chemical reactions can be selected and the diffusion model can be simplified to save computational time without drastic changes in the prediction. Author

**N88-13237#** Deutsche Forschungs- und Versuchsanstalt fuer Luft- und Raumfahrt, Goettingen (West Germany). Inst. for Theoretical Fluid Mechanics.
**ON THE NUMERICAL SIMULATION OF THREE-DIMENSIONAL HYPERSONIC FLOW**
S. Riedelbauch, W. Wetzel, W. Kordulla, and H. Oertel, Jr. *In* AGARD, Aerodynamics of Hypersonic Lifting Vehicles Nov. 1987 16 p (For primary document see N88-13219 05-02)
Copyright Avail: NTIS HC A24/MF A01

The first steps towards the numerical simulation of hypersonic flows is presented. Intentionally, the ideal-gas assumption is used to validate the methods by comparing results with experimentally observed or theoretically obtained data in cold hypersonic flows about simple geometries. The approaches cover the continuum as well as the gas-kinetic flow regime. An implicit finite-difference method with bow-shock fitting is employed to integrate the time-dependent Navier-Stokes equations, while the gas-kinetic flow is simulated by approximations to Boltzmann's equation. The direct-simulation Monte Carlo method is preferred to the molecular-dynamics approach because of its larger computational efficiency. Results are compared with experimental data for the laminar flow past a blunted cone at $M = 10.6$ and past a hemisphere at $M = 4.15$. The decay of Oseen's vortex at $Kn = 0.1$, and the gas-kinetic flow past a cylinder at $M = 5.48$ with $Kn = 0.1$ and 0.3 were simulated, and results are shown in comparison with theoretical data. As an application to more realistic configurations the three-dimensional laminar flow past the nose of a typical spacecraft and the gas-kinetic flow in the symmetry plane of the flow past the same configuration is being discussed. The next steps will include real-gas modelling. For hot hypersonic flows experimental data are badly needed for comparison purpose. Author

**N88-13238#** Glasgow Univ. (Scotland). Dept. of Aeronautics and Fluid Mechanics.
**NUMERICAL EXPERIMENTS WITH HYPERSONIC FLOWS BENEATH A CONE-DELTA-WING COMBINATION**
N. Qin and B. E. Richards *In* AGARD, Aerodynamics of Hypersonic Lifting Vehicles Nov. 1987 14 p (For primary document see N88-13219 05-02)
Copyright Avail: NTIS HC A24/MF A01

Numerical experiments of hypersonic flows beneath a cone-delta-wing combination were carried out by solving the compressible Navier-Stokes equations using an assumption of local conicity. An implicit method is combined with a multigrid scheme in the solution procedure to achieve fast convergence to the steady state. Detailed flow field results provide further insight into the complex flow structures due to interaction between the cone shock

and the wing shock and the interaction of the resulting flow with the wing or cone boundary layer. Flow field pictures reveal phenomena of value in the design of hypersonic lifting vehicles, such as the interference surface pressure and the high local wall heating. Comparisons with experimental data and conical Euler solution are also made. Author

**N88-13239#** Cincinnati Univ., Ohio. Dept. of Aerospace Engineering and Engineering Mechanics.
**A SPATIAL MARCHING TECHNIQUE FOR THE INVISCID BLUNT BODY PROBLEM**
R. T. Davis and Frederick G. Blottner (Sandia National Labs., Albuquerque, N. Mex.) *In* AGARD, Aerodynamics of Hypersonic Lifting Vehicles Nov. 1987 11 p Previously announced as N87-20972 (For primary document see N88-13219 05-02)
Copyright Avail: NTIS HC A24/MF A01

A technique was developed for obtaining approximate solutions of the inviscid, hypersonic flow on a blunt body with a spatial marching scheme. The scheme introduces the Vigneron pressure gradient approximation into the momentum equation in the direction along the body surface. The resulting governing equations are hyperbolic. With a specified shock wave these equations are solved at the stagnation streamline with an iteration procedure and are solved in the downstream direction with a marching scheme. The complete Euler equations are solved with the numerical scheme when the flow is supersonic. A global interation procedure is required to obtain the shock wave location. The approximate results from the spatial marching technique are compared with the complete solution of the Euler equations for flow over a sphere. The two results are shown to be in approximate agreement and the spatial marching technique provides useful engineering predictions while requiring considerably less computational time. Author

**N88-13240#** Messerschmitt-Boelkow-Blohm G.m.b.H., Munich (West Germany). Space Systems Group.
**A 3-D EULER SOLUTION FOR HYPERSONIC MACH NUMBERS**
Michael Pfitzner and Claus Weiland *In* AGARD, Aerodynamics of Hypersonic Lifting Vehicles Nov. 1987 13 p (For primary document see N88-13219 05-02)
Copyright Avail: NTIS HC A24/MF A01

The development of reusable reentry vehicles and hypersonic missiles require the control of aerothermal problems. To that end it is necessary to develop aerothermal prediction methods and to change and extend existing methods, which were developed for subsonic and supersonic flow problems. The integration of three dimensional unsteady and steady Euler equations in the regime of hypersonic flow is discussed. Author

**N88-13241#** Imperial Coll. of Science and Technology, London (England). Dept. of Aeronautics.
**COMPUTATION OF FLOW PAST CONICAL HYPERSONIC WINGS USING A SECOND ORDER GODUNOV METHOD**
R. Hillier *In* AGARD, Aerodynamics of Hypersonic Lifting Vehicles Nov. 1987 15 p (For primary document see N88-13219 05-02)
Copyright Avail: NTIS HC A24/MF A01

Computations of inviscid hypersonic flow past flat plate delta wings during a second order Godunov-type scheme are presented. The governing equations are written in an unsteady conical form and then time marched to a final conical steady state. The core of the calculation is a generalized Riemann problem which is used to determine the flux transfers at the interfaces between computational cells. Results are presented for wings with shock waves both attached at and detached from the leading edges. The leeward surface flows support embedded shock waves and separated vortex flows and the likely influence of real viscous effects on these is discussed. Author

**N88-13242*#** National Aeronautics and Space Administration. Ames Research Center, Moffett Field, Calif.
**AEROTHERMODYNAMICS RESEARCH AT NASA AMES**
George S. Deiwert *In* AGARD, Aerodynamics of Hypersonic Lifting Vehicles Nov. 1987 17 p (For primary document see N88-13219 05-02)
Copyright Avail: NTIS HC A24/MF A01 CSCL 01A

Research activity in the aerothermodynamics branch at NASA Ames Research Center is reviewed. Advanced concepts and mission studies relating to the next generation aerospace transportation systems are summarized and directions for continued research identified. Theoretical and computational studies directed at determining flow fields and radiative and convective heating loads in real gases are described. Included are Navier-Stokes codes for equilibrium and thermochemical nonequilibrium air. Experimental studies in the 3.5 foot hypersonic wind tunnel, the ballistic ranges and the electric arc driven shock tube are described. Tested configurations included generic hypersonic aerospace plane configurations, aeroassisted orbital transfer vehicle shapes and Galileo probe models. Author

**N88-13243#** Messerschmitt-Boelkow-Blohm G.m.b.H., Hamburg (West Germany). Unternehmensbereich Transport- und Verkehrsflugzeuge.
**VORTEX FORMATION OVER DELTA, DOUBLE-DELTA AND WAVE RIDER CONFIGURATIONS AT SUPERSONIC SPEEDS**
Uwe Ganzer and Joachim Szodruch *In* AGARD, Aerodynamics of Hypersonic Lifting Vehicles Nov. 1987 32 p (For primary document see N88-13219 05-02)
Copyright Avail: NTIS HC A24/MF A01

The flow field of the thick delta wing at high subsonic and supersonic speeds was the subject of quite a variety of investigations at the Technical University of Berlin. The research work started as early as in the late 60's and is still going on today. It was triggered off by the initiatives of the late Dietrich Kuchemann-aiming at a hypersonic transport and it was taken as a contribution to the Eurohyp activities. The wing configurations investigated were of simple shape: delta wings with straight leading edges and triangular cross sections of different thicknesses. The interest was focussed on the development of the leeside flow with changes in angle of incidence and main stream Mach number. In addition to that similar delta wings with curved leading edges and also with a jump in leading edge sweep were investigated, as well as two types of wave riders. Besides some theoretical work mainly wind tunnel tests were made applying available test techniques: surface pressure measurements, Pitot measurements in the flow field, flow visualization by Schlieren, vapor and oilfilm techniques, skin friction determination using oilfilm interferrogramm and, finally, laser velocimetry. The experimental investigations were particularly challenging, because of the small models of generally not more than 6 cm span. This limitation arose from the small size of the transonic and supersonic wind tunnel. Author

**N88-13244#** Lockheed-California Co., Burbank.
**THE OFF-DESIGN PERFORMANCE OF HYPERSONIC WAVERIDERS** c05
Lyle N. Long *In* AGARD, Aerodynamics of Hypersonic Lifting Vehicles Nov. 1987 14 p (For primary document see N88-13219 05-02)
Copyright Avail: NTIS HC A24/MF A01

Waveriders are being considered more and more as potential aerospace vehicles. However there are several questions regarding these configurations that must be answered before they can be considered viable designs. The most significant problems are related to aerothermal heating, propulsion integration, and off-design performance. Off-design performance predictions for two generic waveriders are presented. The results are from a numerical method based upon the nonlinear, inviscid Euler equations. Comparisons to experimental data are also shown. Author

**N88-13245*#** Maryland Univ., College Park. Dept. of Aerospace Engineering.
**NUMERICAL OPTIMIZATION OF CONICAL FLOW WAVERIDERS INCLUDING DETAILED VISCOUS EFFECTS** c05
Kevin G. Bowcutt, John D. Anderson, Jr., and Diego Capriotti *In* AGARD, Aerodynamics of Hypersonic Lifting Vehicles Nov. 1987 23 p Sponsored in part by NASA Langley Research Office, Hampton, Va. and Army Research Office, Washington, D.C. (For

primary document see N88-13219 05-02)
Copyright Avail: NTIS HC A24/MF A01 CSCL 01A

A family of optimized hypersonic waveriders is generated and studied wherein detailed viscous effects are included within the optimization process itself. This is in contrast to previous optimized waverider work, wherein purely inviscid flow is used to obtain the waverider shapes. For the present waveriders, the undersurface is a streamsurface of an inviscid conical flowfield, the upper surface is a streamsurface of the inviscid flow over a tapered cylinder (calculated by the axisymmetric method of characteristics), and the viscous effects are treated by integral solutions of the boundary layer equations. Transition from laminar to turbulent flow is included within the viscous calculations. The optimization is carried out using a nonlinear simplex method. The resulting family of viscous hypersonic waveriders yields predicted high values of lift/drag, high enough to break the L/D barrier based on experience with other hypersonic configurations. Moreover, the numerical optimization process for the viscous waveriders results in distinctly different shapes compared to previous work with inviscid-designed waveriders. Also, the fine details of the viscous solution, such as how the shear stress is distributed over the surface, and the location of transition, are crucial to the details of the resulting waverider geometry. Finally, the moment coefficient variations and heat transfer distributions associated with the viscous optimized waveriders are studied. Author

**N88-13246#** Southampton Univ. (England). Dept. of Aeronautics and Astronautics.
**HYPERSONIC STATIC AND DYNAMIC STABILITY OF AXISYMMETRIC SHAPES: A COMPARISON OF PREDICTION METHODS AND EXPERIMENT**
R. A. East and G. R. Hutt *In* AGARD, Aerodynamics of Hypersonic Lifting Vehicles Nov. 1987 15 p Sponsored in part by Ministry of Defence, United Kingdom (For primary document see N88-13219 05-02)
Copyright Avail: NTIS HC A24/MF A01

The stability of oscillatory motions of vehicles flying at hypersonic Mach numbers is of considerable relevance to their initial design. Methods are needed for quick and accurate predictions of stability and control which are applicable over a wide range of body shapes, angles of attack, and flow conditions, without the need to resort to computationally time consuming numerical flow field calculation methods. Experimental data, obtained over a range of angles of attack, concerning the static and dynamic pitching stability of a wide range of both pointed and blunted axisymmetric shapes including cones and blunted cylinder flares are presented. Although Newtonian theory gives inadequate accuracy of prediction, inviscid embedded Newtonian theory, which accounts for the reduced dynamic pressure and lower flow velocity in the embedded flow downstream of the strong bow shock, is shown to provide surprisingly good agreement with the experimental data over a wide range of conditions. Comparisons with experimental results show that the broad flow features and their effect on static and dynamic stability are well described in regimes not containing flow structural change. However, in some cases discrepancies exist between the predictions and experimental observations and these were attributed to a variety of viscous flow phenomena involving boundary layer transition and flow separation, including complex lee-surface vortical flows.
Author

**N88-13247#** Waterloo Univ. (Ontario). Dept. of Applied Mathematics and Mechanical Engineering.
**DYNAMIC STABILITY OF HYPERSONIC CONICAL LIFTING VEHICLES ACCORDING TO NEWTON-BUSEMANN THEORY** **c08**
W. H. Hui and H. J. VanRoessel (University of Western Ontario, London.) *In* AGARD, Aerodynamics of Hypersonic Lifting Vehicles Nov. 1987 13 p Sponsored in part by Natural Science and Engineering Research Council of Canada (For primary document see N88-13219 05-02)
Copyright Avail: NTIS HC A24/MF A01

A theory is given of the aerodynamic stability of hypersonic conical lifting vehicles performing small amplitude pitching motion about its steady flight by using the Newton-Busemann flow theory, which is the rational limit of gas dynamic theory as the flight Mach number M sub infinity yields infinite and the ratio of specific heat Gamma yields 1. This is done by reformulating the gas dynamic equations using a set of material functions as independent variables which are a generalization of the stream functions of steady flow. In this formulation, calculations of the steady flow field are reduced to finding the geodesics of the body surface. The unsteady flow field is then calculated by perturbation of the steady flow; in particular, for conical shapes it requires only numerical quadrature. The theory is applied to conical wings of parabolic cross-section. The dependence of the stiffness and damping-in-pitch derivative on the angle of attack, the slenderness, concavity and convexity of the wing, and on the pivot axis position is studied systematically. Author

**N88-13248#** Air Force Wright Aeronautical Labs., Wright-Patterson AFB, Ohio. Aeromechanics Div.
**LIFTING BODIES: AN ATTRACTIVE AERODYNAMIC CONFIGURATION CHOICE FOR HYPERVELOCITY VEHICLES** **c05**
Alfred C. Draper and Melvin L. Buck *In* AGARD, Aerodynamics of Hypersonic Lifting Vehicles Nov. 1987 44 p (For primary document see N88-13219 05-02)
Copyright Avail: NTIS HC A24/MF A01

A brief chronology is given of the lifting body configurations investigated by the Flight Dynamics Laboratory, along with their aeroperformance capabilities including ASSET, PRIME, the X-24A, and the X-24B. Also included is a brief discussion of lifting body applications at supercircular velocities such as the SORTIE. The impact of basic geometric and component effects on aerodynamic performance parameters is addressed. These results were then translated into an aerodynamic configuration which eliminates the aft vertical fins without degrading the hypersonic lift-to-drag ratio while maintaining directional stability. Additionally, the benefits and applicability are examined. Specifically, the more significant methods such as the Hypersonic Arbitrary Body Program (HABP), PANAIR, Euler, Parabolized Navier-Stokes (PNS), and Navier-Stokes (NS) codes are discussed. Experimental capabilities and needs are discussed and finally, long term goals for future lifting body configurations are assessed. Author

**N88-13249#** British Aerospace Public Ltd. Co., Bristol (England). Aerodynamics Research Dept.
**EXPERIENCES USING THE MARK IV SUPERSONIC HYPERSONIC ARBITRARY BODY PROGRAM**
Carren M. E. Fisher *In* AGARD, Aerodynamics of Hypersonic Lifting Vehicles Nov. 1987 18 p (For primary document see N88-13219 05-02)
Copyright Avail: NTIS HC A24/MF A01

Work done during the last two years in an attempt to gain an understanding of, and to establish a capability for the use of, the Douglas Supersonic/Hypersonic Arbitrary Body Program (S/HABP) is described. This program has a complex structure and offers a large variety of aerodynamic prediction methods to solve many different types of problems. Most of the features of the program were used with success. Aspects of the flowfield routines and viscous options, which could not be utilized correctly, are either under investigation, or updates to the programming are awaited. Some accurate predictions were made using the inviscid pressure methods, which were evaluated for a wide range of configurations, for Mach numbers from 1.7 to 25.0 and from an incidence of -8 to 40 deg. The code was seen to be highly flexible, but the accuracy of the results is user dependent. Relative to computational fluid dynamics codes, S/HABP geometries are easy to prepare and the code is cheap to run. Author

**N88-13250#** Royal Aircraft Establishment, Bedford (England).
**THE RAE EXPERIMENTAL DATA-BASE FOR MISSILES AT HIGH MACH NUMBER AND ITS USE IN ASSESSING CFD METHODS**
J. Hodges and L. C. Ward *In* AGARD, Aerodynamics of

Hypersonic Lifting Vehicles Nov. 1987 14 p (For primary document see N88-13219 05-02)
Copyright Avail: NTIS HC A24/MF A01

Wind tunnel tests are being performed in order to measure overall and panel forces and moments on cruciform body-control and body-wing missile configurations at M = 2.5, 3.5, and 4.5. When completed, the test results will provide a wide ranging data base suitable for inclusion into semi-empirical prediction methods. Additionally it can be used to help validate and assess the computational fluid dynamics (CFD) methods that are available. A detailed description of all the models and the wind tunnel test conditions, and selected results are presented. Comparisons are shown between the experimental data and results from a space-marching Euler code. An outline is given of the extension of these comparisons to surface pressure. Author

**N88-13251#** Avions Marcel Dassault-Breguet Aviation, Saint-Cloud (France).
**GENERAL AERODYNAMIC-AEROTHERMODYNAMIC CONCEPTS FOR HERMES [CONCEPTS GENERAUX AERODYNAMIQUES-AEROTHERMIQUES D'HERMES]**
P. Perrier and Ph. Caupenne *In* AGARD, Aerodynamics of Hypersonic Lifting Vehicles Nov. 1987 7 p In FRENCH (For primary document see N88-13219 05-02)
Copyright Avail: NTIS HC A24/MF A01

Overall aerodynamic and aerothermal design considerations for the Hermes space vehicle are summarized and a general methodology for the development of Hermes is outlined. Examples of specific design objectives are given which address the problems of longitudinal stability and vehicle aerodynamic heating. M.G.

**N88-13252#** British Aerospace Public Ltd. Co., Preston (England). HOTOL Study Team.
**HYPERSONIC AERODYNAMICS: APPLICATIONS FOR HOTOL**
Alison J. Wake *In* AGARD, Aerodynamics of Hypersonic Lifting Vehicles Nov. 1987 12 p (For primary document see N88-13219 05-02)
Copyright Avail: NTIS HC A24/MF A01

HOTOL has emerged from studies between BAe and Rolls-Royce as a totally reusable airframe with a hybrid air-breathing propulsion system. It is aimed at placing payloads into low Earth orbit for 20 percent of the cost of the U.S. Space Shuttle. As part of the current proof-of-concept study an assessment is being made of the aerodynamic characteristics of the vehicle including those in the hypersonic regime. This assessment will also identify areas of high risk and where current methods are deficient. Some of the results obtained, the areas so far identified as requiring further work are detailed and a five year program is proposed to investigate these areas. Author

**N88-13253#** National Aerospace Lab., Tokyo (Japan).
**PROCEEDINGS OF THE 4TH NAL SYMPOSIUM ON AIRCRAFT COMPUTATIONAL AERODYNAMICS**
Dec. 1986 308 p In ENGLISH and JAPANESE Symposium held in Tokyo, Japan, 19-20 Jun. 1986
(NAL-SP-7; ISSN-0452-2982) Avail: NTIS HC A14/MF A01

Thirty-six papers on computational fluid dynamics with aeronautical applications are presented. For individual titles, see N88-13254 through N88-13289.

**N88-13254#** National Aerospace Lab., Tokyo (Japan).
**AN ANALYSIS OF THE COMPRESSIBLE-VISCOUS FLOW FIELD AROUND A 3D-OSCILLATING WING**
Jiro Nakamichi and Koji Isogai *In its* Proceedings of the 4th NAL Symposium on Aircraft Computational Aerodynamics Dec. 1986 p 1-11 In JAPANESE; ENGLISH summary (For primary document see N88-13253 05-02)
Avail: NTIS HC A14/MF A01

A 3D Navier-Stokes program based upon a Beam-Warming diagonalization scheme has been combined with a moving grid system so that it can be applied to the solution around an oscillating wing. The wing is in a pitching motion with an amplitude of 1 deg and a reduced frequency of 0.428 (based upon the root semichord). The free stream Mach number is 0.9 and the mean angle of attack of the wing is 4 deg. To the extent that results have been compared with experimental data, the unsteady flow is successfully simulated and the leading edge separations are observed, which is one of the most significant aspects of the experiment. It is demonstrated that the present code is feasible and applicable to the computation of the unsteady viscous compressible flow field around an oscillating wing. Author

**N88-13255#** Tokyo Univ. (Japan).
**COMPUTATION OF DYNAMIC STALL OF NACA0012 AIRFOIL BY BLOCK PENTADIAGONAL MATRIX SCHEME**
Yoshifumi Shida and Kunio Kawahara *In* National Aerospace Lab., Proceedings of the 4th NAL Symposium on Aircraft Computational Aerodynamics Dec. 1986 p 13-23 In JAPANESE; ENGLISH summary (For primary document see N88-13253 05-02)
Avail: NTIS HC A14/MF A01

The flow field around an oscillating NACA0012 airfoil in pitch at 0.25 chord is analyzed by solving the two-dimensional compressible Navier-Stokes equations. A block pentadiagonal matrix scheme based on the approximate factorization method is adopted. Two meshes, 161 by 40 and 213 by 80, are used. With the coarse mesh, lift stall is captured. With the fine mesh, not only lift stall but also the restoration process of the lift coefficient in the downstroke is captured. Author

**N88-13256#** National Aerospace Lab., Tokyo (Japan).
**NUMERICA CALCULATION IN THE LAPLACE DOMAIN FOR SUBSONIC UNSTEADY AERODYNAMIC FORCES ACTING ON A FINITE WING**
Tetsuhiko Ueda *In its* Proceedings of the 4th NAL Symposium on Aircraft Computational Aerodynamics Dec. 1986 p 25-32 In JAPANESE; ENGLISH summary (For primary document see N88-13253 05-02)
Avail: NTIS HC A14/MF A01

A method of obtaining subsonic unsteady aerodynamic forces in the Laplace domain is presented. The kernel function of singular integral equations based on the lifting surface theory is numerically computed in the exact way for the entire s-plane. In an example calculation of the generalized forces, a singularity appears in the left half of the p-plane at a high Mach number of eight-tenths. It is shown that the singularity is a pole of the order one and that it can be modeled by a simple rational function which is relevant to the aeroelastic analysis. The theory of functions is utilized for obtaining the singularity model for the generalized forces. Author

**N88-13257#** Mitsubishi Heavy-Industries Ltd., Tokyo (Japan).
**PRACTICAL APPLICATION OF TWO-DIMENSIONAL VISCOUS FLOW COMPUTATION**
Takeshi Kaiden, Junichi Miyakawa, Naoki Hirose, and Nobuhiro Kawai (National Aerospace Lab., Tokyo, Japan ) *In* National Aerospace Lab., Proceedings of the 4th NAL Symposium on Aircraft Computational Aerodynamics Dec. 1986 p 33-38 In JAPANESE; ENGLISH summary (For primary document see N88-13253 05-02)
Avail: NTIS HC A14/MF A01

A validative discussion of the NSFOIL code (a high Reynolds number transonic airfoil analysis code) is presented in the region of low speed and high attack angle. The computational results are comapred with results of wind tunnel tests and the vortex method, which is a separated flow analysis method, to investigate the validity of the code and to further the development of future improvements. NSFOIL is found to be able to predict non-linear characteristics, in which conventional numerical methods are powerless. There is still some room for improvement to be able to calculate an exact stall angle. Author

**N88-13258#** Kawasaki Heavy Industries Ltd., Kagamihara (Japan).
**A NUMERICAL INVESTIGATION ON WING/NACELLE INTERFERENCES**
Keisuke Sawada and Susumu Takanashi (National Aerospace Lab.,

Tokyo, Japan ) *In* National Aerospace Lab., Proceedings of the 4th NAL Symposium on Aircraft Computational Aerodynamics Dec. 1986 p 39-44 In JAPANESE; ENGLISH summary (For primary document see N88-13253 05-02)
Avail: NTIS HC A14/MF A01

A numerical investigation of wing/nacelle interferences of upper surface blown (USB) configuration was carried out. A grid system about the realistic configuration of wing/nacelle combination was generated by the multi-block grid generation technique. The Euler equations were solved by the second order accurate upwind scheme. Results were obtained for M sub infinity = 0.7, alpha = 2.0. The existence of channel flows accompanied by strong shock between two engine nacelles was confirmed. Power effects of two engines were examined by modeling both the plane of intake and that of jet exhaust appropriately. Author

**N88-13259#** Kawasaki Heavy Industries Ltd., Kagamihara (Japan).
**THE ROLE OF COMPUTATION FLUID DYNAMICS IN AERONAUTICAL ENGINEERING (4). THE DEVELOPMENT AND APPLICATIONS OF IMPLICIT TVD FINITE VOLUME CODE**
Eiji Shima and Tadamasa Jounouchi *In* National Aerospace Lab., Proceedings of the 4th NAL Symposium on Aircraft Computational Aerodynamics Dec. 1986 p 45-51 In JAPANESE; ENGLISH summary (For primary document see N88-13253 05-02)
Avail: NTIS HC A14/MF A01

An implicit total variation diminishing (TVD) finite volume code was developed. This code applies to van Leer's flux splitting, the Diagonalized Lower/Upper block diagonal Alternating Direction Implicit (LU-ADI) factored algorithm, TVD formulation using characteristic variables and the smooth limiter. The code is more robust and gives sharper shock profile than the conventional central difference scheme, while it takes nearly as much CPU time/step as the Beam-Warming scheme. The computed results are shown for: (1) transonic viscous flow about a NACA0012 airfoil; (2) supersonic inviscid flow about a two-dimensional air intake; and (3) supersonic inviscid flow about an axisymmetric blunt body. Author

**N88-13260#** Fujitsu Ltd., Tokyo (Japan).
**PRACTICAL AND MODERN SIMULATION BY SYSTEMATIC CONNECTION OF THE LU-ADI CODE AND THE SOLUTION ADAPTIVE GRID PROGRAM** **c61**
Kisa Matsuhima, Shigeru Obayashi, Kazuhiro Nakahashi, and Kozo Fujii (National Aerospace Lab., Tokyo, Japan ) *In* National Aerospace Lab., Proceedings of the 4th NAL Symposium on Aircraft Computational Aerodynamics Dec. 1986 p 53-60 In JAPANESE; ENGLISH summary (For primary document see N88-13253 05-02)
Avail: NTIS HC A14/MF A01

In order to develop a practical modern numerical simulation system, an efficient Navier-Stokes solver using the Lower/Upper block diagonal Alternating Direction Implicity (LU-ADI) method and developed as a general-purpose program, has been systematically connected with the Solution-Adaptive-Grid program, a grid generation program and some post processing programs of computational results. The most attractive feature of this simple system is that grid redistribution is accomplished according to the physical phenomena of each problem. It significantly helps to improve the accuracy and quality of numerical results. Through several flow problems, this tiny system has been shown to work effectively. Author

**N88-13261#** Kyoto Univ. (Japan).
**NUMERICAL CALCULATIONS OF THE FLOWFIELD AROUND PROPELLERS**
Makoto Kobayakawa, Hiroyuki Onuma, and Yasuhiro Shiota (Toyota Motor Co., Tokyo, Japan ) *In* National Aerospace Lab., Proceedings of the 4th NAL Symposium on Aircraft Computational Aerodynamics Dec. 1986 p 61-69 In JAPANESE; ENGLISH summary (For primary document see N88-13253 05-02)
Avail: NTIS HC A14/MF A01

In order to examine the flow field around ATP by numerical calculations, the finite difference method is applied. First, the partial differential equation for the disturbance velocity potential is solved by the line relaxation technique. In order to do the calculations, boundary fitted meshes are generated. The transformations between physical and computational space are performed by chain rule. The SR-3 is used for numerical calculations. In the second part of the paper, the Euler equations are solved by non-iterative Alternating Direction Implicit (ADI) schemes in AF algorithm. Boundary fitted meshes are also used for this case. The results show qualitative agreement with the results obtained by Bober et al. Finally, the aerodynamic performances, such as power coefficients and efficiencies, are obtained. Potential calculations show that these quantities are relatively larger than the experimental values obtained by NASA; however, Euler solutions show that the values come closer to the experimental values. Author

**N88-13262#** National Aerospace Lab., Tokyo (Japan).
**NUMERICAL ANALYSIS OF CASCADE FLOW SOLVING NAVIER-STOKES EQUATIONS**
Osamu Nozaki, Naoki Hirose, Nobuhiro Kawai, and Atsuhiro Tamura *In its* Proceedings of the 4th NAL Symposium on Aircraft Computational Aerodynamics Dec. 1986 p 71-75 In JAPANESE; ENGLISH summary (For primary document see N88-13253 05-02)
Avail: NTIS HC A14/MF A01

Numerical analysis based on Navier-Stokes equations was carried out for high Reynolds number flow through two-dimensional cascades using the initial approach fix (IAF) scheme. An algebraic eddy viscosity model of the turbulent boundary layer was used. To make fine orthogonal grids on inner and outer boundaries, C-type grids are generated around a cascade by solving Poisson's equations which have inhomogeneous terms. Several results have been obtained for a compressor and FJR turbine. These results show good agreement with experimental data. Author

**N88-13263#** National Aerospace Lab., Tokyo (Japan).
**INVERSE DESIGN METHOD FOR TWO-DIMENSIONAL TRANSONIC CASCADES**
Susumu Takanashi, Atsuhiro Tamura, Takashi Nakamura, and Naoki Hirose *In its* Proceedings of the 4th NAL Symposium on Aircraft Computational Aerodynamics Dec. 1986 p 77-83 In JAPANESE; ENGLISH summary (For primary document see N88-13253 05-02)
Avail: NTIS HC A14/MF A01

A simple and practical inverse design method is described for two-dimensional transonic cascades with specified target distributions. The design procedure is based on an iterative residual correction concept. The difference between target and computed pressures, at each iteration step, is determined using a cascade analysis code. The blade surface correction corresponding to the pressure difference (or residual) is approximately obtained by transonic integral equations. Typical examples designed by the present method using the full potential solver as the analysis code are presented for subsonic and transonic cascades with specified pressures. Author

**N88-13264#** National Aerospace Lab., Kakuda (Japan).
**DEVELOPMENT OF THE COMPUTER PROGRAM FOR TURBULENT BOUNDARY LAYERS**
Hiroshi Ishigaki and Munekazu Mochizuki *In* National Aerospace Lab., Proceedings of the 4th NAL Symposium on Aircraft Computational Aerodynamics Dec. 1986 p 85-89 In JAPANESE; ENGLISH summary (For primary document see N88-13253 05-02)
Avail: NTIS HC A14/MF A01

A computer program was developed for calculation of the turbulent boundary layer around a two-dimensional or an axisymmetrical body. The method of solving the algorithm and computed results of laminar and turbulent boundary layers are presented Author

**N88-13265#** Ishikawajima-Harima Heavy Industries Co. Ltd., Tokyo (Japan).
**NUMERICAL PREDICTION OF TURBULENT FLOWS IN DUMP DIFFUSERS** c34
Yasunori Ando, Masafumi Kawai, Yukinori Sato, and Hidemi Toh *In* National Aerospace Lab., Proceedings of the 4th NAL Symposium on Aircraft Computational Aerodynamics Dec. 1986 p 91-98 In JAPANESE; ENGLISH summary (For primary document see N88-13253 05-02)
Avail: NTIS HC A14/MF A01

A finite-volume calculation method for the solution of two-dimensional incompressible time-averaged Navier-Stokes equation in a general curvilinear coordinate system is presented. The main calculation algorithm of the method is an extension of the SIMPLE algorithm to present the governing equations based on curvilinear coordinates, maintaining the Cartesian velocity components as dependent variables. The standard k-epsilon turbulence model is used for closure of the Reynolds equation. This method is applied to calculation of turbulent flows in two-dimensional and axisymmetrical dump diffusers with uniform and distorted inlet velocity profiles. General flow pattern and velocity distribution are successfully predicted and the results show good agreement with experimental data, especially when using the QUICKER scheme for convection terms approximation. Pressure loss can also be predicted using the fine grid, but improvement must be achieved in the computational method to be able to predict pressure loss with moderate grid. The treatment of the pressure correction equation in general curvilinear coordinates employed in this work enhances the stability and robustness of calculation. Author

**N88-13266#** Mitsubisi Electric Corp., Tokyo (Japan).
**NUMERICAL ANALYSIS OF SUPERSONIC FLOWS USING PANEL METHOD**
Yuichi Maruyama, Sadao Akishita, and Akihito Nakamura (Mitsubishi Space Software Corp., Japan ) *In* National Aerospace Lab., Proceedings of the 4th NAL Symposium on Aircraft Computational Aerodynamics Dec. 1986 p 99-106 In JAPANESE; ENGLISH summary (For primary document see N88-13253 05-02)
Avail: NTIS HC A14/MF A01

Steady supersonic linearized potential flows about two types of wings and a wing-body configuration were simulated using the panel method program MARCAP. Linearly varying doublet distribution is adopted to ensure the continuity of the strength on panel edges, while constant distribution on each panel is used for source. Morino's scheme is employed for most cases. The velocity boundary condition scheme is also applied to some cases. The results show good agreement with analytical solutions and wind tunnel testings. The computation time is within a reasonable limit, and the program size is comparable to those of panel methods for incompressible or subsonic flows. Author

**N88-13267#** Fuji Heavy Industries Ltd., Utsunomiya (Japan).
**COMPUTATION OF NACELLE INTERFERENCE USING BOUNDARY ELEMENT METHOD**
Masaaki Nakadate, Hidefumi Nagashima, and Mitsunori Yanagizawa (National Aerospace Lab., Tokyo, Japan ) *In* National Aerospace Lab., Proceedings of the 4th NAL Symposium on Aircraft Computational Aerodynamics Dec. 1986 p 107-120 In JAPANESE; ENGLISH summary (For primary document see N88-13253 05-02)
Avail: NTIS HC A14/MF A01

The aerodynamic interference problem of jet transport aircraft due to the close coupling between nacelle and wing is one of the major concerns of aerdynamic engineers. At the research level, the Navier-Stokes code is beginning to be applied to such a problem. At the engineering level the application of the panel method is more practical. This paper presents the results of applying the Boundary Element Method code to the analysis of nacelle interference of a practical jet transport configuration. Correlation between calculated and tested results is also presented. Author

**N88-13268#** National Aerospace Lab., Tokyo (Japan).
**APPLICATION OF DISCRETE VORTEX METHOD TO ANALYSIS OF SEPARATED FLOW AROUND AEROFOILS**
Masashi Shigemi *In its* Proceedings of the 4th NAL Symposium on Aircraft Computational Aerodynamics Dec. 1986 p 121-128 In JAPANESE; ENGLISH summary (For primary document see N88-13253 05-02)
Avail: NTIS HC A14/MF A01

The discrete vortex method was applied to the calculation of the separated flow around aerofoils. A new approach was formulated, in which the strength of the vortex, which is shed off at the separation point, was included in the unknown variables. In order to save computational cost, simplifications were introduced in the formulation, e.g., clusters of the drifting vortices were treated as concentrated single vortices. Because the total pressure in the separated region is less than that in the other region, the pressure distribution around the aerofoil, which is obtained from the velocity distribution through the Bernoulli formula, has to be evaluated individually for the non-separated and separated regions. To define the relativity between the two pressure distributions, a method of estimating the amount of the total pressure loss in the separated region was introduced. The Blasius formula, which is generally used to derive the forces acting on an obstacle, was modified to include the influence of the total pressure loss upon the lift and the drag forces. Author

**N88-13269#** National Aerospace Lab., Tokyo (Japan).
**PROGRAMMING TECHNIQUES FOR HIGH-SPEED PROCESSING OF LARGE SCALE NUMERICAL SIMULATIO ON SUPERCOMPUTERS** c61
Kinuyo Nakamura and Masahiro Yoshida *In its* Proceedings of the 4th NAL Symposium on Aircraft Computational Aerodynamics Dec. 1986 p 129-136 In JAPANESE; ENGLISH summary (For primary document see N88-13253 05-02)
Avail: NTIS HC A14/MF A01

A method is presented for improving algorithms and programming techniques which permits the efficient use of supercomputers. The method is illustrated by an example of a numerical analysis of codes of transonic full potential flows about wings. Author

**N88-13270#** Nippon Electric Co. Ltd., Tokyo (Japan).
**VECTORIZING THE FFTS ON SUPERCOMPUTER SX SYSTEM** c61
Mitsuyasu Hanamura, Junichi Yorozu, Yoshiaki Tsuwa, Tadashi Watanabe, and Norio Masuda *In* National Aerospace Lab., Proceedings of the 4th NAL Symposium on Aircraft Computational Aerodynamics Dec. 1986 p 137-141 In JAPANESE; ENGLISH summary (For primary document see N88-13253 05-02)
Avail: NTIS HC A14/MF A01

One- and two-dimenstional fast Fourier transform (FFT) algorithms for the supercomputer SX system were investigated. Algorithms and calculated CPU-time of two-dimensional FFTs are presented. A time of 9.41 msec is obtained in calculating two-dimensional FFT (256 by 256) at single precision using the SX-2. Author

**N88-13271#** Nippon Electric Co. Ltd., Tokyo (Japan). C and C Information Technology Research Labs.
**TRIDIAGONAL APPROXIMATE FACTORIZATION METHOD: A PRECONDITIONING TECHNIQUE FOR SOLVING NONSYMMETRIC LINEAR SYSTEMS SUITABLE TO SUPERCOMPUTERS** c61
Shun Doi and Norio Harada *In* National Aerospace Lab., Proceedings of the 4th NAL Symposium on Aircraft Computational Aerodynamics Dec. 1986 p 143-149 In JAPANESE; ENGLISH summary (For primary document see N88-13253 05-02)
Avail: NTIS HC A14/MF A01

A tridiagonal approximate factorization (TF) method is proposed as a preconditioning algorithm suitable to vector and parallel computers for solving large sparse nonsymmetric systems of linear equations. In this method, the preconditioning matrix is constructed as a product of component tridiagonal matrices, each of which

consists of matrix elements corresponding to a spatial axis of the original partial differential equation (PDE) problem. The inversion process of this preconditioning matrix is reduced to a series of simple forward-and-backward substitutions, which have inherent parallelism and hence can be easily vectorized. Comparison is made between the TFBCG algorithm, which applies TF preconditioning to the bi-conjugate gradient algorithm, and the ILUBCG/MILUBCG algorithms, the most powerful and popular methods on conventional scale computers. Numerical tests on the SX-2 supercomputer show that the TFBCG program is three to nine times faster than the conventional (M) ILUBCG programs, and also one to four times faster than the sophisticated (M) ILUBCG programs utilizing the list-vector technique. Author

**N88-13272#** Tokyo Metropolitan Univ. (Japan). Coll. of Aeronautical Engineering.
**NUMERICAL ANALYSIS OF AXISYMMETRIC FLOW WITH H2-O2 REACTIONS** **c34**
Shizui Watanabe *In* National Aerospace Lab., Proceedings of the 4th NAL Symposium on Aircraft Computational Aerodynamics Dec. 1986 p 151-157 In JAPANESE; ENGLISH summary (For primary document see N88-13253 05-02)
Avail: NTIS HC A14/MF A01

A numerical method which analyzes unsteady fluid dynamic equations with species transportation and chemical kinetics is presented. It is constructed as follows: Fluid dynamical equations are solved by a Newton-Raphson type iteration method and velocities and fluxes are decided. Species diffusion equations and enthalpy diffusion terms are calculated. Chemical kinetic equations are solved implicitly and thermodynamic quantities are decided. For chemical kinetics, 22 elementary reactions and nine species are considered. This method is applied to analyze hydrogen jet into heated oxygen and argon mixture. Author

**N88-13273#** National Aerospace Lab., Tokyo (Japan).
**RAREFIED GAS NUMERICAL WIND TUNNEL. 2: TWO-DIMENSIONAL AND AXIALLY SYMMETRIC BODIES**
Katsuhisa Koura *In its* Proceedings of the 4th NAL Symposium on Aircraft Computational Aerodynamics Dec. 1986 p 159-164 In JAPANESE; ENGLISH summary (For primary document see N88-13253 05-02)
Avail: NTIS HC A14/MF A01

A rarefied-gas numerical wind tunnel is being developed in order to simulate the rarefied gas flows around space vehicles such as the AOTV and the space plane. The null-collision (NC) technique, which Koura recently introduced into the direct-simulation Monte Carlo method, is used. The NC technique overcomes the principal fault in the time-counter (TC) technique and the difficulties in the collision-frequency (CF) technique and, moreover, the computation time required for the NC technique is comparable to that for the TC technique. The elastic collisions between molecules are taken to be the energy-dependent hard sphere model. The gas-surface interactions are taken to be the Maxwell reflection model. It is confirmed that the numerical wind tunnel works well for two-dimensional and axially symmetric bodies. Author

**N88-13274#** Kyoto Univ. (Japan). Dept. of Aeronautics.
**NUMERICAL ANALYSIS OF FLOW CHARACTERISTICS OF SUPERSONIC FREE-JETS**
Ryuji Ishii and Yoshikuni Umeda *In* National Aerospace Lab., Proceedings of the 4th NAL Symposium on Aircraft Computational Aerodynamics Dec. 1986 p 165-172 In JAPANESE; ENGLISH summary (For primary document see N88-13253 05-02)
Avail: NTIS HC A14/MF A01

Continuum free-jet flows expanding into stagnant and flowing gases are analyzed numerically by the piecewise linear interpolation method (PLM). It is found that the flow structures depend very much on the pressure and the flow Mach number of the ambient gas. A few of the numerical results are compared with the experiments. Author

**N88-13275#** Chiba Univ. (Japan). Faculty of Engineering.
**NUMERICAL SIMULATION OF SPLASH OF DROPLET AT UNIT GRAVITY** **c34**
Nobuhide Nishikawa, Takashi Suzuki, and Satoshi Akiyama *In* National Aerospace Lab., Proceedings of the 4th NAL Symposium on Aircraft Computational Aerodynamics Dec. 1986 p 173-179 In JAPANESE; ENGLISH summary (For primary document see N88-13253 05-02)
Avail: NTIS HC A14/MF A01

Descriptions are given of a numerical calculation carried out in a study of fluid motion of a liquid after impingement of a droplet with a velocity of 3.2 m/s onto the surface of water with a depth of 3 mm in a vessel. A droplet diameter of 2.3 mm was chosen. The numerical scheme developed to calculate the axisymmetric form Navier-Stokes equation was a donor cell version of the SMAC scheme. The typical results are shown in the images of surface model computer graphics for understanding of the dynamics of fluid. Author

**N88-13276#** National Aerospace Lab., Tokyo (Japan).
**COMPUTER GRAPHICS FOR COMPUTATIONAL AERODYNAMICS** **c61**
Kazuyo Suematsu and Tosio Isobe *In its* Proceedings of the 4th NAL Symposium on Aircraft Computational Aerodynamics Dec. 1986 p 181-189 In JAPANESE; ENGLISH summary (For primary document see N88-13253 05-02)
Avail: NTIS HC A14/MF A01

A graphic software package was developed to easily display various kinds of figures, such as grid distributions, pressure contours, oilflow patterns, and streamlines, which are often used in the field of computational aerodynamics. Author

**N88-13277#** Tokyo Univ. (Japan). Dept. of Aeronautics.
**FLOW VISUALIZATION IN COMPUTATIONAL FLUID DYNAMICS** **c34**
Susumu Shirayama and Kunio Kuwahara *In* National Aerospace Lab., Proceedings of the 4th NAL Symposium on Aircraft Computational Aerodynamics Dec. 1986 p 191-195 In JAPANESE; ENGLISH summary (For primary document see N88-13253 05-02)
Avail: NTIS HC A14/MF A01

To better understand the structure of a computed flow field, a visualization system for computational fluid dynamics was developed for color graphic systems. As the quantity of computational results is increasing and both time and spatial scale resolution is getting better, visualization is becoming more important. Visualization helps very much in understanding simulated flows. The contour lines, contour surfaces and particle tracing are important, but, when analyzing the flow fields, many kinds of such techniques must be combined. Often, extra information is obtained by the combination of various techniques. Author

**N88-13278#** Fujitsu Ltd., Tokyo (Japan).
**VISUALIZATION OF AN AIRCRAFT ACCIDENT BASED ON DIGITAL FLIGHT DATA RECORDER INFORMATION** **c61**
Mikio Sasaki, Takamitsu Okada, Kenji Kira, and Toshiyuki Sakamoto (Japan Broadcasting Corp., Tokyo.) *In* National Aerospace Lab., Proceedings of the 4th NAL Symposium on Aircraft Computational Aerodynamics Dec. 1986 p 197-201 In JAPANESE; ENGLISH summary (For primary document see N88-13253 05-02)
Avail: NTIS HC A14/MF A01

An aircraft accident which occurred on August 12th 1985 in Japan was visualized using computer graphics. The animation was made as realistic as possible. The shaking of the aircraft at the outset of the accident and the dutch roll and fugoid oscillation could be observed. The data which were used to make the animation (taken from the onboard digital flight data recorder) and the method by which the animation was generated are given. Author

**N88-13279*#** National Aeronautics and Space Administration. Ames Research Center, Moffett Field, Calif.
**A PERSPECTIVE OF COMPUTATIONAL FLUID DYNAMICS**

Paul Kutler *In* National Aerospace Lab., Proceedings of the 4th NAL Symposium on Aircraft Computational Aerodynamics Dec. 1986 p 203-213 Previously announced as N86-28057 (For primary document see N88-13253 05-02)
Avail: NTIS HC A14/MF A01 CSCL 01A

Computational fluid dynamics (CFD) is maturing, and is at a stage in its technological life cycle where it is now routinely applied to complex problems. It is starting to create an impact on the design cycle of aerospace flight vehicles and their components. CFD is also being used to better understand the fluid physics of flows heretofore not understood, such as three-dimensional separation. CFD is also being used to complement and is complemented by experiments. In this paper, the primary and secondary pacing items that have governed CFD in the past are reviewed and updated. The future prospects of CFD are explored, which will offer people working in the discipline challenges that should extend the technological life cycle to further increase the capabilities of a proven and demonstrated technology. Author

**N88-13280#** Tokyo Univ. (Japan). Dept. of Engineering.
**THREE-DIMENSIONAL FLOW PAST A TWO-DIMENSIONAL BODY**
Susumu Shirayama, Takashi Ota (Keio Univ., Tokyo, Japan ), and Kunio Kuwahara *In* National Aerospace Lab., Proceedings of the 4th NAL Symposium on Aircraft Computational Aerodynamics Dec. 1986 p 215-227 In JAPANESE; ENGLISH summary (For primary document see N88-13253 05-02)
Avail: NTIS HC A14/MF A01

By solving the three-dimensional incompressible Navier-Stokes equations, the development of three-dimensionality was investigated in a flow around a circular cylinder placed between side walls. Also, the case of a circular cylinder with an infinite spanwise length was treated using a periodic boundary condition. Initial vortex development and the development of spanwise vortical pattern are intensively visualized to see the three-dimensional structure. In the initial stage, the flow was almost two-dimensional. The two-dimensionality was kept in the first separation but as the flow developed, the wake became strongly three-dimensional. Also, in the developed stage, a large horseshoe vortex was observed in front of the cylinder near the wall. Author

**N88-13281#** Nissan Motor Co. Ltd., Tokyo (Japan).
**COMPUTATIONAL STUDY OF THREE-DIMENSIONAL WAKE STRUCTURES**
Ryutaro Himeno, Keisuke Kamo, Kazuhiro Tuboi (Japan Information Center of Science and Technology, Tokyo.), Susumu Shirayama, and Kunio Kuwahara *In* National Aerospace Lab., Proceedings of the 4th NAL Symposium on Aircraft Computational Aerodynamics Dec. 1986 p 229-237 In JAPANESE; ENGLISH summary (For primary document see N88-13253 05-02)
(Rept-2) Avail: NTIS HC A14/MF A01

Three-dimensional wake structure past bluff bodies were investigated by solving incompressible Navier-Stokes equations numerically. The effect of the Reynolds number on the flow around a slender body and of the base slant on the flow past a circular cylinder with a base are discussed in this report. The flow around an automobile is also computed. In the high-Reynolds-number flow, a pair of vortex tubes observed in the low-Reynolds-number flow is split into several pairs. A pair of vortex tubes parallel to the free stream, which is observed in the flow past a circular cylinder with a slanted base, becomes stable and influences the drag coefficient. It is found that the third-order upwind differencing scheme in the generalized coordinate system used in this paper is also effective in calculating the flow around a bluff body with a rather complicated geometry, such as an automobile. Author

**N88-13282#** National Aerospace Lab., Tokyo (Japan).
**COMPUTATIONS OF COMPRESSIBLE VISCOUS FLOWS OVER MULTIPLE-BODIES**
Kazuhiro Nakahashi *In its* Proceedings of the 4th NAL Symposium on Aircraft Computational Aerodynamics Dec. 1986 p 239-248 In JAPANESE; ENGLISH summary (For primary document see N88-13253 05-02)
Avail: NTIS HC A14/MF A01

A new technique was developed for computations of compressible, viscous flow over multiple bodies. In this scheme, an implicit finite-difference method (FDM) is applied to regions of near bodies with body-fitted grids, and those FDM regions are patched by solving the remaining regions using an explicit finite element method (FEM). With this zonal approach, the computational efficiency and the solution quality of FDM are retained, while geometric flexibility is gained by using the FEM. The most important advantage the present technique yields is that the flow solver with this FDM-FEM zonal approach can be applied to various kinds of multiple-body flow fields without modifying the basic solution procedure. In this paper, several test problems are computed by the method in order to validate the capabilities of the FDM-FEM zonal approach. Author

**N88-13283#** Tokyo Univ. (Japan). Dept. of Engineering.
**RELAXATION METHOD FOR THE COMPRESSIBLE NAVIER-STOKES EQUATIONS USING UPWIND SCHEMES** **c34**
Shigeru Obayashi, Kozo Fujii (National Aerospace Lab., Tokyo, Japan ), and Kunio Kuwahara *In* National Aerospace Lab., Proceedings of the 4th NAL Symposium on Aircraft Computational Aerodynamics Dec. 1986 p 249-254 In JAPANESE; ENGLISH summary (For primary document see N88-13253 05-02)
Avail: NTIS HC A14/MF A01

A comparison study of total variation diminishing (TVD) schemes using min-mod and differentiable limiters and essentially non-oscillatory (ENO) schemes has been done for a one-dimensional test problem. The one-dimensional steady-state problem, which consists of Euler equations with a source term, is computed in this paper. The computation is carried out by using classical upwind differencing in the implicit part while maintaining a TVD or ENO formulation in the explicit part. Numerical results indicate that the third-order ENO scheme is attractive, since the accuracy is essentially superior to TVD schemes. Author

**N88-13284#** Keio Univ., Tokyo (Japan). Dept. of Engineering.
**COMPUTATION OF FLOW AROUND 2-D CIRCULAR CYLINDER** **c34**
Takashi Ohta, Susumu Shirayama, Kiichirou Takeda, and Kunio Kuwahara (Tokyo Univ., Japan ) *In* National Aerospace Lab., Proceedings of the 4th NAL Symposium on Aircraft Computational Aerodynamics Dec. 1986 p 255-265 In JAPANESE; ENGLISH summary (For primary document see N88-13253 05-02)
Avail: NTIS HC A14/MF A01

Incompressible flows around a two-dimensional circular cylinder were calculated by a finite difference method. Computations were performed in a wide range of Reynolds numbers. Using fine mesh, the varation of flow patterns corresponding to Reynolds numbers was observed. The Karman vortex street was captured well by the C-grid system, which has a large number of grid points in the wake region. Author

**N88-13285#** Tohoku Univ., Sendai (Japan). Dept. of Mechanical Engineering.
**TIME-MARCHING FINITE-DIFFERENCE METHODS FOR THE THREE-DIMENSIONAL EULER EQUATIONS OF CONTRAVARIANT VELOCITY COMPONENTS** **c64**
Hisaaki Daiguji and Satoru Yamamoto *In* National Aerospace Lab., Proceedings of the 4th NAL Symposium on Aircraft Computational Aerodynamics Dec. 1986 p 267-276 In JAPANESE; ENGLISH summary (For primary document see N88-13253 05-02)
Avail: NTIS HC A14/MF A01

Explicit and implicit time-marching methods for solving the three-dimensional compressible Euler equations developed by the authors are presented. The main features of the present methods are employment of the Euler equations of contravariant velocities; that is, the equations of motion in the computational space, and simple and accurate treatment of the solid wall boundary conditions.

In the present paper all the equations required in the computation are shown and compared with the existing methods. Author

**N88-13286#** National Aerospace Lab., Tokyo (Japan).
**NAVIER-STOKES ANALYSIS OF LAMINAR FLOW CONTROL OF A TWO-DIMENSIONAL AIRFOIL**
Nobuhiro Kawai, Naoki Hirose, and Yoji Ishida *In its* Proceedings of the 4th NAL Symposium onAircraft Computational Aerodynamics Dec. 1986 p 277-280 In JAPANESE; ENGLISH summary (For primary document see N88-13253 05-02)
Avail: NTIS HC A14/MF A01

A numerical analysis method for laminar flow control (LFC) based on the Navier-Stokes equations is presented. Suction over the airfoil surfaces is formulated as the velocity boundary condition of the Navier-Stokes solver which uses the implicit approximate factorization scheme. As examples, the present method for LFC was applied to the NACA0012 airfoil at Mach numbers of 0.2 and 0.75. Computational results show that appropriate suction distribution brings about a large amount of recession of the boundary-layer transition point and a great deal of drag reduction. Author

**N88-13287#** National Aerospace Lab., Tokyo (Japan).
**ANALYTICAL METHOD FOR GENERATING COMPUTATIONAL GRIDS ABOUT COMPLETE AIRCRAFT CONFIGURATIONS**
**c61**
Susumu Takanashi and Takao Isawa (Nippon Time Share Co., Japan ) *In its* Proceedings of the 4th NAL Symposium on Aircraft Computational Aerodynamics Dec. 1986 p 281-288 In JAPANESE; ENGLISH summary (For primary document see N88-13253 05-02)
Avail: NTIS HC A14/MF A01

A method for constructing boundary-fitted grids for realistic aircraft configurations is described in this paper. The present grid generation procedure is based on the successive use of Caughey's wind tunnel mapping. The major advantage of the method is that the whole flow field can be transformed into a single rectangular computational domain, even for complex geometries such as that of the ONERA M-5 model. Typical examples of nearly orthogonal grid systems hitherto obtained are also presented. Author

**N88-13288#** National Aerospace Lab., Tokyo (Japan).
**NAVIER-STOKES SIMULATION OF TRANSONIC TRANSPORTATION AIRCRAFT CONFIGURATIONS. 1: FLOW-FIELD SIMULATION OVER WING-FUSELAGE COMBINATIONS**
Kozo Fujii, Susumu Takanashi, and Shigeru Obayashi (Tokyo Univ., Japan ) *In its* Proceedings of the 4th NAL Symposium on Aircraft Computational Aerodynamics Dec. 1986 p 289-298 In JAPANESE; ENGLISH summary (For primary document see N88-13253 05-02)
Avail: NTIS HC A14/MF A01

Viscous transonic flow-field simulations over wing-fuselage combinations were carried out using three-dimensional Reynolds averaged Navier-Stokes equations. the Lower/Upper block diagonal Alternating Direction Implicit (LU-ADI) factorization scheme was used with an implementation of new nonlinear smoothing terms. The computations were done for a practical wing-fuselage combination called W-18 which was designed for the transonic transportation aircraft. The computed results reveal the effect of the existence of the fuselage near the junction of wing and fuselage. Each computation currently requires several hours of computer time, which is, however, quite reasonable when considering the number of grid points to be used for this study. The results indicate that the application of the present Navier-Stokes solution code to the complete aircraft geometries is quite promising. Author

**N88-13289#** Mitsubishi Heavy-Industries Ltd., Tokyo (Japan).
**NUMERICAL SIMULATION OF TRANSONIC AIRCRAFT IN COMPARISON TO WIND TUNNEL TEST**
Junichi Miyakawa, Susumu Takanashi, Kozo Fujii, and Kanichi Amano (Japan Aircraft Development Corp., Tokyo.) *In* National Aerospace Lab., Proceedings of the 4th NAL Symposium on Aircraft Computational Aerodynamics Dec. 1986 p 299-315 In JAPANESE; ENGLISH summary (For primary document see N88-13253 05-02)
Avail: NTIS HC A14/MF A01

Computational aerodynamics has evolved to the point where it has become a practical design tool comparable to wind tunnel testing and has played an important role in actual aircraft design stages. The Navier-Stokes code, however, is still restricted to two-dimensional applications, which have been repeatedly validated. The three-dimensional application, which is a real challenge for the Navier-Stokes code, is discussed. If this three-dimensional application could be perfected, it would be a big step toward the final target of complete aircraft analysis by numerical simulation. Author

**N88-13290*#** National Aeronautics and Space Administration. Ames Research Center, Moffett Field, Calif.
**TIP AERODYNAMICS FROM WIND TUNNEL TEST OF SEMI-SPAN WING**
Johannes M. VanAken (Kansas Univ. Center for Research, Inc., Lawrence.) and Robert H. Stroub Sep. 1986 19 p
(NASA-TM-88253; A-86247; NAS 1.15:88253) Avail: NTIS HC A03/MF A01 CSCL 01A

Presented are the results of a low-speed wind tunnel test on a 5.33-aspect-ratio, semi-span wing with 30- and 35 deg swept tapered tips. The test results include aerodynamic data for the tip itself and for the entire wing including the tip. The metric tip extended inboard 1.58 wing chord lengths. The aerodynamic drag data show the strong influence of tip incidence angle on tip drag for various lift levels. Pitching-moment characteristics show the effect of a moment center at 0.13 c and 0.25 c. Author

**N88-13291*#** Scientific Research Associates, Inc., Glastonbury, Conn.
**CALCULATION OF HELICOPTER ROTOR BLADE/VORTEX INTERACTION BY NAVIER-STOKES PROCEDURES Final Report**
Y.-N. Kim, S. J. Shamroth, and R. C. Buggeln Apr. 1987 38 p
(Contract NAS2-12363)
(NASA-CR-177441; NAS 1.26:177441) Avail: NTIS HC A03/MF A01 CSCL 01A

Interactions of a modern rotor blade with concentrated tip vortices from the previous blades can have a significant influence on the airloads and the aeroacoustics of a helicopter. A better understanding of the blade/vortex interaction process and a method of analyzing its flow field would provide valuable help in the design of helicopters. The work discussed herein represents an initial effort in applying a 3-D, time-dependent Navier-Stokes simulation to the blade vortex interaction problem. The numerical approach is the Linearized Block Implicit (LBI) technique. In this initial effort, consideration is given to the interaction of a wing of idealized geometry and a vortex whose axis is aligned at an arbitrary angle to the wing. The calculations are made for laminar, subsonic flow, and show the time dependent pressure distribution and flow fields resulting from the interaction. Author

**N88-13292*#** Vigyan Research Associates, Inc., Hampton, Va.
**A SWEPT WING PANEL IN A LOW SPEED FLEXIBLE WALLED TEST SECTION Interim Report**
M. J. Goodyer Dec. 1987 20 p
(Contract NAS1-17919)
(NASA-CR-4106; NAS 1.26:4106) Avail: NTIS HC A03/MF A01 CSCL 01A

The testing of two-dimensional airfoil sections in adaptive wall tunnels is relatively widespread and has become routine at all speeds up to transonic. In contrast, the experience with the three-dimensional testing of swept panels in adaptive wall test sections is very limited, except for some activity in the 1940's at NPL, London. The current interest in testing swept wing panels led to the work covered by this report, which describes the design of an adaptive-wall swept-wing test section for a low speed wind tunnel and gives test results for a wing panel swept at 40 deg. The test section has rigid flat sidewalls supporting the panel, and

features flexible top and bottom wall with ribs swept at the same angle as the wing. When streamlined, the walls form waves swept at the same angle as the wing. The C sub L (-) curve for the swept wing, determined from its pressure distributions taken with the walls streamlined, compare well with reference data which was taken on the same model, unswept, in a test section deep enough to avoid wall interference. Author

**N88-13293#** Naval Postgraduate School, Monterey, Calif.
**THE DEVELOPMENT OF A COMPUTER CODE (U2DIIF) FOR THE NUMERICAL SOLUTION OF UNSTEADY, INVISCID AND INCOMPRESSIBLE FLOW OVER AN AIRFOIL M.S. Thesis**
Ngai-Huat Teng Jun. 1987 236 p
(AD-A185033) Avail: NTIS HC A11/MF A01 CSCL 20D

A numerical technique is formulated, in a computer program U2DIIF, for the solution of flow over an airfoil executing an arbitrary unsteady motion in an inviscid and incompressible medium. The technique extends the well known Panel Methods for steady flow into solving a non-linear unsteady flow problem arising from the continuous vortex shedding into the trailing wake due to the unsteady motion of the airfoil. Numerous case-runs are presented to verify U2DIIF computer code against other theoretical and/or numerical methods as well as in cases where limited experimental data are obtainable in literatures. These case-runs include airfoils undergoing a step change or a modified ramp change of angle-of-attack, airfoils executing harmonic oscillation in pitching and plunging motions and airfoils penetrating a sharp edge gust. Author (GRA)

**N88-13294#** Brown Univ., Providence, R. I. Div. of Applied Mathematics.
**COMPUTATIONAL METHODS FOR PROBLEMS IN AERODYNAMICS AND LARGE SPACE STRUCTURE USING PARALLEL AND VECTOR ARCHITECTURES Final Report**
David Gottlieb 1987 7 p
(Contracts AF-AFOSR-85-0303; AF Proj. 2304)
(AD-A185401; AFOSR-87-1189TR) Avail: NTIS HC A02/MF A01 CSCL 01C

One paper produced in this effort dealt with the importance of intermediate boundary conditions for approximate factorization schemes. A second paper derived stability results for spectral methods applied to initial-boundary value problems for hyperbolic systems. The paper demonstrates that one can bound certain weighted L2 spatial norms of the solution in terms of norms of the boundary data. A third paper deals with domain decomposition methods in the content of spectral techniques. Stability and convergence results are obtained for one and two dimensional cases. GRA

**N88-13295#** Institut Franco-Allemand de Recherches, St. Louis (France).
**PRODUCTION OF FLOWS FOR AEROBALLISTIC INVESTIGATIO IN THE SHOCK TUBES OF THE FRANCO-GERMAN RESEARCH INSTITUTE (ISL), SAINT-LOUIS (FRANCE) [ERZEUGUNG VON STROEMUNGEN FUER AEROBALLISTISCHE UNTERSUCHUNGEN IN DEN ISL-STOSSROHREN]**
G. Smeets and K. W. Naumann 2 Jun. 1986 32 p In GERMAN
(ISL-R-113/86; ETN-88-90637) Avail: NTIS HC A03/MF A01

A hypersonic shock tube was modified to allow the production of high density flows for aeroballistic tests. The flow conditions that can be realized at a density corresponding to that of the ground level atmosphere were calculated. The quality of the produced flows was checked in a series of test experiments. A procedure based on direct measurements, enabling a precise determination of the flow characteristics in the measuring cross section, was evaluated. The results promise that, after the realization of a divergent nozzle, an installation will be available that allows aeroballistic investigations under natural flow conditions. For ground level flight conditions, stationary low turbulence flow with velocities up to 2000 m/sec can be obtained during 1msec or longer, in a 20x20 sqcm measuring cross section. ESA

**N88-13296#** Centre d'Etudes Aerodynamiques et Thermiques, Poitiers (France).
**STUDY OF THE EFFECT OF MASS TRANSFER ON A TRANSONIC BOUNDARY LAYER. APPLICATION TO FLOW RELAMINARIZATION Final Report [ETUDE DE L'EFFET DU TRANSFERT DE MASSE SUR UNE COUCHE LIMITE TRANSONIQUE. APPLICATION A LA RELAMINARISATION]**
R. Leblanc, A. Stassinopoulos, and A. ElOuatouati May 1987 45 p In FRENCH
(Contract DRET-85-1414)
(ETN-88-91169) Avail: NTIS HC A03/MF A01

The relaminarization of delta wings in transonic flow is discussed. The transition over a flat plate was studied in a wind tunnel, including analysis of the effects of aspiration on separated flow. The results allows computation with good accuracy a laminar transonic boundary layer. The effects of slots are discussed. ESA

**N88-13297#** Institut de Mecanique des Fluides de Lille (France).
**WAKES OF TWO DIMENSIONAL BLUFF BODIES IN SUBSONIC FLOW. INFLUENCE OF A SEPARATING PLATE AND OF A PULSED INJECTION OF MOMENTUM [SILLAGES DE CULOT BIDIMENSIONNEL EN SUBSONIQUE. INFLUENCE D'UNE PLAQUE SEPARATRICE ET D'UNE INJECTION PULSEE DE QUANTITE DE MOUVEMENT]**
O. Rodriguez, J. M. Desse, C. Ducruet, and J. C. Pegneaux 22 Dec. 1986 84 p In FRENCH
(Contract DRET-85-003)
(IMFL-4200-86/75; ETN-88-91178) Avail: NTIS HC A05/MF A01

The behavior of drag reduction devices was studied. Ultra fast visualization and unsteady pressure measurement were used. Results show the possibility of significant drag reduction due to plate interaction. Pulsed injection experiments show little influence over the average and unsteady pressure. ESA

**N88-13298#** Office National d'Etudes et de Recherches Aerospatiales, Paris (France). Direction de l'Aerodynamique.
**DELTA WING IN INCOMPRESSIBLE FLOW. EXPERIMENTAL STUDY IN F2 [AILE DELTA EN ECOULEMENT INCOMPRESSIBLE. ETUDE EXPERIMENTALE A F2]**
P. Molton Dec. 1986 62 p In FRENCH
(ONERA-RT-36/1147-AN-249-G; ETN-88-91180) Avail: NTIS HC A04/MF A01

Wind tunnel tests were performed using 22 mm thick steel delta wing models. The measuring system includes 252 air intakes distributed over both wing surfaces and two-component laser velocimeters. Velocities from 10 to 70 m/sec and incident angles from 5 to 30 deg were used. The position of the laminar to turbulent transition is characterized. At large incidences (20 deg) the secondary vortices are strong enough to induce a third separation of the boundary layer. The vortices after separation are studied, showing that the main vortex presents a conical distribution which is not affected by the nature of the boundary layers, while the secondary vortex is larger and continues to evolve after transition. ESA

**N88-13299#** Societe Nationale Industrielle Aerospatiale, Toulouse (France). Div. Avions.
**VALIDATION ELEMENTS OF THE COMPUTATION METHODS AND MEASUREMENT TECHNIQUES FOR HIGH LIFT AERODYNAMIC SYSTEMS [ELEMENTS DE VALIDATION DES TECHNIQUES DE MESURE ET DES METHODES DE CALCUL EN AERODYNAMIQUE DES SYSTEMES HYPERSUSTENTES]**
P. Capbern 1987 31 p In FRENCH; ENGLISH summary
(SNIAS-872-111-101; ETN-88-91184) Avail: NTIS HC A03/MF A01

Problems raised by the prediction of the lift and drag coefficients in a high lift system are discussed. The analysis is restricted to two dimensional flow and incompressible subsonic conditions. Cases of single slotted and double slotted flap systems are studied. Wake-drag measurements were carried out in wind tunnel tests.

The results validate the ONERA two dimensional strong interaction method for multielement configurations, but improvements are deemed necessary. ESA

**N88-13300#** Societe Nationale Industrielle Aerospatiale, Toulouse (France). Div. Avions.

**COMPUTATION OF TRANSONIC FLOWS WITH NACELLE SIMULATION**

Y. Vigneron, T. Lejal, and R. Collercandy 1987 34 p
(SNIAS-872-111-117; ETN-88-91198) Avail: NTIS HC A03/MF A01

A method to solve the potential flow equations on an unstructured grid was developed, and tested on a civil aircraft configuration. The basic configuration represents a twin engine aircraft: fuselage + wings + struts + nacelles. The mass flow through the fan is imposed and the exhaust plume is frozen. The grid has 24,558 nodes, of which 1680 are on the surface. The code requires 1 Mwords of central memory, 1050 sec CPU time to reduce the average nonlinear residual by 6 orders of magnitude. Engineering accuracy is obtained in half this time. Configurations of wings + struts + nacelles, wing + nacelles, wing alone are also treated. Surface grids and Mach number contours, focusing on the strut and the nacelle; and pressure distribution on the wing at two stations immediately in board and out board of the strut location are shown. The number of grid points used is not sufficient for a detailed resolution of the flow fields. However the basic trends are predicted correctly, notably the influence of the fuselage and the strut. ESA

**N88-13301#** Aeronautical Research Inst. of Sweden, Stockholm. Aerodynamics Dept.

**COMPUTATION OF RIME ICE ACCRETION ON AIRFOILS**

Staffan Meijer May 1987 15 p Sponsored by National Swedish Board for Technical Development
(FFA-TN-1987-08; ETN-88-91392) Avail: NTIS HC A03/MF A01

A method to calculate rime ice accretion on airfoils is described. The flow field is calculated using incompressible potential theory. In the trajectory equation only the drag and gravity forces acting on the water droplets are retained. The ice accretion is calculated assuming that all droplets freeze at their points of impact and that the ice grows in a direction normal to the surface. Results from two calculations for single airfoils are compared with previous results. Rime ice accretion is also calculated for a two-dimensional high lift wing consisting of a basic wing profile, based on NACA 65-215, a leading edge slat, a trailing edge vane, and a trailing edge flap. Accuracy of the calculated droplet impact points decreases for trajectories that are very close to the airfoil surface for a long time. ESA

**N88-13302#** Aeronautical Research Inst. of Sweden, Stockholm. Aerodynamics Dept.

**LOW SPEED WIND TUNNEL INVESTIGATION OF PROPELLER SLIPSTREAM AERODYNAMIC EFFECTS ON DIFFERENT NACELLE/WING COMBINATIONS. PART 1: TOTAL FORCES AND MOMENTS AND PRESSURE DISTRIBUTIONS ON NACELLE/WING AT DIFFERENT ANGLES OF ATTACK AND YAW AND AT DIFFERENT THRUST COEFFICIENTS**

Ingemar Samuelsson 18 Jun. 1987 74 p Sponsored by Swedish Board for Technical Development
(FFA-TN-1987-22; ETN-88-91393) Avail: NTIS HC A04/MF A01

A wind tunnel investigation of propeller slipstream/nacelle/wing aerodynamic interference effects was carried out for 4 nacelle/wing combinations, with different angles of attack and yaw, freestream speeds (33 to 61 m/sec) and thrust coefficients (CF: 0.05 to 0.57). Results show significant propeller slipstream induced lateral nacelle loads (side force, yawing moment, and rolling moment). For an axisymmetrical nacelle (wing/off) set at incidence at zero yaw, the cyclic thrust variation on the propeller blades creates an asymmetrical pressure field in the slipstream. When this asymmetrical slipstream washes the nacelle surfaces there are lateral loads acting on the nacelle. For an nonaxisymmetrical (high) nacelle lateral nacelle loads develop even at zero incidence and zero yaw, due to asymmetrical interference between the propeller swirl, slipstream, and pressure field and the nacelle surfaces. There are also significant effects of CF on the development of the lateral nacelle loads. ESA

**N88-13303#** Aeronautical Research Inst. of Sweden, Stockholm. Aerodynamics Dept.

**COMPRESSIBLE EULER SOLUTION ON A MULTIBLOCK GRID AROUND A WING-FUSELAGE CONFIGURATION**

Torsten Berglind 27 Jul. 1987 29 p
(Contract FMK-F-K-82260-84-254-73-001)
(FFA-TN-1987-46; ETN-88-91394) Avail: NTIS HC A03/MF A01

A patched multiblock grid around a wing-fuselage configuration was constructed by transfinite interpolation. The wing is enveloped by an 0-0 type of grid with parabolic singularities at the wing tip, and the fuselage is enveloped by an 0-0 type of grid with polar singularities at the nose and the tail, with a slit for the wing grid. This grid is divided into eight computational blocks, so that each coordinate side of a block has one type of boundary condition. A finite volume Euler solver using explicit Runge-Kutta time stepping was coded to handle general multi-block structures. The flow over the 65 deg round leading edge delta wing with a fuselage, at 10 deg angle of attack, and at a free stream Mach number of 0.85 was computed. Results show the capability of the method and the simplicity of the topology input description. ESA

**N88-13304*#** National Aeronautics and Space Administration. Lewis Research Center, Cleveland, Ohio.

**AUTOMATED DESIGN OF CONTROLLED DIFFUSION BLADES**

Jose M. Sanz [1987] 15 p Prepared for presentation at the 33rd International Gas Turbine and Aero-Engine Congress and Exposition, Amsterdam, The Netherlands, 5-9 Jun. 1988
(NASA-TM-100251; E-3877; NAS 1.15:100251) Avail: NTIS HC A03/MF A01 CSCL 01A

A numerical automation procedure has been developed to be used in conjunction with an inverse hodograph method for the design of controlled diffusion blades. With this procedure a cascade of airfoils with a prescribed solidity, inlet Mach number, inlet air flow angle, and air flow turning can be produced automatically. The trailing edge thickness of the airfoil, an important quantity in inverse methods, is also prescribed. The automation procedure consists of a multidimensional Newton iteration in which the objective design conditions are achieved by acting on the hodograph input parameters of the underlying inverse code. The method, although more general in scope, is applied in this paper to the design of axial flow compressor blade sections, and a wide range of examples is presented. Author

**N88-13305*#** National Aeronautics and Space Administration. Ames Research Center, Moffett Field, Calif.

**AN EXPERIMENTAL INVESTIGATION OF THE AERODYNAMICS OF A NACA 64A010 AIRFOIL-FLAP COMBINATION WITH AND WITHOUT FLAP OSCILLATIONS. PART 1: STEADY-STATE CHARACTERISTICS**

Donald A. Buell and Gerald N. Malcolm Jul. 1986 68 p
(NASA-TM-88217; A-86140; NAS 1.15:88217) Avail: NTIS HC A04/MF A01 CSCL 01A

A NACA 64A010 airfoil with a sealed-gap 1/4-chord flap was tested between splitter plates in the NASA Ames 11- by 11-Foot Transonic Wind Tunnel at Mach numbers from 0.50 to 0.85, and Reynolds numbers based on chord from 3 to 13 million. Although the main purpose of the test was to obtain unsteady pressure data with the flap oscillating, no unsteady data are presented in this paper. The steady-state data are presented and compared with other test data to provide a basis for evaluating the results. Pressure data at two span stations are used to deduce early boundary-layer transitions at the midspan at higher Mach numbers, angles of attack, and flap angles. The effects of flap angle on pressures, normal force, pitching moment, and hinge moment are also presented in the report. Mach number errors caused by the splitter-plate configuration and the angle of attack are evaluated

using pressure measurements near the floor and ceiling of the wind tunnel. Author

# 03 AIR TRANSPORTATION AND SAFETY

Includes passenger and cargo air transport operations; and aircraft accidents.

For related information see also *16 Space Transportation* and *85 Urban Technology and Transportation.*

**N88-13306*#** National Aeronautics and Space Administration. Ames Research Center, Moffett Field, Calif.

**INTERFEROMETRIC DATA FOR A SHOCK-WAVE/BOUNDARY-LAYER INTERACTION**

Stephen E. Dunagan, James L. Brown, and John B. Miles (Missouri Univ., Columbia.) Sep. 1986 270 p

(NASA-TM-88227; A-86158; NAS 1.15:88227) Avail: NTIS HC A12/MF A01 CSCL 01A

An experimental study of the axisymmetric shock-wave / boundary-layer strong interaction flow generated in the vicinity of a cylinder-cone intersection was conducted. The study data are useful in the documentation and understanding of compressible turbulent strong interaction flows, and are part of a more general effort to improve turbulence modeling for compressible two- and three-dimensional strong viscous/inviscid interactions. The nominal free stream Mach number was 2.85. Tunnel total pressures of 1.7 and 3.4 atm provided Reynolds number values of 18 x 10(6) and 36 x 10(6) based on model length. Three cone angles were studied giving negligible, incipient, and large scale flow separation. The initial cylinder boundary layer upstream of the interaction had a thickness of 1.0 cm. The subsonic layer of the cylinder boundary layer was quite thin, and in all cases, the shock wave penetrated a significant portion of the boundary layer. Owing to the thickness of the cylinder boundary layer, considerable structural detail was resolved for the three shock-wave / boundary-layer interaction cases considered. The primary emphasis was on the application of the holographic interferometry technique. The density field was deduced from an interferometric analysis based on the Able transform. Supporting data were obtained using a 2-D laser velocimeter, as well as mean wall pressure and oil flow measurements. The attached flow case was observed to be steady, while the separated cases exhibited shock unsteadiness. Comparisons with Navier-Stokes computations using a two-equation turbulence model are presented. M.G.

**N88-13307*#** Lehigh Univ., Bethlehem, Pa. Dept. of Mechanical Engineering and Mechanics.

**VORTEX INTERACTION WITH A LEADING-EDGE OF FINITE THICKNESS Final Technical Report, Feb. 1984 - Apr. 1987**

D. Sohn and Donald Rockwell [1987] 131 p

(Grant NAG1-461)

(NASA-CR-182341; NAS 1.26:182341) Avail: NTIS HC A07/MF A01 CSCL 01A

Vortex interaction with a thick elliptical leading-edge at zero relative offset produces a pronounced secondary vortes of opposite sense that travels with the same phase speed as the primaty vortex along the lower surface of the edge. The edge thickness (scale) relative to the incident vorticity field has a strong effect on the distortion of the incident primary vortex during the impingement processs. When the thickness is sufficiently small, there is a definite severing of the incident vortex and the portion of the incident vortex that travels along the upper part of the elliptical surface has a considerably larger phase speed than that along the lower surface; this suggests that the integrated loading along the upper surface is more strongly correlated. When the thickness becomes too large, then most, if not all, of the incident vortex passes below the leading-edge. On the other hand, the relative tranverse offset of the edge with respect to the center of the incident vortex has a significant effect on the secondary vortex formation. Author

**N88-13308#** Air Force Inst. of Tech., Wright-Patterson AFB, Ohio.

**AIRLINE SAFETY: A COMPARATIVE ANALYSIS M.S. Thesis**

Mary K. Higgins 1987 88 p

(AD-A185358; AFIT/CI/NR-87-68T) Avail: NTIS HC A05/MF A01 CSCL 01C

In this study of airline safety, the focus will be on fatal accidents, considering the records of U.S. domestic airlines and international air carriers over the past ten years. A passenger's probability of being killed on a given flight is estimated using data from each of 157 airlines (35 U.S. domestics and 122 internationals). The calculations suggest substantial divergence of risk across groups of airlines with U.S. domestic trunk lines and large international flag carriers significantly outperforming the small international airlines and children of U.S. airline deregulation. At the same time, the general trend has been toward major reductions over time in air travel risk. GRA

**N88-13309#** Ministry of Transport and Waterways, The Hague (Netherlands).

**CIVIL AERONAUTICS Annual Report, 1985 [RIJKSLUCHTVAART-DIENST]**

1986 67 p In DUTCH

(ETN-88-90616) Avail: NTIS HC A04/MF A01

Activities in aeronautics inspection, airport development, air transportation policy, and aerospace safety are described. The status and activities of the Civil Aeronautics School, the National Aerospace Museum Aviodome, the National Aerospace Laboratory, and the National Aerospace Medical Center are outlined. ESA

**N88-13310*#** Wichita State Univ., Kans.

**THEORETICAL ANALYSIS OF THE ELECTRICAL ASPECTS OF THE BASIC ELECTRO-IMPULSE PROBLEM IN AIRCRAFT DE-ICING APPLICATIONS Final Report**

Robert A. Henderson and Robert L. Schrag Nov. 1987 80 p

(Grant NAG3-284)

(NASA-CR-180845; NAS 1.26:180845) Avail: NTIS HC A05/MF A01 CSCL 01C

A method of modelling a system consisting of a cylindrical coil with its axis perpendicular to a metal plate of finite thickness, and a simple electrical circuit for producing a transient current in the coil, is discussed in the context of using such a system for de-icing aircraft surfaces. A transmission line model of the coil and metal plate is developed as the heart of the system model. It is shown that this transmission model is central to calculation of the coil impedance, the coil current, the magnetic fields established on the surfaces of the metal plate, and the resultant total force between the coil and the plate. FORTRAN algorithms were developed for numerical calculation of each of these quantities, and the algorithms were applied to an experimental prototype system in which these quantities had been measured. Good agreement is seen to exist between the predicted and measured results. Author

# 04 AIRCRAFT COMMUNICATIONS AND NAVIGATION

Includes digital and voice communication with aircraft; air navigation systems (satellite and ground based); and air traffic control.

For related information see also *17 Space Communications, Spacecraft Communications, Command and Tracking* and *Communications and Radar.*

**N88-13311#** Naval Postgraduate School, Monterey, Calif.
**CORRECTION OF INERTIAL NAVIGATION SYSTEM DRIFT ERRORS FOR AN AUTONOMOUS LAND VEHICLE USING OPTICAL RADAR TERRAIN DATA M.S. Thesis**
Mark Douglas Rickenbach Sep. 1987 96 p
(AD-A184973; NPS52-87-039) Avail: NTIS HC A05/MF A01 CSCL 17G

It is generally agreed that some type of vision system capable of providing a preview of terrain is an important attribute of a driverless vehicle. One approach to providing this capability is to use active images such as those obtained by sonar or radar. This thesis is concerned with a computer simulation study of an approach to data processing for range images obtained from an optical radar system using a scanning laser beam. The system studied is modeled after the ERIM scanner mounted on the adaptive Suspension Vehicle walking machine developed at Ohio State University. Both the problem of register successive images in the presence of vehicle motion and of optimally averaging such images to obtain more accurate terrain elevation data are investigated. GRA

**N88-13312#** Naval Research Lab., Washington, D.C.
**ON-ORBIT FREQUENCY STABILITY ANALYSIS OF THE GPS NAVSTAR 8 RUBIDIUM CLOCK AND NAVSTARS 9 AND 10 CESIUM CLOCKS Memorandum Report, Jan. - Dec. 1985**
James A. Buisson and Marie M. Largay 17 Sep. 1987 51 p
(AD-A184984; NRL-MR-6076) Avail: NTIS HC A04/MF A01 CSCL 14B

This report describes the on-orbit frequency stability performance analysis of the Global Positioning System (GPS) NAVSTAR 8 rubidium clock and the NAVSTARs 9 and 10 cesium clocks. Time domain measurements, taken from three GPS monitor sites and from the United States Naval Observatory (USNO), have been analyzed to determine the short and long-term frequency stability performance of the NAVSTAR clocks. The data presented include measurements from 1985. GRA

**N88-13313#** Draper (Charles Stark) Lab., Inc., Cambridge, Mass.
**SATELLITE AUTONOMOUS NAVIGATION WITH SHAD (STELLAR HORIZON ATMOSPHERIC DISPERSION) Final Report, 1 Sep. 1981 - 30 Nov. 1982**
R. L. White and R. B. Gounley Apr. 1987 115 p
(Contract N00014-81-C-0803; ARPA Order 4205)
(AD-A184988; CSDL-R-1982) Avail: NTIS HC A06/MF A01 CSCL 17G

The objective of this study was to test the autonomous navigation accuracy achievable with the SHAD concept for various representative satellite orbits. This was accomplished by conducting a covariance analysis utilizing a Kalman filter to sequentially process the measurements as they occur during orbit operation. GRA

**N88-13314#** Air Force Inst. of Tech., Wright-Patterson AFB, Ohio. School of Engineering.
**USE OF THE GLOBAL POSITIONING SYSTEM FOR TRAJECTORY DETERMINATION OF SRAM 2 MISSILES AT THE EASTERN TEST RANGE M.S. Thesis**
Edwin A. Zehner Dec. 1986 109 p
(AD-A185266; AFIT/GSO/ENS-ENG/86D-2) Avail: NTIS HC A06/MF A01 CSCL 17G

This research was intended to determine the accuracy that can be obtained using the Global Positioning System to track SRAM 2 missiles at the Eastern Test Range. The final goal of the research was to make a definitive calculation of the accuracy offered and compare this against the required accuracy for follow on test and evaluation of SRAM 2 missiles. The scope was limited to use of GPS equipment currently being developed or already available. The results can be applied to tracking other small, dynamic vehicles at other test ranges. Aside from the GPS satellite constellation the equipment configuration included a master receive station with a GPS receiver at a surveyed location to support differential calculations, and a translator on board the SRAM 2. The GPS signals were to be recorded and subjected to post-test processing for increased accuracy. Using this system all error contributions could be adequately estimated except dynamic error and the error due to adequately estimated except dynamic error and the error due to multipath. These two errors could be large and must be studied further before a final error level can be confidently stated. GRA

# 05 AIRCRAFT DESIGN, TESTING AND PERFORMANCE

Includes aircraft simulation technology.

For related information see also *18 Spacecraft Design, Testing and Performance* and *39 Structural Mechanics.* For land transportation vehicles see *85 Urban Technology and Transportation.*

**N88-13315#** Advisory Group for Aerospace Research and Development, Neuilly-Sur-Seine (France). Fluid Dynamics Panel.
**SPECIAL COURSE ON FUNDAMENTALS OF FIGHTER AIRCRAFT DESIGN**
Oct. 1987 290 p Course held in Rhode-St-Genese, Belgium, 17-21 Feb. 1986, in Athens, Greece, 24-25 Feb. 1986, and in Ankara, Turkey, 27-28 Feb. 1986
(AGARD-R-740; ISBN-92-835-1560-9) Copyright Avail: NTIS HC A13/MF A01

The Special Course on the Fundamentals of Fighter Aircraft was sponsored by the AGARD Fluid Dynamics Panel and the von Karman Institute and presented at the latter in Rhode-Saint-Genese, Belgium, 17 to 21 February 1986, at the Greek Air Force Academy, Athens, Greece, 24 to 25 February 1986, and at the ARGE, Ankara, Turkey, 27 to 28 February 1986. The Course presented a comprehensive review of fundamental procedures used during a fighter pre-development phase concentrating on the following: basic mission requirements and aircraft sizing; aerodynamic design including performance, stability and control; materials, structural optimization and aeroelasticity; aircraft dynamics; engine intake and nozzle integration; and airframe store-compatibility. Experimental and theoretical work has been demonstrated to play complementary roles and, in conclusion, recommendations are given for future development of engineering tools. For individual titles, see N88-13316 through N88-13327.

**N88-13316#** Messerschmitt-Boelkow-Blohm G.m.b.H., Munich (West Germany). Helicopter and Military Aircraft Div.
**FUNDAMENTALS OF FIGHTER AIRCRAFT DESIGN**
P. W. Sacher *In* AGARD, Special Course on Fundamentals of Fighter Aircraft Design Oct. 1987 5p (For primary document see N88-13315 05-05)
Copyright Avail: NTIS HC A13/MF A01

Following the technical program of the AGARD Fluid Dynamics Panel (FDP) for the past few years, the aeronautical engineer has found many subjects related to a special technical discipline and directed to industrial applications. But in nearly all cases the analysis of given geometry by experimental or theoretical techniques has overruled the more important engineering task, i.e., the design of a new shape which has desired properties. But in all cases concerning successful flying aircraft the result of engineering work has ben a design compromise achieved by the fruitful cooperation of all technically relevant disciplines. Therefore, one of the most important intentions of this course has been to attract people from different aeronautical disciplines, working in industry and research institutes, and to look for links within the

different branches of aerodynamics such as Wind Tunnel Test Techniques, Computational Fluid Dynamics, Vortex Dynamics, Unsteady Aerodynamics, Viscous Flow Drag Prediction, and their impact on designing aircraft components. Author

**N88-13317#** Air Force Wright Aeronautical Labs., Wright-Patterson AFB, Ohio. Design Branch.
**MISSION REQUIREMENTS AND AIRCRAFT SIZING**
James L. Parker *In* AGARD, Special Course on Fundamentals of Fighter Aircraft Design Oct. 1987 46 p Previously announced in IAA as A87-17881 (For primary document see N88-13315 05-05)
Copyright Avail: NTIS HC A13/MF A01

The development of requirements for new fighter aircraft involves defining threats, targets, and air combat scenarios for the future. Current fighter requirements emphasize the need for close-in combat and beyond-visual-range combat capability to achieve superiority in the air-to-air role. High sortie rates and the ability to perform air-to-surface missions are also primary requirements. Conceptual design and aircraft sizing are used to help define requirements. With conceptual design tools, different fighter designs can be sized for different missions. These configurations allow life cycle cost and effectiveness analysis to be performed, which provide the basis for the definition of the requirement to be constrained to a technologically feasible and economically affordable solution. Author

**N88-13318#** Boeing Military Airplane Development, Seattle, Wash.
**DESIGN OF WINGS AND WING/BODY CONFIGURATIONS FOR TRANSONIC AND SUPERSONIC SPEEDS**
H. Yoshihara *In* AGARD, Special Course on Fundamentals of Fighter Aircraft Design Oct. 1987 19 p (For primary document see N88-13315 05-05)
Copyright Avail: NTIS HC A13/MF A01

Procedures to design wing/fuselage configurations at transonic and supersonic conditions are described. This is preceded by an introductory section sketching the significant flow features as the shock wave and separation patterns for typical fighter wings which affect the performance, followed by a description of the interference effects due to the fuselage. Author

**N88-13319*#** National Aeronautics and Space Administration. Langley Research Center, Hampton, Va.
**NONLINEAR LIFT CONTROL AT HIGH SPEED AND HIGH ANGLE OF ATTACK USING VORTEX FLOW TECHNOLOGY**
**c08**
John E. Lamar *In* AGARD, Special Course on Fundamentals of Fighter Aircraft Design Oct. 1987 23 p Previously announced in IAA as A86-37050 (For primary document see N88-13315 05-05)
Copyright Avail: NTIS HC A13/MF A01 CSCL 01C

Nonlinear lift control at subsonic, transonic and low supersonic speeds owes its origin to the separated but organized vortical flows interacting with the wing upper surface. Since most of this flow originates near the wing or control-surface leading edge, a variety of devices has been studied experimentally which interact with and/or control this flow in order to gain a beneficial effect. The benefits (effects) originally studied were associated only with lift enhancement. Whereas, now the studied benefits encompass performance increase, attention to changes in trimmed conditions and londitudinal stability, improvements in lateral stability, and the attendant variation with changing Mach number. For those devices that can be theoretically modeled, state-of-the-art computer codes have been used for device design and/or analysis. Comparisons at design and off-design conditions are presented for validation purposes. Author

**N88-13320#** National Research Council of Canada, Ottawa (Ontario). Unsteady Aerodynamics Lab.
**AIRCRAFT DYNAMICS: AERODYNAMIC ASPECTS AND WIND TUNNEL TECHNIQUES**
K. J. Orlik-Rueckemann *In* AGARD, Special Course on Fundamentals of Fighter Aircraft Design Oct. 1987 30 p (For primary document see N88-13315 05-05)
Copyright Avail: NTIS HC A13/MF A01

The dynamic behavior of modern fighter aircraft depends more and more on unsteady aerodynamics. Until recently, the designer concentrated on classical problems such as aeroelasticity and flutter. Dynamic stability parameters were most often determined by low angle-of-attack calculation methods, without much recourse to experiment. The results obtained from the few dynamic experiments performed were used to confirm the absence of problems rather than as design parameters. New requirements for fighter aircraft performance include the ability to fly at high angles of attack in the presence of extensive regions of separated or vortical flows, relaxed static stability, greatly increased agility, and an interest in unorthodox geometries such as closely-coupled-canard or tail-first configurations. The time lags and unsteady phenomena associated with flow fields resulting from rapid maneuvers and large amplitude motions significantly affect the dynamic behavior of modern fighter aircraft and become as important for aircraft design as the classical static performance criteria. A review is made of the various aerodynamic aspects affecting aircraft dynamic behavior, followed by a survey of the most pertinent experimental techniques. Author

**N88-13321#** Avions Marcel Dassault-Breguet Aviation, Saint-Cloud (France). Div. des Etudes Avancees.
**TECHNIQUES FOR PERFORMANCE OPTIMISATION IN CRUISE AND MANOEUVERABILITY**
Pierre Perrier *In* AGARD, Special Course on Fundamentals of Fighter Aircraft Design Oct. 1987 12 p (For primary document see N88-13315 05-05)
Copyright Avail: NTIS HC A13/MF A01

The design of a combat aircraft cannot be left to trial and error design when a definite performance target is precisely defined. It is obvious that there is a large variation in the possible aerodynamic aircraft shapes having the internal volume required for fuel, engine, equipment and weapon system accommodation. Among all possible shapes, the best aircraft will have definite advantages over a poor design in terms of performance for a given cost or in terms of cost for given performance. The best aerodynamic definition need no longer be left to the designers in the design office when efficient theoretical-experimental processes of optimization are available in the aircraft industry. Presented is the state of the art of the reflection and application of optimization, i.e., the latter's targets and tools, and some results and perspectives in combat aircraft design are reviewed. Author

**N88-13322#** Office National d'Etudes et de Recherches Aerospatiales, Paris (France).
**FUNDAMENTALS OF FIGHTER AIRCRAFT DESIGN: ENGINE INTAKE AND AFTERBODY**
J. Leynaert *In* AGARD, Special Course on Fundamentals of Fighter Aircraft Design Oct. 1987 39 p Previously announced in IAA as A87-21014 (For primary document see N88-13315 05-05)
Copyright Avail: NTIS HC A13/MF A01

Basic conditions, study parameters, and various solutions of fighter intake and afterbody (except VTOL) are reviewed. Airframe integration and intake adaptation to the flight Mach number are discussed. The following topics of intake flow are analyzed: buzz phenomena, internal bleed flow, high incidence, low speed, mean flow, distortion index, and unsteady distortion. The afterbody discussion covers variable geometry, thrust vectoring, and reverse. Wind tunnel test techniques are also described. Author

**N88-13323#** British Aerospace Public Ltd. Co., Kingston-upon-Thames (England).
**AIRFRAME/STORE COMPATIBILITY**
C. L. Bore *In* AGARD, Special Course on Fundamentals of Fighter Aircraft Design Oct. 1987 27 p (For primary document see N88-13315 05-05)
Copyright Avail: NTIS HC A13/MF A01

By considering the various parameters dominating the value of a fighter air force, those terms can be isolated which respond to influences of store release features. It is shown that stores affect the transport capacity of the air force through the lift/drag ratio, the availability factor through the agility term, and the target-killing factor through the delivery accuracy term. The physical effects of store installation are then examined, and ways identified to minimize undesirable effects. Thus, drag prediction and drag reduction are considered in some depth. The effects of drag on the agility of the aircraft are examined and stability and flutter effects are reviewed. Store release conditions are reviewed. Finally, some recent approaches to store/airframe integration are considered. Author

**N88-13324#** Messerschmitt-Boelkow-Blohm G.m.b.H., Munich (West Germany). Helicopter and Military Aircraft Group.
**AEROELASTICITY AND OPTIMIZATION IN FIGHTER AIRCRAFT DESIGN**
H. Goedel and H. Hoernlein *In* AGARD, Special Course on Fundamentals of Fighter Aircraft Design Oct. 1987 15 p (For primary document see N88-13315 05-05)
Copyright Avail: NTIS HC A13/MF A01

Constraint functions and their differentiations are given for the most interesting physical disciplines of structural optimization and well-known optimization techniques are mentioned. Because of the growing significances of iterative methods a large space has been conceded to the iterative solution of linear equation systems and its use in various algorithms. It is shown that big computer time saving effects would be achieved if the special characteristics of the physical formulation could be exploited mathematically. Author

**N88-13325#** British Aerospace Public Ltd. Co., Preston (England).
**MATERIALS FOR FIGHTER AIRCRAFT**
R. J. Sellars *In* AGARD, Special Course on Fundamentals of Fighter Aircraft Design Oct. 1987 17 p Sponsored in part by Ministry of Defence, United Kingdom (For primary document see N88-13315 05-05)
Copyright Avail: NTIS HC A13/MF A01

Of the many important decisions to be made during the initial conception and design of advanced fighter aircraft, one of the most critical is that made by the materials engineer. Together with the designer, he will recommend the type of material to be incorporated into the aircraft's structure. Such recommendations, while respecting the criteria of minimum mass and minimum cost, must also ensure that the structure will possess a long life and be simple to service and maintain. Discussed are some of the new materials and production processes available for use on advanced fighter aircraft. Comparisons are made between the advanced light alloys now becoming available (i.e., aluminum-lithium), and the latest intermediate modulus fibers for use in carbon fiber components. Author

**N88-13326#** Messerschmitt-Boelkow-Blohm G.m.b.H., Munich (West Germany). Helicopter and Military Aircraft Div.
**THE ROLE OF EXPERIMENTAL INVESTIGATION AND COMPUTATIONAL FLUID DYNAMICS DURING FIGHTER AIRCRAFT DESIGN**
P. W. Sacher *In* AGARD, Special Course on Fundamentals of Fighter Aircraft Design Oct. 1987 26 p (For primary document see N88-13315 05-05)
Copyright Avail: NTIS HC A13/MF A01

In a discussion of the role of experimental investigation and computational fluid dynamics in fighter aircraft design the following topics are reviewed: (1) two ways to simulate compressible flowfields, advantages versus disadvantages of numerical and experimental investigations; (2) general trends in time/speed and costs in experiment and computation; (3) state of the art in numerical aerodynamics; (4) model for numerical simulation; and (5) applications and typical results. In a discussion of wind tunnel technology, the following topics are examined: (1) results from wind tunnel/critical review; (2) effect of Reynolds number; (3) wind tunnel effects; (4) the role of CFD during wind tunnel testing; and (5) the role of wind tunnels during configuration development. In conclusion, it is felt that the computer is not about to replace the wind tunnel, the role of computers is a complementary one to save time and costs and to improve the quality of the final product. F.M.R.

**N88-13327#** Office National d'Etudes et de Recherches Aerospatiales, Paris (France). Aerodynamic Dept.
**REQUIREMENTS AND RECOMMENDATIONS FOR THE DEVELOPMENT OF THEORETICAL CODES AND EXPERIMENTAL FACILITIES IN THE NEAR FUTURE**
B. Costes *In* AGARD, Special Course on Fundamentals of Fighter Aircraft Design Oct. 1987 15 p (For primary document see N88-13315 05-05)
Copyright Avail: NTIS HC A13/MF A01

In order to properly use all available tools, the aircraft designer has to be acquainted with both their good qualities and shortcomings. This guides the improvement studies in a context characterized by the following: the general development of the potential of methods and calculation means, wind tunnels and relevant instrumentation; the new reuirements for aircraft performance and the ever-growing industrial risks. The incoming developments for various levels of calculation codes, used for an industrial design or for fundamental research are examined. Also, the improvements needed for wind tunnels and testing methods are examined, depending on the character of the studies to be carried out. Examples permit a definition of the present state of the art and an examination of the improvements under study which may be exploitable in the not too distant future. Author

**N88-13328#** Materials Research Labs., Ascot Vale (Australia).
**AN EXAMINATION OF COATING FAILURE ON WING PIVOT FITTINGS OF F111 AIRCRAFT**
L. V. Wake May 1987 34 p
(AD-A185028; MRL-R-1060) Avail: NTIS HC A03/MF A01
CSCL 11C

Failure of replacement coatings on the wing pivot fittings in integral wing fuel tanks of F111 aircraft has resulted in serious corrosion and pitting on critical sections of the fittings. Failed paint flakes from the fittings were characterized by adhesive detachment of the epoxy polyamide priming coat. Examination of fuel and moisture resistance of a range of possible coatings has been undertaken against those currently in use. The results suggest that coatings based on epoxy polymide resins are sensitive to glycol ether compounds employed as fuel system icing inhibitors in aviation turbine fuels. A more resistant epoxy polyurethane paint coating has therefore been proposed for use on the inspection areas of the fittings. It is also recommended that respraying over existing coatings inside the wing fuel tanks and on the fittings away from the inspection areas, a practice that has led to a series of intercoat adhesion failures following overhaul, be discontinued. Author (GRA)

**N88-13329#** Societe Nationale Industrielle Aerospatiale, Toulouse (France). Div. Avions.
**AEROELASTIC ANALYSIS OF MODERN TRANSPORT AIRCRAFT [ANALYSE AEROELASTIQUE DES AVIONS MODERNES DE TRANSPORT]**
J. Roustan and M. Curbillon 1987 15 p In FRENCH; ENGLISH summary
(SNIAS-872-111-102; ETN-88-91185) Avail: NTIS HC A02/MF A01

The method used by an aircraft manufacturer to take into consideration static aeroelastic phenomena and to estimate the quantitative effects is described. ESA

**N88-13330#** Societe Nationale Industrielle Aerospatiale, Toulouse (France). Div. Avions.
**DAMAGE CONSIDERATIONS IN SIZING AIRCRAFT CELLS. LIFE PREDICTIONS [PRISE EN COMPTE DE L'ENDOMMAGEMENT DANS LE DIMENSIONNEMENT DES CELLULES D'AVIONS. PREDICTIONS DES DUREES DE VIE]**

J. M. Thomas and B. Heciak 1986 18 p In FRENCH Presented at Conference Endommagement Mecanique des Materiaux et des Structures GAMI, Paris, France, 25-26 Nov. 1986
(SNIAS-872-111-116; ETN-88-91197) Avail: NTIS HC A03/MF A01

Fatigue computation and modeling procedures adopted by an aircraft manufacturer are presented, and a damage tolerance application to A-300 and A-310 aircraft is described. Design and control procedures are listed. ESA

**N88-13244#** Lockheed-California Co., Burbank.
**THE OFF-DESIGN PERFORMANCE OF HYPERSONIC WAVERIDERS**
Lyle N. Long *In* AGARD, Aerodynamics of Hypersonic Lifting Vehicles Nov. 1987 14 (For primary document see N88-13219 05-02)
Copyright Avail: NTIS HC A24/MF A01

**N88-13245*#** Maryland Univ., College Park. Dept. of Aerospace Engineering.
**NUMERICAL OPTIMIZATION OF CONICAL FLOW WAVERIDERS INCLUDING DETAILED VISCOUS EFFECTS**
Kevin G. Bowcutt, John D. Anderson, Jr., and Diego Capriotti *In* AGARD, Aerodynamics of Hypersonic Lifting Vehicles Nov. 1987 23 Sponsored in part by NASA Langley Research Office, Hampton, Va. and Army Research Office, Washington, D.C. (For primary document see N88-13219 05-02)
Copyright Avail: NTIS HC A24/MF A01 CSCL 01A

**N88-13248#** Air Force Wright Aeronautical Labs., Wright-Patterson AFB, Ohio. Aeromechanics Div.
**LIFTING BODIES: AN ATTRACTIVE AERODYNAMIC CONFIGURATION CHOICE FOR HYPERVELOCITY VEHICLES**
Alfred C. Draper and Melvin L. Buck *In* AGARD, Aerodynamics of Hypersonic Lifting Vehicles Nov. 1987 44 (For primary document see N88-13219 05-02)
Copyright Avail: NTIS HC A24/MF A01

# 06 AIRCRAFT INSTRUMENTATION

Includes cockpit and cabin display devices; and flight instruments.

For related information see also *19 Spacecraft Instrumentation* and *35 Instrumentation and Photography.*

**N88-13331#** Advisory Group for Aerospace Research and Development, Neuilly-Sur-Seine (France). Structures and Materials Panel.
**WORKSHOP ON AVIONICS CORROSION CONTROL**
Sep. 1987 80 p Workshop held in Hovik, Norway, 16-17 Apr. 1986 Original contains color illustrations
(AGARD-R-733; ISBN-92-835-0428-3) Copyright Avail: NTIS HC A05/MF A01

This document contains the keynote and other presentations made at a Workshop held by the Structures and Materials Panel on Avionics Corrosion. The discussion covered the problem's extent, the state of the corrosion-prevention art, the prospects for innovative corrosion avoidance techniques, including the substitution of nonmetallic for metallic materials and preventive maintenance techniques. For individual titles, see N88-13332 through N88-13336.

**N88-13332#** Naval Air Development Center, Warminster, Pa.
**AVIONIC CORROSION**
Irving S. Shaffer *In* AGARD Workshop on Avionics Corrosion Control Sep. 1987 10 p (For primary document see N88-13331 05-06)
Copyright Avail: NTIS HC A05/MF A01

The paper discusses the major causes of corrosion in the Navy's avionic equipment and provides specific examples of corrosion failures. Maintenance and readiness data summaries are included to denote further the corrosion problem severity. Corrective measures in design, testing, and maintenance are reviewed. Author

**N88-13333#** Air Force Materials Lab., Wright-Patterson AFB, Ohio. Electronic Failure Analysis Group.
**CORROSION OF ELECTRONIC COMPONENTS**
Bill Dobbs *In* AGARD Workshop on Avionics Corrosion Control Sep. 1987 26 p Original document contains color illustrations (For primary document see N88-13331 05-06)
Copyright Avail: NTIS HC A05/MF A01

The Materials Laboratory Electronic Failure Analysis Group supports US Air Force electronic systems in the areas of materials and manufacturing processes. A large majority of electronic failures is caused my materials and manufacturing process defects. It has been found that corrosion of electronic components is the cause of failure in about 20% of items submitted for testing. Airframe corrosion prevention requirements are well documented. It would be beneficial to the Air Force if corrosion prevention in electronic systems were as well documented. Existing documents, such as T.O. 1-1-689 and NAVAIR 16-1-540, are a step in the right direction. However, compulsory MIL specifications should be applied, since corrosion in Air Force electronic systems contributes significantly to system failure. Failure analysis investigations have been conducted for aircraft circuit breakers, antennas, printed wiring boards, fuses, linear steering position transducers, stepper motors, accelerometers, disk recorder heads, and electrical connectors. The cause of failure is identified and means of preventing future occurrence are presented. Author

**N88-13334#** Commanders Naval Air Forces US Atlantic and Pacific Fleets, Norfolk, Va. Material Advisor.
**US NAVAL AIR FORCE AVIONIC AND ELECTRICAL SYSTEM CORROSION PREVENTION AND CONTROL MAINTENANCE**
G. T. Browne *In* AGARD Workshop on Avionics Corrosion Control Sep. 1987 20 p (For primary document see N88-13331 05-06)
Copyright Avail: NTIS HC A05/MF A01

A study of premature failures of installed avionics, electrical equipment, and systems experienced in US Fleet operational aircraft in the 1960s and 1970s has been reported. These failures were caused by corrosion, water intrusion, and other contaminating agents. To reverse this trend the Commanders Naval Air Forces US Atlantic and Pacific Fleets (COMNAVAIRLANT) (COMNAVAIRPAC) requested that Commander Naval Air System Command (COMNAVAIRSYSCOM) develop a corrosion prevention and control program for avionics, electrical and installed systems used in naval aircraft. COMNAVAIRSYSCOM directed the Naval Air Development Center (NAVAIRDEVCEN) to develop the program together with a technical manual. A conference of interested parties was held in 1976 and action initiated to develop the program and technical manual for use by the fleet technicians. Author

**N88-13335#** Industrial Marine Products Group Ltd., Dartmouth (Nova Scotia). Aerospace Engineering Div.
**CORROSION IN AVIONICS AND ASSOCIATED EQUIPMENT; CAUSE, EFFECT AND PREVENTION**
R. G. Bartlett and E. G. Edgar *In* AGARD Workshop on Avionics Corrosion Control Sep. 1987 9 p (For primary document see N88-13331 05-06)
Copyright Avail: NTIS HC A05/MF A01

Addressed, with examples, are the cause, effect, and prevention of corrosion as it relates to Canadian Forces aircraft. It deals particularly with aircraft operated in a marine environment and is based on the experience of the authors during previous service with the Department of National Defence and in their present employment in industry. The Canadian Forces corrosion prevention treatment program is also mentioned and discussed briefly. Author

**N88-13336#** Societe d'Applications Generales d'Electricite et de Mecanique, Paris (France).
**AVIONICS AND CORROSION**
Alain Pointet and Christophe Turpin-Invernon *In* AGARD

Workshop on Avionics Corrosion Control Sep. 1987 6 p (For primary document see N88-13331 05-06)
Copyright Avail: NTIS HC A05/MF A01

Avionic manufacturing and environmental conditions are responsible for corrosion and/or make easier the action of corrosion in the various parts of an avionics system. A brief survey is made of environmental conditions affecting avionics, how to reproduce them in accordance with norms and which associated problems might occur. All parts of an avionic system are examined, i.e., housings, printed circuit boards, hybrid and integrated circuits. For each component, examples and solutions are given. Author

# 07 AIRCRAFT PROPULSION AND POWER

Includes prime propulsion systems and systems components, e.g., gas turbine engines and compressors; and onboard auxiliary power plants for aircraft.

For related information see also *20 Spacecraft Propulsion and Power, 28 Propellants and Fuels,* and *44 Energy Production and Conversion.*

**N88-13337#** Massachusetts Inst. of Tech., Cambridge. Gas Turbine Lab.
**VELOCITY SCALED AEROELASTIC TESTING OF AN UNDUCTED FAN**
Eric H. Ducharme and Edward F. Crawley Sep. 1987 251 p
Sponsored in part by General Electric Co., Evendale, Ohio
(GTL-191) Avail: NTIS HC A12/MF A01

The aeroelastic behavior of an unducted fan is investigated through a procedure for the sub-velocity scaled testing of anisotropic aeroelastic models. The flutter equations of motion and scaling laws for an anisotropic, rotating model are developed. The scaling laws indicate that by proper choice of model geometry, stiffness, and density, all of the important aeroelastic similarity parameters except for the Mach number can be satisfied in a sub-velocity scaled test. The development of the model building technology to construct reduced stiffness anisotropic models for sub-velocity scaled testing is then described. With the validity of the sub-velocity scaled procedure established, the versatility in the low model stresses was exploited through the construction of models which allowed for the parametric variation of such aeroelastic parameters as: sweep, mass distribution, solidity, blade laminate, and mistuning. The flutter dependence of the models on these parameters was experimentally demonstrated. A flutter model employing the determined blade frequencies and mode shapes for the structural model and a strip theory based on a 2D unsteady cascade theory for the model is presented. Author

**N88-13338*#** National Aeronautics and Space Administration. Lewis Research Center, Cleveland, Ohio.
**COMBUSTION CHARACTERISTICS OF GAS TURBINE ALTERNATIVE FUELS**
R. James Rollbuhler Dec. 1987 20 p Presented at the 25th Automotive Technology Development Contractors' Coordination Meeting (ATD/CCM), Dearborn, Mich., 28-29 Oct. 1987; sponsored by the Society of Automotive Engineers
(Contract DE-AI01-85CE-50111)
(NASA-TM-100247; E-3869; NAS 1.15:100247; DOE/NASA/50111-1) Avail: NTIS HC A03/MF A01 CSCL 21E

An experimental investigation was conducted to obtain combustion performance values for specific heavyend, synthetic hydrocarbon fuels. A flame tube combustor modified to duplicate an advanced gas turbine engine combustor was used for the tests. Each fuel was tested at steady-state operating conditions over a range of mass flow rates, fuel-to-air mass ratio, and inlet air temperatures. The combustion pressure, as well as the hardware, were kept nearly constant over the program test phase. Test results were obtained in regards to geometric temperature pattern factors as a function of combustor wall temperatures, the combustion gas temperature, and the combustion emissions, both as affected by the mass flow rate and fuel-to-air ratio. The synthetic fuels were reacted in the combustor such that for most tests their performance was as good, if not better, than the baseline gasoline or diesel fuel tests. The only detrimental effects were that at high inlet air temperature conditions, fuel decomposition occurred in the fuel atomizing nozzle passages resulting in blockage. And the nitrogen oxide emissions were above EPA limits at low flow rate and high operating temperature conditions. Author

**N88-13339** Iowa State Univ. of Science and Technology, Ames.
**EFFECTS OF FREE STREAM TURBULENCE, REYNOLDS NUMBER AND INCIDENCE ANGLE ON AXIAL TURBINE CASCADE PERFORMANCE Ph.D. Thesis**
S. B. Vijayaraghavan 1987 292 p
Avail: Univ. Microfilms Order No. DA8716834

A large-scale, low-speed, axial turbine cascade was designed using a fast interactive design code and tested over a range of turbulence level and incidence angle for Reynolds numbers typical of gas turbines. Thirty-six tests were done primarily to investigate the profile boundary layer development under different inlet flow conditions. Glue-on hot film gages and surface flow visualizations were used to identify transition and separation over the airfoil surface. In addition to transition measurements, overall cascade performance was determined from static pressure distributions on the airfoil and detailed five-hole pressure probe and hot-wire probe traverses in an exit plane of the cascade. The measured transition start and end points were compared against predictions using existing transition models. Also, the measured losses were compared against predicted losses from boundary layer calculations based on dissipation integral and finite difference analyses.
Dissert. Abstr.

**N88-13340#** Dayton Univ., Ohio.
**CORRELATION OF AIR PRESSURE DROP AND FLAME ARRESTOR CHARACTERISTICS FOR EXPLOSION SUPPRESSION-MATERIALS Final Report, 1 Feb. 1985 - 31 Jan. 1986**
John E. Minardi and Maurice O. Lawson Nov. 1986 55 p
(Contract F33615-84-C-2411)
(AD-A184960; UDR-TR-86-115; AFWAL-TR-86-2087) Avail: NTIS HC A04/MF A01 CSCL 13L

A theory is presented for predicting the pressure rise versus void fraction in the flame tube located at Wright-Patterson Air Force Base. The effects of initial temperature and pressure are included in the theory. A study of the heat losses in the flame tube is presented and an empirical fit to the cool down phase of the pressure time history data is developed. An equation for correlating the friction factors measured in the pressure drop rig with the hydraulic diameter of the foam is developed. An equation for the critical hydraulic diameter (or quenching diameter) as a function of initial pressure and temperature is also given in the report. The theoretical results are compared to experimental data and are shown to compare favorably. GRA

**N88-13341#** Naval Postgraduate School, Monterey, Calif.
**STUDY OF ELECTROSTATIC MODULATION OF FUEL SPRAYS TO ENHANCE COMBUSTION PERFORMANCE IN AN AVIATION GAS TURBINE M.S. Thesis**
Walter W. Manning Jun. 1987 104 p
(AD-A184967) Avail: NTIS HC A06/MF A01 CSCL 21E

The influence of electrostatic and electrohydrodynamic charging on hydrocarbon fuel spray patterns and droplet atomization has been investigated. Research was performed in a combustion environment with an Allison T-56 combustor liner and an unmodified pressure-jet atomizer fuel nozzle. High-voltage probes and a variable-geometry probe insertion device were developed to assess the effectiveness of probe type and location on fuel spray modification and modulation. Exhaust gas temperatures and temperature profiles were measured to determine changes in the combustor's thermal profile and combustion efficiency. JP-4, JET-A and Number-2 Diesel fuels were tested to analyze electrically-assisted atomization effectiveness relative to off-design fuel performance. GRA

**N88-13342#** Naval Postgraduate School, Monterey, Calif.
**AN EXPERIMENTAL INVESTIGATION OF THE IGNITION AND FLAMMABILITY LIMITS OF VARIOUS HYDROCARBON FUELS IN A TWO-DIMENSIONAL SOLID FUEL RAMJET M.S. Thesis**
Richard C. Wooldridge Jun. 1987 43 p
(AD-A184968) Avail: NTIS HC A03/MF A01 CSCL 21D

An experimental investigation was conducted to study the effects of inlet step height on ignition and flammability limits and recirculation zone and boundary layer combustion phenomena of various hydrocarbon fuels. A windowed two-dimensional solid fuel ramjet (SFRJ) was utilized. Hydrocarbon fuels were burned under conditions similar to the actual flight were studied using a variable geometry inlet, an automatic data acquisition system, and high speed motion pictures of the interior of the combustion chamber at the recirculation zone and the boundary layer development region. Data was obtained at a mass flux of 0.2 lbm/sq in/sec at a nominal air inlet temperature of 1000 R with pressures ranging from 100 to 150 psia. GRA

**N88-13343#** National Aerospace Lab., Amsterdam (Netherlands). Structures and Materials Div.
**SIMULATED SERVICE TEST BEHAVIOR OF VARIOUS INTERNAL AND EXTERNAL COATINGS APPLIED ON CF6-50 FIRST STAGE TURBINE BLADES**
A. J. A. Mom and J. A. M. Boogers 4 Mar. 1986 24 p Presented at the Conference on High Temperature Alloys for Gas Turbines and Other Applications, Liege, Belgium, 6-9 Oct. 1986 Previously announced in IAA as A87-49556
(NLR-MP-86018-U; B8709826; ETN-88-91327) Avail: NTIS HC A03/MF A01

Simulated service testing of protective external overcoating and internal coating on the the CF6-50 first stage turbine blade is described. Service life is limited by the external coating life and corrosion attack in the uncoated cooling passages. Results indicate that external overcoats in most cases improve the corrosion behavior of the CF6-50 blades. The best external protection is an Al/Si slurry type of coating on top of Codep B. The application of internal coatings considerably improves corrosion performance of the CF6-50 blade. Internal corrosion is virtually eliminated by the application of Al/Si or Al gas phase coatings. ESA

**N88-13344#** Advisory Group for Aerospace Research and Development, Neuilly-Sur-Seine (France).
**APPLICATION OF MODIFIED LOSS AND DEVIATION CORRELATIONS TO TRANSONIC AXIAL COMPRESSORS**
M. Cetin, A. S. Uecer, Ch. Hirsch, and G. K. Serovy Nov. 1987 74 p
(AGARD-R-745; ISBN-92-835-0346-4) Copyright Avail: NTIS HC A04/MF A01

The goal was to analyze the transonic compressor tests available in the open literature and to propose possible improvements in total loss and turning correlations. From the work performed six conclusions could be drawn for the achievement of better loss predictions. A comparison with results of a two-stage compressor showed that the results of the new correlation set were satisfactory. For more accurate predictions a consistent end-wall boundary layer and secondary loss calculation method must be applied; in multi-stage compressors, spanwise loss mixing procedures must be used. Author

**N88-13345*#** National Aeronautics and Space Administration. Lewis Research Center, Cleveland, Ohio.
**REGRESSED RELATIONS FOR FORCED CONVECTION HEAT TRANSFER IN A DIRECT INJECTION STRATIFIED CHARGE ROTARY ENGINE**
Chi M. Lee and Harold J. Schock (Michigan State Univ., East Lansing.) 1988 24 p Proposed for presentation at the 1988 International Congress and Exposition, Detroit, Mich., 29 Feb. - 4 Mar. 1988; sponsored by the Society of Automotive Engineers, Inc.
(NASA-TM-100124; E-3689; NAS 1.15:100124) Avail: NTIS HC A03/MF A01 CSCL 20E

Currently, the heat transfer equation used in the rotary combustion engine (RCE) simulation model is taken from piston engine studies. These relations have been empirically developed by the experimental input coming from piston engines whose geometry differs considerably from that of the RCE. The objective of this work was to derive equations to estimate heat transfer coefficients in the combustion chamber of an RCE. This was accomplished by making detailed temperature and pressure measurements in a direct injection stratified charge (DISC) RCE under a range of conditions. For each specific measurement point, the local gas velocity was assumed equal to the local rotor tip speed. Local physical properties of the fluids were then calculated. Two types of correlation equations were derived and are described in this paper. The first correlation expresses the Nusselt number as a function of the Prandtl number, Reynolds number, and characteristic temperature ratio; the second correlation expresses the forced convection heat transfer coefficient as a function of fluid temperature, pressure and velocity. Author

**N88-13346*#** National Aeronautics and Space Administration. Lewis Research Center, Cleveland, Ohio.
**UNSTEADY AERODYNAMICS OF AN OSCILLATING CASCADE IN A COMPRESSIBLE FLOW FIELD**
Daniel H. Buffum, Donald R. Boldman, and Sanford Fleeter (Purdue Univ., West Lafayette, Ind.) 1987 22 p Presented at the 4th Symposium on Unsteady Aerodynamics and Aeroelasticity of Turbomachines and Propellers, Aachen, Fed. Republic of Germany, 6-10 Sep. 1987; sponsored by Aachen Univ.
(NASA-TM-100219; E-3830; NAS 1.15:100219) Avail: NTIS HC A03/MF A01 CSCL 20E

Fundamental experiments were performed in the NASA Lewis Transonic Oscillating Cascade Facility to investigate and quantify the unsteady aerodynamics of a cascade of biconvex airfoils executing torsion-mode oscillations at realistic reduced frequencies. Flush-mounted, high-response miniature pressure transducers were used to measure the unsteady airfoil surface pressures. The pressures were measured for three interblade phase angles at two inlet Mach numbers, 0.65 and 0.80, and two incidence angles, 0 and 7 deg. The time-variant pressures were analyzed by means of discrete Fourier transform techniques, and these unique data were then compared with predictions from a linearized unsteady cascade model. The experimental results indicate that the interblade phase angle had a major effect on the chordwise distributions of the airfoil surface unsteady pressure, and that reduced frequency, incidence angle, and Mach number had a somewhat less significant effect. Author

**N88-13347*#** National Aeronautics and Space Administration. Lewis Research Center, Cleveland, Ohio.
**A NUMERICAL STUDY OF THE EFFECTS OF CURVATURE AND CONVERGENCE ON DILUTION JET MIXING**
J. D. Holdeman, R. Reynolds, and C. White (Garrett Turbine Engine Co., Phoenix, Ariz.) 1987 19 p Presented at the 23rd Joint Propulsion Conference, San Diego, Calif., 29 Jun. - 2 Jul. 1987; sponsored by AIAA, SAE, ASME and ASEE
(NASA-TM-89878; E-3548; NAS 1.15:89878) Avail: NTIS HC A03/MF A01 CSCL 21E

An analytical program was conducted to assemble and assess a three-dimensional turbulent viscous flow computer code capable of analyzing the flow field in the transition liners of small gas turbine engines. This code is of the TEACH type with hybrid numerics, and uses the power law and SIMPLER algorithms, an orthogonal curvilinear coordinate system, and an algebraic Reynolds stress turbulence model. The assessments performed in this study, consistent with results in the literature, showed that in its present form this code is capable of predicting trends and qualitative results. The assembled code was used to perform a numerical experiment to investigate the effects of curvature and convergence in the transition liner on the mixing of single and opposed rows of cool dilution jets injected into a hot mainstream flow. Author

**N88-13231#** Johns Hopkins Univ., Laurel, Md. Applied Physics Lab.
**HYPERSONIC AIRBREATHING PROPULSION: EVOLUTION AND OPPORTUNITIES**
P. J. Waltrup *In* AGARD, Aerodynamics of Hypersonic Lifting Vehicles Nov. 1987 29 (For primary document see N88-13219 05-02)
Copyright Avail: NTIS HC A24/MF A01

# 08 AIRCRAFT STABILITY AND CONTROL

Includes aircraft handling qualities; piloting; flight controls; and autopilots.

For related information see also *05 Aircraft Design, Testing and Performance.*

**N88-13348#** Advisory Group for Aerospace Research and Development, Neuilly-Sur-Seine (France). Structures and Materials Panel.
**STATIC AEROELASTIC EFFECTS ON HIGH PERFORMANCE AIRCRAFT**
Jul. 1987 186 p In ENGLISH and FRENCH Meeting held in Athens, Greece, 28 Sep. - 3 Oct. 1986
(AGARD-CP-403; ISBN-92-835-0424-0) Copyright Avail: NTIS HC A09/MF A01

Modern high performance aircraft designs tend to employ very thin airfoils having a degree and a distribution of stiffness far from the ideal; in consequence, there is a loss of control effectiveness and maneuverability. Moreover, the introduction of the highly forward swept wing planform poses a static aeroelastic effect of fundamental importance; these effects are felt at model as well as at full scale. The meeting was organized not only to review instances of these problems but to see how successfully modern tools for structural and aeroelastic analysis can be applied. For individual titles, see N88-13349 through N88-13358.

**N88-13349#** British Aerospace Public Ltd. Co., Preston (England). Military Aircraft Div.
**EXAMPLES OF STATIC AEROELASTIC EFFECTS ON PRESENT COMBAT AIRCRAFT PROJECTS**
W. E. Sharpe and J. B. Newton *In* AGARD Static Aeroelastic Effects on High Performance Aircraft Jul. 1987 10 (For primary document see N88-13348 05-08)
Copyright Avail: NTIS HC A09/MF A01

The results of static aeroelastic calculations for a recent canard/cranked delta fighter project, in which a complete aircraft aerodynamic and structural model is used to demonstrate fully interacted free aircraft deflection modes and resulting stability effects are described. The significance of these results are illustrated by comparison with corresponding fixed root calculations, thereby indicating a requirement for complete aircraft aeroelastic modeling at the earliest possible stage in project design. Aeroelastic modeling of external stores in the context of store/aircraft integration is also discussed. Finally, the correlation of high speed wind tunnel results for aeroelastic distortion is addressed, indicating those parameters which are likely to be significantly affected.
Author

**N88-13350#** Avions Marcel Dassault-Breguet Aviation, Saint-Cloud (France).
**TRENDS IN AEROELASTIC ANALYSIS OF COMBAT AIRCRAFT**
C. Petiau and S. Brun *In* AGARD Static Aeroelastic Effects on High Performance Aircraft Jul. 1987 25 (For primary document see N88-13348 05-08)
Copyright Avail: NTIS HC A09/MF A01

After recalling the general principles of aeroelastic coupling with structural finite element analysis, the simplifying assumptions of static aeroelasticity are explained. The technique of load basis used in a general aircraft structural analysis program is discussed. This technique allows one to separate the big expensive computation of finite element resolutions and theoretical aerodynamic analysis from aeroelastic coupling and flight maneuver computation.
Author

**N88-13351#** Messerschmitt-Boelkow-Blohm G.m.b.H., Munich (West Germany). Helicopter and Airplane Div.
**STATIC AEROELASTIC CONSIDERATIONS IN THE DEFINITION OF DESIGN LOADS FOR FIGHTER AIRPLANES**
G. Schmidinger and O. Sensburg *In* AGARD Static Aeroelastic Effects on High Performance Aircraft Jul. 1987 20 (For primary document see N88-13348 05-08)
Copyright Avail: NTIS HC A09/MF A01

Some typical effects of static aeroelastic correction factors in context with the definition of structural design loads for major aircraft components are discussed. The influences on response parameters and resulting design loads are shown as well as the aeroelastic optimization of trailing edge flaps with respect to geometry, efficiency, and hingemoments.
Author

**N88-13352#** Aerospatiale Usines de Toulouse (France).
**AEROELASTIC ANALYSIS OF MODERN TRANSPORT AIRCRAFT [ANALYSE AEROELASTIQUE DES AVIONS MODERNES DE TRANSPORT]**
J. Roustan and M. Curbillon *In* AGARD Static Aeroelastic Effects on High Performance Aircraft Jul. 1987 27 In FRENCH; ENGLISH summary (For primary document see N88-13348 05-08)
Copyright Avail: NTIS HC A09/MF A01

Static aeroelastic phenomena play a very important role in modern transport aircraft with regard to both handling qualities and loads applied to the structure. Aerospatiale's method for taking these effects into consideration and calculating them is presented.
Author

**N88-13353*#** National Aeronautics and Space Administration. Langley Research Center, Hampton, Va.
**STATIC AEROELASTIC EFFECTS ON THE FLUTTER OF A SUPERCRITICAL WING**
E. Carson Yates, Jr. and Li-Chuan Chu (PRC Kentron, Inc., Hampton, Va.) *In* AGARD Static Aeroelastic Effects on High Performance Aircraft Jul. 1987 14 (For primary document see N88-13348 05-08)
Copyright Avail: NTIS HC A09/MF A01 CSCL 01C

The results of an effort to calculate the effects of angle of attack and the associated aeroelastic deformation on the flutter of a highly swept supercritical wing by use of the modified strip analysis employed in previous studies of this wing are discussed. The spanwise distributions of steady state section lift-curve slope and aerodynamic center required as input for these calculations were obtained from static aeroelastic calculations for the wing by use of the FLO22 transonic code and an assumed dynamic pressure. The process is iterative so that flutter can be obtained at the same dynamic pressure as that used to calculate the statistically deformed shape and loading about which the flutter oscillation occurs (matched conditions). The results of this investigation show that the unconventional backward turn of the transonic dip in the experimental flutter boundary for angles of attack greater than zero is caused by variations in mass ratio and not by static aeroelastic deformation, although inclusion of the latter appears to be required for quantitative accuracy in the calculations.
Author

**N88-13354#** Royal Aircraft Establishment, Farnborough (England).
**WING DIVERGENCE OF TRIMMED AIRCRAFT**
Ll. T. Niblett *In* AGARD Static Aeroelastic Effects on High Performance Aircraft Jul. 1987 9 (For primary document see N88-13348 05-08)
Copyright Avail: NTIS HC A09/MF A01

By means of a simple theoretical model it is shown that wing divergence of a free aircraft can be defined using the static case of trimmed level flight. The same model also shows that the control angle per g goes to zero at a speed near the fixed root divergence

speed and that there is a large change in the spanwise distribution of airload in going from a low speed to speeds above that of fixed root divergence. Author

**N88-13355#** Advisory Group for Aerospace Research and Development, Neuilly-Sur-Seine (France). Helicopter and Airplane Div.

**THE USE OF AEROELASTIC WIND TUNNEL MODELS TO PROVE STRUCTURAL DESIGN**

H. Hoenlinger, J. Schweiger, and G. Schewe (Deutsche Forschungs- und Versuchsanstalt fuer Luft- und Raumfahrt, Goettingen, West Germany ) *In its* Static Aeroelastic Effects on High Performance Aircraft Jul. 1987 15 (For primary document see N88-13348 05-08)

Copyright Avail: NTIS HC A09/MF A01

In a wind tunnel study on an aeroelastic carbon fiber fin/rudder model, it is demonstrated how structural design methods can be checked by experiment beginning in an early stage of the design. Emphasis was put on the static aeroelastic investigations, which became more important in high performance A/C design. Transonic measurements with a rigid balance based on an opto-electronic deformation measurement method were performed. An attempt was made to evaluate rudder efficienies from these aeroelastic measurements. A nonlinear behavior of the rudder based on geometrical coupling with the fin box played an important role in the test evaluation. Author

**N88-13356*#** National Aeronautics and Space Administration. Langley Research Center, Hampton, Va.

**PREDICTION OF WING AEROELASTIC EFFECTS ON AIRCRAFT LIFE AND PITCHING MOMENT CHARACTERISTICS**

Clinton V. Eckstrom *In* AGARD Static Aeroelastic Effects on High Performance Aircraft Jul. 1987 17 Previously announced as N87-15975 (For primary document see N88-13348 05-08)

Copyright Avail: NTIS HC A09/MF A01 CSCL 01C

The distribution of flight loads on an aircraft structure determine the lift and pitching moment characteristics of the aircraft. When the load distribution changes due to the aeroelastic response of the structure, the lift and pitching moment characteristics also change. An estimate of the effect of aeroelasticity on stability and control characteristics is often required for the development of aircraft simulation models of evaluation of flight characteristics. This presentation outlines a procedure for incorporating calculated linear aeroelastic effects into measured nonlinear lift and pitching moment data from wind tunnel tests. Results are presented which were obtained from applying this procedure to data for an aircraft with a very flexible transport type research wing. The procedure described is generally applicable to all types of aircraft. Author

**N88-13357#** Office National d'Etudes et de Recherches Aerospatiales, Paris (France).

**INFLUENCE OF THE STATIC DEFORMATION ON A WING IN THE UNSTEADY AERODYNAMIC**

R. Destuynder *In* AGARD Static Aeroelastic Effects on High Performance Aircraft Jul. 1987 8 Previously announced in IAA as A87-21054 (For primary document see N88-13348 05-08)

Copyright Avail: NTIS HC A09/MF A01

Wind tunnel tests and related calculations were carried out to study the influence of static deformation due to steady loads on the flutter phenomenon experienced by modern civil aircraft. Consideration is also given to the nonlinearity of unsteady forces on an engine as a function of global incidence. It is found that the spanwise untwisting effect associated with positive incidences increases the flutter limits for given Mach number and dynamic pressure values. Author

**N88-13358#** Office National d'Etudes et de Recherches Aerospatiales, Paris (France).

**MEASUREMENT OF MODEL DEFORMATION IN WIND TUNNELS**

M. Charpin, C. Armand, and R. Selvaggini *In* AGARD Static Aeroelastic Effects on High Performance Aircraft Jul. 1987 20 In FRENCH; ENGLISH summary Original language document was announced in IAA as A87-36943 (For primary document see N88-13348 05-08)

Copyright Avail: NTIS HC A09/MF A01

Various techniques used at ONERA for the wind tunnel measurement of the deformation of models undergoing aerodynamic and body loading are presented. Photography of reflecting targets is used to measure trailing edge deformation. Global torsion measurement of a wing at its wing tip is performed by the torsiometer measurement of the angle between the incident and reflected laser beam. An example of the determination of airfoil trailing edge deformation by tracking the position of light sources with an optical detector is presented. Finally, a technique for computing the strain from stress measurements is presented and demonstrated with a helicopter rotor blade model. Author

**N88-13359*#** National Aeronautics and Space Administration. Ames Research Center, Moffett Field, Calif.

**INTEGRATED CONTROL AND DISPLAY RESEARCH FOR TRANSITION AND VERTICAL FLIGHT ON THE NASA V/STOL RESEARCH AIRCRAFT (VSRA)**

John D. Foster, Ernesto Moralez, III, James A. Franklin, and Jeffery A. Schroeder (Army Aviation Research and Development Command, Moffett Field, Calif.) Oct. 1987 35 p (NASA-TM-100029; A-87350; NAS 1.15:100029) Avail: NTIS HC A03/MF A01 CSCL 01C

Results of a substantial body of ground-based simulation experiments indicate that a high degree of precision of operation for recovery aboard small ships in heavy seas and low visibility with acceptable levels of effort by the pilot can be achieved by integrating the aircraft flight and propulsion controls. The availability of digital fly-by-wire controls makes it feasible to implement an integrated control design to achieve and demonstrate in flight the operational benefits promised by the simulation experience. It remains to validate these systems concepts in flight to establish their value for advanced short takeoff vertical landing (STOVL) aircraft designs. This paper summarizes analytical studies and simulation experiments which provide a basis for the flight research program that will develop and validate critical technologies for advanced STOVL aircraft through the development and evaluation of advanced, integrated control and display concepts, and lays out the plan for the flight program that will be conducted on NASA's V/STOL Research Aircraft (VSRA). Author

**N88-13360#** Technische Univ., Brunswick (West Germany). Fakultaet fuer Maschinenbau and Elektrotechnik.

**CONTRIBUTION TO THE IMPROVEMENT OF THE GUIDANCE ACCURACY OF AUTOMATIC PILOTS Ph.D. Thesis [BEITRAEGE ZUER VERBESSERUNG DER FUEHRUNGSGENAUIGKEIT VON FLUGREGLERN]**

Artur Redeker 1986 153 p In GERMAN (ETN-88-90607) Avail: , NTIS HC A08/MF A01

A multiple-quantity configuration controller for aircraft longitudinal motion was developed for the processing and anticipatory control of perturbation and control quantities. A quasi stationary, nonlinear model of the controlled system was used. The deviations between model and flight test data are of the order of a few percent. A computer program of the configuration controller was implemented and tested onboard a research aircraft. A high degree of decoupling between control and eigenbehavior is observed. The flight test results show that an extensive anticipatory control and perturbation compensation for the longitudinal motion can be realized with practical advantages and substantially higher accuracy than in present passenger aircraft. ESA

**N88-13361#** Societe Nationale Industrielle Aerospatiale, Paris (France). Div. Avions.

**ELECTRICAL FLIGHT COMMANDS IN TRANSPORT AIRCRAFT [LES COMMANDES DE VOL ELECTRIQUES DES AVIONS DE TRANSPORT]**

Michel Durandeau and Jacques Troyes 1986 25 p In FRENCH Presented at the Cercle des Officiers Mecaniciens et

Ingenieurs Navigants de l'Aviation Civile (COMINAC), Roissy-en-France, France, 15 Jan. 1986
(SNIAS-872-111-108; ETN-88-91190) Avail: NTIS HC A03/MF A01

The philosophy and implementation of the electrical flight commands adopted for the A320 aircraft are described. The design is very conservative to provide maximum safety, including the design of two-in-one computers where a maximum of asymmetry is provided (components, programs, languages, design teams). ESA

**N88-13362#** Societe Nationale Industrielle Aerospatiale, Toulouse (France). Div. Avions.
**REDUCED ORDER OPTIMAL COMMAND APPLIED TO LONGITUDINAL AUTOMATIC PILOTS [LA COMMANDE OPTIMALE D'ORDRE REDUIT. APPLICATION AU PILOTAGE AUTOMATIQUE LONGITUDINAL]**
O. Herail 1987 21 p In FRENCH
(SNIAS-872-111-114; ETN-88-91195) Avail: NTIS HC A02/MF A01

A flight control method is outlined. The method implies the fixation of the order and structure of the regulator independently of the complexity of the model. The theory provides the coupled matrix equations which give the optimal regulator. The solution is found using nonlinear programming interpreting one of the coupled equations as the expression of the gradient of the quadratic criteria. The technique minimizes a classical quadratic criterion. Examples of models order 11 to 15 are included. ESA

**N88-13363*#** National Aeronautics and Space Administration. Ames Research Center, Moffett Field, Calif.
**FULL-ENVELOPE AERODYNAMIC MODELING OF THE HARRIER AIRCRAFT**
B. David McNally Oct. 1986 18 p Presented at the 17th Annual Symposium Flight Testing: The Continuing Challenge, Washington, D.C., 10-13 Aug. 1986
(NASA-TM-88376; A-86380; NAS 1.15:88376) Avail: NTIS HC A03/MF A01 CSCL 01C

A project to identify a full-envelope model of the YAV-8B Harrier using flight-test and parameter identification techniques is described. As part of the research in advanced control and display concepts for V/STOL aircraft, a full-envelope aerodynamic model of the Harrier is identified, using mathematical model structures and parameter identification methods. A global-polynomial model structure is also used as a basis for the identification of the YAV-8B aerodynamic model. State estimation methods are used to ensure flight data consistency prior to parameter identification. Equation-error methods are used to identify model parameters. A fixed-base simulator is used extensively to develop flight test procedures and to validate parameter identification software. Using simple flight maneuvers, a simulated data set was created covering the YAV-8B flight envelope from about 0.3 to 0.7 Mach and about -5 to 15 deg angle of attack. A singular value decomposition implementation of the equation-error approach produced good parameter estimates based on this simulated data set. Author

**N88-13247#** Waterloo Univ. (Ontario). Dept. of Applied Mathematics and Mechanical Engineering.
**DYNAMIC STABILITY OF HYPERSONIC CONICAL LIFTING VEHICLES ACCORDING TO NEWTON-BUSEMANN THEORY**
W. H. Hui and H. J. VanRoessel (University of Western Ontario, London.) *In* AGARD, Aerodynamics of Hypersonic Lifting Vehicles Nov. 1987 13 Sponsored in part by Natural Science and Engineering Research Council of Canada (For primary document see N88-13219 05-02)
Copyright Avail: NTIS HC A24/MF A01

**N88-13319*#** National Aeronautics and Space Administration. Langley Research Center, Hampton, Va.
**NONLINEAR LIFT CONTROL AT HIGH SPEED AND HIGH ANGLE OF ATTACK USING VORTEX FLOW TECHNOLOGY**
John E. Lamar *In* AGARD, Special Course on Fundamentals of Fighter Aircraft Design Oct. 1987 23 Previously announced in IAA as A86-37050 (For primary document see N86-13315 05-05)
Copyright Avail: NTIS HC A13/MF A01 CSCL 01C

# 09 RESEARCH AND SUPPORT FACILITIES (AIR)

Includes airports, hangars and runways; aircraft repair and overhaul facilities; wind tunnels; shock tubes; and aircraft engine test stands.

For related information see also *14 Ground Support Systems and Facilities (Space).*

**N88-13364#** National Aeronautical Lab., Bangalore (India). Aerodynamics Dv.
**MODEL HELICOPTER ROTOR RIG AND ASSOCIATED STRAIN GAUGE BALANCE FOR PERFORMANCE STUDIES**
S. R. Patil and M. A. Ramaswamy (Indian Inst. of Science, Bangalore.) Aug. 1987 37 p
(NAL-TM-AE-8704) Avail: NTIS HC A03/MF A01 CSCL 14B

The details of a teetering rotor model and the associated strain gage balance and calibration fixtures have been presented. Hovering results for a 1.22-m diameter teetering rotor model evaluated experimentally have been compared with the simple blade element momentum theory. Author

**N88-13365#** National Aeronautical Lab., Bangalore (India). Systems Engineering Div.
**NON-LINEAR MAXIMUM LIKELIHOOD ESTIMATION OF STABILITY DERIVATIVES FROM RANGE DATA**
V. S. Mohan Ram and C. V. Srinath Sastry Dec. 1986 20 p
(NAL-TM-SE-8608) Avail: NTIS HC A03/MF A01

A parameter identification technique of extracting nondimensional stability derivatives for the AGARD standard ballistic correlation model HB-2 from supersonic free-flight data is investigated. Based on the Maximum Likelihood criterion, the identification technique used is a modified Newton-Raphson quasi-linearization minimization procedure with certain extensions for handling general nonlinear systems without involved program changes. A hybrid type formulation for the 6 degrees of freedom nonlinear equations of motion is employed wherein aerodynamic force and moment representations are in wind-axis and body-axis coordinate systems respectively. Results for both the longitudinal and lateral stability derivatives of the AGARD model demonstrate, as borne out by the excellent fit to the measured motions of a typical flight and accuracy of the parameter estimates, the suitability and power of the maximum likelihood method and functional adequacy of the mathematical model used. Author

**N88-13366#** National Aerospace Lab., Amsterdam (Netherlands). Flight Div.
**OVERLOOKED POTENTIAL OF SYSTEMS WITH MARKOVIAN COEFFICIENTS**
H. A. P. Blom 4 Aug. 1986 11 p Presented at the 25th IEEE Conference on Decision and Control, Athens, Greece, 10-12 Dec. 1986
(NLR-MP-86049-U; B8709829; ETN-88-91330) Avail: NTIS HC A03/MF A01

The usual system of linear stochastic difference equations with Markovian coefficients is generalized to cover R sup n valued processes which jump simultaneously with and due to jumps of the coefficients. The additional modeling potential is illustrated for a maneuvering aircraft. To filter partial observations of the generalized system candidate algorithms are reviewed, in particular the generalized pseudo Bayes algorithms and the interacting multiple model (IMM) algorithm. The IMM algorithm for the generalized system is applied to tracking a maneuvering aircraft. The results indicate that the generalized models and the associated IMM algorithm has the potential to yield trackers that perform better than the existing decision-directed trackers. ESA

**N88-13367*#** National Aeronautics and Space Administration. Ames Research Center, Moffett Field, Calif.
**DEVELOPMENT OF AN INTERFACE FOR AN ULTRARELIABLE FAULT-TOLERANT CONTROL SYSTEM AND AN ELECTRONIC SERVO-CONTROL UNIT**
Charles Shaver and Michael Williamson Sep. 1986 37 p
(NASA-TM-88236; A-86196; NAS 1.15:88236) Avail: NTIS HC A03/MF A01 CSCL 14B

The NASA Ames Research Center sponsors a research program for the investigation of Intelligent Flight Control Actuation systems. The use of artificial intelligence techniques in conjunction with algorithmic techniques for autonomous, decentralized fault management of flight-control actuation systems is explored under this program. The design, development, and operation of the interface for laboratory investigation of this program is documented. The interface, architecturally based on the Intel 8751 microcontroller, is an interrupt-driven system designed to receive a digital message from an ultrareliable fault-tolerant control system (UFTCS). The interface links the UFTCS to an electronic servo-control unit, which controls a set of hydraulic actuators. It was necessary to build a UFTCS emulator (also based on the Intel 8751) to provide signal sources for testing the equipment.
Author

**N88-13220#** Calspan Corp., Buffalo, N. Y.
**A SURVEY OF EXISTING HYPERSONIC GROUND TEST FACILITIES: NORTH AMERICA**
C. E. Wittliff *In* AGARD, Aerodynamics of Hypersonic Lifting Vehicles Nov. 1987 17 (For primary document see N88-13219 05-02)
Copyright Avail: NTIS HC A24/MF A01

**N88-13221#** Von Karman Inst. for Fluid Dynamics, Rhode-Saint-Genese (Belgium).
**EUROPEAN HYPERSONIC WIND TUNNELS**
J. F. Wendt *In* AGARD, Aerodynamics of Hypersonic Lifting Vehicles Nov. 1987 24 (For primary document see N88-13219 05-02)
Copyright Avail: NTIS HC A24/MF A01

**N88-13223#** Queensland Univ., Brisbane (Australia). Dept. of Mechanical Engineering.
**SHOCK TUNNELS FOR REAL GAS HYPERSONICS**
R. J. Stalker *In* AGARD, Aerodynamics of Hypersonic Lifting Vehicles Nov. 1987 10 (For primary document see N88-13219 05-02)
Copyright Avail: NTIS HC A24/MF A01

**N88-13612*#** Naval Surface Weapons Center, Silver Spring, Md. Electronics Hardening Branch.
**SCALING THE ELECTROMAGNETICALLY DRIVEN EXPLOSIVE SHOCK SIMULATOR**
Robert I. Persh *In* NASA-Marshall Space Flight Center, The 58th Shock and Vibration Symposium, Volume 1 Oct. 1987 p 49-60 (For primary document see N88-13609 05-39)
Avail: NTIS HC A21/MF A01 CSCL 14B

# 12 ASTRONAUTICS (GENERAL)

For extraterrestrial exploration see *91 Lunar and Planetary Exploration.*

**N88-13368*#** Rockwell International Corp., Downey, Calif. Space Transportation Systems Div.
**ORBITAL SPACECRAFT CONSUMABLES RESUPPLY SYSTEM (OSCRS). VOLUME 1: EXECUTIVE SUMMARY Final Report**
Mar. 1987 73 p
(Contract NAS9-17584)
(NASA-CR-172010; NAS 1.26:172010; STS-86-0302-1A-Vol-1; DRD-10-Vol-1; CDRL-MA-1023T-Vol-1) Avail: NTIS HC A04/MF A01 CSCL 22A

The objective was to establish an earth storable fluid tanker concept which satisfies the initial resupply requirements for the Gamma Ray Observatory (GRO) at a reasonable front end cost while providing growth potential for foreseeable future earth storable fluid resupply mission requirements. The estimated costs required to design, develop, qualify, fabricate, and deliver a flight tanker and its associated control avionics, ground support equipment (GSE), and processing facilities, and the contractors costs to support the first operations mission are reviewed. B.G.

# 13 ASTRODYNAMICS

Includes powered and free-flight trajectories; and orbital and launching dynamics.

No abstracts in this category.

# 14 GROUND SUPPORT SYSTEMS AND FACILITIES (SPACE)

Includes launch complexes, research and production facilities; ground support equipment, e.g., mobile transporters; and simulators.

For related information see also *09 Research and Support Facilities (Air).*

No abstracts in this category.

# 15 LAUNCH VEHICLES AND SPACE VEHICLES

Includes boosters; operating problems of launch/space vehicle systems; and reusable vehicles.

For related information see also *20 Spacecraft Propulsion and Power.*

**N88-13369*#** National Aeronautics and Space Administration. Langley Research Center, Hampton, Va.
**DESIGN AND ASSEMBLY SEQUENCE ANALYSIS OF OPTION 3 FOR CETF REFERENCE SPACE STATION**
L. Bernard Garrett, Gregory C. Andersen, John B. Hall, Jr., Cheryl L. Allen, A. D. Scott, Jr., and Kenneth T. So (Rockwell International Corp., Downey, Calif.) Nov. 1987 83 p
(NASA-TM-100503; NAS 1.15:100503) Avail: NTIS HC A05/MF A01 CSCL 22B

A design and assembly sequence was conducted on one option of the Dual Keel Space Station examined by a NASA Critical Evaluation Task Force to establish viability of several variations of that option. A goal of the study was to produce and analyze technical data to support Task Force decisions to either examine particular Option 3 variations in more depth or eliminate them from further consideration. An analysis of the phasing assembly showed that use of an Expendable Launch Vehicle in conjunction with the Space Transportation System (STS) can accelerate the buildup of the Station and ease the STS launch rate constraints. The study also showed that use of an Orbital Maneuvering Vehicle on the first flight can significantly benefit Station assembly and, by performing Station subsystem functions, can alleviate the need for operational control and reboost systems during the early flights. In addition to launch and assembly sequencing, the study assessed stability and control, and analyzed node-packaging options and the effects of keel removal on the structural dynamics of the Station. Results of these analyses are presented and discussed.
Author

**N88-13370*#** National Aeronautics and Space Administration. Goddard Space Flight Center, Greenbelt, Md.
**COSPAS-SARSAT SATELLITE ORBIT PREDICTOR, VOLUME 10 Technical Memorandum, Apr. - Oct. 1987**
Morton L. Friedman Oct. 1987 108 p
(NASA-TM-85015; Rept-87B0289; NAS 1.15:85015) Avail: NTIS HC A06/MF A01 CSCL 22A

The satellite orbit predictor is a graphical aid for determining the relationship between the satellite (SARSAT or COSPAS) orbit, antenna coverage of the spacecraft and coverage of the local user terminals (LUT's). The predictor allows the user to quickly visualize if a selected position will probably be detected and is composed of a base map and a satellite track overlay for each satellite. This volume contains a table of equator crossings for each satellite covering the period from October 16, 1987 to April 15, 1988. M.G.

# 16 SPACE TRANSPORTATION

Includes passenger and cargo space transportation, e.g., shuttle operations; and space rescue techniques.

For related information see also *03 Air Transportation and Safety* and *18 Spacecraft Design, Testing and Performance*. For space suits see *54 Man/System Technology and Life Support*.

No abstracts in this category.

# 17 SPACE COMM., SPACECRAFT COMM., COMMAND & TRACKING

Includes telemetry; space communications networks; astronavigation and guidance; and radio blackout.

For related information see also *04 Aircraft Communications and Navigation* and *32 Communications and Radar*.

**N88-13371*#** National Aeronautics and Space Administration. Goddard Space Flight Center, Greenbelt, Md.
**A COMPUTER CODE TO PROCESS AND PLOT LASER ALTIMETRY DATA INTERACTIVELY ON A MICROCOMPUTER**
H. G. Safren and J. L. Bufton May 1987 48 p
(NASA-TM-100687; NAS 1.15:100687; 86B0419) Avail: NTIS HC A03/MF A01 CSCL 09F

A computer program, written in FORTRAN, is described which uses a microcomputer to interactively process and plot laser altimetry data taken with a laser altimeter currently under development at the Goddard Space Flight Center. The program uses a plot routine written for a particular microcomputer, so that the program could only be implemented on a different computer by replacing the plot routine. The altimetry data are taken from an aircraft flying over mountainous terrain. The program unpacks the raw data, processes it into along-track distance and ground height and creates plots of the terrain profile. A zoom capability is provided to expand the plot to show greater detail, along either axis, and provision is made to interactively edit out spurious data points. Author

**N88-13372*#** National Aeronautics and Space Administration. Goddard Space Flight Center, Greenbelt, Md.
**A COMPUTER CODE TO CALCULATE LINE BY LINE ATMOSPHERIC TRANSMISSION SPECTRA ON A MICROCOMPUTER**
H. G. Safren Jul. 1987 75 p
(NASA-TM-100686; Rept-86B0201; NAS 1.15:100686) Avail: NTIS HC A04/MF A01 CSCL 09F

A computer program is described which calculates line by line atmospheric transmission spectra on a microcomputer. Radiance calculations are not included. The program is written in FORTRAN and could be modified to run on a microcomputer other than the one on which it was implemented, except that the plotting routine would have to be replaced. The program is based on the 1978 Air Force Geophysics Laboratory LASER routine, and uses absorption line data from the 1982 update of the AFGL Atmospheric Absorption Line Parameters Compilation; segments of needed line data are taken from the tape, preprocessed into the form used by the program and stored on floppy disks. The program calculates transmission spectra over a variety of paths and spanning an arbitrarily chosen wavelength or frequency range; the path may be chosen to be horizontal, vertical or slanted at any zenith angle, and may extend between any two altitudes between 0 and 15 km. Aerosol effects are included, presently based on the 1976 Shettle and Fenn models, plus some molecular continuum effects and Rayleigh scattering. Author

**N88-13373#** Sandia National Labs., Albuquerque, N. Mex.
**NEW APPROACH TO TELEMETRY DEVELOPMENT WILL SIGNIFICANTLY INCREASE PRODUCTIVITY OF JOINT TEST ASSEMBLY (JTA) TEAMS**
K. T. Gee 27 Oct. 1987 10 p Presented at the International Telemetering Conference, San Diego, Calif., 27 Oct. 1987
(Contract DE-AC04-76DP-00789)
(DE88-001676; SAND-87-2623C; CONF-8710171-1) Avail: NTIS HC A02/MF A01

We design telemetry systems which instrument weapons in the Joint DoD/DOE flight test program. These telemetry systems gather data which can be used to determine if a weapon system functioned as intended. A reusable telemetry electronics system to support new programs for the next decade and to replace old telemetry systems which can no longer be produced is being designed. This multisystem Joint Test Assembly, named JTAX, is being designed to be modular, flexible, and testable. The requirements for each program can be met by choosing the necessary circuitry from a list of off-the-shelf, flexible electronics modules. Present day electronics miniaturization will allow these modules to consist of a few integrated circuits. System-specific circuits can be added to the architecture via well-defined interfaces. Off-the-shelf and system-specific circuitry are connected on printed circuit boards which are designed to meet the unique mechanical constraints for each system. DOE

# 18 SPACECRAFT DESIGN, TESTING AND PERFORMANCE

Includes satellites; space platforms; space stations; spacecraft systems and components such as thermal and environmental controls; and attitude controls.

For life support systems see *54 Man/System Technology and Life Support*. For related information see also *05 Aircraft Design, Testing and Performance, 39 Structural Mechanics,* and *16 Space Transportation*.

**N88-13374*#** Massachusetts Inst. of Tech., Cambridge.
**SURVEY ON LARGE SCALE SYSTEM CONTROL METHODS**
Mathieu Mercadal [1987] 20 p
(Grant NAG1-126)
(NASA-CR-181556; NAS 1.26:181556) Avail: NTIS HC A03/MF A01 CSCL 22B

The problem inherent to large scale systems such as power network, communication network and economic or ecological systems were studied. The increase in size and flexibility of future spacecraft has put those dynamical systems into the category of large scale systems, and tools specific to the class of large systems are being sought to design control systems that can guarantee more stability and better performance. Among several survey papers, reference was found to a thorough investigation on decentralized control methods. Especially helpful was the classification made of the different existing approaches to deal with large scale systems. A very similar classification is used, even though the papers surveyed are somehow different from the ones reviewed in other papers. Special attention is brought to the

applicability of the existing methods to controlling large mechanical systems like large space structures. Some recent developments are added to this survey. Author

**N88-13375#** RADEX, Inc., Carlisle, Mass.
**ANALYSIS OF GEOPHYSICAL DATA BASES AND MODELS FOR SPACECRAFT INTERACTIONS Final Technical Report, Aug. 1983 - Oct. 1986**
J. N. Bass, N. A. Bonito, K. G. Cottrell, R. J. Eckhardt, and W. J. McNeil 31 Oct. 1986 276 p
(Contract F19628-83-C-0105)
(AD-A184809; AFGL-TR-86-0221) Avail: NTIS HC A13/MF A01 CSCL 04A

This contract supported on-going as well as planned research into environments and spacecraft interactions in near space. The major projects are summarized. Models and geophysical data bases were investigated for spacecraft charging, shuttle contamination, electrostatic particle pushing codes, beam-plasma interaction in emitting probes, and magnetospheric dynamics. Adiabatic invariance of trapped particles, fluxgate magnetometer simulation and falling sphere accelerometers. In support of the CRRES project, a data management plan has been provided, and a graphics capability developed for the SPAN network. Software development was involved in all phases, using CYBER, VAX and RIDGE computers. GRA

**N88-13376#** Illinois Univ., Urbana. Decision and Control Lab.
**DESIGN OF LOW ORDER CONTROLLERS FOR ROBUST DISTURBANCE REJECTION IN LARGE SPACE STRUCTURES M.S. Thesis**
Russell A. Ramaker Sep. 1987 67 p
(Contract N00014-84-C-0149)
(AD-A185202; DC-97; UILU-ENG-87-2260) Avail: NTIS HC A04/MF A01 CSCL 09A

This thesis will investigate several issues relating to the objective of improving the disturbance rejection of a Large Space Structure (LSS) type system. Due to properties of LSS systems, the design of the controller must address three main issues: 1) improving of the disturbance rejection properties of the system; 2) insuring that the controller is robust to modeling uncertainty; and 3) implementing the design as a low order output feedback controller. The disturbance rejection of the system will be quantified using the H-norm. An arbitrary level of disturbance rejection will then be achieved through a Linear Quadratic (LQ) minimization. This LQ solution produces a state feedback controller which is robust to modeling uncertainty. In order to realize this design, a low order output feedback controller will be designed based on the LQ solution using projective controls. The method described in this thesis will then be applied to a 40th order LSS example. Using a decentralized approach, a controller.will be designed which satisfies the issues discussed above. GRA

**N88-13377#** Stanford Univ., Calif. Dept. of Aeronautics and Astronautics.
**MODELING AND CONTROL OF LARGE FLEXIBLE VEHICLES IN THE ATMOSPHERE AND SPACE Final Report, 15 Dec. 1981 - 14 Dec. 1986**
Holt Ashley 15 Jun. 1987 8 p
(Contracts AF-AFOSR-82-0062; AF Proj. 2302)
(AD-A185368; AFOSR-87-1171TR) Avail: NTIS HC A02/MF A01 CSCL 20K

Summary of major research findings in three topical areas: 1) traveling wave concepts in the dynamics and control of Large Space Structures, 2) passive damping in Large Space Structures Applications, and 3) active control of rigid and flexible Manipulator Arms. The traveling wave concepts for characterizing the dynamics of flexible structures have introduced an alternative to modal synthesis and established a basis for the development of new controls algorithms. Passive damping studies identified various types of damping mechanisms including thermoelastic, and electromagnetic, and quantified their relative contributions. The active control studies generated a number of algorithms and control strategies and demonstration applications. GRA

**N88-13378#** Consiglio Nazionale delle Ricerche, Frascati (Italy). Ist. di Fisica dello Spazio Interplanetario.
**RESEARCH ON ELECTRODYNAMIC TETHER EFFECTS (RETE) EXPERIMENT ELECTRICAL GROUND SUPPORT EQUIPMENT (EGSE)**
U. Guidoni and M. Maggi Jan. 1987 26 p
(IFSI-87-2; ETN-88-91289) Avail: NTIS HC A03/MF A01

The hardware, software, and test procedures of the Electrical Ground Support Equipment (EGSE) to simulate the interfaces of the Orbiter with the tethered satellite and to perform functional tests and data display are described. The main requirement is the possibility to utilize the EGSE, with slight changes, during the subsequent phases of experiment integration and during the Shuttle mission. The EGSE is needed to integrate three experiment subsystems: an ac package to measure three orthogonal components of the electrical field (from 170 Hz to 12 MHz) and 2 orthogonal components of the magnetic field (from 170 Hz to 450 KHz); a dc package which performs Langmuir probe measurements to determine the local plasma characteristic, including the local plasma potential; and a data processing unit for data acquisition and control of interfaces with satellite telemetry. ESA

**N88-13379#** Consiglio Nazionale delle Ricerche, Frascati (Italy). Ist. di Fisica dello Spazio Interplanetario.
**MECHANICAL DESIGN OF THE AC BRACKET PACKAGE FOR THE RETE EXPERIMENT [PROGETTO MECCANICO DELLA UNITA' ACBP PER L'ESPERIMENTO RETE]**
P. Baldetti and M. Candidi Feb. 1987 28 p In ITALIAN
(IFSI-87-4; ETN-88-91291) Avail: NTIS HC A03/MF A01

An element placed at the extremity of the TSSS satellite arm to explore the structure of the zone around the satellite was designed. The unit includes the search coil and electric antennas subsystems. The design specifications and the detailed mechanical design are presented. ESA

**N88-13380#** Consiglio Nazionale delle Ricerche, Frascati (Italy). Ist. di Fisica dello Spazio Interplanetario.
**RETE EXPERIMENT ASSEMBLY, INTEGRATION, AND VERIFICATION (AIV) ACTIVITIES**
U. Guidoni and M. Candidi May 1987 64 p
(IFSI-87-6; ETN-88-91293) Avail: NTIS HC A04/MF A01

The hardware configurations for testing the Research on Electrodynamic Tether Effects experiment at satellite level, and the test sequences adopted at different test levels are outlined. The mechanical and electrical ground support equipment is described. ESA

**N88-13381#** Sandia National Labs., Albuquerque, N. Mex.
**THE EFFECT OF MAXIMUM-ALLOWABLE PAYLOAD TEMPERATURE ON THE MASS OF A MULTIMEGAWATT SPACE-BASED PLATFORM**
D. Dobranich Aug. 1987 48 p
(Contract DE-AC04-76DP-00789)
(DE88-001921; SAND-87-1449) Avail: NTIS HC A03/MF A01

Calculations were performed to determine the mass of a space-based platform as a function of the maximum-allowed operating temperature of the electrical equipment within the platform payload. Two computer programs were used in conjunction to perform these calculations. The first program was used to determine the mass of the platform reactor, shield, and power conversion system. The second program was used to determine the mass of the main and secondary radiators of the platform. The main radiator removes the waste heat associated with the power conversion system and the secondary radiator removes the waste heat associated with the platform payload. These calculations were performed for both Brayton and Rankine cycle platforms with two different types of payload cooling systems: a pumped-loop system (a heat exchanger with a liquid coolant) and a refrigerator system. The results indicate that increases in the maximum-allowed payload temperature offer significant platform mass savings for both the Brayton and Rankine cycle platforms with either the pumped-loop or refrigerator payload cooling systems.

Therefore, with respect to platform mass, the development of high temperature electrical equipment would be advantageous. DOE

**N88-13382*** National Aeronautics and Space Administration, Washington, D.C.
**SPACE STATION SYSTEMS: A BIBLIOGRAPHY WITH INDEXES**
Nov. 1987 245 p
(NASA-SP-7056(05); NAS 1.21:7056(05)) Avail: NTIS HC A11 CSCL 22B

This bibliography lists 967 reports, articles, and other documents introduced into the NASA scientific and technical information system between January 1, 1987 and June 30, 1987. Its purpose is to provide helpful information to the researcher, manager, and designer in technology development and mission design according to system, interactive analysis and design, structural and thermal analysis and design, structural concepts and control systems, electronics, advanced materials, assembly concepts, propulsion, and solar power satellite systems. The coverage includes documents that define major systems and subsystems, servicing and support requirements, procedures and operations, and missions for the current and future space station. Author

# 19 SPACECRAFT INSTRUMENTATION

For related information see also *06 Aircraft Instrumentation* and *35 Instrumentation and Photography.*

No abstracts in this category.

# 20 SPACECRAFT PROPULSION AND POWER

Includes main propulsion systems and components, e.g., rocket engines; and spacecraft auxilliary power sources.

For related information see also *07 Aircraft Propulsion and Power, 28 Propellants and Fuels, 44 Energy Production and Conversion,* and *15 Launch Vehicles and Space Vehicles.*

**N88-13383#** Messerschmitt-Boelkow-Blohm G.m.b.H., Munich (West Germany). Space Systems Group.
**HERMES PROPULSION SYSTEM**
Hans Immich, Helmut Hopmann, and Thierry Caussin (Societe Nationale Industrielle Aerospatiale, Les Mureaux, France ) Paris, France SNIAS 1987 17 p
(SNIAS-872-422-109; ETN-88-91210) Avail: NTIS HC A03/MF A01

The initial baseline concept of the storable bipropellant propulsion system of the Hermes spaceplane is discussed. The general architecture of the propulsion system is shown. The design features of the engines of the main propulsion system and of the thrusters of the auxiliary propulsion system are demonstrated. Operational requirements as safety, reliability, life, and maintainability are discussed. The initial baseline flow scheme of the Hermes propulsion system is described. The main propulsion system consists of 2 reusable pressure fed rocket engines with a nominal steady state thrust of 20 kN per engine in vacuum. An auxiliary system provides thrust for attitude maneuvers and small velocity changes along the vehicle axis. It consists of 28 thrusters (10 to 400 N) distributed forward and aft. ESA

**N88-13384*#** Calspan-Buffalo Univ. Research Center, N.Y.
**DEVELOPMENT OF AN INTEGRATED BEM APPROACH FOR HOT FLUID STRUCTURE INTERACTION Annual Report, Nov. 1986 - Nov. 1987**
Gary F. Dargush, Prasanta K. Banerjee (State Univ. of New York, Buffalo.), and Michael G. Dunn 13 Jan. 1988 96 p Original document contains color illustrations
(Grant NAG7-12)
(NASA-CR-181577; NAS 1.26:181577) Avail: NTIS HC A05/MF A01 CSCL 21H

Significant progress was made toward the goal of developing a general purpose boundary element method for hot fluid-structure interaction. For the solid phase, a boundary-only formulation was developed and implemented for uncoupled transient thermoelasticity in two dimensions. The elimination of volume discretization not only drastically reduces required modeling effort, but also permits uncontrained variation of the through-the-thickness temperature distribution. Meanwhile, for the fluids, fundamental solutions were derived for transient incompressible and compressible flow in the absence of the convective terms. Boundary element formulations were developed and described. For the incompressible case, the necessary kernal functions, under transient and steady-state conditions were derived and fully implemented into a general purpose, multi-region boundary element code. Several examples were examined to study the suitability and convergence characteristics of the various algorithms. Author

**N88-13617*#** Structural Dynamics Research Corp., San Diego, Calif.
**MODAL SURVEY OF THE SPACE SHUTTLE SOLID ROCKET MOTOR USING MULTIPLE INPUT METHODS**
Ralph Brillhart, David L. Hunt, Brent M. Jensen, and Donald R. Mason (Morton Thiokol, Brigham City, Utah.) *In* NASA-Marshall Space Flight Center, The 58th Shock and Vibration Symposium, Volume 1 Oct. 1987 p 155-167 (For primary document see N88-13609 05-39)
Avail: NTIS HC A21/MF A01 CSCL 21H

**N88-13630*#** National Aeronautics and Space Administration. Marshall Space Flight Center, Huntsville, Ala.
**HIGH FREQUENCY DATA ACQUISITION SYSTEM FOR SPACE SHUTTLE MAIN ENGINE TESTING**
Pat Lewallen *In its* The 58th Shock and Vibration Symposium, Volume 1 Oct. 1987 p 349-352 (For primary document see N88-13609 05-39)
Avail: NTIS HC A21/MF A01 CSCL 21H

**N88-13631*#** National Aeronautics and Space Administration. Marshall Space Flight Center, Huntsville, Ala.
**SPACE SHUTTLE MAIN ENGINE VIBRATION DATA BASE**
Pat Lewallen *In its* The 58th Shock and Vibration Symposium, Volume 1 Oct. 1987 p 353-359 (For primary document see N88-13609 05-39)
Avail: NTIS HC A21/MF A01 CSCL 21H

# 23 CHEMISTRY AND MATERIALS (GENERAL)

**N88-13385*#** National Aeronautics and Space Administration. Lewis Research Center, Cleveland, Ohio.
**PHASE PURITY OF NiCo2O4, A CATALYST CANDIDATE FOR ELECTROLYSIS OF WATER**
J. Singer, W. L. Fielder, R. G. Garlick, and T. Negas (Trans Tech, Frederick, Md.) Dec. 1987 11 p
(NASA-TM-100239; E-3754; NAS 1.15:100239) Avail: NTIS HC A03/MF A01 CSCL 07A

NiCo2O4 is shown to be difficult to obtain as a pure phase, and may never have been so obtained. High resolution x-ray diffractometry is required for its precise characterization. Film XRD is not likely to show the asymmetry in the spinel diffraction lines, caused by poorly crystallized NiO, as seen in diffractometer traces. The Co3O4 which is expected to accompany NiO as an impurity in NiCo2O4 syntheses has the same diffraction pattern as the binary oxide. Firings of the co-precipitated hydroxides at 300, 350, and 400 C, including one in pure O2, failed to produce single

phase cobaltate. Scanning electron microscopy showed all the sintered products to range over several orders of magnitude in agglomerate/particle size. Surface areas by BET were all in the range 40 to 110 m sq/g, equivalent to particles of 200 to 100 Angstrom diameter. The spinel diffraction line breadths were compatible with those approximate dimensions. Author

**N88-13386#** Duke Univ., Durham, N. C.
**STUDIES ON SYNTHESES OF AMINE-CARBOXYBORANES (BORON ANALOGUES OF AMINO ACIDS) AND DERIVATIVES Final Report, 1 Sep. 1983 - 31 May 1987**
Bernard F. Spielvogel and Andrew T. McPhail 17 Aug. 1987 5 p
(Contract DAAG29-79-D-1001)
(AD-A184838; ARO-20852.10-CH) Avail: NTIS HC A02/MF A01 CSCL 07C

The principal goal of this research has been the synthesis and characterization of boron analogs of important biologically active molecules such as the amino acids. During this period of research synthesis were developed for esters and amides of a variety of simple boron analogs of amino acids. Also, routes to boron analogs of choline, acetylcholine and substituted acetylcholines were developed. Collaborative studies on the biological activity of many of these compounds were carried out at the University of North Carolina. GRA

# 24 COMPOSITE MATERIALS

Includes physical, chemical, and mechanical properties of laminates and other composite materials.
For ceramic materials see *27 Nonmetallic Materials*.

**N88-13387*#** National Aeronautics and Space Administration. Langley Research Center, Hampton, Va.
**AN ANALYTICAL STUDY OF THE EFFECTS OF TRANSVERSE SHEAR DEFORMATION AND ANISOTROPY ON BUCKLING LOADS OF LAMINATED CYLINDERS M.S. Thesis - George Washington Univ.**
Dawn C. Jegley Oct. 1987 90 p
(NASA-TM-100508; NAS 1.15:100508) Avail: NTIS HC A05/MF A01 CSCL 11D

Buckling loads of thick-walled orthotropic and anisotropic simply supported circular cylinders are predicted using a higher-order transverse-shear deformation theory. A comparison of buckling loads predicted by the conventional first-order transverse-shear deformation theory and the higher-order theory show that the additional allowance for transverse shear deformation has a negligible effect on the predicted buckling loads of medium-thick metallic isotropic cylinders. However, the higher-order theory predicts buckling loads which are significantly lower than those predicted by the first-order transverse-shear deformation theory for certain short, thick-walled cylinders which have low through-the-thickness shear moduli. A parametric study of the effects of ply orientation on the buckling load of axially compressed cylinders indicates that laminates containing 45 degree plies are most sensitive to transverse-shear deformation effects. Interaction curves for buckling loads of cylinders subjected to axial compressive and external pressure loadings indicate that buckling loads due to external pressure loadings are as sensitive to transverse-shear deformation effects as buckling loads due to axial compressive loadings. The effects of anisotropy are important over a much wider range of cylinder geometries than the effects of transverse shear deformation. Author

**N88-13388*#** National Aeronautics and Space Administration. Langley Research Center, Hampton, Va.
**POTENTIAL FOR ON-ORBIT MANUFACTURE OF LARGE SPACE STRUCTURES USING THE PULTRUSION PROCESS**
Maywood L. Wilson, Ian O. MacConochie, and Gary S. Johnson Dec. 1987 20 p Presented at the 46th Conference of Society of Allied Weight Engineers, Inc., Seattle, Wash., 18-20 May 1987
(NASA-TM-4016; L-16356; NAS 1.15:4016; SAWE-Paper-1763)
Avail: NTIS HC A03/MF A01 CSCL 11D

On-orbit manufacture of lightweight, high-strength, advanced-composite structures using the pultrusion process is proposed. This process is adaptable to a zero-gravity environment by using preim-pregnated graphite-fiber reinforcement systems. The reinforcement material is preimpregnated with a high-performance thermoplastic resin at a ground station, is coiled on spools for compact storage, and is transported into Earth orbit. A pultrusion machine is installed in the Shuttle cargo bay from which very long lengths of the desired structure is fabricated on-orbit. Potential structural profiles include rods, angles, channels, hat sections, tubes, honeycomb-cored panels, and T, H, and I beams. A potential pultrudable thermoplastic/graphite composite material is presented as a model for determining the effect on Earth-to-orbit package density of an on-orbit manufacture, the package density is increased by 132 percent, and payload volume requirement is decreased by 56.3 percent. The fabrication method has the potential for on-orbit manufacture of structural members for space platforms, large space antennas, and long tethers. Author

**N88-13389*#** Rensselaer Polytechnic Inst., Troy, N.Y. Dept. of Materials Engineering.
**IMPROVED HIGH MODULUS FIBERS Final Report**
George S. Ansell, Shih-Huei Chen, R. Judd Diefendorf, and Chul-Min Kim Dec. 1987 113 p
(Grant NsG-1510)
(NASA-CR-181539; NAS 1.26:181539) Avail: NTIS HC A06/MF A01 CSCL 11D

The purpose of this investigation was to find ways of reducing the electrical conductivity of carbon fibers without diminishing fiber strength or stiffness, or greatly increasing fiber weight. Polyacrylonitrile (PAN)-based carbon fibers are studied, while pitch-based carbon fibers are only discussed briefly. Two methods of reducing electrical conductivity were investigated. One technique is to put high resistance boron carbide (BN) coatings on carbon fibers. The second method was to reduce the temperature of the stabilization step by performing the stabilization process in a nonoxidizing atmosphere. Author

**N88-13390#** MSNW, Inc., San Marcos, Calif.
**PLASMA JOINING OF METAL MATRIX COMPOSITES Interim Technical Report, Oct. 1986 - Jan. 1987**
G. H. Reynolds and L. Yang Jun. 1987 12 p
(Contract DAAG29-85-C-0027)
(AD-A184828; ARO-22817.6-MS-S) Avail: NTIS HC A02/MF A01 CSCL 11D

Microstructural and microchemical changes occurring in the heat affected zone, at the fusion line, and in the weld metal of low pressure, transferred arc plasma process welds produced with composite powder filler metals are described. GRA

**N88-13391#** National Bureau of Standards, Gaithersburg, Md. Polymers Div.
**IN-SITU CHARACTERIZATION OF THE INTERFACE OF GLASS REINFORCED COMPOSITES Final Report, 25 Dec. 1983 - 24 Dec. 1987**
F. W. Wang and B. M. Fanconi Jun. 1987 63 p
(Contracts MIPR-ARO-111-84; MIPR-ARO-113-85; MIPR-ARO-145-86)
(AD-A185136; NBSIR-87-3581; ARO-21023.4-MS) Avail: NTIS HC A04/MF A01 CSCL 11D

A technique has been developed to monitor the viscosity of curing epoxies. Fluorescence spectroscopy of viscosity-sensitive organic dyes is used together with optic fibers as a means of delivering the probing light to the measurement site and retrieving the modulated light for detection. The technique is adaptable to remote sensing through the use of optic fibers. The evanescent wave of the guided radiation is used to excite probe molecules lying at the interface between the fiber and surrounding matrix. Therefore, the technique is adaptable to in-situ characterization of the interface of glass reinforced composites. GRA

**N88-13392#** Southwest Research Inst., Houston, Tex.
**MICROMECHANISMS OF FATIGUE CRACK GROWTH AND FRACTURE TOUGHNESS IN METAL MATRIX COMPOSITES Technical Report, 29 Apr. 1986 - 31 Jul. 1987**
David L. Davidson Aug. 1987 29 p
(Contract N00014-85-C-0206)
(AD-A185200; SWRI-06-8602) Avail: NTIS HC A03/MF A01 CSCL 11D

Fatigue crack growth and fracture toughness of seven combinations of aluminum matrix alloys reinforced with particulate silicon carbide have been measured. The matrix alloys used were of both the work hardening and heat treatable varieties. Two of the alloys were made by mechanical alloying--powder metallurgy fabrication methods and the remainder were made by ingot metallurgy. Composites were tested in both as-received (extruded) and peakaged conditions. Fractography was done for all the composites, as were cross sections to examine surface roughness. GRA

**N88-13393** British Petroleum Co. Ltd., Sunbury-on-Thames (England).
**CORE MATERIAL Patent Application**
Philip John Turton, inventor 8 Oct. 1986 16 p Filed 4 Apr. 1986 Priority 4 Apr. 1985 GB 8508965
(EP-Patent-0-196-926-A2; EP-Patent-Appl-SN-86302494.9; Int-Patent-Class-E04C-2/22; Int-Patent-Class-E04C-5/07; ETN-88-90723) Avail: UK Patent Office, 25 Southampton Buildings, London WC2A 1AY, United Kingdom

A machine for fabricating a honeycomb core material of resinated filaments was designed. It has a frame with attachment points for filaments arranged linearly and a number of rods spaced apart and substantially parallel to the attachment points. The rods have one or more holes capable of receiving a filament, and the rods are capable of displacement parallel to the plane of the attachment points. There is also a filament supply for passing filament from the attachment points via the rods, and a set of formers having pins capable of being located between the separated filaments following displacement by the rods. By operation of the machine and successive insertion of former, a shaped openwork structure of resinated filaments may be fabricated and which may be cured to produce the core material. ESA

**N88-13394#** Saint-Gobain Recherche, Aubervilliers (France).
**COMPOSITE MATERIALS WITH GLASS MATRIX Final Report [MATERIAUX COMPOSITES A MATRICE VERRE]**
S. Vignesoult Oct. 1986 31 p In FRENCH
(Contract DRET-85-338)
(SGR/PR-4305/86-SV/JC; Study-2512-A; ETN-88-91166)
Copyright Avail: NTIS HC A03/MF A01

Unidirectional glass matrix or vitroceramic matrix composites were produced and tested. The composites were implemented with SiC Nicalon fibers and were manufactured by hot pressing. Good mechanical properties are obtained at room temperature: 600 to 800 MPa breaking strength, 100 to 120 GPa modulus. A degradation of mechanical properties is observed at higher temperatures. A fiber-matrix interaction is suggested. ESA

**N88-13395#** Office National d'Etudes et de Recherches Aerospatiales, Paris (France). Direction Scientifique de la Resistance des Structures.
**MODELS FOR THE DEGRADATION OF STRATIFIED COMPOSITE STRUCTURES Final Report [MODELES DE DEGRADATION DE STRUCTURES COMPOSITES STRATIFIEES]**
D. GillettadeStJoseph Jan. 1987 57 p In FRENCH
(Contract DRET-86-34-001-26)
(ONERA-RT-13/3542-RY-061-R; ETN-88-91179) Avail: NTIS HC A04/MF A01

Two macroscopic degradation models, where the layers are assumed to be homogeneous are described. In the first model each layer presents a linear behavior up to the degradation threshold. In the second model there are damage variables in the layer behavior laws. The results show that the introduction of damage variables leads to a good overall description of the breaking of composite structures. ESA

**N88-13396#** Societe Nationale Industrielle Aerospatiale, Toulouse (France).
**A HYBRID FIBREGLASS-CFRP CLOTH FOR NEW FURNISHINGS**
M. J. Frustie 1987 9 p
(SNIAS-872-111-109; ETN-88-91191) Avail: NTIS HC A02/MF A01

A glass fiber CFRP hybrid was chosen to replace aramid for aircraft cabin furnishings to comply with FAR 25 amendement 61 and FAR 121 amendement 189 concerning heat release. The material has the same weight as 181 style aramids (175 g/sqm) but the use of the carbon fiber glass hybrid with thin fiber glass plies eliminates local reinforcements on parts to obtain a weight slightly lower than obtained with aramid. Mechanical performance is a good as aramid, and production is simpler. ESA

**N88-13397#** Societe Nationale Industrielle Aerospatiale, Toulouse (France). Div. Avions.
**SURFACE TREATMENT PROBLEMS FOUND IN NEW AIRCRAFT DESIGNED USING STRUCTURAL COMPOSITES [PROBLEMES DE TRAITEMENTS DE SURFACE RENCONTRES SUR LES MATERIAUX COMPOSITES STRUCTURAUX DANS LES NOUVEAUX AVIONS]**
G. Hellard 1987 12 p In FRENCH Presented at the 6th Journees Internationales d'Etude sur les Traitements de Surfaces dans l'Industrie Aeronautique et Spatiale
(SNIAS-872-111-113; ETN-88-91194) Avail: NTIS HC A03/MF A01

Problems found in designing aircraft with organic matrix composite materials are presented. The main categories of problems include erosion, lightning, airtightness, and painting. The problems vary with the type of composites and must be treated at the beginning of the aircraft design. ESA

**N88-13398#** Societe Nationale Industrielle Aerospatiale, Les Mureaux (France). Div. Systemes Balistiques et Spatiaux.
**DETERMINATION OF THE FIBER RATIO IN CARBON FIBER/RESIN COMPOSITES BY MEANS OF IMAGE ANALYSIS [MESURE DU TAUX DE FIBRES DES MATERIAUX COMPOSITES FIBRES DE CARBONE: RESINE PAR ANALYSE D'IMAGES]**
Jacques Francois Peltier 1987 17 p In FRENCH
(SNIAS-872-422-101; ETN-88-91202) Avail: NTIS HC A03/MF A01

An image anlysis system was programmed to measure the carbon fiber to resin ratios. The computer program takes into consideration the reflectance variations due to changes in fiber orientation at the polished measurement plane. The results are comparable to those obtained by means of acid attack, except for fibers sensitive to oxidation. ESA

**N88-13399#** Societe Nationale Industrielle Aerospatiale, Les Mureaux (France). Lab. Materiaux et Technologies.
**INFLUENCE OF BONDING SHOP MOISTURE ON METAL-HONEYCOMB JUNCTIONS BONDED WITH ULTRA-THIN ADHESIVE FILMS [INFLUENCE DE L'HYGROMETRIE DES SALLES D'ENCOLLAGE SUR LA QUALITE DES LIAISONS METAL-NIDA COLLEES AVEC FILM ULTRAMINCE]**
J. Chanteranne 1987 7 p In FRENCH; ENGLISH summary Presented at the 29th Colloque of Metallurgy of INSTN
(SNIAS-872-422-112; ETN-88-91212) Avail: NTIS HC A02/MF A01

The optimization of the bonded structure junctions of the Intelsat satellites by the use of an adhesive of very low surface mass (100 g/sqm) for bonding of honeycomb is described. Redux 312 UL' films were tested and a strong influence of the bonding shop moisture is demonstrated, as well as the influence of a primer surface treatment on the geometry and strength of the adhesive menisci formed at the honeycomb junctions. ESA

**N88-13400#** Societe Nationale Industrielle Aerospatiale, Saint-Medard-en-Jalles (France).
**PHILOSOPHY AND PRACTICE OF NONDESTRUCTIVE TESTS OF COMPOSITE MATERIAL STRUCTURES AT AEROSPATIALE AQUITAINE [PHILOSOPHIE ET PRATIQUE DES CND DES STRUCTURES EN MATERIAUX COMPOSITES A L'AEROSPATIALE AQUITAINE]**
C. LeFloch 1987 6 p In FRENCH Presented at the Journees sur Controle Non Destructif et Materiaux Composites, Paris, France, 7 Apr. 1987
(SNIAS-872-430-105; ETN-88-91216) Avail: NTIS HC A02/MF A01

The nondestructive test implementing the quality control procedures of an aircraft manufacturer are described. These are mainly X-ray or ultrasonic procedures. Procedures being studied or in development are discussed, including photothermic analysis, photoacoustics, acoustic microscopy, diffused X-rays, neutrongraphy, and nuclear magnetic resonance. ESA

**N88-13401#** Societe Nationale Industrielle Aerospatiale, Saint-Medard-en-Jalles (France). Div. des Systemes Strategiques et Spatiaux.
**CARBON-CARBON COMPOSITES AND AEROSPATIALE. STATE OF THE ART AND PROSPECTS**
Yves Grenie 1987 11 p
(SNIAS-872-430-108; ETN-88-91219) Avail: NTIS HC A03/MF A01

Three dimensional weaving of carbon fibers is described. Three dimensional carbon-carbon densification is outlined. Applications to reentry vehicle heat shields and rocket motor nozzles are shown. Industrial and biomedical applications are mentioned. ESA

**N88-13402#** Bordeaux 1 Univ., Talence (France). Lab. de Physique Experimentale et des Micro-ondes.
**UTILIZATION OF MICROWAVE MEASURING SYSTEMS FOR NONDESTRUCTIVE CONTROL OF COMPOSITE MATERIALS [UTILISATION DE SYSTEMES DE MESURE MICRO-ONDE POUR LE CONTROLE NON DESTRUCTIF DE RESINES ET COMPOSITES]**
Jean-Louis Miane and Jean-Francis Lacombe (Societe Nationale Industrielle Aerospatiale, Saint-Medard-en-Jalles, France ) Paris, France SNIAS 1987 10 p In FRENCH Presented at the Journee Specialisee Trimestrielle: Controle Non Destructif et Materiaux Composites, 7 Apr. 1987
(SNIAS-872-430-109; ETN-88-91220) Avail: NTIS HC A02/MF A01

Techniques applicable to composite manufacturing process control are described. The goal is to implement automation. The measuring principle is the interaction of centimeter waves (9.5 GHz) with homogeneous dielectrics (resin) or heterogeneous materials (fibers). It is shown that the impregnation rate of Kevlar/epoxy systems can be determined either by the variation of the resonant frequency in the measuring cavity or a variation of the Q coefficient. The degree of polymerization is measured by the variation in complex permittivity. Actual evaluation in real manufacturing conditions is being done. ESA

**N88-13403#** Societe Nationale Industrielle Aerospatiale, Saint-Medard-en-Jalles (France).
**MEASUREMENT AND CONTROL OF DAMAGE IN COMPOSITE MATERIALS: NONDESTRUCTIVE CONTROLS BY THERMOGRAPHY, HOLOGRAPHY, AND RADIOGRAPHY [MESURE ET SUIVI DE L'ENDOMMAGEMENT DES MATERIAUX COMPOSITES. CONTROLES NON DESTRUCTIFS PAR: THERMOGRAPHIE, HOLOGRAPHIE, RADIOGRAPHIE]**
D. Loubet 1987 39 p In FRENCH
(SNIAS-872-430-110; ETN-88-91221) Avail: NTIS HC A03/MF A01

The nondestructive quality control methods used in an aerospace manufacturing plant are discussed. These include thermography, holography, and radiography. Inspection of carbon fiber/epoxy resin composite components used in Airbus aircraft structures and the measuring system are described. ESA

**N88-13404#** Societe Nationale Industrielle Aerospatiale, Saint-Medard-en-Jalles (France).
**MECHANICS OF ANISOTROPIC MEDIA. STUDY OF THE BOUNDARY CONDITIONS [MECANIQUE DES MILIEUX ANISOTROPES. PRISE EN COMPTE DES CONDITIONS AUX LIMITES]**
J. Lamalle 1987 16 p In FRENCH
(SNIAS-872-430-112; ETN-88-91223) Avail: NTIS HC A03/MF A01

Improvements to a global stress/strain computation matrix method are presented. The method may deduce the stress at each layer and predicts the effect of temperature variation. Solutions for cases when couplings between bending strain and extension strain appaar in the global stiffness matrix are suggested. The boundary limits imposed on flat or tubular structures frequently limit strains. An example consisting of a stiffened plate is presented. ESA

**N88-13405#** Societe Nationale Industrielle Aerospatiale, Saint-Medard-en-Jalles (France). Div. Systemes Balistiques et Spatiaux.
**MICROMECHANICS OF THE DEGRADATION OF COMPOSITE MATERIALS [ASPECTS MICROMECANIQUES DE LA DEGRADATION DES MATERIAUX COMPOSITES]**
J. Lamalle 1987 34 p In FRENCH Presented at the 5th Ecole d'Hiver: Calcul des Materiaux Composites Pre-Dimensionnement
(SNIAS-872-430-113; ETN-88-91224) Avail: NTIS HC A03/MF A01

The microscopic degradation processes taking place either in the resin matrix or in the reinforcing fibers are examined in relation to the type of stress. Stress perpendicular to fibers, shear plane stress, stress parallel to fibers, and coupling of stresses with different orientations are discussed. The effects of temperature and the case of multilayer composites are also studied. ESA

**N88-13406#** Societe Nationale Industrielle Aerospatiale, Issac (France).
**THE STRUCTURES OF LARGE WOUND PROPULSION SHELLS [LES STRUCTURES DE GROS PROPULSEURS BOBINES]**
J. P. Denost 1987 21 p In FRENCH Presented at Technospace: Propulsion Spatiale: An 2000, Les Gros Propulseurs Spatiaux Europeens, Issac, France, 12 Nov. 1986
(SNIAS-872-430-118; ETN-88-91229) Avail: NTIS HC A03/MF A01

The history of development of large missile shells manufactured in composite materials by the winding technique is described. The advantages obtained passing from glass fiber to Kevlar and from Kevlar to carbon fibers is discussed. The winding machines, the operating procedures, and the nondestructive quality control techniques are described. ESA

**N88-13407#** Societe Nationale Industrielle Aerospatiale, Saint-Medard-en-Jalles (France).
**CONTRIBUTION OF ACOUSTIC ANALYSIS TO ASSESS DAMAGE IN FLUID STORAGE TANKS UNDER HIGH PRESSURE [CONTRIBUTION DE L'ANALYSE ACOUSTIQUE AU SUIVI DE L'ENDOMMAGEMENT DE RESERVOIRS DE STOCKAGE DE FLUIDE SOUS HAUTE PRESSION]**
C. LeFloch and S. Beziers 1987 6 p In FRENCH Sponsored by Ministere de la Recherche et la Technologie
(SNIAS-872-430-119; ETN-88-91230) Avail: NTIS HC A02/MF A01

Vessels manufactured using glass fiber filament winding and an inner metallic liner were tested. Acoustic emission analysis associated to a damage model discriminates between several types of damage and estimates the damage amplitude. It is also possible to estimate plastic deformation of the metallic liner. Experimental results illustrate this application of acoustic methods. ESA

**N88-13408#** Oak Ridge National Lab., Tenn.
**FABRICATION OF COMPOSITES BY CHEMICAL VAPOR DEPOSITION**

T. M. Besmann, R. A. Lowden, D. P. Stinton, and A. J. Caputo 1987 13 p Presented at the Northeast Regional Meeting of the Metallurgical Society and the Materials Research Society, Hoboken, N.J., 27 May 1987
(Contract DE-AC05-84OR-21400)
(DE87-014565; CONF-8705200-1) Avail: NTIS HC A03/MF A01

Processes for the preparation of composite bodies using chemical vapor deposition have been developed. Composites are prepared by infiltrating ceramic fiber preforms, held at elevated temperatures, with reactant gases that decompose to deposit ceramic matrix material between and around the fibers. The ORNL process is a marked improvement over those commonly in use; preforms that previously required weeks to densify now require approx 24 h. Specimens with densities up to 90% of theoretical and strengths in the range of 300 MPa have been produced. Most importantly, the materials fail noncatastrophically, exhibiting typical composite behavior. The material produced is SiC matrix in SiC (Nicalon) fibers. DOE

**N88-13409*#** National Aeronautics and Space Administration. Lewis Research Center, Cleveland, Ohio.
**FIBER COMPOSITE STRUCTURAL DURABILITY AND DAMAGE TOLERANCE: SIMPLIFIED PREDICTIVE METHODS**
Christos C. Chamis and Carol A. Ginty 1987 28 p Presented at the 2nd Symposium on Composite Materials: Fatigue and Fracture, Cincinnati, Ohio, 26 Apr. - 1 May 1987; sponsored by the American Society for Testing and Materials
(NASA-TM-100179; E-3755; NAS 1.15:100179) Avail: NTIS HC A03/MF A01 CSCL 11D

Simplified predictive methods and models (theory) to evaluate fiber/polymer-matrix composite material for determining structural durability and damage tolerance are presented and described. This theory includes equations for (1) fatigue and fracture of composites without and with defects, (2) impact resistance and residual strength after impact, (3) thermal fatigue, and (4) combined stress fatigue. Several examples are included to illustrate applications of the theory and to identify significant parameters and sensitivities. Comparisons with limited experimental data are made. Author

**N88-13639*#** Feng Chia Univ., Taichung (Taiwan). Dept. of Mechanical Engineering.
**DYNAMIC RESPONSE OF LAMINATED COMPOSITE PLATES USING A THREE-DIMENSIONAL HYBRID-STRESS FINITE-ELEMENT FORMULATION**
W. J. Liou and C. T. Sun (Florida Univ., Gainesville.) *In* NASA-Marshall Space Flight Center, The 58th Shock and Vibration Symposium, Volume 1 Oct. 1987 p 475-485 (For primary document see N88-13609 05-39)
Avail: NTIS HC A21/MF A01 CSCL 11D

**N88-13717#** Northeastern Univ., Boston, Mass. Dept. of Mechanical Engineering.
**EFFECT OF INTERFACE ON MECHANICAL PROPERTIES OF GRAPHITE/201 ALUMINUM COMPOSITES**
J. Seyyedi, H. Nayeb-Hashemi, and J. Blucher *In* Virginia Univ., Fatigue 87, Volume 3 1987 p 1333-1351 Sponsored by NSF, Army Materials and Mechanics Research Center, and the Engineering Foundation (For primary document see N88-13700 05-39)
Avail: NTIS HC A22/MF A01 CSCL 11D

# 25 INORGANIC AND PHYSICAL CHEMISTRY

Includes chemical analysis, e.g., chromatography; combustion theory; electrochemistry; and photochemistry.

For related information see also *77 Thermodynamics and Statistical Physics.*.

**N88-13410** Virginia Polytechnic Inst. and State Univ., Blacksburg.
**IGNITION AND FLAMEHOLDING IN SUPERSONIC FLOW BY INJECTION OF DISSOCIATED HYDROGEN Ph.D. Thesis**
Timothy Charles Wagner 1987 202 p
Avail: Univ. Microfilms Order No. DA8719075

The use of free radicals for ignition and flameholding in supersonic flow was investigated analytically and experimentally. An analytical investigation of the effects of adding small quantities of radicals to a stoichiometric mixture of hydrogen and air was performed using a finite-rate chemical kinetics code. The results of these calculations indicate the small additions of hydrogen atoms, oxygen atoms, nitrogen atoms, or hydroxyl radicals are effective in promoting ignition. These analytical results were qualitatively verified in a Mach 2 flow experiment using hydrogen atoms generated by a plasma torch. The supersonic combustion tests were conducted in a direct-connect mode at atmospheric pressure with either ambient temperature air or burner-heated vitiated air with total temperatures from 1200 to 4000 R. The experimental results indicate that hydrogen atoms from a low-power plasma torch provide an effective ignition and flameholding source for hydrogen-fueled Mach 2 flows at total temperatures as low as 1065 R, the lowest temperature tested. A piloted fuel injector configuration design to take maximum advantage of the hydrogen atoms from the plasma torch was conceived and fabricated. Hydrogen atoms generated by the plasma torch proved to be the most effective ignition source. The combination of hydrogen atoms and the piloted fuel injector was shown to be a very effective igniter and flameholder for scramjet operation over a simulated flight envelope. Dissert. Abstr.

**N88-13411*#** Santa Clara Univ., Calif. Dept. of Chemistry.
**ORGANIC MOLECULES ON METEORITIC SOLID SUBSTRATES Final Report, 1 Jun. 1983 - 31 Mar. 1987**
Michael A. Sweeney 8 Jan. 1988 20 p
(Contract NCC2-271)
(NASA-CR-181570; NAS 1.26:181570) Avail: NTIS HC A03/MF A01 CSCL 07D

The production of C1-C3 monocarboxylic acids from carbonaceous meteorites was investigated by the radiolysis of air-free CO2 and alkane solutions, utilizing a Cs-137 gamma-ray source. Samples were first loaded on a vacuum system, irradiated, and then analyzed by the Hewlett Packard model 5890A gas chromatograph. Moreover, the samples were irradiated with and without added ferrous iron. Author

**N88-13412#** Rochester Univ., N. Y. Dept. of Chemistry.
**REACTIONS OF PORPHYRINS IN SURFACTANT ASSEMBLIES, MICROEMULSIONS AND IN SOLUTIONS Final Report, 1 Dec. 1983 - 30 Apr. 1987**
David G. Whitten 25 Jun. 1987 3 p
(Contract DAAG29-84-K-0011)
(AD-A184797; ARO-20766.7-CH) Avail: NTIS HC A02/MF A01 CSCL 07C

ARO-sponsored research has focused on three different areas, all of which center around photochemical reactions occurring in microheterogeneous media. The first area of investigation has been of photoisomerizations and related processes occurring in spread monolayer films at the air-water interface as well as in supported multilayer assemblies. Studies in this area have demonstrated that reactivity in the spread films can be profoundly different from that occuring in solution. Moreover we have been able to investigate systematically specific factors such as the effect of film compression and the presence of various liquids such as water within or in contact with the film or assembly. A number of findings

in this area have been published and more publications will result from studies not yet completed. GRA

**N88-13413#** Cornell Univ., Ithaca, N.Y.
**TURBULENCE GENERATION IN COMBUSTION Final Report, 15 Sep. 1982 - 31 Mar. 1987**
F. C. Gouldin 22 Jul. 1987 86 p
(Contract DAAG29-82-K-0187)
(AD-A184810; ARO-18738.6-EG) Avail: NTIS HC A05/MF A01 CSCL 21B

Several research programs on turbulent flames have been pursued. The focus has been on low to moderate Reynolds number, premixed flames which are dominated by flamelet structures, i.e., the major heat releasing chemical reactions occur in thin sheets. Large density changes occur across flamelets and it is expected that these structures have an important influence on turbulence generation. The focus of the research has thus been on flamelet characteristics. GRA

**N88-13414#** Army Armament Research and Development Command, Watervliet, N. Y. Weapons Lab.
**THE ANALYSIS OF METAL FINISHING SOLUTIONS BY ION CHROMATOGRAPHY Final Technical Report, Ph.D. Thesis**
Samuel Sopok Aug. 1987 220 p
(AD-A184812; ARCCB-TR-87021) Avail: NTIS HC A10/MF A01 CSCL 11C

Ion chromatography is very effective for ionic and polar species determinations. Separation of the analytes into pure peaks simplifies detection compared to detecting the same species in the unseparated sample matrix. One of the methods provides important improvements on existing methods, while the rest provide new and improved ways to analyze metal finishing solutions. The advantages of these methods are that considerable improvements were made in the areas of: trace ion determinations in the presence of other extremely high ionic concentrations, analysis time, analyst intervention, sensitivity, automation, and multi-ion determinations while maintaining equal precision and specificity compared to traditional chemical methods now in use. GRA

**N88-13415#** SRI International Corp., Menlo Park, Calif.
**LASER PROBES OF PROPELLANT COMBUSTION CHEMISTRY Final Report, 1 Jun. 1984 - 31 May 1987**
David R. Crosley, Gregory P. Smith, and David M. Golden Aug. 1987 130 p
(Contract DAAG29-84-K-0092)
(AD-A184854; ARO-21443.7-CH) Avail: NTIS HC A07/MF A01 CSCL 21B

Laser-induced fluorescence (LIF) can be used to measure the small (diatomic and triatomic) free radicals and other transient species that are intermediates in combustion chemistry. LIF can be coupled with detailed computer models of the chemical reaction networks that incorporate a consistent set of reaction rate constants. Doing so leads to an understanding of that chemistry, of predictive value to describe the combustion under conditions difficult to probe experimentally. This report describes the development of LIF techniques, their applications to flames and laser/pyrolysis (LP) kinetics experiments, and rate constant estimation studies for detailed combustion chemistry modeling. The systems studied were those of hydrocarbons burning in nitrous oxide. These contain some of the chemical networks, individual reactions, and intermediate species present in the gas-phase combustion of nitramine propellants such as HMX and RDX. GRA

**N88-13416#** Pennsylvania State Univ., University Park. Dept. of Chemistry.
**THE FORMATION AND THERMOCHEMICAL PROPERTIES OF MULTILIGAND COMPLEXES Final Report, 1 Jul. 1984 - 30 Jun. 1987**
A. Welford Castleman, Jr. 25 Aug. 1987 31 p
(Contract DAAG29-84-K-0087)
(AD-A184935; ARO-21819.11-CH) Avail: NTIS HC A03/MF A01 CSCL 07C

This research program constituted an investigation of the reactivity and formation of ions that are clustered by molecules. Results are reported for ion-molecule reactions involving sulfides, mercaptans, and dimethyl methylphosphonate with ionic species derived from water and argon. Rate coefficients were measured and product ions identified. Results are also reported for the competitive clustering of water and methanol onto a charged center, namely the potassium cation. The thermochemical parameters for clustering up to three ligands were determined. Relationships of the gas data to properties of condensed phase binary solvent systems is also discussed. GRA

**N88-13417#** Kansas State Univ., Manhattan. Dept. of Chemistry.
**ACTIVATED METAL OXIDE SURFACES AS HIGHLY BASIC AND REDUCING ENVIRONMENTS Final Report, Apr. 1984 - Mar. 1987**
Kenneth J. Klabunde 21 May 1987 11 p
(Contract DAAG29-84-K-0051)
(AD-A184958; ARO-21367.6-CH) Avail: NTIS HC A03/MF A01 CSCL 07B

Alkaline earth oxides of high surface area were thermally activated at 400-1100C. Super base properties and electron transfer sites were generated. These materials serve as catalysts for selective deuteration of hydrocarbons, alkene isomerization, CO telomerization and reduction, carbonyl compound condensation, and as a destructive adsorbent for organophosphorus compounds and other toxic substances. Some fundamental understanding of the reactive sites involved has been gained by studying adsorbed species and by metal ion doping. Studies of single metal oxide molecules in matrices has begun. GRA

**N88-13418#** Air Force Weapons Lab., Kirtland AFB, N. Mex.
**EXTREME ULTRAVIOLET BEAM-FOIL SPECTROSCOPY OF HIGHLY IONIZED NEON AND ARGON Final Report**
John A. Demarest Jun. 1987 190 p
(AD-A185197; AFWL-TR-87-26) Avail: NTIS HC A09/MF A01 CSCL 20G

A study of the extreme ultraviolet radiation emitted by ion beams of highly ionized neon and argon after passage through thin foils was conducted at the variable energy cyclotron at Texas A&M University. A grazing incidence spectrometer was equipped with a position sensitive microchannel plate (MCP) detector which improved the detection efficiency by two orders of magnitude. The position information of the MCP was determined to be linear over 90% of the 50-mm-wide detector. Spectra spanning regions of over 100 angstroms were accumulated at a resolution of less than 1 angstroms. A wavelength calibration based on a second-order equation of spectrometer position was found to result in an accuracy of + 0.1 angstroms. GRA

**N88-13419#** Colorado State Univ., Fort Collins. Dept. of Atmospheric Science.
**ALTERED AND ENHANCED IODARGYRITE WITH BISMUTH TRIIODIDE FOR USE IN PRECIPITATION ENHANCEMENT OPERATIONS Thesis**
Paul Tilden Scott (Air Force Inst. of Tech., Wright-Patterson AFB, Ohio.) Apr. 1987 61 p Sponsored in cooperation with AF
(Contract NA85RAC-05070; Grant NSF AEO-84-20980)
(AD-A185229; CSU-ATSP-410; AFIT-CI/NR-87-64T) Avail: NTIS HC A04/MF A01 CSCL 07D

A new ice nucleant aerosol is developed from the principles of synergism. Two known ice nucleants, silver iodide (AgI) and bismuth triiodide (BiI3) are combined as 2% AgI-NH4I X mole % BiI3 NH4I in a water-acetone solution. The resultant aerosol after combustion is tested for effectiveness in the Colorado State University Isothermal Cloud Chamber (ICC), and the optimum ratio of AgI and BiI3 is determined to be 0.5 mole % BiI3. The effectiveness at this optimum ratio is an order of magnitude greater than AgI alone, although the temperature spectrum, rate, and mechanism are similar. A subsequent x-ray powder analysis identifies the optimum ratio aerosol as the iodargyrite form of AgI having the closet match to ice ever reported for a hexagonal

crystal. Unlike other mixed AgI containing aerosols the resultant aerosol maintained its hexagonal form of AgI at all mole ratios of BiI3 tested. Bismuth is at too small of a ratio to be identified through the method employed although it appears to be fully incorporated into the AgI crystal as an oxide or iodo-oxide. The plausible structure is looked at in light of epitaxial and active site theories of heterogeneous ice nucleation. GRA

**N88-13420** Technische Hogeschool, Eindhoven (Netherlands).
**COAGULATION IN STIRRED TANKS Ph.D. Thesis**
Gerben Berend Johann deBoer 1987 155 p
(B8711373; ISBN-90-71382-08-7; ETN-88-91371) Copyright Avail: Issuing Activity

The clustering process was studied through experiments on the coagulation behavior of aqueous suspensions of monodisperse polystyrene particles to induce coagulation. The average rate of shear in the tank, the volume fraction of solids, the concentration of sodium chloride, and the scale of the tank were varied. Four different stages in the coagulation process are discerned. Primary particles coagulate into doublets. The growth rate of the aggregates is accelerated due to the high collision rate of small particles with the larger aggregates, the presence of large and loose structures that entrap smaller particles and, probably, by aggregates with a chain-like structure. In stage 3 the growth rate of the aggregates decreases, because next to the growth of the smaller particles, the larger particles are disrupted by the action of turbulence. Stage 4 is characterized by a dynamic equilibrium between growth of the aggregates in the zones of high shear. ESA

**N88-13421#** Rutgers - The State Univ., Piscataway, N. J. Center for Ceramics Research.
**COLLOIDAL STABILITY OF OXIDIZED SILICON PARTICLES IN ETHANOLIC AND AQUEOUS MEDIA**
E. M. DeLiso and A. Bleier 1987 24 p Presented at the 18th Annual Meeting of the Fine Particle Society, Boston, Mass., 3 Aug. 1987 Prepared in cooperation with Oak Ridge National Lab., Tenn.
(Contract DE-AC05-84OR-21400)
(DE87-014783; CONF-8708134-1) Avail: NTIS HC A03/MF A01

This work constitutes an initial effort to understand the broad range of surface and colloidal properties exhibited by oxidized silicon powder. We conclude the following: (1) Colloidal stability of oxidized Si powder is of electrostatic origin in 0.15 M NaCl (Aq). The greatest stability exist at pH 9 owing to a sufficiently high zeta potential of -31.8 mV. A critical concentration of electrolyte exists between $10^{-3}$ M and 0.15 M NaCl (Aq) and for the high electrolyte concentration a critical value of zeta exists between -16.5 and -31.8 mV; (2) Stability in $10^{-3}$ M LiCl (ETOH) is high in the absence of KD-2 and is reduced by small additions of this material. These conditions correspond to submonolayer coverage. Adsorption of KD-2 onto oxidized Si appears to arise from the interaction of the basic amine functionality of the dispersant with the acidic oxidized silicon surface; (3) High concentrations of KD-2 reduce the destabilizing effect but do not achieve maximum stability; and (4) Comparison of estimated molecular cross-sectional areas for KD-2 suggest that monolayer coverage corresponds to only about 17% of the available surface. Furthermore, indiscriminate adsorption resulting from reduced solute-solvent interactions is not considered probable. DOE

**N88-13422#** California Univ., Berkeley. Lawrence Berkeley Lab.
**PULSED PLASMA JET IGNITERS: SPECIES MEASUREMENTS IN METHANE COMBUSTION**
J. A. Cavolowsky, P. R. Breber, A. K. Oppenheim, and D. Lucas Aug. 1987 4 p Presented at the Combustion Institute Fall Meeting, Honolulu, Hawaii, 22 Nov. 1987
(Contract DE-AC03-76SF-00098)
(DE88-001389; LBL-23515; CONF-871118-7) Avail: NTIS HC A02

We have determined the mole fractions of the chemical species present in the plume of a pulsed plasma jet igniter during the ignition and subsequent combustion of methane/oxygen/nitrogen and methane/oxygen/argon mixtures. Equivalence ratios of 1.0, 0.6, and 0.4 were used in the jet cavity and in the main combustion chamber to obtain results for both combusting and noncombusting cases. DOE

**N88-13423#** California Univ., Berkeley. Lawrence Berkeley Lab.
**FORMATION AND DESTRUCTION OF NITROUS OXIDE IN LEAN, PREMIXED COMBUSTION**
R. J. Martin and N. J. Brown Aug. 1987 4 p Presented at the Combustion Institute Fall Meeting, Honolulu, Hawaii, 22 Nov. 1987
(Contract DE-AC03-76SF-00098)
(DE88-001390; LBL-23952; CONF-871118-6) Avail: NTIS HC A02

Nitrous oxide is formed in lean CH4/air and H2/air flames doped with various nitrogen compounds, but it does not survive into the post flame region. Nitrous oxide concentration was found to depend inversely upon final flame temperature and equivalence ratio and directly upon nitrogen compound concentration. In decreasing order of observance of early-N2O, four nitrogen-containing dopants can be ranked: N2O, NH3, NO and N2. Nitrous oxide profiles were similar in CH4/air and H2/air flames. Radial profile measurements showed increased amounts of N2O existing near the burner edge. Comparison between calculated NO and N2O profiles and those measured in an H2/air flame showed that NO was satisfactorily predicted by the model, but that significant difficulties exist with the N2O kinetics. DOE

**N88-13424#** Energy and Environmental Research Corp., Irvine, Calif.
**OXYGEN ENRICHED COMBUSTION SYSTEM PERFORMANCE STUDY**
A. R. Abele, Y. Kwan, S. L. Chen, L. S. Silver, and H. Kobayashi 1987 6 p Presented at the Annual Industry and Technology Conference, College Station, Tex., 16 Sep. 1987 Prepared in cooperation with Union Carbide Corp., Tarrytown, N.Y. and Edgerton, Germeshausen and Grier, Inc., Idaho Falls, Idaho
(Contract DE-AC07-76ID-01570)
(DE88-001500; EGG-M-23387; CONF-8709166-2) Avail: NTIS HC A02

Objective of this study is to identify potential industrial applications for which oxygen enriched combustion systems are technically, environmentally and economically feasible and offer significant energy savings and/or productivity improvement, and then to verify the performance of selected systems in research furnaces. Tests of several commercial burner designs have been conducted at scales of 1 x $10^6$ Btu/h and 10 x $10^6$ Btu/h. The burners represent both conventional air fired designs and oxygen/fuel burners designed primarily for very high oxygen levels. Results of these tests indicate that over 50% fuel savings can be achieved with oxygen enrichment compared to air under certain conditions. The different burners demonstrated distinct axial wall temperature distributions which changed by varying degrees as the level of oxygen enrichment was increased. NO sub x emissions increased sharply as the level of oxygen enrichment was increased for conventional air burners up to 35 to 50% oxygen. However, specially designed oxygen/fuel burners showed very low NO sub x emissions for 35 to 100% oxygen. The absolute levels of the NO sub x emissions also depended on the furnace temperature. DOE

**N88-13425#** Clemson Univ., S.C. Dept. of Chemistry.
**INTRAMOLECULAR ENERGY TRANSFER REACTIONS AS A METHOD FOR METAL COMPLEX ASSISTED PRODUCTION OF HYDROGEN Report, 1 Dec. 1983 - Dec. 1986**
J. D. Petersen 1987 17 p
(Contract DE-AS09-80ER-10671)
(DE88-001621; DOE/ER-10671/5; CU-Rept-5) Avail: NTIS HC A03/MF A01

Research is reported on ruthenium(II) antenna fragments,

ruthenium(II) neutral complexes, iron(II) antenna systems, and biimidazolate complexes. DOE

**N88-13426#** Georgetown Univ., Washington, D.C.
**STUDY OF THE PROPERTIES OF A NEW DETECTOR CLASS FOR LIQUID CHROMATOGRAPHY Progress Report**
1987 27 p
(Contract DE-FG05-86ER-13487)
(DE88-001666; DOE/ER-13487/2) Avail: NTIS HC A03/MF A01

The principle of the evaporative light scattering detector (ELSD) detector is that of a transport detector, using a scavenger gas stream rather than a material conveyor. The effluent is nebulized immediately at the exit of the chromatographic column, in a concentric nebulizer, in a stream of warm gas. The solvent vaporizes and leaves a cloud of particles made by the non-volatile content of the eluate. This contains the solutes, as well as the non-volatile residue of the solvent. These particles are carried by the gas stream across an intense light beam. The amount of scattered light collected on a photocell or a photomultiplier is a measure of the amount of non-volatile solute in the effluent stream. A systematic study of the influence of the detector parameters on its response was undertaken, with emphasis on the nebulizer design and operation. This is of special importance in the case of the ELSD, because of some of its particular properties and because of contradictions found in the literature. DOE

**N88-13427#** Sandia National Labs., Albuquerque, N. Mex.
**SHOCK COMPRESSION OF SOLIDS AS A PHYSICAL-CHEMICAL-MECHANICAL PROCESS**
R. A. Graham 1987 8 p Presented at the 5th Topical Conference of the American Physical Society on Shockwaves in Condensed Matter, Monterey, Calif., 20 Jul. 1987
(Contract DE-AC04-76DP-00789)
(DE88-001674; SAND-87-0975C; CONF-870753-78) Avail: NTIS HC A02/MF A01

The changes introduced into solids while being processed through the abrupt stress and particle velocity transitions in the early portion of shock-compression pulses are not well described on a scientific basis, and their description presents perhaps the greatest challenge of modern shock-compression science. Over time scales from hundreds of picoseconds to hundreds of nanoseconds, solids are converted to states in which deformation is fluid-like to certain approximations. Descriptions of the transition regions have traditionally involved both physical and mechanical aspects. With recent studies of shock-induced solid state chemistry, the influence of chemical aspects must now be considered. Unfortunately, any change in chemical composition introduces substantial complications in analysis and interpretation of the shock-compression process. DOE

**N88-13428*#** National Aeronautics and Space Administration. Lewis Research Center, Cleveland, Ohio.
**DETAILED MECHANISM OF TOLUENE OXIDATION AND COMPARISON WITH BENZENE**
David A. Bittker 1988 26 p Proposed for presentation at the 22nd International Symposium on Combustion, Seattle, Wash., 14-18 Aug. 1988; sponsored by the Combustion Inst.
(NASA-TM-100261; E-3889; NAS 1.15:100261) Avail: NTIS HC A03/MF A01 CSCL 07D

A detailed mechanism for the oxidation of toluene in both argon and nitrogen dilutents is presented. The mechanism was used to compute experimentally ignition delay times for shock-heated toluene-oxygen-argon mixtures with resonably good success over a wide range of initial temperatures and pressures. Attempts to compute experimentally measured concentration profiles for toluene oxidation in a turbulent reactor were partially successful. An extensive sensitivity analysis was performed to determine the reactions which control the ignition process and the rates of formation and destruction of various species. The most important step was found to be the reaction of toluene with molecular oxygen, followed by the reactions of hydroperoxyl and atomic oxygen with benzyl radicals. These findings contrast with the benzene oxidation, where the benzene-molecular oxygen reaction is quite unimportant and the reaction of phenyl with molecular oxygen dominates. In the toluene mechanism the corresponding reaction of benzyl radicals with oxygen is unimportant. Two reactions which are important in the oxidation of benzene also influence the oxidation of toluene for several conditions. These are the oxidations of phenyl and cyclopentadienyl radicals by molecular oxygen. The mechanism presented successfully computes the decrease of toluene concentration with time in the nitrogen diluted turbulent reactor. This fact, in addition to the good prediction of ignition delay times, shows that this mechanism can be used for modeling the ignition and combustion process in practical, well-mixed combustion systems. Author

**N88-13429*#** San Diego State Univ., Calif. Dept. of Electrical and Computer Engineering.
**OH(A-X) FLUORESCENCE FROM PHOTODISSOCIATIVE EXCITATION OF HO2 AT 157.5 nm**
M. Suto, C. Ye, M. J. Mitchell, and L. C. Lee [1988] 19 p
(Grant NAGw-661)
(NASA-CR-181580; NAS 1.26:181580) Avail: NTIS HC A03/MF A01 CSCL 07D

The OH(A-X) fluorescence from photodissociative excitation of HO2 by F2 laser photons (157.5 nm) was observed and compared with the OH fluorescence spectra of H2O2 and the O2+CH3OH mixture. The rotational population distributions of OH(A) were obtained from the fluorescence spectra. The most populated levels are J = 4 for photodissociative excitation of HO2, J = 20 for H2O2, and J = 21 for the O2+CH3OH mixture. The fluorescence from the gas mixture is attributed to the O + H recombination for which the atoms are produced from photodissociation of parent molecules. Author

# 26 METALLIC MATERIALS

Includes physical, chemical, and mechanical properties of metals, e.g., corrosion; and metallurgy.

**N88-13430** Brown Univ., Providence, R. I.
**PLASTICITY OF ALUMINUM AND IRON AT HIGH SHEAR STRAIN RATE AND HIGH PRESSURE Ph.D. Thesis**
Richard William Klopp 1987 181 p
Avail: Univ. Microfilms Order No. DA8715522

The results are described of high strain rate pressure shear plate impact experiments performed on 99.99 percent pure mono and polycrystalline aluminum, and 99.99 percent pure polycyrstalline iron. Specimens are deformed in simple shear over a range of shearing rates. A technique for lapping flat, parallel sided specimens is introduced, enabling shearing bulk materials. Higher rates are achieved in specimens prepared by vapor deposition. The flow stress of monocrystalline aluminum is found to increase less than linearly. The measured response of crystals sheared on the (112') plane in the (1'10) direction is used to derive a slip system constitutive relation in which shearing rate depends on resolved shear stress raised to the 0.3 power. This relation predicts the shear stress response of crystals sheared on the (112') plane in the (111) and (1'11) directions to be significantly softer than the (112') (1'10) response at the same shearing rate. These predictions are not supported by the experimental results. A finite difference model shows that flow stress depends on shearing rate raised to the 0.1 power and that the material is essentially strain and temperature independent over the range of parameters considered. Dissert. Abstr.

**N88-13431#** Santa Catarina Univ., Florianopolis (Brazil).
**STUDY OF THE INFLUENCE OF MECHANICAL - THERMAL TREATMENTS ON THE CREEP BEHAVIOR OF A NIOBIUM STAINLESS STEEL**
J. L. Rossi and P. I. Ferreira 1986 4 p In PORTUGUESE; ENGLISH summary Presented at the 7th Brazilian Congress on Engineering and Materials Science, Florianopolis, Brazil, 10 Dec. 1986

(DE87-703506; INIS-BR-756; CONF-861299-2) Avail: NTIS (US Sales Only) HC A02/MF A01

The influence of microstructural parameters controlled by mechanical-thermal treatment on the creep behavior of DIN-Werkstoff-Nr. 1.4981 stainless steel (candidate material for use as cladding of fast breeder reactor fuel elements) is studied. The effects of the solution treatment, predeformation, predeformation plus aging and cycles of predeformation-aging on the creep results obtained at 990 K, for apllied stresses in the range 70 MPa to 310 MPa, are discussed. DOE

**N88-13432#** Santa Catarina Univ., Florianopolis (Brazil).
**MICROSTRUCTURE OF AMORPHOUS AND CRYSTALLINE ZIRCONIUM ALLOYS RAPIDLY SOLIDIFIED**
W. A. Monteiro and G. H. Bezerra 1986 3 p In PORTUGUESE; ENGLISH summary Presented at the 7th Brazilian Congress on Engineering and Materials Science, Florianopolis, Brazil, 10 Dec. 1986
(DE87-703700; INIS-BR-760; CONF-861299-8) Avail: NTIS (US Sales Only) HC A02/MF A01

Microstructural studies of the rapid solidification of Zr-30% in copper alloy was reported. This composition was chosen because it is the Zr concentration limit for the change to the amorphous state. The ribbons were prepared by melt spinning (cooling rate is estimated 10 to the 6th K/s). Under electron microscopy, the microstructure of the ribbon revealed both amorphous and crystalline regions. In the crystalline regions a radial growth morphology occurs with internal stress. The beginning of solidification is a polymorphous reaction and the shape of the micrograins is spherulitic in form. The average diameter of the grains are 0.5 microns or less. DOE

**N88-13433#** National Aeronautical Lab., Bangalore (India). Materials Science Div.
**ANALYSIS OF NICKEL SULPHAMATE BATH USING CHARGING CURRENT COMPENSATED D.C. POLAROGRAPHY**
Bharathi Bai, J. Basu, S. Sreepathy, and S. R. Rajagopalan Aug. 1987 16 p
(NAL-TM-MT-8705) Avail: NTIS HC A03/MF A01

Metallic impurities such as copper, lead, iron, zinc, and cadmium are harmful in the nickel plating bath since they affect the properties of the deposit. The maximum tolerable limit is in the range of 10 to 200 ppm. Application of charging current compensated dc polarography (CCCDCP) to the analysis of trace impurities and nickel in a sulfamate bath is described. Author

**N88-13434#** National Aeronautical Lab., Bangalore (India). Materials Science Div.
**X-RAY ANALYSIS OF POLYCRYSTALLINE ALUMINIUM SUBJECTED TO FATIGUE CYCLING**
Kalyani Vijayan, A. Mani, C. Balasingh, and A. K. Singh Oct. 1987 27 p
(NAL-TM-MT-8706) Avail: NTIS HC A03/MF A01

Variations in the halfwidth values of x-ray reflections from fatigue cycled, polycrystalline aluminum samples have been analyzed. A hitherto unknown oscillatory distribution of the (b/b sub 0) values with fatigue cycling has been observed. The present data also indicate that (1) the broadening due to fatigue cycling increases with increase in glancing angle, (2) the changes in the halfwidth and the integral width values due to fatigue cycling are comparable, and (3) the (b/b sub 0) vs N curves for fatigue cycling under constant stress amplitude and under flight loading conditions are comparable. Author

**N88-13435#** National Aeronautical Lab., Bangalore (India). Materials Science Div.
**ANALYSIS OF WEAR METALS IN ENGINE OILS USING THE ATOMIC ABSORPTION SPECTROPHOTOMETRIC METHOD**
M. Kalyanam, S. Sreepathy, and S. R. Rajagopalan Aug. 1987 39 p
(NAL-TM-MT-8704) Avail: NTIS HC A03/MF A01

The determination of wear metals in certain used automobile engine oil and aircraft engine oil by the atomic absorption spectrophotometric method is described. Preparation of synthetic metal naphthanates for calibration is described.The procedures developed are found to have the required sensitivity for analyzing wear metals at ppm and sub-ppm concentrations. Author

**N88-13436#** British Library Lending Div., Boston Spa (England).
**A MATHEMATICAL MODEL OF HIGH ALLOY NICKEL BASE HIGH TEMPERATURE ALLOYS**
V. T. Zhada, V. A. Osadchii, and Yu. V. Yatsko [1987] 4 p Transl. into ENGLISH from Vysshikh Uchebnykh Zavedeniy Chernaya Mettalurgiya (USSR), no. 2, 1987 p 140
(BLL-M-37381-(5828.4)) Avail: British Library Lending Div., Boston Spa, United Kingdom

A mathematical model linking the properties of high-alloy high-temperature nickel-base alloys at different temperatures with their chemical compositions is described. It is possible to lessen the risk of precipitated embrittling phases causing the properties to deteriorate. The strength and plastic properties of alloys of the type considered can be made consistently higher at high working temperatures. Author

**N88-13437#** British Library Lending Div., Boston Spa (England).
**THE MECHANISM BY WHICH SIGMA-PHASE FORMS IN Fe-Cr-Ni SYSTEM ALLOYS**
N. V. Podobedova, V. P. Ostapenko, and A. V. Rabinovich [1987] 8 p Transl. into ENGLISH from Izvestiya Vysshikh Uchebnykh Zavedeniy Chernaya Metallurgiya (USSR), no. 2, 1987 p 138-140
(BLL-M-37380-(5828.4)) Avail: British Library Lending Div., Boston Spa, United Kingdom

Details are given on how sigma-phase forms in alloys with different compositions. It is found that the mechanism and kinetics of the process are primarily governed by the chemical composition of the initial ferrite phase. Details are given of the temperature and heat treatments at and with which sigma-phase will form. Author

**N88-13438#** British Library Lending Div., Boston Spa (England).
**CORROSION RESISTANCE OF SINTERED ALLOY STEELS**
P. N. Ostrik, I. I. Grigorchuk, and M. M. Gasik [1987] 5 p Transl. into ENGLISH from Vysshikh Uchebnykh Zavedeniy Chernaya Metallurgiya (USSR), no. 2, 1987 p 76-77
(BLL-M-37363-(5828.4)) Avail: British Library Lending Div., Boston Spa, United Kingdom

The results of experimental research into the corrosion resistances of sintered composite materials with the use of a thermogravimetric unit and a microscopic study of the cross sections of oxidized specimens establish that a pronounced deceleration effect can be detected during the oxidation of SPKh3N1MO.25 and SPKh3N2.5MI sintered steel alloys. Oxidation is characterized in this case by the formation of a dense oxide film thoroughly bonded to the surface. Author

**N88-13439#** Naval Postgraduate School, Monterey, Calif.
**INVESTIGATION BY DIFFERENTIAL SCANNING CALORIMETRY OF MICROSTRUCTURE IN A SUPERPLASTIC Al-Mg-Zr ALLOY M.S. Thesis**
Donald L. Stewart, II Jun. 1987 90 p
(AD-A184902) Avail: NTIS HC A05/MF A01 CSCL 11F

The three significant variables identified in thermomechanical processing of an A1-10Mg-0.1Zr alloy to obtain superplastic ductilities are reduction per pass, reheating time between passes, and total strain during warm rolling at 573K. The effect of adjusting these variables on elevated temperature mechanical properties has been evaluated and the microstructures characterized using transmission electron microscopy. Comparison of the differential scanning calorimetry results with mechanical property and microstructural data reveal that the endothermic energy absorbed by the material, which is related to microstructural stability, can be correlated with superplastic behavior. GRA

**N88-13440#** Rensselaer Polytechnic Inst., Troy, N.Y. Dept. of Materials Engineering.
**PROPERTIES OF REFRACTORY METALS PROCESSED BY ENHANCED SINTERING TREATMENTS Final Report**
R. M. German and S. Farooq 29 May 1987 8 p
(Contract DAAG29-84-K-0026)
(AD-A184944; ARO-21294.11-MS) Avail: NTIS HC A02/MF A01 CSCL 11F

This investigation examined the sintering enhancement of refractory metals and attempted to link activator effects to sintering kinetics, microstructure and properties. Work was carried out predominately on the W-Ni-Fe heavy alloy system. In addition, it was recognized that property improvement in heavy alloys could be made possible by understanding impurity-microstructure interactions, fracture behavior, and finally the combined effect of processing conditions and materials characteristics on densification during liquid phase sintering. This report addresses each of the above concerns and presents an overview of the work to date. GRA

**N88-13441#** Naval Postgraduate School, Monterey, Calif.
**THE EFFECT OF TEMPERATURE ON THE TENSILE PROPERTIES OF HSLA-100 STEEL M.S. Thesis**
James E. Hamilton Jun. 1987 115 p
(AD-A184951) Avail: NTIS HC A06/MF A01 CSCL 11F

High Strength Low Alloy (HSLA) steels have been shown to posses high strength and toughness. Additionally, these steels can be welded without the normal preheating required by comparable HY-series steels. HSLA-100, 100 Ksi yield strength, contains increased amounts of copper, manganese and nickel over the currently certified HSLA-80. However, prior to use in Naval ship construction knowledge of the steels toughness behavior is necessary. Existing fracture mechanics models are not applicable to HSLA-100 because HSLA-100 has only 0.04% carbon and these models use carbides as the nucleation sites for cleavage fracture. This research is part of a program to investigate and model the micromechanics of deformation and fracture of HSLA-100. Tensile testing of hourglass shaped specimens was conducted at quasi-static strain rates. Individual tensile test temperatures ranged from 24 C to -196 C. True stress, corrected for necking, and true plastic strain were monitored throughout the tests. This allowed a comparison to be made between the plastic strain behavior of HSLA-100 steel and a traditional constitutive equation used to describe the stress-strain behavior of metals. GRA

**N88-13442#** Army Lab. Command, Watertown, Mass. Material Technology Lab.
**ION PLATING FOR CORROSION CONTROL Final Report**
Welville B. Nowak (Northeastern Univ., Boston, Mass.), Milton Levy, and Frank C. Chang Aug. 1987 12 p
(AD-A185061; MTL-TR-87-41) Avail: NTIS HC A03/MF A01 CSCL 11F

Coatings deposited by ion plating are becoming more widely used for corrosion protection. Aluminum coatings may be the most advanced commercially at this time. Other identified candidates (depending upon the substrate) are iron-chromium, aluminum-magnesium, copper-aluminum, and titanium-nitride. Important characteristics of these coatings are chemical composition and microstructure. An amorphous or microcrystalline structure can result in vastly enhanced resistance to corrosion for metal films that have an inherent tendency toward passivity. These structures can also lead to the formation of a resistant spinel-type oxide layer in certain alloys. The influence of process parameters in achieving these structures is discussed. GRA

**N88-13443#** Aeronautical Research Labs., Melbourne (Australia).
**ENVIRONMENTALLY ASSISTED CRACKING: OVERVIEW OF EVIDENCE FOR AN ADSORPTION-INDUCED LOCALISED-SLIP PROCESS**
S. P. Lynch Dec. 1986 80 p
(AD-A185175; ARL/MAT-R-119) Avail: NTIS HC A05/MF A01 CSCL 11F

Metallographic and fractographic studies of crack growth in aluminum alloys, nickel, magnesium, titanium alloys B-brass iron-hydrogen, and inert environments are reviewed. GRA

**N88-13444#** Massachusetts Inst. of Tech., Cambridge. Dept. of Materials Science and Engineering.
**EFFECT OF RAPID SOLIDIFICATION ON SHORT-RANGE ORDER: A MAGNETIC STUDY Final Report, 1 Apr. 1984 - 31 Mar. 1987**
R. C. OHandley 30 Jun. 1987 11 p
(Contract DAAG29-84-K-0056)
(AD-A185216; ARO-20077.11-MS) Avail: NTIS HC A03/MF A01 CSCL 11F

In this study of the effects of rapid solidification on short-range order and magnetic properties, major progress and significant results were achieved in four specific areas. 1) Short-range order in Co80NbxB20-x amorphous alloys was found to be similar at low x and dissimilar at large x to that of the equilibrium crystal structure. This key observation led to a broader model of magnetic properties in amorphous alloys. 2) Devitrification of two different metallic glasses led to technically and scientifically important discoveries related to the fine microstructures produces. 3) Theoretical cluster calculations of electronic structure significantly advanced our understanding of bonding and magnetism in amorphous alloys. Finally, 4), We found that magnetization reversal could be very well described by the soliton-like solutions to a realistic non-linear wave equation. This approach correctly describes the coupling of the wall motion to its own local strain field, a technically important effect. GRA

**N88-13445#** Drexel Univ., Philadelphia, Pa. Dept. of Materials Engineering.
**A FUNDAMENTAL STUDY OF P/M PROCESSED ELEVATED TEMPERATURE ALUMINUM ALLOYS Final Report, 1 Oct. 1981 - 30 Sep. 1986**
A. Lawley and M. J. Koczak Jul. 1987 38 p
(Contracts AF-AFOSR-82-0010; AF Proj. 2306)
(AD-A185393; AFOSR-87-0964TR) Avail: NTIS HC A03/MF A01 CSCL 11F

Ambient and elevated temperature tensile and creep response, and microstructural stability of a powder processed AL-Fe-Ce alloy have been evaluated. Gas atomized Al-Fe-C was mechanically alloyed (MA) to give a volume fraction of dispersoids of about 0.23. The powder was isostatically pressed in aluminum cans, outgassed and hot extruded to full density. Consistent with improved microstructural stability at elevated temperatures, the MA material is stronger and more creep resistant than the non-MA material. These improvements are attributed to the presence of fine scale oxides and carbides distributed uniformly throughout the structure, and which are introduced during MA; the dispersion inhibits coarsening, recovery and recrystallization. Non-MA Al-Fe-Ce is stronger than non-MA Al-Fe-Ni at all temperatures but it has limited ductility. Qualitatively, the effect of MA on Al-Fe-Ce is similar to that in Al-Fe-Ni. These results suggest that Ce alters the transformation characteristics of Al-Fe and/or that Ce diffuses more slowly that Ni in Al, in the presence of Fe. GRA

**N88-13446#** Ballistic Research Labs., Aberdeen Proving Ground, Md.
**MECHANICAL PROPERTY EVALUATION OF A SERIES OF COMMERCIAL TUNGSTEN ALLOYS**
William J. Bruchey, Jr. and Denise M. Montiel Jun. 1987 30 p
(AD-A185440; BRL-MR-3606) Avail: NTIS HC A03/MF A01 CSCL 11F

A series of commercially available tungsten alloys ranging in tungsten content from 75% to 95% were evaluated. Typical tensile and compressive engineering properties are reported. These tests were conducted in support of penetrator ballistic test programs. GRA

**N88-13447#** Technische Hochschule, Aachen (West Germany). Lehrstuhl fuer Metallurgie der Kernbrennstoffe und Theoretische Huettenkunde.

**PHASE DIAGRAM AND THERMOCHEMICAL PROPERTIES OF THE Al-Cu SYSTEM**

D. Luedecke 1987 28 p Sponsored by Bundesministerium fuer Forschung und Technologie

(ETN-88-91015) Avail: NTIS HC A03/MF A01

Experimental data on the thermochemical properties and the phase diagram of the Al-Cu system are used to establish a set of coefficients which provide a self-consistent representation of the thermochemistry and phase equilibria in this system. For the pure components in their stable and metastable states, and for the stoichiometric compounds, G(T)-functions are given. For the solution phases, the enthalpy and excess entropy of mixing are represented in terms of Redlich-Kister polynomial equations. Results computed with the evaluated data are compared with the experimental information. For the thermochemical properties, there are large discrepancies, particularly for solid alloys; the experimental results, however, exhibit large deviations themselves. There is very good agreement between the simplified experimental phase diagram and the diagram calculated with the optimized set of coefficients. ESA

**N88-13448#** Sandia National Labs., Albuquerque, N. Mex.

**EFFECTIVENESS OF ELECTRODEPOSITED COATINGS IN REDUCING ATMOSPHERIC CORROSION OF COPPER SUBSTRATES**

J. E. Voytko and T. R. Gullinger 1987 9 p Presented at the Symposium on Electronics Finishing for Today and Tomorrow, Wakefield, Mass., 20 Oct. 1987

(Contract DE-AC04-76DP-00789)

(DE87-013651; SAND-87-1718C; CONF-8710154-1) Avail: NTIS HC A02/MF A01

Coatings of gold, nickel, palladium, and nickel with 20 at% phosphorus were electrodeposited on copper substrates at thicknesses of 50 and 150 microinches. These coated samples were exposed in an atmosphere of 100 ppB nitrogen dioxide, 100 ppB hydrogen sulfide, and 10 ppB chlorine, with a relative humidity of 60% and a temperature of 38 C for 332 hours. Weight gain of the samples was monitored to determine corrosion rate. Pore densities and sizes were measured after exposure to compare the performance of each deposit. Although the number of pores in the nickel coatings were fewer than in the other samples, pore sizes were significantly greater. Gold plated on nickel over a copper substrate exhibited smaller pores but a higher density. Palladium at 50 and 150 microinches performed well, thus recommending this coating for use in high reliability contacts. DOE

**N88-13449#** Oak Ridge National Lab., Tenn.

**ADVANCES IN PROCESSING TECHNIQUES FOR NICKEL ALUMINIDES**

V. K. Sikka 1987 12 p Presented at the ASM Europe Technical Conference on Advanced Materials and Processing Techniques for Structural Applications, Paris, France, 7 Sep. 1987

(Contract DE-AC05-84OR-21400)

(DE87-014571; CONF-8709144-1) Avail: NTIS HC A03/MF A01

The status of processing technology at ORNL for three nickel aluminide alloys is presented in the form of flow charts. The technologies discussed include powder processing, melting techniques, near-net-shape processes from molten metal, and cold and hot working of cast products. Tensile properties are compared for one of the three alloys after six different processing techniques. Creep-rupture strength is compared for the three nickel aluminide alloys in the cast and wrought condition. Grain size was the main difference between the material produced by various processing techniques. Significant advances in processing technology of nickel aluminides could find them in use for a range of applications in the future. DOE

**N88-13450#** Edgerton, Germeshausen and Grier, Inc., Idaho Falls, Idaho.

**TENSILE PROPERTIES OF EXTRUSION CONSOLIDATED TYPE 304 SS RAPIDLY SOLIDIFIED POWDERS**

J. E. Flinn, G. E. Korth, and R. N. Wright 1986 25 p Presented at the American Society of Metals Materials Week, Lake Buena Vista, Fla., 6 Oct. 1986

(Contract DE-AC07-76ID-01570)

(DE87-014875; EGG-M-27186; CONF-861063-9) Avail: NTIS HC A03/MF A01

Rapidly solidified Type 304 stainless steel (SS) powders prepared by centrifugal atomization (CA) using helium as a quench gas and having a dendritic microstructure were hot extruded, resulting in fully consolidated bars with a recrystallized fine grain size. The extruded bar, as well as the powder, contained 8 appM of entrapped helium acquired during powder processing. Prior to tensile testing, the specimens were given various preconditioning heat treatments (PCHTs). The tests were conducted in air over a temperature range of 24 to 800 C at a strain rate of approximately 10(-4)/s. The tensile properties of the CA 304 SS extruded powders were compared to an ingot metallurgy (I/M) Type 304 SS material with a similar chemistry. The tensile strengths and reductions in area were superior for the powders, compared to the I/M material, but uniform and total elongations were slightly lower. There were no obvious helium influences associated with the ductilities, e.g., embrittlement. The preconditioning heat treatments for the powder specimens had a significant influence on the strength properties. Strengthening mechanisms are discussed, including grain size, entrapped helium influences and apparent carbide effects. DOE

**N88-13451#** Oak Ridge National Lab., Tenn.

**EFFECT OF RAPID SOLIDIFICATION ON STAINLESS STEEL WELD METAL MICROSTRUCTURES AND ITS IMPLICATIONS ON THE SCHAEFFLER DIAGRAM**

S. A. David, J. M. Vitek, R. W. Reed, and T. L. Hebble Sep. 1987 48 p

(Contract DE-AC05-84OR-21400)

(DE88-001489; ORNL/TM-10487) Avail: NTIS HC A03/MF A01

An investigation was carried out to determine the effect of rapid solidification on the weld metal microstructure of austenitic stainless steels and its implication on the ferrite constitution diagram. Stainless steels were laser welded at different welding speeds and laser power levels. Results show that both weld pool cooling rate and the postsolidification solid state cooling rates have a profound effect on the microstructures. For the steels tested, the microstructures ranged from duplex austenite (gamma) + ferrite (delta) to fully austenitic or fully ferritic. These microstructures were found to be sensitive to both cooling rates and composition. The results are rationalized based on rapid solidification theory. This investigation indicates that solidification rates and postsolidification cooling rates have a profound effect on microstructure, thus making it impossible to predict the microstructures of rapidly cooled weld metal from the conventional constitution diagrams. The influence of the observations made in this investigation on the Schaeffler diagram is demonstrated, and possible corrections to the constitution diagram incorporating the cooling rate effects are proposed. on the Schaeffler diagram is demonstrated, and possible corrections to the constitution diagram incorporating the cooling rate effects are proposed. DOE

**N88-13452#** Cornell Univ., Ithaca, N.Y. Dept. of Materials Science and Engineering.

**CU-2 MECHANICAL PROPERTIES AND MICROSTRUCTURAL STABILITY OF ADVANCED STEAM CYCLE MATERIALS Interim Report, Oct. 1985 - Sep. 1987**

R. A. Carolan, B. Coulombe, and Che-Yu Li 29 Sep. 1987 58 p

(Contract DE-AC05-84OR-21400)

(DE88-001519; ORNL/Sub-85-27488/02) Avail: NTIS HC A04

The aims of this project are, to obtain mechanical property data for the selection of alloys proposed for use in the high temperature steam cycle fossil energy plants, and to characterize

the kinetics of microstructural instability in these alloys, such that long-term microstructural influences on mechanical properties can be described particularly with reference to service conditions. Alloy evaluation is based on the design criteria for advanced steam cycle plants which require a stress to rupture of 96 MPa for a $10^5$ hrs life at 700°C and preferably a rupture strength of 116 MPa under the same conditions. Work to date has emphasized the alloy screening part of the program. The high temperature flow strength of a series of five modified A1S1 316 stainless steels developed at Oak Ridge National Laboratory were evaluated. Candidate alloys CE0-CE2 were Ti V Nb stabilized type 316 stainless steels. Alloys CE3 and AX7 were Ti V Nb stabilized type 316 stainless steels containing copper additions. Alloy AX7 had a lower Ti content. As a reference material a 17/14 CuMo type 316 steel, based on the composition of the alloy used in the Eddystone plant was tested. DOE

# 27 NONMETALLIC MATERIALS

Includes physical, chemical, and mechanical properties of plastics, elastomers, lubricants, polymers, textiles, adhesives, and ceramic materials.

For composite materials see *24 Composite Materials*.

**N88-13453*#** National Aeronautics and Space Administration. Lewis Research Center, Cleveland, Ohio.

**COATINGS FOR HIGH-TEMPERATURE BEARINGS AND SEALS Final Report**

Harold E. Sliney Jul. 1987 14 p Presented at the Workshop on Coatings for Advanced Heat Engines, Castine, Me., 26-30 Jul. 1987; sponsored by DOE

(Contract DE-AI01-85CE-50112)

(NASA-TM-100249; E-3871; NAS 1.15:100249; DOE/NASA-50112-71) Avail: NTIS HC A01/MF A01 CSCL 11G

Criteria are discussed for predicting the probable lubricating ability of candidate solid materials from a consideration of their basic chemical and physical properties. The properties considered to be important in the model are thermochemical potential, adhesion, low hardness, plasticity, yield strength in shear, and brittle-to-ductile transition characteristics. A review of the selection and tribological testing of materials, which were selected for use in self-lubricating composite coatings by employing this model, is given. Two series of plasma-sprayed coatings with good tribological properties over a wide temperature spectrum are described. The PS 100 series of coatings contain oxidatively stable solid lubricants in a nichrome matrix. The PS 200 series contains the same solid lubricants in a very wear resistant metal-bonded chromium carbide matrix. Examples are given of applications of these coatings in high speed shaft seals, sliding contact bearings, and Stirling engine cylinder liners. Author

**N88-13454#** Naval Air Development Center, Warminster, Pa. Air Vehicle and Crew Systems Technology Directorate.

**WATER DISBONDMENT CHARACTERIZATION OF ORGANIC COATING/METAL SUBSTRATE SYSTEMS Interim Report, Oct. 1986 - Jul. 1987**

Stephen J. Spadafora 15 Jul. 1987 53 p

(AD-A184847; NADC-87114-60) Avail: NTIS HC A04/MF A01 CSCL 11C

The adhesion of many organic coatings to metal substrates is adversely affected by exposure to an aqueous environment. Even high relative humidities can cause coating disbondment to occur. The mechanism behind this adhesion loss is the accumulation of water molecules at small pre-existing unbonded areas at the coating under a concentration gradient, condenses in these areas and causes them to grow. As these areas grow laterally, they cause stresses to occur at the coating/substrate interface which eventually leads to the adhesion loss. The more primary chemical adhesive bonds a specific coating makes with the substrate the more resistant that system is to water disbondment. GRA

**N88-13455#** Massachusetts Univ., Amherst. Dept. of Polymer Science and Engineering.

**MOLECULAR-LEVEL SYNTHESIS AND CHARACTERIZATION OF METAL-POLYMER INTERFACES Final Report, 16 Apr. 1984 - 15 Apr. 1987**

Shaw L. Ling and Thomas J. McCarthy 23 Aug. 1987 17 p

(Contract DAAG29-84-K-0052)

(AD-A184956; ARO-20961.4-MS) Avail: NTIS HC A03/MF A01 CSCL 07B

Two separate, but interacting research groups began a program entailing molecular level syntheses and characterization of metal-polymer interfaces. Two general synthetic routes were followed: In one case, a metal surface (platinum) was cleaned of its oxide layer by carrying out a hydrogenation reaction (hexene or cyclohexene) using the metal surface as the catalyst. Under these conditions, platinum oxide is unstable and is reduced to platinum(0) and water. The reaction was then deliberately poisoned with 4-picoline. Monitoring the kinetics of hydrogenation before and after the addition of the poison allowed us to determine that approx. 70% of the hydrogenation sites were ligated. The amount of 4-picoline that adsorbed was determined by elemental analysis, gravimetric analysis and UV-vis analysis of the solution. The surface-confined picoline was then deprotonated to render the ligated lithium reagent which was used to initiate the polymerization of styrene. The thin film of polystyrene prepared in this manner was irreversibly attached to the platinum surface. The platinum-polystyrene interface was studied by a range of analytical techniques. In the other case, a metal-polymer interface was prepared by polymer adsorption: Polystyrene containing one terminal thiol group and styrene-propylene sulfide block copolymers were allowed to adsorb on evaporated gold films supported on glass. GRA

**N88-13456#** Southwest Research Inst., San Antonio, Tex. Belvoir Fuels and Lubricants Research Facility.

**LITERATURE REVIEW OF SOLID LUBRICATION MECHANISMS Interim Report, Jul. 1985 - Nov. 1986**

M. D. Kanakia and M. B. Peterson Jul. 1987 62 p Prepared in cooperation with Wear Sciences, Inc., Arnold, Md.

(Contracts DAAK70-85-C-0007; DA Proj. 1T1-61102-AH-51)

(AD-A185010; BFLRF-213) Avail: NTIS HC A04/MF A01 CSCL 11H

For this report, five phenomenological models are proposed for solid lubrication. These models are: 1) Viscous flow of the solid lubricant due to strong attachment to both surfaces and with uniform shear across the gap; 2) Plastic flow of solid lubricant; 3) Substrate/film slip model in which the sliding takes place between one substrate and the surface of the film; 4) Interfilm slip model when lubricant film is strongly attached to the two substrate surfaces. The sliding take place at the interface; and 5) Intercrystalline slip model which is basically a modification of the plastic flow process. The lubricant film is composed of small crystalline blocks of lubricants which slip past each other. The expected tribological behavior is suggested for each model. A review of the literature was conducted to determine which model could be supported by the evidence available. The report includes a discussion of the following topics: Observation of Film Behavior; Substrate Adhesion; Film Formation, Wear, and Failure; Crystal Structure Effects; Surface Chemical Effects; and Frictional Behavior. GRA

**N88-13457#** California Inst. of Tech., Pasadena.

**DEVELOPMENT OF MICROENCAPSULATION TECHNIQUES Final Report, 1 Sep. 1983 - 31 Aug. 1986**

John D. Baldeschwieler 26 Nov. 1986 3 p

(Contract DAAG29-83-K-0128)

(AD-A185019; ARO-20030.1-CH) Avail: NTIS HC A02/MF A01 CSCL 06A

When vesicles are formed using phospholipids containing terminal sulfhydryl groups it is possible to polymerize the sulfhydryl groups by oxidation to form disulfide linkages. Such cross-links lead to a considerable enhancement in vesicle stability for a given size. An important feature of the sulfhydryl system is that this

type of phospholipid polymer can be readily depolymerized by reducing agents. We have also found formulations which result in spontaneous formation of vesicle structures. Spontaneous vesicle formation reduces many of the difficulties involved in vesicle preparation. Certain combinations of short and long chain lipids give rise to spontaneous vesicle formation. We are currently exploring whether this phenomenon may also occur for short and long chain polymerizable sulfhydryl phospholipids. GRA

**N88-13458#** Materials Research Labs., Ascot Vale (Australia).
**HIGH EXPLOSIVE MOULDING POWDERS FROM RDX AND AQUEOUS POLYURETHANE DISPERSIONS**
I. Dagley, R. J. Spear, and V. Nanut May 1987 34 p
(AD-A185026; MRL-R-1062) Avail: NTIS HC A03/MF A01 CSCL 19A

Eleven commercially available aqueous polyurethane dispersions have been evaluated for use in the preparation of high explosive moulding powders. The polymers were coagulated by addition of electrolytes to aqueous slurries RDX containing the dispersions. In several cases polymer coating of the explosive crystals has been effected. The impact sensitiveness of these compositions and physical mixtures of the polymer particles with RDX have been determined and the effect of coating efficiency, particle size and polymer properties on sensitiveness is discussed. Formulations suitable for use as high explosive moulding powders have been prepared from two dispersions with additional incorporation of zinc stearate. Impact sensitiveness, shock sensitivity and vacuum thermal stability of these formulations have been assessed. GRA

**N88-13459#** Massachusetts Inst. of Tech., Cambridge. Dept. of Chemistry.
**SOLUBLE METAL CHELATE POLYMERS OF COORDINATION NUMBERS SIX, SEVEN AND EIGHT**
Ronald D. Archer, Bing Wang, Valentino J. Tramontano, Annabel Y. Lee, and Ven O. Ochaya 1 Apr. 1987 6 p
(Contract N00014-86-K-0345)
(AD-A185094; TR-8) Avail: NTIS HC A02/MF A01 CSCL 07B

Metal coordination polymers possess certain properties (radiation sensitivity, catalytic activity, unique connectivities, etc.) which can provide advantages over their organic counterparts. However, careful design is necessary to avoid intractability, which has plagued metal chelate macromolecules in the past. Nonrigid coordination centers, bulky groups to prevent stacking, strongly coordinating solvents, oxo-metal centers, non-linear connections in octahedral systems are all being used to counter the insolubility of the more common four-coordinate systems. Circumventing the problems of low ligand solubility, inert metal centers which react too slowly to make good polymers, and labile metal centers which don't produce very inert species will be discussed in connection with new zirconium (IV) adhesives and radiation sensitive cobalt (iii) and dioxouranium (vi) polymers, for which definitive connectivity and chain lengths have been well defined. GRA

**N88-13460#** Keio Univ., Tokyo (Japan).
**UNITED STATES - JAPAN WORKSHOP ON DIELECTRIC AND PIEZOELECTRIC CERAMICS (3RD) HELD IN TOYAMA, JAPAN ON NOVEMBER 9-12, 1986**
30 Jul. 1987 424 p Workshop held in Toyoma, Japan, 9-12 Nov. 1986
(AD-A185113) Avail: NTIS HC A18/MF A01 CSCL 11B

These roundtable discussions were held in the areas of dielectrics, piezoelectrics, processing, and mechanical properties. The value of this series of workshops on dielectric and piezoelectric materials to the United States is twofold: First, the discussions, both formal and private, have provided a source of new research ideas for the individual scientist. Second, the collective knowledge gained by the U.S. attendees, individuals having many different areas of expertise, has aided the Navy in focussing on the newest and most important research directions which the Japanese are taking on these materials. It is clear that the components and devices based on these materials have played an ever increasing role in Naval applications as well as the U.S. technology as a whole. GRA

**N88-13461#** Pratt and Whitney Aircraft, West Palm Beach, Fla. Government Products Div.
**DEVELOPMENT OF IRON ALUMINIDES Final Report, 1 Sep. 1981 - 31 Jan. 1986**
R. G. Bourdeau, C. M. Adam, M. J. Blackburn, C. V. Law, and E. R. Slaughter May 1987 287 p
(Contract F33615-81-C-5110)
(AD-A185190; PW/GRD-FR-18807; AFWAL-TR-87-4009) Avail: NTIS HC A13/MF A01 CSCL 11F

This program addresses the development of iron aluminide base alloys by rapid solidification and the determination of their potential for use in aircraft turbine engines as alternatives to high chromium steels and nickel-base alloys. The program was divided into three tasks. A process and model development task to define thermomechanical processing requirements for Fe3A1 base alloys, a task to produce and deliver to the Air Force Materials Laboratory a number of alloys produced by the P&W rapidly solidified powder process and a task for the development of austenitic Fe-Mn-A1 alloys with improved elevated temperature properties. GRA

**N88-13462#** Air Force Wright Aeronautical Labs., Wright-Patterson AFB, Ohio.
**THERMALLY STABLE AROMATIC STRUCTURES FROM ACYCLIC PRECURSORS. 1. PARA POLYPHENYLENE MODEL COMPOUNDS FROM 3-DIMETHYL AMINO HEX-5-EN-1-YNES Final Report, Mar. 1985 - Mar. 1986**
Marilyn R. Unroe and Bruce A. Reinhardt Jul. 1987 53 p
(AD-A185300; AFWAL-TR-87-4065) Avail: NTIS HC A04/MF A01 CSCL 07C

Condensation of N,N-dimethyl-(3phenylprop-2-ynyl) amines with cinnamyl bromides of various structure afford cinnamyldimethyl-(3-phenylprop-2-vinyl) ammonium bromides in high yield. Without isolation, the ammonium salts can undergo both (3,2) and (1,2) base catalyzed Stevens rearrangements to the corresponding 3-dimethylamno-1,4-diphenylhex-5-en-1-ynes. Subsequent heating of the rearranged products closes the (3,2) linkages preferentially forming the all para-polyphenyls which are isolated easily from the reaction mixtures. GRA

**N88-13463** British Petroleum Co. Ltd., Sunbury-on-Thames (England).
**ANTISTATIC COATING COMPOSITIONS Patent Application**
Malcolm James Graham, inventor 21 Jan. 1987 6 p Filed 26 Jun. 1985
(GB-Patent-2-177-413-A; GB-Patent-Appl-SN-8516168; Int-Patent-Class-C09D-5/00; Int-Patent-Class-C09D-3/00; ETN-88-90517) Avail: UK Patent Office, 25 Southampton Buildings, London WC2A 1AY, United Kingdom

Antistatic coating compositions for plastics substrates, particularly for synthetic paper substrates were developed. They comprise an aqueous system containing a polymeric binder, a pigment, and an antistatic agent. The binder contains carboxyl groups, and the binder:pigment dry weight ratio is in the range 15:100 to 50:100. The antistatic agent is a water soluble ionic compound (e.g., a sodium polyphosphate) present in a dry weight:pigment ratio of from 0.4:100 to 2.5:100. The composition also contains an agent which reacts with carboxyl groups of the binder on drying to insolubilize the binder (e.g., ammonium zirconium carbonate). ESA

**N88-13464** British Petroleum Co. Ltd., Sunbury-on-Thames (England).
**FLAME RETARDANT PHENOLIC FOAMS Patent Application**
Alexander William St Duncan, inventor, Kenneth Charles Thomas, inventor, David George Summers, inventor, and David Charles Wilson, inventor 27 May 1987 13 p Filed 4 Nov. 1986
Priority 16 Nov. 1985 GB 528294
(EP-Patent-0-223-489-A2; EP-Patent-Appl-SN-86308587.4; Int-Patent-Class-C08L-61/06; Int-Patent-Class-C08K-5/00; Int-Patent-Class-C08J-9/06; ETN-88-90722) Avail: UK Patent

Office, 25 Southampton Buildings, London WC2A 1AY, United Kingdom

A method for producing flame retardant phenol aldehyde foams with thermal conductivity (k) value less than 0.020 W/mk was developed. The foams have as flame retardants a blend of a halosubstituted diphenyl oxide and an organic phosphorus compound. Unlike conventional flame retardants, the blend does not adversely affect the low k value, i.e., the low thermal conductivity of the foam. ESA

**N88-13465** British Petroleum Co. Ltd., Sunbury-on-Thames (England).

**PROCESS FOR THE PRODUCTION OF A THERMOPLASTIC ELASTOMER COMPOSITION Patent Application**

Alan Fernyhough, inventor and Sydney George Fogg, inventor 26 Nov. 1986 11 p Filed 23 Apr. 1986 Priority 24 Apr. 1985 GB 8510392

(EP-Patent-0-202-782-A2; EP-Patent-Appl-SN-86303047.4; Int-Patent-Class-C08L-23/04; Int-Patent-Class-C08L-9/02; Int-Patent-Class-C08K-5/14; ETN-88-90725) Avail: UK Patent Office, 25 Southampton Buildings, London WC2A 1AY, United Kingdom

A process for producing a thermoplastic elastomer comprising dynamically curing with a peroxy curing agent nitrile rubber and homopolymer or copolymer of ethylene, which is curable with the peroxy curing agent but excluding copolymers comprising ethylene and an acrylic or methacrylic ester was developed. The thermoplastic elastomer composition produced by the proces is suitable for use in sealant or adhesive compositions, particularly when blended with a tackifying resin. ESA

**N88-13466** Prins Maurits Lab. TNO, Rijswijk (Netherlands).

**RESISTANCE OF CANOPY MATERIALS AGAINST CHEMICALS [BESTENDIGHEID VAN CANOPY-MATERIALEN TEGEN CHEMICALIEEN]**

J. W. VanderSlikke Apr. 1985 39 p In DUTCH; ENGLISH summary

(PML-1985-22; TDCK-93458; ETN-88-90863) Copyright Avail: Issuing Activity

The effects of chemicals on transparent polymers, viz. helicopter and canopy parts as well as commercially available Perspex (polymethyl methacrylate) and Lexan (polycarbonate) were investigated. The used chemicals are liquid chemicals used by the Air Force, chemical warfare agents, and chemicals that can be used as solvent or thickener. The chemicals can adversely affect transparency. Perspex and Lexan react differently with several of the chemicals. The degradation of F-16 canopy material is substantially less than that of commercial sheet Lexan; this finding is not explained. ESA

**N88-13467#** Societe Nationale Industrielle Aerospatiale, Saint-Medard-en-Jalles (France). Division Systemes Balistiques et Spatiaux.

**COMPUTATION OF BONDED ASSEMBLIES. ELASTOPLASTIC ADHESIVES, FIRST PART Progress Report [CALCUL DES ASSEMBLAGES COLLES. ADHESIFS ELASTOPLASTIQUES. RAPPORT D'ETUDES DE LA PREMIERE TRANCHE]**

Maigret, Martin, and Menrath 18 Dec. 1986 57 p In FRENCH

(Contract DRET-84-163)

(SNIAS-NT-18926/AQET; ETN-88-91182) Avail: NTIS HC A04/MF A01

The characterization tests of the Hysol EA 9628 NW adhesive are discussed. The computation methods, developed using the finite element method are analyzed. Elastoplastic study results are presented. ESA

**N88-13468#** Societe Nationale Industrielle Aerospatiale, Saint-Medard-en-Jalles (France).

**FIRST INTERNATIONAL WEEK OF ADHESIVE BONDING AND ASSEMBLING [PREMIERE SEMAINE INTERNATIONALE DE L'ADHESION ET DE L'ASSEMBLAGE]**

Plotard 2 May 1986 10 p In FRENCH; ENGLISH summary

Conference held at Bordeaux, France, 15-18 Apr. 1986

(SNIAS-872-430-106; ETN-88-91217) Avail: NTIS HC A02/MF A01

Techniques used to manufacture structural bonded joints in missiles and satellites are discussed. It is shown that the high level of reliability required imposes technically sophisticated quality control procedures which are mostly nondestructive. ESA

**N88-13469#** Societe Nationale Industrielle Aerospatiale, Saint-Medard-en-Jalles (France). Lab. Materiaux et Procedes Nouveaux.

**STUDY OF CERAMIC-FIBER/CERAMIC SOL-GEL BASED MATRIX COMPOSITES**

B. Capdepuy and P. Lespade 1987 8 p

(SNIAS-872-430-120; ETN-88-91231) Avail: NTIS HC A02/MF A01

Potentials of sol-gel processes in alumina ceramic matrix composite elaboration are evaluated through mechanical tests in flexural configurations. Composites with matrices obtained via pure sol-gel processes present critical behaviors similar to composites obtained using joint sol-gel and conventional powder techniques. The fiber/matrix interface seems to be higher for sol-gel composites, leading to fiber fracture. ESA

**N88-13470#** Societe Nationale Industrielle Aerospatiale, Suresnes (France). Direction Centrale de la Qualite.

**PAINTS REQUIRED FOR AERONAUTICAL CONSTRUCTION [LES BESOINS DE L'AERONAUTIQUE EN MATIERE DE PEINTURES]**

C. Bezaud and J. J. Bodu 7 Apr. 1987 16 p In FRENCH Presented at Journee AFTPV Les Besoins en Peinture de Grandes Administrations, de Quelques Entreprises Nationalisees, et des Unites Urbaines, 8 Apr. 1987

(SNIAS-872-551-102; C-49-541; ETN-88-91234) Avail: NTIS HC A03/MF A01

Aeronautical paint performance required, the main categories of products involved, and the special requirements introduced with the adoption of composite materials are described. Recently designed aircraft, such as the A-320, use mostly epoxy anticorrosion primers and polyurethane finishing. ESA

**N88-13471#** Pacific Northwest Labs., Richland, Wash.

**STATISTICAL PROCESS CONTROL APPLIED TO THE LIQUID-FED CERAMIC MELTER PROCESS**

B. A. Pulsipher and W. L. Kuhn Sep. 1987 41 p

(Contract DE-AC06-76RL-01830)

(DE88-000271; PNL-6268) Avail: NTIS HC A03/MF A01

In this report, an application of control charts to the apparent feed composition of a Liquid-Fed Ceramic Melter (LFCM) is demonstrated by using results from a simulation of the LFCM system. Usual applications of control charts require the assumption of uncorrelated observations over time. This assumption is violated in the LFCM system because of the heels left in tanks from previous batches. Methods for dealing with this problem have been developed to create control charts for individual batches sent to the feed preparation tank (FPT). These control charts are capable of detecting changes in the process average as well as changes in the process variation. All numbers reported in this document were derived from a simulated demonstration of a plausible LFCM system. In practice, site-specific data must be used as input to a simulation tailored to that site. These data directly affect all variance estimates used to develop control charts. DOE

**N88-13472#** Los Alamos National Lab., N. Mex.

**MOLECULAR AND SUPRAMOLECULAR ORIENTATION IN CONDUCTING POLYMERS**

M. Aldissi 1987 13 p Presented at the International Symposium on Polymers for Advanced Technologies, Jerusalem, Israel, 16 Aug. 1987

(Contract W-7405-eng-36)

(DE88-000533; LA-UR-87-3027; CONF-8708139-1) Avail: NTIS HC A03/MF A01

Intrinsic anisotropy in electrical and optical properties of conducting polymers constitutes a unique aspect that derives pi-electron delocalization along the polymer backbone and from the weak inter-chain interaction. To acquire such an intrinsic property, conducting polymers have to be oriented macroscopically and microscopically (at the chain level). A review of the various techniques, including stretch-alignment of the polymer and of precursor polymers, polymerization in ordered media, i.e., in a liquid crystal solvent, and synthesis of liquid crystalline conducting polymers will be given. DOE

**N88-13473#** Sandia National Labs., Albuquerque, N. Mex.
**REACTIVE STICKING COEFFICIENTS OF SILANE ON SILICON**
R. J. Buss, P. Ho, W. G. Breiland, and M. E. Coltrin 1987 10 p Presented at the 34th National Vacuum Symposium and Topical Conference, Anaheim, Calif., 2 Nov. 1987
(Contract DE-AC04-76DP-00789)
(DE88-000601; SAND-87-2321C; CONF-871125-6) Avail: NTIS HC A02/MF A01

The reaction of room-temperature silane and disilane has been investigated on a hot polycrystalline silicon surface using both a collision-free molecular beam and a very low pressure CVD cell. Reactive sticking coefficients were obtained from deposition rate data over a wide range of temperatures and silane (disilane) fluxes. The RSCs are substantially less than one, ranging from 6 x 10 to the -5 power to 4 x 10 to the -2 power. For silane we observed curved Arrhenius plots with slopes decreasing from approx 60 kcal/mol at low temperatures to approx.2 kcal/mol at higher temperatures. The RSCs are independent of flux (pressure) at 1040 C, but vary as flux to the approx -1/2 power at 710 C. A model comprised of a dissociative adsorption mechanism with competing associative desorption and reaction was found to give reasonable agreement. For disilane, we observed RSCs that were roughly ten times higher than those for silane. We also observed a curved Arrhenius plot and a flux dependence at 710 C for disilane. DOE

**N88-13474*#** National Aeronautics and Space Administration. Langley Research Center, Hampton, Va.
**FLEXIBILIZED COPOLYIMIDE ADHESIVES**
Donald J. Progar and Terry L. St.Clair [1988] 40 p Submitted for publication
(NASA-TM-89303; NAS 1.15:89303) Avail: NTIS HC A03/MF A01 CSCL 11A

Two copolyimides, LARC-STPI and STPI-LARC-2, with flexible backbones were processed and characterized as adhesives. The processability and adhesive properties were compared to those of a commercially available form of LARC-TPI. Lap shear specimens were fabricated using adhesive tape prepared from each of the three polymers. Lap shear tests were performed at room temperature, 177 C, and 204 C before and after exposure to water-boil and to thermal aging at 204 C for up to 1000 hours. The three adhesive systems possess exceptional lap shear strengths at room temperature and elevated temperatures both before and after thermal exposure. LARC-STPI, because of its high glass transition temperature provided high lap shear strengths up to 260 C. After water-boil, LARC-TPI exhibited the highest lap shear strengths at room temperature and 177 C, whereas the LARC-STPI retained a higher percentage of its original strength when tested at 204 C. These flexible thermoplastic copolyimides show considerable potential as adhesives based on this study and because of the ease of preparation with low cost, commercially available materials. Author

# 28 PROPELLANTS AND FUELS

Includes rocket propellants, igniters, and oxidizers; their storage and handling procedures; and aircraft fuels.

For related information see also *07 Aircraft Propulsion and Power, 20 Spacecraft Propulsion and Power,* and *44 Energy Production and Conversion.*

**N88-13475#** North Dakota Univ., Grand Forks. Energy Research Center.
**PRODUCTION OF JET FUELS FROM COAL DERIVED LIQUIDS. VOLUME 1: MARKET ASSESSMENT FOR LIQUID BY-PRODUCTS FROM THE GREAT PLAINS GASIFICATION PLANT Interim Report, 20 Jan. - 30 Apr. 1987**
J. E. Sinor Aug. 1987 227 p Prepared in cooperation with Sinor (J. E.) Consultants, Inc. Niwot, Conn.
(Contract MIPR-FY1455-86-N0657; DA Proj. 2480)
(AD-A184846; AFWAL-TR-87-2042-Vol-1) Avail: NTIS HC A11/MF A01 CSCL 21D

In September 1986, the Fuels Branch of the Aero Propulsion Laboratory at Wright-Patterson Air Force Base, Ohio commenced an investigation of the potential of production of jet fuel from the liquid by-product streams produced by the gasification of lignite at the Great Plains Gasification Plant in Buelah, North Dakota. Funding was provided to the Department of Energy (DOE) Pittsburgh Energy Technology Center (PETC) to administer the experimental portion of this effort. This report details the effort of JE Sinor Consultants, who, as a subcontractor to the DOE contract with the University of North Dakota Energy Research Center (UNDERC), determined the market potential of these by-product streams. This report describes the market potential of the by-product streams for the production of phenols, benzene, cresote, cresylic acids, coal tar pitch, paving materials, carbon black, naphthalene, rubber processing oils, as well as jet fuels. GRA

**N88-13476#** Army Armament Research, Development and Engineering Center, Picatinny Arsenal, N.J. Armament Engineering Directorate.
**PERFORMANCE CHARACTERISTICS OF MAGNESIUM-SODIUM NITRATE FLARES IN OXYGEN-NITROGEN ATMOSPHERES**
Patricia L. Farnell and Francis R. Taylor Oct. 1987 29 p
(AD-A185274; ARAED-TR-87027) Avail: NTIS HC A03/MF A01 CSCL 19A

The burning rates and light outputs produced by miniature flares containing magnesium and sodium nitrate have been studied as a function of metal-oxidant ratio and oxygen content of the atmosphere. Also studied were the effects of loading pressure and the use of an organic binder upon the combustion process. In these studies, various atmospheres containing nitrogen and oxygen were used. It was found that the burning rates of the flares were unaffected by the oxygen content of the atmosphere, indicating that radiation feedback from the flame has only a minor influence on the burning rate. It was also found that increasing the loading pressure caused only minor changes in the burning rates of the system indicating that the burning process is not greatly influenced by the reduced gaseous permeability caused by increased loading pressure. However, the burning rate appears to be controlled by exothermic processes occuring at or very near to the burning surface. GRA

**N88-13477#** Societe Nationale Industrielle Aerospatiale, Saint-Medard-en-Jalles (France). Div. Systemes Balistiques et Spatiaux.
**INFLUENCE OF SHOCK WAVE AND GAS PRESSURE ON THE BEHAVIOR OF A PYROTECHNICAL DEVICE [INFLUENCE DE L'ONDE DE CHOC ET DE LA PRESSION GAZEUSE SUR LE FONCTIONNEMENT D'UN PYROMECANISME]**
J. Pascal 5 Feb. 1987 14 p In FRENCH
(SNIAS-872-430-111; ETN-88-91222) Avail: NTIS HC A03/MF A01

The design of explosive actuated plungers is discussed. The preliminary design is made from thermodynamically detonated gas parameters and the estimation of the recoverable energy which may be transmitted to the piston. The results of tests designed to

estimate the overall contribution of shock waves and gas dynamics to piston acceleration are presented. The shock pressure does not appear to have an influence on the gas pressure or piston kinetics. ESA

**N88-13478#** Societe Nationale Industrielle Aerospatiale, Saint-Medard-en-Jalles (France). Div. Systemes Balistiques et Spatiaux.
**ADVANTAGES OF INTERNAL THERMAL PROTECTION IN A PYROTECHNICAL PLUNGER [UTILITE D'UNE PROTECTION THERMIQUE INTERNE DANS UN VERIN PYROTECHNIQUE]**
Michel Pire 8 Jan. 1987 12 p In FRENCH Sponsored by Direction des Engins
(SNIAS-872-430-114; ETN-88-91225) Avail: NTIS HC A03/MF A01

It is shown that for a plunger used in experiments requiring large accelerations for masses up to 200 kg, (powder charge is 300 gr, final velocity of the mass is 4 m/sec) energy exchange between hot gas and walls depends on the internal geometry. The inclusion of an internal thermal protection increases the overall efficiency. ESA

**N88-13479#** Societe Nationale Industrielle Aerospatiale, Saint-Medard-en-Jalles (France). Div. Systemes Balistiques et Spatiaux.
**NUMERICAL SIMULATION APPLIED TO THE DEVELOPMENT OF A PYROTECHNICAL SYSTEM [UTILISATION D'UNE SIMULATION NUMERIQUE LORS DU DEVELOPPEMENT D'UN SYSTEME PYROTECHNIQUE]**
Michel Pire 20 Nov. 1986 18 p In FRENCH Sponsored by Direction des Engins
(SNIAS-872-430-115; ETN-88-91226) Avail: NTIS HC A03/MF A01

A plunger moved by a solid propellant system was designed to be used in experiments requiring the acceleration of masses of up to 200 kg to 4 m/sec. The simulation used in the design phase of such a system is described. The definition of the basic differential equations is discussed. Applications of the model to evaluate the plunger geometry, to contribute to test design, to identify the parameters useful to increase performance, and to guide future plunger design are discussed. ESA

**N88-13480#** Research Inst. of National Defence, Stockholm (Sweden).
**TEST NUMBER 2 OF PROPELLANT FOR ROCKET MOTOR MK52**
Anders Schwartz May 1987 26 p
(PB87-226155; FOA-C-20660-2.1; ISSN-0347-3694; ETN-88-91395) Avail: NTIS HC A03/MF A01

Tensile tests were made on propellants from two rocket motors. Samples from propellants near the motor wall have higher strength than propellant near the bore. Tensile strength decreases with increasing rocket motor age. The tensile strength of propellant cast in carton decreases a little compared with previous measurements. This is valid for low temperatures. Measurement of moisture in propellant from motors indicates that 0.25% to 0.35% moisture is found in the propellant. The moisture may cause decrease of strength with time. A desiccator could be placed in the nozzle to decrease the decomposing effect on propellant of moisture during storing. A new test in 5 yr is recommended. ESA

**N88-13481#** Los Alamos National Lab., N. Mex.
**JET INITIATION OF PBX 9502**
J. M. McAfee Jul. 1987 18 p Presented at the DEA Conference, Schrobenhausen, Fed. Republic of Germany, 1 Jul. 1987
(Contract W-7405-eng-36)
(DE88-000493; LA-UR-87-3169; CONF-8707122-2) Avail: NTIS HC A03/MF A01

Reported is the progress of an effort to determine the quantitative aspects of the initiation of PBX 9502 (95% TATB, 5% Kel-F 800) by copper jets. The particular jet used was that produced by the LAW warhead (66-mm diameter, 42° angle cone, copper-lined, conical shaped charge). Fifteen experiments, in various configurations, have been fired to define the essential parameters for quantitatively measuring the jet performance and initiation of bare PBX 9502. DOE

# 29 MATERIALS PROCESSING

Includes space-based development of products and processes for commercial applications.
For biological materials see *55 Space Biology.*

**N88-13482#** Research Inst. of National Defence, Stockholm (Sweden).
**RESULTS FROM THE MELTING OF TUNGSTEN COMPOSITES UNDER MICROGRAVITY (TEXUS 10 FLIGHT)**
Lars Ekbom Sep. 1987 16 p
(FOA-C-20676-2.1; ISSN-0347-3694; ETN-88-91401) Avail: NTIS HC A03/MF A01

A melting test with tungsten composites on a sounding rocket was done under microgravity. Results show that the particles are evenly distributed and that no segregation due to Marangoni convection occurs. Despite an uneven distribution of the tungsten particles in the performed specimens and the short melting period (12 to 60 sec) the particle distribution becomes even. This shows that the wettability of the molten matrix on tungsten is extreme and thus the capillary force of the liquid is high. The tungsten particles grow from 3 microns to spheres 10 microns in diameter in less than 1 min. This very short time is due to a combination of solving the small tungsten particles in the melt, which increases its tungsten content from 15% to 21%, and the capillary force, which quickly seems to force the particles apart. If the particles can form a low energy boundary they join. In other cases a narrow layer of matrix can stay between the tungsten grains. ESA

# 31 ENGINEERING (GENERAL)

Includes vacuum technology; control engineering; display engineering; cryogenics; and fire prevention.

**N88-13483#** China Nuclear Information Centre, Beijing.
**DEVELOPMENT ON THIN WALL TUBES OF DISPERSION TYPE**
Shien Zhang, Xiyou Wang, Jianshan Li, Rongsheng Zhang, and Zhenshu Xue 1986 11 p In CHINESE; ENGLISH summary Prepared in cooperation with Southwestern Inst. of Nuclear Reactor Engineering, Sichuan, China
(DE87-703384; CNIC-00014; SINRE-0004) Avail: NTIS (US Sales Only) HC A03/MF A01

A method using powder metallurgy and metallic extrusion to manufacture three kinds of magnesium based thin wall tubes of dispersion type is presented. In each case, the composition of dispersed gold, boron and hafnium in magnesium matrix is 0.5 wt%, 1 wt%, 2 wt%, 4 wt% and 8 wt%, respectively. The diameter of the tubes are 20 mm with wall thickness of 1 mm. The process of mixing, compacting, lubricating, heat-extrusion, checking and die designing are described in detail. Measures for controlling tube tolerance and even distribution of dispersion phase, and improving the surface quality are suggested. DOE

**N88-13484#** MMR Technologies, Inc., Mountain View, Calif.
**DEVELOPMENT OF A LOW NOISE 10 K J-T REFRIGERATION SYSTEM Technical Progress Report, 15 Aug. 1986 - 15 Feb. 1987**
William A. Little 15 Feb. 1987 9 p
(Contract N00014-86-C-0301)
(AD-A185258) Avail: NTIS HC A02/MF A01 CSCL 13A

This report summarizes work on the development of a low noise Joule-Thomson, microminiature refrigeration system, designed for 10 K operation. Two events have occurred since the last report which have had an important influence on the confirmation through a series of experimental measurements of

the remarkable cooling power at 80 K to 90 K of the nitrogen-hydrocarbon gas mixtures discussed briefly in the previous report. These experiments confirmed that these mixtures could give a refrigeration an order of magnitude greater than that attainable with argon or nitrogen at the same input pressures. In addition, it was recognized that this high efficiency allowed one to use a heat exchanger of substantially smaller surface area and a compressor designed for operation at much lower pressures. This lower pressure operation would greatly reduce the wear of the piston seals and thereby prolong the life of the system. It was also discovered in the course of these measurements that the use of the gas mixtures resulted in virtually clog-free operation of the refrigerators. GRA

**N88-13485#** British Aerospace Dynamics Group, Bristol (England). Space and Communications Div.
**EVALUATION OF A CRYOGENIC REFRIGERATOR FOR COOLING FOCAL PLANE INSTRUMENTATION Final Report**
B. Joseph, S. T. Werrett, and H. Lowe Paris, France ESA May 1986 147 p
(Contract ESTEC-5098/82-NL-PB)
(BAe-TP-8095-Vol-1; ESA-CR(P)-2424-Vol-1; ETN-88-90884)
Avail: NTIS HC A07/MF A01

The design and performance of a miniature Stirling cycle refrigerator for cooling focal plane instrumentation on ERS and meteorological satellites are described. The accomodation within and the interfaces with three spacecraft payloads are outlined. Causes of two failures which occurred during performance testing were investigated and modifications to prevent any recurrence were made. The design is demonstrated to be suitable for cooling small detector assemblies in a variety of space applications. Although the refrigerator was manufactured in small quantities, no major problems are foreseen with the transfer to commercial quantity production. ESA

**N88-13486#** British Aerospace Dynamics Group, Bristol (England). Space and Communications Div.
**EVALUATION OF A CRYOGENIC REFRIGERATOR FOR COOLING FOCAL PLANE INSTRUMENTATION. APPENDIX B: ACCOMMODATION STUDY Final Report**
B. Joseph, S. T. Werret, and H. Lowe Paris, France ESA May 1986 155 p
(Contract ESTEC-5098/82-NL-PB)
(BAe-TP-8095-Vol-2; BAe-RPT/CCE/014; ESA-CR(P)-2424-Vol-2; ETN-88-90885) Avail: NTIS HC A08/MF A01

It is shown that a miniature Stirling cycle refrigerator can be used to cool an ocean color monitor (OCM) and an optical imaging instrument (OII) on an Earth resources satellite, and an infrared scanner for a meteorological satellite. In the most demanding requirement, cooling the OII detectors, the cooler can cope with a requirement which is impracticable with passive cooling. With less demanding configurations (OCM detectors) adequate spare capacity should be available to permit consideration of detector redundancy provisions. The main requirement of the cooler is for up to 75 W raw electrical power input. That is a two compressor/displacer combination including all control and drive electronics. Study of potential advanced Meteosat requirements shows that accommodation is likely to be easier on a three-axis stabilized spacecraft than on a spin stabilized one. ESA

**N88-13487#** Institut Francais du Petrole, Paris (France).
**DESIGN AND TEST OF HIGH PERFORMANCE COMPOSITE TUBES FOR USE IN DEEP WATER DRILLING AND PRODUCTION SYSTEMS**
Pierre Odru and Yves Massonpierre (Societe Nationale Industrielle Aerospatiale, Saint-Medard-en-Jalles, France ) Paris, France SNIAS 1987 18 p
(SNIAS-872-430-107; ETN-88-91218) Avail: NTIS HC A03/MF A01

High performance composite tubes to be used as marine risers, in deepwater drilling or in production systems were developed. They are composed of several layers with independant functions. Structural layers made of high resistance fibers set in a resin matrix, are filament wound and consist of circumferential layers, perpendicular to the tube axis, to resist bursting stresses, and longitudinal layers, helically wound, to resist axial forces. The tubes are completed with internal and external liners and are terminated at extremities by steel end pieces to which the composite layers are carefully bonded. The concept of high performance composite tubes is described, including their end fittings. Tests were carried out to verify and improve the properties of the pipes, in ultimate conditions (burst pressure up to 170 MPa, ultimate tensile, collapse), as well as fatigue and aging. Results are satisfactory and real applications are envisaged. ESA

**N88-13488#** Societe Nationale Industrielle Aerospatiale, Paris (France).
**HIGH PERFORMANCE COMPOSITE TUBES FOR OFFSHORE APPLICATIONS**
P. J. C. Tamarelle and C. P. Sparks (Institut Francais du Petrole, Paris, France ) 1987 18 p Presented at the Offshore Technology Conference, Houston, Tex. 27-30 Apr. 1987
(SNIAS-872-430-116; ETN-88-91227) Avail: NTIS HC A03/MF A01

The technical aspects of composite tubes are introduced through a series of typical oilfield tubular applications describing design and tests results. The tubes are composed of several layers with independant functions. Structural layers made of high resistance fibers set in a resin matrix, are filament wound and consist of circumferential layers, perpendicular to the tube axis, to resist bursting stresses and longitudinal layers, helically wound, to resist axial forces. The tubes are completed with internal and external liners and are terminated at extremities by steel end pieces to which the composite layers are bonded. Advantages and potential cost savings resulting from the replacement of a conventional steel riser by a composite riser are analyzed for a tension leg platform (TLP) in different water depths, combining the effects on cost of top tension, deck weight, hull size, and mooring loads. ESA

**N88-13489#** Societe Nationale Industrielle Aerospatiale, Suresnes (France). Direction Centrale de la Qualite.
**COMPARISON OF FIRE RESISTANCE OF METALLIC AND NONMETALLIC STRUCTURES [COMPARAISON DE LA RESISTANCE AU FEU DES STRUCTURES METALLIQUES ET NON METALLIQUES]**
C. Kuras 26 Mar. 1986 27 p In FRENCH Presented at Symposium Franco-Sovietique, 5 Dec. 1985
(SNIAS-872-551-101; C-47-888; ETN-88-91233) Avail: NTIS HC A03/MF A01

The behavior of composite materials designed to substitute metallic structural elements is analyzed. Laboratory tests were performed exposing the specimens to fire while subjected to flexure loading. Specimens were either monolithic or sandwich. While light alloy specimens are perforated within 3 to 6 min, the carbon fiber composites hold without perforation in 10 min tests. ESA

**N88-13490#** University of Petroleum and Minerals, Dhahran (Saudi Arabia).
**TRANSIENT DEVELOPMENT OF STRATIFICATION IN A PARTIALLY DIVIDED ENCLOSURE**
D. R. Otis and G. F. Jones 1987 7 p Presented at the Symposium on Technology of Glass, Ceramic, or Glass-Ceramic to Metal Sealing, Boston, Mass., 13 Dec. 1987 Prepared in cooperation with Los Alamos National Lab., N. Mex.
(Contract W-7405-eng-36)
(DE87-011742; LA-UR-87-2135; CONF-871207-8) Avail: NTIS HC A02/MF A01

In passive solar heating of buildings or in compartment fires, we are concerned with the development of thermal stratification when two rooms at different temperatures are connected by the opening of a door. We have performed experiments and numerical calculations aimed at this application. The experiments consist of flow visualization and temperature measurements obtained when isolated halves of a tank containing water at two different temperatures are suddenly connected to allow flow between the

zones. Two significant findings from this work are: (1) the presence of internal waves excited by the onset of flow through the doorway which have not normally been observed in past laboratory experiments, and (2) the equilibration time is found to be in general agreement with that predicted by a formula from a simple orifice model that we describe. Work is progressing on numerical simulations using two core stratification models connected by an orifice including entrainment in the neighborhood of the connection. DOE

**N88-13491#** Los Alamos National Lab., N. Mex.
**COMPUTER CODE SIMULATIONS OF EXPLOSIONS IN FLOW NETWORKS AND COMPARISON WITH EXPERIMENTS**
W. S. Gregory, B. D. Nichols, J. A. Moore, P. R. Smith, R. G. Steinke, and R. D. Idzorek Oct. 1987 70 p
(Contract W-7405-eng-36)
(DE88-001946; LA-11069-MS) Avail: NTIS HC A04

A program of experimental testing and computer code development for predicting the effects of explosions in air-cleaning systems is being carried out for the Department of Energy. This work is a combined effort by the Los Alamos National Laboratory and New Mexico State University (NMSU). Los Alamos has the lead responsibility in the project and develops the computer codes; NMSU performs the experimental testing. The emphasis in the program is on obtaining experimental data to verify the analytical work. The primary benefit of this work will be the development of a verified computer code that safety analysts can use to analyze the effects of hypothetical explosions in nuclear plant air cleaning systems. The experimental data show the combined effects of explosions in air-cleaning systems that contain all of the important air-cleaning elements (blowers, dampers, filters, ductwork, and cells). A small experimental set-up consisting of multiple rooms, ductwork, a damper, a filter, and a blower was constructed. Explosions were simulated with a shock tube, hydrogen/air-filled gas balloons, and blasting caps. Analytical predictions were made using the EVENT84 and NF85 computer codes. The EVENT84 code predictions were in good agreement with the effects of the hydrogen/air explosions, but they did not model the blasting cap explosions adequately. NF85 predicted shock entrance to and within the experimental set-up very well. The NF85 code was not used to model the hydrogen/air or blasting cap explosions. DOE

**N88-13641*#** West Virginia Univ., Morgantown. Dept. of Civil Engineering.
**SIGNIFICANCE OF FOUNDATION-SOIL SEPARATION IN DYNAMIC SOIL-STRUCTURE INTERACTION**
Constantine C. Spyrakos and P. N. Patel *In* NASA-Marshall Space Flight Center, The 58th Shock and Vibration Symposium, Volume 1 Oct. 1987 p 495-506 (For primary document see N88-13609 05-39)
Avail: NTIS HC A21/MF A01 CSCL 13B

# 32 COMMUNICATIONS AND RADAR

Includes radar; land and global communications; communications theory; and optical communications.

For related information see also *04 Aircraft Communications and Navigation* and *17 Space Communications, Spacecraft Communications, Command and Tracking.* For search and rescue see *03 Air Transportation and Safety,* and *16 Space Transportation.*

**N88-13492#** Science Research Council, Chilton (England). Rutherford Appleton Lab.
**NOISE MODELLING IN THE TIME DOMAIN WITH THE AID OF SPICE**
J. Lewis Mar. 1986 42 p
(PB87-221941; RAL-86-104) Avail: NTIS HC E04/MF E04 CSCL 20N

The facility for completely modelling noise in the time domain is not available in a simulator such as Spice. A general technique is detailed for noise having a power law with an index = or greater than (-1) such as shot noise, thermal noise or flicker noise. The technique uses the circuit model created in Spice and shows how Spice can contribute to the computation. Particular reference is made to Field Effect Transistor technology. Author

**N88-13493#** Communications Research Centre, Ottawa (Ontario). Radar and Communications Technology Branch.
**MEASURED CHARACTERISTICS OF 800/900 MHz MOBILE RADIO CHANNELS WITH HIGH-ANGLE PROPAGATION THROUGH MODERATELY DENSE FOLIAGE**
R. J. C. Bultitude Feb. 1986 81 p
(CRC-1398) Avail: NTIS HC A05/MF A01

The digital transmission capacity of randomly fading multipath radio channels is limited to that for which the bandwidth of transmission is much less than the coherence bandwidth (B sub c) of the channel. It is therefore important for system design purposes to determine B sub c in propagation environments where the use of digital radio systems is planned. Experiments that were conducted under conditions similar to those which would be typical on 800/900 MHz satellite-mobile channels in rural environments were detailed. The impulse response functions of measured channels were estimated by operating a pseudo-noise channel probe from a 65 m tower through deciduous trees to a receiver at close range. Measurement results include: channel impulse response estimates, angle of arrival analyses, envelope fading statistics, and double-sided frequency correlation plots. Comparisons are between channel characteristics during the summer and during the autumn when the leaves have fallen from the trees. Estimates of digital channel capacity limitations are also given. Author

**N88-13494** British Broadcasting Corp., Kingswood (England). Engineering Div.
**DIGITAL VIDEO BIT-RATE REDUCTION: DPCM FOR SUB-NYQUIST PAL**
J. H. Stott Oct. 1987 30 p
(BBC-RD-1987/16) Avail: Issuing Activity

Differential pulse-code modulation (DPCM) is a technique for bit-rate reduction. The principles of DPCM and its application to television are discussed. An investigation of the use of DPCM with sub-Nyquist sampled composite PAL video signals is then described. The usefulness of computer optimization techniques is established and practical development work described. It is concluded that three-dimensional predictors, of a complexity not previously envisaged to be worthwhile, offer significant improvements. Two systems meeting practical requirements for 34 and 68 Mbit/s transmission packages were developed and subjectively assessed. Author

**N88-13495** British Broadcasting Corp., Kingswood (England). Engineering Div.
**IMPROVEMENTS TO A UHF REBROADCAST TELEVISION LINK SUFFERING TIDAL FADING: COUNTISBURY UHF RELAY STATION**
J. H. Moore Sep. 1987 10 p
(BBC-RD-1987/14) Avail: Issuing Activity

The Countisbury UHF relay station serves the localities of Lynmouth and Lynton in North Devon. For some time, the problems of co-channel interference and tidal fading have on occasion been evident . Results obtained utilizing a new Rebroadcast LINK (RBL) antenna array are given. The RBL has improved considerably the quality of signals received at this relay station. Details are also given of apparatus which enables sampled television picture sequences to be recorded on a VHS video cassette recorder. The channel identification, date and time are derived from the teletext signal and superimposed at the top of the picture.
Author

**N88-13496** British Broadcasting Corp., Kingswood (England). Engineering Div.
**TELEVISION MOTION MEASUREMENT FOR DATV AND OTHER APPLICATIONS**
G. A. Thomas Sep. 1987 24 p
(BBC-RD-1987/11) Avail: Issuing Activity

G. A. Thomas Sep. 1987 24 p
(BBC-RD-1987/11) Avail: Issuing Activity

Almost all picture processing operations that work in the temporal domain can benefit from knowledge of the speed and direction of moving objects in the scene. Generally, motion vector measurement techniques developed so far do not work well enough for broadcast quality applications. The Report reviews four existing techniques, and suggests some novel extensions to a technique based on phase correlation. The results of simulating this technique on a computer image processing system are reported. Several specific applications have been investigated, including temporal standards conversion and bandwidth reduction in a system using DATV (Digitally Assisted Television). The results are encouraging, and suggest that the proposed vector measurement technique can be used successfully in critical broadcast quality applications.
Author

**N88-13497** Rice Univ., Houston, Tex.
**HF SIDEBANDS IN THE IONOSPHERE Ph.D. Thesis**
Zhong-Hao Huang 1987 146 p
Avail: Univ. Microfilms Order No. DA8718727

Sidebands on the high frequency (HF) waves received from two transmitted waves separated by small frequency intervals were first observed by Gordon and Ganguly in January, 1984 at Arecibo, Puerto Rico. Papadopoulos proposed that HF sidebands would arise from the nonlinear interaction of an ELF wave with the two high frequency waves. The nonlinear mechanism for ELF and HF sideband generation is parametric decay of a HF radio wave into a low frequency compression Alfven wave and a high frequency sideband. In 1984 Fejer proposed another nonlinear mechanism (phase modulation theory) for HF sideband generation. Fejer points out that the effect of the ponderomotive force is a reduction in the electron density and an increase in the phase delay which is greater for more powerful waves. Numerical solutions show that the phase decay would relate to the power density of the HF wave. This modulation index theory using the WKB approximation shows that the amplitude of sidebands is related to: the effective HF power; the HF frequency; the temperature of the electrons; the scale height of the ionosphere; and the difference frequency of the two pump waves. Observations of HF sidebands were again made in January, 1986. The 430 MHz incoherent radar provided the ionospheric background measurements. The modulation index theory provides the most complete interpretation of the observations.
Dissert. Abstr.

**N88-13498#** Georgia Inst. of Tech., Atlanta.
**AN INVESTIGATION OF MILLIMETER WAVE PROPAGATION IN THE ATMOSPHERE: MEASUREMENT PROGRAM Final Report, 21 Sep. 1981 - 31 Mar. 1987**
R. W. McMillan and R. A. Bohlander 17 Jun. 1987 188 p
(Contract DAAG29-81-K-0173)
(AD-A184837; ARO-18457.12-GS) Avail: NTIS HC A09/MF A01 CSCL 20N

This report describes work done on Contract DAAG29-81-K-0173, An Investigation of Millimeter Wave Propagation in the Atmosphere: Measure Program, conducted by the Georgia Tech Research Institute during the period September 1981 through May 1987. The objective was to measure the effects of atmospheric turbulence on the propagation of millimeter wave radiation, with emphasis on inclement weather effects. Five separate measurement sessions were conducted at a site near Urbana, Illinois, and these measurements were made jointly with personnel from the National Oceanic and Atmospheric Administration, who furnished meteorological instrumentation and information on experiment design. Personnel from the Atmospheric Sciences Laboratory at White Sands Missile Range also contributed to this program. Measurements were made at frequencies near 118, 142, 173, and 230 GHz to cover all of the major atmospheric features in the millimeter wave spectral range, and were made during clear air, rain, fog, and snow. The equipment comprised a small step-van transmitter truck and an array of four receivers, pumped by a common local oscillator, mounted on a semi-trailer.
GRA

**N88-13499#** Naval Postgraduate School, Monterey, Calif.
**THE USE OF COAXIAL TRANSMISSION LINE ELEMENTS IN LOG-PERIODIC DIPOLE ARRAYS M.S. Thesis**
Robert E. Tarleton, Jr. Jun. 1987 170 p
(AD-A184864) Avail: NTIS HC A08/MF A01 CSCL 09A

This thesis examines the feasibility of designing a log-periodic dipole array (LPDA) with coaxial transmission line elements and comparing the resulting operational bandwidth with that of a conventional LPDA. Using the Numerical Electromagnetics Code (NEC), a coaxial dipole was modeled to optimize the bandwidth and then used as the element in a variety of uniform arrays. Different types of element connections were examined including switched series, switched parallel, and unswitched parallel. The results of NEC for each of the arrays are plotted as K-BETA diagrams to compare to the standard arrays. The results of the investigation show that the Snyder dipole provides more operational bandwidth than a standard dipole, but when placed in a uniform array there is no more bandwidth than that of a conventional uniform array.
GRA

**N88-13500#** Naval Research Lab., Washington, D.C.
**AN EXACT ANALYSIS AND PERFORMANCE OF FRAMED ALOHA WITH CAPTURE Interim Report**
J. E. Wieselthier, A. Ephremides, and L. A. Michaels 4 Sep. 1987 41 p
(AD-A185006; NRL-MR-6056) Avail: NTIS HC A03/MF A01 CSCL 15B

This paper presents an exact analysis of Framed ALOHA that is based on the use of a new combinatorial technique. This model can accommodate a general model for capture, in which the probability that one packet is received successfully depends on the number of packets involved in the collision. Performance results are presented for both uncontrolled and dynamically controlled systems.
GRA

**N88-13501#** Office of Naval Research, London (England).
**ITALY'S INSTITUTE OF RESEARCH ON ELECTROMAGNETIC WAVES--THE ISTITUTO DI RICERCA SULLE ONDE ELETTROMAGNETICHE**
Daniel J. Collins 10 Aug. 1987 6 p
(AD-A185020; ONRL-7-021-R) Avail: NTIS HC A02/MF A01 CSCL 17E

The activity of this laboratory are reviewed. Of particular interest is the work in micro-optics and optical sensors, integrated optics, remote sensing, and signal processing.
GRA

**N88-13502#** Massachusetts Inst. of Tech., Cambridge. Research Lab. of Electronics.
**TIME DOMAIN ELECTROMAGNETIC WAVES IN MULTILAYERED MEDIA Final Report, 1 Apr. 1985 - 31 Mar. 1987**
Jin-Au Kong Jun. 1987 7 p
(Contract DAAG29-85-K-0079)
(AD-A185055; ARO-21375.2-EL) Avail: NTIS HC A02/MF A01 CSCL 20N

This work has (1) modeled and calculated the impedance parameters of strip lines with perpendicularly crossing strips and computed the transient response on such structures, (2) analyzed the effects of periodical meshed ground planes on signal propagation, (3) generalized the method of characteristics for signal propagation on nonuniformly coupled transmission lines, (4) studied the transient response of arbitrary source excitation on two-layer media, and (5) studied the models of vias for interchip connections.
GRA

**N88-13503#** Spectral Sciences, Inc., Burlington, Mass.
**MODTRAN: A MODERATE RESOLUTION MODEL FOR LOWTRAN Technical Report, 12 May 1986 - 11 May 1987**
Alexander Berk, Lawrence S. Bernstein, and David C. Robertson 8 Jul. 1987 40 p
(Contract F19628-86-C-0079)
(AD-A185384; SSI-TR-124; AFGL-TR-87-0220; SR-1) Avail: NTIS HC A03/MF A01 CSCL 20N

This interim technical report describes a new band model formulation for the LOWTRAN 6 atmospheric transmittance/radiation computer code. Band model parameters for H2O, CO2, O3, CO, CH4, O2, and N2 were calculated using the 1986 HITRAN line atlas. They were calculated for 1/cm bins from 0 - 17,900/cm and at five temperatures from 200 to 300K. This transmittance model and associated subroutines have been integrated into LOWTRAN 6. The spectral resolution of this new option is better than 5/cm (FWHM). A preliminary version of the code has been delivered to AFGL for testing. Validation against FASCOD2 calculations will be the emphasis for the remainder of this effort. GRA

**N88-13504#** Illinois Univ., Urbana. Coordinated Science Lab.
**EIGENVALUE PROJECTION THEORY FOR LINEAR OPERATOR EQUATIONS OF ELECTROMAGNETICS**
A. F. Peterson Sep. 1987 54 p
(Contract N00014-84-C-0149)
(AD-A185434; UILU-ENG-87-2252) Avail: NTIS HC A04/MF A01 CSCL 20C

Equations representing realistic electromagnetics problems seldom yield exact solutions, and thus are usually treated numerically. In general, a discretization procedure such as the method of moments (also known as the weighted residual method) is used to convert the original continuous equation to a finite-dimensional matrix equation. A theory is presented that demonstrates the relation between the eigenvalue spectrum of the original, continuous operator and the eigenvalues of the method-of-moments matrix. In addition, an equivalence between the finite difference method and the method of moments is developed that permits the theory to be applied to finite-difference equations. Examples involving differential and integral equations are used to confirm the theory and to illustrate the typical eigenvalue spectrum arising in electromagnetic field problems. GRA

**N88-13505#** Satel Conseil, Paris (France).
**STUDY OF THE FEASIBILITY OF A SATELLITE COMMUNICATION SYSTEM FOR ROAD TRANSPORTATION HOME OFFICE TO VEHICLE COMMUNICATION. VOLUME 1: CONCEPTUAL ANALYSIS Final Report [ETUDE DE L'INTERET DES TRANSPORTEURS ROUTIERS POUR UN SYSTEME DE COMMUNICATION PAR SATELLITE AVEC LES VEHICULES. TOME 1: ANALYSE DE CONCEPTS]**
Paris, France ESA Jul. 1987 68 p In FRENCH Prepared in cooperation with the Institut du Transport Aerien
(Contract ESA-6023/84-F-RD(SC))
(SC/87-E/6-Vol-1; ESA-CR(P)-2458-Vol-1; ETN-88-91152) Avail: NTIS HC A04/MF A01

Several scenarios were proposed to potential users, including extension of the ground cell system, the INMARSAT public system, the LOCSTAR system (localization and transmission of short messages), and the adapted SYCOMORES and LAMEX satellite systems. Road vehicle long distance communication with central office is discussed. The feasibility, covering area, investment, and costs are discussed for each of the scenarios. No final choice is made. The balance of each scenario is nevertheless presented. ESA

**N88-13506#** Satel Conseil, Paris (France).
**STUDY OF THE FEASIBILITY OF A SATELLITE COMMUNICATION SYSTEM FOR ROAD TRANSPORTATION HOME OFFICE TO VEHICLE COMMUNICATION. VOLUME 2: MARKET STUDY Final Report [ETUDE DE L'INTERET DES TRANSPORTEURS ROUTIERS POUR UN SYSTEME DE COMMUNICATION PAR SATELLITE AVEC LES VEHICULES. TOME 2: ETUDES DE MARCHE]**
Georges Haessig and Catherine Pouessel Paris, France ESA Jul. 1987 82 p In FRENCH Prepared in cooperation with the Institut du Transport Aerien
(Contract ESA-6023/84-F-RD(SC))
(SC/87-E/6-Vol-2; ESA-CR(P)-2458-Vol-2; ETN-88-91153) Avail: NTIS HC A05/MF A01

Road vehicle long distance communication (Mediterranean or Arab countries) with their central office is considered. Satellite communication provides a means for private networks operating with slightly degraded quality so as not to compete with public telecommunication networks. It is concluded that the real prospective market in this area is from a minimum of 2500 to a maximum of 7500 private channels. ESA

**N88-13507#** Societe Nationale Industrielle Aerospatiale, Saint-Medard-en-Jalles (France). Lab. d'Essais Electromagnetiques.
**MEASUREMENTS IN AN ELECTROMAGNETIC TEST LABORATORY [LES MESURES DANS UN LABORATOIRE D'ESSAIS ELECTROMAGNETIQUES]**
Bernard Raveu 18 Jan. 1987 7 p In FRENCH
(SNIAS-872-430-102; ETN-88-91213) Avail: NTIS HC A02/MF A01

Electromagnetic compatibility test equipment and the specially built strong electromagnetic pulses immunity test system, developed in order to control the characteristics of aerospace communication systems, are described. The compatability tests are carried out at frequencies from 10KHz to 10GHz in a Faraday cage. Measurement is implemented with an optical transmission bus. The extremely high voltage pulse generator assembled for immunity testing is based on Marx generators. Measurement and command are made via optical circuits. ESA

**N88-13508#** Societe Nationale Industrielle Aerospatiale, Saint-Medard-en-Jalles (France). Lab. d'Essais Electromagnetiques.
**ELECTROMAGNETIC TESTS [LES ESSAIS ELECTROMAGNETIQUES]**
Bernard Raveu 29 Jan. 1987 8 p In FRENCH Sponsored by Direction des Engins
(SNIAS-872-430-103; ETN-88-91214) Avail: NTIS HC A02/MF A01

The laboratory measuring instruments and the measuring method used to determine the frequency dependent transfer impedance of a transmission cable and connection defects in a cable network are described. It is shown that the procedure accuracy and reproducibility are excellent. The implementation of high voltage pulses (several megavolt) generators based on a Marx type device and its various applications are also described. ESA

**N88-13509#** Societe Nationale Industrielle Aerospatiale, Saint-Medard-en-Jalles (France). Div. des Systemes Strategiques et Spatiaux.
**NUMERICAL AND ANALYTICAL STUDY OF THE EQUIVALENT PERMITTIVITY OR PERMEABILITY OF NONHOMOGENEOUS MATERIALS. APPLICATION TO THE EXPERIMENTAL ELECTROMAGNETIC CHARACTERIZATION OF COMPOSITES [ETUDE NUMERIQUE ET ANALYTIQUE DE LA PERMITTIVITE ET DE LA PERMEABILITE EQUIVALENTES DES MATERIAUX NON-HOMOGENES. APPLICATION A LA CARACTERISATION ELECTROMAGNETIQUE EXPERIMENTALE DES COMPOSITES]**
Bernard Guillou 27 Jan. 1987 20 p In FRENCH; ENGLISH summary
(SNIAS-872-430-104; ETN-88-91215) Avail: NTIS HC A03/MF A01

A method to infer a general formulation for the real part of the equivalent permittivity in the case of large wavelengths is presented. In the general cases of flat dielectric multilayers, a numerical method is described. It is based on multiplying the matrix corresponding to each slab and the transmission coefficients of a homogeneous material with the equivalent permittivity and permeability. Numerical results for typical two layer composites which allow to find the behavior of imaginary parts of the dielectric constants of the inhomogeneous specimen are shown. ESA

**N88-13510#** Centre National de la Recherche Scientifique, Toulouse (France). Lab. d'Automatique et d'Analyse des Systemes.

**CONTRIBUTION TO OPTIMAL FLOW IN NETWORKS. A EXPERIMENTAL MULTIPROCESSOR FOR ASYNCHRONOUS ITERATION IMPLEMENTATION Ph.D. Thesis - Toulouse. Univ., France**

Gerard Authie 1987 210 p In FRENCH; ENGLISH summary
(LAAS-87-269; ETN-88-91236) Avail: NTIS HC A10/MF A01

The problem of optimal flow determination is considered in relation with packet-switched communication networks. For linear cost problems, a unifying presentation of classical methods is done, enabling graphic interpretations. For convex cost, a dual approach which incorporates an iteration control mechanism and stopping test based on a comparison between the dual function and the associated primal cost is derived. An extension to optimal multicommodity network flow problems is proposed. Parallelism and asynchronous iterations are also discussed. ESA

**N88-13511#** Research Inst. of National Defence, Stockholm (Sweden).

**LARGE BANDWIDTH GROUND SCATTERING MODEL**

Hans Hellsten Jul. 1987 20 p
(FOA-C-30458-3.2; ISSN-0347-3708; ETN-88-91405) Avail: NTIS HC A03/MF A01; Research Institute of National Defence, Stockholm, Sweden KR 50

A model for diffraction limited radar backscatter from natural terrain is outlined. The radar is assumed capable of achieving linear resolution on the ground of wavelength order, as for a SAR adopting a large synthetic aperture length and a low frequency radar band of large relative bandwidth. The frequencies are so low that the ground surface may be assumed reasonably smooth and well defined. Vegetation is invisible. Physical optics is well suited for the computation. The radar signal is represented by complex numbers, while the scattering amplitude is split into a complex linear and a complex skew-linear part. Polarization effects may be completely accounted for, by a minimum of notation. The freedom from notational redundancy is important in treatment of inverse scattering, retrieving the ground topography on the basis of diffraction limited SAR data. It is demonstrated that for scalar Kirchoff theory to be even approximately correct, the ground must undulate only gently with respect to the chosen state of linear polarization. ESA

**N88-13512#** Research Inst. of National Defence, Linkoeping (Sweden).

**INVERSE SCATTERING ANALYSIS OF DIFFRACTION LIMITED SAR**

Hans Hellsten Jul. 1987 21 p
(FOA-C-30459-3.2; ISSN-0347-3708; ETN-88-91406) Avail: NTIS HC A03/MF A01; Research Institute of National Defence, Stockholm, Sweden KR 50

The inverse problem of reconstructing the ground topography on the basis of SAR data is set up and solved analytically. The solution incorporates compensation for antenna effects. An interferometric antenna configuration is understood, since a single antenna cannot illuminate the ground on just one side of the aircraft over the frequency band intended. The inversion process leads to a two dimensional Poisson equation for the ground surface angular height function, the source density of the equation corresponding to the conventional SAR ground reflectivity. Because the shape of the ground is described relative to the aircraft, there is a certain latitude in this description, relating to aircraft motions, which do not affect radar data. The boundary conditions of the equation are invoked accordingly. A topographic map at the resolution of the radar bandwidth is obtained (1 m resolution for a 10 to 100 MHz signal). ESA

**N88-13513*#** National Aeronautics and Space Administration. Lewis Research Center, Cleveland, Ohio.

**COMMUNICATIONS PAYLOAD CONCEPTS FOR GEOSTATIONARY FACILITIES**

William A. Poley and Jack Lekan Dec. 1987 96 p
(NASA-TM-100154; E-3353; NAS 1.15:100154) Avail: NTIS HC A05/MF A01 CSCL 17B

Summarized and compared are the major results of two NASA sponsored studies that defined potential communication payload concepts to meet the satellite traffic forecast for the turn of the century for the continental US and Region 2 of the International Telecommunications Union. The studies were performed by the Ford Aerospace and Communications Corporation and RCA Astro-Electronics (now GE-RCA Astro-Space Division). Future scenarios of aggregations of communications services are presented. Payload concepts are developed and defined in detail for nine of the scenarios. Payload costs and critical technologies per payload are also presented. Finally the payload concepts are compared and the findings of the reports are discussed. Author

**N88-13514#** Federal Communications Commission, Columbia, Md. Engineering Evaluation Branch.

**TWO-SIGNAL CROSS MODULATION EFFECTS, HALF-IF EFFECTS AND INTERFERENCE CRITERIA IN LAND MOBILE SHARING WITH UHF (ULTRA HIGH FREQUENCY) TELEVISION**

H. Davis Feb. 1987 27 p
(PB87-228037; EEB-86-5) Avail: NTIS HC A03/MF A01 CSCL 20N

Interference effects were observed from two interference signals in the second adjacent channel (cross modulation) and from interference signals in or related to the fourth upper adjacent channel (half-IF effects). Data on these interference effects were obtained in connection with an FCC docket on further sharing of the UHF television band by private land mobile radio services. Statistically, the half-IF effects appear to result in desired to undesired signal ratios which are similar to those found for cross modulation. GRA

**N88-13515*#** National Aeronautics and Space Administration. Lewis Research Center, Cleveland, Ohio.

**AN EVOLUTIONARY COMMUNICATIONS SCENARIO FOR MARS EXPLORATION**

Steven M. Stevenson 1987 31 p Presented at The Case For Mars 3, Boulder, Colo., 18-22 Jul. 1987; sponsored by the American Astronautical Society
(NASA-TM-100263; E-3892; NAS 1.15:100263) Avail: NTIS HC A03/MF A01 CSCL 17B

As Mars exploration grows in complexity with time, the corresponding communication needs will grow in variety and complexity also. From initial Earth/Mars links, further needs will arise for complete surface connectivity for the provision of navigation, position location, and voice, data, and video communications services among multiple Mars bases and remote exploration sites. This paper addresses the likely required communication functions over the first few decades of Martian exploration and postulates systems for providing these services. Required technologies are identified and development requirements indicated. Author

**N88-13516*#** Notre Dame Univ., Ind. Dept. of Electrical Engineering.

**ERROR CONTROL TECHNIQUES FOR SATELLITE AND SPACE COMMUNICATIONS Semiannual Status Report**

Daniel J. Costello, Jr. Jan. 1988 90 p
(Grant NAG5-557)
(NASA-CR-181581; NAS 1.26:181581) Avail: NTIS HC A05/MF A01 CSCL 17B

Progress made in the following areas is discussed: concatenated codes using bandwidth efficient Trellis inner codes; bounds on the minimum free Euclidean distance of bandwidth efficient Trellis inner codes; performance analysis of bandwidth Trellis codes on channels with phase jitter; construction of bandwidth efficient Trellis codes; and parity retransmission hybrid ARQ using convolutional codes. B.G.

# 33 ELECTRONICS AND ELECTRICAL ENGINEERING

Includes test equipment and maintainability; components, e.g., tunnel diodes and transistors; microminiaturization; and integrated circuitry.

For related information see also *60 Computer Operations and Hardware* and *76 Solid-State Physics.*

**N88-13517#** Enviro-Management and Research, Inc., Springfield, Va.
**SURVEY STATE OF THE ART: ELECTRICAL LOAD MANAGEMENT TECHNIQUES AND EQUIPMENT Final Report, 2 May - 23 Oct. 1986**
N. Khosla 31 Oct. 1986 230 p
(Contract DAAK70-86-C-0035)
(AD-A184083) Avail: NTIS HC A11/MF A01 CSCL 10B

The feasibility of solid state cells based on lithium ion conducting polymer electrolytes has been demonstrated. A preliminary investigation of sodium and magnesium ion conductors in polymer electrolyte cells is summarized. Cell types were Li/V6O13, Na/V6O13, and Mg/V6O13 with polymer electrolytes based on polyethylene oxide and salts of the anode element. GRA

**N88-13518*#** Prairie View Agricultural and Mechanical Coll., Tex. Dept. of Electrical Engineering.
**A STUDY OF CHARGED PARTICLES/RADIATION DAMAGE TO VLSI DEVICE MATERIALS Final Report**
John G. Okyere Sep. 1987 139 p
(Contract NAS9-17136)
(NASA-CR-172036; NAS 1.26:172036; DRL-T-1862; DRD-SE-1118T; PVAMU-EE093087JGO1A) Avail: NTIS HC A07/MF A01 CSCL 09C

Future spacecraft systems such as the manned space station will be subjected to low-dose long term radiation particles. Most electronic systems are affected by such particles. There is therefore a great need to understand device physics and failure mechanisms affected by radiation and to design circuits that would be less susceptible to radiation. Using 2 MeV electron radiation and bias temperature aging, it was found that MOS capacitors that were prepositively biased have lower flatband voltage shift and lesser increase in density of surface state charge than those that were not prepositively biased. In addition, it was shown that there is continued recovery of flatband voltage and density of state charge in irradiated capacitors during both room temperature anneal and 137 degree anneal. When nMOS transistors were subjected to 1 MeV proton radiation, charge pumping and current versus voltage measurements indicated that transconductance degradation, threshold voltage shifts and changes in interface states density may be the primary cause of nMOS transistor failure after radiation. Simulation studies using SPICE were performed on CMOS SRAM cells of various transistor sizes. It is shown that transistor sizing affects the noise margins of CMOS SRAM cells, and that as the beta ratio of the transistors of the CMOS SRAM cell decreases, the effective noise margin of the SRAM cell increases. Some suggestions were made in connection with the design of CMOS SRAMS that are hardened against single event upsets. Author

**N88-13519#** Aerospace Corp., El Segundo, Calif. Lab. Operations.
**HIGH ENERGY DENSITY RECHARGEABLE BATTERIES FOR AEROSPACE POWER REQUIREMENTS**
Albert H. Zimmerman and D. M. Speckman 3 Aug. 1987 37 p
(Contract F04701-85-C-0086)
(AD-A184883; TR-0086A(2945-01)-1; SD-TR-87-43) Avail: NTIS HC A03/MF A01 CSCL 10C

In light of power requirements for search missions the rechargeable battery and fuel cell technologies that are expected to be available for these missions are identified, and areas of technology development that will be required for each energy storage system are indicated. The general conclusions are that the nickel cadmium and nickel hydrogen battery systems will be able to satisfy the space power needs through the early 1990s, after which a significantly higher energy density system will be required, particularly for geosynchronous and mid-altitude orbit missions. The sodium sulfur battery is the only system projected to meet the requirements of the most power intensive missions that are expected to operate in higher orbits by the mid-1990s. For low earth orbit missions the nickel hydrogen battery system is expected to provide the required power levels, except in situations where very high peak power levels are required. The hydrogen oxygen regenerative fuel cell is best suited to satisfying the high peak power needs in large power systems, but must undergo significant development to obtain the needed system life. GRA

**N88-13520#** Naval Postgraduate School, Monterey, Calif.
**EVALUATION OF DEVICE FIGURE OF MERIT IN MICROWAVE SWITCHING CIRCUIT DESIGN M.S. Thesis**
Pitak Pibultip Jun. 1987 93 p
(AD-A184896) Avail: NTIS HC A05/MF A01 CSCL 09A

In microwave switching circuit design, a switching-semiconductor figure of merit can be defined and used as the measure of device switching effectiveness. Research switching-semiconductor figures of merit were applied to general switching circuits. Computer-aided circuit analysis program (Touchstone), and a Fortran program were used for the computation of switching circuit performance. GRA

**N88-13521#** Naval Postgraduate School, Monterey, Calif.
**AN INVESTIGATION OF UNIPOLAR ARCING AT ATMOSPHERIC PRESSURE IN ALUMINUM 2024 AND ALUMINUM COATED GLASS SLIDES M.S. Thesis**
Steven W. Woodson Jun. 1987 54 p
(AD-A184903) Avail: NTIS HC A04/MF A01 CSCL 20I

An experimental investigation of unipolar arcing at atmospheric pressure was conducted using Aluminum 2024 and glass slides with a thin coating of pure aluminum. The plasma was produced on the surface using a neodymium-glass laser in the Q-switched mode. It was found that the power density required for the onset of unipolar arcing was similar to that of samples irradiated in a vacuum, although the size and density of the resulting craters were significantly different. GRA

**N88-13522#** Rit Research Corp., Rochester, N.Y.
**ELECTROMAGNETICS AND ELECTROTHERMAL APPROACH TO EVALUATE FAILURES IN MICROELECTRONIC DEVICES CAUSED BY ELECTROSTATIC DISCHARGES: STOCHASTICAL ASPECTS OF THE DEVICE RELIABILITY Final Report, for 1984 - 1987**
Perambur S. Neelakantaswamy Aug. 1987 364 p
(Contract N00014-84-K-0532)
(AD-A184906; RITRC-014) Avail: NTIS HC A16/MF A01 CSCL 20C

Summarized are the following research projects: Interaction of electromagnetic overstresses, such as electrostatic discharge (ESD) from microelectronic devices, resulting IC damage(s) and methods of preventing related failures. GRA

**N88-13523#** Marconi Electronic Devices Ltd., Lincoln (England).
**OPTICALLY TUNED MM-WAVE IMPATT SOURCE Final Report**
D. A. Williams Jul. 1987 81 p
(Contract DAJA45-84-C-0045; DA Proj. 1L1-61102-BH-57)
(AD-A185250) Avail: NTIS HC A05/MF A01 CSCL 09A

The analytic theory of optical tuning in IMPATT oscillators developed in the initial phase of the work has been extended and generalised. Accuracy of the theory in predicting tuning at the higher oscillator voltage swings has been greatly improved by reformulating the Bessel function series used to express avalanche gain. A model for optical injection locking, where the oscillator output is locked to a microwave intensity modulated optical signal, has also been developed. The computer model for optical control has been modified to study the tuning behaviour of Ku-Band IMPATTs, as used in the recent experimental work. Work on optical tuning speed studies has also been extended. The experimental program has produced a number of developments. A delay line discriminator has been used to measure the tuning speed in

response to a step change in illumination level. It has been found that a frequency shift of 1.4mhz at W-Band could be achieved in less than 20ns and a frequency shift of 5.6MHz at Ka-Band in less than 10ns. GRA

**N88-13524#** Calculon Corp., Rockville, Md.
**HUMAN ENGINEERING LABORATORY GROUNDING ANALYSIS (HELGA)-2 Final Report**
Walter N. McJilton and Charles R. Beek Jul. 1987 79 p
(Contracts DAAK11-84-D-0008; DA Proj. 1L1-62716-AH-70)
(AD-A185367; HEL-TN-4-87) Avail: NTIS HC A05/MF A01
CSCL 13L

This report documents the development of an alternate earth grounding technique for tactical applications, specifically to correct the human factors issues associated with the 6-foot ground rod currently in wide use throughout the Army. Three alternate grounding systems were identified and tested at several field sites that represented a broad variety of environments. The three alternate designs tested were copper screen mats, horizontal surface wire with ground pegs, and horizontal buried wire. The results showed that the surface wire configuration is the best overall design. The study also indicated that, the performance of installed ground systems and potential grounding sites should be measured. A null-balance earth tester would serve that purpose. The Army should publish revised guidance on tactical grounding practices. GRA

**N88-13525#** Air Force Systems Command, Wright-Patterson AFB, Ohio. Foreign Technology Div.
**NEW BREAKTHROUGH IN CHINESE INTEGRATED CIRCUITS: SUCCESSFUL DEVELOPMENT OF HIGH-SPEED CMOS CIRCUITS**
Suifu Wang 23 Sep. 1987 7 p
(AD-A185381; FTD-ID(RS)T-0008-87) Avail: NTIS HC A02/MF A01 CSCL 09A

In the field of high-speed logic circuits, the new bipolar type integrated circuits have held a prominent position for some time now. Unfortunately, a fatal flaw of the bipolar type circuit is that power dissipation is high and, consequently, they are greatly limited in application. Since CMOS circuits have the distinctive advantages of low power dissipation and good anti-interference properties they are looked upon with favor. The shortcoming of the CMOS circuit is that its speed is rather low. In the early 80's, integrated circuits entered the VLSI era and were successfully developed one after another using micro-processing technology as the core, thus improving the CMOS circuits so that they entered the ranks of the high-speed logic circuits. GRA

**N88-13526#** Technische Univ., Munich (West Germany). Lehrstuhl fuer Elektrische Messtechnik.
**ESTABLISHMENT OF COMPLETE MINIMUM TEST SETS FOR DIGITAL CIRCUITS WITH SAFETY ENGINEERING SIGNIFICANCE Ph.D. Thesis [ERSTELLUNG VOLLSTAENDIGER MINDESTTESTMENGEN FUER DIGITALE SCHALTUNGEN MIT SICHERHEITSTECHNISCHER BEDEUTUNG]**
Gerhard Kadzioch 1986 152 p In GERMAN
(ETN-88-90599) Avail: NTIS HC A08/MF A01

A method that provides minimum test sets for switching networks and minimum test sequences for sequential switching circuits was developed. The method represents the digital circuits in equivalent circuits where testing is simpler. The method was realized in a FORTRAN 5 program on a Cyber computer. Minimum test sets can be calculated for switching networks with a size of up to 100 gates, 14 inputs, and 14 outputs, and for sequential circuits with 4 times smaller dimensions. Minimum test sets for switching networks with the option of recognition of short circuit faults and terminal faults are presented. ESA

**N88-13527#** Centre National de la Recherche Scientifique, Toulouse (France). Lab. d'Automatique et d'Analyse des Systemes.
**DIGITAL CONTROL OF A DIRECT CURRENT CONVERTER FOR A HYBRID VEHICLE Ph.D. Thesis - Inst. National Polytechnique de Toulouse, France**
Juan Manuel Hernandez 1987 96 p In FRENCH; ENGLISH summary Sponsored by CONACYT, Mexico
(LAAS-87-266; ETN-88-91235) Avail: NTIS HC A05/MF A01

The nonlinear feedback loops permitting the large signal control of pulse width modulators in direct current converters are discussed. A digital feedback loop on a converter controlling the coupling of a direct current machine is described. It is used in the propulsion of a hybrid vehicle (thermal-electric) with regenerative braking. The protection of the power switches is also studied. An active protection of the MOST bipolar transistor association is proposed. ESA

**N88-13528#** Consiglio Nazionale delle Ricerche, Frascati (Italy). Ist. di Fisica dello Spazio Interplanetario.
**CAPACITIVE RESONANT TRANSDUCER FOR THE FRASCATI GRAVITATIONAL ANTENNA [TRASDUTTORE RISONANTE CAPACITIVO PER L'ANTENNA GRAVITAZIONALE DI FRASCATI]**
M. Visco Jul. 1986 27 p In ITALIAN
(IFSI-86-9; ETN-88-91281) Avail: NTIS HC A03/MF A01

The design of the transducer for the 390 kg cryogenic gravitational antenna is described. A SQUID amplifier which is a Josephson junction superconductor amplifying device was adopted. The noise temperature is thus reduced to near the quantic limit. ESA

**N88-13529#** Technische Hogeschool, Eindhoven (Netherlands).
**LOW-CURRENT BEHAVIOR AND CURRENT CHOPPING OF VACUUM ARCS Ph.D. Thesis**
Rene Peter Paul Smeets 1987 146 p
(ISBN-90-9001649-X; ETN-88-91364) Avail: NTIS HC A07/MF A01

A connection between microscopic processes in the cathode spot of a vacuum (copper) discharge, and the phenomenon of current chopping, inherent to the interruption of ac power currents, is illustrated. It is shown that current chopping of an ac current is equivalent to the inability of a dc arc to maintain itself indefinitely at low currents. After a lifetime ranging over 6 orders of magnitude at arc currents from 4 to 40A, a dc arc always extinguishes spontaneously. Instabilities occur over the whole arc lifetime, aggravated the lower the arc current is. The phenomena that accompany an instability can be described by a transient arc resistance. To assure a continued operation of the discharge as a whole, a sufficient amount of metal vapor must be supplied. A large inductance enhances arc stability. ESA

**N88-13530#** Communications Satellite Corp., Clarksburg, Md.
**MAKING SPACE NICKEL/HYDROGEN BATTERIES LIGHTER AND LESS EXPENSIVE**
J. D. Dunlop and R. Beauchamp 1987 23 p Presented at the DARPA Conference, Monterey, Calif., 6 Aug. 1987 Prepared in cooperation with Johnson Controls, Inc., Milwaukee, Wis.
(Contract DE-AC04-76DP-00789)
(DE88-000168; SAND-87-7153C; CONF-8708157-1) Avail: NTIS HC A03/MF A01

A multi-kilowatt-hour nickel/hydrogen battery was designed and developed for terrestrial applications. This battery consists of individual Ni/H cells contained within a common pressure vessel (IC-CPV). Cost studies projected a substantial reduction in manufacturing costs over present aerospace Ni/H batteries. This same design approach is recommended for development of aerospace batteries. An aerospace design concept of an IC-CPV battery is presented. The objective was to make a comparison between this new design approach and the present aerospace technology using individual pressure vessel (IPV) cells. Results of this study show the following potential advantages for this IC-CPV

design approach: a 15/1 reduction in cost, a 50% improvement in energy density, and a 3/1 reduction in volume. DOE

# 34 FLUID MECHANICS AND HEAT TRANSFER

Includes boundary layers; hydrodynamics; fluidics; mass transfer; and ablation cooling.

For related information see also *02 Aerodynamics* and *77 Thermodynamics and Statistical Physics.*

**N88-13531#** Toronto Univ. (Ontario). Inst. for Aerospace Studies.
**A COMPLETE LINEARIZED THEORY FOR THE ANALYSIS AND DESIGN OF TWO-DIMENSIONAL HYDROFOILS NEAR A FREE SURFACE**
P. Piperni Oct. 1987 154 p
(UTIAS-TN-264; ISSN-0082-5263) Avail: NTIS HC A08/MF A01

The results of a limited application of the theory are also included. Specifically, the separate effects of hydrofoil thickness, camber, angle of incidence, and trailing edge flap effectiveness are investigated. Pressure distributions on a NACA 4 digit series hydrofoil are also computed and discussed. In addition, hydrofoil sections are designed for two specified pressure loadings. The effects of depth and Froude number on the resulting section designs are investigated. Finally, the analytical method presented is utilized to calculate the free surface waves generated by a near-surface hydrofoil. In addition, an expression for the wave resistance is also presented. In essence, the present theory demonstrates that the free surface acts as a coupling agent between the symmetric and asymmetric components of the hydrofoil geometry and loading. In particular it is shown that the vorticity density is dependent on the sectional thickness as well as on the camberline geometry, in contrast to the infinite fluid case. In the design problem, the thickness function is found to be dependent on both the even and odd components of the pressure distribution. For Froude numbers greater than approximately 1.0, the free surface has the effects of decreasing the lift of the hydrofoil significantly. For Froude numbers lower than this, the free surface is shown to have the opposite effect. Author

**N88-13532** Virginia Polytechnic Inst. and State Univ., Blacksburg.
**A CARTESIAN FINITE-VOLUME METHOD FOR THE EULER EQUATIONS Ph.D. Thesis**
Sang Keun Choi 1987 100 p
Avail: Univ. Microfilms Order No. DA8718994

A numerical procedure was developed for the computation of inviscid flows over arbitary, complex two-dimensional geometries. The Euler equations are solved using a finite volume method with a nonbody-fitted Cartesian grid. A numerical formulation for complicated body geometries is developed in conjunction with implicit flux-splitting schemes. A variety of numerical computations were performed to validate the numerical methodologies developed. Computations for supersonic flow over a flat plate with an impinging shock wave are used to verify the numerical algorithm, without geometric considerations. The supersonic flow over a blunt body is utilized to show the accuracy of the nonbody-fitted Cartesian grid, along with the shock resolution of the flux-vector splitting scheme. Geometric complexities are illustrated with the flow through a two-dimensional supersonic inlet with and without an open bleed door. The ability of the method to deal with subsonic and transonic flows is illustrated by computations over a nonlifting NACA 0012 airfoil. The method is shown to be accurate, efficient, and robust and should prove to be particularly useful in a preliminary design mode, where flows past a wide variety of complex geometries can be computed without complicated grid generation procedures. Dissert. Abstr.

**N88-13533** Georgia Inst. of Tech., Atlanta.
**SOLUTION PROCEDURE FOR THE NAVIER-STOKES EQUATIONS APPLIED TO ROTORS Ph.D. Thesis**
Brian Ernest Wake 1987 204 p
Avail: Univ. Microfilms Order No. DA8718407

A solution procedure for the unsteady, three-dimensional Navier-Stokes equations was developed and applied to helicopter rotors. The procedure is an efficient hybrid ADI scheme in which the radial and viscous terms are treated explicitly. This procedure solves the Navier-Stokes equations in a time-accurate manner. Steady solutions are obtained by marching through time and asymptotically converging to steady state. Turbulence is included by an algebraic eddy-viscosity model. An unsteady grid is utilized to incorporate the blade motion. Arbitrary motions due to cyclic pitch, flapping, lead-lag motions, and aeroelastic deflections can also be incorporated into the unsteady grid terms. The equations are formulated for a curvilinear coordinate system, enabling completely arbitrary rotor-blade geometries. To account for the effect of the rotor wake, the transpiration-velocity technique is used. Quasi-steady Euler calculations were made for a high-speed nonlifting ONERA blade. Unsteady Euler and Navier-Stokes calculations were also performed for this configuration to examine the viscous and unsteady effects. Lifting hover results were made for a two-bladed rotor with 0012 blade airfoil sections. For this case, a detailed qualitative comparison with experimental results in the tip region is done. Also, unsteady Euler results were obtained for a lifting OLS rotor. Dissert. Abstr.

**N88-13534** California Univ., Berkeley.
**THE SIMULATION OF THE VISCOUS FLOW AROUND A CYLINDER BY THE RANDOM VORTEX METHOD Ph.D. Thesis**
Erik Charles Tiemroth 1986 244 p
Avail: Univ. Microfilms Order No. DA8718185

The ability to calculate the loads on cylindrical members is of great importance in offshore engineering. The random vortex method (RVM) is applied to simulate steady, uniform incident flow over a cylinder and the flow about a cylinder in a free surface wave field. Tent functions are used to model the vortex sheets at the boundary and a Rankine core function is used for the vortex blobs. Second-order accurate time integration and random walk diffusion algorithms are used. One of the most difficult problems with the RVM is the computational requirements of the convection calculations. The exact solution to this problem involves O(N sup 2) calculations, where N is the number of vortex blobs. A highly accurate method based on series expansion is introduced that is capable of reducing the computational requirements to O(N sup 1.4). Simulations for the case of steady, uniform incident flow were made for Reynolds numbers of 4,000 to 95,000. Comparison was made with experiments and finite difference calculations for the case of Reynolds number 9,500. The observed flow structures agreed well with the simulated flow. Simulations of the wave flows was also successful. The predicted forces agreed with experimental results within 10 to 20 percent for a range of incident wave lengths and amplitudes. The simulated vorticity fields provided an interpretation of the typical shapes seen in experimentally derive force curves, in which the various regions could be associated with the degree of vorticity formation and shedding.
Dissert. Abstr.

**N88-13535#** Los Alamos National Lab., N. Mex.
**STATISTICAL THEORY OF TURBULENT INCOMPRESSIBLE MULTIMATERIAL FLOW Ph.D. Thesis**
B. Kashiwa Oct. 1987 217 p
(Contract W-7405-eng-36)
(DE88-000435; LA-11088-T) Avail: NTIS HC A11/MF A01

Interpenetrating motion of incompressible materials is considered. Turbulence is defined as any deviation from the mean motion. Accordingly a nominally stationary fluid will exhibit turbulent fluctuations due to a single, slowly moving sphere. Mean conservation equations for interpenetrating materials in arbitrary proportions are derived using an ensemble averaging procedure, beginning with the exact equations of motion. The result is a set of conservation equations for the mean mass, momentum and

fluctuational kinetic energy of each material. The equation system is at first unclosed due to integral terms involving unknown one-point and two-point probability distribution functions. In the mean momentum equation, the unclosed terms are clearly identified as representing two physical processes. One is transport of momentum by multimaterial Reynolds stresses, and the other is momentum exchange due to pressure fluctuations and viscous stress at material interfaces. Closure is approached by combining careful examination of multipoint statistical correlations with the traditional physical technique of kappa-epsilon modeling for single-material turbulence. This involves representing the multimaterial Reynolds stress for each material as a turbulent viscosity times the rate of strain based on the mean velocity of that material. The multimaterial turbulent viscosity is related to the fluctuational kinetic energy kappa, and the rate of fluctuational energy dissipation epsilon, for each material. Hence a set of kappa and epsilon equations must be solved, together with mean mass and momentum conservation equations, for each material. Both kappa and the turbulent viscosities enter into the momentum exchange force. The theory is applied to: (1) calculation of the drag force on a sphere fixed in a uniform flow, (2) calculation of the settling rate in a suspension, and (3) calculation of velocity profiles in the pneumatic transport of solid particles in a pipe. DOE

**N88-13536#** Stanford Univ., Calif. Thermosciences Div.
**EXPERIMENTAL STUDY OF THE FLUID MECHANICS OF UNSTEADY TURBULENT BOUNDARY LAYERS Final Report, 3 Jul. 1983 - 6 Jan. 1986**
G. J. Brereton and W. C. Reynolds May 1987 258 p
(Contract DAAG29-83-K-0056)
(AD-A184856; TF-29; ARO-19976.4-EG) Avail: NTIS HC A12/MF A01 CSCL 20D

An experimental study of the effects of forced, free-stream unsteadiness on turbulent boundary layers was undertaken in an effort to characterize the nature of such flows and to provide guidance for turbulence modelers. A turbulent boundary layer, which had developed under steady, constant-pressure conditions, was locally subjected to a range of frequencies of sinusoidal free-stream unsteadiness. The response of the boundary layer to these free-stream effects was studied through simultaneous measurements of the u and v components of the velocity field, using a two-color laser-doppler anemometer. To focus on the distinct behaviors of the deterministic and time-averaged fields of flow, the equations of fluid motion were reformulated according to a triple decomposition of velocity and pressure into (1) a time-averaged measure, (2) a deterministic or organized, unsteady measure, and (3) a turbulent measure. GRA

**N88-13537#** Air Force Inst. of Tech., Wright-Patterson AFB, Ohio.
**DYNAMICS OF PROPELLANT FEEDLINE SYSTEMS M.S. Thesis**
William F. Berrier, Jr. May 1987 119 p
(AD-A184865; AFIT/GA/AA/85D-2) Avail: NTIS HC A06/MF A01 CSCL 21H

A generalized computer code for the simulation of fluid transients is assembled, verified, and applied. The solution method developed for the program is based on a method of characteristics solution of the equations of motion for one-dimensional fluid flow in pipelines. The differential equations were solved using a first-order finite difference technique. Boundary conditions for the equations of motion were developed or directly included from available component models. The computer routines were verified from several sources. The agreement between the results of this study and the published data was quite good for a wide range of boundary conditions and pipe systems. Recommendations were made for improvement of some models and the replacement of others to further improve the accuracy of the results. GRA

**N88-13538#** North Carolina State Univ., Raleigh. Dept. of Mathematics.
**NONLINEAR HYPERBOLIC CONSERVATION LAWS Final Technical Report, 1 Oct. 1985 - 31 May 1987**
Michael Shearer 17 Aug. 1987 6 p
(Contract DAAL03-86-K-0004)
(AD-A184963; ARO-23326.6-MA) Avail: NTIS HC A02/MF A01 CSCL 07D

The focus of this research project has been the study of systems of conservation laws that lose strict hyperbolicity. Two areas of application, namely isentropic gas dynamics for a van der Waals gas, and multiphase flow in a porous medium were considered. Additionally, a numerical study of the elastic string equations using Glimm's random choice method has been completed. GRA

**N88-13539#** Naval Ship Research and Development Center, Bethesda, Md.
**AN EXPERIMENTAL INVESTIGATION OF APPENDAGE-FLAT PLATE JUNCTION FLOW. VOLUME 2. ELLIPTICAL NOSE APPENDAGE DATA BASE Final Report**
Stuart C. Dickinson Dec. 1986 45 p
(AD-A184974; DTNSRDC-86/052-Vol-2) Avail: NTIS HC A03/MF A01 CSCL 20D

A horseshoe root vortex secondary flow forms at the junction of a flat plate and an appendage, creating a three-dimensional, separated flow. Flow visualizations and pressure measurements were made for two appendage shapes at zero angle of attack with a turbulent incoming boundary layer. The entire data base for this flow is presented in this report. The velocity data are presented graphically as boundary-layer traverses, and in tabular form. These data are intended for researchers interested in the specific details of the flow or as a test case for numerical modeling. GRA

**N88-13540#** Stanford Univ., Calif. Center for Large Scale Scientific Computation.
**A NOTE ON THE USE OF SYMMETRIC LINE GAUSS-SEIDEL FOR THE STEADY UPWIND DIFFERENCED EULER EQUATIONS**
William A. Mulder 29 Jul. 1987 11 p
(Contract N00014-82-K-0335)
(AD-A185223; CLASSIC-87-20) Avail: NTIS HC A03/MF A01 CSCL 20D

Symmetric Line Gauss-Seidel (SLGS) relaxation, when used to compute steady solutions to the upwind differences Euler equations of gas dynamics, is shown to be unstable. The instability occurs for the long waves. If SLGS is used in a multigrid scheme, stability is restored. However, the use of an unstable relaxation scheme will not provide a robust multigrid code. Damped Symmetric Point Gauss-Seidel relaxation is stable and provides similar multigrid convergence rates at much lower cost. However, it fails if the flow is aligned with the grid over a substantial part of the computational domain. Damped Alternating Direction Line Jacobi relaxation can overcome this problem. GRA

**N88-13541#** Alabama Univ., Birmingham. Dept. of Mathematics.
**DISPLAYING THREE-DIMENSIONAL DATA Final Report, 1 Jul. 1983 - 30 Jun. 1984**
Letitia Korbly and Peter V. ONeil 1987 2 p
(Contracts AF-AFOSR-83-0247; AF Proj. 2304)
(AD-A185347; AFOSR-87-1190TR) Avail: NTIS HC A02/MF A01 CSCL 20D

The objective of the project was to graphically represent data obtained in the course of solving equations of fluid dynamics. Studies of three-dimensional data were done with data arising from a fluid dynamics problem involving high temperatures and velocities. Three representational methods were used: (1) particle tracings showing vectors pointing in the direction of flow at a point, 2) representation of contours, and 3) ray tracing, with color values assigned to a cell depending on the values of some quantity such as density. GRA

**N88-13542#** California Univ., Davis. Dept. of Mechanical Engineering.
**CONDITIONAL SECOND ORDER CLOSURE FOR TURBULENT SHEAR FLOWS Final Report, Jul. 1984 - Jun. 1987**
W. Kollman 26 Aug. 1987 59 p
(Contracts AF-AFOSR-84-0219; AF Proj. 2307)
(AD-A185369; AFOSR-87-0992TR) Avail: NTIS HC A04/MF A01 CSCL 20D

Second order turbulence closure models for conditional moments and the intermittency factor were developed. Methods for the treatment of turbulent/non-turbulent and other scalar interfaces were applied to the plane mixing layer and round jet. Multiscale closure models based on the dissipation rate were developed and applied to homogeneous turbulence and the plane jet. Scalar transport was investigated using the separation probability of clusters of particles and numerical solutions based on stochastic simulation techniques. A direct extension of conditional closure to velocity-scalar pdf equations was also developed. GRA

**N88-13543#** Dayton Univ., Ohio.
**ASYMPTOTIC ANALYSIS OF A TURBULENT BOUNDARY LAYER IN A STRONG ADVERSE PRESSURE GRADIENT Interim Report, 1 Jan. - 31 Jul. 1987**
William B. Bush and L. Krishnamurthy Jul. 1987 57 p
(Contract F49420-85-C-0137)
(AD-A185406; AFOSR-87-0962TR) Avail: NTIS HC A04/MF A01 CSCL 20D

The structure of an incompressible turbulent boundary layer subjected to a strong adverse pressure gradient is studied by means of an asymptotic analysis of the Reynolds time-averaged equations. Limit-process expansions developed in the limit of large Reynolds number reveal a relatively thick nondefect layer in the outer region of the boundary layer near the exterior inviscid flow, and a relatively thin layer near the wall. To leading orders of approximation, the momentum balance involves convection, pressure gradient, and turbulent stress in the outer layer, and pressure gradient, and turbulent and viscous stresses in the inner layer. The asymptotic expansions for these two layers are matched in an arbitrary intermediate region, wherein the streamwise velocity has a square-root dependence and the Reynolds stress has a corresponding linear dependence on the normal coordinate. The leading-order approximations for the outer and inner layers give rise to similarity formulations, from which appropriate similarity formulations for the distinguished intermediate layer have been identified and developed. These latter formulations are employed to analyze available experimental data. GRA

**N88-13544#** Institut Franco-Allemand de Recherches, St. Louis (France).
**TRAJECTORY CONTROL USING LATERALLY EJECTED JETS. LITERATURE REVIEW [DIE FLUGBAHNSTEUERUNG MITTELS SEITLICH AUSTRETENDER STRAHLEN. LITERATURUEBERSICHT]**
K. W. Naumann and J. Srulijes 7 Oct. 1985 140 p In GERMAN
(ISL-R-117/85; ETN-88-90633) Avail: NTIS HC A07/MF A01

Trajectory control by jets from the fluid mechanics point of view is reviewed. The most important models are presented and discussed. ESA

**N88-13545#** Institut Franco-Allemand de Recherches, St. Louis (France).
**INVESTIGATION OF THE EFFECT OF LATERALLY EJECTED GAS JETS ON FLOWS Final Report [UNTERSUCHUNG UEBER DIE BEEINFLUSSUNG VON STROEMUNGEN DURCH SEITLICH AUSTRETENDE GASSTRAHLEN]**
G. Patz 14 Feb. 1986 28 p In GERMAN
(Contract BMVg-T/R-760/F-0001/F-1701)
(ISL-R-107/86; ETN-88-90635) Avail: NTIS HC A03/MF A01

The effect of a gas jet, ejected through a hole in the wall, on the supersonic flow along that wall was simulated in a model measuring chamber in a shock tube. A head wave with an obliquely detaching shock was formed, accompanied by a pressure increase in front of the jet. This effect can be used for missile control. In the shock tube, the flow about a plane plate with a slit through which a gas jet was laterally ejected, was simulated. Flow visualization and wall pressure measurements in front of and behind the nozzle slit show the effect of the jet on the flow, and allow the analysis of the initial phase and the evaluation of the forces resulting from the wall pressure which add to the jet thrust. ESA

**N88-13546#** Royal Netherlands Meteorological Inst., De Bilt. Afdeling Fysische Meteorologie.
**ACTIVE AND PASSIVE PLUME DISTRIBUTION MODELS IN THE CONVECTIVE BOUNDARY LAYER USING A LARGE EDDY SIMULATION MODEL [ACTIEVE EN PASSIEVE PLUIMVERSPREIDINGSMODELLEN IN DE CONVECTIEVE GRENSLAAG MET EEN LARGE EDDY SIMULATIEMODEL]**
Paul deValk Aug. 1986 84 p In DUTCH; ENGLISH summary
(KNMI-TR-90; B8700739; ISSN-0169-1708; ETN-88-90816)
Copyright Avail: NTIS HC A05/MF A01

The behavior of byoyant and nonbuoyant plumes in a convective boundary layer is described using a large eddy model. The equation, domain, boundary conditions, numerical solution methods and shortcomings, and organization of the model are discussed. For various stack heights, the results for nonbuoyant plumes agree with laboratory results and parameterizations within the standard deviation. These parameterizations are probably also applicable for the distribution of a buoyant plume near the source. The plume-rise formula of Briggs overestimates the plume rising in comparison with the results of the large eddy model. However, the plume-rise formula describes the model results satisfactorily if it is (after correction) applied to a line source, used in the large eddy model. The extra turbulence, due to the buoyancy of the warm plume, seems to lead to an extra distribution in the lateral direction at a long distance from the source. ESA

**N88-13547#** Universite de Technologie de Compiegne (France).
**UTILIZATION OF A HIGH RATE VECTOR COMPUTER IN COMPUTATIONAL FLUID MECHANICS FOR AERONAUTICS Final Report [UTILISATION D'UN PROCESSEUR VECTORIEL A GRAND DEBIT POUR DES CALCULS EN MECANIQUE DES FLUIDES A FINALITE AERONAUTIQUE]**
Michel Vayssade 1986 68 p In FRENCH
(Contract DRET-84-164)
(ETN-88-91171) Avail: NTIS HC A04/MF A01

A finite element numerical model, used for the solution of Navier-Stokes equation for incompressible flow was adapted to the FPS-164 vector computer and optimized. The computer capacity is 99 megaflops and is equipped with 4 matrix algebra acceleration (MAX) cards operating in SIMD mode. The results obtained are limited due to disk unit input-output delay and problems derived from the MAX card architecture. ESA

**N88-13548#** Institut de Mecanique des Fluides de Toulouse (France). Transferts en Ecoulements Laminaires et Turbulents.
**PHYSICAL ANALYSIS AND NUMERICAL SIMULATION OF COHERENT TURBULENT STRUCTURES IN MIXED LAYERS, JETS, AND WAKES Final Report [ANALYSE PHYSIQUE ET SIMULATION NUMERIQUE DES STRUCTURES TOURBILLONNAIRES COHERENTES DES COUCHES DE MELANGE, DES JETS ET DES SILLAGES]**
M. Braza, H. HaMinh, A. Kourta, and A. Sevrain 1987 256 p In FRENCH and ENGLISH
(Contract DRET-84-190)
(ETN-88-91183) Avail: NTIS HC A12/MF A01

The numerical analysis of flow configurations, characterized by the fact that unsteady flow appears naturally, is studied in order to contribute to the development of unsteady turbulent flow in complex geometric configurations. The method used to solve the Navier-Stokes equation for cases including complex geometries is discussed. Viscous unsteady flow of a flat jet, the unsteady viscous flow of a mixing layer, the unsteady viscous turbulent flow around a cylinder, and the unsteady turbulent and viscous flow around a wing profile are described. ESA

**N88-13549*#** National Aeronautics and Space Administration. Ames Research Center, Moffett Field, Calif.
**VORTICAL FLOWS RESEARCH PROGRAM OF THE FLUID DYNAMICS RESEARCH BRANCH**
Aug. 1986 28 p
(NASA-TM-88332; A-86324; NAS 1.15:88332) Avail: NTIS HC A03/MF A01 CSCL 20D

The research interests of the staff of the Fluid Dynamics Research Branch in the general area of vortex flows are summarized. A major factor in the development of enchanced maneuverability and reduced drag by aerodynamic means is the use of effective vortex control devices. The key to control is the use of emerging computational tools for predicting viscous fluid flow in close coordination with fundamental experiments. In fact, the extremely complex flow fields resulting from numerical solutions to boundary value problems based on the Navier-Stokes equations requires an intimate relationship between computation and experiment. The field of vortex flows is important in so many practical areas that a concerted effort in this area is justified. A brief background of the research activity undertaken is presented, including a proposed classification of the research areas. The classification makes a distinction between issues related to vortex formation and structure, and work on vortex interactions and evolution. Examples of current research results are provided, along with references where available. Based upon the current status of research and planning, speculation on future research directions of the group is also given. Author

**N88-13550#** California Inst. of Tech., Pasadena. Firestone Lab.
**NUMERICAL ANALYSIS, COMPUTING AND FUNDAMENTAL STUDIES IN FLUID MECHANICS Summary Report, 1 Apr. 1986 - 31 Mar. 1987**
1987 7 p
(Contract DE-AS03-76ER-72012)
(DE88-001912; DOE/ER-72012/T5; SR-12) Avail: NTIS HC A02/MF A01

This report describes work completed and work in progress on the following topics: vortex dynamics and vortical flows; Hele-Shaw fingering at small values of surface tension; numerical methods for stiff differential equations; pattern formation in solidifying systems; path instability in rising bubbles; and multigrid solvers for partial differential equations. DOE

**N88-13551*#** Alabama A & M Univ., Normal. School of Engineering and Technology.
**LOW THRUST VISCOUS NOZZLE FLOW FIELDS PREDICTION Annual Report No. 1, 1986-1987**
Goang-Shin Liaw Dec. 1987 34 p
(Grant NAG8-064)
(NASA-CR-182334; NAS 1.26:182334) Avail: NTIS HC A03/MF A01 CSCL 20D

An existing Navier-Stokes code (PARC2D) was used to compute the nozzle flow field. Grids were generated by the interactive grid generator codes TBGG and GENIE. All computations were made on the NASA/MSFC CRAY X-MP computer. Comparisons were made between the computations and MSFC in-house wall pressure measurements for CO2 flow through a conical nozzle having an area ratio of 40. Satisfactory agreements exist between the computations and measurements for different stagnation pressures of 29.4, 14.7, and 7.4 psia, at stagnation temperature of 1060 R. However, agreements did not match precisely near the nozzle exit. Several reasons for the lack of agreement are possible. The computational code assumes a constant gas gamma, whereas the gamma i.e. the specific heat ratio for CO2 varied from 1.22 in the plenum chamber to 1.38 at the nozzle exit. The computations also assumes adiabatic and no-slip walls. Both assumptions may not be correct. Finally, it is possible that condensation occurs during the nozzle expansion at the low stagnation pressure. The next phase of the work will incorporate variable gamma and slip wall boundary conditions in the computational code and develop a more accurate computer code. Author

**N88-13552*#** National Aeronautics and Space Administration. Lewis Research Center, Cleveland, Ohio.
**MEASUREMENT OF LOCAL CONVECTIVE HEAT TRANSFER COEFFICIENTS FROM A SMOOTH AND ROUGHENED NACA-0012 AIRFOIL: FLIGHT TEST DATA**
James E. Newton, G. James VanFossen, Phillip E. Poinsatte, and Kenneth J. DeWitt (Toledo Univ., Ohio.) 1988 17 p Presented at the 26th Aerospace Sciences Meeting, Reno, Nev., 11-14 Jan. 1988; sponsored by AIAA
(NASA-TM-100284; E-3924; NAS 1.15:100284; AIAA-88-0287)
Avail: NTIS HC A03/MF A01 CSCL 20D

Wind tunnels typically have higher free stream turbulence levels than are found in flight. Turbulence intensity was measured to be 0.5 percent in the NASA Lewis Icing Research Tunnel (IRT) with the cloud making sprays off and around 2 percent with cloud making equipment on. Turbulence intensity for flight conditions was found to be too low to make meaningful measurements for smooth air. This difference between free stream and wing tunnel conditions has raised questions as to the validity of results obtained in the IRT. One objective of these tests was to determine the effect of free stream turbulence on convective heat transfer for the NASA Lewis LEWICE ice growth prediction code. These tests provide in-flight heat transfer data for a NASA-0012 airfoil with a 533 cm chord. Future tests will measure heat transfer data from the same airfoil in the Lewis Icing Research Tunnel. Roughness was obtained by the attachment of small, 2 mm diameter hemispheres of uniform size to the airfoil in three different patterns. Heat transfer measurements were recorded in flight on the NASA Lewis Twin Otter Icing Research Aircraft. Measurements were taken for the smooth and roughened surfaces at various aircraft speeds and angles of attack up to four degrees. Results are presented as Frossling number versus position on the airfoil for various roughnesses and angles of attack. Author

**N88-13265#** Ishikawajima-Harima Heavy Industries Co. Ltd., Tokyo (Japan).
**NUMERICAL PREDICTION OF TURBULENT FLOWS IN DUMP DIFFUSERS**
Yasunori Ando, Masafumi Kawai, Yukinori Sato, and Hidemi Toh *In* National Aerospace Lab., Proceedings of the 4th NAL Symposium on Aircraft Computational Aerodynamics Dec. 1986 p 91-98 In JAPANESE; ENGLISH summary (For primary document see N88-13253 05-02)
Avail: NTIS HC A14/MF A01

**N88-13272#** Tokyo Metropolitan Univ. (Japan). Coll. of Aeronautical Engineering.
**NUMERICAL ANALYSIS OF AXISYMMETRIC FLOW WITH H2-O2 REACTIONS**
Shizui Watanabe *In* National Aerospace Lab., Proceedings of the 4th NAL Symposium on Aircraft Computational Aerodynamics Dec. 1986 p 151-157 In JAPANESE; ENGLISH summary (For primary document see N88-13253 05-02)
Avail: NTIS HC A14/MF A01

**N88-13275#** Chiba Univ. (Japan). Faculty of Engineering.
**NUMERICAL SIMULATION OF SPLASH OF DROPLET AT UNIT GRAVITY**
Nobuhide Nishikawa, Takashi Suzuki, and Satoshi Akiyama *In* National Aerospace Lab., Proceedings of the 4th NAL Symposium on Aircraft Computational Aerodynamics Dec. 1986 p 173-179 In JAPANESE; ENGLISH summary (For primary document see N88-13253 05-02)
Avail: NTIS HC A14/MF A01

**N88-13277#** Tokyo Univ. (Japan). Dept. of Aeronautics.
**FLOW VISUALIZATION IN COMPUTATIONAL FLUID DYNAMICS**
Susumu Shirayama and Kunio Kuwahara *In* National Aerospace Lab., Proceedings of the 4th NAL Symposium on Aircraft Computational Aerodynamics Dec. 1986 p 191-195 In JAPANESE; ENGLISH summary (For primary document see N88-13253 05-02)
Avail: NTIS HC A14/MF A01

**N88-13283#** Tokyo Univ. (Japan). Dept. of Engineering.
**RELAXATION METHOD FOR THE COMPRESSIBLE NAVIER-STOKES EQUATIONS USING UPWIND SCHEMES**
Shigeru Obayashi, Kozo Fujii (National Aerospace Lab., Tokyo, Japan ), and Kunio Kuwahara *In* National Aerospace Lab., Proceedings of the 4th NAL Symposium on Aircraft Computational Aerodynamics Dec. 1986 p 249-254 In JAPANESE; ENGLISH summary (For primary document see N88-13253 05-02)
Avail: NTIS HC A14/MF A01

**N88-13284#** Keio Univ., Tokyo (Japan). Dept. of Engineering.
**COMPUTATION OF FLOW AROUND 2-D CIRCULAR CYLINDER**
Takashi Ohta, Susumu Shirayama, Kiichirou Takeda, and Kunio Kuwahara (Tokyo Univ., Japan ) *In* National Aerospace Lab., Proceedings of the 4th NAL Symposium on Aircraft Computational Aerodynamics Dec. 1986 p 255-265 In JAPANESE; ENGLISH summary (For primary document see N88-13253 05-02)
Avail: NTIS HC A14/MF A01

# 35 INSTRUMENTATION AND PHOTOGRAPHY

Includes remote sensors; measuring instruments and gages; detectors; cameras and photographic supplies; and holography.

For aerial photography see *43 Earth Resources and Remote Sensing*. For related information see also *06 Aircraft Instrumentation*, and *19 Spacecraft Instrumentation*.

**N88-13553*#** Information and Control Systems, Inc., Hampton, Va.
**DEVELOPMENT OF RESPONSE MODELS FOR THE EARTH RADIATION BUDGET EXPERIMENT (ERBE) SENSORS. PART 3: ERBE SCANNER MEASUREMENT ACCURACY ANALYSIS DUE TO REDUCED HOUSEKEEPING DATA Final Report**
Sang H. Choi, Dan A. Chrisman, Jr., and Nesim Halyo 20 Mar. 1987 45 p
(Contract NAS1-16130)
(NASA-CR-178294; NAS 1.26:178294; FR-687105-Pt-3) Avail: NTIS HC A03/MF A01 CSCL 14E

The accuracy of scanner measurements was evaluated when the sampling frequency of sensor housekeeping (HK) data was reduced from once every scan to once every eight scans. The resulting increase in uncertainty was greatest for sources with rapid or extreme temperature changes. This analysis focused on the mirror attenuator mosaic (MAM) baffle and plate and scanner radiometer baffle due to their relatively high temperature changes during solar calibrations. Since only solar simulator data were available, the solar temperatures were approximated on these components and the radiative and thermal gradients in the MAM baffle due to reflected sunlight. Of the two cases considered for the MAM plate and baffle temperatures, one uses temperatures obtained from the ground calibration. The other attempt uses temperatures computed from the MAM baffle model. This analysis shows that the heat input variations due largely to the solar radiance and irradiance during a scan cycle are small. It also demonstrates that reasonable intervals longer than the current HK data acquisition interval should not significantly affect the estimation of a radiation field in the sensor field-of-view. Author

**N88-13554#** Institut Franco-Allemand de Recherches, St. Louis (France).
**OPTOELECTRONIC MEASUREMENT METHODS FOR BALLISTIC EXPERIMENTS [OPTOELEKTRONISCHE MESSMETHODEN FUER BALLISTICHE EXPERIMENTE]**
K. Sterzelmeier and H. J. Roessner 19 May 1986 18 p In GERMAN; FRENCH summary
(PB87-110706; ISL-CO-207/86) AVAIL: NTIS HC E03/MF E03 CSCL 14B

Two optoelectronic methods are presented for determining the speed, contour, flight, and angles of incidence/precession of bar shaped projectiles. These methods can be used in tight spaces, contactless, without influence on, nor needing adjustment and/or attachment to projectiles. One method used a unique optical barrier to measure speed and to determine geometric form; also to analyze expansion and deformation of projectiles. A very narrow light band is used transversely to the firing axis. Speed is derived from projectile length and its transit time. Contour is deduced directly from the temporal variation of light flux during its passage through the light band. The other method known as OMEGA, measures the angle of incidence of projectile on its trajectory while it traverses a narrow light band. A luminous spot observed on projectile during the traverse is reproduced on a lateral diode. Variation of light flux is recorded again, simultaneously marking changes of position of light spot on the measurement plane. Speed is determined as before from length and transit time. Spatial situation of projectile is determined by differentiating the position functions. Author

**N88-13555#** EG and G Energy Measurements, Inc., Woburn, Mass.
**A FOCUSSED MCP (MICROCHANNEL PLATE) IMAGE INTENSIFIER TYPE FOR HIGH SPEED GATING**
Ben Vine and George Yates 1987 9 p Presented at the 31st SPIE Annual International Technical Symposium on Optical and Optoelectronic Applied Science and Engineering, San Diego, Calif., 16 Aug. 1987 Prepared in cooperation with Los Alamos National Lab., N. Mex.
(Contract W-7405-eng-36)
(DE88-000480; LA-UR-87-3305; CONF-8708110-20) Avail: NTIS HC A02/MF A01

This tube is aimed at shuttering speeds faster than 200 picoseconds, with required electrical gate pulse less than 80 volts. Similar tubes were described in a 1984 paper at this meeting. One new feature is the use of a microchannel plate (MCP) to provide high and adjustable signal gain. This tube, in comparison with proximity-focussed tubes, conserves resolution by using an electrostatic focus lens. Also new is the use of transfer photocathode technique to eliminate stray emission from the gate mesh. Measured performance: Gating speed, Gain, On-Off signal ratio will be presented. Tube construction and the transfer photocathode technique will be discussed. The noise which shows up in high-gain imaging systems will be discussed. DOE

**N88-13556*#** Rockwell International Science Center, Anaheim, Calif.
**STUDY OF SOLID STATE PHOTOMULTIPLIER Final Contractor Report, 1 Jun. 1986 - 30 Apr. 1987**
K. M. Hays and R. A. LaViolette Aug. 1987 55 p
(Contract NAS2-12400)
(NASA-CR-177465; NAS 1.26:177465; SC5464.FR) Avail: NTIS HC A04/MF A01 CSCL 14B

Available solid state photomultiplier (SSPM) detectors were tested under low-background, low temperature conditions to determine the conditions producing optimal sensitivity in a space-based astronomy system such as a liquid cooled helium telescope in orbit. Detector temperatures varied between 6 and 9 K, with background flux ranging from 10 to the 13th power to less than 10 to the 6th power photons/square cm-s. Measured parameters included quantum efficiency, noise, dark current, and spectral response. Experimental data were reduced, analyzed, and combined with existing data to build the SSPM data base included herein. The results were compared to analytical models of SSPM performance where appropriate models existed. Analytical models presented here were developed to be as consistent with the data base as practicable. Significant differences between the theory and data are described. Some models were developed or updated as a result of this study. Author

**N88-13557*#** Information and Control Systems, Inc., Hampton, Va.

**DEVELOPMENT OF RESPONSE MODELS FOR THE EARTH RADIATION BUDGET EXPERIMENT (ERBE) SENSORS. PART 1: DYNAMIC MODELS AND COMPUTER SIMULATIONS FOR THE ERBE NONSCANNER, SCANNER AND SOLAR MONITOR SENSORS**

Nesim Halyo, Sang H. Choi, Dan A. Chrisman, Jr., and Richard W. Samms 20 Mar. 1987 296 p

(Contract NAS1-16130)

(NASA-CR-178292; NAS 1.26:178292) Avail: NTIS HC A13/MF A01 CSCL 14B

Dynamic models and computer simulations were developed for the radiometric sensors utilized in the Earth Radiation Budget Experiment (ERBE). The models were developed to understand performance, improve measurement accuracy by updating model parameters and provide the constants needed for the count conversion algorithms. Model simulations were compared with the sensor's actual responses demonstrated in the ground and inflight calibrations. The models consider thermal and radiative exchange effects, surface specularity, spectral dependence of a filter, radiative interactions among an enclosure's nodes, partial specular and diffuse enclosure surface characteristics and steady-state and transient sensor responses. Relatively few sensor nodes were chosen for the models since there is an accuracy tradeoff between increasing the number of nodes and approximating parameters such as the sensor's size, material properties, geometry, and enclosure surface characteristics. Given that the temperature gradients within a node and between nodes are small enough, approximating with only a few nodes does not jeopardize the accuracy required to perform the parameter estimates and error analyses. Author

**N88-13558#** Massachusetts Inst. of Tech., Cambridge. Research Labs. of Electronics.

**MODEL-BASED MOTION ESTIMATION AND ITS APPLICATION TO RESTORATION AND INTERPOLATION OF MOTION PICTURES**

Dennis Michael Martinez Jun. 1987 167 p

(Contract N00014-81-K-0742; Grant NSF ECS-84-07285)

(AD-A185054; TR-530) Avail: NTIS HC A08/MF A01 CSCL 14B

This report is concerned with the problem of motion estimation from digitally sampled motion pictures. Several models are developed that describe object motion with velocity fields. Given an image sequence, the velocity field is underconstrained and therefore cannot be determined uniquely. However, by imposing structural constraints on the velocity field in the form of a parametric model, it is possible to determine the model parameters uniquely. This report describes parametric models which form the basis for two motion estimation algorithms. Experimental results demonstrate that these algorithms determine velocity fields more accurately than conventional region matching methods. One of the algorithms, based on the least squares error criterion, also has the desirable property of being computationally efficient. To demonstrate the performance of the least square motion estimation algorithm, a motion-compensated noise reduction system was implemented. Experiments demonstrate that the motion-compensated noise reduction system can yield better results than conventional restoration methods. A motion-compensated frame interpolation system, also implemented, permits frame rate conversion by arbitrary rates. GRA

**N88-13559#** Army Research Inst. of Environmental Medicine, Natick, Mass.

**ASSESSMENT OF THE RELIABILITY OF A CORRECTION PROCEDURE FOR WGT (WET GLOBE THERMOMETER) (BOTSBALL) MEASUREMENTS OF HEAT STRESS**

William T. Matthew, Glenn J. Thomas, Lawrence E. Armstrong, and Roger W. Hubbard Aug. 1987 26 p

(AD-A185193; USARIEM-T-17/87) Avail: NTIS HC A03/MF A01 CSCL 14B

The Botsball or WGT (Wet Globe Thermometer) has been widely distributed to military users as a rugged, simple, and inexpensive alternative to WBGT (Wet Bulb-Globe Temperature) instruments. Existing hot weather guidelines for the Botsball presumed that the Botsball would always read approximately 2 F (1.6C) lower than the prevailing WBGT index. Following reports from the field of Botsball readings as much as 10F (5.6 C) lower than the prevailing WBGT index during hot, dry, and windy conditions, a wind tunnel study was conducted to assess Botsball performance characteristics over a broad range of temperatures, humidities, and wind speeds. The wind tunnel study confirmed that substantial and potentially dangerous underestimates of heat stress on the order of 11F (6.1C) may be obtained with the Botsball under very hot, dry, and windy conditions. In an effort to derive a practical correction process that would, with reasonable precision, correct the Botsball reading to parity with the prevailing WBGT index, the wind tunnel data were reexamined. GRA

**N88-13560#** Army Research Inst. of Environmental Medicine, Natick, Mass.

**COOLING ELECTRONIC EQUIPMENT AT SIMULATED HIGH ALTITUDE IN HYPOBARIC CHAMBERS Technical Report, Sep. 1985 - Aug. 1987**

James A. Devine 25 Aug. 1987 20 p

(AD-A185196; USARIEM-T-33/87) Avail: NTIS HC A03/MF A01 CSCL 13A

An air cooling system has been designed to minimize electronic equipment failures during simulated exposures to 9,000 meters (29,000 ft) in hypobaric chambers. Air density, critical to convective heat transfer during electronic equipment operations, diminishes rapidly below 830 grams cubic meter (16,000 ft, 5,000 meters) resulting in equipment failures. Forced convection, using fans, can be effective up to 6,000meters but extensive equipment failures occur at higher altitudes. A newly designed cooling system incorporates a micrometer-like air flow control nozzle that directs compressed air onto the subject area. The design also accelerates surrounding air molecules to create a highly amplified flow by adding the entrained ambient air to the compressed air. Air flows may be directed on heat exchangers, power supplies, through ventilation ports, ports, to assist fan units, and for general in-cabinet cooling. GRA

**N88-13561#** Air Force Inst. of Tech., Wright-Patterson AFB, Ohio.

**FIBER-OPTIC ACCELEROMETER INVESTIGATION M.S. Thesis**

Waldemar Zukauskas 1987 85 p

(AD-A185359; AFIT/CI/NR-87-59T) Avail: NTIS HC A05/MF A01 CSCL 17G

A fiber-optic accelerometer concept based on the radial displacement of a hollow cylinder subject to acceleration is experimentally investigated. The accelerometer configuration consists of two PZT cylinders wrapped with 2.3 meters of high birefringent single mode fiber placed in a differential configuration. Cylinder radial displacement induces an axial strain into the fiber which stretches the fiber, causing a simultaneous optical path length and index of refraction change. The result is an overall phase change of the light propagating in the fiber, causing a simultaneous optical path length and index of refraction change. The result is an overall phase change of the light propagating in the fiber. Acceleration is hence measured by ac detecting and scaling the phase change. Optical common mode rejection is achieved via a 90 degree fiber rotation and splice. Polarization, phase, and temperature stability for the system with and without optical common moding is investigated. A theoretical system scale factor and bias is calculated and used to determine the minimum detectable acceleration sensed for a 50 volt dc step input simulating induced acceleration. System noise is compared to the photon shot noise limit. GRA

**N88-13562#** Oregon Univ., Eugene. Inst. of Theoretical Science.
**THE PRODUCTION OF ULTRASMALL AND SUPERFINE HOLOGRAPHIC DIFFRACTION GRATINGS USING SYNCHROTRON RADIATION AND LITHOGRAPHIC TECHNIQUES Final Annual Report, 1 Sep. 1985 - 31 Dec. 1986**
Paul L. Csonka Feb. 1987 21 p
(Contracts AF-AFOSR-85-0326; AF Proj. 2301)
(AD-A185395; AFOSR-87-0963TR) Avail: NTIS HC A02/MF A01 CSCL 20F

The research effort was directed toward the production of superfine X-ray gratings by holographic means, i.e. generating an interference pattern by X-rays emitted in the form of synchrotron radiation from a high energy electron storage ring, recording the pattern on a resist, such as PMMA, and subsequently transferring it onto metal. GRA

**N88-13563#** Naval Research Lab., Washington, D.C.
**HIGH PEAK POWER KA-BAND GYROTRON OSCILLATOR EXPERIMENT Interim Report, Mar. 1985 - Mar. 1986**
S. H. Gold, A. W. Fliflet, W. M. Manheimer, R. B. McCowan, and W. M. Black 21 Sep. 1987 65 p Prepared in cooperation with Science Applications International Corp., McLean, Va., JAYCOR, Vienna, Va., and Maryland Univ., College Park
(AD-A185424; NRL-MR-5923) Avail: NTIS HC A04/MF A01 CSCL 09A

A Ka-band gyrotron oscillator powered by a 600 kV pulseline accelerator has produced approximately 100 kW at 35 GHz in a circular TE62 mode. It has also demonstrated frequency tuning over the range 28 to 49 GHz by operating in a family of TEm2 modes, with the azimuthal index m ranging from 4 to 10, by variation of the guide magnetic field. Operation is in general agreement with the predictions of theory. GRA

**N88-13564#** Panametrics, Inc., Waltham, Mass.
**FABRICATE, CALIBRATE AND TEST A DOSIMETER FOR INTEGRATION INTO THE CRRES (COMBINED RELEASE AND RADIATION EFFECTS SATELLITE) SATELLITE Technical Report**
Paul R. Morel, Frederick A. Hanser, Bach Sellers, and Ram Cohen Jun. 1987 34 p
(Contract F19628-82-C-0090)
(AD-A185439; AFGL-TR-87-0232; SR-4) Avail: NTIS HC A03/MF A01 CSCL 08D

A space-radiation Dosimeter has been fabricated, calibrated , and tested, and will be integrated into the CRRES spacecraft. This Dosimeter is essentially identical to that previously installed on the DMSP F7 satellite. These dosimeters are primarily designed to measure the dose from electrons of greater than 1 MeV to greater than 10 MeV in four channels. Each channel has a different thickness aluminum dome. The solid state detector outputs are processed to provide the dose from electrons (low energy loss), the dose from protons (high energy loss), the flux from electrons, the flux of protons, and the rate of high energy loss nuclear star events. The dosimeter also has a calibration mode in which the alpha particles from a weak source behind each detector are used to check for total detector depletion and proper operation of the electronics. A high energy electron Fluxmeter to measure electrons from 1-10 meV in ten differential channels will also be integrated into the CRRES spacecraft. The Fluxmeter will be modified to provide a low voltage continuous bias to the solid state detectors to reduce the possibility of detector degradation in storage and in vacuum. The Fluxmeter will be retested as necessary, and then be delivered and integrated into the CRRES spacecraft. GRA

**N88-13565#** Institut de Mecanique des Fluides de Lille (France).
**DETERMINATION OF A FLOW VELOCITY FIELD USING FOUR-EXPOSURE LASER HOLOGRAPHY [DETERMINATION DU CHAMP DE VITESSES D'UN ECOULEMENT PAR HOLOGRAPHIE LASER A QUATRE EXPOSITIONS]**
O. Rodriguez, T. Laden, and M. Dadi 22 Jul. 1985 41 p In FRENCH
(Contract DRET-83-250)
(IMFL-3114-85/32; ETN-88-91170) Avail: NTIS HC A03/MF A01

The application of four pulse laser holography to flow measurement is explored. The four particle images allow an estimation of velocity, acceleration, and rotational fields. Polystyrene particles, 40 to 50 microns diameter, were used. Deviations of 12 percent between observation and computation are explained. The method is useful at low velocities and high velocity gradients. It is not possible to solve the motion equation, based on Stokes drag, to compute the fluid velocity from the experimental particle velocity and acceleration data. ESA

**N88-13566#** Centre National de la Recherche Scientifique, Marseilles (France). Inst. de Mecanique Statistique de la Turbulence.
**HOT WIRE AND LASER VELOCIMETER STUDIES OF TURBULENT FLOW AT SUPERSONIC VELOCITIES Final Report [ETUDE PAR VELOCIMETRIE LASER ET FIL CHAUD DES ECOULEMENTS TURBULENTS AUX VITESSES SUPERSONIQUES]**
Nov. 1984 64 p In FRENCH
(Contract DRET-83-460)
(ETN-88-91172) Avail: NTIS HC A04/MF A01

The set-up of the application of a two dimensional laser Doppler velocimeter to measure supersonic turbulent flow distribution is described. Normal and tangent components of the Reynolds tensor are determined for the case of a turbulent boundary layer and the results are compared with those obtained by hot wire anemometry. Laser data shows lower variance and better reliability. ESA

**N88-13567#** Societe Nationale Industrielle Aerospatiale, Les Mureaux (France).
**AN ELECTRIC FIELD METER BASED UPON A NEW PRINCIPLE: A DUMMY DISPLACEMENT ELECTRODE. APPLICATION TO AEROSPACE VEHICLES**
P. Andre and G. Boulanger 1986 11 p In FRENCH; ENGLISH summary
(SNIAS-872-422-106; ETN-88-91207) Avail: NTIS HC A03/MF A01

An electrical field measuring instrument which significantly improves the rejection of noise due to collected electric charges (ionized particles) is presented. Using the principle (dummy displacement electrode), a complete field meter was manufactured. The test results show accurate field measurements in points submitted to a very significant charged particle flux. Instrument data processing and data transmission are also described. ESA

**N88-13568#** Rome Univ. (Italy). Dipartimento di Fisica.
**THE TECHNICAL EVOLUTION OF THE WILSON CAMERA: THE BEGINNINGS (1895-1925) [EVOLUZIONE DELLA TECNICA DELLA CAMERA DI WILSON: LE ORIGINI (1895-1925)]**
R. Carullo 16 Jan. 1987 63 p In ITALIAN
(Nota-Interna-876; ETN-88-91238) Avail: NTIS HC A04/MF A01

The history of the technical evolution of the Wilson camera from 1895 to 1925 is presented, paying particular attention to the period before 1911, when the alpha and beta particle traces were observed for the first time in a condensation chamber. ESA

**N88-13569#** Consiglio Nazionale delle Ricerche, Frascati (Italy). Ist. di Fisica dello Spazio Interplanetario.
**THE TAIL LOBE ION SPECTROMETER: THEORY AND OBSERVATIONS**
M. Candidi, S. Orsini, and J. L. Horwitz (Alabama Univ., Huntsville.) Nov. 1986 34 p
(IFSI-86-12; ETN-88-91283) Avail: NTIS HC A03/MF A01

The properties of the O(+) ionospheric ion streams in the Earth's magnetotail as measured by ISEE-2, and the predictions of a two-dimensional kinetic model for the transport of ionospheric ions from the cleft topside ionosphere into the tail lobes are

compared. General agreement between average data and model with intermediate parameters is apparent. However, variations associated with varying magnetic activity levels do not appear to be well modeled. Model sophistication and data coverage and organization have to be improved. ESA

**N88-13570** Technische Hogeschool Twente, Enschede (Netherlands).
**SIMULATION OF THE PERPENDICULAR MAGNETIC RECORDING PROCESS Ph.D. Thesis**
Martin Frank Beusekamp 1987 209 p
(B8713537; ISBN-90-9001655-4; ETN-88-91356) Copyright
Avail: Issuing Activity

A simulation model of the complete perpendicular magnetic recording process, from write current to readback voltage, that is neither analytical nor iterative, is described. The actual physical process is piecewisely linearized during every stage of recording. The influence of the so-called image-charge effect, caused by the presence of a head and a keeper layer in the vicinity of a magnetized recording layer, is emphasized. The effect is treated quantitatively and the influence of the obliquity of the recording layer's intrinsic hysteresis loop is investigated. The influences of the bit density and the head field to coercive field ratio are described. The thicknesses of the recording layer and the air gap were varied, showing that the air gap should be as small as possible. ESA

**N88-13571#** Lawrence Livermore National Lab., Calif.
**STREAK CAMERA DYNAMIC RANGE OPTIMIZATION**
J. D. Wiedwald and R. A. Lerche Sep. 1987 8 p Presented at the 31st SPIE Annual International Technical Symposium on Optical and Optoelectronic Applied Science and Engineering, San Diego, Calif., 16 Aug. 1987
(Contract W-7405-eng-48)
(DE88-001632; UCRL-96518; CONF-8708110-24) Avail: NTIS HC A02/MF A01

The Lawrence Livermore National Laboratory (LLNL) optical streak camera is used by the Laser Fusion Program in a wide range of applications. Many of these applications require a large recorded dynamic range. Recent work has focused on maximizing the dynamic range of the streak camera recording system. For our streak cameras, image intensifier saturation limits the upper end of the dynamic range. We have developed procedures to set the image intensifier gain such that the system dynamic range is maximized. Specifically, the gain is set such that a single streak tube photoelectron is recorded with an exposure of about five times the recording system noise. This ensures detection of single photoelectrons, while not consuming intensifier or recording system dynamic range through excessive intensifier gain. The optimum intensifier gain has been determined for two types of film and for a lens-coupled CCD camera. We have determined that by recording the streak camera image with a CCD camera, the system is shot-noise limited up to the onset of image intensifier nonlinearity. When recording on film, the film determines the noise at high exposure levels. There is discussion of the effects of slit width and image intensifier saturation on dynamic range. DOE

**N88-13572#** Lawrence Livermore National Lab., Calif.
**RESOLUTION LIMITATIONS AND OPTIMIZATION OF THE LLNL STREAK CAMERA FOCUS**
R. A. Lerche and R. L. Griffith Sep. 1987 11 p Presented at the 31st SPIE Annual International Technical Symposium on Optical and Optoelectronic Applied Sciences and Engineering, San Diego, Calif., 16 Aug. 1987
(Contract W-7405-eng-48)
(DE88-001633; UCRL-96519; CONF-8708110-23) Avail: NTIS HC A02/MF A01

The RCA C73435 image tube is biased at voltages far from its original design in the Lawrence Livermore National Laboratory (LLNL) ultrafast (10 ps) streak camera. Its output resolution at streak camera operating potentials has been measured as a function of input slit width, incident-light wavelength, and focus-grid voltage. The temporal resolution is insensitive to focus-grid voltage for a narrow (100 micron) input slit, but is very sensitive to focus-grid voltage for a wide (2 mm) input slit. At the optimum wide-slit focus voltage, temporal resolution is insensitive to slit width. Spatial resolution is nearly independent of focus-grid voltage for values that give good temporal resolution. Both temporal and spatial resolution depend on the incident-light wavelength. Data for 1.06 micron light show significantly better focusing than for 0.53 micron light. Streak camera operation is simulated with a computer program that calculates photoelectron trajectories. Electron ray tracing describes all of the observed effects of slit width, incident-light wavelength, and focus-grid voltage on output resolution. DOE

**N88-13573*#** Sverdrup Technology, Inc., Cleveland, Ohio.
**OPERATING ENVELOPES OF PARTICLE SIZING INSTRUMENTATION USED FOR ICING RESEARCH Final Contractor Report**
Edward A. Hovenac Dec. 1987 16 p
(Contract NAS3-24105)
(NASA-CR-180870; E-3886; NAS 1.26:180870; AIAA-88-0291)
Avail: NTIS HC A03/MF A01 CSCL 14B

The Forward Scattering Spectrometer Probe and the Optical Array Probe are analyzed in terms of their ability to make accurate determinations of water droplet size distributions. Sources of counting and sizing errors are explained. The paper describes ways of identifying these errors and how they can affect measurement. Author

**N88-13756*#** Colorado Univ., Boulder. Center for the Study of Earth from Space.
**THE PORTABLE INSTANT DISPLAY AND ANALYSIS SPECTROMETER (PIDAS)**
Alexander F. H. Goetz *In* JPL Proceedings of the 3rd Airborne Imaging Spectrometer Data Analysis Workshop 15 Aug. 1987 p 8-17 (For primary document see N88-13755 05-42)
Avail: NTIS HC A09/MF A01 CSCL 14B

# 36 LASERS AND MASERS

Includes parametric amplifiers.
For related information see also *76 Solid-State Physics*.

**N88-13574#** Cambridge Univ. (England). Dept. of Engineering.
**MASTER PLOTS FOR PREDICTING THE CASE-DEPTH IN LASER SURFACE TREATMENTS**
H. R. Shercliff and M. F. Ashby Oct. 1986 31 p
(PB87-221875; CUED/C-MATS/TR-134) Avail: NTIS HC E05/MF E05 CSCL 20E

Diagrams are proposed that show the case depth in laser surface transformation hardening as a function of the process variables (beam power, size and speed) and thermal constraints (thermal conductivity, specific heat and so forth). It is shown that most fail to use the dimensionless relationship which exists between case depth and these variables. A new master plot (showing the case depth for all values of the variables) is derived and demonstrated using recent experimental measurements from laser hardened steel surfaces. It is constructed by using an approximate analytical solution for the temperature field in the solid, which is shown to be in good agreement with the more tedious numerical computations. Author

**N88-13575#** Sandia National Labs., Albuquerque, N. Mex.
**NARROW LINEWIDTH GAIN MEASUREMENTS IN A KrF EXCIMER AMPLIFIER PUMPED LONGITUDINALLY BY A HIGH-POWER ELECTRON BEAM**
R. G. Adams, M. M. Dillon, and R. A. Gerber 1987 13 p Presented at the SDIO/DARPA Services Annual Propagation Review, Monterey, Calif., 29 Sep. 1987
(Contract DE-AC04-76DP-00789)
(DE88-001365; SAND-87-2202C; CONF-8709146-13) Avail: NTIS HC A03/MF A01

Single-pulse gain measurements have been performed on an excimer amplifier pumped longitudinally by a high-power (approx.

4 MW/cm²) electron beam. This amplifier maintained the narrow linewidth (less than 10 GHz) characteristic of the probe laser beam produced by a grating-tuned, discharge excimer laser. Gain was measured at 248.45 nm, the center of the KrF laser gain profile, over four orders of magnitude of input intensity for a laser pulse of 20-ns FWHM. The data can be represented by the Rigrod-Rice steady state analysis and yield values over this data range for the small signal gain, the nonsaturable absorption, and saturation intensity of g sub 0 = 12.6%/cm, alpha approx. 0.45%/cm, and I sub s = 4.1 MW/sq cm, respectively, for a 750 torr laser mix. DOE

**N88-13576#** Sandia National Labs., Albuquerque, N. Mex.
**LOW JITTER LASER-TRIGGERED HIGH-VOLTAGE VACUUM SWITCH USING LOW LASER ENERGIES**
P. J. Brannon and D. F. Cowgill Oct. 1987 18 p
(Contract DE-AC04-76DP-00789)
(DE88-001922; SAND-87-1997) Avail: NTIS HC A03/MF A01

A laser-triggered high voltage vacuum switch with a unique composite target pellet has been developed. The target pellet is fabricated from a compressed mixture of equal weights of 8-micron titanium and 300-micron KCl powders. The switch triggers reliably for 532-nm laser input energies of 20 microJ corresponding to a peak irradiance of 1 MW/ sq cm. Jitter times of less than +/- 15 ns are observed. The delay time of the switch increases as the gap voltage decreases. A delay time of less than 100 ns is observed for a gap voltage of 6000 V and a gap spacing of 0.5 mm. The trigger energies and peak irradiances reported here are smaller by an order of magnitude or more than previously reported for laser-triggered vacuum switches. DOE

**N88-13577*#** Old Dominion Univ., Norfolk, Va. Dept. of Mathematical Sciences.
**THEORETICAL STUDIES OF SOLAR LASERS AND CONVERTERS Progress Report, 15 May - 31 Dec. 1987**
John Heinbockel Jan. 1988 29 p
(Grant NAG1-757)
(NASA-CR-181569; NAS 1.26:181569) Avail: NTIS HC A03/MF A01 CSCL 20E

The geometry and setup for the n-C3F7I iodine laser are illustrated. The mathematical modeling of this system is described. The chemical kinetics are summarized. A sensitivity analysis was performed on the parameters occurring in the differential equations describing the chemical kinetics. B.G.

**N88-13578#** Texas Univ., Dallas. Center for Quantum Electronics and Applications.
**THE GAMMA-RAY LASER PROJECT Quarterly Technical Progress Report, 1 Apr. - 30 Jun. 1987**
Carl B. Collins Jul. 1987 60 p
(Contract N00014-86-C-2488)
(AD-A184824; UTD-GRL-8701; QTPR-1) Avail: NTIS HC A04/MF A01 CSCL 09C

Recent approaches to the problem of the gamma-ray laser have focused on upconversion techniques in which metastable nuclei are pumped with long wavelength radiation. At the nuclear level the storage of energy can approach tera-Joules (10 to the 12th power J) per liter for thousands of years. However, any plan to use such a resource for a gamma-ray laser poses problems of a broad interdisciplinary nature requiring the fusion of concepts taken from relatively unrelated fields of physics. GRA

**N88-13579#** Naval Postgraduate School, Monterey, Calif.
**PHOTOCURRENT GENERATION FROM BASIC METALS, UTILIZING A SHORT PULSED ArF EXCIMER LASER M.S. Thesis**
Thomas J. Ringler Sep. 1987 62 p
(AD-A184928) Avail: NTIS HC A04/MF A01 CSCL 09C

An excimer laser used to produce cold photoelectrons from common metal surfaces offers an improvement over a standard heated (thermionic) cathode electron source. Photoelectrons accelerated across an anode cathode gap were observed under both space charge limited and emission limited conditions. Temporal characteristics of the resulting electron beam showed fast rise times of 3-5 nano seconds (ns) for space charge limited and 8-12ns (full width half maximum) for emission limited cases. Spatial characteristics of the output pulse shape revealed a classic clipped peak amplitude in the space charge pulse but identical characteristics in the emission limited pulse output. Both types of emission produced large current densities up to 91 amps/sq cm. Varying the cathode metal used for the photocathode indicates Zinc (Zn) produced the largest current density, and therefore, the highest quantum efficiency in both space charge and emission limited cases. GRA

**N88-13580#** Wisconsin Univ., Madison. Dept. of Chemistry.
**APPLICATIONS OF NONLINEAR HOLE BURNING SPECTROSCOPY Final Report, 1 Jul. 1985 - 30 Jun. 1987**
John C. Wright 31 Aug. 1987 4 p
(Contract DAAG29-85-K-0001)
(AD-A184943) Avail: NTIS HC A02/MF A01 CSCL 20E

A new method for generating spectral holes was studied. The method used nonlinear four wave mixing to create an excited state population from which relaxation created a hole. After studies to define a suitable system for the experiments, it was found that polymethyl methacrylate (PMMA) provided a host material where hole burning was extremely efficient. The high efficiency in fact limited the ability to measure the hole. A new technique is presently being developed that can dynamically access the holes created without interference from additional hole burning. GRA

**N88-13581#** Illinois Univ., Urbana. Dept. of Aeronautical and Astronautical Engineering.
**COMPUTER SIMULATION OF cw HF CHEMICAL LASER UNSTABLE RESONATOR PERFORMANCE**
L. H. Sentman and J. O. Gilmore Aug. 1987 102 p
(Contract N00014-85-K-0326)
(AD-A185059; AAE-TR-87-5; UILU-ENG-87-0505) Avail: NTIS HC A06/MF A01 CSCL 09C

Inadequacies in the treatment of the fluid dynamic mixing that were not apparent in Fabry-Perot or stable resonator models were revealed with a wave optics unstable resonator model. The unstable resonator data as a function of resonator size and size of the laser were shown to provide a severe test of a couples, wave optics, chemical kinetic, fluid dynamic model of a chemical laser. A mechanism for the observed time-dependent oscillations that occur on lines whose saturated gain does not fill the unstable resonator was proposed. According to the proposed mechanism, the time-dependent oscillations are the result of a competition between chemical pumping and radiative deactivation of upper laser levels of HF. The oscillations occur only if the media is not strongly coupled to the optical fields diffractively or geometrically. Computer calculations supported the proposed mechanism and new unstable resonator experiments were suggested. GRA

**N88-13582#** Ballistic Research Labs., Aberdeen Proving Ground, Md.
**A STUDY OF THE INTERACTION OF LASER LIGHT WITH LIQUID PROPELLANT DROPS Final Memo. Report, Apr. - Jul. 1986**
Richard A. Beyer and Linda C. Maas 7 Apr. 1987 24 p
(AD-A185117; BRL-MR-3579) Avail: NTIS HC A03/MF A01 CSCL 19A

The interaction of liquid propellant drops with the beam from a modest power carbon dioxide laser has been used to observe evidence of strong internal circulation and corresponding instability of these drops. The drops appear to relax, but characteristic times may extend to as much as 0.1 sec. The drops are found to break up under relatively small perturbations when highly circulating. The implications in gun environments where interdrop collisions may occur shortly after drop formation, as well as the potential importance to possible research configurations, are discussed. GRA

**N88-13583#** Massachusetts Inst. of Tech., Cambridge. Research Lab. of Electronics.
**PHASE-LOCKED SEMICONDUCTOR QUANTUM WELL LASER ARRAYS Ph.D. Thesis**
Elias Towe Mar. 1987 192 p
(Contract DAAL03-86-K-0002; Grant NSF ECS-83-05448)
(AD-A185155; TR-526; ARO-23223.26-EL) Avail: NTIS HC A09/MF A01 CSCL 09C

This dissertation presents the experimental study of quantum well heterostructures in the III-V compound semiconductor system of (Al,Ga)As/GaAs. This study was conducted with a view to applying these structures in heterostructure lasers; specifically, phase-locked laser arrays. Broad area lasers fabricated from the quantum well microstructures exhibited threshold current densities as low as 200 Amp/sq. cm. The major contribution of this work is a new monolithic laser array structure which achieves phase-locking through coupling by diffraction in a central mode-mixing region where the light is unguided. The propagating eigen-modes are index-guided on either side of the mode-mixing region in parallel-element ridge waveguides. The new array displays narrow, single-lobe far-field patterns. The narrowest far-field pattern observed is 2 deg wide. An analytic model which explains the characteristics of the observed far-field patterns is presented. This model is developed from a premise with experimental basis. GRA

**N88-13584#** Illinois Univ., Urbana. Dept. of Aeronautical and Astronautical Engineering.
**AN EXPERIMENTAL STUDY OF CW HF CHEMICAL LASER AMPLIFIER PERFORMANCE AND ZERO POWER GAIN**
L. H. Sentman, P. Theodoropoulos, R. Waldo, T. Nguyen, and R. Snipes Aug. 1987 122 p
(Contract N00014-85-K-0326)
(AD-A185241; AAE-TR-87-6; UILU-ENG-87-0506) Avail: NTIS HC A06/MF A01 CSCL 09C

The multiline and single-line amplifier performance of a two channel Helios CL II laser was studied. Flow channel aperturing of the input beam was found to cause a significant reduction in the measured amplification ratio. The absorption of the the multiline input beam by SF6 was found to be negligible (less than 0.5%/cm). Maximum multiline and single line amplification was obtained when the input beam was passed through the amplifier at the XC corresponding to maximum zero power gain. Single-line amplification ratios were considerably lower than multiline amplification ratios obtained for the same input power. The P2(6) amplification ratios were lower than the P1(6) amplification ratios, even though the P2(6) zero power gain was considerably higher than the P1(6) zero power gain. The data suggested that about 1/3 of the oscillator output needs to be input to obtain amplifier output equal to the device's oscillator performance. GRA

**N88-13585#** Naval Surface Weapons Center, Silver Spring, Md.
**PHENOMENA AT A FOCUS IN A LASER SYSTEM Final Report**
H. R. Reiss 31 Jul. 1987 17 p
(AD-A185442; NSWC/TR-87-184) Avail: NTIS HC A02/MF A01 CSCL 09C

A high-powered, continuous beam laser system is examined in terms of the physical conditions which exist if the laser beam is brought to a diffraction-limited, real focus in a moderate vacuum environment. Ionization of the gas at the focus by multiphoton processes is extensive, but it is shown that neither reflection of the beam by the plasma at the focus nor absorption by ionization is sufficient to disrupt propagation of the beam through the focus. GRA

**N88-13586#** Institut Franco-Allemand de Recherches, St. Louis (France).
**TRANSIENT PROCESSES IN THE INTERACTION BETWEEN PROZESSE DER WECHSELWIRKUNG GEPULSTER LASER-STRAHLUNG MIT MATERIE]**
**LASERSTRAHLUNG MIT MATERIE]**
M. Hugenschmidt and J. Wey 20 Jun. 1986 27 p In GERMAN
(ISL-R-115/86; ETN-88-90638) Avail: NTIS HC A03/MF A01

Aspects brought about by the use of highpower pulsed lasers for the treatment of materials are treated. A TEA-CO2 laser delivering single pulses of a few 100 J, and a repetitive CO2 laser (100Hz, 2kW) were used for the measurement. The production of a plasma at the material surface and its effect on the energy transfer were determined; the energy transfer can be enhanced 10 times with respect to a continuous laser. The induced thermal and thermomechanical processes were visualized by high frequency cinematography. Further investigations for the technical application of high power pulsed laser are suggested. ESA

**N88-13587#** Pacific Northwest Labs., Richland, Wash.
**RAMAN MICROPROBE CHARACTERIZATION OF DIELECTRIC FILMS FOLLOWING HIGH-ENERGY PULSED LASER IRRADIATION**
G. J. Exarhos and D. M. Friedrich Feb. 1987 13 p Presented at the 22nd Annual Meeting of the Microbeam Analysis Society, Kailua-Kona, Hawaii, 13 Jul. 1987
(Contract DE-AC06-76RL-01830)
(DE88-000559; PNL-SA-14795; CONF-870725-13) Avail: NTIS HC A03/MF A01

The interaction of intense laser radiation with thin oxide films often results in degradation of their optical properties through the formation of regions characterized by stress inhomogeneity, phase transformation/recrystallization, or marked material ablation. A Raman microprobe investigation of several sputter-deposited single and multi-layer films was initiated to study in greater detail the molecular changes induced by high energy irradiation. Catastrophic damage was observed in submillimeter regions whose shape and depth depend upon laser energy, wavelength, and the cumulative number of incident pulses. Spatially resolved Raman spectra acquired with a resolution of a few micrometers were correlated with a specific damage morphology. Microprobe measurements also reveal nonuniform stress in the coatings. DOE

**N88-13588#** Lawrence Livermore National Lab., Calif.
**THEORY OF MULTIPHOTON IONIZATION OF ATOMS BY STRONG, SHORT PULSED LASERS**
K. C. Kulander 10 Jul. 1987 16 p Presented at the International Conference on Multiphoton Processes, Boulder, Colo., 13 Jul. 1987
(Contract W-7405-eng-48)
(DE88-000963; UCRL-96631; CONF-870789-3) Avail: NTIS HC A03/MF A01

A numerical technique for investigating the behavior of many electron atoms in intense laser fields is presented. A description of the method is followed by results of an illustrative, application to helium for a number of wavelengths and intensities. A discussion of high order ionization dynamics for this system based on these calculations is provided. DOE

**N88-13589#** Lawrence Livermore National Lab., Calif.
**A LONG ELECTROMAGNETIC WIGGLER FOR THE PALADIN FREE-ELECTRON LASER EXPERIMENTS**
G. A. Deis, A. R. Harvey, C. D. Parkison, D. Prosnitz, J. Rego, E. T. Scharlemann, and K. Halbach 1987 6 p Presented at the 10th International Conference on Magnet Technology (MT-10), Boston, Mass., 21 Sep. 1987 Prepared in cooperation with California Univ., Berkeley, Lawrence Berkeley Lab.
(Contract W-7405-eng-48)
(DE88-000970; UCRL-96292; CONF-870901-8) Avail: NTIS HC A02/MF A01

A 25.6-m-long wiggler for a free-electron-laser (FEL) experiment has been designed, built, and tested. It is a DC iron-core electromagnetic wiggler that incorporates a number of important and unique features. Permanent magnets are used to suppress saturation in the iron and extend the linear operating range. Steering-free excitation allows real-time adjustment of the field taper without causing beam steering. Wiggle-plane focusing is produced by curved pole tips. The magnitude of random pole-to-pole field errors is minimized by a mechanical design

concept that reduces tolerance stackup in critical locations. To date, 15 m of this wiggler has been tested, and measurements have shown exceptionally low levels of random errors. DOE

**N88-13590#** Sandia National Labs., Albuquerque, N. Mex.
**ANTI-STOKES GENERATION OF 226 nm LIGHT**
C. Reiser 1987 3 p Presented at the SDIO/DARPA Services Annual Propagation Review, Monterey, Calif., 29 Sep. 1987
(Contract DE-AC04-76DP-00789)
(DE88-001612; SAND-87-2285C; CONF-8709146-16) Avail: NTIS HC A02/MF A01

To ionize atmospheric atomic oxygen efficiently, the DELPHI mission requires high energy lasers at a few key wavelengths. The mission also constrains the weight and volume of the laser devices. Our work centers on the efficient generation of oxygen two-photon resonant light at 226 nm from the output of efficient KrF excimer lasers emitting near 249 nm by utilizing an anti-Stokes vibrational shift in H. DOE

**N88-13591#** Los Alamos National Lab., N. Mex.
**CHEMICAL ANALYSIS FOR EXCIMER LASER SYSTEMS**
R. C. Heaton, P. H. Hemberger, and W. F. Sandoval Sep. 1987 15 p
(Contract W-7405-eng-36)
(DE88-001941; LA-11008-MS) Avail: NTIS HC A02/MF A01

Analytical methods and procedures used to determine fluorine, krypton, xenon, and argon in fill gases for excimer lasers are described. Fluorine was determined by gas chromatography, mass spectrometry, and wet chemical (iodine liberation) methods. The noble gases were determined by gas chromatography and mass spectrometry, and attempts to identify impurities were made using mass spectrometry. Analytical results for 26 gas cylinders are reported. Limitations of the methods are discussed and recommendations for future efforts are presented. DOE

**N88-13228#** Institut Franco-Allemand de Recherches, St. Louis (France). Dept. d'Aerodynamique.
**AN ULTRA-HIGH-SPEED CINEMATOGRAPHIC METHOD FOR THE STUDY OF WAKES IN HYPERSONIC BALLISTIC RANGES [UNE METHODE CINEMATOGRAPHIQUE ULTRA-RAPIDE POUR L'ETUDE DES SILLAGES EN TUNNEL DE TIR HYPERSONIQUE]**
Axel Koeneke, Bernard Charles Jaeggy, and Germain Koerber *In* AGARD, Aerodynamics of Hypersonic Lifting Vehicles Nov. 1987 13 p
In FRENCH (For primary document see N88-13219 05-02)
Copyright Avail: NTIS HC A24/MF A01

# 37 MECHANICAL ENGINEERING

Includes auxiliary systems (nonpower); machine elements and processes; and mechanical equipment.

**N88-13592#** Laboratorio de Computacao Cientifica, Rio de Janeiro (Brazil).
**QUALIFICATION OF EXPANSION AND JOINT WELDING PROCEDURES OF TUBE-TO-TUBESHEET JOINTS FOR HEAT EXCHANGERS IN NUCLEAR POWER PLANTS**
G. A. M. Camargo, J. G. V. Couto, and L. A. S. deCastro 1986 1 p In PORTUGUESE; ENGLISH summary Presented at the 4th Brazilian Symposium on Piping and Pressure Vessels, Salvador, Brazil, 28 Oct. 1986
(DE87-703526; INIS-BR-779; CONF-8610317-1-Summ) Avail: NTIS (US Sales Only) HC A02/MF A01

Leaking tube-to-tubesheet joints are about the most frequent defects detected in the operation of tubular heat exchangers. This kind of problem requires special treatment in the case of heat exchangers installed in nuclear power plants, aimed at a minimum of leakages and further repair outages. The criteria used for the prequalification of tube-to-tubesheet joints are described and the experience already gathered during the test and fabrication of several components supplied by national manufacturers are summarized. DOE

**N88-13593#** Firma Ficht G.m.b.H., Kirchseeon (West Germany).
**DEVELOPMENT, CONSTRUCTION AND TESTING OF A NOVEL INTERNAL COMBUSTION ENGINE WITH CONICAL ROTATING SLIDE VALVE**
1986 44 p In GERMAN; ENGLISH summary
(DE88-900071; EUR-10733-DE) Avail: NTIS (US Sales Only) HC A03/MF A01

Four different multi-cylinder two-stroke engines of a new design ranging from 100 cc. to 200 cc. in capacity and with different power outputs have been developed and have successfully completed trials. The trials proved that this type of engine has many advantages over conventional design. Distinctive features are its rigidly connected pistons, the seals between the base of the cylinders and the crankcase, and the slotted linkage system to convert the reciprocating motion of the pistons into the rotary motion of the crankshaft. The expected advantages are a very high power-to-weight ratio, reduced mechanical losses which provide an extended working life and reduced fuel consumption with low pollution. The design and construction of the basic-cooled two-cylinder unit has been completed. Experimental measurements confirm theoretical predictions. Measurements in the power range of 3.3 kW to 9.2 kW have been made. The minimum fuel consumption was found to be 200 gr of fuel per HPh to 1700 rpm. DOE

**N88-13594#** BL Technology Ltd., Warwick (England).
**THE DEVELOPMENT AND EVALUATION OF THREE-DIMENSIONAL MODELS OF COLD FLOW IN INTERNAL COMBUSTION ENGINES Final Summary Report, 1 Mar. 1983 - 31 Dec. 1984**
1986 14 p
(DE88-900077; EUR-10812-EN) Avail: NTIS (US Sales Only) HC A03/MF A01

Described is the first phase of a program aimed at developing a series of computer models capable of describing the air flow and turbulence in cylinders of internal combustion engines. During the course of this first phase program a computer code has been developed which is capable of simulating the flow and turbulence field within a limited but useful range of chamber geometries. The Computer code allows for the description of simple cylinder head recesses and offset bowl-in-pistons along with two possible representations of valves. Velocity and turbulence measurements have been made using laser doppler anemometry on plexi-glass engines for code evaluation. Flow measurements at the valve have been made to establish inlet conditions for steady and unsteady flows and in-cylinder data acquired for a range of chamber geometries. DOE

**N88-13595*#** University of South Florida, Tampa. Dept. of Computer Science and Engineering.
**TOWARDS BUILDING A TEAM OF INTELLIGENT ROBOTS Final Report**
Murali R. Varanasi and R. Mehrotra 28 Dec. 1987 100 p
(Grant NAG1-772)
(NASA-CR-181538; NAS 1.26:181538; CSE-87-00005) Avail: NTIS HC A05/MF A01 CSCL 13I

Topics addressed include: collision-free motion planning of multiple robot arms; two-dimensional object recognition; and pictorial databases (storage and sharing of the representations of three-dimensional objects). For individual titles, see N88-13596 through N88-13597.

**N88-13596*#** University of South Florida, Tampa. Dept. of Computer Science and Engineering.
**COLLISION-FREE MOTION OF TWO ROBOT ARMS IN A COMMON WORKSPACE**
Robert A. Basta, Rajiv Mehrotra, and Murali R. Varanasi *In its* Towards Building a Team of Intelligent Robots 28 Dec. 1987 67 (For primary document see N88-13595 05-37)
(Grant NAG1-632)
(CSE-87-00002) Avail: NTIS HC A05/MF A01 CSCL 13I

Collision-free motion of two robot arms in a common workspace is investigated. A collision-free motion is obtained by detecting collisions along the preplanned trajectories using a sphere model for the wrist of each robot and then modifying the paths and/or trajectories of one or both robots to avoid the collision. Detecting and avoiding collisions are based on the premise that: preplanned trajectories of the robots follow a straight line; collisions are restricted to between the wrists of the two robots (which corresponds to the upper three links of PUMA manipulators); and collisions never occur between the beginning points or end points on the straight line paths. The collision detection algorithm is described and some approaches to collision avoidance are discussed. Author

**N88-13597*#** University of South Florida, Tampa.
**A RUDIMENTARY DATABASE FOR THREE-DIMENSIONAL OBJECTS USING STRUCTURAL REPRESENTATION c61**
James P. Sowers *In its* Towards Building a Team of Intelligent Robots 28 Dec. 1987 26 (For primary document see N88-13595 05-37)
(Grant NAG1-632)
(CSE-87-00004) Avail: NTIS HC A05/MF A01 CSCL 09B

A database which enables users to store and share the description of three-dimensional objects in a research environment is presented. The main objective of the design is to make it a compact structure that holds sufficient information to reconstruct the object. The database design is based on an object representation scheme which is information preserving, reasonably efficient, and yet economical in terms of the storage requirement. The determination of the needed data for the reconstruction process is guided by the belief that it is faster to do simple computations to generate needed data/information for construction than to retrieve everything from memory. Some recent techniques of three-dimensional representation that influenced the design of the database are discussed. The schema for the database and the structural definition used to define an object are given. The user manual for the software developed to create and maintain the contents of the database is included. Author

**N88-13598#** Naval Postgraduate School, Monterey, Calif.
**CONTROL OF A FLEXIBLE ONE-LINK MANIPULATOR M.S. Thesis**
Ioannis E. Zouzias Jun. 1987 188 p
(AD-A185035) Avail: NTIS HC A09/MF A01 CSCL 13I

The feasibility of controlling a flexible one-link manipulator with an adaptive computer simulation model, called a curve following system, is investigated. At the beginning a very flexible unloaded arm is used. Later the stiffness of the arm is increased, until we reach the case of a flexible arm that can be used in practice. Finally load is added to the arm and its behavior is studied. Author (GRA)

**N88-13599#** Scientific Research Associates, Inc., Glastonbury, Conn.
**THREE-DIMENSIONAL DYNAMIC LABYRINTH SEAL ANALYSIS Final Report, 1 Jul. - 31 Dec. 1986**
Y. T. Chan, R. C. Buggeln, and H. McDonald 2 Jan. 1987 50 p
(Contract F33615-86-C-2665)
(AD-A185353; SRA-910017; AFWAL-TR-87-2009) Avail: NTIS HC A03/MF A01 CSCL 11A

A transient capability has been developed for fluid flow analysis in a labyrinth seal configuration with a whirling rotor. The technique utilizes a moving coordinate system that allows transient calculations of the flow and pressure fields. Two sample calculations with different rotor oscillation displacements are presented and the results demonstrate the potential of this analysis. GRA

**N88-13600#** Technische Hochschule, Darmstadt (West Germany). Fachbereich Maschinenbau.
**IDENTIFICATION OF PERTURBATIONS IN TURBOMACHINES BY THE ANALYSIS OF PRESSURE SIGNALS, VIBRATIONS AND WAVELIKE MOTIONS Ph.D. Thesis [IDENTIFIZIERUNG VON STOERUNGEN IN TURBOMASCHINEN DURCH ANALYSE VON DRUCKSIGNALEN, KOEPERSCHALL UND WELLENSCHWINGUNGEN]**
Marcial Valero Martinez 1985 134 p In GERMAN
(ETN-88-90602) Avail: NTIS HC A07/MF A01

Simulated perturbations in five different turbomachines were investigated to identify the perturbations by their effects on the different characteristics. The identification capability of the statistical standard deviation of a rotor-rotation-average time signal from its mean value, and of the coherence function of a signal with a constant reference signal were determined. It is shown that the signal giving the radial motion of the wave with respect to the bearings provides information concerning the detection of damage. If sufficient suitable characteristics are available, the identification via decision trees can provide a comparable statistical safety as the pattern recognition method, with an important time saving. The results show that pressure signals are most suited for turbomachine monitoring. ESA

**N88-13601#** Technische Hogeschool, Eindhoven (Netherlands).
**TRIBOLOGY OF THIN FILM SYSTEMS Ph.D. Thesis**
Antonius Gerardus Tangena 1987 141 p
(ETN-88-91365) Avail: NTIS HC A07/MF A01

The correlation between mechanical stresses and tribological behavior for thin films on different substrates is studied. It is shown that the geometry of the system, the mechanical properties of the substrate, and the contact load determine the mechanical deformations of the top layer and thus its tribological behavior. Plastic deformation of the film is emphasized. A method to deduce the stress-strain curve of a thin film from a Brinell indentation test is presented. Experiments were conducted on an electrical contact system. A noble metal layer was applied on different substrates. A simple low cycle fatigue model gives a good description of the wear behavior as a function of the average von Mises stress. A magnetic coating was applied on various substrates. Calculations and experiments investigating the influence of the substrate on deformations of surface asperities of the coating correlate well. ESA

**N88-13602#** Oak Ridge National Lab., Tenn.
**DEALING WITH UNANTICIPATED EVENTS IN AUTONOMOUS NAVIGATION**
B. L. Burks, D. L. Barnett, S. M. Killough, R. C. Mann, and F. G. Pin Sep. 1987 7 p Presented at the 26th IEEE CDC Conference, Los Angeles, Calif., 9 Dec. 1987
(Contract DE-AC05-84OR-21400)
(DE88-000590; CONF-871211-3) Avail: NTIS HC A02

Advances are described in the mobile robot series (currently HERMIES-IIB) to include 8 NCUBE processors onboard (computationally equivalent to 8 Vax 11/780's) operating in parallel, and augmentation of the sensor suite with cameras to facilitate on-board vision analysis and goal finding. The essential capabilities of the expert system described in an earlier paper have also been ported to the on-board HERMIES-IIB computers thereby eliminating off-board computation. A successful experiment is described in which a robot is placed in an initial arbitrary location without prior specification of the room contents, successfully discovers and navigates around stationary and occasionally moving obstacles, picks up and moves small obstacles, searches for a control panel, and reads the meters found on the panel. The success of this experiment encourages more complex on-board vision analysis and expert system control in dynamic environments. The experiment will be expanded to include research in robot learning as the robot attempts to adjust the meter reading to a particular value without a prior knowledge of the control panel system dynamics. DOE

**N88-13603*#** Mechanical Technology, Inc., Latham, N. Y. Research and Development Div.
**SEAL TECHNOLOGY FOR LIQUID OXYGEN (LOX) TURBOPUMPS Final Report, Feb. 1982 - Nov. 1985**
Wilbur Shapiro and Robert Hamm Nov. 1985 388 p
(Contract NAS3-23260)
(NASA-CR-174866; NAS 1.26:174866; Rept-85TR20) Avail: NTIS HC A17/MF A01 CSCL 11A

Two types of advanced seals for liquid oxygen (LOX) turbopumps were investigated. One was a spiral-groove face seal whose function is to seal high-pressure LOX at the impeller end of the turbopump. The other was a floating-ring, Rayleigh-step, helium buffered seal used to prevent LOX ingress to the turbine side of the unit. For each seal type, two sizes were investigated (50 and 20 mm). A turbine-driven test rig was designed and manufactured, and a test program was completed on the 50 mm floating-ring, Rayleigh-step, helium buffered seal. Significant results were: vaporization in the flow path could cause failure by overheating; therefore, the spiral-groove pumping portion of the seal that provides the fluid film must circulate fluid without disruption if vaporization occurs in the sealing dam. This is successfully accomplished by a pressure-balanced spiral-groove concept that is described. The spiral-groove configuration is affected by turbulence in the fluid film and pressure drops due to fluid inertia at sudden contractions. The net results of these effects are deep grooves, large operating films, and high power loss when compared against seals operating with laminar films. Turbulence and inertia are induced by the high-density and low-viscosity characteristics of LOX. The program clearly pointed out the need to consider system environmental factors such as thermal and centrifugal distortions and rotor vibrations in the seal design. Author

**N88-13604*#** National Aeronautics and Space Administration. Lewis Research Center, Cleveland, Ohio.
**FINITE-ELEMENT GRID IMPROVEMENT BY MINIMIZATION OF STIFFNESS MATRIX TRACE**
Madan G. Kittur, Ronald L. Huston (Cincinnati Univ., Ohio.), and Fred B. Oswald Dec. 1987 17 p Prepared in cooperation with Army Aviation Research and Development Command, St. Louis, Mo.
(NASA-TM-100255; E-3827; NAS 1.15:100255) Avail: NTIS HC A03/MF A01 CSCL 20K

A new and simple method of finite-element grid improvement is presented. The objective is to improve the accuracy of the analysis. The procedure is based on a minimization of the trace of the stiffness matrix. For a broad class of problems this minimization is seen to be equivalent to minimizing the potential energy. The method is illustrated with the classical tapered bar problem examined earlier by Prager and Masur. Identical results are obtained. Author

**N88-13605*#** National Aeronautics and Space Administration. Goddard Space Flight Center, Greenbelt, Md.
**TRAJECTORY CONTROL OF ROBOT MANIPULATORS WITH CLOSED-KINEMATIC CHAIN MECHANISM**
Charles C. Nguyen, Farhad J. Pooran (Catholic Univ. of America, Washington, D.C.), and Timothy Premack [1987] 5 p
(Grant NAG5-780)
(NASA-TM-89305; NAS 1.15:89305) Avail: NTIS HC A02/MF A01 CSCL 13I

The problem of Cartesian trajectory control of a closed-kinematic chain mechanism robot manipulator, recently built at CAIR to study the assembly of NASA hardware for the future Space Station, is considered. The study is performed by both computer simulation and experimentation for tracking of three different paths: a straight line, a sinusoid, and a circle. Linearization and pole placement methods are employed to design controller gains. Results show that the controllers are robust and there are good agreements between simulation and experimentation. The results also show excellent tracking quality and small overshoots. Author

**N88-13637*#** Army Engineer Waterways Experiment Station, Vicksburg, Miss. Instrumentation Services Div.
**MEASUREMENT OF SUSPENSION AND RIDE CHARACTERISTICS OF THE M1 MAIN BATTLE TANK**
Bobby E. Reed, Billy Palmertree, and C. W. Bobbitt (Mississippi State Univ., Miss.) *In* NASA-Marshall Space Flight Center, The 58th Shock and Vibration Symposium, Volume 1 Oct. 1987 p 441-457 (For primary document see N88-13609 05-39)
Avail: NTIS HC A21/MF A01 CSCL 13I

**N88-13640*#** Institut National des Sciences Appliquees de Lyon, Villeurbanne (France). Lab. de Mecanique des Structures.
**DYNAMIC BEHAVIOR OF DISSYMMETRIC ROTOR BEARINGS MODELLED WITH A PERIODIC COEFFICIENT LARGE SYSTEM**
P. M. Guilhen, P. Berthier, G. Ferraris, and M. Lalanne *In* NASA-Marshall Space Flight Center, The 58th Shock and Vibration Symposium, Volume 1 Oct. 1987 p 487-494 (For primary document see N88-13609 05-39)
Avail: NTIS HC A21/MF A01 CSCL 13I

# 38 QUALITY ASSURANCE AND RELIABILITY

Includes product sampling procedures and techniques; and quality control.

**N88-13629*#** Rockwell International Corp., Huntsville, Ala. Space Transportation Systems Div.
**INCIPIENT FAILURE DETECTION OF SPACE SHUTTLE MAIN ENGINE TURBOPUMP BEARINGS USING VIBRATION ENVELOPE DETECTION**
Charles B. Hopson *In* NASA-Marshall Space Flight Center, The 58th Shock and Vibration Symposium, Volume 1 Oct. 1987 p 337-347 (For primary document see N88-13609 05-39)
(Contract NAS8-36700)
Avail: NTIS HC A21/MF A01 CSCL 14D

# 39 STRUCTURAL MECHANICS

Includes structural element design and weight analysis; fatigue; and thermal stress.

For applications see *05 Aircraft Design, Testing and Performance* and *18 Spacecraft Design, Testing and Performance.*

**N88-13606#** Structureal Integrity Associates, Inc., San Jose, Calif.
**STRESS INTENSITY FACTORS FOR CRACKING METAL STRUCTURES UNDER RAPID THERMAL LOADING, PHASE 1 Final Report, Jul. 1986 - Feb. 1987**
An-Yu Kuo, P. C. Riccardella, and Joseph P. Gallagher Jun. 1987 88 p
(Contract F33615-86-C-3219)
(AD-A184112; SIR-87-005; AFWAL-TR-87-3022) Avail: NTIS HC A05/MF A01 CSCL 11F

An SBIR Phase I feasibility study has been conducted on a novel method of calculating cracktip stress intensity factors for cracked metal structures under rapid thermal pulse loadings. The work couples a Green's function integration technique for transient thermal stresses with the well-known influence function approach for calculating stress intensity factors. A preliminary version of a computer program implementing the methodology designated AF-CRACK, was developed and delivered with the Phase I project report. Operable on an IBM-pc or compatible, the program demonstrates the ability to accurately calculate stress intensity factors, with very short turnaround times, and immediate graphics visualization of the results. GRA

**N88-13607#** Laboratorio de Computacao Cientifica, Rio de Janeiro (Brazil).
**WELDED JOINT FATIGUE OF A AISI 304 L TYPE STAINLESS STEEL**
N. K. Kuramoto, A. S. Guimaraes, P. E. V. deMiranda, and R. Pascual 1986 1 p In PORTUGUESE; ENGLISH summary Presented at the 4th Brazilian Symposium on Piping and Pressure Vessels, Salvador, Brazil, 28 Oct. 1986
(DE87-703530; INIS-BR-784; CONF-8610317-5-Summ) Avail: NTIS (US Sales Only) HC A02/MF A01

The flexing fatigue behavior for the base metal and welded joints of a type AISI 304 L stainless steel was characterized. An automatic welding process was used with improved procedures in order to warrant better welding metallurgy. Fatigue test sample reinforcements were machined to enable the characterization of the metallurgical variables, especially the role physics played by delta ferrite. The resulting welded joints showed better fatigue life than the base metal. Delta ferrite was found to play an important role on the initiation and propagation processes of the fatigue cracks. DOE

**N88-13608#** Laboratorio de Computacao Cientifica, Rio de Janeiro (Brazil).
**FINITE ELEMENT MODEL FOR THE STRESS AND FLEXIBILITY ANALYSIS OF CURVED PIPES**
J. N. C. Guerreiro Mar. 1987 20 p In PORTUGUESE; ENGLISH summary
(DE87-703632; LNCC-008/87) Avail: NTIS (US Sales Only) HC A03/MF A01

We present a finite element model for the analysis of pipe bends with flanged ends or flanged tangents. Comments are made on the consideration of the internal pressure load. Flexibility and stress intensification factores obtained with the present model are compared with others available. DOE

**N88-13609*#** National Aeronautics and Space Administration. Marshall Space Flight Center, Huntsville, Ala.
**THE 58TH SHOCK AND VIBRATION SYMPOSIUM, VOLUME 1**
Walter D. Pilkey, comp. and Barbara F. Pilkey, comp. (Virginia Univ., Charlottesville.) Oct. 1987 476 p Symposium held in Huntsville, Ala., 13-15 Oct. 1987
(NASA-CP-2488-Vol-1; M-571-Vol-1; NAS 1.55:2488-Vol-1) Avail: NTIS HC A21/MF A01 CSCL 20K

The proceedings of the 58th Shock and Vibration Symposium, held in Huntsville, Alabama, October 13 to 15, 1987 are given. Mechanical shock, dynamic analysis, space shuttle main engine vibration, isolation and damping, and analytical methods are discussed. For individual titles, see N88-13610 through N88-13641.

**N88-13610*#** Astron Research and Engineering, Santa Monica, Calif.
**THE ANALYSIS OF NONSTATIONARY VIBRATION DATA**
Allan G. Piersol *In* NASA-Marshall Space Flight Center, The 58th Shock and Vibration Symposium, Volume 1 Oct. 1987 p 3-2 (For primary document see N88-13609 05-39)
Avail: NTIS HC A21/MF A01 CSCL 20K

The general methodology for the analysis of arbitrary nonstationary random data is reviewed. A specific parametric model, called the product model, that has applications to space vehicle launch vibration data analysis is discussed. Illustrations are given using the nonstationary launch vibration data measured on the Space Shuttle orbiter vehicle. Author

**N88-13611*#** Sandia National Labs., Albuquerque, N. Mex.
**CONSERVATISM IMPLICATIONS OF SHOCK TEST TAILORING FOR MULTIPLE DESIGN ENVIRONMENTS**
Thomas J. Baca, R. Glenn Bell, and Susan A. Robbins *In* NASA-Marshall Space Flight Center, The 58th Shock and Vibration Symposium, Volume 1 Oct. 1987 p 29-47 (For primary document see N88-13609 05-39)
Avail: NTIS HC A21/MF A01 CSCL 20K

A method for analyzing shock conservation in test specifications that have been tailored to qualify a structure for multiple design environments is discussed. Shock test conservation is qualified for shock response spectra, shock intensity spectra and ranked peak acceleration data in terms of an Index of Conservation (IOC) and an Overtest Factor (OTF). The multi-environment conservation analysis addresses the issue of both absolute and average conservation. The method is demonstrated in a case where four laboratory tests have been specified to qualify a component which must survive seven different field environments. Final judgment of the tailored test specification is shown to require an understanding of the predominant failure modes of the test item. Author

**N88-13612*#** Naval Surface Weapons Center, Silver Spring, Md. Electronics Hardening Branch.
**SCALING THE ELECTROMAGNETICALLY DRIVEN EXPLOSIVE SHOCK SIMULATOR** **c09**
Robert I. Persh *In* NASA-Marshall Space Flight Center, The 58th Shock and Vibration Symposium, Volume 1 Oct. 1987 p 49-60 (For primary document see N88-13609 05-39)
Avail: NTIS HC A21/MF A01 CSCL 14B

A heavy payload electromagnetically driven explosive shock simulator, referred to as EDESS-3, has been assembled and characterized at the Navel research Weapons Center. EDESS-3 is the logical outgrowth of the earlier EDESS 1 and 2 simulator work which explored the use of electrical pulse power technology for the generation of explosive like shocks. The features of the EDESS-3 are presented, and designs for the next generation of EDESS machines are introduced. Author

**N88-13613*#** Naval Postgraduate School, Monterey, Calif. Dept. of Mechanical Engineering.
**EXPERIMENTAL STUDIES ON THE TRIPPING BEHAVIOR OF NARROW T-STIFFENED FLAT PLATES SUBJECTED TO HYDROSTATIC PRESSURE AND UNDERWATER SHOCK**
H. L. Budweg and Y. S. Shin *In* NASA-Marshall Space Flight Center, The 58th Shock and Vibration Symposium, Volume 1 Oct. 1987 p 61-95 (For primary document see N88-13609 05-39)
Avail: NTIS HC A21/MF A01 CSCL 20K

An experimental investigation was conducted to determine the static and dynamic responses of a specific stiffened flat plate design. The air-backed rectangular flat plates of 6061-T6 aluminum with an externally machined longitudinal narrow-flanged T-stiffener and clamped boundary conditions were subjected to static loading by water hydropump pressure and shock loading from an eight pound TNT charge detonated underwater. The dynamic test plate was instrumented to measure transient strains and free field pressure. The static test plate was instrumented to measure transient strains, plate deflection, and pressure. Emphasis was placed upon forcing static and dynamic stiffener tripping, obtaining relevant strain and pressure data, and studying the associated plate-stiffener behavior. Author

**N88-13614*#** Advanced Technology and Research, Inc., Laurel, Md.
**NON-LINEAR SHIPBOARD SHOCK ANALYSIS OF THE TOMAHAWK MISSILE SHOCK ISOLATION SYSTEM**
Joel Leifer and Michael Gross *In* NASA-Marshall Space Flight Center, The 58th Shock and Vibration Symposium, Volume 1 Oct. 1987 p 97-117 (For primary document see N88-13609 05-39)
Avail: NTIS HC A21/MF A01 CSCL 20K

The identification, quantification, computer modeling and verification of the Tomahawk nonlinear liquid spring shock isolation system in a surface ship Vertical Launch System (VLS) are discussed. The isolation system hardware and mode of operation is detailed in an effort to understand the nonlinearities. These nonlinearities are then quantified and modeled using the MSC/NASTRAN finite element code. The model was verified using experimental data from the Navel Ordnance Systems Center MIL-S-901 medium weight shock tests of August 1986. The model was then used to predict the Tomahawk response to the CG-53 USS Mobile Bay shock trials of May-June 1987. Results indicate that the model is an accurate mathematical representation of the

physical system either functioning as designed or in an impaired condition due to spring failure. Author

**N88-13615*#** Industrieanlagen-Betriebsgesellschaft m.b.H., Ottobrunn (West Germany).
**ON THE SIMULATION OF BALLISTIC SHOCK LOADS**
Uwe Hollburg *In* NASA-Marshall Space Flight Center, The 58th Shock and Vibration Symposium, Volume 1 Oct. 1987 p 119-135 (For primary document see N88-13609 05-39)
Avail: NTIS HC A21/MF A01 CSCL 20K

Blast or penetrator-impact induced shocks are characterized by high acceleration levels, particularly in the higher frequency range and for a short time duration. These shocks are dangerous for the equipment of ships, combat vehicles, airplanes or spacecraft structures. As ballistic shock loads are insufficiently simulated by laboratory test machines, researchers designed a ballistic shock simulator. The impact induced shocks are simulated by an explosive and the vehicle to be bombarded is replaced by a simplified structure. This structure is suitable to accomodate any equipment which can be tested up to their load limits. Author

**N88-13616*#** Army Engineer Waterways Experiment Station, Vicksburg, Miss.
**ANALYSIS OF PHOTOPOLE DATA REDUCTION MODELS**
James B. Cheek *In* NASA-Marshall Space Flight Center, The 58th Shock and Vibration Symposium, Volume 1 Oct. 1987 p 137-151 (For primary document see N88-13609 05-39)
Avail: NTIS HC A21/MF A01 CSCL 20K

An analysis of the total impulse obtained from a buried explosive charge can be calculated from displacement versus time points taken from successive film frames of high speed motion pictures of the explosive event. The indicator of that motion is a pole and baseplate (photopole), which is placed on or within the soil overburden. Here, researchers are concerned with the precision of the impulse calculation and ways to improve that precision. Also examined here is the effect of each initial condition on the curve fitting process. It is shown that the zero initial velocity criteria should not be applied due to the linear acceleration versus time character of the cubic power series. The applicability of the new method to photopole data records whose early time motions are obscured is illustrated. Author

**N88-13617*#** Structural Dynamics Research Corp., San Diego, Calif.
**MODAL SURVEY OF THE SPACE SHUTTLE SOLID ROCKET MOTOR USING MULTIPLE INPUT METHODS** **c20**
Ralph Brillhart, David L. Hunt, Brent M. Jensen, and Donald R. Mason (Morton Thiokol, Brigham City, Utah.) *In* NASA-Marshall Space Flight Center, The 58th Shock and Vibration Symposium, Volume 1 Oct. 1987 p 155-167 (For primary document see N88-13609 05-39)
Avail: NTIS HC A21/MF A01 CSCL 21H

The ability to accurately characterize propellant in a finite element model is a concern of engineers tasked with studying the dynamic response of the Space Shuttle Solid Rocket Motor (SRM). THe uncertainties arising from propellant characterization through specimem testing led to the decision to perform a model survey and model correlation of a single segment of the Shuttle SRM. Multiple input methods were used to excite and define case/propellant modes of both an inert segment and, later, a live propellant segment. These tests were successful at defining highly damped, flexible modes, several pairs of which occured with frequency spacing of less than two percent. Author

**N88-13618*#** Cincinnati Univ., Ohio. Structural Dynamics Research Lab.
**A NEW METHOD TO REAL-NORMALIZE MEASURED COMPLEX MODES**
Max L. Wei, Randall J. Allemang, Qiang Zhang, and David L. Brown *In* NASA-Marshall Space Flight Center, The 58th Shock and Vibration Symposium, Volume 1 Oct. 1987 p 169-180 (For primary document see N88-13609 05-39)
Avail: NTIS HC A21/MF A01 CSCL 20K

A time domain subspace iteration technique is presented to compute a set of normal modes from the measured complex modes. By using the proposed method, a large number of physical coordinates are reduced to a smaller number of model or principal coordinates. Subspace free decay time responses are computed using properly scaled complex modal vectors. Companion matrix for the general case of nonproportional damping is then derived in the selected vector subspace. Subspace normal modes are obtained through eigenvalue solution of the (M sub N) sup -1 (K sub N) matrix and transformed back to the physical coordinates to get a set of normal modes. A numerical example is presented to demonstrate the outlined theory. Author

**N88-13619*#** Clarkson Univ., Potsdam, N.Y. Dept. of Civil and Environmental Engineering.
**THE MATRIX EXPONENTIAL IN TRANSIENT STRUCTURAL ANALYSIS**
Levon Minnetyan *In* NASA-Marshall Space Flight Center, The 58th Shock and Vibration Symposium, Volume 1 Oct. 1987 p 181-192 (For primary document see N88-13609 05-39)
Avail: NTIS HC A21/MF A01 CSCL 20K

The primary usefulness of the presented theory is in the ability to represent the effects of high frequency linear response with accuracy, without requiring very small time steps in the analysis of dynamic response. The matrix exponential contains a series approximation to the dynamic model. However, unlike the usual analysis procedure which truncates the high frequency response, the approximation in the exponential matrix solution is in the time domain. By truncating the series solution to the matrix exponential short, the solution is made inaccurate after a certain time. Yet, up to that time the solution is extremely accurate, including all high frequency effects. By taking finite time increments, the exponential matrix solution can compute the response very accurately. Use of the exponential matrix in structural dynamics is demonstrated by simulating the free vibration response of multi degree of freedom models of cantilever beams. Author

**N88-13620*#** Cincinnati Univ., Ohio. Structural Dynamics Research Lab.
**IMPROVEMENT OF MODAL SCALING FACTORS USING MASS ADDITIVE TECHNIQUE**
Qiang Zhang, Randall J. Allemang, Max L. Wei, and David L. Brown *In* NASA-Marshall Space Flight Center, The 58th Shock and Vibration Symposium, Volume 1 Oct. 1987 p 193-202 (For primary document see N88-13609 05-39)
Avail: NTIS HC A21/MF A01 CSCL 20K

A general investigation into the improvement of modal scaling factors of an experimental modal model using additive technique is discussed. Data base required by the proposed method consists of an experimental modal model (a set of complex eigenvalues and eigenvectors) of the original structure and a corresponding set of complex eigenvalues of the mass-added structure. Three analytical methods,i.e., first order and second order perturbation methods, and local eigenvalue modification technique, are proposed to predict the improved modal scaling factors. Difficulties encountered in scaling closely spaced modes are discussed. Methods to compute the necessary rotational modal vectors at the mass additive points are also proposed to increase the accuracy of the analytical prediction. Author

**N88-13621*#** Assurance Technology Corp., Carlisle, Mass.
**INITIAL DYNAMIC LOAD ESTIMATES DURING CONFIGURATION DESIGN**
Daniel Schiff *In* NASA-Marshall Space Flight Center, The 58th Shock and Vibration Symposium, Volume 1 Oct. 1987 p 203-223 Sponsored by NRL (For primary document see N88-13609 05-39)
Avail: NTIS HC A21/MF A01 CSCL 20K

This analysis includes the structural response to shock and vibration and evaluates the maximum deflections and material stresses and the potential for the occurrence of elastic instability, fatigue and fracture. The required computations are often performed by means of finite element analysis (FEA) computer programs in

which the structure is simulated by a finite element model which may contain thousands of elements. The formulation of a finite element model can be time consuming, and substantial additional modeling effort may be necessary if the structure requires significant changes after initial analysis. Rapid methods for obtaining rough estimates of the structural response to shock and vibration are presented for the purpose of providing guidance during the initial mechanical design configuration stage. Author

**N88-13622*#** Cincinnati Univ., Ohio. Dept. of Aerospace Engineering and Engineering Mechanics.

**SIMULTANEOUS STRUCTURAL AND CONTROL OPTIMIZATION VIA LINEAR QUADRATIC REGULATOR EIGENSTRUCTURE ASSIGNMENT**

G. A. Becus, C. Y. Lui, V. B. Venkayya, and V. A. Tischler (Air Force Wright Aeronautical Labs., Wright-Patterson AFB, Ohio.) *In* NASA-Marshall Space Flight Center, The 58th Shock and Vibration Symposium, Volume 1 Oct. 1987 p 225-232 (For primary document see N88-13609 05-39)

Avail: NTIS HC A21/MF A01 CSCL 20K

A method for simultaneous structural and control design of large flexible space structures (LFSS) to reduce vibration generated by disturbances is presented. Desired natural frequencies and damping ratios for the closed loop system are achieved by using a combination of linear quadratic regulator (LQR) synthesis and numerical optimization techniques. The state and control weighing matrices (Q and R) are expressed in terms of structural parameters such as mass and stiffness. The design parameters are selected by numerical optimization so as to minimize the weight of the structure and to achieve the desired closed-loop eigenvalues. An illustrative example of the design of a two bar truss is presented. Author

**N88-13623*#** Honeywell, Inc., Glendale, Ariz.

**VISCOUS DAMPED SPACE STRUCTURE FOR REDUCED JITTER**

James F. Wilson and L. Porter Davis *In* NASA-Marshall Space Flight Center, The 58th Shock and Vibration Symposium, Volume 1 Oct. 1987 p 233-243 (For primary document see N88-13609 05-39)

Avail: NTIS HC A21/MF A01 CSCL 20K

A technique to provide modal vibration damping in high performance space structures was developed which uses less than one once of incompressible fluid. Up to 50 percent damping can be achieved which can reduce the settling times of the lowest structural mode by as much as 50 to 1. This concept allows the designers to reduce the weight of the structure while improving its dynamic performance. Damping by this technique is purely viscous and has been shown by test to be linear over 5 orders of input magnitude. Amplitudes as low as 0.2 microinch were demonstrated. Damping in the system is independent of stiffness and relatively insensitive to temperature. Author

**N88-13624*#** Mechanical Technology, Inc., Latham, N. Y. Advanced Technology Operation.

**ON THE GLITCHES IN THE FORCE TRANSMITTED BY AN ELECTRODYNAMIC EXCITER TO A STRUCTURE**

Dantam K. Rao *In* NASA-Marshall Space Flight Center, The 58th Shock and Vibration Symposium, Volume 1 Oct. 1987 p 245-255 (For primary document see N88-13609 05-39)

Avail: NTIS HC A21/MF A01 CSCL 20K

Around resonance, the force transmitted by an exciter into a structure will be smaller or greater than a reference force generated by its coils due to electromechanical interaction. A simple analysis is presented which reveals how this phenomenon of force drop-off is controlled by three factors. The first factor, called Armature Mass Factor, describes a purely mechanical interaction between the structure and the exciter. The electromechanical energy conversion and its interaction with the structure yields two additional factors, called Electrical Resistance and Electrical Inductance Factors. They describe the effects of coil resistance, inductance and magnetic field strength relative to structural damping and stiffness. Present analysis indicates that, under proper circumstances, more than 90 percent of the force drop-off can be eliminated if armature-to-structure mass ratio is smaller or equal to half of modal loss factor. Author

**N88-13625*#** Advanced Technology and Research, Inc., Laurel, Md.

**A SYSTEM IDENTIFICATION TECHNIQUE BASED ON THE RANDOM DECREMENT SIGNATURES. PART 2: EXPERIMENTAL RESULTS**

Nabih E. Bedewi and Jackson C. S. Yang (Maryland Univ., College Park.) *In* NASA-Marshall Space Flight Center, The 58th Shock and Vibration Symposium, Volume 1 Oct. 1987 p 257-273 (For primary document see N88-13609 05-39)

Avail: NTIS HC A21/MF A01 CSCL 20K

Identification of the system parameters of a randomly excited structure may be treated using a variety of statistical techniques. Of all these techniques, the Random Decrement is unique in that it providcs the homogeneous component of the system response. Using this quality, a system identification technique was developed based on a least-squares fit of the signatures to estimate the mass, damping, and stiffness matrices of a linear randomly excited system. The mathematics of the technique is presented in addition to the results of computer simulations conducted to demonstrate the prediction of the response of the system and the random forcing function initially introduced to excite the system. Author

**N88-13626*#** Advanced Technology and Research, Inc., Laurel, Md.

**A SYSTEM IDENTIFICATION TECHNIQUE BASED ON THE RANDOM DECREMENT SIGNATURES. PART 2: EXPERIMENTAL RESULTS**

Nabih E. Bedewi and Jackson C. S. Yang (Maryland Univ., College Park.) *In* NASA-Marshall Space Flight Center, The 58th Shock and Vibration Symposium, Volume 1 Oct. 1987 p 275-287 (For primary document see N88-13609 05-39)

Avail: NTIS HC A21/MF A01 CSCL 20K

Identification of the system parameters of a randomly excited structure may be treated using a variety of statistical techniques. Of all these techniques, the Random Decrement is unique in that it provides the homogeneous component of the system response. Using this quality, a system identification technique was developed based on a least-squares fit of the signatures to estimate the mass, damping, and stiffness matrices of a linear randomly excited system. The results of an experiment conducted on an offshore platform scale model to verify the validity of the technique and to demonstrate its application in damage detection are presented. Author

**N88-13627*#** Sandia National Labs., Albuquerque, N. Mex. Modal and Structural Dynamics Div.

**STRUCTURAL FREQUENCY FUNCTIONS FOR AN IMPULSIVE, DISTRIBUTED FORCING FUNCTION**

Vesta I. Bateman *In* NASA-Marshall Space Flight Center, The 58th Shock and Vibration Symposium, Volume 1 Oct. 1987 p 291-319 (For primary document see N88-13609 05-39)

Avail: NTIS HC A21/MF A01 CSCL 20K

The response of a penetrator structure to a spatially distributed mechanical impulse with a magnitude approaching field test force levels (1-2 Mlb) were measured. The frequency response function calculated from the response to this unique forcing function is compared to frequency response functions calculated from response to point forces of about 2000 pounds. The results show that the strain gages installed on the penetrator case respond similiarly to a point, axial force and to a spatially distributed, axial force. This result suggests that the distributed axial force generated in a penetration event may be reconstructed as a point axial force when the penetrator behaves in linear manner. Author

**N88-13628*#** Rockwell International Corp., Canoga Park, Calif. Rocketdyne Div.

**FLUID MASS AND THERMAL LOADING EFFECTS ON THE MODAL CHARACTERISTICS OF SPACE SHUTTLE MAIN ENGINE LIQUID OXYGEN INLET SPLITTER VANES**

H. V. Panossian and J. J. Boehnlein *In* NASA-Marshall Space Flight Center, The 58th Shock and Vibration Symposium, Volume 1 Oct. 1987 p 323-335 (For primary document see N88-13609 05-39)
(Contract NAS8-40000)
Avail: NTIS HC A21/MF A01 CSCL 20K

An analysis and evaluation of experimental modal survey test data on the variations of modal characteristics induced by pressure and thermal loading events are presented. Extensive modal survey tests were carried out on a Space Shuttle Main Engine (SSME) test article using liquid nitrogen under cryogenic temperatures and high pressures. The results suggest that an increase of pressure under constant cryogenic temperature or a decrease of temperature under high pressure induces an upward shift of frequencies of various modes of the structures. Author

**N88-13629*#** Rockwell International Corp., Huntsville, Ala. Space Transportation Systems Div.
**INCIPIENT FAILURE DETECTION OF SPACE SHUTTLE MAIN ENGINE TURBOPUMP BEARINGS USING VIBRATION ENVELOPE DETECTION** c38
Charles B. Hopson *In* NASA-Marshall Space Flight Center, The 58th Shock and Vibration Symposium, Volume 1 Oct. 1987 p 337-347 (For primary document see N88-13609 05-39)
(Contract NAS8-36700)
Avail: NTIS HC A21/MF A01 CSCL 14D

The results of an analysis performed on seven successive Space Shuttle Main Engine (SSME) static test firings, utilizing envelope detection of external accelerometer data are discussed. The results clearly show the great potential for using envelope detection techniques in SSME incipient failure detection. Author

**N88-13630*#** National Aeronautics and Space Administration. Marshall Space Flight Center, Huntsville, Ala.
**HIGH FREQUENCY DATA ACQUISITION SYSTEM FOR SPACE SHUTTLE MAIN ENGINE TESTING** c20
Pat Lewallen *In its* The 58th Shock and Vibration Symposium, Volume 1 Oct. 1987 p 349-352 (For primary document see N88-13609 05-39)
Avail: NTIS HC A21/MF A01 CSCL 21H

The high frequency data acquisition system developed for the Space Shuttle Main Engine (SSME) single engine test facility at the National Space Technology Laboratories is discussed. The real time system will provide engineering data for a complete set of SSME instrumentation (approx. 100 measurements) within 4 hours following engine cutoff, a decrease of over 48 hours from the previous analog tape based system. Author

**N88-13631*#** National Aeronautics and Space Administration. Marshall Space Flight Center, Huntsville, Ala.
**SPACE SHUTTLE MAIN ENGINE VIBRATION DATA BASE** c20
Pat Lewallen *In its* The 58th Shock and Vibration Symposium, Volume 1 Oct. 1987 p 353-359 (For primary document see N88-13609 05-39)
Avail: NTIS HC A21/MF A01 CSCL 21H

In order to evaluate Space Shuttle Main Engine (SSME) vibration data without having to constantly replay analog tapes, the SSME Vibration Data Base was developed. This data base contains data that have been digitized at a high sample rate for the entire test duration. It provides quick and efficient recall capabilities for numerious computation and display routines. The data base components are described as well as some of the compution and display features. Author

**N88-13632*#** West Virginia Univ., Morgantown. Dept. of Civil Engineering.
**EXACT FINITE ELEMENT METHOD ANALYSIS OF VISCOELASTIC TAPERED STRUCTURES TO TRANSIENT LOADS**
Constantine Chris Spyrakos *In* NASA-Marshall Space Flight Center, The 58th Shock and Vibration Symposium, Volume 1 Oct. 1987 p 361-375 (For primary document see N88-13609 05-39)
Avail: NTIS HC A21/MF A01 CSCL 20K

A general method is presented for determining the dynamic torsional/axial response of linear structures composed of either tapered bars or shafts to transient excitations. The method consists of formulating and solving the dynamic problem in the Laplace transform domain by the finite element method and obtaining the response by a numerical inversion of the transformed solution. The derivation of the torsional and axial stiffness matrices is based on the exact solution of the transformed governing equation of motion, and it consequently leads to the exact solution of the problem. The solution permits treatment of the most practical cases of linear tapered bars and shafts, and employs modeling of structures with only one element per member which reduces the number of degrees of freedom involved. The effects of external viscous or internal viscoelastic damping are also taken into account. Author

**N88-13633*#** Virginia Univ., Charlottesville. Dept. of Mechanical and Aerospace Engineering.
**OPTIMAL SHOCK ISOLATION WITH MINIMUM SETTLING TIME**
W. D. Pilkey and T. W. Lim *In* NASA-Marshall Space Flight Center, The 58th Shock and Vibration Symposium, Volume 1 Oct. 1987 p 379-388 (For primary document see N88-13609 05-39)
Avail: NTIS HC A21/MF A01 CSCL 20K

It is shown how unique isolator forces and corresponding forces can be chosen by superimposing a minimum settling time onto the limiting performance of the shock isolation system. Basically, this means that the system which has reached the peak value of the performance index is settled to rest in minimum time. Author

**N88-13634*#** Structural Dynamics Research Corp., Milford, Ohio.
**AN EFFICIENT FREQUENCY RESPONSE SOLUTION FOR NONPROPORTIONALLY DAMPED SYSTEMS**
Paul Conti and William K. Rule *In* NASA-Marshall Space Flight Center, The 58th Shock and Vibration Symposium, Volume 1 Oct. 1987 p 389-394 (For primary document see N88-13609 05-39)
Avail: NTIS HC A21/MF A01 CSCL 20K

A method is presented to accurately and economically calculate steady state frequency responses based on the analysis of large finite element models with nonproportional damping effects. The new method is a hybrid of the traditional nonproportional and proportional damping solution methods. It captures the advantages of each computational approach without the burden of their respective shortcomings, as demonstrated with comparative analysis performed on a large finite element model. Author

**N88-13635*#** Michigan Univ., Ann Arbor. Dept. of Mechanical Engineering and Applied Mechanics.
**SHAPE OPTIMIZATION OF DAMPING LAYERS**
T.-C. Lin and R. A. Scott *In* NASA-Marshall Space Flight Center, The 58th Shock and Vibration Symposium, Volume Oct. 1987 p 395-409 (For primary document see N88-13609 05-39)
Avail: NTIS HC A21/MF A01 CSCL 20K

Shape optimization of unconstrained and constrained damping layers is completed. The specific problem analyzed is a cantilever beam loaded at its tip by a harmonic force. Finite element modeling and mathematical programming techniques are used to obtain the solution. Performance measures are taken to be reduction of maximum diplacement and increase in fatigue lifetime. Results include the improvement, over the uniform treatment case, of these measures when the profile of the damping layer is optimized. Author

**N88-13636*#** Acoustical Research and Applications, Vienna, Va.
**A PASSIVE VIBRATION-CANCELLING ISOLATION MOUNT**
Alan O. Sykes *In* NASA-Marshall Space Flight Center, The

58th Shock and Vibration Symposium, Volume 1 Oct. 1987 p 411-439 (For primary document see N88-13609 05-39)
Avail: NTIS HC A21/MF A01 CSCL 20K

An analysis of an idealized passive vibration-cancelling two-terminal mount with one degree of freedom at each mechanical terminal isolating a nonrigid machine from a nonrigid foundation is presented. To evaluate a vibration-cancelling (VC) mount, its effectiveness as a function of frequency is compared with the effectiveness of both conventional and compound mounts isolating a rigid machine from a nonrigid foundation. The comparisons indicate that a carefully designed and manufactured VC mount should provide substantially greater vibration reduction at its cancellation frequency than either a conventional or compound mount having the same low frequency stiffness, i.e., stiffness at the natural frequency of the machine mount system. Author

**N88-13637*#** Army Engineer Waterways Experiment Station, Vicksburg, Miss. Instrumentation Services Div.
**MEASUREMENT OF SUSPENSION AND RIDE CHARACTERICS OF THE M1 MAIN BATTLE TANK** **c37**
Bobby E. Reed, Billy Palmertree, and C. W. Bobbitt (Mississippi State Univ., Mississippi State.) *In* NASA-Marshall Space Flight Center, The 58th Shock and Vibration Symposium, Volume 1 Oct. 1987 p 441-457 (For primary document see N88-13609 05-39)
Avail: NTIS HC A21/MF A01 CSCL 13I

Means were developed to measure the effect of vibration on human beings in a tank vehicle so as to determine the limits to which they might be taken in terms of operating effectiveness and also in terms of well being. Improved hardware for making these measurements, a method for relating tank hull input forces to ride quality, and installation and calibration of instrumentation to measure the hull forces are discussed. Author

**N88-13638*#** West Virginia Univ., Morgantown. Dept. of Mechanical and Aerospace Engineering.
**ADVANCED JOINING CONCEPTS FOR PASSIVE VIBRATION CONTROL**
Jacky C. Prucz and Constantine Spyrakos *In* NASA-Marshall Space Flight Center, The 58th Shock and Vibration Symposium, Volume 1 Oct. 1987 p 459-471 (For primary document see N88-13609 05-39)
Avail: NTIS HC A21/MF A01 CSCL 20K

A comprehensive parametric study was carried out to establish design guidelines for favorable tradeoffs between damping benefits and the associated stiffness, strength and weight penalties in a rhombic joint. The results are compared with the corresponding tradeoffs for a double-lap joint made of the same materials. Author

**N88-13639*#** Feng Chia Univ., Taichung (Taiwan). Dept. of Mechanical Engineering.
**DYNAMIC RESPONSE OF LAMINATED COMPOSITE PLATES USING A THREE-DIMENSIONAL HYBRID-STRESS FINITE-ELEMENT FORMULATION** **c24**
W. J. Liou and C. T. Sun (Florida Univ., Gainesville.) *In* NASA-Marshall Space Flight Center, The 58th Shock and Vibration Symposium, Volume 1 Oct. 1987 p 475-485 (For primary document see N88-13609 05-39)
Avail: NTIS HC A21/MF A01 CSCL 11D

A method of analysis of dynamic response of laminated composite plates is presented. The analysis is carried by using a hybrid-stress finite element numerical technique. By using this approach, the response of simply supported laminated plates subjected to sinusoidal loading are investigated. For the solution of the finite element equations of motion of free vibrations and dynamic response problems, two effective methods of solution, the space iteration method and the Newmark direct integration method are used. These two methods are discussed here. Author

**N88-13640*#** Institut National des Sciences Appliquees de Lyon, Villeurbanne (France). Lab. de Mecanique des Structures.
**DYNAMIC BEHAVIOR OF DISSYMMETRIC ROTOR BEARINGS MODELLED WITH A PERIODIC COEFFICIENT LARGE SYSTEM** **c37**
P. M. Guilhen, P. Berthier, G. Ferraris, and M. Lalanne *In* NASA-Marshall Space Flight Center, The 58th Shock and Vibration Symposium, Volume 1 Oct. 1987 p 487-494 (For primary document see N88-13609 05-39)
Avail: NTIS HC A21/MF A01 CSCL 13I

The instability and unbalance response of dissymmetric rotor-bearing systems containing periodic coefficients when modeling produces matrices with a large number of degrees of freedom are discussed. It is important to solve the equations and then predict the dynamic behavior of the system. This can be done knowing the instability areas and the unbalance response in the stable areas. One deals here with a large number of equations and a reduction of the number of degrees of freedom of the system is achieved through a pseudo modal method. This method is shown to give satisfactory results. Author

**N88-13641*#** West Virginia Univ., Morgantown. Dept. of Civil Engineering.
**SIGNIFICANCE OF FOUNDATION-SOIL SEPARATION IN DYNAMIC SOIL-STRUCTURE INTERACTION** **c31**
Constantine C. Spyrakos and P. N. Patel *In* NASA-Marshall Space Flight Center, The 58th Shock and Vibration Symposium, Volume 1 Oct. 1987 p 495-506 (For primary document see N88-13609 05-39)
Avail: NTIS HC A21/MF A01 CSCL 13B

THe dynamic response of flexible surface strip-foundations allowed to uplift is numerically obtained for externally applied forces of a transient time variation. The soil medium is represented by an isotropic, homogeneous and linear half-space. The soil is treated by a time domain boundary element method, while the flexible foundation is treated by the finite element method. It was concluded that intermediate relative stiffness leads to moderate deformations when uplift is permitted. Very flexible footings produce higher deformations in unilateral contact compared to bilateral contact, and thus should be considered in their design. Unilateral contact does not significantly increase deformations for stiff footings subjected to concentrated central loading. However, relatively large deformation differences occur when the loading is eccentric, necessitating consideration of uplift in their design. Author

**N88-13642#** Materials Research Labs., Melbourne (Australia).
**APPLICATION OF FINITE ELEMENT METHODS WITH CYCLIC ELASTO-PLASTIC STRAIN ANALYSIS TO LOW CYCLE FATIGUE ANALYSIS OF ENGINE COMPONENTS**
N. S. Swansson Dec. 1986 37 p
(AR-004-512; ARL-AERO-PROP-R-174) Avail: NTIS HC A03/MF A01

Low Cycle Fatigue (LCF) in engine components involves macroscopic cyclic plastic strains (with a stress-strain hysteresis loop) over a significant portion of the failure region. Characterizing elasto-plastic behavior in potential failure regions is a necessary step in estimating LCF life. The equations governing elasto-plastic behavior are summarized, and the methods for their implementation in Finite Element (FE) stress analysis programs discussed. An extension of the PAFEC program to include mixed isotropic-kinematic hardening is outlined, and verified by examples for which alternative FE solutions were available. A sample application has been made to holes in a plate with biaxial stress fields similar to those in disc webs, and the results compared with the Neuber and modified Stowell rules commonly used for design life estimation; these rules tend to overestimate the strain in biaxial stress conditions, leading to conservative life estimates. Author

**N88-13643** Georgia Inst. of Tech., Atlanta.
**COUPLED ELASTIC ROTOR/BODY VIBRATIONS WITH INPLANE DEGREES OF FREEDOM Ph.D. Thesis**
Ming-Sheng Huang 1987 132 p
Avail: Univ. Microfilms Order No. DA8718452

A complete set of nonlinear, integro-partial differential equations of motion is derived for an elastic rotor with inplane degrees of freedom in both hover and forward flight conditions. The hub equations are also derived. The coupled elastic rotor-fuselage vibrations are solved by harmonic balance and impedance matching for a soft-inplane rotor (Lambda sub 1 = 0.008, Lambda sub 2 = 0.012), and stiff inplane rotor (Lambda sub 1=0.08, Lambda sub 2 =0.12). The results are presented as functions of both fuselage vertical constrained frequency and fuselage pitch constrained frequency. For comparison purposes, the results are also given as a function of vertical constrained frequency with no nonlinear terms. Also, vibrations with hub offsets h bar =0.4, d bar sub p =0.0, d bar sub f=0.2) are presented. All calculations are in forward flight conditions (mu = 0.3). Dissert. Abstr.

**N88-13644** Duke Univ., Durham, N. C.
**AN EXAMINATION OF CHAOTIC MOTION FOR THE BUCKLED BEAM Ph.D. Thesis**
Charles Pezeshki 1987 212 p
Avail: Univ. Microfilms Order No. DA8718429

The dynamics of a magnetically buckled beam are analyzed with a particular slant towards determining why the system exhibits chaotic behavior. The system behavior is analyzed by considering both an experimental and theoretical model. The theoretical model consists of a Rayleigh-Ritz modal expansion. For this theoretical model, chaos boundaries in the parameter space are mapped. Time histories and Poincare maps are calculated. Initial condition maps of different types are also generated. Lyapunov exponents are calculated for one, two, and three mode approximations to the partial differential equation describing the motion. In the experimental analysis, power spectra are calculated from experimentally recorded time histories. Lyapunov exponents are also calculated from these experimental time histories and compared with the theoretical work. Majors results include a verification of the accuracy of the theoretical model for predicting physical behavior. The initial condition maps demonstrate fractal behavior, giving an insight into why chaotic motion occurs. The Lyapunov exponents generated from the theoretical model expansions were also shown to converge. The Lyapunov exponents calculated from the experimentally obtained time histories compared well with the theoretical values. The power spectra obtained from experimental time histories also compared well with power spectra calculated from the modal expansion.
Dissert. Abstr.

**N88-13645#** Virginia Univ., Charlottesville.
**FATIGUE 87, VOLUME 1 Final Report, 1 Jun. 1987 - 1 May 1988**
R. O. Ritchie, ed. and E. A. Starke, Jr., ed. 1987 615 p Presented at the Third International Conference on Fatigue and Fatigue Thresholds, Charlottesville, Va., 28 Jun. - 3 Jul. 1987
(Grant DAAL03-87-G-0102)
(AD-A184045; ARO-24134.1-MS-CF-Vol-1) Avail: NTIS HC A99/MF A01 CSCL 20K

A wide range of diverse views of the fundamental and applied aspects of fatigue are discussed. Questions of cyclic deformation, crack initiation and propagation, small cracks, crack closure, variable amplitude effects, and environmentally influenced behavior are covered. For individual titles, see N88-13646 through N88-13699.

**N88-13646#** Virginia Univ., Charlottesville.
**CYCLIC DEFORMATION AND CRACK INITIATION**
P. Neumann and A. Tonnessen (Max-Planck-Inst. fuer Eisenforschung, Duesseldorf, West Germany ) *In its* Fatigue 87, Volume 1 1987 p 1-22 (For primary document see N88-13645 05-39)
Avail: NTIS HC A99/MF A01 CSCL 20K

Fatigue loading hardens most metals in a peculiar way, forming metastable dislocation configurations and favoring strain localization. Therefore, fatigue crack nucleation usually occurs at highly localized slip bands. Modern sectioning techniques revealed preferred crack initiation sites within these slip bands which are not yet understood. In common microstructures, fatigue crack nucleation can also occur at weak inclusions or special grain boundaries. In spite of their low energy, twin boundaries were found to be predominant crack nucleation sites in high cycle fatigue. Usually, the environment is found to be important in the formation of fatigue cracks. Author

**N88-13647#** Ritsumeikan Univ., Kyoto (Japan). Dept. of Mechanical Engineering.
**EFFECT OF GRAIN ORIENTATION ON THE ORIGINATION AND THE INITIAL GROWTH OF FATIGUE CRACKS IN PURE IRON**
Tsuneshichi Tanaka *In* Virginia Univ., Fatigue 87, Volume 1 1987 p 23-42 (For primary document see N88-13645 05-39)
Avail: NTIS HC A99/MF A01 CSCL 20K

Nucleation and initial growth of fatigue cracks in pure iron plate specimens were observed under reversed bending, axial stresses, and alternating tension. Grain orientation was determined by the etch pit method. It was found that cracks originated at grain boundaries under reversed stress, but they nucleated along slip bands under alternating tension. The shift of the crack nucleation sites may be caused by the degree of development of slip bands activated by the maximum applied stress. Another finding was that the morphology of early cracks was the same as that of the pencil glide observed in the slip motion of b.c.c. metals.
Author

**N88-13648#** General Motors Research Labs., Warren, Mich.
**THE GROWTH OF PERSISTENT SLIP BANDS**
W. J. Baxter *In* Virginia Univ., Fatigue 87, Volume 1 1987 p 43-51 (For primary document see N88-13645 05-39)
Avail: NTIS HC A99/MF A01 CSCL 20K

The growth of persistent slip bands (PSB) in 6061-T6 aluminum was measured with a photoelectron microscope equipped with a fatigue stage. The PSB appeared initially as a small extrusion and elongated across the surface by the sequential addition of new extrusions. As the PSB elongated, the initial extrusion became more pronounced. The rate of elongation in polycrystalline material varied inversely with length, whereas in a single crystal the rate remained constant. This difference is attributed to the constraints imposed upon a small grain by the surrounding material. The growth laws are described by a simple model in which the PSB is softer than the matrix of the grain. Author

**N88-13649#** Salford Univ. (England). Dept. of Aeronautical and Mechanical Engineering.
**THE MECHANICS OF FATIGUE-CRACK NUCLEATION IN A LOW-ALLOY STEEL UNDER FRETTING CONDITIONS**
J. Beard and P. F. Thomason *In* Virginia Univ., Fatigue 87, Volume 1 1987 p 53-62 (For primary document see N88-13645 05-39)
Avail: NTIS HC A99/MF A01 CSCL 20K

A novel fretting-fatigue test rig, giving close control and monitoring of contact stresses and slip amplitude at a Hertzian fretting contact, was used to establish the progressive mechanism of fretting fatigue. Metallographic analysis by electron microscopy methods revealed the presence of very hard white etching layers which were found to fragment and break away from the fretting contact surface at regular intervals. Tentative proposals are given for the mechanism of fatigue crack nucleation under fretting conditions in the presence of white etching layers. Author

**N88-13650#** Michigan Univ., Ann Arbor. Dept. of Materials Science and Engineering.
**THE EFFECTS OF THIN ANODIC FILMS ON THE CYCLIC MICROSTRAIN/MACROSTRAIN BEHAVIOR OF TUNGSTEN**
Keith J. Bowman and Ronald Gibala *In* Virginia Univ., Fatigue 87, Volume 1 1987 p 63-72 (For primary document see N88-13645 05-39)
(Grant NSF DMR-85-0675)
Avail: NTIS HC A99/MF A01 CSCL 20K

The occurrence of film hardening or softening effects in bcc metals is dependent on the relative mobilities of edge and screw dislocations at different homologous temperatures. In this investigation, the difference in the contributions of edge and screw dislocations to plastic flow at different strain levels is used to evaluate the role of thin anodic films in cyclic deformation of W at 298 K. Large reversible hardening effects observed at cyclic microstrains and smaller softening effects which occur at cyclic macrostrains are described in terms of the dominant dislocation species for the two plastic strain regimes. Author

**N88-13651#** Virginia Univ., Charlottesville.
**SURFACE DEFORMATION AND FATIGUE CRACK INITIATION OF ALPHA-IRON**
C. S. Kim, Y. W. Chung, and M. E. Fine (Northwestern Univ., Evanston, Ill.) *In its* Fatigue 87, Volume 1 1987 p 73-82 (For primary document see N88-13645 05-39)
(Grants NSF DMR-83-03904; NSF DMR-82-16972; NSF DMR-85-20280)
Avail: NTIS HC A99/MF A01 CSCL 20K

Cyclic deformation and fatigue crack initiation properties of alpha-iron fatigued under plastic strain control are investigated as a function of orientation. Single slip, double slip, and localized deformation in the form of macroscopic deformation bands brought about by plastic instability were observed. Cracks were found to initiate at slip lines anywhere from 100 to 20,000 cycles depending on crystal orientation at a plastic strain amplitude of 5 times 10 to the minus 4th power. Author

**N88-13652#** Michigan State Univ., East Lansing. Dept. of Metallurgy, Mechanics and Materials Science.
**THE EFFECT OF ION BEAM MIXED Ni-Al SURFACE LAYERS ON PSB EXTRUSION MORPHOLOGY IN FATIGUED NICKEL**
D. S. Grummon and J. W. Jones (Michigan Univ., Ann Arbor.) *In* Virginia Univ., Fatigue 87, Volume 1 1987 p 83-92 (For primary document see N88-13645 05-39)
Avail: NTIS HC A99/MF A01 CSCL 20K

Experiments were performed to study the effect of ion beam mixed Ni-Al surface layers on mechanical behavior and surface damage accumulation associated with crack initiation during fatigue of nickel. Supersaturated solid solutions of Al in Ni and Ni sub 3 Al structures were produced in layers less than 100 mm thick by ballistic mixing of vacuum evaporated films. Such surface alloying altered the number, distribution and morphology of persistant slip band extrusions. The results are discussed in terms of the stresses imposed on the surface film in response to plastic strain localization in the bulk. Author

**N88-13653#** Rockwell International Science Center, Thousand Oaks, Calif.
**THE EVOLUTION OF LOCAL MECHANICAL PROPERTIES OF Al 2219-T851 DURING FATIGUE**
W. L. Morris, M. R. James, and B. N. Cox *In* Virginia Univ., Fatigue 87, Volume 1 1987 p 93-101 (For primary document see N88-13645 05-39)
(Contract N62269-86-C-0261)
Avail: NTIS HC A99/MF A01 CSCL 20K

Local strain amplitudes were measured in individual grains of Al 2219-T851 alloy during fatigue. The alloy has a 360 MPa bulk cyclic yield strength, but its surface is microplastic at cyclic stresses greater than 70 MPa. With fatigue at plus or minus 275 MPa, an upper flow stress of -200 MPa develops in grains much larger than mean size. Large residual stresses caused by the localized deformation severely limit the total strain at these softened sites. The use of a load reduction sequence to minimize these residual stresses during strain measurements, so as to obtain more accurate values for the local flow stresses, is discussed. Author

**N88-13654#** Norges Tekniske Hoegskole, Trondheim. Div. of Metallurgy.
**CYCLIC DEFORMATION OF AN EXTRUDED AlMgSi ALLOY**
Ketill Pedersen *In* Virginia Univ., Fatigue 87, Volume 1 1987 p 103-112 (For primary document see N88-13645 05-39)
Avail: NTIS HC A99/MF A01 CSCL 20K

Specimens in under-, peak- and overaged conditions of an extruded commercial AlMgSi alloy have been cycled under constant plastic strain amplitudes. In the underaged condition, cyclic hardening to a saturation stress was observed. The cyclic hardening was due to formation of a high density of dislocation loops. In the peak aged condition, a saturation stress was obtained after a short period of hardening. Persistent slip bands were not observed on the polished specimen surfaces. If the material is recrystallized and aged to peak hardness, cyclic softening occurs and persistent slip bands are formed. Author

**N88-13655#** Ecole Polytechnique, Montreal (Quebec). Dept. de Genie Metallurgique.
**THE ORIENTATIONS OF DIPOLAR WALLS PRODUCED BY CYCLIC DEFORMATION**
J. I. Dickson, S. Turenne, L. Handfield, and G. LEsperance *In* Virginia Univ., Fatigue 87, Volume 1 1987 p 113-122 Sponsored by NSERC (Canada), and FCAR (Quebec) (For primary document see N88-13645 05-39)
Avail: NTIS HC A99/MF A01 CSCL 20K

Dipolar walls produced by cyclic deformation consist largely of dipole loops and can be modeled as a geometrical network of stacked loops formed by edge trapping and/or jog-dragging mechanisms and swept together by edge dislocations. Such a model helps in understanding the orientations and certain other aspects of dipolar walls in i.c.c., b.c.c. and h.c.p. metals. Author

**N88-13656#** General Dynamics Corp., Fort Worth, Tex.
**CLOSURE BEHAVIOR UNDER CONSTANT EFFECTIVE STRESS INTENSITY LOADING CONDITIONS**
C. D. Carman and B. M. Hillberry (Purdue Univ., West Lafayette, Ind.) *In* Virginia Univ., Fatigue 87, Volume 1 1987 p 125-134 (For primary document see N88-13645 05-39)
Avail: NTIS HC A99/MF A01 CSCL 20K

Crack closure was measured over a wide range of stress intensity levels and stress ratios for 7475-T6 aluminum alloy. These results were used to generate a block loading program that would produce a constant delta kappa sub eff which was then shown experimentally to produce a constant fatigue crack growth rate. Author

**N88-13657#** Volvo A.B., Goeteborg (Sweden). Lab. for Metallic Materials.
**THE INFLUENCE OF THE TOPOGRAPHY OF FRACTURE SURFACES ON CRACK CLOSURE**
K. Hamberg, J. Wasen, and B. Karlsson (Chalmers Univ. of Technology, Goeteborg, Sweden ) *In* Virginia Univ., Fatigue 87, Volume 1 1987 p 135-144 Sponsored by the Swedish Board of Technical Development (For primary document see N88-13645 05-39)
Avail: NTIS HC A99/MF A01 CSCL 20K

This investigation of steels with microstructures of ferrite, ferrite/pearlite, ferrite/martensite and pearlite lead to the conclusions that, in the case of single phase materials, the fracture surface toughness increases linearly with the size of the micro structural unit; both the volume fraction and the hardness of second phase inclusions are determining factors for the fracture surface roughness in coarse grained steels; the closure level is closely related to fracture surface roughness. Author

**N88-13658#** Virginia Univ., Charlottesville.
**GROWTH OF SHORT FATIGUE CRACKS IN A SQUEEZE FORMED ALUMINUM ALLOY**
B. P. D. OConnor and A. Plumtree (Waterloo Univ., Ontario ) *In its* Fatigue 87, Volume 1 1987 p 145-154 (For primary document see N88-13645 05-39)
Avail: NTIS HC A99/MF A01 CSCL 20K

The initiation and early growth of fatigue cracks in strain cycled squeeze formed 6066-T6 aluminum alloy was investigated using single stage replication techniques. Cracks initiated at the second phase particles in the interdendritic region. Fatigue cracks

propagated through these regions. Short crack growth behavior may be expressed using a model based on crack tip plasticity where the barriers are second phase particles at triple junctions. These barriers influenced the growth at low strain amplitudes more than at higher amplitudes. Author

**N88-13659#** Virginia Univ., Charlottesville.
**INFLUENCE OF MICROSTRUCTURE AND AGING CONDITION ON THE FATIGUE CRACK PROPAGATION IN AGE HARDENED ALUMINIUM ALLOYS**
R. Scheffel, O. Ibas, and K. Detert (Siegen Univ., West Germany) *In its* Fatigue 87, Volume 1 1987 p 155-164 (For primary document see N88-13645 05-39)
Avail: NTIS HC A99/MF A01 CSCL 20K

Fatigue crack growth rates of age hardened aluminum alloys with different grain sizes were studied. The tests were conducted on specimens at increasing delta kappa values and on bend specimens at increasing as well as decreasing delta kappa. The stress ratio varied between 0.1 and 0.8. An influence of stress ratio below 0.6 was found with increasing grain size. This could be explained by roughness induced closure which occurs in coarse grained materials. By taking closure into account, good agreement of the data at all stress ratios and for different aluminum alloys could be obtained. An absolute threshold value is found to be below 1.5 MPa square root of m. Author

**N88-13660#** Iowa Univ., Iowa City. Dept. of Mechanical Engineering.
**FATIGUE CRACK GROWTH BEHAVIOR OF A356-T6 CAST ALUMINUM ALLOY**
C. C. Wigant and R. I. Stephens *In* Virginia Univ., Fatigue 87, Volume 1 1987 p 165-174 (For primary document see N88-13645 05-39)
Avail: NTIS HC A99/MF A01 CSCL 20K

Constant amplitude fatigue crack growth behavior was obtained for A356-T6 (Al7SiMg) cast aluminum alloy for crack growth rates between 10 to the minus 11th power and 10 to the minus 6th power m/cycle with R ratios of 0.1 and 0.5. Three different mold temperatures resulted in secondary dendritic arm spacings to vary from about 80 to 90 microns, resulting in only coarse microstructure. Threshold levels, delta kappa sub th, and the Paris exponent, m, were approximately twice the values usually found for wrought aluminum alloys. The influence of R ratio was quite pronounced, and crack closure did not eliminate threshold and near threshold R ratio differences. Roughness induced crack closure was no doubt more important than plasticity induced closure. Author

**N88-13661#** Norges Tekniske Hoegskole, Trondheim. Div. of Metallurgy.
**STRIATIONS AND THE FATIGUE GROWTH MECHANISM IN A MICRO-ALLOYED STEEL**
H. J. Roven, M. A. Langoy, and E. Nes *In* Virginia Univ., Fatigue 87, Volume 1 1987 p 175-184 (For primary document see N88-13645 05-39)
Avail: NTIS HC A99/MF A01 CSCL 20K

The fatigue crack growth mechanism was studied in a micro-alloyed steel in laboratory air at constant load ratio. A striation mechanism was found to dominate both the delta kappa sub th and Paris law region. The striation spacing was found to be constant over four orders of magnitude of crack growth rates, whereas the classical one cycle per striation spacing only occurred in a small fraction of the Paris law regime. The crack deformation zone contained subgrains with a decreasing size as the fracture plane was approached. A model was developed to describe the observed empirical connection between delta kappa and N sub s (number of cycles per striation). The crack growth equation in this model is in accordance with the accumulated damage philosophy. Author GR

**N88-13662#** Air Force Materials Lab., Wright-Patterson AFB, Ohio.
**SIGNIFICANCE OF FATIGUE CRACK CLOSURE UNDER SPECTRUM LOADING**
R. Sunder *In* Virginia Univ., Fatigue 87, Volume 1 1987 p 185-194 (For primary document see N88-13645 05-39)
Avail: NTIS HC A99/MF A01 CSCL 20K

A numerical study was made to evaluate the significance of fatigue crack closure under spectrum loading. It uses a reasonably accurate crack growth prediction model to assess the effect of variation in crack closure stress on predicted life. It is shown that precise knowledge of crack closure stress can be crucial to life estimates. The degree to which this precision will affect accuracy of life estimates depends on crack growth properties of the material as well as the nature of the load spectrum. The dK/da and net stress effects on crack growth are also considered. Author

**N88-13663#** Portsmouth Polytechnic (England). Dept. of Mechanical Engineering.
**NEAR-THRESHOLD SHORT CRACK GROWTH BEHAVIOR IN NIMONIC 105**
J. Byrne *In* Virginia Univ., Fatigue 87, Volume 1 1987 p 195-204 (For primary document see N88-13645 05-39)
Avail: NTIS HC A99/MF A01 CSCL 20K

Physically short semi-elliptic and through cracks, 0.1 to 0.4 mm in depth, were generated in Nimonic 105. These short cracks propagated in less than the nominal delta kappa sub th for long cracks at R = 0.1 and crack growth rates blended with the long crack results at between 0.5 to 0.65 mm crack depth. A similar crystallographic fatigue crack growth mechanism was observed for both the short and long cracks. It is proposed that this physically short crack growth behavior is due to a reduced effect of crack closure on the short crack results. Author

**N88-13664#** Virginia Univ., Charlottesville.
**FATIGUE CRACK PROPAGATION OF SHORT AND LONG CRACKS: PHYS. BASIS, PREDICTION METHODS AND ENGINEERING SIGNIFICANCE**
H. Nowack and R. Marissen (Deutsche Forschungs- und Versuchsanstalt fuer Luft- und Raumfahrt, Cologne, West Germany) *In its* Fatigue 87, Volume 1 1987 p 207-299 Sponsored in part by Deutsche Forschungsgemainschaft, (For primary document see N88-13645 05-39)
Avail: NTIS HC A99/MF A01 CSCL 20K

Recent developments regarding the microcrack stage and the short crack stage are described. It is shown that the advanced macrocrack propagation analysis schemes are based upon the effective stress intensity factor, but it is also shown that the mere consideration of delta kappa sub eff was not always sufficient. Author

**N88-13665#** Centro Informazioni Studi Esperienze, Milan (Italy).
**LOW CYCLE FATIGUE LIFE PREDICTIONS OF A 1CrMoV STEEL IN TERMS OF A J-CONTROLLED SHORT CRACK GROWTH MODEL**
V. Bicego *In* Virginia Univ., Fatigue 87, Volume 1 1987 p 231-240 (For primary document see N88-13645 05-39)
Avail: NTIS HC A99/MF A01 CSCL 20K

The propagation of cracks under low cycle fatigue (LCF) conditions is modeled in terms of Rice's cyclic parameter delta J, specifically formulated for short cracks. Simply relying on the values of Paris coefficients from conventional fatigue crack growth tests under elastic conditions, it is shown that life predictions obtained by integrating the crack growth expressions for the LCF cracks comply quite favorably with actual lives found in tests at 480 and 540 C on a 1CrMoV steel. Author

**N88-13666#** Rockwell International Science Center, Thousand Oaks, Calif.
**THE STATISTICS OF THE SHAPE OF SMALL FATIGUE CRACKS**
B. N. Cox and W. L. Morris *In* Virginia Univ., Fatigue 87, Volume 1 1987 p 241-250 (For primary document see N88-13645 05-39)
(Contract F49620-85-C-0034)
Avail: NTIS HC A99/MF A01 CSCL 20K

Monte Carlo simulations of the growth of small fatigue cracks through stochastic microstructures are discussed. The simulations are based on canonical formulae for the stress intensity factor around an irregular crack front and the laws of crack growth extracted from prior experiments or theories to describe the influence of the microstructural environment. The magnitude and persistence of fluctuations in crack shape may be used to test postulated laws of growth. The physical insight available from the Monte Carlo simulations will ultimately permit more accurate predictions of fatigue lifetime. Author

**N88-13667#** Nottingham Univ. (England). Dept. of Metallurgy and Materials Science.

**THE EFFECT OF ALPHA PLATELET MORPHOLOGY AND BETA-GRAIN SIZE ON THE INITIATION AND GROWTH OF SHORT FATIGUE CRACKS IN TI65S**

P. J. Hastings, M. A. Hicks (Rolls-Royce Ltd., Derby, England ), and J. E. King *In* Virginia Univ., Fatigue 87, Volume 1 1987 p 251-259 Sponsored in part by Rolls Royce Ltd. (For primary document see N88-13645 05-39)

Avail: NTIS HC A99/MF A01 CSCL 20K

The effects of alpha-platelet alignment and prior beta grain size on short fatigue crack growth in a beta-treated titanium alloy Ti65S was investigated. At crack depth of the order of the beta colony size, faster crack growth was seen in aligned structures than in basketweave structures, although the shortest cracks grew at similar rates in both. Large increases in prior beta grain size appear to increase crack growth rates. Author

**N88-13668#** Virginia Univ., Charlottesville.

**THE INITIATION AND GROWTH OF SMALL FATIGUE CRACKS IN COPPER AT ROOM AND CRYOGENIC TEMPERATURES**

I. B. Kwon, J. Weertman, and M. E. Fine (Northwestern Univ., Evanston, Ill.) *In its* Fatigue 87, Volume 1 1987 p 261-270 (For primary document see N88-13645 05-39)

(Grant NSF DMR-82-16972)

Avail: NTIS HC A99/MF A01 CSCL 20K

The microstructural evolution of small fatigue cracks in copper, both polycrystals and single crystals, were investigated by microscopy techniques using surface replicas at 298 K, 77 K and 4.2 K. The basic initiation processes of small fatigue cracks are unchanged at different test temperatures and in different environments, even though the lower temperatures and inert environments retard the fatigue crack initiation. The temperature and environmental dependences of fatigue damage during the early stages of fatigue are discussed based on the microscopic observations. Author

**N88-13669#** Lisbon Univ. (Portugal). CEMUL/IST.

**BEHAVIOR OF SHORT CRACKS IN A 2024 ALUMINUM ALLOY SHEET TESTED AT SEVERAL STRESS RATIOS**

A. Andrade and M. Freitas *In* Virginia Univ., Fatigue 87, Volume 1 1987 p 271-279 (For primary document see N88-13645 05-39)

Avail: NTIS HC A99/MF A01 CSCL 20K

The initiation and growth of small cracks (greater than 3 microns) from edge notches in 2024 T3 aluminum alloy sheets were studied under constant amplitude loading for a wide range of stress ratio. The surface crack length was monitored by taking surface replicas at regular intervals. Crack initiation was located at voids associated with inclusions due to decohesion or at cracked inclusions. Crack growth rates were plotted against the stress intensity factor ranges. Results show that small cracks grow faster than large cracks at the same stress intensity factor range. An effect of the stress range on the number of initiated cracks was detected as being a more significant factor than stress ratio or maximum stress by themselves. Author

**N88-13670#** Nottingham Univ. (England). Dept. of Metallurgy and Materials Science.

**THE EFFECT OF MICROSTRUCTURE ON THE SURFACE CRACK LENGTH: CRACK DEPTH RELATIONSHIP FOR SHORT CRACKS**

R. K. Bolingbroke and J. E. King *In* Virginia Univ., Fatigue 87, Volume 1 1987 p 281-290 Sponsored in part by MOD (For primary document see N88-13645 05-39)

Avail: NTIS HC A99/MF A01 CSCL 20K

Observations of crack shape development were made for surface cracks varying in length from between 40 microns and several mm in aluminum and titanium alloys. In the aluminum alloy, aspect ratio was found to vary with specimen orientation for short cracks. However, when the change in aspect ratio was taken into account, the da/dN vs. a (or delta kappa) curves were not shifted very significantly. Similar behavior was seen in alpha/transformed beta microstructures in Ti alloys. However, in coarse grained beta-annealed microstructures, very high a/c ratios can be obtained, indicating that growth rate comparisons based on surface crack length could be very misleading in some cases. Author

**N88-13671#** Virginia Univ., Charlottesville.

**ON THE ROLE OF CRACK TIP SHIELDING IN INFLUENCING THE BEHAVIOR OF LONG AND SMALL FATIGUE CRACKS IN ALUMINUM-LITHIUM ALLOY 2090**

K. T. Venkateswara Rao, W. Yu, and R. O. Ritchie (California Univ., Berkeley.) *In its* Fatigue 87, Volume 1 1987 p 291-301 (For primary document see N88-13645 05-39)

(Contract DE-AC03-76SF-00098)

Avail: NTIS HC A99/MF A01 CSCL 20K

The fatigue crack growth behavior of long (approximately greater than 5 mm) through thickness cracks is compared with that of microstructurally small (2 to 1000 microns) surface cracks in aluminum-lithium alloy 2090-T8E41. Although long crack growth rates are in general significantly slower than in traditional high strength aluminum alloys and show marked anisotropy, corresponding growth rates of small cracks are up to 3 orders of magnitude faster, and propagate at stress intensities far below the long crack threshold delta kappa sub th. Such behavior is attributed to the role of crack tip shielding, primarily from crack deflection and asperity induced crack closure. Author

**N88-13672#** McDonnell-Douglas Research Labs., St. Louis, Mo.

**THE INFLUENCE OF SLIP MECHANISM ON FATIGUE OF Mg AND Mg-2.3Li**

J. K. Gregory *In* Virginia Univ., Fatigue 87, Volume 1 1987 p 303-312 (For primary document see N88-13645 05-39)

Avail: NTIS HC A99/MF A01 CSCL 20K

The fatigue behavior of pure magnesium is compared with that of Mg-2.3Li on smooth S-N specimens. To obtain a lifetime of 10 to the 5th power cycles at R = 0.1, sigma sub max is 80 MPa for Mg, and 125 MPa for Mg-2.3Li. Surface cracks nucleate at roughly the same fraction of the total life, and grow at the same rates. The similarity in behavior, despite the difference in stress levels, is explained by two effects: (1) the proportional limit is increased from 4 MPa to 32 MPa by the addition of lithium, reducing the effective stress range driving crack growth; and (2) crack orientations in Mg-2.3Li are more strongly influenced by slip, resulting in deflection to unfavorable growth directions. Author

**N88-13673#** Gifu Univ. (Japan). Dept. of Mechanical Engineering.

**THE GROWTH BEHAVIOR OF SMALL FATIGUE CRACKS; THE EFFECT OF MICROSTRUCTURE AND CRACK CLOSURE**

K. Tokaji, T. Ogawa, S. Osako, and Y. Harada (Nippon Sharyo Ltd., Nagoya, Japan ) *In* Virginia Univ., Fatigue 87, Volume 1 1987 p 313-322 (For primary document see N88-13645 05-39)

Avail: NTIS HC A99/MF A01 CSCL 20K

Small fatigue crack growth behavior was studied under rotary bending in low carbon steel prepared with two ferrite grain sizes, and was compared with the growth behavior of large through cracks. The critical crack length above which linear elastic fracture mechanics is applicable was evaluated for small crack growth, and the effect of microstructure on crack growth rates and crack closure were examined experimentally. It was found that small cracks grew much faster than large cracks and also showed growth

rate perturbations due to grain boundaries. Crack opening stress increased with increasing crack length and tended to be constant near the critical crack length. The anomalous or rapid growth behavior of small cracks is discussed in terms of growth mechanisms and crack closure. Author

**N88-13674#** Virginia Univ., Charlottesville.
**THE INFLUENCE OF MICROSTRUCTURE AND RESIDUAL STRESSES ON THE INITIATION AND PROPAGATION OF SHORT SURFACE CRACKS ON AlMgSi1**
B. Meier and V. Gerold (Max-Planck-Inst. fuer Metallforschung, Stuttgart, West Germany ) *In its* Fatigue 87, Volume 1 1987 p 323-332 (For primary document see N88-13645 05-39)
Avail: NTIS HC A99/MF A01 CSCL 20K

The effect of microstructural features and residual compression stresses on crack initiation and growth of short surface cracks in Al-1 wt. percent Mg-1 wt. percent Si alloys in the peak-aged condition was investigated. A clear influence of slip distribution on crack initiation mechanisms was found. In the high cycle regime, the interface inclusion matrix transverse to the loading direction plays a dominant role in crack initiation. In the growth behavior of surface cracks, there exists a regime with a slop m equals 2 (Paris). In that regime, nearly no influence of microstructural features and residual compression on the growth rate in contrast to that found by through-thickness cracks could be observed. Author

**N88-13675#** Kyushu Univ., Fukuoka (Japan). Dept. of Mechanics and Strength of Solids.
**THRESHOLD STRESS FOR FATIGUE CRACK INITIATION FROM A SMALL CRACK**
Y. Murakami and K. Matsuda *In* Virginia Univ., Fatigue 87, Volume 1 1987 p 333-342 (For primary document see N88-13645 05-39)
Avail: NTIS HC A99/MF A01 CSCL 20K

The critical stress for crack initiation from a small crack and effective threshold stress intensity factor range of 0.46 percent steel were determined by the annealing method. The specimens containing small cracks were annealed in order to relieve residual stress and were again subjected to the fatigue test at a different stress level. The length of nonpropagation crack from the initial crack was measured. The critical stress for fatigue crack initiation from an ideal crack and delta kappa sub eff, th were determined. Author

**N88-13676*#** Academia Sinica, Beijing (China). Inst. of Aeronautical Materials.
**AN EXPERIMENTAL STUDY OF CLOSURE BEHAVIOR OF NATURALLY INITIATED SMALL CRACKS**
X. Su and W. N. Sharpe, Jr. (Johns Hopkins Univ., Baltimore, Md.) *In* Virginia Univ., Fatigue 87, Volume 1 1987 p 343-350 (For primary document see N88-13645 05-39)
(Grant NAG1-526)
Avail: NTIS HC A99/MF A01 CSCL 20K

Small cracks were initiated on the edges of 2024-T3 aluminum specimens by fatigue loading with various R-ratios. The crack opening displacement was then measured with a laser based interferometric technique and used to determine the operating load ratio. This ratio decreased with increasing distance from the tip. However, it remained essentially constant as the crack grew if a constant measuring system was used. Author

**N88-13677#** Virginia Univ., Charlottesville.
**BEHAVIOR OF LONG AND SHORT FATIGUE CRACKS IN A POWDER METALLURGY SUPERALLOY AT ROOM AND AT HIGH TEMPERATURE**
F. Soniak and L. Remy (Centre National de la Recherche Scientifique, Paris, France ) *In its* Fatigue 87, Volume 1 1987 p 351-360 (For primary document see N88-13645 05-39)
Avail: NTIS HC A99/MF A01 CSCL 20K

Fatigue crack growth behavior of long and short cracks at room temperature and at 650 C for different stress ratios are discussed. At room temperature for long cracks, closure was found to depend upon the stress ratio. Short cracks were found to grow faster than long cracks, and no intrinsic threshold was observed at room temperature. At 650 C closure was found to depend upon the maximum stress intensity factor. Unstable crack propagation was observed in short cracks. Fatigue crack growth rates could be rationalized by crack closure analysis and the intrinsic crack growth law da/dN versus delta kappa sub eff should lead to conservative predictions of fatigue crack growth life at room and high temperatures. Author

**N88-13678#** Kyoto Univ. (Japan). Dept. of Engineering Science.
**PROPAGATION OF SMALL FATIGUE CRACKS IN 2024-T3 ALUMINUM ALLOY**
K. Tanaka, Y. Akiniwa, and E. Matsui *In* Virginia Univ., Fatigue 87, Volume 1 1987 p 361-370 (For primary document see N88-13645 05-39)
Avail: NTIS HC A99/MF A01 CSCL 20K

Smooth specimens of 2024-T3 aluminum alloy were fatigued under nominally elastic conditions with several mean stresses. The propagation behavior of many small cracks were analyzed statistically. The relation between crack growth rate and the crack length was divided into three regions. The characteristics in each region were examined, and the growth behavior of the main crack was discussed in relation to life prediction. Author

**N88-13679#** Ecole Polytechnique, Montreal (Quebec). Dept. of Metallurgy Engineering.
**CLOSURE AND PROPAGATION BEHAVIOR OF SHORT FATIGUE CRACKS AT DIFFERENT R-RATIOS**
Y. Verreman, J.-P. Bailon, and J. Masounave (National Research Council of Canada, Boucherville, Quebec ) *In* Virginia Univ., Fatigue 87, Volume 1 1987 p 371-380 Sponsored by Natural Science and Engineering Research Council (For primary document see N88-13645 05-39)
Avail: NTIS HC A99/MF A01 CSCL 20K

A previous investigation on V-notched specimens in plane strain showed that the short crack behavior at R = -1 is essentially due to an initial transient variation of the crack opening level within the notch plastic zone. Here, new results at R = 0 and -2 are given. Similar closure and propagation behaviors were observed. It was found that the lower the R-ratio, the more pronounced the short crack effect. This results from important differences between the amplitudes of the opening level variation. Micro-strain gages installed close to the crack plane were used to monitor the length and the opening level of short cracks. The notch monotonic and cyclic plastic zone extents were computed from finite element analysis. Author

**N88-13680#** Stanford Univ., Calif. Dept. of Materials Science and Engineering.
**A UNIFIED MODEL FOR FATIGUE CRACK INITIATION, SHORT CRACK GROWTH, LONG CRACK PROPAGATION, AND CLOSURE EFFECTS**
A. O. Obabueki, C. H. Lee, T. Tanaka, and A. K. Miller *In* Virginia Univ., Fatigue 87, Volume 1 1987 p 381-391 (For primary document see N88-13645 05-39)
(Contract DE-FG03-84ER-45119)
Avail: NTIS HC A99/MF A01 CSCL 20K

A unified, physical-phenomenological model was developed for predicting fatigue crack initiation and growth under uniaxial far-field loading. In the model, Stage 1 fatigue crack advance (initiation and growth) is predicted using the range in crack tip non-elastic shearing displacement, whereas Stage 2 fatigue crack advance (initiation and growth) is calculated using the range in non-elastic crack tip opening displacement and the local peak tensile stress. The effects of weak surface grains, grain boundaries or relevant microstructural features, and redistribution of the local stresses during crack closure and reopening were incorporated into the model in order to represent the local mechanical conditions in the crack tip under various loading conditions. Author GR

**N88-13681#** Cambridge Univ. (England). Dept. of Materials Science and Metallurgy.
**FATIGUE CRACK RETARDATION IN ALUMINIUM ALLOYS**
D. J. Alexander and J. F. Knott *In* Virginia Univ., Fatigue 87, Volume 1 1987 p 395-406 Sponsored by Natural Science and Engineering Research Council of Canada (For primary document see N88-13645 05-39)
Avail: NTIS HC A99/MF A01 CSCL 20K

Fatigue crack retardation due to single tensile overloads were studied in aluminum alloys 7010-T7651 and 8090-T851, for delta kappa equals 7 MPa square root m, R equals 0.1 and 0.5, and specimen thicknesses of 6.35, 13 and 35 mm. Retardation lasts for many more cycles and extends over a greater distance in the 8090 alloy for similar test conditions. Crack closure cannot explain retardation in the 7010 alloy. Retardation is apparently due to residual stress effects and crack deflection. In the 8090 alloy at R equals 0.1, closure is a significant factor in the retardation, but not at R equals 0.5. Crack deflection appears to be the primary mechanism of retardation in this case. Author

**N88-13682#** Technion Research and Development Foundation Ltd., Haifa (Israel).
**FATIGUE CRACK GROWTH UNDER RANDOM OVERLOADS**
R. Arone *In* Virginia Univ., Fatigue 87, Volume 1 1987 p 407-413 (For primary document see N88-13645 05-39)
Avail: NTIS HC A99/MF A01 CSCL 20K

Retardation effects associated with random overload peaks are considered. A Poisson flow of overloads superimposed on a baseline constant amplitude cyclic load is assumed. Under the above assumptions the total retardation time is presented as a stochastic process governed by the intensity of overloads. Expressions estimating reliability level for a given lifetime are derived. Author

**N88-13683#** Metz Univ. (France). Lab. de Fiabilite Mecanique.
**A DISLOCATION MODEL FOR FATIGUE CRACK PROPAGATION UNDER VARIABLE AMPLITUDE LOADING**
A. Bia, C. Robin, and G. Pluvinage *In* Virginia Univ., Fatigue 87, Volume 1 1987 p 415-424 (For primary document see N88-13645 05-39)
Avail: NTIS HC A99/MF A01 CSCL 20K

A dislocation model based on the Bilby-Cottrel-Swinden model is proposed to describe the fatigue crack propagation under variable amplitude loading. Only the simple case of overload applications is investigated. The determination of the crack tip opening displacement enables researchers to calculate the fatigue crack propagation through the overload plastic zone. The results are respectively compared with experimental data, analytical and numerical analysis. Author

**N88-13684#** Metallurgical Consulting Services Ltd., Saskatoon (Saskatchewan).
**OBSERVATIONS ON THE EFFECT OF OVERLOADS ON FATIGUE CRACK GROWTH**
S. K. P. Cheung-Mak and I. LeMay *In* Virginia Univ., Fatigue 87, Volume 1 1987 p 425-434 (For primary document see N88-13645 05-39)
Avail: NTIS HC A99/MF A01 CSCL 20K

The crack growth behavior of an aluminum 2219-T851 alloy was studied under variable amplitude loading. Experimental data were obtained for both single spike and repeated overloads. The retardation following overload application depended on the overload ratio and the number of overload cycles. Analytical studies using Chang's model demonstrated good agreement with the experimental data for a number of delay cycles and overload plastic zone size. Author

**N88-13685#** Xian Jiaotong Univ. (China). Dept. of Engineering Mechanics.
**A STUDY OF FATIGUE CRACK GROWTH LIFE UNDER RANDOM STRESSES**
J. M. Hu, W. P. Yao, and K. X. Li *In* Virginia Univ., Fatigue 87, Volume 1 1987 p 435-441 (For primary document see N88-13645 05-39)
Avail: NTIS HC A99/MF A01 CSCL 20K

In view of statistics, the expressions of characteristic stress intensity range delta kappa sub char which is related to da/dt are discussed by using the MTS-880 material test system. The central crack tests of low carbon steel were controlled by pseudo random signal in order to investigate the influences of different delta kappa sub char on da/dt. A formula by which the fatigue crack growth life under narrow band random stress can be estimated is derived. The result of calculation using the formula is in accord with the experimental result. Author

**N88-13686#** Portsmouth Polytechnic (England). Dept. of Mechanical Engineering.
**CRACK GROWTH IN CONTRASTING TITANIUM ALLOYS UNDER THE CONJOINT ACTION OF HIGH AND LOW CYCLE FATIGUE**
B. E. Powell *In* Virginia Univ., Fatigue 87, Volume 1 1987 p 443-452 (For primary document see N88-13645 05-39)
(Contract F49620-85-C-0116; Grant AF-AFOSR-0077-82)
Avail: NTIS HC A99/MF A01 CSCL 20K

Fatigue crack propagation rates were measured for Ti-6Al-4V and Ti-5331S aircraft engine disc materials using compact tension and corner notched tensile test pieces. The loadings used simulate both the start-stop operations of aircraft engines which lead to low cycle fatigue and the in-flight vibrations which may cause high cycle fatigue. It is suggested that the different fatigue crack growth behavior of Ti-5331S, relative to that of Ti-6Al-4V, arises largely from the greater proportion of crack closure and short crack growth occurring in this alloy. Author

**N88-13687#** Coast Guard Academy, New London, Conn.
**VARIABLE AMPLITUDE FATIGUE CRACK GROWTH IN ALUMINUM ALLOYS 2090-T8E41 AND 7075-T651**
J. S. Thomas, Jr., J. C. VanSice, and A. F. Grandt, Jr. (Purdue Univ., West Lafayette, Ind.) *In* Virginia Univ., Fatigue 87, Volume 1 1987 p 453-460 (For primary document see N88-13645 05-39)
Avail: NTIS HC A99/MF A01 CSCL 20K

Fatigue crack growth experiments were conducted to compare the variable amplitude fatigue crack growth behavior of aluminum-lithium alloy 2090-T8E41 and aluminum alloy 7075-T651. Fixed-end single edge-notch tension specimens were subjected to the MINITWIST loading spectrum. The results indicate that the 2090-T8E41 alloy has significantly superior fatigue crack growth resistance to the MINITWIST load history. Author

**N88-13688#** Virginia Univ., Charlottesville.
**CRACK GROWTH PREDICTION IN 3D STRUCTURES UNDER AERONAUTICAL-TYPE SPECTRUM LOADINGS**
R. Labourdette, G. Baudin, and M. Robert (Office National d'Etudes et de Recherches Aerospatiales, Paris, France ) *In its* Fatigue 87, Volume 1 1987 p 461-470 (For primary document see N88-13645 05-39)
Avail: NTIS HC A99/MF A01 CSCL 20K

A model describing crack growth in 3D structures submitted to aeronautical spectrum loadings is presented. Examples of predictions for 7075-T7351 alloy bending specimens undergoing FALSTAFF and mini-TWIST sequences are compared with experimental results. The general accuracy of predictions appears reasonably good since almost all points fall in the classical area. Suggested improvements can result from a description of plastic behavior. Author

**N88-13689#** Academia Sinica, Beijing (China). Inst. of Mechanics.
**FATIGUE OF 30CrMnSiNi2A NOTCHED SPECIMENS UNDER SPECTRUM LOADING**
Y. S. Wu, J. H. Huan, and A. H. Zhou *In* Virginia Univ., Fatigue 87, Volume 1 1987 p 471-478 (For primary document see N88-13645 05-39)
Avail: NTIS HC A99/MF A01 CSCL 20K

The fatigue tests of 30CrMnSiNi2A notched specimens were performed under a maneuver loading spectrum. The stress-strain behavior at the notch under the load spectrum was studied. The fatigue crack initiation and growth was observed microscopically and macroscopically. The fatigue crack initiation life was estimated by a simplified local stress-strain method. The fatigue crack growth life was estimated by the fracture mechanics method. The estimated results and the test results were compared. The size of the initiation crack was determined based on the size of fatigue crack initiation zone in the fracture surface of the specimen.
Author

**N88-13690#** Industrieanlagen-Betriebsgesellschaft m.b.H., Ottobrunn (West Germany). Dept. of Fatigue and Fracture Mechanics.
**THE HOW AND WHY OF VARIABLE AMPLITUDE TESTING**
W. Schuetz and P. Heuler *In* Virginia Univ., Fatigue 87, Volume 1 1987 p 479-494 (For primary document see N88-13645 05-39)
Avail: NTIS HC A99/MF A01 CSCL 20K

Fatigue life prediction by experiment, that is, variable amplitude testing, is becoming more and more widespread in industry. The many engineering decisions necessary before a useful variable amplitude test can be carried out are explained in detail, such as measurement of stress time history in service, which counting procedure to use and why, scatter of measured stress spectra, manipulation of measured stress spectra, reconstruction (synthesis) of the test spectrum as a basis for a realistic variable amplitude test sequence, and predicted fatigue life under this sequence.
Author

**N88-13691#** Cambridge Univ. (England). Dept. of Materials Science and Metallurgy.
**NEAR-THRESHOLD GROWTH OF DEFECTS IN ENGINEERING MATERIALS**
J. F. Knott *In* Virginia Univ., Fatigue 87, Volume 1 1987 p 497-515 (For primary document see N88-13645 05-39)
Avail: NTIS HC A99/MF A01 CSCL 20K

Recent work on fatigue crack growth in the near threshold region, with particular reference to the behavior of short cracks is discussed. Attention is drawn to the importance of closure, and it is suggested that a lower bound to behavior in steels is associated with a closure free threshold stress intensity factor of approx. 3 MPa(1/2). Engineering design is considered with respect to two areas: structures and machine components. Closure-free threshold values are appropriate for structures. For machine components, engineering design must rest on the endurance limit. This is a function of the material's defect content. A simple statistical model is described to demonstrate the sensitivity of behavior to input variables.
Author

**N88-13692#** Virginia Univ., Charlottesville.
**EFFECTS OF MN DISPERSOIDS ON NEAR THRESHOLD FATIGUE CRACK GROWTH IN 2134 TYPE ALLOYS**
K. V. Jata, J. A. Walsh, and E. A. Starke, Jr. *In its* Fatigue 87, Volume 1 1987 p 517-526 (For primary document see N88-13645 05-39)
(Grant AF-AFOSR-0061-83)
Avail: NTIS HC A99/MF A01 CSCL 20K

The near threshold fatigue crack resistance of high purity 2134 type alloys with Zr as the major dispersoid forming element was examined in the under and overaged conditions as a function of Mn additions ranging from 0 to 1.02 weight percent. The additions of manganese resulted in a continuous decrease of the nominal threshold in both the aging conditions, with the effect more pronounced in the overaged condition. Crack deflections, closure and fractography suggest that roughness induced crack closure is dominant in all alloys. Besides, fractographic evidence suggests that large Mn particles could contribute to local microcrack acceleration resulting in an intrinsic lowering of the fatigue thresholds and faster crack propagation rates.
Author

**N88-13693#** Ruhr Univ., Bochum (West Germany). Inst. fuer Werkstoffe.
**INTERACTION OF MICROSTRUCTURE AND FATIGUE IN TOOL STEELS**
H. Berns *In* Virginia Univ., Fatigue 87, Volume 1 1987 p 527-536 (For primary document see N88-13645 05-39)
Avail: NTIS HC A99/MF A01 CSCL 20K

Different grades of cold working, hot working and high speed steels were investigated as to their behavior in rotating bending and stable crack growth tests with longitudinal and transverse specimens. Hard phases like carbides and nonmetallic inclusions vary in size and content because of carbon contents ranging from 0.27 to 2.25 percent. The tempered matrix consists of martensite and/or bainite with some retained austenite. The macrohardness ranges from 400 to 900 HV.
Author

**N88-13694#** Purdue Univ., West Lafayette, Ind. Dept. of Mechanical Engineering.
**TENSILE MEAN STRESS EFFECTS ON UNIAXIAL FATIGUE BEHAVIOR OF 1045 HR STEEL**
A. Fatemi and R. I. Stephens (Iowa Univ., Iowa City.) *In* Virginia Univ., Fatigue 87, Volume 1 1987 p 537-546 (For primary document see N88-13645 05-39)
Avail: NTIS HC A99/MF A01 CSCL 20K

The effect of tensile mean stress/strain on axial fatigue and cyclic deformation behavior of SAE 1045 steel in the hot rolled condition was investigated using strain controlled smooth specimens at room temperature. It was found that mean strain was not detrimental to fatigue life unless it produces a mean stress. In tests where the mean stress was significant, a reduction in fatigue lives up to a factor of three was observed. Mean stress relaxation and mean strain effect on the stress-strain curve are discussed and the use of several damage parameters to predict the mean stress effect on fatigue life is examined.
Author

**N88-13695#** Mitsubishi Electric Co., Amagasaki (Japan). Central Research Lab.
**FATIGUE STRENGTH OF ALLOY A286 AT CRYOGENIC TEMPERATURE**
A. Inoue, S. Yoshioka, S. Takayanagi, K. Hiraga, T. Ogata, K. Nagai, T. Yuri, and K. Ishikawa (National Research Inst. for Metals, Niihari, Japan ) *In* Virginia Univ., Fatigue 87, Volume 1 1987 p 547-555 (For primary document see N88-13645 05-39)
Avail: NTIS HC A99/MF A01 CSCL 20K

The fatigue strength at 4 and 300K of alloy A286 and its weld was investigated. Load controlled low cycle fatigue tests were carried out on the base material, weldment and heat treated weldment of the alloy by using smooth and notched specimens. Results revealed a close correlation between fatigue strength of these specimens and their tensile strength. The notch sensitivity for fatigue strength of the base and welded materials was low even at 4K.
Author

**N88-13696#** United Kingdom Atomic Energy Authority, Risley (England).
**THE INITIATION AND GROWTH OF FATIGUE CRACKS IN CARBURISED 9Cr1Mo STEEL**
P. J. Jeffcoat *In* Virginia Univ., Fatigue 87, Volume 1 1987 p 557-566 (For primary document see N88-13645 05-39)
Avail: NTIS HC A99/MF A01 CSCL 20K

The high temperature fatigue endurance of carburized 9Cr1Mo ferritic steel was determined by conditions under which fatigue cracks were initiated. At high loads, cracks are initiated at the carburized surface and endurance is little changed. By contrast, at lower loads, cracks are initiated internally at oxide inclusions randomly distributed in the steel, and marked improvements in endurance are measured. A simple semi-empirical model is presented which relates fatigue endurance to the inclusion population of the steel.
Author

**N88-13697#** Ecole Centrale de Lyon (France). Dept. de Mecanique des Solides.
**FRETTING WEAR AND FRETTING FATIGUE DAMAGE**

C. Colombie, Y. Berthier, L. Vincent, and M. Godet (Institut National des Sciences Appliquees de Lyon, Villeurbanne, France ) *In* Virginia Univ., Fatigue 87, Volume 1 1987 p 567-575 (For primary document see N88-13645 05-39)
Avail: NTIS HC A99/MF A01 CSCL 20K

Fretting wear and fretting fatigue are studied from a combined mechanical and material point of view. Each phase of the degradation process is described by considering boundary conditions in the contact and material properties. The role of debris is shown to be very important to predicting failures. Author

**N88-13698#** Chalmers Univ. of Technology, Goeteborg (Sweden). Dept. of Engineering Metals.
**CRACK PROPAGATION PROPERTIES OF SINTERED STEEL**
I. Bertilsson and B. Karlsson *In* Virginia Univ., Fatigue 87, Volume 1 1987 p 577-586 Sponsored by the Swedish Board for Technical Development (For primary document see N88-13645 05-39)
Avail: NTIS HC A99/MF A01 CSCL 20K

The crack propagation properties of sintered steels with porosities ranging from 0 to 16 percent are discussed. The most important variable affecting the crack propagating resistance was found to be the porosity. A higher porosity normally leads to lower resistance. The microstructure has a smaller influence. The crack mainly follows the pore system. Most of the straining is concentrated on the sintering necks between the original powder particles. The localized deformations give rise to a large number of microcracks. These microcracks increase the crack closure which leads to lower propagation rates. Author

**N88-13699#** Virginia Univ., Charlottesville.
**THE ROLE OF INCLUSIONS IN CORROSION FATIGUE CRACK INITIATION IN Q1N**
R. A. Cottis and A. Markfield (Manchester Coll. of Science and Technology, England ) *In its* Fatigue 87, Volume 1 1987 p 587-596 (For primary document see N88-13645 05-39)
Avail: NTIS HC A99/MF A01 CSCL 20K

The role of inclusions in the initiation and early stages of fatigue cracks was studied for Q1N in sodium chloride solution. The test conditions are such that the effect of corrosion is exclusively the dissolution associated with the crack, with no hydrogen embrittlement. Oxide inclusions are found to initiate fatigue cracks in air, while sulfides are more effective in corrosion. This is attributed to the effect of sulfur species produced by dissolution of the inclusions in enhancing the rate of corrosion of the steel around the inclusion. The addition of thiosulphate spreads the enhanced corrosion over a larger surface area, and thereby reduces the local rates of attack, and transfers the initiation site back to the oxide inclusions. Corrosion is thought to accelerate the growth of short cracks by the dissolution of microstructural barriers and by the elimination of closure effects. Author

**N88-13700#** Virginia Univ., Charlottesville.
**FATIGUE 87, VOLUME 3 Final Report, 1 Jun. 1987 - 1 May 1988**
R. O. Ritchie, ed. and E. A. Starke, Jr., ed. 1987 501 p Presented at the Third International conference on Fatigue and Fatigue thresholds, Charlottesville, Va., 28 Jun. - 3 Jul. 1987
(Grant DAAL03-87-G-0102)
(AD-A184047; ARO-24134.3-MS-CF-Vol-3) Avail: NTIS HC A22/MF A01 CSCL 20K

A wide range of diverse views of the fundamental and applied aspects of fatigue are presented. This includes questions of cyclic deformation, crack initiation and propagation, small cracks, crack closure, variable amplitude effects, and environmentally influenced behavior. A comprehensive review of state of the art of fatigue behavior is presented in detail. For individual titles, see N88-13701 through N88-13734.

**N88-13701#** British Steel Corp., Rotherham (England). Swinden Labs.
**A STUDY OF CORROSION FATIGUE CRACK INITIATION, GROWTH AND THE THRESHOLD CONDITION UNDER VARIABLE AMPLITUDE LOADING**
I. M. Austen and E. F. Walker *In* Virginia Univ., Fatigue 87, Volume 3 1987 p 1155-1168 Sponsored by European Coal and Steel Community (For primary document see N88-13700 05-39)
Avail: NTIS HC A22/MF A01 CSCL 20K

Variable amplitude corrosion fatigue is the major cause of service failures and fatigue life is dominated by crack initiation and growth at low rates. Life predictions require research into mechanisms and modelling and work is described in these three areas. These are initiation from notches, crack growth rates and threshold stress intensity, each under constant and variable amplitude loading. Results are considered in terms of quantitative models based on mechanistic understanding. Author

**N88-13702#** Manchester Coll. of Science and Technology (England). Corrosion and Protection Centre.
**THE INFLUENCE OF CRACK CONDITIONS ON HYDROGEN UPTAKE BY STEELS**
R. A. Cottis, E. A. Taqi, and M. Haji-Ghassemi *In* Virginia Univ., Fatigue 87, Volume 3 1987 p 1179-1188 (For primary document see N88-13700 05-39)
Avail: NTIS HC A22/MF A01 CSCL 20K

Investigations into the chemical conditions existing within simulated cracks have shown that an increased hydrogen overpotential may be obtained when the external surface of a sample is anodically polarized. The hydrogen uptake by the steel directly is examined using a conventional hydrogen permeation electrode set into the wall of a simulated crack. This has confirmed that high hydrogen uptake rates may be obtained with anodic polarization. Additional tests using an occluded cell around a slow strain test-piece have demonstrated the possibility of hydrogen embrittlement under anodic polarization, the fractographic features observed at -500 mV (SCE) and -1200 mV (SCE) being essentially identical. Author

**N88-13703#** General Electric Co., Schenectady, N.Y.
**MODELING THE EFFECT OF SULFUR ON THE THRESHOLD ENVIRONMENTAL CRACKING RATE OF STEELS IN HIGH TEMPERATURE WATER**
Peter L. Andresen *In* Virginia Univ., Fatigue 87, Volume 3 1987 p 1189-1200 (For primary document see N88-13700 05-39)
Avail: NTIS HC A22/MF A01 CSCL 20K

The effect of metallurgical sulfur on the environmental crack growth rates of steels in high temperature water is modeled based on crack tip transport considerations. Contributions of sulfide dissolution are integrated with the effects of water chemistry (corrosion potential, solution conductivity, and convection) to determine the crack tip chemistry. This knowledge is coupled with oxidation kinetics measurements for various materials and calculated crack tip strain rates to provide predictions of steady state and threshold crack growth rates. The model provides a unified understanding of water and material chemistry effects in low alloy, carbon, and stainless steels as well as Inconels.
Author

**N88-13704#** Ljubljana Univ. (Yugoslavia). Dept. of Mechanical Engineering.
**OCCURANCE AND GROWTH OF FATIGUE CRACKS IN CORROSION ENVIRONMENT**
F. Kosel and L. Kosec *In* Virginia Univ., Fatigue 87, Volume 3 1987 p 1201-1210 (For primary document see N88-13700 05-39)
Avail: NTIS HC A22/MF A01 CSCL 20K

The mechanism of the development and growth of defects occurring due to metal oxidation at the conditions of changing temperature field is explained. The analysis is made on two examples: the breaking of a growing oxide wedge, and crack

closure by a composite layer between the metal and the oxide. Finally the effect of the number of cracks on their growth is also analyzed. Author

**N88-13705#** Northwestern Univ., Evanston, Ill. Dept. of Materials Science and Engineering
**THE EFFECT OF ENVIRONMENT ON LOW CYCLE FATIGUE PROPERTIES IN HSLA STEEL**
W. J. Lee, S. P. Bhat (Inland Steel Co., Chicago, Ill.), Y. W. Chung, and M. E. Fine *In* Virginia Univ., Fatigue 87, Volume 3 1987 p 1211-1220 (For primary document see N88-13700 05-39)
Avail: NTIS HC A22/MF A01 CSCL 20K

The influence of gaseous environment on low cycle fatigue properties and microcrack initiation mechanisms was studied in 0.11 wt. percent Nb high strength low alloy steels. Completely reversed push-pull fatigue tests at various plastic strain amplitudes were performed both in air and in ultrahigh vacuum (UHV). A two stage surface replication technique for transmission electron microscopy was used to determine the initial microcracks which when formed are less than one micron in length. Microcracks are initiated along slip lines both in air and in UHV. The increase in fatigue resistance in UHV is attributed to a delay in microcrack initiation and, more importantly, decrease in the microcrack growth rate. The environmental effect becomes more severe as the plastic strain amplitude decreases. Author

**N88-13706#** Ecole Nationale Superieure de la Metallurgie et de l'Industrie des Mines, Ste. Etienne (France).
**COUPLING EFFECTS BETWEEN THE FERRITE AND AUSTENITE PHASES DURING CORROSION FATIGUE OF A FERRITE/AUSTENITE DUPLEX STAINLESS STEEL**
T. Magnin, J. M. Lardon, and C. Amzallag (Creusot-Loire, Firminy, France ) *In* Virginia Univ., Fatigue 87, Volume 3 1987 p 1221-1228 (For primary document see N88-13700 05-39)
Avail: NTIS HC A22/MF A01 CSCL 20K

The corrosion fatigue behavior in a 3.5 percent NaCl solution at pH 2 of an alpha/gamma duplex stainless steel with 50 percent ferrite content is studied and compared with those of the alpha and gamma phases considered separately. The better resistance to corrosion fatigue of the duplex alloy in comparison to those of its individual phases is emphasized and explained by both mechanical and electrochemical coupling effects between the alpha and gamma phases in the duplex alloy. Author

**N88-13707#** Max-Planck-Inst. fuer Metallforschung, Stuttgart (West Germany). Inst. fuer Werkstoffwissenschaften.
**FATIGUE CRACK PROPAGATION IN Al-Zn-Mg BICRYSTALS AND ITS DEPENDENCE ON THE ENVIRONMENT**
A. Niegel, H.-J. Gudladt, and V. Gerold *In* Virginia Univ., Fatigue 87, Volume 3 1987 p 1229-1238 Sponsored by Deutsche Forschungsgemeinschaft (For primary document see N88-13700 05-39)
Avail: NTIS HC A22/MF A01 CSCL 20K

High cycle fatigue crack propagation was studied in precipitation hardened Al-Zn-Mg specimens containing a single grain boundary perpendicular or at 45 deg to the load axis. In peak aged bicrystals tested in laboratory air as well as wet nitrogen the crack propagates intergranular. In dry nitrogen and wet atmospheres containing less than 0.8 kPa wetness the crack initiation and propagation becomes transgranular and is 100 times slower than intercrystalline crack propagation. The influence of moisture affecting the intergranular crack propagation is discussed in terms of stress corrosion cracking and stress corrosion fatigue. Author

**N88-13708#** Ottawa Univ. (Ontario). Dept. of Mechanical Engineering.
**FRACTURE KINETICS OF CORROSION FATIGUE**
K. Krausz and A. S. Krausz *In* Virginia Univ., Fatigue 87, Volume 3 1987 p 1239-1248 Sponsored by Natural Sciences and Engineering Research Council (For primary document see N88-13700 05-39)
Avail: NTIS HC A22/MF A01 CSCL 20K

Thermally activated threshold effects in fatigue originate from atomic vibration induced rebonding and crack closure induced growth rate reduction. Fracture kinetics analyses of fatigue carried out for a wide range of metals and some polymers indicate that in about two thirds of these materials the threshold effect is controlled by thermal vibration rebonding and the rest by closure effects. The interrelations among mechanical and corrosion fatigue, and stress corrosion cracking are recognized. Author

**N88-13709#** Atomic Energy Research Establishment, Harwell (England). Materials Physics and Metallurgy Div.
**THE INFLUENCE OF TEMPER EMBRITTLEMENT ON FATIGUE CRACK GROWTH IN HYDROGEN**
C. A. Hippsley *In* Virginia Univ., Fatigue 87, Volume 3 1987 p 1249-1258 Sponsored by UKAEA (For primary document see N88-13700 05-39)
Avail: NTIS HC A22/MF A01 CSCL 20K

The effects of temper embrittlement on fatigue crack growth in gaseous hydrogen were examined for 2.25Cr 1Mo steel. A range of tempered and aged conditions was examined, using vacuum as the control environment. In the unembrittled state, hydrogen encouraged intergranular cracking at intermediate stress intensity and transgranular cracking at high stress intensity. Reversible temper embrittlement promoted the intergranular mode, and one-step temper embrittlement promoted the transgranular mode, thus reflecting lower shelf fracture mechanisms. Author

**N88-13710#** Sheffield Univ. (England). Dept. of Metallurgy.
**CRACK INITIATION STUDIES IN HYDROGEN EMBRITTLED SPRING STEEL STRIP**
L. W. Lack, R. Brook, G. W. Greenwood, and I. C. Howard *In* Virginia Univ., Fatigue 87, Volume 3 1987 p 1259-1268 Sponsored by Science and Engineering Research Council (For primary document see N88-13700 05-39)
Avail: NTIS HC A22/MF A01 CSCL 20K

Fatigue tests in bending are described on high carbon spring steels over a frequency range from 2 to 0.02 Hz on material with and without an electro deposited zinc coating. It is shown that the hydrogen embrittlement introduced through the zinc plating had a particularly severe effect at the lowest frequency and its effect was further enhanced by increase in the content of residual elements. Fracture initiation appeared to be influenced by impurity particles, notably, MnS, and by defects at the strip surface produced by arcing in the electroplating barrel. Conversely elongated stringers in the strip interior tended to arrest and deflect the crack path. Author

**N88-13711#** Deutsche Forschungs- und Versuchsanstalt fuer Luft- und Raumfahrt, Cologne (West Germany). Inst. for Materials Research.
**FATIGUE MECHANISMS IN ARALL, A FATIGUE RESISTANT HYBRID ALUMINUM ARAMID COMPOSITE MATERIAL**
R. Marissen *In* Virginia Univ., Fatigue 87, Volume 3 1987 p 1271-1279 Sponsored by Deutsche Forschungsgemeinschaft (For primary document see N88-13700 05-39)
Avail: NTIS HC A22/MF A01 CSCL 20K

ARALL (Aramid Reinforced Aluminum Laminates) is a hybrid composite containing thin high strength aluminum alloy sheets, which are laminated using a structural epoxy adhesive containing about 50 percent aramid fibers. ARALL shows an excellent resistance against fatigue crack growth, due to intact fibers bridging fatigue cracks in the aluminum sheet material. Author

**N88-13712#** Ecole des Mines, Paris (France). Centre des Materiaux.
**LOW CYCLE FATIGUE BEHAVIOUR OF NOTCHED SPECIMENS OF NICKEL BASED SUPERALLOY SINGLE CRYSTAL**
A. Defresne and L. Remy *In* Virginia Univ., Fatigue 87, Volume 3 1987 p 1281-1290 Sponsored by DRET (For primary document see N88-13700 05-39)
Avail: NTIS HC A22/MF A01 CSCL 20K

The low cycle fatigue behavior of notched specimen was studied for two nickel superalloy single crystals MAR-M 200 and CMSX 2

at 650 C in the life range 1000 to 100,000 cycles. The initiation and growth of cracks were monitored throughout cycling using a replication technique at the notch root as well as the potential drop technique. Initiation was found to occur in the early cycles. Cracking in CMSX 2 involves the development of a single crack whereas several cracks grow and coalesce in MAR-M 200. Low cycle fatigue data on smooth specimen were shown to be unable to account for an engineering definition of life to crack initiation on notch specimen. The fatigue life of notched specimen was computed therefore using fatigue crack growth data. The calculated life was found to be in pretty good agreement with experimental data and a fatigue limit was actually predicted. Author

**N88-13713#** Indian Inst. of Tech., Madras. Dept. of Mechanical Engineering.
**FATIGUE CHARACTERISTICS OF ION TREATED SURFACES**
R. Krishnamurthy and H. V. Somasundar (NIE, Mysore, India ) *In* Virginia Univ., Fatigue 87, Volume 3 1987 p 1291-1299 (For primary document see N88-13700 05-39)
Avail: NTIS HC A22/MF A01 CSCL 20K

Surface technologists aim to develop suitable surface coatings to enhance the fatigue life of engineering materials. Most of the coatings would influence the substrate material with undersirable effects such as thermal softening, interface transitions, and other substrate defects. Of late, ion treatments have found increasing applications. These include ion nitriding and ion implantation. Where ion nitriding is plating of surfaces with N+ ion bombardment, resulting in formation of compound surfacial layers, ion implantation is a cool surface treatment resulting in little change in surface characteristics. The fatigue characteristics of ion implanted and ion nitrided high strength low alloy steel are discussed. Author

**N88-13714#** Utah Univ., Salt Lake City. Dept. of Mechanical and Industrial Engineering.
**THE EFFECT OF HEAT TREATMENT ON FATIGUE CRACK GROWTH IN POLYCARBONATE**
L. E. Hornberger and K. L. DeVries *In* Virginia Univ., Fatigue 87, Volume 3 1987 p 1301-1311 (For primary document see N88-13700 05-39)
Avail: NTIS HC A22/MF A01 CSCL 20K

Residual stresses are known to have pronounced effects on the mechanical properties of materials. Previous studies have shown that the quenching of polycarbonate from above its glass transition temperature produced sizeable surface stresses and these stresses were accompanied by a tenfold increase in Izod impact strength and a twentyfold increase in the mean fatigue life of the material at a maximum flexural stress of 62 MPa. More recently, studies on the effect of heat treatment was accomplished either prior to or subsequent to the introduction of a crack and the crack growth then monitored as a function of the number of fatigue cycles. Author

**N88-13715#** Lehigh Univ., Bethlehem, Pa. Dept. of Materials Science and Engineering.
**EFFECT OF TEST TEMPERATURE AND FREQUENCY ON FATIGUE CRACK PROPAGATION IN PVC**
J. D. Phillips, R. W. Hertzberg, and J. A. Manson *In* Virginia Univ., Fatigue 87, Volume 3 1987 p 1313-1322 (For primary document see N88-13700 05-39)
(Grant NSF DMR-84-12357)
Avail: NTIS HC A22/MF A01 CSCL 20K

The effect of frequency and temperature on the fatigue crack propagation (FCP) behavior of poly(vinyl chloride) was studied. An Arrhenius relationship between the crack growth rate and the reciprocal of the absolute temperature was found, leading to an estimate of the activation energy for the FCP propagation process. Examination of the fracture surfaces revealed the presence of discontinuous growth bands, which correspond to the size of the crack tip plastic zone during each test. Dimensions of the stretch zones separating these bands coincide with the calculated values of the crack opening displacement. Also, J integral values, inferred from stretch zone size measurements, agree with values calculated from material properties. Author

**N88-13716#** Tohoku Univ., Sendai (Japan). Dept. of Mechanical Engineering.
**ENVIRONMENTAL FRACTURE TOUGHNESS AND STATIC FATIGUE CRACK PROPAGATION OF SILICA GLASS**
Y. Sawaki, K. Kobayashi, S. Sakaguchi, and T. Kawasaki (Hiroshima Inst. of Tech., Japan ) *In* Virginia Univ., Fatigue 87, Volume 3 1987 p 1323-1332 (For primary document see N88-13700 05-39)
Avail: NTIS HC A22/MF A01 CSCL 20K

The region 1 static fatigue crack growth curve, da/dt- K, of silica glass determined by precracked CT specimen can be characterized by the parallel curves of each other, shifting into higher stress intensity region by decreasing the humidity in the air. This can be rationalized by introducing the newly proposed parameter, environmental fracture toughness, Kie, which is the measure of the degree of degradation of the material at the crack tip caused by the interaction with water. This Kie is linearly related to the water vapor pressure on the log-log paper and successfully explains the fatigue cracking behavior. Author

**N88-13717#** Northeastern Univ., Boston, Mass. Dept. of Mechanical Engineering.
**EFFECT OF INTERFACE ON MECHANICAL PROPERTIES OF GRAPHITE/201 ALUMINUM COMPOSITES** **c24**
J. Seyyedi, H. Nayeb-Hashemi, and J. Blucher *In* Virginia Univ., Fatigue 87, Volume 3 1987 p 1333-1351 Sponsored by NSF, Army Materials and Mechanics Research Center, and the Engineering Foundation (For primary document see N88-13700 05-39)
Avail: NTIS HC A22/MF A01 CSCL 11D

The effect of interface on mechanical properties of Gr/201 Al composite material, was investigated after being heat treated in vacuum for 24 hrs at 450, 500, and 545 C. The longitudinal tensile and compressive strengths declined as a result of heat treatment. However, an increase in the interfacial shear strength was observed through a steady decrease in the amount of fiber pullout with an increase of the heat treatment temperature. Transmission electron microscopic studies revealed the formation and growth of Al4C3 and Al4O4C in the interface which degraded the fiber surface. This fiber surface appears to be responsible for a decrease in strength at elevated temperatures. Tension-tension fatigue behavior of these composites were evaluated. The results showed that the failure was controlled by a combination of matrix and interfacial zone properties. Author

**N88-13718#** Aeronautical Research Inst. of Sweden, Bromma. Structures Dept.
**FATIGUE CRACK GROWTH: STATISTICAL CONSIDERATIONS**
A. F. Blom and B. Palmberg *In* Virginia Univ., Fatigue 87, Volume 3 1987 p 1365-1399 Previously announced as N87-24718 Sponsored by Swedish Defence Material Administration and Swedish Board for Technical Development (For primary document see N88-13700 05-39)
Avail: NTIS HC A22/MF A01 CSCL 20K

All the parameters of importance in a damage tolerance analysis are treated. Sources of scatter in fatigue crack growth during service loading are reviewed. Stochastic fatigue crack growth models are discussed. Limitations in such models are pointed out and are partly accounted for by modification of models. Author

**N88-13719#** Illinois Univ., Urbana. Dept. of Mechanical and Industrial Engineering.
**CONSTRAINT EFFECTS IN FATIGUE CRACK GROWTH**
R. C. McClung and H. Sehitoglu *In* Virginia Univ., Fatigue 87, Volume 3 1987 p 1401-1410 (For primary document see N88-13700 05-39)
Avail: NTIS HC A22/MF A01 CSCL 20K

Fatigue crack opening levels for different applied stress levels and stress states are determined with an elastic-plastic finite element simulation of fatigue crack growth. Both out-of-plane constraint (plane stress versus plane strain) and in-plane constaint (due to applied stress biaxiality) are shown to influence crack opening levels. These influences vary significantly with stress level.

The trends in opening levels determined analytically compare favorably with experimental crack growth data from the literature on thickness effects and stress biaxiality effects. Changes in opening levels are interpreted in terms of the interaction between residual displacements and crack opening displacements.
Author

**N88-13720#** International Business Machines Corp., Poughkeepsie, N.Y.
**COMPUTER AIDED MODELING AND FATIGUE FAILURE FORECAST UNDER STOCHASTIC LOADING**
B. D. Notohardjono and D. S. Ermer (Wisconsin Univ., Madison.) *In* Virginia Univ., Fatigue 87, Volume 3 1987 p 1411-1419 (For primary document see N88-13700 05-39)
Avail: NTIS HC A22/MF A01 CSCL 20K

A methodology for an on-line fatigue failure forecast (FFF) for stochastic loading is presented here. Autoregressive moving average (ARMA) models which are discrete representations of the underlying differential equations, are fitted to strain data for different times. Damping factors, that are estimated from the model parameters, decrease with time, and after generating a relationship between the normalized value of the damping factor, the remaining life or life ratio is found off-line. Several examples of on-line life prediction for the same kind of material that was tested off-line are given.
Author

**N88-13721#** Rochester Univ., N. Y. Materials Science Program.
**EMBRITTLING EFFECT OF THE PLASTIC ZONE**
J. C. M. Li *In* Virginia Univ., Fatigue 87, Volume 3 1987 p 1421-1429 (For primary document see N88-13700 05-39)
(Contract DE-FG02-85ER-45201)
Avail: NTIS HC A22/MF A01 CSCL 20K

The plastic zone developed in Mode 2 and Mode 3 loading can shield the crack tip from the applied stress and increases the toughness of the material. However, upon loading, it embrittles the material by providing the driving force for crack propagation. In Mode 1 loading, an asymmetric plastic zone can cause mixed mode crack propagation and crack branching and can also embrittle the material by the above Mode 2 effect. Plastic zones produced by chemical means such as hydrogen charging also can enhance crack propagation and may be the cause for hydrogen embrittlement.
Author

**N88-13722#** Missouri Univ., Kansas City. Dept. of Mechanical and Aerospace Engineering.
**A COMPARISON OF PLASTIC WORK ENERGY AND EXTERNAL INPUT FOR FATIGUE CRACK PROPAGATION**
C. Q. Bowles and E. G. Wenski (Allied Bendix Aerospace, Kansas City, Mo.) *In* Virginia Univ., Fatigue 87, Volume 3 1987 p 1431-1437 (For primary document see N88-13700 05-39)
Avail: NTIS HC A22/MF A01 CSCL 20K

The plastic work and the external energy required for fatigue crack propagation are discussed. Both energy values are experimentally determined for 2024-T351 Al. The values of plastic work are in agreement with those of Fine et al. The external energy input to the specimen as determined from hysteresis loops measured by a load line clip is approximately three time larger than the plastic work.
Author

**N88-13723#** Xian Jiaotong Univ. (China). Dept. of Engineering Mechanics.
**FATIGUE UNDER NONNORMAL RANDOM STRESSES USING MONTE CARLO METHOD**
H. J. Liu and S. R. Hu *In* Virginia Univ., Fatigue 87, Volume 3 1987 p 1439-1448 (For primary document see N88-13700 05-39)
Avail: NTIS HC A22/MF A01 CSCL 20K

A fatigue life prediction model is proposed for the structural elements subjected to a stress process, modeled as a stationary wide band nonnormal process. This model is restricted to high cycle fatigue design and evaluation, uses available constant amplitude material fatigue data and Palmgren-Miner rule. The test results suggest that the model give a reasonable life estimates. Secondly, Monte Carlo method is discussed in some depth. The different time histories simulated by Monte Carlo method for a given spectral density was shown to be equivalent in the meaning of effects on fatigue damage in high cycle fatigue.
Author

**N88-13724#** Georgia Inst. of Tech., Atlanta. Fracture and Fatigue Research Lab.
**TELEMETRIC LASER EXTENSOMETRY TECHNIQUE FOR MONITORING DEFLECTIONS IN SMALL CRACKS**
M. L. Bartlett, A. Saxena, and R. C. Brown *In* Virginia Univ., Fatigue 87, Volume 3 1987 p 1449-1458 (For primary document see N88-13700 05-39)
Avail: NTIS HC A22/MF A01 CSCL 20K

Crack mouth opening displacement for small fatigue cracks were studied using a telemetric laser extensometry system. The resolution of measurement for this system was at least 1.27 x 10 to the -7 m (.000005 in). The measured compliances for small edge cracks in a uniformly stressed specimen were much larger than the analytically predicted values based on the assumption that K completely characterizes the crack tip stress field. These measurements suggest that for small cracks the strain energy release rate, G, is not equal to K sup 2/E and a crack driving force based on G may be more reasonable than K.
Author

**N88-13725#** Rutgers - The State Univ., Piscataway, N. J. Dept. of Mechanics and Materials Science.
**X-RAY FATIGUE FAILURE PREDICTION BASED ON PLASTICITY RESPONSE TO MICROCRACKS**
S. Weissmann *In* Virginia Univ., Fatigue 87, Volume 3 1987 p 1459-1468 (For primary document see N88-13700 05-39)
(Grant NSF DMR-81-04985)
Avail: NTIS HC A22/MF A01 CSCL 20K

Cyclic deformation of aluminum crystals and Al 2024 alloys gives rise to surface intrusions which develop into microcracks. Microplastic zones at the crack tips get strain hardened upon cycling and by impeding the advancing crack fronts induce new formation of surface intrusions. Associated with the strain hardened zones at the crack tips is a pronounced induced lattice misorientation which serves as an important criterion to predict fatigue failure in the alloys. The X-ray CARCA method is used to determine the critical lattice misalignment when catastrophic failure is imminent.
Author

**N88-13726#** Southern Methodist Univ., Dallas, Tex. Dept. of Civil and Mechanical Engineering.
**AN OPTICAL INTERFEROMETRY TECHNIQUE TO EVALUATE CLOSURE ALONG A CRACK FRONT**
Angela A. Steffen and Paul F. Packman *In* Virginia Univ., Fatigue 87, Volume 3 1987 p 1469-1477 (For primary document see N88-13700 05-39)
Avail: NTIS HC A22/MF A01 CSCL 20K

Fatigue crack closure was observed in PMMA SEN fatigue cracked three point bend specimen. Optical interference profiles indicate that a portion of the crack face can be approximated by a straight line and extended to obtain a rotation factor which indicated that the crack tip was open along the centerline for all loading conditions. The interference profiles along the edge showed that portions of the crack were closed for low loads and open under increasing loads. Crack opening profiles taken in the thickness direction indicate the closure of the crack face extends into the thickness of the material at low loads. With increasing loads the interference profile indicates a transverse bending similar to anticlastic bending which vanishes at high applied loads.
Author

**N88-13727#** Chalmers Univ. of Technology, Goeteborg (Sweden). Dept. of Engineering Metals.
**ON THE GEOMETRICAL DESCRIPTION OF FATIGUE CRACK SURFACES**
B. Karlsson, J. Wasen, and K. Hamberg (Volvo A.B., Goeteborg, Sweden ) *In* Virginia Univ., Fatigue 87, Volume 3 1987 p 1479-1492 (For primary document see N88-13700 05-39)
Avail: NTIS HC A22/MF A01 CSCL 20K

Fatigue crack surfaces generally have a stochastic character requiring statistical descriptions. The simple distributions often found are conveniently characterized by means and standard deviations. The fracture surfaces are effectively described by angular distributions, height distributions, and wavelength spectra. Such distributions develop during the fracture process as a result of the stochastic interactions between the stress field and the microstructure at the crack front. A new model based on stochastic cracking is presented. The model describes the essential characteristics of the fracture surface geometry and naturally relates to the underlying microstructure. Author

**N88-13728#** Yokohama National Univ. (Japan). Dept. of Engineering.
**DEVELOPMENT OF RESEARCH ON FATIGUE OF SPOT-WELD IN AUTOMOBILE STRUCTURES IN JAPAN**
Hideo Kitagawa, Tsugihiko Satoh, Satoshi Nishijima, Masao Fujimoto, and Nobuyuki Mori (Toyota Motor Co., Tokyo, Japan ) *In* Virginia Univ., Fatigue 87, Volume 3 1987 p 1493-1501 (For primary document see N88-13700 05-39)
Avail: NTIS HC A22/MF A01 CSCL 20K

Research in Japan on the fatigue strength or fatigue life of spot welds and/or spot welded automobile structures seems to be one the most systematic and characteristic activities in this technical field. The trace of development of the research is reviewed and discussed from a historical and technological viewpoint. E.R.

**N88-13729#** Connecticut Univ., Storrs. Dept. of Metallurgy.
**AN OVERVIEW OF FATIGUE**
A. J. McEvily *In* Virginia Univ., Fatigue 87, Volume 3 1987 p 1503-1516 (For primary document see N88-13700 05-39)
(Contract DE-FG02-84ER-45109)
Avail: NTIS HC A22/MF A01 CSCL 20K

An overview of fatigue research is presented. Four topics are briefly discussed: (1) fatigue crack initiation and growth in a nickel based superalloy single crystal, (2) the effect of the ambient environment on near threshold fatigue crack growth behavior, (3) the role of crack closure in load interaction effects in fatigue crack growth, and (4) the nature of creep fatigue interactions, if any, during fatigue crack growth. Author

**N88-13730#** Max-Planck-Inst. fuer Metallforschung, Stuttgart (West Germany). Inst. fuer Werkstoffwissenschaften.
**DEFORMATION MECHANISMS AND CRACK INITIATION IN FATIGUE**
V. Gerold and B. Meier *In* Virginia Univ., Fatigue 87, Volume 3 1987 p 1517-1540 (For primary document see N88-13700 05-39)
Avail: NTIS HC A22/MF A01 CSCL 20K

Fatigue crack initiation of metals and alloys as the onset of failure is a very complex phenomenon which is influenced by many interacting parameters such as microstructure, loading conditions, environment, etc. Fatigue deformation mechanisms preceeding crack initiation is discussed. A review is given on recent research on fcc material on both single phase and precipitation hardened single and polycrystals. Following is a survey on new results in the area of crack nucleation. Because of the outstanding importance of fatigue crack initiation in common service, the initiation mechanisms in commercial aluminum based alloys are included. Author

**N88-13731#** Lehigh Univ., Bethlehem, Pa. Dept. of Mechanical Engineering and Mechanics.
**ENVIRONMENTALLY ASSISTED FATIGUE CRACK GROWTH**
R. P. Wei *In* Virginia Univ., Fatigue 87, Volume 3 1987 p 1541-1560 (For primary document see N88-13700 05-39)
(Contract DE-FG02-84ER-45138)
Avail: NTIS HC A22/MF A01 CSCL 20K

A framework is presented for understanding the role of environmental variables and of microstructure through modeling of environmentally assisted fatigue crack growth. The principal features of fatigue crack growth response and the current state of understanding are illustrated by data on structurally important alloys. The interaction between environment and microstructure are illustrated by recent results on a high strength steel and an aluminum alloy. The need for environmental control in studies of fatigue mechanisms is emphasized. Author

**N88-13732*#** Georgia Inst. of Tech., Atlanta. Fracture and Fatigue Research Lab.
**DEFORMATION, FATIGUE AND FRACTURE BEHAVIOR OF TWO CAST ANISOTROPIC SUPERALLOYS**
Walter W. Milligan, Eric S. Huron (Pratt and Whitney Aircraft, East Hartford, Conn.), and Stephen D. Antolovich *In* Virginia Univ., Fatigue 87, Volume 3 1987 p 1561-1591 (For primary document see N88-13700 05-39)
(Grant NAG3-503)
Avail: NTIS HC A22/MF A01 CSCL 20K

Tensile and low cycle fatigue (LCF) tests were conducted on two cast anisotropic superalloys. The effects of temperature, strain rate and stress range were investigated. Deformation behavior was extensively characterized and modeled. LCF and fracture behavior were studied and correlated with deformation behavior. Author

**N88-13733#** Ford Motor Co., Dearborn, Mich.
**APPLICATIONS OF FATIGUE ANALYSES: TRANSPORTATION**
R. W. Landgraf *In* Virginia Univ., Fatigue 87, Volume 3 1987 p 1593-1610 (For primary document see N88-13700 05-39)
Avail: NTIS HC A22/MF A01 CSCL 20K

Progress in the implementation of modern fatigue methodology in ground vehicle design is reviewed in the context of recent advances in data acquisition, computer modeling and laboratory simulation testing technologies. A fatigue analysis program, designed specifically for ground vehicle problems, is described and example applications presented. The trend towards integration of this methodology into computer workstation environment is discussed and future needs and refinement are identified. Author

**N88-13734#** Birmingham Univ. (England). Dept. of Metallurgy and Materials.
**FATIGUE CRACK GROWTH**
C. J. Beevers *In* Virginia Univ., Fatigue 87, Volume 3 1987 p 1611-1635 (For primary document see N88-13700 05-39)
Avail: NTIS HC A22/MF A01 CSCL 20K

The growth of both small and long fatigue cracks in a range of engineering metals and alloys are considered. Both intergranular and transgranular modes of small crack growth in aluminum alloys are analyzed. The relationship between small and long crack growth are considered and these lead to the conclusion that the effective stress intensity curve for long cracks can present an upper bound range of growth rates for both small and long cracks when the crack length is greater than the grain size or the basic microstructural element. Author

**N88-13735*#** National Aeronautics and Space Administration. Langley Research Center, Hampton, Va.
**STRAIN-ENERGY-RELEASE RATE ANALYSIS OF THE END-NOTCHED FLEXURE SPECIMEN USING THE FININTE-ELEMENT METHOD**
S. A. Salpekar, I. S. Raju, and T. K. OBrien (Army Aviation Research and Development Command, Hampton, Va.) Nov. 1987 33 p
(NASA-TM-100494; NAS 1.15:100494; USAAVSCOM-TM-87-B-12)
Avail: NTIS HC A03/MF A01 CSCL 20K

Two-dimensional finite-element analysis of the end-notched flexure specimen was performed using 8-node isoparametric, parabolic elements to evaluate compliance and mode II strain energy release rates, G sub II. The G sub II values were computed using two different techniques: the virtural crack-closure technique (VCCT) and the rate of change of compliance with crack length (compliance derivative method). The analysis was performed for various crack-length-to-semi-span (a/L) ratios ranging from 0.2 to

0.9. Three material systems representing a wide range of material properties were analyzed. The compliance and strain energy release rates of the specimen calculated with the present finite-element analysis agree very well with beam theory equations including transverse shear. The G sub II values calculated using the compliance derivative method compared extremely well with those calculated using the VCCT. The G sub II values obtained by the compliance derivative method using the top or bottom beam deflections agreed closely with each other. The strain energy release rates from a plane-stress analysis were higher than the plane-strain values by only a small percentage, indicating that either assumption may be used in the analysis. The G sub II values for one material system calculated from the finite-element analysis agreed with one solution in the literature and disagreed with the other solution in the literature. Author

**N88-13736#** Virginia Polytechnic Inst. and State Univ., Blacksburg. Center for Adhesion Science.

**BENDING OF A BONDED BEAM AS A TEST METHOD FOR ADHESIVE PROPERTIES Report, Sep. 1986 - Jun. 1987**

E. Moussiaux, H. F. Brinson, and A. H. Cardon Aug. 1987 91 p

(Contract N00014-82-K-0185)

(AD-A184813; CAS/EMS-87-2; VPI-E-87-9) Avail: NTIS HC A05/MF A01 CSCL 13M

A strength-of-materials type solution is obtained for the shear stress state in the adhesive layer of a bonded cantilever beam subjected to an end load. The shear stress is constant through the thickness of the adhesive layer and varies from zero at the fixed end to a maximum value at the free end. This maximum value can, under certain conditions, be calculated from knowledge of the load and the beam geometry under certain conditions, be calculated from knowledge of the load and the beam geometry only. The adhesive's shear modulus can then be determined from a measurement of the shear strain in the adhesive layer. An expression for the beam deflection is also obtained. It contains a coefficient of adhesion which is potentially useful in evaluating surface treatments or other factors leading to different states of adhesion. Fracture mechanics application of the specimen, and nonlinear and viscoelastic adhesive behavior are briefly mentioned. GRA

**N88-13737#** Naval Ship Research and Development Center, Bethesda, Md.

**BASIC DESK-TOP COMPUTER PROGRAM FOR THE THREE-DIMENSIONAL STATIC CONFIGURATION OF AN EXTENSIBLE FLEXIBLE CABLE IN A UNIFORM STREAM**

Richard K. Knutson Aug. 1987 54 p

(AD-A184852; DTNSRSDC-87/029) Avail: NTIS HC A04/MF A01 CSCL 20D

A generalized computer program for predicting the three-dimensional, static configurations and tensions of extensible, flexible cable systems is described. The program is written in BASIC language for use on desktop computers. The report includes development of the equations, descriptions of the program, instruction for program usage, sample programs, and a program listing for a Hewlett-Packard 9836 desktop computer.

Author (GRA)

**N88-13738#** Naval Ship Research and Development Center, Bethesda, Md.

**RADSPHERE: A COMPUTER PROGRAM FOR CALCULATING THE STEADY-STATE, AXIALLY SYMMETRIC, FORCED RESPONSE AND RADIATION FIELD OF A SUBMERGED SPHERICAL SHELL Final Report, Mar. - Jun. 1985**

Francis M. Henderson Aug. 1987 73 p

(AD-A185025; DTNSRDC-87/031) Avail: NTIS HC A04/MF A01 CSCL 20A

A computer program, RADSPHERE, has been developed for calculating the axisymmetric forced vibration response and sound radiation of a thin, elastic, spherical shell, submerged in an infinite fluid. Four cases of excitation are provided: (1) a concentrated radial load acting at a point on the shell surface, (2) two such loads acting simultaneously at antipodal surface points, (3) a uniform load distributed over a sector of the surface, and (4) two sector loads acting simultaneously with respect to an axis of the sphere. The calculated quantities are the shell surface radial velocity and the acoustic pressure at both the shell surface and in the far-field. RADSPHERE results are generated in tabular form and in graphic form, the latter through use of a companion program PLOTTER which provides an interface with the facilities of the software package DISSPLA. GRA

**N88-13739#** Naval Research Lab., Orlando, Fla. Underwater Sound Reference Div.

**DAMPING ANALYSIS OF FLEXURAL WAVES IN FLUID-LOADED SINGLE AND CONSTRAINED PLATES Interim Memo. Report, Oct. 1986 - Jul. 1987**

Pieter S. Dubbelday 1 Sep. 1987 31 p

(AD-A185116; NRL-MR-6067) Avail: NTIS HC A03/MF A01 CSCL 20D

A hybrid model was developed for the analysis of constrained-layer damping whereby the base plate is described by exact elasticity theory, while the elastomer and constraining layers are analogous to Kerwin's model. Under fluid loading, the success of the technique is measured by a damping efficiency, the ratio of loss in the elastomer to the total loss due to viscoelastic loss from a composite plate in vacuum, for antisymmetric and symmetric waves separately with the radiation loss from a single fluid-loaded plate. This ignores the interaction of fluid and constrained plate. This study shows that at high and low frequencies discrepancies occur. Inclusion in the hybrid model of both flexural and extensional waves shows that at higher frequencies the presence of the two types of waves redistributes the energy across the plate. Thus it proves necessary to compute damping efficiency from analysis of the fluid-loaded composite plate with inclusion of both antisymmetric and symmetric waves. GRA

**N88-13740#** State Univ. of New York, Buffalo. Dept. of Chemistry.

**PURE DEPHASING OF A VIBRATIONAL ADBOND**

Sander VanSmaalen and Thomas F. George Aug. 1987 45 p

(Contract N00014-86-C-0043)

(AD-A185222; UBUFFALO/DC/87/TR-49) Avail: NTIS HC A03/MF A01 CSCL 20E

A theoretical study of the vibrational relaxation of the adbond between a physisorbed molecule and a crystalline substrate is presented. The bond between the admolecule and substrate is described as a one-dimensional Morse-oscillator. Using standard perturbation theory, expressions for the relaxation of the vibrational adbond due to its interaction with the substrate lattice vibrations are derived. Both energy relaxation and pure dephasing are considered. A numerical evaluation of the resulting expressions for the relaxation constants is given for a Debye spectrum for the phonons and for a surface phonon spectrum. The relative importance of pure dephasing and energy relaxation in determining the absorption linewidth is derived as a function of the fundamental frequency of the active mode. GRA

**N88-13741#** Technische Univ., Aachen (West Germany). Fakultaet fuer Maschinenbau und Elektrotechnik.

**OPTICAL DEFORMATION MEASUREMENT ON SHELLS FOLLOWING THE RASTER PRINCIPLE Ph.D. Thesis [OPTISCHE VERFORMUNGSMESSUNG AN SCHALEN NACH DEM RASTERPRINZIP]**

Claus Schulze 1986 132 p In GERMAN

(ETN-88-90608) Avail: NTIS HC A07/MF A01

The in-plane, out-of-plane, and hybrid raster methods for deformation measurements are presented. The optical registration of raster pictures is explained. Measuring techniques for the deformation analysis of shell components using single-picture recording are examined. Deforation analysis of shell components following a time average method is presented. The experiments show that raster methods are a suitable and accurate instrument for the complex acquisition of motion or deformation phenomena.

ESA

**N88-13742#** Office National d'Etudes et de Recherches Aerospatiales, Paris (France). Direction Scientifique de la Resistance des Structures.
**AN ELEMENT OF A MULTILAYER SHELL FOR THE COMPUTATION OF COMPOSITE STRUCTURES Final Report [UN ELEMENT DE COQUE MULTICOUCHE POUR LE CALCUL DES STRUCTURES COMPOSITES]**
R. Girard Jan. 1987 46 p In FRENCH
(Contract DRET-85-34-001-29-8-3-2)
(ONERA-RT-14/3542-RY-051-R; ETN-88-91181) Avail: NTIS HC A03/MF A01

A macro-element model with 40 degrees of freedom was developed to be used as a classical shell or plate homogeneous element. The elementary elasticity, mass, and geometrical rigidity matrices were computed for the numerical solution of static and dynamic problems. The overall program was tested on various problems. Comparison with existing analytical solutions shows the reliability of the proposed element. ESA

**N88-13743#** Societe Nationale Industrielle Aerospatiale, Paris (France). Div. des Engins Tactiques.
**UTILIZATION OF DYNAMIC CHARACTERISTICS OF MATERIALS TO OPTIMIZE MILITARY EXPLOSIVE CHARGES. APPLICATION TO ANTISHIP DEVICES [DE L'UTILISATION DES CARACTERISTIQUES DYNAMIQUES DES MATERIAUX POUR L'OPTIMISATION DES CHARGES MILITAIRES. APPLICATION AUX ANTI-NAVIRES]**
Alain Grave 1987 32 p In FRENCH Presented at the Comite des Relations Industrielles (CRIN) du CNRS, Bellevue, France, 11 Mar. 1987
(SNIAS-872-320-101; ETN-88-91200) Avail: NTIS HC A03/MF A01

The study of the military explosive heads of sea-skimming devices of the Exocet (300 m/sec) family or its successors (800 m/sec) is presented. The head must protect the explosive charge through impact to a calibrated delay. Choice of materials, dynamic behavior, numerical simulation modeling of the explosive charge, and the final design of the military head are discussed. Verification tests made with inert loads show good agreement for missile nose deformation and a slight underestimation of cylinder deformation. ESA

**N88-13744#** Societe Nationale Industrielle Aerospatiale, Paris (France). Div. des Engins Tactiques.
**NUMERICAL SIMULATIONS OF IMPACT TESTS ON A RIGID WALL**
D. Bois, A. Grave, and M. L. Meyniel 1987 9 p
(SNIAS-872-320-102; ETN-88-91201) Avail: NTIS HC A02/MF A01

The behavior at impact of steel 30NCD16 is evaluated using the isothermal Johnson-Cook and Lindholm dynamic models. The numerical simulation of the impact tests against a rigid wall and the comparison to the experimental results highlight the interest of these models compared with the elastoplastic model with static properties. These two macroscopic models seem to be well suited to simulate dynamic phenomena of very different scales involving large deformations. The results of the simulations are little sensitive to the initial adopted modeling. The two models appear to be equivalent. ESA

**N88-13745*#** National Aeronautics and Space Administration. Lewis Research Center, Cleveland, Ohio.
**THERMAL FINITE-ELEMENT ANALYSIS OF SPACE SHUTTLE MAIN ENGINE TURBINE BLADE**
Ali Abdul-Aziz, Michael T. Tong (Sverdrup Technology, Inc., Cleveland, Ohio.), and Albert Kaufman Oct. 1987 11 p
(NASA-TM-100117; E-3535; NAS 1.15:100117) Avail: NTIS HC A03/MF A01 CSCL 20K

Finite-element, transient heat transfer analyses were performed for the first-stage blades of the space shuttle main engine (SSME) high-pressure fuel turbopump. The analyses were based on test engine data provided by Rocketdyne. Heat transfer coefficients were predicted by performing a boundary-layer analysis at steady-state conditions with the STAN5 boundary-layer code. Two different peak-temperature overshoots were evaluated for the startup transient. Cutoff transient conditions were also analyzed. A reduced gas temperature profile based on actual thermocouple data was also considered. Transient heat transfer analyses were conducted with the MARC finite-element computer code. Author

**N88-13746#** Vibration Inst., Clarendon Hills, Ill.
**THE SHOCK AND VIBRATION DIGEST, VOLUME 19, NO. 12 Monthly Report**
Judith Nagle-Eshleman, ed. Dec. 1987 112 p
Avail: NTIS HC A06/MF A01

Included are abstracts from current literature; book reviews; reviews of meetings; annual indexes; calendar; and feature articles and reviews. For individual titles, see N88-13747 through N88-13748.

**N88-13747#** Massachusetts Inst. of Tech., Cambridge. Dept. of Ocean Engineering.
**DYNAMICS OF CABLES AND CHAINS**
M. S. Triantafyllou *In* Vibration Inst., The Shock and Vibration Digest, Volume 19, No. 12 Dec. 1987 p 3-5 (For primary document see N88-13746 05-39)
Avail: NTIS HC A06/MF A01

This review covers some basic areas of cable and chain dynamics. Both linear and nonlinear dynamics are included. Author

**N88-13748#** China Ship Scientific Research Center, Wuxi.
**EXPERIMENTAL STUDIES ON ACOUSTIC EMISSION MONITORING OF CRACK PROPAGATION IN OFFSHORE STRUCTURES: A LITERATURE SURVEY c71**
Zhiyu Liu *In* Vibration Inst., The Shock and Vibration Digest, Volume 19, No. 12 Dec. 1987 p 6-17 (For primary document see N88-13746 05-39)
Avail: NTIS HC A06/MF A01

A comprehensive survey of experimental studies on acoustic emission (AE) monitoring of crack propagation in offshore steel structures and assesses relevant developments and applications of research work is presented. Criteria for the design of AE monitoring systems for detecting and characterizing fatigue cracks in offshore structures and interpreting relevant data are also given. Author

**N88-13749#** Helsinki Univ. (Finland). Inst. of Mathematics.
**TWO LOW-ORDER MIXED METHODS FOR THE ELASTICITY PROBLEM**
R. Stenberg 1987 15 p
(PB87-225272; HTKK-MAT-A-247; ISBN-951-754-162-7) Avail: NTIS HC A03/MF A01 CSCL 20K

The finite element approximation of the equations of linear elasticity is considered, where the bounded domain is assumed to have a polygonal or polyhedral boundary. The unknowns of the proglem are the displacement and the stress tensor, and the data is given by the body force and the boundary traction. GRA

**N88-13750#** Sandia National Labs., Albuquerque, N. Mex.
**ANALYSIS OF END STRESSES IN GLASS-METAL BIMATERIAL STRIPS**
F. P. Gerstle, Jr. and R. S. Chambers 1987 40 p Presented at the Symposium on Technology of Glass, Ceramic, Or Glass-ceramic To Metal Sealing, Boston, Mass., 13 Dec. 1987
(Contract DE-AC04-76DP-00789)
(DE87-007848; SAND-87-0432C; CONF-871207-1) Avail: NTIS HC A03/MF A01

We have analyzed the shear and normal residual stresses which build up along the interface near the end of a glass-metal seal during cooling. These stresses strongly affect the measured strength of a seal. Previous treatments of this problem have identified the presence of large interfacial transverse normal and shear stresses at the ends of bimaterial joints. We show the presence of maxima and minima in both force and moment. We demonstrate that, for certain material property combinations and

relative thicknesses, the interfacial moment can induce either a peel or a pinch condition at the ends of this strip. We tested this with strips of high expansion glass-ceramic sealed to 304 stainless steel and obtained qualitative agreement. Careful finite element modeling of the strips showed that peel and pinch conditions do not necessarily coincide with the sign of the singular transverse normal stress at the strip end. This sign appears to be controlled by differences in thermoelastic properties and not by relative thickness. DOE

**N88-13751#** Edgerton, Germeshausen and Grier, Inc., Idaho Falls, Idaho.
**ACOUSTIC EMISSIONS AT AN OPEN CRACK**
J. A. Johnson 1987 11 p Presented at the Review of Progress in Quantitative NDE, Williamsburg, Va., 21 Jun. 1987
(Contract DE-AC07-76ID-01570)
(DE88-001504; EGG-M-08987; CONF-870691-5) Avail: NTIS HC A03

Both finite difference and finite element techniques have been shown to be capable of modeling the propagation of acoustic emissions (AE) from a simple source to any close point in the part. However, the calculations done to date could also be done using the simpler Green's function methods. In this work the capabilities of the numerical methods are used to model problems that include the complexities that cannot be handled using the Green's function methods. In particular, the effect of the presence of the macrocrack on the received signal is investigated. We assume that the macrocrack interacts only as a geometric structure from which sound may reflect and mode convert, thereby complicating the signal at the receiving transducer. Numerical calculations of the AE field due to an open crack are compared to the Green's function results in a solid with no flaw. DOE

**N88-13752#** Lawrence Livermore National Lab., Calif.
**FREE LAGRANGE RECONNECTION ALGORITHMS FOR HYDROCODES USING A QUADRILATERAL MESH**
A. V. Attia Sep. 1987 45 p
(Contract W-7405-eng-48)
(DE88-001580; UCID-21203) Avail: NTIS HC A03/MF A01

In the dynamic response of materials to intense impulsive loading, material behavior may span both solid and fluid phases. Large relative motions may occur either because a solid fragment or a fluid region undergoes complex motions, or because of interactions at the interface between different materials. In order to address such complex motions, the computational technique should allow the mesh connectivity to vary. The Free Lagrange Method extends the classical Lagrangian continuum discretization by allowing changes in connectivity. This report covers the development of Free Lagrange reconnection algorithms for finite-difference or finite-element hydrocodes which use arbitrary mesh connectivity, but require the option to maintain a quadrilateral mesh as much as possible. Local mesh reconnection algorithms have been developed to allow general modifications to connectivity. These modifications are driven by algorithms for detecting local zone defects caused by excessive squeezing, stretching, or shearing of the mesh, such as can occur during Lagrangian simulation of large relative fluid motions. Several examples are given of the application of these algorithms for each of these types of mesh deformation. relative fluid motions. Several examples are given of the application of these algorithms for each of these types of mesh deformation. DOE

**N88-13753*#** National Aeronautics and Space Administration. Lewis Research Center, Cleveland, Ohio.
**A COMPUTER PROGRAM FOR CALCULATING UNSTEADY AERODYNAMIC COEFFICIENTS FOR CASCADES IN SUPERSONIC AXIAL FLOW**
John K. Ramsey and Robert E. Kielb Dec. 1987 54 p
(NASA-TM-100204; E-3801; NAS 1.15:100204) Avail: NTIS HC A04/MF A01 CSCL 01A

Recent interest in supersonic and hypersonic flight has renewed interst in developing propulsion systems which include a supersonic axial flow compressor. An important design consideration for the blades in such a compressor is aeroelastic stability. Described is a computer program which calculates the lift and moment coefficients for an oscillating cascade with a supersonic leading edge locus. A brief discussion of the theory (Lane's method) is presented, along with program logic, user instructions, and test cases. Author

**N88-13754*#** National Aeronautics and Space Administration. Lewis Research Center, Cleveland, Ohio.
**STAEBL/GENERAL COMPOSITES WITH HYGROTHERMAL EFFECTS (STAEBL/GENCOM)**
Robert Rubenstein (Sverdrup Technology, Inc., Cleveland, Ohio.) and Christos C. Chamis Dec. 1987 14 p
(NASA-TM-100266; E-3896; NAS 1.15:100266) Avail: NTIS HC A03/MF A01 CSCL 11D

A computer code has been developed to perform structural optimization of turbine blades made from angle ply fiber composite laminates. Design variables available for optimization include geometric parameters such as blade thickness distribution and root chord, and composite material parameters such as ply angles and numbers of plies of each constituent material. Design constraints include resonance margins, forced response margins, maximum stress, and maximum ply combined stress. A general description of this code is given. Design optimization studies for typical blades are presented. Author

# 42 GEOSCIENCES (GENERAL)

**N88-13755*#** Jet Propulsion Lab., California Inst. of Tech., Pasadena.
**PROCEEDINGS OF THE THIRD AIRBORNE IMAGING SPECTROMETER DATA ANALYSIS WORKSHOP**
Gregg Vane, ed. 15 Aug. 1987 190 p Workshop held in Pasadena, Calif., 2-4 Jun. 1987 Film slides as supplement
(Contract NAS7-918)
(NASA-CR-181552; JPL-Pub-87-30; NAS 1.26:181552) Avail: NTIS HC A09/MF A01 CSCL 08B

Summaries of 17 papers presented at the workshop are published. After an overview of the imaging spectrometer program, time was spent discussing AIS calibration, performance, information extraction techniques, and the application of high spectral resolution imagery to problems of geology and botany. For individual titles, see N88-13756 through N88-13772.

**N88-13756*#** Colorado Univ., Boulder. Center for the Study of Earth from Space.
**THE PORTABLE INSTANT DISPLAY AND ANALYSIS SPECTROMETER (PIDAS)** c35
Alexander F. H. Goetz *In* JPL Proceedings of the 3rd Airborne Imaging Spectrometer Data Analysis Workshop 15 Aug. 1987 p 8-17 (For primary document see N88-13755 05-42)
Avail: NTIS HC A09/MF A01 CSCL 14B

A field spectrometer covering the range 0.4 to 2.5 microns was developed that acquires spectra in 2 seconds at 872 points within the spectrum. The Portable Instant Display and Analysis Spectrometer (PIDAS) can acquire spectra every 8 seconds and stores up to 288 spectra in bubble memory. A hand held display unit allows for display of the current spectrum acquired and superimposed on one of 128 permanently stored library spectra. PIDAS represents a major advance in the technology of field spectral data acquisition and for the first time makes possible the acquisition of enough spectra to characterize the mean and intraclass variance within a LANDSAT MSS or TM pixel. Author

**N88-13757*#** Jet Propulsion Lab., California Inst. of Tech., Pasadena.
**AIS-2 RADIOMETRY AND A COMPARISON OF METHODS FOR THE RECOVERY OF GROUND REFLECTANCE** c43
James E. Conel, Robert O. Green, Gregg Vane, Carol J. Bruegge, Ronald E. Alley, and Brian J. Curtiss (Colorado Univ., Boulder.)

*In its* Proceedings of the 3rd Airborne Imaging Spectrometer Data Analysis Workshop 15 Aug. 1987 p 18-47 (For primary document see N88-13755 05-42)
Avail: NTIS HC A09/MF A01 CSCL 14B

A field experiment and its results involving Airborne Imaging Spectrometer-2 data are described. The radiometry and spectral calibration of the instrument are critically examined in light of laboratory and field measurements. Three methods of compensating for the atmosphere in the search for ground reflectance are compared. It was found that laboratory determined responsitivities are 30 to 50 percent less than expected for conditions of the flight for both short and long wavelength observations. The combined system atmosphere surface signal to noise ratio, as indexed by the mean response divided by the standard deviation for selected areas, lies between 40 and 110, depending upon how scene averages are taken, and is 30 percent less for flight conditions than for laboratory. Atmospheric and surface variations may contribute to this difference. It is not possible to isolate instrument performance from the present data. As for methods of data reduction, the so-called scene average or log-residual method fails to recover any feature present in the surface reflectance, probably because of the extreme homogeneity of the scene. Author

**N88-13758*#** Nevada Univ., Reno. School of Mines.
**EFFECTIVE USE OF PRINCIPAL COMPONENT ANALYSIS WITH HIGH RESOLUTION REMOTE SENSING DATA TO DELINEATE HYDROTHERMAL ALTERATION AND CARBONATE ROCKS** **c43**
Sandra C. Feldman *In* JPL Proceedings of the 3rd Airborne Imaging Spectrometer Data Analysis Workshop 15 Aug. 1987 p 48-55 (For primary document see N88-13755 05-42)
Avail: NTIS HC A09/MF A01 CSCL 08B

Methods of applying principal component (PC) analysis to high resolution remote sensing imagery were examined. Using Airborne Imaging Spectrometer (AIS) data, PC analysis was found to be useful for removing the effects of albedo and noise and for isolating the significant information on argillic alteration, zeolite, and carbonate minerals. An effective technique for using PC analysis using an input the first 16 AIS bands, 7 intermediate bands, and the last 16 AIS bands from the 32 flat field corrected bands between 2048 and 2337 nm. Most of the significant mineralogical information resided in the second PC. PC color composites and density sliced images provided a good mineralogical separation when applied to a AIS data set. Although computer intensive, the advantage of PC analysis is that it employs algorithms which already exist on most image processing systems. Author

**N88-13759*#** Autometric Corp., Inc., Falls Church, Va.
**LAND COVER/USE CLASSIFICATION OF CAIRNS, QUEENSLAND, AUSTRALIA: A REMOTE SENSING STUDY INVOLVING THE CONJUNCTIVE USE OF THE AIRBORNE IMAGING SPECTROMETER, THE LARGE FORMAT CAMERA AND THE THEMATIC MAPPER SIMULATOR** **c43**
Matthew Heric, William Cox, and Daniel K. Gordon *In* JPL Proceedings of the 3rd Airborne Imaging Spectrometer Data Analysis Workshop 15 Aug. 1987 p 56-62 (For primary document see N88-13755 05-42)
Avail: NTIS HC A09/MF A01 CSCL 08B

In an attempt to improve the land cover/use classification accuracy obtainable from remotely sensed multispectral imagery, Airborne Imaging Spectrometer-1 (AIS-1) images were analyzed in conjunction with Thematic Mapper Simulator (NS001) Large Format Camera color infrared photography and black and white aerial photography. Specific portions of the combined data set were registered and used for classification. Following this procedure, the resulting derived data was tested using an overall accuracy assessment method. Precise photogrammetric 2D-3D-2D geometric modeling techniques is not the basis for this study. Instead, the discussion exposes resultant spectral findings from the image-to-image registrations. Problems associated with the AIS-1 TMS integration are considered, and useful applications of the imagery combination are presented. More advanced methodologies for imagery integration are needed if multisystem data sets are to be utilized fully. Nevertheless, research, described herein, provides a formulation for future Earth Observation Station related multisensor studies. Author

**N88-13760*#** Washington Univ., Seattle.
**CALIBRATING AIS IMAGES USING THE SURFACE AS A REFERENCE** **c43**
M. O. Smith, D. A. Roberts, H. M. Shipman, J. B. Adams, S. C. Willis, and A. R. Gillespie *In* JPL Proceedings of the 3rd Airborne Imaging Spectrometer Data Analysis Workshop 15 Aug. 1987 p 63-69 (For primary document see N88-13755 05-42)
Avail: NTIS HC A09/MF A01 CSCL 08B

A method of evaluating the initial assumptions and uncertainties of the physical connection between Airborne Imaging Spectrometer (AIS) image data and laboratory/field spectrometer data was tested. The Tuscon AIS-2 image connects to lab reference spectra by an alignment to the image spectral endmembers through a system gain and offset for each band. Images were calibrated to reflectance so as to transform the image into a measure that is independent of the solar radiant flux. This transformation also makes the image spectra directly comparable to data from lab and field spectrometers. A method was tested for calibrating AIS images using the surface as a reference. The surface heterogeneity is defined by lab/field spectral measurements. It was found that the Tuscon AIS-2 image is consistent with each of the initial hypotheses: (1) that the AIS-2 instrument calibration is nearly linear; (2) the spectral variance is caused by sub-pixel mixtures of spectrally distinct materials and shade, and (3) that sub-pixel mixtures can be treated as linear mixtures of pure endmembers. It was also found that the image can be characterized by relatively few endmembers using the AIS-2 spectra. Author

**N88-13761*#** National Aeronautics and Space Administration. Ames Research Center, Moffett Field, Calif.
**THE USE OF AIRBORNE IMAGING SPECTROMETER DATA TO DETERMINE EXPERIMENTALLY INDUCED VARIATION IN CONIFEROUS CANOPY CHEMISTRY** **c43**
Nancy A. Swanberg (TGS Technology, Inc., Moffett Field, Calif.) and Pamela A. Matson *In* JPL Proceedings of the 3rd Airborne Imaging Spectrometer Data Analysis Workshop 15 Aug. 1987 p 70-74 (For primary document see N88-13755 05-42)
Avail: NTIS HC A09/MF A01 CSCL 08B

It was experimentally determined whether induced differences in forest canopy chemical composition can be detected using data from the Airborne Imaging Spectrometer (AIS). Treatments were applied to an even-aged forest of Douglas fir trees. Work to date has stressed wet chemical analysis of foliage samples and correction of AIS data. Plot treatments were successful in providing a range of foliar N2 concentrations. Much time was spent investigating and correcting problems with the raw AIS data. Initial problems with groups of drop out lines in the AIS data were traced to the tape recorder and the tape drive. Custom adjustment of the tape drive led to recovery of most missing lines. Remaining individual drop out lines were replaced using average of adjacent lines. Application of a notch filter to the Fourier transform of the image in each band satisfactorily removed vertical striping. The aspect ratio was corrected by resampling the image in the line direction using nearest neighbor interpolation. Author

**N88-13762*#** Research Center Graz (Austria).
**OVERVIEW OF AUSTRIAN AIRBORNE IMAGING SPECTROMETER (AIS) PROGRAMME AND FIRST RESULTS** **c43**
C. Banninger *In* JPL Proceedings of the 3rd Airborne Imaging Spectrometer Data Analysis Workshop 15 Aug. 1987 p 75-82 (For primary document see N88-13755 05-42)
Avail: NTIS HC A09/MF A01 CSCL 08B

Airborne Imaging Spectrometer (AIS) data collected from eight test areas in Austria were evaluated for their usefulness in forest damage assessment, geobotany, alpine vegetation mapping, and land use classification. Difficulties encountered in installing the SPAM spectral analysis software for use on the image display

system and the necessity to adapt existing programs for this task impeded and delayed the analysis of the AIS data. Spectral reflectance curves obtained from a geobotanical test site show a marked increase in reflectance across most of the measured spectrum for metal stressed spruce trees compared with nonstressed spruce trees. Author

**N88-13763*#** Delaware Univ., Newark. Coll. of Marine Studies.
**AIS-2 SPECTRA OF CALIFORNIA WETLAND VEGETATION c43**
Michael F. Gross, Susan L. Ustin (California Univ., Davis.), and Vytautas Klemas *In* JPL Proceedings of the 3rd Airborne Imaging Spectrometer Data Analysis Workshop 15 Aug. 1987 p 83-90 Prepared in cooperation with California Univ., Berkeley (For primary document see N88-13755 05-42)
(Grant NAGw-950)
Avail: NTIS HC A09/MF A01 CSCL 08B

Spectral data gathered by Airborne Imaging Spectrometers-2 from wetlands were analyzed. Spectra representing stands of green Salicornia virginica, green Sesuvium verrucosum, senescing Distichlis spicata, a mixture of senescing Scirpus acutus and Scirpus californicus, senescing Scirpus paludosus, senescent S. paludosus, mowed senescent S. paludosus, and soil were isolated. No difference among narrowband spectral reflectance of the cover types was apparent between 0.8 to 1.6 micron. There were, however, broadband differences in brightness. These differences were sufficient to permit a fairly accurate decomposition of the image into its major cover type components using a procedure that assumes an additive linear mixture of surface spectra. Author

**N88-13764*#** National Aeronautics and Space Administration. Ames Research Center, Moffett Field, Calif.
**TOWARD DETECTING CALIFORNIA SHRUBLAND CANOPY CHEMISTRY WITH AIS DATA c43**
Curtis V. Price and Walter E. Westman *In* JPL Proceedings of the 3rd Airborne Imaging Spectrometer Data Analysis Workshop 15 Aug. 1987 p 91-97 (For primary document see N88-13755 05-42)
Avail: NTIS HC A09/MF A01 CSCL 08B

Airborne Imaging Spectrometer (AIS)-2 data of coastal sage scrub vegetation were examined for fine spectral features that might be used to predict concentrations of certain canopy chemical constituents. A Fourier notch filter was applied to the AIS data and the TREE and ROCK mode spectra were ratioed to a flat field. Portions of the resulting spectra resemble spectra for plant cellulose and starch in that both show reduced reflectance at 2100 and 2270 nm. The latter are regions of absorption of energy by organic bonds found in starch and cellulose. Whether the relationship is sufficient to predict the concentration of these chemicals from AIS spectra will require testing of the predictive ability of these wavebands with large field sample sizes. Author

**N88-13765*#** Montana Univ., Missoula.
**MEASURING NEAR INFRARED SPECTRAL REFLECTANCE CHANGES FROM WATER STRESSED CONIFER STANDS WITH AIS-2 c43**
George Riggs and Steven W. Running *In* JPL Proceedings of the 3rd Airborne Imaging Spectrometer Data Analysis Workshop 15 Aug. 1987 p 100-106 (For primary document see N88-13755 05-42)
Avail: NTIS HC A09/MF A01 CSCL 08B

Airborne Imaging Spectrometer-2 (AIS-2) data was acquired over two paired conifer stands for the purpose of detecting differences in spectral reflectance between stressed and natural canopies. Water stress was induced in a stand of Norway spruce and white pine by severing the sapwood near the ground. Water stress during the AIS flights was evaluated through shoot water potential and relative water content measurements. Preliminary analysis with raw AIS-2 data using SPAM indicates that there were small, inconsistent differences in absolute spectral reflectance in the near infrared 0.97 to 1.3 micron between the stressed and natural canopies. Author

**N88-13766*#** Brown Univ., Providence, R. I. Dept. of Geological Sciences.
**ABUNDANCE AND DISTRIBUTION OF ULTRAMAFIC MICROBRECCIA IN MOSES ROCK DIKE: QUANTITATIVE APPLICATION OF AIS DATA Abstract Only c43**
John F. Mustard and Carle M. Pieters *In* JPL Proceedings of the 3rd Airborne Imaging Spectrometer Data Analysis Workshop 15 Aug. 1987 p 105-106 (For primary document see N88-13755 05-42)
Avail: NTIS HC A09/MF A01 CSCL 08B

Moses Rock dike is a Tertiary diatreme containing serpentinized ultramafic microbreccia (SUM). Field evidence indicates the SUM was emplaced first followed by breccias derived from the Permian strata exposed in the walls of the diatreme and finally by complex breccias containing basement and mantle derived rocks. SUM is found primarily dispersed throughout the matrix of the diatreme. Moses Rock dike was examined with Airborne Imaging Spectrometer (AIS) to map the distribution and excess of SUM in the matrix and to better understand the nature of the eruption which formed this explosive volcanic feature. AIS data was calibrated by dividing the suite of AIS data by data from an internal standard area and then multiplying this relative reflectance data by the absolute bidirectional reflectance of a selected sample from the standard area which was measured in the lab. From the calibrated AIS data the minerals serpentine, gypsum, and illite as well as desert varnish and the lithologies SUM and other sandstones were identified. SUM distribution and abundance in the matrix of the diatreme were examined in detail and two distinct styles of SUM dispersion were observed. The two styles are discussed in detail. Author

**N88-13767*#** Stanford Univ., Calif. Dept. of Applied Earth Sciences.
**EVALUATION OF AIS-2 (1986) DATA OVER HYDROTHERMALLY ALTERED GRANITOID ROCKS OF THE SINGATSE RANGE (YERINGTON) NEVADA AND COMPARISON WITH 1985 AIS-1 DATA c43**
R. J. P. Lyon *In* JPL Proceedings of the 3rd Airborne Imaging Spectrometer Data Analysis Workshop 15 Aug. 1987 p 107-119 (For primary document see N88-13755 05-42)
Avail: NTIS HC A09/MF A01 CSCL 08B

The Airborne Imaging Spectrometer-2 (AIS-2) flights along 2 subparallel lines (bearing 013) were designed to traverse 3 major rock assemblages - the Triassic sedimentary sequence; the granitoid rocks of the Yerington batholith and the Tertiary ignimbritic ash flow and ash fall tuffs. The first 2 sites are hydrothermally altered to a quartz-sericite-tourmaline mineralogy. The first AIS-2 data set showed numerous line dropouts and a considerable number of randomly distributed dark pixels. A second decommutation reduced the dropout essentially to near zero and the dark pixels by about 75 percent. Vertical striping was removed by histogram matching, column by column. A log residual spectrum was calculated which showed the departure of a 2 x 2 pixel area from the spatially and spectrally averaged scene. A 1:1 correlation was found with the log residual AIS-2 data and a large open pit area of gypsum. An area with known sericite agreed with the overflight data, and an area known to be free of any significant amount of O-H bearing materials showed no evidence of any in the AIS-2 log residuals. Author

**N88-13768*#** Durham Univ. (England). Dept. of Geological Sciences.
**PRELIMINARY RESULTS FROM AN INVESTIGATION OF AIS-1 DATA OVER AN AREA OF EPITHERMAL ALTERATION: PLATEAU, NORTHERN QUEENSLAND, AUSTRALIA c43**
Steve Mackin, Tim Munday, and Simon Hook *In* JPL Proceedings of the 3rd Airborne Imaging Spectrometer Data Analysis Workshop (date) 120-131 (SEE N88-13755 05-42) 15 Aug. 1987 (For primary document see N88-13755 05-42)
Avail: NTIS HC A09/MF A01 CSCL 08B

Airborne Imaging Spectrometer-1 (AIS-1) data were flown over undifferentiated sequences of acid to intermediate volcanics and intrusives; meta-sediments; and a series of partially lateritized

sedimentary rocks. The area exhibits a considerable spectral variability, after the suppression of striping effects. Log residual, and Internal Average Relative Reflectance (IARR) analytical techniques were used to enhance mineralogically related spectral features. Both methods produce similar results, but did not visually highlight mineral absorption features due to processing artifacts in areas of significant vegetation cover. The enhancement of mineral related absorption features was achieved using a hybrid processing approach based on the relative reflectance differences between vegetated and non-vegetated surfaces at 1.2 and 2.1 micron. The result is an image with little overall contrast, but which enhances the more subtle spectral features believed to be associated with clays and epidote. The AIS data was subject to interactive analysis using SPAM. Clear separation of clay and epidote related absorption features was apparent, and the identification of kaolinite was possible despite detrimental spectral effects. Author

**N88-13769*#** Geological Survey, Denver, Colo.
**CAUSES OF SPURIOUS FEATURES IN SPECTRAL REFLECTANCE DATA** **c43**
Roger N. Clark and Trude V. V. King *In* JPL Proceedings of the 3rd Airborne Imaging Spectrometer Data Analysis Workshop 15 Aug. 1987 p 132-137 (For primary document see N88-13755 05-42)
Avail: NTIS HC A09/MF A01 CSCL 08B

Several techniques are becoming common in the analysis of imaging spectrometer data that can lead to spurious absorption features or to changes in the position, width, and shape of actual absorption features. It is a common practice to calibrate AIS or other imaging spectrometer data by averaging each pixel along the flight line. The average is used to calibrate the spectral data by dividing the spectrum at each pixel by the average. If some pixels in the data set contain an absorption, then the average will also show an absorption. Some AIS data has had problems with wavelength stability from one scan line to the next which can produce spurious features with some analysis methods. If a pixel has a spectrum with an absorption having a different position or width than the spectrum used in a ratio, then the ratio can produce a spurious absorption at a different position and width than the true absorption feature. An average spectrum ratioed to each pixel will produce band shifts, and changes in width or shape. If continuum removal is performed by substraction rather than division, band positions can also be shifted. Author

**N88-13770*#** Geological Survey, Denver, Colo.
**AUTOMATIC CONTINUUM ANALYSIS OF REFLECTANCE SPECTRA** **c43**
Roger N. Clark and Trude V. V. King *In* JPL Proceedings of the 3rd Airborne Imaging Spectrometer Data Analysis Workshop 15 Aug. 1987 p 138-142 (For primary document see N88-13755 05-42)
Avail: NTIS HC A09/MF A01 CSCL 08B

A continuum algorithm based on a Segmented Upper Hull method (SUH) is described. An upper hull is performed on segments of a spectrum defined by local minima and maxima. The segments making a complete spectrum are then combined. The definition of the upper hull allows the continuum to be both concave and/or convex, adapting to the shape of the spectrum. The method performs multiple passes on a spectrum by segmenting each local maximum to minimum and performing an upper hull. The algorithm naturally adapts to the widths of absorption features, so that all features are found, including the nature of doublets, triplets, etc. The algorithm is also reasonably fast on common minicomputers so that it might be applied to the large data sets from imaging spectrometers. Author

**N88-13771*#** Geological Survey, Reston, Va.
**ANALYSIS OF AIRBORNE IMAGING SPECTROMETER DATA FOR THE RUBY MOUNTAINS, MONTANA, BY USE OF ABSORPTION-BAND-DEPTH IMAGES** **c43**
David W. Brickey, James K. Crowley, and Lawrence C. Rowan *In* JPL Proceedings of the 3rd Airborne Imaging Spectrometer Data Analysis Workshop 15 Aug. 1987 p 143-147 (For primary document see N88-13755 05-42)
Avail: NTIS HC A09/MF A01 CSCL 08B

Airborne Imaging Spectrometer-1 (AIS-1) data were obtained for an area of amphibolite grade metamorphic rocks that have moderate rangeland vegetation cover. Although rock exposures are sparse and patchy at this site, soils are visible through the vegetation and typically comprise 20 to 30 percent of the surface area. Channel averaged low band depth images for diagnostic soil rock absorption bands. Sets of three such images were combined to produce color composite band depth images. This relative simple approach did not require extensive calibration efforts and was effective for discerning a number of spectrally distinctive rocks and soils, including soils having high talc concentrations. The results show that the high spectral and spatial resolution of AIS-1 and future sensors hold considerable promise for mapping mineral variations in soil, even in moderately vegetated areas. Author

**N88-13772*#** Colorado Univ., Boulder. Center for the Study of Earth from Space.
**MAPPING HYDROTHERMALLY ALTERED ROCKS IN THE NORTHERN GRAPEVINE MOUNTAINS, NEVADA AND CALIFORNIA WITH THE AIRBORNE IMAGING SPECTROMETER** **c43**
Fred A. Kruse *In* JPL Proceedings of the 3rd Airborne Imaging Spectrometer Data Analysis Workshop 15 Aug. 1987 p 148-166 (For primary document see N88-13755 05-42)
Avail: NTIS HC A09/MF A01 CSCL 08B

Seven flightlines of Airborne Imaging Spectrometer (AIS) data were analyzed for an area of hydrothermally altered rocks. The data were reduced to reflectance relative to an average spectrum, and an automated procedure was used to produce a color coded image displaying absorption band information. Individual spectra were extracted from the AIS images to determine the detailed mineralogy. Two alteration types were mapped based upon mineralogy identified using the AIS data. The primary alteration type is quartz sericite pyrite alteration which occurs in northwest-trending zones in quartz monzonite porphyry. The AIS data allow identification of sericite (muscovite) based upon a strong absorption feature near 2.21 micron and weaker absorption features near 2.35 and 2.45 micron. The second alteration type occurs as a zone of argillic alteration associated with a granitic intrusion. Montmorillonite was identified based on a weak to moderate absorption feature near 2.2 micron and the absence of the two absorption features at longer wavelengths characteristic of sericite. Montmorillonite could be identified only where concentrations of sericite did not mask the montmorillonite spectrum. Author

**N88-13773*#** National Aeronautics and Space Administration. Goddard Space Flight Center, Greenbelt, Md.
**IN-ORBIT CALIBRATION ADJUSTMENT OF THE NIMBUS-7 SMMR**
Per Gloersen Sep. 1987 43 p
(NASA-TM-100678; Rept-87B0413; NAS 1.15:100678) Avail: NTIS HC A03/MF A01 CSCL 08B

The procedure for converting raw antenna signals (counts) from the Nimbus-7 Scanning Multichannel Microwave Radiometer (SMMR) to microwave radiances is described. The procedure entails taking the raw data stored on TAT data tapes, applying an interim prelaunch calibration, correcting for polarization mixing, and finally adjusting the calibration so that the observations conform to model calculations of oceanic radiances. The results are stored on TCT data tapes with the same format as the TATs, i.e., the basic sampling interval of the SMMR is retained. The properties of the TCTs are compared with those of the other basic SMMR radiance data product, the CELL tapes, in which the integrated fields-of-view (IFOVs) have been averaged into cells with coarser sampling intervals and in which the prelaunch calibration is the final one used. Author

**N88-13774*#** National Aeronautics and Space Administration. Goddard Space Flight Center, Greenbelt, Md.
**SCIENTIFIC AND OPERATIONAL REQUIREMENTS FOR TOMS DATA**
Arlin J. Krueger, ed. Dec. 1987 112 p Conference held in Greenbelt, Md., 10-11 Sep. 1986
(NASA-CP-2497; Rept-87B0206; NAS 1.55:2497) Avail: NTIS HC A06/MF A01 CSCL 04A

Global total ozone and sulfur dioxide data from the Nimbus 7 Total Ozone Mapping Spectrometer (TOMS) instrument have applications in a broad range of disciplines. The presentations of 29 speakers who are using the data in research or who have operational needs for the data are summarized. Five sessions addressed topics in stratospheric processes, tropospheric dynamics and chemistry, remote sensing, volcanology, and future instrument requirements. Stratospheric and some volcanology requirements can be met by a continuation of polar orbit satellites using a slightly modified TOMS but weather related research, tropospheric sulfur budget studies, and most operational needs require the time resolution of a geostationary instrument. For individual titles, see N88-13775 through N88-13802.

**N88-13775*#** National Aeronautics and Space Administration. Goddard Space Flight Center, Greenbelt, Md.
**TOMS: THE ANTARCTIC OZONE HOLE AND OZONE TRENDS Abstract Only** **c45**
Richard S. Stolarski *In its* Scientific and Operational Requirements for TOMS Data Dec. 1987 p 5-7 (For primary document see N88-13774 05-42)
Avail: NTIS HC A06/MF A01 CSCL 13B

The Total Ozone Mapping Spectrometer (TOMS) instrument aboard Nimbus 7 has proved invaluable for the investigation of the recent rapid decline in the springtime total ozone over the Antarctic. The principle problem discussed is that of observing the atmosphere over long periods of time to determine whether or not trends and/or slow oscillations are taking place. Total ozone is an excellent summary parameter for the state of the stratosphere. It responds to temperature changes, and in the long term, is expected to respond to chemical changes. Thus, when changes take place in total ozone, such as the springtime Antarctic decrease it is a clear indication of an important problem, both because of environmental potential and scientific importance. TOMS is actually an overkill for this problem. Significantly more data is taken than is necessary. Tests have shown that maps produced on a 2 by 4 degree grid are essentially equivalent to those produced from the entire gridded data set. Because the critical aspect of the search for changes in ozone is continuous data, reflight of a polar orbiting TOMS is important. Included in the flight should be a stratospheric temperature sensor and, if possible, a modification to obtain some ozone altitude information. A critical aspect of the problem is timeliness of the data. This is the only drawback of the existing TOMS. It is expected that in the very near future the processing will be done within two weeks of real time. This is critical to the process of discovery of phenomena such as the Antarctic ozone hole. Author

**N88-13776*#** National Aeronautics and Space Administration. Goddard Space Flight Center, Greenbelt, Md.
**OCTOBER LOWER STRATOSPHERIC ANTARCTIC TEMPERTURE AND TOTAL OZONE FROM 1979-1985 Abstract Only** **c45**
Paul A. Newman (Applied Research Corp., Landover, Md.) and Mark R. Schoeberl *In its* Scientific and Operational Requirements for TOMS Data Dec. 1987 p 8-9 (For primary document see N88-13774 05-42)
Avail: NTIS HC A06/MF A01 CSCL 13B

During October, from 1979 to 1985, Southern Hemisphere daily plots of TOMS total ozone and lower stratospheric temperature are shown to be strongly correlated. The same result is found for the monthly averages. Additionally, these data reveal strong wave events during the ozone hole period. October zonal means of TOMS total ozone and NMC temperature are well correlated from year to year, and both are decreasing. Finally, the mid-latitude temperature maximum is found to be radically cooler in 1985 than in either 1979 (a dynamically active year) or in 1980 (a dynamically quiescent year). Author

**N88-13777*#** Wisconsin Univ., Madison.
**SYSTEMATIC STRATOSPHERIC-TROPOSPHERIC EXCHANGE VIEWED FROM ISENTROPIC COORDINATES Abstract Only** **c46**
Donald Johnson *In* NASA. Goddard Space Flight Center, Scientific and Operational Requirements for TOMS Data Dec. 1987 p 10 (For primary document see N88-13774 05-42)
Avail: NTIS HC A06/MF A01 CSCL 04A

Within the atmosphere's stratification, stratospheric-tropospheric exchange of mass and other properties occurs primarily through quasi-horizontal transport processes within baroclinic wave regimes and through diabatic processes either in the form of deep convection or through systematic meridional variation of incoming and outgoing radiation. These exchange processes include both extrusions of stratospheric air into the troposphere and intrusions of tropospheric air into the stratosphere. The physical processes that govern both meridional and vertical exchange processes within isentropic coordinates are summarized for the global circulation. Author

**N88-13778*#** National Aeronautics and Space Administration. Goddard Space Flight Center, Greenbelt, Md.
**PHOTOCHEMICAL OZONE OVERBURDEN CORRECTION Abstract Only** **c45**
Michael Stefanick (Science Systems and Applications, Inc., Seabrook, Md.) and Arlin J. Krueger *In its* Scientific and Operational Requirements for TOMS Data Dec. 1987 p 11 (For primary document see N88-13774 05-42)
Avail: NTIS HC A06/MF A01 CSCL 13B

One-half of the total ozone column is predominantly under photochemical control under all conditions except polar winter. The other half is dynamically controlled. Since the photochemical forcing is phased with the solar declination and modulated by air temperature variation in the upper stratosphere and the dynamic forcing is tied to wave activity in the upper troposphere, the total ozone column is a mixture of the two drivers. If the total ozone is used to infer a property of the dynamic field, namely the tropopause height, it is necessary to correct for the photochemical variations. It should be possible to remove the photochemical component of the total ozone by using SBUV profile information along the orbital track as long as the spatial variations are low frequency. The column integral above the Umkehr levels in the lower stratosphere are examined to determine the level where the spatial variability decreases to the expected photochemical range to find an approximate dividing line between photochemical and dynamic control. Given this a spherical harmonic function will be fitted to the ozone field and subtracted from the TOMS total ozone field. This residual field will then be correlated with tropopause height to determine whether an improvement is obtained over the total ozone correlation. Author

**N88-13779*#** Illinois Univ., Urbana. Dept. of Atmospheric Science.
**ANALYSIS OF THE BREAKDOWN OF THE ANTARCTIC CIRCUMPOLAR VORTEX USING TOMS OZONE DATA Abstract Only** **c45**
Kenneth P. Bowman *In* NASA. Goddard Space Flight Center, Scientific and Operational Requirements for TOMS Data Dec. 1987 p 12-13 (For primary document see N88-13774 05-42)
Avail: NTIS HC A06/MF A01 CSCL 13B

Climatological analysis of data from the Total Ozone Mapping Spectrometer (TOMS) on the Nimbus 7 satellite has shown that the annual cycles of ozone are very different in the Arctic and Antarctic. The annual cycle in the Arctic is a relatively smooth annual sine wave; but in the Antarctic the circumpolar vortex breaks down rapidly during the Southern Hemisphere spring (September through November), producing a rapid rise in total ozone and a sawtooth-shaped annual cycle. The evolution of the Antarctic total ozone field during the vortex breakdown was studied by computing

areally-integrated ozone amounts from the TOMS data. This technique avoids substantial difficulties with using zonally-averaged ozone amounts to study the asymmetric breakdown phenomenon. Variability of total ozone is found to be large both within an individual year and between different years. During the last decade monthly-mean total ozone values in the Antarctic during the springtime vortex breakdown period have decreased dramatically. The ozone-area statistics indicate that the decrease has resulted in part from changes in the timing of the vortex breakdown and resultant ozone increase, which have occurred later during recent years. Analysis of the spatial scales involved in the ozone transport and mixing that occur during the vortex breakdown is now underway. Reliable calculation of diagnostic quantities like areally-integrated ozone is possible only with the high-resolution, two-dimensional, daily coverage provided by the TOMS instrument. Author

**N88-13780*#** National Aeronautics and Space Administration. Goddard Space Flight Center, Greenbelt, Md.
**INSIGHTS INTO THE GENERAL CIRCULATION OF THE LOWER STRATOSPHERE FROM TOMS Abstract Only c46**
Mark R. Schoeberl *In its* Scientific and Operational Requirements for TOMS Data Dec. 1987 p 14 (For primary document see N88-13774 05-42)
Avail: NTIS HC A06/MF A01 CSCL 04A

Total ozone is controlled by dynamical advection as well as chemistry. At least for day-to-day variations, dynamical processes appear to be in control of total ozone. There also appears to be good evidence that seasonal and secular changes in total ozone are also dynamically controlled. For example, the zonal mean changes in total ozone in the two hemispheres in spring appear to be quite different. The TOMS total ozone data suggest a south polar spring upwelling while the Northern Hemisphere shows a clear downwelling in the same period. Radiative transfer computations support this conclusion. The secular changes in total ozone over the South Pole in spring indicate a change in dynamics rather than chemistry. Author

**N88-13781*#** National Aeronautics and Space Administration. Goddard Space Flight Center, Greenbelt, Md.
**OZONE, JET STREAKS AND SEVERE WEATHER Abstract Only c47**
Frank S. Sechrist, Ralph A. Petersen, Keith F. Brill (General Sciences Corp., Landover, Md.), Arlin J. Krueger, and Louis W. Uccellini *In its* Scientific and Operational Requirements for TOMS Data Dec. 1987 p 20 (For primary document see N88-13774 05-42)
Avail: NTIS HC A06/MF A01 CSCL 04B

Data from three independent observing platforms are synthesized to study the role of jet streaks in severe weather. The three data types are: conventional radiosondes; 6.7 micron water vapor imagery from the GOES satellite; and total ozone imagery from Nimbus 7. Diagnoses are then made of potential vorticity, mid-tropospheric moisture, and total ozone at and below the level of jet streaks. Potential vorticity and total ozone distributions are both tracers of stratospheric air. Theoretically, both should respond to the transverse, vertical circulations expected in the vicinity of jet streaks. Both should increase due to the sinking above the left front quadrant of the streaks. Moisture, on the other hand, increases in the ascent under the left front quadrant. This study shows striking agreement between the three parameters independently observed from three different observing platforms. Moreover, the three severe weather case studies suggest a unique distribution of ozone, potential vorticity, and mid-tropospheric moisture relative to a jet streak. This, in turn, led to the creation of a new ozone/jet streak model which shows that the total ozone distribution provides a signature in the vicinity of jet streaks and permits identification of areas most likely to experience severe weather at a later time. The value of such observations to operational forecasting is discussed. Author

**N88-13782*#** National Aeronautics and Space Administration. Goddard Space Flight Center, Greenbelt, Md.
**LOWER-STRATOSPHERIC/UPPER-TROPOSPHERIC E PROCESSES ASSOCIATED WITH TROPICAL CYCLONES AS OBSERVED BY TOMS Abstract Only c46**
Edward B. Rodgers *In its* Scientific and Operational Requirements for TOMS Data Dec. 1987 p 21-22 (For primary document see N88-13774 05-42)
Avail: NTIS HC A06/MF A01 CSCL 04A

Total ozone associated with western Atlantic and Pacific tropical cyclones at various stages of development were analyzed for the purpose of monitoring storm intensity and/or intensity changes. The analysis is based on total ozone measurements from the Nimbus 7 Total Ozone Mapping Spectrometer (TOMS). Since ozone may be considered a passive tracer in the lower stratosphere and the ozone gradients are strongest just above the tropopause, fluctuations of total ozone are due to variations in tropopause height and/or changes in concentration within the column caused by vertical and horizontal advection. In the subtropical northern Pacific during August and September 1981, a negative correlation greater than 0.60 was found between upper-tropospheric geopotential heights near the tropopause level and total ozone. Preliminary results suggest that TOMS can be used to resolve the upper-troposphere structure in and around tropical cyclones and can provide an indication of those processes that help to intensify and maintain these storms. Author

**N88-13783*#** Saint Louis Univ., Mo.
**TROPICAL EASTERLY JET LOCATED USING TOMS DATA Abstract Only c46**
William C. Bolhofer *In* NASA. Goddard Space Flight Center, Scientific and Operational Requirements for TOMS Data Dec. 1987 p 23 (For primary document see N88-13774 05-42)
Avail: NTIS HC A06/MF A01 CSCL 04A

The formative stages of the onset of the 1979 southwest monsoon was marked by a WNW-ESE oriented band of marine convection over the South Arabian Sea. This convection was first observed on June 10, 1979 using satellite cloud imagery. The marine convection appeared during a major acceleration of the upper troposphere easterly wind field. A composite vertical meridional cross-section of upper level winds for June 11, revealed the core of the Tropical Easterly Jet (TEJ) at 115 mb, 9.5 deg N. Time analysis of the upper level wind field over the Tropical Wind Observing Ship (TWOS) polygon show a lowering of both the pressure level of maximum wind and tropopause level with acceleration of the upper level easterlies. The tropopause was as much as 20 mb lower on the equatorial side of the TEJ. Streamline analysis of the maximum observed easterly winds over India did not reveal the horizontal position of the TEJ. Careful analysis of Total Ozone Mapping Spectrometer (TOMS) data for June 11, 1979 showed relatively high values of ozone south of India. It was observed that the latitudinal position of the TEJ on June 11, at approximately 70 deg E coincided with the northern edge of relatively high ozone values. Using this as a reference, the TEJ core was identified as far as NE Bay of Bengal (the limits of the available TOMS data). Author

**N88-13784*#** National Aeronautics and Space Administration. Langley Research Center, Hampton, Va.
**THE USE OF TOMS DATA FOR TROPOSPHERIC OZONE STUDIES Abstract Only c45**
Jack Fishman and Edward V. Browell *In* NASA. Goddard Space Flight Center, Scientific and Operational Requirements for TOMS Data Dec. 1987 p 26 (For primary document see N88-13774 05-42)
Avail: NTIS HC A06/MF A01 CSCL 13B

Instances were identified where enhancements of tropical ozone are associated with sporadic widespread biomass burning. A strong positive correlation exists between total ozone and the distribution of carbon monoxide in the tropics, indicating that total ozone data can be used for tropospheric ozone studies. Using ozone profiles derived from the Stratospheric Aerosol and Gas Experiment (SAGE), preliminary findings show enhanced tropospheric ozone

concentrations over Africa and the eastern Atlantic at tropical latitudes. Other preliminary studies also suggest that Total Ozone Mapping Spectrometer (TOMS) data may provide a means of identifying widespread air pollution episodes over the United States during the summer. Author

**N88-13785*#** Chicago Univ., Ill. Dept. of Geophysical Science.
**TOMS AS A MONITOR OF THE ULTRAVIOLET RADIATION ENVIRONMENT: APPLICATIONS TO PHOTOBIOLOGY Abstract Only c45**
John E. Frederick *In* NASA. Goddard Space Flight Center, Scientific and Operational Requirements for TOMS Data Dec. 1987 p 27-30 (For primary document see N88-13774 05-42)
Avail: NTIS HC A06/MF A01 CSCL 13B

The flux of biologically relevant ultraviolet radiation that reaches the surface of the Earth varies with the ozone amount, surface reflectivity, and cloudcover. The Total Ozone Mapping Spectrometer (TOMS) provides information relevant to all three items. A recent application of satellite-based ozone measurements has been to develop climatologies of the biologically significant UV-B radiation reaching the Earth's surface. A growing body of research suggests that UV-B radiation tends to suppress the immune system of laboratory mice. At tropical latitudes, it is likely that parasitical diseases develop most readily in people who have experienced immune system suppression from UV-B exposure. The computed distribution of surface radiation combined with information on disease incidence may clarify the role of UV-B as a suppressor of the human immune system. TOMS used in conjunction with radiative transfer calculations can provide information of relevance in photobiology. Author

**N88-13786*#** National Aeronautics and Space Administration. Goddard Space Flight Center, Greenbelt, Md.
**NORTHWEST AIRLINES FLIGHT EXPERIMENTS Abstract Only c45**
Arlin J. Krueger *In its* Scientific and Operational Requirements for TOMS Data Dec. 1987 p 31 (For primary document see N88-13774 05-42)
Avail: NTIS HC A06/MF A01 CSCL 13B

An experiment was conducted in which real-time Total Ozone Mapping Spectrometer (TOMS) data was compared with Northwest Airlines upper air charts. It was demonstrated that the regions of steep gradient in total ozone corresponded with fronts in the upper troposphere, specifically breaks in the tropopause associated with jet streams. Other small scale structures in the ozone could be related to minor trough and ridge lines. This suggests that the relation between total ozone and tropopause height might apply even on relatively small scales, and an analysis produced high correlation coefficients provided that the air mass origin was considered. In a second test, cabin ozone mixing at 37,000 ft. varied from less than 100 ppb (300 DU total ozone) to greater than 300 ppb in a trough (400 DU total ozone). A third analysis showed that clear air turbulence was located where upper air fronts were in rapid motion as suggested by comparison of the 1200 UT synoptic charts and the ozone map taken about six hours later. Author

**N88-13787*#** Control Data Corp., Minneapolis, Minn.
**APPLICATION OF TOMS DATA TO WEATHER ANALYSIS MODELS Abstract Only c47**
Gregory D. Nastrom *In* NASA. Goddard Space Flight Center, Scientific and Operational Requirements for TOMS Data Dec. 1987 p 32 (For primary document see N88-13774 05-42)
Avail: NTIS HC A06/MF A01 CSCL 04B

Recent studies of the errors of analysis reflected by numerical weather analysis models are reviewed. Despite the improvements in data coverage and data ingestion methods in the past decade, it is found that significant errors of analysis persist. A case study comparison of Total Ozone Mapping Spectrometer (TOMS) data and aircraft data with the NMC analysis over the North Atlantic is used to illustrate the size of local errors encountered. The possibility of using TOMS images to locate meteorologically significant features such as troughs and ridges near the tropopause is discussed. Author

**N88-13788*#** National Aeronautics and Space Administration. Goddard Space Flight Center, Greenbelt, Md.
**CORRELATIONS OF TOMS TOTAL OZONE DATA (NIMBUS-7 SATELLITE) WITH TROPOPAUSE HEIGHT Abstract Only c45**
Marie-Jeanne Munteanu *In its* Scientific and Operational Requirements for TOMS Data Dec. 1987 p 37 (For primary document see N88-13774 05-42)
Avail: NTIS HC A06/MF A01 CSCL 13B

Two correlation studies of Total Ozone Mapping Spectrometer (TOMS) data with tropopause height from radiosondes performed over Europe showed a correlation coefficient of 0.94 and 0.96. As a result, the rms error in the prediction of tropopause height from total ozone was found to be 20 mb. Correlation between tropopause height and TOMS data was the highest of all the other correlations with variables directly derived from radiosondes or simulated thermal radiances over the location of radiosondes. Comparing the two dimensional fields of TOMS, tropopause height from radiosondes and tropopause height field from TIROS-N retrievals, we can say that the first field is much closer to the true field from radiosondes than the third. The correlation coefficient for a ten-day study between TOMS data and tropopause height from radiosondes is between 0.85 and 0.9 for 30-70N. Tropopause analysis provided by GLA model also shows a very high correlation with TOMS data. Author

**N88-13789*#** National Aeronautics and Space Administration. Goddard Space Flight Center, Greenbelt, Md.
**AN ANALYSIS OF TROPOPAUSE PRESSURE AND TOTAL OZONE CORRELATIONS Abstract Only c46**
Siegfried D. Schubert and Marie-Jeanne Munteanu *In its* Scientific and Operational Requirements for TOMS Data Dec. 1987 p 38 (For primary document see N88-13774 05-42)
Avail: NTIS HC A06/MF A01 CSCL 04A

A study of the relationship between total ozone and tropopause pressure was carried out using Total Ozone Mapping Spectrometer (TOMS) data and National Meteorological Center (NMC) global analyses. The medium scales generally show correlations greater than 0.6 throughout the middle latitudes of both hemispheres with some regions exceeding 0.8. The areas of highest correlations seem to be associated with the storm track regions of both the Northern and Southern Hemispheres. A detailed spectral analysis is performed for the medium scales on five pairs of time series of area averaged tropopause pressure and total ozone. In middle latitudes, total ozone and tropopause pressure exhibit generally similar distributions in the power spectrum. In the subtropics and tropics the power in ozone drops off more rapidly with increasing frequency than the power in tropopause pressure. Only in the Northern Hemisphere middle latitudes does one find a clear association between increased power in ozone and tropopause pressure and maxima in the coherency spectrum. Results for large scales are more complicated, showing generally positive correlations at middle latitudes. Author

**N88-13790*#** National Aeronautics and Space Administration. Goddard Space Flight Center, Greenbelt, Md.
**TOMS OZONE DATA COMPARED AT MESOSCALE RESOLUTION TO TROPOPAUSE HEIGHTS FROM THE AVE RADIOSONDE NETWORK AND TO VAS RADIANCES OVER THE SOUTH-CENTRAL UNITED STATES Abstract Only c46**
Dennis Chesters, Louis Uccellini, and David Larko *In its* Scientific and Operational Requirements for TOMS Data Dec. 1987 p 39 (For primary document see N88-13774 05-42)
Avail: NTIS HC A06/MF A01 CSCL 04A

Observations from 1982 are being compared between the Total Ozone Mapping Spectrometer (TOMS), the Atmospheric Variability Experiment (AVE), and the VISSR Atmospheric Sounder (VAS) across Texas and Oklahoma. TOMS data show a significant ozone maximum over northeastern Texas. AVE radiosonde analysis shows tropopause heights with the highest pressure (lowest altitudes) over central Oklahoma accompanied by a mid-level jet across

northern Mexico exiting above the Texas-Gulf coast. Corresponding VAS radiances show a dry slot in the middle tropopause across central Texas accompanied by a secondary slot over Oklahoma. The maxima are separated by 100 to 500 km. The impact of TOMS data on tropopause analysis is preliminarily seen as insignificant because TOMS data is not registered with respect to AVE tropopause heights. Author

**N88-13791*#** National Aeronautics and Space Administration. Goddard Space Flight Center, Greenbelt, Md.
**THE USE OF TOMS-MODIFIED VAS DATA FOR LARGE-SCALE NWP c46**
Wayman E. Baker, Marie-Jeanne Munteanu, Joel Susskind, and D. Reuter *In its* Scientific and Operational Requirements for TOMS Data Dec. 1987 p 40-45 (For primary document see N88-13774 05-42)
Avail: NTIS HC A06/MF A01 CSCL 04A

Collocation statistics obtained by comparing VISSR Atmospheric Sounder (VAS) temperature soundings with those from nearby rawinsondes indicate good agreement. However, the VAS soundings exhibited a substantial cold bias in the middle and upper troposphere. The error makes promising the use of the Total Ozone Mapping Spectrometer (TOMS) to obtain an independent estimate of tropopause pressure for use in the retrieval program. Good agreement is found between TOMS data and tropopause pressure. A quantitative assessment for the correlation of tropopause pressure, obtained from TOMS by regression and from rawinsondes over Europe, is reported. Author

**N88-13792*#** Atmospheric Environment Service, Downsview (Ontario).
**DOBSON-STATIONS PERFORMANCE ASSESSMENT USING TOMS DATA Abstract Only c45**
Rumen D. Bojkov and Carl L. Mateer *In* NASA. Goddard Space Flight Center, Scientific and Operational Requirements for TOMS Data Dec. 1987 p 47 (For primary document see N88-13774 05-42)
Avail: NTIS HC A06/MF A01 CSCL 13B

Examples of comparisons of monthly summaries (based on daily measurements) of some of the regularly operating Dobson stations, with the values deduced from the Total Ozone Mapping Spectrometer (TOMS) overpass are given. Shortcomings in certain Dobson stations are identified, such as: use of an incorrect value for the extraterrestrial constant (HOBART); sudden large volume changes (Brisbane); unusually low Dobson readings (Mauna Loa); and use of inaccurate cloud blue sky charts, causing fictitious differences with direct sun measurements (Toronto). Author

**N88-13793*#** National Aeronautics and Space Administration. Goddard Space Flight Center, Greenbelt, Md.
**VOLCANIC ERUPTION DETECTION WITH TOMS c46**
Arlin J. Krueger *In its* Scientific and Operational Requirements for TOMS Data Dec. 1987 p 54-56 (For primary document see N88-13774 05-42)
Avail: NTIS HC A06/MF A01 CSCL 04A

The Nimbus 7 Total Ozone Mapping Spectrometer (TOMS) is designed for mapping of the atmospheric ozone distribution. Absorption by sulfur dioxide at the same ultraviolet spectral wavelengths makes it possible to observe and resolve the size of volcanic clouds. The sulfur dioxide absorption is discriminated from ozone and water clouds in the data processing by their spectral signatures. Thus, the sulfur dioxide can serve as a tracer which appears in volcanic eruption clouds because it is not present in other clouds. The detection limit with TOMS is close to the theoretical limit due to telemetry signal quantization of 1000 metric tons (5-sigma threshold) within the instrument field of view (50 by 50 km near the nadir). Requirements concerning the use of TOMS in detection of eruptions, geochemical cycles, and volcanic climatic effects are discussed. R.J.F.

**N88-13794*#** National Aeronautics and Space Administration. Goddard Space Flight Center, Greenbelt, Md.
**ANALYSIS OF SO2 SIGNALS IN SBUV/TOMS DATA Abstract Only c45**
Richard McPeters *In its* Scientific and Operational Requirements for TOMS Data Dec. 1987 p 57-59 (For primary document see N88-13774 05-42)
Avail: NTIS HC A06/MF A01 CSCL 13B

Absorption bands between 300 nm and 315 nm were observed in spectral scans of the atmospheric albedo made by the Solar Backscatter Ultraviolet (SBUV) spectrometer following the eruption of El Chichon. It is shown that those bands coincide with peaks in the absorption coefficient spectrum of SO sub 2. The magnitude of the absorption is used to the column content of present SO sub 2. These observations confirm that the differential absorption between 312.5 nm and 317.5 nm in Total Ozone Mapping Spectrometer (TOMS) data can be used to measure SO sub 2 with high spatial resolution. A maximum concentration of SO sub 2 of 15 matm-cm was observed by SBUV on April 15, 1982. The measurement based on direct measurement of band intensity can be used to calibrate the TOMS algorithm for deriving SO sub 2 amounts. Author

**N88-13795*#** Atmospheric Environment Service, Downsview (Ontario).
**COMPARISON OF GROUND BASED AND TOMS MEASUREMENTS OF SO2 FROM VOLCANIC EMISSIONS c46**
James B. Kerr and Wayne J. Evans *In* NASA. Goddard Space Flight Center, Scientific and Operational Requirements for TOMS Data Dec. 1987 p 60-69 (For primary document see N88-13774 05-42)
Avail: NTIS HC A06/MF A01 CSCL 04A

The Brewer Ozone Spectrometer is being used in the World Ozone Network to monitor ozone and SO sub 2. SO sub 2 from natural as well as anthropogenic sources are measured. It has been demonstrated that SO sub 2 interferes with total ozone values as measured by the Dobson Spectrophotometer and the Total Ozone Mapping Spectrometer (TOMS). A small amount of manmade SO sub 2 is difficult to detect and quantify by TOMS because it is located near the surface. However, larger amounts of SO sub 2 injected into the stratosphere from volcanic emissions are detected by TOMS. Author

**N88-13796*#** National Oceanic and Atmospheric Administration, Washington, D. C.
**TOMS AND THE NOAA/FAA VOLCANO SUPPORT PLAN Abstract Only c46**
Michael Matson *In* NASA. Goddard Space Flight Center, Scientific and Operational Requirements for TOMS Data Dec. 1987 p 70 (For primary document see N88-13774 05-42)
Avail: NTIS HC A06/MF A01 CSCL 04A

A plan to detect volcanic ash clouds that are aircraft hazards is discussed. The plan utilizes NOAA satellite data and trajectory analysis. Because current operational satellite sensors cannot unambiguously distinguish volcanic eruptions from meteorological clouds, the plan is designed to react to known eruptions rather than detect eruptions. However, the Total Ozone Mapping Spectrometer (TOMS) instrument has been used to detect sulfur dioxide clouds from volcanic eruptions regardless of cloudiness. If TOMS was flown on an operational NOAA satellite, NOAA would have an automated volcanic eruption detection system which could more effectively support the Federal Aviation Administration. Author

**N88-13797*#** Smithsonian Institution, Washington, D. C.
**USE OF SATELLITE DATA IN VOLCANO MONITORING c46**
Lindsay McClelland *In* NASA. Goddard Space Flight Center, Scientific and Operational Requirements for TOMS Data Dec. 1987 p 71-76 (For primary document see N88-13774 05-42)
Avail: NTIS HC A06/MF A01 CSCL 04A

It is argued that Total Ozone Mapping Spectrometer (TOMS) data, especially data on sulfur dioxide detection in volcanic clouds, and weather satellite data complement each other. TOMS data is

most useful for discovering previously unknown eruptions and indicating a minimum volume of SO sub 2 produced by a given eruption. Once an eruption has been reported, weather satellite data can be used to accurately monitor its progress. To be used effectively, these data need to be analyzed jointly and in real time. Toward this end, it is hoped that full and timely utilization can be made of existing TOMS data, a polar orbiting TOMS can be launched in the near future, and that TOMS type instruments can be included on future geostationary satellites. Author

**N88-13798*#** SASC Technologies, Inc., Hyattsville, Md.
**SELECTION OF OPTIMUM WAVELENGTHS FOR OZONE MAPPING FROM SATELLITES Abstract Only** **c43**
P. K. Bhartia *In* NASA. Goddard Space Flight Center, Scientific and Operational Requirements for TOMS Data Dec. 1987 p 83 (For primary document see N88-13774 05-42)
Avail: NTIS HC A06/MF A01 CSCL 08B

Faced with conflicting requirements for measuring total ozone with the Solar Backscatter Ultraviolet Spectrometer/Total Ozone Mapping Spectrometer (SBUV/TOMS), a recommended strategy is to select three wavelengths: one at the peak of the ozone absorption cross section spectrum, another at a nearby minimum and a third wavelength that lies just outside the absorption spectrum. A pair formed using the first two wavelengths are then used under most observing conditions; another pair formed using the last two wavelengths are used near the terminator. There is no evidence that the use of additional wavelengths provides any benefit for measuring total ozone. Additional wavelengths, however, are necessary if other atmospheric species, such as SO sub 2, need to be measured. Author

**N88-13799*#** National Aeronautics and Space Administration. Goddard Space Flight Center, Greenbelt, Md.
**DETERMINATION OF TOTAL OZONE FROM HIRS2/MSU SOUNDING DATA Abstract Only** **c43**
Joel Susskind *In its* Scientific and Operational Requirements for TOMS Data Dec. 1987 p 84 (For primary document see N88-13774 05-42)
Avail: NTIS HC A06/MF A01 CSCL 08B

The total ozone fields computed from the High Resolution Infrared Sounder 2/Microwave Sounding Unit (HIRS2/MSU) are somewhat noisy compared to Total Ozone Mapping Spectrometer (TOMS) results and show latitude dependent systematic errors which vary slowly in time. Researchers used systematic errors from previous time periods to correct the HIRS2 soundings. Comparison of fields of HIRS2 and TOMS derived ozone are shown. Results are encouraging and indicate useful soundings of total O sub 3 burden can be done at night and in the polar winter. Ideally, joint infrared, microwave, and ultraviolet systems should be flown on low Earth orbiting and geostationary satellites to best utilize the complementary nature of the observations. Author

**N88-13800*#** National Aeronautics and Space Administration. Goddard Space Flight Center, Greenbelt, Md.
**COMPLEMENTARY INFORMATION BETWEEN UV AND IR FOR REMOTE SENSING OF TOTAL OZONE Abstract Only** **c43**
Prabhakara Cuddapah *In its* Scientific and Operational Requirements for TOMS Data Dec. 1987 p 85 (For primary document see N88-13774 05-42)
Avail: NTIS HC A06/MF A01 CSCL 08B

When infrared and ultraviolet measurements are available simultaneously with the same field of view, it is possible to minimize some of the errors in measuring the total ozone. The addition of the infrared technique to Total Ozone Mapping Spectrometer (TOMS) operation can aid in getting measurements of ozone in the nighttime and during the polar night. A radiometer with a channel in the window region around 11 microns, a channel in the 9-6 micron O sub 3 band, and three channels in the 15 micron CO sub 2 band should be adequate to retrieve total ozone. Such a radiometer could be designed to do cross track scanning. This combination of ultraviolet and infrared instruments could be flown on a geostationary or polar orbiting satellite. Author

**N88-13801*#** National Aeronautics and Space Administration. Goddard Space Flight Center, Greenbelt, Md.
**OBSERVATION GUIDELINES FOR A TOTAL OZONE MAPPING SPECTROMETER (TOMS) IN GEOSYNCHRONOUS ORBIT** **c43**
William E. Shenk *In its* Scientific and Operational Requirements for TOMS Data Dec. 1987 p 86-87 (For primary document see N88-13774 05-42)
Avail: NTIS HC A06/MF A01 CSCL 08B

The successful utilization of Total Ozone Mapping Spectrometer (TOMS) measurements in low Earth orbit for the analysis of rapidly changing events has led to the consideration of a TOMS in geosynchronous orbit. This orbit should allow for the selection of temporal and spatial resolutions that are specifically designed for these events, plus the flexibility of selecting different sized areas and pointing the sensor to focus on the most interesting events. Separate temporal and spatial resolution guidelines plus recommended areal coverage have been developed for tropical cyclones, jet streams, the interaction between strong convection and the environment, and the surveillance of volcanoes. It is also suggested that the most effective use of TOMS would be simultaneous flights with microwave and high spatial resolution infrared temperature profiles. Author

**N88-13802*#** National Aeronautics and Space Administration. Goddard Space Flight Center, Greenbelt, Md.
**A GEOSTATIONARY IMAGING SPECTROMETER TOMS INSTRUMENT** **c43**
Arlin J. Krueger, J. Owen Maloy, and H. B. Roeder (Perkin-Elmer Corp., Garden Grove, Calif.) *In its* Scientific and Operational Requirements for TOMS Data Dec. 1987 p 88-89 (For primary document see N88-13774 05-42)
Avail: NTIS HC A06/MF A01 CSCL 08B

One design for a geostationary Total Ozone Mapping Spectrometer (TOMS) with many desirable features is an imaging spectrometer. A preliminary study makes use of a 0.25 m Czerny-Turner spectrometer with which the Earth is imaged on a charge-coupled device (CCD) in dispersed light. The wavelength is determined by a movable grating which can be set arbitrarily by ground control. The signal integration time depends on wavelength but this system allows arbitrary timing by command. Special circumstances such as a requirement to track a low-lying sulfur dioxide cloud or a need to discriminate high level ozone from total ozone at midlatitudes could be obtained by adding a particular wavelength to the normally pre-programmed time sequence. The incident solar irradiance is measured by deploying a diffuser plate in the field of view. Individual detector elements correspond to scene elements in which the several wavelengths are serially sampled and the Earth radiance is compared to the incident sunlight. Thus the problem of uncorrelated drift of multiple detectors is removed. Author

# 43 EARTH RESOURCES AND REMOTE SENSING

Includes remote sensing of earth resources by aircraft and spacecraft; photogrammetry; and aerial photography.

For instrumentation see *35 Instrumentation and Photography.*

**N88-13803** Ohio State Univ., Columbus.
**DETECTION OF CRITICAL POINTS: THE FIRST STEP TO AUTOMATIC LINE GENERALIZATION Ph.D. Thesis**
Khagendra Thapa 1987 198 p
Avail: Univ. Microfilms Order No. DA8717736

The process of map production by computers especially when a change in scale is required cannot be made automatic despite the efforts by many mapping agencies. There does not exist a satisfactory method which can generalize lines automatically as the scale of the map changes. The problems of data compression and raster to vector conversion are solved by the process of finding critical points in the raster data by using the method of zero crossings of the convoluted values of the second derivative

of the Gaussian with the signal derived from the digitized data. The problem of automatic line generalization from an larger scale to any smaller scale is also solved by finding the zero crossings. The data compaction in vector data is achieved by analyzing the eigenvalues of the normalized symmetric scatter matrix derived from the data. The evaluation of the generalized lines is performed by comparing the corresponding lines generalized by zero crossings algorithm with those performed by cartographers. Results are given and discussed. Dissert. Abstr.

**N88-13804#** Naval Postgraduate School, Monterey, Calif.
**ESTIMATION OF MARINE BOUNDARY LAYER DEPTH AND RELATIVE HUMIDITY WITH MULTISPECTRAL SATELLITE MEASUREMENTS M.S. Thesis**
Richard J. Kren Jun. 1987 74 p
(AD-A184881) Avail: NTIS HC A04/MF A01 CSCL 04B

This study presents a technique for estimating marine boundary layer depth and relative humidity structure from satellite inferred measurements of aerosol optical depth, total water vapor and sea surface temperature. The data originates from radiance measurements by channels 1, 4 and 5 of NOAA's AVHRR instrument. The technique assumes that the atmospheric optical depth and total water vapor are primarily confined within the boundary layer, and that the layer is well-mixed. These inputs are combined through the relative humidity dependent variables of extinction and vapor density. Relative humidity is parameterized as an increasing linear function with height, resulting in an equation for the near surface relative humidity. This equation is solved, enabling estimation of boundary layer depth and humidity structure. The technique is iterative in nature, requiring 5 to 10 iterations for convergence. GRA

**N88-13805#** Naval Ocean Systems Center, San Diego, Calif.
**VARIFRONT 3 EXPEDITION DATA REPORT (USNS DE STEIGUER CRUISE 1202-82). BIOLUMINESCENCE, HYDROGRAPHIC, NUTRIENT, AND SATELLITE DATA FROM THE GULF OF CALIFORNIA (NOVEMBER-DECEMBER 1981) Final Report**
Stephen H. Lieberman and Suzana Potuznik Oct. 1986 105 p
Prepared in cooperation with San Diego State Univ., Calif.
(AD-A185011; NOSC/TD-992) Avail: NTIS HC A06/MF A01 CSCL 08C

This report presents data from the expedition Varifront 3, which measured stimulated planktonic bioluminescence and related physical, chemical, and biological parameters. Satellite imagery of sea surface temperature and chlorophyll was also collected. The study established a data base to develop correlates for a productive model of the distribution and intensity of planktonic bioluminescence in surface and near-surface ocean waters. GRA

**N88-13806#** Technische Hogeschool, Delft (Netherlands). Afdeling der Geodesie.
**PRECISION ANALYSIS OF REGULAR NETWORKS Thesis [PRECISIE ANALYSE VAN REGELMATIGE NETTEN]**
Guy Marc Hogenhout Nov. 1986 117 p In DUTCH
(B8709808; ETN-88-90622) Avail: NTIS HC A06/MF A01

The precision of regular networks was investigated with a view to practical applications in land registration. The precision analysis method following the Delft method is presented. The description and eigenvalues of block networks are discussed. The deviation between the precision of block networks and the model precision of the Delft artificial matrix is explained. The global precision of a network can be substantially improved by a favorable position of connection points for the second phase adjustment. The elimination of intermediate points from very regular block networks to save computer time and memory is discussed. ESA

**N88-13807#** National Aerospace Lab., Amsterdam (Netherlands). Afdeling Ruimtevaart.
**NATIONAL POINT OF CONTACT (NPOC)-SPOT INQUIRY 1986**
O. H. M. deVries 1986 24 p In DUTCH; ENGLISH summary
(NLR-MP-86055-U; B8707399; ETN-88-90830) Avail: NTIS HC A02/MF A01

The Dutch market for remote sensing satellite data was surveyed. Results show that the application is not on a large enough scale to maintain a completely commercial market. A reasonable market expansion is expected due to the interest in SPOT; an extra stimulus could be the development of a National Data Archive. ESA

**N88-13808#** National Aerospace Lab., Amsterdam (Netherlands). Space Div.
**STUDY ON DATA COMPRESSION SYSTEMS FOR OPERATIONAL REMOTE SENSING**
J. B. Boerger, W. C. Huisman, J. C. A. vanderLubbe, and A. Rosema (European Association of Remote Sensing Labs., Paris, France ) Paris, France ESA 1986 134 p
(Contract ESOC-6141/84-D-IM(SC))
(NLR-TR-86029-L; ESA-CR(P)-2439; ETN-88-91136) Avail: NTIS HC A07/MF A01

The consequence of data compression on the Meteosat imagery data dissemination mission were studied. User and operational requirements were reviewed and data compression algorithms were assessed. Operational requirements such as the amount of memory needed to execute decompression and the prevention of error propagation favor one dimensional intraframe encoding. Operation requirements indicate a lower bound on the compression ratio of Meteosat imagery data of 2. This ratio is achievable. A higher compression ratio is possible at the cost of a small reconstruction error. From performance and implementation points of view a small preference is given to the MEANDER-1 algorithm for compression/decompression of imagery data. The suggested on-line data decompression method should be integrated with the operational preprocessing steps. ESA

**N88-13809#** Societe Nationale Industrielle Aerospatiale, Les Mureaux (France).
**MATCHING SEGMENTS FROM A MAP AND AN AERIAL IMAGE USING RELAXATION TECHNIQUES**
Eva Salmeron and Maurice Milgram 1986 14 p In FRENCH; ENGLISH summary
(SNIAS-872-422-103; ETN-88-91204) Avail: NTIS HC A03/MF A01

A method for the matching of an aerial image and an ordnance survey map is presented. Entities such as contrast lines are used. The method is based on probabilistic relaxation. Labels (image segments) are given to objects (map segments) using probabilities and constraints specific to the problem. The method leads to good results with real complex images comprising 100 map-segments and 200 image-segments. ESA

**N88-13810#** Research Inst. of National Defence, Stockholm (Sweden).
**HIGH RESOLUTION SATELLITE IMAGERY SIMULATION**
Ulf Ekblad Jul. 1987 35 p
(FOA-C-30462-3.3,9.3; ISSN-0347-3708; ETN-88-91408) Avail: NTIS HC A03/MF A01; Research Institute of National Defence, Stockholm, Sweden KR 50

In order to investigate the possibility of using satellites in verification of military and disarmament treaties, simulations of satellite images are presented. A column of tanks on a road in a terrain model was used as an example of military activities. With the half-width of the point spread function as a measure of resolution, the spatial resolution needed for detection is 8 m. ESA

**N88-13811*#** National Air and Space Museum, Washington, D.C. Center for Earth and Planetary Studies.
**ENVIRONMENTAL PROCESSES AND SPECTRAL REFLECTANCE CHARACTERISTICS ASSOCIATED WITH SOIL EROSION IN DESERT FRINGE REGIONS**
P. A. Jacobberger 20 Oct. 1987 28 p
(Contract NAS5-28774)
(NASA-CR-182332; NAS 1.26:182332) Avail: NTIS HC A03/MF A01 CSCL 08B

(NASA-CR-182332; NAS 1.26:182332) Avail: NTIS HC A03/MF A01 CSCL 08B

Results of analysis of spectral variation of sand dunes in El Ghorabi, Bahariya, Egypt; Tombouctou/Azaouad, Mali; and Tsodilo Hills, western Botswana are presented. Seasonal variations in dune extent and location of dune crests and their relationship to such factors as wind and weather variations are emphasized. J.P.B.

**N88-13757*#** Jet Propulsion Lab., California Inst. of Tech., Pasadena.
**AIS-2 RADIOMETRY AND A COMPARISON OF METHODS FOR THE RECOVERY OF GROUND REFLECTANCE**
James E. Conel, Robert O. Green, Gregg Vane, Carol J. Bruegge, Ronald E. Alley, and Brian J. Curtiss (Colorado Univ., Boulder.) *In its* Proceedings of the 3rd Airborne Imaging Spectrometer Data Analysis Workshop 15 Aug. 1987 p 18-47 (For primary document see N88-13755 05-42)
Avail: NTIS HC A09/MF A01 CSCL 14B

**N88-13758*#** Nevada Univ., Reno. School of Mines.
**EFFECTIVE USE OF PRINCIPAL COMPONENT ANALYSIS WITH HIGH RESOLUTION REMOTE SENSING DATA TO DELINEATE HYDROTHERMAL ALTERATION AND CARBONATE ROCKS**
Sandra C. Feldman *In* JPL Proceedings of the 3rd Airborne Imaging Spectrometer Data Analysis Workshop 15 Aug. 1987 p 48-55 (For primary document see N88-13755 05-42)
Avail: NTIS HC A09/MF A01 CSCL 08B

**N88-13759*#** Autometric Corp., Inc., Falls Church, Va.
**LAND COVER/USE CLASSIFICATION OF CAIRNS, QUEENSLAND, AUSTRALIA: A REMOTE SENSING STUDY INVOLVING THE CONJUNCTIVE USE OF THE AIRBORNE IMAGING SPECTROMETER, THE LARGE FORMAT CAMERA AND THE THEMATIC MAPPER SIMULATOR**
Matthew Heric, William Cox, and Daniel K. Gordon *In* JPL Proceedings of the 3rd Airborne Imaging Spectrometer Data Analysis Workshop 15 Aug. 1987 p 56-62 (For primary document see N88-13755 05-42)
Avail: NTIS HC A09/MF A01 CSCL 08B

**N88-13760*#** Washington Univ., Seattle.
**CALIBRATING AIS IMAGES USING THE SURFACE AS A REFERENCE**
M. O. Smith, D. A. Roberts, H. M. Shipman, J. B. Adams, S. C. Willis, and A. R. Gillespie *In* JPL Proceedings of the 3rd Airborne Imaging Spectrometer Data Analysis Workshop 15 Aug. 1987 p 63-69 (For primary document see N88-13755 05-42)
Avail: NTIS HC A09/MF A01 CSCL 08B

**N88-13761*#** National Aeronautics and Space Administration. Ames Research Center, Moffett Field, Calif.
**THE USE OF AIRBORNE IMAGING SPECTROMETER DATA TO DETERMINE EXPERIMENTALLY INDUCED VARIATION IN CONIFEROUS CANOPY CHEMISTRY**
Nancy A. Swanberg (TGS Technology, Inc., Moffett Field, Calif.) and Pamela A. Matson *In* JPL Proceedings of the 3rd Airborne Imaging Spectrometer Data Analysis Workshop 15 Aug. 1987 p 70-74 (For primary document see N88-13755 05-42)
Avail: NTIS HC A09/MF A01 CSCL 08B

**N88-13762*#** Research Center Graz (Austria).
**OVERVIEW OF AUSTRIAN AIRBORNE IMAGING SPECTROMETER (AIS) PROGRAMME AND FIRST RESULTS**
C. Banninger *In* JPL Proceedings of the 3rd Airborne Imaging Spectrometer Data Analysis Workshop 15 Aug. 1987 p 75-82 (For primary document see N88-13755 05-42)
Avail: NTIS HC A09/MF A01 CSCL 08B

**N88-13763*#** Delaware Univ., Newark. Coll. of Marine Studies.
**AIS-2 SPECTRA OF CALIFORNIA WETLAND VEGETATION**
Michael F. Gross, Susan L. Ustin (California Univ., Davis.), and Vytautas Klemas *In* JPL Proceedings of the 3rd Airborne Imaging Spectrometer Data Analysis Workshop 15 Aug. 1987 p 83-90 Prepared in cooperation with California Univ., Berkeley (For primary document see N88-13755 05-42)
(Grant NAGw-950)
Avail: NTIS HC A09/MF A01 CSCL 08B

**N88-13764*#** National Aeronautics and Space Administration. Ames Research Center, Moffett Field, Calif.
**TOWARD DETECTING CALIFORNIA SHRUBLAND CANOPY CHEMISTRY WITH AIS DATA**
Curtis V. Price and Walter E. Westman *In* JPL Proceedings of the 3rd Airborne Imaging Spectrometer Data Analysis Workshop 15 Aug. 1987 p 91-97 (For primary document see N88-13755 05-42)
Avail: NTIS HC A09/MF A01 CSCL 08B

**N88-13765*#** Montana Univ., Missoula.
**MEASURING NEAR INFRARED SPECTRAL REFLECTANCE CHANGES FROM WATER STRESSED CONIFER STANDS WITH AIS-2**
George Riggs and Steven W. Running *In* JPL Proceedings of the 3rd Airborne Imaging Spectrometer Data Analysis Workshop 15 Aug. 1987 p 100-106 (For primary document see N88-13755 05-42)
Avail: NTIS HC A09/MF A01 CSCL 08B

**N88-13766*#** Brown Univ., Providence, R. I. Dept. of Geological Sciences.
**ABUNDANCE AND DISTRIBUTION OF ULTRAMAFIC MICROBRECCIA IN MOSES ROCK DIKE: QUANTITATIVE APPLICATION OF AIS DATA Abstract Only**
John F. Mustard and Carle M. Pieters *In* JPL Proceedings of the 3rd Airborne Imaging Spectrometer Data Analysis Workshop 15 Aug. 1987 p 105-106 (For primary document see N88-13755 05-42)
Avail: NTIS HC A09/MF A01 CSCL 08B

**N88-13767*#** Stanford Univ., Calif. Dept. of Applied Earth Sciences.
**EVALUATION OF AIS-2 (1986) DATA OVER HYDROTHERMALLY ALTERED GRANITOID ROCKS OF THE SINGATSE RANGE (YERINGTON) NEVADA AND COMPARISON WITH 1985 AIS-1 DATA**
R. J. P. Lyon *In* JPL Proceedings of the 3rd Airborne Imaging Spectrometer Data Analysis Workshop 15 Aug. 1987 p 107-119 (For primary document see N88-13755 05-42)
Avail: NTIS HC A09/MF A01 CSCL 08B

**N88-13768*#** Durham Univ. (England). Dept. of Geological Sciences.
**PRELIMINARY RESULTS FROM AN INVESTIGATION OF AIS-1 DATA OVER AN AREA OF EPITHERMAL ALTERATION: PLATEAU, NORTHERN QUEENSLAND, AUSTRALIA**
Steve Mackin, Tim Munday, and Simon Hook *In* JPL Proceedings of the 3rd Airborne Imaging Spectrometer Data Analysis Workshop 15 Aug. 1987 p 120-131 (For primary document see N88-13755 05-42)
Avail: NTIS HC A09/MF A01 CSCL 08B

**N88-13769*#** Geological Survey, Denver, Colo.
**CAUSES OF SPURIOUS FEATURES IN SPECTRAL REFLECTANCE DATA**
Roger N. Clark and Trude V. V. King *In* JPL Proceedings of the 3rd Airborne Imaging Spectrometer Data Analysis Workshop (date) 15 Aug. 1987 p 132-137 (For primary document see N88-13755 05-42)
Avail: NTIS HC A09/MF A01 CSCL 08B

**N88-13770*#** Geological Survey, Denver, Colo.
**AUTOMATIC CONTINUUM ANALYSIS OF REFLECTANCE SPECTRA**
Roger N. Clark and Trude V. V. King *In* JPL Proceedings of the 3rd Airborne Imaging Spectrometer Data Analysis Workshop 15 Aug. 1987 p 138-142 (For primary document see N88-13755 05-42)
Avail: NTIS HC A09/MF A01 CSCL 08B

**N88-13771*#** Geological Survey, Reston, Va.
**ANALYSIS OF AIRBORNE IMAGING SPECTROMETER DATA FOR THE RUBY MOUNTAINS, MONTANA, BY USE OF ABSORPTION-BAND-DEPTH IMAGES**
David W. Brickey, James K. Crowley, and Lawrence C. Rowan *In* JPL Proceedings of the 3rd Airborne Imaging Spectrometer Data Analysis Workshop 15 Aug. 1987 p 143-147 (For primary document see N88-13755 05-42)
Avail: NTIS HC A09/MF A01 CSCL 08B

**N88-13772*#** Colorado Univ., Boulder. Center for the Study of Earth from Space.
**MAPPING HYDROTHERMALLY ALTERED ROCKS IN THE NORTHERN GRAPEVINE MOUNTAINS, NEVADA AND CALIFORNIA WITH THE AIRBORNE IMAGING SPECTROMETER**
Fred A. Kruse *In* JPL Proceedings of the 3rd Airborne Imaging Spectrometer Data Analysis Workshop 15 Aug. 1987 p 148-166 (For primary document see N88-13755 05-42)
Avail: NTIS HC A09/MF A01 CSCL 08B

**N88-13798*#** SASC Technologies, Inc., Hyattsville, Md.
**SELECTION OF OPTIMUM WAVELENGTHS FOR OZONE MAPPING FROM SATELLITES Abstract Only**
P. K. Bhartia *In* NASA. Goddard Space Flight Center, Scientific and Operational Requirements for TOMS Data Dec. 1987 p 83 (For primary document see N88-13774 05-42)
Avail: NTIS HC A06/MF A01 CSCL 08B

**N88-13799*#** National Aeronautics and Space Administration. Goddard Space Flight Center, Greenbelt, Md.
**DETERMINATION OF TOTAL OZONE FROM HIRS2/MSU SOUNDING DATA Abstract Only**
Joel Susskind *In its* Scientific and Operational Requirements for TOMS Data Dec. 1987 p 84 (For primary document see N88-13774 05-42)
Avail: NTIS HC A06/MF A01 CSCL 08B

**N88-13800*#** National Aeronautics and Space Administration. Goddard Space Flight Center, Greenbelt, Md.
**COMPLEMENTARY INFORMATION BETWEEN UV AND IR FOR REMOTE SENSING OF TOTAL OZONE Abstract Only**
Prabhakara Cuddapah *In its* Scientific and Operational Requirements for TOMS Data Dec. 1987 p 85 (For primary document see N88-13774 05-42)
Avail: NTIS HC A06/MF A01 CSCL 08B

**N88-13801*#** National Aeronautics and Space Administration. Goddard Space Flight Center, Greenbelt, Md.
**OBSERVATION GUIDELINES FOR A TOTAL OZONE MAPPING SPECTROMETER (TOMS) IN GEOSYNCHRONOUS ORBIT**
William E. Shenk *In its* Scientific and Operational Requirements for TOMS Data Dec. 1987 p 86-87 (For primary document see N88-13774 05-42)
Avail: NTIS HC A06/MF A01 CSCL 08B

**N88-13802*#** National Aeronautics and Space Administration. Goddard Space Flight Center, Greenbelt, Md.
**A GEOSTATIONARY IMAGING SPECTROMETER TOMS INSTRUMENT**
Arlin J. Krueger, J. Owen Maloy, and H. B. Roeder (Perkin-Elmer Corp., Garden Grove, Calif.) *In its* Scientific and Operational Requirements for TOMS Data Dec. 1987 p 88-89 (For primary document see N88-13774 05-42)
Avail: NTIS HC A06/MF A01 CSCL 08B

# 44 ENERGY PRODUCTION AND CONVERSION

Includes specific energy conversion systems, e.g., fuel cells; global sources of energy; geophysical conversion; and windpower.

For related information see also *07 Aircraft Propulsion and Power, 20 Spacecraft Propulsion and Power,* and *28 Propellants and Fuels.*

**N88-13812#** Sandia National Labs., Albuquerque, N. Mex.
**AN OVERVIEW OF THE DOE/SANDIA/USDA VERTICAL AXIS WIND TURBINE TEST BED PROJECT**
P. C. Klimas, H. M. Dodd, and R. N. Clark 1987 7 p Presented at Windpower '87, San Francisco, Calif., 5 Oct. 1987 Prepared in cooperation with Department of Agriculture, Bushland, Tex.
(Contract DE-AC04-76DP-00789)
(DE88-000604; SAND-87-1131C; CONF-871062-2) Avail: NTIS HC A02/MF A01

Sandia National Laboratories (SNL) is presently erecting its Department of Energy (DOE) funded 34-m diameter vertical axis wind turbine (VAWT) Test Bed on a Department of Agriculture (USDA) site near Amarillo, Texas. This versatile VAWT, rated at 500 kW in a 12.5 m/s (28 mph) wind, has been designed to demonstrate aerodynamic, structural dynamic, and control strategies intended to improve the effectiveness of VAWT systems. The paper addresses all aspects of this major wind energy project. The need for a turbine in this general physical size range, the choice of a modular fabrication scheme, and the reasons for component materials and subsystems are all discussed. The selection of the Bushland, Texas, site and the motivation behind the involvement of the USDA Agricultural Research Service is described. The SNL organization and management plan assembled to design, procure, erect, and operate the Test Bed is detailed. The technical features in the areas of aerodynamics, structures, power systems, control philosophies, instrumentation, data acquisition, and data analysis are highlighted. DOE

**N88-13813** Prins Maurits Lab. TNO, Rijswijk (Netherlands).
**FUEL CELLS [BRANDSTOFCELLEN]**
C. A. vanBeest Sep. 1986 42 p In DUTCH; ENGLISH summary
(Contract A78/KL/125)
(PML-1986-43; TD-86-3976; ETN-88-90865) Copyright Avail: Issuing Activity

Literature on fuel cells was reviewed in the framework of research on energy sources for the military. The principles, advantages, and practical limitations of fuel cells are reviewed. The main types of fuel cells are discussed. It is recommended to let the armed forces gain experience with fuel cell systems to replace diesel generators. ESA

**N88-13814#** Centre National d'Etudes Spatiales, Toulouse (France).
**THE HIGH PERFORMANCE SOLAR ARRAY GSR3**
A. Mamode, J. Bartevian, J. L. Bastard, P. Auffray, and A. Plagne (Societe Nationale Industrielle Aerospatiale, Les Mureaux, France) Paris, France SNIAS 1987 10 p Previously announced as N87-28972
(SNIAS-872-422-108; ETN-88-91209) Avail: NTIS HC A02/MF A01

A foldout solar array for communication satellites was developed. A wing composed of 4 panels of 1.6 x 1.5 m and a Y-shaped yoke, and a wing with 3 panels of 2.4 x 2.4 m were made. End of life performance goal is greater than 35 W/kg with BSR 180 micron solar cells, and 50 W/kg using 50 micron BSFR cells. Analysis shows that all identified requirements can be covered with current skin made of open weave very high modulus carbon fiber; reinforcements of unidirectional carbon fiber; honeycomb in current section; hold-down inserts made of wound carbon fibers; titanium hinge fitting; and Kapton foil (25 or 50 micron thickness). Tests confirm performance predictions. ESA

**N88-13815#** Midwest Research Inst., Golden, Colo. Solar Energy Research Inst.
**ACCURATE ROTOR LOADS PREDICTION USING THE FLAP (FORCE AND LOADS ANALYSIS PROGRAM) DYNAMICS CODE**
A. D. Wright and R. W. Thresher Oct. 1987 10 p Presented at the Windpower '87, San Francisco, Calif., 5 Oct. 1987
(Contract DE-AC02-83CH-10093)
(DE88-001109; SERI/TP-217-3223; CONF-871062-5) Avail: NTIS HC A02

Accurately predicting wind turbine blade loads and response is very important in predicting the fatigue life of wind turbines. There is a clear need in the wind turbine community for validated and user-friendly structural dynamics codes for predicting blade loads and response. At the Solar Energy Research Institute (SERI), a Force and Loads Analysis Program (FLAP) has been refined and validated and is ready for general use. Currently, FLAP is operational on an IBM-PC compatible computer and can be used to analyze both rigid- and teetering-hub configurations. The results of this paper show that FLAP can be used to accurately predict the deterministic loads for rigid-hub rotors. This paper compares analytical predictions to field test measurements for a three-bladed, upwind turbine with a rigid-hub configuration. The deterministic loads predicted by FLAP are compared with 10-min azimuth averages of blade root flapwise bending moments for different wind speeds. DOE

# 45 ENVIRONMENT POLLUTION

Includes atmospheric, noise, thermal, and water pollution.

**N88-13816** Prins Maurits Lab. TNO, Rijswijk (Netherlands).
**INVESTIGATION OF THE EXPOSURE TO HARMFUL COMPOUNDS IN THE WORKSHOP OF NONDESTRUCTIVE MATERIALS TESTING AT GILZE-RIJEN (NETHERLANDS) [ONDERZOEK NAAR DE BLOOTSTELLING AAN SCHADELIJKE VERBINDINGEN IN HET WERKCENTRUM VOOR NIET-DESTRUCTIEF MATERIAALONDERZOEK TE GILZE-RIJEN]**
J. Kaaijk Nov. 1986 19 p In DUTCH; ENGLISH summary
(Contract A78/KLu/065)
(PML-1985-42; TDCK-93808; ETN-88-90862) Copyright Avail: Issuing Activity

The nature and concentration of toxic vapor and dust, to which persons are exposed in the atmosphere of the nondestructive materials research workshops were investigated. Organic vapors were collected on the absorbent Tenax-GC, and analyzed by gas chromatography/mass spectrometry. Amine concentration was measured using Draeger detection tubes. Dust was collected on filters and analyzed by X-ray fluorescence and scaning electron microscopy/energy-dispersive X-ray spectrometry. The concentrations of the identified compounds as well as the dust concentration are below the Dutch hygienic standards (MAC values). Short transgressions of the MAC value of ethanolamine (8 mg/cum) are likely to occur. ESA

**N88-13817** Prins Maurits Lab. TNO, Rijswijk (Netherlands).
**INVESTIGATION OF THE NATURE AND CONCENTRATION OF VAPOR AND MIST DURING THE CLEANING OF AIRCRAFT [ONDERZOEK NAAR DE AARD EN DE CONCENTRATIE VAN DAMP EN NEVEL BIJ HET REINIGEN VAN VLIEGTUIGEN]**
J. Kaaijk Sep. 1985 17 p In DUTCH; ENGLISH summary
(Contract A78/KLu/065)
(PML-1985-29; TDCK-93540; ETN-88-90864) Copyright Avail: Issuing Activity

The nature and quantity of toxic vapor and mist in the atmosphere of a hangar during the cleaning of airplanes were investigated. Organic vapors were collected on the adsorbent Tenax-GC, and analyzed by gas chromatography and mass spectrometry. Mist was collected on filters and analyzed by X-ray fluorescence and scanning electron microscopy/energy-dispersive X-ray spectrometry. The concentrations of the identified compounds are below the Dutch hygiene standards. ESA

**N88-13818#** Environmental Protection Agency, Washington, D.C. Office of Municipal Pollution Control.
**INNOVATIVE AND ALTERNATIVE TECHNOLOGY PROJECTS Progress Report, 1987**
Sep. 1987 71 p
(PB87-230165) Avail: NTIS HC A04/MF A01 CSCL 13B

The publication is issued annually to provide interested parties with an overview of progress in the implementation of innovative and alternative technologies under provisions of the Clean Water Act. The report is based upon information from grant awards through April of the issue year as provided by state agencies and EPA regional offices. GRA

**N88-13775*#** National Aeronautics and Space Administration. Goddard Space Flight Center, Greenbelt, Md.
**TOMS: THE ANTARCTIC OZONE HOLE AND OZONE TRENDS Abstract Only**
Richard S. Stolarski *In its* Scientific and Operational Requirements for TOMS Data Dec. 1987 p 5-7 (For primary document see N88-13774 05-42)
Avail: NTIS HC A06/MF A01 CSCL 13B

**N88-13776*#** National Aeronautics and Space Administration. Goddard Space Flight Center, Greenbelt, Md.
**OCTOBER LOWER STRATOSPHERIC ANTARCTIC TEMPERTURE AND TOTAL OZONE FROM 1979-1985 Abstract Only**
Paul A. Newman (Applied Research Corp., Landover, Md.) and Mark R. Schoeberl *In its* Scientific and Operational Requirements for TOMS Data Dec. 1987 p 8-9 (For primary document see N88-13774 05-42)
Avail: NTIS HC A06/MF A01 CSCL 13B

**N88-13778*#** National Aeronautics and Space Administration. Goddard Space Flight Center, Greenbelt, Md.
**PHOTOCHEMICAL OZONE OVERBURDEN CORRECTION Abstract Only**
Michael Stefanick (Science Systems and Applications, Inc., Seabrook, Md.) and Arlin J. Krueger *In its* Scientific and Operational Requirements for TOMS Data Dec. 1987 p 11 (For primary document see N88-13774 05-42)
Avail: NTIS HC A06/MF A01 CSCL 13B

**N88-13779*#** Illinois Univ., Urbana. Dept. of Atmospheric Science.
**ANALYSIS OF THE BREAKDOWN OF THE ANTARCTIC CIRCUMPOLAR VORTEX USING TOMS OZONE DATA Abstract Only**
Kenneth P. Bowman *In* NASA. Goddard Space Flight Center, Scientific and Operational Requirements for TOMS Data Dec. 1987 p 12-13 (For primary document see N88-13774 05-42)
Avail: NTIS HC A06/MF A01 CSCL 13B

**N88-13784*#** National Aeronautics and Space Administration. Langley Research Center, Hampton, Va.
**THE USE OF TOMS DATA FOR TROPOSPHERIC OZONE STUDIES Abstract Only**
Jack Fishman and Edward V. Browell *In* NASA. Goddard Space Flight Center, Scientific and Operational Requirements for TOMS Data Dec. 1987 p 26 (For primary document see N88-13774 05-42)
Avail: NTIS HC A06/MF A01 CSCL 13B

**N88-13785*#** Chicago Univ., Ill. Dept. of Geophysical Science.
**TOMS AS A MONITOR OF THE ULTRAVIOLET RADIATION ENVIRONMENT: APPLICATIONS TO PHOTOBIOLOGY Abstract Only**
John E. Frederick *In* NASA. Goddard Space Flight Center, Scientific and Operational Requirements for TOMS Data Dec. 1987 p 27-30 (For primary document see N88-13774 05-42)
Avail: NTIS HC A06/MF A01 CSCL 13B

**N88-13786*#** National Aeronautics and Space Administration. Goddard Space Flight Center, Greenbelt, Md.
**NORTHWEST AIRLINES FLIGHT EXPERIMENTS Abstract Only**
Arlin J. Krueger *In its* Scientific and Operational Requirements for TOMS Data Dec. 1987 p 31 (For primary document see N88-13774 05-42)
Avail: NTIS HC A06/MF A01 CSCL 13B

**N88-13788*#** National Aeronautics and Space Administration. Goddard Space Flight Center, Greenbelt, Md.
**CORRELATIONS OF TOMS TOTAL OZONE DATA (NIMBUS-7 SATELLITE) WITH TROPOPAUSE HEIGHT Abstract Only**
Marie-Jeanne Munteanu *In its* Scientific and Operational Requirements for TOMS Data Dec. 1987 p 37 (For primary document see N88-13774 05-42)
Avail: NTIS HC A06/MF A01 CSCL 13B

**N88-13792*#** Atmospheric Environment Service, Downsview (Ontario).
**DOBSON-STATIONS PERFORMANCE ASSESSMENT USING TOMS DATA Abstract Only**
Rumen D. Bojkov and Carl L. Mateer *In* NASA. Goddard Space Flight Center, Scientific and Operational Requirements for TOMS Data Dec. 1987 p 47 (For primary document see N88-13774 05-42)
Avail: NTIS HC A06/MF A01 CSCL 13B

**N88-13794*#** National Aeronautics and Space Administration. Goddard Space Flight Center, Greenbelt, Md.
**ANALYSIS OF SO2 SIGNALS IN SBUV/TOMS DATA Abstract Only**
Richard McPeters *In its* Scientific and Operational Requirements for TOMS Data Dec. 1987 p 57-59 (For primary document see N88-13774 05-42)
Avail: NTIS HC A06/MF A01 CSCL 13B

# 46 GEOPHYSICS

Includes aeronomy; upper and lower atmosphere studies; ionospheric and magnetospheric physics; and geomagnetism.

For space radiation see *93 Space Radiation.*

**N88-13819#** Centro Brasileiro de Pesquisas Fisicas, Rio de Janeiro.
**NON-MINIMAL INTERACTION OF GRAVITY WITH OTHER PHYSICAL FIELDS: AN OVERVIEW**
M. Novello and L. A. R. deOliveira 1986 34 p
(DE87-703362; CBPF-NF-033/86) Avail: NTIS (US Sales Only) HC A03/MF A01

A review on some modern developments concerning the interaction of gravity with other physical fields was presented. It is argued that a suitable context for an account of their dynamical interplay is that of the non-minimal (e.g., conformal) coupling of these fields to gravity. Some interesting features of non-minimal coupling, such as the connection with Weyl-integrable spacetime (WIST) structure, the generation of eternal Universes, the appearance of a cosmological constant and the possible induction of repulsive gravity via spontaneous symmetry breaking (SSB) mechanisms, are discussed. In particular, a simple case of strong interacting scalar particles (such as the well-known elastic reaction pi kappa yields pi kappa) is examined in a curved background, thereby obtaining the curious result that the actual, observed value of the strong coupling constant and the minimum value allowable, in order to preclude antigravity, are related by Eddington's number 10 to the 39th power. DOE

**N88-13820*#** California Univ., San Diego, La Jolla. Inst. of Geophysics and Planetary Physics.
**COMPARING HARD AND SOFT PRIOR BOUNDS IN GEOPHYSICAL INVERSE PROBLEMS**
George E. Backus 28 Dec. 1987 33 p
(Grants NAG5-818; NSF EAR-85-21543)
(NASA-CR-181557; NAS 1.26:181557) Avail: NTIS HC A03/MF A01 CSCL 08G

In linear inversion of a finite-dimensional data vector y to estimate a finite-dimensional prediction vector z, prior information about X sub E is essential if y is to supply useful limits for z. The one exception occurs when all the prediction functionals are linear combinations of the data functionals. Two forms of prior information are compared: a soft bound on X sub E is a probability distribution p sub x on X which describeds the observer's opinion about where X sub E is likely to be in X; a hard bound on X sub E is an inequality Q sub x(X sub E, X sub E) is equal to or less than 1, where Q sub x is a positive definite quadratic form on X. A hard bound Q sub x can be softened to many different probability distributions p sub x, but all these p sub x's carry much new information about X sub E which is absent from Q sub x, and some information which contradicts Q sub x. Both stochastic inversion (SI) and Bayesian inference (BI) estimate z from y and a soft prior bound p sub x. If that probability distribution was obtained by softening a hard prior bound Q sub x, rather than by objective statistical inference independent of y, then p sub x contains so much unsupported new information absent from Q sub x that conclusions about z obtained with SI or BI would seen to be suspect. Author

**N88-13821#** Naval Postgraduate School, Monterey, Calif.
**DEVELOPMENT OF A DATA ANALYSIS SYSTEM FOR THE DETECTION OF LOWER LEVEL ATMOSPHERIC TURBULENCE WITH AN ACOUSTIC SOUNDER M.S. Thesis**
Michael Raymond Wroblewski Jun. 1987 100 p
(AD-A184972) Avail: NTIS HC A05/MF A01 CSCL 04A

Atmospheric density fluctuations induce phase perturbations that degrade the spatial coherence of a laser beam propagating through the atmosphere. These degradations spread the laser beam and alter the centroid and are found at virtually all levels of the atmosphere. A substantial fraction of the optical turbulence along a vertical path arises from the heat flux between the atmosphere and the Earth's surface. This type of turbulence is typically within the first 100 to 200 meters above the surface. During this research, a high frequency acoustic sounder was developed to analyze this turbulent layer. The primary focus was the development of the command and control software required to coordinate the data collection and reduction. The system was used at two sites and should prove useful in quantifying the effects of optical turbulence within the surface boundary layer on laser and optical system performance. Author (GRA)

**N88-13822#** Alaska Univ., Fairbanks. Geophysical Inst.
**THE POLAR IONOSPHERE AND INTERPLANETARY FIELD Final Report, 1 Jul. 1985 - 30 Jun. 1987**
B. J. Watkins and S. I. Akasofu Aug. 1987 42 p
(Contracts AF-AFOSR-85-0258; AF Proj. 2310)
(AD-A185386; AFOSR-87-1342TR) Avail: NTIS HC A03/MF A01 CSCL 04A

The model ionosphere was developed that is coupled to a magnetospheric model for investigating time dependent behavior of the Polar F-region ionosphere in response to varying interplanetary magnetic field (IMF) configurations. The numerical ionospheric model covers a latitude range from 50 to 90 degrees and an altitude range of 150 to 600 KM. The purpose of the magnetospheric model is to define the location and geometry of the polar cap, which is defined as the region of open field lines. The polar cap configuration has been coupled to a model electric field pattern that in turn may vary in size and strength in response to the IMF. The ionosphere model assumes only oxygen ions; the ion density is solved vertically along many magnetic field lines as they move horizontally under the influence of the large-scale convective electric fields. The lower boundary is defined by the local chemistry and the upper boundary condition has been set by applying an outward flux of ions appropriate for open field line conditions. The model has been used to illustrate ionospheric behavior during geomagnetic storm conditions. Future model applications may include ionospheric prediction using IMF inputs improved understanding of polar ionization structures. GRA

**N88-13823#** Air Force Geophysics Lab., Hanscom AFB, Mass.
**AN ANALYTICAL SOIL THERMODYNAMIC MODEL FOR THE DIURNAL VARIATION OF GROUND SURFACE TEMPERATURE Environmental Research Papers Oct. 1985 - Sep. 1986**
Samuel Y. Yee and George D. Modica 5 Jan. 1987 27 p
(AD-A185388; AFGL-TR-87-0007; AFGL-ERP-965) Avail: NTIS HC A03/MF A01 CSCL 08G

An analytical expression is given for time variations of temperature within a model soil slab that is subjected to idealized heating at the supper surface and maintained at constant temperature at the lower surface. Applied at the upper surface, the model temperature may be considered to be the ground surface temperature of the earth. An important feature of this model is that phase-shifted nonlinear responses to the forcing are allowed at the upper boundary. The analytical nature of the solution enables us to easily study the relative importance of various physical processes in the model surface energy budget equation. For example, evaporational cooling is found to be an important feedback process under model summer conditions, accounting for a change of about 6K in the daily mean surface temperature; under winter conditions, the change attributable to evaporation is only about 1K. The perturbation method used in the approach to linearize the model upper boundary condition is shown to be applicable to more complicated and more realistic upper boundary conditions. GRA

**N88-13824#** Paris VI Univ. (France).
**CONTRIBUTIONS OF LIDAR MEASUREMENTS TO THE STUDY OF LONG TERM VARIATIONS OF THE MIDDLE ATMOSPHERE Ph.D. Thesis [CONTRIBUTION DES MESURES LIDAR A L'ETUDE DES VARIATIONS A LONG TERME DE L'ETAT THERMIQUE DE L'ATMOSPHERE MOYENNE]**
Najib Smires 1986 123 p In FRENCH
(ETN-88-91237) Avail: NTIS HC A06/MF A01

The long term evolution of the middle atmosphere is deduced from Rayleigh lidar measurement. Correlations with solar activity and the relation between temperature variations and ozone concentration are studied. The negative correlation of ozone-temperature, as predicted by models, is confirmed. A seasonal variation related to planetary waves is suggested. The correlation between temperature and solar activity is also wholly confirmed. Other perturbations and correlations are also discussed. ESA

**N88-13825#** Consiglio Nazionale delle Ricerche, Frascati (Italy). Ist. di Fisica dello Spazio Interplanetario.
**MEDIA CALIBRATIONS OF THE DOPPLER SIGNAL FOR A GRAVITATIONAL WAVE EXPERIMENT**
R. Agresti, L. less, and P. Bonifazi Dec. 1986 139 p
(IFSI-86-13; ETN-88-91284) Avail: NTIS HC A07/MF A01

A computer procedure for the calibration of propagation effects on the Doppler signal of an interplanetary spacecraft is presented. The effects are due to the troposphere, the inosphere, and the interplanetary plasma. The package was developed for the analysis of the gravitational wave experiment planned for Ulysses. It was tested upon REGRESS and ATDF data of the Voyager 1 spacecraft. ESA

**N88-13826#** Royal Inst. of Tech., Stockholm (Sweden). Dept. of Plasma Physics.
**ELECTRIC FIELD MEASUREMENTS ON VIKING: FIRST RESULTS**
L. P. Block, C.-G. Faelthammar, P.-A. Lindqvist, G. Marklund, F. S. Mozer, A. Pedersen, T. A. Potemra, and L. J. Zanetti (Johns Hopkins Univ., Laurel, Md.) Mar. 1987 21 p Submitted for publication
(TRITA-EPP-87-04; ISSN-0348-7539; ETN-88-91385) Avail: NTIS HC A03/MF A01

Two Viking (Swedish satellite) passes over the northern auroral oval and polar cap, one noon-midnight, and one evening-morning pass are discussed. An example of a Pi2 pulsation event is given and interpreted in terms of a damped resonant oscillation, probably caused by a sudden impulse. A ULF wave is shown, which, due to the high Alfven velocity, can be seen only in the electric field. An auroral arc crossing, where the electric and magnetic field data are consistent with an upward directed magnetic-field aligned electric field associated with an upward Birkeland current, is presented. ESA

**N88-13827#** Uppsala Ionospheric Observatory (Sweden).
**[ACTIVITIES REPORT OF THE IONOSPHERIC OBSERVATORY] Annual Report, 1986**
1987 53 p
(UIO-SR-87-01; ISSN-0349-2699; ETN-88-91391) Avail: NTIS HC A04/MF A01

Research in space plasma physics, particularly high latitude ionospheric phenomena and phenomena related to the interaction of the ionosphere with the magnetosphere and with the neutral atmosphere, is described. In situ experiments are performed using sounding rockets and the Swedish Viking satellite. Ground-based, remote-sensing experiments are also performed, using radar and radio techniques, in particular EISCAT, backscatter radars, and equipment for observing stimulated electromagnetic emissions from heating experiments. Routine monitoring of ionospheric conditions is conducted using the ionosonde, riometer, and backscatter radar techniques. The SABRE VHF radar is operated. The influence of ionospheric phenomena on radio wave propagation is studied. ESA

**N88-13828*#** Arizona State Univ., Tempe. Dept. of Geology.
**STUDIES IN AEOLIAN GEOLOGY Final Technical Report, 1 Dec. 1977 - 28 Feb. 1986**
Ronald Greeley 15 Jan. 1988 12 p
(Grant NsG-2284)
(NASA-CR-182328; NAS 1.26:182328) Avail: NTIS HC A03/MF A01 CSCL 08G

The objective of the research was to assess the significance of aeolian (windblown) processes in the evolution of planetary surfaces. The approach was to use wind tunnel simulations, field studies of possible analogs, and analyses of spacecraft data. Author

**N88-13777*#** Wisconsin Univ., Madison.
**SYSTEMATIC STRATOSPHERIC-TROPOSPHERIC EXCHANGE VIEWED FROM ISENTROPIC COORDINATES Abstract Only**
Donald Johnson *In* NASA. Goddard Space Flight Center, Scientific and Operational Requirements for TOMS Data Dec. 1987 p 10 (For primary document see N88-13774 05-42)
Avail: NTIS HC A06/MF A01 CSCL 04A

**N88-13780*#** National Aeronautics and Space Administration. Goddard Space Flight Center, Greenbelt, Md.
**INSIGHTS INTO THE GENERAL CIRCULATION OF THE LOWER STRATOSPHERE FROM TOMS Abstract Only**
Mark R. Schoeberl *In its* Scientific and Operational Requirements for TOMS Data Dec. 1987 p 14 (For primary document see N88-13774 05-42)
Avail: NTIS HC A06/MF A01 CSCL 04A

**N88-13782*#** National Aeronautics and Space Administration. Goddard Space Flight Center, Greenbelt, Md.
**LOWER-STRATOSPHERIC/UPPER-TROPOSPHERIC E PROCESSES ASSOCIATED WITH TROPICAL CYCLONES AS OBSERVED BY TOMS Abstract Only**
Edward B. Rodgers *In its* Scientific and Operational Requirements for TOMS Data Dec. 1987 p 21-22 (For primary document see N88-13774 05-42)
Avail: NTIS HC A06/MF A01 CSCL 04A

**N88-13783*#** Saint Louis Univ., Mo.
**TROPICAL EASTERLY JET LOCATED USING TOMS DATA Abstract Only**
William C. Bolhofer *In* NASA. Goddard Space Flight Center, Scientific and Operational Requirements for TOMS Data Dec. 1987 p 23 (For primary document see N88-13774 05-42)
Avail: NTIS HC A06/MF A01 CSCL 04A

**N88-13789*#** National Aeronautics and Space Administration. Goddard Space Flight Center, Greenbelt, Md.
**AN ANALYSIS OF TROPOPAUSE PRESSURE AND TOTAL OZONE CORRELATIONS Abstract Only**
Siegfried D. Schubert and Marie-Jeanne Munteanu *In its* Scientific and Operational Requirements for TOMS Data Dec. 1987 p 38 (For primary document see N88-13774 05-42)
Avail: NTIS HC A06/MF A01 CSCL 04A

**N88-13790*#** National Aeronautics and Space Administration. Goddard Space Flight Center, Greenbelt, Md.
**TOMS OZONE DATA COMPARED AT MESOSCALE RESOLUTION TO TROPOPAUSE HEIGHTS FROM THE AVE RADIOSONDE NETWORK AND TO VAS RADIANCES OVER THE SOUTH-CENTRAL UNITED STATES Abstract Only**
Dennis Chesters, Louis Uccellini, and David Larko *In its* Scientific and Operational Requirements for TOMS Data Dec. 1987 p 39 (For primary document see N88-13774 05-42)
Avail: NTIS HC A06/MF A01 CSCL 04A

**N88-13791*#** National Aeronautics and Space Administration. Goddard Space Flight Center, Greenbelt, Md.
**THE USE OF TOMS-MODIFIED VAS DATA FOR LARGE-SCALE NWP**
Wayman E. Baker, Marie-Jeanne Munteanu, Joel Susskind, and D. Reuter *In its* Scientific and Operational Requirements for TOMS Data Dec. 1987 p 40-45 (For primary document see N88-13774 05-42)
Avail: NTIS HC A06/MF A01 CSCL 04A

**N88-13793*#** National Aeronautics and Space Administration. Goddard Space Flight Center, Greenbelt, Md.
**VOLCANIC ERUPTION DETECTION WITH TOMS**
Arlin J. Krueger *In its* Scientific and Operational Requirements for TOMS Data Dec. 1987 p 54-56 (For primary document see N88-13774 05-42)
Avail: NTIS HC A06/MF A01 CSCL 04A

**N88-13795*#** Atmospheric Environment Service, Downsview (Ontario).
**COMPARISON OF GROUND BASED AND TOMS MEASUREMENTS OF SO2 FROM VOLCANIC EMISSIONS**
James B. Kerr and Wayne J. Evans *In* NASA. Goddard Space Flight Center, Scientific and Operational Requirements for TOMS Data Dec. 1987 p 60-69 (For primary document see N88-13774 05-42)
Avail: NTIS HC A06/MF A01 CSCL 04A

**N88-13796*#** National Oceanic and Atmospheric Administration, Washington, D. C.
**TOMS AND THE NOAA/FAA VOLCANO SUPPORT PLAN Abstract Only**
Michael Matson *In* NASA. Goddard Space Flight Center, Scientific and Operational Requirements for TOMS Data Dec. 1987 p 70 (For primary document see N88-13774 05-42)
Avail: NTIS HC A06/MF A01 CSCL 04A

**N88-13797*#** Smithsonian Institution, Washington, D. C.
**USE OF SATELLITE DATA IN VOLCANO MONITORING**
Lindsay McClelland *In* NASA. Goddard Space Flight Center, Scientific and Operational Requirements for TOMS Data Dec. 1987 p 71-76 (For primary document see N88-13774 05-42)
Avail: NTIS HC A06/MF A01 CSCL 04A

# 47 METEOROLOGY AND CLIMATOLOGY

Includes weather forecasting and modification.

**N88-13829#** GEOMET Technologies, Inc., Germantown, Md.
**ZEUS: A KNOWLEDGE-BASED EXPERT SYSTEM THAT ASSISTS IN PREDICTING VISIBILITY AT AIRBASES Final Report, Dec. 1985 - Dec. 1986**
Mark J. Stunder, Robert C. Koch, Timothy N. Sletten, and Sang M. Lee 15 Jan. 1987 162 p
(Contract F19628-86-C-0033)
(AD-A184197; GEOMET-EAF-1725; AFGL-TR-87-0019) Avail: NTIS HC A08/MF A01 CSCL 04B

Artificial Intelligence (AI) knowledge-based expert system (KBES) was developed to demonstrate the feasibility of using this approach to assist forecasters in predicting local visibility. The study developed a knowledge structure for handling rules and data needed to advise on advective and radiation fog formation processes. A review of alternatives for developing the needed software led to selection of the EXSYS, AI programming shell for developing and running a KBES on PC-compatible computers. The KBES for advising forecasters is called Zeus and was developed in three versions to be used at each of three airbases: Dover, Seymour Johnson, and Fort Bragg. The system was enthusiastically used at the bases for a 2-mo period as reported in a user survey. The Zeus forecast produced overall skill scores of 0.35 and 0.38, respectively. The skill scores were significantly better than for forecasters (at one of the bases) during the user test period. A drawback of the system is a tendancy to underpredict the frequency of occurrences of low-visibility categories. The good performance and the high user acceptance demonstrates a successful proof-of-concept. Further development of the approach is recommended. Author (GRA)

**N88-13830#** Air Weather Service, Scott AFB, Ill.
**ISENTROPIC ANALYSIS AND INTERPRETATION: OPERATIONAL APPLICATIONS TO SYNOPTIC AND MESOSCALE FORECAST PROBLEMS**
James T. Moore Aug. 1987 89 p
(AD-A184814; AWS/TN-87/002) Avail: NTIS HC A05/MF A01 CSCL 04B

A basic review of the isentropic coordinate system, including its advantages and disadvantages for operational use. The primitive equations in isentropic coordinate form are discussed with emphasis on their physical meaning and interpretation. Isentropic analysis techniques for horizontal and cross sectional perspectives are described as aids for diagnostic analysis of synoptic scale weather systems. Numerous diagnostic variables are discussed; all can be excellent tools in identifying synoptic scale features helpful in forecasting cyclogenesis and regions susceptible to strong convection. The final section presents specialized applications of isentropic techniques to weather analysis and forecasting, including: trajectory analysis, tropopause folding process, short-term forecasting of severe weather threat areas, and aviation forecasting. GRA

**N88-13831#** Naval Postgraduate School, Monterey, Calif.
**DEVELOPMENT OF AN ACOUSTIC ECHOSOUNDER FOR DETECTION OF LOWER LEVEL ATMOSPHERIC TURBULENCE M.S. Thesis**
Frank J. Weingartner Jun. 1987 98 p
(AD-A184877) Avail: NTIS HC A05/MF A01 CSCL 04B

Atmospheric density fluctuations induce phase perturbations that upgrade the spatial coherence of a laser beam propagating through the atmosphere. These degradations spread the laser beam and alter the centroid and intensity profile stochastically. Turbulent conditions arising from various environmental situations and meteorological phenomena are found at virtually all levels of the atmosphere. A substantial fraction of the optical turbulence along a vertical path arises from the surface heat flux within the first 100-200 meters above the ground. This thesis seeks to measure and analyze atmospheric turbulence within the first 100-200 meters above the ground with extremely high accuracy. The echosounder design incorporated a 25 element, square, planar array housed within a lead and foam insulated, acoustic shroud. This acoustic echosounder was employed to collect real-time, low level atmospheric data at two sites. This data should prove useful in determining whether the performance of laser and electro-optical systems could be increased by raising sensors and transmitters well above the local turbulent layer through the use of towers or other such structures. GRA

**N88-13832#** Control Data Corp., Minneapolis, Minn. Meteorology Research Center.
**A SINGLE-STATION WEATHER FORECASTING EXPERT SYSTEM Final Report, 21 Dec. 1985 - 21 Jun. 1987**
William H. Jasperson and David E. Venne 1 Aug. 1987 36 p (Contract F19628-86-C-0030)
(AD-A184889; AFGL-TR-87-0194) Avail: NTIS HC A03/MF A01 CSCL 04B

This report describes the development of an early prototype expert system for the classical single-station weather forecasting problem. The skills required to maximize forecast quality based on such limited data are being lost though they continue to have application to certain military scenarios which include communications interruptions. Knowledge for the expert system was obtained from a meteorologist experienced in single-station weather forecasting by working through case study data. The prototype was developed on a microcomputer and uses forward and backward chaining rules, frames, and other functions and procedures written in LISP. The expert system is able to emulate the expert for a several day case study used in the development, although much more work must be done to make the system useful for the general meteorological situation. GRA

**N88-13833#** Naval Postgraduate School, Monterey, Calif.
**MESOSCALE APPLICATIONS OF HIGH RESOLUTION IMAGERY M.S. Thesis**
Randy J. Scanlon Sep. 1987 133 p
(AD-A185039) Avail: NTIS HC A07/MF A01 CSCL 04B

Analysis of two mesoscale phenomena, a dry slot in stratocumulus over the eastern North Pacific (June 1985) and an enhanced-V cloud formation over the Gulf of Mexico (April 1984) is performed using very-high resolution photographs taken from the Space Transportation System (STS) 41-C and 51-G missions. Collocated meteorological satellite imagery (GOES, NOAA AVHRR, DMSP) and conventional meteorological data are utilized with the shuttle photography to better understand the microscale and mesoscale features of these two events. GRA

**N88-13834#** Naval Postgraduate School, Monterey, Calif.
**OPPORTUNITIES FOR TROPICAL CYCLONE MOTION RESEARCH IN THE NORTHWEST PACIFIC REGION Interim Report, Oct. 1986 - Sep. 1987**
Scott A. Sandgathe Aug. 1987 81 p
(AD-A185068; NPS-63-87-006) Avail: NTIS HC A05/MF A01 CSCL 04B

Tropical cyclone track prediction problems in the Northwest Pacific region that need to be researched are reviewed from the perspective of the operational forecaster. This information is provided as background for the upcoming Office of Naval Research field experiment on tropical cyclone motion. A short-term climatology of the frequency and spatial distribution of tropical cyclones is provided. Seven classes of operationally interested track forecast situations are described. Each cyclone from 1982 through 1985 is tabulated in terms of these classes. GRA

**N88-13835#** Air Force Inst. of Tech., Wright-Patterson AFB, Ohio.
**ENVIRONMENTAL AND CONVECTIVE INFLUENCE ON TROPICAL CYCLONE DEVELOPMENT VERSUS NON-DEVELOPMENTAL M.S. Thesis - Colorado State Univ.**
Patrick A. Lunney 1987 110 p
(AD-A185231; AFIT/CI/NR-87-60T) Avail: NTIS HC A06/MF A01 CSCL 04A

Composite and individual case analyses were made with USAF northwestern Pacific 950 mb (approx 1500 feet) investigative reconnaissance flights into tropical disturbances. Physical processes associated with early-stage tropical cyclone development vs. non-development were studied. Analysis of a 7-year period provides about 100 cases of development vs. 100 cases of non-development. Significantly higher radial inflow is observed in the inner-core of developing cases as compared to non-developing cases. Many formation cases had strong packets of radial momentum surges to inner-core radii at selective azimuthal locations. These wind surges were related to satellite-observed concentrations of deep convectuon near the inner- core of the developing disturbances and appear to be environmentally induced. Another factor influencing tropical disturbance's upper-tropospheric (250 mb) relative wind blowthrough or ventilation. The direction of the 250 mb relative wind to the tropical disturbance's moving center was found to have a major influence on the location of the distrurbance's meso-scale vortex ( 1-2 deg in diameter) or Low-Level Circulation Center (LLCC) in relation to the center of the parent cloud cluster convection. A fundamental characteristic of developing disturbances over non-developing disturbances was their ability to generate more LLCC's. GRA

**N88-13836#** Air Force Geophysics Lab., Hanscom AFB, Mass.
**THE APPLICATION OF DOUBLY-TRUNCATED HYDROMETEOR DISTRIBUTIONS TO NUMERICAL CLOUD MODELS Environmental Research Papers, 1985-1986**
Robert O. Berthel, Robert M. Banta, and Vernon G. Plank 9 Feb. 1987 34 p Supersedes US-PATENT-APPL-SN-420451 (AF Proj. 6670)
(AD-A185273; AFGL-TR-87-0050; AFGL-ERP-966; US-PATENT-APPL-SN-420451) Avail: NTIS HC A03/MF A01 CSCL 04A

A number of meteorological applications involving clouds require being able to determine a reasonable hydrometeor particle size distribution when given the mean hydrometeor mass density (liquid- or ice-water content) over a region of space. Such applications include numerical cloud model with parameterized or bulk microphysics, which have often assumed exponential size distributions. This study proposes a parameterization scheme based on a doubly-truncated exponential particle size distribution, i.e. a distribution that is truncated at both the large and small diameter ends. The necessary inputs to the scheme are the liquid or ice water content and the temperature of the sample, and, in some circumstances, an estimate of the lower truncation limit. Outputs include the parameters of the exponential distribution, including the upper truncation limit. A special set of relationships is used for rain when the largest particles exceed the assumed breakup diameter of 6 mm. The scheme relies on theoretical relationships derived from the equation for the double-truncated distribution, and on empirically-derived relationships. The empirical expressions include relationships between M and Z (where M is the liquid or ice water content and Z is the radar reflectivity) and values for the product Lambda D sum M (where Lambda is the parameter of the exponential distribution and D sub M is the upper truncation limit). GRA

**N88-13837#** Air Force Inst. of Tech., Wright-Patterson AFB, Ohio.
**MODELING CLOUDY AND CLEAR INTERVAL LENGTH PROBABILITIES USING SPACE SHUTTLE IMAGERY M.S. Thesis**
George F. Howard, III 1987 81 p
(AD-A185290; AFIT/CI/NR-87-36T) Avail: NTIS HC A05/MF A01 CSCL 04B

Interval length probabilities provide an alternative to other characterizations of cloudy and clear regions as viewed from atop the atmosphere. This work attempts to accurately model these probabilities using very high resolution space shuttle orbiter images. Probabilities extracted from these images are compared with three model representations. Metric and congruent statistical methods based on absolute deviations are used to determine model goodness-of-fit. An exponential model is shown to exhibit the least error of the three. Further examination shows that the parameters used to fit the exponential model to observed probabilities can be obtained from the cloud field itself (in the form of mean cloudy and mean clear interval lengths). These mean values are determined for image fractions as small as 1/32 and used to predict probabilities for the entire image. GRA

**N88-13838#** Air Force Inst. of Tech., Wright-Patterson AFB, Ohio.
**SPECIFICATION OF PREDICTORS NECESSARY FOR THE DETERMINATION OF OVER OR UNDERESTIMATION OF RADAR DERIVED TOTAL RAINFALL M.S. Thesis**
Vincent P. Holbrook Aug. 1987 76 p
(AD-A185363; AFIT/CI/NR-87-63T) Avail: NTIS HC A05/MF A01 CSCL 04B

A study was performed to produce a set of empirical predictors useful in identifying over or underestimation of radar determined rainfall rates. Two radar sampling procedures, systematic and irregular, were employed against light and heavy rain events to calculate rainfall rates for 10 km x 10 km grid boxes. Sampling intervals used were 10, 15, 20, 30, 40, and 50 minutes. The sampled rainfall rates were compared against the rainfall rates for 5-minute sampled data and the error was determined. The predictors were then used to determine whether the error was an over or underestimation. There was no significant difference in results as a function of the sampling interval used. Different sets of predictors were required for the category of precipitation as well as over or underestimation. The percentage of correct identifications, whether for over or underestimation, approached 80%. Allowing for error associated with the 5-minute sampling interval, the correct decision approached and sometimes exceeded 90%. The predictors which produced the best results utilized percent coverage of the grid box by precipitation, temporal and spatial homogeneity, and the mean rainfall rate. GRA

**N88-13839#** Royal Netherlands Meteorological Inst., De Bilt.
**THE LENGTHENING AND SHORTENING OF THE DAY [LENGEN EN KORTEN VAN DE DAGEN]**
J. denHeijer 1987 18 p In DUTCH
(KNMI-TR-91; B8700740; ISSN-0169-1708; ETN-88-90817)
Copyright Avail: NTIS HC A03/MF A01

The phenomena that lead to the fact that the lengthening and shortening of the day is not synchronous with clocks are discussed. The instants of sunrise and sunset, the length of the days in the Netherlands and the different kinds of time indication are outlined, and their effect on the complexity of the length of the days is pointed out. ESA

**N88-13840#** Royal Netherlands Meteorological Inst., De Bilt.
**EXPECTATIONS FOR WATER LEVEL DEVIATIONS AT THE DELTA WORKS: ZIERIKZEE (NETHERLANDS), NOVEMBER 1981-FEBRUARY 1986 [VERWACHTINGEN VOOR WATERSTAND-SAFWIJKINGEN DELTAWERKEN: ZIERIKZEE, NOVEMBER 1981-FEBRUARI 1986]**
A. W. Donker 1987 25 p In DUTCH
(KNMI-TR-93; B8709747; ISSN-0169-1708; ETN-88-90819)
Copyright Avail: NTIS HC A03/MF A01

The water level forecasting for the East-Scheldt (Netherlands) mouth during the conduct of delta works is discussed. The forecasting term was 24 hr, with further prospects for 36 hr. For water level deviation forecasting the weather service paid special attention to the announcement of quiet water, combinations of low level increases during high tide and low decreases during low tide, decreases of 50 cm or more during low tide, and substantial water level increases. The instruments used by the weather service are presented. The program for the verification of the 24 hr forecasts is explained. The usefulness of the results is demonstrated. ESA

**N88-13841#** Royal Netherlands Meteorological Inst., De Bilt.
**INVENTORY OF WEATHER STATIONS. CLIMATOLOGICAL DATA FROM DUTCH STATIONS, NO. 26 [INVENTARISATIE METEO-STATIONS. KLIMATOLOGISCHE GEGEVENS VAN NEDERLANDSE STATIONS NO. 26]**
J. C. M. Duivenvoorden 1987 112 p In DUTCH
(KNMI-150-26; B8707547; ISSN-0169-3581; ETN-88-90820)
Copyright Avail: NTIS HC A06/MF A01

Meteorological data from Dutch weather stations were inventoried with a view to agricultural research. The different kinds of meteorological data and weather stations, the storage of data, and the quality, availability and cost of the data are discussed. A user manual for the data and the location of the stations is given. Tables with the different meteorological parameters are presented. The meteorological data provided by weather amateurs and river boards are also inventoried. ESA

**N88-13842*#** National Aeronautics and Space Administration. Goddard Space Flight Center, Greenbelt, Md.
**GLOBAL ATMOSPHERIC CIRCULATION STATISTICS: FOUR YEAR AVERAGES**
M. F. Wu, M. A. Geller, E. R. Nash, and M. E. Gelman (National Oceanic and Atmospheric Administration, Washington, D. C.) Jun. 1987 74 p
(NASA-TM-100690; Rept-87B0437; NAS 1.15:100690) Avail: NTIS HC A04/MF A01 CSCL 04B

Four year averages of the monthly mean global structure of the general circulation of the atmosphere are presented in the form of latitude-altitude, time-altitude, and time-latitude cross sections. The numerical values are given in tables. Basic parameters utilized include daily global maps of temperature and geopotential height for 18 pressure levels between 1000 and 0.4 mb for the period December 1, 1978 through November 30, 1982 supplied by NOAA/NMC. Geopotential heights and geostrophic winds are constructed using hydrostatic and geostrophic formulae. Meridional and vertical velocities are calculated using thermodynamic and continuity equations. Fields presented in this report are zonally averaged temperature, zonal, meridional, and vertical winds, and amplitude of the planetary waves in geopotential height with zonal wave numbers 1-3. The northward fluxes of sensible heat and eastward momentum by the standing and transient eddies along with their wavenumber decomposition and Eliassen-Palm flux propagation vectors and divergences by the standing and transient eddies along with their wavenumber decomposition are also given. Large interhemispheric differences and year-to-year variations are found to originate in the changes in the planetary wave activity. Author

**N88-13843#** Pacific Northwest Labs., Richland, Wash.
**HANFORD METEOROLOGICAL STATION COMPUTER CODES. VOLUME 5: THE TOWER COMPUTER CODE**
J. W. Buck and G. L. Andrews Oct. 1987 34 p
(Contract DE-AC06-76RL-01830)
(DE88-001610; PNL-6279-Vol-5) Avail: NTIS HC A03/MF A01

The Hanford Meteorological Station (HMS), operated by Pacific Northwest Laboratory, records and stores wind, dry bulb temperature, and soil temperature data gathered each hour from the 410-ft meteorological tower. These data include measurements of wind speed and wind direction for seven heights, eight dry bulb temperatures, and three soil temperatures. The TOWER computer code is used to process and store those measurements and apply quality assurance checks to the data. The code accesses an input file, which contains the previous archive's date and hour, and an output file, which contains tower weather observations for the current month. A data entry form consisting of 25 fields is included in the program. The fields must be filled in by the user. The information entered is appended to the monthly file, which provides an archive for the tower data gathered hourly. This volume describes the implementation and operation of the TOWER computer code at the HMS. DOE

**N88-13781*#** National Aeronautics and Space Administration. Goddard Space Flight Center, Greenbelt, Md.
**OZONE, JET STREAKS AND SEVERE WEATHER Abstract Only**
Frank S. Sechrist, Ralph A. Petersen, Keith F. Brill (General Sciences Corp., Landover, Md.), Arlin J. Krueger, and Louis W. Uccellini *In its* Scientific and Operational Requirements for TOMS Data Dec. 1987 p 20 (For primary document see N88-13774 05-42)
Avail: NTIS HC A06/MF A01 CSCL 04B

**N88-13787*#** Control Data Corp., Minneapolis, Minn.
**APPLICATION OF TOMS DATA TO WEATHER ANALYSIS MODELS Abstract Only**
Gregory D. Nastrom *In* NASA. Goddard Space Flight Center, Scientific and Operational Requirements for TOMS Data Dec. 1987 p 32 (For primary document see N88-13774 05-42)
Avail: NTIS HC A06/MF A01 CSCL 04B

# 48 OCEANOGRAPHY

Includes biological, dynamic, and physical oceanography; and marine resources.

For related information see also *43 Earth Resources and Remote Sensing.*

**N88-13844#** Danish Meteorological Inst., Copenhagen.
**THE ICE CONDITIONS IN THE GREENLAND WATERS, 1981**
Dec. 1986 167 p In DANISH and ENGLISH
(ISBN-87-7478-276-2; ETN-88-90756) Avail: NTIS HC A08/MF A01

Monthly ice charts for the entire Greenland region and local reconnaissance charts are presented. ESA

# 51 LIFE SCIENCES (GENERAL)

**N88-13845#** Environmental Protection Agency, Research Triangle Park, N.C. Inhalation Toxicology Div.
**SHORT-TERM IN VITRO SCREENING STUDIES RELATED TO THE INHALATION TOXICOLOGY OF POTENTIALLY TOXIC AEROSOLS Final Report, Jun. 1984 - Apr. 1986**
Elaine C. Grose and Judith A. Graham Aug. 1987 27 p
(AD-A184815) Avail: NTIS HC A03/MF A01 CSCL 06K

The toxicity of JCE001 particles was tested using the rabbit alveolvar macrophage (RAM) test, hamster tracheal cultures and in vivo pulmonary bactericidal activity in mice. In the RAM test, incubation of alveolar macrophages (AM) with the JCE001 particles decreased AM viability, cellular adenosine 5' -triphosphate (ATP) and total protein levels. The lowest effective dose as determined by Williams' test was 50 micrograms/mL of JCE001 particles for all parameters examined. The presence of soluble cytotoxic components was established. The nature and rate of release of soluble toxic components from the JCE001 particles were important contributing factors in the mechanism by which these particles produced their toxic effects. A single 1-hr in vitro exposure of hamster tracheal ring organ cultures to the JCE001 particles was conducted to determine the dose response on ciliated respiratory epithelium. JCE001 particles caused a significant decrease in cilia beating frequency and an increase in cytopathological alterations. Morphological alterations in the tracheal epithelium were observed with light microscopy and scanning electron microscopy. The effect of the JCE001 particles on the ability of AM to kill inhaled pneumoniae was also measured. Bactericidal activity of all groups treated with the JCE001 particles was markedly reduced compared to that of controls. GRA

**N88-13846#** Army Research Inst. of Environmental Medicine, Natick, Mass.
**A PLETHYSMOGRAPH FOR MEASURING PULMONARY VENTILATION IN SMALL ANIMALS**
Vincent Forte, Jr., Stephen Muza, Reed Hoyt, and Allen Cymerman 3 Jun. 1987 31 p
(AD-A184978; USARIEM-T-18-87) Avail: NTIS HC A03/MF A01 CSCL 06D

A plethysmograph was developed to permit non-invasive measurement of pulmonary ventilation in small animals. In this system, precise measurements of temperature, humidity, and barometric pressure are used to calculate tidal volume, while a BASIC computer program directs the collection and display of data on tidal volume, frequency, body temperature, chamber temperature, and relative humidity. The long acoustical time constant of the plethysmograph permits accurate measurement of tidal volume in a wide variety of small unrestrained animals such as mice, rats, and hamsters. GRA

**N88-13847#** John B. Pierce Foundation of Connecticut, New Haven.
**MICROWAVE CHALLENGES TO THE THERMOREGULATORY SYSTEM**
Eleanor R. Adair Aug. 1987 98 p
(Contract F33615-85-C-4500)
(AD-A185391; USAFSAM-TR-87-7) Avail: NTIS HC A05/MF A01 CSCL 06G

Three experiments were conducted to measure the upper tolerance limit for maintaining thermal balance in squirrel monkeys during exposure to 2450-MHz radiofrequency radiation (RFR). During microwave exposure at high intensity, thermoregulatory behavior, metabolic, vasomotor, and sudomotor responses were mobilized in normal fashion, but the capacity to lose heat through sweating found to be the limiting factor in microwave tolerance. The major conclusion drawn from these studies is that the thermoregulatory system deals with energy absorbed from microwave fields in exactly the same way as energy produced in the body by normal metabolic processes or absorbed during exposure to conventional radiant or convective heat sources. GRA

# 52 AEROSPACE MEDICINE

Includes physiological factors; biological effects of radiation; and effects of weightlessness on man and animals.

**N88-13848#** Army Research Inst. of Environmental Medicine, Natick, Mass.
**PHYSIOLOGICAL DETERMINANTS OF LOAD BEARING CAPACITY Technical Report, Nov. - Dec. 1986**
Joseph E. Dziados, Andrew I. Damokosh, Robert P. Mello, James A. Vogel, and Kenneth L. Farmer, Jr. Jun. 1987 34 p
(AD-A184977; USARIEM-T-19-87) Avail: NTIS HC A03/MF A01 CSCL 06J

This study identifies some of the physiological determinants of load bearing capacity. Although it is reasonanble to assume that maximal aerobic capacity (VO2) is an important determinant of load bearing ability, research implicating the importance of muscular strength and endurance of the lower extremities in load bearing activity has not been reported. To address this deficiency, 49 infantrymen were measured for: 1) aerobic capacity, 2) muscular strength of the quadriceps and hamstrings 3) muscular endurance of the quadriceps and hamstrings and 4) body composition. Following these measures, the infantrymen made a maximal effort 10-mile road march with battle dress equipment. These data suggest that hamstring muscle strength may be an important determinant of prolonged load bearing performance. Further research may elucidate the degree to which aerobic capacity, muscle strength, and other physiological variables independently and/or interactively influence load bearing capacity. GRA

**N88-13849#** Army Research Inst. of Environmental Medicine, Natick, Mass.
**HUMAN THERMOREGULATORY MODEL FOR WHOLE BODY IMMERSION IN WATER AT 20 AND 28 C**
Peter Tikuisis, Richard R. Gonzalez, and Kent B. Pandolf Jun. 1987 55 p
(AD-A185052; USARIEM-T-23-87) Avail: NTIS HC A04/MF A01 CSCL 06J

The mathematical models of thermoregulation of Stolwijk and Hardy and Montgomery were used to develop a model suitable for the simulation of human physiological responses to cold-water immersion. Data were obtained from experiments where thirteen healthy male volunteers were totally immersed under resting and nude conditions for 1 h in water temperatures of 20 and 28 C. Mean measured rectal temperature (Tre) fell by about 0.9 and 0.5

C in 20 and 28 C water for all subjects, yet mean measured metabolic rate (M) rose by about 275 and 90 W for the low body fat group (n=7) and 195 and 45 W for the moderate body fat group (n=6). To predict the observed Tre and M values, the present model a) included thermal inputs for shivering from the skin independent of their inclusion with the central temperature to account for the observed initial rapid rise in M, b) determined a thermally neutral body temperature profile such that the measured and predicted initial values of Tre and M were matched, c) confined the initial shivering to the trunk region to avoid an overly large predicted initial rate of rectal cooling, and d) calculated the steady-state convective heat loss by assuming a zero heat storage in the skin compartment to circumvent the acute sensitivity to the small skin-water temperature difference when using conventional methods. The last three modifications are unique to thermoregulatory modeling. A BASIC computer listing of the model and a sample simulation are provided. GRA

**N88-13850#** Army Research Inst. of Environmental Medicine, Natick, Mass.
**A DEVICE AND METHODOLOGY FOR MEASURING REPETITIVE LIFTING VO2MAX (OXYGEN CONSUMPTION RATE) Technical Report, Aug. 1983 - Aug. 1986**
Marilyn A. Sharp, Joseph M. McGrath, Everett Harman, Joseph J. Knapik, and William A. Sawyer Aug. 1987 45 p
(AD-A185195; USARIEM-T-31/87) Avail: NTIS HC A03/MF A01 CSCL 14B

A repetitive lifting device capable of reliably operation under heavy loads for prolonged periods was designed to study manual material handling problems unique to the Army. The device consists of a pneumatically driven platform which can lift or lower loads up to 100 kg, from 0 to 200 cm above floor level. The device was utilized to develop a multi-stage repetitive lifting maximal oxygen uptake procedure and is suitable to be used for a wide variety of lifting and lowering tasks. GRA

# 53 BEHAVIORAL SCIENCES

Includes psychological factors; individual and group behavior; crew training and evaluation; and psychiatric research.

**N88-13851#** Institute for Perception RVO-TNO, Soesterberg (Netherlands). Afdeling Verrichtingspsychologie.
**TASKOMAT, A TASK BATTERY FOR INFORMATION PROCESSING**
L. C. Boer, A. W. K. Gaillard, and P. G. A. M. Jorna 1987 124 p In DUTCH; ENGLISH summary
(Contract A83/K/045)
(IZF-1987-2; TD-87-1776; ETN-88-90860) Avail: NTIS HC A06/MF A01

The construction of, and experience with Taskomat, a standardized task battery for the testing of human information processing are reviewed. Administration procedures and fields of application are discussed, including selection of personnel, measurement of psychological fitness, effects of mental loads, and stress. A manual for the operator, and instructions for the test subject are included. ESA

# 54 MAN/SYSTEM TECHNOLOGY AND LIFE SUPPORT

Includes human engineering; biotechnology; and space suits and protective clothing.

For related information see also *16 Space Transportation.*

**N88-13852*#** National Aeronautics and Space Administration. Ames Research Center, Moffett Field, Calif.
**CONTROLLED ECOLOGICAL LIFE SUPPORT SYSTEM. DESIGN, DEVELOPMENT, AND USE OF A GROUND-BASED PLANT GROWTH MODULE**
Robert D. MacElroy, David T. Smernoff (New Hampshire Univ., Durham.), and John D. Rummel Sep. 1987 83 p Meeting held at Moffett Field, Calif., Sep. 1984, in Cocoa Beach, Fla., Apr. 1985 and in Carmel, Calif., 23-25 Apr. 1986
(Contract NCC2-27)
(NASA-CP-2479; A-87255; NAS 1.55:2479) Avail: NTIS HC A05/MF A01 CSCL 06K

Problems of food production by higher plants are addressed. Experimentation requirements and necessary equipment for designing an experimental Controlled Ecological Life Support System (CELSS) Plant Growth Module are defined. A framework is provided for the design of laboratory sized plant growth chambers. The rationale for the development of an informal collaborative effort between investigators from universities and industry and those at Ames is evaluated. Specific research problems appropriate for collaborative efforts are identified. For individual titles, see N88-13853 through N88-13855.

**N88-13853*#** National Aeronautics and Space Administration. Ames Research Center, Moffett Field, Calif.
**CELSS PROGRAM MEETING**
John W. Tremor and Robert D. MacElroy *In its* Controlled Ecological Life Support System. Design, Development, and Use of a Ground-Based Plant Growth Module Sep. 1987 p 1-9 Meeting held in Carmel Valley Inn, Calif., 23-25 Apr. 1986 (For primary document see N88-13852 05-54)
Avail: NTIS HC A05/MF A01 CSCL 06K

A meeting on the potential contributions of plant science to the goals of Controlled Ecological Life Support System (CELSS) research produced discussions that helped to focus on a variety of topics. In the area of volatiles and soluble organics, microbial activity, disease, and productivity, participants emphasized the need to know more about the consequences of closure for the growth of plants. Under nutrient delivery systems, the problems focus on the need to maintain a stable, optimum nutrient system. Lighting systems discussions emphasized unique methods of direct lighting and development of improved irradiation sources. Flight experiment opportunities were outlined by one speaker. Documentation of the Plant Growth Module was discussed. The last day's discussion focused on the organization of the research group to be involved in the development and use of a two to three cubic meter sealed chamber and ancillary equipment. J.P.B.

**N88-13854*#** National Aeronautics and Space Administration. Ames Research Center, Moffett Field, Calif.
**CONTROLLED ECOLOGICAL LIFE SUPPORT SYSTEMS: DEVELOPMENT OF A PLANT GROWTH MODULE**
Mel M. Averner, Robert D. MacElroy, and David T. Smernoff (New Hampshire Univ., Durham.) *In its* Controlled Ecological Life Support System. Design, Development, and Use of a Ground-Based Plant Growth Module Sep. 1987 p 11-40 (For primary document see N88-13852 05-54)
Avail: NTIS HC A05/MF A01 CSCL 06K

An effort was made to begin defining the scientific and technical requirements for the design and construction of a ground-based plant growth facility. In particular, science design criteria for the Plant Growth Module (PGM) of the Controlled Ecological Life Support System (CELSS) were determined in the following areas: (1) irradiation parameters and associated equipment affecting plant growth; (2) air flow; (3) planting, culture, and harvest techniques;

(4) carbon dioxide; (5) temperature and relative humidity; (6) oxygen; (7) construction materials and access; (8) volatile compounds; (9) bacteria, sterilization, and filtration; (10) nutrient application systems; (11) nutrient monitoring; and (12) nutrient pH and conductivity. J.P.B.

**N88-13855*#** National Aeronautics and Space Administration. Ames Research Center, Moffett Field, Calif.
**PLANT GROWTH MODULE (PGM) CONCEPTUAL DESIGN**
Steven H. Schwartzkopf (California Univ., Davis.) and Daryl Rasmussen *In its* Controlled Ecological Life Support System. Design, Development, and Use of a Ground-Based Plant Growth Module Sep. 1987 p 41-70 (For primary document see N88-13852 05-54)
Avail: NTIS HC A05/MF A01 CSCL 06K

The Plant Growth Module for the Controlled Ecological Life Support System (CELSS), designed to answer basic science questions related to growing plants in closed systems, is described functionally with artist's conception drawings. Subsystems are also described, including enclosure and access; data acquisition and control; gas monitor and control; heating, ventilation, and air conditioning; air delivery; nutrient monitor and control; microbial monitoring and control; plant support and nutrient delivery; illumination; and internal operations. The hardware development plan is outlined. J.P.B.

**N88-13856#** Arizona State Univ., Tempe.
**EXAMINING THE RELATIVE EFFICIENCY OF PART- VERSUS WHOLE-TASK PRACTICE FOR MULTIPLE-TASK SITUATIONS Final Report, 1 Sep. 1984 - 31 Jul. 1987**
Diane L. Damos Aug. 1987 18 p
(Contract DAAG29-84-K-0197)
(AD-A185056; ARO-22256.4-LS) Avail: NTIS HC A03/MF A01 CSCL 05F

The primary purpose was to compare part-task training to whole-task training for a variety of dual-task combinations. Four experiments were performed. The first experiment examined the speed and accuracy of manual responses vs vocal responses when subjects performed a Stroop task. The second experiment was directly concerned with comparing the relative efficiency of part- versus whole-task training for multiple-task situations. The third experiment was designed to fill one of the more important gaps concerning combinations consisting of two tracking tasks. The fourth experiment examined the effect of response mode (manual vs vocal) on single- and dual-task performance as a function of task pacing. The first experiment provided some useful data while experiments 2 and 3 were inconclusive. Data from experiment 4 indicated that the use of voice recognition systems offers a number of advantages, particularly under dual-task conditions. GRA

**N88-13857#** Institute for Perception RVO-TNO, Soesterberg (Netherlands). Ergonomics Group.
**SITTING POSTURE OF HELICOPTER PILOTS OF THE ROYAL NETHERLANDS AIR FORCE; PRELIMINARY RECOMMENDATIONS**
D. S. C. Osinga and H. Schuffel Aug. 1986 32 p
(Contract A82/KLu/113)
(IZF-1986-16; TD-86-3428-II; ETN-88-91716) Avail: NTIS HC A03/MF A01

Ergonomic recommendations emphasizing helicopter pilot sitting posture are provided. The recommendations are based on an anthropometric survey and a study on causes of helicopter pilot back pain complaints. Sitting posture dimensions of male military personnel with guidelines for the location of displays and controls, and a checklist for evaluating future cockpit lay-out are included. ESA

**N88-13858#** Pacific Northwest Labs., Richland, Wash.
**IRRADIATION PRESERVATION OF SEAFOOD: LITERATURE REVIEW**
P. M. Molton Oct. 1987 60 p
(Contract DE-AC06-76RL-01830)
(DE88-001691; PNL-6311) Avail: NTIS HC A04/MF A01

The application of gamma-irradiation for extending the shelf life of seafood has been of interest for many years. This report reviews a number of studies on seafood irradiation conducted over the past several years. Topics covered include seafood irradiation techniques and dosages, species applicability and differences, the effects of packaging on seafood preservation, and changes in organoleptic acceptability as a result of irradiation. Particular attention is given to radiation effects (likely and unlikely) of concern to the public. These include the potential for generation of toxic chemical products, botulinum toxin production, and other health concerns. No scientifically defensible evidence of any kind was found for any harmful effect of irradiation of seafoods at the doses being considered (less than 300 krad), and all indications are that irradiation is an acceptable and needed additional tool for seafood preservation. DOE

# 55 SPACE BIOLOGY

Includes exobiology; planetary biology; and extraterrestrial life.

No abstracts in this category.

# 59 MATHEMATICAL AND COMPUTER SCIENCES (GENERAL)

No abstracts in this category.

# 60 COMPUTER OPERATIONS AND HARDWARE

Includes hardware for computer graphics, firmware, and data processing.

For components see *33 Electronics and Electrical Engineering.*

**N88-13859#** Naval Postgraduate School, Monterey, Calif.
**TEST AND EVALUATION OF THE TRANSPUTER IN A MULTI-TRANSPUTER SYSTEM M.S. Thesis**
Jose Vanni Filho Jun. 1987 200 p
(AD-A184969) Avail: NTIS HC A09/MF A01 CSCL 09B

The purpose of this thesis is to start the evaluation of the Transputer, a 32 bit microprocessor on a chip, to verify its potentials and limitations for real time applications in distributed systems. The evaluation concentrates on the four physical communication links, and its advertised capability to operate in parallel with the main processor (CPU), each one of them at a rate of 10 mbit/sec in each direction. It also presents to the reader an introduction to the machine itself, to the Occam Programming Language, a description of the environment at the Naval Postgraduate School (NPS), and suggests to the novice a learning sequence. The evaluation programs and other example programs presented were implemented using the Occam Programming Language (Proto-Occam) in either the Occam Programming System (OPS) or the Transputer Development System (TDS), both resident on the VAX 11/780 computer under the VMS Operating System (VAX/VMS). GRA

**N88-13860#** Saab-Space A.B., Linkoeping (Sweden).
**STUDY OF FAULT TOLERANT TECHNIQUES FOR SATELLITE DATA HANDLING Final Report, Dec. 1986**
J. Hanje, J. Torin, T. Eliasson, M. Sveningsson, J. Contet, J. P. Sotta, P. H. Lebouar, D. Perarnaud, P. Vlimant, and D. Powell (Laboratoire d'Automatique et de Ses Applications Spatiales, Toulouse, France ) et al. Paris, France ESA 26 Jan. 1987 149 p Prepared in cooperation with Chalmers Univ. of Technology, Goeteborg (Sweden)
(Contract ESTEC-6074/84-NL-PB)
(FTT/REP/0001/SAAB; ESA-CR(P)-2427; ETN-88-90886) Avail: NTIS HC A07/MF A01

Orbital transfer vehicle and deep space probe missions were analyzed to identify the requirements of a target Data Handling Subsystem (DHS). Fault tolerant techniques were assessed to catalog the fault tolerant features especially applicable for space use. Transient faults due to heavy ion induced single event upsets were emphasized, because of their very large influence on space applications. Candidate solutions were analyzed and synthesized into a design architecture of the Target DHS. The fault tolerant features of the Target DHS are found to reside in a central on board computer. Two DHS architectures were established, one for each mission. The different requirements of dependability led to different architectures of the fault tolerant computers. ESA

**N88-13861** Politecnico di Milano (Italy). Dipartamento di Elettronica.
**ARRAYS FOR DISCRETE FOURIER TRANSFORM**
Anna Antola, Roberto Negrini, and Nello Scarabottollo 1987 47 p Sponsored by Selenia SpA
(Rept-87-019; ETN-88-91301) Avail: Issuing Activity

Structures for parallel and pipelined direct or fast transforms are detailed. Circuit complexities are evaluated. Application of Fourier transform arrays to digital signal processing for a synthetic aperature radar real time terrain mapping system is described. ESA

# 61 COMPUTER PROGRAMMING AND SOFTWARE

Includes computer programs, routines, alogorithms, and specific applications, e.g., CAD/CAM.

**N88-13862#** Massachusetts Inst. of Tech., Cambridge.
**LEARNING A COLOR ALGORITHM FROM EXAMPLES**
Anya Hurlbert and Tomaso Poggio Jun. 1987 32 p Prepared in cooperation with Whitaker Coll., Mass.
(Contract N00014-85-K-0124)
(AD-A184385; AI-M-909; CBIP-M-25) Avail: NTIS HC A03/MF A01 CSCL 09B

It is shown that a color algorithm capable of separating illumination from reflectance in a Mondrian world can be learned from a set of examples. The learned algorithm is equivalent to filtering the image data (in which reflectance and illumination are intermixed) through a center-surround receptive field in individual chromatic channels. The operation resembles the retinex algorithm recently proposed by Edwin Land. This result is a specific instance of our earlier result that a standard regularization algorithm can be learned from examples. It illustrates that the natural constraints needed to solve a problem in inverse optics can be extracted directly from a sufficient set of input data and the corresponding solutions. The learning procedure has been implemented as a parallel algorithm on the Connection Machine System. GRA

**N88-13863*#** North Carolina State Univ., Raleigh. Dept. of Computer Science.
**EXPERIMENTS IN FAULT TOLERANT SOFTWARE RELIABILITY Semiannual Progress Report, 1 Apr. - 30 Sep. 1987**
David F. McAllister, K. C. Tai, and Mladen A. Vouk Oct. 1987 100 p
(Grant NAG1-667)
(NASA-CR-181554; NAS 1.26:181554) Avail: NTIS HC A05/MF A01 CSCL 09B

The reliability of voting was evaluated in a fault-tolerant software system for small output spaces. The effectiveness of the back-to-back testing process was investigated. Version 3.0 of the RSDIMU-ATS, a semi-automated test bed for certification testing of RSDIMU software, was prepared and distributed. Software reliability estimation methods based on non-random sampling are being studied. The investigation of existing fault-tolerance models was continued and formulation of new models was initiated. For individual titles, see N88-13864 through N88-13866.

**N88-13864*#** North Carolina State Univ., Raleigh. Dept. of Computer Science.
**RELIABILITY OF VOTING IN FAULT-TOLERANT SOFTWARE SYSTEMS FOR SMALL OUTPUT SPACES**
David F. McAllister, Chien-En Sun, and Mladen A. Vouk *In its* Experiments in Fault Tolerant Software Reliability Oct. 1987 31 (For primary document see N88-13863 05-61)
(Grant NAG1-667)
(TR-87-16) Avail: NTIS HC A05/MF A01 CSCL 09B

Under a voting strategy in a fault-tolerant software system there is a difference between correctness and agreement. An independent N-version programming reliability model is proposed for treating small output spaces which distinguishes between correctness and agreement. System reliability is investigated using analytical relationships and simulation. A consensus majority voting strategy is proposed and its performance is analyzed and compared with other voting strategies. Consensus majority strategy automatically adapts the voting to different component reliability and output space cardinality characteristics. It is shown that absolute majority voting strategy provides a lower bound on the reliability provided by the consensus majority, and 2-of-n voting strategy an upper bound. If r is the cardinality of the output space it is proved the 1/r is a lower bound on the average reliability of fault-tolerant system components below which the system reliability begins to deteriorate as more versions are added. Author

**N88-13865*#** National Aeronautics and Space Administration. Langley Research Center, Hampton, Va.
**EFFECTIVENESS OF BACK-TO-BACK TESTING**
Mladen A. Vouk, David F. McAllister, David E. Eckhardt, Alper Caglayan, and John P. J. Kelly (California Univ., Santa Barbara.) *In* North Carolina State Univ., Experiments in Fault Tolerant Software Reliability Oct. 1987 25 (For primary document see N88-13863 05-61)
(Contract NAS1-17705; Grants NAG1-667; NAG1-512)
(TR-87-08) Avail: NTIS HC A05/MF A01 CSCL 09B

Three models of back-to-back testing processes are described. Two models treat the case where there is no intercomponent failure dependence. The third model describes the more realistic case where there is correlation among the failure probabilities of the functionally equivalent components. The theory indicates that back-to-back testing can, under the right conditions, provide a considerable gain in software reliability. The models are used to analyze the data obtained in a fault-tolerant software experiment. It is shown that the expected gain is indeed achieved, and exceeded, provided the intercomponent failure dependence is sufficiently small. However, even with the relatively high correlation the use of several functionally equivalent components coupled with back-to-back testing may provide a considerable reliability gain. Implications of this finding are that the multiversion software development is a feasible and cost effective approach to providing highly reliable software components intended for fault-tolerant software systems, on condition that special attention is directed at early detection and elimination of correlated faults. Author

**N88-13866*#** North Carolina State Univ., Raleigh.
**RSDIMU ACCEPTANCE TESTING SYSTEM: OVERVIEW OF ACCEPTANCE SOFTWARE AND PROCEDURES**
*In its* Experiments in Fault Tolerant Software Reliability Oct. 1987 36 (For primary document see N88-13863 05-61)
Avail: NTIS HC A05/MF A01 CSCL 09B

An overview of the acceptance software and certification testing procedures is presented. Author

**N88-13867*#** Illinois Univ., Urbana-Champaign. Coordinated Science Lab.
**FILE USAGE ANALYSIS AND RESOURCE USAGE PREDICTION: A MEASUREMENT-BASED STUDY Ph.D. Thesis**
Murthy V.-S. Devarakonda Dec. 1987 91 p
(Grant NAG1-613)
(NASA-CR-181553; NAS 1.26:181553; UILU-ENG-87-2275; CSG-79) Avail: NTIS HC A05/MF A01 CSCL 09B

A probabilistic scheme was developed to predict process resource usage in UNIX. Given the identity of the program being run, the scheme predicts CPU time, file I/O, and memory requirements of a process at the beginning of its life. The scheme uses a state-transition model of the program's resource usage in its past executions for prediction. The states of the model are the resource regions obtained from an off-line cluster analysis of processes run on the system. The proposed method is shown to work on data collected from a VAX 11/780 running 4.3 BSD UNIX. The results show that the predicted values correlate well with the actual. The coefficient of correlation between the predicted and actual values of CPU time is 0.84. Errors in prediction are mostly small. Some 82% of errors in CPU time prediction are less than 0.5 standard deviations of process CPU time. Author

**N88-13868*#** Illinois Univ., Urbana-Champaign. Coordinated Science Lab.
**USAGE ANALYSIS OF USER FILES IN UNIX**
Murthy V. Devarakonda and Ravishankar K. Iyer Dec. 1987 45 p Sponsored in part by AT and T
(Grant NAG1-613)
(NASA-CR-181561; NAS 1.26:181561; UILU-ENG-87-2274; CSG-78) Avail: NTIS HC A03/MF A01 CSCL 09B

Presented is a user-oriented analysis of short term file usage in a 4.2 BSD UNIX environment. The key aspect of this analysis is a characterization of users and files, which is a departure from the traditional approach of analyzing file references. Two characterization measures are employed: accesses-per-byte (combining fraction of a file referenced and number of references) and file size. This new approach is shown to distinguish differences in files as well as users, which cam be used in efficient file system design, and in creating realistic test workloads for simulations. A multi-stage gamma distribution is shown to closely model the file usage measures. Even though overall file sharing is small, some files belonging to a bulletin board system are accessed by many users, simultaneously and otherwise. Over 50% of users referenced files owned by other users, and over 80% of all files were involved in such references. Based on the differences in files and users, suggestions to improve the system performance were also made. Author

**N88-13869*#** Illinois Univ., Urbana-Champaign. Coordinated Science Lab.
**PREDICTABILITY OF PROCESS RESOURCE USAGE: A MEASUREMENT-BASED STUDY OF UNIX**
Murthy V. Devarakonda and Ravishankar K. Iyer Dec. 1987 32 p Sponsored in part by AT and T
(Grant NAG1-613)
(NASA-CR-181562; NAS 1.26:181562; UILU-ENG-87-2273; CSG-77) Avail: NTIS HC A03/MF A01 CSCL 09B

A probabilistic scheme is developed to predict process resource usage in UNIX. Given the identity of the program being run, the scheme predicts CPU time, file I/O, and memory requirements of a process at the beginning of its life. The scheme uses a state-transition model of the program's resource usage in its past executions for prediction. The states of the model are the resource regions obtained from an off-line cluster analysis of processes run on the system. The proposed method is shown to work on data collected from a VAX 11/780 running 4.3 BSD UNIX. The results show that the predicted values correlate well with the actual. The correlation coefficient between the predicted and actual values of CPU time is 0.84. Errors in prediction are mostly small. Some 82% of errors in CPU time prediction are less than 0.5 standard deviations of process CPU time. Author

**N88-13870*#** Illinois Univ., Urbana-Champaign. Coordinated Science Lab.
**PERFORMABILITY MODELING BASED ON REAL DATA: A CASESTUDY**
M. C. Hsueh, R. K. Iyer, and K. S. Trivedi (Duke Univ., Durham, N. C.) Dec. 1987 24 p Submitted for publication
(Grant NAG1-613)
(NASA-CR-181563; NAS 1.26:181563; UILU-ENG-87-2272; CSG-76) Avail: NTIS HC A03/MF A01 CSCL 09B

Described is a measurement-based performability model based on error and resource usage data collected on a multiprocessor system. A method for identifying the model structure is introduced and the resulting model is validated against real data. Model development from the collection of raw data to the estimation of the expected reward is described. Both normal and error behavior of the system are characterized. The measured data show that the holding times in key operational and error states are not simple exponentials and that a semi-Markov process is necessary to model the system behavior. A reward function, based on the service rate and the error rate in each state, is then defined in order to estimate the performability of the system and to depict the cost of different types of errors. Author

**N88-13871*#** Illinois Univ., Urbana-Champaign. Coordinated Science Lab.
**DIAGNOSTIC REASONING IN DIGITAL SYSTEMS M.S. Thesis**
Kurt Henry Thearling Dec. 1987 45 p
(Grant NAG1-613)
(NASA-CR-181564; NAS 1.26:181564; UILU-ENG-87-2271; CSG-75) Avail: NTIS HC A03/MF A01 CSCL 09B

Described is an efficient method for fault diagnosis in digital systems based on the technique of reasoning. The methodology operates on the observed erroneous behavior and the structure of the system. The behavior consists of the error(s) observed on the circuit's output lines and specific values on the circuit's input lines. The techniques described improve on previously published research on diagnostic reasoning in two ways. Previous work has stressed system independent techniques which could be used to diagnose any faulty system whose structure can be represented. By concentrating on the specific case of diagnosing faulty digital circuits, it is possible to simplify the representation of the structure of the system. This representation, in the form of an AND/OR fault tree, efficiently abstracts the structure of a faulty digital system. More importantly, a method for partitioning the digital system is introduced which can considerably reduce the runtime complexity of a diagnosis. Author

**N88-13872*#** Illinois Univ., Urbana-Champaign. Coordinated Science Lab.
**ERROR PROPAGATION IN A DIGITAL AVIONIC MINI PROCESSOR M.S. Thesis**
Dale L. Lomelino Dec. 1987 47 p
(Grant NAG1-602)
(NASA-CR-181565; NAS 1.26:181565; UILU-ENG-87-2270; CSG-74) Avail: NTIS HC A03/MF A01 CSCL 09B

A methodology is introduced and demonstrated for the study of error propagation from the gate to the chip level. The importance of understanding error propagation derives from its close tie with system activity. In this system the target system is BDX-930, a digital avionic multiprocessor. The simulator used was developed at NASA-Langley, and is a gate level, event-driven, unit delay, software logic simulator. An approach is highly structured and easily adapted to other systems. The analysis shows the nature and extent of the dependency of error propagation on microinstruction type, assembly level instruction, and fault-free gate activity. Author

**N88-13873#** Illinois Univ., Chicago. Biometric Lab.
**APPROXIMATING MULTIVARIATE NORMAL ORTHANT PROBABILITIES USING THE CLARK ALGORITHM Technical Report, 1 Aug. 1985 - 1 Jan. 1987**
Robert D. Gibbons, R. D. Bock, and Donald Hedeker 15 Jul. 1987 33 p
(Contract N00014-85-K-0586; DA Proj. RR0-4206)
(AD-A184855; Rept-87-1) Avail: NTIS HC A03/MF A01 CSCL 09B

The probability of m correlated random variables is drawn from a multivariate normal distribution being non-negative. Exact results for this probability integral are unavailable for m greater than 3. Approximations for higher dimensional problems have generally yielded poor results except for special cases, such as compound symmetry, which is of limited value in practice. The purpose of this paper is to present a general approximation of this probability integral. The algorithm developed here is computationally tractable for m = 50 and accurate for very general correlational structures. The performance of this algorithm is compared to results based on Clark's (1961) original approximation, Gaussian quadrature formulae, and Monte Carlo simulation methods. Application of this approximation to problems of conditional dependence in IRT estimation problems is discussed. GRA

**N88-13874#** Naval Postgraduate School, Monterey, Calif.
**A PROTOTYPE RAY TRACER M.S. Thesis**
Paul G. Smith Jun. 1987 138 p
(AD-A184863) Avail: NTIS HC A07/MF A01 CSCL 20F

The ability to make computer images more realistic is becoming more important as the hardware for producing such images is becoming less expensive and hence more available. The key to producing realistic images lies in the algorithms that can take full advantage of the hardware to produce them. In this study, we look at a prototype of one ray tracer. Ray tracing, in combination with a global illumination model, currently provides the most realistic images that can be generated on general purpose computing hardware. The prototype was successfully implemented on an IBM AT clone. GRA

**N88-13875#** Naval Postgraduate School, Monterey, Calif.
**IMPLEMENTATION OF AN FIR BAND PASS FILTER USING A BIT-SLICE PROCESSOR M.S. Thesis**
Darrel W. Purdy Jun. 1987 164 p
(AD-A184895) Avail: NTIS HC A08/MF A01 CSCL 09B

A 13th order FIR filter for digital image processing is implemented in microcode using the Am29203 bit-slice evaluation Board of Advanced Micro Devices. To meet this requirement, the filter is first implemented in FORTRAN. Then the results of both implementations are used for timing comparisons. Although non-optimal bit-slice devices are used on the evaluation board, a time of 11 microseconds is achieved, as compared to the 100 microseconds achieved in the FORTRAN implementation. Theoretical estimates of 2.65 microseconds and 0.78 microseconds are obtained for high speed Am2900 bit-slice devices and Vitesse's Gallium Arsenide bit-slice devices, respectively. It is shown that, although the initial learning period for bit-slice devices is high, once learned, a skillful bit-slice designed can implement a simple filter design in minimal time with significant results in time savings. GRA

**N88-13876#** Naval Postgraduate School, Monterey, Calif.
**AN ADAPTIVE LATTICE ALGORITHM FOR SPECTRAL LINE ESTIMATION M.S. Thesis**
Ill Koo Park Jun. 1987 103 p
(AD-A184970) Avail: NTIS HC A06/MF A01 CSCL 12A

A lattice structure is derived to realize linear phase transfer functions and to develop an adaptive algorithm for continuously updating the lattice reflection coefficients. The lattice structure is considered because of its superior finite wordlength performance compared to transversal structures. The adaptive lattice algorithm developed has been applied to estimate the sinusoidal frequencies as part of Prony's method. Results of computer simulation supporting the theory are reported. GRA

**N88-13877#** Naval Postgraduate School, Monterey, Calif.
**AN APL WORKSPACE FOR CONDUCTING NONPARAMETRIC STATISTICAL INFERENCE M.S. Thesis**
Wayne Franz Vagts Jun. 1987 116 p
(AD-A184971) Avail: NTIS HC A06/MF A01 CSCL 09B

This thesis contains programs written in APL and documentation for performing certain nonparametric tests and computing nonparametric confidence intervals. These methods of inference are particularly useful in dealing with Department of Defense related problems as illustrated in the several military examples worked in Appendix C. The following nonparametric tests are considered: Sign Test, Wilcoxon Signed-rank Test, Mann-Whitney Test, Kruskal-Wallis test, Kendall's B, Spearman's R and Nonparametric Linear Regression. The tests are based on the exact distributions of the respective test statistics unless a large sample approximation is determined to provide at least a three decimal place accuracy. The software consists of two APL workspaces; one, which is designed for microcomputers (IBM PC's or compatibles) and is menu-driven, and the other, without menus, is designed for the mainframe computer (IBM 3033) at the Naval Postgraduate School. GRA

**N88-13878#** Naval Research Lab., Washington, D.C.
**SOFTWARE DESIGN FOR AN AIRBORNE GRAVITY MEASUREMENT SYSTEM Final Report, 1 Jul. 1986 - 28 Feb. 1987**
Mary F. Peters, John M. Brozena, and J. D. Clamons 12 Aug. 1987 37 p
(AD-A185000; NRL-9049) Avail: NTIS HC A03/MF A01 CSCL 09B

This report describes the results of a software design study for an airborne gravity measurement system. The software is intended for data acquisition and monitoring aboard a fixed-wing aircraft over oceanic areas, and for the postflight processing required to compute gravity along a flight track. Various requirements of the postflight processing system are discussed. A method to compute gravity from airborne measurements is outlined; as some quantities can be derived from more than one measurement, alternative algorithms, to be used in cases of poor quality or missing data, are given. Author (GRA)

**N88-13879#** Naval Postgraduate School, Monterey, Calif.
**AN EXTENSION TO THE MULTILEVEL LOGIC SIMULATOR FOR MICROCOMPUTERS M.S. Thesis**
Julio Cesar Lopes deAlbuquerque Jun. 1987 256 p
(AD-A185032) Avail: NTIS HC A12/MF A01 CSCL 09B

One of the most time consuming parts of the design process is the debugging of the project. This happens when simple modifications to a circuit require recompilation of the whole circuit. In the CAD tool currently available for digital systems design, compilation is a bottle neck. The VOHL system has an extremely efficient simulator phase and a reasonable but slower compilation phase. This thesis investigates a mechanism for eliminating the need to recompile the complete circuit when small changes are needed. GRA

**N88-13880#** Duke Univ., Durham, N. C. Dept. of Computer Science.
**NEAR-HORN PROLOG**
D. W. Loveland 5 May 1987 16 p
(Contract DAAG29-84-K-0072)
(AD-A185172; CS-1987-14; ARO-21213.3-MA) Avail: NTIS HC A03/MF A01 CSCL 09B

The author proposes an extension to Prolog that handles clause sets that are Horn and almost-Horn in a manner that emphasizes clarity, efficiency, and minimal deviation from standard prolog. Although one version of near-Horn Prolog is complete under appropriate search strategies, we focus on incomplete variants that allow fast processing. Negation in the program is handled correctly, although within a positive implication logic extension of Horn logic. Processing speed degradation is directly proportional to the distance the program is from a Horn clause set. GRA

**N88-13881#** Cornell Univ., Ithaca, N.Y. Mathematical Sciences Inst.
**ILLUSTRATIVE EXAMPLES OF PRINCIPAL COMPONENT ANALYSIS USING BMDP/4M Interim Technical Report**
W. T. Federer, C. E. McCulloch, and N. J. Miles-McDermott 25 May 1987 54 p
(Contract DAAG29-85-C-0018)
(AD-A185179; TR-87-51; BU-929-M; ARO-23306.86-MA) Avail: NTIS HC A04/MF A01 CSCL 09B

In order to provide a deeper understanding of the workings of principal components, four data sets were constructed by taking linear combinations of values of two uncorrelated variables to form the X-variates for the principal component analysis. The examples highlight some of the properties and limitations of the principal component analysis. This is part of a continuing project that produces annotated computer output for principal component analysis. The complete project will involve processing four examples on SAS/PRINCOMP, BMDP/4M, SPSS-X/FACTOR, GENSTAT/PCP, and SYSTAT/FACTOR. We show here the results from BMDP/4M, Version 85. GRA

**N88-13882#** Institute for Perception RVO-TNO, Soesterberg (Netherlands). Afdeling Visuologie.
**THE USE OF COLOR IN ELECTRONIC MAPS. PART 1: GENERATION AND ANALYSIS OF COLOR ON THE GOULD/DEANZA IMAGE PROCESSING SYSTEM**
J. Walraven and W. A. G. vanderHoeven Dec. 1986 33 p In DUTCH; ENGLISH summary
(Contract A84/KLu/089)
(IZF-1986-32; TD-87-0045; ETN-88-90859) Avail: NTIS HC A03/MF A01

The problem of using color on computer controlled displays was studied in a project dealing with the visual-ergonomical aspects of electronic maps. The components and operational facilities of the image processing system, and the calibration of the system are outlined. The colorimetric basis for the specification and generation of colors on a display is discussed. Examples of color processing illustrate the potential of the system. ESA

**N88-13883#** Societe Nationale Industrielle Aerospatiale, Toulouse (France). Div. Avions.
**OVERALL DESCRIPTION OF THE COMPUTER AIDED DESIGN AND MANUFACTURING SYSTEMS ASSOCIATED WITH THE A320 PROGRAM AT AEROSPATIALE AND ITS PARTNERS [PRESENTATION GENERALE DES SYSTEMES CFAO ASSOCIES AU PROGRAMME A320 DE L'AEROSPATIALE ET CHEZ LES PARTENAIRES]**
Roger Bergoend 1987 13 p In FRENCH
(SNIAS-872-111-104; ETN-88-91186) Avail: NTIS HC A03/MF A01

Computer aided design and manufacturing of the A-320 aircraft is described. It is used along all design and manufacturing steps including preliminary design, aerodynamics, shape design, structural computation, electrical design, specifications, tool design, quality control, and final technical documentation. Several data banks are described including the design bank, running on a CDC computer and a total of 8500 megaoctets. ESA

**N88-13884#** Societe Nationale Industrielle Aerospatiale, Toulouse (France). Div. Avions.
**PRESENTATION OF SIGMA (INTERACTIVE ASSISTED GEOMETRY SYSTEM). A COMPUTER ASSISTED SHAPE DESIGN PROGRAM DEVELOPED AT THE AEROSPATIALE AIRCRAFT DIVISION [PRESENTATION DE SIGMA (SYSTEME INTERACTIF DE GEOMETRIE ASSISTEE). LOGICIEL DE CFAO DEVELOPPE A LA DIVISION AVIONS DE L'AEROSPATIALE]**
Rene Gandou 1987 27 p In FRENCH
(SNIAS-872-111-110; ETN-88-91192) Avail: NTIS HC A03/MF A01

A real time highly interactive shape design program which does not require computer operation training is described. A local knowledge data bank which grows with accumulated experience is available. The geometrical design of ATR42 and A-320 aircraft was done with this system. ESA

**N88-13885#** Societe Nationale Industrielle Aerospatiale, Toulouse (France). Div. Avions.
**STRUCTURAL OPTIMIZATION IN THE DESIGN PROCESS**
J. Locatelli 1987 15 p
(SNIAS-872-111-115; ETN-88-91196) Avail: NTIS HC A03/MF A01

Computer aided design of aircraft structures to assure static and dynamic behavior control in order to reduce operating costs is reviewed. The evaluation of interactions of the external shape, aerodynamic loads, structural geometry, internal loads, and mass distributions needs different black boxes, which are executed consecutively: a strength analysis program, a modal analysis for characteristic vibration behavior (each based on the finite element method) and an aeroelastic investigation program using matrix methods (and in particular the stiffness matrix of the structural model). Each program performs successive analyses and resizing functions for the optimization run, in a single computer submission. They are prerequisites for performance of the sensitivity analysis and the computation of constraint derivatives. ESA

**N88-13886#** Societe Nationale Industrielle Aerospatiale, Les Mureaux (France). Div. Systemes Balistiques et Spatiaux.
**INTRODUCTION TO LOCAL AREA NETWORK DESIGN ON ARIANE 5 AND FUTURE LAUNCHERS**
Yves Durand and Jean-Michel Pic 17 Jan. 1986 11 p
(SNIAS-872-422-102; ETN-88-91203) Avail: NTIS HC A03/MF A01

The impact of real time local area networks (LAN) on launchers is discussed. Communication needs of a launch vehicle that call for distributed processing techniques are reviewed. The design drivers of the system are identified. A method to ensure the fulfillment of design goals, i.e., to benefit from the potentials of real time LAN is outlined. ESA

**N88-13887#** Technische Hogeschool, Eindhoven (Netherlands).
**DIGITIZATION FUNCTIONS IN COMPUTER GRAPHICS Ph.D. Thesis**
Maria Lucia Petronel vanLierop 1987 175 p Sponsored by the Netherlands Technology Foundation
(ETN-88-91363) Avail: NTIS HC A08/MF A01

A framework in which desirable properties of graphics digitization functions are formulated formally is presented. For digitization functions that are not close, a measure is introduced to express the quality of these functions with regard to closeness; this measure is called the vicinity function. Digitization functions for line segments are considered. For these functions a vicinity measure called the deviation function is introduced. A minimality property for line functions is introduced. It is proved that translation invariant, minimal, close line functions are not convex. It is conjectured that closeness and convexity are conflicting properties. It is shown that on a restricted domain D, a convex line function can be constructed from any translation invariant, minimal line function that satisfies certain conditions. It is proved that there is a one-to-one correspondence between line functions satisfying these conditions and permutations. Consequently, each permutation induces a convex line function on domain D. None of these functions is close. ESA

**N88-13888#** Technische Hogeschool, Eindhoven (Netherlands).
**SOME DISTANCE PROBLEMS IN CODING THEORY Ph.D. Thesis**
Cornelis Leonardus M vanPul 1987 107 p
(B8711398; ETN-88-91370) Avail: NTIS HC A06/MF A01

Coding in an imperfect computer memory with stuck-at-defects and random errors is treated. Two constructions for constant weight codes are considered. These constructions result in improved lower bounds on the function A(n,d,w) i.e., the largest size of any binary constant weight code of length n, minimum distance d, and constant weight w. This function plays an important role in determining upper bounds on the function A(n,d) (e.g., linear programming

bound and Johnson bound). The complete solution of a problem formulated by Ahlswede, El Gamal and Pang in 1984 is given. A problem connected with comma-free codes is tackled. ESA

**N88-13889#** Sandia National Labs., Albuquerque, N. Mex.
**INDIRECT SOLUTION OF STATIC PROBLEMS USING CONCURRENT VECTOR PROCESSING COMPUTERS**
J. H. Biffle 1987 17 p Presented at the Symposium on Technology of Glass, Ceramic, or Glass-Ceramic to Metal Sealing, Boston, Mass., 13 Dec. 1987
(Contract DE-AC04-76DP-00789)
(DE87-012105; SAND-86-2294C; CONF-871207-9) Avail: NTIS HC A03/MF A01

Indirect equation solvers such as the conjugate gradient method have been successfully vectorized and are capable of efficiently solving very large three-dimensional nonlinear static problems. A further reduction in job turn around time may be accomplished with concurrent vector processing computers. The nonlinear conjugate gradient algorithm is adapted to concurrent vector processing computers while striving to preserve the vector processing speed of the algorithm. It is critical that the nonlinear capabilities of the code are still efficiently processed under the concurrent algorithm. The algorithmic performance for two highly nonlinear three-dimensional problems is discussed. DOE

**N88-13890#** Sandia National Labs., Albuquerque, N. Mex.
**STRUCTURING DATA FOR CONCURRENT VECTORIZED PROCESSING IN A TRANSIENT DYNAMICS FINITE ELEMENT PROGRAM**
D. P. Flanagan and L. M. Taylor 1987 9 p Presented at the Symposium on Technology of Glass, Ceramic, or Glass-Ceramic to Metal Sealing, Boston, Mass., 13 Dec. 1987
(Contract DE-AC04-76DP-00789)
(DE87-013082; SAND-86-2173C; CONF-871207-12) Avail: NTIS HC A02/MF A01

Most transient dynamics analysis programs employ explicit time integration with a lumped (diagonalized) mass matrix. These programs predict the response of solids to intense dynamic loads, such as crash, penetration, or explosive loads. The explicit integration architecture avoids the solution of coupled matrix equations, which is of great advantage in these highly nonlinear problems. Explicit integration algorithms are naturally well suited to both vector and concurrent processing. However, to realize the advantage of concurrent vector processors, many traditional schemes for managing finite element data in memory must be changed. Optimal performance requires vectorization of as much code as possible. Finite element programs must be designed from a data flow perspective in order to fit comfortably into the architectures of modern computing hardware. A synopsis of how this approach was taken for production transient dynamic analysis programs PRONTO 2D and PRONTO 3D is presented. There are two points in the explicit integration loop where each finite element cannot be processed independently. The first is the gathering of nodal data (coordinates, displacements, velocities, etc.) via the element connectivity table. The second is the assembly of nodal force contributions from each element. These two processes dominate overall performance. The implications of the hardware architecture of concurrent processors on these crucial areas will be discussed. DOE

**N88-13891#** Sandia National Labs., Albuquerque, N. Mex.
**AN ADA GRAPHICAL TOOL TO SUPPORT SOFTWARE DEVELOPMENT**
A. Maxted and J. C. Rowe Sep. 1987 9 p Presented at the ACM SIGAda International Conference on the Ada Programming, Boston, Mass., 9 Dec. 1987
(Contract DE-AC04-76DP-00789)
(DE87-014854; SAND-87-2009C; CONF-871225-1) Avail: NTIS HC A02/MF A01

Significant work has been done by others on tools that allow software engineers to graphically illustrate software designs and, in some cases, to produce code automatically from the graphical design. What we posit here is that, given the current technology available in the marketplace, over the life of a typical software project it is more beneficial to produce accurate graphical representations of a software design from the code. We have developed a prototype tool that will take as input any legal Ada compilation unit, or set of units, and produce a precise graphical representation of those units. Because of the inherent suitability of Ada as a compilable Program Design Language (PDL), our tool is usable virtually throughout the software development life-cycle. This tool has been used successfully at Sandia National Laboratories during the preliminary and detailed design phases of a medium-sized software development project; moreover, we believe benefits will continue to accrue during the later stages of the life-cycle, particularly software maintenance and enhancement. DOE

**N88-13892#** California Univ., Berkeley. Lawrence Berkeley Lab.
**THE MAXIMUM LIKELIHOOD ESTIMATOR METHOD OF IMAGE RECONSTRUCTION: ITS FUNDAMENTAL CHARACTERISTICS AND THEIR ORIGIN**
J. Llacer and E. Veklerov May 1987 16 p Presented at the 10th Information Processing in medical Imaging International Conference, Utrecht, Netherlands, 22 Jun. 1987
(Contract DE-AC03-76SF-00098)
(DE88-000462; LBL-22417; CONF-8706213-1) Avail: NTIS HC A03/MF A01

Work is reviewed which characterizes the image reconstruction properties of the MLE algorithm. Its convergence properties are studied and the onset of image deterioration confirmed, a function of the number of counts in the source. By modulating the weight given to projection tubes with high numbers with respect to those with low numbers of counts in the reconstruction processes, it is confirmed that image deterioration is due to an attempt by the algorithm to match projection data tubes with high numbers of counts too closely to the iterative image projections. A stopping rule is developed for the algorithm testing the hypothesis that a reconstructed image could have given the initial projection data in a manner consistent with the underlying assumption of Poisson distributed variables. The rule was applied successfully to two mathematically generated phantoms and to a third phantom with exact (no statistical fluctuations) projection data. It is concluded that the behavior of the target functions whose extrema are sought in iterative schemes is more important in the early stages of the reconstruction than in the later stages, when the extrema are being approached but with the Poisson nature of the measurement. DOE

**N88-13893#** California Univ., Berkeley. Lawrence Berkeley Lab.
**SUSIE REFERENCE MANUAL**
R. A. Belshe Sep. 1987 24 p
(Contract DE-AC03-76SF-00098)
(DE88-001462; LBL-PUB-3061-Rev) Avail: NTIS HC A03/MF A01

SUSIE is a program for interactive analysis of one and two dimensional spectra. It runs on the Modcomp Classic computers, using a Tektronix 4014 CRT display unit with a high-speed DMA interface and an LBL designed supplemental control panel. The original Modcomp version was written by M. Neiman (LBL PUB-3014, Feb. 1981). The current version is the result of a number of major revisions and extensions, the most significant being the addition of 2-D spectra, and the ability to access spectra which are created by the EVA event sorting program. DOE

**N88-13894#** Sandia National Labs., Albuquerque, N. Mex.
**SANDIA SOFTWARE GUIDELINES: SOFTWARE QUALITY PLANNING**
Aug. 1987 61 p
(Contract DE-AC04-76DP-00789)
(DE88-001931; SAND-85-2344) Avail: NTIS HC A04/MF A01

This volume is one in a series of Sandia Software Guidelines intended for use in producing quality software within Sandia National Laboratories. In consonance with the IEEE Standard for

Software Quality Assurance Plans, this volume identifies procedures to follow in producing a software quality assurance (SQA) plan for an organization or a project, and provides an example project SQA plan. DOE

**N88-13895#** Los Alamos National Lab., N. Mex.
**MIXING MICROSOFT C AND MICROSOFT FORTRAN PROGRAM MODULES ON THE IBM PERSONAL COMPUTER**
F. McGirt Sep. 1987 31 p
(Contract W-7405-eng-36)
(DE88-001947; LA-11098-MS) Avail: NTIS HC A03/MF A01

Techniques that enable the interchangeable use of C or FORTRAN subprograms with either C or FORTRAN main programs are described. These techniques allow subprograms to be written in one of the languages and then called as subprograms with the other language. DOE

**N88-13896*#** College of William and Mary, Williamsburg, Va. Dept. of Computer Science.
**A REQUIREMENTS SPECIFICATION FOR A SOFTWARE DESIGN SUPPORT SYSTEM Final Report**
Robert E. Noonan 8 Jan. 1988 13 p
(Grant NAG1-647)
(NASA-CR-182333; NAS 1.26:182333) Avail: NTIS HC A03/MF A01 CSCL 09B

Most existing software design systems (SDSS) support the use of only a single design methodology. A good SDSS should support a wide variety of design methods and languages including structured design, object-oriented design, and finite state machines. It might seem that a multiparadigm SDSS would be expensive in both time and money to construct. However, it is proposed that instead an extensible SDSS that directly implements only minimal database and graphical facilities be constructed. In particular, it should not directly implement tools to faciliate language definition and analysis. It is believed that such a system could be rapidly developed and put into limited production use, with the experience gained used to refine and evolve the systems over time. Author

**N88-13260#** Fujitsu Ltd., Tokyo (Japan).
**PRACTICAL AND MODERN SIMULATION BY SYSTEMATIC CONNECTION OF THE LU-ADI CODE AND THE SOLUTION ADAPTIVE GRID PROGRAM**
Kisa Matsuhima, Shigeru Obayashi, Kazuhiro Nakahashi, and Kozo Fujii (National Aerospace Lab., Tokyo, Japan ) *In* National Aerospace Lab., Proceedings of the 4th NAL Symposium on Aircraft Computational Aerodynamics Dec. 1986 p 53-60 In JAPANESE; ENGLISH summary (For primary document see N88-13253 05-02)
Avail: NTIS HC A14/MF A01

**N88-13269#** National Aerospace Lab., Tokyo (Japan).
**PROGRAMMING TECHNIQUES FOR HIGH-SPEED PROCESSING OF LARGE SCALE NUMERICAL SIMULATION ON SUPERCOMPUTERS**
Kinuyo Nakamura and Masahiro Yoshida *In its* Proceedings of the 4th NAL Symposium on Aircraft Computational Aerodynamics Dec. 1986 p 129-136 In JAPANESE; ENGLISH summary (For primary document see N88-13253 05-02)
Avail: NTIS HC A14/MF A01

**N88-13270#** Nippon Electric Co. Ltd., Tokyo (Japan).
**VECTORIZING THE FFTS ON SUPERCOMPUTER SX SYSTEM**
Mitsuyasu Hanamura, Junichi Yorozu, Yoshiaki Tsuwa, Tadashi Watanabe, and Norio Masuda *In* National Aerospace Lab., Proceedings of the 4th NAL Symposium on Aircraft Computational Aerodynamics Dec. 1986 p 137-141 In JAPANESE; ENGLISH summary (For primary document see N88-13253 05-02)
Avail: NTIS HC A14/MF A01

**N88-13271#** Nippon Electric Co. Ltd., Tokyo (Japan). C and C Information Technology Research Labs.
**TRIDIAGONAL APPROXIMATE FACTORIZATION METHOD: A PRECONDITIONING TECHNIQUE FOR SOLVING NONSYMMETRIC LINEAR SYSTEMS SUITABLE TO SUPERCOMPUTERS**
Shun Doi and Norio Harada *In* National Aerospace Lab., Proceedings of the 4th NAL Symposium on Aircraft Computational Aerodynamics Dec. 1986 p 143-149 In JAPANESE; ENGLISH summary (For primary document see N88-13253 05-02)
Avail: NTIS HC A14/MF A01

**N88-13276#** National Aerospace Lab., Tokyo (Japan).
**COMPUTER GRAPHICS FOR COMPUTATIONAL AERODYNAMICS**
Kazuyo Suematsu and Tosio Isobe *In its* Proceedings of the 4th NAL Symposium on Aircraft Computational Aerodynamics Dec. 1986 p 181-189 In JAPANESE; ENGLISH summary (For primary document see N88-13253 05-02)
Avail: NTIS HC A14/MF A01

**N88-13278#** Fujitsu Ltd., Tokyo (Japan).
**VISUALIZATION OF AN AIRCRAFT ACCIDENT BASED ON DIGITAL FLIGHT DATA RECORDER INFORMATION**
Mikio Sasaki, Takamitsu Okada, Kenji Kira, and Toshiyuki Sakamoto (Japan Broadcasting Corp., Tokyo.) *In* National Aerospace Lab., Proceedings of the 4th NAL Symposium on Aircraft Computational Aerodynamics Dec. 1986 p 197-201 In JAPANESE; ENGLISH summary (For primary document see N88-13253 05-02)
Avail: NTIS HC A14/MF A01

**N88-13287#** National Aerospace Lab., Tokyo (Japan).
**ANALYTICAL METHOD FOR GENERATING COMPUTATIONAL GRIDS ABOUT COMPLETE AIRCRAFT CONFIGURATIONS**
Susumu Takanashi and Takao Isawa (Nippon Time Share Co., Japan ) *In its* Proceedings of the 4th NAL Symposium on Aircraft Computational Aerodynamics Dec. 1986 p 281-288 In JAPANESE; ENGLISH summary (For primary document see N88-13253 05-02)
Avail: NTIS HC A14/MF A01

**N88-13597*#** University of South Florida, Tampa.
**A RUDIMENTARY DATABASE FOR THREE-DIMENSIONAL OBJECTS USING STRUCTURAL REPRESENTATION**
James P. Sowers *In its* Towards Building a Team of Intelligent Robots 28 Dec. 1987 26 (For primary document see N88-13595 05-37)
(Grant NAG1-632)
(CSE-87-00004) Avail: NTIS HC A05/MF A01 CSCL 09B

# 62 COMPUTER SYSTEMS

Includes computer networks and special application computer systems.

**N88-13897#** Brown Univ., Providence, R. I. Center for Neural Science.
**STORING AND RETRIEVING DATA IN A PARALLEL DISTRIBUTED MEMORY SYSTEM Ph.D. Thesis**
Terry W. Potter 9 Jun. 1987 11 p
(Contract DAAG29-84-K-0202)
(AD-A185177; ARO-22000.6-LS) Avail: NTIS HC A03/MF A01 CSCL 09B

The storage and retrieval of patterns in a Hopfield-like Parallel Distributed Memory is investigated experimentally with a view toward increasing its storage capacity. The first two Chapters give an overview of distributed memories and in particular the Hopfield distributed memory. This dissertation then experimentally investigates new and untested methods to increase the storage capabilities of a Hopfield-like neural net. Increasing the storage capacity by using the continuous-valued Hopfield memory is explored in Chapter 3 and the impact on capacity of data representation is experimentally investigated in Chapter 4. We then

focus on new ways of storing data (changing the interconnect strengths) including in Chapter 7 developing a new method called Modifying the Energy Contour or MEC. In addition, this Chapter also outlines how to increase error-tolerance through the use of noisy patterns. The Hopfield distributed memory is then contrasted to another intelligent memory subsystem based on more of a traditional computer technology. In Chapter 8 we see that traditional computer technology using data-parallel techniques has a greater storage efficiency than possible with current Hopfield-like distributed memories. GRA

**N88-13898#** Lawrence Livermore National Lab., Calif.
**CONCEPTUAL ISSUES IN MEASURING THE BEHAVIOR OF A DISTRIBUTED REAL-TIME PROCESS-CONTROL COMPUTER SYSTEM**
J. D. Lawrence May 1987 23 p Presented at the International Conference on the Management and Performance Evaluation of Computer Systems, Orlando, Fla., 8 Dec. 1987
(Contract W-7405-eng-48)
(DE87-009748; UCRL-96426; CONF-871209-1) Avail: NTIS HC A03/MF A01

Measuring the performance, reliability and availability of a distributed real-time process-control fault-tolerant computer system presents a variety of interesting problems. A method is described by which this task can be organized efficiently, and by which appropriate measures can be delivered to a variety of different user groups. This involves constructing a system structure tree that organizes all of the hardware and software of the computer system. Subtrees are identified that provide information to the various users. Some of the problems that one can expect to encounter are discussed. DOE

**N88-13899#** Lawrence Livermore National Lab., Calif.
**CONCEPTUAL ISSUES IN MEASURING THE BEHAVIOR OF A DISTRIBUTED REAL-TIME PROCESS-CONTROL COMPUTER SYSTEM**
J. D. Lawrence 14 Aug. 1987 18 p Presented at the International Conference on the Management and Performance Evaluation of Computer Systems, Orlando, Fla., 8 Dec. 1987
(Contract W-7405-eng-48)
(DE87-014251; UCRL-96426-Rev-1; CONF-871209-1-Rev-1)
Avail: NTIS HC A03/MF A01

Measuring the performance, reliability and availability of a distributed real-time process-control fault-tolerant computer system presents a variety of interesting problems. A method is described by which this task can be organized efficiently, and by which appropriate measurements can be provided for a variety of different user groups. This involves constructing a system structure graph that organizes all of the hardware and software of the computer system. Subgraphs are identified that provide information to the various users. A particularly important type of user is the equipment, or process, being controlled. Some of the problems that one can expect to encounter are discussed. DOE

# 63 CYBERNETICS

Includes feedback and control theory, artificial intelligence, robotics and expert systems.

For related information see also *54 Man/System Technology and Life Support.*

**N88-13900*#** Information and Control Systems, Inc., Hampton, Va.
**INVESTIGATION, DEVELOPMENT, AND APPLICATION OF OPTIMAL OUTPUT FEEDBACK THEORY. VOLUME 3: THE RELATIONSHIP BETWEEN DYNAMIC COMPENSATORS AND OBSERVERS AND KALMAN FILTERS Final Report**
John R. Broussard Dec. 1987 26 p
(Contract NAS1-15759)
(NASA-CR-4107; NAS 1.26:4107) Avail: NTIS HC A03/MF A01 CSCL 09B

Relationships between observers, Kalman Filters and dynamic compensators using feedforward control theory are investigated. In particular, the relationship, if any, between the dynamic compensator state and linear functions of a discrete plane state are investigated. It is shown that, in steady state, a dynamic compensator driven by the plant output can be expressed as the sum of two terms. The first term is a linear combination of the plant state. The second term depends on plant and measurement noise, and the plant control. Thus, the state of the dynamic compensator can be expressed as an estimator of the first term with additive error given by the second term. Conditions under which a dynamic compensator is a Kalman filter are presented, and reduced-order optimal estimaters are investigated. Author

**N88-13901#** Societe Nationale Industrielle Aerospatiale, Les Mureaux (France). Div. Systemes Balistiques et Spatiaux.
**CONTROL OF AN UNSTABLE LAUNCHER IN ATMOSPHERIC FLIGHT USING MINIMAX OPTIMAL CONTROL LAWS**
J. Dupont, G. Pignie, and J. P. Cornu 1987 11 p
(Contract CT/104/D.En/84)
(SNIAS-872-422-107; ETN-88-91208) Avail: NTIS HC A03/MF A01

A class of composed laws, using linear and minimax controlers leading to better dimensioned control devices and easy to tune control processes for unstable launchers was developed. This type of composed control law reduces optimally the maximum deflection and angular rate of the swiveled engine, and thus cost and weight of the device. It gives a natural decoupling between stability and set-point following requirements, and control against wind gusts. Such a scheme is not much more complex to implement in real time than a classical linear controler. A generalization to the case where the aerodynamic torque is not a linear function of the angle of attack, though leading to more complex computations, can be considered. Even if the solution of the game is not entirely explicit, it may lead to usable control policies, via numerical approximations. ESA

**N88-13902** Politecnico di Milano (Italy). Dipartamento di Elettronica.
**BEHAVIORAL ARCHITECTURE ROBOT CONTROL SYSTEM (BARCS): A NEW WAY OF BUILDING ROBOTS**
R. Cassinis Sep. 1987 39 p
(Rept-87-036; ETN-88-91304) Avail: Issuing Activity

A modular method of building robot control systems, especially suitable for mobile machines, is described. Traditional programming is completely abandoned, and a system based on a behavioral architecture and on smart sensor data handling is implemented. All modules are conceptually at the same level: no fixed hierarchies are established. All information in the system is public, i.e., every module can access all information, because the needs of each module cannot be foreseen: a suitable data structure must therefore be implemented. At any time, each module knows what the other modules are doing. An experimental realization is described. ESA

**N88-13903#** Groningen Rijksuniversiteit (Netherlands). Dept. of Mathematics.
**EQUIVALENCE OF INPUT-OUTPUT STABILITY AND EXPONENTIAL STABILITY FOR INFINITE DIMENSIONAL SYSTEMS**
R. F. Curtain 1987 45 p
(TW-276; B8705873; ETN-88-91346) Avail: NTIS HC A03/MF A01

For a wide class of infinite dimensional linear systems it is shown that if the state space realization is exponentially stabilizable and detectable, then exponential stability is equivalent to input-output stability of the transfer function. The equivalence conditions are readily checked for spectral and delay systems. While one would expect that systems with a well defined nuclear Hankel operator would be included in the above class, it is not proved. Output feedback control may result in a weaker form of exponential stability, but this is a consequence of the well

posedness question in state space and seems unavoidable. ESA

**N88-13904#** Michigan Univ., Ann Arbor. Dept. of Electrical Engineering and Computer Science.
**ON LINEAR PERIODIC CONTROLLERS**
S. Lee and S. M. Meerkov Dec. 1987 5 p Presented at the 26th IEEE CDC Conference, Los Angeles, Calif., 9 Dec. 1987
(Contract DE-FG02-85ER-13315)
(DE87-011174; CONF-871211-2) Avail: NTIS HC A02/MF A01

A necessary and sufficient condition for existence of a linear periodic controller which is advantageous in problems of robust, strong and simultaneous stabilization is formulated. DOE

**N88-13905#** Allied Bendix Corp., Kansas City, Mo.
**XCUT: A RULE-BASED EXPERT SYSTEM FOR THE AUTOMATED PROCESS PLANNING OF MACHINED PARTS**
S. L. Brooks, K. E. Hummel, and M. L. Wolf Jun. 1987 17 p Presented at the Symposium on Technology of Glass, Ceramic, or Glass-Ceramic to Metal Sealing, Boston, Mass., 13 Dec. 1987
(Contract DE-AC04-76DP-00613)
(DE87-011638; BDX-613-3768; CONF-871207-6) Avail: NTIS HC A03/MF A01

Automated process planning is becoming a popular research and development topic in engineering and applied artificial intelligence. It is generally defined as the automatic planning of the manufacturing procedures for producing a part from a computer aided design (CAD) based product definition. An automated process planning system, XCUT, is currently being developed using rule-based expert system techniques. XCUT will generate process plans for the production of machined piece-parts, given a geometric description of a part's features. The system currently is focused on operation planning for prismatic parts on multi-axis milling machines. To date, moderately complex 2-1/2D prismatic parts have successfully been planned for with approximately 300 rules in the knowledge base. This paper will describe the XCUT system, system architecture, knowledge representation, plan development sequence, and issues in applying expert system technology to automated process planning. DOE

**N88-13906#** Allied Bendix Corp., Kansas City, Mo.
**USING HIERARCHICALLY STRUCTURED PROBLEM-SOLVING KNOWLEDGE IN A RULE-BASED PROCESS PLANNING SYSTEM**
K. E. Hummel and S. L. Brooks Jun. 1987 17 p Presented at the Symposium on Technology of Glass, Ceramic, or Glass-Ceramic To Metal Sealing, Boston, Mass., 13 Dec. 1987
(Contract DE-AC04-76DP-00613)
(DE87-011639; BDX-6133769; CONF-871207-10) Avail: NTIS HC A03/MF A01

A rule-based expert system, XCUT, currently is being developed which will generate process plans for the production of machined parts, given a feature-based part description. Due to the vast and dynamic nature of process planning knowledge, a technique has been used in the development of XCUT that segments problem solving knowledge into multiple rule bases. These rule bases are structured in a hierarchical manner that is reflective of the problem decomposition procedure used to generate a plan. An inference engine, HERB (Hierarchical Expert Rule Bases), has been developed which supports the manipulation of multiple rule bases during the planning process. This paper illustrates the hierarchical nature of problem-solving knowledge in the XCUT system and describes the use of HERB for programming with hierarchically structured rule bases. DOE

**N88-13907*#** Catholic Univ. of America, Washington, D.C. Dept. of Electrical Engineering.
**OPTIMAL CONTROL OF LARGE SPACE STRUCTURES VIA GENERALIZED INVERSE MATRIX**
Charles C. Nguyen and Xiaowen Fang [1987] 5 p
(Grant NAG5-949)
(NASA-CR-182336; NAS 1.26:182336) Avail: NTIS HC A02/MF A01 CSCL 09B

Independent Modal Space Control (IMSC) is a control scheme that decouples the space structure into n independent second-order subsystems according to n controlled modes and controls each mode independently. It is well-known that the IMSC eliminates control and observation spillover caused when the conventional coupled modal control scheme is employed. The independent control of each mode requires that the number of actuators be equal to the number of modelled modes, which is very high for a faithful modeling of large space structures. A control scheme is proposed that allows one to use a reduced number of actuators to control all modeled modes suboptimally. In particular, the method of generalized inverse matrices is employed to implement the actuators such that the eigenvalues of the closed-loop system are as closed as possible to those specified by the optimal IMSC. Computer simulation of the proposed control scheme on a simply supported beam is given. Author

**N88-13908*#** Catholic Univ. of America, Washington, D.C. Dept. of Electrical Engineering.
**CARTESIAN PATH CONTROL OF A TWO-DEGREE-OF-FREEDOM ROBOT MAINPULATOR Semiannual Report**
Charles C. Nguyen and Farhad J. Pooran Jan. 1988 24 p
(Grant NAG5-780)
(NASA-CR-182331; NAS 1.26:182331) Avail: NTIS HC A03/MF A01 CSCL 09B

The problem of cartesian trajectory control of a closed-kinematic chain mechanism robot manipulator with possible space station applications is considered. The study was performed by both computer simulation and experimentation for tracking of three different paths: a straight line, a sinusoid and a circle. Linearization and pole placement methods are employed to design controller gains. Results show that the controllers are robust and there are good agreements between simulation and experimentation. Excellent tracking quality and small overshoots are also evident. Author

# 64 NUMERICAL ANALYSIS

Includes iteration, difference equations, and numerical approximation.

**N88-13909#** Warwick Univ. Coventry (England). Control Theory Centre.
**ROBUSTNESS OF LINEAR SYSTEMS**
A. J. Pritchard and S. Townley Apr. 1987 62 p
(PB87-220042; Rept-141) Avail: NTIS HC E06/MF E06 CSCL 12A

Linear systems which are stable are considered. Perturbations are assumed to have unbounded structure and the smallest perturbation was determined which destroys the stability. The first section is an abstract analysis of the problem, but in later sections specialize to three types of systems; those whose mild solutions are given in terms of: (1) strongly continuous semigroups, (2) resolvent operators - integro differential systems, and (3) evolution operators - time varying systems. Author

**N88-13910#** Warwick Univ. Coventry (England). Control Theory Centre.
**STABILITY PROPERTIES OF SPLINE APPROXIMATIONS FOR RETARDED SYSTEMS**
F. Kappel and D. Salamon Dec. 1986 59 p
(Grant NSF MCS-82-10950)
(PB87-220919; Rept-136) Avail: NTIS HC E06/MF A06 CSCL 12A

Qualitative properties of the spline approximation scheme for retarded functional differential equations introduced in AD-A142963 are studied. It is shown that the approximating systems are stable for large N if the underlying retarded functional differential equation is stable. In this case the approximating equations are uniformly (with respect to the approximation index) stable in the vector component of the state but not so in the complete state. Author

**N88-13911#** Centro Brasileiro de Pesquisas Fisicas, Rio de Janeiro.
**LAGRANGIAN PROCEDURES FOR HIGHER ORDER FIELD EQUATIONS**
C. G. Bollini and J. J. Giambiagi 1986 24 p
(DE87-703365; CBPF-NF-037/86) Avail: NTIS (US Sales Only) HC A03/MF A01

A Lagrangian procedure for the treatment of higher order field equations is presented. The energy-momentum tensor and the conserved density current are constructed. In particular, the case in which the derivatives appear only in the invariant D'Alembertian operator is discussed. Also discussed are examples. The fields are quantized and the corresponding Hamiltonian constructed, which is shown not to be positive definite. Rules for causal propagators are given. DOE

**N88-13912#** Illinois Univ., Urbana. Coordinated Science Lab.
**EFFICIENT COMPUTATION OF PERIODIC GREEN'S FUNCTIONS WITH APPLICATION TO GRATING STRUCTURES**
Roy Jorgenson and Raj Mittra Aug. 1987 90 p
(Contract N00014-84-C-0149)
(AD-A184853; UILU-ENG-87-2249) Avail: NTIS HC A05/MF A01 CSCL 20C

It is shown tht electromagnetic scattering from periodic structures may be formulated in terms of an integral equation that has its kernel a periodic Green's function. The periodic Green's function may be derived from two points of view: as a response to an array of line/point sources (spatial domain) or as a response from a series of current sheets (spectral domain). These responses are a Fourier transform pair and are slowly convergent summations. The convergence problems in each domain arise from unavoidable singularities in the reciprocal domain. A method is discussed to overcome the slow convergence by using the Poisson summation formula and summing in a combination of spectral and spatial domains. A parameter study is performed to determine an optimum way to weight the combination of domains. Simple examples of scattering from a one-dimensional array of strips and two-dimensional array of plates are used to illustrate the concepts. GRA

**N88-13913#** Naval Postgraduate School, Monterey, Calif.
**CROSS-CORRELATION OF UNIFORM CYCLIC DIFFERENCE SET SEQUENCES M.S. Thesis**
David L. Rogers Jun. 1987 96 p
(AD-A184879) Avail: NTIS HC A05/MF A01 CSCL 12A

The incidence vector or characteristic function of a cyclic difference set can be viewed as a full period of a cyclic binary sequence. These cyclic difference set sequences possess certain desirable properties for applications in digital communications, radar ranging and some aspects of mathematical modeling. One particularly desirable property unique to cyclic difference set sequences is their two-level auto-correlation function. In this thesis, the cross-correlation functions of a sample of uniform cyclic difference set sequences are investigated. The cross-correlations involve equivalent and inequivalent uniform cyclic difference set sequences. In addition, the span and cyclotomic cosets are determined for each sequence in the sample. GRA

**N88-13914#** George Washington Univ., Washington, D.C. Inst. for Management Science and Engineering.
**EXPLICIT FORMULATE FOR THE DISTRIBUTIONS OF STOPPING VARIABLES UNDER WALD'S TRUNCATED SPRT (SEQUENTIAL PROBABILITY RADIO TESTS) FOR A POISSON PROCESS**
S. Zacks 6 May 1987 21 p
(Contract N00014-83-K-0216)
(AD-A185053; GWU/IMSE/SERIAL-T-516/87) Avail: NTIS HC A03/MF A01 CSCL 12A

Explicit formulae are developed for the distributions of the stopping variables associated with truncated versions of the Wald sequential probability ratio tests (SPRT) of hypothesis about the mean time between failures (MTBF) of a poisson process. These formulae are based on newly derived expressions for linear boundaries crossing probabilities under Poisson processes. The results of the present study can also be applied for determining confidence intervals for the MTBF after sequential stopping. Author (GRA)

**N88-13915#** Naval Research Lab., Washington, D.C. Acoustics Div.
**ON A BOUNDARY DATA OPERATOR AND GENERALIZED EXTERIOR ROBIN PROBLEMS FOR THE HELMHOLTZ EQUATION Interim Report**
Allan G. Dallas 5 Aug. 1987 40 p
(AD-A185124; NRL-9008) Avail: NTIS HC A03/MF A01 CSCL 20A

This report deals with boundary-value problems for the equation Delta u + kappa(2) u = 0 in an exterior domain Omega(+) in euclidean three-space, with a boundary condition of the form delta u / delta nu + B(u bar gamma) = g; gamma: = delta Omega(+) is smooth, nu is the unit normal for gamma, g an element of L sub 2 (gamma), and B is bounded linear operator in L sub 2 (gamma) such that i bar-zeta B is dissipative for some zeta lying in a certain set depending upon kappa. It is required that the Neumann data delta u / delta nu and Dirichlet data u bar gamma in L sub 2 (gamma) be taken on in the normal L sub 2 sense. The study is based upon the boundary-data operator A in L sub 2 (gamma), mapping delta u / delta nu to u bar gamma for appropriate outgoing solutions u in Omega(+). By studying the operator I + BA, it is proven that the problem is well-posed and various construction techniques are established. GRA

**N88-13916#** Ballistic Research Labs., Aberdeen Proving Ground, Md.
**MULTIDIMENSIONAL LEAST SQUARES FITTING OF FUZZY MODELS Technical Report, Jun. 1985 - Jun. 1986**
Aivars K. R. Celmins 10 Apr. 1987 54 p
(AD-A185148; BRL-TR-2803) Avail: NTIS HC A04/MF A01 CSCL 12A

We describe a new method for the fitting of differentiable fuzzy model functions to crisp data. The model functions can be either scalar or multi-dimensional and need not be linear. The data are n-component vectors. An efficient algorithm is achieved by restricting the fuzzy model functions to sets which depend on fuzzy parameter vector and assuming that the vector has a conical membership function. A fuzzy model function, equated to zero, defines in the n-space a fuzzy hypersurface. Simple properties of such surfaces are established and a structure in the space of fuzzy manifolds is introduced by defining a discord and collocation between any two fuzzy manifolds. Using these concepts and the restriction to conical membership functions, we derive a simple spread propagation formula for arbitrary functions of fuzzy variables. The model fitting is done in a least squares sense by minimizing the squares of the deviations from one of the membership values of the fitted hypersurface at the observations. Under the outlined restriction, the problem can be reduced to an ordinary least squares formulation for which software is available. squares formulation for which software is available. GRA

**N88-13917#** Ballistic Research Labs., Aberdeen Proving Ground, Md.
**LEAST SQUARES FOR FUZZY VECTOR DATA REGRESSION**
Aivars K. Celmins Jun. 1987 48 p
(AD-A185156; BRL-TR-2817) Avail: NTIS HC A03/MF A01 CSCL 12A

We consider model fitting problems in which the mathematical model of an observed event is a system of equations involving model parameters and observables, and in which the data are fuzzy vectors. Such problems naturally arise in applications when data are scarce and information is vague about distributions of variances that are contained in the observations. Then it may only be possible to obtain estimates of membership functions of the data. A model can be fitted to such data by maximizing the membership values of the adjusted observations. We achieve this by minimizing the sum of squares of the the deviations of the membership values from one. The optimization problem simplifies

significantly if the membership functions of the fuzzy vectors belong to a class of conical functions, which are defined in terms of an elliptic norm. Properties of these functions are discussed and a membership propagation formula derived which component-wise obeys the extension principle. Author (GRA)

**N88-13918#** Wyoming Univ., Laramie.
**NUMERICAL AND ANALYTICAL METHODS IN NONLINEAR PARTIAL DIFFERENTIAL EQUATIONS Final Technical Report, 1 Nov. 1983 - 30 Apr. 1987**
Richard E. Ewing 30 Apr. 1987 18 p
(Contract DAAG29-84-K-0002)
(AD-A185210; ARO-19855.40-MA) Avail: NTIS HC A03/MF A01 CSCL 12A

Complex physical phenomena involving chemically reacting systems or the transport of heat or fluids are often modeled by coupled systems of time-dependent, nonlinear partial differential equations. The difficulties in understanding the stability of the differential equation systems and in designing efficient, accurate numerical methods for their solution are widely recognized and were the focus of this research. We have worked on four general aspects of the analysis and numerical approximation of systems of partial differential equations. These areas of research are: (1) modeling aspects and stability analysis for nonlinear time-dependent partial differential equations; (2) use and analysis of finite element or finite difference methods to discretize coupled systems of nonlinear differential equations; (3) development of adaptive or local grid refinement capabilities to resolve local phenomena in large-scale applications; and (4) development of data structures, preconditioners, and efficient solution algorithms for large-scale problems on new computer architectures. Emphasis has been placed upon multiphase or multicomponent, transport-dominated flow processes with dynamic local phenomena. The research also involved a mix of analysis, algorithm development, and large-scale computation using newer computer architectures. GRA

**N88-13919#** Clarkson Univ., Potsdam, N.Y. Dept. of Mathematics and Computer Science.
**EIGENVECTORS OF DISTANCE-REGULAR GRAPHS**
David L. Powers 1987 26 p
(Contract N00014-85-K-0497)
(AD-A185375; AD-E500888) Avail: NTIS HC A03/MF A01 CSCL 12B

The objective of this work is to find properties of a distance-regular graph G that are expressed in the eigenvectors of its adjacency matrix. The approach is to consider the rows of a matrix of orthogonal eigencolumns as (coordinates of) points in euclidean space, each one corresponding to a vertex of G. For the second eigenvalue, the symmetry group of the points is isomorphic to the automorphism group of G. Adjacency of vertices is related to linear dependence, linear independence and proximity of points. Relative position of points studied by way of the polytope that is their convex hull. Several families of examples are included. GRA

**N88-13920#** WEA, Cambridge, Mass.
**COMPUTATION OF NATURAL FREQUENCIES OF PLANAR LATTICE STRUCTURE Technical Report, 1 Sep. 1985 - 1 Mar. 1987**
James H. Williams, Jr. and Raymond J. Nagem 1 Mar. 1987 65 p
(Contract F49620-85-C-0148)
(AD-A185387; AFOSR-87-1006TR) Avail: NTIS HC A04/MF A01 CSCL 22B

Transfer matrices and joint coupling matrices are used to compute natural frequencies of vibration of a five-bay planar lattice structure. The method of analysis may be applied to general two- and three-dimensional lattices. The necessary numerical computations may be performed easily with a personal computer. Numerical results for the first twenty-five nonzero natural frequencies of the five-bay planar lattice structure are given for the case when the members of the lattice are modeled as Bernoulli-Euler beams, and for the case when the members of the lattice are modeled as Timoshenko beams. The maximum difference in the computed natural frequencies of the two models occurs in the twenty-fifth mode and is less than one-half of one percent. The natural frequencies obtained here agree within six percent with the natural frequencies obtained in a previous analysis using a finite element method and an experimental modal analysis. GRA

**N88-13921#** North Carolina Univ., Chapel Hill. Center for Stochastic Processes.
**POINT PROCESSES Technical Report, Sep. 1986 - Sep. 1987**
Richard F. Serfozo May 1987 88 p
(Contracts F49620-85-C-0144; AF-AFOSR-84-0367)
(AD-A185398; TR-185; AFOSR-87-1105TR) Avail: NTIS HC A05/MF A01 CSCL 12A

This document describes the structure of most point processes and discusses some of their basic properties. The coverage does not include several important topics requiring lengthy mathematical development (e.g. martingale theory of point processes, general Palm probabilities, and ergodic and spectral analysis of stationary processes). The emphasis will be one presenting tools for modeling stochastic systems rather than on applications of the tools. Although the theory of point processes is intimately connected with the subject of measure and integration (a point process is a random counting measure). The author focused on results that can be understood without a deep knowledge of measure theory. On the other hand, the presentation will be rigorous and at the level of the applied probability literature that one would encounter in studying point processes. Author (GRA)

**N88-13922#** North Carolina State Univ., Raleigh. Dept. of Mathematics.
**THE NUMERICAL AND ANALYTIC OF IMPLICIT DIFFERENTIAL EQUATIONS AND THEIR APPLICATION TO CONTROL AND CIRCUIT PROBLEMS Final Report, 16 Jul. 1984 - 15 Jan. 1987**
Stephen L. Campbell 1 Feb. 1987 14 p
(Contracts AF-AFOSR-84-0240; AF Proj. 2304)
(AD-A185404; AFOSR-87-1151TR) Avail: NTIS HC A02/MF A01 CSCL 12B

Results on the numerical and analytic solution of implicit systems of differential equations and their application to circuit and control problems were developed. In particular, the first general algorithm for the linear time varying case was developed along with an analysis of how to apply it to certain control problems. New structure theorems provide insight on the convergence of backward differentiation formulas and guidelines for their use. Author (GRA)

**N88-13923#** Maryland Univ. Baltimore County, Catonsville. Dept. of Mathematics
**NUMERICAL METHODS FOR REACTION-DIFFUSION PROBLEMS WITH NON-DIFFERENTIABLE KINETICS Summary Report**
A. K. Aziz, A. B. Stephens, and Manil Suri 7 Nov. 1986 23 p
(Contracts AF-AFOSR-85-0322; AF Proj. 2304)
(AD-A185405; UMBC-MRR-86-2; AFOSR-87-1036TR) Avail: NTIS HC A02/MF A01 CSCL 12A

This document considers a class of steady-state semi- linear reaction-diffusion problems with non-differentiable kinetics. The analytical properties of these problems have received considerable attention in the literature. The first step in analyzing their numerical approximation is taken. The authors present a finite element method and establish error bounds which are optimal for some of the problems. In addition, a finite difference approach is also discussed. Numerical experiments for one-and two-dimensional problems are reported. Author (GRA)

**N88-13924#** Virginia Univ., Charlottesville. Dept. of Electrical Engineering.
**ROBUST PREDICTION OPERATIONS FOR STATIONARY PROCESSES**
P. P. Kazakos 18 Aug. 1987 28 p

(Contracts AF-AFOSR-87-0224; AF Proj. 2304)
(AD-A185408; UVA/525682/EE88/101; AFOSR-87-1085TR)
Avail: NTIS HC A03/MF A01 CSCL 12A

Considered is a prediction for stationary processes, in environments where data outliers may be present. Developed is a sequence of outlier resistant prediction operations, which is uniformly qualitatively robust. Studied are the asymptotic mean-squared performance of the developed operations, both in the absence and the presence of i.i.d. data outliers. Important performance characteristics studied include the breakdown point and the influence function. Author (GRA)

**N88-13925#** North Carolina Univ., Chapel Hill. Center for Stochastic Processes.
**EXTREMA OF SKEWED STABLE PROCESSES**
Gennady Samorodnitsky Jun. 1987 38 p
(Contract F49620-85-C-0144)
(AD-A185422; TR-189; AFOSR-87-1143TR) Avail: NTIS HC A03/MF A01 CSCL 12A

Examined are extremes of (generally) skewed stable processes. In particular the author finds the asymptotic behavior of the distribution function of the order statistics from a (dependent) stable sample. Given are necessary conditions for a.s. boundedness of general stable processes. These conditions turn out to be sufficient when O is less than alpha less than 1. Further, asymptotic lower bounds O less than alpha less than 1 those bounds are shown to give the exact asymptotic behavior of the supremum and infimum distribution functions. GRA

**N88-13926#** Technische Hogeschool, Delft (Netherlands). Faculteit der Wiskunde en Informatica.
**THE ESTIMATION OF BASIC MATRICES USING TRAVEL INTENSITY THEOREMS [HET SCHATTEN VAN BASISMATRICES MET INTENSITEITSTELLINGEN]**
R. Hamerslag 1987 29 p In DUTCH
(Rept-87-13; B8711346; ISSN-0920-2358; ETN-88-90846)
Copyright Avail: NTIS HC A03/MF A01

Four modeling methods for the estimation of basic matrices, i.e., travel origin and destination tables, are presented. The first method, that is related to the weighted Poisson estimate, cannot be used together with intensity theorems, but provides preliminary information for the three other methods. This preliminary information is essential, but is lost in the second method, namely the information minimization method and entropy method. This objection can be circumvented in the information minimization method with elastic boundary conditions. The fourth method (binary calibration) considers the observations as stochastic quantities, in contrast with the second method. The coefficients in the forecasting models are estimated using all available data, including the intensity theorems. ESA

**N88-13927#** Rome Univ. (Italy). Dipartimento di Fisica.
**APPLICATION OF THE VON KARMAN EQUATION TO THE BIFURCATION THEORY [APPLICAZIONI DELLA TEORIA DELLE BIFORCAZIONI PER LE EQUAZIONI DI VON KARMAN]**
A. M. Allega and M. Rosati (Consiglio Nazionale delle Ricerche, Rome, Italy ) 13 Jul. 1987 48 p In ITALIAN Sponsored by CNR
(Nota-Interna-891; ETN-88-91252) Avail: NTIS HC A03/MF A01

It is proved that a given bifurcation problem described by an equation system in an infinite dimensional space can be frequently reduced to an equation system of Von Karman type. For the double eigenvalue case, the stability conditions are given as a function of the signs of the real parts of the 2 eigenvalues of the 2x2 jacobian matrix ESA

**N88-13928#** Technische Hogeschool Twente, Enschede (Netherlands). Center for Theoretical Physics.
**TRANSIENT PERIODIC BEHAVIOR RELATED TO A SADDLE-NODE BIFURCATION**
Ruud vanDamme and Theo P. Valkering Jun. 1986 21 p Sponsored by Stichting voor Zuiver Wetenschappelijk Onderzoek
(ETN-88-91321) Avail: NTIS HC A03/MF A01

Transient periodic orbits of dissipative invertible maps of R sq are obtained. Such orbits occur just before, in parameter space, a saddle-node bifurcation takes place. Simple scaling laws for the duration of the transient, and for the region of initial conditions which evolve into transient periodic orbits are obtained. An estimate of this region is obtained by the construction, after extension of the map to Csq, of the stable manifolds of the two complex saddles in Csq that bifurcate into the real saddle-node pair. ESA

**N88-13929#** Groningen Rijksuniversiteit (Netherlands). Dept. of Mathematics.
**A CONSTRUCTION OF SIMPLE ABELIAN VARIETIES**
F. Oort and M. vanderPut 1987 17 p
(ZW-8702; B8705703; ETN-88-91345) Avail: NTIS HC A03/MF A01

A result for (Y, mu) a polarized abelian variety over a field k is proved. ESA

**N88-13930#** Technische Hogeschool, Eindhoven (Netherlands).
**ON A NUMERICAL METHOD TO SOLVE CONTACT PROBLEMS Ph.D. Thesis**
Franiscus Petrus Tho Baaijens 1987 119 p
(B8711403; ETN-88-91367) Avail: NTIS HC A06/MF A01

A general formulation of the contact constraints, valid for each magnitude of the relative displacements, is given. Based on the method of weighted residuals a weak formulation that incorporates these constraints is given. A constitutive equation with which a large class of frictional phenomena can be described is derived. The model shows a strong analogy with models for elastoplastic material behavior. Reversible (micro-) slip and irreversible slip are distinguished. The amount of irreversible slip is determined with a slip criterion, while the direction follows from a quasi-associated slip rule. Based on the finite element method numerical simulations are made. In the discretization of the governing equations difficulties arise with respect to the contact constraints. A solution is described. The resulting system of nonlinear (vector) equations is solved iteratively by application of Newton's method. ESA

**N88-13931*#** National Aeronautics and Space Administration. Lewis Research Center, Cleveland, Ohio.
**SHARP SIMULATION OF DISCONTINUITIES IN HIGHLY CONVECTIVE STEADY FLOW**
B. P. Leonard Dec. 1987 35 p Prepared in cooperation with Akron Univ., Ohio.
(NASA-TM-100240; E-3863; ICOMP-87-9; NAS 1.15:100240)
Avail: NTIS HC A03/MF A01 CSCL 20D

For steady multidimesional convection, the Quadratic Upstream Interpolation for Convective Kinematics (QUICK) scheme has several attractive properties. However, for highly convective simulation of step profiles, QUICK produces unphysical overshoots and a few oscillations, and this may cause serious problems in nonlinear flows. Fortunately, it is possible to modify the convective flux by writing the normalized convected control-volume face value as a function of the normalized adjacent upstream node value, developing criteria for monotonic resolution without sacrificing formal accuracy. This results in a nonlinear functional relationship between the normalized variables, whereas standard methods are all linear in this sense. The resulting Simple High Accuracy Resolution Program (SHARP) can be applied to steady multidimensional flows containing thin shear or mixing layers, shock waves, and other frontal phenomena. This represents a significant advance in modeling highly convective flows of engineering and geophysical importance. SHARP is based on an explicit, conservative, control-volume flux formation, equally applicable to one, two, or three dimensional elliptic, parabolic, hyperbolic, or mixed-flow regimes. Results are given for the bench-mark purely convective first-order results and the nonmonotonic predictions of second- and third-order upwinding. Author

**N88-13932#** Sandia National Labs., Albuquerque, N. Mex.
**TUTORIAL ON ELEMENTARY BIFURCATION THEORY**

L. A. Romero Sep. 1987 10 p Presented at the Symposium on Technology of Glass, Ceramic, or Glass-Ceramic to Metal Sealing, Boston, Mass., 13 Dec. 1987
(Contract DE-AC04-76DP-00789)
(DE87-014849; SAND-87-1859C; CONF-871207-16) Avail: NTIS HC A02/MF A01

Elementary results on bifurcations of equilibrium and periodic solutions are presented. When solving equations of motion equilibrium conditions of second order systems, two stable regimes can be found. The point at which the two solutions intersect is called a bifurcation point. Bifurcation theory is concerned with multiple solutions to nonlinear equations and how these solutions appear, disappear, and intersect as equation parameters are changed. DOE

**N88-13933#** Los Alamos National Lab., N. Mex. Center for Nonlinear Studies.
**CHAOS: CHTO DELAT? (WHAT IS TO BE DONE?)**
David Campbell 1987 23 p Presented at the International Conference on Physics of Chaos and Systems Far From Equilibrium, Monterey, Calif., 11 Jan. 1987
(Contract W-7405-eng-36)
(DE88-000513; LA-UR-87-2942; CONF-870159-5) Avail: NTIS HC A03/MF A01

Provided is a brief overview of the current status of the field of deterministic chaos, stressing its interrelations and applications to other fields and suggesting a number of important open problems for future study. DOE

**N88-13934#** Texas Univ., Austin.
**RESEARCH AND DEVELOPMENT OF FINITE ELEMENTS AND ITERATIVE ALGORITHMS FOR ELLIPTIC PARTIAL DIFFERENTIAL EQUATIONS Final Report, 1 Aug. 1984 - 31 Aug. 1987**
G. F. Carey and D. M. Young 31 Aug. 1987 36 p
(Contract DE-AS05-81ER-10954)
(DE88-001381; DOE/ER-10954/4) Avail: NTIS HC A03/MF A01

This study deals with the use of iterative solution algorithms in conjunction with finite element methods for solving partial differential equations arising in mechanics. Some aspects of the work are directed to the question of suitability of classes of techniques for computations on advanced vector and parallel architectures. DOE

**N88-13935*#** Old Dominion Univ., Norfolk, Va. Dept. of Electrical and Computer Engineering.
**GUIDANCE AND CONTROL STRATEGIES FOR AEROSPACE VEHICLES Progress Report, 1 Jul. - 31 Dec. 1987**
Joseph L. Hibey and D. S. Naidu Jan. 1987 39 p
(Grant NAG1-736)
(NASA-CR-181579; NAS 1.26:181579) Avail: NTIS HC A03/MF A01 CSCL 12A

A simplified method of matched asymptotic expansions was developed where the common part in composite solution is generated as a polynomial in stretched variable instead of actually evaluating the same from the outer solution. This methodology was applied to the solution of the exact equations for three dimensional atmospheric entry problems. Compared to previous works, the present simplified methodology yields explicit analytical expressions for various components of the composite solution without resorting to any type of transcendental equations to be solved only by numerical methods. The optimal control problem arising in the noncoplanar orbital transfer employing aeroassist was also addressed. B.G.

**N88-13285#** Tohoku Univ., Sendai (Japan). Dept. of Mechanical Engineering.
**TIME-MARCHING FINITE-DIFFERENCE METHODS FOR THE THREE-DIMENSIONAL EULER EQUATIONS OF CONTRAVARIANT VELOCITY COMPONENTS**
Hisaaki Daiguji and Satoru Yamamoto *In* National Aerospace Lab., Proceedings of the 4th NAL Symposium on Aircraft Computational Aerodynamics Dec. 1986 p 267-276 In JAPANESE; ENGLISH summary (For primary document see N88-13253 05-02)
Avail: NTIS HC A14/MF A01

# 65 STATISTICS AND PROBABILITY

Includes data sampling and smoothing; Monte Carlo method; and stochastic processes.

**N88-13936*#** California Univ., San Diego, La Jolla. Inst. of Geophysics and Planetary Physics.
**ISOTROPIC PROBABILITY MEASURES IN INFINITE DIMENSIONAL SPACES: INVERSE PROBLEMS/PRIOR INFORMATION/ STOCHASTIC INVERSION**
George Backus 4 Sep. 1987 10 p
(Grants NAG5-818; NSF EAR-85-21543)
(NASA-CR-181555; NAS 1.26:181555) Avail: NTIS HC A02/MF A01 CSCL 12A

Let R be the real numbers, R(n) the linear space of all real n-tuples, and R(infinity) the linear space of all infinite real sequences x = (x sub 1, x sub 2,...). Let P sub n :R(infinity) approaches R(n) be the projection operator with P sub n (x) = (x sub 1,...,x sub n). Let p(infinity) be a probability measure on the smallest sigma-ring of subsets of R(infinity) which includes all of the cylinder sets P sub n(-1) (B sub n), where B sub n is an arbitrary Borel subset of R(n). Let p sub n be the marginal distribution of p(infinity) on R(n), so p sub n(B sub n) = p(infinity)(P sub n to the -1(B sub n)) for each B sub n. A measure on R(n) is isotropic if it is invariant under all orthogonal transformations of R(n). All members of the set of all isotropic probability distributions on R(n) are described. The result calls into question both stochastic inversion and Bayesian inference, as currently used in many geophysical inverse problems. M.G.

**N88-13937#** South Carolina Univ., Columbia. Dept. of Statistics.
**FURTHER STUDIES IN ESTIMATION OF LIFE DISTRIBUTION CHARACTERISTICS FROM CENSORED DATA Final Technical Report, 1 Jun. 1984 - 31 May 1987**
W. J. Padgett Jun. 1987 19 p
(Contract MIPR-ARO-139-85)
(AD-A184862; ARO-21245.26-MA) Avail: NTIS HC A02/MF A01 CSCL 12A

The main objectives of this research have been the development of smooth nonparametric estimators of quantile functions from right-censored data and the further study of smooth density estimators from censored observations. In particular, kernel-type and generalized quantile estimators have been obtained under censoring which give better estimates of percentiles of the lifetime distribution than the usual product-limit quantile estimator. Asymptotic properties of these quantile estimators have been developed, including asymptotic normality and consistency. Also, the mean-square convergence and mean squared error of the kernel quantile estimators have been investigated. A data-based procedure for selecting the bandwidth has been studied using the bootstrap, and approximate confidence intervals for the true quantile have been proposed using bootstrap estimates of the sampling distribution. Theoretical results on the optimal bandwidth selection for kernel density estimators under random right censorship have also been obtained. GRA

**N88-13938#** Southern Methodist Univ., Dallas, Tex. Dept. of Statistical Science.
**SAMPLE REUSE IN STATISTICAL REMODELING Final Technical Report**
William R. Schucany Aug. 1987 9 p
(Contract N00014-85-K-0340)
(AD-A184916) Avail: NTIS HC A02/MF A01 CSCL 12A

The primary objective of this contract has been the development and extension of sample reuse techniques in statistical modeling. To a great extent the models that have been examined are

nonparametric or non-Gaussian. The resampling schemes that have been employed and extended are the jackknife, the bootstrap and generalized cross validation. Many new and potentially important results have been established. These are summarized in the next section. In section 4 our technical proposal presents a continuation of the discussion of some of these topics. In that section are outlined research objectives and the approaches to be taken during the proposed two-year renewal of the project. GRA

**N88-13939#** Cornell Univ., Ithaca, N.Y. Mathematical Sciences Inst.

**ILLUSTRATIVE EXAMPLES OF PRINCIPAL COMPONENT ANALYSIS USING SYSTAT/FACTOR Interim Technical Report**

W. T. Federer, C. E. McCulloch, and J. J. Miles-McDermott 20 May 1987 34 p

(Contract DAAG29-85-C-0018)

(AD-A184920; TR-87-50; ARO-23306.87-MA) Avail: NTIS HC A03/MF A01 CSCL 12A

In order to provide a deeper understanding of the workings of principal components, four data sets were constructed by taking linear combinations of values of two correlated variables to form the X-variates for the principal component analysis. The examples highlight some of the properties and limitations of principal component analysis. This is part of a continuing project that produces annotated computer output for principal component analysis. The complete project will involve processing four examples on SAS/PRINCOMP, BMDP/4M, SPSS-X/FACTOR, GENSTAT / PCP, and SYSTAT / FACTOR. We show here the results from SYSTAT/FACTOR, Version 3. Author (GRA)

**N88-13940#** Naval Research Lab., Washington, D.C.

**DETERMINING DIFFERENCES IN RATES CORRESPONDING TO A GIVEN SIGNIFICANCE LEVEL Final Memo. Report, Oct. 1986 - Mar. 1987**

Allen R. Miller and Martin Feuerman 4 Sep. 1987 9 p Prepared in cooperation with New Jersey Medical School, Newark

(AD-A185004; NRL-MR-6060) Avail: NTIS HC A02/MF A01 CSCL 12A

The well-known Chi-square test can be used to determine whether the difference in two rates is statistically significant, and if so, at what level of significance. This paper discusses the related question of how large a difference in rates must be (when one rate is held constant) in order to show statistical significance at a given level of significance. An illustrative example, adapted from data appearing in the biostatistical literature, is provided. GRA

**N88-13941#** Cornell Univ., Ithaca, N.Y. Mathematical Sciences Inst.

**ILLUSTRATIVE EXAMPLES OF PRINCIPAL COMPONENT ANALYSIS USING GENSTAT/PCP Interim Report**

W. T. Federer, Z. D. Feng, and C. E. McCulloch 26 Jun. 1987 42 p

(Contract DAAG29-85-C-0018)

(AD-A185085; ARO-23306.93-MA) Avail: NTIS HC A03/MF A01 CSCL 12A

In order to provide a deeper understanding of the workings of principal components, four data sets were constructed by taking linear combinations of values of two uncorrelated variables to form the X-variates for the principal component analysis. This is part of a continuing project that produces annotated computer output for principal components analysis. The complete project will involve processing four examples on SAS/PRINCOMP, BMDP/4M, SPSS-X/FACTOR, GENSTAT/PCP, and SYSTAT/FACTOR. We show here the results from GENSTAT/PCP, Version 4.04. GRA

**N88-13942#** Texas A&M Univ., College Station. Dept. of Statistics.

**QUANTILE BASED UNIFIED DISTRIBUTION OF EXTREME VALUES AND ORDER STATISTICS**

Emanuel Parzen Jun. 1987 32 p

(Contract DAAL03-87-K-0003)

(AD-A185171; TR-Q-2; ARO-23010.2-MA) Avail: NTIS HC A03/MF A01 CSCL 12A

This paper presents ideas leading to unified formulas for exact and asympotic distributions of central and extreme order statistics of random samples and stationary time series X(t) in terms of quantile functions Q(u), density quantile functions fQ(u), left and right hazard quantile functions hQ(u), defined to equal respectively fQ(u)/u and fQ(u)/(1-u), tail exponents, and the spectral density near zero frequency of a two-valued time series c(x(t);u), equal to 1-u or -u as X(t) less than Q(u) or X(t) greater than Q(u). Author (GRA)

**N88-13943#** Texas A&M Univ., College Station. Dept. of Statistics.

**QUANTILE STATISTICAL DATA ANALYSIS**

Emanuel Parzen Feb. 1987 13 p

(Contract DAAL03-87-K-0003)

(AD-A185181; TR-Q-1; ARO-23010.1-MA) Avail: NTIS HC A03/MF A01 CSCL 12A

This paper presents some reasons why theoretical and sample quantile functions would be routinely used by contemporary statistical data analysts. Quantile methods are introduced in the context of the exponential distribution as a fit to the historically important life table data of Graunt (1661). Section titles are: history of statistics and contemporary textbooks; quantile concepts; identification quantile function; identification quantile box plot; tail classification of probability laws; goodness of fit plots; IQQ plot; cumulative weighted spacings function D (u); quantile simulations and distribution of extreme values; comparison quantile function; nonparametric estimation of probability density; conclusion. Author (GRA)

**N88-13944#** North Carolina Univ., Chapel Hill. Center for Stochastic Processes.

**FREIDLIN-WENTZELL TYPE ESTIMATES AND THE LAW OF THE ITERATED LOGARITHM FOR A CLASS OF STOCHASTIC PROCESSES RELATED TO SYMMETRIC STATISTICS Report, Sep. 1986 - Sep. 1987**

Toshio Mori and Hiroshi Oodaira May 1987 13 p

(Contract F49620-85-C-0144)

(AD-A185366; TR-184; AFOSR-87-1106TR) Avail: NTIS HC A02/MF A01 CSCL 12A

Analogues of Freidlin and Wentzell's estimates for diffusion processes and the functional law of the iterated logarithm are obtained for a class of stochastic processes represented by multiple Wiener integrals with respect to two parameter Wiener processes, which arise as the limit processes of sequences of normalized symmetric statistics. Author (GRA)

**N88-13945#** Societe Nationale Industrielle Aerospatiale, Saint-Medard-en-Jalles (France).

**PRESENTATION OF A COMPUTER PROGRAM PERMITTING THE EXPLOITATION OF TESTS DESIGNED TO DETERMINE THE SENSITIVITY OF ONE SHOT DEVICES TO A PARAMETER. APPLICATION TO A DEGENERATE ONE SHOT SEQUENCE [PRESENTATION D'UN LOGICIEL PERMETTANT L'EXPLOITATION DES TESTS VISANT A DETERMINER LA SENSIBILITE DES DISPOSITIFS MONOCOUP VIS A VIS D'UN PARAMETRE. APPLICATION AU CAS D'UNE SEQUENCE ONE SHOT DEGENEREE]**

Ch. Saubade 1987 18 p In FRENCH

(SNIAS-872-430-117; ETN-88-91228) Avail: NTIS HC A03/MF A01

A computational principle derived from confidence interval determination and maximum likelihood is described. The computation of standard deviation, safety level, and operating level associated to a given risk is discussed. A computer program in which the mentioned principles are developed with the help of Monte Carlo techniques is presented. ESA

**N88-13946** Politecnico di Milano (Italy). Dipartamento di Elettronica.
**A FUNCTIONAL INTERPRETATION OF THE LOGISTIC EQUATION**
Marino Gatto, Simona Muratori, and Sergio Rinaldi 1987 8 p
(Rept-87-037; ETN-88-91305) Avail: Issuing Activity

The Verhulst-Pearl equation (logistic equation), used to describe the growth of populations, is interpreted from a functional point of view. A simple problem of optimal growth is formulated, then solved with the Euler-Lagrange equation. The analysis of the solution shows that the optimal growth is logistic if the functional to be minimized is defined over an infinite time horizon. Logistic growth represents the best trade-off between deviation from optimal size and cost of growing of a population over its entire life. Such a functional interpretation of the Verhulst-Pearl equation is simpler and more intuitive than those given by Volterra (1939) and Leitmann (1972) which were not formulated over an infinite time horizon. ESA

**N88-13947#** Michigan Univ., Ann Arbor. Dept. of Electrical Engineering and Computer Science.
**ON THE CORRELATION FREE FORMS FOR NONLINEAR STOCHASTIC SYSTEMS**
S. M. Meerkov, T. Runolfsson, and Z. Schuss Dec. 1987 19 p Presented at the 26nd IEEE CDC Conference, Los Angeles, Calif., 9 Dec. 1987 Prepared in cooperation with Tel Aviv Univ., Israel
(Contract DE-FG02-85ER-13315)
(DE87-011169; CONF-871211-1) Avail: NTIS HC A03/MF A01

A method for analysis of nonlinear systems with wide-band and high-frequency stochastic parametric oscillations is developed and a correlation free description is obtained. Several illustrative examples are considered. DOE

**N88-13948#** Los Alamos National Lab., N. Mex.
**MODELING AND GENERATING INPUT PROCESSES**
M. E. Johnson 1987 4 p Presented at the Winter Simulation Conference, Atlanta, Ga., 14 Dec. 1987
(Contract W-7405-eng-36)
(DE87-013162; LA-UR-87-2453; CONF-871216-1) Avail: NTIS HC A02

This tutorial paper provides information relevant to the selection and generation of stochastic inputs to simulation studies. The primary area considered is multivariate but much of the philosophy at least is relevant to univariate inputs as well. DOE

# 66 SYSTEMS ANALYSIS

Includes mathematical modeling; network analysis; and operations research.

**N88-13949** Technische Hogeschool, Delft (Netherlands). Faculty of Mathematics and Informatics/Computer Science.
**THE ISOTROPIC ROCKET: A SURVEILLANCE EVASION GAME**
Joseph Lewin and Geert Jan Olsder 1987 47 p
(Rept-87-21; B8713114; ETN-88-91341) Copyright Avail: Issuing Activity

A vehicle, with bounded speed and the capability of instantaneous turns, that tries to escape from a circular region (such as from a radar) attached to a pursuer who has a bounded magnitude of acceleration, but who has the capability to direct the acceleration in any direction instantaneously, is considered. The central question is under what circumstances, i.e., for which parameter values and initial conditions, can the pursuer keep the vehicle (also called the evader) forever under surveillance. A subset of the state space from where the evader cannot escape is given. The state space is three-dimensional and the problem has analogies with the isotropic rocket game treated by Isaacs and Bernhard (1966, 1970). ESA

# 67 THEORETICAL MATHEMATICS

Includes topology and number theory.

**N88-13950#** Centro Brasileiro de Pesquisas Fisicas, Rio de Janeiro.
**COMPUTER-AIDED STUDY OF A CLASS OF RIEMANNIAN SPACE-TIMES**
M. J. Reboucas and J. E. Aman 1986 22 p
(DE87-703367; CBPF-NF-041/86) Avail: NTIS (US Sales Only) HC A03/MF A01

The Riemannian Goedel-type manifolds are examined in the light of the equivalence problem techniques by using algebric computing. The conditions for space-time homogeneity of a Riemannian manifold with a Goedel-type metric are derived, generalizing previous work on this subject matter. A classification of the Goedel-type Riemannian manifolds based on two relevant parameters m and Omega is formulated. It is shown that apart from the m(sup 2)=4 Omega (sup 2) case they are all Petrov type D with a five-parameter group of motions. The special m(sup 2)=4 Omega (sup 2) manifold is shown to be conformally flat and to admit a seven-parameter group of isometries. An algebric classification of the Ricci spinor of all Goedel-type Riemannian manifolds is discussed. Possible sources for these space-times are examined. A generalization of the Reboucas-Tiomno theorem on Goedel-type manifolds is given. DOE

**N88-13951*#** National Aeronautics and Space Administration. Ames Research Center, Moffett Field, Calif.
**A SYSTEM OF THREE-DIMENSIONAL COMPLEX VARIABLES**
E. Dale Martin Jun. 1986 7 p
(NASA-TM-88318; A-86302; NAS 1.15:88318) Avail: NTIS HC A02/MF A01 CSCL 12A

Some results of a new theory of multidimensional complex variables are reported, including analytic functions of a three-dimensional (3-D) complex variable. Three-dimensional complex numbers are defined, including vector properties and rules of multiplication. The necessary conditions for a function of a 3-D variable to be analytic are given and shown to be analogous to the 2-D Cauchy-Riemann equations. A simple example also demonstrates the analogy between the newly defined 3-D complex velocity and 3-D complex potential and the corresponding ordinary complex velocity and complex potential in two dimensions. Author

# 70 PHYSICS (GENERAL)

For precision time and time interval (PTTI) see *35 Instrumentation and Photography;* for geophysics, astrophysics or solar physics see *46 Geophysics, 90 Astrophysics,* or *92 Solar Physics.*

**N88-13952#** Lawrence Livermore National Lab., Calif.
**DEVELOPMENT OF A STRONG ELECTROMAGNET WIGGLER**
M. J. Burns, G. A. Deis, R. H. Holmes, R. D. VanMaren, and K. Halbach 1987 6 p Presented at the 10th International Conference on Magnet Technology (MT-10), Boston, Mass., 21 Sep. 1987 Prepared in cooperation with California Univ., Berkeley, Lawrence Berkeley Lab.
(Contract W-7405-eng-48)
(DE88-000971; UCRL-96289; CONF-870901-9) Avail: NTIS HC A02/MF A01

The Strong Electromagnet (SEM) wiggler is a permanent magnet-assisted electromagnet under development at the Lawrence Livermore National Laboratory (LLNL) as part of the Induction Linac Free-Electron-Laser (IFEL) program. This concept uses permanent magnets within the wiggler to provide a reverse bias flux in the iron and thus delay the onset of magnetic saturation. The electromagnet coils determine the wiggler field and operate at low current densities by virtue of their placement away from the midplane. We describe here the design approach used and test data from a 7-period wiggler prototype that includes curved pole tips to provide wiggle-plane focusing. DOE

**N88-13953#** Lawrence Livermore National Lab., Calif.
**DEVELOPMENT OF A LACED ELECTROMAGNETIC WIGGLER**
T. C. Christensen, M. J. Burns, G. A. Deis, C. D. Parkison, D. Prosnitz, and K. Halbach 1987 6 p Presented at the 10th International Conference on Magnet Technology (MT-10), Boston, Mass., 21 Sep. 1987 Prepared in cooperation with California Univ., Berkeley, Lawrence Berkeley Lab.
(Contract W-7405-eng-48)
(DE88-000972; UCRL-96288; CONF-870901-7) Avail: NTIS HC A02/MF A01

The laced electromagnetic wiggler is a new concept being developed to attain higher magnetic fields, shorter wavelengths, and larger gaps for the induction-linear accelerator, free-electron-laser (FEL) program. In the laced wiggler design, permanent magnets are located (laced) between the electromagnetic coils to increase the reverse-bias flux in the iron pole beyond that possible with only pole-edge (side) permanent magnets. This increase in reverse-bias flux allows wiggler operation at midplane magnetic field intensities comparable to those of a hybrid permanent magnet/steel wiggler, but with field adjustability over a specified range. The maximum field intensity and tuning range are selected, within limits, for specific design requirements. A one-period prototype of this concept has been designed and tested with promising results. DOE

**N88-13954*#** Martin Marietta Corp., Denver, Colo. Astronautics Group.
**FEASIBILITY STUDY FOR GAS-GRAIN SIMULATION FACILITY Final Contractor Report**
J. B. Miller and B. C. Clark Sep. 1987 104 p
(Contract NAS2-11370)
(NASA-CR-177468; NAS 1.26:177468) Avail: NTIS HC A06/MF A01 CSCL 14B

Presented are the results of a feasibility study conducted to examine physical phenomena involved in gas-grain interactions using a Gas-Grain Simulation Facility (GGSF). Author

# 71 ACOUSTICS

Includes sound generation, transmission and attenuation. For noise pollution see *45 Environmental Pollution.*

**N88-13955** British Broadcasting Corp., Kingswood (England). Engineering Div.
**THEORETICAL AND PRACTICAL ASPECTS OF THE FUNCTIONAL ABSORBER METHOD OF ARRANGING SOUND ABSORBING PANELS**
E. W. Taylor Oct. 1987 22 p
(BBC-RD-1987/15) Avail: Issuing Activity

Measurements of the absorption of sound by functional absorbers (panels of porous material mounted so that both sides are exposed to the sound field) are described, the absorbers being arranged in a number of different configurations. The effect of increasing the surface density of the absorbing panels without significantly changing their thickness or porosity is examined, and deductions are made about the mechanisms of absorption at different frequencies. Author

**N88-13956#** Texas Univ., Austin. Applied Research Lab.
**APPLICATION OF VANDERMONDE DECOMPOSITION TO DIRECTIONAL AND MODAL ANALYSIS OF BROADBAND TRANSIENTS Final Report, 1 Jun. 1985 - 30 Nov. 1986**
Terry L. Henderson 11 Jun. 1987 29 p
(Contract N00014-85-K-0501)
(AD-A185007; ARL-TR-87-29) Avail: NTIS HC A03/MF A01 CSCL 12A

Progress in the theory and applications of Vandermonde decomposition is briefly summarized. The broadband direction finding application is outlined. A step-by-step description of the factorization algorithm is given. Efforts to localize broadband acoustic transients are summarized. GRA

**N88-13957#** Naval Postgraduate School, Monterey, Calif.
**DEVELOPMENT OF A NEW METHOD OF MEASURING THE CHARACTERISTIC IMPEDANCE AND COMPLEX WAVE NUMBER OF A POROUS ACOUSTIC MATERIAL M.S. Thesis**
Frederick Fay Schulz Jun. 1987 128 p
(AD-A185038) Avail: NTIS HC A07/MF A01 CSCL 20A

The specific DC flow resistance, characteristic impedance and complex wave number of air-filled fiberglass have been extracted from measurements of the peak and half-power frequencies of the two lowest-frequency normal modes of a rectangular plexiglass cavity partially filled with fiberglass. Using Biot theory (Ref's. 8, 9 and 10) to describe the sound field within the fiberglass, a dispersion relation for the allowed modes in the cavity was derived, from which the above properties were extracted. The values determined by this new method compared favorably (within 25%) with the results of measurements using classical methods. The new method differs from the classical resonance tube method (Ref. 4) by 1) the use of a wave theory to describe the sound field within the fiberglass 2) the use of a mode with particle velocity parallel to the air-fiberglass interface. The differences make it possible to extract the acoustic properties of bulk fiberglass using only a thin sample. GRA

**N88-13958#** Johns Hopkins Univ., Baltimore, Md. Dept. of Materials Science and Engineering.
**FULL FIELD VISUALIZATION OF SURFACE AND BULK ACOUSTIC WAVES USING HETERODYNE HOLOGRAPHIC INTERFEROMETRY Annual Summary Report, 1 Dec. 1986 - 15 Sep. 1987**
James W. Wagner and Robert E. Green, Jr. 15 Sep. 1987 11 p
(Contract N00014-82-K-0741)
(AD-A185071) Avail: NTIS HC A03/MF A01 CSCL 09D

The objective of this research has been to apply optical holographic techniques coupled with electronic signal and image processing to provide quantitative, full field measurements of acoustic wave disturbances. This program has sought to establish the limits of sensitivity with which surface acoustic waves might be measured and mapped. In addition, an effort to extend heterodyne holographic measurements to the examination of acoustic energy flow in optically transparent bulk materials has begun. GRA

**N88-13959#** Metraflu, Ecully (France).
**COMPRESSOR LARGE BANDWIDTH NOISE EMISSION MECHANISMS Final Report [MECANISMES D'EMISSION LARGE BANDE DES COMPRESSEURS]**
Michel Roger Apr. 1987 37 p In FRENCH
(Contract DRET-83-34-497-00-470-75-01)
(ETN-88-91177) Avail: NTIS HC A03/MF A01

Noise generated by a double flow turboreactor fan was studied. Results of a numerical analysis of the noise due to preturbulence, the noise irradiated by turbulent wakes, a modal analysis of the propagation of noise through a rotating flow, and the analysis of the inertial stability of the rotating flow at the fan outlet and the noise generated by those instabilities are described. It is shown that the propagation of noise through a rotating flow is not limited to the acoustic modes, and the cut-off frequencies of the acoustic modes are different from those in steady flow. ESA

**N88-13960*#** National Aeronautics and Space Administration. Lewis Research Center, Cleveland, Ohio.
**HIGH SPEED PROPELLER PERFORMANCE AND NOISE PREDICTIONS AT TAKEOFF/LANDING CONDITIONS**
M. Nallasamy (Sverdrup Technology, Inc., Cleveland, Ohio.), R. P. Woodward, and J. F. Groeneweg [1987] 17 p Prepared for presentation at the 26th Aerospace Sciences Meeting, Reno, Nev., 11-14, Jan. 1988; sponsored by AIAA
(NASA-TM-100267; E-3898; NAS 1.15:100267) Avail: NTIS HC A03/MF A01 CSCL 20A

The performance and noise of a high speed SR-7A model propeller under takeoff/landing conditions are considered. The blade loading distributions are obtained by solving the

three-dimensional Euler equations and the sound pressure levels are computed using a time domain approach. At the nominal takeoff operating point, the blade sections near the hub are lightly or negatively loaded. The chordwise loading distributions are distinctly different from those of cruise conditions. The noise of the SR-7A model propeller at takeoff is dominated by the loading noise, similar to that at cruise conditions. The waveforms of the acoustic pressure signature are nearly sinusoidal in the plane of the propeller. The computed directivity of the blade passing frequency tone agrees fairly well with the data at nominal takeoff blade angle. Author

**N88-13961*#** National Aeronautics and Space Administration. Lewis Research Center, Cleveland, Ohio.
**NOISE OF A MODEL COUNTERROTATION PROPELLER WITH REDUCED AFT ROTOR DIAMETER AT SIMULATED TAKEOFF/APPROACH CONDITIONS (F7/A3)**
Richard P. Woodward and Eliott B. Gordon (Sverdrup Technology, Inc., Cleveland, Ohio.) 1988 31 p Presented at the 26th Aerospace Sciences Meeting, Reno, Nev., 11-14 Jan. 1988; sponsored by AIAA
(NASA-TM-100254; E-3880; NAS 1.15:100254; AIAA-88-0263) Avail: NTIS HC A03/MF A01 CSCL 20A

A model high-speed advanced counterrotation propeller, F7/A3, was tested in the NASA Lewis Research Center 9 by 15 foot Anechoic Wind Tunnel at simulated takeoff/approach conditions of 0.2 Mach number. Acoustic measurements were taken with an axially translating microphone probe, and with a polar microphone probe which was fixed to the propeller nacelle and could take both sideline and circumferential acoustic surveys. Aerodynamic measurements were also made to establish propeller operating conditions. The propeller was run at two setting angles (front angle/rear angle) of 36.4/43.5 and 41.1/46.4 degrees, forward rotor tip speeds from 165 to 259 m/sec, rotor spacings from 8.48 to 14.99 cm based on pitch change axis separation, and angles of attack to 16 degrees. The aft rotor diameter was 85 percent of the forward rotor diameter to reduce tip vortex-aft rotor interaction as a major interaction noise source. Results are compared with equal diameter F7/A7 data which was previously obtained under similar operating conditions. The aft rotor-alone tone was 7 dB lower for the reduced diameter aft rotor, due to reduced tip speed at constant rpm. Interaction tone levels for the F7/A3 propeller were higher at minimum row spacing and lower at maximum spacing. Author

**N88-13962*#** National Aeronautics and Space Administration. Langley Research Center, Hampton, Va.
**FLUCTUATING PRESSURE LOADS UNDER HIGH SPEED BOUNDARY LAYERS**
William E. Zorumski Oct. 1987 15 p Presented at the AIAA 11th Aeroacoustics Conference Workshop on Sonic Fatigue and Hypersonic Acoustic Loads, Sunnyvale, Calif. 19-21 Oct. 1987
(NASA-TM-100517; NAS 1.15:100517) Avail: NTIS HC A03/MF A01 CSCL 20A

Aeroacoustic fatigue is anticipated to control the design of significant portions of the structures of high-speed vehicles. This is due to contemplated long-duration flights at high dynamic pressures and Mach numbers with related high skin temperatures. Fluctuating pressure loads are comparatively small beneath attached turbulent boundary layers, but become important in regions of flow separation such as compression and expansion corners on elevons and rudders. The most intense loads are due to shock/boundary-layer interaction. These flows may occur in the engine-exhaust wall jet and in flows over control surfaces. A brief review is given of available research in these areas with a description of work under way at Langley Research Center. Author

**N88-13748#** China Ship Scientific Research Center, Wuxi.
**EXPERIMENTAL STUDIES ON ACOUSTIC EMISSION MONITORING OF CRACK PROPAGATION IN OFFSHORE STRUCTURES: A LITERATURE SURVEY**
Zhiyu Liu *In* Vibration Inst., The Shock and Vibration Digest, Volume 19, No. 12 Dec. 1987 p 6-17 (For primary document see N88-13746 05-39)
Avail: NTIS HC A06/MF A01

# 72 ATOMIC AND MOLECULAR PHYSICS

Includes atomic structure, electron properties, and molecular spectra.

**N88-13963#** Brookhaven National Lab., Upton, N. Y.
**THE ROLE OF ELECTRONIC STRUCTURE CALCULATION IN MECHANISTIC ANALYSIS OF ELECTRON TRANSFER REACTIONS IN THE LIQUID PHASE**
M. D. Newton Aug. 1987 16 p Presented at the Chemical Reactions in the Liquid State Center for Computational Chemistry Workshop, Orsay, France, 7 Sep. 1987
(Contract DE-AC02-76CH-00016)
(DE87-014395; BNL-40183; CONF-8709136-1) Avail: NTIS HC A03

Model calculations have been employed to elucidate the mechanism of electron transfer reactions in aqueous solution. The contribution of inner shell OH bonds to activation barriers has been estimated from calculation for metal ion hydrates. Calculated electron transfer matrix elements H sub if for redox processes of the type, ML sub 6 sup 2(+)+ ML sub 6 sup 3(+) in equilibrium ML sub 6 sup 3(+) + ML sub 6 sup 2(+), M = Fe, Co, or Ru, L = H2O or NH3, have been analyzed in terms of various orbital concepts. The matrix elements are based on ab initio wavefunctions for model supermolecule clusters of the type, (ML sub n ...L sub n M) sup 5(+), with n = 1 or 3. The analysis shows that the many-electron H sub if quantities can in fact be expressed to good approximation as effective 1-electron expressions of the type, H sub if proportional to lambda' sup 2 N sub c h sub L1Lr, where lambda' is the metal-ligand covalency parameter, h sub L1Lr is a local 1-electron matrix element for ligand orbitals in contact in the transition state, and N sub c is the number of such contacts. A least-squares fit of the data implies a value of approx. 5000/cm for h sub L1Lr, showing that significant coupling can occur in the absence of formal bonding between reactants. DOE

**N88-13964#** State Univ. of New York at Buffalo, Amherst.
**DYNAMICAL ANALYSIS OF MOLECULAR DECAY AT SPHERICAL SURFACES**
P. T. Leung and Thomas F. George Aug. 1987 19 p
(Contract N00014-86-K-0043)
(AD-A184908; TR-50) Avail: NTIS HC A03/MF A01 CSCL 07D

A dynamical approach to the classical decay rates for molecules near a dielectric sphere is presented through the application of the diffraction theory for a dipole antenna established by Van del Pol and Bremmer. This theory is somewhat simpler than but formally equivalent to that established by Ruppin and preserves a feature which is closer to the method of the theory established by Chance, Prock and Silbey for a flat surface. The results, when compared to those obtained from the static image theory, show that this latter theory can be very inaccurate for large molecule-sphere distances or highly-conducting spheres, consistent with previous findings for surfaces with perfect flatness or small roughness. GRA

**N88-13965#** United Technologies Corp., San Jose, Calif. Chemical Systems.
**HIGH ENERGY MOLECULES OF HIGH SYMMETRY Final Report, Mar. 1985 - Feb. 1987**
J. M. Guimont and W. S. Anderson Aug. 1987 71 p
(Contract F049620-85-C-0056)
(AD-A185385; AFOSR-87-1009TR) Avail: NTIS HC A04/MF A01 CSCL 07C

The first phase of this program was investigation of triquinoyl hydrate (hexaketocyclohexane octahydrate, C6H16O14) which is formed when certain cyclohexane derivatives are treated with cold nitric acid. This ketone hydrate has now been characterized by measurements of its elemental composition, X-ray diffraction

pattern, density, infrared and Raman spectrum, carbon thirteen NMP pattern, ultraviolet absorption and fluorescence spectra, ion chromatogram, potentiometric titration curve, solubility, rate of weight loss at several temperatures, heat of decomposition and of combustion, and reactivity toward several different nucleophiles, reducing agents and oxidizing agents. The ketone hydrate is an unusually dense, tightly hydrogen-bonded, acidic, crystalline material which in solution rapidly undergoes dehydration, disproportionation and ring-opening reactions. It may be regarded as a graphite oxide (graphitic acid) having the maximum oxygen-to-carbon ratio. GRA

**N88-13966#** Rome Univ. (Italy). Dipartimento di Fisica.
**W DECAYS**
K. Kleinknecht, B. Renk, G. Barbiellini, F. Cavallo, C. Chiccoli, G. Kalmus, C. Matteuzzi, P. Pasini, M. Tyndel, and M. Diemoz et al. 3 Feb. 1987 36 p Presented at the LEP200 ECFA-Workshop, Aachen, Fed. Republic of Germany, 29 Sep. - 1 Oct. 1986
(Nota-Interna-877; ETN-88-91239) Avail: NTIS HC A03/MF A01

The determination of the W decay branching ratios as a general test of the universality of the weak charged current, predicted by the standard model, is discussed. Ways to identify the three possible combinations of W decay modes, and how to separate the different flavor contributions, in the lepton and in the quark sector are considered. It is concluded that the Large Electron-Proton collider (LEP) experiment will give a significant test of fermion universality, based on a clean and direct determination of the W couplings to all the flavors. All the fermions will be measured at the same time in the same reaction, namely the W decay, with the considerable advantage that most of the systematic uncertainties will tend to cancel out. In the second phase of LEP the missing energy will have a crucial role not only for the identification of new, nonstandard, particles, but also in the WW decays, to identify the unseen neutrinos. ESA

**N88-13967#** Rome Univ. (Italy). Dipartimento di Fisica.
**THE BIRTH OF BIG SCIENCE: NUCLEAR PHYSICS AS ADVANCED TECHNOLOGY SOURCE [LA NASCITA DELLA BIG SCIENCE: LA FISICA NUCLEARE COME FONTE DI TECHNOLOGIA DI PUNTA]**
Angelo Baracca and Michelangelo DeMaria 13 May 1987 41 p In ITALIAN Submitted for publication
(Nota-Interna-881; ETN-88-91242) Avail: NTIS HC A03/MF A01

The history of science development is discussed. The sudden change of scale of scientific activities in the United States as a consequence of World War 2 is considered. ESA

**N88-13968#** Los Alamos National Lab., N. Mex.
**THEORY OF NEUTRON SCATTERING EXPERIMENTS ON MOMEN TUM DISTRIBUTIONS IN QUANTUM FLUIDS**
R. N. Silver 1987 13 p Presented at the 11th International Workshop on Condensed Matter Theories, Oulu, Finland, 27 Jul. 1987
(Contract W-7405-eng-36)
(DE87-01369; LA-UR-87-2534; CONF-8707110-1) Avail: NTIS HC A03/MF A01

The first perturbative derivation of the final state corrections to the impulse approximation for deep inelastic neutron scattering experiments was presented. The final state broadening is found to depend on g(r) and the He-He phase shifts. The theory satisfies the f-sum rule, the omega sup 2 sum rule (kinetic energy) valid at high Q, and the omega sup 3 sum rule. In the structure of the theory, the self-energy terms alone would lead to quasi-Lorentzian broadening. However, these are exactly cancelled by a part of the vertex terms which introduce g(r). Numerical results are presented for superfluid He. DOE

**N88-13969#** Aerospace Corp., El Segundo, Calif. Space Sciences Lab.
**RESTORATION OF PARTICLE PITCH ANGLE DISTRIBUTION FUNCTIONS BY A MAXIMUM ENTROPY ALGORITHM**
J. L. Roeder and D. J. Gorney 1 Nov. 1986 31 p
(Grant NSF ATM-83-13655)
(ATR-86(7098)-3) Avail: NTIS HC A03/MF A01

A technique is presented with which to analyze particle flux data in order to resolve features in the pitch angle distribution which are smaller than the angular response width of the detector. This process uses a large number of data points which overlap in pitch angle to construct a maximum entropy criterion for the true angular distribution at constant energy. Statistical arrors in the measured fluxes are allowed by the inclusion of a Chi-squared constraint in the calculation. Example electron distribution functions computed from SCATHA observation show loss cone gradients with widths of less than two degrees, with an instrument response of approximately six degrees. Models of both the original and the restored distributions are constructed as sums of bi-Maxwellians. The differences in the electrostatic stability of these models due to changes in the velocity gradients are discussed. This analysis may have applications for estimating beam, conic, and loss cone features in particle velocity distributions throughout the ionosphere and magnetosphere with significant consequences for wave-particle interactions. Author

**N88-13970#** Boston Univ., Mass.
**ATOMIC BEAM STUDIES OF THE INTERACTION OF HYDROGEN WITH TRANSITION METAL SURFACES Technical Progress Report**
M. E. Batanouny 1987 17 p
(Contract DE-FG02-85ER-45222)
(DE88-000208; DOE/ER-45222/05) Avail: NTIS HC A03/MF A01

This progress report discusses improvements in the helium scattering facility performance and in using a spin-polarized metastable helium beam as a new probe of surface magnetism. DOE

**N88-13971#** Rockefeller Univ., New York.
**EXPERIMENTAL STUDIES OF ELEMENTARY PARTICLE INTERACTIONS AT HIGH ENERGIES Technical Progress Report**
21 Sep. 1987 80 p
(Contract DE-AC02-87ER-40325)
(DE88-000804; DOE/ER-40325/1) Avail: NTIS HC A05/MF A01

This paper discusses progress of experiments at CERN and Fermilab. At CERN, data accumulation and analysis is discussed for the UA-6 experiment, which involves proton-antiproton collisions. At Fermilab, the testing of a collider detector for the Tevatron is discussed. DOE

**N88-13972#** Kansas State Univ., Manhattan. Atomic and Nuclear Science Lab.
**ATOMIC PHYSICS WITH HIGHLY CHARGED IONS Progress Report**
P. Richard 1987 18 p
(Contract DE-FG02-86ER-13491)
(DE88-000894; DOE/ER-13491/335) Avail: NTIS HC A03/MF A01

This progress report covers the following topics: angular distributions of reaction products from capture by slow multiply charged projectiles; capture from aligned molecules; production of molecular fragments by fast heavy-ion bombardment; F(8+) + Ne collisions; few body collisions; and other charge exchange, electron capture, ion colliding topics. DOE

**N88-13973#** Louisiana State Univ., Baton Rouge. Dept. of Chemical Engineering.
**MOLECULAR DYNAMICS STUDIES OF AROMATIC HYDROCARBON LIQUIDS Annual Progress Report, 1 Sep. 1986 - 31 Aug. 1987**
E. McLaughlin and S. Gupta 1987 23 p
(Contract DE-FG05-86ER-13632)
(DE88-001473; DOE/ER-13632/1) Avail: NTIS HC A03/MF A01

Algorithms for molecular dynamics simulations on supercomputers have been developed and simulations performed for fluids of nonspherical molecules modeled using the following potentials: two center and three-center Lennard-Jones potentials in order to study phase-equilibria in these fluids, oblate and prolate Gaussian overlap potential (original and modified potentials), and dipolar and quadrupolar spheres. Simulation results have been used to test predictive methods: a nonspherical reference potential based thermodynamic perturbation theory and a sphericalized potential method. Both these methods work well for fluids modeled using the modified Gaussian overlap potential. The sphericalized potential method is, surprisingly, shown to work well for polar fluids also. Work is underway to model liquid benzene. DOE

**N88-13974#** Rice Univ., Houston, Tex. Dept. of Physics.
**THEORETICAL ATOMIC AND MOLECULAR PHYSICS Progress Report**
N. F. Lane 1986 7 p
(Contract DE-AS05-84ER-13168)
(DE88-001625; DOE/ER-13168/3) Avail: NTIS HC A02/MF A01

The theoretical atomic and molecular physics program at Rice University addresses basic problems on the structure and collision dynamics of electrons, atoms, ions and molecules, emphasizing processes related to possible new energy technologies and other applications. The program focuses on collision processes under disturbed conditions, i.e., high levels of excitation, ionization, energy transfer, and external influences. Research projects include: collision processes in ICF plasmas; excitation and charge-transfer processes; Rydberg atom collisions; Penning ionization of atoms; excitation in electron-molecule collisions; and related topics. DOE

# 73 NUCLEAR AND HIGH-ENERGY PHYSICS

Includes elementary and nuclear particles; and reactor theory.

For space radiation see *93 Space Radiation.*

**N88-13975#** California Univ., Los Angeles.
**THEORETICAL AND EXPERIMENTAL INVESTIGATION OF ELECTRON BEAM ACCELERATION AND SUB-MILLIMETER WAVE GENERATION IN CYCLOTRON RESONANT CAVITIES Final Technical Report, Feb. 1984 - 30 Apr. 1987**
N. C. Luhmann, Jr., D. B. McDermott, and P. Vitello 24 Jul. 1987 8 p
(Contract DAAG29-84-K-0015)
(AD-A184806; ARO-21020.6-PH) Avail: NTIS HC A02/MF A01 CSCL 09A

The high energy, axis-encircling electron beam produced by the TE sub 111 gyro-resonant accelerator has been used to drive two varieties of high cyclotron harmonic amplifiers, the high harmonic gyro-klystron and the high harmonic gyro-TWT. The gyro-klystron has been tested in three configurations. The first was a simple two cavity gyro-klystron where the energy of the rotating beam is modulated in the buncher cavity. Bunches develop in the drift tube and radiate in the catcher cavity. The fifth harmonic device yielded a gain of 20 dB and a saturated power of 90 W. A multi-cavity system can be expected to yield considerably more gain because intermediate cavities will enhance the bunch formation. Using the same overall length as the two cavity device, the four cavity gyro-klystron yielded a gain of 37 dB, but saturated at roughly the same output power. GRA

**N88-13976#** Naval Postgraduate School, Monterey, Calif.
**CERENKOV RADIATION FIELD ANALYSIS DUE TO A PASSING ELECTRON BEAM M.S. Thesis**
Byron K. Price Jun. 1987 115 p
(AD-A184870) Avail: NTIS HC A06/MF A01 CSCL 20H

This paper is a continuation of a preliminary study which investigated the magnetic field radiated from a charge bunch traveling over a finite path. One of the recommendations of the preliminary study was to investigate how the magnitude and shape of the radiated field depends on the location of the observer relative to certain time boundaries defined by relationships between the arrival times of different parts of a pulse. This recommendation was followed by studying the signals radiated from charge bunches with two different ratios of rise time to path length. Within the Cerenkov cone and near a time boundary, the observed pulses are shaped like spikes. The time boundaries were found to be hyperbolas in the plane defined by the direction of travel of the charge bunch and the direction of propagation of radiation. GRA

**N88-13977#** Consiglio Nazionale delle Ricerche, Frascati (Italy). Ist. di Fisica dello Spazio Interplanetario.
**PROCEDURE AND PROGRAM USED FOR DATA PROCESSING IN A POLL ON NUCLEAR ENERGY UTILIZATION [PROCEDURE E PROGRAMMI PER ELABORE I DATI DI UN SONDAGGIO SUL NUCLEARE]**
C. Signorini Jan. 1987 35 p In ITALIAN Prepared in cooperation with Rome Univ., Italy
(IFSI-87-3; ETN-88-91290) Avail: NTIS HC A03/MF A01

Five questions about the utilization of nuclear energy, and 7 about knowledge of nuclear energy were answered by 597 subjects. General information for subject characterization is included. The Fortran computer prorgam for poll evaluation is detailed. The results are not given. ESA

# 74 OPTICS

Includes light phenomena; and optical devices.

For lasers see *36 Lasers and Masers.*

**N88-13978#** Direction des Recherches Etudes et Techniques, Paris (France). Centre de Documentation de LArmement.
**ULTRAFAST INTRINSIC BISTABLE DEVICES Final Report [DISPOSITIFS BISTABLES INTRINSEQUES ULTRARAPIDES]**
S. Laval and A. Koster May 1986 49 p In FRENCH
(PB87-109310; DRET-84/1376) AVAIL: NTIS HC E04/MF E04

The study is proposed of an original, intrinsic bistable optical device, in which is foregone the presence of a Fabry-Perot cavity. The principle is based on resonant excitation of a nonlinear waveguide formed by a thin silicon layer epitaxially grown on a sapphire substrate. The different stages are described of the work done concerning conception and implementation of the device, as well as the first experimental results obtained. Author

**N88-13979#** Microcoatings, Westford, Mass.
**HIGH RESOLUTION ULTRAVIOLET FILTER DEVELOPMENT Final Report, 7 Aug. 1986 - 7 Feb. 1987**
John C. Simons 7 Feb. 1987 43 p
(Contract F19628-86-C-0173)
(AD-A184183; AFGL-TR-87-0090) Avail: NTIS HC A03/MF A01 CSCL 20F

The SBIR Phase I research reported herein arose out of the AFGL interest in acquiring high-resolution images of missile plumes and similar phenomena, and the lack of ultraviolet filters of adequate resolution quality. The task objectives were first to develop filter spectral designs capable of rejecting (to better than six to eight orders of magnitude) all visible radiation, providing a clear window below 4000A and down to as near 2000A as reasonbly feasible, or such narrower band as needed, without degrading the resolution of the transmitted image by more than 5 line-pairs per mm, or the transmittance by more than three orders of magnitude. GRA

**N88-13980#** Lawrence Livermore National Lab., Calif.
**X-RAY IMAGING: STATUS AND TRENDS**
R. W. Ryon, H. E. Martz, J. M. Hernandez, J. J. Haskins, R. A. Day, J. M. Brase, B. Cross, and D. Wherry Aug. 1987 19 p Presented at the 36th Annual Denver X-Ray Conference, Denver, Colo., 3 Aug. 1987 Prepared in cooperation with Kevex, Inc., Foster City, Calif.

(Contract W-7405-eng-48)
(DE88-000756; UCRL-96517; CONF-8708150-1) Avail: NTIS HC A03/MF A01

There is a veritable renaissance occurring in x-ray imaging. X-ray imaging by radiography has been a highly developed technology in medicine and industry for many years. However, high resolution imaging has not generally been practical because sources have been relatively dim and diffuse, optical elements have been nonexistent for most applications, and detectors have been slow and of low resolution. Materials analysis needs have therefore gone unmet. Rapid progress is now taking place because we are able to exploit developments in microelectronics and related material fabrication techniques, and because of the availability of intense x-ray sources. This report describes the methods and uses of x-ray imaging along with a discussion of technology advances in these areas. DOE

**N88-13981#** Clarkson Coll. of Technology, Potsdam, N.Y. Dept. of Electrical and Computer Engineering.
**EXTINCTION BY DIELECTRIC PARTICLES AT OPTICAL AND INFRARED WAVELENGTH Final Report, 1 Jun. 1984 - 30 Jun. 1987**
Peter W. Barber 31 Aug. 1987 6 p
(Contract DAAG29-84-K-0054)
(AD-A184818; ARO-21262.6-GS) Avail: NTIS HC A02/MF A01 CSCL 20F

Light scattering calculations for spheroidal particles have determined a relationship between the scattering matrix and the physical features of the particles. Multiple scattering calculations for parallel cylinders show that the coupling is greatest when one cylinder is in the shadow of the other. Slightly distorted spherical droplets exhibit new resonances which are caused by mode coupling. GRA

**N88-13982#** Tacan Aerospace Corp., Carlsbad, Calif.
**NONCONVENTIONAL OPTICAL TECHNIQUES FOR OPTICAL WAVEFRONT PROCESSING Final Report, Jun. 1985 - Jul. 1986**
M. M. Salour Jun. 1987 42 p
(Contract F29601-85-C-0082)
(AD-A185099; AFWL-TR-86-45) Avail: NTIS HC A03/MF A01 CSCL 20F

This report describes the design and construction of an optically pumped semiconductor laser oscillator with the following specifications: 1) Operating wavelengths, 414 nm and 680nm, interchangeable (i.e., requires a change in optical setup and the pump source, but no change in the cavity design); 2) CW power, nominal 30 mW each line; and 3) Tuning range of + or - 30 nm. The laser includes all external ring cavity components, cooling (nonliquid n2), and provisions were made for mounting line narrowing and tuning elements. Ancillary equipment list, operating and instruction manuals were also provided. GRA

**N88-13983#** Maharishi International Univ., Fairfield, Iowa. Dept. of Physics.
**SOLITONS IN STIMULATED RAMAN SCATTERING: GENERATION AND CONTROL OF ULTRASHORT OPTICAL PULSES Final Report, 15 Sep. 1986 - 15 Jun. 1987**
Kai J. Druhl 15 Jun. 1987 66 p
(Contracts DAAL03-86-K-0167; DAAG29-85-K-0031)
(AD-A185141; ARO-24396.1-PH) Avail: NTIS HC A04/MF A01 CSCL 20F

The propagation of Raman solitons in media with homogeneous and inhomogeneous broadening is studied. Results are obtained for the amplitude and temporal width of solitons as functions of propagation distance and detuning from exact Raman resonance. The analytical treatment uses differential conservation laws, which give good quantitative estimates as well as a detailed understanding of the balance of physical processes responsible for soliton evolution. Numerical calculations are used to verify the analytical results and to extend them to the transient regime, where the soliton width is comparable to the coherence time of the medium. Solitons are found to be more stable for inhomogeneous broadening than for homogeneous broadening. In order to obtain both good pulse narrowing and soliton stability, the detuning from exact Raman resonance should not exceed 5% of the Raman line width. These results make media with broad inhomogeneous Raman lines like optical fibers the most promising candidates for the application of Raman solitons. GRA

**N88-13984** British Petroleum Co. Ltd., Sunbury-on-Thames (England).
**OPTICAL PROBE Patent Application**
Barry Baker, inventor and Lorelli Alison Hilliard, inventor 4 Feb. 1987 9 p Filed 31 Jul. 1986 Priority 1 Aug. 1985 GB 8519387
(EP-Patent-0-210-869-A1; EP-Patent-Appl-SN-86305908.5; Int-Patent-Class-G01N-21/85; ETN-88-90724) Avail: UK Patent Office, 25 Southampton Buildings, London WC2A 1AY, United Kingdom

An optical probe for measuring absorption and transmission of light through a fluid was designed. It comprises two fiber optic filaments which are adjacent for at least part of their length and which terminate at one end in a sample portion of the probe. The ends of the fiber optic filaments in the sample portion of the probe are separated by a gap capable of receiving fluid. The fiber optic filaments are single optical fibers and the ends of the optical fibers in the sample portion of the probe are bevelled and have light reflecting end surfaces such that light transmitted along one optical fiber is reflected by the light reflecting end surface across the gap and then along the other optical fiber. The end surfaces of the optical fibers may be at an angle of 45 deg relative to the longitudinal axis of the fibers. ESA

**N88-13985#** Consiglio Nazionale delle Ricerche, Frascati (Italy). Ist. di Fisica dello Spazio Interplanetario.
**OPTICAL PHOTOMETER FOR THE TIRGO TELESCOPE [FOTOMETRO OTTICO PER IL TELESCOPIO TIRGO]**
P. Baldetti, A. DiGiorgio, A. Morbidini, S. Nozzoli, R. Orfei, and P. Saraceno Mar. 1987 98 p In ITALIAN
(IFSI-87-5; ETN-88-91292) Avail: NTIS HC A05/MF A01

The optical photometer developed for a 150 cm Cassegrain type telescope is described. The instrument can measure in the UBV band. It allows the extension of the original infrared-dedicated telescope to observations up to the 0.3 microns ultraviolet region. The control electronics, the mechanical design, and the optical path are detailed. ESA

**N88-13986#** Pacific Northwest Labs., Richland, Wash.
**DEVELOP TECHNIQUES FOR ION IMPLANTATION OF (LEAD-LANTHANUM-ZIRCONATE-TITANATE) FOR ADAPTIVE OPTICS**
C. R. Batishko, J. L. Brimhall, W. T. Pawlewicz, K. A. Stahl, and L. H. Toburen Sep. 1987 76 p
(Contract DE-AC06-76RL-01830)
(DE88-000642; PNL-6264) Avail: NTIS HC A05/MF A01

Research was conducted at Pacific Northwest Laboratory to develop high photosensitivity adaptive optical elements utilizing ion implanted lanthanum-doped lead-zirconate-titanate (PLZT). One centimeter square samples were prepared by implanting ferroelectric and anti-ferroelectric PLZT with a variety of species or combinations of species. These included Ne, O, Ni, Ne/Cr, Ne/Al, Ne/Ni, Ne/O, and Ni/O, at a variety of energies and fluences. An indium-tin oxide (ITO) electrode coating was designed to give a balance of high conductivity and optical transmission at near uv to near ir wavelengths. Samples were characterized for photosensitivity; implanted layer thickness, index of refraction, and density; electrode (ITO) conductivity; and in some cases, residual stress curvature. Thin film anti-ferroelectric PLZT was deposited in a preliminary experiment. The structure was amorphous with x-ray diffraction showing the beginnings of a structure at substrate temperatures of approximately 550 C. This report summarizes the research and provides a sampling of the data taken during the report period. DOE

# 75 PLASMA PHYSICS

Includes magnetohydrodynamics and plasma fusion. For ionospheric plasmas see *46 Geophysics*. For space plasmas see *90 Astrophysics*.

**N88-13987#** Eoetvoes Lorand Fizikai Tarsulat, Budapest (Hungary).
**PROCEEDINGS OF THE 17TH INTERNATIONAL CONFERENCE ON PHENOMENA IN IONIZED GASES HELD IN BUDAPEST, HUNGARY, JULY 8-12, 1985: INVITED PAPERS**
J. S. Bakos, ed. and Zsuzsa Soerlei, ed. Mar. 1986 361 p Conference held in Budapest, Hungary, 8-12 Jul. 1985 Prepared in cooperation with Hungarian Academy of Sciences, Budapest
(DE87-703562; INIS-mf-10971; CONF-850718) Avail: NTIS (US Sales Only) HC A16/MF A01

The invited papers of the 17th International Conference on Phenomena in Ionized Gases are published containing papers on kinetic theory of ionized gases. The topics cover plasma kinetics, plasma diagnostic methods, arc and discharge physics, magnetic properties of plasmas, new plasma models, laser-plasma physics, and transport phenomena in ionized gases. DOE

**N88-13988#** Nagoya Univ. (Japan). Inst. of Plasma Physics.
**ENERGY DEPENDENCE OF ION-INDUCED SPUTTERING YIELDS OF MONATOMIC SOLIDS IN THE LOW ENERGY REGION**
N. Matsunami, Y. Yamamura (Okayama Univ. of Science, Japan ), N. Itoh, H. Tawara, and T. Kawamura Jul. 1987 40 p
(IPPJ-AM-52) Avail: NTIS HC A03/MF A01

The theory of sputtering thresholds for not-too-oblique incidence is developed, considering several collision sequences near the surface. A version of the empirical formula is proposed in order to obtain the sputtering yield in the near threshold energy region. B.G.

**N88-13989#** California Univ., Los Angeles. Dept. of Mechanical, Aerospace and Nuclear Engineering.
**ALT-1 PUMP LIMITER EXPERIMENTS**
D. M. Goebel, R. W. Conn, G. A. Campbell, W. K. Leung, K. H. Dippel, K. H. Finken, G. H. Wolf, G. J. Thomas, A. E. Pontau, and W. Hsu Sep. 1987 36 p Prepared in cooperation with Kernforschungsanlage, Juelich, Fed. Republic of Germany and Sandia National Labs., Livermore, Calif.
(Contract DE-FG03-85ER-51069)
(DE88-000822; UCLA/PPG-1084) Avail: NTIS HC A03/MF A01

Results from the ALT-1 pump limiter experiments in TEXTOR are presented. ALT-1 has demonstrated control of the plasma density in a high recycling tokamak by pumping up to 15% of the core efflux. The closed pump limiter designs with restricted entrance geometries to reduce the backflow of neutral gas to the plasma remove over 50% of the ion flux incident on the collection slot. Up to 80% of the entrance ion flux is removed when the edge electron temperature is less than 10 eV and plasma-neutral gas interactions are minimized inside the limiter. Results from a 3-D Monte Carlo neutral gas transport code agree closely with these experimental results. The compound curvature of the head is found to distribute the heat over the surface as predicted in the original designs. Impurity removal experiments demonstrate that significant helium exhaust can be achieved with a pump limiter. During ohmic heating in TEXTOR, the energy and particle confinement times are proportional to the line averaged core density. With ICRH auxiliary heating, tau/sub E/ follow L-mode scaling independent of particle removal by the pump limiter. Pump limiter operation does not directly modify the SOL plasma density and electron temperature, but controls the core plasma density by changing the global recycling at the boundary. The global particle confinement, the particle flux to the limiter, and the edge electron temperature follow the changes in the core density and auxiliary heating power. DOE

**N88-13990#** Naval Research Lab., Washington, D.C. Lab. for Computational Physics and Fluid Dynamics.
**EVOLUTION OF MEAN SQUARE MAGNETIC VECTOR POTENTIAL IN COMPRESSIBLE, TWO-DIMENSIONAL, MAGNETOFLUID TURBULENCE**
R. B. Dahlburg 8 Sep. 1987 11 p
(AD-A184985; NRL-MR-6012) Avail: NTIS HC A03/MF A01 CSCL 20I

The mean square magnetic vector potential is not invariant in ideal, two dimensional, compressible, magnetohydrodynamic turbulence. A new, related invariant for the compressible case is given. The results are demonstrated by numerical simulation. In the compressible case large amplitude fluctuations in the mean square magnetic vector potential are observed. GRA

**N88-13991#** Naval Research Lab., Washington, D.C. Plasma Physics Div.
**ADVANCED CONCEPTS THEORY ANNUAL REPORT 1986 Memorandum Report, Jan. - Dec. 1986**
12 Aug. 1987 107 p
(Contract MIPR-86-570)
(AD-A184986; NRL-MR-6051) Avail: NTIS HC A06/MF A01 CSCL 20I

Reported is the work of the Plasma Radiation Branch conducted in FY 86 with respect to several critical problems concerning the design of Z pinch implosions and the optimization of their radiative output. Separate sections describe progress in atomic modeling of K shell copper radiation, radiation hydrodynamics, argon implosions, design of anti-zippering nozzles, and analyses of anomalous resistivity and plasma opening switches. GRA

**N88-13992#** Naval Research Lab., Washington, D.C.
**THEORY OF INDUCED SPATIAL INCOHERENCE Interim Report**
R. H. Lehmberg, A. J. Schmitt, and S. E. Bodner 16 Sep. 1987 60 p
(AD-A185005; NRL-MR-5980) Avail: NTIS HC A04/MF A01 CSCL 18A

Described are theoretical and experimental investigations of induced spatial incoherence (ISI), a technique for achieving the smooth and controllable target beam profiles required for direct-drive laser fusion. Analytic and numerical calculations show that nonuniformities due to interference among the beamlets are smoothed by both thermal diffusion and temporal averaging. Under laser-plasma conditions of interest to ICF, average ablation pressure nonuniformities of about 1% should be readily attainable. A partial ISI scheme is also investigated, which allows widely-spaced beamlets to remain mutually coherent; the resulting high spatial frequency interference structure can be effectively smoothed by thermal diffusion alone. A perturbation analysis shows that the average target profile (I(x)) remains relatively insensitive to laser beam aberration when the scalelength of that aberration is larger than the initial beamlet width. This aberration will tend to broaden and smooth (I(x)), rather than introduce any small-scale structure. The broadening is largely controllable because it depends only upon spatial averages of the aberrated quantities over the entire laser aperture; the uncontrollable perturbations can be reduced to about 1% in practical cases. GRA

**N88-13993#** Massachusetts Inst. of Tech., Cambridge. Dept. of Materials Science and Engineering.
**THE INTERACTION OF DC PLASMA JET WITH A MELTING METAL: EXPERIMENTAL MEASUREMENTS AND MATHEMATICAL DESCRIPTION Final Report, 1 Jan. 1983 - 31 Jul. 1986**
Julian Szekely 21 May 1987 10 p
(Contract DAAG29-83-K-0022)
(AD-A185173; ARO-19929.3-MS) Avail: NTIS HC A02/MF A01 CSCL 13H

This investigation was concerned with the experimental and theoretical study of the interaction of a transferred arc plasma jet with a metal block onto which this jet impinges. Problems of this type are of interest in plasma arc remelting processes and also in

welding. The study had both experimental and analytical (mathematical) modelling components. The experimental work involved the construction of an apparatus which is essence consisted of a 20 kW plasma jet impinging onto a hemispherical steel block of 200 mm diameter. The experiment measured the voltage, the current, the plasma gas flow rate and the evolution of the temperature fields as the metal block was heated up and partially melted. GRA

**N88-13994#** Air Force Weapons Lab., Kirtland AFB, N. Mex.
**ANALYTICAL SOLUTION OF THE EQUATIONS FOR A COAXIAL PLASMA GUN OPERATING IN THE SNOWPLOW MODE. 1. WEAK COUPLING LIMIT Final Report, 1 Feb. - 30 May 1986**
David Dietz Jun. 1987 29 p
(AD-A185370; AD-E500888; AFWL-TR-86-137) Avail: NTIS HC A03/MF A01 CSCL 20I

The analysis solution of the system of coupled ordinary differential equations which describes the time evolution of an ideal coaxial plasma gun operating in the snowplow mode is obtained in the weak coupling limit, i.e., when the gun is fully influenced by the driving (RLC) circuit but the circuit is negligibly influenced by the gun. Criteria are derived for the validity of this limit and numerical examples are presented. GRA

**N88-13995#** Royal Inst. of Tech., Stockholm (Sweden). Dept. of Plasma Physics.
**A SYNTHETIC PLASMA SOURCE**
Lennart Lindberg Dec. 1986 11 p Presented at the 18th Int. Conf. on Phenomena in Ionized Gases, Swansea, United Kingdom, 13-17 Jul. 1987
(TRITA-EPP-86-15; ISSN-0348-7539; ETN-88-91384) Avail: NTIS HC A03/MF A01

A synthetic plasma source producing a plasma beam with low temperature (0.3 to 0.5 eV, in the central column, but 3 to 5 eV with a tail of energetic electrons at r = 33 mm) and nearly maxwellian electron distribution is described. Two thermionic cathodes are used, one supplying energetic electrons that ionize the gas, the other, a lanthanum hexaboride plate in contact with the plasma, supplying thermal electrons. ESA

**N88-13996#** Royal Inst. of Tech., Stockholm (Sweden). Dept. of Plasma Physics.
**LABORATORY AND NEAR-EARTH SPACE PLASMA AS A KEY TO THE PLASMA UNIVERSE**
C.-G. Faelthammar Jun. 1987 35 p Presented at IEEE Interntional Conference on Plasma Science, Arlington, Va., 1-3 Jun. 1987
(TRITA-EPP-87-09; ISSN-0348-7539; ETN-88-91389) Avail: NTIS HC A03/MF A01

It is argued that experiments in the laboratory and in situ measurements in space represent an essential key to reliable understanding of the plasma Universe. This is illustrated by discussing fundamental electrophysical aspects of matter in the plasma state. Conduction of electric current; magnetic-field aligned electric fields; acceleration of charged particles to high energy; coupling between magnetic field and the motion of matter; rapid release of magnetically stored energy; chemical separation; and critical-velocity interaction between plasma and neutral gas are considered. ESA

**N88-13997#** Royal Inst. of Tech., Stockholm (Sweden). Dept. of Plasma Physics.
**OBSERVATIONS OF PROPAGATING DOUBLE LAYERS IN A HIGH CURRENT DISCHARGE**
Lennart Lindberg Aug. 1987 23 p Presented at the 18th Int. Conf. on Phenomena in Ionized Gases, Swansea, United Kingdom, 13-17 Jul. 1987
(TRITA-EPP-87-10; ISSN-0348-7539; ETN-88-91390) Avail: NTIS HC A03/MF A01

Observations of current disruptions and propagating electric double layers (3 to 5 kV) in a high density (2 times 10 to the 19th power/cu m) highly ionized, moving, and expanding plasma column are reported. An initial plasma column is formed in an axial magnetic field (0.1T) by a conical theta-pinch plasma gun. When an axial current (max 5 kA, 3 to 5 kV) is drawn through the column, spontaneous disruptions and double layer formation occur within a few microseconds. Floating, secondary emitting Langmuir probes indicate very high positive potential peaks (1 to 2 kV above the anode potential during a few microseconds) in the plasma on the positive side of the double layer. Short, intense bursts of HF radiation are detected at the disruptions. ESA

**N88-13998#** Los Alamos National Laboratory, N. Mex.
**DYNAMIC PROCESSES IN FIELD-REVERSED-CONFIGURATION COMPACT TOROIDS**
D. J. Rej 1987 21 p Presented at the Course and Workshop on Physics of Mirrors, Reversed Field Pinches and Compact Tori, Varenna, Italy, 1 Sep. 1987
(Contract W-7405-eng-36)
(DE87-014756; LA-UR-87-2854; CONF-870908-12) Avail: NTIS HC A03/MF A01

The dynamic processes involved in field-reversed configuration (FRC) formation, translation, and compression are reviewed. Though the FRC is related to the field-reversed mirror concept, the formation method used in most experiments is a variant of the field-reversed THETA-pinch. Formation of the FRC eqilibrium occurs rapidly, usually in less than 20 microsec. The formation sequence consists of several coupled processes: preionization; radial implosion and compression; magnetic field line closure; axial contraction; equilibrium formation. Recent experiments and theory have led to a significantly improved understanding of these processes; however, the experimental method still relies on a somewhat empirical approach which involves the optimization of initial preionization plasma parameters and symmetry. New improvements in FRC formation methods include the use of lower voltages which extrapolate better to larger devices. The axial translation of compact toroid plasmas offers an attractive engineering convenience in a fusion reactor. FRC translation has been demonstrated in experiments worldwide, and these plasmas are found to be robust, moving at speeds up to the Alfven velocity over distances of up to 16 m, with no degradation in the confinement. Compact toroids are ideal for magnetic compression. Translated FRCs have been compressed and heated by imploding liners. Upcoming experiments will rely on external flux compression to heat a translater FRC at 1-GW power levels. DOE

**N88-13999#** Los Alamos National Laboratory, N. Mex.
**A SHORT INTRODUCTION TO THE STATUS AND MOTIVATION FOR REVERSED FIELD PINCH AND COMPACT TOROID RESEARCH**
H. Dreicer Sep. 1987 22 p Presented at the Course and Workshop on Physics of Mirrors, Reversed Field Pinches and Compact Tori, Varenna, Italy, 1 Sep. 1987
(Contract W-7405-eng-36)
(DE88-000487; LA-UR-87-3209; CONF-870908-10) Avail: NTIS HC A03/MF A01

Potential commercial fusion power systems must be acceptable from a safety and environmental standpoint. They must also promise to be competitive with other sources of energy (i.e., fossil, fission, etc.) when considered from the standpoint of the cost of electricity (COE) and the unit direct cost (UDC) in dollars/kWe. These costs are affected by a host of factors including recirculating power, plant availability, construction time, capital cost, etc., and are influenced by technological complexity. In an attempt to meet these requirements, the emphasis of fusion research in the United States has been moving toward smaller, lower-cost systems. There is increased interest in higher beta tokamaks and stellarators, and in compact alternate concepts such as the Reversed Field Pinch (RFP) and the Compact Toroids (CTs) which are, in part, the subject of this paper. DOE

**N88-14000#** Los Alamos National Laboratory, N. Mex.
**A REVIEW OF THE EXPERIMENTAL AND THEORETICAL STATUS OF THE REVERSED-FIELD PINCH**
D. A. Baker 1987 25 p Presented at the Energy Independence Conference, Rio de Janeiro, Brazil, 17 Aug. 1987

(Contract W-7405-eng-36)
(DE88-000529; LA-UR-87-3042; CONF-870836-1) Avail: NTIS HC A03/MF A01

This paper reviews the status of the reversed-field pinch (RFP) approach to the development of a compact nuclear fusion reactor. Two RFP papers in this conference are complementary; the first paper contains the historical origins and basic concepts concerning MHD instabilities, relaxation and RFP confinement properties as well as a discussion of future prospects of the RFP. This paper gives an overview of the status of plasma parameters of the present main RFP experiments and of the status of theory and experiment of the interesting RFP plasma phenomena of relaxation, self reversal and flux generation (these effects are often referred to as the dynamo effect). The low frequency oscillating-field current drive concept which exploits these effects is discussed. Particular emphasis is given to the theoretical results obtained from plasma simulation codes used in these active areas of study. Selected topics of recent research on the Los Alamos ZT-40M experiments are reported. The paper concludes with descriptions of the next generation Los Alamos RFP experiment ZTH, to be located in the new Confinement Physics Research Facility presently under construction, and the characteristics of an RFP compact reactor. DOE

**N88-14001#** California Univ., Berkeley. Lawrence Berkeley Lab.
**HEAVY-ION ACCELERATOR RESEARCH FOR INERTIAL FUSION**
Aug. 1987 10 p
(Contract DE-AC03-76SF-00098)
(DE88-000541; LBL-PUB-621-8/87) Avail: NTIS HC A02/MF A01

Thermonuclear fusion offers a most attractive long-term solution to the problem of future energy supplies: The fuel is virtually inexhaustible and the fusion reaction is notably free of long-lived radioactive by-products. Also, because the fuel is in the form of a plasma, there is no solid fuel core that could melt down. The DOE supports two major fusion research programs to exploit these virtues, one based on magnetic confinement and a second on inertial confinement. One part of the program aimed at inertial fusion is known as Heavy Ion Fusion Accelerator Research, or HIFAR. In this booklet, the aim is to place this effort in the context of fusion research generally, to review the brief history of heavy-ion fusion, and to describe the current status of the HIFAR program. DOE

**N88-14002#** Oak Ridge National Lab., Tenn.
**ECONOMICS OF FUSION REACTORS**
J. Sheffield 24 Sep. 1987 20 p
(Contract DE-AC05-84OR-21400)
(DE88-000580; DOE/OR-21400/T316) Avail: NTIS HC A03/MF A01

This paper contains viewgraphs on the cost effectiveness of fusion reactors. Some conclusions made in this paper are: the generic reactor model is a useful tool for determining the general features required to make a competitive fusion reactor; the cost of electricity is not a sensitive function of any particular reactor element - either technology or physics; the competitive reactors require moderate advances in physics and technology; key factors to be addressed in the long term are development of low activation materials and overall reactor availability; and a number of magnetic configurations have the potential physics capability to make a competitive reactor. DOE

**N88-14003#** Oak Ridge National Lab., Tenn.
**SUBCOMMITTEE FOR MHD THEORY Status Report**
R. A. Dory 1987 21 p Presented at the Ignition Physics Study Group Meeting, San Diego, Calif., 21 Sep. 1987
(Contract DE-AC05-84OR-21400)
(DE88-000596; CONF-8709142-3) Avail: NTIS HC A03/MF A01

This progress report contains viewgraphs on the limits of the beta value and the safety factor for tokamak magnetohydrodynamic flows. DOE

**N88-14004#** Wisconsin Univ., Madison. Plasma Physics Research.
**REVERSED FIELD PINCH PLASMAS WITH VARIOUS BOUNDARY CONDITIONS**
A. F. Almagri, S. Assadi, R. N. Dexter, Y. L. Ho, S. C. Proger, J. S. Sarff, D. A. Skinner, and J. C. Sprott Sep. 1987 24 p Presented at the Course and Workshop on Physics of Mirrors, Reversed Field Pinches and Compact Tori, Varenna, Italy, 1 Sep. 1987
(Contract DE-FG02-85ER-53212)
(DE88-000832; DOE/ER-53212/113; CONF-870908-11) Avail: NTIS HC A03/MF A01

Reversed field pinch (RFP) behavior with boundary conditions which deviate from the perfectly conducting circular shell are investigated theoretically and experimentally. Interchange (Mercier) stability and the resulting beta limits are evaluated for various noncircular shapes. Growth rates are calculated for various current-driven magnetohydrodynamic instabilities for both resistive and distant walls. A sustained noncircular RFP experiment is operated to investigate magnetic fluctuations in regions of good and bad curvature. Behavior of a nonsustained RFP is investigated, in which the plasma is situated far from the conducting shell in a poloidal divertor configuration. DOE

**N88-14005#** Sandia National Labs., Albuquerque, N. Mex.
**RIIM TWO-PULSE INJECTOR EXPERIMENTS**
M. G. Mazarakis, D. L. Smith, E. E. Jones, D. E. Hasti, J. M. Jojola, and M. Lehmann 1987 5 p Presented at the SDIO/DARPA Services Annual Propagation Review, Monterey, Calif., 29 Sep. 1987
(Contract DE-AC04-76DP-00789)
(DE88-000926; SAND-87-2344C; CONF-8709146-5) Avail: NTIS HC A02/MF A01

The RADLAC-II foilless diode injector was operated under double pulse conditions utilizing the RIIM accelerator as the test bed. The original RIIM accelerator pulse-power network was modified to provide for the generation, transmission, and delivery to the foilless diode of two distinct voltage pulses with variable interpulse separation from 0 to 2 ms. Two pulse-power assemblies were investigated and will be presented in connection with the diode performance. In both cases, the generated plasma and an excessive neutral gas release, following the first pulse, prevented the diode from producing a second beam pulse for interpulse separations larger than approx 1 microsec. DOE

**N88-14006#** Oak Ridge National Lab., Tenn.
**TRANSPORT SCALING IN THE COLLISIONLESS-DETRAPPING REGIME IN STELLARATORS**
E. C. Crume, Jr., K. C. Shaing, S. P. Hirshman, and W. I. vanRij Sep. 1987 16 p
(Contract DE-AC05-84OR-21400)
(DE88-001511; ORNL/TM-10574) Avail: NTIS HC A03/MF A01

Stellarator transport scalings with electric field, geometry, and collision frequency in the reactor-relevant collisionless-detrapping regime are determined from numerical solutions of the drift kinetic equation. A new geometrical scaling, proportional to epsilon(sub t sup 3/2) rather than epsilon(sub t)epsilon(sub h sup 1/2), is found, where epsilon(sub t) is the inverse aspect ratio and epsilon(sub h) is the helical ripple. With the new scaling, no reduction in energy confinement time is associated with large helical ripple, which provides design flexibility. Integral expressions for the particle and heat fluxes that are useful for transport simulations are given. DOE

**N88-14007#** TRW, Inc., Redondo Beach, Calif.
**MICROWAVE SUPERHEATERS FOR FUSION**
R. B. Campbell, M. A. Hoffman, and B. G. Logan (Lawrence Livermore National Lab., Calif.) 16 Oct. 1987 5 p Presented at the Symposium on Fusion Engineering, Monterey, Calif., 12

Oct. 1987
(Contract W-7405-eng-48)
(DE88-001656; UCRL-96720; CONF-871007-27) Avail: NTIS HC A02

The microwave superheater uses the synchrotron radiation from a thermonuclear plasma to heat gas seeded with an alkali metal to temperatures far above the temperature of material walls. It can improve the efficiency of the Compact Fusion Advanced Rankine (CFAR) cycle described elsewhere in these proceedings. For a proof-of-principle experiment using helium, calculations show that a gas superheat delta T of 2000 K is possible when the wall temperature is maintained at 1000 K. The concept can be scaled to reactor grade systems. Because of the need for synchrotron radiation, the microwave superheater is best suited for use with plasmas burning an advanced fuel such as D He-3. DOE

**N88-14008#** Los Alamos National Lab., N. Mex.
**NUMERICAL MODELS FOR HIGH BETA MAGNETOHYDRODYNAMIC FLOW**
J. U. Brackbill 1987 42 p Presented at the IEEE Minicourse on Computer Applications in Plasma Science, Arlington, Va., 3 Jun. 1987
(Contract W-7405-eng-36)
(DE88-001850; LA-UR-87-3326; CONF-8706154-2) Avail: NTIS HC A03/MF A01

The fundamentals of numerical magnetohydrodynamics for highly conducting, high-beta plasmas are outlined. The discussions emphasize the physical properties of the flow, and how elementary concepts in numerical analysis can be applied to the construction of finite difference approximations that capture these features. The linear and nonlinear stability of explicit and implicit differencing in time is examined, the origin and effect of numerical diffusion in the calculation of convective transport is described, and a technique for maintaining solenoidality in the magnetic field is developed. Many of the points are illustrated by numerical examples. The techniques described are applicable to the time-dependent, high-beta flows normally encountered in magnetically confined plasmas, plasma switches, and space and astrophysical plasmas. DOE

**N88-13222#** Office National d'Etudes et de Recherches Aerospatiales, Paris (France).
**PREPARATION OF QUALIFICATION TESTS OF A PLASMA GENERATOR FOR THE FEEDING OF A HYPERSONIC WIND TUNNEL [PREPARATION D'ESSAIS PROBATOIRES D'UN GENERATEUR DE PLASMA POUR L'ALIMENTATION D'UNE SOUFFLERIE HYPERSONIQUE]**
H. Consigny, C. Pacou, O. Papirnyk, Ph. Sagnier, and J. P. Chevallier *In* AGARD, Aerodynamics of Hypersonic Lifting Vehicles Nov. 1987 14 p In FRENCH Previously announced in IAA as A87-44341 (For primary document see N88-13219 05-02)
Copyright Avail: NTIS HC A24/MF A01

# 76 SOLID-STATE PHYSICS

Includes superconductivity.

For related information, see also *33 Electronics and Electrical Engineering* and *36 Lasers and Masers.*

**N88-14009#** Florida State Univ., Tallahassee.
**SUPERCOMPUTING AT FLORIDA STATE UNIVERSITY (FSU)**
D. Levinthal, H. Goldman, C. Georgiopoulos, J. L. DeKeyser, S. Linn, S. Youssef, and M. F. Hodous 1987 21 p Presented at the Computing High Energy Physics, Pacific Grove, Calif., 2 Feb. 1987 Prepared in cooperation with ETA Systems, Inc., St. Paul, Minn.
(Contracts DE-FG05-87ER-40319; DE-FC05-85ER-25000)
(DE87-013900; CONF-870249-10; FSU-SCRU-87-08) Avail: NTIS HC A02/MF A01

Over the last several months the experimental physicists at FSU and SCRI have investigated the use of properties of the CYBER-205 on pattern recognition and Monte Carlo calculations. It was found that extremely large performance enhancements can be achieved with such machines if the algorithms are assembled out of intrinsicly vector constructs. This usually requires changes of algorithms. These changes almost always produce codes of a simpler nature emphasizing the rule rather than the exception as is the case in scalar codes. The use of predefined look-up tables allows the exceptions to be handled within the structure of the more common cases making the structure of the algorithm more apparent. This gives speed increases as large as a factor of ten. DOE

**N88-14010#** China Nuclear Information Centre, Beijing.
**ANOMALOUS PHONON BEHAVIOR OF SUPERCONDUCTOR Y-Ba-Cu-O**
Jinghui Ruan, Jizhou Li, Ansun Yu, Shu Gan, Shiwen Niu, Chen Gou, Chuntang Ye, Zhenyi Liu, Xiangmiao Zheng (Beijing Univ., China ), and Bingxiong Lin, bh630440 1987 5 p In CHINESE; ENGLISH summary
(DE87-703401; CNIC-00054; IAE-0016) Avail: NTIS (US Sales Only) HC A02/MF A01

The generalized phonon density of states of Y-Ba-Cu-O superconductor (T(sub c) = 90.5 K) have been measured at 289 K and 87 K respectively, by using Be filter detector neutron inelastic scattering spectrometer at Institute of Atomic Energy. At 87 K, the optical mode at 76 MeV which is estimated owing to Cu-O-Cu breathing mode and a stronger acoustic mode below 6 MeV are observed, and the low frequency modes at 10 MeV and 19 MeV in 289 K seems to have disappeared, or to be softened. It is possible that the anomalous change of phonon density of states below T(sub c) is responsible for the higher superconducting transition temperature of Y-Ba-Cu-O. DOE

**N88-14011#** Sandia National Labs., Albuquerque, N. Mex.
**MBE GROWTH OF InAsSb STRAINED-LAYER SUPERLATTICES**
L. R. Dawson 1987 5 p Presented at the 14th International Symposium on Gallium Arsenide and Related Compounds, Crete, Greece, 28 Sep. 1987
(Contract DE-AC04-76DP-00789)
(DE88-000365; SAND-87-1239C; CONF-8709133-1) Avail: NTIS HC A02/MF A01

The use of tensile strain parallel to (100) interfaces in InAs(sub x) Sb (sub 1-x) strained-layer superlattices (SLSs) has been used to reduce the energy gap below that of unstrained alloys. Dislocation-free SLSs with x = .10 have been prepared. Cracking in structures with x greater than .10 has been overcome by the initial growth of a severely mismatched InAs (sub .35) Sb (sub .65) buffer layer, followed by compressively strained InAs (sub .27) Sb (sub .73) and InAs (sub .20 Sb (sub .80) buffer layers. SLSs with x = .20 show substantial dislocation filtering and significant optical absorption at wavelengths beyond that of equivalent bulk alloys. DOE

**N88-14012#** Stanford Univ., Calif.
**COMPUTER MODELING OF COMPLETE IC FABRICATION PROCESS Final Report, 1 Oct. 1983 - 1 Feb. 1987**
Robert W. Dutton 28 May 1987 34 p
(Contract DAAG29-83-K-0125)
(AD-A184807; ARO-20569.8-EL) Avail: NTIS HC A03/MF A01 CSCL 13H

The development of fundamental algorithms for process and device modeling as well as novel integration of the tools for advanced Integrated Circuit (IC) technology design is discussed. The development of the first complete 2D process simulator, SUPREM 4, is reported. The algorithms are discussed as well as application to local-oxidation and extrinsic diffusion conditions which occur in CMOS AND BiCMOS technologies. The evolution of 1D (SEDAN) and 2D (PISCES) device analysis is discussed. The application of SEDAN to a variety of non-silicon technologies (GaAs and HgCdTe) are considered. A new multi-window analysis capability for PISCES which exploits Monte Carlo analysis of hot carriers has been demonstrated and used to characterize a variety

of silicon MOSFET and GaAs MESFET effects. A parallel computer implementation of PISCES has been achieved using a Hypercube architecture. The PISCES program has been used for a range of important device studies including: latchup, analog switch analysis, MOSFET capacitance studies and bipolar transient device for ECL gates. The program is broadly applicable to RAM and BiCMOS technology analysis and design. In the analog switch technology area this research effort has produced a variety of important modeling and advances. GRA

**N88-14013#** Washington Univ., Seattle. Dept. of Materials Science and Engineering.
**STUDY OF BOUNDARY STRUCTURES Final Report, 1 Apr. 1983 - 31 Jul. 1987**
Ryoichi Kikuchi 31 Jul. 1987 17 p Prepared in cooperation with Hughes Aircraft Co.
(Contracts DAAG29-85-K-0166; DAAG29-83-C-0011)
(AD-A184808; ARO-19904.3-PH; ARO-23188.1-PH) Avail: NTIS HC A02/MF A01 CSCL 11F

The project extends previous studies on structures of a 2-D grain boundary (GB). The basic analytical tool is the cluster variation method (CVM) and the path probability method (PPM). In the CVM, the free energy is minimized with respect to a large number of variables using a linear iteration method called the natural iteration method (NIM). A square lattice is chosen as the basic lattice (DSC lattice) of the analysis. The first, second, and third nearest neighbor pairs are excluded due to a large repulsion. The fourth and fifth neighbors contribute interaction potentials E(4,AB) and E(5,AB), and so on. In the DSC lattice the CVM is formulated using a cluster made of nine lattice points in the form of a quadruple square. The QS formulation leads to numerical results that are reliable compared with the MC method. In low temperatures, atoms hardly deviate from the skeletal stable crystalline structure. The pair method is found to give reliable numerical results practically the same as those of QS for low temperatures including the entire ordered phase in the work D. This result is significant because when the pair method is used, the two sides of the GB do not need to be oriented symmetrically as was done here. GRA

**N88-14014#** North Carolina State Univ., Raleigh. Dept. of Electrical and Computer Engineering.
**FUNDAMENTAL STUDIES IN THE OM-CVD GROWTH OF Ga-In-As-Sb Final Report, 1 Sep. 1983 - 28 Feb. 1987**
S. M. Bedair and J. R. Hauser May 1987 47 p
(Contract DAAG29-83-K-0118)
(AD-A184822; ARO-19788.10-MS) Avail: NTIS HC A03/MF A01 CSCL 11C

The fundamental OM-CVD growth processes are studied. Several ternary and quaternary alloys have been synthesized and their structural, optical and electrical properties are studied. Atomic Layer Epitaxy is developed to control the deposition process to the atomic level. Strained layer superlattices have been used as buffer layers to reduce defects originating from GaAs substrates. GRA

**N88-14015#** Aerospace Corp., El Segundo, Calif. Electronics Research Lab.
**A GaAs MESFET BALANCED MIXER WITH VERY LOW INTERMODULATION**
Stephen A. Maas 31 Aug. 1987 18 p
(Contract F04701-85-C-0086)
(AD-A184848; TR-0086A(2925-02)-3; SD-TR-87-39) Avail: NTIS HC A02/MF A01 CSCL 09A

A new type of balanced mixer has been realized by using the unbiased channel of a GaAs MESFET as the mixing element. Because this resistance is only very weakly nonlinear, very low intermodulation results. State-of-the-art second- and third-order output intercept points of 34 and 21 dBm, respectively, are achieved, with a 7-dB conversion loss at X band. GRA

**N88-14016#** Naval Postgraduate School, Monterey, Calif.
**TECHNOLOGY UPGRADE OF A SILICON COMPILER M.S. Thesis**
Eva G. Malagon Jun. 1987 119 p
(AD-A184873) Avail: NTIS HC A06/MF A01 CSCL 20L

A 1.5 micron dual layer metal scaleable CMOS standard cell library is inserted into the NMOS based silicon compiler, MacPitts. The MacPitts data-path consisting of a collection of registers and arithmetic/logic units (organelles) and sequenced by a three phase clock was modified to accept two phase clocking and SCMOSMOS organelles. GRA

**N88-14017#** Systems Research Labs., Inc., Dayton, Ohio. Research Applications Div.
**CHARACTERIZATION OF THE MICROSTRUCTURES OF VARIOUS MATERIALS Final Report, 1 Sep. 1983 - 31 Aug. 1986**
Allen G. Jackson Jun. 1987 65 p
(Contract F33615-83-C-5073)
(AD-A184961; SRL-6810; AFWAL-TR-87-4041) Avail: NTIS HC A04/MF A01 CSCL 11F

Characterization research was conducted on Ti-, Al-, and Mg-base alloys and nonmetallic polymers using electron-optical and light optical methods, including transmission, scanning transmission and scanning electron microscopy, electron microprobe, interference layer microscopy, and various light optical methods. Rapid solidification research was done on Ti-, Al-, and Mg-base alloys using pendant-drop-melt-extraction, melt-spinning, and splat cooling methods. Apparatus to produce the alloys was constructed. GRA

**N88-14018#** Rice Univ., Houston, Tex.
**SUPERSONIC BEAM OBSERVATIONS OF SEMICONDUCTOR CLUSTERS Final Report, 1 Jan. 1985 - 30 Jun. 1987**
R. E. Smalley, R. F. Curl, and F. K. Tittel 31 Aug. 1987 12 p
(Contract DAAG29-85-K-0029)
(AD-A184991; ARO-21724.10-CH) Avail: NTIS HC A03/MF A01 CSCL 20H

The research carried out during this grant is concerned with the study of cluster beam spectroscopy of semiconducting elements (Si and Ge), as well as III-V semiconductors (GaxAsy) based on rapid advances in the art of generating and probing supersonic cluster beams developed at Rice University. This approach allows the study of small, bare clusters in the high vacuum of a molecular beam apparatus in much the same way that the more conventional type of surface science uses perfect single crystals in an ultra high vacuum surface machine. In both cases the object of study is a highly idealized model of the real polycrystalline surfaces of practical importance, but in the case of the clusters beam approach, this model has the advantage of a far more immediate connection to high level ab initio theory. It can be argued that cluster beam techniques are a means of getting away from the macroscopic, low symmetry aspects of surfaces and bringing surface science experiments into the microscopic, molecular realm ideal for theory. Although there have been substantial studies of metal and rare gas clusters, only recently has attention begun to focus on clusters of semiconductor elements. GRA

**N88-14019#** Brown Univ., Providence, R. I. Dept. of Chemistry.
**PREPARATION AND CHARACTERIZATION OF MEMBERS OF THE SYSTEM (Zn,Se)1-xGaPx**
H-S. Shen, G-Q. Yao, X-C He, K. Dwight, and A. Wold 26 Aug. 1987 9 p Sponsored in cooperation with NSF
(Contract N00014-85-K-0177)
(AD-A185073; TR-4) Avail: NTIS HC A02/MF A01 CSCL 20B

Single crystals of members of the system (ZnSe)1-xGaPx were grown by chemical vapor transport using iodine as the transport agent. The IR spectrum of (ZnSe), 905 (GaP) .095 is not appreciaty changed from that of pure ZnSe; however, the hardness and stability towards oxidation are greatly enhanced. GRA

**N88-14020#** Harry Diamond Labs., Adelphi, Md.
**RESONANT LEVEL LIFETIME IN GaAs/ AlGaAs DOUBLE-BARRIER STRUCTURES Final Report, Feb. - Jun. 1987**

Thomas B. Bahder, Clyde A. Morrison, and John D. Bruno Aug. 1987 9 p
(AD-A185376; AD-E500888; HDL-TR-2125) Avail: NTIS HC A02/MF A01 CSCL 20L

The lifetime of the lowest quasi-bound state localized between the barriers of a GaAs/AlGaAs double-barrier structure is calculated as a function of barrier and well dimensions. The results are consistent with high-frequency experiments. Author (GRA)

**N88-14021#** University of Southern California, Los Angeles.
**MOLECULAR BEAM EPITAXIAL GROWTH AND CHARACTERIZATION OF 3-5 COMPOUND SEMICONDUCTOR SINGLE AND MULTIPLE INTERFACE STRUCTURES Final Report, 30 Jul. 1984 - 29 Oct. 1986**
Anupam Madhukar 29 Oct. 1986 6 p
(Contracts AF-AFOSR-84-0279; AF Proj. 2917)
(AD-A185400; AFOSR-87-1177TR) Avail: NTIS HC A02/MF A01 CSCL 20G

A brief description of equipment acquired under the present grant is provided, along with a list of equipment. The equipment has enhanced molecular beam epitaxial growth and characterization capabilities in the principal investigator's laboratory. GRA

**N88-14022** British Petroleum Co. Ltd., Sunbury-on-Thames (England).
**PREPARATION OF AMORPHOUS SILICON SEMICONDUCTORS Patent Application**
Michael John Thwaites, inventor and John Howard Purnell, inventor 10 Dec. 1986 3 p Filed 29 May 1986 Priority 31 May 1985 GB 8513733
(GB-Patent-2-176-054-A; GB-Patent-Appl-SN-8613076; Int-Patent-Class-H01L-21/205; Int-Patent-Class-C23C-16/24; ETN-88-90716) Avail: UK Patent Office, 25 Southampton Buildings, London WC2A 1AY, United Kingdom

A film of hydrogenated amorphous silicon was made by thermally decomposing a monosilane at elevated temperature in the presence of a substrate and depositing a layer of amorphous silicon which contains hydrogen on the substrate. ESA

**N88-14023#** Massachusetts Inst. of Tech., Cambridge.
**T.E.M. STUDY OF BOEHMITE GELS AND OF THEIR TRANSFORMATION INTO ALPHA-ALUMINA**
X. Yang, A. C. Pierre (Societe Nationale Industrielle Aerospatiale, Saint-Medard-en-Jalles, France ), and D. R. Uhlmann Paris, France SNIAS 1987 21 p
(SNIAS-872-430-121; ETN-88-91232) Avail: NTIS HC A03/MF A01

The evolution in the crystallites organization of boehmite gels transforming into alpha alumina was observed after heat treatment up to 1150 C, for up to 24 hr. It is found that the initial colloidal boehmite crystallites do not grow during the transition alumina stages, but reorder to give parallel strings of pores in large domains. It is suggested that these domains pre-existed in the gel, the limit between two domains corresponding to inevitable mismatches in the edge to face perpendicular linkage. It is argued that each domain results in one paracrystal in the transition aluminas. ESA

**N88-14024#** Technische Hogeschool, Eindhoven (Netherlands).
**THE PSEUDOPOTENTIAL DENSITY FUNCTIONAL METHOD APPLIED TO SEMICONDUCTING CRYSTALS Ph.D. Thesis**
Peter Jan Hendrik Denteneer 1987 153 p
(ETN-88-91362) Avail: NTIS HC A08/MF A01

The pseudopotential density functional method to calculate from first principles the electronic and atomic structure of the ground state of crystals is described. Density-functional theory necessitates the self-consistent solution of the one-electron Schrodinger equation, whereas pseudopotentials allow for the inclusion in the calculation of valence electrons only, and for the expansion of the functions of interest in plane waves. The application of the technique of special points in the first Brillouin zone to perform integrations over reciprocal space is emphasized. The exploitation of space-group symmetry in the solution of the Schrodinger equation is discussed. Results of calculations for silicon, diamond, and two structurally extreme polytypes of silicon carbide illustrate the method. ESA

**N88-14025#** Sandia National Labs., Albuquerque, N. Mex.
**COMPARISON OF 2D MEMORY SEU TRANSPORT SIMULATION WITH EXPERIMENTS**
J. S. Fu, H. T. Weaver, R. Koga, and W. A. Kolasinski (Aerospace Corp., El Segundo, Calif.) 1 Dec. 1986 27 p Supersedes ATR-86(8139)-2
(ATR-86(8139)-2-Rev-A; ATR-86(8139)-2) Avail: NTIS HC A03/MF A01

Single event upset (SEU) simulations in SRAM cells have been carried out, and the results are compared to experimental data on 16K bit memories. The simulations consisted of simultaneous calculations of charge transport and transient circuit response for four cross-coupled CMOS transistors following the introduction of a slab of excess carriers into the off p-channel drain. The experiments collected upset rates produced in the memories by 163 MeV argon ions directed normally to the chip surface. Agreement between experiment and calculation was achieved when (1) the p-channel transistors were integrated into a single block of silicon as in the memory cell layout and (2) scaling was done on the Auger coefficients to compensate for an inherent 2D effect. Author

**N88-14026#** Sandia National Labs., Albuquerque, N. Mex.
**NOVEL HETEROJUNCTION DEVICES**
V. Narayanamurti 1987 2 p Presented at the Institute of Electrical and Electronics Engineering International Electron Devices Meeting, Washington, D.C., 6 Dec. 1987
(Contract DE-AC04-76DP-00789)
(DE87-013716; SAND-87-1691C; CONF-871220-1) Avail: NTIS HC A02

Recent progress in the fabrication and realization of novel heterojunction devices based on band structure engineering is described. The fact that strained layer epitaxy can be used to create entirely new structures illustrated through such diverse examples as ordered growth of Ge/Si on Si, strained p-type quantum-well FETs with light-hole dominated transconductance on GaAs, and high speed strained InGaAs/GaAs MODFETs. Recent calculations involving molecular dynamic simulations of strained layer growth, with mismatches of up to 4%, is described and the outstanding puzzle of crystal thicknesses much larger than allowed by equilibrium theories for coherent crystal growth is resolved. Some recent examples of the perfection of quantum-well structures is illustrated through the fabrication of devices based on perpendicular transport such as the resonant tunneling bipolar transistor and 10 micron superlattice ir detectors. DOE

**N88-14027#** North Carolina State Univ., Raleigh. Dept. of Materials Science and Engineering.
**STRUCTURAL CHARACTERIZATION OF ION IMPLANTED BETA-SIC THIN FILMS**
J. A. Edmond, R. F. Davis, and S. P. Withrow 1987 17 p Presented at the Silicon Carbide Symposium, Columbus, Ohio, 2 Aug. 1987 Prepared in cooperation with Oak Ridge National Lab., Tenn.
(Contract DE-AC05-84OR-21400)
(DE87-014567; CONF-8708151-1) Avail: NTIS HC A03/MF A01

Thin films of beta-SiC (100) grown on Si have been implanted with Al, P, Si and Si plus C. The temperature dependence of implantation-induced damage was studied between 77K and 1023K using transmission electron microscopy and Rutherford backscattering/channeling. Amorphous layers resulting from implantation of any of the above species recrystallized via solid phase epitaxy during post-implantation annealing between 1973K and 2073K. As such, this latter process necessitated the prior removal of the Si substrate. However, the resultant layers were very defective. Increasing the sample temperature to 1023K during implantation allowed in situ dynamic annealing of the samples and therefore, greatly reduced the residual damage to the lattice.

No additional annealing was required for structural recovery. DOE

**N88-14028#** Catholic Univ. of America, Washington, D.C.
**IONIC TRANSPORT AND ELECTRICAL RELAXATION IN GLASS Final Report**
C. T. Moynihan and A. Barkatt, comp. 28 Sep. 1987 22 p
(Contract DE-AS05-78ER-05781)
(DE88-000887; DOE/ER-05781/1) Avail: NTIS HC A03/MF A01

The basic purpose of the work described was to achieve extensive and quantitative understanding of ionic transport processes in melts and glasses by means of a combination of experimental measurements and theoretical modeling. Two major subjects of the study were the mechanism of dielectric relaxation in ionically conducting glasses and the large retardation of ionic transport in mixed alkali systems. DOE

# 77 THERMODYNAMICS AND STATISTICAL PHYSICS

Includes quantum mechanics; theoretical physics; and Bose and Fermi statistics.

For related information see also *25 Inorganic and Physical Chemistry* and *34 Fluid Mechanics and Heat Transfer.*

**N88-14029#** Centro Brasileiro de Pesquisas Fisicas, Rio de Janeiro.
**SEPARABLE ORTHOGONAL COORDINATES AND PARTICLE CREATION FOR AN ACCELERATING OBSERVER**
I. Costa 1986 29 p
(DE87-703358; CBPF-NF-026/86) Avail: NTIS (US Sales Only) HC A03/MF A01

An exactly solvable example of a non-stationary system, which has an inertial and a uniform accelerated asymptotic region is presented. A set of solutions that are quasi-classical in these two regions is constructed and the two sets are compared. The Bogoliubov coefficients have a thermal character and show a temperature of a(sub infinity)/2 pi, where a(sub infinity)is the asymptotic acceleration in the out-region. This result is much what one would expect on the basis of the Hawking effect. It implies that the natural particle number is not conserved in free Minkowski space. DOE

**N88-14030#** Centro Brasileiro de Pesquisas Fisicas, Rio de Janeiro.
**EXAMPLE OF CORRELATION BETWEEN SPACE AND SPIN COORDINATES**
J. S. Helman 1986 25 p
(DE87-703366; CBPF-NF-039/86) Avail: NTIS (US Sales Only) HC A03/MF A01

An elementary, exactly solvable, quantum mechanical model in which space and spin coordinates are correlated is fully developed. It clearly illustrates aspects which are seldom treated in elementary courses. Furthermore, it provides simple examples for the concepts of bonding, antibonding, Franck-Condon effect and effective spin-spin interaction. DOE

**N88-14031#** Technische Hogeschool Twente, Enschede (Netherlands). Center for Theoretical Physics.
**A MECHANISM FOR SYMMETRY BREAKING IN ANTIFERROMAGNETIC HEISENBERG SYSTEMS**
P. L. Iske and W. J. Caspers Jul. 1986 20 p
(ETN-88-91320) Avail: NTIS HC A03/MF A01

An approximation method, based on dimer coverings, for the ground state of the antiferromagnetic Heisenberg lattice is described. Finite system calculations suggest the validity of the approximation, which accounts for symmetry breaking for two and more dimensional systems. ESA

**N88-14032#** Florida Univ., Gainesville. Dept. of Physics.
**INTRODUCTION TO STRING FIELD THEORY**
P. Ramond and M. Ruiz-Altaba May 1987 54 p Presented at the 2nd Mexican School on Particles and Fields, Cuernavaca, Mexico, 1 Dec. 1986
(Contract DE-FG05-86ER-40272)
(DE87-014583; DOE/ER-40272/30; CONF-8612111-1; UFTP-87-2) Avail: NTIS HC A04/MF A01

A pedagogical introduction to the field theory of open strings, non-commutative geometry, and some geometrical notions on loop space is given. DOE

# 80 SOCIAL SCIENCES (GENERAL)

Includes educational matters.

No abstracts in this category.

# 81 ADMINISTRATION AND MANAGEMENT

Includes management planning and research.

**N88-14033** Advisory Group for Aerospace Research and Development, Neuilly-Sur-Seine (France).
**CALENDAR OF SELECTED AERONAUTICAL AND SPACE MEETINGS**
Jul. 1987 144 p In ENGLISH and FRENCH
(AGARD-CAL-87/1; ISBN-92-835-0427-5) Copyright Avail: NTIS HC A07/MF A01

Three kinds of events are presented by the calendar: technical meetings, conferences, and synposia; exhibitions and technical displays; and educational courses. For each meeting, exhibition, or course, the following information is given: reference number, date, location, title and sponsor, keywords indicating main topics covered; and contact code for inquiries. The list of topics include: aerospace medicine and biology; electronics, optic, and metrology; flight mechanics; fluid dynamics and acoustics; navigation, guidance, and control; thermodynamics, combustion, propulsion and energetics; structures, materials, and applied mechanics; atmospheric physics and earth environment; information, documentation, and data processing; exhibitions and displays; and educational courses. B.G.

**N88-14034#** Naval Postgraduate School, Monterey, Calif.
**A STUDY OF THE DEPARTMENT OF DEFENSE CONFIGURATION MANAGEMENT POLICIES AND PROCEDURES AS APPLIED TO THE FA-18 STRIKE/FIGHTER PROGRAM M.S. Thesis**
Christopher J. Roum Jun. 1987 89 p
(AD-A184872) Avail: NTIS HC A05/MF A01 CSCL 05A

The costs and benefits of the Department of Defense and the Department of the Navy Configuration Management (CM) program are appraised but only to identify the present costs and benefits and their relationship. The FA-18 program is utilized as the research vehicle and is examined in terms of configuration management and control policies and procedures. The focus is on post-production-baseline configuration control. An overview of critical CM issues in the government/contractor relationship is presented and their impact on the FA-18 program is analyzed. It was determined that current policies and procedures cannot insure control of the product baseline in highly sophisticated and broadly integrated weapon systems. Responsibility for CM is too fragmented and the system too cumbersome to allow effective and efficient information flow. In most cases, CM inefficiencies identified in the FA-18 program were previously addressed by program management and extraordinary work-arounds implemented to ensure future FA-18 supportability. Recommendations for improvement of Configuration Management and Control for future programs are made. Author (GRA)

**N88-14035#** Department of Defense, Washington, D. C.
**UNIVERSITY RESEARCH INITIATIVE RESEARCH PROGRAM SUMMARIES**
Jun. 1987 22 p
(AD-A184876) Avail: NTIS HC A02/MF A01 CSCL 05A

This compilation of University Research Initiative (URI) program summaries has been prepared in response to numerous requests for information about the URI, the newest basic research program of the Department of Defense (DoD). This document directly addresses the most frequently asked, general questions about URI research programs and provides points of contact where more specific information about each program may be sought. It is hoped that this document will stimulate further interest among university researchers, who may be inspired to participate in DoD basic research programs in the future; among researchers in federal laboratories or in industry, who may be encouraged to initiate mutually beneficial collaborations with the programs described herein; and among defense and research policymakers, who may wish to track the progress of the innovative URI program. GRA

**N88-14036#** Societe Nationale Industrielle Aerospatiale, Toulouse (France). Div. Avions.
**OPERATIONAL GROUPS AT THE AEROSPATIALE AIRCRAFT DIVISION [LES GROUPES OPERATIONNELS A LA DIVISION AVIONS DE L'AEROSPATIALE]**
R. Deque 1987 9 p In FRENCH Presented at the 8th Congres AFCIQ: Porte Ouverte sur la Reconquete
(SNIAS-872-111-107; ETN-88-91189) Avail: NTIS HC A02/MF A01

The design to cost method and the role of operational groups, adopted by aircraft construction management as the basic organization tool for design groups are explained. The system was used for the design of A310 and ATR42 aircraft. ESA

**N88-14037#** Advisory Group for Aerospace Research and Development, Neuilly-Sur-Seine (France).
**CALENDAR OF SELECTED AERONAUTICAL AND SPACE MEETINGS**
Dec. 1987 134 p
(AGARD-CAL-88/1; ISBN-92-835-0440-2) Copyright Avail: NTIS HC A07/MF A01

For each meeting, exhibition, or course, the following information is given: reference number, data, location, title and sponsor, keywords indicating the main topics covered, and contact code for inquiries. Topics covered include: aerospace medicine and biology; electronics, optics, and metrology; flight mechanics; fluid dynamics and acoustics; navigation, guidance, and control; thermodynamics, combustion, propulsion, and energetics; structures, materials, and applied mechanics; atmospheric physics and earth environment; and information, documentation, and data processing. B.G.

## 82 DOCUMENTATION AND INFORMATION SCIENCE

Includes information management; information storage and retrieval technology; technical writing; graphic arts; and micrography.

For computer documentation see *61 Computer Programming and Software.*

**N88-14038#** Science Research Council, Chilton (England). Rutherford Appleton Lab.
**RELATIONAL DATA HANDLING SYSTEM FOR SCIENTISTS**
B. J. Read [1986] 21 p
(PB87-223426; RAL-86-053) Copyright Avail: NTIS HC E03/MF E03 CSCL 05B

Scientific applications may make special demands of a data base management system. It must not just cope with arrays and floating point numbers, but rather, recognize the different style in which data are used compared with ordinary commercial systems. R-EXEC was developed in response to the need for a simple, portable, relational file manipulation package in the FORTRAN environment. Relational algebra provides a firm theoretical foundation. This is then necessarily extended to handle data input, output, sorting, reports and graphs. The novel command interface is precedural and user efficient. The development of R-EXEC was strongly influenced by the immediate demands of applications in physics and astronomy. Apart from character strings, there are five numeric data types, all of which can be vectors. The data relations are self describing files, owned and managed by users without reference to a database administrator, and with no central schema to maintain. Particularly powerful data manipulation tools are the grouping operation, the outer join and the way functions of attributes are permitted in projection. Null, or default, values are optional. However, perhaps the most important attraction is the ease of adding new functions. Author

**N88-14039#** National Technical Information Service, Springfield, Va.
**ROLE OF TECHNICAL INFORMATION IN INNOVATION**
J. E. Clark and A. R. Wenberg 30 Aug. 1987 17 p Presented at the 194th American Chemical Society National Meeting, New Orleans, La., 30 Aug. - 4 Sep. 1987
(PB87-235388) Avail: NTIS HC A03/MF A01 CSCL 05B

Innovation results from the acquisition and use of technical information are presented. Scientific journals are frequently used by academic and other researchers to summarize their research results while technical reports are used widely by academics, governments, and business to document their research and development results in more detail. Other products of research and development efforts such as patents, computer software, and technical data complete the toolbox which innovators and entrepreneurs need to accomplish change. The complementary roles of these various types of scientific and technical information are described. GRA

**N88-14040#** National Technical Information Service, Springfield, Va.
**ROLE OF THE TECHNICAL REPORT IN TECHNOLOGICAL INNOVATION**
J. F. Caponio and D. D. Bracken 1987 21 p Presented at the 5th International Conference of Scientific Editors, Hamburg, Fed. Republic of Germany, 14-19 Jun. 1987
(PB87-232500) Avail: NTIS HC A03/MF A01 CSCL 05B

The United States has followed a policy since World War II of permitting and encouraging the flow of technology to the free world nations. For more than forty years, the National Technical Information Service (NTIS) has served as the primary source for the collection and distribution of Government-sponsored research and engineering reports (TR's), research in progress summaries, computer programs, machine-readable data files, and applied technology. The scientific paper and the TR are examined, compared, and appraised as carriers of scientific and technical knowledge. In addition to characterizing the taxonomy of the TR, the respective roles and functions of the published paper and the unpublished TR are identified in the diffusion of scientific and technological knowledge. More importantly, arguments are advanced and evidence presented to prove why the TR is more important than the scientific paper in stimulating technological innovation in the United States today. GRA

**N88-14041#** Vrije Universiteit, Amsterdam (Netherlands). Subfaculteit Wiskunde en Informatica.
**CONNECTING RPC (REMOTE PROCEDURE CALL)-BASED DISTRIBUTED SYSTEMS USING WIDE-AREA NETWORKS**
R. vanRenesse, A. S. Tanenbaum, H. vanStaveren, and J. Hall Dec. 1986 14 p Sponsored by Nederlandse Organisatie voor Zuiver Wetenschappelijk Onderzoek, The Hague
(PB87-234423; IR-118) Avail: NTIS HC A03/MF A01 CSCL 09B

Remote Procedure Call (RPC) is a widely used communication mechanism in local network based distributed operating systems. It is simple, fast, and straight forward to implement. However, when two or more distant distributed systems are connected,

problems arise concerning the protocols, locating services, and other issues. To solve these problems, gateways are introduced. The authors discuss various ways in which these gateways can be organized and show how their application in the Amoeba Distributed Operating System has solved the problems cited above. GRA

**N88-14042*#** Jet Propulsion Lab., California Inst. of Tech., Pasadena.
**GUIDANCE FOR CONFERENCE RAPPORTEURS**
Leo R. Lunine 15 Nov. 1987 7 p
(NASA-CR-182338; JPL-D-4956; NAS 1.26:182338) Avail: NTIS HC A02/MF A01 CSCL 05B

Guidance is provided for rapporteurs at the National Conference on Strategic Management of Research and Development (Arlington, Va., 14-16 June 1988). J.P.B.

# 83 ECONOMICS AND COST ANALYSIS

Includes cost effectiveness studies.

No abstracts in this category.

# 84 LAW, POLITICAL SCIENCE AND SPACE POLICY

Includes NASA appropriation hearings; aviation law; space law and policy; international law; international cooperation; and patent policy.

**N88-14043#** Committee on Appropriations (U.S. Senate).
**NATIONAL AERONAUTICS AND SPACE ADMINISTRATION SPACE STATION PROPOSAL, FISCAL YEAR 1988**
Washington GPO 1987 281 p Hearings before the Committee on Appropriations, 100th Congress, 1st Session, 1 and 20 May 1987
(S-Hrg-100-328; GPO-76-948) Avail: Committee on Appropriations

Hearings were held to ascertain non-NASA expert opinion on the advisability of and options for a U.S. orbital space station. Scientists, academics, engineers, and businessmen expressed opinions on the desirability of funding a space station as opposed to other possible space priorities. The second day of hearings concentrated on opinions regarding the commercial potential of a space-station. J.P.B.

**N88-14044#** Committee on Science, Space and Technology (U.S. House).
**THE 1988 NASA (NATIONAL AERONAUTICS AND SPACE ADMINISTRATION) AUTHORIZATION**
Washington GPO 1988 77 p Hearing before the Subcommittee on Space Science and Applications of the Committee on Science, Space and Technology, 100th Congress, 1st Session, No. 43, 8 Apr. 1987
(GPO-80-245) Avail: Subcommittee on Space Science and Applications

Space Stations configuration and cost reviews are discussed in terms of the commitment of the United States to a permanently manned Space Station. Congressional approval to release Request for Proposals to industry for a phased development of the space station is sought, including estimates for an enhanced capability configuration. Also described is the revised baseline and the enhanced configuration. B.G.

# 85 URBAN TECHNOLOGY AND TRANSPORTATION

Includes applications of space technology to urban problems; technology transfer; technology assessment; and surface and mass transportation.

For related information see also *03 Air Transportation and Safety, 16 Space Transportation,* and *44 Energy Production and Conversion.*

**N88-14045#** Maryland Univ., College Park. Center for Automation Research.
**RANGE IMAGERY ALGORITHMS FOR THE DETECTION OF OBSTACLES BY AUTONOMOUS VEHICLES**
Phillip A. Veatch and Larry S. Davis Jul. 1987 76 p
(Contract DACA76-84-C-0004)
(AD-A185421; CAR-TR-309; CS-TR-1888; ETL-0461) Avail: NTIS HC A05/MF A01 CSCL 17G

Algorithms are presented which segment range images and classify regions as being navigable or unnavigable by a land vehicle. The algorithms are applied to data collected from an active laser range sensor mounted on an autonomous land vehicle and their comparative results are analyzed. The sensitivity of various algorithms to uncertainty in the orientation of the range sensor is studied. Experiments on sensor calibration and image enhancement are also presented. A computer model of an autonomous land vehicle and its environment is described which provides a valuable tool for investigating issues of navigation with range sensors. Obstacle detection algorithms are used in conjunction with the model to demonstrate a vehicle navigating itself through an obstacle strewn world to a goal location. GRA

**N88-14046*#** National Aeronautics and Space Administration. Lewis Research Center, Cleveland, Ohio.
**PROGRESS TOWARD THE EVOLUTION OF A STIRLING SPACE ENGINE**
Donald L. Alger [1987] 15 p Prepared for presentation at the 1988 International Congress and Exposition, Detroit, Mich., 29-Feb. - 4 Mar. 1988; sponsored by Society of Automotive Engineers, Inc.
(NASA-TM-100221; E-3833; NAS 1.15:100221) Avail: NTIS HC A03/MF A01 CSCL 10B

Following the successful testing of the 25 kWe Space Power Demonstrator (SPD) engine in 1985, a Stirling Space Engine (SSE) technology advancement program was initiated. The program's objective was to advance free-piston Stirling engine/linear alternator technolgy sufficiently so that a Stirling engine system may become a viable candidate for space power applications. Evolution of the SSE technology is planned to occur at three different engine heater temperature levels: 650, 1050, and 1300 K. These temperatures define three phases of technology development with the first phase involving the 650 K SPD engine. Technology development of the 650 K engine and preliminary design of the 1050 K engine will be discussed. Author

# 88 SPACE SCIENCES (GENERAL)

**N88-14047#** Consiglio Nazionale delle Ricerche, Frascati (Italy). Ist. di Fisica dello Spazio Interplanetario.
**[ACTIVITIES REPORT IN INTERPLANETARY SPACE PHYSICS] Annual Report, 1985 [RELAZIONE SULL'ATTIVITA' SVOLTA NELL'ANNO 1985]**
Mar. 1986 92 p In ITALIAN
(IFSI-86-5; ETN-88-91279) Avail: NTIS HC A05/MF A01

Research concerning cosmic rays, infrared astronomy, gravitational waves, and interplanetary space is summarized. ESA

**N88-14048#** Consiglio Nazionale delle Ricerche, Frascati (Italy). Ist. di Fisica dello Spazio Interplanetario.
**BUDGET AND PROGRAMS FOR 1986 RESEARCH [PROGRAMMI DI RICERCA PREVISTI PER IL 1986 E RELATIVI PREVENTIVI DI SPESA]**
Dec. 1986 57 p In ITALIAN
(IFSI-86-16; ETN-88-91287) Avail: NTIS HC A04/MF A01

Cosmic ray research, analysis of solar neutron events, interplanetary effects of solar activity, processing of solar images, experiments with Giotto and TSS satellites, laboratory experiments, gravitational waves, Earth observation, and theoretical studies are summarized. ESA

# 89 ASTRONOMY

Includes radio, gamma-ray, and infrared astronomy, and astrometry.

**N88-14049*#** Princeton Univ. Observatory, N. J.
**PHOTON COUNTING IMAGE SENSOR DEVELOPMENT FOR ASTRONOMICAL APPLICATIONS Final Project Report, 1 Jul. 1979 - 14 Sep. 1987**
Edward B. Jenkins 15 Nov. 1987 61 p
(Grant NsG-7618)
(NASA-CR-181507; NAS 1.26:181507) Avail: NTIS HC A04/MF A01 CSCL 03A

Specially built intensified CCD (ICCD) detector tubes were purchased and the performance of the electron bombardment process was investigated. In addition to studying the signal characteristics of the photoevents, there was interest in demonstrating that back-illuminated chips were not susceptible to radiation damage to their clocking electrodes. How to perform a centroid analysis for a 2-dimensional Gaussian distribution of charge is described. Measurement of the projection (along columns or rows) of the average charge spread profile is discussed. The development and flight of the Interstellar Medium Absorption Profile Spectrograph (IMAPS) is discussed. B.G.

**N88-14050#** Air Force Systems Command, Wright-Patterson AFB, Ohio. Foreign Technology Div.
**ASTROPHYSICS OBSERVATORY IN BYURAKAN**
E. Ye. Khachikyan 14 Aug. 1987 28 p Transl. into ENGLISH from Vemiya i Vselennaya (USSR), no. 2, Mar. - Apr. 1967 p 59-67
(AD-A185144; FTD-ID(RS)T-0627-87) Avail: NTIS HC A03/MF A01 CSCL 03A

In the past two decades the Byurakan Astrophysics Observatory in Soviet Armenia has enriched science with a series of discoveries acknowledged by the entire world. A description is given of how it was created and what the Byurakan Observatory is now doing. GRA

**N88-14051#** Los Alamos National Lab., N. Mex.
**AN AUTOMATED SUPERNOVA SEARCH AND THE DESIGN STRATEGY**
S. A. Colgate 1987 16 p Presented at the Summer Workshop, Santa Cruz, Calif., 13 Jul. 1987 Prepared in cooperation with New Mexico Inst. of Mining and Technology, Socorro.
(Contract W-7405-eng-36)
(DE88-001827; LA-UR-87-3457; CONF-8707126-1) Avail: NTIS HC A02/MF A01

The design considerations for an automated supernova search are reviewed. If supernova are to be found a week after explosion well before light maximum of both Types I and II, and if a rate of finding of 52 per year is justified, then one needs to keep roughly 5000 galaxies under surveillance out of a full set of 15,000 galaxies at approx. 50 Mpc distance. For detection at 1% of Type I maximum light requires a 30-inch telescope, 10 photoelectrons per pixel threshold, a 128 x 128 pixel photodetector operating with a 3-second integration time, and 2 seconds to slew and settle approx. 1 deg. A system designed to perform this function in real-time is described. DOE

# 90 ASTROPHYSICS

Includes cosmology; celestial mechanics; space plasmas; and interstellar and interplanetary gases and dust.
For related information see also *75 Plasma Physics.*

**N88-14052#** Royal Inst. of Tech., Stockholm (Sweden). Dept. of Plasma Physics.
**COMMENTS ON H. ARP THE PERSISTENT PROBLEM OF SPIRAL GALAXIES**
Hannes Alfven Apr. 1987 12 p
(TRITA-EPP-87-05; ISSN-0348-7539; ETN-88-91386) Avail: NTIS HC A03/MF A01

Arp's (1986) criticism of the standard theory of spiral galaxies is supported. Introduction of plasma theory is necessary in order to understand the structure of spiral galaxies. An important result of Arp's approach is that there is no convincing argument for the belief that there is a missing mass. Ways in which laboratory studies on plasma can contribute to galactic theory are discussed. ESA

**N88-14053#** Royal Inst. of Tech., Stockholm (Sweden). Dept. of Plasma Physics.
**COSMOLOGY IN THE PLASMA UNIVERSE**
Hannes Alfven May 1987 24 p Lecture presented at the Inst. of Space Research, Academy of Sciences, Moscow, USSR, May 1987
(TRITA-EPP-87-07; ISSN-0348-7539; ETN-88-91388) Avail: NTIS HC A03/MF A01

Criteria a cosmological theory must satisfy in order to be acceptable in the plasma Universe are considered. Matter-antimatter symmetry, and Klein's cosmological model are discussed. Prophetic and actualistic approaches to adopting Big Bang cosmology to the plasma Universe are assessed. Traditional Big Bang theory leads to difficulties due to the prophetic nature of its predictions. Actualistic approaches, extrapolating backwards from present conditions lead to increasing uncertainty the further they go. It is stressed, however that the Hubble expansion was caused by annihilation in a large region (1 billion light years) called Bigger Big Bang. ESA

# 91 LUNAR AND PLANETARY EXPLORATION

Includes planetology; and manned and unmanned flights.
For spacecraft design or space stations see *18 Spacecraft Design, Testing and Performance.*

**N88-14054*#** National Aeronautics and Space Administration. Lewis Research Center, Cleveland, Ohio.
**SMALL SPACE REACTOR POWER SYSTEMS FOR UNMANNED SOLAR SYSTEM EXPLORATION MISSIONS**
Harvey S. Bloomfield Dec. 1987 117 p
(NASA-TM-100228; E-3847; NAS 1.15:100228) Avail: NTIS HC A06/MF A01 CSCL 03B

A preliminary feasibility study of the application of small nuclear reactor space power systems to the Mariner Mark II Cassini spacecraft/mission was conducted. The purpose of the study was to identify and assess the technology and performance issues associated with the reactor power system/spacecraft/mission integration. The Cassini mission was selected because study of the Saturn system was identified as a high priority outer planet exploration objective. Reactor power systems applied to this mission were evaluated for two different uses. First, a very small 1 kWe reactor power system was used as an RTG replacement for the nominal spacecraft mission science payload power requirements while still retaining the spacecraft's usual bipropellant chemical propulsion system. The second use of reactor power involved the additional replacement of the chemical propulsion system with a small reactor power system and an electric propulsion system. The study also provides an examination of potential applications for the additional power available for scientific data

collection. The reactor power system characteristics utilized in the study were based on a parametric mass model that was developed specifically for these low power applications. The model was generated following a neutronic safety and operational feasibility assessment of six small reactor concepts solicited from U.S. industry. This assessment provided the validation of reactor safety for all mission phases and generatad the reactor mass and dimensional data needed for the system mass model. Author

# 92 SOLAR PHYSICS

Includes solar activity, solar flares, solar radiation and sunspots.

For related information see *93 Space Radiation.*

**N88-14055#** California Inst. of Tech., Pasadena. Solar Astronomy Group.

**THE APPEARANCE AND DISAPPEARANCE OF MAGNETIC FLUX ON THE QUIET SUN Final Report, 1 Oct. 1981 - 31 Dec. 1986**

Harold Zirin and Sara F. Martin Jul. 1987 19 p

(Contracts AF-AFOSR-82-0018; AF Proj. 2311)

(AD-A185432; AFOSR-87-1346TR) Avail: NTIS HC A02/MF A01 CSCL 03B

Significant new discoveries and findings were made concerning solar magnetic fields. The majority of magnetic flux on the sun is observed to disappear when magnetic fields of one polarity migrate into or develop in juxtaposition with fields of opposite polarity. The cancellation of magnetic fields can be interpreted as: (a) submergence (b) reconnection or (c) dissipation (annihilation). Large-scale filaments are observed to form in the chromosphere immediately above the boundaries between areas of network magnetic field of opposite polarity where network cancellation occurs. Small-scale filaments develop in association with small-scale cancelling magnetic fields at the rate of hundreds per day. Magnetic fields associated with large-scale solar convection cells, known as intranetwork magnetic fields, can be detected everywhere on the visible disk of the sun by using the videomagnetograph to integrate successive, 1/15 sec. magnetic field images for intervals of 1 to 10 minutes. The intranetwork field appears to be a few seconds of arc in diameter, and have field strengths of the order of a few to tens of Gauss. The intranetwork fields appear to originate at the centers of supergranules and flow to the boundaries of the cells in approximately radial patterns. GRA

**N88-14056#** Academy of Sciences, Berlin (East Germany). Inst. fuer Kosmosforschung.

**A FLUID SIMULATION OF THE AMPTE LITHIUM GAS RELEASES IN THE SOLAR WIND**

K. Sauer, K. Bauhgaertel, I. Axnaes, and Nils Brenning (Royal Inst. of Tech., Stockholm, Sweden ) Stockholm, Sweden Royal Inst. of Tech. Aug. 1987 21 p

(TRITA-EPP-87-06; ISSN-0348-7539; ETN-88-91387) Avail: NTIS HC A02/MF A01

The effect of the AMPTE Li releases in the solar wind on the plasma dynamics and magnetic field structure is studied on the basis of a quasi one-dimensional fluid model, which includes a first-order correction for the lateral flow around the obstacle. The seeding rate and initial velocity of Li ions is calculated from photoionization in a spherically expanding Li cloud. In spite of the expected limited applicability of one-fluid modeling to the problem, the model reproduces the quantitative details of the magnetic field and plasma density variations, as well as the time sequence when the whole structure is swept past the satellites by the solar wind. A qualitative agreement is also found for the velocity profile and shock-like transition where the undisturbed solar wind enters the region influenced by the Li cloud. ESA

**N88-14057#** Los Alamos National Lab., N. Mex.

**MAGNETIC FIELD DRAPING ABOUT CORONAL MASS EJECTA**

D. J. McComas and J. T. Gosling 1987 6 p Presented at the 6th Meeting of Solar Wind, Estes Park, Colo., 24 Aug. 1987

(Contract W-7405-eng-36)

(DE88-001805; LA-UR-87-3643; CONF-8708141-4) Avail: NTIS HC A02/MF A01

Fast coronal mass ejecta (CMEs) accelerate and deflect the slower moving solar wind plasma which piles up ahead of them as they propagate out through the heliosphere. This acceleration and deflection, in turn, causes the interplanetary magnetic field (IMF) imbedded in the upstream solar wind to drape about the ejecta. Draping should cause substantial out-of-the-ecliptic magnetic fields at some locations ahead of CMEs, and radial fields behind and along the flanks. At the Earth, draping can be an important factor in the generation of some magnetic storms and substorms, while in the outer heliosphere draping may produce very large magnetotail-like configurations, somewhat analogous to those observed behind Venus and comets. DOE

# 93 SPACE RADIATION

Includes cosmic radiation; and inner and outer earth's radiation belts.

For biological effects of radiation see *52 Aerospace Medicine.* For theory see *73 Nuclear and High-Energy Physics.*

**N88-14058*#** National Aeronautics and Space Administration. Langley Research Center, Hampton, Va.

**PRELIMINARY ESTIMATES OF GALACTIC COSMIC RAY EXPOSURES FOR MANNED INTERPLANETARY MISSIONS**

John W. Wilson, Lawrence W. Townsend, and William Atwell (Rockwell International Corp., Houston, Tex.) Oct. 1987 15 p

(NASA-TM-100519; NAS 1.15:100519) Avail: NTIS HC A03/MF A01 CSCL 03B

Preliminary estimates of radiation exposures resulting from galactic cosmic rays are presented for interplanetary missions. The calculations use the Naval Research Laboratory cosmic ray transport code. The heavy ion portion of the transport code can be used with any number of layers of target material, consisting of up to five different constituents per layer. The nucleonic portion of the transport code can be used with any number of layers of target material of arbitrary composition except hydrogen. Calculated galactic cosmic ray particle fluxes, doses, and dose equivalents behind various thicknesses of aluminum shielding are presented for solar maximum and solar minimum periods. Author

**N88-14059#** California Univ., Berkeley.

**SATELLITE OBSERVATIONS OF EXTREME ULTRAVIOLET RADIATION Final Report, 22 Apr. - 31 May 1976**

Stuart Bowyer 11 May 1987 8 p

(Contract DAAG29-77-C-0031)

(AD-A185043; ARO-13706.5-GS) Avail: NTIS HC A02/MF A01 CSCL 20E

The first Extreme UltraViolet (EUV) spectrometer (ECOM-721) was flown on the DOD satellite P78-1. The instrument collected a large amount of high quality data on the Earth's atmosphere, ionosphere and magnetosphere. It is still the only such experiment performed from a satellite. Because the instrument was on a spinning satellite, in a noon-midnight polar orbit at 600km altitude, it obtained a huge amount of unique data of geophysical interest. A substantial number of important geophysical observations were made, including the first spectrum of the polar cusp under sunlight, the first spectrum of the EUV nightglow emissions, the first spectrum of the tropical airglow in the EUV, the first spectrum of the nightside aurora below 800A, the detection of dielectronic recombination emissions in the atmosphere, and the first spectrum of the polar cap emissions in the EUV. GRA

**N88-14060#** Consiglio Nazionale delle Ricerche, Frascati (Italy). Ist. di Fisica dello Spazio Interplanetario.

**COSMIC RAY NM-64 NEUTRON MONITOR DATA 14, ROME, ITALY, JANUARY - DECEMBER 1985**

N. Iucci, R. Buccellato, F. Re, F. Signoretti, C. Signorini, G. Villoresi, and N. L. Zangrilli Jul. 1987 55 p
(IFSI-87-8; ETN-88-91294) Avail: NTIS HC A04/MF A01

Pressure corrected data from the neutron monitor and barometric pressure data for 1985, together with the graphs of the corrected intensity are given. Devices employed, operational mode, and data handling are described. ESA

**N88-14061#** Consiglio Nazionale delle Ricerche, Rome (Italy). Reparto Raggi Cosmici.

**AXIAL ANISOTROPY OF THE INTENSITY OF THE COSMIC RAY NUCLEAR COMPONENT [ANISOTROPIA ASSIALE NELL'INTENSITA'DELLA COMPONENTE NUCLEONICA DELLA RADIAZIONE COSMICA]**

N. Iucci, S. Pase, and M. Storini Frascati, Italy Jul. 1987 62 p In ITALIAN
(IFSI-87-7; ETN-88-91296) Avail: NTIS HC A04/MF A01

The anisotropy of the galactic cosmic radiation in the direction of Earth axis was computed. It shows a 12 month wave of 0.45% average amplitude. The reason seems to be geophysical: the annual temperature variation in the measuring location. Suggestions to eliminate this modulation are given. ESA

## 99 GENERAL

**N88-14062*** National Aeronautics and Space Administration, Washington, D.C.

**ASTRONAUTICS AND AERONAUTICS, 1978: A CHRONOLOGY**

Bette R. Janson (Creative Resources and Planning, Fairfax, Va.) 1986 394 p *Its* NASA History Series
(NASA Order W-73289)
(NASA-SP-4023; NAS 1.21:4023) Avail: SOD HC $13.00 as 033-000-01010-9; NTIS MF A01 CSCL 05D

This is the 18th in a series of annual chronologies of significant events in the fields of astronautics and aeronautics. Events covered are international as well as national and political as well as scientific and technical. This series is a reference work for historians, NASA personnel, government agencies, congressional staffs, and the media. Author

**N88-14063#** Office of Naval Research, London (England).

**AGARD: THE NATO ADVISORY GROUP FOR AEROSPACE RESEARCH AND DEVELOPMENT**

Dennis R. Sadowski 18 Aug. 1987 4 p
(AD-A185062; ONRL-7-025-C) Avail: NTIS HC A02/MF A01 CSCL 05A

The AGARD origin, mission, organization, and list of AGARD Panels are presented in this brief summary of an important aerospace advisory body. GRA

☆ U.S. GOVERNMENT PRINTING OFFICE: 1988—202-150/80003

## Typical Subject Index Listing

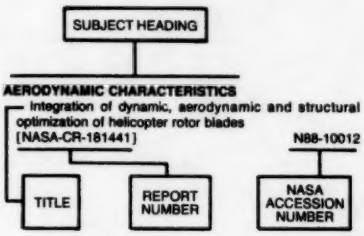


The subject heading is the key to the subject content of the document. Titles, report numbers, and accession numbers of pertinent documents are provided under each subject heading. When the title is insufficiently descriptive of the document content, a title extension has been added, separated from the title by three hyphens. The report number helps to indicate the type of document cited (e.g., NASA report, NASA translation, NASA contractor report). The NASA accession number is the number by which the document abstracts are arranged in this journal and by which the document is sold or requested. The titles, with title extensions if present, are arranged under each subject heading in ascending accession number order. The subject headings have been selected from the latest revision of the *NASA Thesaurus* (NASA SP-7053).

# A

**A-320 AIRCRAFT**
The A320 Airbus program
[SNIAS-872-111-105] N88-13215
Electrical flight commands in transport aircraft
[SNIAS-872-111-108] N88-13361
Overall description of the computer aided design and manufacturing systems associated with the A320 program at Aeroepatiale and its partners
[SNIAS-872-111-104] N88-13883
Presentation of SIGMA (Interactive Assisted Geometry System). A computer assisted shape-design program developed at the Aerospatiale Aircraft Division
[SNIAS-872-111-110] N88-13884

**ABEL FUNCTION**
A construction of simple Abelian varieties
[ZW-8702] N88-13929

**ABSORPTION SPECTRA**
Pure dephasing of a vibrational adbond
[AD-A185222] N88-13740
Proceedings of the Third Airborne Imaging Spectrometer Data Analysis Workshop
[NASA-CR-181552] N88-13755
Preliminary results from an investigation of AIS-1 data over an area of epithermal alteration: Plateau, Northern Queensland, Australia N88-13768
Causes of spurious features in spectral reflectance data N88-13769
Automatic continuum analysis of reflectance spectra N88-13770
Analysis of airborne imaging spectrometer data for the Ruby Mountains, Montana, by use of absorption-band-depth images N88-13771
Mapping hydrothermally altered rocks in the Northern Grapevine Mountains, Nevada and California with the airborne imaging spectrometer N88-13772
Analysis of SO2 signals in SBUV/TOMS data N88-13794
Comparison of ground based and TOMS measurements of SO2 from volcanic emissions N88-13795

**ABSORPTIVITY**
Optical probe
[EP-PATENT-0-210-869-A1] N88-13984

**ABUNDANCE**
Abundance and distribution of ultramafic microbreccia in Moses Rock Dike: Quantitative application of AIS data N88-13766

**ACCELERATION (PHYSICS)**
Fiber-optic accelerometer investigation
[AD-A185359] N88-13561
Separable orthogonal coordinates and particle creation for an accelerating observer
[DE87-703358] N88-14029

**ACCELEROMETERS**
Fiber-optic accelerometer investigation
[AD-A185359] N88-13561

**ACCESS CONTROL**
Usage analysis of user files in UNIX
[NASA-CR-181561] N88-13868

**ACCIDENTS**
Visualization of an aircraft accident based on digital flight data recorder information N88-13278

**ACCOMMODATION**
Evaluation of a cryogenic refrigerator for cooling focal plane instrumentation. Appendix B: Accommodation study --- satellite instruments
[BAE-TP-8095-VOL-2] N88-13486

**ACCURACY**
Contribution to the improvement of the guidance accuracy of automatic pilots
[ETN-88-90607] N88-13360
Operating envelopes of particle sizing instrumentation used for icing research
[NASA-CR-180870] N88-13573

**ACOUSTIC ATTENUATION**
Theoretical and practical aspects of the functional absorber method of arranging sound absorbing panels
[BBC-RD-1987/15] N88-13955

**ACOUSTIC EMISSION**
Contribution of acoustic analysis to assess damage in fluid storage tanks under high pressure --- composite materials, filament winding
[SNIAS-872-430-119] N88-13407
The Shock and Vibration Digest, Volume 19, No. 12 N88-13746
Experimental studies on acoustic emission monitoring of crack propagation in offshore structures: A literature survey N88-13748
Acoustic emissions at an open crack
[DE88-001504] N88-13751

**ACOUSTIC IMPEDANCE**
Development of a new method of measuring the characteristic impedance and complex wave number of a porous acoustic material
[AD-A185038] N88-13957

**ACOUSTIC MEASUREMENT**
Development of an acoustic echosounder for detection of lower level atmospheric turbulence
[AD-A184877] N88-13831

**ACOUSTIC PROPAGATION**
Compressor large bandwidth noise emission mechanisms
[ETN-88-91177] N88-13959

**ACOUSTIC PROPERTIES**
Development of a new method of measuring the characteristic impedance and complex wave number of a porous acoustic material
[AD-A185038] N88-13957

**ACOUSTIC SCATTERING**
On a boundary data operator and generalized exterior Robin problems for the Helmholtz equation
[AD-A185124] N88-13915

**ACOUSTICS**
Development of an acoustic echosounder for detection of lower level atmospheric turbulence
[AD-A184877] N88-13831
Application of Vandermonde decomposition to directional and modal analysis of broadband transients
[AD-A185007] N88-13956

**ACTIVE CONTROL**
Modeling and control of large flexible vehicles in the atmosphere and space
[AD-A185388] N88-13377
Cartesian path control of a two-degree-of-freedom robot manipulator
[NASA-CR-182331] N88-13908

**ADA (PROGRAMMING LANGUAGE)**
An Ada graphical tool to support software development
[DE87-014854] N88-13891

**ADAPTIVE CONTROL**
Correction of inertial navigation system drift errors for an autonomous land vehicle using optical radar terrain data
[AD-A184973] N88-13311

**ADAPTIVE FILTERS**
An adaptive lattice algorithm for spectral line estimation
[AD-A184970] N88-13876

**ADAPTIVE OPTICS**
Develop techniques for ion implantation of (lead-lanthanum-zirconate-titanate) for adaptive optics
[DE88-000642] N88-13986

**ADHESIVE BONDING**
Influence of bonding shop moisture on metal-honeycomb junctions bonded with ultra-thin adheeive films
[SNIAS-872-422-112] N88-13399
Water disbondment characterization of organic Coating/metal substrate systems
[AD-A184847] N88-13454
Computation of bonded assemblies. Elastoplastic adhesives, first part
[SNIAS-NT-18926/AQET] N88-13467
First International Week of Adhesive Bonding and Assembling
[SNIAS-872-430-106] N88-13468
Flexibilized copolyimide adhesives
[NASA-TM-89303] N88-13474
Bending of a bonded beam as a test method for adhesive properties
[AD-A184813] N88-13736

**ADHESIVES**
Process for the production of a thermoplastic elastomer composition
[EP-PATENT-0-202-782-A2] N88-13485
Flexibilized copolyimide adhesives
[NASA-TM-89303] N88-13474

**ADSORPTION**
Pure dephasing of a vibrational adbond
[AD-A185222] N88-13740

**AERIAL PHOTOGRAPHY**
Matching segments from a map and an aerial image using relaxation techniques
[SNIAS-872-422-103] N88-13809

**AEROACOUSTICS**
Fluctuating pressure loads under high speed boundary layers
[NASA-TM-100517] N88-13962

**AERODYNAMIC CHARACTERISTICS**
Aerodynamics of Hypersonic Lifting Vehicles
[AGARD-CP-428] N88-13219
The drag of slender axisymmetric cones in rarefied hypersonic flow N88-13229
Low Reynolds number influence on aerodynamic performance of hypersonic lifting vehicles N88-13230
Hypersonic airbreathing propulsion: Evolution and opportunities N88-13231
Hypersonic aerodynamics: Applications for HOTOL N88-13252
A perspective of computational fluid dynamics N88-13279
Computational methods for problems in aerodynamics and large space structure using parallel and vector architectures
[AD-A185401] N88-13294
An experimental investigation of the aerodynamics of a NACA 64A010 airfoil-flap combination with and without flap oscillations. Part 1: Steady-state characteristics
[NASA-TM-88217] N88-13305

Nonlinear lift control at high speed and high angle of attack using vortex flow technology N88-13319
Aircraft dynamics: Aerodynamic aspects and wind tunnel techniques N88-13320
Full-envelope aerodynamic modeling of the Harrier aircraft
[NASA-TM-88376] N88-13363
Vortical Flows Research Program of the Fluid Dynamics Research Branch
[NASA-TM-88332] N88-13549

**AERODYNAMIC COEFFICIENTS**
Numerical calculations of the flowfield around propellers N88-13261

**AERODYNAMIC CONFIGURATIONS**
Numerical simulation of the hypersonic flow around lifting vehicles N88-13234
Lifting bodies: An attractive aerodynamic configuration choice for hypervelocity vehicles N88-13248
General aerodynamic-aerothermodynamic concepts for Hermes N88-13251
Numerical analysis of supersonic flows using panel method N88-13266
Tip aerodynamics from wind tunnel test of semi-span wing
[NASA-TM-88253] N88-13290
Fundamentals of fighter aircraft design N88-13316

**AERODYNAMIC FORCES**
Numerica calculation in the Laplace domain for subsonic unsteady aerodynamic forces acting on a finite wing N88-13256
Computational methods for problems in aerodynamics and large space structure using parallel and vector architectures
[AD-A185401] N88-13294

**AERODYNAMIC INTERFERENCE**
Computation of nacelle interference using boundary element method N88-13267

**AERODYNAMIC LOADS**
Numerical optimization of conical flow waveriders including detailed viscous effects N88-13245
Aeroelastic analysis of modern transport aircraft N88-13352
Wing divergence of trimmed aircraft N88-13354
Measurement of model deformation in wind tunnels N88-13358
Crack growth prediction in 3D structures under aeronautical-type spectrum loadings N88-13688

**AERODYNAMIC STABILITY**
Predictions of F-111 TACT aircraft buffet response and correlations of fluctuating pressures measured on aluminum and steel models and the aircraft
[NASA-CR-4069] N88-13218

**AERODYNAMICS**
Proceedings of the 4th NAL Symposium on Aircraft Computational Aerodynamics
[NAL-SP-7] N88-13253
Unsteady aerodynamics of an oscillating cascade in a compressible flow field
[NASA-TM-100219] N88-13346
A computer program for calculating unsteady aerodynamic coefficients for cascades in supersonic axial flow
[NASA-TM-100204] N88-13753

**AEROELASTIC RESEARCH WINGS**
Prediction of wing aeroelastic effects on aircraft life and pitching moment characteristics N88-13356

**AEROELASTICITY**
Numerica calculation in the Laplace domain for subsonic unsteady aerodynamic forces acting on a finite wing N88-13256
Aeroelasticity and optimization in fighter aircraft design N88-13324
Aeroelastic analysis of modern transport aircraft — European Airbus
[SNIAS-872-111-102] N88-13329
Velocity scaled aeroelastic testing of an unducted fan
[GTL-191] N88-13337
Static Aeroelastic Effects on High Performance Aircraft
[AGARD-CP-403] N88-13348
Examples of static aeroelastic effects on present combat aircraft projects N88-13349
Trends in aeroelastic analysis of combat aircraft N88-13350
Static aeroelastic considerations in the definition of design loads for fighter airplanes N88-13351
Static aeroelastic effects on the flutter of a supercritical wing N88-13353
The use of aeroelastic wind tunnel models to prove structural design N88-13355
Prediction of wing aeroelastic effects on aircraft life and pitching moment characteristics N88-13356
Influence of the static deformation on a wing in the unsteady aerodynamic N88-13357
Solution procedure for the Navier-Stokes equations applied to rotors N88-13533

**AERONAUTICAL ENGINEERING**
Fundamentals of fighter aircraft design N88-13316
Astronautics and aeronautics, 1978: A chronology
[NASA-SP-4023] N88-14062

**AEROSOLS**
Altered and enhanced iodargyrite with bismuth triiodide for use in precipitation enhancement operations
[AD-A185229] N88-13419
Comparison of ground based and TOMS measurements of SO2 from volcanic emissions N88-13795
Short-term in vitro screening studies related to the inhalation toxicology of potentially toxic aerosols
[AD-A184815] N88-13845

**AEROSPACE ENGINEERING**
Astronautics and aeronautics, 1978: A chronology
[NASA-SP-4023] N88-14062

**AEROSPACE INDUSTRY**
Fundamentals of fighter aircraft design N88-13316
Requirements and recommendations for the development of theoretical codes and experimental facilities in the near future N88-13327
Measurements in an electromagnetic test laboratory
[SNIAS-872-430-102] N88-13507
Operational groups at the Aerospatiale Aircraft Division
[SNIAS-872-111-107] N88-14036

**AEROSPACE SAFETY**
Civil aeronautics
[ETN-88-90616] N88-13309

**AEROSPACE SYSTEMS**
Initial dynamic load estimates during configuration design N88-13621
AGARD: The NATO Advisory Group for Aerospace Research and Development
[AD-A185062] N88-14063

**AEROSPACE TECHNOLOGY TRANSFER**
AGARD: The NATO Advisory Group for Aerospace Research and Development
[AD-A185062] N88-14063

**AEROSPACE VEHICLES**
Computational methods for problems in aerodynamics and large space structure using parallel and vector architectures
[AD-A185401] N88-13294
Guidance and control strategies for aerospace vehicles
[NASA-CR-181579] N88-13935

**AEROSTATICS**
Static Aeroelastic Effects on High Performance Aircraft
[AGARD-CP-403] N88-13348

**AEROTHERMODYNAMICS**
A 3-D Euler solution for hypersonic Mach numbers N88-13240
Aerothermodynamics research at NASA Ames N88-13242
The off-design performance of hypersonic waveriders N88-13244
General aerodynamic-aerothermodynamic concepts for Hermes N88-13251

**AFRICA**
Environmental processes and spectral reflectance characteristics associated with soil erosion in desert fringe regions
[NASA-CR-182332] N88-13811

**AGING (METALLURGY)**
Influence of microstructure and aging condition on the fatigue crack propagation in age hardened aluminium alloys N88-13659

**AGREEMENTS**
High resolution satellite imagery simulation — treaty verification
[FOA-C-30462-3.3,9.3] N88-13810

**AIR CONDITIONING EQUIPMENT**
Plant Growth Module (PGM) conceptual design N88-13855

**AIR COOLING**
Cooling electronic equipment at simulated high altitude in hypobaric chambers
[AD-A185196] N88-13560

**AIR FILTERS**
Computer code simulations of explosions in flow networks and comparison with experiments
[DE88-001946] N88-13491

**AIR FLOW**
Practical application of two-dimensional viscous flow computation N88-13257
The development and evaluation of three-dimensional models of cold flow in internal combustion engines
[DE88-900077] N88-13594
Controlled ecological life support systems: Development of a plant growth module N88-13854

**AIR INTAKES**
The role of computation fluid dynamics in aeronautical engineering (4). The development and applications of implicit TVD finite volume code N88-13259

**AIR POLLUTION**
The use of TOMS data for tropospheric ozone studies N88-13784

**AIR TRANSPORTATION**
Airline safety: A comparative analysis
[AD-A185358] N88-13308

**AIR WATER INTERACTIONS**
Reactions of porphyrins in surfactant assemblies, microemulsions and in solutions
[AD-A184797] N88-13412
Estimation of marine boundary layer depth and relative humidity with multispectral satellite measurements
[AD-A184881] N88-13804

**AIRBORNE/SPACEBORNE COMPUTERS**
Electrical flight commands in transport aircraft
[SNIAS-872-111-108] N88-13361
Study of fault tolerant techniques for satellite data handling
[FTT/REP/0001/SAAB] N88-13860

**AIRCRAFT ACCIDENTS**
Airline safety: A comparative analysis
[AD-A185358] N88-13308

**AIRCRAFT COMPARTMENTS**
A hybrid fibreglass-CFRP cloth for new furnishings — aircraft cabins
[SNIAS-872-111-109] N88-13396

**AIRCRAFT CONFIGURATIONS**
Analytical method for generating computational grids about complete aircraft configurations N88-13287
Navier-Stokes simulation of transonic transportation aircraft configurations. 1: Flow-field simulation over wing-fuselage combinations N88-13288
Computation of transonic flows with nacelle simulation
[SNIAS-872-111-117] N88-13300

**AIRCRAFT CONSTRUCTION MATERIALS**
The use of aeroelastic wind tunnel models to prove structural design N88-13355
A hybrid fibreglass-CFRP cloth for new furnishings — aircraft cabins
[SNIAS-872-111-109] N88-13396
Paints required for aeronautical construction
[SNIAS-872-551-102] N88-13470

**AIRCRAFT CONTROL**
Structural optimization in the design process — aircraft
[SNIAS-872-111-115] N88-13885

**AIRCRAFT DESIGN**
The A320 Airbus program
[SNIAS-872-111-105] N88-13215
Validation elements of the computation methods and measurement techniques for high lift aerodynamic systems
[SNIAS-872-111-101] N88-13299
Special Course on Fundamentals of Fighter Aircraft Design
[AGARD-R-740] N88-13315
Fundamentals of fighter aircraft design N88-13316
Mission requirements and aircraft sizing N88-13317
Design of wings and wing/body configurations for transonic and supersonic speeds N88-13318
Aircraft dynamics: Aerodynamic aspects and wind tunnel techniques N88-13320
Fundamentals of fighter aircraft design: Engine intake and afterbody N88-13322
Aeroelasticity and optimization in fighter aircraft design N88-13324
Materials for fighter aircraft N88-13325
Requirements and recommendations for the development of theoretical codes and experimental facilities in the near future N88-13327
Aeroelastic analysis of modern transport aircraft — European Airbus
[SNIAS-872-111-102] N88-13329
Damage considerations in sizing aircraft cells. Life predictions
[SNIAS-872-111-116] N88-13330
Static Aeroelastic Effects on High Performance Aircraft
[AGARD-CP-403] N88-13348
Static aeroelastic considerations in the definition of design loads for fighter airplanes N88-13351
The use of aeroelastic wind tunnel models to prove structural design N88-13355
Surface treatment problems found in new aircraft designed using structural composites
[SNIAS-872-111-113] N88-13397
Utilization of a high rate vector computer in computational fluid mechanics for aeronautics
[ETN-88-91171] N88-13547
Overall description of the computer aided design and manufacturing systems associated with the A320 program at Aerospatiale and its partners
[SNIAS-872-111-104] N88-13883

Presentation of SIGMA (Interactive Assisted Geometry System). A computer assisted shape design program developed at the Aerospatiale Aircraft Division
[SNIAS-872-111-110] N88-13884
Structural optimization in the design process — aircraft
[SNIAS-872-111-115] N88-13885
Operational groups at the Aerospatiale Aircraft Division
[SNIAS-872-111-107] N88-14036

**AIRCRAFT ENGINES**
A numerical investigation on wing/nacelle interferences N88-13258
Correlation of air pressure drop and flame arrestor characteristics for explosion suppression materials
[AD-A184960] N88-13340

**AIRCRAFT FUELS**
Correlation of air pressure drop and flame arrestor characteristics for explosion suppression materials
[AD-A184960] N88-13340
Study of electrostatic modulation of fuel sprays to enhance combustion performance in an aviation gas turbine
[AD-A184967] N88-13341

**AIRCRAFT GUIDANCE**
Contribution to the improvement of the guidance accuracy of automatic pilots
[ETN-88-90607] N88-13360

**AIRCRAFT HAZARDS**
TOMS and the NOAA/FAA volcano support plan N88-13796

**AIRCRAFT MAINTENANCE**
A project of an intelligent system to help on-line trouble shooting — aircraft maintenance
[SNIAS-872-111-106] N88-13216
Design and control of repairs of carbon fiber lift augmentation flaps in the ATR42 aircraft
[SNIAS-872-111-112] N88-13217
Simulated service test behavior of various internal and external coatings applied on CF6-50 first stage turbine blades
[NLR-MP-86018-U] N88-13343
Investigation of the nature and concentration of vapor and mist during the cleaning of aircraft
[PML-1985-29] N88-13817

**AIRCRAFT MANEUVERS**
Trends in aeroelastic analysis of combat aircraft N88-13350
Overlooked potential of systems with Markovian coefficients
[NLR-MP-86049-U] N88-13366

**AIRCRAFT MODELS**
Measurement of model deformation in wind tunnels N88-13358

**AIRCRAFT PERFORMANCE**
The A320 Airbus program
[SNIAS-872-111-105] N88-13215
Aircraft dynamics: Aerodynamic aspects and wind tunnel techniques N88-13320
Techniques for performance optimisation in cruise and manoeuverability N88-13321
Requirements and recommendations for the development of theoretical codes and experimental facilities in the near future N88-13327
Aeroelastic analysis of modern transport aircraft N88-13352

**AIRCRAFT PILOTS**
Sitting posture of helicopter pilots of the Royal Netherlands Air Force; preliminary recommendations
[IZF-1986-16] N88-13857

**AIRCRAFT SAFETY**
Airline safety: A comparative analysis
[AD-A185358] N88-13308
Theoretical analysis of the electrical aspects of the basic electro-impulse problem in aircraft de-icing applications
[NASA-CR-180845] N88-13310
Corrosion in avionics and associated equipment; cause, effect and prevention N88-13335

**AIRCRAFT STABILITY**
Examples of static aeroelastic effects on present combat aircraft projects N88-13349

**AIRCRAFT STRUCTURES**
Materials for fighter aircraft N88-13325
Surface treatment problems found in new aircraft designed using structural composites
[SNIAS-872-111-113] N88-13397
Philosophy and practice of nondestructive tests of composite material structures at Aerospatiale Aquitaine
[SNIAS-872-430-105] N88-13400
Measurement and control of damage in composite materials: Nondestructive controls by thermography, holography, and radiography
[SNIAS-872-430-110] N88-13403
Structural optimization in the design process — aircraft
[SNIAS-872-111-115] N88-13885

**AIRFOILS**
Computation of dynamic stall of NACA0012 airfoil by block pentadiagonal matrix scheme N88-13255
Practical application of two-dimensional viscous flow computation N88-13257
The role of computation fluid dynamics in aeronautical engineering (4). The development and applications of implicit TVD finite volume code N88-13259
Application of discrete vortex method to analysis of separated flow around aerofoils N88-13268
Navier-Stokes analysis of laminar flow control of a two-dimensional airfoil N88-13286
A swept wing panel in a low speed flexible walled test section
[NASA-CR-4106] N88-13292
The development of a computer code (U2DIIF) for the numerical solution of unsteady, inviscid and incompressible flow over an airfoil
[AD-A185033] N88-13293
Computation of rime ice accretion on airfoils
[FFA-TN-1987-08] N88-13301
An experimental investigation of the aerodynamics of a NACA 64A010 airfoil-flap combination with and without flap oscillations. Part 1: Steady-state characteristics
[NASA-TM-88217] N88-13305
Measurement of local convective heat transfer coefficients from a smooth and roughened NACA-0012 airfoil: Flight test data
[NASA-TM-100284] N88-13552

**AIRFRAMES**
Fundamentals of fighter aircraft design: Engine intake and afterbody N88-13322

**AIRLINE OPERATIONS**
Civil aeronautics
[ETN-88-90616] N88-13309

**AIRPORTS**
ZEUS: A knowledge-based expert system that assists in predicting visibility at airbases
[AD-A184197] N88-13829

**ALGEBRA**
A system of three-dimensional complex variables
[NASA-TM-88318] N88-13951

**ALGORITHMS**
Driving mechanism of unsteady separation shock motion in hypersonic interactive flow N88-13226
Numerical prediction of turbulent flows in dump diffusers N88-13265
Programming techniques for high-speed processing of large scale numerical simulation on supercomputers N88-13269
Vectorizing the FFTs on supercomputer SX system N88-13270
Tridiagonal approximate factorization method: A preconditioning technique for solving nonsymmetric linear systems suitable to supercomputers N88-13271
MODTRAN: A moderate resolution model for LOWTRAN
[AD-A185384] N88-13503
Model-based motion estimation and its application to restoration and interpolation of motion pictures
[AD-A185054] N88-13558
Free Lagrange reconnection algorithms for hydrocodes using a quadrilateral mesh
[DE88-001580] N88-13752
Automatic continuum analysis of reflectance spectra N88-13770
Learning a color algorithm from examples
[AD-A184385] N88-13862
Approximating multivariate normal orthant probabilities using the Clark algorithm
[AD-A184855] N88-13873
An adaptive lattice algorithm for spectral line estimation
[AD-A184970] N88-13876
Indirect solution of static problems using concurrent vector processing computers
[DE87-012105] N88-13889
The maximum likelihood estimator method of image reconstruction: Its fundamental characteristics and their origin
[DE88-000462] N88-13892
Research and development of finite elements and iterative algorithms for elliptic partial differential equations
[DE88-001381] N88-13934
Restoration of particle pitch angle distribution functions by a maximum entropy algorithm
[ATR-86(7098)-3] N88-13969
Molecular dynamics studies of aromatic hydrocarbon liquids
[DE88-001473] N88-13973
Supercomputing at Florida State University (FSU)
[DE87-013900] N88-14009
Range imagery algorithms for the detection of obstacles by autonomous vehicles
[AD-A185421] N88-14045

**ALKALINE EARTH OXIDES**
Activated metal oxide surfaces as highly basic and reducing environments
[AD-A184958] N88-13417

**ALKANES**
Organic molecules on meteoritic solid substrates
[NASA-CR-181570] N88-13411

**ALLOYS**
The mechanism by which sigma-phase forms in Fe-Cr-Ni system alloys
[BLL-M-37380-(5828.4)] N88-13437
Corrosion resistance of sintered alloy steels
[BLL-M-37363-(5828.4)] N88-13438

**ALTITUDE SIMULATION**
Cooling electronic equipment at simulated high altitude in hypobaric chambers
[AD-A185196] N88-13560

**ALUMINIDES**
Advances in processing techniques for nickel aluminides
[DE87-014571] N88-13449
Development of iron aluminides
[AD-A185190] N88-13461

**ALUMINUM**
Plasticity of aluminum and iron at high shear strain rate and high pressure N88-13430
X-ray analysis of polycrystalline aluminium subjected to fatigue cycling
[NAL-TM-MT-8706] N88-13434
The growth of persistent slip bands N88-13648

**ALUMINUM ALLOYS**
Investigation by differential scanning calorimetry of microstructure in a superplastic Al-Mg-Zr alloy
[AD-A184902] N88-13439
A fundamental study of P/M processed elevated temperature aluminum alloys
[AD-A185393] N88-13445
Phase diagram and thermochemical properties of the Al-Cu system
[ETN-88-91015] N88-13447
An investigation of unipolar arcing at atmospheric pressure in aluminum 2024 and aluminum coated glass slides
[AD-A184903] N88-13521
The effect of ion beam mixed Ni-Al surface layers on PSB extrusion morphology in fatigued nickel N88-13652
The evolution of local mechanical properties of Al 2219-T851 during fatigue N88-13653
Cyclic deformation of an extruded AlMgSi alloy N88-13654
Closure behavior under constant effective stress intensity loading conditions N88-13656
Growth of short fatigue cracks in a squeeze formed aluminum alloy N88-13658
Influence of microstructure and aging condition on the fatigue crack propagation in age hardened aluminium alloys N88-13659
Fatigue crack growth behavior of A356-T6 cast aluminum alloy N88-13660
Behavior of short cracks in a 2024 aluminum alloy sheet tested at several stress ratios N88-13669
The effect of microstructure on the surface crack length: Crack depth relationship for short cracks N88-13670
On the role of crack tip shielding in influencing the behavior of long and small fatigue cracks in aluminum-lithium alloy 2090 N88-13671
The influence of microstructure and residual stresses on the initiation and propagation of short surface cracks on AlMgSi1 N88-13674
An experimental study of closure behavior of naturally initiated small cracks N88-13676
Propagation of small fatigue cracks in 2024-T3 aluminum alloy N88-13678
Fatigue crack retardation in aluminium alloys N88-13681
Observations on the effect of overloads on fatigue crack growth N88-13684
Crack growth in contrasting titanium alloys under the conjoint action of high and low cycle fatigue N88-13686
Variable amplitude fatigue crack growth in aluminum alloys 2090-T8E41 and 7075-T651 N88-13687
Effects of MN dispersoids on near threshold fatigue crack growth in 2134 type alloys N88-13692
Fatigue mechanisms in ARALL, a fatigue resistant hybrid aluminum aramid composite material N88-13711
A comparison of plastic work energy and external input for fatigue crack propagation N88-13722
X-ray fatigue failure prediction based on plasticity response to microcracks N88-13725
Environmentally assisted fatigue crack growth N88-13731
Fatigue crack growth N88-13734

Characterization of the microstructures of various materials
[AD-A184961] N88-14017

**ALUMINUM COATINGS**
Ion plating for corrosion control
[AD-A185061] N88-13442

**ALUMINUM GALLIUM ARSENIDES**
Resonant level lifetime in GaAs/ AlGaAs double-barrier structures
[AD-A185376] N88-14020

**ALUMINUM GRAPHITE COMPOSITES**
Effect of interface on mechanical properties of graphite/201 aluminum composites N88-13717

**ALUMINUM OXIDES**
T.E.M. study of boehmite gels and of their transformation into alpha-alumina
[SNIAS-872-430-121] N88-14023

**AMINES**
Studies on syntheses of amine-carboxyboranes (boron analogues of amino acids) and derivatives
[AD-A184838] N88-13386
Thermally stable aromatic structures from acyclic precursors. 1. Para polyphenylene model compounds from 3-Dimethyl amino hex-5-EN-1-YNES
[AD-A185300] N88-13462

**AMORPHOUS MATERIALS**
Microstructure of amorphous and crystalline zirconium alloys rapidly solidified
[DE87-703700] N88-13432

**AMORPHOUS SEMICONDUCTORS**
Preparation of amorphous silicon semiconductors
[GB-PATENT-2-176-054-A] N88-14022

**AMPLIFICATION**
A focussed MCP (microchannel plate) image intensifier type for high speed gating
[DE88-000480] N88-13555
Narrow linewidth gain measurements in a KrF excimer amplifier pumped longitudinally by a high-power electron beam
[DE88-001365] N88-13575

**AMPLIFIERS**
Narrow linewidth gain measurements in a KrF excimer amplifier pumped longitudinally by a high-power electron beam
[DE88-001365] N88-13575

**AMPLITUDE MODULATION**
Axial anisotropy of the intensity of the cosmic ray nuclear component
[IFSI-87-7] N88-14061

**AMPLITUDES**
Fatigue 87, volume 1
[AD-A184045] N88-13645
A dislocation model for fatigue crack propagation under variable amplitude loading N88-13683
The how and why of variable amplitude testing N88-13690

**AMPTE (SATELLITES)**
A fluid simulation of the AMPTE lithium gas releases in the solar wind
[TRITA-EPP-87-06] N88-14056

**ANALOG TO DIGITAL CONVERTERS**
Digitization functions in computer graphics
[ETN-88-91363] N88-13887

**ANALOGS**
Studies on syntheses of amine-carboxyboranes (boron analogues of amino acids) and derivatives
[AD-A184838] N88-13386

**ANALYTIC FUNCTIONS**
A system of three-dimensional complex variables
[NASA-TM-88318] N88-13951

**ANGLE OF ATTACK**
Low speed wind tunnel investigation of propeller slipstream aerodynamic effects on different nacelle/wing combinations. Part 1: Total forces and moments and pressure distributions on nacelle/wing at different angles of attack and yaw and at different thrust coefficients
[FFA-TN-1987-22] N88-13302

**ANGLES (GEOMETRY)**
Effects of free stream turbulence, Reynolds number and incidence angle on axial turbine cascade performance N88-13339

**ANIMALS**
A plethysmograph for measuring pulmonary ventilation in small animals
[AD-A184978] N88-13846

**ANISOTROPIC MEDIA**
Mechanics of anisotropic media. Study of the boundary conditions --- stratified composites
[SNIAS-872-430-112] N88-13404

**ANISOTROPY**
Velocity scaled aeroelastic testing of an unducted fan
[GTL-191] N88-13337
Molecular and supramolecular orientation in conducting polymers
[DE88-000533] N88-13472
Axial anisotropy of the intensity of the cosmic ray nuclear component
[IFSI-87-7] N88-14061

**ANNEALING**
Threshold stress for fatigue crack initiation from a small crack N88-13675
Structural characterization of ion implanted beta-SiC thin films
[DE87-014567] N88-14027

**ANNUAL VARIATIONS**
Environmental processes and spectral reflectance characteristics associated with soil erosion in desert fringe regions
[NASA-CR-182332] N88-13811

**ANOMALIES**
Anomalous phonon behavior of superconductor Y-Ba-Cu-O
[DE87-703401] N88-14010

**ANTARCTIC REGIONS**
TOMS: The Antarctic ozone hole and ozone trends N88-13775

**ANTENNA ARRAYS**
The use of coaxial transmission line elements in log-periodic dipole arrays
[AD-A184864] N88-13499

**ANTENNA DESIGN**
Capacitive resonant transducer for the Frascati gravitational antenna
[IFSI-86-9] N88-13528

**ANTHROPOMETRY**
Physiological determinants of load bearing capacity
[AD-A184977] N88-13848

**ANTIFERROMAGNETISM**
A mechanism for symmetry breaking in antiferromagnetic Heisenberg systems
[ETN-88-91320] N88-14031

**ANTIGRAVITY**
Non-minimal interaction of gravity with other physical fields: An overview
[DE87-703362] N88-13819

**ANTIMONY ALLOYS**
MBE growth of InAsSb strained-layer superlattices
[DE88-000365] N88-14011

**ANTIPROTONS**
Experimental studies of elementary particle interactions at high energies
[DE88-000804] N88-13971

**ANTISHIP MISSILES**
Utilization of dynamic characteristics of materials to optimize military explosive charges. Application to antiship devices
[SNIAS-872-320-101] N88-13743

**APPENDAGES**
An experimental investigation of appendage-flat plate junction flow. Volume 2. Elliptical nose appendage data base
[AD-A184974] N88-13539

**APPLICATIONS PROGRAMS (COMPUTERS)**
Experiences using the Mark IV supersonic hypersonic arbitrary body program N88-13249
Practical application of two-dimensional viscous flow computation N88-13257
The role of computation fluid dynamics in aeronautical engineering (4). The development and applications of implicit TVD finite volume code N88-13259
Practical and modern simulation by systematic connection of the LU-ADI code and the solution adaptive grid program N88-13260
Development of the computer program for turbulent boundary layers N88-13264
Numerical analysis of supersonic flows using panel method N88-13266
Computation of nacelle interference using boundary element method N88-13267
Computer graphics for computational aerodynamics N88-13276
A numerical study of the effects of curvature and convergence on dilution jet mixing
[NASA-TM-89878] N88-13347
MODTRAN: A moderate resolution model for LOWTRAN
[AD-A185384] N88-13503

**APPROXIMATION**
Tridiagonal approximate factorization method: A preconditioning technique for solving nonsymmetric linear systems suitable to supercomputers N88-13271
Master plots for predicting the case-depth in laser surface treatments
[PB87-221875] N88-13574
Approximating multivariate normal orthant probabilities using the Clark algorithm
[AD-A184855] N88-13873
Stability properties of spline approximations for retarded systems
[PB87-220919] N88-13910
Numerical and analytical methods in nonlinear partial differential equations
[AD-A185210] N88-13918

**AQUEOUS SOLUTIONS**
Organic molecules on meteoritic solid substrates
[NASA-CR-181570] N88-13411
Coagulation in stirred tanks
[88711373] N88-13420

**ARC DISCHARGES**
Low-current behavior and current chopping of vacuum arcs
[ISBN-90-9001649-X] N88-13529

**ARCHITECTURE (COMPUTERS)**
Utilization of a high rate vector computer in computational fluid mechanics for aeronautics
[ETN-88-91171] N88-13547
Test and evaluation of the transputer in a multi-transputer system
[AD-A184969] N88-13859
Arrays for discrete Fourier transform
[REPT-87-019] N88-13861
XCUT: A rule-based expert system for the automated process planning of machined parts
[DE87-011638] N88-13905

**ARGON**
Extreme ultraviolet beam-foil spectroscopy of highly ionized neon and argon
[AD-A185197] N88-13418

**ARGON LASERS**
Photocurrent generation from basic metals, utilizing a short pulsed ArF excimer laser
[AD-A184928] N88-13579

**ARIANE LAUNCH VEHICLE**
Introduction to local area network design on Ariane 5 and future launchers
[SNIAS-872-422-102] N88-13886

**ARMATURES**
On the glitches in the force transmitted by an electrodynamic exciter to a structure N88-13624

**ARMED FORCES (FOREIGN)**
Corrosion in avionics and associated equipment; cause, effect and prevention N88-13335

**ARMOR**
Numerical simulations of impact tests on a rigid wall --- armor steel
[SNIAS-872-320-102] N88-13744

**ARRAYS**
Arrays for discrete Fourier transform
[REPT-87-019] N88-13861

**ARTIFICIAL INTELLIGENCE**
A project of an intelligent system to help on-line trouble shooting --- aircraft maintenance
[SNIAS-872-111-106] N88-13216
Towards building a team of intelligent robots
[NASA-CR-181538] N88-13595
Collision-free motion of two robot arms in a common workspace
[CSE-87-00002] N88-13596
Dealing with unanticipated events in autonomous navigation
[DE88-000590] N88-13602
ZEUS: A knowledge-based expert system that assists in predicting visibility at airbases
[AD-A184197] N88-13829
Diagnostic reasoning in digital systems
[NASA-CR-181564] N88-13871
Behavioral Architecture Robot Control System (BARCS): A new way of building robots
[REPT-87-036] N88-13902

**ARTIFICIAL SATELLITES**
Satellite autonomous navigation with SHAD (Stellar Horizon Atmospheric Dispersion)
[AD-A184988] N88-13313

**ASHES**
TOMS and the NOAA/FAA volcano support plan N88-13796

**ASPECT RATIO**
The effect of microstructure on the surface crack length: Crack depth relationship for short cracks N88-13670

**ASSEMBLIES**
Reactions of porphyrins in surfactant assemblies, microemulsions and in solutions
[AD-A184797] N88-13412
Computation of bonded assemblies. Elastoplastic adhesives, first part
[SNIAS-NT-18926/AQET] N88-13467

**ASSEMBLING**
Design and assembly sequence analysis of option 3 for CETF reference space station
[NASA-TM-100503] N88-13369
RETE experiment Assembly, Integration, and Verification (AIV) activities
[IFSI-87-6] N88-13380

**ASTRONOMICAL MODELS**
Comments on H. Arp The persistent problem of spiral galaxies
[TRITA-EPP-87-05] N88-14052
**ASTRONOMICAL TELESCOPES**
Optical photometer for the Tirgo telescope
[IFSI-87-5] N88-13985
**ASTROPHYSICS**
Photon counting image sensor development for astronomical applications
[NASA-CR-181507] N88-14049
Astrophysics observatory in Byurakan
[AD-A185144] N88-14050
**ASYMMETRY**
Dynamic behavior of dissymmetric rotor bearings modelled with a periodic coefficient large system N88-13640
**ASYMPTOTIC METHODS**
Extrema of skewed stable processes
[AD-A185422] N88-13925
**ASYMPTOTIC SERIES**
Asymptotic analysis of a turbulent boundary layer in a strong adverse pressure gradient
[AD-A185406] N88-13543
**ATMOSPHERIC BOUNDARY LAYER**
Estimation of marine boundary layer depth and relative humidity with multispectral satellite measurements
[AD-A184881] N88-13804
**ATMOSPHERIC CHEMISTRY**
Scientific and Operational Requirements for TOMS Data
[NASA-CP-2497] N88-13774
The use of TOMS data for tropospheric ozone studies N88-13784
The polar ionosphere and interplanetary field
[AD-A185386] N88-13822
**ATMOSPHERIC CIRCULATION**
Systematic stratospheric-tropospheric exchange viewed from isentropic coordinates N88-13777
Insights into the general circulation of the lower stratosphere from TOMS N88-13780
Lower-stratospheric/upper-tropospheric exchange processes associated with tropical cyclones as observed by TOMS N88-13782
Environmental and convective influence on tropical cyclone development versus non-development
[AD-A185231] N88-13835
Global atmospheric circulation statistics: Four year averages
[NASA-TM-100690] N88-13842
**ATMOSPHERIC COMPOSITION**
OH(A-X) fluorescence from photodissociative excitation of HO2 at 157.5 nm
[NASA-CR-181580] N88-13429
TOMS: The Antarctic ozone hole and ozone trends N88-13775
October lower stratospheric Antarctic temperature and total ozone from 1979-1985 N88-13776
Photochemical ozone overburden correction N88-13778
Analysis of the breakdown of the Antarctic circumpolar vortex using TOMS ozone data N88-13779
Insights into the general circulation of the lower stratosphere from TOMS N88-13780
Lower-stratospheric/upper-tropospheric exchange processes associated with tropical cyclones as observed by TOMS N88-13782
Volcanic eruption detection with TOMS N88-13793
Analysis of SO2 signals in SBUV/TOMS data N88-13794
Comparison of ground based and TOMS measurements of SO2 from volcanic emissions N88-13795
Use of satellite data in volcano monitoring N88-13797
Complementary information between UV and IR for remote sensing of total ozone N88-13800
**ATMOSPHERIC DIFFUSION**
A computer code to calculate line by line atmospheric transmission spectra on a microcomputer
[NASA-TM-100686] N88-13372
**ATMOSPHERIC EFFECTS**
The effect of environment on low cycle fatigue properties in HSLA steel N88-13705
Fatigue crack propagation in Al-Zn-Mg bicrystals and its dependence on the environment N88-13707
Environmental fracture toughness and static fatigue crack propagation of silica glass N88-13716
Environmentally assisted fatigue crack growth N88-13731
AIS-2 radiometry and a comparison of methods for the recovery of ground reflectance N88-13757
Calibrating AIS images using the surface as a reference N88-13760
Causes of spurious features in spectral reflectance data N88-13769
**ATMOSPHERIC ENTRY**
Guidance and control strategies for aerospace vehicles
[NASA-CR-181579] N88-13935
**ATMOSPHERIC MODELS**
Analysis of geophysical data bases and models for spacecraft interactions
[AD-A184809] N88-13375
MODTRAN: A moderate resolution model for LOWTRAN
[AD-A185384] N88-13503
Ozone, jet streaks and severe weather N88-13781
Application of TOMS data to weather analysis models N88-13787
The polar ionosphere and interplanetary field
[AD-A185386] N88-13822
**ATMOSPHERIC MOISTURE**
Influence of bonding shop moisture on metal-honeycomb junctions bonded with ultra-thin adhesive films
[SNIAS-872-422-112] N88-13399
**ATMOSPHERIC PHYSICS**
Analysis of geophysical data bases and models for spacecraft interactions
[AD-A184809] N88-13375
**ATMOSPHERIC PRESSURE**
An investigation of unipolar arcing at atmospheric pressure in aluminum 2024 and aluminum coated glass slides
[AD-A184903] N88-13521
An analysis of tropopause pressure and total ozone correlations N88-13789
The use of TOMS-modified VAS data for large-scale NWP N88-13791
Cosmic ray NM-64 neutron monitor data 14, Rome, Italy, January - December 1985
[IFSI-87-8] N88-14060
**ATMOSPHERIC REFRACTION**
Satellite autonomous navigation with SHAD (Stellar Horizon Atmospheric Dispersion)
[AD-A184988] N88-13313
An investigation of millimeter wave propagation in the atmosphere: Measurement program
[AD-A184837] N88-13498
**ATMOSPHERIC SOUNDING**
Development of a data analysis system for the detection of lower level atmospheric turbulence with an acoustic sounder
[AD-A184972] N88-13821
Development of an acoustic echosounder for detection of lower level atmospheric turbulence
[AD-A184877] N88-13831
**ATMOSPHERIC STRATIFICATION**
Systematic stratospheric-tropospheric exchange viewed from isentropic coordinates N88-13777
**ATMOSPHERIC TEMPERATURE**
Contributions of lidar measurements to the study of long term variations of the middle atmosphere
[ETN-88-91237] N88-13824
**ATMOSPHERIC TURBULENCE**
Development of a data analysis system for the detection of lower level atmospheric turbulence with an acoustic sounder
[AD-A184972] N88-13821
Development of an acoustic echosounder for detection of lower level atmospheric turbulence
[AD-A184877] N88-13831
**ATOMIC BEAMS**
Atomic beam studies of the interaction of hydrogen with transition metal surfaces
[DE88-000208] N88-13970
**ATOMIC CLOCKS**
On-orbit frequency stability analysis of the GPS NAVSTAR 8 rubidium clock and NAVSTARs 9 and 10 cesium clocks
[AD-A184964] N88-13312
**ATOMIC PHYSICS**
Atomic physics with highly charged ions
[DE88-000894] N88-13972
Theoretical atomic and molecular physics
[DE88-001625] N88-13974
**ATOMIC STRUCTURE**
The role of electronic structure calculation in mechanistic analysis of electron transfer reactions in the liquid phase
[DE87-014395] N88-13963
**ATOMIZING**
Study of electrostatic modulation of fuel sprays to enhance combustion performance in an aviation gas turbine
[AD-A184967] N88-13341
**ATOMS**
Theory of multiphoton ionization of atoms by strong, short pulsed lasers
[DE88-000963] N88-13588
**AUGMENTATION**
Improvements to a UHF rebroadcast television link suffering tidal fading: Countisbury UHF relay station
[BBC-RD-1987/14] N88-13495
**AURORAL ZONES**
Electric field measurements on Viking: First results
[TRITA-EPP-87-04] N88-13826
**AUSTENITIC STAINLESS STEELS**
Welded joint fatigue of a AISI 304 L type stainless steel
[DE87-703530] N88-13607
**AUTOMATIC CONTROL**
Automated design of controlled diffusion blades
[NASA-TM-100251] N88-13304
**AUTOMATIC PILOTS**
Contribution to the improvement of the guidance accuracy of automatic pilots
[ETN-88-90607] N88-13360
Reduced order optimal command applied to longitudinal automatic pilots
[SNIAS-872-111-114] N88-13362
**AUTOMOBILES**
Computational study of three-dimensional wake structures
[REPT-2] N88-13281
Applications of fatigue analyses: Transportation N88-13733
**AUTOMORPHISMS**
A construction of simple Abelian varieties
[ZW-8702] N88-13929
**AUTONOMOUS NAVIGATION**
Satellite autonomous navigation with SHAD (Stellar Horizon Atmospheric Dispersion)
[AD-A184988] N88-13313
Dealing with unanticipated events in autonomous navigation
[DE88-000590] N88-13602
Range imagery algorithms for the detection of obstacles by autonomous vehicles
[AD-A185421] N88-14045
**AVALANCHE DIODES**
Optically tuned MM-wave IMPATT source
[AD-A185250] N88-13523
**AVERAGE**
Causes of spurious features in spectral reflectance data N88-13769
**AVIONICS**
Workshop on Avionics Corrosion Control
[AGARD-R-733] N88-13331
Avionic corrosion N88-13332
Corrosion of electronic components N88-13333
US Naval Air Force avionic and electrical system corrosion prevention and control maintenance N88-13334
Avionics and corrosion N88-13336
Error propagation in a digital avionic mini processor
[NASA-CR-181565] N88-13872
**AXIAL FLOW**
Application of modified loss and deviation correlations to transonic axial compressors
[AGARD-R-745] N88-13344
**AXISYMMETRIC BODIES**
The drag of slender axisymmetric cones in rarefied hypersonic flow N88-13229
Hypersonic static and dynamic stability of axisymmetric shapes: A comparison of prediction methods and experiment N88-13245
The role of computation fluid dynamics in aeronautical engineering (4). The development and applications of implicit TVD finite volume code N88-13259
Development of the computer program for turbulent boundary layers N88-13264
Rarefied gas numerical wind tunnel. 2: Two-dimensional and axially symmetric bodies N88-13273
**AXISYMMETRIC FLOW**
Numerical analysis of axisymmetric flow with H2-O2 reactions N88-13272

## B

**BACKSCATTERING**
Large bandwidth ground scattering model --- radar scattering
[FOA-C-30458-3.2] N88-13511
**BALANCE**
A GaAs MESFET balanced mixer with very low intermodulation
[AD-A184848] N88-14015
**BALLISTICS**
An ultra-high-speed cinematographic method for the study of wakes in hypersonic ballistic ranges N88-13228

Production of flows for aeroballistic investigation in the shock tubes of the Franco-German Research Institute (ISL), Saint-Louis (France)
[ISL-R-113/86] N88-13295
Optoelectronic measurement methods for ballistic experiments
[PB87-110706] N88-13554

**BANDPASS FILTERS**
Implementation of an FIR band pass filter using a bit-slice processor
[AD-A184895] N88-13875

**BARS**
Exact finite element method analysis of viscoelastic tapered structures to transient loads N88-13632

**BAYES THEOREM**
Comparing hard and soft prior bounds in geophysical inverse problems
[NASA-CR-181557] N88-13820

**BEAM INTERACTIONS**
Atomic beam studies of the interaction of hydrogen with transition metal surfaces
[DE88-000206] N88-13970

**BEAMS (RADIATION)**
Phenomena at a focus in a laser system
[AD-A185442] N88-13585

**BEAMS (SUPPORTS)**
Shape optimization of damping layers N88-13635
An examination of chaotic motion for the buckled beam N88-13644
Optimal control of large space structures via generalized inverse matrix
[NASA-CR-182336] N88-13907

**BEARINGS**
Coatings for high-temperature bearings and seals
[NASA-TM-100249] N88-13453
Dynamic behavior of dissymmetric rotor bearings modelled with a periodic coefficient large system N88-13640

**BEND TESTS**
Crack initiation studies in hydrogen embrittled spring steel strip N88-13710
An optical interferometry technique to evaluate closure along a crack front N88-13726

**BENDING**
Crack growth prediction in 3D structures under aeronautical-type spectrum loadings N88-13688

**BENDING FATIGUE**
Bending of a bonded beam as a test method for adhesive properties
[AD-A184813] N88-13736

**BENZENE**
Detailed mechanism of toluene oxidation and comparison with benzene
[NASA-TM-100261] N88-13428

**BIBLIOGRAPHIES**
Literature review of solid lubrication mechanisms
[AD-A185010] N88-13456

**BICRYSTALS**
Fatigue crack propagation in Al-Zn-Mg bicrystals and its dependence on the environment N88-13707

**BIG BANG COSMOLOGY**
Cosmology in the plasma universe
[TRITA-EPP-87-07] N88-14053

**BIOLOGICAL EFFECTS**
TOMS as a monitor of the ultraviolet radiation environment: Applications to photobiology N88-13785

**BIOLOGICAL MODELS (MATHEMATICS)**
A functional interpretation of the logistic equation
[REPT-87-037] N88-13946

**BIOLUMINESCENCE**
Varifront 3 iexpedition data report (USNS DE STEIGUER CRUISE 1202-82). Bioluminescence, hydrographic, nutrient, and satellite data from the Gulf of California (November-December 1981)
[AD-A185011] N88-13805

**BISMUTH COMPOUNDS**
Altered and enhanced iodargyrite with bismuth triiodide for use in precipitation enhancement operations
[AD-A185229] N88-13419

**BITS**
Digital video bit-rate reduction: DPCM for sub-Nyquist PAL
[BBC-RD-1987/16] N88-13494

**BLADE TIPS**
Calculation of helicopter rotor blade/vortex interaction by Navier-Stokes procedures
[NASA-CR-177441] N88-13291

**BLADE-VORTEX INTERACTION**
Calculation of helicopter rotor blade/vortex interaction by Navier-Stokes procedures
[NASA-CR-177441] N88-13291

**BLOWING**
Experimental investigations on blunt bodies and corner configurations in hypersonic flow N88-13225

**BLUFF BODIES**
Computational study of three-dimensional wake structures
[REPT-2] N88-13281
Wakes of two dimensional bluff bodies in subsonic flow. Influence of a separating plate and of a pulsed injection of momentum
[IMFL-4200-86/75] N88-13297

**BLUNT BODIES**
Experimental investigations on blunt bodies and corner configurations in hypersonic flow N88-13225
The effects of sweep and bluntness on a glancing shock wave turbulent boundary layer interaction N88-13227
A spatial marching technique for the inviscid blunt body problem N88-13239
The role of computation fluid dynamics in aeronautical engineering (4). The development and applications of implicit TVD finite volume code N88-13259

**BODY TEMPERATURE**
Human thermoregulatory model for whole body immersion in water at 20 and 28 C
[AD-A185052] N88-13849

**BODY-WING AND TAIL CONFIGURATIONS**
Design of wings and wing/body configurations for transonic and supersonic speeds N88-13318

**BODY-WING CONFIGURATIONS**
Numerical simulation of the hypersonic flow around lifting vehicles N88-13234
Vortex formation over delta, double-delta and wave rider configurations at supersonic speeds N88-13243
The RAE experimental data-base for missiles at high Mach number and its use in assessing CFD methods N88-13250
Low speed wind tunnel investigation of propeller slipstream aerodynamic effects on different nacelle/wing combinations. Part 1: Total forces and moments and pressure distributions on nacelle/wing at different angles of attack and yaw and at different thrust coefficients
[FFA-TN-1987-22] N88-13302
Compressible Euler solution on a multiblock grid around a wing-fuselage configuration
[FFA-TN-1987-46] N88-13303

**BORIDES**
A synthetic plasma source
[TRITA-EPP-86-15] N88-13995

**BORON**
Studies on syntheses of amine-carboxyboranes (boron analogues of amino acids) and derivatives
[AD-A184838] N88-13386

**BOSONS**
W decays
[NOTA-INTERNA-877] N88-13966

**BOUNDARY ELEMENT METHOD**
Computation of nacelle interference using boundary element method N88-13267
Significance of foundation-soil separation in dynamic soil-structure interaction N88-13641

**BOUNDARY LAYER CONTROL**
Navier-Stokes analysis of laminar flow control of a two-dimensional airfoil N88-13286
Study of the effect of mass transfer on a transonic boundary layer. Application to flow relaminarization
[ETN-88-91169] N88-13296

**BOUNDARY LAYER FLOW**
Active and passive plume distribution models in the convective boundary layer using a large eddy simulation model
[KNMI-TR-90] N88-13546

**BOUNDARY LAYER SEPARATION**
Study of the effect of mass transfer on a transonic boundary layer. Application to flow relaminarization
[ETN-88-91169] N88-13296
Delta wing in incompressible flow. Experimental study in F2
[ONERA-RT-36/1147-AN-249-G] N88-13298
Vortical Flows Research Program of the Fluid Dynamics Research Branch
[NASA-TM-88332] N88-13549

**BOUNDARY LAYER TRANSITION**
Numerical optimization of conical flow waveriders including detailed viscous effects N88-13245
Hypersonic static and dynamic stability of axisymmetric shapes: A comparison of prediction methods and experiment N88-13246

**BOUNDARY VALUE PROBLEMS**
Solution of some 3-D viscous and inviscid supersonic flow problems by finite-volume space-marching schemes N88-13235
Numerical experiments with hypersonic flows beneath a cone-delta-wing combination N88-13238
Development of an integrated BEM approach for hot fluid structure interaction
[NASA-CR-181577] N88-13384
Mechanics of anisotropic media. Study of the boundary conditions --- stratified composites
[SNIAS-872-430-112] N88-13404
An examination of chaotic motion for the buckled beam N88-13844
On a boundary data operator and generalized exterior Robin problems for the Helmholtz equation
[AD-A185124] N88-13915
Guidance and control strategies for aerospace vehicles
[NASA-CR-181579] N88-13935

**BOW WAVES**
On the numerical simulation of three-dimensional hypersonic flow N88-13237
The off-design performance of hypersonic waveriders N88-13244

**BRACKETS**
Mechanical design of the ac bracket package for the RETE experiment
[IFSI-87-4] N88-13379

**BRANCHING (MATHEMATICS)**
Application of the Von Karman equation to the bifurcation theory
[NOTA-INTERNA-891] N88-13927
Transient periodic behavior related to a saddle-node bifurcation
[ETN-88-91321] N88-13928
Tutorial on elementary bifurcation theory
[DE87-014849] N88-13932

**BRANCHING (PHYSICS)**
W decays
[NOTA-INTERNA-877] N88-13966

**BREAKING**
Models for the degradation of stratified composite structures
[ONERA-RT-13/3542-RY-061-R] N88-13395

**BREATHING APPARATUS**
A plethysmograph for measuring pulmonary ventilation in small animals
[AD-A184978] N88-13846

**BRECCIA**
Abundance and distribution of ultramafic microbreccia in Moses Rock Dike: Quantitative application of AIS data N88-13766

**BRIGHTNESS**
Performance characteristics of magnesium-sodium nitrate flares in oxygen-nitrogen atmospheres
[AD-A185274] N88-13476
AIS-2 spectra of California wetland vegetation N88-13763

**BROADBAND**
Application of Vandermonde decomposition to directional and modal analysis of broadband transients
[AD-A185007] N88-13956

**BROADCASTING**
Improvements to a UHF rebroadcast television link suffering tidal fading: Countisbury UHF relay station
[BBC-RD-1987/14] N88-13495

**BROKEN SYMMETRY**
A mechanism for symmetry breaking in antiferromagnetic Heisenberg systems
[ETN-88-91320] N88-14031

**BUCKLING**
An analytical study of the effects of transverse shear deformation and anisotropy on buckling loads of laminated cylinders
[NASA-TM-100508] N88-13387
An examination of chaotic motion for the buckled beam N88-13844

**BUDGETING**
Budget and programs for 1986 research
[IFSI-86-16] N88-14048

**BUFFETING**
Predictions of F-111 TACT aircraft buffet response and correlations of fluctuating pressures measured on aluminum and steel models and the aircraft
[NASA-CR-4069] N88-13218

**BURNERS**
Oxygen enriched combustion system performance study
[DE88-001500] N88-13424

**BURNING RATE**
Performance characteristics of magnesium-sodium nitrate flares in oxygen-nitrogen atmospheres
[AD-A185274] N88-13476

**BY-PRODUCTS**
Production of jet fuels from coal derived liquids. Volume 1: Market assessment for liquid by-products from the Great Plains gasification plant
[AD-A184846] N88-13475
CELSS Program Meeting N88-13853
Controlled ecological life support systems: Development of a plant growth module N88-13854


## C


**CABIN ATMOSPHERES**
Northwest Airlines flight experiments N88-13786

**CABLES (ROPES)**
BASIC desk-top computer program for the three-dimensional static configuration of an extensible flexible cable in a uniform stream
[AD-A184852] N88-13737
The Shock and Vibration Digest, Volume 19, No. 12 N88-13746
Dynamics of cables and chains N88-13747
**CALCULUS OF VARIATIONS**
The role of computation fluid dynamics in aeronautical engineering (4). The development and applications of implicit TVD finite volume code N88-13259
**CALENDARS**
Calendar of selected aeronautical and space meetings
[AGARD-CAL-87/1] N88-14033
Calendar of selected aeronautical and space meetings
[AGARD-CAL-88/1] N88-14037
**CALIBRATING**
Development of response models for the Earth Radiation Budget Experiment (ERBE) sensors. Part 3: ERBE scanner measurement accuracy analysis due to reduced housekeeping data
[NASA-CR-178294] N88-13553
Fabricate, calibrate and test a dosimeter for integration into the CRRES (Combined Release and Radiation Effects Satellite) satellite
[AD-A185439] N88-13564
Improvement of modal scaling factors using mass additive technique N88-13620
AIS-2 radiometry and a comparison of methods for the recovery of ground reflectance N88-13757
Calibrating AIS images using the surface as a reference N88-13760
Causes of spurious features in spectral reflectance data N88-13769
Analysis of SO2 signals in SBUV/TOMS data N88-13794
Media calibrations of the Doppler signal for a gravitational wave experiment — interplanetary medium
[IFSI-86-13] N88-13825
**CALORIMETERS**
Investigation by differential scanning calorimetry of microstructure in a superplastic Al-Mg-Zr alloy
[AD-A184902] N88-13439
**CAMERAS**
The technical evolution of the Wilson camera: The beginnings (1895-1925)
[NOTA-INTERNA-876] N88-13568
**CANADA**
Corrosion in avionics and associated equipment; cause, effect and prevention N88-13335
**CANARD CONFIGURATIONS**
Examples of static aeroelastic effects on present combat aircraft projects N88-13349
**CANOPIES**
Resistance of canopy materials against chemicals
[PML-1985-22] N88-13466
**CANOPIES (VEGETATION)**
Proceedings of the Third Airborne Imaging Spectrometer Data Analysis Workshop
[NASA-CR-181552] N88-13755
The use of airborne imaging spectrometer data to determine experimentally induced variation in coniferous canopy chemistry N88-13761
Toward detecting California shrubland canopy chemistry with AIS data N88-13764
Analysis of airborne imaging spectrometer data for the Ruby Mountains, Montana, by use of absorption-band-depth images N88-13771
**CANTILEVER BEAMS**
The matrix exponential in transient structural analysis N88-13619
Bending of a bonded beam as a test method for adhesive properties
[AD-A184813] N88-13736
**CARBON**
The initiation and growth of fatigue cracks in carburised 9Cr1Mo steel N88-13696
**CARBON DIOXIDE**
Organic molecules on meteoritic solid substrates
[NASA-CR-181570] N88-13411
Controlled ecological life support systems: Development of a plant growth module N88-13654
**CARBON FIBER REINFORCED PLASTICS**
Design and control of repairs of carbon fiber lift augmentation flaps in the ATR42 aircraft
[SNIAS-872-111-112] N88-13217
A hybrid fibreglass-CFRP cloth for new furnishings — aircraft cabins
[SNIAS-872-111-109] N88-13396
Determination of the fiber ratio in carbon fiber/resin composites by means of image analysis
[SNIAS-872-422-101] N88-13398
Measurement and control of damage in composite materials: Nondestructive controls by thermography, holography, and radiography
[SNIAS-872-430-110] N88-13403
Comparison of fire resistance of metallic and nonmetallic structures
[SNIAS-872-551-101] N88-13489
**CARBON FIBERS**
The use of aeroelastic wind tunnel models to prove structural design N88-13355
Improved high modulus fibers
[NASA-CR-181539] N88-13389
**CARBON STEELS**
Crack initiation studies in hydrogen embrittled spring steel strip N88-13710
**CARBON-CARBON COMPOSITES**
Carbon-carbon composites and Aerospatiale. State of the art and prospects
[SNIAS-872-430-108] N88-13401
**CARBONACEOUS METEORITES**
Organic molecules on meteoritic solid substrates
[NASA-CR-181570] N88-13411
**CARBONACEOUS ROCKS**
Effective use of principal component analysis with high resolution remote sensing data to delineate hydrothermal alteration and carbonate rocks N88-13758
**CARBOXYL GROUP**
Studies on syntheses of amine-carboxyboranes (boron analogues of amino acids) and derivatives
[AD-A184838] N88-13386
**CARBOXYLIC ACIDS**
Organic molecules on meteoritic solid substrates
[NASA-CR-181570] N88-13411
**CARBURETORS**
A study of the interaction of laser light with liquid propellant drops
[AD-A185117] N88-13582
**CASCADE FLOW**
Numerical analysis of cascade flow solving Navier-Stokes equations N88-13262
Inverse design method for two-dimensional transonic cascades N88-13263
Effects of free stream turbulence, Reynolds number and incidence angle on axial turbine cascade performance N88-13339
Unsteady aerodynamics of an oscillating cascade in a compressible flow field
[NASA-TM-100219] N88-13346
A computer program for calculating unsteady aerodynamic coefficients for cascades in supersonic axial flow
[NASA-TM-100204] N88-13753
**CASES (CONTAINERS)**
Structural frequency functions for an impulsive, distributed forcing function N88-13627
**CASSEGRAIN OPTICS**
Optical photometer for the Tirgo telescope
[IFSI-87-5] N88-13965
**CAST ALLOYS**
Fatigue crack growth behavior of A356-T6 cast aluminum alloy N88-13660
**CASTING**
Advances in processing techniques for nickel aluminides
[DE87-014571] N88-13449
**CATALYSTS**
Phase purity of $NiCo_2O_4$, a catalyst candidate for electrolysis of water
[NASA-TM-100239] N88-13385
Activated metal oxide surfaces as highly basic and reducing environments
[AD-A184958] N88-13417
**CAUCHY PROBLEM**
Computation of flow past conical hypersonic wings using a second order Godunov method N88-13241
**CAVITATION CORROSION**
Simulated service test behavior of various internal and external coatings applied on CF6-50 first stage turbine blades
[NLR-MP-86018-U] N88-13343
**CAVITY RESONATORS**
Theoretical and experimental investigation of electron beam acceleration and sub-millimeter wave generation in cyclotron resonant cavities
[AD-A184806] N88-13975
**CENSORED DATA (MATHEMATICS)**
Further studies in estimation of life distribution characteristics from censored data
[AD-A184862] N88-13937
**CENTIMETER WAVES**
Utilization of microwave measuring systems for nondestructive control of composite materials
[SNIAS-872-430-109] N88-13402
**CENTRAL PROCESSING UNITS**
File usage analysis and resource usage prediction: A measurement-based study
[NASA-CR-181553] N88-13867
Predictability of process resource usage: A measurement-based study of UNIX
[NASA-CR-181562] N88-13869
**CERAMIC BONDING**
Analysis of end stresses in glass-metal bimaterial strips
[DE87-007848] N88-13750
**CERAMIC MATRIX COMPOSITES**
Study of ceramic-fiber/ceramic sol-gel based matrix composites
[SNIAS-872-430-120] N88-13489
**CERAMICS**
Statistical process control applied to the liquid-fed ceramic melter process
[DE86-000271] N88-13471
**CERENKOV RADIATION**
Cerenkov radiation field analysis due to a passing electron beam
[AD-A184870] N88-13976
**CHAINS**
Trajectory control of robot manipulators with closed-kinematic chain mechanism
[NASA-TM-89305] N88-13605
The Shock and Vibration Digest, Volume 19, No. 12 N88-13746
Dynamics of cables and chains N88-13747
**CHANNEL FLOW**
A numerical investigation on wing/nacelle interferences N88-13258
**CHANNELS (DATA TRANSMISSION)**
An exact analysis and performance of framed ALOHA with capture
[AD-A185006] N88-13500
**CHAOS**
Chaos: Chto Delat? (What is to be done?)
[DE88-000513] N88-13933
**CHARACTERIZATION**
Molecular-level synthesis and characterization of metal-polymer interfaces
[AD-A184958] N88-13455
Characterization of the microstructures of various materials
[AD-A184961] N88-14017
**CHARGE COUPLED DEVICES**
Photon counting image sensor development for astronomical applications
[NASA-CR-181507] N88-14049
**CHARGE TRANSFER**
Comparison of 2D memory SEU transport simulation with experiments
[ATR-86(8139)-2-REV-A] N88-14025
**CHARGED PARTICLES**
An electric field meter based upon a new principle: A dummy displacement electrode. Application to aerospace vehicles
[SNIAS-872-422-106] N88-13567
**CHECKOUT**
A project of an intelligent system to help on-line trouble shooting — aircraft maintenance
[SNIAS-872-111-106] N88-13216
**CHELATES**
Soluble metal chelate polymers of coordination numbers six, seven and eight
[AD-A185094] N88-13459
**CHEMICAL ANALYSIS**
The analysis of metal finishing solutions by ion chromatography
[AD-A184812] N88-13414
Chemical analysis for excimer laser systems
[DE88-001941] N88-13591
Evaluation of AIS-2 (1986) data over hydrothermally altered granitoid rocks of the Singatse Range (Yerington) Nevada and comparison with 1985 AIS-1 data N88-13767
**CHEMICAL ATTACK**
Resistance of canopy materials against chemicals
[PML-1985-22] N88-13466
**CHEMICAL BONDS**
Pure dephasing of a vibrational adbond
[AD-A185222] N88-13740
**CHEMICAL CLOUDS**
A fluid simulation of the AMPTE lithium gas releases in the solar wind
[TRITA-EPP-87-06] N88-14056
**CHEMICAL COMPOSITION**
A mathematical model of high alloy nickel base high temperature alloys
[BLL-M-37381-(5828.4)] N88-13436
Ion plating for corrosion control
[AD-A185061] N88-13442

The use of airborne imaging spectrometer data to determine experimentally induced variation in coniferous canopy chemistry N88-13761
Toward detecting California shrubland canopy chemistry with AIS data N88-13764
High energy molecules of high symmetry [AD-A185365] N88-13965
**CHEMICAL LASERS**
Computer simulation of cw HF chemical laser unstable resonator performance [AD-A185059] N88-13581
An experimental study of CW HF chemical laser amplifier performance and zero power gain [AD-A185241] N88-13584
**CHEMICAL REACTIONS**
Hypersonic laminar boundary layer: Parametric study for the representation of real gas effects N88-13236
Numerical analysis of axisymmetric flow with H2-O2 reactions N88-13272
Plasma joining of metal matrix composites [AD-A184828] N88-13390
Fabrication of composites by chemical vapor deposition [DE87-014565] N88-13408
Shock compression of solids as a physical-chemical-mechanical process [DE88-001674] N88-13427
Modeling the effect of sulfur on the threshold environmental cracking rate of steels in high temperature water N88-13703
The role of electronic structure calculation in mechanistic analysis of electron transfer reactions in the liquid phase [DE87-014395] N88-13963
**CHEMISORPTION**
The influence of crack conditions on hydrogen uptake by steels N88-13702
**CHIPS (ELECTRONICS)**
Technology upgrade of a silicon compiler [AD-A184873] N88-14016
**CHLOROPHYLLS**
Varifront 3 expedition data report (USNS DE STEIGUER CRUISE 1202-82). Bioluminescence, hydrographic, nutrient, and satellite data from the Gulf of California (November-December 1981) [AD-A185011] N88-13805
**CHONDRITES**
Organic molecules on meteoritic solid substrates [NASA-CR-181570] N88-13411
**CHROMATOGRAPHY**
The analysis of metal finishing solutions by ion chromatography [AD-A184812] N88-13414
High energy molecules of high symmetry [AD-A185365] N88-13965
**CHROMIUM**
The mechanism by which sigma-phase forms in Fe-Cr-Ni system alloys [BLL-M-37380-(5828.4)] N88-13437
**CHROMIUM STEELS**
Tensile properties of extrusion consolidated Type 304 SS rapidly solidified powders [DE87-014875] N88-13450
Low cycle fatigue life predictions of a 1CrMoV steel in terms of a J-controlled short crack growth model N88-13665
the influence of temper embrittlement on fatigue crack growth in hydrogen N88-13709
**CHRONOLOGY**
Astronautics and aeronautics, 1978: A chronology [NASA-SP-4023] N88-14062
**CIRCUIT BREAKERS**
Low-current behavior and current chopping of vacuum arcs [ISBN-90-9001649-X] N88-13529
**CIRCUITS**
Diagnostic reasoning in digital systems [NASA-CR-181564] N88-13871
The numerical and analytic of implicit differential equations and their application to control and circuit problems [AD-A185404] N88-13922
**CIVIL AVIATION**
Airline safety: A comparative analysis [AD-A185358] N88-13308
Civil aeronautics [ETN-88-90616] N88-13309
**CLEANING**
Investigation of the nature and concentration of vapor and mist during the cleaning of aircraft [PML-1985-29] N88-13817
**CLEAR AIR TURBULENCE**
Northwest Airlines flight experiments N88-13786
**CLIMATOLOGY**
Inventory of weather stations. Climatological data from Dutch stations, no. 26 [KNMI-150-26] N88-13841
**CLOSED ECOLOGICAL SYSTEMS**
Controlled Ecological Life Support System. Design, Development, and Use of a Ground-Based Plant Growth Module [NASA-CP-2479] N88-13852
CELSS Program Meeting N88-13853
Controlled ecological life support systems: Development of a plant growth module N88-13854
Plant Growth Module (PGM) conceptual design N88-13855
**CLOSURES**
Conditional second order closure for turbulent shear flows [AD-A185369] N88-13542
**CLOUD CHAMBERS**
The technical evolution of the Wilson camera: The beginnings (1895-1925) [NOTA-INTERNA-876] N88-13568
**CLOUD COVER**
Mesoscale applications of high resolution imagery [AD-A185039] N88-13833
Modeling cloudy and clear interval length probabilities using space shuttle imagery [AD-A185290] N88-13837
**CLOUD PHYSICS**
The application of doubly-truncated hydrometeor distributions to numerical cloud models [AD-A185273] N88-13836
**CLOUD SEEDING**
Altered and enhanced iodargyrite with bismuth triiodide for use in precipitation enhancement operations [AD-A185229] N88-13419
**CLOUDS**
Volcanic eruption detection with TOMS N88-13793
Analysis of SO2 signals in SBUV/TOMS data N88-13794
**CLOUDS (METEOROLOGY)**
Tropical easterly jet located using TOMS data N88-13783
**CLUMPS**
Supersonic beam observations of semiconductor clusters [AD-A184991] N88-14018
**CMOS**
A study of charged particles/radiation damage to VLSI device materials [NASA-CR-172036] N88-13518
New breakthrough in Chinese integrated circuits: Successful development of high-speed CMOS circuits [AD-A185381] N88-13525
**COAGULATION**
Coagulation in stirred tanks [B8711373] N88-13420
**COAL**
Production of jet fuels from coal derived liquids. Volume 1: Market assessment for liquid by-products from the Great Plains gasification plant [AD-A184846] N88-13475
**COAL DERIVED LIQUIDS**
Production of jet fuels from coal derived liquids. Volume 1: Market assessment for liquid by-products from the Great Plains gasification plant [AD-A184846] N88-13475
**COASTS**
Varifront 3 expedition data report (USNS DE STEIGUER CRUISE 1202-82). Bioluminescence, hydrographic, nutrient, and satellite data from the Gulf of California (November-December 1981) [AD-A185011] N88-13805
**COATINGS**
Effectiveness of electrodeposited coatings in reducing atmospheric corrosion of copper substrates [DE87-013651] N88-13448
Raman microprobe characterization of dielectric films following high-energy pulsed laser irradiation [DE88-000559] N88-13587
Fatigue characteristics of ion treated surfaces N88-13713
**COAXIAL CABLES**
The use of coaxial transmission line elements in log-periodic dipole arrays [AD-A184864] N88-13499
**COBALT OXIDES**
Phase purity of NiCo2O4, a catalyst candidate for electrolysis of water [NASA-TM-100239] N88-13385
**CODING**
A computer code to process and plot laser altimetry data interactively on a microcomputer [NASA-TM-100687] N88-13371
A computer code to calculate line by line atmospheric tranamission spectra on a microcomputer [NASA-TM-100686] N88-13372
Hanford Meteorological Station computer codes. Volume 5: The TOWER computer code [DE88-001610] N88-13843
Some distance problems in coding theory [B8711396] N88-13888
**COEFFICIENTS**
Reactive sticking coefficients of silane on silicon [DE88-000601] N88-13473
**COLD FLOW TESTS**
The development and evaluation of three-dimensional models of cold flow in internal combustion engines [DE88-900077] N88-13594
**COLLISION AVOIDANCE**
Towards building a team of intelligent robots [NASA-CR-181538] N88-13595
Collision-free motion of two robot arms in a common workspace [CSE-87-00002] N88-13596
**COLLISIONS**
A study of the interaction of laser light with liquid propellant drops [AD-A185117] N88-13582
**COLLOIDS**
Colloidal stability of oxidized silicon particles in ethanolic and aqueous media [DE87-014783] N88-13421
**COLOR**
The use of color in electronic maps. Part 1: Generation and analysis of color on the Gould/DeAnza image processing system [IZF-1986-32] N88-13882
**COLOR VISION**
Learning a color algorithm from examples [AD-A184385] N88-13862
**COMBINATORIAL ANALYSIS**
An exact analysis and performance of framed ALOHA with capture [AD-A185006] N88-13500
**COMBUSTION**
Combustion related shear-flow dynamics in elliptic supersonic jets N88-13232
Correlation of air pressure drop and flame arrestor characteristics for explosion suppression materials [AD-A184960] N88-13340
Turbulence generation in combustion [AD-A184810] N88-13413
A study of the interaction of laser light with liquid propellant drops [AD-A185117] N88-13582
**COMBUSTION CHEMISTRY**
Laser probes of propellant combustion chemistry [AD-A184854] N88-13415
Detailed mechanism of toluene oxidation and comparison with benzene [NASA-TM-100261] N88-13428
**COMBUSTION EFFICIENCY**
Study of electrostatic modulation of fuel sprays to enhance combustion performance in an aviation gas turbine [AD-A184967] N88-13341
Oxygen enriched combustion system performance study [DE88-001500] N88-13424
**COMBUSTION PHYSICS**
Combustion characteristics of gas turbine alternative fuels [NASA-TM-100247] N88-13338
**COMBUSTION PRODUCTS**
Laser probes of propellant combustion chemistry [AD-A184854] N88-13415
Pulsed plasma jet igniters: Species measurements in methane combustion [DE88-001389] N88-13422
Formation and destruction of nitrous oxide in lean, premixed combustion [DE88-001390] N88-13423
**COMMAND GUIDANCE**
Reduced order optimal command applied to longitudinal automatic pilots [SNIAS-872-111-114] N88-13362
**COMMERCIAL AIRCRAFT**
Design and control of repairs of carbon fiber lift augmentation flaps in the ATR42 aircraft [SNIAS-872-111-112] N88-13217
Airline safety: A comparative analysis [AD-A185358] N88-13308
**COMMUNICATION NETWORKS**
Contribution to optimal flow in networks. A experimental multiprocessor for asynchronous iteration implementation [LAAS-87-269] N88-13510
Communications payload concepts for geostationary facilities [NASA-TM-100154] N88-13513
An evolutionary communications scenario for Mars exploration [NASA-TM-100263] N88-13515

Connecting RPC (Remote Procedure Call)-based distributed systems using wide-area networks
[PB87-234423] N88-14041

**COMPENSATORS**
Investigation, development, and application of optimal output feedback theory. Volume 3: The relationship between dynamic compensators and observers and Kalman filters
[NASA-CR-4107] N88-13900

**COMPILERS**
Mixing Microsoft C and Microsoft FORTRAN program modules on the IBM Personal Computer
[DE88-001947] N88-13895
Technology upgrade of a silicon compiler
[AD-A184873] N88-14016

**COMPONENT RELIABILITY**
Conservatism implications of shock test tailoring for multiple design environments N88-13611
Small space reactor power systems for unmanned solar system exploration missions
[NASA-TM-100228] N88-14054

**COMPOSITE MATERIALS**
Materials for fighter aircraft N88-13325
Fabrication of composites by chemical vapor deposition
[DE87-014565] N88-13408
Bending of a bonded beam as a test method for adhesive properties
[AD-A184813] N88-13736
Damping analysis of flexural waves in fluid-loaded single and constrained plates
[AD-A185116] N88-13739
An element of a multilayer shell for the computation of composite structures
[ONERA-RT-14/3542-RY-051-R] N88-13742

**COMPOSITE STRUCTURES**
Models for the degradation of stratified composite structures
[ONERA-RT-13/3542-RY-061-R] N88-13395
Surface treatment problems found in new aircraft designed using structural composites
[SNIAS-872-111-113] N88-13397
Philosophy and practice of nondestructive tests of composite material structures at Aerospatiale Aquitaine
[SNIAS-872-430-105] N88-13400
Measurement and control of damage in composite materials: Nondestructive controls by thermography, holography, and radiography
[SNIAS-872-430-110] N88-13403
Mechanics of anisotropic media. Study of the boundary conditions — stratified composites
[SNIAS-872-430-112] N88-13404
Micromechanics of the degradation of composite materials
[SNIAS-872-430-113] N88-13405
The structures of large wound propulsion shells — carbon fiber composites filament winding
[SNIAS-872-430-118] N88-13406
Design and test of high performance composite tubes for use in deep water drilling and production systems
[SNIAS-872-430-107] N88-13487
High performance composite tubes for offshore applications
[SNIAS-872-430-116] N88-13488
Strain-energy-release rate analysis of the end-notched flexure specimen using the finite-element method
[NASA-TM-100494] N88-13735
Bending of a bonded beam as a test method for adhesive properties
[AD-A184813] N88-13736

**COMPRESSIBLE FLOW**
An analysis of the compressible-viscous flow field around a 3D-oscillating wing N88-13254
Computation of dynamic stall of NACA0012 airfoil by block pentadiagonal matrix scheme N88-13255
Computations of compressible viscous flows over multiple-bodies N88-13282
Relaxation method for the compressible Navier-Stokes equations using upwind schemes N88-13283
Interferometric data for a shock-wave/boundary-layer interaction
[NASA-TM-88227] N88-13306
Unsteady aerodynamics of an oscillating cascade in a compressible flow field
[NASA-TM-100219] N88-13346
A note on the use of symmetric line Gauss-Seidel for the steady upwind differenced Euler equations
[AD-A185223] N88-13540
Evolution of mean square magnetic vector potential in compressible, two-dimensional, magnetofluid turbulence
[AD-A184965] N88-13990

**COMPRESSING**
Shock compression of solids as a physical-chemical-mechanical process
[DE88-001674] N88-13427

**COMPRESSION LOADS**
Shock compression of solids as a physical-chemical-mechanical process
[DE88-001674] N88-13427

**COMPRESSIVE STRENGTH**
Effect of interface on mechanical properties of graphite/201 aluminum composites N88-13717

**COMPRESSOR BLADES**
Automated design of controlled diffusion blades
[NASA-TM-100251] N88-13304

**COMPRESSORS**
Application of modified loss and deviation correlations to transonic axial compressors
[AGARD-R-745] N88-13344
Compressor large bandwidth noise emission mechanisms
[ETN-88-91177] N88-13959

**COMPUTATION**
Calculation of helicopter rotor blade/vortex interaction by Navier-Stokes procedures
[NASA-CR-177441] N88-13291
Efficient computation of periodic Green's functions with application to grating structures
[AD-A184853] N88-13912

**COMPUTATIONAL FLUID DYNAMICS**
Aerodynamics of Hypersonic Lifting Vehicles
[AGARD-CP-428] N88-13219
Numerical simulation of the hypersonic flow around lifting vehicles N88-13234
On the numerical simulation of three-dimensional hypersonic flow N88-13237
Aerothermodynamics research at NASA Ames N88-13242
The RAE experimental data-base for missiles at high Mach number and its use in assessing CFD methods N88-13250
Proceedings of the 4th NAL Symposium on Aircraft Computational Aerodynamics
[NAL-SP-7] N88-13253
An analysis of the compressible-viscous flow field around a 3D-oscillating wing N88-13254
Computation of dynamic stall of NACA0012 airfoil by block pentadiagonal matrix scheme N88-13255
Numerica calculation in the Laplace domain for subsonic unsteady aerodynamic forces acting on a finite wing N88-13256
Practical application of two-dimensional viscous flow computation N88-13257
A numerical investigation on wing/nacelle interferences N88-13258
The role of computation fluid dynamics in aeronautical engineering (4). The development and applications of implicit TVD finite volume code N88-13259
Practical and modern simulation by systematic connection of the LU-ADI code and the solution adaptive grid program N88-13260
Numerical calculations of the flowfield around propellers N88-13261
Numerical analysis of cascade flow solving Navier-Stokes equations N88-13262
Inverse design method for two-dimensional transonic cascades N88-13263
Development of the computer program for turbulent boundary layers N88-13264
Numerical prediction of turbulent flows in dump diffusers N88-13265
Numerical analysis of supersonic flows using panel method N88-13266
Computation of nacelle interference using boundary element method N88-13267
Application of discrete vortex method to analysis of separated flow around aerofoils N88-13268
Programming techniques for high-speed processing of large scale numerical simulation on supercomputers N88-13269
Vectorizing the FFTs on supercomputer SX system N88-13270
Tridiagonal approximate factorization method: A preconditioning technique for solving nonsymmetric linear systems suitable to supercomputers N88-13271
Numerical analysis of axisymmetric flow with H2-O2 reactions N88-13272
Rarefied gas numerical wind tunnel. 2: Two-dimensional and axially symmetric bodies N88-13273
Numerical analysis of flow characteristics of supersonic free-jets N88-13274
Numerical simulation of splash of droplet at unit gravity N88-13275
Computer graphics for computational aerodynamics N88-13276
Flow visualization in computational fluid dynamics N88-13277
Visualization of an aircraft accident based on digital flight data recorder information N88-13278
A perspective of computational fluid dynamics N88-13279
Three-dimensional flow past a two-dimensional body N88-13280
Computational study of three-dimensional wake structures
[REPT-2] N88-13281
Computations of compressible viscous flows over multiple-bodies N88-13282
Relaxation method for the compressible Navier-Stokes equations using upwind schemes N88-13283
Computation of flow around 2-D circular cylinder N88-13284
Time-marching finite-difference methods for the three-dimensional Euler equations of contravariant velocity components N88-13285
Navier-Stokes analysis of laminar flow control of a two-dimensional airfoil N88-13286
Analytical method for generating computational grids about complete aircraft configurations N88-13287
Navier-Stokes simulation of transonic transportation aircraft configurations. 1: Flow-field simulation over wing-fuselage combinations N88-13288
Numerical simulation of transonic aircraft in comparison to wind tunnel test N88-13289
Validation elements of the computation methods and measurement techniques for high lift aerodynamic systems
[SNIAS-872-111-101] N88-13299
Compressible Euler solution on a multiblock grid around a wing-fuselage configuration
[FFA-TN-1987-46] N88-13303
The role of experimental investigation and computational fluid dynamics during fighter aircraft design N88-13326
A numerical study of the effects of curvature and convergence on dilution jet mixing
[NASA-TM-89878] N88-13347
A note on the use of symmetric line Gauss-Seidel for the steady upwind differenced Euler equations
[AD-A185223] N88-13540
Utilization of a high rate vector computer in computational fluid mechanics for aeronautics
[ETN-88-91171] N88-13547
Physical analysis and numerical simulation of coherent turbulent structures in mixed layers, jets, and wakes
[ETN-88-91169] N88-13548
Vortical Flows Research Program of the Fluid Dynamics Research Branch
[NASA-TM-88332] N88-13549
Numerical analysis, computing and fundamental studies in fluid mechanics
[DE88-001912] N88-13550
Low thrust viscous nozzle flow fields prediction
[NASA-CR-182334] N88-13551
SHARP simulation of discontinuities in highly convective steady flow
[NASA-TM-100240] N88-13931

**COMPUTATIONAL GRIDS**
Numerical simulation of the hypersonic flow around lifting vehicles N88-13234
Computation of dynamic stall of NACA0012 airfoil by block pentadiagonal matrix scheme N88-13255
Practical and modern simulation by systematic connection of the LU-ADI code and the solution adaptive grid program N88-13260
A perspective of computational fluid dynamics N88-13279
Computation of flow around 2-D circular cylinder N88-13284
Analytical method for generating computational grids about complete aircraft configurations N88-13287
Compressible Euler solution on a multiblock grid around a wing-fuselage configuration
[FFA-TN-1987-46] N88-13303
A Cartesian finite-volume method for the Euler equations N88-13532
Finite-element grid improvement by minimization of stiffness matrix trace
[NASA-TM-100255] N88-13604
Free Lagrange reconnection algorithms for hydrocodes using a quadrilateral mesh
[DE88-001580] N88-13752

**COMPUTER AIDED DESIGN**
Numerical simulation applied to the development of a pyrotechnical system
[SNIAS-872-430-115] N88-13479
Applications of fatigue analyses: Transportation N88-13733
An extension to the multilevel logic simulator for microcomputers
[AD-A185032] N88-13879
Overall description of the computer aided design and manufacturing systems associated with the A320 program at Aerospatiale and its partners
[SNIAS-872-111-104] N88-13883

Presentation of SIGMA (Interactive Assisted Geometry System). A computer assisted shape design program developed at the Aerospatiale Aircraft Division
[SNIAS-872-111-110] N88-13884
Structural optimization in the design process --- aircraft
[SNIAS-872-111-115] N88-13885
XCUT: A rule-based expert system for the automated process planning of machined parts
[DE87-011638] N88-13905
Using hierarchically structured problem-solving knowledge in a rule-based process planning system
[DE87-011639] N88-13906
Computer modeling of complete IC fabrication process
[AD-A184807] N88-14012

**COMPUTER AIDED MANUFACTURING**
Overall description of the computer aided design and manufacturing systems associated with the A320 program at Aerospatiale and its partners
[SNIAS-872-111-104] N88-13883
XCUT: A rule-based expert system for the automated process planning of machined parts
[DE87-011638] N88-13905
Using hierarchically structured problem-solving knowledge in a rule-based process planning system
[DE87-011639] N88-13906
Computer modeling of complete IC fabrication process
[AD-A184807] N88-14012

**COMPUTER AIDED MAPPING**
Detection of critical points: The first step to automatic line generalization N88-13803
Matching segments from a map and an aerial image using relaxation techniques
[SNIAS-872-422-103] N88-13809
The use of color in electronic maps. Part 1: Generation and analysis of color on the Gould/DeAnza image processing system
[IZF-1986-32] N88-13882

**COMPUTER ANIMATION**
Visualization of an aircraft accident based on digital flight data recorder information N88-13278

**COMPUTER GRAPHICS**
Computer graphics for computational aerodynamics N88-13276
Flow visualization in computational fluid dynamics N88-13277
Visualization of an aircraft accident based on digital flight data recorder information N88-13278
Implementation of an FIR band pass filter using a bit-slice processor
[AD-A184895] N88-13875
The use of color in electronic maps. Part 1: Generation and analysis of color on the Gould/DeAnza image processing system
[IZF-1986-32] N88-13882
Digitization functions in computer graphics
[ETN-88-91363] N88-13887
An Ada graphical tool to support software development
[DE87-014854] N88-13891

**COMPUTER NETWORKS**
Relational data handling system for scientists
[PB87-223426] N88-14038
Connecting RPC (Remote Procedure Call)-based distributed systems using wide-area networks
[PB87-234423] N88-14041

**COMPUTER PROGRAMMING**
Programming techniques for high-speed processing of large scale numerical simulation on supercomputers N88-13269
Vectorizing the FFTs on supercomputer SX system N88-13270
An APL workspace for conducting nonparametric statistical inference
[AD-A184971] N88-13877
Digitization functions in computer graphics
[ETN-88-91363] N88-13887
Some distance problems in coding theory
[B8711398] N88-13888
A requirements specification for a software design support system
[NASA-CR-182333] N88-13896
Presentation of a computer program permitting the exploitation of tests designed to determine the sensitivity of one shot devices to a parameter. Application to a degenerate one shot sequence
[SNIAS-872-430-117] N88-13945

**COMPUTER PROGRAMS**
The development of a computer code (U2DIIF) for the numerical solution of unsteady, inviscid and incompressible flow over an airfoil
[AD-A185033] N88-13293
Development of an interface for an ultrareliable fault-tolerant control system and an electronic servo-control unit
[NASA-TM-88236] N88-13367
A computer code to process and plot laser altimetry data interactively on a microcomputer
[NASA-TM-100687] N88-13371
A computer code to calculate line by line atmospheric transmission spectra on a microcomputer
[NASA-TM-100686] N88-13372
Stress intensity factors for cracking metal structures under rapid thermal loading, phase 1
[AD-A184112] N88-13606
BASIC desk-top computer program for the three-dimensional static configuration of an extensible flexible cable in a uniform stream
[AD-A184852] N88-13737
RADSPHERE: A computer program for calculating the steady-state, axially symmetric, forced response and radiation field of a submerged spherical shell
[AD-A185025] N88-13738
A computer program for calculating unsteady aerodynamic coefficients for cascades in supersonic axial flow
[NASA-TM-100204] N88-13753
Development of a data analysis system for the detection of lower level atmospheric turbulence with an acoustic sounder
[AD-A184972] N88-13821
Media calibrations of the Doppler signal for a gravitational wave experiment --- interplanetary medium
[IFSI-86-13] N88-13825
ZEUS: A knowledge-based expert system that assists in predicting visibility at airbases
[AD-A184197] N88-13829
Hanford Meteorological Station computer codes. Volume 5: The TOWER computer code
[DE88-001610] N88-13843
Usage analysis of user files in UNIX
[NASA-CR-181561] N88-13868
Performability modeling based on real data: A casestudy
[NASA-CR-181563] N88-13870
A prototype ray tracer
[AD-A184863] N88-13874
Implementation of an FIR band pass filter using a bit-slice processor
[AD-A184895] N88-13875
Software design for an airborne gravity measurement system
[AD-A185000] N88-13878
Illustrative examples of principal component analysis using BMDP/4M
[AD-A185179] N88-13881
Sandia software guidelines: Software quality planning
[DE88-001931] N88-13894
Illustrative examples of principal component analysis using GENSTAT/PCP
[AD-A185085] N88-13941
Modeling and generating input processes
[DE87-013162] N88-13948
Technology upgrade of a silicon compiler
[AD-A184873] N88-14016

**COMPUTER STORAGE DEVICES**
Some distance problems in coding theory
[B8711398] N88-13888

**COMPUTER SYSTEMS DESIGN**
Study of fault tolerant techniques for satellite data handling
[FTT/REP/0001/SAAB] N88-13880
Introduction to local area network design on Ariane 5 and future launchers
[SNIAS-872-422-102] N88-13886
Conceptual issues in measuring the behavior of a distributed real-time process-control computer system
[DE87-009748] N88-13898
Connecting RPC (Remote Procedu ~ Call)-based distributed systems using wide-area networks
[PB87-234423] N88-14041

**COMPUTER SYSTEMS PROGRAMS**
A requirements specification for a software design support system
[NASA-CR-182333] N88-13896

**COMPUTER TECHNIQUES**
Stress intensity factors for cracking metal structures under rapid thermal loading, phase 1
[AD-A184112] N88-13606
Computer aided modeling and fatigue failure forecast under stochastic loading N88-13720
Development of a data analysis system for the detection of lower level atmoapheric turbulence with an acoustic sounder
[AD-A184972] N88-13821
Efficient computation of periodic Green's functions with application to grating structures
[AD-A184853] N88-13912
Computer-aided study of a class of Riemannian space-times
[DE87-703967] N88-13950
Relational data handling system for scientists
[PB87-223426] N88-14038
An automated supernova search and the design strategy
[DE88-001827] N88-14051

**COMPUTER VISION**
Dealing with unanticipated events in autonomous navigation
[DE88-000590] N88-13602

**COMPUTERIZED SIMULATION**
Practical and modern simulation by systematic connection of the LU-ADI code and the solution adaptive grid program N88-13260
Programming techniques for high-speed processing of large scale numerical simulation on supercomputers N88-13269
Rarefied gas numerical wind tunnel. 2: Two-dimensional and axially symmetric bodies N88-13273
Numerical simulation of splash of droplet at unit gravity N88-13275
A perspective of computational fluid dynamics N88-13279
Navier-Stokes simulation of transonic transportation aircraft configurations. 1: Flow-field simulation over wing-fuselage combinations N88-13288
Numerical simulation of transonic aircraft in comparison to wind tunnel test N88-13289
Computation of transonic flows with nacelle simulation
[SNIAS-872-111-117] N88-13300
Correction of inertial navigation system drift errors for an autonomous land vehicle using optical radar terrain data
[AD-A184973] N88-13311
The role of experimental investigation and computational fluid dynamics during fighter aircraft design N88-13326
A numerical study of the effects of curvature and convergence on dilution jet mixing
[NASA-TM-89878] N88-13347
Computer code simulations of explosions in flow networks and comparison with experiments
[DE88-001946] N88-13491
Noise modelling in the time domain with the aid of Spice
[PB87-221941] N88-13492
Numerical and analytical study of the equivalent permittivity or permeability of nonhomogeneous materials. Application to the experimental electromagnetic characterization of composites
[SNIAS-872-430-104] N88-13509
Dynamics of propellant feedline systems
[AD-A184865] N88-13537
Physical analysis and numerical simulation of coherent turbulent structures in mixed layers, jets, and wakes
[ETN-88-91183] N88-13548
Low thrust viscous nozzle flow fields prediction
[NASA-CR-182334] N88-13551
Development of response models for the Earth Radiation Budget Experiment (ERBE) sensors. Part 1: Dynamic models and computer simulations for the ERBE nonscanner, scanner and solar monitor sensors
[NASA-CR-178292] N88-13557
Collision-free motion of two robot arms in a common workspace
[CSE-87-00002] N88-13596
Trajectory control of robot manipulators with closed-kinematic chain mechanism
[NASA-TM-89305] N88-13605
Applications of fatigue analyses: Transportation N88-13733
Free Lagrange reconnection algorithms for hydrocodes using a quadrilateral mesh
[DE88-001580] N88-13752
An adaptive lattice algorithm for spectral line estimation
[AD-A184970] N88-13876
SUSIE reference manual
[DE88-001462] N88-13893
Optimal control of large space structures via generalized inverse matrix
[NASA-CR-182336] N88-13907
Modeling and generating input processes
[DE87-013162] N88-13948
Molecular dynamics studies of aromatic hydrocarbon liquids
[DE88-001473] N88-13973
Computer modeling of complete IC fabrication process
[AD-A184807] N88-14012
Range imagery algorithms for the detection of obstacles by autonomous vehicles
[AD-A185421] N88-14045

**CONCATENATED CODES**
Error control techniques for satellite and space communications
[NASA-CR-181581] N88-13516

**CONCENTRATION (COMPOSITION)**
Investigation of the nature and concentration of vapor and mist during the cleaning of aircraft
[PML-1985-29] N88-13817
**CONCURRENT PROCESSING**
Indirect solution of static problems using concurrent vector processing computers
[DE87-012105] N88-13889
Structuring data for concurrent vectorized processing in a transient dynamics finite element program
[DE87-013082] N88-13890
**CONFERENCES**
Aerodynamics of Hypersonic Lifting Vehicles
[AGARD-CP-428] N88-13219
Proceedings of the 4th NAL Symposium on Aircraft Computational Aerodynamics
[NAL-SP-7] N88-13253
Special Course on Fundamentals of Fighter Aircraft Design
[AGARD-R-740] N88-13315
Workshop on Avionics Corrosion Control
[AGARD-R-733] N88-13331
Static Aeroelastic Effects on High Performance Aircraft
[AGARD-CP-403] N88-13348
The 58th Shock and Vibration Symposium, volume 1
[NASA-CP-2468-VOL-1] N88-13609
Fatigue 87, volume 1
[AD-A184045] N88-13645
Scientific and Operational Requirements for TOMS Data
[NASA-CP-2497] N88-13774
Proceedings of the 17th International Conference on Phenomena in Ionized Gases held in Budapest, Hungary, July 8-12, 1985: Invited papers
[DE87-703562] N88-13987
Calendar of selected aeronautical and space meetings
[AGARD-CAL-87/1] N88-14033
Calendar of selected aeronautical and space meetings
[AGARD-CAL-88/1] N88-14037
Guidance for conference rapporteurs
[NASA-CR-182338] N88-14042
**CONFIDENCE LIMITS**
An APL workspace for conducting nonparametric statistical inference
[AD-A184971] N88-13877
Determining differences in rates corresponding to a given significance level
[AD-A185004] N88-13940
**CONFIGURATION MANAGEMENT**
A study of the Department of Defense configuration management policies and procedures as applied to the FA-18 Strike/Fighter program
[AD-A184872] N88-14034
**CONGRESSIONAL REPORTS**
National Aeronautics and Space Administration space station proposal, fiscal year 1988
[S-HRG-100-328] N88-14043
The 1988 NASA (National Aeronautics and Space Administration) authorization
[GPO-80-245] N88-14044
**CONICAL BODIES**
Dynamic stability of hypersonic conical lifting vehicles according to Newton-Busemann theory N88-13247
Interferometric data for a shock-wave/boundary-layer interaction
[NASA-TM-88227] N88-13306
Development, construction and testing of a novel internal combustion engine with conical rotating slide valve
[DE88-900071] N88-13593
**CONIFERS**
The use of airborne imaging spectrometer data to determine experimentally induced variation in coniferous canopy chemistry N88-13761
Measuring near infrared spectral reflectance changes from water stressed conifer stands with AIS-2 N88-13765
**CONJUGATE GRADIENT METHOD**
Indirect solution of static problems using concurrent vector processing computers
[DE87-012105] N88-13889
**CONSERVATION**
Conservatism implications of shock test tailoring for multiple design environments N88-13611
**CONSERVATION LAWS**
Nonlinear hyperbolic conservation laws
[AD-A184963] N88-13538
**CONSTITUTIVE EQUATIONS**
On a numerical method to solve contact problems — forming processes
[B8711403] N88-13930
**CONSTRUCTION**
Development, construction and testing of a novel internal combustion engine with conical rotating slide valve
[DE88-900071] N88-13593
Controlled ecological life support systems: Development of a plant growth module N88-13854
**CONTACT LOADS**
On a numerical method to solve contact problems — forming processes
[B8711403] N88-13930
**CONTINUOUS RADIATION**
Phenomena at a focus in a laser system
[AD-A185442] N88-13585
**CONTINUOUS WAVE LASERS**
Computer simulation of cw HF chemical laser unstable resonator performance
[AD-A185059] N88-13581
An experimental study of CW HF chemical laser amplifier performance and zero power gain
[AD-A185241] N88-13584
**CONTINUUMS**
Automatic continuum analysis of reflectance spectra N88-13770
**CONTOURS**
Detection of critical points: The first step to automatic line generalization N88-13803
**CONTROL**
Conceptual issues in measuring the behavior of a distributed real-time process-control computer system
[DE87-009748] N88-13898
Conceptual issues in measuring the behavior of a distributed real-time process-control computer system
[DE87-014251] N88-13899
**CONTROL STABILITY**
Survey on large scale system control methods
[NASA-CR-181556] N88-13374
Equivalence of input-output stability and exponential stability for infinite dimensional systems
[TW-276] N88-13903
**CONTROL SYSTEMS DESIGN**
US Naval Air Force avionic and electrical system corrosion prevention and control maintenance N88-13334
Development of an interface for an ultrareliable fault-tolerant control system and an electronic servo-control unit
[NASA-TM-88236] N88-13367
Survey on large scale system control methods
[NASA-CR-181556] N88-13374
Design of low order controllers for robust disturbance rejection in large space structures
[AD-A185202] N88-13376
Plant Growth Module (PGM) conceptual design N88-13855
Behavioral Architecture Robot Control System (BARCS): A new way of building robots
[REPT-87-036] N88-13902
**CONTROL THEORY**
Survey on large scale system control methods
[NASA-CR-181556] N88-13374
Error control techniques for satellite and space communications
[NASA-CR-181581] N88-13516
Trajectory control of robot manipulators with closed-kinematic chain mechanism
[NASA-TM-89305] N88-13605
Control of an unstable launcher in atmospheric flight using minimax optimal control laws
[SNIAS-872-422-107] N88-13901
Equivalence of input-output stability and exponential stability for infinite dimensional systems
[TW-276] N88-13903
On linear periodic controllers
[DE87-011174] N88-13904
**CONTROLLABILITY**
Control of a flexible one-link manipulator
[AD-A185035] N88-13598
**CONTROLLED ATMOSPHERES**
Performance characteristics of magnesium-sodium nitrate flares in oxygen-nitrogen atmospheres
[AD-A185274] N88-13476
**CONTROLLERS**
On linear periodic controllers
[DE87-011174] N88-13904
**CONVECTION CURRENTS**
Environmental and convective influence on tropical cyclone development versus non-development
[AD-A185231] N88-13835
**CONVECTIVE FLOW**
SHARP simulation of discontinuities in highly convective steady flow
[NASA-TM-100240] N88-13931
**CONVECTIVE HEAT TRANSFER**
Measurement of local convective heat transfer coefficients from a smooth and roughened NACA-0012 airfoil: Flight test data
[NASA-TM-100284] N88-13552
Cooling electronic equipment at simulated high altitude in hypobaric chambers
[AD-A185196] N88-13560
**CONVERGENCE**
A numerical study of the effects of curvature and convergence on dilution jet mixing
[NASA-TM-89878] N88-13347
A note on the use of symmetric line Gauss-Seidel for the steady upwind differenced Euler equations
[AD-A185223] N88-13540
**COOLING SYSTEMS**
The effect of maximum-allowable payload temperature on the mass of a multimegawatt space-based platform
[DE88-001921] N88-13381
**COORDINATES**
Separable orthogonal coordinates and particle creation for an accelerating observer
[DE87-703358] N88-14029
Example of correlation between space and spin coordinates
[DE87-703366] N88-14030
**COORDINATION POLYMERS**
Soluble metal chelate polymers of coordination numbers six, seven and eight
[AD-A185094] N88-13459
**COPOLYMERS**
Flexibilized copolyimide adhesives
[NASA-TM-89303] N88-13474
**COPPER**
Jet initiation of PBX 9502
[DE88-000493] N88-13481
The initiation and growth of small fatigue cracks in copper at room and cryogenic temperatures N88-13668
**COPPER ALLOYS**
Phase diagram and thermochemical properties of the Al-Cu system
[ETN-88-91015] N88-13447
Effectiveness of electrodeposited coatings in reducing atmospheric corrosion of copper substrates
[DE87-013651] N88-13448
**CORRECTION**
Correction of inertial navigation system drift errors for an autonomous land vehicle using optical radar terrain data
[AD-A184973] N88-13311
Photochemical ozone overburden correction N88-13778
**CORRELATION**
Illustrative examples of principal component analysis using SYSTAT/FACTOR
[AD-A184920] N88-13939
Example of correlation between space and spin coordinates
[DE87-703366] N88-14030
**CORROSION**
The role of inclusions in corrosion fatigue crack initiation in Q1N N88-13699
Modeling the effect of sulfur on the threshold environmental cracking rate of steels in high temperature water N88-13703
**CORROSION PREVENTION**
Workshop on Avionics Corrosion Control
[AGARD-R-733] N88-13331
Avionic corrosion N88-13332
Corrosion of electronic components N88-13333
US Naval Air Force avionic and electrical system corrosion prevention and control maintenance N88-13334
Corrosion in avionics and associated equipment; cause, effect and prevention N88-13335
Avionics and corrosion N88-13336
Simulated service test behavior of various internal and external coatings applied on CF6-50 first stage turbine blades
[NLR-MP-86018-U] N88-13343
Ion plating for corrosion control
[AD-A185061] N88-13442
Paints required for aeronautical construction
[SNIAS-872-551-102] N88-13470
**CORROSION RESISTANCE**
An examination of coating failure on wing pivot fittings of f111 aircraft
[AD-A185028] N88-13328
Corrosion resistance of sintered alloy steels
[BLL-M-37363-(5828.4)] N88-13438
Effectiveness of electrodeposited coatings in reducing atmospheric corrosion of copper substrates
[DE87-013651] N88-13448
Resistance of canopy materials against chemicals
[PML-1985-22] N88-13486
Coupling effects between the ferrite and austenite phases during corrosion fatigue of a ferrite/austenite duplex stainless steel N88-13706
**COSMIC PLASMA**
Cosmology in the plasma universe
[TRITA-EPP-87-07] N88-14053
**COSMIC RAYS**
Activities report in interplanetary space physics
[IFSI-86-5] N88-14047

Budget and programs for 1986 research [IFSI-86-16] N88-14048
Cosmic ray NM-64 neutron monitor data 14, Rome, Italy, January - December 1985 [IFSI-87-8] N88-14060

**COSPAS**
COSPAS-SARSAT satellite orbit predictor, volume 10 [NASA-TM-85015] N88-13370

**COST ANALYSIS**
Hypersonic aerodynamics: Applications for HOTOL N88-13252
A study of the Department of Defense configuration management policies and procedures as applied to the FA-18 Strike/Fighter program [AD-A184872] N88-14034
The 1988 NASA (National Aeronautics and Space Administration) authorization [GPO-80-245] N88-14044

**COST EFFECTIVENESS**
Experiments in fault tolerant software reliability [NASA-CR-181554] N88-13863

**COST REDUCTION**
Making space nickel/hydrogen batteries lighter and less expensive [DE88-000168] N88-13530

**COUNTER ROTATION**
Noise of a model counterrotation propeller with reduced aft rotor diameter at simulated takeoff/approach conditions (F7/A3) [NASA-TM-100254] N88-13961

**COUPLING**
Coupled elastic rotor/body vibrations with inplane degrees of freedom N88-13643
Non-minimal interaction of gravity with other physical fields: An overview [DE87-703362] N88-13819

**COVARIANCE**
Illustrative examples of principal component analysis using BMDP/4M [AD-A185179] N88-13881
Illustrative examples of principal component analysis using SYSTAT/FACTOR [AD-A184920] N88-13939

**CRACK CLOSURE**
Fatigue 87, volume 1 [AD-A184045] N88-13645
Closure behavior under constant effective stress intensity loading conditions N88-13656
The influence of the topography of fracture surfaces on crack closure N88-13657
Significance of fatigue crack closure under spectrum loading N88-13662
Fatigue crack propagation of short and long cracks: Phys. basis, prediction methods and engineering significance N88-13664
The growth behavior of small fatigue cracks; the effect of microstructure and crack closure N88-13673
An experimental study of closure behavior of naturally initiated small cracks N88-13676
Behavior of long and short fatigue cracks in a powder metallurgy superalloy at room and at high temperature N88-13677
Closure and propagation behavior of short fatigue cracks at different R-ratios N88-13679
A unified model for fatigue crack initiation, short crack growth, long crack propagation, and closure effects N88-13680
Observations on the effect of overloads on fatigue crack growth N88-13684
Crack growth in contrasting titanium alloys under the conjoint action of high and low cycle fatigue N88-13686
Near-threshold growth of defects in engineering materials N88-13691
Effects of MN dispersoids on near threshold fatigue crack growth in 2134 type alloys N88-13692
Fatigue 87, volume 3 [AD-A184047] N88-13700
Occurance and growth of fatigue cracks in corrosion environment N88-13704
Fracture kinetics of corrosion fatigue N88-13708
Constraint effects in fatigue crack growth N88-13719
An optical interferometry technique to evaluate closure along a crack front N88-13726

**CRACK GEOMETRY**
Fatigue crack growth N88-13734

**CRACK INITIATION**
Fatigue 87, volume 1 [AD-A184045] N88-13645
Cyclic deformation and crack initiation N88-13646
Effect of grain orientation on the origination and the initial growth of fatigue cracks in pure iron N88-13647
The mechanics of fatigue-crack nucleation in a low-alloy steel under fretting conditions N88-13649
Surface deformation and fatigue crack initiation of alpha-iron N88-13651
The effect of ion beam mixed Ni-Al surface layers on PSB extrusion morphology in fatigued nickel N88-13652
The orientations of dipolar walls produced by cyclic deformation N88-13655
Growth of short fatigue cracks in a squeeze formed aluminum alloy N88-13658
The effect of alpha platelet morphology and beta-grain size on the initiation and growth of short fatigue cracks in Ti65S N88-13667
The initiation and growth of small fatigue cracks in copper at room and cryogenic temperatures N88-13668
Behavior of short cracks in a 2024 aluminum alloy sheet tested at several stress ratios N88-13669
The influence of microstructure and residual stresses on the initiation and propagation of short surface cracks on AlMgSi1 N88-13674
Threshold stress for fatigue crack initiation from a small crack N88-13675
A unified model for fatigue crack initiation, short crack growth, long crack propagation, and closure effects N88-13680
Fatigue of 30CrMnSiNi2A notched specimens under spectrum loading N88-13689
The initiation and growth of fatigue cracks in carburised 9Cr1Mo steel N88-13696
The role of inclusions in corrosion fatigue crack initiation in Q1N N88-13699
Fatigue 87, volume 3 [AD-A184047] N88-13700
A study of corrosion fatigue crack initiation, growth and the threshold condition under variable amplitude loading N88-13701
The effect of environment on low cycle fatigue properties in HSLA steel N88-13705
Coupling effects between the ferrite and austenite phases during corrosion fatigue of a ferrite/austenite duplex stainless steel N88-13706
Fatigue crack propagation in Al-Zn-Mg bicrystals and its dependence on the environment N88-13707
Crack initiation studies in hydrogen embrittled spring steel strip N88-13710
Telemetric laser extensometry technique for monitoring deflections in small cracks N88-13724
An overview of fatigue N88-13729
Deformation mechanisms and crack initiation in fatigue N88-13730

**CRACK PROPAGATION**
Micromechanisms of fatigue crack growth and fracture toughness in metal matrix composites [AD-A185200] N88-13392
Environmentally assisted cracking: Overview of evidence for an adsorption-induced localised-slip process [AD-A185175] N88-13443
Stress intensity factors for cracking metal structures under rapid thermal loading, phase 1 [AD-A184112] N88-13606
Fatigue 87, volume 1 [AD-A184045] N88-13645
Effect of grain orientation on the origination and the initial growth of fatigue cracks in pure iron N88-13647
The growth of persistent slip bands N88-13648
Closure behavior under constant effective stress intensity loading conditions N88-13656
Growth of short fatigue cracks in a squeeze formed aluminum alloy N88-13658
Influence of microstructure and aging condition on the fatigue crack propagation in age hardened aluminium alloys N88-13659
Fatigue crack growth behavior of A356-T6 cast aluminum alloy N88-13660
Striations and the fatigue growth mechanism in a micro-alloyed steel N88-13661
Near-threshold short crack growth behavior in Nimonic 105 N88-13663
Fatigue crack propagation of short and long cracks: Phys. basis, prediction methods and engineering significance N88-13664
Low cycle fatigue life predictions of a 1CrMoV steel in terms of a J-controlled short crack growth model N88-13665
The statistics of the shape of small fatigue cracks N88-13666
The effect of alpha platelet morphology and beta-grain size on the initiation and growth of short fatigue cracks in Ti65S N88-13667
Behavior of short cracks in a 2024 aluminum alloy sheet tested at several stress ratios N88-13669
On the role of crack tip shielding in influencing the behavior of long and small fatigue cracks in aluminum-lithium alloy 2090 N88-13671
The influence of slip mechanism on fatigue of Mg and Mg-2.3Li N88-13672
The growth behavior of small fatigue cracks; the effect of microstructure and crack closure N88-13673
The influence of microstructure and residual stresses on the initiation and propagation of short surface cracks on AlMgSi1 N88-13674
Threshold stress for fatigue crack initiation from a small crack N88-13675
Behavior of long and short fatigue cracks in a powder metallurgy superalloy at room and at high temperature N88-13677
Propagation of small fatigue cracks in 2024-T3 aluminum alloy N88-13678
Closure and propagation behavior of short fatigue cracks at different R-ratios N88-13679
A unified model for fatigue crack initiation, short crack growth, long crack propagation, and closure effects N88-13680
Fatigue crack retardation in aluminium alloys N88-13681
Fatigue crack growth under random overloads N88-13682
A dislocation model for fatigue crack propagation under variable amplitude loading N88-13683
Observations on the effect of overloads on fatigue crack growth N88-13684
A study of fatigue crack growth life under random stresses N88-13685
Crack growth in contrasting titanium alloys under the conjoint action of high and low cycle fatigue N88-13686
Variable amplitude fatigue crack growth in aluminum alloys 2090-T8E41 and 7075-T651 N88-13687
Crack growth prediction in 3D structures under aeronautical-type spectrum loadings N88-13688
Near-threshold growth of defects in engineering materials N88-13691
Effects of MN dispersoids on near threshold fatigue crack growth in 2134 type alloys N88-13692
Crack propagation properties of sintered steel N88-13698
The role of inclusions in corrosion fatigue crack initiation in Q1N N88-13699
Fatigue 87, volume 3 [AD-A184047] N88-13700
A study of corrosion fatigue crack initiation, growth and the threshold condition under variable amplitude loading N88-13701
The influence of crack conditions on hydrogen uptake by steels N88-13702
Modeling the effect of sulfur on the threshold environmental cracking rate of steels in high temperature water N88-13703
Occurance and growth of fatigue cracks in corrosion environment N88-13704
Coupling effects between the ferrite and austenite phases during corrosion fatigue of a ferrite/austenite duplex stainless steel N88-13706
Fatigue crack propagation in Al-Zn-Mg bicrystals and its dependence on the environment N88-13707
the influence of temper embrittlement on fatigue crack growth in hydrogen N88-13709
Crack initiation studies in hydrogen embrittled spring steel strip N88-13710
Fatigue mechanisms in ARALL, a fatigue resistant hybrid aluminum aramid composite material N88-13711
The effect of heat treatment on fatigue crack growth in polycarbonate N88-13714
Effect of test temperature and frequency on fatigue crack propagation in PVC N88-13715
Environmental fracture toughness and static fatigue crack propagation of silica glass N88-13716
Fatigue crack growth: Statistical considerations N88-13718
Constraint effects in fatigue crack growth N88-13719
A comparison of plastic work energy and external input for fatigue crack propagation N88-13722
On the geometrical description of fatigue crack surfaces N88-13727
An overview of fatigue N88-13729
Environmentally assisted fatigue crack growth N88-13731
Fatigue crack growth N88-13734
The Shock and Vibration Digest, Volume 19, No. 12 N88-13746
Experimental studies on acoustic emission monitoring of crack propagation in offshore structures: A literature survey N88-13748
Acoustic emissions at an open crack [DE88-001504] N88-13751

**CRACK TIPS**
On the role of crack tip shielding in influencing the behavior of long and small fatigue cracks in aluminum-lithium alloy 2090 N88-13671
A unified model for fatigue crack initiation, short crack growth, long crack propagation, and closure effects N88-13680
A dislocation model for fatigue crack propagation under variable amplitude loading N88-13683

Observations on the effect of overloads on fatigue crack growth N88-13684
Modeling the effect of sulfur on the threshold environmental cracking rate of steels in high temperature water N88-13703
Effect of test temperature and frequency on fatigue crack propagation in PVC N88-13715
Constraint effects in fatigue crack growth N88-13719
Embrittling effect of the plastic zone N88-13721
Telemetric laser extensometry technique for monitoring deflections in small cracks N88-13724
An optical interferometry technique to evaluate closure along a crack front N88-13726

**CRACKING (FRACTURING)**
Fracture kinetics of corrosion fatigue N88-13708
On the geometrical description of fatigue crack surfaces N88-13727

**CRACKS**
Fatigue 87, volume 1
[AD-A184045] N88-13645
Cyclic deformation and crack initiation N88-13646
Effect of grain orientation on the origination and the initial growth of fatigue cracks in pure iron N88-13647
The mechanics of fatigue-crack nucleation in a low-alloy steel under fretting conditions N88-13649
Growth of short fatigue cracks in a squeeze formed aluminum alloy N88-13658
Fatigue crack growth behavior of A356-T6 cast aluminum alloy N88-13660
Near-threshold short crack growth behavior in Nimonic 105 N88-13663
Fatigue crack propagation of short and long cracks: Phys. basis, prediction methods and engineering significance N88-13664
Low cycle fatigue life predictions of a 1CrMoV steel in terms of a J-controlled short crack growth model N88-13665
The statistics of the shape of small fatigue cracks N88-13666
The effect of alpha platelet morphology and beta-grain size on the initiation and growth of short fatigue cracks in Ti65S N88-13667
The initiation and growth of small fatigue cracks in copper at room and cryogenic temperatures N88-13668
Behavior of short cracks in a 2024 aluminum alloy sheet tested at several stress ratios N88-13669
On the role of crack tip shielding in influencing the behavior of long and small fatigue cracks in aluminum-lithium alloy 2090 N88-13671
The influence of slip mechanism on fatigue of Mg and Mg-2.3Li N88-13672
Threshold stress for fatigue crack initiation from a small crack N88-13675
An experimental study of closure behavior of naturally initiated small cracks N88-13676
Behavior of long and short fatigue cracks in a powder metallurgy superalloy at room and at high temperature N88-13677
Closure and propagation behavior of short fatigue cracks at different R-ratios N88-13679
A unified model for fatigue crack initiation, short crack growth, long crack propagation, and closure effects N88-13680
Fatigue crack retardation in aluminium alloys N88-13681
Fatigue crack growth under random overloads N88-13682
A dislocation model for fatigue crack propagation under variable amplitude loading N88-13683
Variable amplitude fatigue crack growth in aluminum alloys 2090-T8E41 and 7075-T651 N88-13687
Near-threshold growth of defects in engineering materials N88-13691
Effects of MN dispersoids on near threshold fatigue crack growth in 2134 type alloys N88-13692
The initiation and growth of fatigue cracks in carburised 9Cr1Mo steel N88-13696
The role of inclusions in corrosion fatigue crack initiation in Q1N N88-13699
Acoustic emissions at an open crack
[DE88-001504] N88-13751

**CREATIVITY**
Separable orthogonal coordinates and particle creation for an accelerating observer
[DE87-703358] N88-14029

**CREEP PROPERTIES**
Study of the influence of mechanical - thermal treatments on the creep behavior of a niobium stainless steel
[DE87-703506] N88-13431
Cu-2 mechanical properties and microstructural stability of advanced steam cycle materials
[DE88-001519] N88-13452

**CRITICAL POINT**
Detection of critical points: The first step to automatic line generalization N88-13803

**CROP GROWTH**
Controlled Ecological Life Support System. Design, Development, and Use of a Ground-Based Plant Growth Module
[NASA-CP-2479] N88-13852
CELSS Program Meeting N88-13853
Controlled ecological life support systems: Development of a plant growth module N88-13854
Plant Growth Module (PGM) conceptual design N88-13855

**CROSS CORRELATION**
Cross-correlation of uniform cyclic difference set sequences
[AD-A184879] N88-13913

**CROSSLINKING**
Development of microencapsulation techniques
[AD-A185019] N88-13457

**CRUISING FLIGHT**
Techniques for performance optimisation in cruise and manoeuverability N88-13321

**CRYOGENIC COOLING**
Evaluation of a cryogenic refrigerator for cooling focal plane instrumentation — satellite instruments
[BAE-TP-8095-VOL-1] N88-13485
Evaluation of a cryogenic refrigerator for cooling focal plane instrumentation. Appendix B: Accommodation study — satellite instruments
[BAE-TP-8095-VOL-2] N88-13486

**CRYOGENIC EQUIPMENT**
Evaluation of a cryogenic refrigerator for cooling focal plane instrumentation — satellite instruments
[BAE-TP-8095-VOL-1] N88-13485
Evaluation of a cryogenic refrigerator for cooling focal plane instrumentation. Appendix B: Accommodation study — satellite instruments
[BAE-TP-8095-VOL-2] N88-13486
Capacitive resonant transducer for the Frascati gravitational antenna
[IFSI-86-9] N88-13528

**CRYOGENICS**
Fatigue strength of alloy A286 at cryogenic temperature N88-13695

**CRYSTAL DEFECTS**
Structural characterization of ion implanted beta-SiC thin films
[DE87-014567] N88-14027

**CRYSTAL GROWTH**
United States - Japan Workshop on Dielectric and Piezoelectric Ceramics (3rd) held in Toyama, Japan on November 9-12, 1986
[AD-A185113] N88-13460
MBE growth of InAsSb strained-layer superlattices
[DE88-000365] N88-14011
Molecular beam epitaxial growth and characterization of 3-5 compound semiconductor single and multiple interface structures
[AD-A185400] N88-14021
Novel heterojunction devices
[DE87-013716] N88-14026

**CRYSTAL LATTICES**
MBE growth of InAsSb strained-layer superlattices
[DE88-000365] N88-14011
The pseudopotential density functional method applied to semiconducting crystals
[ETN-88-91362] N88-14024
Novel heterojunction devices
[DE87-013716] N88-14026

**CRYSTAL STRUCTURE**
Properties of refractory metals processed by enhanced sintering treatments
[AD-A184944] N88-13440
Study of boundary structures
[AD-A184808] N88-14013

**CRYSTAL SURFACES**
Surface deformation and fatigue crack initiation of alpha-iron N88-13651

**CRYSTALLINITY**
Microstructure of amorphous and crystalline zirconium alloys rapidly solidified
[DE87-703700] N88-13432

**CRYSTALLIZATION**
T.E.M. study of boehmite gels and of their transformation into alpha-alumina
[SNIAS-872-430-121] N88-14023

**CRYSTALLOGRAPHY**
Effect of grain orientation on the origination and the initial growth of fatigue cracks in pure iron N88-13647
The growth of persistent slip bands N88-13648
The orientations of dipolar walls produced by cyclic deformation N88-13655
The influence of slip mechanism on fatigue of Mg and Mg-2.3Li N88-13672

**CRYSTALS**
Cyclic deformation of an extruded AlMgSi alloy N88-13654

**CULTIVATION**
Controlled ecological life support systems: Development of a plant growth module N88-13854

**CUMULATIVE DAMAGE**
Damage considerations in sizing aircraft cells. Life predictions
[SNIAS-872-111-116] N88-13330

**CURRENT DENSITY**
Reversed field pinch plasmas with various boundary conditions
[DE88-000832] N88-14004

**CURVATURE**
A numerical study of the effects of curvature and convergence on dilution jet mixing
[NASA-TM-89878] N88-13347

**CUTTERS**
XCUT: A rule-based expert system for the automated process planning of machined parts
[DE87-011638] N88-13905

**CYCLES**
Cross-correlation of uniform cyclic difference set sequences
[AD-A184879] N88-13913

**CYCLIC LOADS**
X-ray analysis of polycrystalline aluminium subjected to fatigue cycling
[NAL-TM-MT-8706] N88-13434
Application of finite element methods with cyclic elasto-plastic strain analysis to low cycle fatigue analysis of engine components
[AR-004-512] N88-13642
Fatigue 87, volume 3
[AD-A184047] N88-13700
A study of corrosion fatigue crack initiation, growth and the threshold condition under variable amplitude loading N88-13701
The effect of environment on low cycle fatigue properties in HSLA steel N88-13705
Fatigue crack propagation in Al-Zn-Mg bicrystals and its dependence on the environment N88-13707
Low cycle fatigue behaviour of notched specimens of nickel based superalloy single crystal N88-13712
Computer aided modeling and fatigue failure forecast under stochastic loading N88-13720
Embrittling effect of the plastic zone N88-13721
X-ray fatigue failure prediction based on plasticity response to microcracks N88-13725

**CYCLOGENESIS**
Environmental and convective influence on tropical cyclone development versus non-development
[AD-A185231] N88-13835

**CYCLONES**
Lower-stratospheric/upper-tropospheric exchange processes associated with tropical cyclones as observed by TOMS N88-13782
Opportunities for tropical cyclone motion research in the Northwest Pacific region
[AD-A185068] N88-13834

**CYCLOTRON RESONANCE DEVICES**
High peak power ka-band gyrotron oscillator experiment
[AD-A185424] N88-13563
Theoretical and experimental investigation of electron beam acceleration and sub-millimeter wave generation in cyclotron resonant cavities
[AD-A184806] N88-13975

**CYLINDRICAL BODIES**
Driving mechanism of unsteady separation shock motion in hypersonic interactive flow N88-13226
Three-dimensional flow past a two-dimensional body N88-13280
Computational study of three-dimensional wake structures
[REPT-2] N88-13281
Computation of flow around 2-D circular cylinder N88-13284
Interferometric data for a shock-wave/boundary-layer interaction
[NASA-TM-88227] N88-13306
An analytical study of the effects of transverse shear deformation and anisotropy on buckling loads of laminated cylinders
[NASA-TM-100508] N88-13387
The simulation of the viscous flow around a cylinder by the random vortex method N88-13534
Fiber-optic accelerometer investigation
[AD-A185359] N88-13561

**CYLINDRICAL SHELLS**
Experimental studies on the tripping behavior of narrow T-stiffened flat plates subjected to hydrostatic pressure and underwater shock N88-13613

# D


**DAMAGE**
Fiber composite structural durability and damage tolerance: Simplified predictive methods
[NASA-TM-100179] N88-13409
Raman microprobe characterization of dielectric films following high-energy pulsed laser irradiation
[DE88-000559] N88-13587
Fretting wear and fretting fatigue damage N88-13697

**DAMAGE ASSESSMENT**
Contribution of acoustic analysis to assess damage in fluid storage tanks under high pressure — composite materials, filament winding
[SNIAS-872-430-119] N88-13407
Overview of Austrian Airborne Imaging Spectrometer (AIS) programme and first results N88-13762

**DAMPING**
Non-linear shipboard shock analysis of the Tomahawk missile shock isolation system N88-13614
Improvement of modal scaling factors using mass additive technique N88-13620

**DATA ACQUISITION**
High frequency data acquisition system for space shuttle main engine testing N88-13630
The Portable Instant Display and Analysis Spectrometer (PIDAS) N88-13756
Plant Growth Module (PGM) conceptual design N88-13855
Software design for an airborne gravity measurement system
[AD-A185000] N88-13878

**DATA BASE MANAGEMENT SYSTEMS**
Relational data handling system for scientists
[PB87-223426] N88-14038

**DATA BASES**
The RAE experimental data-base for missiles at high Mach number and its use in assessing CFD methods N88-13250
A rudimentary database for three-dimensional objects using structural representation
[CSE-87-00004] N88-13597
Improvement of modal scaling factors using mass additive technique N88-13620
Space shuttle main engine vibration data base N88-13631
Role of technical information in innovation
[PB87-235388] N88-14039

**DATA COMPRESSION**
Study on data compression systems for operational remote sensing — meteosat imagery
[NLR-TR-86029-L] N88-13808

**DATA LINKS**
Test and evaluation of the transputer in a multi-transputer system
[AD-A184969] N88-13859

**DATA MANAGEMENT**
Relational data handling system for scientists
[PB87-223426] N88-14038

**DATA PROCESSING**
A computer code to process and plot laser altimetry data interactively on a microcomputer
[NASA-TM-100667] N88-13371
The analysis of nonstationary vibration data N88-13610
A new method to real-normalize measured complex modes N88-13618
TOMS: The Antarctic ozone hole and ozone trends N88-13775
Application of TOMS data to weather analysis models N88-13787
TOMS ozone data compared at mesoscale resolution to tropopause heights from the AVE radiosonde network and to VAS radiances over the south-central United States N88-13790
Development of a data analysis system for the detection of lower level atmospheric turbulence with an acoustic sounder
[AD-A184972] N88-13821
Hanford Meteorological Station computer codes. Volume 5: The TOWER computer code
[DE88-001610] N88-13843
File usage analysis and resource usage prediction: A measurement-based study
[NASA-CR-181553] N88-13867
Predictability of process resource usage: A measurement-based study of UNIX
[NASA-CR-181562] N88-13869
Performability modeling based on real data: A casestudy
[NASA-CR-181563] N88-13870
Conceptual issues in measuring the behavior of a distributed real-time process-control computer system
[DE87-014251] N88-13899

**DATA REDUCTION**
Analysis of photopole data reduction models N88-13616
The Portable Instant Display and Analysis Spectrometer (PIDAS) N88-13756
AIS-2 radiometry and a comparison of methods for the recovery of ground reflectance N88-13757
Software design for an airborne gravity measurement system
[AD-A185000] N88-13878

**DATA SIMULATION**
High resolution satellite imagery simulation — treaty verification
[FOA-C-30462-3.3,9.3] N88-13810

**DATA STORAGE**
A rudimentary database for three-dimensional objects using structural representation
[CSE-87-00004] N88-13597
Storing and retrieving data in a parallel distributed memory system
[AD-A185177] N88-13897

**DATA TRANSMISSION**
An exact analysis and performance of framed ALOHA with capture
[AD-A185006] N88-13500
Test and evaluation of the transputer in a multi-transputer system
[AD-A184969] N88-13859

**DAYTIME**
The lengthening and shortening of the day
[KNMI-TR-91] N88-13839

**DEBRIS**
Fretting wear and fretting fatigue damage N88-13697

**DECAY**
Dynamical analysis of molecular decay at spherical surfaces
[AD-A184908] N88-13964

**DECOMPOSITION**
Application of Vandermonde decomposition to directional and modal analysis of broadband transients
[AD-A185007] N88-13956

**DEFENSE PROGRAM**
University research initiative research program summaries
[AD-A184876] N88-14035

**DEFLECTION**
Telemetric laser extensometry technique for monitoring deflections in small cracks N88-13724

**DEFORMATION**
Measurement of model deformation in wind tunnels N88-13358
An analytical study of the effects of transverse shear deformation and anisotropy on buckling loads of laminated cylinders
[NASA-TM-100508] N88-13387
Cyclic deformation and crack initiation N88-13646
The orientations of dipolar walls produced by cyclic deformation N88-13655
Striations and the fatigue growth mechanism in a micro-alloyed steel N88-13661
The influence of slip mechanism on fatigue of Mg and Mg-2.3Li N88-13672
Fatigue 87, volume 3
[AD-A184047] N88-13700
Deformation mechanisms and crack initiation in fatigue N88-13730
Deformation, fatigue and fracture behavior of two cast anisotropic superalloys N88-13732

**DEGRADATION**
Models for the degradation of stratified composite structures
[ONERA-RT-13/3542-RY-061-R] N88-13395
Micromechanics of the degradation of composite materials
[SNIAS-872-430-113] N88-13405
Development of a data analysis system for the detection of lower level atmospheric turbulence with an acoustic sounder
[AD-A184972] N88-13821

**DEGREES OF FREEDOM**
Coupled elastic rotor/body vibrations with inplane degrees of freedom N88-13643

**DEICING**
Theoretical analysis of the electrical aspects of the basic electro-impulse problem in aircraft de-icing applications
[NASA-CR-180845] N88-13310

**DELAMINATING**
Strain-energy-release rate analysis of the end-notched flexure specimen using the finite-element method
[NASA-TM-100494] N88-13735

**DELTA WINGS**
Computation of flow past conical hypersonic wings using a second order Godunov method N88-13241
Vortex formation over delta, double-delta and wave rider configurations at supersonic speeds N88-13243
Study of the effect of mass transfer on a transonic boundary layer. Application to flow relaminarization
[ETN-88-91169] N88-13296
Delta wing in incompressible flow. Experimental study in F2
[ONERA-RT-36/1147-AN-249-G] N88-13298
Examples of static aeroelastic effects on present combat aircraft projects N88-13349

**DELTAS**
Expectations for water level deviations at the delta works: Zierikzee (Netherlands), November 1981-February 1986
[KNMI-TR-93] N88-13840

**DENSITY DISTRIBUTION**
The pseudopotential density functional method applied to semiconducting crystals
[ETN-88-91362] N88-14024

**DEPOSITION**
Computation of rime ice accretion on airfoils
[FFA-TN-1987-08] N88-13301

**DEPTH**
Master plots for predicting the case-depth in laser surface treatments
[PB87-221875] N88-13574
The effect of microstructure on the surface crack length: Crack depth relationship for short cracks N88-13670

**DEPTH MEASUREMENT**
Estimation of marine boundary layer depth and relative humidity with multispectral satellite measurements
[AD-A184881] N88-13804

**DERIVATION**
Studies on syntheses of amine-carboxyboranes (boron analogues of amino acids) and derivatives
[AD-A184838] N88-13386

**DESERTIFICATION**
Environmental processes and spectral reflectance characteristics associated with soil erosion in desert fringe regions
[NASA-CR-182332] N88-13811

**DESERTS**
Environmental processes and spectral reflectance characteristics associated with soil erosion in desert fringe regions
[NASA-CR-182332] N88-13811

**DESIGN ANALYSIS**
Aerodynamics of Hypersonic Lifting Vehicles
[AGARD-CP-428] N88-13219
Lifting bodies: An attractive aerodynamic configuration choice for hypervelocity vehicles N88-13248
Design of wings and wing/body configurations for transonic and supersonic speeds N88-13318
Aeroelastic analysis of modern transport aircraft — European Airbus
[SNIAS-872-111-102] N88-13329
Design and assembly sequence analysis of option 3 for CETF reference space station
[NASA-TM-100503] N88-13369
Evaluation of device figure of merit in microwave switching circuit design
[AD-A184896] N88-13520
A complete linearized theory for the analysis and design of two-dimensional hydrofoils near a free surface
[UTIAS-TN-264] N88-13531
Conservatism implications of shock test tailoring for multiple design environments N88-13611
Near-threshold growth of defects in engineering materials N88-13691
Utilization of dynamic characteristics of materials to optimize military explosive charges. Application to antiship devices
[SNIAS-872-320-101] N88-13743
STAEBL/general composites with hygrothermal effects (STAEBL/GENCOM)
[NASA-TM-100266] N88-13754
High speed propeller performance and noise predictions at takeoff/landing conditions
[NASA-TM-100267] N88-13960
Photon counting image sensor development for astronomical applications
[NASA-CR-181507] N88-14049

**DESIGN TO COST**
Operational groups at the Aerospatiale Aircraft Division
[SNIAS-872-111-107] N88-14036

**DESTRUCTION**
Formation and destruction of nitrous oxide in lean, premixed combustion
[DE88-001390] N88-13423

**DETECTION**
Incipient failure detection of space shuttle main engine turbopump bearings using vibration envelope detection N88-13629

**DIAGNOSIS**
Diagnostic reasoning in digital systems
[NASA-CR-181564] N88-13871

**DIELECTRIC PROPERTIES**
United States - Japan Workshop on Dielectric and Piezoelectric Ceramics (3rd) held in Toyama, Japan on November 9-12, 1986
[AD-A185113] N88-13460
Numerical and analytical study of the equivalent permittivity or permeability of nonhomogeneous materials. Application to the experimental electromagnetic characterization of composites
[SNIAS-872-430-104] N88-13509
Ionic transport and electrical relaxation in glass
[DE88-000887] N88-14028
**DIELECTRICS**
Raman microprobe characterization of dielectric films following high-energy pulsed laser irradiation
[DE88-000559] N88-13587
Extinction by dielectric particles at optical and infrared wavelength
[AD-A184818] N88-13981
**DIFFERENCE EQUATIONS**
Cross-correlation of uniform cyclic difference set sequences
[AD-A184879] N88-13913
**DIFFERENTIAL EQUATIONS**
A note on the use of symmetric line Gauss-Seidel for the steady upwind differenced Euler equations
[AD-A185223] N88-13540
The numerical and analytic of implicit differential equations and their application to control and circuit problems
[AD-A185404] N88-13922
**DIFFRACTION LIMITED CAMERAS**
Inverse scattering analysis of diffraction limited SAR
[FOA-C-30459-3.2] N88-13512
**DIFFRACTION PATTERNS**
Phase-locked semiconductor quantum well laser arrays
[AD-A185155] N88-13583
**DIFFUSERS**
Numerical prediction of turbulent flows in dump diffusers N88-13265
**DIFFUSION**
Automated design of controlled diffusion blades
[NASA-TM-100251] N88-13304
Numerical methods for reaction-diffusion problems with non-differentiable kinetics
[AD-A185405] N88-13923
Freidlin-Wentzell type estimates and the law of the iterated logarithm for a class of stochastic processes related to symmetric statistics
[AD-A185366] N88-13944
On the correlation free forms for nonlinear stochastic systems
[DE87-011169] N88-13947
**DIGITAL COMPUTERS**
Technology upgrade of a silicon compiler
[AD-A184873] N88-14016
**DIGITAL DATA**
High frequency data acquisition system for space shuttle main engine testing N88-13630
Space shuttle main engine vibration data base N88-13631
**DIGITAL ELECTRONICS**
Establishment of complete minimum test sets for digital circuits with safety engineering significance
[ETN-88-90599] N88-13526
**DIGITAL FILTERS**
Implementation of an FIR band pass filter using a bit-slice processor
[AD-A184895] N88-13875
**DIGITAL SIMULATION**
Numerical simulation of the hypersonic flow around lifting vehicles N88-13234
The polar ionosphere and interplanetary field
[AD-A185388] N88-13822
An extension to the multilevel logic simulator for microcomputers
[AD-A185032] N88-13879
**DIGITAL SYSTEMS**
Diagnostic reasoning in digital systems
[NASA-CR-181564] N88-13871
Error propagation in a digital avionic mini processor
[NASA-CR-181565] N88-13872
**DIGITAL TECHNIQUES**
Measured characteristics of 800/900 MHz mobile radio channels with high-angle propagation through moderately dense foliage
[CRC-1398] N88-13493
**DIGITAL TELEVISION**
Digital video bit-rate reduction: DPCM for sub-Nyquist PAL
[BBC-RD-1987/16] N88-13494
Television motion measurement for DATV and other applications
[BBC-RD-1987/11] N88-13496
**DILUTION**
A numerical study of the effects of curvature and convergence on dilution jet mixing
[NASA-TM-88878] N88-13347
**DIMENSIONS**
BASIC desk-top computer program for the three-dimensional static configuration of an extensible flexible cable in a uniform stream
[AD-A184852] N88-13737
Evolution of mean square magnetic vector potential in compressible, two-dimensional, magnetofluid turbulence
[AD-A184985] N88-13990
Comparison of 2D memory SEU transport simulation with experiments
[ATR-86(8139)-2-REV-A] N88-14025
**DIPOLE ANTENNAS**
The use of coaxial transmission line elements in log-periodic dipole arrays
[AD-A184864] N88-13499
**DIRECT CURRENT**
Analysis of nickel sulphamate bath using charging current compensated D.C. polarography
[NAL-TM-MT-8705] N88-13433
Digital control of a direct current converter for a hybrid vehicle
[LAAS-87-266] N88-13527
**DISCONTINUITY**
SHARP simulation of discontinuities in highly convective steady flow
[NASA-TM-100240] N88-13931
**DISLOCATIONS (MATERIALS)**
A dislocation model for fatigue crack propagation under variable amplitude loading N88-13683
**DISPERSION**
Development on thin wall tubes of dispersion type
[DE87-703384] N88-13483
**DISPERSIONS**
High explosive moulding powders from RDX and aqueous polyurethane dispersions
[AD-A185026] N88-13458
**DISPLACEMENT**
Hypersonic laminar boundary layer: Parametric study for the representation of real gas effects N88-13236
Telemetric laser extensometry technique for monitoring deflections in small cracks N88-13724
**DISPLAY DEVICES**
Displaying three-dimensional data
[AD-A185347] N88-13541
The Portable Instant Display and Analysis Spectrometer (PIDAS) N88-13756
The use of color in electronic maps. Part 1: Generation and analysis of color on the Gould/DeAnza image processing system
[IZF-1986-32] N88-13882
**DISTRIBUTED PROCESSING**
Storing and retrieving data in a parallel distributed memory system
[AD-A185177] N88-13897
Conceptual issues in measuring the behavior of a distributed real-time process-control computer system
[DE87-009748] N88-13898
Conceptual issues in measuring the behavior of a distributed real-time process-control computer system
[DE87-014251] N88-13899
Connecting RPC (Remote Procedure Call)-based distributed systems using wide-area networks
[PB87-234423] N88-14041
**DISTRIBUTION FUNCTIONS**
Extrema of skewed stable processes
[AD-A185422] N88-13925
Further studies in estimation of life distribution characteristics from censored data
[AD-A184862] N88-13937
Restoration of particle pitch angle distribution functions by a maximum entropy algorithm
[ATR-86(7096)-3] N88-13969
**DIURNAL VARIATIONS**
An analytical soil thermodynamic model for the diurnal variation of ground surface temperature
[AD-A185388] N88-13823
The lengthening and shortening of the day
[KNMI-TR-91] N88-13839
**DIVERGENCE**
Wing divergence of trimmed aircraft N88-13354
**DOCUMENTATION**
Guidance for conference rapporteurs
[NASA-CR-182338] N88-14042
**DOPED CRYSTALS**
Structural characterization of ion implanted beta-SiC thin films
[DE87-014567] N88-14027
**DOPPLER RADAR**
Media calibrations of the Doppler signal for a gravitational wave experiment --- interplanetary medium
[IFSI-86-13] N88-13825
**DOSIMETERS**
Fabricate, calibrate and test a dosimeter for integration into the CRRES (Combined Release and Radiation Effects Satellite) satellite
[AD-A185439] N88-13564
**DRAG**
The drag of slender axisymmetric cones in rarefied hypersonic flow N88-13229
**DRAG REDUCTION**
Navier-Stokes analysis of laminar flow control of a two-dimensional airfoil N88-13286
Wakes of two dimensional bluff bodies in subsonic flow. Influence of a separating plate and of a pulsed injection of momentum
[IMFL-4200-86/75] N88-13297
**DRILLING**
Design and test of high performance composite tubes for use in deep water drilling and production systems
[SNIAS-872-430-107] N88-13487
High performance composite tubes for offshore applications
[SNIAS-872-430-116] N88-13488
**DROPS (LIQUIDS)**
Numerical simulation of splash of droplet at unit gravity N88-13275
Operating envelopes of particle sizing instrumentation used for icing research
[NASA-CR-180870] N88-13573
A study of the interaction of laser light with liquid propellant drops
[AD-A185117] N88-13582
Extinction by dielectric particles at optical and infrared wavelength
[AD-A184818] N88-13981
**DUCTED FANS**
Velocity scaled aeroelastic testing of an unducted fan
[GTL-191] N88-13337
**DUCTILITY**
Investigation by differential scanning calorimetry of microstructure in a superplastic Al-Mg-Zr alloy
[AD-A184902] N88-13439
**DUNES**
Environmental processes and spectral reflectance characteristics associated with soil erosion in desert fringe regions
[NASA-CR-182332] N88-13811
**DYNAMIC CHARACTERISTICS**
Dynamics of cables and chains N88-13747
Molecular dynamics studies of aromatic hydrocarbon liquids
[DE88-001473] N88-13973
Dynamic processes in field-reversed-configuration compact toroids
[DE87-014756] N88-13998
**DYNAMIC CONTROL**
Photochemical ozone overburden correction N88-13778
Investigation, development, and application of optimal output feedback theory. Volume 3: The relationship between dynamic compensators and observers and Kalman filters
[NASA-CR-4107] N88-13900
**DYNAMIC LOADS**
Experimental studies on the tripping behavior of narrow T-stiffened flat plates subjected to hydrostatic pressure and underwater shock N88-13613
BASIC desk-top computer program for the three-dimensional static configuration of an extensible flexible cable in a uniform stream
[AD-A184852] N88-13737
RADSPHERE: A computer program for calculating the steady-state, axially symmetric, forced response and radiation field of a submerged spherical shell
[AD-A185025] N88-13738
Accurate rotor loads prediction using the FLAP (Force and Loads Analysis Program) dynamics code
[DE88-001109] N88-13815
Structuring data for concurrent vectorized processing in a transient dynamics finite element program
[DE87-013082] N88-13890
**DYNAMIC MODELS**
Development of response models for the Earth Radiation Budget Experiment (ERBE) sensors. Part 1: Dynamic models and computer simulations for the ERBE nonscanner, scanner and solar monitor sensors
[NASA-CR-178292] N88-13557
The tail lobe ion spectrometer: Theory and observations
[IFSI-86-12] N88-13569
**DYNAMIC RESPONSE**
Aircraft dynamics: Aerodynamic aspects and wind tunnel techniques N88-13320
Modal survey of the space shuttle solid rocket motor using multiple input methods N88-13617

Dynamical analysis of molecular decay at spherical surfaces
[AD-A184908] N88-13964

**DYNAMIC STABILITY**
Hypersonic static and dynamic stability of axisymmetric shapes: A comparison of prediction methods and experiment N88-13246
Dynamic stability of hypersonic conical lifting vehicles according to Newton-Busemann theory N88-13247
Dynamic behavior of dissymmetric rotor bearings modelled with a periodic coefficient large system N88-13640

**DYNAMIC STRUCTURAL ANALYSIS**
Predictions of F-111 TACT aircraft buffet response and correlations of fluctuating pressures measured on aluminum and steel models and the aircraft
[NASA-CR-4089] N88-13218
The 56th Shock and Vibration Symposium, volume 1
[NASA-CP-2486-VOL-1] N88-13609
Improvement of modal scaling factors using mass additive technique N88-13620
Initial dynamic load estimates during configuration design N88-13621
Viscous damped space structure for reduced jitter N88-13623
A system identification technique based on the random decrement signatures. Part 1: Theory and simulation N88-13625
A system identification technique based on the random decrement signatures. Part 2: Experimental results N88-13626
An efficient frequency response solution for nonproportionally damped systems N88-13634
Shape optimization of damping layers N88-13635
Dynamic response of laminated composite plates using a three-dimensional hybrid-stress finite-element formulation N88-13639
Dynamic behavior of dissymmetric rotor bearings modelled with a periodic coefficient large system N88-13640
Utilization of dynamic characteristics of materials to optimize military explosive charges. Application to antiship devices
[SNIAS-872-320-101] N88-13743
Accurate rotor loads prediction using the FLAP (Force and Loads Analysis Program) dynamics code
[DE88-001109] N88-13815

**DYNAMICAL SYSTEMS**
Non-minimal interaction of gravity with other physical fields: An overview
[DE87-703362] N88-13819

**DYNAMICS**
Dynamics of propellant feedline systems
[AD-A184865] N88-13537


## E


**EARTH ATMOSPHERE**
Anti-Stokes generation of 226 nm light
[DE88-001612] N88-13590

**EARTH AXIS**
Axial anisotropy of the intensity of the cosmic ray nuclear component
[IFSI-87-7] N88-14061

**EARTH IONOSPHERE**
Activities report of the Ionospheric Observatory
[UIO-SR-87-01] N88-13827

**EARTH RADIATION BUDGET EXPERIMENT**
Development of response models for the Earth Radiation Budget Experiment (ERBE) sensors. Part 3: ERBE scanner measurement accuracy analysis due to reduced housekeeping data
[NASA-CR-178294] N88-13553
Development of response models for the Earth Radiation Budget Experiment (ERBE) sensors. Part 1: Dynamic models and computer simulations for the ERBE nonscanner, scanner and solar monitor sensors
[NASA-CR-178292] N88-13557

**EARTHNET**
National Point Of Contact (NPOC)-SPOT inquiry 1986
[NLR-MP-86055-U] N88-13807

**ECONOMIC ANALYSIS**
Economics of fusion reactors
[DE88-000580] N88-14002

**ECONOMICS**
Economics of fusion reactors
[DE88-000580] N88-14002

**EDGE DISLOCATIONS**
The growth of persistent slip bands N88-13648
The effects of thin anodic films on the cyclic microstrain/macrostrain behavior of tungsten N88-13650
Cyclic deformation of an extruded AlMgSi alloy N88-13654
The orientations of dipolar walls produced by cyclic deformation N88-13655

**EDUCATION**
Special Course on Fundamentals of Fighter Aircraft Design
[AGARD-R-740] N88-13315
Calendar of selected aeronautical and space meetings
[AGARD-CAL-87/1] N88-14033

**EFFECTIVENESS**
Effectiveness of electrodeposited coatings in reducing atmospheric corrosion of copper substrates
[DE87-013651] N88-13448

**EIGENVALUES**
Eigenvalue projection theory for linear operator equations of electromagnetics
[AD-A185434] N88-13504
Simultaneous structural and control optimization via linear quadratic regulator eigenstructure assignment N88-13622

**EIGENVECTORS**
Eigenvectors of distance-regular graphs
[AD-A185375] N88-13919

**EJECTA**
Magnetic field draping about coronal mass ejecta
[DE88-001805] N88-14057

**ELASTIC PROPERTIES**
Coupled elastic rotor/body vibrations with inplane degrees of freedom N88-13643
Two low-order mixed methods for the elasticity problem
[PB87-225272] N88-13749

**ELASTIC SHELLS**
RADSPHERE: A computer program for calculating the steady-state, axially symmetric, forced response and radiation field of a submerged spherical shell
[AD-A185025] N88-13738

**ELASTOMERS**
Process for the production of a thermoplastic elastomer composition
[EP-PATENT-0-202-782-A2] N88-13465

**ELASTOPLASTICITY**
Computation of bonded assemblies. Elastoplastic adhesives, first part
[SNIAS-NT-18926/AQET] N88-13467
Application of finite element methods with cyclic elasto-plastic strain analysis to low cycle fatigue analysis of engine components
[AR-004-512] N88-13642

**ELECTRIC ARCS**
An investigation of unipolar arcing at atmospheric pressure in aluminum 2024 and aluminum coated glass slides
[AD-A184903] N88-13521

**ELECTRIC BATTERIES**
High energy density rechargeable batteries for aerospace power requirements
[AD-A184883] N88-13519

**ELECTRIC CHARGE**
Analysis of nickel sulphamate bath using charging current compensated D.C. polarography
[NAL-TM-MT-8705] N88-13433

**ELECTRIC CHOPPERS**
Low-current behavior and current chopping of vacuum arcs
[ISBN-90-9001649-X] N88-13529

**ELECTRIC CONDUCTORS**
Molecular and supramolecular orientation in conducting polymers
[DE88-000533] N88-13472

**ELECTRIC CONTROL**
Electrical flight commands in transport aircraft
[SNIAS-872-111-108] N88-13361

**ELECTRIC DISCHARGES**
Electromagnetics and electrothermal approach to evaluate failures in microelectronic devices caused by electrostatic discharges: Stochastical aspects of the device reliability
[AD-A184906] N88-13522

**ELECTRIC EQUIPMENT**
US Naval Air Force avionic and electrical system corrosion prevention and control maintenance N88-13334

**ELECTRIC FIELDS**
An electric field meter based upon a new principle: A dummy displacement electrode. Application to aerospace vehicles
[SNIAS-872-422-106] N88-13567
Electric field measurements on Viking: First results
[TRITA-EPP-87-04] N88-13826

**ELECTRIC MOTOR VEHICLES**
Digital control of a direct current converter for a hybrid vehicle
[LAAS-87-266] N88-13527

**ELECTRIC POTENTIAL**
High energy density rechargeable batteries for aerospace power requirements
[AD-A184883] N88-13519

**ELECTRIC POWER PLANTS**
Cu-2 mechanical properties and microstructural stability of advanced steam cycle materials
[DE88-001519] N88-13452

**ELECTRICAL FAULTS**
Low-current behavior and current chopping of vacuum arcs
[ISBN-90-9001649-X] N88-13529

**ELECTRICAL GROUNDING**
Human engineering laboratory grounding analysis (HELGA)-2
[AD-A185367] N88-13524

**ELECTRICAL IMPEDANCE**
Time domain electromagnetic waves in multilayered media
[AD-A185055] N88-13502
Analytical solution of the equations for a coaxial plasma gun operating in the snowplow mode. 1. Weak coupling limit
[AD-A185370] N88-13994

**ELECTRICAL MEASUREMENT**
Electromagnetic tests
[SNIAS-872-430-103] N88-13508
An electric field meter based upon a new principle: A dummy displacement electrode. Application to aerospace vehicles
[SNIAS-872-422-106] N88-13567
Electric field measurements on Viking: First results
[TRITA-EPP-87-04] N88-13826

**ELECTRICAL PROPERTIES**
A study of charged particles/radiation damage to VLSI device materials
[NASA-CR-172036] N88-13518

**ELECTRICAL RESISTIVITY**
Improved high modulus fibers
[NASA-CR-181539] N88-13389
Human engineering laboratory grounding analysis (HELGA)-2
[AD-A185367] N88-13524

**ELECTRO-OPTICS**
Optoelectronic measurement methods for ballistic experiments
[PB87-110706] N88-13554

**ELECTRODEPOSITION**
Effectiveness of electrodeposited coatings in reducing atmospheric corrosion of copper substrates
[DE87-013651] N88-13448

**ELECTRODES**
An electric field meter based upon a new principle: A dummy displacement electrode. Application to aerospace vehicles
[SNIAS-872-422-106] N88-13567

**ELECTRODYNAMICS**
Theoretical analysis of the electrical aspects of the basic electro-impulse problem in aircraft de-icing applications
[NASA-CR-180845] N88-13310
Colloidal stability of oxidized silicon particles in ethanolic and aqueous media
[DE87-014783] N88-13421

**ELECTROLYSIS**
Phase purity of NiCo2O4, a catalyst candidate for electrolysis of water
[NASA-TM-100239] N88-13385

**ELECTROLYTES**
Colloidal stability of oxidized silicon particles in ethanolic and aqueous media
[DE87-014783] N88-13421
Analysis of nickel sulphamate bath using charging current compensated D.C. polarography
[NAL-TM-MT-8705] N88-13433
Ionic transport and electrical relaxation in glass
[DE88-000887] N88-14028

**ELECTROLYTIC CELLS**
Survey state of the art: Electrical load management techniques and equipment
[AD-A184083] N88-13517

**ELECTROMAGNETIC ABSORPTION**
Pure dephasing of a vibrational adbond
[AD-A185222] N88-13740

**ELECTROMAGNETIC COMPATIBILITY**
Measurements in an electromagnetic test laboratory
[SNIAS-872-430-102] N88-13507

**ELECTROMAGNETIC INTERFERENCE**
Two-signal cross modulation effects, half-IF effects and interference criteria in land mobile sharing with UHF (Ultra High Frequency) television
[PB87-228037] N88-13514

**ELECTROMAGNETIC MEASUREMENT**
Measurements in an electromagnetic test laboratory
[SNIAS-872-430-102] N88-13507
Electromagnetic tests
[SNIAS-872-430-103] N88-13508

Numerical and analytical study of the equivalent permittivity or permeability of nonhomogeneous materials. Application to the experimental electromagnetic characterization of composites
[SNIAS-872-430-104] N88-13509

**ELECTROMAGNETIC PULSES**
Theoretical analysis of the electrical aspects of the basic electro-impulse problem in aircraft de-icing applications
[NASA-CR-180645] N88-13310
Solitons in stimulated Raman scattering: Generation and control of ultrashort optical pulses
[AD-A185141] N88-13983

**ELECTROMAGNETIC RADIATION**
Scaling the electromagnetically driven explosive shock simulator N88-13612
Cerenkov radiation field analysis due to a passing electron beam
[AD-A184870] N88-13976

**ELECTROMAGNETIC SCATTERING**
Efficient computation of periodic Green's functions with application to grating structures
[AD-A184853] N88-13912

**ELECTROMAGNETIC SPECTRA**
Extreme ultraviolet beam-foil spectroscopy of highly ionized neon and argon
[AD-A185197] N88-13418

**ELECTROMAGNETIC WAVE TRANSMISSION**
A computer code to calculate line by line atmospheric transmission spectra on a microcomputer
[NASA-TM-100686] N88-13372
An investigation of millimeter wave propagation in the atmosphere: Measurement program
[AD-A184837] N88-13498
Time domain electromagnetic waves in multilayered media
[AD-A185055] N88-13502

**ELECTROMAGNETISM**
Eigenvalue projection theory for linear operator equations of electromagnetics
[AD-A185434] N88-13504

**ELECTROMAGNETS**
A long electromagnetic wiggler for the paladin free-electron laser experiments
[DE88-000970] N88-13589
Development of a strong electromagnet wiggler
[DE88-000971] N88-13952
Development of a laced electromagnetic wiggler
[DE88-000972] N88-13953

**ELECTROMECHANICS**
On the glitches in the force transmitted by an electrodynamic exciter to a structure N88-13624

**ELECTRON BEAMS**
Narrow linewidth gain measurements in a KrF excimer amplifier pumped longitudinally by a high-power electron beam
[DE88-001365] N88-13575
Theoretical and experimental investigation of electron beam acceleration and sub-millimeter wave generation in cyclotron resonant cavities
[AD-A184806] N88-13975
Cerenkov radiation field analysis due to a passing electron beam
[AD-A184870] N88-13976

**ELECTRON STATES**
Effect of rapid solidification on short-range order: A magnetic study
[AD-A185216] N88-13444

**ELECTRON TRANSFER**
The role of electronic structure calculation in mechanistic analysis of electron transfer reactions in the liquid phase
[DE87-014395] N88-13963

**ELECTRONIC EQUIPMENT**
Corrosion of electronic components N88-13333
Development of an interface for an ultrareliable fault-tolerant control system and an electronic servo-control unit
[NASA-TM-88236] N88-13367
Electromagnetics and electrothermal approach to evaluate failures in microelectronic devices caused by electrostatic discharges: Stochastical aspects of the device reliability
[AD-A184906] N88-13522
Fabricate, calibrate and test a dosimeter for integration into the CRRES (Combined Release and Radiation Effects Satellite) satellite
[AD-A185439] N88-13564

**ELECTRONIC MODULES**
New approach to telemetry development will significantly increase productivity of Joint Test Assembly (JTA) teams
[DE88-001676] N88-13373

**ELECTROSTATIC CHARGE**
Study of electrostatic modulation of fuel sprays to enhance combustion performance in an aviation gas turbine
[AD-A184967] N88-13341

Electromagnetics and electrothermal approach to evaluate failures in microelectronic devices caused by electrostatic discharges: Stochastical aspects of the device reliability
[AD-A184906] N88-13522

**ELECTROSTATICS**
Analysis of geophysical data bases and models for spacecraft interactions
[AD-A184809] N88-13375

**ELEMENTARY PARTICLE INTERACTIONS**
Experimental studies of elementary particle interactions at high energies
[DE88-000804] N88-13971

**ELEVATORS (LIFTS)**
A device and methodology for measuring repetitive lifting VO2max (oxygen consumption rate)
[AD-A185195] N88-13850

**ELLIPTIC DIFFERENTIAL EQUATIONS**
Research and development of finite elements and iterative algorithms for elliptic partial differential equations
[DE88-001381] N88-13934

**ELLIPTICAL CYLINDERS**
An experimental investigation of appendage-flat plate junction flow. Volume 2. Elliptical nose appendage data base
[AD-A184974] N88-13539

**ELONGATION**
BASIC desk-top computer program for the three-dimensional static configuration of an extensible flexible cable in a uniform stream
[AD-A184852] N88-13737

**EMBRITTLEMENT**
Tensile properties of extrusion consolidated Type 304 SS rapidly solidified powders
[DE87-014875] N88-13450

**EMISSION SPECTRA**
Atomic beam studies of the interaction of hydrogen with transition metal surfaces
[DE88-000208] N88-13970
Satellite observations of extreme ultraviolet radiation
[AD-A185043] N88-14059

**EMULSIONS**
Reactions of porphyrins in surfactant assemblies, microemulsions and in solutions
[AD-A184797] N88-13412

**ENCAPSULATING**
Development of microencapsulation techniques
[AD-A185019] N88-13457

**ENCLOSURES**
Plant Growth Module (PGM) conceptual design N88-13855

**ENDOTHERMIC REACTIONS**
Investigation by differential scanning calorimetry of microstructure in a superplastic Al-Mg-Zr alloy
[AD-A184902] N88-13439

**ENERGY ABSORPTION**
Toward detecting California shrubland canopy chemistry with AIS data N88-13764

**ENERGY CONSERVATION**
Oxygen enriched combustion system performance study
[DE88-001500] N88-13424

**ENERGY CONVERSION EFFICIENCY**
An overview of the DOE/SANDIA/USDA vertical axis wind turbine Test Bed Project
[DE88-000604] N88-13812
The high performance solar array GSR3
[SNIAS-872-422-108] N88-13814

**ENERGY DISTRIBUTION**
Lagrangian procedures for higher order field equations
[DE87-703365] N88-13911

**ENERGY POLICY**
Fuel cells --- military applications
[PML-1986-43] N88-13813

**ENERGY TRANSFER**
Intramolecular energy transfer reactions as a method for metal complex assisted production of hydrogen
[DE88-001621] N88-13425
Energy dependence of ion-induced sputtering yields of monatomic solids in the low energy region
[IPPJ-AM-52] N88-13988

**ENGINE DESIGN**
Automated design of controlled diffusion blades
[NASA-TM-100251] N88-13304
Development of an integrated BEM approach for hot fluid structure interaction
[NASA-CR-181577] N88-13384

**ENGINE FAILURE**
Incipient failure detection of space shuttle main engine turbopump bearings using vibration envelope detection N88-13629

**ENGINE PARTS**
Application of finite element methods with cyclic elasto-plastic strain analysis to low cycle fatigue analysis of engine components
[AR-004-512] N88-13642

**ENGINE TESTS**
Incipient failure detection of space shuttle main engine turbopump bearings using vibration envelope detection N88-13629
High frequency data acquisition system for space shuttle main engine testing N88-13630

**ENGINES**
Analysis of wear metals in engine oils using the atomic absorption spectrophotometric method
[NAL-TM-MT-8704] N88-13435

**ENVIRONMENTS**
Avionics and corrosion N88-13336

**EPITAXY**
Novel heterojunction devices
[DE87-013716] N88-14026

**EPOXY MATRIX COMPOSITES**
In-situ characterization of the interface of glass reinforced composites
[AD-A185136] N88-13391
Utilization of microwave measuring systems for nondestructive control of composite materials
[SNIAS-872-430-109] N88-13402

**EQUATIONS OF MOTION**
Non-linear maximum likelihood estimation of stability derivatives from range data
[NAL-TM-SE-8606] N88-13385
Dynamics of propellant feedline systems
[AD-A184865] N88-13537
Tutorial on elementary bifurcation theory
[DE87-014849] N88-13932
Analytical solution of the equations for a coaxial plasma gun operating in the snowplow mode. 1. Weak coupling limit
[AD-A185370] N88-13994

**EQUIPMENT SPECIFICATIONS**
Photon counting image sensor development for astronomical applications
[NASA-CR-181507] N88-14049

**EROSION**
Studies in Aeolian geology
[NASA-CR-182328] N88-13828

**ERROR ANALYSIS**
Correction of inertial navigation system drift errors for an autonomous land vehicle using optical radar terrain data
[AD-A184973] N88-13311
Error control techniques for satellite and space communications
[NASA-CR-181581] N88-13516
Assessment of the reliability of a correction procedure for WGT (Wet Globe Thermometer) (Botsball) measurements of heat stress
[AD-A185193] N88-13559
Operating envelopes of particle sizing instrumentation used for icing research
[NASA-CR-180870] N88-13573
Experiments in fault tolerant software reliability
[NASA-CR-181554] N88-13863
Reliability of voting in fault-tolerant software systems for small output spaces
[TR-87-16] N88-13864
Effectiveness of back-to-back testing
[TR-87-08] N88-13865
Diagnostic reasoning in digital systems
[NASA-CR-181564] N88-13871
Error propagation in a digital avionic mini processor
[NASA-CR-181565] N88-13872

**ERRORS**
Determination of total ozone from HIRS2/MSU sounding data N88-13799

**ESTIMATES**
Model-based motion estimation and its application to restoration and interpolation of motion pictures
[AD-A185054] N88-13558
Estimation of marine boundary layer depth and relative humidity with multispectral satellite measurements
[AD-A184881] N88-13804
An adaptive lattice algorithm for spectral line estimation
[AD-A184970] N88-13876
Further studies in estimation of life distribution characteristics from censored data
[AD-A184862] N88-13937
Freidlin-Wentzell type estimates and the law of the iterated logarithm for a class of stochastic processes related to symmetric statistics
[AD-A185366] N88-13944

**ESTIMATING**
The maximum likelihood estimator method of image reconstruction: its fundamental characteristics and their origin
[DE88-000462] N88-13892
**EULER EQUATIONS OF MOTION**
Numerical analysis of flow through scramjet engine inlets N88-13233
A 3-D Euler solution for hypersonic Mach numbers N88-13240
The off-design performance of hypersonic waveriders N88-13244
Time-marching finite-difference methods for the three-dimensional Euler equations of contravariant velocity components N88-13285
A Cartesian finite-volume method for the Euler equations N88-13532
Solution procedure for the Navier-Stokes equations applied to rotors N88-13533
A note on the use of symmetric line Gauss-Seidel for the steady upwind differenced Euler equations
[AD-A185223] N88-13540
SHARP simulation of discontinuities in highly convective steady flow
[NASA-TM-100240] N88-13931
**EULER-LAGRANGE EQUATION**
Free Lagrange reconnection algorithms for hydrocodes using a quadrilateral mesh
[DE88-001580] N88-13752
**EUROPEAN AIRBUS**
Aeroelastic analysis of modern transport aircraft — European Airbus
[SNIAS-872-111-102] N88-13329
**EUROPEAN SPACE PROGRAMS**
Mechanical design of the ac bracket package for the RETE experiment
[IFSI-87-4] N88-13379
Budget and programs for 1986 research
[IFSI-86-16] N88-14048
**EVALUATION**
Evaluation of device figure of merit in microwave switching circuit design
[AD-A184896] N88-13520
Test and evaluation of the transputer in a multi-transputer system
[AD-A184969] N88-13859
**EVASIVE ACTIONS**
The isotropic rocket: A surveillance evasion game
[REPT-87-21] N88-13949
**EVOLUTION (DEVELOPMENT)**
The evolution of local mechanical properties of Al 2219-T851 during fatigue N88-13653
**EXCHANGING**
Lower-stratospheric/upper-tropospheric exchange processes associated with tropical cyclones as observed by TOMS N88-13762
**EXCIMER LASERS**
Narrow linewidth gain measurements in a KrF excimer amplifier pumped longitudinally by a high-power electron beam
[DE88-001365] N88-13575
Photocurrent generation from basic metals, utilizing a short pulsed ArF excimer laser
[AD-A184928] N88-13579
Anti-Stokes generation of 226 nm light
[DE88-001612] N88-13590
Chemical analysis for excimer laser systems
[DE88-001941] N88-13591
**EXCITATION**
On the glitches in the force transmitted by an electrodynamic exciter to a structure N88-13624
**EXHAUST FLOW SIMULATION**
Investigation of the effect of laterally ejected gas jets on flows
[ISL-R-107/86] N88-13545
**EXPANSION**
Qualification of expansion and joint welding procedures of tube-to-tubesheet joints for heat exchangers in nuclear power plants
[DE87-703526] N88-13592
**EXPECTATION**
Expectations for water level deviations at the delta works: Zierikzee (Netherlands), November 1981-February 1986
[KNMI-TR-93] N88-13640
**EXPEDITIONS**
Varifront 3 expedition data report (USNS DE STEIGUER CRUISE 1202-82). Bioluminescence, hydrographic, nutrient, and satellite data from the Gulf of California (November-December 1981)
[AD-A185011] N88-13805
**EXPERIMENT DESIGN**
Controlled Ecological Life Support System. Design, Development, and Use of a Ground-Based Plant Growth Module
[NASA-CP-2479] N88-13852
CELSS Program Meeting N88-13853
Controlled ecological life support systems: Development of a plant growth module N88-13854
**EXPERIMENTATION**
A plethysmograph for measuring pulmonary ventilation in small animals
[AD-A184978] N88-13846
**EXPERT SYSTEMS**
ZEUS: A knowledge-based expert system that assists in predicting visibility at airbases
[AD-A184197] N88-13829
A single-station weather forecasting expert system
[AD-A184889] N88-13832
XCUT: A rule-based expert system for the automated process planning of machined parts
[DE87-011638] N88-13905
Using hierarchically structured problem-solving knowledge in a rule-based process planning system
[DE87-011639] N88-13906
**EXPLOSION SUPPRESSION**
Correlation of air pressure drop and flame arrestor characteristics for explosion suppression materials
[AD-A184960] N88-13340
**EXPLOSIONS**
Scaling the electromagnetically driven explosive shock simulator N88-13612
On the simulation of ballistic shock loads N88-13615
**EXPLOSIVE DEVICES**
Influence of shock wave and gas pressure on the behavior of a pyrotechnical device
[SNIAS-872-430-111] N88-13477
**EXPLOSIVES**
High explosive moulding powders from RDX and aqueous polyurethane dispersions
[AD-A185026] N88-13458
**EXPONENTIAL FUNCTIONS**
The matrix exponential in transient structural analysis N88-13619
**EXPOSURE**
Investigation of the exposure to harmful compounds in the workshop of nondestructive materials testing at Gilze-Rijen (Netherlands)
[PML-1985-42] N88-13616
**EXTERNAL STORE SEPARATION**
Airframe/store compatibility N88-13323
**EXTRATERRESTRIAL RADIATION**
Fabricate, calibrate and test a dosimeter for integration into the CRRES (Combined Release and Radiation Effects Satellite) satellite
[AD-A185439] N88-13564
**EXTREME ULTRAVIOLET RADIATION**
Extreme ultraviolet beam-foil spectroscopy of highly ionized neon and argon
[AD-A185197] N88-13418
Satellite observations of extreme ultraviolet radiation
[AD-A185043] N88-14059
**EXTREMELY HIGH FREQUENCIES**
High peak power ka-band gyrotron oscillator experiment
[AD-A185424] N88-13563
**EXTRUDING**
Tensile properties of extrusion consolidated Type 304 SS rapidly solidified powders
[DE87-014875] N88-13450
Development on thin wall tubes of dispersion type
[DE87-703384] N88-13483
Cyclic deformation of an extruded AlMgSi alloy N88-13654

## F

**F REGION**
The polar ionosphere and interplanetary field
[AD-A185386] N88-13822
**F-18 AIRCRAFT**
A study of the Department of Defense configuration management policies and procedures as applied to the FA-18 Strike/Fighter program
[AD-A184872] N88-14034
**F-111 AIRCRAFT**
Predictions of F-111 TACT aircraft buffet response and correlations of fluctuating pressures measured on aluminum and steel models and the aircraft
[NASA-CR-4069] N88-13218
**FABRICATION**
Fabrication of composites by chemical vapor deposition
[DE87-014565] N88-13408
The production of ultrasmall and superfine holographic diffraction gratings using synchrotron radiation and lithographic techniques
[AD-A185395] N88-13562
Fabricate, calibrate and test a dosimeter for integration into the CRRES (Combined Release and Radiation Effects Satellite) satellite
[AD-A185439] N88-13564
Computer modeling of complete IC fabrication process
[AD-A184807] N88-14012
**FABRICS**
A hybrid fibreglass-CFRP cloth for new furnishings — aircraft cabins
[SNIAS-872-111-109] N88-13396
**FACTOR ANALYSIS**
Application of Vandermonde decomposition to directional and modal analysis of broadband transients
[AD-A185007] N88-13956
**FAILURE**
An examination of coating failure on wing pivot fittings of f111 aircraft
[AD-A185028] N88-13328
Electromagnetics and electrothermal approach to evaluate failures in microelectronic devices caused by electrostatic discharges: Stochastical aspects of the device reliability
[AD-A184906] N88-13522
Computer aided modeling and fatigue failure forecast under stochastic loading N88-13720
Deformation mechanisms and crack initiation in fatigue N88-13730
**FAILURE ANALYSIS**
Corrosion of electronic components N88-13333
Applications of fatigue analyses: Transportation N88-13733
**FATIGUE (MATERIALS)**
Micromechanisms of fatigue crack growth and fracture toughness in metal matrix composites
[AD-A185200] N88-13392
X-ray analysis of polycrystalline aluminium subjected to fatigue cycling
[NAL-TM-MT-8706] N88-13434
Fatigue 87, volume 3
[AD-A184047] N88-13700
Fracture kinetics of corrosion fatigue N88-13706
Fatigue crack growth: Statistical considerations N88-13718
Telemetric laser extensometry technique for monitoring deflections in small cracks N88-13724
An optical interferometry technique to evaluate closure along a crack front N88-13726
On the geometrical description of fatigue crack surfaces N88-13727
An overview of fatigue N88-13729
Deformation mechanisms and crack initiation in fatigue N88-13730
Experimental studies on acoustic emission monitoring of crack propagation in offshore structures: A literature survey N88-13748
**FATIGUE LIFE**
Damage considerations in sizing aircraft cells. Life predictions
[SNIAS-872-111-116] N88-13330
Welded joint fatigue of a AISI 304 L type stainless steel
[DE87-703530] N88-13607
A study of fatigue crack growth life under random stresses N88-13685
The how and why of variable amplitude testing N88-13690
Tensile mean stress effects on uniaxial fatigue behavior of 1045 HR steel N88-13694
Fretting wear and fretting fatigue damage N88-13697
A study of corrosion fatigue crack initiation, growth and the threshold condition under variable amplitude loading N88-13701
Low cycle fatigue behaviour of notched specimens of nickel based superalloy single crystal N88-13712
Fatigue characteristics of ion treated surfaces N88-13713
The effect of heat treatment on fatigue crack growth in polycarbonate N88-13714
Effect of test temperature and frequency on fatigue crack propagation in PVC N88-13715
Environmental fracture toughness and static fatigue crack propagation of silica glass N88-13716
Effect of interface on mechanical properties of graphite/201 aluminum composites N88-13717
Constraint effects in fatigue crack growth N88-13719
Computer aided modeling and fatigue failure forecast under stochastic loading N88-13720
A comparison of plastic work energy and external input for fatigue crack propagation N88-13722
Fatigue under nonnormal random stresses using Monte Carlo method N88-13723
X-ray fatigue failure prediction based on plasticity response to microcracks N88-13725
Development of research on fatigue of spot-weld in automobile structures in Japan N88-13728

Accurate rotor loads prediction using the FLAP (Force and Loads Analysis Program) dynamics code
[DE88-001109] N88-13815

**FATIGUE TESTS**
Application of finite element methods with cyclic elasto-plastic strain analysis to low cycle fatigue analysis of engine components
[AR-004-512] N88-13642
Fatigue 87, volume 1
[AD-A184045] N88-13645
The mechanics of fatigue-crack nucleation in a low-alloy steel under fretting conditions N88-13649
Fatigue crack growth behavior of A356-T6 cast aluminum alloy N88-13660
Variable amplitude fatigue crack growth in aluminum alloys 2090-T8E41 and 7075-T651 N88-13687
Fatigue of 30CrMnSiNi2A notched specimens under spectrum loading N88-13689
The how and why of variable amplitude testing N88-13690
Fatigue strength of alloy A286 at cryogenic temperature N88-13695
The role of inclusions in corrosion fatigue crack initiation in Q1N N88-13699
Crack initiation studies in hydrogen embrittled spring steel strip N88-13710
Applications of fatigue analyses: Transportation N88-13733
Fatigue crack growth N88-13734

**FAULT TOLERANCE**
Development of an interface for an ultrareliable fault-tolerant control system and an electronic servo-control unit
[NASA-TM-88236] N88-13367
Study of fault tolerant techniques for satellite data handling
[FTT/REP/0001/SAAB] N88-13860
Experiments in fault tolerant software reliability
[NASA-CR-181554] N88-13863
Reliability of voting in fault-tolerant software systems for small output spaces
[TR-87-16] N88-13864
Effectiveness of back-to-back testing
[TR-87-06] N88-13865
RSDIMU acceptance testing system: Overview of acceptance software and procedures N88-13866

**FAULT TREES**
Diagnostic reasoning in digital systems
[NASA-CR-181564] N88-13871
Conceptual issues in measuring the behavior of a distributed real-time process-control computer system
[DE87-009748] N88-13898

**FEASIBILITY ANALYSIS**
Study of the feasibility of a satellite communication system for road transportation home office to vehicle communication. Volume 1: Conceptual analysis
[SC/87-E/6-VOL-1] N88-13505
Study of the feasibility of a satellite communication system for road transportation home office to vehicle communication. Volume 2: Market study
[SC/87-E/6-VOL-2] N88-13506
The gamma-ray laser project
[AD-A184824] N88-13578
Stress intensity factors for cracking metal structures under rapid thermal loading, phase 1
[AD-A184112] N88-13606
Feasibility study for gas-grain simulation facility
[NASA-CR-177468] N88-13954

**FEDERAL BUDGETS**
The 1988 NASA (National Aeronautics and Space Administration) authorization
[GPO-80-245] N88-14044

**FEED SYSTEMS**
Dynamics of propellant feedline systems
[AD-A184865] N88-13537

**FEEDBACK CONTROL**
Design of low order controllers for robust disturbance rejection in large space structures
[AD-A185202] N88-13376
Simultaneous structural and control optimization via linear quadratic regulator eigenstructure assignment N88-13622
On linear periodic controllers
[DE87-011174] N88-13904

**FEEDFORWARD CONTROL**
Investigation, development, and application of optimal output feedback theory. Volume 3: The relationship between dynamic compensators and observers and Kalman filters
[NASA-CR-4107] N88-13900

**FERRITES**
The initiation and growth of fatigue cracks in carburised 9Cr1Mo steel N88-13896

**FIBER COMPOSITES**
Fiber composite structural durability and damage tolerance: Simplified predictive methods
[NASA-TM-100179] N88-13409
Study of ceramic-fiber/ceramic sol-gel based matrix composites
[SNIAS-872-430-120] N88-13469

**FIBER OPTICS**
In-situ characterization of the interface of glass reinforced composites
[AD-A185136] N88-13391
Fiber-optic accelerometer investigation
[AD-A185359] N88-13561
Streak camera dynamic range optimization
[DE88-001632] N88-13571
Optical probe
[EP-PATENT-0-210-869-A1] N88-13984

**FIBER ORIENTATION**
Determination of the fiber ratio in carbon fiber/resin composites by means of image analysis
[SNIAS-872-422-101] N88-13398

**FIBER REINFORCED COMPOSITES**
In-situ characterization of the interface of glass reinforced composites
[AD-A185136] N88-13391
Design and test of high performance composite tubes for use in deep water drilling and production systems
[SNIAS-872-430-107] N88-13487
Fatigue mechanisms in ARALL, a fatigue resistant hybrid aluminum aramid composite material N88-13711

**FIELD EFFECT TRANSISTORS**
A study of charged particles/radiation damage to VLSI device materials
[NASA-CR-172036] N88-13518
A GaAs MESFET balanced mixer with very low intermodulation
[AD-A184848] N88-14015

**FIELD THEORY (PHYSICS)**
Non-minimal interaction of gravity with other physical fields: An overview
[DE87-703362] N88-13819
Lagrangian procedures for higher order field equations
[DE87-703365] N88-13911
Introduction to string field theory
[DE87-014583] N88-14032

**FIGHTER AIRCRAFT**
Special Course on Fundamentals of Fighter Aircraft Design
[AGARD-R-740] N88-13315
Fundamentals of fighter aircraft design N88-13316
Mission requirements and aircraft sizing N88-13317
Design of wings and wing/body configurations for transonic and supersonic speeds N88-13318
Aircraft dynamics: Aerodynamic aspects and wind tunnel techniques N88-13320
Techniques for performance optimisation in cruise and manoeuverability N88-13321
Fundamentals of fighter aircraft design: Engine intake and afterbody N88-13322
Airframe/store compatibility N88-13323
Aeroelasticity and optimization in fighter aircraft design N88-13324
Materials for fighter aircraft N88-13325
Requirements and recommendations for the development of theoretical codes and experimental facilities in the near future N88-13327
Examples of static aeroelastic effects on present combat aircraft projects N88-13349
Trends in aeroelastic analysis of combat aircraft N88-13350
A study of the Department of Defense configuration management policies and procedures as applied to the FA-18 Strike/Fighter program
[AD-A184872] N88-14034

**FIGURE OF MERIT**
Evaluation of device figure of merit in microwave switching circuit design
[AD-A184896] N88-13520

**FILAMENT WINDING**
Core material — honeycombs
[EP-PATENT-0-196-926-A2] N88-13393
The structures of large wound propulsion shells --- carbon fiber composites filament winding
[SNIAS-872-430-118] N88-13406

**FILE MAINTENANCE (COMPUTERS)**
File usage analysis and resource usage prediction: A measurement-based study
[NASA-CR-181553] N88-13867
Usage analysis of user files in UNIX
[NASA-CR-181561] N88-13868
Relational data handling system for scientists
[PB87-223426] N88-14038

**FINITE DIFFERENCE THEORY**
Time-marching finite-difference methods for the three-dimensional Euler equations of contravariant velocity components N88-13285

**FINITE ELEMENT METHOD**
Trends in aeroelastic analysis of combat aircraft N88-13350
Finite-element grid improvement by minimization of stiffness matrix trace
[NASA-TM-100255] N88-13604
Finite element model for the stress and flexibility analysis of curved pipes
[DE87-703632] N88-13608
Non-linear shipboard shock analysis of the Tomahawk missile shock isolation system N88-13614
Modal survey of the space shuttle solid rocket motor using multiple input methods N88-13617
Initial dynamic load estimates during configuration design N88-13621
Exact finite element method analysis of viscoelastic tapered structures to transient loads N88-13632
An efficient frequency response solution for nonproportionally damped systems N88-13634
Shape optimization of damping layers N88-13635
Dynamic response of laminated composite plates using a three-dimensional hybrid-stress finite-element formulation N88-13639
Significance of foundation-soil separation in dynamic soil-structure interaction N88-13641
Application of finite element methods with cyclic elasto-plastic strain analysis to low cycle fatigue analysis of engine components
[AR-004-512] N88-13642
Strain-energy-release rate analysis of the end-notched flexure specimen using the finite-element method
[NASA-TM-100494] N88-13735
An element of a multilayer shell for the computation of composite structures
[ONERA-RT-14/3542-RY-051-R] N88-13742
Thermal finite-element analysis of space shuttle main engine turbine blade
[NASA-TM-100117] N88-13745
Two low-order mixed methods for the elasticity problem
[PB87-225272] N88-13749
Structuring data for concurrent vectorized processing in a transient dynamics finite element program
[DE87-013082] N88-13890
Research and development of finite elements and iterative algorithms for elliptic partial differential equations
[DE88-001361] N88-13934

**FINITE VOLUME METHOD**
Solution of some 3-D viscous and inviscid supersonic flow problems by finite-volume space-marching schemes N88-13235
The role of computation fluid dynamics in aeronautical engineering (4). The development and applications of implicit TVD finite volume code N88-13259
Compressible Euler solution on a multiblock grid around a wing-fuselage configuration
[FFA-TN-1987-46] N88-13303
A Cartesian finite-volume method for the Euler equations N88-13532

**FINS**
The effects of sweep and bluntness on a glancing shock wave turbulent boundary layer interaction N88-13227
The use of aeroelastic wind tunnel models to prove structural design N88-13355

**FIR FILTERS**
Implementation of an FIR band pass filter using a bit-slice processor
[AD-A184895] N88-13875

**FIRE PREVENTION**
Comparison of fire resistance of metallic and nonmetallic structures
[SNIAS-872-551-101] N88-13489

**FIREPROOFING**
Comparison of fire resistance of metallic and nonmetallic structures
[SNIAS-872-551-101] N88-13489

**FISHES**
Irradiation preservation of seafood: Literature review
[DE88-001691] N88-13858

**FITTINGS**
An examination of coating failure on wing pivot fittings of f111 aircraft
[AD-A185028] N88-13328

**FLAME HOLDERS**
Ignition and flameholding in supersonic flow by injection of dissociated hydrogen N88-13410

**FLAME RETARDANTS**
Flame retardant phenolic foams
[EP-PATENT-0-223-489-A2] N88-13464

**FLAME STABILITY**
Combustion related shear-flow dynamics in elliptic supersonic jets N88-13232

**FLAMES**
Correlation of air pressure drop and flame arrestor characteristics for explosion suppression materials
[AD-A184960] N88-13340
Formation and destruction of nitrous oxide in lean, premixed combustion
[DE88-001390] N88-13423
**FLAMMABILITY**
An experimental investigation of the ignition and flammability limits of various hydrocarbon fuels in a two-dimensional solid fuel ramjet
[AD-A184968] N88-13342
**FLAPS (CONTROL SURFACES)**
Design and control of repairs of carbon fiber lift augmentation flaps in the ATR42 aircraft
[SNIAS-872-111-112] N88-13217
Validation elements of the computation methods and measurement techniques for high lift aerodynamic systems
[SNIAS-872-111-101] N88-13299
An experimental investigation of the aerodynamics of a NACA 64A010 airfoil-flap combination with and without flap oscillations. Part 1: Steady-state characteristics
[NASA-TM-88217] N88-13305
**FLAT PLATES**
A Cartesian finite-volume method for the Euler equations N88-13532
An experimental investigation of appendage-flat plate junction flow. Volume 2. Elliptical nose appendage data base
[AD-A184974] N88-13539
Experimental studies on the tripping behavior of narrow T-stiffened flat plates subjected to hydrostatic pressure and underwater shock N88-13613
Analysis of photopole data reduction models N88-13616
Dynamic response of laminated composite plates using a three-dimensional hybrid-stress finite-element formulation N88-13639
**FLEXIBILITY**
A swept wing panel in a low speed flexible walled test section
[NASA-CR-4106] N88-13292
Flexibilized copolyimide adhesives
[NASA-TM-89303] N88-13474
Control of a flexible one-link manipulator
[AD-A185035] N88-13598
Finite element model for the stress and flexibility analysis of curved pipes
[DE87-703632] N88-13608
**FLEXIBLE SPACECRAFT**
Simultaneous structural and control optimization via linear quadratic regulator eigenstructure assignment N88-13622
**FLEXING**
Strain-energy-release rate analysis of the end-notched flexure specimen using the finite-element method
[NASA-TM-100494] N88-13735
**FLIGHT CHARACTERISTICS**
Model helicopter rotor rig and associated strain gauge balance for performance studies
[NAL-TM-AE-8704] N88-13364
**FLIGHT CONTROL**
Nonlinear lift control at high speed and high angle of attack using vortex flow technology N88-13319
Integrated control and display research for transition and vertical flight on the NASA V/STOL Research Aircraft (VSRA)
[NASA-TM-100029] N88-13359
Electrical flight commands in transport aircraft
[SNIAS-872-111-108] N88-13361
Reduced order optimal command applied to longitudinal automatic pilots
[SNIAS-872-111-114] N88-13362
Control of an unstable launcher in atmospheric flight using minimax optimal control laws
[SNIAS-872-422-107] N88-13901
**FLIGHT ENVELOPES**
Full-envelope aerodynamic modeling of the Harrier aircraft
[NASA-TM-88376] N88-13363
**FLIGHT MECHANICS**
Aerodynamics of Hypersonic Lifting Vehicles
[AGARD-CP-428] N88-13219
Calendar of selected aeronautical and space meetings
[AGARD-CAL-87/1] N88-14033
**FLIGHT SAFETY**
Airline safety: A comparative analysis
[AD-A185358] N88-13308
**FLIGHT SIMULATION**
Shock tunnels for real gas hypersonics N88-13223
Overlooked potential of systems with Markovian coefficients
[NLR-MP-86049-U] N88-13366
Noise of a model counterrotation propeller with reduced aft rotor diameter at simulated takeoff/approach conditions (F7/A3)
[NASA-TM-100254] N88-13961
**FLIGHT TESTS**
Full-envelope aerodynamic modeling of the Harrier aircraft
[NASA-TM-88376] N88-13363
**FLOW DISTRIBUTION**
Experimental investigations on blunt bodies and corner configurations in hypersonic flow N88-13225
Driving mechanism of unsteady separation shock motion in hypersonic interactive flow N88-13226
Numerical simulation of the hypersonic flow around lifting vehicles N88-13234
Solution of some 3-D viscous and inviscid supersonic flow problems by finite-volume space-marching schemes N88-13235
Numerical experiments with hypersonic flows beneath a cone-delta-wing combination N88-13238
A 3-D Euler solution for hypersonic Mach numbers N88-13240
Computation of flow past conical hypersonic wings using a second order Godunov method N88-13241
Aerothermodynamics research at NASA Ames N88-13242
Vortex formation over delta, double-delta and wave rider configurations at supersonic speeds N88-13243
Numerical optimization of conical flow waveriders including detailed viscous effects N88-13245
An analysis of the compressible-viscous flow field around a 3D-oscillating wing N88-13254
Computation of dynamic stall of NACA0012 airfoil by block pentadiagonal matrix scheme N88-13255
Numerical calculations of the flowfield around propellers N88-13261
Navier-Stokes simulation of transonic transportation aircraft configurations. 1: Flow-field simulation over wing-fuselage combinations N88-13288
Computation of transonic flows with nacelle simulation
[SNIAS-872-111-117] N88-13300
Compressible Euler solution on a multiblock grid around a wing-fuselage configuration
[FFA-TN-1987-46] N88-13303
Vortex interaction with a leading-edge of finite thickness
[NASA-CR-182341] N88-13307
Unsteady aerodynamics of an oscillating cascade in a compressible flow field
[NASA-TM-100219] N88-13346
A numerical study of the effects of curvature and convergence on dilution jet mixing
[NASA-TM-89878] N88-13347
The simulation of the viscous flow around a cylinder by the random vortex method N88-13534
An experimental investigation of appendage-flat plate junction flow. Volume 2. Elliptical nose appendage data base
[AD-A184974] N88-13539
Conditional second order closure for turbulent shear flows
[AD-A185369] N88-13542
Low thrust viscous nozzle flow fields prediction
[NASA-CR-182334] N88-13551
**FLOW EQUATIONS**
Computation of transonic flows with nacelle simulation
[SNIAS-872-111-117] N88-13300
**FLOW MEASUREMENT**
Interferometric data for a shock-wave/boundary-layer interaction
[NASA-TM-88227] N88-13306
Determination of a flow velocity field using four-exposure laser holography
[IMFL-3114-85/32] N88-13565
**FLOW VISUALIZATION**
Experimental investigations on blunt bodies and corner configurations in hypersonic flow N88-13225
An ultra-high-speed cinematographic method for the study of wakes in hypersonic ballistic ranges N88-13228
Flow visualization in computational fluid dynamics N88-13277
Visualization of an aircraft accident based on digital flight data recorder information N88-13278
Transient development of stratification in a partially divided enclosure
[DE87-011742] N88-13490
Vortical Flows Research Program of the Fluid Dynamics Research Branch
[NASA-TM-88332] N88-13549
**FLUID DYNAMICS**
European hypersonic wind tunnels N88-13221
Combustion related shear-flow dynamics in elliptic supersonic jets N88-13232
Application of modified loss and deviation correlations to transonic axial compressors
[AGARD-R-745] N88-13344
Static aeroelastic effects on the flutter of a supercritical wing N88-13353
Displaying three-dimensional data
[AD-A185347] N88-13541
A system of three-dimensional complex variables
[NASA-TM-88318] N88-13951
Calendar of selected aeronautical and space meetings
[AGARD-CAL-87/1] N88-14033
**FLUID FILMS**
Literature review of solid lubrication mechanisms
[AD-A185010] N88-13456
**FLUID FLOW**
A spatial marching technique for the inviscid blunt body problem N88-13239
A perspective of computational fluid dynamics N88-13279
Development of an integrated BEM approach for hot fluid structure interaction
[NASA-CR-181577] N88-13384
Three-dimensional dynamic labyrinth seal analysis
[AD-A185353] N88-13599
Fluid mass and thermal loading effects on the modal characteristics of space shuttle main engine liquid oxygen inlet splitter vanes N88-13628
**FLUID MECHANICS**
A spatial marching technique for the inviscid blunt body problem N88-13239
Experimental study of the fluid mechanics of unsteady turbulent boundary layers
[AD-A184856] N88-13536
Numerical analysis, computing and fundamental studies in fluid mechanics
[DE88-001912] N88-13550
Damping analysis of flexural waves in fluid-loaded single and constrained plates
[AD-A185116] N88-13739
**FLUIDS**
Theory of neutron scattering experiments on momentum distributions in quantum fluids
[DE87-01369] N88-13968
**FLUORESCENCE**
OH(A-X) fluorescence from photodissociative excitation of HO2 at 157.5 nm
[NASA-CR-181580] N88-13429
**FLUORINE COMPOUNDS**
Photocurrent generation from basic metals, utilizing a short pulsed ArF excimer laser
[AD-A184928] N88-13579
**FLUTTER**
Static aeroelastic effects on the flutter of a supercritical wing N88-13353
**FLUTTER ANALYSIS**
Velocity scaled aeroelastic testing of an unducted fan
[GTL-191] N88-13337
Influence of the static deformation on a wing in the unsteady aerodynamic N88-13357
**FLUX VECTOR SPLITTING**
Numerical simulation of the hypersonic flow around lifting vehicles N88-13234
A Cartesian finite-volume method for the Euler equations N88-13532
**FOAMS**
Flame retardant phenolic foams
[EP-PATENT-0-223-489-A2] N88-13464
**FOCUSING**
Resolution limitations and optimization of the LLNL streak camera focus
[DE88-001633] N88-13572
Phenomena at a focus in a laser system
[AD-A185442] N88-13585
Theory of induced spatial incoherence
[AD-A185005] N88-13982
**FOILS (MATERIALS)**
RIIM two-pulse injector experiments
[DE88-000926] N88-14005
**FOOD**
Controlled Ecological Life Support System. Design, Development, and Use of a Ground-Based Plant Growth Module
[NASA-CP-2479] N88-13852
Irradiation preservation of seafood: Literature review
[DE88-001691] N88-13858
**FORCED CONVECTION**
Regressed relations for forced convection heat transfer in a direct injection stratified charge rotary engine
[NASA-TM-100124] N88-13345
**FORESTS**
Proceedings of the Third Airborne Imaging Spectrometer Data Analysis Workshop
[NASA-CR-181552] N88-13755
The use of airborne imaging spectrometer data to determine experimentally induced variation in coniferous canopy chemistry N88-13761

Overview of Austrian Airborne Imaging Spectrometer (AIS) programme and first results N88-13762

**FORMING TECHNIQUES**
Growth of short fatigue cracks in a squeeze formed aluminum alloy N88-13658

**FORTRAN**
Mixing Microsoft C and Microsoft FORTRAN program modules on the IBM Personal Computer [DE88-001947] N88-13895

**FOUNDATIONS**
A passive vibration-cancelling isolation mount N88-13636
Significance of foundation-soil separation in dynamic soil-structure interaction N88-13641

**FOURIER TRANSFORMATION**
Vectorizing the FFTs on supercomputer SX system N88-13270
Arrays for discrete Fourier transform [REPT-87-019] N88-13861

**FRACTURE MECHANICS**
Models for the degradation of stratified composite structures [ONERA-RT-13/3542-RY-061-R] N88-13395
Environmentally assisted cracking: Overview of evidence for an adsorption-induced localised-slip process [AD-A185175] N88-13443
Stress intensity factors for cracking metal structures under rapid thermal loading, phase 1 [AD-A184112] N88-13606
Near-threshold growth of defects in engineering materials N88-13691
Interaction of microstructure and fatigue in tool steels N88-13693
Environmental fracture toughness and static fatigue crack propagation of silica glass N88-13716
Deformation, fatigue and fracture behavior of two cast anisotropic superalloys N88-13732
Strain-energy-release rate analysis of the end-notched flexure specimen using the finite-element method [NASA-TM-100494] N88-13735

**FRACTURE STRENGTH**
Micromechanisms of fatigue crack growth and fracture toughness in metal matrix composites [AD-A185200] N88-13392
Fatigue mechanisms in ARALL, a fatigue resistant hybrid aluminum aramid composite material N88-13711
Environmental fracture toughness and static fatigue crack propagation of silica glass N88-13716
Embrittling effect of the plastic zone N88-13721

**FRACTURING**
The influence of the topography of fracture surfaces on crack closure N88-13657

**FRAGMENTATION**
The mechanics of fatigue-crack nucleation in a low-alloy steel under fretting conditions N88-13649

**FREE ELECTRON LASERS**
A long electromagnetic wiggler for the paladin free-electron laser experiments [DE88-000970] N88-13589
Development of a strong electromagnet wiggler [DE88-000971] N88-13952
Development of a laced electromagnetic wiggler [DE88-000972] N88-13953

**FREE FLIGHT**
Non-linear maximum likelihood estimation of stability derivatives from range data [NAL-TM-SE-8608] N88-13365

**FREE FLOW**
Effects of free stream turbulence, Reynolds number and incidence angle on axial turbine cascade performance N88-13339

**FREE JETS**
Numerical analysis of flow characteristics of supersonic free-jets N88-13274
Investigation of the effect of laterally ejected gas jets on flows [ISL-R-107/86] N88-13545

**FREE MOLECULAR FLOW**
Experiences using the Mark IV supersonic hypersonic arbitrary body program N88-13249

**FREE-PISTON ENGINES**
Shock tunnels for real gas hypersonics N88-13223

**FREQUENCY CONTROL**
Optically tuned MM-wave IMPATT source [AD-A185250] N88-13523

**FREQUENCY RESPONSE**
An efficient frequency response solution for nonproportionally damped systems N88-13634

**FREQUENCY STABILITY**
On-orbit frequency stability analysis of the GPS NAVSTAR 8 rubidium clock and NAVSTARs 9 and 10 cesium clocks [AD-A184984] N88-13312

**FRETTING**
The mechanics of fatigue-crack nucleation in a low-alloy steel under fretting conditions N88-13649
Fretting wear and fretting fatigue damage N88-13697

**FRICTION**
On a numerical method to solve contact problems — forming processes [B8711403] N88-13930

**FROUDE NUMBER**
A complete linearized theory for the analysis and design of two-dimensional hydrofoils near a free surface [UTIAS-TN-264] N88-13531

**FUEL CELLS**
Phase purity of NiCo2O4, a catalyst candidate for electrolysis of water [NASA-TM-100239] N88-13385
High energy density rechargeable batteries for aerospace power requirements [AD-A184883] N88-13519
Fuel cells — military applications [PML-1986-43] N88-13813

**FUEL COMBUSTION**
Oxygen enriched combustion system performance study [DE88-001500] N88-13424

**FUEL FLOW**
Dynamics of propellant feedline systems [AD-A184865] N88-13537

**FUEL INJECTION**
Regressed relations for forced convection heat transfer in a direct injection stratified charge rotary engine [NASA-TM-100124] N88-13345
Ignition and flameholding in supersonic flow by injection of dissociated hydrogen N88-13410
A study of the interaction of laser light with liquid propellant drops [AD-A185117] N88-13582

**FUEL SPRAYS**
Study of electrostatic modulation of fuel sprays to enhance combustion performance in an aviation gas turbine [AD-A184967] N88-13341

**FUEL TANKS**
Orbital Spacecraft Consumables Resupply System (OSCRS). Volume 1: Executive summary [NASA-CR-172010] N88-13368

**FUNCTION SPACE**
Isotropic probability measures in infinite dimensional spaces: Inverse problems/prior information/stochastic inversion [NASA-CR-181555] N88-13936

**FUNCTIONAL ANALYSIS**
On the correlation free forms for nonlinear stochastic systems [DE87-011169] N88-13947

**FUNCTIONALS**
A functional interpretation of the logistic equation [REPT-87-037] N88-13946

**FURNACES**
Oxygen enriched combustion system performance study [DE88-001500] N88-13424

**FUSELAGES**
Navier-Stokes simulation of transonic transportation aircraft configurations. 1: Flow-field simulation over wing-fuselage combinations N88-13288
Compressible Euler solution on a multiblock grid around a wing-fuselage configuration [FFA-TN-1987-46] N88-13303
Coupled elastic rotor/body vibrations with inplane degrees of freedom N88-13643

**FUSION REACTORS**
Advanced concepts theory annual report 1986 [AD-A184986] N88-13991
Dynamic processes in field-reversed-configuration compact toroids [DE87-014756] N88-13998
A short introduction to the status and motivation for reversed field pinch and compact toroid research [DE88-000487] N88-13999
A review of the experimental and theoretical status of the reversed-field pinch [DE88-000529] N88-14000
Economics of fusion reactors [DE88-000580] N88-14002
Subcommittee for MHD theory [DE88-000598] N88-14003
Transport scaling in the collisionless-detrapping regime in stellarators [DE88-001511] N88-14006
Microwave superheaters for fusion [DE88-001656] N88-14007

**FUZZY SETS**
Multidimensional least squares fitting of fuzzy models [AD-A185148] N88-13916
Least squares for fuzzy vector data regression [AD-A185156] N88-13917

## G

**GALACTIC COSMIC RAYS**
Preliminary estimates of galactic cosmic ray exposures for manned interplanetary missions [NASA-TM-100519] N88-14058
Axial anisotropy of the intensity of the cosmic ray nuclear component [IFSI-87-7] N88-14061

**GALACTIC STRUCTURE**
Comments on H. Arp The persistent problem of spiral galaxies [TRITA-EPP-87-05] N88-14052

**GALLIUM ARSENIDES**
Fundamental studies in the OM-CVD growth of Ga-In-As-Sb [AD-A184822] N88-14014
A GaAs MESFET balanced mixer with very low intermodulation [AD-A184848] N88-14015
Resonant level lifetime in GaAs/ AlGaAs double-barrier structures [AD-A185376] N88-14020

**GALLIUM PHOSPHIDES**
Preparation and characterization of members of the system (Zn,Se)1-xGaPx [AD-A185073] N88-14019

**GAME THEORY**
The isotropic rocket: A surveillance evasion game [REPT-87-21] N88-13949

**GAMMA RAY LASERS**
The gamma-ray laser project [AD-A184824] N88-13578

**GAS CHROMATOGRAPHY**
Laser probes of propellant combustion chemistry [AD-A184854] N88-13415
Chemical analysis for excimer laser systems [DE88-001941] N88-13591

**GAS DETECTORS**
Plant Growth Module (PGM) conceptual design N88-13855

**GAS DYNAMICS**
Dynamic stability of hypersonic conical lifting vehicles according to Newton-Busemann theory N88-13247
Influence of shock wave and gas pressure on the behavior of a pyrotechnical device [SNIAS-872-430-111] N88-13477

**GAS EXPANSION**
A fluid simulation of the AMPTE lithium gas releases in the solar wind [TRITA-EPP-87-06] N88-14056

**GAS EXPLOSIONS**
Computer code simulations of explosions in flow networks and comparison with experiments [DE88-001946] N88-13491

**GAS FLOW**
On the numerical simulation of three-dimensional hypersonic flow N88-13237
Rarefied gas numerical wind tunnel. 2: Two-dimensional and axially symmetric bodies N88-13273

**GAS HEATING**
Microwave superheaters for fusion [DE88-001656] N88-14007

**GAS JETS**
Investigation of the effect of laterally ejected gas jets on flows [ISL-R-107/86] N88-13545

**GAS MIXTURES**
Development of a low noise 10 K J-T refrigeration system [AD-A185258] N88-13484
Chemical analysis for excimer laser systems [DE88-001941] N88-13591

**GAS PRESSURE**
Correlation of air pressure drop and flame arrestor characteristics for explosion suppression materials [AD-A184960] N88-13340

**GAS TURBINE ENGINES**
A numerical study of the effects of curvature and convergence on dilution jet mixing [NASA-TM-89878] N88-13347

**GAS TURBINES**
Combustion characteristics of gas turbine alternative fuels [NASA-TM-100247] N88-13338
Effects of free stream turbulence, Reynolds number and incidence angle on axial turbine cascade performance N88-13339
Study of electrostatic modulation of fuel sprays to enhance combustion performance in an aviation gas turbine [AD-A184967] N88-13341

**GAS-SOLID INTERACTIONS**
Feasibility study for gas-grain simulation facility
[NASA-CR-177468] N88-13954
**GASES**
The effect of environment on low cycle fatigue properties in HSLA steel N88-13705
**GELS**
T.E.M. study of boehmite gels and of their transformation into alpha-alumina
[SNIAS-872-430-121] N88-14023
**GEOBOTANY**
Overview of Austrian Airborne Imaging Spectrometer (AIS) programme and first results N88-13762
**GEODESY**
Software design for an airborne gravity measurement system
[AD-A185000] N88-13878
**GEODETIC ACCURACY**
Precision analysis of regular networks
[B8709808] N88-13806
**GEODETIC SURVEYS**
Precision analysis of regular networks
[B8709808] N88-13806
**GEOMAGNETIC TAIL**
The tail lobe ion spectrometer: Theory and observations
[IFSI-86-12] N88-13569
**GEOMETRICAL OPTICS**
A prototype ray tracer
[AD-A184863] N88-13874
**GEOMETRY**
Introduction to string field theory
[DE87-014583] N88-14032
**GEOPHYSICS**
Isotropic probability measures in infinite dimensional spaces: Inverse problems/prior information/stochastic inversion
[NASA-CR-181555] N88-13936
**GEOSYNCHRONOUS ORBITS**
Observation guidelines for a Total Ozone Mapping Spectrometer (TOMS) in geosynchronous orbit N88-13801
**GLASS**
Composite materials with glass matrix
[SGR/PR-4305/86-SV/JC] N88-13394
Ionic transport and electrical relaxation in glass
[DE88-000887] N88-14028
**GLASS FIBER REINFORCED PLASTICS**
In-situ characterization of the interface of glass reinforced composites
[AD-A185136] N88-13391
**GLASS FIBERS**
A hybrid fibreglass-CFRP cloth for new furnishings — aircraft cabins
[SNIAS-872-111-109] N88-13396
**GLASS LASERS**
An investigation of unipolar arcing at atmospheric pressure in aluminum 2024 and aluminum coated glass slides
[AD-A184903] N88-13521
**GLOBAL POSITIONING SYSTEM**
On-orbit frequency stability analysis of the GPS NAVSTAR 8 rubidium clock and NAVSTARs 9 and 10 cesium clocks
[AD-A184984] N88-13312
Use of the global positioning system for trajectory determination of SRAM 2 missiles at the Eastern Test Range
[AD-A185266] N88-13314
**GOALS**
Lifting bodies: An attractive aerodynamic configuration choice for hypervelocity vehicles N88-13248
**GOVERNMENTS**
University research initiative research program summaries
[AD-A184878] N88-14035
Role of the technical report in technological innovation
[PB87-232500] N88-14040
**GRAIN BOUNDARIES**
Cyclic deformation and crack initiation N88-13646
Effect of grain orientation on the origination and the initial growth of fatigue cracks in pure iron N88-13647
Study of boundary structures
[AD-A184808] N88-14013
**GRAIN SIZE**
Influence of microstructure and aging condition on the fatigue crack propagation in age hardened aluminium alloys N88-13659
The effect of alpha platelet morphology and beta-grain size on the initiation and growth of short fatigue cracks in Ti6S5 N88-13667
**GRANITE**
Evaluation of AIS-2 (1986) data over hydrothermally altered granitoid rocks of the Singatse Range (Yerington) Nevada and comparison with 1985 AIS-1 data N88-13767
**GRAPH THEORY**
Eigenvectors of distance-regular graphs
[AD-A185375] N88-13919
**GRATINGS (SPECTRA)**
The production of ultrasmall and superfine holographic diffraction gratings using synchrotron radiation and lithographic techniques
[AD-A185395] N88-13562
Efficient computation of periodic Green's functions with application to grating structures
[AD-A184853] N88-13912
**GRAVITATION**
Software design for an airborne gravity measurement system
[AD-A185000] N88-13878
**GRAVITATION THEORY**
Non-minimal interaction of gravity with other physical fields: An overview
[DE87-703362] N88-13819
**GRAVITATIONAL FIELDS**
Non-minimal interaction of gravity with other physical fields: An overview
[DE87-703362] N88-13819
**GRAVITATIONAL WAVE ANTENNAS**
Capacitive resonant transducer for the Frascati gravitational antenna
[IFSI-86-9] N88-13528
**GRAVITATIONAL WAVES**
Media calibrations of the Doppler signal for a gravitational wave experiment — interplanetary medium
[IFSI-86-13] N88-13825
Activities report in interplanetary space physics
[IFSI-86-5] N88-14047
Budget and programs for 1986 research
[IFSI-86-16] N88-14048
**GREEN'S FUNCTIONS**
Efficient computation of periodic Green's functions with application to grating structures
[AD-A184853] N88-13912
**GREENLAND**
The ice conditions in the Greenland waters, 1981
[ISBN-87-7478-276-2] N88-13844
**GROUND STATE**
A mechanism for symmetry breaking in antiferromagnetic Heisenberg systems
[ETN-88-91320] N88-14031
**GROUND STATIONS**
Dobson-stations performance assessment using TOMS data N88-13792
A single-station weather forecasting expert system
[AD-A184889] N88-13832
**GROUND SUPPORT EQUIPMENT**
Research on Electrodynamic Tether Effects (RETE) experiment Electrical Ground Support Equipment (EGSE) — tethered satellite
[IFSI-87-2] N88-13378
RETE experiment Assembly, Integration, and Verification (AIV) activities
[IFSI-87-6] N88-13380
**GROWTH**
A functional interpretation of the logistic equation
[REPT-87-037] N88-13946

## H

**HANGARS**
Investigation of the nature and concentration of vapor and mist during the cleaning of aircraft
[PML-1985-29] N88-13817
**HARDENING**
The effects of thin anodic films on the cyclic microstrain/macrostrain behavior of tungsten N88-13650
**HARDENING (MATERIALS)**
Master plots for predicting the case-depth in laser surface treatments
[PB87-221875] N88-13574
Influence of microstructure and aging condition on the fatigue crack propagation in age hardened aluminium alloys N88-13659
**HARDWARE**
Plant Growth Module (PGM) conceptual design N88-13855
**HARMONIC EXCITATION**
A system identification technique based on the random decrement signatures. Part 1: Theory and simulation N88-13625
A system identification technique based on the random decrement signatures. Part 2: Experimental results N88-13626
**HARRIER AIRCRAFT**
Full-envelope aerodynamic modeling of the Harrier aircraft
[NASA-TM-88376] N88-13363
**HEAT**
Assessment of the reliability of a correction procedure for WGT (Wet Globe Thermometer) (Botsball) measurements of heat stress
[AD-A185193] N88-13559
**HEAT FLUX**
Hypersonic laminar boundary layer: Parametric study for the representation of real gas effects N88-13236
**HEAT MEASUREMENT**
Investigation by differential scanning calorimetry of microstructure in a superplastic Al-Mg-Zr alloy
[AD-A184902] N88-13439
**HEAT RESISTANT ALLOYS**
A mathematical model of high alloy nickel base high temperature alloys
[BLL-M-37381-(5828.4)] N88-13436
Behavior of long and short fatigue cracks in a powder metallurgy superalloy at room and at high temperature N88-13677
Fatigue strength of alloy A286 at cryogenic temperature N88-13695
Low cycle fatigue behaviour of notched specimens of nickel based superalloy single crystal N88-13712
An overview of fatigue N88-13729
Deformation, fatigue and fracture behavior of two cast anisotropic superalloys N88-13732
Characterization of the microstructures of various materials
[AD-A184961] N88-14017
**HEAT TOLERANCE**
Assessment of the reliability of a correction procedure for WGT (Wet Globe Thermometer) (Botsball) measurements of heat stress
[AD-A185193] N88-13559
**HEAT TRANSFER**
Experimental investigations on blunt bodies and corner configurations in hypersonic flow N88-13225
**HEAT TRANSFER COEFFICIENTS**
Regressed relations for forced convection heat transfer in a direct injection stratified charge rotary engine
[NASA-TM-100124] N88-13345
**HEAT TREATMENT**
Study of the influence of mechanical - thermal treatments on the creep behavior of a niobium stainless steel
[DE87-703506] N88-13431
The effect of heat treatment on fatigue crack growth in polycarbonate N88-13714
**HEATING EQUIPMENT**
Plant Growth Module (PGM) conceptual design N88-13855
**HEAVY IONS**
Heavy-ion accelerator research for inertial fusion
[DE88-000541] N88-14001
**HEISENBERG THEORY**
A mechanism for symmetry breaking in antiferromagnetic Heisenberg systems
[ETN-88-91320] N88-14031
**HELICOPTER DESIGN**
Model helicopter rotor rig and associated strain gauge balance for performance studies
[NAL-TM-AE-8704] N88-13364
Sitting posture of helicopter pilots of the Royal Netherlands Air Force; preliminary recommendations
[IZF-1986-16] N88-13857
**HELICOPTERS**
Calculation of helicopter rotor blade/vortex interaction by Navier-Stokes procedures
[NASA-CR-177441] N88-13291
Coupled elastic rotor/body vibrations with inplane degrees of freedom N88-13643
Sitting posture of helicopter pilots of the Royal Netherlands Air Force; preliminary recommendations
[IZF-1986-16] N88-13857
**HELMHOLTZ EQUATIONS**
On a boundary data operator and generalized exterior Robin problems for the Helmholtz equation
[AD-A185124] N88-13915
**HERMES MANNED SPACEPLANE**
Preparation of qualification tests of a plasma generator for the feeding of a hypersonic wind tunnel N88-13222
General aerodynamic-aerothermodynamic concepts for Hermes N88-13251
Hermes propulsion system
[SNIAS-872-422-109] N88-13383
**HETEROJUNCTION DEVICES**
Novel heterojunction devices
[DE87-013716] N88-14026
**HETEROJUNCTIONS**
Phase-locked semiconductor quantum well laser arrays
[AD-A185155] N88-13583
**HF LASERS**
Computer simulation of cw HF chemical laser unstable resonator performance
[AD-A185059] N88-13581

An experimental study of CW HF chemical laser amplifier performance and zero power gain
[AD-A185241] N88-13584

**HIGH ENERGY INTERACTIONS**
Analysis of geophysical data bases and models for spacecraft interactions
[AD-A184809] N88-13375

**HIGH POWER LASERS**
Phenomena at a focus in a laser system
[AD-A185442] N88-13585

**HIGH RESOLUTION**
High resolution satellite imagery simulation --- treaty verification
[FOA-C-30462-3.3,9.3] N88-13810
High resolution ultraviolet filter development
[AD-A184183] N88-13979

**HIGH REYNOLDS NUMBER**
Practical application of two-dimensional viscous flow computation N88-13257
Numerical analysis of cascade flow solving Navier-Stokes equations N88-13262

**HIGH SPEED**
Fluctuating pressure loads under high speed boundary layers
[NASA-TM-100517] N88-13962

**HIGH SPEED PHOTOGRAPHY**
An ultra-high-speed cinematographic method for the study of wakes in hypersonic ballistic ranges N88-13228
Analysis of photopole data reduction models N88-13616

**HIGH STRENGTH ALLOYS**
The effect of temperature on the tensile properties of HSLA-100 steel
[AD-A184951] N88-13441

**HIGH STRENGTH STEELS**
The effect of temperature on the tensile properties of HSLA-100 steel
[AD-A184951] N88-13441
Fatigue characteristics of ion treated surfaces N88-13713
Environmentally assisted fatigue crack growth N88-13731
Numerical simulations of impact tests on a rigid wall --- armor steel
[SNIAS-872-320-102] N88-13744

**HIGH TEMPERATURE**
A fundamental study of P/M processed elevated temperature aluminum alloys
[AD-A185393] N88-13445
Coatings for high-temperature bearings and seals
[NASA-TM-100249] N88-13453
Behavior of long and short fatigue cracks in a powder metallurgy superalloy at room and at high temperature N88-13677

**HIGH TEMPERATURE PLASMAS**
Advanced concepts theory annual report 1986
[AD-A184986] N88-13991

**HIGH VOLTAGES**
Measurements in an electromagnetic test laboratory
[SNIAS-872-430-102] N88-13507
Low jitter laser-triggered high-voltage vacuum switch using low laser energies
[DE88-001922] N88-13576

**HISTORIES**
Hypersonic airbreathing propulsion: Evolution and opportunities N88-13231
The technical evolution of the Wilson camera: The beginnings (1895-1925)
[NOTA-INTERNA-876] N88-13568
The birth of big science: Nuclear physics as advanced technology source
[NOTA-INTERNA-881] N88-13967

**HOLE BURNING**
Applications of nonlinear hole burning spectroscopy
[AD-A184943] N88-13580

**HOLOGRAPHIC INTERFEROMETRY**
Interferometric data for a shock-wave/boundary-layer interaction
[NASA-TM-88227] N88-13306
Full field visualization of surface and bulk acoustic waves using heterodyne holographic interferometry
[AD-A185071] N88-13958

**HOLOGRAPHY**
Measurement and control of damage in composite materials: Nondestructive controls by thermography, holography, and radiography
[SNIAS-872-430-110] N88-13403
The production of ultrasmall and superfine holographic diffraction gratings using synchrotron radiation and lithographic techniques
[AD-A185395] N88-13562
Determination of a flow velocity field using four-exposure laser holography
[IMFL-3114-85/32] N88-13565

**HONEYCOMB CORES**
Core material --- honeycombs
[EP-PATENT-0-196-926-A2] N88-13393

**HONEYCOMB STRUCTURES**
Influence of bonding shop moisture on metal-honeycomb junctions bonded with ultra-thin adhesive films
[SNIAS-872-422-112] N88-13399

**HORIZON**
Satellite autonomous navigation with SHAD (Stellar Horizon Atmospheric Dispersion)
[AD-A184988] N88-13313

**HOT WORKING**
Advances in processing techniques for nickel aluminides
[DE87-014571] N88-13449

**HOT-WIRE ANEMOMETERS**
Turbulence measurement in hypersonic flow N88-13224
Hot wire and laser velocimeter studies of turbulent flow at supersonic velocities
[ETN-88-91172] N88-13566

**HOTOL LAUNCH VEHICLE**
Hypersonic aerodynamics: Applications for HOTOL N88-13252

**HOUSEKEEPING (SPACECRAFT)**
Development of response models for the Earth Radiation Budget Experiment (ERBE) sensors. Part 3: ERBE scanner measurement accuracy analysis due to reduced housekeeping data
[NASA-CR-178294] N88-13553

**HOVERING**
Solution procedure for the Navier-Stokes equations applied to rotors N88-13533

**HUMAN FACTORS ENGINEERING**
Human engineering laboratory grounding analysis (HELGA)-2
[AD-A185367] N88-13524
Sitting posture of helicopter pilots of the Royal Netherlands Air Force; preliminary recommendations
[IZF-1986-16] N88-13857

**HUMAN PERFORMANCE**
Examining the relative efficiency of Part- versus whole-task practice for multiple-task situations
[AD-A185056] N88-13856

**HUMAN TOLERANCES**
Measurement of suspension and ride characteristics of the M1 main battle tank N88-13637
Investigation of the exposure to harmful compounds in the workshop of nondestructive materials testing at Gilze-Rijen (Netherlands)
[PML-1985-42] N88-13816

**HUMIDITY**
Estimation of marine boundary layer depth and relative humidity with multispectral satellite measurements
[AD-A184881] N88-13804
Controlled ecological life support systems: Development of a plant growth module N88-13854

**HUMIDITY MEASUREMENT**
Estimation of marine boundary layer depth and relative humidity with multispectral satellite measurements
[AD-A184881] N88-13804

**HUNGARY**
Proceedings of the 17th International Conference on Phenomena in Ionized Gases held in Budapest, Hungary, July 8-12, 1985: Invited papers
[DE87-703562] N88-13987

**HYDROCARBON COMBUSTION**
Laser probes of propellant combustion chemistry
[AD-A184854] N88-13415

**HYDROCARBON FUELS**
An experimental investigation of the ignition and flammability limits of various hydrocarbon fuels in a two-dimensional solid fuel ramjet
[AD-A184968] N88-13342

**HYDROCARBONS**
Development of a low noise 10 K J-T refrigeration system
[AD-A185258] N88-13484
Molecular dynamics studies of aromatic hydrocarbon liquids
[DE88-001473] N88-13973

**HYDRODYNAMIC COEFFICIENTS**
Free Lagrange reconnection algorithms for hydrocodes using a quadrilateral mesh
[DE88-001580] N88-13752

**HYDRODYNAMICS**
A complete linearized theory for the analysis and design of two-dimensional hydrofoils near a free surface
[UTIAS-TN-264] N88-13531
Advanced concepts theory annual report 1986
[AD-A184986] N88-13991

**HYDROFOILS**
A complete linearized theory for the analysis and design of two-dimensional hydrofoils near a free surface
[UTIAS-TN-264] N88-13531

**HYDROGEN EMBRITTLEMENT**
Environmentally assisted cracking: Overview of evidence for an adsorption-induced localised-slip process
[AD-A185175] N88-13443
The influence of crack conditions on hydrogen uptake by steels N88-13702
the influence of temper embrittlement on fatigue crack growth in hydrogen N88-13709
Crack initiation studies in hydrogen embrittled spring steel strip N88-13710
Embrittling effect of the plastic zone N88-13721

**HYDROGEN PRODUCTION**
Intramolecular energy transfer reactions as a method for metal complex assisted production of hydrogen
[DE88-001621] N88-13425

**HYDROGRAPHY**
Varifront 3 expedition data report (USNS DE STEIGUER CRUISE 1202-82). Bioluminescence, hydrographic, nutrient, and satellite data from the Gulf of California (November-December 1981)
[AD-A185011] N88-13805

**HYDROMETEOROLOGY**
The application of doubly-truncated hydrometeor distributions to numerical cloud models
[AD-A185273] N88-13636

**HYDROSTATIC PRESSURE**
Experimental studies on the tripping behavior of narrow T-stiffened flat plates subjected to hydrostatic pressure and underwater shock N88-13613

**HYDROTHERMAL STRESS ANALYSIS**
STAEBL/general composites with hygrothermal effects (STAEBL/GENCOM)
[NASA-TM-100266] N88-13754

**HYDROTHERMAL SYSTEMS**
Effective use of principal component analysis with high resolution remote sensing data to delineate hydrothermal alteration and carbonate rocks N88-13758
Evaluation of AIS-2 (1986) data over hydrothermally altered granitoid rocks of the Singatse Range (Yerington) Nevada and comparison with 1985 AIS-1 data N88-13767
Mapping hydrothermally altered rocks in the Northern Grapevine Mountains, Nevada and California with the airborne imaging spectrometer N88-13772

**HYGRAL PROPERTIES**
STAEBL/general composites with hygrothermal effects (STAEBL/GENCOM)
[NASA-TM-100266] N88-13754

**HYPERBOLIC FUNCTIONS**
Nonlinear hyperbolic conservation laws
[AD-A184963] N88-13538

**HYPERSONIC AIRCRAFT**
The off-design performance of hypersonic waveriders N88-13244
Numerical optimization of conical flow waveriders including detailed viscous effects N88-13245
Dynamic stability of hypersonic conical lifting vehicles according to Newton-Busemann theory N88-13247
Lifting bodies: An attractive aerodynamic configuration choice for hypervelocity vehicles N88-13248

**HYPERSONIC FLIGHT**
Shock tunnels for real gas hypersonics N88-13223
Driving mechanism of unsteady separation shock motion in hypersonic interactive flow N88-13226

**HYPERSONIC FLOW**
Experimental investigations on blunt bodies and corner configurations in hypersonic flow N88-13225
An ultra-high-speed cinematographic method for the study of wakes in hypersonic ballistic ranges N88-13228
Numerical simulation of the hypersonic flow around lifting vehicles N88-13234
Hypersonic laminar boundary layer: Parametric study for the representation of real gas effects N88-13236
On the numerical simulation of three-dimensional hypersonic flow N88-13237
Numerical experiments with hypersonic flows beneath a cone-delta-wing combination N88-13238
A spatial marching technique for the inviscid blunt body problem N88-13239
A 3-D Euler solution for hypersonic Mach numbers N88-13240
Computation of flow past conical hypersonic wings using a second order Godunov method N88-13241

**HYPERSONIC VEHICLES**
The effects of sweep and bluntness on a glancing shock wave turbulent boundary layer interaction N88-13227
Hypersonic static and dynamic stability of axisymmetric shapes: A comparison of prediction methods and experiment N88-13246

**HYPERSONIC WIND TUNNELS**
A survey of existing hypersonic ground test facilities: North America N88-13220
European hypersonic wind tunnels N88-13221

Preparation of qualification tests of a plasma generator for the feeding of a hypersonic wind tunnel N88-13222
Turbulence measurement in hypersonic flow N88-13224
The drag of slender axisymmetric cones in rarefied hypersonic flow N88-13229
Low Reynolds number influence on aerodynamic performance of hypersonic lifting vehicles N88-13230
Aerothermodynamics research at NASA Ames N88-13242

**HYPOBARIC ATMOSPHERES**
Cooling electronic equipment at simulated high altitude in hypobaric chambers
[AD-A185196] N88-13560

## I

**ICE**
Altered and enhanced iodargyrite with bismuth triodide for use in precipitation enhancement operations
[AD-A185229] N88-13419

**ICE FORMATION**
Computation of rime ice accretion on airfoils
[FFA-TN-1987-08] N88-13301
Measurement of local convective heat transfer coefficients from a smooth and roughened NACA-0012 airfoil: Flight test data
[NASA-TM-100264] N88-13552
Operating envelopes of particle sizing instrumentation used for icing research
[NASA-CR-180870] N88-13573
The ice conditions in the Greenland waters, 1981
[ISBN-87-7478-276-2] N88-13844

**ICE PREVENTION**
Theoretical analysis of the electrical aspects of the basic electro-impulse problem in aircraft de-icing applications
[NASA-CR-180845] N88-13310

**ICE REPORTING**
The ice conditions in the Greenland waters, 1981
[ISBN-87-7478-276-2] N88-13844

**IGNEOUS ROCKS**
Abundance and distribution of ultramafic microbreccia in Moses Rock Dike: Quantitative application of AIS data N88-13766

**IGNITERS**
Pulsed plasma jet igniters: Species measurements in methane combustion
[DE88-001389] N88-13422

**IGNITION**
An experimental investigation of the ignition and flammability limits of various hydrocarbon fuels in a two-dimensional solid fuel ramjet
[AD-A184968] N88-13342
Ignition and flameholding in supersonic flow by injection of dissociated hydrogen N88-13410
Pulsed plasma jet igniters: Species measurements in methane combustion
[DE88-001389] N88-13422
Detailed mechanism of toluene oxidation and comparison with benzene
[NASA-TM-100261] N88-13428
Jet initiation of PBX 9502
[DE88-000493] N88-13481
A study of the interaction of laser light with liquid propellant drops
[AD-A185117] N88-13582

**IGNITION LIMITS**
An experimental investigation of the ignition and flammability limits of various hydrocarbon fuels in a two-dimensional solid fuel ramjet
[AD-A184968] N88-13342

**ILLUMINATION**
Plant Growth Module (PGM) conceptual design N88-13855

**IMAGE ANALYSIS**
Determination of the fiber ratio in carbon fiber/resin composites by means of image analysis
[SNIAS-872-422-101] N88-13398
Land cover/use classification of Cairns, Queensland, Australia: A remote sensing study involving the conjunctive use of the airborne imaging spectrometer, the large format camera and the thematic mapper simulator N88-13759

**IMAGE INTENSIFIERS**
A focussed MCP (microchannel plate) image intensifier type for high speed gating
[DE88-000480] N88-13555
Streak camera dynamic range optimization
[DE88-001632] N88-13571

**IMAGE PROCESSING**
Correction of inertial navigation system drift errors for an autonomous land vehicle using optical radar terrain data
[AD-A184973] N88-13311
Television motion measurement for DATV and other applications
[BBC-RD-1987/11] N88-13496
Italy's Institute of Research on Electromagnetic Waves--the Istituto di Ricerca sulle Onde Elettromagnetiche
[AD-A185020] N88-13501
Study on data compression systems for operational remote sensing — meteosat imagery
[NLR-TR-86029-L] N88-13808
Matching segments from a map and an aerial image using relaxation techniques
[SNIAS-872-422-103] N88-13809
Learning a color algorithm from examples
[AD-A184385] N88-13862
A prototype ray tracer
[AD-A184863] N88-13874
The use of color in electronic maps. Part 1: Generation and analysis of color on the Gould/DeAnza image processing system
[IZF-1986-32] N88-13882
The maximum likelihood estimator method of image reconstruction: Its fundamental characteristics and their origin
[DE88-000462] N88-13892
Full field visualization of surface and bulk acoustic waves using heterodyne holographic interferometry
[AD-A185071] N88-13958
X-ray imaging: Status and trends
[DE88-000756] N88-13980

**IMAGE RECONSTRUCTION**
The maximum likelihood estimator method of image reconstruction: Its fundamental characteristics and their origin
[DE88-000462] N88-13892

**IMAGE RESOLUTION**
High resolution ultraviolet filter development
[AD-A184183] N88-13979

**IMAGE TUBES**
Resolution limitations and optimization of the LLNL streak camera focus
[DE88-001633] N88-13572

**IMAGERY**
Modeling cloudy and clear interval length probabilities using space shuttle imagery
[AD-A185290] N88-13837
Range imagery algorithms for the detection of obstacles by autonomous vehicles
[AD-A185421] N88-14045

**IMAGING SPECTROMETERS**
Proceedings of the Third Airborne Imaging Spectrometer Data Analysis Workshop
[NASA-CR-181552] N88-13755
The Portable Instant Display and Analysis Spectrometer (PIDAS) N88-13756
AIS-2 radiometry and a comparison of methods for the recovery of ground reflectance N88-13757
Effective use of principal component analysis with high resolution remote sensing data to delineate hydrothermal alteration and carbonate rocks N88-13758
Land cover/use classification of Cairns, Queensland, Australia: A remote sensing study involving the conjunctive use of the airborne imaging spectrometer, the large format camera and the thematic mapper simulator N88-13759
Calibrating AIS images using the surface as a reference N88-13760
The use of airborne imaging spectrometer data to determine experimentally induced variation in coniferous canopy chemistry N88-13761
Overview of Austrian Airborne Imaging Spectrometer (AIS) programme and first results N88-13762
AIS-2 spectra of California wetland vegetation N88-13763
Toward detecting California shrubland canopy chemistry with AIS data N88-13764
Measuring near infrared spectral reflectance changes from water stressed conifer stands with AIS-2 N88-13765
Abundance and distribution of ultramafic microbreccia in Moses Rock Dike: Quantitative application of AIS data N88-13766
Evaluation of AIS-2 (1986) data over hydrothermally altered granitoid rocks of the Singatse Range (Yerington) Nevada and comparison with 1985 AIS-1 data N88-13767
Preliminary results from an investigation of AIS-1 data over an area of epithermal alteration: Plateau, Northern Queensland, Australia N88-13768
Causes of spurious features in spectral reflectance data N88-13769
Automatic continuum analysis of reflectance spectra N88-13770
Analysis of airborne imaging spectrometer data for the Ruby Mountains, Montana, by use of absorption-band-depth images N88-13771
Mapping hydrothermally altered rocks in the Northern Grapevine Mountains, Nevada and California with the airborne imaging spectrometer N88-13772
A geostationary imaging spectrometer TOMS instrument N88-13802

**IMAGING TECHNIQUES**
Photon counting image sensor development for astronomical applications
[NASA-CR-181507] N88-14049

**IMMUNOLOGY**
TOMS as a monitor of the ultraviolet radiation environment: Applications to photobiology N88-13785

**IMPACT PREDICTION**
Utilization of dynamic characteristics of materials to optimize military explosive charges. Application to antiship devices
[SNIAS-872-320-101] N88-13743

**IMPACT TESTS**
High explosive moulding powders from RDX and aqueous polyurethane dispersions
[AD-A185026] N88-13458
Numerical simulations of impact tests on a rigid wall --- armor steel
[SNIAS-872-320-102] N88-13744

**IMPEDANCE MATCHING**
Electromagnetic tests
[SNIAS-872-430-103] N88-13508

**IMPLOSIONS**
Advanced concepts theory annual report 1986
[AD-A184986] N88-13991

**IMPULSES**
Analysis of photopole data reduction models N88-13616

**IMPURITIES**
Chemical analysis for excimer laser systems
[DE88-001941] N88-13591

**INCIDENCE**
Effects of free stream turbulence, Reynolds number and incidence angle on axial turbine cascade performance N88-13339

**INCOHERENCE**
Theory of induced spatial incoherence
[AD-A185005] N88-13992

**INCOMPRESSIBLE FLOW**
Numerical prediction of turbulent flows in dump diffusers N88-13265
Computation of flow around 2-D circular cylinder N88-13284
The development of a computer code (U2DIF) for the numerical solution of unsteady, inviscid and incompressible flow over an airfoil
[AD-A185033] N88-13293
Delta wing in incompressible flow. Experimental study in F2
[ONERA-RT-36/1147-AN-249-G] N88-13298
Statistical theory of turbulent incompressible multimaterial flow
[DE88-000435] N88-13535

**INCOMPRESSIBLE FLUIDS**
Viscous damped space structure for reduced jitter N88-13623

**INDIUM ARSENIDES**
MBE growth of InAsSb strained-layer superlattices
[DE88-000365] N88-14011

**INERTIAL FUSION (REACTOR)**
Heavy-ion accelerator research for inertial fusion
[DE88-000541] N88-14001

**INERTIAL NAVIGATION**
Correction of inertial navigation system drift errors for an autonomous land vehicle using optical radar terrain data
[AD-A184973] N88-13311

**INFERENCE**
An APL workspace for conducting nonparametric statistical inference
[AD-A184971] N88-13877

**INFINITY**
Equivalence of input-output stability and exponential stability for infinite dimensional systems
[TW-276] N88-13903

**INFORMATION DISSEMINATION**
Role of technical information in innovation
[PB87-235388] N88-14039
Role of the technical report in technological innovation
[PB87-232500] N88-14040

**INFORMATION PROCESSING (BIOLOGY)**
Taskomat, a task battery for information processing
[IZF-1987-2] N88-13851

**INFORMATION RETRIEVAL**
Storing and retrieving data in a parallel distributed memory system
[AD-A185177] N88-13897

**INFRARED ASTRONOMY**
Study of solid state photomultiplier
[NASA-CR-177465] N88-13556

Activities report in interplanetary space physics
[IFSI-86-5] N88-14047

**INFRARED DETECTORS**
Evaluation of a cryogenic refrigerator for cooling focal plane instrumentation --- satellite instruments
[BAE-TP-8095-VOL-1] N88-13485
Evaluation of a cryogenic refrigerator for cooling focal plane instrumentation. Appendix B: Accommodation study --- satellite instruments
[BAE-TP-8095-VOL-2] N88-13486

**INFRARED SPECTRA**
Measuring near infrared spectral reflectance changes from water stressed conifer stands with AIS-2 N88-13765
High energy molecules of high symmetry
[AD-A185385] N88-13965
Extinction by dielectric particles at optical and infrared wavelength
[AD-A184818] N88-13981

**INFRARED SPECTROMETERS**
Complementary information between UV and IR for remote sensing of total ozone N88-13800

**INJECTORS**
RIIM two-pulse injector experiments
[DE88-000926] N88-14005

**INPUT**
Equivalence of input-output stability and exponential stability for infinite dimensional systems
[TW-276] N88-13903
Modeling and generating input processes
[DE87-013162] N88-13948

**INSTALLING**
Airframe/store compatibility N88-13323
Human engineering laboratory grounding analysis (HELGA)-2
[AD-A185367] N88-13524

**INTAKE SYSTEMS**
Fundamentals of fighter aircraft design: Engine intake and afterbody N88-13322
Fluid mass and thermal loading effects on the modal characteristics of space shuttle main engine liquid oxygen inlet splitter vanes N88-13628

**INTEGRATED CIRCUITS**
Electromagnetics and electrothermal approach to evaluate failures in microelectronic devices caused by electrostatic discharges: Stochastical aspects of the device reliability
[AD-A184906] N88-13522
An extension to the multilevel logic simulator for microcomputers
[AD-A185032] N88-13879
Computer modeling of complete IC fabrication process
[AD-A184807] N88-14012
Technology upgrade of a silicon compiler
[AD-A184873] N88-14016

**INTERACTIVE CONTROL**
A computer code to process and plot laser altimetry data interactively on a microcomputer
[NASA-TM-100687] N88-13371

**INTERFACES**
Development of an interface for an ultrareliable fault-tolerant control system and an electronic servo-control unit
[NASA-TM-88236] N88-13367
Reactions of porphyrins in surfactant assemblies, microemulsions and in solutions
[AD-A184797] N88-13412
Water disbondment characterization of organic Coating/metal substrate systems
[AD-A184847] N88-13454
Molecular-level synthesis and characterization of metal-polymer interfaces
[AD-A184956] N88-13455
Bending of a bonded beam as a test method for adhesive properties
[AD-A184813] N88-13736
Molecular beam epitaxial growth and characterization of 3-5 compound semiconductor single and multiple interface structures
[AD-A185400] N88-14021

**INTERFACIAL TENSION**
Effect of interface on mechanical properties of graphite/201 aluminum composites N88-13717

**INTERFEROMETRY**
An optical interferometry technique to evaluate closure along a crack front N88-13726

**INTERIOR BALLISTICS**
A study of the interaction of laser light with liquid propellant drops
[AD-A185117] N88-13582

**INTERMODULATION**
A GaAs MESFET balanced mixer with very low intermodulation
[AD-A184848] N88-14015

**INTERNAL COMBUSTION ENGINES**
Development, construction and testing of a novel internal combustion engine with conical rotating slide valve
[DE88-900071] N88-13593
The development and evaluation of three-dimensional models of cold flow in internal combustion engines
[DE88-900077] N88-13594

**INTERNATIONAL COOPERATION**
The A320 Airbus program
[SNIAS-872-111-105] N88-13215

**INTERPLANETARY FLIGHT**
Preliminary estimates of galactic cosmic ray exposures for manned interplanetary missions
[NASA-TM-100519] N88-14058

**INTERPLANETARY MAGNETIC FIELDS**
The polar ionosphere and interplanetary field
[AD-A185386] N88-13822
Magnetic field draping about coronal mass ejecta
[DE88-001805] N88-14057

**INTERPLANETARY MEDIUM**
Media calibrations of the Doppler signal for a gravitational wave experiment --- interplanetary medium
[IFSI-86-13] N88-13825

**INTERPLANETARY SPACE**
Activities report in interplanetary space physics
[IFSI-86-5] N88-14047

**INVENTORIES**
Inventory of weather stations. Climatological data from Dutch stations, no. 26
[KNMI-150-26] N88-13841

**INVERSE SCATTERING**
Inverse scattering analysis of diffraction limited SAR
[FOA-C-30459-3.2] N88-13512
Solitons in stimulated Raman scattering: Generation and control of ultrashort optical pulses
[AD-A185141] N88-13983

**INVERSIONS**
Comparing hard and soft prior bounds in geophysical inverse problems
[NASA-CR-181557] N88-13820

**INVERTED CONVERTERS (DC TO AC)**
Digital control of a direct current converter for a hybrid vehicle
[LAAS-87-266] N88-13527

**INVISCID FLOW**
A spatial marching technique for the inviscid blunt body problem N88-13239
Numerical optimization of conical flow waveriders including detailed viscous effects N88-13245
The role of computation fluid dynamics in aeronautical engineering (4). The development and applications of implicit TVD finite volume code N88-13259
The development of a computer code (U2DIIF) for the numerical solution of unsteady, inviscid and incompressible flow over an airfoil
[AD-A185033] N88-13293
A Cartesian finite-volume method for the Euler equations N88-13532
A note on the use of symmetric line Gauss-Seidel for the steady upwind differenced Euler equations
[AD-A185223] N88-13540

**IODIDES**
Altered and enhanced iodargyrite with bismuth triiodide for use in precipitation enhancement operations
[AD-A185229] N88-13419

**IODINE LASERS**
Theoretical studies of solar lasers and converters
[NASA-CR-181569] N88-13577

**ION BEAMS**
Extreme ultraviolet beam-foil spectroscopy of highly ionized neon and argon
[AD-A185197] N88-13418
The effect of ion beam mixed Ni-Al surface layers on PSB extrusion morphology in fatigued nickel N88-13652

**ION CONCENTRATION**
The formation and thermochemical properties of multiligand complexes
[AD-A184935] N88-13416
Activated metal oxide surfaces as highly basic and reducing environments
[AD-A184958] N88-13417

**ION CYCLOTRON RADIATION**
Theoretical atomic and molecular physics
[DE88-001625] N88-13974

**ION IMPLANTATION**
Fatigue characteristics of ion treated surfaces N88-13713
Develop techniques for ion implantation of (lead-lanthanum-zirconate-titanate) for adaptive optics
[DE88-000842] N88-13986
Structural characterization of ion implanted beta-SiC thin films
[DE87-014567] N88-14027

**ION PLATING**
Ion plating for corrosion control
[AD-A185061] N88-13442

**ION SCATTERING**
Atomic physics with highly charged ions
[DE88-000894] N88-13972

**ION SOURCES**
Theoretical atomic and molecular physics
[DE88-001625] N88-13974

**IONIC COLLISIONS**
Atomic physics with highly charged ions
[DE88-000894] N88-13972

**IONIC MOBILITY**
Ionic transport and electrical relaxation in glass
[DE88-000887] N88-14028

**IONIC REACTIONS**
Atomic physics with highly charged ions
[DE88-000894] N88-13972

**IONIZATION**
Anti-Stokes generation of 226 nm light
[DE88-001612] N88-13590

**IONIZED GASES**
Proceedings of the 17th International Conference on Phenomena in Ionized Gases held in Budapest, Hungary, July 8-12, 1985: Invited papers
[DE87-703562] N88-13987

**IONS**
The analysis of metal finishing solutions by ion chromatography
[AD-A184812] N88-13414
Survey state of the art: Electrical load management techniques and equipment
[AD-A184083] N88-13517
Atomic physics with highly charged ions
[DE88-000894] N88-13972
Ionic transport and electrical relaxation in glass
[DE88-000887] N88-14028

**IRON**
Plasticity of aluminum and iron at high shear strain rate and high pressure N88-13430
The mechanism by which sigma-phase forms in Fe-Cr-Ni system alloys
[BLL-M-37380-(5828.4)] N88-13437
Effect of grain orientation on the origination and the initial growth of fatigue cracks in pure iron N88-13647
Surface deformation and fatigue crack initiation of alpha-iron N88-13651

**IRON ALLOYS**
Fatigue strength of alloy A286 at cryogenic temperature N88-13695

**IRON COMPOUNDS**
Development of iron aluminides
[AD-A185190] N88-13461

**IRRADIATION**
An investigation of unipolar arcing at atmospheric pressure in aluminum 2024 and aluminum coated glass slides
[AD-A184903] N88-13521
Raman microprobe characterization of dielectric films following high-energy pulsed laser irradiation
[DE88-000559] N88-13587
Pure dephasing of a vibrational adbond
[AD-A185222] N88-13740
Controlled ecological life support systems: Development of a plant growth module N88-13854
Irradiation preservation of seafood: Literature review
[DE88-001691] N88-13858

**ISENTROPE**
Isentropic analysis and interpretation: Operational applications to synoptic and mesoscale forecast problems
[AD-A184814] N88-13830

**ITERATION**
A new method to real-normalize measured complex modes N88-13618
Near-horn prolog
[AD-A185172] N88-13880
Research and development of finite elements and iterative algorithms for elliptic partial differential equations
[DE88-001381] N88-13934
Freidlin-Wentzell type estimates and the law of the iterated logarithm for a class of stochastic processes related to symmetric statistics
[AD-A185366] N88-13944

**ITERATIVE NETWORKS**
Contribution to optimal flow in networks. A experimental multiprocessor for asynchronous iteration implementation
[LAAS-87-269] N88-13510

## J


**JET AIRCRAFT**
Computation of nacelle interference using boundary element method N88-13267
**JET ENGINE FUELS**
Study of electrostatic modulation of fuel sprays to enhance combustion performance in an aviation gas turbine
[AD-A184967] N88-13341
An experimental investigation of the ignition and flammability limits of various hydrocarbon fuels in a two-dimensional solid fuel ramjet
[AD-A184968] N88-13342
Production of jet fuels from coal derived liquids. Volume 1: Market assessment for liquid by-products from the Great Plains gasification plant
[AD-A184846] N88-13475
**JET FLOW**
Combustion related shear-flow dynamics in elliptic supersonic jets N88-13232
Jet initiation of PBX 9502
[DE88-000493] N88-13481
Trajectory control using laterally ejected jets. Literature review
[ISL-R-117/85] N88-13514
**JET MIXING FLOW**
A numerical study of the effects of curvature and convergence on dilution jet mixing
[NASA-TM-89878] N88-13347
**JET STREAMS (METEOROLOGY)**
Ozone, jet streaks and severe weather N88-13781
**JOINTS (JUNCTIONS)**
Advanced joining concepts for passive vibration control N88-13638
**JOULE-THOMSON EFFECT**
Development of a low noise 10 K J-T refrigeration system
[AD-A185258] N88-13484


## K


**KALMAN FILTERS**
Investigation, development, and application of optimal output feedback theory. Volume 3: The relationship between dynamic compensators and observers and Kalman filters
[NASA-CR-4107] N88-13900
**KINEMATICS**
Non-linear maximum likelihood estimation of stability derivatives from range data
[NAL-TM-SE-8608] N88-13365
SHARP simulation of discontinuities in highly convective steady flow
[NASA-TM-100240] N88-13931
**KINETIC ENERGY**
Mechanical property evaluation of a series of commercial tungsten alloys
[AD-A185440] N88-13446
**KRYPTON FLUORIDE LASERS**
Narrow linewidth gain measurements in a KrF excimer amplifier pumped longitudinally by a high-power electron beam
[DE88-001365] N88-13575


## L


**LABORATORY EQUIPMENT**
Measurements in an electromagnetic test laboratory
[SNIAS-872-430-102] N88-13507
Electromagnetic tests
[SNIAS-872-430-103] N88-13508
Controlled Ecological Life Support System. Design, Development, and Use of a Ground-Based Plant Growth Module
[NASA-CP-2479] N88-13852
CELSS Program Meeting N88-13853
**LABYRINTH SEALS**
Three-dimensional dynamic labyrinth seal analysis
[AD-A185353] N88-13599
**LAGRANGE MULTIPLIERS**
Lagrangian procedures for higher order field equations
[DE87-703365] N88-13911
**LAMINAR BOUNDARY LAYER**
Hypersonic laminar boundary layer: Parametric study for the representation of real gas effects N88-13236
Navier-Stokes analysis of laminar flow control of a two-dimensional airfoil N88-13286
**LAMINAR FLOW**
On the numerical simulation of three-dimensional hypersonic flow N88-13237
**LAMINATES**
Dynamic response of laminated composite plates using a three-dimensional hybrid-stress finite-element formulation N88-13639
Fatigue mechanisms in ARALL, a fatigue resistant hybrid aluminum aramid composite material N88-13711
**LAND MOBILE SATELLITE SERVICE**
Study of the feasibility of a satellite communication system for road transportation home office to vehicle communication. Volume 1: Conceptual analysis
[SC/87-E/6-VOL-1] N88-13505
Study of the feasibility of a satellite communication system for road transportation home office to vehicle communication. Volume 2: Market study
[SC/87-E/6-VOL-2] N88-13506
**LAND USE**
Land cover/use classification of Cairns, Queensland, Australia: A remote sensing study involving the conjunctive use of the airborne imaging spectrometer, the large format camera and the thematic mapper simulator N88-13759
Overview of Austrian Airborne Imaging Spectrometer (AIS) programme and first results N88-13762
**LANDING**
High speed propeller performance and noise predictions at takeoff/landing conditions
[NASA-TM-100267] N88-13860
**LANTHANUM**
Develop techniques for ion implantation of (lead-lanthanum-zirconate-titanate) for adaptive optics
[DE88-000642] N88-13986
**LANTHANUM COMPOUNDS**
A synthetic plasma source
[TRITA-EPP-86-15] N88-13995
**LAPLACE TRANSFORMATION**
Numerica calculation in the Laplace domain for subsonic unsteady aerodynamic forces acting on a finite wing N88-13256
**LARGE SPACE STRUCTURES**
Computational methods for problems in aerodynamics and large space structure using parallel and vector architectures
[AD-A185401] N88-13294
Survey on large scale system control methods
[NASA-CR-181556] N88-13374
Design of low order controllers for robust disturbance rejection in large space structures
[AD-A185202] N88-13376
Modeling and control of large flexible vehicles in the atmosphere and space
[AD-A185368] N88-13377
Potential for on-orbit manufacture of large space structures using the pultrusion process
[NASA-TM-4016] N88-13388
Optimal control of large space structures via generalized inverse matrix
[NASA-CR-182336] N88-13907
**LASER ALTIMETERS**
A computer code to process and plot laser altimetry data interactively on a microcomputer
[NASA-TM-100687] N88-13371
**LASER ANEMOMETERS**
Turbulence measurement in hypersonic flow N88-13224
**LASER APPLICATIONS**
An ultra-high-speed cinematographic method for the study of wakes in hypersonic ballistic ranges N88-13228
Master plots for predicting the case-depth in laser surface treatments
[PB87-221675] N88-13574
**LASER CAVITIES**
Nonconventional optical techniques for optical wavefront processing
[AD-A185099] N88-13982
**LASER DOPPLER VELOCIMETERS**
Determination of a flow velocity field using four-exposure laser holography
[IMFL-3114-85/32] N88-13565
Hot wire and laser velocimeter studies of turbulent flow at supersonic velocities
[ETN-88-91172] N88-13566
**LASER FUSION**
Theory of induced spatial incoherence
[AD-A185005] N88-13992
**LASER GUIDANCE**
Range imagery algorithms for the detection of obstacles by autonomous vehicles
[AD-A185421] N88-14045
**LASER INDUCED FLUORESCENCE**
Laser probes of propellant combustion chemistry
[AD-A184854] N88-13415
**LASER OUTPUTS**
Low jitter laser-triggered high-voltage vacuum switch using low laser energies
[DE88-001922] N88-13576
Theoretical studies of solar lasers and converters
[NASA-CR-181569] N88-13577
A study of the interaction of laser light with liquid propellant drops
[AD-A185117] N88-13582
An experimental study of CW HF chemical laser amplifier performance and zero power gain
[AD-A185241] N88-13584
Raman microprobe characterization of dielectric films following high-energy pulsed laser irradiation
[DE88-000559] N88-13587
Development of a data analysis system for the detection of lower level atmospheric turbulence with an acoustic sounder
[AD-A184972] N88-13821
**LASER PLASMAS**
An investigation of unipolar arcing at atmospheric pressure in aluminum 2024 and aluminum coated glass slides
[AD-A184903] N88-13521
**LASER PUMPING**
Nonconventional optical techniques for optical wavefront processing
[AD-A185099] N88-13982
Theory of induced spatial incoherence
[AD-A185005] N88-13992
**LASER TARGET INTERACTIONS**
Transient processes in the interaction between pulsed laser radiation and matter
[ISL-R-115/86] N88-13586
**LASER TARGETS**
Low jitter laser-triggered high-voltage vacuum switch using low laser energies
[DE88-001922] N88-13576
**LASER WELDING**
Effect of rapid solidification on stainless steel weld metal microstructures and its implications on the Schaeffler diagram
[DE88-001489] N88-13451
**LATTICE VIBRATIONS**
Pure dephasing of a vibrational adbond
[AD-A185222] N88-13740
Computation of natural frequencies of planar lattice structure
[AD-A185387] N88-13920
Study of boundary structures
[AD-A184808] N88-14013
**LAUNCH VEHICLES**
Control of an unstable launcher in atmospheric flight using minimax optimal control laws
[SNIAS-872-422-107] N88-13901
**LAUNCHING**
Non-linear shipboard shock analysis of the Tomahawk missile shock isolation system N88-13614
**LEAD (METAL)**
Develop techniques for ion implantation of (lead-lanthanum-zirconate-titanate) for adaptive optics
[DE88-000642] N88-13986
**LEADING EDGES**
Vortex interaction with a leading-edge of finite thickness
[NASA-CR-182341] N88-13307
**LEARNING**
Learning a color algorithm from examples
[AD-A184385] N88-13862
**LEAST SQUARES METHOD**
Model-based motion estimation and its application to restoration and interpolation of motion pictures
[AD-A185054] N88-13558
A system identification technique based on the random decrement signatures. Part 1: Theory and simulation N88-13625
A system identification technique based on the random decrement signatures. Part 2: Experimental results N88-13626
Multidimensional least squares fitting of fuzzy models
[AD-A185148] N88-13916
Least squares for fuzzy vector data regression
[AD-A185156] N88-13917
**LENGTH**
The effect of microstructure on the surface crack length: Crack depth relationship for short cracks N88-13670
**LIFE (DURABILITY)**
Fiber composite structural durability and damage tolerance: Simplified predictive methods
[NASA-TM-100179] N88-13409
Significance of fatigue crack closure under spectrum loading N88-13662
Further studies in estimation of life distribution characteristics from censored data
[AD-A184862] N88-13937
**LIFE CYCLE COSTS**
Simulated service test behavior of various internal and external coatings applied on CF6-50 first stage turbine blades
[NLR-MP-86018-U] N88-13343

**LIFT**
Nonlinear lift control at high speed and high angle of attack using vortex flow technology N88-13319
Prediction of wing aeroelastic effects on aircraft life and pitching moment characteristics N88-13358
**LIFT AUGMENTATION**
Validation elements of the computation methods and measurement techniques for high lift aerodynamic systems
[SNIAS-872-111-101] N88-13299
**LIFT DRAG RATIO**
Airframe/store compatibility N88-13323
**LIFTING BODIES**
Aerodynamics of Hypersonic Lifting Vehicles
[AGARD-CP-428] N88-13219
Numerical experiments with hypersonic flows beneath a cone-delta-wing combination N88-13238
Numerical optimization of conical flow waveriders including detailed viscous effects N88-13245
Dynamic stability of hypersonic conical lifting vehicles according to Newton-Busemann theory N88-13247
Lifting bodies: An attractive aerodynamic configuration choice for hypervelocity vehicles N88-13248
**LIFTING REENTRY VEHICLES**
European hypersonic wind tunnels N88-13221
Shock tunnels for real gas hypersonics N88-13223
Low Reynolds number influence on aerodynamic performance of hypersonic lifting vehicles N88-13230
**LIGANDS**
The formation and thermochemical properties of multiligand complexes
[AD-A184935] N88-13416
Intramolecular energy transfer reactions as a method for metal complex assisted production of hydrogen
[DE88-001621] N88-13425
Soluble metal chelate polymers of coordination numbers six, seven and eight
[AD-A185094] N88-13459
The role of electronic structure calculation in mechanistic analysis of electron transfer reactions in the liquid phase
[DE87-014395] N88-13963
**LIGHT (VISIBLE RADIATION)**
Solitons in stimulated Raman scattering: Generation and control of ultrashort optical pulses
[AD-A185141] N88-13983
**LIGHT ALLOYS**
Materials for fighter aircraft N88-13325
**LIGHT AMPLIFIERS**
An experimental study of CW HF chemical laser amplifier performance and zero power gain
[AD-A185241] N88-13584
**LIGHT BEAMS**
Optoelectronic measurement methods for ballistic experiments
[PB87-110706] N88-13554
**LIGHT IONS**
Energy dependence of ion-induced sputtering yields of monatomic solids in the low energy region
[IPPJ-AM-52] N88-13988
**LIGHT SCATTERING**
Extinction by dielectric particles at optical and infrared wavelength
[AD-A184818] N88-13981
**LIGHT SCATTERING METERS**
Study of the properties of a new detector class for liquid chromatography
[DE88-001666] N88-13426
**LIGHT SOURCES**
Anti-Stokes generation of 226 nm light
[DE88-001612] N88-13590
**LIGHT TRANSMISSION**
Optical probe
[EP-PATENT-0-210-869-A1] N88-13984
**LIMITERS (FUSION REACTORS)**
ALT-1 pump limiter experiments
[DE88-000822] N88-13989
**LINE SPECTRA**
A computer code to calculate line by line atmospheric transmission spectra on a microcomputer
[NASA-TM-100686] N88-13372
Narrow linewidth gain measurements in a KrF excimer amplifier pumped longitudinally by a high-power electron beam
[DE88-001365] N88-13575
An adaptive lattice algorithm for spectral line estimation
[AD-A184970] N88-13876
**LINEAR ACCELERATORS**
Development of a laced electromagnetic wiggler
[DE88-000972] N88-13953
Heavy-ion accelerator research for inertial fusion
[DE88-000541] N88-14001
**LINEAR EQUATIONS**
Eigenvalue projection theory for linear operator equations of electromagnetics
[AD-A185434] N88-13504
**LINEAR QUADRATIC GAUSSIAN CONTROL**
Design of low order controllers for robust disturbance rejection in large space structures
[AD-A185202] N88-13376
**LINEAR SYSTEMS**
Tridiagonal approximate factorization method: A preconditioning technique for solving nonsymmetric linear systems suitable to supercomputers N88-13271
Equivalence of input-output stability and exponential stability for infinite dimensional systems
[TW-276] N88-13903
Robustness of linear systems
[PB87-220042] N88-13909
**LINEARITY**
Numerical methods for reaction-diffusion problems with non-differentiable kinetics
[AD-A185405] N88-13923
**LINEARIZATION**
Numerical analysis of supersonic flows using panel method N88-13266
**LIPIDS**
Development of microencapsulation techniques
[AD-A185019] N88-13457
**LIQUID CHROMATOGRAPHY**
Study of the properties of a new detector class for liquid chromatography
[DE88-001666] N88-13426
**LIQUID OXYGEN**
Seal technology for liquid oxygen (LOX) turbopumps
[NASA-CR-174866] N88-13603
Fluid mass and thermal loading effects on the modal characteristics of space shuttle main engine liquid oxygen inlet splitter vanes N88-13628
**LIQUID PHASES**
The role of electronic structure calculation in mechanistic analysis of electron transfer reactions in the liquid phase
[DE87-014395] N88-13963
**LIQUID ROCKET PROPELLANTS**
Dynamics of propellant feedline systems
[AD-A184865] N88-13537
**LIQUIDS**
Statistical process control applied to the liquid-fed ceramic melter process
[DE88-000271] N88-13471
Molecular dynamics studies of aromatic hydrocarbon liquids
[DE88-001473] N88-13973
**LITHIUM**
Survey state of the art: Electrical load management techniques and equipment
[AD-A184083] N88-13517
A fluid simulation of the AMPTE lithium gas releases in the solar wind
[TRITA-EPP-87-06] N88-14056
**LITHIUM ALLOYS**
On the role of crack tip shielding in influencing the behavior of long and small fatigue cracks in aluminum-lithium alloy 2090 N88-13671
Variable amplitude fatigue crack growth in aluminum alloys 2090-T8E41 and 7075-T651 N88-13687
**LOAD DISTRIBUTION (FORCES)**
Physiological determinants of load bearing capacity
[AD-A184977] N88-13848
**LOAD TESTS**
Control of a flexible one-link manipulator
[AD-A185035] N88-13598
An optical interferometry technique to evaluate closure along a crack front N88-13726
Deformation, fatigue and fracture behavior of two cast anisotropic superalloys N88-13732
**LOADS (FORCES)**
Static aeroelastic considerations in the definition of design loads for fighter airplanes N88-13351
An analytical study of the effects of transverse shear deformation and anisotropy on buckling loads of laminated cylinders
[NASA-TM-100508] N88-13387
The simulation of the viscous flow around a cylinder by the random vortex method N88-13534
A dislocation model for fatigue crack propagation under variable amplitude loading N88-13683
Observations on the effect of overloads on fatigue crack growth N88-13684
Variable amplitude fatigue crack growth in aluminum alloys 2090-T8E41 and 7075-T651 N88-13687
Fatigue of 30CrMnSiNi2A notched specimens under spectrum loading N88-13689
Damping analysis of flexural waves in fluid-loaded single and constrained plates
[AD-A185116] N88-13739
Fluctuating pressure loads under high speed boundary layers
[NASA-TM-100517] N88-13962
**LOCAL AREA NETWORKS**
Introduction to local area network design on Ariane 5 and future launchers
[SNIAS-872-422-102] N88-13886
**LOG PERIODIC ANTENNAS**
The use of coaxial transmission line elements in log-periodic dipole arrays
[AD-A184864] N88-13499
**LOGARITHMS**
Freidlin-Wentzell type estimates and the law of the iterated logarithm for a class of stochastic processes related to symmetric statistics
[AD-A185366] N88-13944
**LOGIC CIRCUITS**
An exact analysis and performance of framed ALOHA with capture
[AD-A185006] N88-13500
New breakthrough in Chinese integrated circuits: Successful development of high-speed CMOS circuits
[AD-A185381] N88-13525
Implementation of an FIR band pass filter using a bit-slice processor
[AD-A184895] N88-13875
**LOGIC PROGRAMMING**
Near-horn prolog
[AD-A185172] N88-13880
**LOGISTICS**
A functional interpretation of the logistic equation
[REPT-87-037] N88-13946
**LONG TERM EFFECTS**
Lifting bodies: An attractive aerodynamic configuration choice for hypervelocity vehicles N88-13248
A study of charged particles/radiation damage to VLSI device materials
[NASA-CR-172036] N88-13518
Contributions of lidar measurements to the study of long term variations of the middle atmosphere
[ETN-88-91237] N88-13824
**LOW ALTITUDE**
Development of an acoustic echosounder for detection of lower level atmospheric turbulence
[AD-A184877] N88-13831
**LOW CARBON STEELS**
The growth behavior of small fatigue cracks; the effect of microstructure and crack closure N88-13673
A study of fatigue crack growth life under random stresses N88-13685
**LOW CURRENTS**
Low-current behavior and current chopping of vacuum arcs
[ISBN-90-9001649-X] N88-13529
**LOW REYNOLDS NUMBER**
Low Reynolds number influence on aerodynamic performance of hypersonic lifting vehicles N88-13230
**LOW SPEED**
A swept wing panel in a low speed flexible walled test section
[NASA-CR-4106] N88-13292
**LOW TEMPERATURE ENVIRONMENTS**
The initiation and growth of small fatigue cracks in copper at room and cryogenic temperatures N88-13668
**LOW VACUUM**
Low jitter laser-triggered high-voltage vacuum switch using low laser energies
[DE88-001922] N88-13576
**LUBRICANTS**
Analysis of wear metals in engine oils using the atomic absorption spectrophotometric method
[NAL-TM-MT-8704] N88-13435
**LUBRICATION SYSTEMS**
Literature review of solid lubrication mechanisms
[AD-A185010] N88-13456
**LUMINESCENCE**
Performance characteristics of magnesium-sodium nitrate flares in oxygen-nitrogen atmospheres
[AD-A185274] N88-13476

## M

**MACH NUMBER**
Fundamentals of fighter aircraft design: Engine intake and afterbody N88-13322
**MACHINE TOOLS**
A passive vibration-cancelling isolation mount N88-13636
**MAGNESIUM**
Investigation by differential scanning calorimetry of microstructure in a superplastic Al-Mg-Zr alloy
[AD-A184902] N88-13439
The influence of slip mechanism on fatigue of Mg and Mg-2.3Li N88-13672
**MAGNESIUM ALLOYS**
Cyclic deformation of an extruded AlMgSi alloy N88-13654

The influence of microstructure and residual stresses on the initiation and propagation of short surface cracks on AlMgSi1 N88-13674

Characterization of the microstructures of various materials
[AD-A184961] N88-14017

**MAGNESIUM COMPOUNDS**

Performance characteristics of magnesium-sodium nitrate flares in oxygen-nitrogen atmospheres
[AD-A185274] N88-13476

**MAGNET COILS**

Development of a strong electromagnet wiggler
[DE88-000971] N88-13952

**MAGNETIC COILS**

Scaling the electromagnetically driven explosive shock simulator N88-13612

**MAGNETIC FIELD CONFIGURATIONS**

Reversed field pinch plasmas with various boundary conditions
[DE88-000832] N88-14004

A fluid simulation of the AMPTE lithium gas releases in the solar wind
[TRITA-EPP-87-06] N88-14056

Magnetic field draping about coronal mass ejecta
[DE88-001805] N88-14057

**MAGNETIC FLUX**

Reversed field pinch plasmas with various boundary conditions
[DE88-000832] N88-14004

The appearance and disappearance of magnetic flux on the quiet sun
[AD-A185432] N88-14055

**MAGNETIC PROPERTIES**

Effect of rapid solidification on short-range order: A magnetic study
[AD-A185216] N88-13444

**MAGNETIC RECORDING**

Simulation of the perpendicular magnetic recording process
[B8713537] N88-13570

**MAGNETOHYDRODYNAMIC FLOW**

Subcommittee for MHD theory
[DE88-000596] N88-14003

Numerical models for high beta magnetohydrodynamic flow
[DE88-001850] N88-14008

**MAGNETOHYDRODYNAMIC STABILITY**

A review of the experimental and theoretical status of the reversed-field pinch
[DE88-000529] N88-14000

Reversed field pinch plasmas with various boundary conditions
[DE88-000832] N88-14004

**MAGNETOHYDRODYNAMIC TURBULENCE**

Evolution of mean square magnetic vector potential in compressible, two-dimensional, magnetofluid turbulence
[AD-A184985] N88-13990

**MAGNETOSPHERE**

Activities report of the Ionospheric Observatory
[UIO-SR-87-01] N88-13827

Laboratory and near-earth space plasma as a key to the plasma universe
[TRITA-EPP-87-09] N88-13996

**MAGNETOSPHERIC ION DENSITY**

The polar ionosphere and interplanetary field
[AD-A185386] N88-13822

**MAINTENANCE**

Avionic corrosion N88-13332

US Naval Air Force avionic and electrical system corrosion prevention and control maintenance N88-13334

**MANAGEMENT INFORMATION SYSTEMS**

University research initiative research program summaries
[AD-A184876] N88-14035

**MANAGEMENT METHODS**

A study of the Department of Defense configuration management policies and procedures as applied to the FA-18 Strike/Fighter program
[AD-A184872] N88-14034

**MANEUVERABILITY**

Airframe/store compatibility N88-13323

**MANGANESE**

Effects of MN dispersoids on near threshold fatigue crack growth in 2134 type alloys N88-13692

**MANIFOLDS (MATHEMATICS)**

Transient periodic behavior related to a saddle-node bifurcation
[ETN-88-91321] N88-13928

**MANIPULATORS**

Modeling and control of large flexible vehicles in the atmosphere and space
[AD-A185368] N88-13377

Control of a flexible one-link manipulator
[AD-A185035] N88-13598

Trajectory control of robot manipulators with closed-kinematic chain mechanism
[NASA-TM-89305] N88-13605

Cartesian path control of a two-degree-of-freedom robot manipulator
[NASA-CR-182331] N88-13908

**MANNED SPACE FLIGHT**

National Aeronautics and Space Administration space station proposal, fiscal year 1988
[S-HRG-100-328] N88-14043

Preliminary estimates of galactic cosmic ray exposures for manned interplanetary missions
[NASA-TM-100519] N88-14058

**MANUALS**

US Naval Air Force avionic and electrical system corrosion prevention and control maintenance N88-13334

**MANUFACTURING**

Avionics and corrosion N88-13336

**MAPPING**

Scientific and Operational Requirements for TOMS Data
[NASA-CP-2497] N88-13774

Observation guidelines for a Total Ozone Mapping Spectrometer (TOMS) in geosynchronous orbit N88-13801

**MARINE BIOLOGY**

Varifront 3 expedition data report (USNS DE STEIGUER CRUISE 1202-82). Bioluminescence, hydrographic, nutrient, and satellite data from the Gulf of California (November-December 1981)
[AD-A185011] N88-13805

**MARINE ENVIRONMENTS**

Estimation of marine boundary layer depth and relative humidity with multispectral satellite measurements
[AD-A184881] N88-13804

**MARKET RESEARCH**

Study of the feasibility of a satellite communication system for road transportation home office to vehicle communication. Volume 2: Market study
[SC/87-E/6-VOL-2] N88-13506

National Point Of Contact (NPOC)-SPOT inquiry 1986
[NLR-MP-86055-U] N88-13807

**MARKETING**

Production of jet fuels from coal derived liquids. Volume 1: Market assessment for liquid by-products from the Great Plains gasification plant
[AD-A184846] N88-13475

**MARKOV PROCESSES**

Overlooked potential of systems with Markovian coefficients
[NLR-MP-86049-U] N88-13366

**MARS (PLANET)**

An evolutionary communications scenario for Mars exploration
[NASA-TM-100263] N88-13515

**MARS SURFACE**

An evolutionary communications scenario for Mars exploration
[NASA-TM-100263] N88-13515

**MASS**

The effect of maximum-allowable payload temperature on the mass of a multimegawatt space-based platform
[DE88-001921] N88-13381

Fluid mass and thermal loading effects on the modal characteristics of space shuttle main engine liquid oxygen inlet splitter vanes N88-13628

**MASS FLOW**

Combustion characteristics of gas turbine alternative fuels
[NASA-TM-100247] N88-13338

**MASS SPECTROMETERS**

The tail lobe ion spectrometer: Theory and observations
[IFSI-86-12] N88-13569

**MASS SPECTROSCOPY**

Supersonic beam observations of semiconductor clusters
[AD-A184991] N88-14018

**MASS TRANSFER**

Study of the effect of mass transfer on a transonic boundary layer. Application to flow relaminarization
[ETN-88-91169] N88-13296

Systematic stratospheric-tropospheric exchange viewed from isentropic coordinates N88-13777

**MATHEMATICAL MODELS**

Computation of rime ice accretion on airfoils
[FFA-TN-1987-08] N88-13301

Non-linear maximum likelihood estimation of stability derivatives from range data
[NAL-TM-SE-8608] N88-13365

Development of an integrated BEM approach for hot fluid structure interaction
[NASA-CR-181577] N88-13384

Models for the degradation of stratified composite structures
[ONERA-RT-13/3542-RY-061-R] N88-13395

OH(A-X) fluorescence from photodissociative excitation of HO2 at 157.5 nm
[NASA-CR-181580] N88-13429

A mathematical model of high alloy nickel base high temperature alloys
[BLL-M-37381-(5828.4)] N88-13436

Noise modelling in the time domain with the aid of Spice
[PB87-221941] N88-13492

Large bandwidth ground scattering model --- radar scattering
[FOA-C-30458-3.2] N88-13511

Conditional second order closure for turbulent shear flows
[AD-A185369] N88-13542

Active and passive plume distribution models in the convective boundary layer using a large eddy simulation model
[KNMI-TR-90] N88-13546

Model-based motion estimation and its application to restoration and interpolation of motion pictures
[AD-A185054] N88-13558

Simulation of the perpendicular magnetic recording process
[B8713537] N88-13570

Theoretical studies of solar lasers and converters
[NASA-CR-181569] N88-13577

Control of a flexible one-link manipulator
[AD-A185035] N88-13598

Non-linear shipboard shock analysis of the Tomahawk missile shock isolation system N88-13614

Analysis of photopole data reduction models N88-13616

Initial dynamic load estimates during configuration design N88-13621

Significance of fatigue crack closure under spectrum loading N88-13662

Low cycle fatigue life predictions of a 1CrMoV steel in terms of a J-controlled short crack growth model N88-13665

A unified model for fatigue crack initiation, short crack growth, long crack propagation, and closure effects N88-13680

A dislocation model for fatigue crack propagation under variable amplitude loading N88-13683

Observations on the effect of overloads on fatigue crack growth N88-13684

Computer aided modeling and fatigue failure forecast under stochastic loading N88-13720

Fatigue under nonnormal random stresses using Monte Carlo method N88-13723

Applications of fatigue analyses: Transportation N88-13733

The application of doubly-truncated hydrometeor distributions to numerical cloud models
[AD-A185273] N88-13836

Modeling cloudy and clear interval length probabilities using space shuttle imagery
[AD-A185290] N88-13837

Human thermoregulatory model for whole body immersion in water at 20 and 28 C
[AD-A185052] N88-13849

Optimal control of large space structures via generalized inverse matrix
[NASA-CR-182336] N88-13907

Multidimensional least squares fitting of fuzzy models
[AD-A185148] N88-13916

The estimation of basic matrices using travel intensity theorems
[REPT-87-13] N88-13926

SHARP simulation of discontinuities in highly convective steady flow
[NASA-TM-100240] N88-13931

Sample reuse in statistical remodeling
[AD-A184916] N88-13938

Presentation of a computer program permitting the exploitation of tests designed to determine the sensitivity of one shot devices to a parameter. Application to a degenerate one shot sequence
[SNIAS-872-430-117] N88-13945

The interaction of DC plasma jet with a melting metal: Experimental measurements and mathematical description
[AD-A185173] N88-13993

Numerical models for high beta magnetohydrodynamic flow
[DE88-001850] N88-14008

**MATRICES (MATHEMATICS)**

Reduced order optimal command applied to longitudinal automatic pilots
[SNIAS-872-111-114] N88-13362

Mechanics of anisotropic media. Study of the boundary conditions --- stratified composites
[SNIAS-872-430-112] N88-13404
The matrix exponential in transient structural analysis N88-13619
Simultaneous structural and control optimization via linear quadratic regulator eigenstructure assignment N88-13622
Illustrative examples of principal component analysis using BMDP/4M
[AD-A185179] N88-13881
Structuring data for concurrent vectorized processing in a transient dynamics finite element program
[DE87-013082] N88-13890
Optimal control of large space structures via generalized inverse matrix
[NASA-CR-182336] N88-13907
Eigenvectors of distance-regular graphs
[AD-A185375] N88-13919
Computation of natural frequencies of planar lattice structure
[AD-A185387] N88-13920
The estimation of basic matrices using travel intensity theorems
[REPT-87-13] N88-13926
Illustrative examples of principal component analysis using SYSTAT/FACTOR
[AD-A184920] N88-13939

**MATRIX MATERIALS**
Composite materials with glass matrix
[SGR/PR-4305/86-SV/JC] N88-13394
Fabrication of composites by chemical vapor deposition
[DE87-014565] N88-13408

**MATRIX METHODS**
Structural optimization in the design process --- aircraft
[SNIAS-872-111-115] N88-13885

**MATRIX THEORY**
The matrix exponential in transient structural analysis N88-13619

**MAXIMUM ENTROPY METHOD**
Restoration of particle pitch angle distribution functions by a maximum entropy algorithm
[ATR-86(7098)-3] N88-13969

**MAXIMUM LIKELIHOOD ESTIMATES**
Non-linear maximum likelihood estimation of stability derivatives from range data
[NAL-TM-SE-8608] N88-13365
Approximating multivariate normal orthant probabilities using the Clark algorithm
[AD-A184855] N88-13873
The maximum likelihood estimator method of image reconstruction: Its fundamental characteristics and their origin
[DE88-000462] N88-13892
Presentation of a computer program permitting the exploitation of tests designed to determine the sensitivity of one shot devices to a parameter. Application to a degenerate one shot sequence
[SNIAS-872-430-117] N88-13945

**MEAN SQUARE VALUES**
Evolution of mean square magnetic vector potential in compressible, two-dimensional, magnetofluid turbulence
[AD-A184985] N88-13990

**MEASURING INSTRUMENTS**
New approach to telemetry development will significantly increase productivity of Joint Test Assembly (JTA) teams
[DE88-001676] N88-13373

**MECHANICAL DEVICES**
Mechanical design of the ac bracket package for the RETE experiment
[IFSI-87-4] N88-13379

**MECHANICAL PROPERTIES**
Micromechanics of the degradation of composite materials
[SNIAS-872-430-113] N88-13405
Mechanical property evaluation of a series of commercial tungsten alloys
[AD-A185440] N88-13446
The evolution of local mechanical properties of Al 2219-T851 during fatigue N88-13653

**MECHANICAL SHOCK**
The 58th Shock and Vibration Symposium, volume 1
[NASA-CP-2488-VOL-1] N88-13809
Conservatism implications of shock test tailoring for multiple design environments N88-13811
Scaling the electromagnetically driven explosive shock simulator N88-13812
Initial dynamic load estimates during configuration design N88-13821
Optimal shock isolation with minimum settling time N88-13833

**MELTING**
Advances in processing techniques for nickel aluminides
[DE87-014571] N88-13449
Statistical process control applied to the liquid-fed ceramic melter process
[DE88-000271] N88-13471
Results from the melting of tungsten composites under microgravity (TEXUS 10 flight)
[FOA-C-20676-2.1] N88-13482

**MEMORY (COMPUTERS)**
A rudimentary database for three-dimensional objects using structural representation
[CSE-87-00004] N88-13597
Storing and retrieving data in a parallel distributed memory system
[AD-A185177] N88-13897

**MENTAL PERFORMANCE**
Taskomat, a task battery for information processing
[IZF-1987-2] N88-13851

**MERIDIONAL FLOW**
Systematic stratospheric-tropospheric exchange viewed from isentropic coordinates N88-13777

**MESOSCALE PHENOMENA**
Mesoscale applications of high resolution imagery
[AD-A185039] N88-13833

**METABOLISM**
Human thermoregulatory model for whole body immersion in water at 20 and 28 C
[AD-A185052] N88-13849

**METAL BONDING**
Analysis of end stresses in glass-metal bimaterial strips
[DE87-007848] N88-13750

**METAL COATINGS**
The analysis of metal finishing solutions by ion chromatography
[AD-A184812] N88-13414
Ion plating for corrosion control
[AD-A185061] N88-13442

**METAL FATIGUE**
Welded joint fatigue of a AISI 304 L type stainless steel
[DE87-703530] N88-13607
Fatigue 87, volume 1
[AD-A184045] N88-13645
Cyclic deformation and crack initiation N88-13646
Effect of grain orientation on the origination and the initial growth of fatigue cracks in pure iron N88-13647
The growth of persistent slip bands N88-13648
The mechanics of fatigue-crack nucleation in a low-alloy steel under fretting conditions N88-13649
Surface deformation and fatigue crack initiation of alpha-iron N88-13651
The effect of ion beam mixed Ni-Al surface layers on PSB extrusion morphology in fatigued nickel N88-13652
The evolution of local mechanical properties of Al 2219-T851 during fatigue N88-13653
Cyclic deformation of an extruded AlMgSi alloy N88-13654
Closure behavior under constant effective stress intensity loading conditions N88-13656
Growth of short fatigue cracks in a squeeze formed aluminum alloy N88-13658
Influence of microstructure and aging condition on the fatigue crack propagation in age hardened aluminium alloys N88-13659
Fatigue crack growth behavior of A356-T6 cast aluminum alloy N88-13660
Striations and the fatigue growth mechanism in a micro-alloyed steel N88-13661
Significance of fatigue crack closure under spectrum loading N88-13662
Near-threshold short crack growth behavior in Nimonic 105 N88-13663
Fatigue crack propagation of short and long cracks: Phys. basis, prediction methods and engineering significance N88-13664
Low cycle fatigue life predictions of a 1CrMoV steel in terms of a J-controlled short crack growth model N88-13665
The statistics of the shape of small fatigue cracks N88-13666
The effect of alpha platelet morphology and beta-grain size on the initiation and growth of short fatigue cracks in Ti65S N88-13667
The initiation and growth of small fatigue cracks in copper at room and cryogenic temperatures N88-13668
On the role of crack tip shielding in influencing the behavior of long and small fatigue cracks in aluminum-lithium alloy 2090 N88-13671
The influence of slip mechanism on fatigue of Mg and Mg-2.3Li N88-13672
The growth behavior of small fatigue cracks; the effect of microstructure and crack closure N88-13673
The influence of microstructure and residual stresses on the initiation and propagation of short surface cracks on AlMgSi1 N88-13674
Threshold stress for fatigue crack initiation from a small crack N88-13675
An experimental study of closure behavior of naturally initiated small cracks N88-13676
Behavior of long and short fatigue cracks in a powder metallurgy superalloy at room and at high temperature N88-13677
Propagation of small fatigue cracks in 2024-T3 aluminum alloy N88-13678
Closure and propagation behavior of short fatigue cracks at different R-ratios N88-13679
A unified model for fatigue crack initiation, short crack growth, long crack propagation, and closure effects N88-13680
Fatigue crack retardation in aluminium alloys N88-13681
Fatigue crack growth under random overloads N88-13682
A dislocation model for fatigue crack propagation under variable amplitude loading N88-13683
Observations on the effect of overloads on fatigue crack growth N88-13684
A study of fatigue crack growth life under random stresses N88-13685
Crack growth in contrasting titanium alloys under the conjoint action of high and low cycle fatigue N88-13686
Variable amplitude fatigue crack growth in aluminum alloys 2090-T8E41 and 7075-T651 N88-13687
Fatigue of 30CrMnSiNi2A notched specimens under spectrum loading N88-13689
The how and why of variable amplitude testing N88-13690
Near-threshold growth of defects in engineering materials N88-13691
Interaction of microstructure and fatigue in tool steels N88-13693
Tensile mean stress effects on uniaxial fatigue behavior of 1045 HR steel N88-13694
Fatigue strength of alloy A286 at cryogenic temperature N88-13695
The initiation and growth of fatigue cracks in carburised 9Cr1Mo steel N88-13696
Fretting wear and fretting fatigue damage N88-13697
The role of inclusions in corrosion fatigue crack initiation in Q1N N88-13699
A study of corrosion fatigue crack initiation, growth and the threshold condition under variable amplitude loading N88-13701
The influence of crack conditions on hydrogen uptake by steels N88-13702
Occurance and growth of fatigue cracks in corrosion environment N88-13704
The effect of environment on low cycle fatigue properties in HSLA steel N88-13705
Coupling effects between the ferrite and austenite phases during corrosion fatigue of a ferrite/austenite duplex stainless steel N88-13706
Development of research on fatigue of spot-weld in automobile structures in Japan N88-13728
Environmentally assisted fatigue crack growth N88-13731
Deformation, fatigue and fracture behavior of two cast anisotropic superalloys N88-13732
Fatigue crack growth N88-13734

**METAL FINISHING**
The analysis of metal finishing solutions by ion chromatography
[AD-A184812] N88-13414

**METAL MATRIX COMPOSITES**
Plasma joining of metal matrix composites
[AD-A184828] N88-13390
Micromechanisms of fatigue crack growth and fracture toughness in metal matrix composites
[AD-A185200] N88-13392

**METAL OXIDE SEMICONDUCTORS**
A study of charged particles/radiation damage to VLSI device materials
[NASA-CR-172036] N88-13518

**METAL OXIDES**
Activated metal oxide surfaces as highly basic and reducing environments
[AD-A184958] N88-13417

**METAL PLATES**
Water disbondment characterization of organic Coating/metal substrate systems
[AD-A184847] N88-13454
Numerical simulations of impact tests on a rigid wall --- armor steel
[SNIAS-872-320-102] N88-13744

**METAL SHEETS**
Behavior of short cracks in a 2024 aluminum alloy sheet tested at several stress ratios N88-13669

**METAL SURFACES**
Master plots for predicting the case-depth in laser surface treatments
[PB87-221875] N88-13574
The effect of ion beam mixed Ni-Al surface layers on PSB extrusion morphology in fatigued nickel
N88-13652
The influence of the topography of fracture surfaces on crack closure N88-13657
Atomic beam studies of the interaction of hydrogen with transition metal surfaces
[DE88-000208] N88-13970

**METALS**
Analysis of wear metals in engine oils using the atomic absorption spectrophotometric method
[NAL-TM-MT-8704] N88-13435
Molecular-level synthesis and characterization of metal-polymer interfaces
[AD-A184956] N88-13455
Photocurrent generation from basic metals, utilizing a short pulsed ArF excimer laser
[AD-A184928] N88-13579
The orientations of dipolar walls produced by cyclic deformation N88-13655
The interaction of DC plasma jet with a melting metal: Experimental measurements and mathematical description
[AD-A185173] N88-13993

**METASTABLE STATE**
The gamma-ray laser project
[AD-A184824] N88-13578

**METEOROLOGICAL PARAMETERS**
Global atmospheric circulation statistics: Four year averages
[NASA-TM-100690] N88-13842

**METEOROLOGICAL RADAR**
Specification of predictors necessary for the determination of over or underestimation of radar derived total rainfall
[AD-A185383] N88-13838

**METEOROLOGICAL SATELLITES**
Fabricate, calibrate and test a dosimeter for integration into the CRRES (Combined Release and Radiation Effects Satellite) satellite
[AD-A185439] N88-13564
Estimation of marine boundary layer depth and relative humidity with multispectral satellite measurements
[AD-A184881] N88-13804

**METEOROLOGY**
Application of TOMS data to weather analysis models
N88-13787

**METEOSAT SATELLITE**
Study on data compression systems for operational remote sensing --- meteosat imagery
[NLR-TR-86029-L] N88-13808

**METHANE**
Pulsed plasma jet igniters: Species measurements in methane combustion
[DE88-001389] N88-13422

**METHYL COMPOUNDS**
Thermally stable aromatic structures from acyclic precursors. 1. Para polyphenylene model compounds from 3-Dimethyl amino hex-5-EN-1-YNES
[AD-A185300] N88-13462

**MEXICO**
Varifront 3 expedition data report (USNS DE STEIGUER CRUISE 1202-82). Bioluminescence, hydrographic, nutrient, and satellite data from the Gulf of California (November-December 1981)
[AD-A185011] N88-13805

**MICROCHANNELS**
A focussed MCP (microchannel plate) image intensifier type for high speed gating
[DE88-000480] N88-13555

**MICROCOMPUTERS**
A computer code to calculate line by line atmospheric transmission spectra on a microcomputer
[NASA-TM-100686] N88-13372
An extension to the multilevel logic simulator for microcomputers
[AD-A185032] N88-13879

**MICROCRACKS**
Environmentally assisted cracking: Overview of evidence for an adsorption-induced localised-slip process
[AD-A185175] N88-13443
The orientations of dipolar walls produced by cyclic deformation N88-13655
Crack propagation properties of sintered steel
N88-13698
The effect of environment on low cycle fatigue properties in HSLA steel N88-13705
X-ray fatigue failure prediction based on plasticity response to microcracks N88-13725

**MICROELECTRONICS**
Electromagnetics and electrothermal approach to evaluate failures in microelectronic devices caused by electrostatic discharges: Stochastical aspects of the device reliability
[AD-A184906] N88-13522

**MICROPROCESSORS**
Test and evaluation of the transputer in a multi-transputer system
[AD-A184969] N88-13859

**MICROSTRUCTURE**
Study of the influence of mechanical - thermal treatments on the creep behavior of a niobium stainless steel
[DE87-703506] N88-13431
Investigation by differential scanning calorimetry of microstructure in a superplastic Al-Mg-Zr alloy
[AD-A184902] N88-13439
Ion plating for corrosion control
[AD-A185061] N88-13442
Effect of rapid solidification on short-range order: A magnetic study
[AD-A185216] N88-13444
Effect of rapid solidification on stainless steel weld metal microstructures and its implications on the Schaeffler diagram
[DE88-001489] N88-13451
United States - Japan Workshop on Dielectric and Piezoelectric Ceramics (3rd) held in Toyama, Japan on November 9-12, 1986
[AD-A185113] N88-13460
Fatigue 87, volume 1
[AD-A184045] N88-13645
The influence of the topography of fracture surfaces on crack closure N88-13657
Influence of microstructure and aging condition on the fatigue crack propagation in age hardened aluminium alloys N88-13659
The effect of microstructure on the surface crack length: Crack depth relationship for short cracks N88-13670
The growth behavior of small fatigue cracks; the effect of microstructure and crack closure N88-13673
The influence of microstructure and residual stresses on the initiation and propagation of short surface cracks on AlMgSi1 N88-13674
Propagation of small fatigue cracks in 2024-T3 aluminum alloy N88-13678
Interaction of microstructure and fatigue in tool steels
N88-13693
Deformation mechanisms and crack initiation in fatigue N88-13730
Environmentally assisted fatigue crack growth
N88-13731
Fatigue crack growth N88-13734
Characterization of the microstructures of various materials
[AD-A184961] N88-14017

**MICROWAVE EQUIPMENT**
Evaluation of device figure of merit in microwave switching circuit design
[AD-A184896] N88-13520
Observation guidelines for a Total Ozone Mapping Spectrometer (TOMS) in geosynchronous orbit
N88-13801

**MICROWAVE OSCILLATORS**
Optically tuned MM-wave IMPATT source
[AD-A185250] N88-13523
High peak power ka-band gyrotron oscillator experiment
[AD-A185424] N88-13563

**MICROWAVE RADIOMETERS**
In-orbit calibration adjustment of the Nimbus-7 SMMR
[NASA-TM-100678] N88-13773

**MICROWAVE SOUNDING**
Determination of total ozone from HIRS2/MSU sounding data N88-13799

**MICROWAVE SWITCHING**
Evaluation of device figure of merit in microwave switching circuit design
[AD-A184896] N88-13520

**MICROWAVES**
United States - Japan Workshop on Dielectric and Piezoelectric Ceramics (3rd) held in Toyama, Japan on November 9-12, 1986
[AD-A185113] N88-13460
Microwave challenges to the thermoregulatory system
[AD-A185391] N88-13847
Microwave superheaters for fusion
[DE88-001656] N88-14007

**MIDDLE ATMOSPHERE**
Contributions of lidar measurements to the study of long term variations of the middle atmosphere
[ETN-88-91237] N88-13824

**MIE SCATTERING**
Extinction by dielectric particles at optical and infrared wavelength
[AD-A184818] N88-13981

**MILITARY AIR FACILITIES**
ZEUS: A knowledge-based expert system that assists in predicting visibility at airbases
[AD-A184197] N88-13829

**MILITARY OPERATIONS**
High resolution satellite imagery simulation --- treaty verification
[FOA-C-30462-3.3,9.3] N88-13810

**MILITARY TECHNOLOGY**
Fuel cells --- military applications
[PML-1986-43] N88-13813
University research initiative research program summaries
[AD-A184876] N88-14035

**MILLIMETER WAVES**
An investigation of millimeter wave propagation in the atmosphere: Measurement program
[AD-A184837] N88-13498
Optically tuned MM-wave IMPATT source
[AD-A185250] N88-13523

**MINERAL DEPOSITS**
Proceedings of the Third Airborne Imaging Spectrometer Data Analysis Workshop
[NASA-CR-181552] N88-13755
Preliminary results from an investigation of AIS-1 data over an area of epithermal alteration: Plateau, Northern Queensland, Australia N88-13768

**MINICOMPUTERS**
Error propagation in a digital avionic mini processor
[NASA-CR-181565] N88-13872

**MINIMAX TECHNIQUE**
Control of an unstable launcher in atmospheric flight using minimax optimal control laws
[SNIAS-872-422-107] N88-13901

**MISSILE CONFIGURATIONS**
Utilization of dynamic characteristics of materials to optimize military explosive charges. Application to antiship devices
[SNIAS-872-320-101] N88-13743

**MISSILE TRACKING**
Use of the global positioning system for trajectory determination of SRAM 2 missiles at the Eastern Test Range
[AD-A185266] N88-13314

**MISSILE TRAJECTORIES**
Use of the global positioning system for trajectory determination of SRAM 2 missiles at the Eastern Test Range
[AD-A185266] N88-13314

**MISSILES**
High resolution ultraviolet filter development
[AD-A184183] N88-13979

**MISSING MASS (ASTROPHYSICS)**
Comments on H. Arp The persistent problem of spiral galaxies
[TRITA-EPP-87-05] N88-14052

**MISSION PLANNING**
Mission requirements and aircraft sizing N88-13317
Space station systems: A bibliography with indexes
[NASA-SP-7056(05)] N88-13382

**MIST**
Investigation of the nature and concentration of vapor and mist during the cleaning of aircraft
[PML-1985-29] N88-13817

**MIXERS**
A GaAs MESFET balanced mixer with very low intermodulation
[AD-A184848] N88-14015

**MIXING**
The effect of ion beam mixed Ni-Al surface layers on PSB extrusion morphology in fatigued nickel
N88-13652

**MOBILE COMMUNICATION SYSTEMS**
Measured characteristics of 800/900 MHz mobile radio channels with high-angle propagation through moderately dense foliage
[CRC-1398] N88-13493
Two-signal cross modulation effects, half-IF effects and interference criteria in land mobile sharing with UHF (Ultra High Frequency) television
[PB87-228037] N88-13514

**MOBILITY**
Dealing with unanticipated events in autonomous navigation
[DE88-000590] N88-13602

**MODAL RESPONSE**
Modal survey of the space shuttle solid rocket motor using multiple input methods N88-13617
A new method to real-normalize measured complex modes N88-13618
Improvement of modal scaling factors using mass additive technique N88-13620
Viscous damped space structure for reduced jitter
N88-13623
On the glitches in the force transmitted by an electrodynamic exciter to a structure N88-13624

**MODELS**
Full-envelope aerodynamic modeling of the Harrier aircraft
[NASA-TM-88376] N88-13363
Model helicopter rotor rig and associated strain gauge balance for performance studies
[NAL-TM-AE-8704] N88-13364
Damping analysis of flexural waves in fluid-loaded single and constrained plates
[AD-A185116] N88-13739
Performability modeling based on real data: A casestudy
[NASA-CR-181563] N88-13870
Example of correlation between space and spin coordinates
[DE87-703366] N88-14030
**MODULATION**
Study of electrostatic modulation of fuel sprays to enhance combustion performance in an aviation gas turbine
[AD-A184967] N88-13341
Two-signal cross modulation effects, half-IF effects and interference criteria in land mobile sharing with UHF (Ultra High Frequency) television
[PB87-228037] N88-13514
**MOIRE FRINGES**
Optical deformation measurement on shells following the raster principle
[ETN-88-90608] N88-13741
**MOLDING MATERIALS**
High explosive moulding powders from RDX and aqueous polyurethane dispersions
[AD-A185026] N88-13458
**MOLECULAR ABSORPTION**
MODTRAN: A moderate resolution model for LOWTRAN
[AD-A185384] N88-13503
**MOLECULAR BEAM EPITAXY**
MBE growth of InAsSb strained-layer superlattices
[DE88-000365] N88-14011
Molecular beam epitaxial growth and characterization of 3-5 compound semiconductor single and multiple interface structures
[AD-A185400] N88-14021
**MOLECULAR BEAMS**
Reactive sticking coefficients of silane on silicon
[DE88-000601] N88-13473
Supersonic beam observations of semiconductor clusters
[AD-A184991] N88-14018
**MOLECULAR COLLISIONS**
Theoretical atomic and molecular physics
[DE88-001625] N88-13974
**MOLECULAR ENERGY LEVELS**
Intramolecular energy transfer reactions as a method for metal complex assisted production of hydrogen
[DE88-001621] N88-13425
Molecular-level synthesis and characterization of metal-polymer interfaces
[AD-A184956] N88-13455
**MOLECULAR EXCITATION**
Intramolecular energy transfer reactions as a method for metal complex assisted production of hydrogen
[DE88-001621] N88-13425
Pure dephasing of a vibrational adbond
[AD-A185222] N88-13740
**MOLECULAR INTERACTIONS**
Soluble metal chelate polymers of coordination numbers six, seven and eight
[AD-A185094] N88-13459
**MOLECULAR OSCILLATIONS**
Pure dephasing of a vibrational adbond
[AD-A185222] N88-13740
**MOLECULAR ROTATION**
Dynamical analysis of molecular decay at spherical surfaces
[AD-A184908] N88-13964
**MOLECULAR SPECTROSCOPY**
Supersonic beam observations of semiconductor clusters
[AD-A184991] N88-14018
**MOLECULAR STRUCTURE**
Molecular and supramolecular orientation in conducting polymers
[DE88-000533] N88-13472
**MOLECULES**
The formation and thermochemical properties of multiligand complexes
[AD-A184935] N88-13416
High energy molecules of high symmetry
[AD-A185385] N88-13965
**MOMENTUM**
Lagrangian procedures for higher order field equations
[DE87-703365] N88-13911
Theory of neutron scattering experiments on momen tum distributions in quantum fluids
[DE87-01369] N88-13968
**MOMENTUM TRANSFER**
Statistical theory of turbulent incompressible multimaterial flow
[DE88-000435] N88-13535
**MONITORS**
Plant Growth Module (PGM) conceptual design N88-13855
**MONKEYS**
Microwave challenges to the thermoregulatory system
[AD-A185391] N88-13847
**MONTE CARLO METHOD**
The statistics of the shape of small fatigue cracks N88-13666
Fatigue under nonnormal random stresses using Monte Carlo method N88-13723
Approximating multivariate normal orthant probabilities using the Clark algorithm
[AD-A184855] N88-13873
**MORPHOLOGY**
Molecular and supramolecular orientation in conducting polymers
[DE88-000533] N88-13472
The effect of alpha platelet morphology and beta-grain size on the initiation and growth of short fatigue cracks in Ti6S N88-13667
Characterization of the microstructures of various materials
[AD-A184961] N88-14017
**MOTION PERCEPTION**
Television motion measurement for DATV and other applications
[BBC-RD-1987/11] N88-13496
**MOTION PICTURES**
Model-based motion estimation and its application to restoration and interpolation of motion pictures
[AD-A185054] N88-13558
**MTBF**
Explicit formulate for the distributions of stopping variables under Wald's truncated SPRT (Sequential Probability Radio Tests) for a poisson process
[AD-A185053] N88-13914
**MULTICHANNEL COMMUNICATION**
In-orbit calibration adjustment of the Nimbus-7 SMMR
[NASA-TM-100678] N88-13773
**MULTIPROCESSING (COMPUTERS)**
Contribution to optimal flow in networks. A experimental multiprocessor for asynchronous iteration implementation
[LAAS-87-269] N88-13510
**MULTISPECTRAL BAND CAMERAS**
Land cover/use classification of Cairns, Queensland, Australia: A remote sensing study involving the conjunctive use of the airborne imaging spectrometer, the large format camera and the thematic mapper simulator N88-13759
**MULTIVARIATE STATISTICAL ANALYSIS**
Approximating multivariate normal orthant probabilities using the Clark algorithm
[AD-A184855] N88-13873
Illustrative examples of principal component analysis using BMDP/4M
[AD-A185179] N88-13881
Illustrative examples of principal component analysis using SYSTAT/FACTOR
[AD-A184920] N88-13939
Illustrative examples of principal component analysis using GENSTAT/PCP
[AD-A185085] N88-13941
Modeling and generating input processes
[DE87-013162] N88-13948
**MUSCULOSKELETAL SYSTEM**
Physiological determinants of load bearing capacity
[AD-A184977] N88-13848

## N

**NACELLES**
Computation of transonic flows with nacelle simulation
[SNIAS-872-111-117] N88-13300
Low speed wind tunnel investigation of propeller slipstream aerodynamic effects on different nacelle/wing combinations. Part 1: Total forces and moments and pressure distributions on nacelle/wing at different angles of attack and yaw and at different thrust coefficients
[FFA-TN-1987-22] N88-13302
**NASA PROGRAMS**
National Aeronautics and Space Administration space station proposal, fiscal year 1988
[S-HRG-100-328] N88-14043
The 1988 NASA (National Aeronautics and Space Administration) authorization
[GPO-80-245] N88-14044
**NAVIER-STOKES EQUATION**
Numerical analysis of flow through scramjet engine inlets N88-13233
Numerical simulation of the hypersonic flow around lifting vehicles N88-13234
Solution of some 3-D viscous and inviscid supersonic flow problems by finite-volume space-marching schemes N88-13235
Numerical experiments with hypersonic flows beneath a cone-delta-wing combination N88-13236
Numerical analysis of cascade flow solving Navier-Stokes equations N88-13262
Relaxation method for the compressible Navier-Stokes equations using upwind schemes N88-13283
Navier-Stokes analysis of laminar flow control of a two-dimensional airfoil N88-13286
Navier-Stokes simulation of transonic transportation aircraft configurations. 1: Flow-field simulation over wing-fuselage combinations N88-13288
Numerical simulation of transonic aircraft in comparison to wind tunnel test N88-13289
Calculation of helicopter rotor blade/vortex interaction by Navier-Stokes procedures
[NASA-CR-177441] N88-13291
Solution procedure for the Navier-Stokes equations applied to rotors N88-13533
Physical analysis and numerical simulation of coherent turbulent structures in mixed layers, jets, and wakes
[ETN-88-91183] N88-13548
Low thrust viscous nozzle flow fields prediction
[NASA-CR-182334] N88-13551
The interaction of DC plasma jet with a melting metal: Experimental measurements and mathematical description
[AD-A185173] N88-13993
**NAVIGATION**
Calendar of selected aeronautical and space meetings
[AGARD-CAL-87/1] N88-14033
**NAVIGATION SATELLITES**
Use of the global positioning system for trajectory determination of SRAM 2 missiles at the Eastern Test Range
[AD-A185266] N88-13314
**NAVSTAR SATELLITES**
On-orbit frequency stability analysis of the GPS NAVSTAR 8 rubidium clock and NAVSTARs 9 and 10 cesium clocks
[AD-A184984] N88-13312
**NAVY**
Avionic corrosion N88-13332
**NEAR INFRARED RADIATION**
Measuring near infrared spectral reflectance changes from water stressed conifer stands with AIS-2 N88-13765
**NEODYMIUM LASERS**
An investigation of unipolar arcing at atmospheric pressure in aluminum 2024 and aluminum coated glass slides
[AD-A184903] N88-13521
**NEON**
Extreme ultraviolet beam-foil spectroscopy of highly ionized neon and argon
[AD-A185197] N88-13418
**NETHERLANDS**
Civil aeronautics
[ETN-88-90616] N88-13309
Inventory of weather stations. Climatological data from Dutch stations, no. 26
[KNMI-150-26] N88-13841
**NETWORK CONTROL**
Survey on large scale system control methods
[NASA-CR-181556] N88-13374
**NEUTRON COUNTERS**
Cosmic ray NM-64 neutron monitor data 14, Rome, Italy, January - December 1985
[IFSI-87-8] N88-14060
**NEUTRON SCATTERING**
Theory of neutron scattering experiments on momen tum distributions in quantum fluids
[DE87-01369] N88-13968
**NICKEL**
The mechanism by which sigma-phase forms in Fe-Cr-Ni system alloys
[BLL-M-37380-(5828.4)] N88-13437
Advances in processing techniques for nickel aluminides
[DE87-014571] N88-13449
**NICKEL ALLOYS**
A mathematical model of high alloy nickel base high temperature alloys
[BLL-M-37381-(5828.4)] N88-13436
The effect of ion beam mixed Ni-Al surface layers on PSB extrusion morphology in fatigued nickel N88-13652
Low cycle fatigue behaviour of notched specimens of nickel based superalloy single crystal N88-13712

An overview of fatigue N88-13729
**NICKEL CADMIUM BATTERIES**
High energy density rechargeable batteries for aerospace power requirements
[AD-A184883] N88-13519
**NICKEL COMPOUNDS**
Phase purity of NiCo2O4, a catalyst candidate for electrolysis of water
[NASA-TM-100239] N88-13385
**NICKEL HYDROGEN BATTERIES**
Making space nickel/hydrogen batteries lighter and less expensive
[DE88-000168] N88-13530
**NICKEL PLATE**
Analysis of nickel sulphamate bath using charging current compensated D.C. polarography
[NAL-TM-MT-8705] N88-13433
**NIMBUS 7 SATELLITE**
In-orbit calibration adjustment of the Nimbus-7 SMMR
[NASA-TM-100678] N88-13773
Volcanic eruption detection with TOMS N88-13793
Selection of optimum wavelengths for ozone mapping from satellites N88-13798
Determination of total ozone from HIRS2/MSU sounding data N88-13799
**NIMONIC ALLOYS**
Near-threshold short crack growth behavior in Nimonic 105 N88-13663
**NIOBIUM**
Study of the influence of mechanical - thermal treatments on the creep behavior of a niobium stainless steel
[DE87-703506] N88-13431
**NITRIDING**
Fatigue characteristics of ion treated surfaces N88-13713
**NITROGEN**
Development of a low noise 10 K J-T refrigeration system
[AD-A185258] N88-13484
**NITROUS OXIDES**
Formation and destruction of nitrous oxide in lean, premixed combustion
[DE88-001390] N88-13423
**NOAA SATELLITES**
TOMS and the NOAA/FAA volcano support plan N88-13796
**NOISE (SOUND)**
Noise modelling in the time domain with the aid of Spice
[PB87-221941] N88-13492
**NOISE PREDICTION**
High speed propeller performance and noise predictions at takeoff/landing conditions
[NASA-TM-100267] N88-13960
**NOISE PREDICTION (AIRCRAFT)**
Compressor large bandwidth noise emission mechanisms
[ETN-88-91177] N88-13959
**NOISE REDUCTION**
Noise of a model counterrotation propeller with reduced aft rotor diameter at simulated takeoff/approach conditions (F7/A3)
[NASA-TM-100254] N88-13961
**NOISE SPECTRA**
Compressor large bandwidth noise emission mechanisms
[ETN-88-91177] N88-13959
**NOISE TEMPERATURE**
Capacitive resonant transducer for the Frascati gravitational antenna
[IFSI-88-9] N88-13528
**NONDESTRUCTIVE TESTS**
Philosophy and practice of nondestructive tests of composite material structures at Aerospatiale Aquitaine
[SNIAS-872-430-105] N88-13400
Utilization of microwave measuring systems for nondestructive control of composite materials
[SNIAS-872-430-109] N88-13402
Measurement and control of damage in composite materials: Nondestructive controls by thermography, holography, and radiography
[SNIAS-872-430-110] N88-13403
Contribution of acoustic analysis to assess damage in fluid storage tanks under high pressure — composite materials, filament winding
[SNIAS-872-430-119] N88-13407
Water disbondment characterization of organic Coating/metal substrate systems
[AD-A184847] N88-13454
First International Week of Adhesive Bonding and Assembling
[SNIAS-872-430-106] N88-13468
Investigation of the exposure to harmful compounds in the workshop of nondestructive materials testing at Gilze-Rijen (Netherlands)
[PML-1985-42] N88-13816
**NONLINEAR OPTICS**
Anti-Stokes generation of 226 nm light
[DE88-001612] N88-13590
**NONLINEAR SYSTEMS**
On the correlation free forms for nonlinear stochastic systems
[DE87-011169] N88-13947
**NONLINEARITY**
Non-linear maximum likelihood estimation of stability derivatives from range data
[NAL-TM-SE-8608] N88-13365
HF sidebands in the ionosphere N88-13497
Nonlinear hyperbolic conservation laws
[AD-A184963] N88-13538
Applications of nonlinear hole burning spectroscopy
[AD-A184943] N88-13580
Dynamics of cables and chains N88-13747
**NONPARAMETRIC STATISTICS**
An APL workspace for conducting nonparametric statistical inference
[AD-A184971] N88-13877
Further studies in estimation of life distribution characteristics from censored data
[AD-A134882] N88-13937
Sample reuse in statistical remodeling
[AD-A184916] N88-13938
Quantile statistical data analysis
[AD-A185181] N88-13943
**NORTH AMERICA**
A survey of existing hypersonic ground test facilities: North America N88-13220
**NORTH ATLANTIC TREATY ORGANIZATION (NATO)**
Special Course on Fundamentals of Fighter Aircraft Design
[AGARD-R-740] N88-13315
Calendar of selected aeronautical and space meetings
[AGARD-CAL-88/1] N88-14037
**NOSE CONES**
A spatial marching technique for the inviscid blunt body problem N88-13239
**NOSES (FOREBODIES)**
An experimental investigation of appendage-flat plate junction flow. Volume 2. Elliptical nose appendage data base
[AD-A184974] N88-13539
**NOTCH SENSITIVITY**
Fatigue strength of alloy A286 at cryogenic temperature N88-13695
**NOTCH STRENGTH**
Low cycle fatigue behaviour of notched specimens of nickel based superalloy single crystal N88-13712
**NOTCH TESTS**
Closure and propagation behavior of short fatigue cracks at different R-ratios N88-13679
Crack growth in contrasting titanium alloys under the conjoint action of high and low cycle fatigue N88-13686
Fatigue of 30CrMnSiNi2A notched specimens under spectrum loading N88-13689
**NOZZLE GEOMETRY**
Combustion related shear-flow dynamics in elliptic supersonic jets N88-13232
**NUCLEAR ELECTRIC POWER GENERATION**
Procedure and program used for data processing in a poli on nuclear energy utilization
[IFSI-87-3] N88-13977
**NUCLEAR FUSION**
A review of the experimental and theoretical status of the reversed-field pinch
[DE88-000529] N88-14000
**NUCLEAR POWER PLANTS**
Computer code simulations of explosions in flow networks and comparison with experiments
[DE88-001946] N88-13491
**NUCLEAR REACTIONS**
Anomalous phonon behavior of superconductor Y-Ba-Cu-O
[DE87-703401] N88-14010
**NUCLEAR RELAXATION**
A review of the experimental and theoretical status of the reversed-field pinch
[DE88-000529] N88-14000
**NUCLEAR RESEARCH**
The birth of big science: Nuclear physics as advanced technology source
[NOTA-INTERNA-881] N88-13967
**NUCLEAR WEAPONS**
New approach to telemetry development will significantly increase productivity of Joint Test Assembly (JTA) teams
[DE88-001676] N88-13373
**NUCLEATION**
The mechanics of fatigue-crack nucleation in a low-alloy steel under fretting conditions N88-13649
**NUMERICAL ANALYSIS**
Numerical analysis of flow through scramjet engine inlets N88-13233
Eigenvalue projection theory for linear operator equations of electromagnetics
[AD-A185434] N88-13504
Numerical analysis, computing and fundamental studies in fluid mechanics
[DE88-001912] N88-13550
The numerical and analytic of implicit differential equations and their application to control and circuit problems
[AD-A185404] N88-13922
Numerical methods for reaction-diffusion problems with non-differentiable kinetics
[AD-A185405] N88-13923
**NUMERICAL CONTROL**
Digital control of a direct current converter for a hybrid vehicle
[LAAS-87-266] N88-13527
The numerical and analytic of implicit differential equations and their application to control and circuit problems
[AD-A185404] N88-13922
**NUMERICAL STABILITY**
Numerical and analytical methods in nonlinear partial differential equations
[AD-A185210] N88-13918
**NUTRITION**
Controlled ecological life support systems: Development of a plant growth module N88-13854
Plant Growth Module (PGM) conceptual design N88-13855

## O

**OBSERVATORIES**
Astrophysics observatory in Byurakan
[AD-A185144] N88-14050
**OCEAN SURFACE**
Varifront 3 expedition data report (USNS DE STEIGUER CRUISE 1202-82). Bioluminescence, hydrographic, nutrient, and satellite data from the Gulf of California (November-December 1981)
[AD-A185011] N88-13805
**OFFSHORE PLATFORMS**
High performance composite tubes for offshore applications
[SNIAS-872-430-116] N88-13488
A system identification technique based on the random decrement signatures. Part 2: Experimental results N88-13626
Experimental studies on acoustic emission monitoring of crack propagation in offshore structures: A literature survey N88-13748
**OILS**
Analysis of wear metals in engine oils using the atomic absorption spectrophotometric method
[NAL-TM-MT-8704] N88-13435
**ONBOARD DATA PROCESSING**
Study of fault tolerant techniques for satellite data handling
[FTT/REP/0001/SAAB] N88-13860
**ONBOARD EQUIPMENT**
A project of an intelligent system to help on-line trouble shooting — aircraft maintenance
[SNIAS-872-111-106] N88-13216
**ONE DIMENSIONAL FLOW**
Relaxation method for the compressible Navier-Stokes equations using upwind schemes N88-13283
**OPERATING SYSTEMS (COMPUTERS)**
Connecting RPC (Remote Procedure Call)-based distributed systems using wide-area networks
[PB87-234423] N88-14041
**OPERATORS (MATHEMATICS)**
Eigenvalue projection theory for linear operator equations of electromagnetics
[AD-A185434] N88-13504
On a boundary data operator and generalized exterior Robin problems for the Helmholtz equation
[AD-A185124] N88-13915
Introduction to string field theory
[DE87-014583] N88-14032
**OPERATORS (PERSONNEL)**
Measurement of suspension and ride characteristics of the M1 main battle tank N88-13637
**OPTICAL BISTABILITY**
Ultrafast intrinsic bistable devices
[PB87-109310] N88-13978
**OPTICAL DATA PROCESSING**
Nonconventional optical techniques for optical wavefront processing
[AD-A185099] N88-13982

**OPTICAL MEASUREMENT**
Optical deformation measurement on shells following the raster principle
[ETN-88-90608] N88-13741
**OPTICAL MEASURING INSTRUMENTS**
Determination of the fiber ratio in carbon fiber/resin composites by means of image analysis
[SNIAS-872-422-101] N88-13398
**OPTICAL PROPERTIES**
Fundamental studies in the OM-CVD growth of Ga-In-As-Sb
[AD-A184822] N88-14014
**OPTICAL PUMPING**
Nonconventional optical techniques for optical wavefront processing
[AD-A185099] N88-13982
Solitons in stimulated Raman scattering: Generation and control of ultrashort optical pulses
[AD-A185141] N88-13983
**OPTICAL RADAR**
Italy's Institute of Research on Electromagnetic Waves--the Istituto di Ricerca sulle Onde Elettromagnetiche
[AD-A185020] N88-13501
Contributions of lidar measurements to the study of long term variations of the middle atmosphere
[ETN-88-91237] N88-13824
**OPTICAL RESONANCE**
Ultrafast intrinsic bistable devices
[PB87-109310] N88-13978
**OPTICAL RESONATORS**
Computer simulation of cw HF chemical laser unstable resonator performance
[AD-A185059] N88-13581
**OPTICAL SCANNERS**
Applications of nonlinear hole burning spectroscopy
[AD-A184943] N88-13580
Range imagery algorithms for the detection of obstacles by autonomous vehicles
[AD-A185421] N88-14045
**OPTICAL WAVEGUIDES**
Ultrafast intrinsic bistable devices
[PB87-109310] N88-13978
**OPTIMAL CONTROL**
Investigation, development, and application of optimal output feedback theory. Volume 3: The relationship between dynamic compensators and observers and Kalman filters
[NASA-CR-4107] N88-13900
Control of an unstable launcher in atmospheric flight using minimax optimal control laws
[SNIAS-872-422-107] N88-13901
Guidance and control strategies for aerospace vehicles
[NASA-CR-181579] N88-13935
**OPTIMIZATION**
Techniques for performance optimisation in cruise and manoeuverability N88-13321
Aeroelasticity and optimization in fighter aircraft design N88-13324
Reduced order optimal command applied to longitudinal automatic pilots
[SNIAS-872-111-114] N88-13362
Design of low order controllers for robust disturbance rejection in large space structures
[AD-A185202] N88-13376
Digital video bit-rate reduction: DPCM for sub-Nyquist PAL
[BBC-RD-1987/16] N88-13494
Contribution to optimal flow in networks. A experimental multiprocessor for asynchronous iteration implementation
[LAAS-87-269] N88-13510
Establishment of complete minimum test sets for digital circuits with safety engineering significance
[ETN-88-90599] N88-13526
Finite-element grid improvement by minimization of stiffness matrix trace
[NASA-TM-100255] N88-13604
Simultaneous structural and control optimization via linear quadratic regulator eigenstructure assignment N88-13622
Shape optimization of damping layers N88-13635
STAEBL/general composites with hygrothermal effects (STAEBL/GENCOM)
[NASA-TM-100266] N88-13754
Structural optimization in the design process --- aircraft
[SNIAS-872-111-115] N88-13885
**OPTOELECTRONIC DEVICES**
Optoelectronic measurement methods for ballistic experiments
[PB87-110706] N88-13554
**ORBIT TRANSFER VEHICLES**
Study of fault tolerant techniques for satellite data handling
[FTT/REP/0001/SAAB] N88-13860
**ORBITAL ASSEMBLY**
Potential for on-orbit manufacture of large space structures using the pultrusion process
[NASA-TM-4016] N88-13388
**ORBITAL MANEUVERING VEHICLES**
Orbital Spacecraft Consumables Resupply System (OSCRS). Volume 1: Executive summary
[NASA-CR-172010] N88-13368
**ORBITAL SERVICING**
Orbital Spacecraft Consumables Resupply System (OSCRS). Volume 1: Executive summary
[NASA-CR-172010] N88-13368
In-orbit calibration adjustment of the Nimbus-7 SMMR
[NASA-TM-100678] N88-13773
**ORBITAL SPACE STATIONS**
Orbital Spacecraft Consumables Resupply System (OSCRS). Volume 1: Executive summary
[NASA-CR-172010] N88-13368
Design and assembly sequence analysis of option 3 for CETF reference space station
[NASA-TM-100503] N88-13369
Space station systems: A bibliography with indexes
[NASA-SP-7056(05)] N88-13382
National Aeronautics and Space Administration space station proposal, fiscal year 1988
[S-HRG-100-328] N88-14043
The 1988 NASA (National Aeronautics and Space Administration) authorization
[GPO-80-245] N88-14044
**ORGANOMETALLIC COMPOUNDS**
United States - Japan Workshop on Dielectric and Piezoelectric Ceramics (3rd) held in Toyama, Japan on November 9-12, 1986
[AD-A185113] N88-13460
**ORGANOMETALLIC POLYMERS**
Soluble metal chelate polymers of coordination numbers six, seven and eight
[AD-A185094] N88-13459
**ORTHOGONALITY**
Eigenvectors of distance-regular graphs
[AD-A185375] N88-13919
Separable orthogonal coordinates and particle creation for an accelerating observer
[DE87-703358] N88-14029
**OSCILLATING FLOW**
Unsteady aerodynamics of an oscillating cascade in a compressible flow field
[NASA-TM-100219] N88-13346
**OSCILLATIONS**
An experimental investigation of the aerodynamics of a NACA 64A010 airfoil-flap combination with and without flap oscillations. Part 1: Steady-state characteristics
[NASA-TM-88217] N88-13305
**OUTLIERS (STATISTICS)**
Robust prediction operations for stationary processes
[AD-A185408] N88-13924
**OUTPUT**
Equivalence of input-output stability and exponential stability for infinite dimensional systems
[TW-276] N88-13903
**OXIDATION**
Detailed mechanism of toluene oxidation and comparison with benzene
[NASA-TM-100261] N88-13428
Occurance and growth of fatigue cracks in corrosion environment N88-13704
High energy molecules of high symmetry
[AD-A185385] N88-13965
**OXIDE FILMS**
The effects of thin anodic films on the cyclic microstrain/macrostrain behavior of tungsten N88-13650
**OXYGEN**
Oxygen enriched combustion system performance study
[DE88-001500] N88-13424
Anti-Stokes generation of 226 nm light
[DE88-001612] N88-13590
Controlled ecological life support systems: Development of a plant growth module N88-13854
**OXYGEN CONSUMPTION**
A device and methodology for measuring repetitive lifting VO2max (oxygen consumption rate)
[AD-A185195] N88-13850
**OXYGEN IONS**
The tail lobe ion spectrometer: Theory and observations
[IFSI-86-12] N88-13569
**OZONE**
Photochemical ozone overburden correction N88-13778
Analysis of the breakdown of the Antarctic circumpolar vortex using TOMS ozone data N88-13779
Insights into the general circulation of the lower stratosphere from TOMS N88-13780
Ozone, jet streaks and severe weather N88-13781
Lower-stratospheric/upper-tropospheric exchange processes associated with tropical cyclones as observed by TOMS N88-13782
Tropical easterly jet located using TOMS data N88-13783
The use of TOMS data for tropospheric ozone studies N88-13784
Northwest Airlines flight experiments N88-13786
An analysis of tropopause pressure and total ozone correlations N88-13789
TOMS ozone data compared at mesoscale resolution to tropopause heights from the AVE radiosonde network and to VAS radiances over the south-central United States N88-13790
Dobson-stations performance assessment using TOMS data N88-13792
Comparison of ground based and TOMS measurements of SO2 from volcanic emissions N88-13795
Selection of optimum wavelengths for ozone mapping from satellites N88-13798
Determination of total ozone from HIRS2/MSU sounding data N88-13799
Complementary information between UV and IR for remote sensing of total ozone N88-13800
Observation guidelines for a Total Ozone Mapping Spectrometer (TOMS) in geosynchronous orbit N88-13801
A geostationary imaging spectrometer TOMS instrument N88-13802
**OZONE DEPLETION**
Scientific and Operational Requirements for TOMS Data
[NASA-CP-2497] N88-13774
TOMS: The Antarctic ozone hole and ozone trends N88-13775
October lower stratospheric Antarctic temperature and total ozone from 1979-1985 N88-13776
**OZONOMETRY**
Scientific and Operational Requirements for TOMS Data
[NASA-CP-2497] N88-13774
TOMS: The Antarctic ozone hole and ozone trends N88-13775
Analysis of the breakdown of the Antarctic circumpolar vortex using TOMS ozone data N88-13779
The use of TOMS data for tropospheric ozone studies N88-13784


## P


**PADE APPROXIMATION**
The matrix exponential in transient structural analysis N88-13619
**PAINTS**
Paints required for aeronautical construction
[SNIAS-872-551-102] N88-13470
**PANELS**
Theoretical and practical aspects of the functional absorber method of arranging sound absorbing panels
[BBC-RD-1987/15] N88-13955
**PARALLEL PROCESSING (COMPUTERS)**
Computational methods for problems in aerodynamics and large space structure using parallel and vector architectures
[AD-A185401] N88-13294
Arrays for discrete Fourier transform
[REPT-87-019] N88-13861
Storing and retrieving data in a parallel distributed memory system
[AD-A185177] N88-13897
Research and development of finite elements and iterative algorithms for elliptic partial differential equations
[DE88-001381] N88-13934
**PARAMETER IDENTIFICATION**
Full-envelope aerodynamic modeling of the Harrier aircraft
[NASA-TM-88376] N88-13363
Non-linear maximum likelihood estimation of stability derivatives from range data
[NAL-TM-SE-8608] N88-13365
**PARAMETERIZATION**
A system identification technique based on the random decrement signatures. Part 1: Theory and simulation N88-13625
Fatigue crack growth: Statistical considerations N88-13718
**PARASITIC DISEASES**
TOMS as a monitor of the ultraviolet radiation environment: Applications to photobiology N88-13785

**PARTIAL DIFFERENTIAL EQUATIONS**
Numerical and analytical methods in nonlinear partial differential equations
[AD-A185210] N88-13918
**PARTICLE ACCELERATORS**
Experimental studies of elementary particle interactions at high energies
[DE88-000804] N88-13971
**PARTICLE COLLISIONS**
W decays
[NOTA-INTERNA-877] N88-13966
**PARTICLE DENSITY (CONCENTRATION)**
Restoration of particle pitch angle distribution functions by a maximum entropy algorithm
[ATR-86(7098)-3] N88-13969
**PARTICLE INTERACTIONS**
The formation and thermochemical properties of multiligand complexes
[AD-A184935] N88-13416
Feasibility study for gas-grain simulation facility
[NASA-CR-177468] N88-13954
**PARTICLE SIZE DISTRIBUTION**
Operating envelopes of particle sizing instrumentation used for icing research
[NASA-CR-180870] N88-13573
The application of doubly-truncated hydrometeor distributions to numerical cloud models
[AD-A185273] N88-13838
**PARTICLES**
Separable orthogonal coordinates and particle creation for an accelerating observer
[DE87-703358] N88-14029
**PASSENGER AIRCRAFT**
Contribution to the improvement of the guidance accuracy of automatic pilots
[ETN-88-90607] N88-13360
**PATENT POLICY**
Core material — honeycombs
[EP-PATENT-0-196-926-A2] N88-13393
Antistatic coating compositions
[GB-PATENT-2-177-413-A] N88-13463
Flame retardant phenolic foams
[EP-PATENT-0-223-489-A2] N88-13464
Process for the production of a thermoplastic elastomer composition
[EP-PATENT-0-202-782-A2] N88-13465
Optical probe
[EP-PATENT-0-210-869-A1] N88-13984
Preparation of amorphous silicon semiconductors
[GB-PATENT-2-176-054-A] N88-14022
**PATTERN RECOGNITION**
Towards building a team of intelligent robots
[NASA-CR-181538] N88-13595
A rudimentary database for three-dimensional objects using structural representation
[CSE-87-00004] N88-13597
Supercomputing at Florida State University (FSU)
[DE87-013900] N88-14009
**PAYLOAD INTEGRATION**
RETE experiment Assembly, Integration, and Verification (AIV) activities
[IFSI-87-6] N88-13380
**PAYLOADS**
The effect of maximum-allowable payload temperature on the mass of a multimegawatt space-based platform
[DE88-001921] N88-13381
**PENETRATION**
Mechanical property evaluation of a series of commercial tungsten alloys
[AD-A185440] N88-13446
Structural frequency functions for an impulsive, distributed forcing function N88-13627
**PERFORMANCE PREDICTION**
Predictions of F-111 TACT aircraft buffet response and correlations of fluctuating pressures measured on aluminum and steel models and the aircraft
[NASA-CR-4069] N88-13218
The off-design performance of hypersonic waveriders N88-13244
Numerical optimization of conical flow waveriders including detailed viscous effects N88-13245
Dynamic stability of hypersonic conical lifting vehicles according to Newton-Busemann theory N88-13247
Experiences using the Mark IV supersonic hypersonic arbitrary body program N88-13249
The RAE experimental data-base for missiles at high Mach number and its use in assessing CFD methods N88-13250
Damage considerations in sizing aircraft cells. Life predictions
[SNIAS-872-111-116] N88-13330
Model helicopter rotor rig and associated strain gauge balance for performance studies
[NAL-TM-AE-8704] N88-13364
Performability modeling based on real data: A casestudy
[NASA-CR-181563] N88-13870
**PERFORMANCE TESTS**
Application of modified loss and deviation correlations to transonic axial compressors
[AGARD-R-745] N88-13344
Error control techniques for satellite and space communications
[NASA-CR-181581] N88-13516
Establishment of complete minimum test sets for digital circuits with safety engineering significance
[ETN-88-90599] N88-13526
Seal technology for liquid oxygen (LOX) turbopumps
[NASA-CR-174866] N88-13603
Trajectory control of robot manipulators with closed-kinematic chain mechanism
[NASA-TM-89305] N88-13605
Test and evaluation of the transputer in a multi-transputer system
[AD-A184969] N88-13859
High speed propeller performance and noise predictions at takeoff/landing conditions
[NASA-TM-100267] N88-13960
**PERIODIC FUNCTIONS**
Efficient computation of periodic Green's functions with application to grating structures
[AD-A184853] N88-13912
**PERMANENT MAGNETS**
A long electromagnetic wiggler for the paladin free-electron laser experiments
[DE88-000970] N88-13589
Development of a laced electromagnetic wiggler
[DE88-000972] N88-13953
**PERSONAL COMPUTERS**
BASIC desk-top computer program for the three-dimensional static configuration of an extensible flexible cable in a uniform stream
[AD-A184852] N88-13737
Mixing Microsoft C and Microsoft FORTRAN program modules on the IBM Personal Computer
[DE88-001947] N88-13895
**PERTURBATION**
Identification of perturbations in turbomachines by the analysis of pressure signals, vibrations and wavelike motions
[ETN-88-90602] N88-13600
Improvement of modal scaling factors using mass additive technique N88-13620
Development of a data analysis system for the detection of lower level atmospheric turbulence with an acoustic sounder
[AD-A184972] N88-13821
**PERTURBATION THEORY**
Design of low order controllers for robust disturbance rejection in large space structures
[AD-A185202] N88-13376
Robustness of linear systems
[PB87-220042] N88-13909
Molecular dynamics studies of aromatic hydrocarbon liquids
[DE88-001473] N88-13973
**PHASE DIAGRAMS**
The mechanism by which sigma-phase forms in Fe-Cr-Ni system alloys
[BLL-M-37380-(5828.4)] N88-13437
Phase diagram and thermochemical properties of the Al-Cu system
[ETN-88-91015] N88-13447
**PHASE LOCKED SYSTEMS**
Phase-locked semiconductor quantum well laser arrays
[AD-A185155] N88-13583
**PHASE MODULATION**
HF sidebands in the ionosphere N88-13497
Error control techniques for satellite and space communications
[NASA-CR-181581] N88-13516
**PHASE TRANSFORMATIONS**
The mechanism by which sigma-phase forms in Fe-Cr-Ni system alloys
[BLL-M-37380-(5828.4)] N88-13437
Coupling effects between the ferrite and austenite phases during corrosion fatigue of a ferrite/austenite duplex stainless steel N88-13706
**PHENOLS**
Flame retardant phenolic foams
[EP-PATENT-0-223-489-A2] N88-13464
Production of jet fuels from coal derived liquids. Volume 1: Market assessment for liquid by-products from the Great Plains gasification plant
[AD-A184846] N88-13475
**PHENYLS**
Thermally stable aromatic structures from acyclic precursors. 1. Para polyphenylene model compounds from 3-Dimethyl amino hex-5-EN-1-YNES
[AD-A185300] N88-13462
**PHONONS**
Anomalous phonon behavior of superconductor Y-Ba-Cu-O
[DE87-703401] N88-14010
**PHOTOABSORPTION**
Intramolecular energy transfer reactions as a method for metal complex assisted production of hydrogen
[DE88-001621] N88-13425
**PHOTOCATHODES**
A focussed MCP (microchannel plate) image intensifier type for high speed gating
[DE88-000480] N88-13555
Streak camera dynamic range optimization
[DE88-001632] N88-13571
**PHOTOCHEMICAL REACTIONS**
Intramolecular energy transfer reactions as a method for metal complex assisted production of hydrogen
[DE88-001621] N88-13425
Scientific and Operational Requirements for TOMS Data
[NASA-CP-2497] N88-13774
Photochemical ozone overburden correction N88-13778
**PHOTODISSOCIATION**
OH(A-X) fluorescence from photodissociative excitation of HO2 at 157.5 nm
[NASA-CR-181580] N88-13429
**PHOTOELECTRIC EMISSION**
Photocurrent generation from basic metals, utilizing a short pulsed ArF excimer laser
[AD-A184928] N88-13579
**PHOTOIONIZATION**
Theory of multiphoton ionization of atoms by strong, short pulsed lasers
[DE88-000963] N88-13588
**PHOTOLITHOGRAPHY**
The production of ultrasmall and superfine holographic diffraction gratings using synchrotron radiation and lithographic techniques
[AD-A185395] N88-13562
**PHOTOMETERS**
Optical probe
[EP-PATENT-0-210-869-A1] N88-13984
Optical photometer for the Tirgo telescope
[IFSI-87-5] N88-13985
**PHOTOMULTIPLIER TUBES**
Study of solid state photomultiplier
[NASA-CR-177465] N88-13556
Streak camera dynamic range optimization
[DE88-001632] N88-13571
**PHOTONS**
Study of solid state photomultiplier
[NASA-CR-177465] N88-13556
Photon counting image sensor development for astronomical applications
[NASA-CR-181507] N88-14049
**PHOTOSENSITIVITY**
Develop techniques for ion implantation of (lead-lanthanum-zirconate-titanate) for adaptive optics
[DE88-000642] N88-13986
**PHYSICAL FITNESS**
Physiological determinants of load bearing capacity
[AD-A184977] N88-13848
**PHYSICAL OPTICS**
Large bandwidth ground scattering model — radar scattering
[FOA-C-30458-3.2] N88-13511
**PHYSIOLOGICAL RESPONSES**
Human thermoregulatory model for whole body immersion in water at 20 and 28 C
[AD-A185052] N88-13849
**PIEZOELECTRIC CERAMICS**
United States - Japan Workshop on Dielectric and Piezoelectric Ceramics (3rd) held in Toyama, Japan on November 9-12, 1986
[AD-A185113] N88-13460
**PIONS**
Experimental studies of elementary particle interactions at high energies
[DE88-000804] N88-13971
**PIPELINES**
Dynamics of propellant feedline systems
[AD-A184865] N88-13537
**PIPELINING (COMPUTERS)**
Arrays for discrete Fourier transform
[REPT-87-019] N88-13861
**PIPES (TUBES)**
Development on thin wall tubes of dispersion type
[DE87-703384] N88-13483

Design and test of high performance composite tubes for use in deep water drilling and production systems [SNIAS-872-430-107] N88-13487
High performance composite tubes for offshore applications [SNIAS-872-430-116] N88-13488
Qualification of expansion and joint welding procedures of tube-to-tubesheet joints for heat exchangers in nuclear power plants [DE87-703526] N88-13592
Finite element model for the stress and flexibility analysis of curved pipes [DE87-703632] N88-13606
Analysis of photopole data reduction models N88-13616

**PITCH (INCLINATION)**
Restoration of particle pitch angle distribution functions by a maximum entropy algorithm [ATR-86(7098)-3] N88-13969

**PITCHING MOMENTS**
Dynamic stability of hypersonic conical lifting vehicles according to Newton-Busemann theory N88-13247
Prediction of wing aeroelastic effects on aircraft life and pitching moment characteristics N88-13356

**PIVOTS**
An examination of coating failure on wing pivot fittings of f111 aircraft [AD-A185028] N88-13328

**PLANAR STRUCTURES**
Computation of natural frequencies of planar lattice structure [AD-A185387] N88-13920

**PLANE STRAIN**
Closure and propagation behavior of short fatigue cracks at different R-ratios N88-13679

**PLANETARY EVOLUTION**
Studies in Aeolian geology [NASA-CR-182328] N88-13828

**PLANETARY SURFACES**
Studies in Aeolian geology [NASA-CR-182328] N88-13828

**PLANKTON**
Varifront 3 expedition data report (USNS DE STEIGUER CRUISE 1202-82). Bioluminescence, hydrographic, nutrient, and satellite data from the Gulf of California (November-December 1981) [AD-A185011] N88-13805

**PLANT STRESS**
Overview of Austrian Airborne Imaging Spectrometer (AIS) programme and first results N88-13762
Measuring near infrared spectral reflectance changes from water stressed conifer stands with AIS-2 N88-13765

**PLANTING**
Controlled ecological life support systems: Development of a plant growth module N88-13854

**PLANTS (BOTANY)**
Controlled Ecological Life Support System. Design, Development, and Use of a Ground-Based Plant Growth Module [NASA-CP-2479] N88-13852

**PLASMA ARC WELDING**
Plasma joining of metal matrix composites [AD-A184828] N88-13390
The interaction of DC plasma jet with a melting metal: Experimental measurements and mathematical description [AD-A185173] N88-13993

**PLASMA CONTROL**
ALT-1 pump limiter experiments [DE88-000822] N88-13989
A review of the experimental and theoretical status of the reversed-field pinch [DE88-000529] N88-14000

**PLASMA CURRENTS**
Observations of propagating double layers in a high current discharge [TRITA-EPP-87-10] N88-13997

**PLASMA DENSITY**
ALT-1 pump limiter experiments [DE88-000822] N88-13989

**PLASMA DIAGNOSTICS**
Proceedings of the 17th International Conference on Phenomena in Ionized Gases held in Budapest, Hungary, July 8-12, 1985: Invited papers [DE87-703562] N88-13987

**PLASMA DYNAMICS**
Laboratory and near-earth space plasma as a key to the plasma universe [TRITA-EPP-87-09] N88-13996
Numerical models for high beta magnetohydrodynamic flow [DE88-001850] N88-14008
A fluid simulation of the AMPTE lithium gas releases in the solar wind [TRITA-EPP-87-06] N88-14056

**PLASMA GENERATORS**
Preparation of qualification tests of a plasma generator for the feeding of a hypersonic wind tunnel N88-13222
High peak power ka-band gyrotron oscillator experiment [AD-A185424] N88-13563
A synthetic plasma source [TRITA-EPP-86-15] N88-13995

**PLASMA GUNS**
Analytical solution of the equations for a coaxial plasma gun operating in the snowplow mode. 1. Weak coupling limit [AD-A185370] N88-13994

**PLASMA HEATING**
ALT-1 pump limiter experiments [DE88-000822] N88-13989

**PLASMA INTERACTIONS**
Analysis of geophysical data bases and models for spacecraft interactions [AD-A184809] N88-13375
Laboratory and near-earth space plasma as a key to the plasma universe [TRITA-EPP-87-09] N88-13996

**PLASMA JETS**
Pulsed plasma jet igniters: Species measurements in methane combustion [DE88-001389] N88-13422
The interaction of DC plasma jet with a melting metal: Experimental measurements and mathematical description [AD-A185173] N88-13993
Observations of propagating double layers in a high current discharge [TRITA-EPP-87-10] N88-13997

**PLASMA LAYERS**
Observations of propagating double layers in a high current discharge [TRITA-EPP-87-10] N88-13997

**PLASMA PHYSICS**
Activities report of the Ionospheric Observatory [UIO-SR-87-01] N88-13827
Energy dependence of ion-induced sputtering yields of monatomic solids in the low energy region [IPPJ-AM-52] N88-13988
Laboratory and near-earth space plasma as a key to the plasma universe [TRITA-EPP-87-09] N88-13996
Comments on H. Arp The persistent problem of spiral galaxies [TRITA-EPP-87-05] N88-14052
Cosmology in the plasma universe [TRITA-EPP-87-07] N88-14053

**PLASMA PINCH**
Advanced concepts theory annual report 1986 [AD-A184986] N88-13991

**PLASMA PROBES**
Preparation of qualification tests of a plasma generator for the feeding of a hypersonic wind tunnel N88-13222

**PLASMA RADIATION**
Advanced concepts theory annual report 1986 [AD-A184986] N88-13991

**PLASMA SHEATHS**
Analytical solution of the equations for a coaxial plasma gun operating in the snowplow mode. 1. Weak coupling limit [AD-A185370] N88-13994

**PLASMA TURBULENCE**
Evolution of mean square magnetic vector potential in compressible, two-dimensional, magnetofluid turbulence [AD-A184985] N88-13990

**PLASMAS (PHYSICS)**
Theoretical atomic and molecular physics [DE88-001625] N88-13974
Reversed field pinch plasmas with various boundary conditions [DE88-000832] N88-14004

**PLASTIC COATINGS**
Water disbondment characterization of organic Coating/metal substrate systems [AD-A184847] N88-13454

**PLASTIC DEFORMATION**
Plasticity of aluminum and iron at high shear strain rate and high pressure N88-13430
Tribology of thin film systems [ETN-88-91365] N88-13601
Surface deformation and fatigue crack initiation of alpha-iron N88-13651
X-ray fatigue failure prediction based on plasticity response to microcracks N88-13725

**PLASTIC PROPERTIES**
Surface deformation and fatigue crack initiation of alpha-iron N88-13651
Embrittling effect of the plastic zone N88-13721
A comparison of plastic work energy and external input for fatigue crack propagation N88-13722

**PLATES (STRUCTURAL MEMBERS)**
Damping analysis of flexural waves in fluid-loaded single and constrained plates [AD-A185116] N88-13739

**PLATING**
The analysis of metal finishing solutions by ion chromatography [AD-A184812] N88-13414
Analysis of nickel sulphamate bath using charging current compensated D.C. polarography [NAL-TM-MT-8705] N88-13433

**PLETHYSMOGRAPHY**
A plethysmograph for measuring pulmonary ventilation in small animals [AD-A184978] N88-13846

**PLOTTING**
A computer code to process and plot laser altimetry data interactively on a microcomputer [NASA-TM-100687] N88-13371

**PLUMES**
Active and passive plume distribution models in the convective boundary layer using a large eddy simulation model [KNMI-TR-90] N88-13546
High resolution ultraviolet filter development [AD-A184183] N88-13979

**PLUNGERS**
Influence of shock wave and gas pressure on the behavior of a pyrotechnical device [SNIAS-872-430-111] N88-13477
Advantages of internal thermal protection in a pyrotechnical plunger [SNIAS-872-430-114] N88-13478
Numerical simulation applied to the development of a pyrotechnical system [SNIAS-872-430-115] N88-13479

**PNEUMATIC EQUIPMENT**
A device and methodology for measuring repetitive lifting VO2max (oxygen consumption rate) [AD-A185195] N88-13650

**POINTS (MATHEMATICS)**
Point processes [AD-A185398] N88-13921

**POISSON DENSITY FUNCTIONS**
Explicit formulate for the distributions of stopping variables under Wald's truncated SPRT (Sequential Probability Radio Tests) for a poisson process [AD-A185053] N88-13914

**POLAR REGIONS**
The polar ionosphere and interplanetary field [AD-A185386] N88-13822
Electric field measurements on Viking: First results [TRITA-EPP-87-04] N88-13826
Activities report of the Ionospheric Observatory [UIO-SR-87-01] N88-13827
Axial anisotropy of the intensity of the cosmic ray nuclear component [IFSI-87-7] N88-14061

**POLAROGRAPHY**
Analysis of nickel sulphamate bath using charging current compensated D.C. polarography [NAL-TM-MT-8705] N88-13433

**POLICIES**
A study of the Department of Defense configuration management policies and procedures as applied to the FA-18 Strike/Fighter program [AD-A184872] N88-14034
National Aeronautics and Space Administration space station proposal, fiscal year 1988 [S-HRG-100-328] N88-14043

**POLLUTION CONTROL**
Innovative and alternative technology projects [PB87-230165] N88-13818

**POLYACETYLENE**
Molecular and supramolecular orientation in conducting polymers [DE88-000533] N88-13472

**POLYCARBONATES**
The effect of heat treatment on fatigue crack growth in polycarbonate N88-13714

**POLYCRYSTALS**
X-ray analysis of polycrystalline aluminium subjected to fatigue cycling [NAL-TM-MT-8706] N88-13434

**POLYGONS**
Two low-order mixed methods for the elasticity problem [PB87-225272] N88-13749

**POLYHEDRONS**
Two low-order mixed methods for the elasticity problem [PB87-225272] N88-13749

**POLYIMIDE RESINS**
In-situ characterization of the interface of glass reinforced composites [AD-A185136] N88-13391

**POLYIMIDES**
Flexibilized copolyimide adhesives
[NASA-TM-89303] N88-13474
**POLYMER CHEMISTRY**
Characterization of the microstructures of various materials
[AD-A184961] N88-14017
**POLYMERIZATION**
Molecular-level synthesis and characterization of metal-polymer interfaces
[AD-A184956] N88-13455
Molecular and supramolecular orientation in conducting polymers
[DE88-000533] N88-13472
**POLYURETHANE RESINS**
High explosive moulding powders from RDX and aqueous polyurethane dispersions
[AD-A185026] N88-13458
**POLYVINYL CHLORIDE**
Effect of test temperature and frequency on fatigue crack propagation in PVC N88-13715
**PONDEROMOTIVE FORCES**
HF sidebands in the ionosphere N88-13497
**POPULATION THEORY**
A functional interpretation of the logistic equation
[REPT-87-037] N88-13946
**POROSITY**
Crack propagation properties of sintered steel N88-13698
**POROUS MATERIALS**
Development of a new method of measuring the characteristic impedance and complex wave number of a porous acoustic material
[AD-A185038] N88-13957
**PORPHYRINS**
Reactions of porphyrins in surfactant assemblies, microemulsions and in solutions
[AD-A184797] N88-13412
**PORTABLE EQUIPMENT**
The Portable Instant Display and Analysis Spectrometer (PIDAS) N88-13756
**POSITIONING**
Theoretical and practical aspects of the functional absorber method of arranging sound absorbing panels
[BBC-RD-1987/15] N88-13955
**POSTURE**
Sitting posture of helicopter pilots of the Royal Netherlands Air Force; preliminary recommendations
[IZF-1986-16] N88-13857
**POTENTIAL FLOW**
Numerical analysis of supersonic flows using panel method N88-13266
Computation of transonic flows with nacelle simulation
[SNIAS-872-111-117] N88-13300
**POTENTIAL THEORY**
Resonant level lifetime in GaAs/ AlGaAs double-barrier structures
[AD-A185376] N88-14020
**POTENTIOMETRIC ANALYSIS**
High energy molecules of high symmetry
[AD-A185365] N88-13965
**POWDER (PARTICLES)**
Colloidal stability of oxidized silicon particles in ethanolic and aqueous media
[DE87-014783] N88-13421
High explosive moulding powders from RDX and aqueous polyurethane dispersions
[AD-A185025] N88-13458
**POWDER METALLURGY**
A fundamental study of P/M processed elevated temperature aluminum alloys
[AD-A185393] N88-13445
Tensile properties of extrusion consolidated Type 304 SS rapidly solidified powders
[DE87-014875] N88-13450
Development on thin wall tubes of dispersion type
[DE87-703384] N88-13483
Behavior of long and short fatigue cracks in a powder metallurgy superalloy at room and at high temperature N88-13677
**POWER AMPLIFIERS**
Theoretical and experimental investigation of electron beam acceleration and sub-millimeter wave generation in cyclotron resonant cavities
[AD-A184806] N88-13975
**POWER CONDITIONING**
High energy density rechargeable batteries for aerospace power requirements
[AD-A184883] N88-13519
**POWER GAIN**
An experimental study of CW HF chemical laser amplifier performance and zero power gain
[AD-A185241] N88-13584
**POWER SPECTRA**
An examination of chaotic motion for the buckled beam N88-13644
**PRECISION**
Precision analysis of regular networks
[B8709606] N88-13806
**PREDICTION ANALYSIS TECHNIQUES**
Hypersonic static and dynamic stability of axisymmetric shapes: A comparison of prediction methods and experiment N88-13246
Experiences using the Mark IV supersonic hypersonic arbitrary body program N88-13249
Application of modified loss and deviation correlations to transonic axial compressors
[AGARD-R-745] N88-13344
An analytical study of the effects of transverse shear deformation and anisotropy on buckling loads of laminated cylinders
[NASA-TM-100508] N88-13387
The simulation of the viscous flow around a cylinder by the random vortex method N88-13534
Low thrust viscous nozzle flow fields prediction
[NASA-CR-182334] N88-13551
An examination of chaotic motion for the buckled beam N88-13644
Fatigue crack growth: Statistical considerations N88-13718
Comparing hard and soft prior bounds in geophysical inverse problems
[NASA-CR-181557] N88-13820
Specification of predictors necessary for the determination of over or underestimation of radar derived total rainfall
[AD-A185363] N88-13838
**PREDICTIONS**
Numerical prediction of turbulent flows in dump diffusers N88-13265
Prediction of wing aeroelastic effects on aircraft life and pitching moment characteristics N88-13356
Fiber composite structural durability and damage tolerance: Simplified predictive methods
[NASA-TM-100179] N88-13409
Master plots for predicting the case-depth in laser surface treatments
[PB87-221875] N88-13574
Significance of fatigue crack closure under spectrum loading N88-13662
Low cycle fatigue life predictions of a 1CrMoV steel in terms of a J-controlled short crack growth model N88-13665
Crack growth prediction in 3D structures under aeronautical-type spectrum loadings N88-13688
Accurate rotor loads prediction using the FLAP (Force and Loads Analysis Program) dynamics code
[DE88-001109] N88-13815
File usage analysis and resource usage prediction: A measurement-based study
[NASA-CR-181553] N88-13867
Predictability of process resource usage: A measurement-based study of UNIX
[NASA-CR-181562] N88-13869
Robust prediction operations for stationary processes
[AD-A185408] N88-13924
**PREMIXED FLAMES**
Turbulence generation in combustion
[AD-A184810] N88-13413
**PREMIXING**
Formation and destruction of nitrous oxide in lean, premixed combustion
[DE88-001390] N88-13423
**PRESERVING**
Irradiation preservation of seafood: Literature review
[DE88-001691] N88-13858
**PRESSURE CHAMBERS**
Cooling electronic equipment at simulated high altitude in hypobaric chambers
[AD-A185196] N88-13560
**PRESSURE DISTRIBUTION**
Application of discrete vortex method to analysis of separated flow around aerofoils N88-13268
Low speed wind tunnel investigation of propeller slipstream aerodynamic effects on different nacelle/wing combinations. Part 1: Total forces and moments and pressure distributions on nacelle/wing at different angles of attack and yaw and at different thrust coefficients
[FFA-TN-1987-22] N88-13302
Plasticity of aluminum and iron at high shear strain rate and high pressure N88-13430
Identification of perturbations in turbomachines by the analysis of pressure signals, vibrations and wavelike motions
[ETN-88-90602] N88-13600
**PRESSURE EFFECTS**
Fluid mass and thermal loading effects on the modal characteristics of space shuttle main engine liquid oxygen inlet splitter vanes N88-13628
**PRESSURE GRADIENTS**
Statistical theory of turbulent incompressible multimaterial flow
[DE88-000435] N88-13535
Asymptotic analysis of a turbulent boundary layer in a strong adverse pressure gradient
[AD-A185406] N88-13543
**PRESSURE MEASUREMENT**
Fluctuating pressure loads under high speed boundary layers
[NASA-TM-100517] N88-13962
**PRESSURE OSCILLATIONS**
Predictions of F-111 TACT aircraft buffet response and correlations of fluctuating pressures measured on aluminum and steel models and the aircraft
[NASA-CR-4069] N88-13218
**PRESSURE RATIO**
Performance characteristics of magnesium-sodium nitrate flares in oxygen-nitrogen atmospheres
[AD-A185274] N88-13476
**PRESSURE VESSEL DESIGN**
The structures of large wound propulsion shells --- carbon fiber composites filament winding
[SNIAS-872-430-118] N88-13406
**PRESSURE VESSELS**
Making space nickel/hydrogen batteries lighter and less expensive
[DE88-000168] N88-13530
**PRINCIPAL COMPONENTS ANALYSIS**
Effective use of principal component analysis with high resolution remote sensing data to delineate hydrothermal alteration and carbonate rocks N88-13758
Illustrative examples of principal component analysis using GENSTAT/PCP
[AD-A185085] N88-13941
**PROBABILITY DENSITY FUNCTIONS**
Conditional second order closure for turbulent shear flows
[AD-A185369] N88-13542
**PROBABILITY DISTRIBUTION FUNCTIONS**
Comparing hard and soft prior bounds in geophysical inverse problems
[NASA-CR-181557] N88-13820
Explicit formulate for the distributions of stopping variables under Wald's truncated SPRT (Sequential Probability Radio Tests) for a poisson process
[AD-A185053] N88-13914
**PROBABILITY THEORY**
Approximating multivariate normal orthant probabilities using the Clark algorithm
[AD-A184855] N88-13873
Point processes
[AD-A185398] N88-13921
Isotropic probability measures in infinite dimensional spaces: Inverse problems/prior information/stochastic inversion
[NASA-CR-181555] N88-13936
**PROBLEM SOLVING**
A 3-D Euler solution for hypersonic Mach numbers N88-13240
Two low-order mixed methods for the elasticity problem
[PB87-225272] N88-13749
Indirect solution of static problems using concurrent vector processing computers
[DE87-012105] N88-13889
Application of the Von Karman equation to the bifurcation theory
[NOTA-INTERNA-891] N88-13927
**PROCEDURES**
The how and why of variable amplitude testing N88-13690
**PROCESS CONTROL (INDUSTRY)**
Avionics and corrosion N88-13336
Improved high modulus fibers
[NASA-CR-181539] N88-13389
Advances in processing techniques for nickel aluminides
[DE87-014571] N88-13449
Statistical process control applied to the liquid-fed ceramic melter process
[DE88-000271] N88-13471
Master plots for predicting the case-depth in laser surface treatments
[PB87-221875] N88-13574
Using hierarchically structured problem-solving knowledge in a rule-based process planning system
[DE87-011639] N88-13906
A study of the Department of Defense configuration management policies and procedures as applied to the FA-18 Strike/Fighter program
[AD-A184872] N88-14034

**PRODUCT DEVELOPMENT**
Production of flows for aeroballistic investigation in the shock tubes of the Franco-German Research Institute (ISL), Saint-Louis (France)
[ISL-R-113/86] N88-13295
Carbon-carbon composites and Aerospatiale. State of the art and prospects
[SNIAS-872-430-108] N88-13401
**PRODUCTION COSTS**
Making space nickel/hydrogen batteries lighter and less expensive
[DE88-000168] N88-13530
**PRODUCTION PLANNING**
XCUT: A rule-based expert system for the automated process planning of machined parts
[DE87-011638] N88-13905
Using hierarchically structured problem-solving knowledge in a rule-based process planning system
[DE87-011639] N88-13906
**PROGRAM VERIFICATION (COMPUTERS)**
Effectiveness of back-to-back testing
[TR-87-08] N88-13865
RSDIMU acceptance testing system: Overview of acceptance software and procedures N88-13866
An extension to the multilevel logic simulator for microcomputers
[AD-A185032] N88-13879
**PROGRAMMING LANGUAGES**
Near-hom prolog
[AD-A185172] N88-13880
Mixing Microsoft C and Microsoft FORTRAN program modules on the IBM Personal Computer
[DE88-001947] N88-13895
A requirements specification for a software design support system
[NASA-CR-182333] N88-13896
**PROJECTILES**
Mechanical property evaluation of a series of commercial tungsten alloys
[AD-A185440] N88-13446
Optoelectronic measurement methods for ballistic experiments
[PB87-110706] N88-13554
**PROPAGATION (EXTENSION)**
Error propagation in a digital avionic mini processor
[NASA-CR-181565] N88-13872
**PROPANE**
Molecular dynamics studies of aromatic hydrocarbon liquids
[DE88-001473] N88-13973
**PROPELLANT COMBUSTION**
Laser probes of propellant combustion chemistry
[AD-A184854] N88-13415
**PROPELLANT DECOMPOSITION**
Test number 2 of propellant for rocket motor MK52
[PB87-226155] N88-13480
**PROPELLANT PROPERTIES**
Modal survey of the space shuttle solid rocket motor using multiple input methods N88-13617
**PROPELLANT STORAGE**
Test number 2 of propellant for rocket motor MK52
[PB87-226155] N88-13480
**PROPELLANT TRANSFER**
Orbital Spacecraft Consumables Resupply System (OSCRS). Volume 1: Executive summary
[NASA-CR-172010] N88-13368
**PROPELLER BLADES**
High speed propeller performance and noise predictions at takeoff/landing conditions
[NASA-TM-100267] N88-13960
**PROPELLER SLIPSTREAMS**
Low speed wind tunnel investigation of propeller slipstream aerodynamic effects on different nacelle/wing combinations. Part 1: Total forces and moments and pressure distributions on nacelle/wing at different angles of attack and yaw and at different thrust coefficients
[FFA-TN-1987-22] N88-13302
**PROPELLERS**
Numerical calculations of the flowfield around propellers N88-13261
**PROPULSION**
Calendar of selected aeronautical and space meetings
[AGARD-CAL-87/1] N88-14033
**PROPULSION SYSTEM CONFIGURATIONS**
Integrated control and display research for transition and vertical flight on the NASA V/STOL Research Aircraft (VSRA)
[NASA-TM-100029] N88-13359
Hermes propulsion system
[SNIAS-872-422-109] N88-13383
**PROTECTIVE COATINGS**
An examination of coating failure on wing pivot fittings of f111 aircraft
[AD-A185028] N88-13328
Simulated service test behavior of various internal and external coatings applied on CF6-50 first stage turbine blades
[NLR-MP-86018-U] N88-13343
Coatings for high-temperature bearings and seals
[NASA-TM-100249] N88-13453
Water disbondment characterization of organic Coating/metal substrate systems
[AD-A184847] N88-13454
Antistatic coating compositions
[GB-PATENT-2-177-413-A] N88-13463
**PROTONS**
Experimental studies of elementary particle interactions at high energies
[DE88-000804] N88-13971
**PROTOTYPES**
A single-station weather forecasting expert system
[AD-A184889] N88-13832
A prototype ray tracer
[AD-A184863] N88-13874
**PROVING**
High resolution satellite imagery simulation --- treaty verification
[FOA-C-30462-3.3,9.3] N88-13810
**PSEUDOPOTENTIALS**
The pseudopotential density functional method applied to semiconducting crystals
[ETN-88-91362] N88-14024
**PUBLIC RELATIONS**
Procedure and program used for data processing in a poll on nuclear energy utilization
[IFSI-87-3] N88-13977
**PULMONARY FUNCTIONS**
A plethysmograph for measuring pulmonary ventilation in small animals
[AD-A184978] N88-13846
**PULSE COMMUNICATION**
Cross-correlation of uniform cyclic difference set sequences
[AD-A184879] N88-13913
**PULSE DURATION MODULATION**
Digital control of a direct current converter for a hybrid vehicle
[LAAS-87-266] N88-13527
**PULSE GENERATORS**
RIIM two-pulse injector experiments
[DE88-000926] N88-14005
**PULSED LASERS**
Determination of a flow velocity field using four-exposure laser holography
[IMFL-3114-85/32] N88-13565
Transient processes in the interaction between pulsed laser radiation and matter
[ISL-R-115/86] N88-13586
Raman microprobe characterization of dielectric films following high-energy pulsed laser irradiation
[DE88-000559] N88-13587
Theory of multiphoton ionization of atoms by strong, short pulsed lasers
[DE88-000963] N88-13588
**PULSES**
Cerenkov radiation field analysis due to a passing electron beam
[AD-A184870] N88-13976
**PULTRUSION**
Potential for on-orbit manufacture of large space structures using the pultrusion process
[NASA-TM-4016] N88-13388
**PURSUIT TRACKING**
The isotropic rocket: A surveillance evasion game
[REPT-87-21] N88-13949
**PYROLYSIS**
Laser probes of propellant combustion chemistry
[AD-A184854] N88-13415
Detailed mechanism of toluene oxidation and comparison with benzene
[NASA-TM-100261] N88-13428
A study of the interaction of laser light with liquid propellant drops
[AD-A185117] N88-13582
**PYROTECHNICS**
Performance characteristics of magnesium-sodium nitrate flares in oxygen-nitrogen atmospheres
[AD-A185274] N88-13476
Advantages of internal thermal protection in a pyrotechnical plunger
[SNIAS-872-430-114] N88-13478
Numerical simulation applied to the development of a pyrotechnical system
[SNIAS-872-430-115] N88-13479

## Q

**Q SWITCHED LASERS**
An investigation of unipolar arcing at atmospheric pressure in aluminum 2024 and aluminum coated glass slides
[AD-A184903] N88-13521
**QUALITY CONTROL**
Avionics and corrosion N88-13336
Philosophy and practice of nondestructive tests of composite material structures at Aerospatiale Aquitaine
[SNIAS-872-430-105] N88-13400
Chemical analysis for excimer laser systems
[DE88-001941] N88-13591
Sandia software guidelines: Software quality planning
[DE88-001931] N88-13894
**QUANTILES**
Quantile based unified distribution of extreme values and order statistics
[AD-A185171] N88-13942
Quantile statistical data analysis
[AD-A185181] N88-13943
**QUANTITATIVE ANALYSIS**
Abundance and distribution of ultramafic microbreccia in Moses Rock Dike: Quantitative application of AIS data N88-13766
**QUANTUM EFFICIENCY**
Study of solid state photomultiplier
[NASA-CR-177465] N88-13556
**QUANTUM MECHANICS**
Theory of neutron scattering experiments on momen tum distributions in quantum fluids
[DE87-01369] N88-13968
Resonant level lifetime in GaAs/ AlGaAs double-barrier structures
[AD-A185376] N88-14020
Example of correlation between space and spin coordinates
[DE87-703366] N88-14030
A mechanism for symmetry breaking in antiferromagnetic Heisenberg systems
[ETN-88-91320] N88-14031
**QUANTUM WELLS**
Phase-locked semiconductor quantum well laser arrays
[AD-A185155] N88-13583

## R

**RADAR IMAGERY**
Correction of inertial navigation system drift errors for an autonomous land vehicle using optical radar terrain data
[AD-A184973] N88-13311
**RADAR MAPS**
Inverse scattering analysis of diffraction limited SAR
[FOA-C-30459-3.2] N88-13512
**RADAR MEASUREMENT**
Contributions of lidar measurements to the study of long term variations of the middle atmosphere
[ETN-88-91237] N88-13824
**RADAR PHOTOGRAPHY**
Inverse scattering analysis of diffraction limited SAR
[FOA-C-30459-3.2] N88-13512
**RADAR SCATTERING**
Large bandwidth ground scattering model — radar scattering
[FOA-C-30458-3.2] N88-13511
Inverse scattering analysis of diffraction limited SAR
[FOA-C-30459-3.2] N88-13512
**RADAR TRACKING**
Media calibrations of the Doppler signal for a gravitational wave experiment — interplanetary medium
[IFSI-86-13] N88-13825
**RADIAL DISTRIBUTION**
Fiber-optic accelerometer investigation
[AD-A185359] N88-13561
**RADIANCE**
Calibrating AIS images using the surface as a reference N88-13760
**RADIATION BELTS**
Analysis of geophysical data bases and models for spacecraft interactions
[AD-A184809] N88-13375
**RADIATION DETECTORS**
Study of solid state photomultiplier
[NASA-CR-177465] N88-13556
**RADIATION DISTRIBUTION**
RADSPHERE: A computer program for calculating the steady-state, axially symmetric, forced response and radiation field of a submerged spherical shell
[AD-A185025] N88-13738

Cerenkov radiation field analysis due to a passing electron beam
[AD-A184870] N88-13976
**RADIATION DOSAGE**
Fabricate, calibrate and test a dosimeter for integration into the CRRES (Combined Release and Radiation Effects Satellite) satellite
[AD-A185439] N88-13564
**RADIATION EFFECTS**
A study of charged particles/radiation damage to VLSI device materials
[NASA-CR-172036] N88-13518
Fabricate, calibrate and test a dosimeter for integration into the CRRES (Combined Release and Radiation Effects Satellite) satellite
[AD-A185439] N88-13564
TOMS as a monitor of the ultraviolet radiation environment: Applications to photobiology N88-13785
Irradiation preservation of seafood: Literature review
[DE88-001691] N88-13858
**RADIATION HAZARDS**
Preliminary estimates of galactic cosmic ray exposures for manned interplanetary missions
[NASA-TM-100519] N88-14058
**RADIATIVE HEAT TRANSFER**
A hybrid fibreglass-CFRP cloth for new furnishings --- aircraft cabins
[SNIAS-872-111-109] N88-13396
**RADIATIVE TRANSFER**
MODTRAN: A moderate resolution model for LOWTRAN
[AD-A185364] N88-13503
**RADIO COMMUNICATION**
Two-signal cross modulation effects, half-IF effects and interference criteria in land mobile sharing with UHF (Ultra High Frequency) television
[PB87-228037] N88-13514
**RADIO FREQUENCY HEATING**
Microwave superheaters for fusion
[DE88-001656] N88-14007
**RADIO RELAY SYSTEMS**
Improvements to a UHF rebroadcast television link suffering tidal fading: Countisbury UHF relay station
[BBC-RD-1987/14] N88-13495
**RADIO SIGNALS**
Two-signal cross modulation effects, half-IF effects and interference criteria in land mobile sharing with UHF (Ultra High Frequency) television
[PB87-228037] N88-13514
**RADIO WAVES**
Measured characteristics of 800/900 MHz mobile radio channels with high-angle propagation through moderately dense foliage
[CRC-1398] N88-13493
**RADIOACTIVE DECAY**
W decays
[NOTA-INTERNA-877] N88-13966
**RADIOGRAPHY**
Measurement and control of damage in composite materials: Nondestructive controls by thermography, holography, and radiography
[SNIAS-872-430-110] N88-13403
X-ray imaging: Status and trends
[DE88-000756] N88-13960
**RADIOLYSIS**
Organic molecules on meteoritic solid substrates
[NASA-CR-181570] N88-13411
**RADIOMETERS**
Development of response models for the Earth Radiation Budget Experiment (ERBE) sensors. Part 3: ERBE scanner measurement accuracy analysis due to reduced housekeeping data
[NASA-CR-178294] N88-13553
**RADIOSONDES**
Correlations of TOMS total ozone data (Nimbus-7 satellite) with tropopause height N88-13788
**RAIN**
Specification of predictors necessary for the determination of over or underestimation of radar derived total rainfall
[AD-A185363] N88-13838
**RAMAN LASERS**
Raman microprobe characterization of dielectric films following high-energy pulsed laser irradiation
[DE88-000559] N88-13587
**RAMAN SPECTRA**
High energy molecules of high symmetry
[AD-A185385] N88-13965
Solitons in stimulated Raman scattering: Generation and control of ultrashort optical pulses
[AD-A185141] N88-13983
**RAMJET ENGINES**
An experimental investigation of the ignition and flammability limits of various hydrocarbon fuels in a two-dimensional solid fuel ramjet
[AD-A184968] N88-13342
**RANDOM LOADS**
Fatigue under nonnormal random stresses using Monte Carlo method N88-13723
**RANDOM VIBRATION**
The analysis of nonstationary vibration data N88-13610
**RANGE (EXTREMES)**
Extrema of skewed stable processes
[AD-A185422] N88-13925
**RANGEFINDING**
Range imagery algorithms for the detection of obstacles by autonomous vehicles
[AD-A185421] N88-14045
**RANKINE CYCLE**
Microwave superheaters for fusion
[DE88-001656] N88-14007
**RAPID QUENCHING (METALLURGY)**
Effect of rapid solidification on short-range order: A magnetic study
[AD-A185218] N88-13444
Tensile properties of extrusion consolidated Type 304 SS rapidly solidified powders
[DE87-014875] N88-13450
Development of iron aluminides
[AD-A185190] N88-13461
**RAREFACTION**
Low Reynolds number influence on aerodynamic performance of hypersonic lifting vehicles N88-13230
**RAREFIED GAS DYNAMICS**
Rarefied gas numerical wind tunnel. 2: Two-dimensional and axially symmetric bodies N88-13273
**RATIOS**
Determination of the fiber ratio in carbon fiber/resin composites by means of image analysis
[SNIAS-872-422-101] N88-13398
**RAWINSONDES**
The use of TOMS-modified VAS data for large-scale NWP N88-13791
**RAY TRACING**
A prototype ray tracer
[AD-A184863] N88-13874
**RDX**
High explosive moulding powders from RDX and aqueous polyurethane dispersions
[AD-A185026] N88-13458
**REACTION KINETICS**
Numerical analysis of axisymmetric flow with H2-O2 reactions N88-13272
Laser probes of propellant combustion chemistry
[AD-A184854] N88-13415
Detailed mechanism of toluene oxidation and comparison with benzene
[NASA-TM-100261] N88-13428
Effect of rapid solidification on stainless steel weld metal microstructures and its implications on the Schaeffler diagram
[DE88-001489] N88-13451
Reactive sticking coefficients of silane on silicon
[DE88-000601] N88-13473
Theoretical studies of solar lasers and converters
[NASA-CR-181569] N88-13577
Fracture kinetics of corrosion fatigue N88-13708
Numerical methods for reaction-diffusion problems with non-differentiable kinetics
[AD-A185405] N88-13923
**REACTIVITY**
Reactions of porphyrins in surfactant assemblies, microemulsions and in solutions
[AD-A184797] N88-13412
**REAL GASES**
Hypersonic laminar boundary layer: Parametric study for the representation of real gas effects N88-13236
On the numerical simulation of three-dimensional hypersonic flow N88-13237
**REAL TIME OPERATION**
Performability modeling based on real data: A casestudy
[NASA-CR-181563] N88-13870
Presentation of SIGMA (Interactive Assisted Geometry System). A computer assisted shape design program developed at the Aerospatiale Aircraft Division
[SNIAS-872-111-110] N88-13884
Conceptual issues in measuring the behavior of a distributed real-time process-control computer system
[DE87-009748] N88-13898
Conceptual issues in measuring the behavior of a distributed real-time process-control computer system
[DE87-014251] N88-13899
**RECOMBINATION REACTIONS**
OH(A-X) fluorescence from photodissociative excitation of HO2 at 157.5 nm
[NASA-CR-181580] N88-13429
**RECOMMENDATIONS**
Observation guidelines for a Total Ozone Mapping Spectrometer (TOMS) in geosynchronous orbit N88-13801
**RECRYSTALLIZATION**
Cyclic deformation of an extruded AlMgSi alloy N88-13654
**REDUCED GRAVITY**
Results from the melting of tungsten composites under microgravity (TEXUS 10 flight)
[FOA-C-20676-2.1] N88-13482
Feasibility study for gas-grain simulation facility
[NASA-CR-177468] N88-13954
**REDUCTION (CHEMISTRY)**
Activated metal oxide surfaces as highly basic and reducing environments
[AD-A184958] N88-13417
**REENTRY EFFECTS**
Hypersonic aerodynamics: Applications for HOTOL N88-13252
**REFRACTORY MATERIALS**
Cu-2 mechanical properties and microstructural stability of advanced steam cycle materials
[DE88-001519] N88-13452
**REFRACTORY METAL ALLOYS**
Properties of refractory metals processed by enhanced sintering treatments
[AD-A184944] N88-13440
**REFRACTORY METALS**
Properties of refractory metals processed by enhanced sintering treatments
[AD-A184944] N88-13440
**REFRIGERANTS**
Development of a low noise 10 K J-T refrigeration system
[AD-A185258] N88-13484
**REFRIGERATORS**
Development of a low noise 10 K J-T refrigeration system
[AD-A185258] N88-13484
Evaluation of a cryogenic refrigerator for cooling focal plane instrumentation --- satellite instruments
[BAE-TP-8095-VOL-1] N88-13485
Evaluation of a cryogenic refrigerator for cooling focal plane instrumentation. Appendix B: Accommodation study --- satellite instruments
[BAE-TP-8095-VOL-2] N88-13486
**REFUELING**
Orbital Spacecraft Consumables Resupply System (OSCRS). Volume 1: Executive summary
[NASA-CR-172010] N88-13368
**REGRESSION ANALYSIS**
Regressed relations for forced convection heat transfer in a direct injection stratified charge rotary engine
[NASA-TM-100124] N88-13345
An APL workspace for conducting nonparametric statistical inference
[AD-A184971] N88-13877
Least squares for fuzzy vector data regression
[AD-A185156] N88-13917
**REINFORCED SHELLS**
Experimental studies on the tripping behavior of narrow T-stiffened flat plates subjected to hydrostatic pressure and underwater shock N88-13613
**RELAXATION (MECHANICS)**
Pure dephasing of a vibrational adbond
[AD-A185222] N88-13740
**RELAXATION METHOD (MATHEMATICS)**
A note on the use of symmetric line Gauss-Seidel for the steady upwind differenced Euler equations
[AD-A185223] N88-13540
Matching segments from a map and an aerial image using relaxation techniques
[SNIAS-872-422-103] N88-13809
**RELIABILITY**
Development of an interface for an ultrareliable fault-tolerant control system and an electronic servo-control unit
[NASA-TM-88236] N88-13367
Electromagnetics and electrothermal approach to evaluate failures in microelectronic devices caused by electrostatic discharges: Stochastical aspects of the device reliability
[AD-A184906] N88-13522
**RELIABILITY ENGINEERING**
Reliability of voting in fault-tolerant software systems for small output spaces
[TR-87-16] N88-13864
Effectiveness of back-to-back testing
[TR-87-08] N88-13865
**REMOTE SENSING**
The Portable Instant Display and Analysis Spectrometer (PIDAS) N88-13756
Effective use of principal component analysis with high resolution remote sensing data to delineate hydrothermal alteration and carbonate rocks N88-13758
Land cover/use classification of Cairns, Queensland, Australia: A remote sensing study involving the conjunctive use of the airborne imaging spectrometer, the large format camera and the thematic mapper simulator N88-13759

In-orbit calibration adjustment of the Nimbus-7 SMMR
[NASA-TM-100678] N88-13773
Study on data compression systems for operational remote sensing — meteosat imagery
[NLR-TR-86029-L] N88-13808

**REMOTE SENSORS**
In-situ characterization of the interface of glass reinforced composites
[AD-A185136] N88-13391
Italy's Institute of Research on Electromagnetic Waves–the Istituto di Ricerca sulle Onde Elettromagnetiche
[AD-A185020] N88-13501
Development of response models for the Earth Radiation Budget Experiment (ERBE) sensors. Part 3: ERBE scanner measurement accuracy analysis due to reduced housekeeping data
[NASA-CR-178294] N88-13553
Estimation of marine boundary layer depth and relative humidity with multispectral satellite measurements
[AD-A184881] N88-13804
Software design for an airborne gravity measurement system
[AD-A185000] N88-13878

**REPORTS**
Workshop on Avionics Corrosion Control
[AGARD-R-733] N88-13331
Role of technical information in innovation
[PB87-235388] N88-14039
Role of the technical report in technological innovation
[PB87-232500] N88-14040

**REQUIREMENTS**
Design and assembly sequence analysis of option 3 for CETF reference space station
[NASA-TM-100503] N88-13369

**RESEARCH**
Procedure and program used for data processing in a poll on nuclear energy utilization
[IFSI-87-3] N88-13977
Budget and programs for 1986 research
[IFSI-86-16] N88-14048

**RESEARCH AND DEVELOPMENT**
Aerothermodynamics research at NASA Ames N88-13242
Innovative and alternative technology projects
[PB87-230165] N88-13818
CELSS Program Meeting N88-13853
The birth of big science: Nuclear physics as advanced technology source
[NOTA-INTERNA-881] N88-13967
Role of technical information in innovation
[PB87-235388] N88-14039
Role of the technical report in technological innovation
[PB87-232500] N88-14040
AGARD: The NATO Advisory Group for Aerospace Research and Development
[AD-A185062] N88-14063

**RESEARCH FACILITIES**
Aerothermodynamics research at NASA Ames N88-13242

**RESEARCH MANAGEMENT**
The birth of big science: Nuclear physics as advanced technology source
[NOTA-INTERNA-881] N88-13967
A short introduction to the status and motivation for reversed field pinch and compact toroid research
[DE88-000487] N88-13999
University research initiative research program summaries
[AD-A184876] N88-14035

**RESIDENTIAL ENERGY**
Transient development of stratification in a partially divided enclosure
[DE87-011742] N88-13490

**RESIDUAL STRENGTH**
Fiber composite structural durability and damage tolerance: Simplified predictive methods
[NASA-TM-100179] N88-13409

**RESIDUAL STRESS**
The evolution of local mechanical properties of Al 2219-T851 during fatigue N88-13653
The influence of microstructure and residual stresses on the initiation and propagation of short surface cracks on AlMgSi1 N88-13674
Observations on the effect of overloads on fatigue crack growth N88-13684
The effect of heat treatment on fatigue crack growth in polycarbonate N88-13714
Analysis of end stresses in glass-metal bimaterial strips
[DE87-007848] N88-13750

**RESONANCE**
Resonant level lifetime in GaAs/ AlGaAs double-barrier structures
[AD-A185376] N88-14020

**RESONANCE FLUORESCENCE**
Solitons in stimulated Raman scattering: Generation and control of ultrashort optical pulses
[AD-A185141] N88-13983

**RESONANT FREQUENCIES**
A new method to real-normalize measured complex modes N88-13618
Initial dynamic load estimates during configuration design N88-13621
Dynamic behavior of dissymmetric rotor bearings modelled with a periodic coefficient large system N88-13640
Computation of natural frequencies of planar lattice structure
[AD-A185387] N88-13920

**RESOURCES MANAGEMENT**
University research initiative research program summaries
[AD-A184876] N88-14035

**RESPIRATION**
Short-term in vitro screening studies related to the inhalation toxicology of potentially toxic aerosols
[AD-A184815] N88-13845
A plethysmograph for measuring pulmonary ventilation in small animals
[AD-A184978] N88-13848

**RESPONSE TIME (COMPUTERS)**
Indirect solution of static problems using concurrent vector processing computers
[DE87-012105] N88-13889

**RETARDING**
Fatigue crack retardation in aluminium alloys N88-13681

**REVERSE FIELD PINCH**
Dynamic processes in field-reversed-configuration compact toroids
[DE87-014756] N88-13998
A short introduction to the status and motivation for reversed field pinch and compact toroid research
[DE88-000487] N88-13999
A review of the experimental and theoretical status of the reversed-field pinch
[DE88-000529] N88-14000
Reversed field pinch plasmas with various boundary conditions
[DE88-000832] N88-14004

**REYNOLDS NUMBER**
The drag of slender axisymmetric cones in rarefied hypersonic flow N88-13229
Computational study of three-dimensional wake structures
[REPT-2] N88-13281
Effects of free stream turbulence, Reynolds number and incidence angle on axial turbine cascade performance N88-13339
Regressed relations for forced convection heat transfer in a direct injection stratified charge rotary engine
[NASA-TM-100124] N88-13345

**RIDING QUALITY**
Measurement of suspension and ride characteristics of the M1 main battle tank N88-13637

**RIEMANN MANIFOLD**
Computer-aided study of a class of Riemannian space-times
[DE87-703367] N88-13950

**RIGID STRUCTURES**
Numerical simulations of impact tests on a rigid wall — armor steel
[SNIAS-872-320-102] N88-13744

**RISK**
Hypersonic aerodynamics: Applications for HOTOL N88-13252

**ROBOTICS**
Correction of inertial navigation system drift errors for an autonomous land vehicle using optical radar terrain data
[AD-A184973] N88-13311
Towards building a team of intelligent robots
[NASA-CR-181538] N88-13595
Collision-free motion of two robot arms in a common workspace
[CSE-87-00002] N88-13596
Behavioral Architecture Robot Control System (BARCS): A new way of building robots
[REPT-87-036] N88-13902

**ROBOTS**
Towards building a team of intelligent robots
[NASA-CR-181538] N88-13595
Collision-free motion of two robot arms in a common workspace
[CSE-87-00002] N88-13596
Dealing with unanticipated events in autonomous navigation
[DE88-000590] N88-13602
Trajectory control of robot manipulators with closed-kinematic chain mechanism
[NASA-TM-89305] N88-13605
Cartesian path control of a two-degree-of-freedom robot manipulator
[NASA-CR-182331] N88-13908
Range imagery algorithms for the detection of obstacles by autonomous vehicles
[AD-A185421] N88-14045

**ROBUSTNESS (MATHEMATICS)**
Solution of some 3-D viscous and inviscid supersonic flow problems by finite-volume space-marching schemes N88-13235
Robustness of linear systems
[PB87-220042] N88-13909
Robust prediction operations for stationary processes
[AD-A185406] N88-13924

**ROCKET ENGINE CASES**
The structures of large wound propulsion shells — carbon fiber composites filament winding
[SNIAS-872-430-118] N88-13406

**ROCKET ENGINE DESIGN**
Hermes propulsion system
[SNIAS-872-422-109] N88-13383

**ROCKET PROPELLANTS**
Test number 2 of propellant for rocket motor MK52
[PB87-226155] N88-13480

**ROCKS**
Analysis of airborne imaging spectrometer data for the Ruby Mountains, Montana, by use of absorption-band-depth images N88-13771
Mapping hydrothermally altered rocks in the Northern Grapevine Mountains, Nevada and California with the airborne imaging spectrometer N88-13772

**ROOM TEMPERATURE**
Behavior of long and short fatigue cracks in a powder metallurgy superalloy at room and at high temperature N88-13677

**ROOTS OF EQUATIONS**
Detection of critical points: The first step to automatic line generalization N88-13803

**ROTARY ENGINES**
Regressed relations for forced convection heat transfer in a direct injection stratified charge rotary engine
[NASA-TM-100124] N88-13345

**ROTARY WINGS**
Velocity scaled aeroelastic testing of an unducted fan
[GTL-191] N88-13337

**ROTATING FLUIDS**
Compressor large bandwidth noise emission mechanisms
[ETN-88-91177] N88-13959

**ROTATION**
Development, construction and testing of a novel internal combustion engine with conical rotating slide valve
[DE88-900071] N88-13593

**ROTOR BLADES (TURBOMACHINERY)**
Solution procedure for the Navier-Stokes equations applied to rotors N88-13533
Noise of a model counterrotation propeller with reduced aft rotor diameter at simulated takeoff/approach conditions (F7/A3)
[NASA-TM-100254] N88-13961

**ROTORS**
Calculation of helicopter rotor blade/vortex interaction by Navier-Stokes procedures
[NASA-CR-177441] N88-13291
Model helicopter rotor rig and associated strain gauge balance for performance studies
[NAL-TM-AE-8704] N88-13364
Dynamic behavior of dissymmetric rotor bearings modelled with a periodic coefficient large system N88-13640
Coupled elastic rotor/body vibrations with inplane degrees of freedom N88-13643

**RUBIDIUM**
On-orbit frequency stability analysis of the GPS NAVSTAR 8 rubidium clock and NAVSTARs 9 and 10 cesium clocks
[AD-A184984] N88-13312

**RUDDERS**
The use of aeroelastic wind tunnel models to prove structural design N88-13355

**RUN TIME (COMPUTERS)**
File usage analysis and resource usage prediction: A measurement-based study
[NASA-CR-181553] N88-13867
Predictability of process resource usage: A measurement-based study of UNIX
[NASA-CR-181562] N88-13869

**RUTHENIUM COMPOUNDS**
Intramolecular energy transfer reactions as a method for metal complex assisted production of hydrogen
[DE88-001621] N88-13425

# S


**SADDLE POINTS**
Transient periodic behavior related to a saddle-node bifurcation
[ETN-88-91321] N88-13928
**SAFETY**
Comparison of fire resistance of metallic and nonmetallic structures
[SNIAS-872-551-101] N88-13489
Establishment of complete minimum test sets for digital circuits with safety engineering significance
[ETN-88-90569] N88-13526
**SAFETY FACTORS**
Small space reactor power systems for unmanned solar system exploration missions
[NASA-TM-100228] N88-14054
**SAMPLING**
Sample reuse in statistical remodeling
[AD-A184916] N88-13938
**SANDS**
Environmental processes and spectral reflectance characteristics associated with soil erosion in desert fringe regions
[NASA-CR-182332] N88-13811
**SANDSTONES**
Abundance and distribution of ultramafic microbreccia in Moses Rock Dike: Quantitative application of AIS data N88-13766
**SARSAT**
COSPAS-SARSAT satellite orbit predictor, volume 10
[NASA-TM-85015] N88-13370
**SATELLITE COMMUNICATION**
Error control techniques for satellite and space communications
[NASA-CR-181581] N88-13516
**SATELLITE CONFIGURATIONS**
Evaluation of a cryogenic refrigerator for cooling focal plane instrumentation. Appendix B: Accommodation study — satellite instruments
[BAE-TP-8095-VOL-2] N88-13486
**SATELLITE DESIGN**
Mechanical design of the ac bracket package for the RETE experiment
[IFSI-87-4] N88-13379
A geostationary imaging spectrometer TOMS instrument N88-13802
**SATELLITE GROUND TRACKS**
COSPAS-SARSAT satellite orbit predictor, volume 10
[NASA-TM-85015] N88-13370
**SATELLITE IMAGERY**
Tropical easterly jet located using TOMS data N88-13783
Application of TOMS data to weather analysis models N88-13787
National Point Of Contact (NPOC)-SPOT inquiry 1986
[NLR-MP-86055-U] N88-13807
Study on data compression systems for operational remote sensing — meteosat imagery
[NLR-TR-86029-L] N88-13808
High resolution satellite imagery simulation — treaty verification
[FOA-C-30462-3.3,9.3] N88-13810
Mesoscale applications of high resolution imagery
[AD-A185039] N88-13833
**SATELLITE NETWORKS**
Study of the feasiblity of a satellite communication system for road transportation home office to vehicle communication. Volume 1: Conceptual analysis
[SC/87-E/6-VOL-1] N88-13505
Study of the feasibility of a satellite communication system for road transportation home office to vehicle communication. Volume 2: Market study
[SC/87-E/6-VOL-2] N88-13506
**SATELLITE OBSERVATION**
Budget and programs for 1986 research
[IFSI-86-16] N88-14048
Satellite observations of extreme ultraviolet radiation
[AD-A185043] N88-14059
**SATELLITE ORBITS**
COSPAS-SARSAT satellite orbit predictor, volume 10
[NASA-TM-85015] N88-13370
**SATELLITE SOUNDING**
Scientific and Operational Requirements for TOMS Data
[NASA-CP-2497] N88-13774
Dobson-stations performance assessment using TOMS data N88-13792
Volcanic eruption detection with TOMS N88-13793
Analysis of SO2 signals in SBUV/TOMS data N88-13794
Comparison of ground based and TOMS measurements of SO2 from volcanic emissions N88-13795
Use of satellite data in volcano monitoring N88-13797
Selection of optimum wavelengths for ozone mapping from satellites N88-13798
Determination of total ozone from HIRS2/MSU sounding data N88-13799
Complementary information between UV and IR for remote sensing of total ozone N88-13800
Observation guidelines for a Total Ozone Mapping Spectrometer (TOMS) in geosynchronous orbit N88-13801
Electric field measurements on Viking: First results
[TRITA-EPP-87-04] N88-13826
**SATELLITE-BORNE INSTRUMENTS**
Evaluation of a cryogenic refrigerator for cooling focal plane instrumentation — satellite instruments
[BAE-TP-8095-VOL-1] N88-13485
Evaluation of a cryogenic refrigerator for cooling focal plane instrumentation. Appendix B: Accommodation study — satellite instruments
[BAE-TP-8095-VOL-2] N88-13486
Development of response models for the Earth Radiation Budget Experiment (ERBE) sensors. Part 3: ERBE scanner measurement accuracy analysis due to reduced housekeeping data
[NASA-CR-178294] N88-13553
**SATELLITE-BORNE PHOTOGRAPHY**
Varifront 3 expedition data report (USNS DE STEIGUER CRUISE 1202-82). Bioluminescence, hydrographic, nutrient, and satellite data from the Gulf of California (November-December 1981)
[AD-A185011] N88-13805
Modeling cloudy and clear interval length probabilities using space shuttle imagery
[AD-A185290] N88-13837
**SCALE (RATIO)**
Detection of critical points: The first step to automatic line generalization N88-13803
**SCALE MODELS**
Measurement of model deformation in wind tunnels N88-13358
A system identification technique based on the random decrement signatures. Part 2: Experimental results N88-13626
**SCALING**
Transport scaling in the collisionless-detrapping regime in stellarators
[DE88-001511] N88-14006
**SCALING LAWS**
Improvement of modal scaling factors using mass additive technique N88-13620
**SCANNERS**
Development of response models for the Earth Radiation Budget Experiment (ERBE) sensors. Part 3: ERBE scanner measurement accuracy analysis due to reduced housekeeping data
[NASA-CR-178294] N88-13553
**SCANNING**
In-orbit calibration adjustment of the Nimbus-7 SMMR
[NASA-TM-100678] N88-13773
**SCATTERING**
Anti-Stokes generation of 226 nm light
[DE88-001612] N88-13590
Atomic beam studies of the interaction of hydrogen with transition metal surfaces
[DE88-000208] N88-13970
Energy dependence of ion-induced sputtering yields of monatomic solids in the low energy region
[IPPJ-AM-52] N88-13988
**SCENE ANALYSIS**
Television motion measurement for DATV and other applications
[BBC-RD-1987/11] N88-13496
**SCREW DISLOCATIONS**
The effects of thin anodic films on the cyclic microstrain/macrostrain behavior of tungsten N88-13650
**SEA ICE**
The ice conditions in the Greenland waters, 1981
[ISBN-87-7478-276-2] N88-13844
**SEA LEVEL**
Expectations for water level deviations at the delta works: Zierikzee (Netherlands), November 1981-February 1986
[KNMI-TR-93] N88-13840
**SEALERS**
Process for the production of a thermoplastic elastomer composition
[EP-PATENT-0-202-782-A2] N88-13485
**SEALS (STOPPERS)**
Coatings for high-temperature bearings and seals
[NASA-TM-100249] N88-13453
Three-dimensional dynamic labyrinth seal analysis
[AD-A185353] N88-13599
Seal technology for liquid oxygen (LOX) turbopumps
[NASA-CR-174866] N88-13603
**SEARCHING**
An automated supernova search and the design strategy
[DE88-001827] N88-14051
**SEDIMENTARY ROCKS**
Preliminary results from an investigation of AIS-1 data over an area of epithermal alteration: Plateau, Northern Queensland, Australia N88-13768
**SEDIMENTS**
Colloidal stability of oxidized silicon particles in ethanolic and aqueous media
[DE87-014783] N88-13421
**SELF LUBRICATION**
Coatings for high-temperature bearings and seals
[NASA-TM-100249] N88-13453
**SEMANTICS**
Near-horn prolog
[AD-A185172] N88-13880
**SEMICONDUCTOR DEVICES**
Molecular beam epitaxial growth and characterization of 3-5 compound semiconductor single and multiple interface structures
[AD-A185400] N88-14021
**SEMICONDUCTOR LASERS**
Phase-locked semiconductor quantum well laser arrays
[AD-A185155] N88-13583
Nonconventional optical techniques for optical wavefront processing
[AD-A185099] N88-13982
**SEMICONDUCTORS (MATERIALS)**
Supersonic beam observations of semiconductor clusters
[AD-A184991] N88-14018
The pseudopotential density functional method applied to semiconducting crystals
[ETN-88-91362] N88-14024
**SEMISPAN MODELS**
Tip aerodynamics from wind tunnel test of semi-span wing
[NASA-TM-88253] N88-13290
**SEPARATED FLOW**
Driving mechanism of unsteady separation shock motion in hypersonic interactive flow N88-13226
Application of discrete vortex method to analysis of separated flow around aerofoils N88-13268
**SEQUENCING**
Cross-correlation of uniform cyclic difference set sequences
[AD-A184879] N88-13913
**SEQUENTIAL ANALYSIS**
Explicit formulate for the distributions of stopping variables under Wald's truncated SPRT (Sequential Probability Radio Tests) for a poisson process
[AD-A185053] N88-13914
**SERIES EXPANSION**
The simulation of the viscous flow around a cylinder by the random vortex method N88-13534
**SERVOCONTROL**
Development of an interface for an ultrareliable fault-tolerant control system and an electronic servo-control unit
[NASA-TM-88236] N88-13367
**SHAFTS (MACHINE ELEMENTS)**
Exact finite element method analysis of viscoelastic tapered structures to transient loads N88-13632
**SHAPED CHARGES**
Jet initiation of PBX 9502
[DE88-000493] N88-13481
**SHAPES**
Shape optimization of damping layers N88-13635
The statistics of the shape of small fatigue cracks N88-13666
**SHEAR**
An analytical study of the effects of transverse shear deformation and anisotropy on buckling loads of laminated cylinders
[NASA-TM-100508] N88-13387
**SHEAR LAYERS**
Combustion related shear-flow dynamics in elliptic supersonic jets N88-13232
**SHEAR STRAIN**
Plasticity of aluminum and iron at high shear strain rate and high pressure N88-13430
**SHEAR STRENGTH**
Flexibilized copolyimide adhesives
[NASA-TM-89303] N88-13474
Effect of interface on mechanical properties of graphite/201 aluminum composites N88-13717
**SHEAR STRESS**
Analysis of end stresses in glass-metal bimaterial strips
[DE87-007848] N88-13750
**SHELLFISH**
Irradiation preservation of seafood: Literature review
[DE88-001691] N88-13858

**SHELLS (STRUCTURAL FORMS)**
The structures of large wound propulsion shells --- carbon fiber composites filament winding
[SNIAS-872-430-118] N88-13406
Optical deformation measurement on shells following the raster principle
[ETN-88-90608] N88-13741
An element of a multilayer shell for the computation of composite structures
[ONERA-RT-14/3542-RY-051-R] N88-13742
**SHIELDING**
On the role of crack tip shielding in influencing the behavior of long and small fatigue cracks in aluminum-lithium alloy 2090 N88-13671
**SHIP HULLS**
Experimental studies on the tripping behavior of narrow T-stiffened flat plates subjected to hydrostatic pressure and underwater shock N88-13613
**SHIPS**
Integrated control and display research for transition and vertical flight on the NASA V/STOL Research Aircraft (VSRA)
[NASA-TM-100029] N88-13359
**SHOCK ABSORBERS**
Non-linear shipboard shock analysis of the Tomahawk missile shock isolation system N88-13614
**SHOCK LOADS**
Shock compression of solids as a physical-chemical-mechanical process
[DE88-001674] N88-13427
Experimental studies on the tripping behavior of narrow T-stiffened flat plates subjected to hydrostatic pressure and underwater shock N88-13613
On the simulation of ballistic shock loads N88-13615
**SHOCK SIMULATORS**
Scaling the electromagnetically driven explosive shock simulator N88-13612
**SHOCK SPECTRA**
Conservatism implications of shock test tailoring for multiple design environments N88-13611
**SHOCK TESTS**
The 58th Shock and Vibration Symposium, volume 1
[NASA-CP-2488-VOL-1] N88-13609
Conservatism implications of shock test tailoring for multiple design environments N88-13611
Scaling the electromagnetically driven explosive shock simulator N88-13612
Non-linear shipboard shock analysis of the Tomahawk missile shock isolation system N88-13614
**SHOCK TUBES**
Production of flows for aeroballistic investigation in the shock tubes of the Franco-German Research Institute (ISL), Saint-Louis (France)
[ISL-R-113/86] N88-13295
**SHOCK TUNNELS**
Shock tunnels for real gas hypersonics N88-13223
**SHOCK WAVE INTERACTION**
The effects of sweep and bluntness on a glancing shock wave turbulent boundary layer interaction N88-13227
Interferometric data for a shock-wave/boundary-layer interaction
[NASA-TM-88227] N88-13306
**SHOCK WAVES**
Driving mechanism of unsteady separation shock motion in hypersonic interactive flow N88-13226
On the numerical simulation of three-dimensional hypersonic flow N88-13237
Numerical experiments with hypersonic flows beneath a cone-delta-wing combination N88-13238
The off-design performance of hypersonic waveriders N88-13244
Influence of shock wave and gas pressure on the behavior of a pyrotechnical device
[SNIAS-872-430-111] N88-13477
On the simulation of ballistic shock loads N88-13615
The Shock and Vibration Digest, Volume 19, No. 12 N88-13746
**SIDEBANDS**
HF sidebands in the ionosphere N88-13497
**SIGNAL DETECTION**
Development of an acoustic echosounder for detection of lower level atmospheric turbulence
[AD-A184877] N88-13831
**SIGNAL FADING**
Measured characteristics of 800/900 MHz mobile radio channels with high-angle propagation through moderately dense foliage
[CRC-1398] N88-13493
Improvements to a UHF rebroadcast television link suffering tidal fading: Countisbury UHF relay station
[BBC-RD-1987/14] N88-13495
**SIGNAL PROCESSING**
Measured characteristics of 800/900 MHz mobile radio channels with high-angle propagation through moderately dense foliage
[CRC-1398] N88-13493
Italy's Institute of Research on Electromagnetic Waves--the Istituto di Ricerca sulle Onde Elettromagnetiche
[AD-A185020] N88-13501
Analysis of SO2 signals in SBUV/TOMS data N88-13794
Estimation of marine boundary layer depth and relative humidity with multispectral satellite measurements
[AD-A184881] N88-13804
Cross-correlation of uniform cyclic difference set sequences
[AD-A184879] N88-13913
**SIGNAL TRANSMISSION**
Measured characteristics of 800/900 MHz mobile radio channels with high-angle propagation through moderately dense foliage
[CRC-1398] N88-13493
Time domain electromagnetic waves in multilayered media
[AD-A185055] N88-13502
**SIGNATURES**
A system identification technique based on the random decrement signatures. Part 1: Theory and simulation N88-13625
A system identification technique based on the random decrement signatures. Part 2: Experimental results N88-13626
**SIGNIFICANCE**
Determining differences in rates corresponding to a given significance level
[AD-A185004] N88-13940
**SILANES**
Reactive sticking coefficients of silane on silicon
[DE88-000601] N88-13473
**SILICA GLASS**
Environmental fracture toughness and static fatigue crack propagation of silica glass N88-13716
**SILICON**
Colloidal stability of oxidized silicon particles in ethanolic and aqueous media
[DE87-014783] N88-13421
Reactive sticking coefficients of silane on silicon
[DE88-000601] N88-13473
Technology upgrade of a silicon compiler
[AD-A184873] N88-14016
Preparation of amorphous silicon semiconductors
[GB-PATENT-2-176-054-A] N88-14022
**SILICON ALLOYS**
Cyclic deformation of an extruded AlMgSi alloy N88-13654
**SILICON CARBIDES**
Composite materials with glass matrix
[SGR/PR-4305/86-SV/JC] N88-13394
Fabrication of composites by chemical vapor deposition
[DE87-014565] N88-13408
Structural characterization of ion implanted beta-SiC thin films
[DE87-014567] N88-14027
**SILVER IODIDES**
Altered and enhanced iodargyrite with bismuth triiodide for use in precipitation enhancement operations
[AD-A185229] N88-13419
**SIMULATION**
European hypersonic wind tunnels N88-13221
The simulation of the viscous flow around a cylinder by the random vortex method N88-13534
The statistics of the shape of small fatigue cracks N88-13666
Numerical simulations of impact tests on a rigid wall --- armor steel
[SNIAS-872-320-102] N88-13744
Feasibility study for gas-grain simulation facility
[NASA-CR-177468] N88-13954
Comparison of 2D memory SEU transport simulation with experiments
[ATR-86(8139)-2-REV-A] N88-14025
**SIMULATORS**
On the simulation of ballistic shock loads N88-13615
**SINGLE CRYSTALS**
Environmentally assisted cracking: Overview of evidence for an adsorption-induced localised-slip process
[AD-A185175] N88-13443
Surface deformation and fatigue crack initiation of alpha-iron N88-13651
Low cycle fatigue behaviour of notched specimens of nickel based superalloy single crystal N88-13712
An overview of fatigue N88-13729
Preparation and characterization of members of the system (Zn,Se)1-xGaPx
[AD-A185073] N88-14019
**SINGLE EVENT UPSETS**
Comparison of 2D memory SEU transport simulation with experiments
[ATR-86(8139)-2-REV-A] N88-14025
**SINTERING**
Corrosion resistance of sintered alloy steels
[BLL-M-37363-(5828.4)] N88-13438
Properties of refractory metals processed by enhanced sintering treatments
[AD-A184944] N88-13440
Results from the melting of tungsten composites under microgravity (TEXUS 10 flight)
[FOA-C-20676-2.1] N88-13482
Crack propagation properties of sintered steel N88-13696
**SITTING POSITION**
Sitting posture of helicopter pilots of the Royal Netherlands Air Force; preliminary recommendations
[IZF-1986-16] N88-13857
**SIZING (SHAPING)**
Mission requirements and aircraft sizing N88-13317
**SKEWNESS**
Extrema of skewed stable processes
[AD-A185422] N88-13925
**SKY SURVEYS (ASTRONOMY)**
An automated supernova search and the design strategy
[DE88-001827] N88-14051
**SLENDER BODIES**
Computational study of three-dimensional wake structures
[REPT-2] N88-13281
**SLENDER CONES**
The drag of slender axisymmetric cones in rarefied hypersonic flow N88-13229
**SLIDING FRICTION**
Literature review of solid lubrication mechanisms
[AD-A185010] N88-13456
**SLOPES**
Computational study of three-dimensional wake structures
[REPT-2] N88-13281
**SODIUM CHLORIDES**
The role of inclusions in corrosion fatigue crack initiation in Q1N N88-13699
**SODIUM NITRATES**
Performance characteristics of magnesium-sodium nitrate flares in oxygen-nitrogen atmospheres
[AD-A185274] N88-13476
**SOFTWARE ENGINEERING**
Towards building a team of intelligent robots
[NASA-CR-181538] N88-13595
A rudimentary database for three-dimensional objects using structural representation
[CSE-87-00004] N88-13597
Experiments in fault tolerant software reliability
[NASA-CR-181554] N88-13863
Reliability of voting in fault-tolerant software systems for small output spaces
[TR-87-16] N88-13864
Effectiveness of back-to-back testing
[TR-87-08] N88-13865
RSDIMU acceptance testing system: Overview of acceptance software and procedures N88-13866
Software design for an airborne gravity measurement system
[AD-A185000] N88-13878
An Ada graphical tool to support software development
[DE87-014854] N88-13891
Sandia software guidelines: Software quality planning
[DE88-001931] N88-13894
A requirements specification for a software design support system
[NASA-CR-182333] N88-13896
Role of technical information in innovation
[PB87-235388] N88-14039
**SOFTWARE TOOLS**
A requirements specification for a software design support system
[NASA-CR-182333] N88-13896
**SOIL EROSION**
Environmental processes and spectral reflectance characteristics associated with soil erosion in desert fringe regions
[NASA-CR-182332] N88-13811
**SOIL SCIENCE**
Significance of foundation-soil separation in dynamic soil-structure interaction N88-13641
**SOILS**
Significance of foundation-soil separation in dynamic soil-structure interaction N88-13641
Analysis of airborne imaging spectrometer data for the Ruby Mountains, Montana, by use of absorption-band-depth images N88-13771
An analytical soil thermodynamic model for the diurnal variation of ground surface temperature
[AD-A185388] N88-13823

**SOL-GEL PROCESSES**
Study of ceramic-fiber/ceramic sol-gel based matrix composites
[SNIAS-872-430-120] N88-13469
**SOLAR ACTIVITY**
The appearance and disappearance of magnetic flux on the quiet sun
[AD-A185432] N88-14055
**SOLAR ACTIVITY EFFECTS**
Contributions of lidar measurements to the study of long term variations of the middle atmosphere
[ETN-88-91237] N88-13824
**SOLAR ARRAYS**
The high performance solar array GSR3
[SNIAS-872-422-108] N88-13814
**SOLAR CELLS**
The high performance solar array GSR3
[SNIAS-872-422-108] N88-13814
**SOLAR CORONA**
Magnetic field draping about coronal mass ejecta
[DE88-001805] N88-14057
**SOLAR FLARES**
The appearance and disappearance of magnetic flux on the quiet sun
[AD-A185432] N88-14055
**SOLAR HEATING**
Transient development of stratification in a partially divided enclosure
[DE87-011742] N88-13490
**SOLAR MAGNETIC FIELD**
The appearance and disappearance of magnetic flux on the quiet sun
[AD-A185432] N88-14055
**SOLAR SPECTRA**
Calibrating AIS images using the surface as a reference N88-13760
**SOLAR WIND**
A fluid simulation of the AMPTE lithium gas releases in the solar wind
[TRITA-EPP-87-06] N88-14056
Magnetic field draping about coronal mass ejecta
[DE88-001805] N88-14057
**SOLID LUBRICANTS**
Coatings for high-temperature bearings and seals
[NASA-TM-100249] N88-13453
Literature review of solid lubrication mechanisms
[AD-A185010] N88-13456
**SOLID PROPELLANT COMBUSTION**
Influence of shock wave and gas pressure on the behavior of a pyrotechnical device
[SNIAS-872-430-111] N88-13477
Advantages of internal thermal protection in a pyrotechnical plunger
[SNIAS-872-430-114] N88-13478
Numerical simulation applied to the development of a pyrotechnical system
[SNIAS-872-430-115] N88-13479
**SOLID PROPELLANT ROCKET ENGINES**
Modal survey of the space shuttle solid rocket motor using multiple input methods N88-13617
**SOLID ROCKET PROPELLANTS**
Modal survey of the space shuttle solid rocket motor using multiple input methods N88-13617
**SOLID STATE**
Survey state of the art: Electrical load management techniques and equipment
[AD-A184083] N88-13517
Study of solid state photomultiplier
[NASA-CR-177465] N88-13556
**SOLID STATE DEVICES**
Fabricate, calibrate and test a dosimeter for integration into the CRRES (Combined Release and Radiation Effects Satellite) satellite
[AD-A185439] N88-13564
**SOLID SURFACES**
Pure dephasing of a vibrational adbond
[AD-A185222] N88-13740
**SOLIDIFICATION**
Microstructure of amorphous and crystalline zirconium alloys rapidly solidified
[DE87-703700] N88-13432
Effect of rapid solidification on short-range order: A magnetic study
[AD-A185216] N88-13444
Tensile properties of extrusion consolidated Type 304 SS rapidly solidified powders
[DE87-014875] N88-13450
Effect of rapid solidification on stainless steel weld metal microstructures and its implications on the Schaeffler diagram
[DE88-001489] N88-13451
Development of iron aluminides
[AD-A185190] N88-13461
**SOLIDS**
Shock compression of solids as a physical-chemical-mechanical process
[DE88-001674] N88-13427
**SOLITARY WAVES**
Solitons in stimulated Raman scattering: Generation and control of ultrashort optical pulses
[AD-A185141] N88-13983
**SONAR**
Correction of inertial navigation system drift errors for an autonomous land vehicle using optical radar terrain data
[AD-A184973] N88-13311
**SOUND FIELDS**
RADSPHERE: A computer program for calculating the steady-state, axially symmetric, forced response and radiation field of a submerged spherical shell
[AD-A185025] N88-13738
Development of a new method of measuring the characteristic impedance and complex wave number of a porous acoustic material
[AD-A185038] N88-13957
**SOUND TRANSMISSION**
Theoretical and practical aspects of the functional absorber method of arranging sound absorbing panels
[BBC-RD-1987/15] N88-13955
**SOUND WAVES**
Theoretical and practical aspects of the functional absorber method of arranging sound absorbing panels
[BBC-RD-1987/15] N88-13955
Full field visualization of surface and bulk acoustic waves using heterodyne holographic interferometry
[AD-A185071] N88-13958
**SOUTHERN HEMISPHERE**
October lower stratospheric Antarctic temperature and total ozone from 1979-1985 N88-13776
**SPACE COMMUNICATION**
An evolutionary communications scenario for Mars exploration
[NASA-TM-100263] N88-13515
**SPACE EXPLORATION**
An evolutionary communications scenario for Mars exploration
[NASA-TM-100263] N88-13515
Small space reactor power systems for unmanned solar system exploration missions
[NASA-TM-100228] N88-14054
**SPACE MANUFACTURING**
Potential for on-orbit manufacture of large space structures using the pultrusion process
[NASA-TM-4016] N88-13388
**SPACE NAVIGATION**
Satellite autonomous navigation with SHAD (Stellar Horizon Atmospheric Dispersion)
[AD-A184988] N88-13313
**SPACE OBSERVATIONS (FROM EARTH)**
An automated supernova search and the design strategy
[DE88-001827] N88-14051
**SPACE PLASMAS**
Activities report of the Ionospheric Observatory
[UIO-SR-87-01] N88-13827
**SPACE PLATFORMS**
The effect of maximum-allowable payload temperature on the mass of a multimegawatt space-based platform
[DE88-001921] N88-13381
Communications payload concepts for geostationary facilities
[NASA-TM-100154] N88-13513
**SPACE POWER REACTORS**
Small space reactor power systems for unmanned solar system exploration missions
[NASA-TM-100228] N88-14054
**SPACE PROBES**
Study of fault tolerant techniques for satellite data handling
[FTT/REP/0001/SAAB] N88-13860
**SPACE PROGRAMS**
National Aeronautics and Space Administration space station proposal, fiscal year 1988
[S-HRG-100-328] N88-14043
**SPACE SHUTTLE MAIN ENGINE**
The 58th Shock and Vibration Symposium, volume 1
[NASA-CP-2488-VOL-1] N88-13609
Fluid mass and thermal loading effects on the modal characteristics of space shuttle main engine liquid oxygen inlet splitter vanes N88-13628
Incipient failure detection of space shuttle main engine turbopump bearings using vibration envelope detection N88-13629
High frequency data acquisition system for space shuttle main engine testing N88-13630
Space shuttle main engine vibration data base N88-13631
Thermal finite-element analysis of space shuttle main engine turbine blade
[NASA-TM-100117] N88-13745
**SPACE SHUTTLE ORBITERS**
Numerical simulation of the hypersonic flow around lifting vehicles N88-13234
**SPACE SHUTTLE PAYLOADS**
Potential for on-orbit manufacture of large space structures using the pultrusion process
[NASA-TM-4016] N88-13388
**SPACE SHUTTLES**
The analysis of nonstationary vibration data N88-13610
Modal survey of the space shuttle solid rocket motor using multiple input methods N88-13617
Modeling cloudy and clear interval length probabilities using space shuttle imagery
[AD-A185290] N88-13837
**SPACE STATION PAYLOADS**
Communications payload concepts for geostationary facilities
[NASA-TM-100154] N88-13513
**SPACE STATION POWER SUPPLIES**
Space station systems: A bibliography with indexes
[NASA-SP-7056(05)] N88-13382
**SPACE STATION PROPULSION**
Space station systems: A bibliography with indexes
[NASA-SP-7056(05)] N88-13382
**SPACE STATION STRUCTURES**
Space station systems: A bibliography with indexes
[NASA-SP-7056(05)] N88-13382
**SPACE STATIONS**
Feasibility study for gas-grain simulation facility
[NASA-CR-177468] N88-13954
**SPACE VEHICLE CHECKOUT PROGRAM**
RETE experiment Assembly, Integration, and Verification (AIV) activities
[IFSI-87-6] N88-13380
**SPACE-TIME FUNCTIONS**
Computer-aided study of a class of Riemannian space-times
[DE87-703367] N88-13950
**SPACEBORNE EXPERIMENTS**
Research on Electrodynamic Tether Effects (RETE) experiment Electrical Ground Support Equipment (EGSE) --- tethered satellite
[IFSI-87-2] N88-13378
RETE experiment Assembly, Integration, and Verification (AIV) activities
[IFSI-87-6] N88-13380
**SPACEBORNE TELESCOPES**
Study of solid state photomultiplier
[NASA-CR-177465] N88-13556
**SPACECRAFT COMMUNICATION**
Error control techniques for satellite and space communications
[NASA-CR-181581] N88-13516
**SPACECRAFT COMPONENTS**
High energy density rechargeable batteries for aerospace power requirements
[AD-A184883] N88-13519
**SPACECRAFT CONFIGURATIONS**
The 1988 NASA (National Aeronautics and Space Administration) authorization
[GPO-80-245] N88-14044
**SPACECRAFT CONSTRUCTION MATERIALS**
Influence of bonding shop moisture on metal-honeycomb junctions bonded with ultra-thin adhesive films
[SNIAS-872-422-112] N88-13399
First International Week of Adhesive Bonding and Assembling
[SNIAS-872-430-106] N88-13468
**SPACECRAFT CONTAMINATION**
Analysis of geophysical data bases and models for spacecraft interactions
[AD-A184809] N88-13375
**SPACECRAFT CONTROL**
Modeling and control of large flexible vehicles in the atmosphere and space
[AD-A185368] N88-13377
Optimal control of large space structures via generalized inverse matrix
[NASA-CR-182336] N88-13907
Guidance and control strategies for aerospace vehicles
[NASA-CR-181579] N88-13935
**SPACECRAFT DESIGN**
General aerodynamic-aerothermodynamic concepts for Hermes N88-13251
Hermes propulsion system
[SNIAS-872-422-109] N88-13383
Introduction to local area network design on Ariane 5 and future launchers
[SNIAS-872-422-102] N88-13886

**SPACECRAFT ENVIRONMENTS**
Analysis of geophysical data bases and models for spacecraft interactions
[AD-A184809] N88-13375
**SPACECRAFT GUIDANCE**
Guidance and control strategies for aerospace vehicles
[NASA-CR-181579] N88-13935
**SPACECRAFT PERFORMANCE**
RETE experiment Assembly, Integration, and Verification (AIV) activities
[IFSI-87-6] N88-13380
**SPACECRAFT POWER SUPPLIES**
The effect of maximum-allowable payload temperature on the mass of a multimegawatt space-based platform
[DE88-001921] N88-13381
Making space nickel/hydrogen batteries lighter and less expensive
[DE88-000168] N88-13530
The high performance solar array GSR3
[SNIAS-872-422-108] N88-13814
Progress toward the evolution of a Stirling space engine
[NASA-TM-100221] N88-14046
**SPACECRAFT RADIATORS**
The effect of maximum-allowable payload temperature on the mass of a multimegawatt space-based platform
[DE88-001921] N88-13381
**SPACECRAFT STRUCTURES**
Computational methods for problems in aerodynamics and large space structure using parallel and vector architectures
[AD-A185401] N88-13294
Viscous damped space structure for reduced jitter N88-13623
**SPACECRAFT TEMPERATURE**
The effect of maximum-allowable payload temperature on the mass of a multimegawatt space-based platform
[DE88-001921] N88-13381
**SPACECRAFT TRACKING**
Media calibrations of the Doppler signal for a gravitational wave experiment — interplanetary medium
[IFSI-86-13] N88-13825
**SPATIAL DISTRIBUTION**
Structural frequency functions for an impulsive, distributed forcing function N88-13627
**SPATIAL FILTERING**
Analysis of airborne imaging spectrometer data for the Ruby Mountains, Montana, by use of absorption-band-depth images N88-13771
**SPATIAL MARCHING**
A spatial marching technique for the inviscid blunt body problem N88-13239
**SPATIAL RESOLUTION**
Resolution limitations and optimization of the LLNL streak camera focus
[DE88-001633] N88-13572
**SPECIFICATIONS**
Conservatism implications of shock test tailoring for multiple design environments N88-13611
**SPECTRA**
SUSIE reference manual
[DE88-001462] N88-13893
**SPECTRAL BANDS**
Analysis of SO2 signals in SBUV/TOMS data N88-13794
**SPECTRAL REFLECTANCE**
AIS-2 radiometry and a comparison of methods for the recovery of ground reflectance N88-13757
Calibrating AIS images using the surface as a reference N88-13760
AIS-2 spectra of California wetland vegetation N88-13763
Toward detecting California shrubland canopy chemistry with AIS data N88-13764
Measuring near infrared spectral reflectance changes from water stressed conifer stands with AIS-2 N88-13765
Preliminary results from an investigation of AIS-1 data over an area of epithermal alteration: Plateau, Northern Queensland, Australia N88-13768
Causes of spurious features in spectral reflectance data N88-13769
Automatic continuum analysis of reflectance spectra N88-13770
Mapping hydrothermally altered rocks in the Northern Grapevine Mountains, Nevada and California with the airborne imaging spectrometer N88-13772
Environmental processes and spectral reflectance characteristics associated with soil erosion in desert fringe regions
[NASA-CR-182332] N88-13811
**SPECTRAL RESOLUTION**
Preliminary results from an investigation of AIS-1 data over an area of epithermal alteration: Plateau, Northern Queensland, Australia N88-13768
**SPECTROPHOTOMETERS**
Comparison of ground based and TOMS measurements of SO2 from volcanic emissions N88-13795
**SPECTRORADIOMETERS**
AIS-2 radiometry and a comparison of methods for the recovery of ground reflectance N88-13757
**SPECTROSCOPIC ANALYSIS**
Chemical analysis for excimer laser systems
[DE88-001941] N88-13591
**SPECTROSCOPY**
Applications of nonlinear hole burning spectroscopy
[AD-A184943] N88-13580
**SPECTRUM ANALYSIS**
Proceedings of the Third Airborne Imaging Spectrometer Data Analysis Workshop
[NASA-CR-181552] N88-13755
Evaluation of AIS-2 (1986) data over hydrothermally altered granitoid rocks of the Singatse Range (Yerington) Nevada and comparison with 1985 AIS-1 data N88-13767
Application of Vandermonde decomposition to directional and modal analysis of broadband transients
[AD-A185007] N88-13956
**SPHERES**
Dynamical analysis of molecular decay at spherical surfaces
[AD-A184908] N88-13964
**SPHERICAL SHELLS**
RADSPHERE: A computer program for calculating the steady-state, axially symmetric, forced response and radiation field of a submerged spherical shell
[AD-A185025] N88-13738
**SPIN-SPIN COUPLING**
Example of correlation between space and spin coordinates
[DE87-703366] N88-14030
**SPIRAL GALAXIES**
Comments on H. Arp The persistent problem of spiral galaxies
[TRITA-EPP-87-05] N88-14052
**SPLASHING**
Numerical simulation of splash of droplet at unit gravity N88-13275
**SPLINE FUNCTIONS**
Stability properties of spline approximations for retarded systems
[PB87-220919] N88-13910
**SPOT (FRENCH SATELLITE)**
National Point Of Contact (NPOC)-SPOT inquiry 1986
[NLR-MP-86055-U] N88-13807
**SPOT WELDS**
Development of research on fatigue of spot-weld in automobile structures in Japan N88-13728
**SPRING (SEASON)**
Insights into the general circulation of the lower stratosphere from TOMS N88-13780
**SPRINGS (ELASTIC)**
Non-linear shipboard shock analysis of the Tomahawk missile shock isolation system N88-13614
**SPUTTERING**
An investigation of unipolar arcing at atmospheric pressure in aluminum 2024 and aluminum coated glass slides
[AD-A184903] N88-13521
Energy dependence of ion-induced sputtering yields of monatomic solids in the low energy region
[IPPJ-AM-52] N88-13986
**SQUID (DETECTORS)**
Capacitive resonant transducer for the Frascati gravitational antenna
[IFSI-86-9] N88-13528
**STABILITY**
Computational methods for problems in aerodynamics and large space structure using parallel and vector architectures
[AD-A185401] N88-13294
Colloidal stability of oxidized silicon particles in ethanolic and aqueous media
[DE87-014783] N88-13421
Stability properties of spline approximations for retarded systems
[PB87-220919] N88-13910
Extrema of skewed stable processes
[AD-A185422] N88-13925
Tutorial on elementary bifurcation theory
[DE87-014849] N88-13932
**STABILITY DERIVATIVES**
Low speed wind tunnel investigation of propeller slipstream aerodynamic effects on different nacelle/wing combinations. Part 1: Total forces and moments and pressure distributions on nacelle/wing at different angles of attack and yaw and at different thrust coefficients
[FFA-TN-1987-22] N88-13302
**STAGNATION PRESSURE**
Low thrust viscous nozzle flow fields prediction
[NASA-CR-182334] N88-13551
**STAINLESS STEELS**
Study of the influence of mechanical - thermal treatments on the creep behavior of a niobium stainless steel
[DE87-703506] N88-13431
Tensile properties of extrusion consolidated Type 304 SS rapidly solidified powders
[DE87-014875] N88-13450
Effect of rapid solidification on stainless steel weld metal microstructures and its implications on the Schaeffler diagram
[DE88-001489] N88-13451
Cu-2 mechanical properties and microstructural stability of advanced steam cycle materials
[DE88-001519] N88-13452
Coupling effects between the ferrite and austenite phases during corrosion fatigue of a ferrite/austenite duplex stainless steel N88-13706
**STAR TRACKERS**
Satellite autonomous navigation with SHAD (Stellar Horizon Atmospheric Dispersion)
[AD-A184988] N88-13313
**STATIC DEFORMATION**
Influence of the static deformation on a wing in the unsteady aerodynamic N88-13357
**STATIC DISCHARGERS**
Antistatic coating compositions
[GB-PATENT-2-177-413-A] N88-13463
**STATIC LOADS**
Experimental studies on the tripping behavior of narrow T-stiffened flat plates subjected to hydrostatic pressure and underwater shock N88-13613
**STATICS**
Static aeroelastic considerations in the definition of design loads for fighter airplanes N88-13351
**STATISTICAL ANALYSIS**
Statistical process control applied to the liquid-fed ceramic melter process
[DE88-000271] N88-13471
A system identification technique based on the random decrement signatures. Part 1: Theory and simulation N88-13625
A system identification technique based on the random decrement signatures. Part 2: Experimental results N88-13626
Fatigue crack growth: Statistical considerations N88-13718
Global atmospheric circulation statistics: Four year averages
[NASA-TM-100890] N88-13842
An APL workspace for conducting nonparametric statistical inference
[AD-A184971] N88-13877
Sample reuse in statistical remodeling
[AD-A184916] N88-13936
Quantile based unified distribution of extreme values and order statistics
[AD-A185171] N88-13942
Quantile statistical data analysis
[AD-A185181] N88-13943
Presentation of a computer program permitting the exploitation of tests designed to determine the sensitivity of one shot devices to a parameter. Application to a degenerate one shot sequence
[SNIAS-872-430-117] N88-13945
**STATISTICAL DISTRIBUTIONS**
On the geometrical description of fatigue crack surfaces N88-13727
The application of doubly-truncated hydrometeor distributions to numerical cloud models
[AD-A185273] N88-13836
Quantile based unified distribution of extreme values and order statistics
[AD-A185171] N88-13942
**STATISTICAL MECHANICS**
Chaos: Chto Delat? (What is to be done?)
[DE88-000513] N88-13933
**STATISTICAL TESTS**
Determining differences in rates corresponding to a given significance level
[AD-A185004] N88-13940
**STEADY FLOW**
SHARP simulation of discontinuities in highly convective steady flow
[NASA-TM-100240] N88-13931
**STEADY STATE**
An experimental investigation of the aerodynamics of a NACA 64A010 airfoil-flap combination with and without flap oscillations. Part 1: Steady-state characteristics
[NASA-TM-88217] N88-13305
RADSPHERE: A computer program for calculating the steady-state, axially symmetric, forced response and radiation field of a submerged spherical shell
[AD-A185025] N88-13738
Numerical methods for reaction-diffusion problems with non-differentiable kinetics
[AD-A185405] N88-13923

**STEAM**
Cu-2 mechanical properties and microstructural stability of advanced steam cycle materials
[DE88-001519] N88-13452

**STEELS**
Corrosion resistance of sintered alloy steels
[BLL-M-37363-(5828.4)] N88-13438
Master plots for predicting the case-depth in laser surface treatments
[PB87-221875] N88-13574
The mechanics of fatigue-crack nucleation in a low-alloy steel under fretting conditions N88-13649
The influence of the topography of fracture surfaces on crack closure N88-13657
Striations and the fatigue growth mechanism in a micro-alloyed steel N88-13661
Fatigue of 30CrMnSiNi2A notched specimens under spectrum loading N88-13689
Interaction of microstructure and fatigue in tool steels N88-13693
Tensile mean stress effects on uniaxial fatigue behavior of 1045 HR steel N88-13694
The initiation and growth of fatigue cracks in carburised 9Cr1Mo steel N88-13696
Crack propagation properties of sintered steel N88-13696
The role of inclusions in corrosion fatigue crack initiation in Q1N N88-13699
The influence of crack conditions on hydrogen uptake by steels N88-13702
Modeling the effect of sulfur on the threshold environmental cracking rate of steels in high temperature water N88-13703

**STELLAR MASS EJECTION**
Magnetic field draping about coronal mass ejecta
[DE88-001805] N88-14057

**STELLARATORS**
Transport scaling in the collisionless-detrapping regime in stellarators
[DE88-001511] N88-14006

**STERILIZATION**
Controlled ecological life support systems: Development of a plant growth module N88-13854

**STIFFENING**
Experimental studies on the tripping behavior of narrow T-stiffened flat plates subjected to hydrostatic pressure and underwater shock N88-13613

**STIFFNESS**
Control of a flexible one-link manipulator
[AD-A185035] N88-13598

**STIRLING ENGINES**
Progress toward the evolution of a Stirling space engine
[NASA-TM-100221] N88-14046

**STIRRING**
Coagulation in stirred tanks
[B8711373] N88-13420

**STOCHASTIC PROCESSES**
Electromagnetics and electrothermal approach to evaluate failures in microelectronic devices caused by electrostatic discharges: Stochastical aspects of the device reliability
[AD-A184906] N88-13522
Conditional second order closure for turbulent shear flows
[AD-A185369] N88-13542
Fatigue crack growth under random overloads N88-13682
Computer aided modeling and fatigue failure forecast under stochastic loading N88-13720
On the geometrical description of fatigue crack surfaces N88-13727
Comparing hard and soft prior bounds in geophysical inverse problems
[NASA-CR-181557] N88-13820
Explicit formulate for the distributions of stopping variables under Wald's truncated SPRT (Sequential Probability Radio Tests) for a poisson process
[AD-A185053] N88-13914
Point processes
[AD-A185398] N88-13921
Robust prediction operations for stationary processes
[AD-A185408] N88-13924
Isotropic probability measures in infinite dimensional spaces: Inverse problems/prior information/stochastic inversion
[NASA-CR-181555] N88-13936
Freidlin-Wentzell type estimates and the law of the iterated logarithm for a class of stochastic processes related to symmetric statistics
[AD-A185366] N88-13944
On the correlation free forms for nonlinear stochastic systems
[DE87-011169] N88-13947

**STORAGE BATTERIES**
High energy density rechargeable batteries for aerospace power requirements
[AD-A184883] N88-13519

**STORAGE TANKS**
Contribution of acoustic analysis to assess damage in fluid storage tanks under high pressure — composite materials, filament winding
[SNIAS-872-430-119] N88-13407

**STORMS**
Ozone, jet streaks and severe weather N88-13781

**STRAIN ENERGY METHODS**
A comparison of plastic work energy and external input for fatigue crack propagation N88-13722

**STRAIN ENERGY RELEASE RATE**
Strain-energy-release rate analysis of the end-notched flexure specimen using the finite-element method
[NASA-TM-100494] N88-13735

**STRAIN GAGES**
Model helicopter rotor rig and associated strain gauge balance for performance studies
[NAL-TM-AE-8704] N88-13364

**STRAIN MEASUREMENT**
Measurement of model deformation in wind tunnels N88-13358
Application of finite element methods with cyclic elasto-plastic strain analysis to low cycle fatigue analysis of engine components
[AR-004-512] N88-13642

**STRAIN RATE**
Plasticity of aluminum and iron at high shear strain rate and high pressure N88-13430

**STRATIFICATION**
Transient development of stratification in a partially divided enclosure
[DE87-011742] N88-13490

**STRATIFIED FLOW**
Regressed relations for forced convection heat transfer in a direct injection stratified charge rotary engine
[NASA-TM-100124] N88-13345

**STRATOCUMULUS CLOUDS**
Mesoscale applications of high resolution imagery
[AD-A185039] N88-13833

**STRATOSPHERE**
October lower stratospheric Antarctic temperature and total ozone from 1979-1985 N88-13776
Insights into the general circulation of the lower stratosphere from TOMS N88-13780
Lower-stratospheric/upper-tropospheric exchange processes associated with tropical cyclones as observed by TOMS N88-13782
Comparison of ground based and TOMS measurements of SO2 from volcanic emissions N88-13795

**STREAK CAMERAS**
Streak camera dynamic range optimization
[DE88-001632] N88-13571
Resolution limitations and optimization of the LLNL streak camera focus
[DE88-001633] N88-13572

**STRESS (PHYSIOLOGY)**
Assessment of the reliability of a correction procedure for WGT (Wet Globe Thermometer) (Botsball) measurements of heat stress
[AD-A185193] N88-13559
Microwave challenges to the thermoregulatory system
[AD-A185391] N88-13647
Physiological determinants of load bearing capacity
[AD-A184977] N88-13848
A device and methodology for measuring repetitive lifting VO2max (oxygen consumption rate)
[AD-A185195] N88-13850

**STRESS ANALYSIS**
Development of an integrated BEM approach for hot fluid structure interaction
[NASA-CR-181577] N88-13384
Micromechanics of the degradation of composite materials
[SNIAS-872-430-113] N88-13405
Finite element model for the stress and flexibility analysis of curved pipes
[DE87-703632] N88-13608
Fatigue under nonnormal random stresses using Monte Carlo method N88-13723
Analysis of end stresses in glass-metal bimaterial strips
[DE87-007848] N88-13750

**STRESS CONCENTRATION**
Constraint effects in fatigue crack growth N88-13719

**STRESS CORROSION**
A study of corroion fatigue crack initiation, growth and the threshold condition under variable amplitude loading N88-13701
The influence of crack conditions on hydrogen uptake by steels N88-13702
Occurance and growth of fatigue cracks in corroion environment N88-13704

**STRESS CORROSION CRACKING**
Environmenta'ly assisted cracking: Overview of evidence for an adsorption-induced localised-slip process
[AD-A185175] N88-13443
Fatigue crack propagation in Al-Zn-Mg bicrystals and its dependence on the environment N88-13707
Fracture kinetics of corroion fatigue N88-13708

**STRESS DISTRIBUTION**
Telemetric laser extensometry technique for monitoring deflections in small cracks N88-13724
On the geometrical description of fatigue crack surfaces N88-13727

**STRESS INTENSITY FACTORS**
Stress intensity factors for cracking metal structures under rapid thermal loading, phase 1
[AD-A184112] N88-13606
Finite element model for the stress and flexibility analysis of curved pipes
[DE87-703632] N88-13608
Closure behavior under constant effective stress intensity loading conditions N88-13656
Fatigue crack propagation of short and long cracks: Phys. basis, prediction methods and engineering significance N88-13664
Behavior of short cracks in a 2024 aluminum alloy sheet tested at several stress ratios N88-13669
the influence of temper embrittlement on fatigue crack growth in hydrogen N88-13709
Constraint effects in fatigue crack growth N88-13719
Development of research on fatigue of spot-weld in automobile structures in Japan N88-13728
Fatigue crack growth N88-13734

**STRESS RELAXATION**
Tensile mean stress effects on uniaxial fatigue behavior of 1045 HR steel N88-13694

**STRESS-STRAIN RELATIONSHIPS**
The effect of temperature on the tensile properties of HSLA-100 steel
[AD-A184951] N88-13441
Cyclic deformation and crack initiation N88-13646
Fatigue of 30CrMnSiNi2A notched specimens under spectrum loading N88-13689

**STRESSES**
Initial dynamic load estimates during configuration design N88-13621
A study of fatigue crack growth life under random stresses N88-13685
Tensile mean stress effects on uniaxial fatigue behavior of 1045 HR steel N88-13694

**STRING THEORY**
Introduction to string field theory
[DE87-014583] N88-14032

**STRIP TRANSMISSION LINES**
Time domain electromagnetic waves in multilayered media
[AD-A185055] N88-13502

**STRUCTURAL ANALYSIS**
Static Aeroelastic Effects on High Performance Aircraft
[AGARD-CP-403] N88-13348
Space station systems: A bibliography with indexes
[NASA-SP-7056(05)] N88-13382
Micromechanics of the degradation of composite materials
[SNIAS-872-430-113] N88-13405
Fiber composite structural durability and damage tolerance: Simplified predictive methods
[NASA-TM-100179] N88-13409
Mechanical property evaluation of a series of commercial tungsten alloys
[AD-A185440] N88-13446
The matrix exponential in transient structural analysis N88-13619
Simultaneous structural and control optimization via linear quadratic regulator eigenstructure assignment N88-13622
Structural frequency functions for an impulsive, distributed forcing function N88-13627
Exact finite element method analysis of viscoelastic tapered structures to transient loads N88-13632
Optimal shock isolation with minimum settling time N88-13633
Significance of foundation-soil separation in dynamic soil-structure interaction N88-13641
An element of a multilayer shell for the computation of composite structures
[ONERA-RT-14/3542-RY-051-R] N88-13742
Experimental studies on acoustic emission monitoring of crack propagation in offshore structures: A literature survey N88-13748

**STRUCTURAL DESIGN**
Lifting bodies: An attractive aerodynamic configuration choice for hypervelocity vehicles N88-13248
Static aeroelastic considerations in the definition of design loads for fighter airplanes N88-13351

The use of aeroelastic wind tunnel models to prove structural design N88-13355
Design and assembly sequence analysis of option 3 for CETF reference space station [NASA-TM-100503] N88-13369
Space station systems: A bibliography with indexes [NASA-SP-7056(05)] N88-13382
Surface treatment problems found in new aircraft designed using structural composites [SNIAS-872-111-113] N88-13397
A complete linearized theory for the analysis and design of two-dimensional hydrofoils near a free surface [UTIAS-TN-264] N88-13531
Initial dynamic load estimates during configuration design N88-13621
The high performance solar array GSR3 [SNIAS-872-422-108] N88-13814
Structural optimization in the design process — aircraft [SNIAS-872-111-115] N88-13885
Small space reactor power systems for unmanned solar system exploration missions [NASA-TM-100228] N88-14054

**STRUCTURAL DESIGN CRITERIA**
Simultaneous structural and control optimization via linear quadratic regulator eigenstructure assignment N88-13622

**STRUCTURAL MEMBERS**
Potential for on-orbit manufacture of large space structures using the pultrusion process [NASA-TM-4016] N88-13388

**STRUCTURAL PROPERTIES (GEOLOGY)**
Studies in Aeolian geology [NASA-CR-182328] N88-13828

**STRUCTURAL VIBRATION**
Identification of perturbations in turbomachines by the analysis of pressure signals, vibrations and wavelike motions [ETN-88-90602] N88-13600
The 58th Shock and Vibration Symposium, volume 1 [NASA-CP-2488-VOL-1] N88-13609
The analysis of nonstationary vibration data N88-13610
Simultaneous structural and control optimization via linear quadratic regulator eigenstructure assignment N88-13622
Viscous damped space structure for reduced jitter N88-13623
On the glitches in the force transmitted by an electrodynamic exciter to a structure N88-13624
Fluid mass and thermal loading effects on the modal characteristics of space shuttle main engine liquid oxygen inlet splitter vanes N88-13628
Incipient failure detection of space shuttle main engine turbopump bearings using vibration envelope detection N88-13629
Space shuttle main engine vibration data base N88-13631
Optimal shock isolation with minimum settling time N88-13633
A passive vibration-cancelling isolation mount N88-13636
Advanced joining concepts for passive vibration control N88-13638
Dynamic response of laminated composite plates using a three-dimensional hybrid-stress finite-element formulation N88-13639

**SUBMARINES**
Experimental studies on the tripping behavior of narrow T-stiffened flat plates subjected to hydrostatic pressure and underwater shock N88-13613

**SUBROUTINES**
MODTRAN: A moderate resolution model for LOWTRAN [AD-A185384] N88-13503
Mixing Microsoft C and Microsoft FORTRAN program modules on the IBM Personal Computer [DE88-001947] N88-13895

**SUBSONIC FLOW**
Wakes of two dimensional bluff bodies in subsonic flow. Influence of a separating plate and of a pulsed injection of momentum [IMFL-4200-86/75] N88-13297

**SUBSTRATES**
Effectiveness of electrodeposited coatings in reducing atmospheric corrosion of copper substrates [DE87-013651] N88-13448
Water disbondment characterization of organic Coating/metal substrate systems [AD-A184847] N88-13454
Reactive sticking coefficients of silane on silicon [DE88-000601] N88-13473
Raman microprobe characterization of dielectric films following high-energy pulsed laser irradiation [DE88-000559] N88-13587
Tribology of thin film systems [ETN-88-91365] N88-13601

**SULFUR**
Modeling the effect of sulfur on the threshold environmental cracking rate of steels in high temperature water N88-13703

**SULFUR DIOXIDES**
Volcanic eruption detection with TOMS N88-13793
Analysis of SO2 signals in SBUV/TOMS data N88-13794
TOMS and the NOAA/FAA volcano support plan N88-13796
Use of satellite data in volcano monitoring N88-13797

**SUMMARIES**
University research initiative research program summaries [AD-A184876] N88-14035

**SUN**
The appearance and disappearance of magnetic flux on the quiet sun [AD-A185432] N88-14055

**SUNRISE**
The lengthening and shortening of the day [KNMI-TR-91] N88-13839

**SUNSET**
The lengthening and shortening of the day [KNMI-TR-91] N88-13839

**SUPERCOMPUTERS**
Programming techniques for high-speed processing of large scale numerical simulation on supercomputers N88-13269
Vectorizing the FFTs on supercomputer SX system N88-13270
Tridiagonal approximate factorization method: A preconditioning technique for solving nonsymmetric linear systems suitable to supercomputers N88-13271
Supercomputing at Florida State University (FSU) [DE87-013900] N88-14009

**SUPERCONDUCTORS**
Anomalous phonon behavior of superconductor Y-Ba-Cu-O [DE87-703401] N88-14010

**SUPERCRITICAL AIRFOILS**
Influence of the static deformation on a wing in the unsteady aerodynamic N88-13357

**SUPERCRITICAL WINGS**
Static aeroelastic effects on the flutter of a supercritical wing N88-13353

**SUPERHEATING**
Microwave superheaters for fusion [DE88-001656] N88-14007

**SUPERHIGH FREQUENCIES**
Optically tuned MM-wave IMPATT source [AD-A185250] N88-13523

**SUPERLATTICES**
MBE growth of InAsSb strained-layer superlattices [DE88-000365] N88-14011

**SUPERNOVAE**
An automated supernova search and the design strategy [DE88-001827] N88-14051

**SUPERPLASTICITY**
Investigation by differential scanning calorimetry of microstructure in a superplastic Al-Mg-Zr alloy [AD-A184902] N88-13439

**SUPERSONIC AIRCRAFT**
Experiences using the Mark IV supersonic hypersonic arbitrary body program N88-13249

**SUPERSONIC COMBUSTION RAMJET ENGINES**
Aerodynamics of Hypersonic Lifting Vehicles [AGARD-CP-428] N88-13219
Hypersonic airbreathing propulsion: Evolution and opportunities N88-13231
Numerical analysis of flow through scramjet engine inlets N88-13233
Ignition and flameholding in supersonic flow by injection of dissociated hydrogen N88-13410

**SUPERSONIC FLOW**
Combustion related shear-flow dynamics in elliptic supersonic jets N88-13232
Solution of some 3-D viscous and inviscid supersonic flow problems by finite-volume space-marching schemes N88-13235
The role of computation fluid dynamics in aeronautical engineering (4). The development and applications of implicit TVD finite volume code N88-13259
Numerical analysis of supersonic flows using panel method N88-13266
Interferometric data for a shock-wave/boundary-layer interaction [NASA-TM-88227] N88-13306
Ignition and flameholding in supersonic flow by injection of dissociated hydrogen N88-13410
A Cartesian finite-volume method for the Euler equations N88-13532
Investigation of the effect of laterally ejected gas jets on flows [ISL-R-107/86] N88-13545
Hot wire and laser velocimeter studies of turbulent flow at supersonic velocities [ETN-88-91172] N88-13566
A computer program for calculating unsteady aerodynamic coefficients for cascades in supersonic axial flow [NASA-TM-100204] N88-13753

**SUPERSONIC JET FLOW**
Numerical analysis of flow characteristics of supersonic free-jets N88-13274

**SUPERSONIC SPEED**
Vortex formation over delta, double-delta and wave rider configurations at supersonic speeds N88-13243
Design of wings and wing/body configurations for transonic and supersonic speeds N88-13318
Supersonic beam observations of semiconductor clusters [AD-A184991] N88-14018

**SUPPORTS**
A passive vibration-cancelling isolation mount N88-13636

**SURFACE CRACKS**
The effect of microstructure on the surface crack length: Crack depth relationship for short cracks N88-13670

**SURFACE FINISHING**
Surface treatment problems found in new aircraft designed using structural composites [SNIAS-872-111-113] N88-13397
The analysis of metal finishing solutions by ion chromatography [AD-A184812] N88-13414
Fatigue characteristics of ion treated surfaces N88-13713

**SURFACE LAYERS**
The effect of ion beam mixed Ni-Al surface layers on PSB extrusion morphology in fatigued nickel N88-13652

**SURFACE PROPERTIES**
A complete linearized theory for the analysis and design of two-dimensional hydrofoils near a free surface [UTIAS-TN-264] N88-13531
Dynamical analysis of molecular decay at spherical surfaces [AD-A184908] N88-13964

**SURFACE REACTIONS**
Reactions of porphyrins in surfactant assemblies, microemulsions and in solutions [AD-A184797] N88-13412
A study of the interaction of laser light with liquid propellant drops [AD-A185117] N88-13582
Pure dephasing of a vibrational adbond [AD-A185222] N88-13740
Energy dependence of ion-induced sputtering yields of monatomic solids in the low energy region [IPPJ-AM-52] N88-13988

**SURFACE STABILITY**
Colloidal stability of oxidized silicon particles in ethanolic and aqueous media [DE87-014783] N88-13421

**SURFACE TEMPERATURE**
An analytical soil thermodynamic model for the diurnal variation of ground surface temperature [AD-A185388] N88-13823

**SURFACE VEHICLES**
Correction of inertial navigation system drift errors for an autonomous land vehicle using optical radar terrain data [AD-A184973] N88-13311
Range imagery algorithms for the detection of obstacles by autonomous vehicles [AD-A185421] N88-14045

**SURFACTANTS**
Reactions of porphyrins in surfactant assemblies, microemulsions and in solutions [AD-A184797] N88-13412

**SURGES**
Transient processes in the interaction between pulsed laser radiation and matter [ISL-R-115/86] N88-13586
Application of Vandermonde decomposition to directional and modal analysis of broadband transients [AD-A185007] N88-13956

**SURVEYS**
A survey of existing hypersonic ground test facilities: North America N88-13220
Survey state of the art: Electrical load management techniques and equipment [AD-A184083] N88-13517

Varifront 3 expedition data report (USNS DE STEIGUER CRUISE 1202-82). Bioluminescence, hydrographic, nutrient, and satellite data from the Gulf of California (November-December 1981)
[AD-A185011] N88-13805
**SUSPENSION SYSTEMS (VEHICLES)**
Measurement of suspension and ride characteristics of the M1 main battle tank N88-13637
**SWEDISH SPACE PROGRAM**
Electric field measurements on Viking: First results
[TRITA-EPP-87-04] N88-13826
**SWEEP ANGLE**
The effects of sweep and bluntness on a glancing shock wave turbulent boundary layer interaction N88-13227
**SWEPT FORWARD WINGS**
Wing divergence of trimmed aircraft N88-13354
**SWEPT WINGS**
A swept wing panel in a low speed flexible walled test section
[NASA-CR-4106] N88-13292
Static aeroelastic effects on the flutter of a supercritical wing N88-13353
**SWITCHES**
Low jitter laser-triggered high-voltage vacuum switch using low laser energies
[DE88-001922] N88-13576
**SWITCHING CIRCUITS**
Evaluation of device figure of merit in microwave switching circuit design
[AD-A184896] N88-13520
Digital control of a direct current converter for a hybrid vehicle
[LAAS-87-266] N88-13527
**SWITCHING THEORY**
An exact analysis and performance of framed ALOHA with capture
[AD-A185006] N88-13500
**SYMMETRY**
Conditional second order closure for turbulent shear flows
[AD-A185369] N88-13542
RADSPHERE: A computer program for calculating the steady-state, axially symmetric, forced response and radiation field of a submerged spherical shell
[AD-A185025] N88-13738
High energy molecules of high symmetry
[AD-A185385] N88-13965
**SYNCHRONOUS PLATFORMS**
Communications payload concepts for geostationary facilities
[NASA-TM-100154] N88-13513
**SYNCHROTRON RADIATION**
The production of ultrasmall and superfine holographic diffraction gratings using synchrotron radiation and lithographic techniques
[AD-A185395] N88-13562
Microwave superheaters for fusion
[DE88-001656] N88-14007
**SYNOPTIC METEOROLOGY**
Isentropic analysis and interpretation: Operational applications to synoptic and mesoscale forecast problems
[AD-A184814] N88-13830
Global atmospheric circulation statistics: Four year averages
[NASA-TM-100690] N88-13842
**SYNTHESIS (CHEMISTRY)**
Studies on syntheses of amine-carboxyboranes (boron analogues of amino acids) and derivatives
[AD-A184838] N88-13386
Molecular-level synthesis and characterization of metal-polymer interfaces
[AD-A184956] N88-13455
Preparation and characterization of members of the system (Zn,Se)1-xGaPx
[AD-A185073] N88-14019
**SYNTHETIC APERTURE RADAR**
Inverse scattering analysis of diffraction limited SAR
[FOA-C-30459-3.2] N88-13512
Arrays for discrete Fourier transform
[REPT-87-019] N88-13661
**SYNTHETIC FUELS**
Combustion characteristics of gas turbine alternative fuels
[NASA-TM-100247] N88-13338
**SYSTEM EFFECTIVENESS**
Experiments in fault tolerant software reliability
[NASA-CR-181554] N88-13663
**SYSTEM IDENTIFICATION**
A system identification technique based on the random decrement signatures. Part 1: Theory and simulation N88-13625
A system identification technique based on the random decrement signatures. Part 2: Experimental results N88-13626
**SYSTEMS ANALYSIS**
RSDIMU acceptance testing system: Overview of acceptance software and procedures N88-13866
**SYSTEMS ENGINEERING**
Plant Growth Module (PGM) conceptual design N88-13855
**SYSTEMS INTEGRATION**
Small space reactor power systems for unmanned solar system exploration missions
[NASA-TM-100228] N88-14054
**SYSTEMS SIMULATION**
Simulation of the perpendicular magnetic recording process
[B8713537] N88-13570
**SYSTEMS STABILITY**
Robustness of linear systems
[PB87-220042] N88-13909

## T

**TAKEOFF**
High speed propeller performance and noise predictions at takeoff/landing conditions
[NASA-TM-100267] N88-13860
**TANKS (COMBAT VEHICLES)**
Measurement of suspension and ride characteristics of the M1 main battle tank N88-13637
**TAPERING**
Exact finite element method analysis of viscoelastic tapered structures to transient loads N88-13632
**TASK COMPLEXITY**
Examining the relative efficiency of Part- versus whole-task practice for multiple-task situations
[AD-A185056] N88-13856
**TASKS**
Taskomat, a task battery for information processing
[IZF-1987-2] N88-13851
Examining the relative efficiency of Part- versus whole-task practice for multiple-task situations
[AD-A185056] N88-13856
**TEAMS**
Operational groups at the Aerospatiale Aircraft Division
[SNIAS-872-111-107] N88-14036
**TECHNICAL WRITING**
Role of the technical report in technological innovation
[PB87-232500] N88-14040
**TECHNOLOGY ASSESSMENT**
Hypersonic airbreathing propulsion: Evolution and opportunities N88-13231
The RAE experimental data-base for missiles at high Mach number and its use in assessing CFD methods N88-13250
Hypersonic aerodynamics: Applications for HOTOL N88-13252
A perspective of computational fluid dynamics N88-13279
Fundamentals of fighter aircraft design N88-13316
Progress toward the evolution of a Stirling space engine
[NASA-TM-100221] N88-14046
Astronautics and aeronautics, 1978: A chronology
[NASA-SP-4023] N88-14062
**TECHNOLOGY TRANSFER**
University research initiative research program summaries
[AD-A184876] N88-14035
**TECHNOLOGY UTILIZATION**
Carbon-carbon composites and Aerospatiale. State of the art and prospects
[SNIAS-872-430-108] N88-13401
**TELEMETRY**
New approach to telemetry development will significantly increase productivity of Joint Test Assembly (JTA) teams
[DE88-001676] N88-13373
**TELESCOPES**
An automated supernova search and the design strategy
[DE88-001827] N88-14051
**TELEVISION TRANSMISSION**
Improvements to a UHF rebroadcast television link suffering tidal fading: Countisbury UHF relay station
[BBC-RD-1987/14] N88-13495
Television motion measurement for DATV and other applications
[BBC-RD-1987/11] N88-13496
Two-signal cross modulation effects, half-IF effects and interference criteria in land mobile sharing with UHF (Ultra High Frequency) television
[PB87-228037] N88-13514
**TEMPER (METALLURGY)**
the influence of temper embrittlement on fatigue crack growth in hydrogen N88-13709
**TEMPERATURE**
Controlled ecological life support systems: Development of a plant growth module N88-13854
**TEMPERATURE DISTRIBUTION**
Occurance and growth of fatigue cracks in corrosion environment N88-13704
**TEMPERATURE EFFECTS**
Combustion characteristics of gas turbine alternative fuels
[NASA-TM-100247] N88-13338
The effect of temperature on the tensile properties of HSLA-100 steel
[AD-A184951] N88-13441
Development of response models for the Earth Radiation Budget Experiment (ERBE) sensors. Part 1: Dynamic models and computer simulations for the ERBE nonscanner, scanner and solar monitor sensors
[NASA-CR-178292] N88-13557
The initiation and growth of small fatigue cracks in copper at room and cryogenic temperatures N88-13668
Effect of test temperature and frequency on fatigue crack propagation in PVC N88-13715
**TEMPERATURE GRADIENTS**
An analytical soil thermodynamic model for the diurnal variation of ground surface temperature
[AD-A185386] N88-13823
**TEMPERATURE MEASUREMENT**
A mathematical model of high alloy nickel base high temperature alloys
[BLL-M-37381-(5828.4)] N88-13436
October lower stratospheric Antarctic temperature and total ozone from 1979-1985 N88-13776
**TEMPORAL RESOLUTION**
Resolution limitations and optimization of the LLNL streak camera focus
[DE88-001633] N88-13572
**TENSILE PROPERTIES**
The effect of temperature on the tensile properties of HSLA-100 steel
[AD-A184951] N88-13441
Tensile properties of extrusion consolidated Type 304 SS rapidly solidified powders
[DE87-014875] N88-13450
**TENSILE STRENGTH**
Fatigue strength of alloy A286 at cryogenic temperature N88-13695
Effect of interface on mechanical properties of graphite/201 aluminum composites N88-13717
Deformation, fatigue and fracture behavior of two cast anisotropic superalloys N88-13732
**TENSILE STRESS**
Tensile mean stress effects on uniaxial fatigue behavior of 1045 HR steel N88-13694
**TENSILE TESTS**
Test number 2 of propellant for rocket motor MK52
[PB87-226155] N88-13480
Crack growth in contrasting titanium alloys under the conjoint action of high and low cycle fatigue N88-13686
**TENSORS**
Lagrangian procedures for higher order field equations
[DE87-703365] N88-13911
**TERMINAL BALLISTICS**
Mechanical property evaluation of a series of commercial tungsten alloys
[AD-A185440] N88-13446
On the simulation of ballistic shock loads N88-13615
Structural frequency functions for an impulsive, distributed forcing function N88-13627
**TERRAIN**
Large bandwidth ground scattering model — radar scattering
[FOA-C-30458-3.2] N88-13511
**TERRAIN ANALYSIS**
Correction of inertial navigation system drift errors for an autonomous land vehicle using optical radar terrain data
[AD-A184973] N88-13311
**TEST FACILITIES**
A survey of existing hypersonic ground test facilities: North America N88-13220
High frequency data acquisition system for space shuttle main engine testing N88-13630
An overview of the DOE/SANDIA/USDA vertical axis wind turbine Test Bed Project
[DE88-000604] N88-13812
Feasibility study for gas-grain simulation facility
[NASA-CR-177468] N88-13954
Atomic beam studies of the interaction of hydrogen with transition metal surfaces
[DE88-000208] N88-13970
**TEST FIRING**
Mechanical property evaluation of a series of commercial tungsten alloys
[AD-A185440] N88-13446

**TETHERED SATELLITES**
Research on Electrodynamic Tether Effects (RETE) experiment Electrical Ground Support Equipment (EGSE) — tethered satellite
[IFSI-87-2] N88-13378
RETE experiment Assembly, Integration, and Verification (AIV) activities
[IFSI-87-6] N88-13380

**TEXAS**
An overview of the DOE/SANDIA/USDA vertical axis wind turbine Test Bed Project
[DE88-000604] N88-13812

**THEMATIC MAPPING**
Land cover/use classification of Cairns, Queensland, Australia: A remote sensing study involving the conjunctive use of the airborne imaging spectrometer, the large format camera and the thematic mapper simulator N88-13759
Overview of Austrian Airborne Imaging Spectrometer (AIS) programme and first results N88-13762
Mapping hydrothermally altered rocks in the Northern Grapevine Mountains, Nevada and California with the airborne imaging spectrometer N88-13772

**THEORETICAL PHYSICS**
Theoretical atomic and molecular physics
[DE88-001625] N88-13974

**THERMAL ANALYSIS**
Space station systems: A bibliography with indexes
[NASA-SP-7056(05)] N88-13382
Development of an integrated BEM approach for hot fluid structure interaction
[NASA-CR-181577] N88-13384
Investigation by differential scanning calorimetry of microstructure in a superplastic Al-Mg-Zr alloy
[AD-A184902] N88-13439
Thermal finite-element analysis of space shuttle main engine turbine blade
[NASA-TM-100117] N88-13745

**THERMAL CONDUCTIVITY**
Development of response models for the Earth Radiation Budget Experiment (ERBE) sensors. Part 1: Dynamic models and computer simulations for the ERBE nonscanner, scanner and solar monitor sensors
[NASA-CR-178292] N88-13557

**THERMAL CYCLING TESTS**
Stress intensity factors for cracking metal structures under rapid thermal loading, phase 1
[AD-A184112] N88-13606

**THERMAL DIFFUSION**
Transient development of stratification in a partially divided enclosure
[DE87-011742] N88-13490

**THERMAL PROTECTION**
Advantages of internal thermal protection in a pyrotechnical plunger
[SNIAS-872-430-114] N88-13478

**THERMAL STABILITY**
Thermally stable aromatic structures from acyclic precursors. 1. Para polyphenylene model compounds from 3-Dimethyl amino hex-5-EN-1-YNES
[AD-A185300] N88-13462

**THERMAL STRESSES**
United States - Japan Workshop on Dielectric and Piezoelectric Ceramics (3rd) held in Toyama, Japan on November 9-12, 1986
[AD-A185113] N88-13460
Fluid mass and thermal loading effects on the modal characteristics of space shuttle main engine liquid oxygen inlet splitter vanes N88-13628
Fracture kinetics of corrosion fatigue N88-13708
The effect of heat treatment on fatigue crack growth in polycarbonate N88-13714

**THERMIONIC CATHODES**
A synthetic plasma source
[TRITA-EPP-86-15] N88-13995

**THERMOCHEMICAL PROPERTIES**
The formation and thermochemical properties of multiligand complexes
[AD-A184935] N88-13416

**THERMOCHEMISTRY**
Phase diagram and thermochemical properties of the Al-Cu system
[ETN-88-91015] N88-13447

**THERMODYNAMIC PROPERTIES**
An analytical soil thermodynamic model for the diurnal variation of ground surface temperature
[AD-A185388] N88-13823
Molecular dynamics studies of aromatic hydrocarbon liquids
[DE88-001473] N88-13973

**THERMODYNAMICS**
Ionic transport and electrical relaxation in glass
[DE88-000887] N88-14028
Calendar of selected aeronautical and space meetings
[AGARD-CAL-87/1] N88-14033

**THERMOGRAPHY**
Measurement and control of damage in composite materials: Nondestructive controls by thermography, holography, and radiography
[SNIAS-872-430-110] N88-13403

**THERMOMECHANICAL TREATMENT**
Development of iron aluminides
[AD-A185190] N88-13461

**THERMOMETERS**
Assessment of the reliability of a correction procedure for WGT (Wet Globe Thermometer) (Botsball) measurements of heat stress
[AD-A185193] N88-13559

**THERMOPLASTIC RESINS**
Process for the production of a thermoplastic elastomer composition
[EP-PATENT-0-202-782-A2] N88-13465
Flexibilized copolyimide adhesives
[NASA-TM-89303] N88-13474

**THERMOREGULATION**
Microwave challenges to the thermoregulatory system
[AD-A185391] N88-13847
Human thermoregulatory model for whole body immersion in water at 20 and 26 C
[AD-A185052] N88-13849

**THIN FILMS**
Influence of bonding shop moisture on metal-honeycomb junctions bonded with ultra-thin adhesive films
[SNIAS-872-422-112] N88-13399
Raman microprobe characterization of dielectric films following high-energy pulsed laser irradiation
[DE88-000559] N88-13587
Tribology of thin film systems
[ETN-88-91385] N88-13601
The effects of thin anodic films on the cyclic microstrain/macrostrain behavior of tungsten N88-13650
Develop techniques for ion implantation of (lead-lanthanum-zirconate-titanate) for adaptive optics
[DE88-000642] N88-13986
Structural characterization of ion implanted beta-SiC thin films
[DE87-014567] N88-14027

**THIN WALLS**
Development on thin wall tubes of dispersion type
[DE87-703384] N88-13483

**THREE DIMENSIONAL FLOW**
An analysis of the compressible-viscous flow field around a 3D-oscillating wing N88-13254
Three-dimensional flow past a two-dimensional body N88-13280
Computational study of three-dimensional wake structures
[REPT-2] N88-13281
Time-marching finite-difference methods for the three-dimensional Euler equations of contravariant velocity components N88-13285
Numerical simulation of transonic aircraft in comparison to wind tunnel test N88-13289
A numerical study of the effects of curvature and convergence on dilution jet mixing
[NASA-TM-89878] N88-13347
Displaying three-dimensional data
[AD-A185347] N88-13541
The development and evaluation of three-dimensional models of cold flow in internal combustion engines
[DE88-900077] N88-13594
Three-dimensional dynamic labyrinth seal analysis
[AD-A185353] N88-13599
A system of three-dimensional complex variables
[NASA-TM-88318] N88-13951

**THRUST DISTRIBUTION**
Low speed wind tunnel investigation of propeller slipstream aerodynamic effects on different nacelle/wing combinations. Part 1: Total forces and moments and pressure distributions on nacelle/wing at different angles of attack and yaw and at different thrust coefficients
[FFA-TN-1987-22] N88-13302

**TIME**
On-orbit frequency stability analysis of the GPS NAVSTAR 8 rubidium clock and NAVSTARs 9 and 10 cesium clocks
[AD-A184984] N88-13312
Time domain electromagnetic waves in multilayered media
[AD-A185055] N88-13502

**TIME DEPENDENCE**
On the numerical simulation of three-dimensional hypersonic flow N88-13237
Noise modelling in the time domain with the aid of Spice
[PB87-221941] N88-13492
Numerical and analytical methods in nonlinear partial differential equations
[AD-A185210] N88-13918

**TIME MARCHING**
Computation of flow past conical hypersonic wings using a second order Godunov method N88-13241
Time-marching finite-difference methods for the three-dimensional Euler equations of contravariant velocity components N88-13285

**TIME SERIES ANALYSIS**
Quantile based unified distribution of extreme values and order statistics
[AD-A185171] N88-13942

**TITANATES**
Develop techniques for ion implantation of (lead-lanthanum-zirconate-titanate) for adaptive optics
[DE88-000642] N88-13986

**TITANIUM ALLOYS**
The effect of microstructure on the surface crack length: Crack depth relationship for short cracks N88-13670
Crack growth in contrasting titanium alloys under the conjoint action of high and low cycle fatigue N88-13686
Characterization of the microstructures of various materials
[AD-A184961] N88-14017

**TOKAMAK DEVICES**
ALT-1 pump limiter experiments
[DE88-000822] N88-13989
Subcommittee for MHD theory
[DE88-000596] N88-14003

**TOLERANCES (MECHANICS)**
Damage considerations in sizing aircraft cells. Life predictions
[SNIAS-872-111-116] N88-13330

**TOLERANCES (PHYSIOLOGY)**
Microwave challenges to the thermoregulatory system
[AD-A185391] N88-13847

**TOLUENE**
Detailed mechanism of toluene oxidation and comparison with benzene
[NASA-TM-100261] N88-13428

**TOMAHAWK MISSILES**
Non-linear shipboard shock analysis of the Tomahawk missile shock isolation system N88-13614

**TOOLS**
Human engineering laboratory grounding analysis (HELGA)-2
[AD-A185367] N88-13524
Interaction of microstructure and fatigue in tool steels N88-13693

**TOPOGRAPHY**
The influence of the topography of fracture surfaces on crack closure N88-13657

**TOROIDAL PLASMAS**
Dynamic processes in field-reversed-configuration compact toroids
[DE87-014756] N88-13999

**TOROIDS**
A short introduction to the status and motivation for reversed field pinch and compact toroid research
[DE88-000487] N88-13999

**TOUGHNESS**
The effect of temperature on the tensile properties of HSLA-100 steel
[AD-A184951] N88-13441

**TOXIC HAZARDS**
Investigation of the exposure to harmful compounds in the workshop of nondestructive materials testing at Gilze-Rijen (Netherlands)
[PML-1985-42] N88-13816

**TOXICITY**
Short-term in vitro screening studies related to the inhalation toxicology of potentially toxic aerosols
[AD-A184815] N88-13845

**TOXICITY AND SAFETY HAZARD**
Investigation of the exposure to harmful compounds in the workshop of nondestructive materials testing at Gilze-Rijen (Netherlands)
[PML-1985-42] N88-13816
Investigation of the nature and concentration of vapor and mist during the cleaning of aircraft
[PML-1985-29] N88-13817

**TRACKING (POSITION)**
Opportunities for tropical cyclone motion research in the Northwest Pacific region
[AD-A185068] N88-13834

**TRAFFIC CONTROL**
The estimation of basic matrices using travel intensity theorems
[REPT-87-13] N88-13926

**TRAILING EDGE FLAPS**
Static aeroelastic considerations in the definition of design loads for fighter airplanes N88-13351

**TRAINING DEVICES**
Examining the relative efficiency of Part- versus whole-task practice for multiple-task situations
[AD-A185056] N88-13858

**TRAJECTORIES**
Trajectory control of robot manipulators with closed-kinematic chain mechanism
[NASA-TM-89305] N88-13605
Cartesian path control of a two-degree-of-freedom robot manipulator
[NASA-CR-182331] N88-13906
**TRAJECTORY ANALYSIS**
Optoelectronic measurement methods for ballistic experiments
[PB87-110706] N88-13554
**TRAJECTORY CONTROL**
Trajectory control using laterally ejected jets. Literature review
[ISL-R-117/85] N88-13544
Cartesian path control of a two-degree-of-freedom robot manipulator
[NASA-CR-182331] N88-13906
**TRANSDUCERS**
Capacitive resonant transducer for the Frascati gravitational antenna
[IFSI-86-9] N88-13528
**TRANSFER FUNCTIONS**
Electromagnetic tests
[SNIAS-872-430-103] N88-13508
Equivalence of input-output stability and exponential stability for infinite dimensional systems
[TW-276] N88-13903
**TRANSIENT LOADS**
Exact finite element method analysis of viscoelastic tapered structures to transient loads N88-13632
**TRANSIENT RESPONSE**
Time domain electromagnetic waves in multilayered media
[AD-A185055] N88-13502
Structuring data for concurrent vectorized processing in a transient dynamics finite element program
[DE87-013062] N88-13890
**TRANSITION FLOW**
A numerical study of the effects of curvature and convergence on dilution jet mixing
[NASA-TM-89878] N88-13347
**TRANSITION METALS**
Atomic beam studies of the interaction of hydrogen with transition metal surfaces
[DE88-000206] N88-13970
**TRANSMISSION LINES**
The use of coaxial transmission line elements in log-periodic dipole arrays
[AD-A184864] N88-13499
**TRANSONIC FLOW**
The role of computation fluid dynamics in aeronautical engineering (4). The development and applications of implicit TVD finite volume code N88-13259
Navier-Stokes simulation of transonic transportation aircraft configurations. 1: Flow-field simulation over wing-fuselage combinations N88-13288
Numerical simulation of transonic aircraft in comparison to wind tunnel test N88-13289
Study of the effect of mass transfer on a transonic boundary layer. Application to flow relaminarization
[ETN-88-91169] N88-13296
Computation of transonic flows with nacelle simulation
[SNIAS-872-111-117] N88-13300
**TRANSONIC SPEED**
Design of wings and wing/body configurations for transonic and supersonic speeds N88-13318
**TRANSPARENCE**
Resistance of canopy materials against chemicals
[PML-1985-22] N88-13466
**TRANSPORT AIRCRAFT**
Computation of nacelle interference using boundary element method N88-13267
Navier-Stokes simulation of transonic transportation aircraft configurations. 1: Flow-field simulation over wing-fuselage combinations N88-13288
Aeroelastic analysis of modern transport aircraft N88-13352
**TRANSPORT PROPERTIES**
Numerical analysis of axisymmetric flow with H2-O2 reactions N88-13272
Conditional second order closure for turbulent shear flows
[AD-A185369] N88-13542
**TRANSPORT THEORY**
Transport scaling in the collisionless-detrapping regime in stellarators
[DE88-001511] N88-14006
Comparison of 2D memory SEU transport simulation with experiments
[ATR-86(8139)-2-REV-A] N88-14025
**TRANSPORTATION NETWORKS**
Study of the feasibility of a satellite communication system for road transportation home office to vehicle communication. Volume 1: Conceptual analysis
[SC/87-E/6-VOL-1] N88-13505
Study of the feasibility of a satellite communication system for road transportation home office to vehicle communication. Volume 2: Market study
[SC/87-E/6-VOL-2] N88-13506
**TRAVELING WAVES**
Modeling and control of large flexible vehicles in the atmosphere and space
[AD-A185368] N88-13377
**TRIBOLOGY**
Tribology of thin film systems
[ETN-88-91365] N88-13601
**TROPICAL REGIONS**
The use of TOMS data for tropospheric ozone studies N88-13784
**TROPICAL STORMS**
Opportunities for tropical cyclone motion research in the Northwest Pacific region
[AD-A185068] N88-13834
Environmental and convective influence on tropical cyclone development versus non-development
[AD-A185231] N88-13835
**TROPOPAUSE**
Photochemical ozone overburden correction N88-13778
Northwest Airlines flight experiments N88-13786
Application of TOMS data to weather analysis models N88-13787
Correlations of TOMS total ozone data (Nimbus-7 satellite) with tropopause height N88-13788
An analysis of tropopause pressure and total ozone correlations N88-13789
TOMS ozone data compared at mesoscale resolution to tropopause heights from the AVE radiosonde network and to VAS radiances over the south-central United States N88-13790
The use of TOMS-modified VAS data for large-scale NWP N88-13791
**TROPOSPHERE**
Scientific and Operational Requirements for TOMS Data
[NASA-CP-2497] N88-13774
Lower-stratospheric/upper-tropospheric exchange processes associated with tropical cyclones as observed by TOMS N88-13782
Tropical easterly jet located using TOMS data N88-13785
The use of TOMS data for tropospheric ozone studies N88-13784
**TRUSSES**
Simultaneous structural and control optimization via linear quadratic regulator eigenstructure assignment N88-13622
**TUBE HEAT EXCHANGERS**
Qualification of expansion and joint welding procedures of tube-to-tubesheet joints for heat exchangers in nuclear power plants
[DE87-703526] N88-13592
**TUNGSTEN**
The effects of thin anodic films on the cyclic microstrain/macrostrain behavior of tungsten N88-13650
**TUNGSTEN ALLOYS**
Mechanical property evaluation of a series of commercial tungsten alloys
[AD-A185440] N88-13446
**TUNGSTEN COMPOUNDS**
Results from the melting of tungsten composites under microgravity (TEXUS 10 flight)
[FOA-C-20676-2.1] N88-13482
**TUNING**
Optically tuned MM-wave IMPATT source
[AD-A185250] N88-13523
**TURBINE BLADES**
Simulated service test behavior of various internal and external coatings applied on CF6-50 first stage turbine blades
[NLR-MP-86018-U] N88-13343
Thermal finite-element analysis of space shuttle main engine turbine blade
[NASA-TM-100117] N88-13745
A computer program for calculating unsteady aerodynamic coefficients for cascades in supersonic axial flow
[NASA-TM-100204] N88-13753
STAEBL/general composites with hygrothermal effects (STAEBL/GENCOM)
[NASA-TM-100266] N88-13754
Accurate rotor loads prediction using the FLAP (Force and Loads Analysis Program) dynamics code
[DE88-001109] N88-13815
**TURBINE ENGINES**
Thermal finite-element analysis of space shuttle main engine turbine blade
[NASA-TM-100117] N88-13745
**TURBINE PUMPS**
Seal technology for liquid oxygen (LOX) turbopumps
[NASA-CR-174866] N88-13603
Incipient failure detection of space shuttle main engine turbopump bearings using vibration envelope detection N88-13629
Thermal finite-element analysis of space shuttle main engine turbine blade
[NASA-TM-100117] N88-13745
STAEBL/general composites with hygrothermal effects (STAEBL/GENCOM)
[NASA-TM-100266] N88-13754
**TURBOCOMPRESSORS**
Automated design of controlled diffusion blades
[NASA-TM-100251] N88-13304
Effects of free stream turbulence, Reynolds number and incidence angle on axial turbine cascade performance N88-13339
**TURBOMACHINERY**
Identification of perturbations in turbomachines by the analysis of pressure signals, vibrations and wavelike motions
[ETN-88-90602] N88-13600
**TURBOPROP AIRCRAFT**
Noise of a model counterrotation propeller with reduced aft rotor diameter at simulated takeoff/approach conditions (F7/A3)
[NASA-TM-100254] N88-13961
**TURBULENCE**
A perspective of computational fluid dynamics N88-13279
Effects of free stream turbulence, Reynolds number and incidence angle on axial turbine cascade performance N88-13339
Vortical Flows Research Program of the Fluid Dynamics Research Branch
[NASA-TM-88332] N88-13549
Measurement of local convective heat transfer coefficients from a smooth and roughened NACA-0012 airfoil: Flight test data
[NASA-TM-100284] N88-13552
Isentropic analysis and interpretation: Operational applications to synoptic and mesoscale forecast problems
[AD-A184814] N88-13830
Chaos: Chto Delat? (What is to be done?)
[DE88-000513] N88-13933
**TURBULENCE EFFECTS**
Turbulence generation in combustion
[AD-A184810] N88-13413
**TURBULENT BOUNDARY LAYER**
The effects of sweep and bluntness on a glancing shock wave turbulent boundary layer interaction N88-13227
Development of the computer program for turbulent boundary layers N88-13264
Interferometric data for a shock-wave/boundary-layer interaction
[NASA-TM-88227] N88-13306
Experimental study of the fluid mechanics of unsteady turbulent boundary layers
[AD-A184856] N88-13536
Asymptotic analysis of a turbulent boundary layer in a strong adverse pressure gradient
[AD-A185406] N88-13543
Fluctuating pressure loads under high speed boundary layers
[NASA-TM-100517] N88-13962
**TURBULENT DIFFUSION**
Active and passive plume distribution models in the convective boundary layer using a large eddy simulation model
[KNMI-TR-90] N88-13546
**TURBULENT FLOW**
Numerical analysis of flow through scramjet engine inlets N88-13233
Numerical prediction of turbulent flows in dump diffusers N88-13265
Delta wing in incompressible flow. Experimental study in F2
[ONERA-RT-36/1147-AN-249-G] N88-13298
Interferometric data for a shock-wave/boundary-layer interaction
[NASA-TM-88227] N88-13306
A numerical study of the effects of curvature and convergence on dilution jet mixing
[NASA-TM-89878] N88-13347
Statistical theory of turbulent incompressible multimaterial flow
[DE88-000435] N88-13535
Physical analysis and numerical simulation of coherent turbulent structures in mixed layers, jets, and wakes
[ETN-88-91183] N88-13548
Hot wire and laser velocimeter studies of turbulent flow at supersonic velocities
[ETN-88-91172] N88-13566

**TURBULENT HEAT TRANSFER**
The development and evaluation of three-dimensional models of cold flow in internal combustion engines [DE88-900077] N88-13594
**TURBULENT JETS**
Conditional second order closure for turbulent shear flows [AD-A185369] N88-13542
**TWO DIMENSIONAL BODIES**
Development of the computer program for turbulent boundary layers N88-13264
Rarefied gas numerical wind tunnel. 2: Two-dimensional and axially symmetric bodies N88-13273
Three-dimensional flow past a two-dimensional body N88-13280
Computation of flow around 2-D circular cylinder N88-13284
Navier-Stokes analysis of laminar flow control of a two-dimensional airfoil N88-13286
SUSIE reference manual [DE88-001462] N88-13893
**TWO DIMENSIONAL BOUNDARY LAYER**
An experimental investigation of the ignition and flammability limits of various hydrocarbon fuels in a two-dimensional solid fuel ramjet [AD-A184968] N88-13342
**TWO DIMENSIONAL FLOW**
Computation of dynamic stall of NACA0012 airfoil by block pentadiagonal matrix scheme N88-13255
Practical application of two-dimensional viscous flow computation N88-13257
The role of computation fluid dynamics in aeronautical engineering (4). The development and applications of implicit TVD finite volume code N88-13259
Numerical analysis of cascade flow solving Navier-Stokes equations N88-13262
Inverse design method for two-dimensional transonic cascades N88-13263
Numerical prediction of turbulent flows in dump diffusers N88-13265
**TYPHOONS**
Opportunities for tropical cyclone motion research in the Northwest Pacific region [AD-A185068] N88-13834

## U

**U.S.S.R.**
Astrophysics observatory in Byurakan [AD-A185144] N88-14050
**ULTRAHIGH FREQUENCIES**
Improvements to a UHF rebroadcast television link suffering tidal fading: Countisbury UHF relay station [BBC-RD-1987/14] N88-13495
Two-signal cross modulation effects, half-IF effects and interference criteria in land mobile sharing with UHF (Ultra High Frequency) television [PB87-228037] N88-13514
**ULTRAVIOLET ASTRONOMY**
Optical photometer for the Tirgo telescope [IFSI-87-5] N88-13985
**ULTRAVIOLET RADIATION**
TOMS as a monitor of the ultraviolet radiation environment: Applications to photobiology N88-13785
**ULTRAVIOLET SPECTRA**
Satellite observations of extreme ultraviolet radiation [AD-A185043] N88-14059
**ULTRAVIOLET SPECTROMETERS**
Dobson-stations performance assessment using TOMS data N88-13792
Volcanic eruption detection with TOMS N88-13793
Analysis of SO2 signals in SBUV/TOMS data N88-13794
Comparison of ground based and TOMS measurements of SO2 from volcanic emissions N88-13795
TOMS and the NOAA/FAA volcano support plan N88-13796
Use of satellite data in volcano monitoring N88-13797
Selection of optimum wavelengths for ozone mapping from satellites N88-13798
Determination of total ozone from HIRS2/MSU sounding data N88-13799
Complementary information between UV and IR for remote sensing of total ozone N88-13800
Observation guidelines for a Total Ozone Mapping Spectrometer (TOMS) in geosynchronous orbit N88-13801
Satellite observations of extreme ultraviolet radiation [AD-A185043] N88-14059
**ULTRAVIOLET SPECTROSCOPY**
Extreme ultraviolet beam-foil spectroscopy of highly ionized neon and argon [AD-A185197] N88-13418
**ULYSSES MISSION**
Media calibrations of the Doppler signal for a gravitational wave experiment — interplanetary medium [IFSI-86-13] N88-13825
**UNDERGROUND EXPLOSIONS**
Analysis of photopole data reduction models N88-13616
**UNDERWATER STRUCTURES**
Design and test of high performance composite tubes for use in deep water drilling and production systems [SNIAS-872-430-107] N88-13487
High performance composite tubes for offshore applications [SNIAS-872-430-116] N88-13488
**UNDERWATER TESTS**
Experimental studies on the tripping behavior of narrow T-stiffened flat plates subjected to hydrostatic pressure and underwater shock N88-13613
**UNIVERSE**
Laboratory and near-earth space plasma as a key to the plasma universe [TRITA-EPP-87-09] N88-13996
Cosmology in the plasma universe [TRITA-EPP-87-07] N88-14053
**UNIVERSITIES**
University research initiative research program summaries [AD-A184876] N88-14035
**UNSTEADY FLOW**
Driving mechanism of unsteady separation shock motion in hypersonic interactive flow N88-13226
Numerica calculation in the Laplace domain for subsonic unsteady aerodynamic forces acting on a finite wing N88-13256
The development of a computer code (U2DIIF) for the numerical solution of unsteady, inviscid and incompressible flow over an airfoil [AD-A185033] N88-13293
Unsteady aerodynamics of an oscillating cascade in a compressible flow field [NASA-TM-100219] N88-13346
Influence of the static deformation on a wing in the unsteady aerodynamic N88-13357
Experimental study of the fluid mechanics of unsteady turbulent boundary layers [AD-A184856] N88-13536
Physical analysis and numerical simulation of coherent turbulent structures in mixed layers, jets, and wakes [ETN-88-91183] N88-13548
A computer program for calculating unsteady aerodynamic coefficients for cascades in supersonic axial flow [NASA-TM-100204] N88-13753
**UNSTEADY STATE**
Aircraft dynamics: Aerodynamic aspects and wind tunnel techniques N88-13320
**UPPER SURFACE BLOWN FLAPS**
A numerical investigation on wing/nacelle interferences N88-13258
**UPSTREAM**
Relaxation method for the compressible Navier-Stokes equations using upwind schemes N88-13283
**USER MANUALS (COMPUTER PROGRAMS)**
SUSIE reference manual [DE88-001462] N88-13893
**USER REQUIREMENTS**
Orbital Spacecraft Consumables Resupply System (OSCRS). Volume 1: Executive summary [NASA-CR-172010] N88-13368
File usage analysis and resource usage prediction: A measurement-based study [NASA-CR-181553] N88-13867
Usage analysis of user files in UNIX [NASA-CR-181561] N88-13868
**UTILIZATION**
Photocurrent generation from basic metals, utilizing a short pulsed ArF excimer laser [AD-A184928] N88-13579

## V

**V/STOL AIRCRAFT**
Integrated control and display research for transition and vertical flight on the NASA V/STOL Research Aircraft (VSRA) [NASA-TM-100029] N88-13359
Full-envelope aerodynamic modeling of the Harrier aircraft [NASA-TM-88376] N88-13363
**VACUUM ARC SWITCHES**
Low-current behavior and current chopping of vacuum arcs [ISBN-90-9001649-X] N88-13529
**VALVES**
Development, construction and testing of a novel internal combustion engine with conical rotating slide valve [DE88-900071] N88-13593
**VANES**
Fluid mass and thermal loading effects on the modal characteristics of space shuttle main engine liquid oxygen inlet splitter vanes N88-13628
**VAPOR DEPOSITION**
Fabrication of composites by chemical vapor deposition [DE87-014565] N88-13408
Reactive sticking coefficients of silane on silicon [DE88-000601] N88-13473
Fundamental studies in the OM-CVD growth of Ga-In-As-Sb [AD-A184822] N88-14014
**VAPORS**
Investigation of the nature and concentration of vapor and mist during the cleaning of aircraft [PML-1985-29] N88-13817
**VECTOR ANALYSIS**
Computational methods for problems in aerodynamics and large space structure using parallel and vector architectures [AD-A185401] N88-13294
Utilization of a high rate vector computer in computational fluid mechanics for aeronautics [ETN-88-91171] N88-13547
**VECTORS (MATHEMATICS)**
Solution of some 3-D viscous and inviscid supersonic flow problems by finite-volume space-marching schemes N88-13235
Multidimensional least squares fitting of fuzzy models [AD-A185148] N88-13918
Least squares for fuzzy vector data regression [AD-A185156] N88-13917
**VEGETATIVE INDEX**
AIS-2 spectra of California wetland vegetation N88-13783
**VELOCITY**
Time-marching finite-difference methods for the three-dimensional Euler equations of contravariant velocity components N88-13285
Velocity scaled aeroelastic testing of an unducted fan [GTL-191] N88-13337
Wing divergence of trimmed aircraft N88-13354
**VELOCITY DISTRIBUTION**
Model-based motion estimation and its application to restoration and interpolation of motion pictures [AD-A185054] N88-13558
**VENTILATION**
A plethysmograph for measuring pulmonary ventilation in small animals [AD-A184978] N88-13846
Plant Growth Module (PGM) conceptual design N88-13855
**VENTILATORS**
Computer code simulations of explosions in flow networks and comparison with experiments [DE88-001946] N88-13491
**VERTICAL FLIGHT**
Integrated control and display research for transition and vertical flight on the NASA V/STOL Research Aircraft (VSRA) [NASA-TM-100029] N88-13359
**VERY LARGE SCALE INTEGRATION**
A study of charged particles/radiation damage to VLSI device materials [NASA-CR-172036] N88-13518
New breakthrough in Chinese integrated circuits: Successful development of high-speed CMOS circuits [AD-A185381] N88-13525
**VIBRATION**
Initial dynamic load estimates during configuration design N88-13621
The Shock and Vibration Digest, Volume 19, No. 12 N88-13746
Dynamics of cables and chains N88-13747
Computation of natural frequencies of planar lattice structure [AD-A185387] N88-13920
**VIBRATION DAMPING**
The 58th Shock and Vibration Symposium, volume 1 [NASA-CP-2488-VOL-1] N88-13609
Viscous damped space structure for reduced jitter N88-13623
A system identification technique based on the random decrement signatures. Part 1: Theory and simulation N88-13625
A system identification technique based on the random decrement signatures. Part 2: Experimental results N88-13626
An efficient frequency response solution for nonproportionally damped systems N88-13634
Shape optimization of damping layers N88-13635

Advanced joining concepts for passive vibration control N88-13638

**VIBRATION ISOLATORS**
Modeling and control of large flexible vehicles in the atmosphere and space
[AD-A185368] N88-13377
The 58th Shock and Vibration Symposium, volume 1
[NASA-CP-2488-VOL-1] N88-13609
Optimal shock isolation with minimum settling time N88-13633
A passive vibration-cancelling isolation mount N88-13636

**VIBRATION MEASUREMENT**
Measurement of suspension and ride characteristics of the M1 main battle tank N88-13637
Coupled elastic rotor/body vibrations with inplane degrees of freedom N88-13643

**VIBRATIONAL SPECTRA**
Pure dephasing of a vibrational adbond
[AD-A185222] N88-13740

**VIDEO SIGNALS**
Digital video bit-rate reduction: DPCM for sub-Nyquist PAL
[BBC-RD-1987/16] N88-13494
Improvements to a UHF rebroadcast television link suffering tidal fading: Countisbury UHF relay station
[BBC-RD-1987/14] N88-13495
Two-signal cross modulation effects, half-IF effects and interference criteria in land mobile sharing with UHF (Ultra High Frequency) television
[PB87-228037] N88-13514

**VISCOELASTIC DAMPING**
Damping analysis of flexural waves in fluid-loaded single and constrained plates
[AD-A185116] N88-13739

**VISCOELASTICITY**
Exact finite element method analysis of viscoelastic tapered structures to transient loads N88-13632
Bending of a bonded beam as a test method for adhesive properties
[AD-A184813] N88-13736

**VISCOSITY**
In-situ characterization of the interface of glass reinforced composites
[AD-A185136] N88-13391
Colloidal stability of oxidized silicon particles in ethanolic and aqueous media
[DE87-014783] N88-13421

**VISCOUS DAMPING**
Viscous damped space structure for reduced jitter N88-13623
Exact finite element method analysis of viscoelastic tapered structures to transient loads N88-13632

**VISCOUS FLOW**
Low Reynolds number influence on aerodynamic performance of hypersonic lifting vehicles N88-13230
Numerical simulation of the hypersonic flow around lifting vehicles N88-13234
Numerical optimization of conical flow waveriders including detailed viscous effects N88-13245
An analysis of the compressible-viscous flow field around a 3D-oscillating wing N88-13254
Practical application of two-dimensional viscous flow computation N88-13257
The role of computation fluid dynamics in aeronautical engineering (4). The development and applications of implicit TVD finite volume code N88-13259
Computations of compressible viscous flows over multiple-bodies N88-13282
A numerical study of the effects of curvature and convergence on dilution jet mixing
[NASA-TM-89878] N88-13347
The simulation of the viscous flow around a cylinder by the random vortex method N88-13534
Low thrust viscous nozzle flow fields prediction
[NASA-CR-182334] N88-13551

**VISIBILITY**
ZEUS: A knowledge-based expert system that assists in predicting visibility at airbases
[AD-A184197] N88-13829

**VISUAL PERCEPTION**
Learning a color algorithm from examples
[AD-A184385] N88-13862

**VOLCANOES**
Volcanic eruption detection with TOMS N88-13793
Analysis of SO2 signals in SBUV/TOMS data N88-13794
Comparison of ground based and TOMS measurements of SO2 from volcanic emissions N88-13795
TOMS and the NOAA/FAA volcano support plan N88-13796
Use of satellite data in volcano monitoring N88-13797

**VOLCANOLOGY**
Volcanic eruption detection with TOMS N88-13793

**VON KARMAN EQUATION**
Application of the Von Karman equation to the bifurcation theory
[NOTA-INTERNA-891] N88-13927

**VORTEX BREAKDOWN**
Analysis of the breakdown of the Antarctic circumpolar vortex using TOMS ozone data N88-13779

**VORTEX SHEDDING**
Vortex interaction with a leading-edge of finite thickness
[NASA-CR-182341] N88-13307

**VORTICES**
Vortex formation over delta, double-delta and wave rider configurations at supersonic speeds N88-13243
The off-design performance of hypersonic waveriders N88-13244
Application of discrete vortex method to analysis of separated flow around aerofoils N88-13268
Three-dimensional flow past a two-dimensional body N88-13280
Vortex interaction with a leading-edge of finite thickness
[NASA-CR-182341] N88-13307
Nonlinear lift control at high speed and high angle of attack using vortex flow technology N88-13319
Vortical Flows Research Program of the Fluid Dynamics Research Branch
[NASA-TM-88332] N88-13549
Isentropic analysis and interpretation: Operational applications to synoptic and mesoscale forecast problems
[AD-A184814] N88-13830


## W


**WAKES**
An ultra-high-speed cinematographic method for the study of wakes in hypersonic ballistic ranges N88-13228
Computational study of three-dimensional wake structures
[REPT-2] N88-13261
Wakes of two dimensional bluff bodies in subsonic flow. Influence of a separating plate and of a pulsed injection of momentum
[IMFL-4200-86/75] N88-13297

**WALKING MACHINES**
Correction of inertial navigation system drift errors for an autonomous land vehicle using optical radar terrain data
[AD-A184973] N88-13311

**WALLS**
The orientations of dipolar walls produced by cyclic deformation N88-13655
Reversed field pinch plasmas with various boundary conditions
[DE88-000832] N88-14004

**WASTE TREATMENT**
Innovative and alternative technology projects
[PB87-230165] N88-13818

**WASTE WATER**
Innovative and alternative technology projects
[PB87-230165] N88-13818

**WATER**
Phase purity of NiCo2O4, a catalyst candidate for electrolysis of water
[NASA-TM-100239] N88-13385
Operating envelopes of particle sizing instrumentation used for icing research
[NASA-CR-180670] N88-13573

**WATER IMMERSION**
Human thermoregulatory model for whole body immersion in water at 20 and 28 C
[AD-A185052] N88-13849

**WATER TREATMENT**
Innovative and alternative technology projects
[PB87-230165] N88-13818

**WATERPROOFING**
Water disbondment characterization of organic Coating/metal substrate systems
[AD-A184847] N88-13454

**WAVE ATTENUATION**
Experimental studies on acoustic emission monitoring of crack propagation in offshore structures: A literature survey N88-13748

**WAVE EXCITATION**
Ultrafast intrinsic bistable devices
[PB87-109310] N88-13978

**WAVE FRONTS**
Nonconventional optical techniques for optical wavefront processing
[AD-A185099] N88-13982

**WAVE FUNCTIONS**
Development of a new method of measuring the characteristic impedance and complex wave number of a porous acoustic material
[AD-A185038] N88-13957

**WAVE GENERATION**
HF sidebands in the ionosphere N88-13497

**WAVE INTERACTION**
Numerical experiments with hypersonic flows beneath a cone-delta-wing combination N88-13238
Computation of flow past conical hypersonic wings using a second order Godunov method N88-13241

**WAVE PROPAGATION**
Vortex interaction with a leading-edge of finite thickness
[NASA-CR-182341] N88-13307
Measured characteristics of 800/900 MHz mobile radio channels with high-angle propagation through moderately dense foliage
[CRC-1398] N88-13493
An investigation of millimeter wave propagation in the atmosphere: Measurement program
[AD-A184837] N88-13498
Damping analysis of flexural waves in fluid-loaded single and constrained plates
[AD-A185116] N88-13739
Theoretical and practical aspects of the functional absorber method of arranging sound absorbing panels
[BBC-RD-1987/15] N88-13955

**WAVELENGTHS**
Selection of optimum wavelengths for ozone mapping from satellites N88-13798

**WEAR**
Analysis of wear metals in engine oils using the atomic absorption spectrophotometric method
[NAL-TM-MT-8704] N88-13435
Fretting wear and fretting fatigue damage N88-13697

**WEATHER**
Application of TOMS data to weather analysis models N88-13787
The use of TOMS-modified VAS data for large-scale NWP N88-13791
Use of satellite data in volcano monitoring N88-13797

**WEATHER FORECASTING**
Ozone, jet streaks and severe weather N88-13781
ZEUS: A knowledge-based expert system that assists in predicting visibility at airbases
[AD-A184197] N88-13829
Isentropic analysis and interpretation: Operational applications to synoptic and mesoscale forecast problems
[AD-A184814] N88-13830
Mesoscale applications of high resolution imagery
[AD-A185039] N88-13833
Opportunities for tropical cyclone motion research in the Northwest Pacific region
[AD-A185068] N88-13834

**WEATHER MODIFICATION**
Altered and enhanced iodargyrite with bismuth triiodide for use in precipitation enhancement operations
[AD-A185229] N88-13419

**WEATHER STATIONS**
A single-station weather forecasting expert system
[AD-A184889] N88-13832
Inventory of weather stations. Climatological data from Dutch stations, no. 26
[KNMI-150-26] N88-13841
Hanford Meteorological Station computer codes. Volume 5: The TOWER computer code
[DE88-001610] N88-13843

**WEAVING**
Carbon-carbon composites and Aerospatiale. State of the art and prospects
[SNIAS-872-430-108] N88-13401

**WEIGHT REDUCTION**
Making space nickel/hydrogen batteries lighter and less expensive
[DE88-000168] N88-13530

**WELDABILITY**
The effect of temperature on the tensile properties of HSLA-100 steel
[AD-A184951] N88-13441

**WELDED JOINTS**
Qualification of expansion and joint welding procedures of tube-to-tubesheet joints for heat exchangers in nuclear power plants
[DE87-703526] N88-13592
Welded joint fatigue of a AISI 304 L type stainless steel
[DE87-703530] N88-13607
Fatigue strength of alloy A286 at cryogenic temperature N88-13695
Development of research on fatigue of spot-weld in automobile structures in Japan N88-13728

**WETLANDS**
AIS-2 spectra of California wetland vegetation N88-13763
**WIGGLER MAGNETS**
A long electromagnetic wiggler for the paladin free-electron laser experiments
[DE88-000970] N88-13589
Development of a strong electromagnet wiggler
[DE88-000971] N88-13952
Development of a laced electromagnetic wiggler
[DE88-000972] N88-13953
**WIND (METEOROLOGY)**
Tropical easterly jet located using TOMS data N88-13783
Studies in Aeolian geology
[NASA-CR-182328] N88-13828
**WIND EFFECTS**
Environmental processes and spectral reflectance characteristics associated with soil erosion in desert fringe regions
[NASA-CR-182332] N88-13811
**WIND TUNNEL MODELS**
Static Aeroelastic Effects on High Performance Aircraft
[AGARD-CP-403] N88-13348
The use of aeroelastic wind tunnel models to prove structural design N88-13355
**WIND TUNNEL TESTS**
European hypersonic wind tunnels N88-13221
Turbulence measurement in hypersonic flow N88-13224
The drag of slender axisymmetric cones in rarefied hypersonic flow N88-13229
Low Reynolds number influence on aerodynamic performance of hypersonic lifting vehicles N88-13230
Vortex formation over delta, double-delta and wave rider configurations at supersonic speeds N88-13243
The RAE experimental data-base for missiles at high Mach number and its use in assessing CFD methods N88-13250
Tip aerodynamics from wind tunnel test of semi-span wing
[NASA-TM-88253] N88-13290
A swept wing panel in a low speed flexible walled test section
[NASA-CR-4106] N88-13292
Study of the effect of mass transfer on a transonic boundary layer. Application to flow relaminarization
[ETN-88-91169] N88-13296
Delta wing in incompressible flow. Experimental study in F2
[ONERA-RT-36/1147-AN-249-G] N88-13298
Low speed wind tunnel investigation of propeller slipstream aerodynamic effects on different nacelle/wing combinations. Part 1: Total forces and moments and pressure distributions on nacelle/wing at different angles of attack and yaw and at different thrust coefficients
[FFA-TN-1987-22] N88-13302
Aircraft dynamics: Aerodynamic aspects and wind tunnel techniques N88-13320
Fundamentals of fighter aircraft design: Engine intake and afterbody N88-13322
The role of experimental investigation and computational fluid dynamics during fighter aircraft design N88-13326
Requirements and recommendations for the development of theoretical codes and experimental facilities in the near future N88-13327
Static Aeroelastic Effects on High Performance Aircraft
[AGARD-CP-403] N88-13348
The use of aeroelastic wind tunnel models to prove structural design N88-13355
Measurement of model deformation in wind tunnels N88-13358
Measurement of local convective heat transfer coefficients from a smooth and roughened NACA-0012 airfoil: Flight test data
[NASA-TM-100264] N88-13552
Assessment of the reliability of a correction procedure for WGT (Wet Globe Thermometer) (Botsball) measurements of heat stress
[AD-A185193] N88-13559
**WIND TUNNEL WALLS**
A swept wing panel in a low speed flexible walled test section
[NASA-CR-4106] N88-13292
**WIND TUNNELS**
Rarefied gas numerical wind tunnel. 2: Two-dimensional and axially symmetric bodies N88-13273
**WIND TURBINES**
An overview of the DOE/SANDIA/USDA vertical axis wind turbine Test Bed Project
[DE88-000604] N88-13812
Accurate rotor loads prediction using the FLAP (Force and Loads Analysis Program) dynamics code
[DE88-001109] N88-13815
**WINDPOWER UTILIZATION**
An overview of the DOE/SANDIA/USDA vertical axis wind turbine Test Bed Project
[DE88-000604] N88-13812
**WING LOADING**
The RAE experimental data-base for missiles at high Mach number and its use in assessing CFD methods N88-13250
**WING NACELLE CONFIGURATIONS**
A numerical investigation on wing/nacelle interferences N88-13258
Computation of nacelle interference using boundary element method N88-13267
**WING OSCILLATIONS**
An analysis of the compressible-viscous flow field around a 3D-oscillating wing N88-13254
Computation of dynamic stall of NACA0012 airfoil by block pentadiagonal matrix scheme N88-13255
Influence of the static deformation on a wing in the unsteady aerodynamic N88-13357
**WING TIPS**
Tip aerodynamics from wind tunnel test of semi-span wing
[NASA-TM-88253] N88-13290
**WINGS**
Numerica calculation in the Laplace domain for subsonic unsteady aerodynamic forces acting on a finite wing N88-13256
Numerical analysis of supersonic flows using panel method N88-13266
Navier-Stokes simulation of transonic transportation aircraft configurations. 1: Flow-field simulation over wing-fuselage combinations N88-13288
Design of wings and wing/body configurations for transonic and supersonic speeds N88-13318
An examination of coating failure on wing pivot fittings of f111 aircraft
[AD-A185028] N88-13328
**WORK**
A comparison of plastic work energy and external input for fatigue crack propagation N88-13722
**WORKLOADS (PSYCHOPHYSIOLOGY)**
Taskomat, a task battery for information processing
[IZF-1987-2] N88-13851

## X

**X RAY ANALYSIS**
X-ray analysis of polycrystalline aluminium subjected to fatigue cycling
[NAL-TM-MT-8706] N88-13434
X-ray fatigue failure prediction based on plasticity response to microcracks N88-13725
**X RAY DIFFRACTION**
The production of ultrasmall and superfine holographic diffraction gratings using synchrotron radiation and lithographic techniques
[AD-A185395] N88-13562
**X RAY IMAGERY**
X-ray imaging: Status and trends
[DE88-000756] N88-13980
**X RAY LASERS**
The gamma-ray laser project
[AD-A184824] N88-13578

## Y

**YAW**
Low speed wind tunnel investigation of propeller slipstream aerodynamic effects on different nacelle/wing combinations. Part 1: Total forces and moments and pressure distributions on nacelle/wing at different angles of attack and yaw and at different thrust coefficients
[FFA-TN-1987-22] N88-13302
**YIELD POINT**
Fiber composite structural durability and damage tolerance: Simplified predictive methods
[NASA-TM-100179] N88-13409
**YIELD STRENGTH**
Analysis of end stresses in glass-metal bimaterial strips
[DE87-007848] N88-13750

## Z

**ZINC SELENIDES**
Preparation and characterization of members of the system (Zn,Se)1-xGaPx
[AD-A185073] N88-14019
**ZIRCONATES**
Develop techniques for ion implantation of (lead-lanthanum-zirconate-titanate) for adaptive optics
[DE88-000642] N88-13986
**ZIRCONIUM**
Investigation by differential scanning calorimetry of microstructure in a superplastic Al-Mg-Zr alloy
[AD-A184902] N88-13439
**ZIRCONIUM ALLOYS**
Microstructure of amorphous and crystalline zirconium alloys rapidly solidified
[DE87-703700] N88-13432

### Typical Personal Author Index Listing

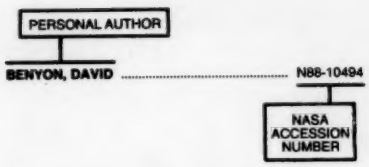


Listings in this index are arranged alphabetically by personal author. The NASA accession number denotes the number by which the citation is identified.

## A


ABDUL-AZIZ, ALI ..... N88-13745
ABELE, A. R. ..... N88-13424
ADAIR, ELEANOR R. ..... N88-13847
ADAM, C. M. ..... N88-13461
ADAMS, J. B. ..... N88-13760
ADAMS, R. G. ..... N88-13575
AGRESTI, R. ..... N88-13825
AKASOFU, S. I. ..... N88-13822
AKINIWA, Y. ..... N88-13678
AKISHITA, SADAO ..... N88-13266
AKIYAMA, SATOSHI ..... N88-13275
ALDISSI, M. ..... N88-13472
ALEXANDER, D. J. ..... N88-13681
ALFVEN, HANNES ..... N88-14052
N88-14053
ALGER, DONALD L. ..... N88-14046
ALLEGA, A. M. ..... N88-13927
ALLEMANG, RANDALL J. ..... N88-13618
N88-13620
ALLEN, CHERYL L. ..... N88-13369
ALLEY, RONALD E. ..... N88-13757
ALMAGRI, A. F. ..... N88-14004
AMAN, J. E. ..... N88-13950
AMANO, KANICHI ..... N88-13289
AMZALLAG, C. ..... N88-13706
ANDERSEN, GREGORY C. ..... N88-13369
ANDERSON, JOHN D., JR. ..... N88-13245
ANDERSON, W. S. ..... N88-13965
ANDO, YASUNORI ..... N88-13265
ANDRADE, A. ..... N88-13669
ANDRE, P. ..... N88-13567
ANDRESEN, PETER L. ..... N88-13703
ANDREWS, G. L. ..... N88-13843
ANSELL, GEORGE S. ..... N88-13389
ANTOLA, ANNA ..... N88-13861
ANTOLOVICH, STEPHEN D. ..... N88-13732
ARCHER, RONALD D. ..... N88-13459
ARMAND, C. ..... N88-13358
ARMSTRONG, LAWRENCE E. ..... N88-13559
ARONE, R. ..... N88-13682
ASHBY, M. F. ..... N88-13574
ASHLEY, HOLT ..... N88-13377
ASSADI, S. ..... N88-14004
ATTIA, A. V. ..... N88-13752
ATWELL, WILLIAM ..... N88-14058
AUFFRAY, P. ..... N88-13814
AUPOIX, B. ..... N88-13236
AUSTEN, I. M. ..... N88-13701
AUTHIE, GERARD ..... N88-13510
AVERNER, MEL M. ..... N88-13854
AXNAES, I. ..... N88-14056
AZIZ, A. K. ..... N88-13923


## B


BAAIJENS, FRANISCUS PETRUS THOMAS ..... N88-13930
BACA, THOMAS J. ..... N88-13611
BACKUS, GEORGE ..... N88-13936
BACKUS, GEORGE E. ..... N88-13820
BAHDER, THOMAS B. ..... N88-14020
BAI, BHARATHI ..... N88-13433
BAILON, J.-P. ..... N88-13679
BAKER, BARRY ..... N88-13984
BAKER, D. A. ..... N88-14000
BAKER, WAYMAN E. ..... N88-13791
BAKOS, J. S. ..... N88-13987
BALASINGH, C. ..... N88-13434
BALDESCHWIELER, JOHN D. ..... N88-13457
BALDETTI, P. ..... N88-13379
N88-13985
BANERJEE, PRASANTA K. ..... N88-13384
BANNINGER, C. ..... N88-13762
BANTA, ROBERT M. ..... N88-13836
BARACCA, ANGELO ..... N88-13967
BARBER, PETER W. ..... N88-13981
BARBIELLINI, G. ..... N88-13966
BARKATT, A. ..... N88-14028
BARNETT, D. L. ..... N88-13602
BARTEVIAN, J. ..... N88-13614
BARTLETT, M. L. ..... N88-13724
BARTLETT, R. G. ..... N88-13335
BASS, J. N. ..... N88-13375
BASTA, ROBERT A. ..... N88-13596
BASTARD, J. L. ..... N88-13814
BASU, J. ..... N88-13433
BATANOUNY, M. E. ..... N88-13970
BATEMAN, VESTA I. ..... N88-13627
BATISHKO, C. R. ..... N88-13986
BAUDIN, G. ..... N88-13688
BAUHGAERTEL, K. ..... N88-14056
BAXTER, W. J. ..... N88-13648
BEARD, J. ..... N88-13649
BEAUCHAMP, R. ..... N86-13530
BECUS, G. A. ..... N88-13622
BEDAIR, S. M. ..... N88-14014
BEDEWI, NABIH E. ..... N88-13625
N88-13626
BEEK, CHARLES R. ..... N88-13524
BEEVERS, C. J. ..... N88-13734
BELL, R. GLENN ..... N88-13611
BELSHE, R. A. ..... N88-13893
BERGLIND, TORSTEN ..... N88-13303
BERGOEND, ROGER ..... N88-13215
N88-13883
BERK, ALEXANDER ..... N88-13503
BERNS, H. ..... N88-13693
BERNSTEIN, LAWRENCE S. ..... N88-13503
BERRIER, WILLIAM F., JR. ..... N88-13537
BERTHEL, ROBERT O. ..... N88-13836
BERTHIER, P. ..... N88-13640
BERTHIER, Y. ..... N88-13697
BERTILSSON, I. ..... N88-13698
BESMANN, T. M. ..... N88-13408
BEUSEKAMP, MARTIN FRANK ..... N88-13570
BEYER, RICHARD A. ..... N88-13582
BEZAUD, C. ..... N88-13470
BEZERRA, G. H. ..... N88-13432
BEZIERS, S. ..... N88-13407
BHARTIA, P. K. ..... N88-13798
BHAT, S. P. ..... N88-13705
BIA, A. ..... N88-13683
BICEGO, V. ..... N88-13665
BIFFLE, J. H. ..... N88-13889
BITTKER, DAVID A. ..... N88-13428
BLACK, W. M. ..... N88-13563
BLACKBURN, M. J. ..... N88-13461
BLEIER, A. ..... N88-13421
BLOCK, L. P. ..... N88-13826
BLOM, A. F. ..... N88-13718
BLOM, H. A. P. ..... N88-13366
BLOOMFIELD, HARVEY S. ..... N88-14054
BLOTTNER, FREDERICK G. ..... N88-13239
BLUCHER, J. ..... N88-13717
BOBBITT, C. W. ..... N88-13637
BOCK, R. D. ..... N88-13873
BODNER, S. E. ..... N88-13992
BODU, J. J. ..... N88-13470
BOEHNLEIN, J. J. ..... N88-13628
BOER, L. C. ..... N88-13851
BOERGER, J. B. ..... N88-13808
BOHLANDER, R. A. ..... N88-13498
BOIS, D. ..... N88-13744
BOJKOV, RUMEN D. ..... N88-13792
BOLDMAN, DONALD R. ..... N88-13346
BOLHOFER, WILLIAM C. ..... N88-13783
BOLINGBROKE, R. K. ..... N88-13670
BOLLINI, C. G. ..... N88-13911
BONIFAZI, P. ..... N88-13825
BONITO, N. A. ..... N88-13375
BOOGERS, J. A. M. ..... N88-13343
BORE, C. L. ..... N88-13323
BOULANGER, G. ..... N88-13567
BOURDEAU, R. G. ..... N88-13461
BOWCUTT, KEVIN G. ..... N88-13245
BOWLES, C. Q. ..... N88-13722
BOWMAN, KEITH J. ..... N88-13650
BOWMAN, KENNETH P. ..... N88-13779
BOWYER, STUART ..... N88-14059
BRACKBILL, J. U. ..... N88-14006
BRACKEN, D. D. ..... N88-14040
BRANNON, P. J. ..... N88-13576
BRASE, J. M. ..... N88-13960
BRAZA, M. ..... N88-13548
BREBER, P. R. ..... N88-13422
BREILAND, W. G. ..... N88-13473
BRENNING, NILS ..... N88-14056
BRERETON, G. J. ..... N88-13536
BRICKEY, DAVID W. ..... N88-13771
BRILL, KEITH F. ..... N88-13781
BRILLHART, RALPH ..... N88-13617
BRIMHALL, J. L. ..... N88-13966
BRINSON, H. F. ..... N88-13736
BROOK, R. ..... N88-13710
BROOKS, S. L. ..... N88-13905
N88-13906
BROUSSARD, JOHN R. ..... N88-13900
BROWELL, EDWARD V. ..... N88-13784
BROWN, DAVID L. ..... N88-13618
N88-13620
BROWN, JAMES L. ..... N88-13306
BROWN, N. J. ..... N88-13423
BROWN, R. C. ..... N88-13724
BROWNE, G. T. ..... N88-13334
BROZENA, JOHN M. ..... N88-13878
BRUCHEY, WILLIAM J., JR. ..... N88-13446
BRUEGGE, CAROL J. ..... N88-13757
BRUN, S. ..... N88-13350
BRUNO, JOHN D. ..... N88-14020
BUCCELLATO, R. ..... N88-14060
BUCK, J. W. ..... N88-13843
BUCK, MELVIN L. ..... N88-13248
BUDWEG, H. L. ..... N88-13613
BUELL, DONALD A. ..... N88-13305
BUFFUM, DANIEL H. ..... N88-13346
BUFTON, J. L. ..... N88-13371
BUGGELN, R. C. ..... N88-13291
N88-13599
BUISSON, JAMES A. ..... N88-13312
BULTITUDE, R. J. C. ..... N88-13493
BURKS, B. L. ..... N88-13602
BURNS, M. J. ..... N88-13952
N88-13953
BUSH, WILLIAM B. ..... N88-13543
BUSS, R. J. ..... N88-13473
BYRNE, J. ..... N88-13863


## C


CAGLAYAN, ALPER ..... N88-13865
CALARESE, W. ..... N88-13224
CAMARGO, G. A. M. ..... N88-13592
CAMPBELL, DAVID ..... N88-13933
CAMPBELL, G. A. ..... N88-13989
CAMPBELL, R. B. ..... N88-14007
CAMPBELL, STEPHEN L. ..... N88-13922
CANDIDI, M. ..... N88-13379
N88-13380
N88-13569
CAPBERN, P. ..... N88-13299
CAPDEPUY, B. ..... N88-13469
CAPONIO, J. F. ..... N88-14040
CAPRIOTTI, DIEGO ..... N88-13245
CAPUTO, A. J. ..... N88-13408
CARDON, A. H. ..... N88-13736

CAREY, G. F. ..... N88-13934
CARMAN, C. D. ..... N88-13656
CAROLAN, R. A. ..... N88-13452
CARULLO, R. ..... N88-13588
CASPERS, W. J. ..... N88-14031
CASSINIS, R. ..... N88-13902
CASTLEMAN, A. WELFORD, JR. ..... N88-13416
CAUPENNE, PH. ..... N88-13251
CAUSSIN, THIERRY ..... N88-13383
CAVALLO, F. ..... N88-13966
CAVOLOWSKY, J. A. ..... N88-13422
CELMINS, AIVARS K. ..... N88-13917
CELMINS, AIVARS K. R. ..... N88-13916
CETIN, M. ..... N88-13344
CHAMBERS, R. S. ..... N88-13750
CHAMIS, CHRISTOS C. ..... N88-13409
N88-13754
CHAN, Y. T. ..... N88-13599
CHANET, P. ..... N88-13216
CHANG, FRANK C. ..... N88-13442
CHANTERANNE, J. ..... N88-13399
CHARPIN, M. ..... N88-13358
CHAUSSEE, DENNY ..... N88-13234
CHEEK, JAMES B. ..... N88-13616
CHEN, S. L. ..... N88-13424
CHEN, SHIH-HUEI ..... N88-13389
CHESTERS, DENNIS ..... N88-13790
CHEUNG-MAK, S. K. P. ..... N88-13684
CHEVALLIER, J. P. ..... N88-13222
CHICCOLI, C. ..... N88-13966
CHOI, SANG H. ..... N88-13553
N88-13557
CHOI, SANG KEUN ..... N88-13532
CHRISMAN, DAN A., JR. ..... N88-13553
N88-13557
CHRISTENSEN, T. C. ..... N88-13953
CHU, LI-CHUAN ..... N88-13353
CHUNG, Y. W. ..... N88-13651
N88-13705
CLAMONS, J. D. ..... N88-13878
CLARK, B. C. ..... N88-13954
CLARK, J. E. ..... N88-14039
CLARK, R. N. ..... N88-13812
CLARK, ROGER N. ..... N88-13769
N88-13770
COE, CHARLES F. ..... N88-13218
COHEN, RAM ..... N88-13564
COLGATE, S. A. ..... N88-14051
COLLERCANDY, R. ..... N88-13300
COLLINS, CARL B. ..... N88-13578
COLLINS, DANIEL J. ..... N88-13501
COLOMBIE, C. ..... N88-13697
COLTRIN, M. E. ..... N88-13473
CONEL, JAMES E. ..... N88-13757
CONN, R. W. ..... N88-13969
CONSIGNY, H. ..... N88-13222
CONTET, J. ..... N88-13860
CONTI, PAUL ..... N88-13634
CORNU, J. P. ..... N88-13901
COSTA, I. ..... N88-14029
COSTELLO, DANIEL J., JR. ..... N88-13516
COSTES, B. ..... N88-13327
COTTIS, R. A. ..... N88-13699
N88-13702
COTTRELL, K. G. ..... N88-13375
COULOMBE, B. ..... N88-13452
COUSTEIX, J. ..... N88-13236
COUTO, J. G. V. ..... N88-13592
COWGILL, D. F. ..... N88-13576
COX, B. N. ..... N88-13653
N88-13666
COX, WILLIAM ..... N88-13759
CRAWLEY, EDWARD F. ..... N88-13337
CROSLEY, DAVID R. ..... N88-13415
CROSS, B. ..... N88-13980
CROWLEY, JAMES K. ..... N88-13771
CRUME, E. C., JR. ..... N88-14006
CSONKA, PAUL L. ..... N88-13562
CUDDAPAH, PRABHAKARA ..... N88-13800
CUNNINGHAM, ATLEE M., JR. ..... N88-13218
CURBILLON, M. ..... N88-13329
N88-13352
CURL, R. F. ..... N88-14018
CURTAIN, R. F. ..... N88-13903
CURTISS, BRIAN J. ..... N88-13757
CYMERMAN, ALLEN ..... N88-13846

## D

DADI, M. ..... N88-13565
DAGLEY, I. ..... N88-13458
DAHLBURG, R. B. ..... N88-13990
DAIGUJI, HISAAKI ..... N88-13285
DALLAS, ALLAN G. ..... N88-13915
DAMOKOSH, ANDREW I. ..... N88-13848
DAMOS, DIANE L. ..... N88-13856
DARGUSH, GARY F. ..... N88-13384
DAVID, S. A. ..... N88-13451
DAVIDSON, DAVID L. ..... N88-13392
DAVIS, H. ..... N88-13514
DAVIS, L. PORTER ..... N88-13623
DAVIS, LARRY S. ..... N88-14045
DAVIS, R. F. ..... N88-14027
DAVIS, R. T. ..... N88-13239
DAWSON, L. R. ..... N88-14011
DAY, R. A. ..... N88-13980
DEALBUQUERQUE, JULIO CESAR LOPES ..... N88-13879
DEBOER, GERBEN BEREND JOHANNES ..... N88-13420
DECASTRO, L. A. S. ..... N88-13592
DEFRESNE, A. ..... N88-13712
DEIS, G. A. ..... N88-13589
N88-13952
N88-13953
DEIWERT, GEORGE S. ..... N88-13242
DEKEYSER, J. L. ..... N88-14009
DELISO, E. M. ..... N88-13421
DEMAREST, JOHN A. ..... N88-13418
DEMARIA, MICHELANGELO ..... N88-13967
DEMIRANDA, P. E. V. ..... N88-13607
DENHEIJER, J. ..... N88-13839
DENOST, J. P. ..... N88-13406
DENTENEER, PETER JAN HENDRIK ..... N88-14024
DEOLIVEIRA, L. A. R. ..... N88-13819
DEQUE, R. ..... N88-14036
DESSE, J. M. ..... N88-13297
DESTUYNDER, R. ..... N88-13357
DETERT, K. ..... N88-13659
DEVALK, PAUL ..... N88-13546
DEVARAKONDA, MURTHY V. ..... N88-13868
N88-13869
DEVARAKONDA, MURTHY V.-S. ..... N88-13867
DEVINE, JAMES A. ..... N88-13560
DEVRIES, K. L. ..... N88-13714
DEVRIES, O. H. M. ..... N88-13807
DEWITT, KENNETH J. ..... N88-13552
DEXTER, R. N. ..... N88-14004
DICKINSON, STUART C. ..... N88-13539
DICKSON, J. I. ..... N88-13655
DIEFENDORF, R. JUDD ..... N88-13389
DIEMOZ, M. ..... N88-13966
DIETZ, DAVID ..... N88-13994
DIGIORGIO, A. ..... N88-13985
DILLON, M. M. ..... N88-13575
DIPPEL, K. H. ..... N88-13989
DOBBS, BILL ..... N88-13333
DOBRANICH, D. ..... N88-13381
DODD, H. M. ..... N88-13812
DOI, SHUN ..... N88-13271
DOLLING, D. S. ..... N88-13226
DONKER, A. W. ..... N88-13840
DORY, R. A. ..... N88-14003
DRAPER, ALFRED C. ..... N88-13248
DREICER, H. ..... N88-13999
DRUHL, KAI J. ..... N88-13983
DUBBELDAY, PIETER S. ..... N88-13739
DUCHARME, ERIC H. ..... N88-13337
DUCRUET, C. ..... N88-13297
DUIVENVOORDEN, J. C. M. ..... N88-13841
DUNAGAN, STEPHEN E. ..... N88-13306
DUNCAN, ALEXANDER WILLIAM STUART ..... N88-13464
DUNLOP, J. D. ..... N88-13530
DUNN, MICHAEL G. ..... N88-13384
DUPONT, J. ..... N88-13901
DURAND, YVES ..... N88-13886
DURANDEAU, MICHEL ..... N88-13361
DUTTON, ROBERT W. ..... N88-14012
DWIGHT, K. ..... N88-14019
DZIADOS, JOSEPH E. ..... N88-13848

## E

EAST, R. A. ..... N88-13246
ECKHARDT, DAVID E. ..... N88-13865
ECKHARDT, R. J. ..... N88-13375
ECKSTROM, CLINTON V. ..... N88-13356
EDGAR, E. G. ..... N88-13335
EDMOND, J. A. ..... N88-14027
EKBLAD, ULF ..... N88-13810
EKBOM, LARS ..... N88-13482
ELDEM, C. ..... N88-13236
ELIASSON, T. ..... N88-13860
ELOUATOUATI, A. ..... N88-13296
EPHREMIDES, A. ..... N88-13500
ERMER, D. S. ..... N88-13720
EVANS, WAYNE J. ..... N88-13795
EWING, RICHARD E. ..... N88-13918
EXARHOS, G. J. ..... N88-13587

## F

FAELTHAMMAR, C.-G. ..... N88-13826
N88-13996
FANCONI, B. M. ..... N88-13391
FANG, XIAOWEN ..... N88-13907
FARMER, KENNETH L., JR. ..... N88-13848
FARNELL, PATRICIA L. ..... N88-13476
FAROOQ, S. ..... N88-13440
FATEMI, A. ..... N88-13694
FEDERER, W. T. ..... N88-13881
N88-13939
N88-13941
FELDMAN, SANDRA C. ..... N88-13758
FENG, Z. D. ..... N88-13941
FERNYHOUGH, ALAN ..... N88-13485
FERRARIS, G. ..... N88-13640
FERREIRA, P. I. ..... N88-13431
FEUERMAN, MARTIN ..... N88-13940
FIELDER, W. L. ..... N88-13385
FILHO, JOSE VANNI ..... N88-13859
FINE, M. E. ..... N88-13651
N88-13668
N88-13705
FINKEN, K. H. ..... N88-13989
FISHER, CARREN M. E. ..... N88-13249
FISHMAN, JACK ..... N88-13784
FLANAGAN, D. P. ..... N88-13890
FLEETER, SANFORD ..... N88-13346
FLIFLET, A. W. ..... N88-13563
FLINN, J. E. ..... N88-13450
FOGG, SYDNEY GEORGE ..... N88-13485
FOMISON, N. R. ..... N88-13227
FORTE, VINCENT, JR. ..... N88-13846
FOSTER, JOHN D. ..... N88-13359
FOURNIER, J. P. ..... N88-13216
FRANKLIN, JAMES A. ..... N88-13359
FREDERICK, JOHN E. ..... N88-13785
FREITAS, M. ..... N88-13669
FRIEDMAN, MORTON L. ..... N88-13370
FRIEDRICH, D. M. ..... N88-13587
FRUSTIE, M. J. ..... N88-13396
FU, J. S. ..... N88-14025
FUJII, KOZO ..... N88-13260
N88-13283
N88-13288
N88-13289
FUJIMOTO, MASAO ..... N88-13728

## G

GAILLARD, A. W. K. ..... N88-13851
GALLAGHER, JOSEPH P. ..... N88-13606
GAN, SHU ..... N88-14010
GANDOU, RENE ..... N88-13884
GANZER, UWE ..... N88-13243
GARLICK, R. G. ..... N88-13385
GARRETT, L. BERNARD ..... N88-13369
GASIK, M. M. ..... N88-13438
GATTO, MARINO ..... N88-13946
GEE, K. T. ..... N88-13373
GELLER, M. A. ..... N88-13842
GELMAN, M. E. ..... N88-13842
GEORGE, THOMAS F. ..... N88-13740
N88-13964
GEORGIOPOULOS, C. ..... N88-14009
GERBER, R. A. ..... N88-13575
GERMAN, R. M. ..... N88-13440
GEROLD, V. ..... N88-13674
N88-13707
N88-13730
GERSTLE, F. P., JR. ..... N88-13750
GIAMBIAGI, J. J. ..... N88-13911
GIBALA, RONALD ..... N88-13650
GIBBONS, ROBERT D. ..... N88-13873
GILLESPIE, A. R. ..... N88-13760
GILLETTADESTJOSEPH, D. ..... N88-13395
GILMORE, J. O. ..... N88-13581
GINTY, CAROL A. ..... N88-13409
GIRARD, R. ..... N88-13742
GLOERSEN, PER ..... N88-13773
GODET, M. ..... N88-13697
GOEBEL, D. M. ..... N88-13989
GOEDEL, H. ..... N88-13324
GOETZ, ALEXANDER F. H. ..... N88-13756
GOLD, S. H. ..... N88-13563
GOLDEN, DAVID M. ..... N88-13415
GOLDMAN, H. ..... N88-14009
GONZALEZ, RICHARD R. ..... N88-13849
GOODYER, M. J. ..... N88-13292
GORDON, DANIEL K. ..... N88-13759
GORDON, ELIOTT B. ..... N83-13961
GORNEY, D. J. ..... N88-13969
GOSLING, J. T. ..... N88-14057

GOTTLIEB, DAVID ..... N88-13294
GOU, CHEN ..... N88-14010
GOULDIN, F. C. ..... N88-13413
GOUNLEY, R. B. ..... N88-13313
GRAHAM, JUDITH A. ..... N88-13845
GRAHAM, MALCOLM JAMES ..... N88-13463
GRAHAM, R. A. ..... N88-13427
GRANDT, A. F., JR. ..... N88-13687
GRAVE, A. ..... N88-13744
GRAVE, ALAIN ..... N88-13743
GREELEY, RONALD ..... N88-13828
GREEN, ROBERT E., JR. ..... N88-13958
GREEN, ROBERT O. ..... N88-13757
GREENWOOD, G. W. ..... N88-13710
GREGORY, J. K. ..... N88-13672
GREGORY, W. S. ..... N88-13491
GRENIE, YVES ..... N88-13401
GRIFFITH, R. L. ..... N88-13572
GRIGORCHUK, I. I. ..... N88-13438
GROENEWEG, J. F. ..... N88-13960
GROSE, ELAINE C. ..... N88-13845
GROSS, MICHAEL ..... N88-13614
GROSS, MICHAEL F. ..... N88-13763
GRUMMON, D. S. ..... N88-13652
GUDLADT, H.-J. ..... N88-13707
GUERREIRO, J. N. C. ..... N88-13608
GUIDONI, U. ..... N88-13378
N88-13380
GUILHEN, P. M. ..... N88-13640
GUILINGER, T. R. ..... N88-13448
GUILLOU, BERNARD ..... N88-13509
GUIMARAES, A. S. ..... N88-13607
GUIMONT, J. M. ..... N88-13965
GUPTA, S. ..... N88-13973
GUTMARK, E. ..... N88-13232

## H

HAESSIG, GEORGES ..... N88-13506
HAJI-GHASSEMI, M. ..... N88-13702
HALBACH, K. ..... N88-13589
N88-13952
N88-13953
HALL, J. ..... N88-14041
HALL, JOHN B., JR. ..... N88-13369
HALYO, NESIM ..... N88-13553
N88-13557
HAMBERG, K. ..... N88-13657
N88-13727
HAMERSLAG, R. ..... N88-13926
HAMILTON, JAMES E. ..... N88-13441
HAMINH, H. ..... N88-13548
HAMM, ROBERT ..... N88-13603
HANAMURA, MITSUYASU ..... N88-13270
HANDFIELD, L. ..... N88-13655
HANJE, J. ..... N88-13860
HANSER, FREDERICK A. ..... N88-13564
HARADA, NORIO ..... N88-13271
HARADA, Y. ..... N88-13673
HARMAN, EVERETT ..... N88-13850
HARVEY, A. R. ..... N88-13589
HASKINS, J. J. ..... N88-13980
HASTI, D. E. ..... N88-14005
HASTINGS, P. J. ..... N88-13667
HAUSER, J. R. ..... N88-14014
HAYS, K. M. ..... N88-13556
HE, X-C ..... N88-14019
HEATON, R. C. ..... N88-13591
HEBBLE, T. L. ..... N88-13451
HECIAK, B. ..... N88-13330
HEDEKER, DONALD ..... N88-13873
HEINBOCKEL, JOHN ..... N88-13577
HELLARD, G. ..... N88-13397
HELLARD, GUY ..... N88-13217
HELLSTEN, HANS ..... N88-13511
N88-13512
HELMAN, J. S. ..... N88-14030
HEMBERGER, P. H. ..... N88-13591
HENDERSON, FRANCIS M. ..... N88-13738
HENDERSON, ROBERT A. ..... N88-13310
HENDERSON, TERRY L. ..... N88-13956
HERAIL, O. ..... N88-13362
HERIC, MATTHEW ..... N88-13759
HERNANDEZ, J. M. ..... N88-13980
HERNANDEZ, JUAN MANUEL ..... N88-13527
HERTZBERG, R. W. ..... N88-13715
HEULER, P. ..... N88-13690
HIBEY, JOSEPH L. ..... N88-13935
HICKS, M. A. ..... N88-13667
HIGGINS, MARY K. ..... N88-13308
HILLBERRY, B. M. ..... N88-13656
HILLIARD, LORELLI ALISON ..... N88-13984
HILLIER, R. ..... N88-13241
HIMENO, RYUTARO ..... N88-13281
HIPPSLEY, C. A. ..... N88-13709
HIRAGA, K. ..... N88-13695
HIROSE, NAOKI ..... N88-13257
N88-13262
N88-13263
N88-13286
HIRSCH, CH. ..... N88-13344
HIRSHMAN, S. P. ..... N88-14006
HO, P. ..... N88-13473
HO, Y. L. ..... N88-14004
HODGES, J. ..... N88-13250
HODOUS, M. F. ..... N88-14009
HOENLINGER, H. ..... N88-13355
HOERNLEIN, H. ..... N88-13324
HOFFMAN, M. A. ..... N88-14007
HOGENHOUT, GUY MARC ..... N88-13806
HOLBROOK, VINCENT P. ..... N88-13838
HOLDEMAN, J. D. ..... N88-13347
HOLLBURG, UWE ..... N88-13615
HOLMES, R. H. ..... N88-13952
HOOK, SIMON ..... N88-13768
HOPMANN, HELMUT ..... N88-13383
HOPSON, CHARLES B. ..... N88-13629
HORNBERGER, L. E. ..... N88-13714
HORWITZ, J. L. ..... N88-13569
HOVENAC, EDWARD A. ..... N88-13573
HOWARD, GEORGE F., III ..... N88-13837
HOWARD, I. C. ..... N88-13710
HOYT, REED ..... N88-13846
HSU, W. ..... N88-13989
HSUEH, M. C. ..... N88-13870
HU, J. M. ..... N88-13685
HU, S. R. ..... N88-13723
HUAN, J. H. ..... N88-13689
HUANG, MING-SHENG ..... N88-13643
HUANG, ZHONG-HAO ..... N88-13497
HUBBARD, ROGER W. ..... N88-13559
HUGENSCHMIDT, M. ..... N88-13586
HUI, W. H. ..... N88-13247
HUISMAN, W. C. ..... N88-13808
HUMMEL, DIETRICH ..... N88-13225
HUMMEL, K. E. ..... N88-13905
N88-13906
HUNT, DAVID L. ..... N88-13617
HURLBERT, ANYA ..... N88-13862
HURON, ERIC S. ..... N88-13732
HUSTON, RONALD L. ..... N88-13604
HUTT, G. R. ..... N88-13246

## I

IBAS, O. ..... N88-13659
IDZOREK, R. D. ..... N88-13491
IESS, L. ..... N88-13825
IMMICH, HANS ..... N88-13383
INOUE, A. ..... N88-13695
ISAWA, TAKAO ..... N88-13287
ISHIDA, YOJI ..... N88-13286
ISHIGAKI, HIROSHI ..... N88-13264
ISHII, RYUJI ..... N88-13274
ISHIKAWA, K. ..... N88-13695
ISKE, P. L. ..... N88-14031
ISOBE, TOSIO ..... N88-13276
ISOGAI, KOJI ..... N88-13254
ITOH, N. ..... N88-13988
IUCCI, N. ..... N88-14060
N88-14061
IYER, R. K. ..... N88-13870
IYER, RAVISHANKAR K. ..... N88-13868
N88-13869

## J

JACKSON, ALLEN G. ..... N88-14017
JACOBBERGER, P. A. ..... N88-13811
JAEGGY, BERNARD CHARLES ..... N88-13228
JAMES, M. R. ..... N88-13653
JANSON, BETTE R. ..... N88-14062
JASPERSON, WILLIAM H. ..... N88-13832
JATA, K. V. ..... N88-13692
JEFFCOAT, P. J. ..... N88-13896
JEGLEY, DAWN C. ..... N88-13387
JENKINS, EDWARD B. ..... N88-14049
JENSEN, BRENT M. ..... N88-13617
JOHNSON, DONALD ..... N88-13777
JOHNSON, GARY S. ..... N88-13388
JOHNSON, J. A. ..... N88-13751
JOHNSON, M. E. ..... N88-13948
JOJOLA, J. M. ..... N88-14005
JONES, E. E. ..... N88-14005
JONES, G. F. ..... N88-13490
JONES, J. W. ..... N88-13652
JORGENSON, ROY ..... N88-13912
JORNA, P. G. A. M. ..... N88-13851
JOSEPH, B. ..... N88-13485
N88-13486
JOUNOUCHI, TADAMASA ..... N88-13259

## K

KAAIJK, J. ..... N88-13816
N88-13817
KADZIOCH, GERHARD ..... N88-13526
KAIDEN, TAKESHI ..... N88-13257
KALMUS, G. ..... N88-13966
KALYANAM, M. ..... N88-13435
KAMO, KEISUKE ..... N88-13281
KANAKIA, M. D. ..... N88-13456
KAPPEL, F. ..... N88-13910
KARLSSON, B. ..... N88-13657
N88-13698
N88-13727
KASHIWA, B. ..... N88-13535
KAUFMAN, ALBERT ..... N88-13745
KAWAHARA, KUNIO ..... N88-13255
KAWAI, MASAFUMI ..... N88-13265
KAWAI, NOBUHIRO ..... N88-13257
N88-13262
N88-13286
KAWAMURA, T. ..... N88-13988
KAWASAKI, T. ..... N88-13716
KAZAKOS, P. P. ..... N88-13924
KELLY, JOHN P. J. ..... N88-13865
KERR, JAMES B. ..... N88-13795
KHACHIKYAN, E. YE. ..... N88-14050
KHOSLA, N. ..... N88-13517
KIELB, ROBERT E. ..... N88-13753
KIKUCHI, RYOICHI ..... N88-14013
KILLOUGH, S. M. ..... N88-13602
KIM, C. S. ..... N88-13651
KIM, CHUL-MIN ..... N88-13389
KIM, Y.-N. ..... N88-13291
KING, J. E. ..... N88-13667
N88-13670
KING, TRUDE V. V. ..... N88-13769
N88-13770
KIRA, KENJI ..... N88-13278
KITAGAWA, HIDEO ..... N88-13728
KITTUR, MADAN G. ..... N88-13804
KLABUNDE, KENNETH J. ..... N88-13417
KLEINKNECHT, K. ..... N88-13966
KLEMAS, VYTAUTAS ..... N88-13783
KLIMAS, P. C. ..... N88-13812
KLOPP, RICHARD WILLIAM ..... N88-13430
KNAPIK, JOSEPH J. ..... N88-13850
KNOTT, J. F. ..... N88-13681
N88-13691
KNUTSON, RICHARD K. ..... N88-13737
KOBAYAKAWA, MAKOTO ..... N88-13261
KOBAYASHI, H. ..... N88-13424
KOBAYASHI, K. ..... N88-13716
KOCH, ROBERT C. ..... N88-13829
KOCZAK, M. J. ..... N88-13445
KOENEKE, AXEL ..... N88-13228
KOERBER, GERMAIN ..... N88-13228
KOGA, R. ..... N88-14025
KOLASINSKI, W. A. ..... N88-14025
KOLLMAN, W. ..... N88-13542
KONG, JIN-AU ..... N88-13502
KOPPENWALLNER, GEORG ..... N88-13230
KORBLY, LETITIA ..... N88-13541
KORDULLA, W. ..... N88-13237
KORTH, G. E. ..... N88-13450
KOSEC, L. ..... N88-13704
KOSEL, F. ..... N88-13704
KOSHIGOE, S. ..... N88-13232
KOSTER, A. ..... N88-13978
KOURA, KATSUHISA ..... N88-13273
KOURTA, A. ..... N88-13548
KRAUSZ, A. S. ..... N88-13708
KRAUSZ, K. ..... N88-13708
KREN, RICHARD J. ..... N88-13804
KRISHNAMURTHY, L. ..... N88-13543
KRISHNAMURTHY, R. ..... N88-13713
KRUEGER, ARLIN J. ..... N88-13774
N88-13778
N88-13781
N88-13786
N88-13793
N88-13802
KRUSE, FRED A. ..... N88-13772
KUHN, W. L. ..... N88-13471
KULANDER, K. C. ..... N88-13588
KUMAR, AJAY ..... N88-13233
KUO, AN-YU ..... N88-13606
KURAMOTO, N. K. ..... N88-13607
KURAS, C. ..... N88-13489
KUTLER, PAUL ..... N88-13279
KUWAHARA, KUNIO ..... N88-13277
N88-13280
N88-13281
N88-13283

N88-13284
KWAN, Y. ..... N88-13424
KWON, I. B. ..... N88-13668

## L

LABOURDETTE, R. ..... N88-13688
LACK, L. W. ..... N88-13710
LACOMBE, JEAN-FRANCIS ..... N88-13402
LADEN, T. ..... N88-13565
LALANNE, M. ..... N88-13640
LAMALLE, J. ..... N88-13404
N88-13405
LAMAR, JOHN E. ..... N88-13319
LANDGRAF, R. W. ..... N88-13733
LANE, N. F. ..... N88-13974
LANGOY, M. A. ..... N88-13661
LARDON, J. M. ..... N88-13706
LARGAY, MARIE M. ..... N88-13312
LARKO, DAVID ..... N88-13790
LAVAL, S. ..... N88-13978
LAVIOLETTE, R. A. ..... N88-13556
LAW, C. V. ..... N88-13461
LAWLEY, A. ..... N88-13445
LAWRENCE, J. D. ..... N88-13898
N88-13899
LAWSON, MAURICE O. ..... N88-13340
LEBLANC, R. ..... N88-13296
LEBOUAR, P. H. ..... N88-13860
LEE, ANNABEL Y. ..... N88-13459
LEE, C. H. ..... N88-13680
LEE, CHI M. ..... N88-13345
LEE, L. C. ..... N88-13429
LEE, S. ..... N88-13904
LEE, SANG M. ..... N88-13629
LEE, W. J. ..... N88-13705
LEFLOCH, C. ..... N88-13400
N88-13407
LEHMANN, M. ..... N88-14005
LEHMBERG, R. H. ..... N88-13992
LEIFER, JOEL ..... N88-13614
LEJAL, T. ..... N88-13300
LEKAN, JACK ..... N88-13513
LEMAY, I. ..... N88-13684
LEONARD, B. P. ..... N88-13931
LERCHE, R. A. ..... N88-13571
N88-13572
LESPADE, P. ..... N88-13469
LESPERANCE, G. ..... N88-13655
LEUNG, P. T. ..... N88-13964
LEUNG, W. K. ..... N88-13969
LEVINTHAL, D. ..... N88-14009
LEVY, MILTON ..... N88-13442
LEWALLEN, PAT ..... N88-13630
N88-13631
LEWIN, JOSEPH ..... N88-13949
LEWIS, J. ..... N88-13492
LEYNAERT, J. ..... N88-13322
LI, CHE-YU ..... N88-13452
LI, J. C. M. ..... N88-13721
LI, JIANSHAN ..... N88-13483
LI, JIZHOU ..... N88-14010
LI, K. X. ..... N88-13685
LIAW, GOANG-SHIN ..... N88-13551
LIEBERMAN, STEPHEN H. ..... N88-13805
LIM, T. W. ..... N88-13633
LIN, BINGXIONG ..... N88-14010
LIN, T.-C. ..... N88-13635
LINDBERG, LENNART ..... N88-13995
N88-13997
LINDQVIST, P.-A. ..... N88-13826
LING, SHAW L. ..... N88-13455
LINN, S. ..... N88-14009
LIOU, W. J. ..... N88-13639
LITTLE, WILLIAM A. ..... N88-13484
LIU, H. J. ..... N88-13723
LIU, ZHENYI ..... N88-14010
LIU, ZHIYU ..... N88-13748
LLACER, J. ..... N88-13892
LOCATELLI, J. ..... N88-13885
LOGAN, B. G. ..... N88-14007
LOMELINO, DALE L. ..... N88-13872
LONG, LYLE N. ..... N88-13244
LOUBET, D. ..... N88-13403
LOVELAND, D. W. ..... N88-13880
LOWDEN, R. A. ..... N88-13408
LOWE, H. ..... N88-13485
N88-13486
LUCAS, D. ..... N88-13422
LUEDECKE, D. ..... N88-13447
LUHMANN, N. C., JR. ..... N88-13975
LUI, C. Y. ..... N88-13622
LUNINE, LEO R. ..... N88-14042
LUNNEY, PATRICK A. ..... N88-13835
LYNCH, S. P. ..... N88-13443
LYON, R. J. P. ..... N88-13767

## M

MAAS, LINDA C. ..... N88-13582
MAAS, STEPHEN A. ..... N88-14015
MACCONOCHIE, IAN O. ..... N88-13388
MACELROY, ROBERT D. ..... N88-13852
N88-13853
N88-13854
MACKIN, STEVE ..... N88-13768
MADHUKAR, ANUPAM ..... N88-14021
MAGGI, M. ..... N88-13378
MAGNIN, T. ..... N88-13706
MAIGRET ..... N88-13467
MALAGON, EVA G. ..... N88-14016
MALCOLM, GERALD N. ..... N88-13305
MALOY, J. OWEN ..... N88-13802
MAMODE, A. ..... N88-13814
MANHEIMER, W. M. ..... N88-13563
MANI, A. ..... N88-13434
MANN, R. C. ..... N88-13602
MANNING, WALTER W. ..... N88-13341
MANSON, J. A. ..... N88-13715
MARISSEN, R. ..... N88-13664
N88-13711
MARKFIELD, A. ..... N88-13699
MARKLUND, G. ..... N88-13826
MARTIN ..... N88-13467
MARTIN, E. DALE ..... N88-13951
MARTIN, R. J. ..... N88-13423
MARTIN, SARA F. ..... N88-14055
MARTINEZ, DENNIS MICHAEL ..... N88-13558
MARTINEZ, MARCIAL VALERO ..... N88-13600
MARTZ, H. E. ..... N88-13980
MARUYAMA, YUICHI ..... N88-13266
MASON, DONALD R. ..... N88-13617
MASOUNAVE, J. ..... N88-13679
MASSONPIERRE, YVES ..... N88-13487
MASUDA, NORIO ..... N88-13270
MATEER, CARL L. ..... N88-13792
MATSON, MICHAEL ..... N88-13796
MATSON, PAMELA A. ..... N88-13761
MATSUDA, K. ..... N88-13675
MATSUHIMA, KISA ..... N88-13260
MATSUI, E. ..... N88-13678
MATSUNAMI, N. ..... N88-13988
MATTEUZZI, C. ..... N88-13966
MATTHEW, WILLIAM T. ..... N88-13559
MAXTED, A. ..... N88-13891
MAZARAKIS, M. G. ..... N88-14005
MCAFEE, J. M. ..... N88-13481
MCALLISTER, DAVID F. ..... N88-13863
N88-13864
N88-13865
MCCARTHY, THOMAS J. ..... N88-13455
MCCLELLAND, LINDSAY ..... N88-13797
MCCLUNG, R. C. ..... N88-13719
MCCOMAS, D. J. ..... N88-14057
MCCOWAN, R. B. ..... N88-13563
MCCULLOCH, C. E. ..... N88-13881
N88-13939
N88-13941
MCDERMOTT, D. B. ..... N88-13975
MCDONALD, H. ..... N88-13599
MCEVILY, A. J. ..... N88-13729
MCGIRT, F. ..... N88-13895
MCGRATH, JOSEPH M. ..... N88-13850
MCJILTON, WALTER N. ..... N88-13524
MCLAUGHLIN, E. ..... N88-13973
MCMILLAN, R. W. ..... N88-13498
MCNALLY, B. DAVID ..... N88-13363
MCNEIL, W. J. ..... N88-13375
MCPETERS, RICHARD ..... N88-13794
MCPHAIL, ANDREW T. ..... N88-13386
MEERKOV, S. M. ..... N88-13904
N88-13947
MEHROTRA, R. ..... N88-13595
MEHROTRA, RAJIV ..... N88-13596
MEIER, B. ..... N88-13674
N88-13730
MEIJER, STAFFAN ..... N88-13301
MELLO, ROBERT P. ..... N88-13848
MENRATH ..... N88-13467
MERCADAL, MATHIEU ..... N88-13374
MEYNIEL, M. L. ..... N88-13744
MIANE, JEAN-LOUIS ..... N88-13402
MICHAELS, L. A. ..... N88-13500
MILES-MCDERMOTT, J. J. ..... N88-13939
MILES-MCDERMOTT, N. J. ..... N88-13881
MILES, JOHN B. ..... N88-13306
MILGRAM, MAURICE ..... N88-13809
MILLER, A. K. ..... N88-13680
MILLER, ALLEN R. ..... N88-13940
MILLER, J. B. ..... N88-13954
MILLIGAN, WALTER W. ..... N88-13732
MINARDI, JOHN E. ..... N88-13340
MINNETYAN, LEVON ..... N88-13619
MITCHELL, M. J. ..... N88-13429
MITTRA, RAJ ..... N88-13912
MIYAKAWA, JUNICHI ..... N88-13257
N88-13289
MOCHIZUKI, MUNEKAZU ..... N88-13264
MODICA, GEORGE D. ..... N88-13823
MOLTON, P. ..... N88-13296
MOLTON, P. M. ..... N88-13658
MOM, A. J. A. ..... N88-13343
MONTEIRO, W. A. ..... N88-13432
MONTIEL, DENISE M. ..... N88-13446
MOORE, J. A. ..... N88-13491
MOORE, J. H. ..... N88-13495
MOORE, JAMES T. ..... N88-13830
MORALEZ, ERNESTO, III ..... N88-13359
MORBIDINI, A. ..... N88-13985
MOREL, PAUL R. ..... N88-13564
MORI, NOBUYUKI ..... N88-13728
MORI, TOSHIO ..... N88-13944
MORRIS, W. L. ..... N88-13653
N88-13666
MORRISON, CLYDE A. ..... N88-14020
MOUSSIAUX, E. ..... N88-13736
MOYNIHAN, C. T. ..... N88-14028
MOZER, F. S. ..... N88-13826
MULDER, WILLIAM A. ..... N88-13540
MUNDAY, TIM ..... N88-13768
MUNTEANU, MARIE-JEANNE ..... N88-13788
N88-13789
N88-13791
MURAKAMI, Y. ..... N88-13675
MURATORI, SIMONA ..... N88-13946
MUSTARD, JOHN F. ..... N88-13768
MUZA, STEPHEN ..... N88-13848

## N

NAGAI, K. ..... N88-13695
NAGASHIMA, HIDEFUMI ..... N88-13267
NAGEM, RAYMOND J. ..... N88-13920
NAGLE-ESHLEMAN, JUDITH ..... N88-13746
NAIDU, D. S. ..... N88-13935
NAKADATE, MASAAKI ..... N88-13267
NAKAHASHI, KAZUHIRO ..... N88-13260
N88-13282
NAKAMICHI, JIRO ..... N88-13254
NAKAMURA, AKIHITO ..... N88-13266
NAKAMURA, KINUYO ..... N88-13269
NAKAMURA, TAKASHI ..... N88-13263
NALLASAMY, M. ..... N88-13960
NANUT, V. ..... N88-13458
NARAYANAMURTI, V. ..... N88-14026
NARLO, J. C., II ..... N88-13226
NASH, E. R. ..... N88-13842
NASTROM, GREGORY D. ..... N88-13787
NAUMANN, K. W. ..... N88-13295
N88-13544
NAYEB-HASHEMI, H. ..... N88-13717
NEELAKANTASWAMY, PERAMBUR S. ..... N88-13522
NEGAS, T. ..... N88-13365
NEGRINI, ROBERTO ..... N88-13861
NES, E. ..... N88-13661
NEUMANN, P. ..... N88-13648
NEWMAN, PAUL A. ..... N88-13776
NEWTON, J. B. ..... N88-13349
NEWTON, JAMES E. ..... N88-13552
NEWTON, M. D. ..... N88-13963
NGUYEN, CHARLES C. ..... N88-13605
N88-13907
N88-13908
NGUYEN, T. ..... N88-13584
NIBLETT, L.L. T. ..... N88-13354
NICHOLS, B. D. ..... N88-13491
NIEGEL, A. ..... N88-13707
NISHIJIMA, SATOSHI ..... N88-13728
NISHIKAWA, NOBUHIDE ..... N88-13275
NIU, SHIWEN ..... N88-14010
NOONAN, ROBERT E. ..... N88-13896
NOTOHARDJONO, B. D. ..... N88-13720
NOVELLO, M. ..... N88-13819
NOWACK, H. ..... N88-13664
NOWAK, WELVILLE B. ..... N88-13442
NOZAKI, OSAMU ..... N88-13262
NOZZOLI, S. ..... N88-13985

## O

OBABUEKI, A. O. ..... N88-13680
OBAYASHI, SHIGERU ..... N88-13260
N88-13283
N88-13288

OBRIEN, T. K. ..... N88-13735
OCHAYA, VEN O. ..... N88-13459
OCONNOR, B. P. D. ..... N88-13658
OORU, PIERRE ..... N88-13487
OERTEL, H., JR. ..... N88-13237
OGATA, T. ..... N88-13695
OGAWA, T. ..... N88-13673
OHANDLEY, R. C. ..... N88-13444
OHTA, TAKASHI ..... N88-13284
OKADA, TAKAMITSU ..... N88-13278
OKYERE, JOHN G. ..... N88-13518
OLSDER, GEERT JAN ..... N88-13949
ONEIL, PETER V. ..... N88-13541
ONUMA, HIROYUKI ..... N88-13261
OODAIRA, HIROSHI ..... N88-13944
OORT, F. ..... N88-13929
OPPENHEIM, A. K. ..... N88-13422
ORFEI, R. ..... N88-13985
ORLIK-RUECKEMANN, K. J. ..... N88-13320
ORSINI, S. ..... N88-13569
OSADCHII, V. A. ..... N88-13436
OSAKO, S. ..... N88-13673
OSINGA, D. S. C. ..... N88-13857
OSTAPENKO, V. P. ..... N88-13437
OSTRIK, P. N. ..... N88-13438
OSWALD, FRED B. ..... N88-13604
OTA, TAKASHI ..... N88-13280
OTIS, D. R. ..... N88-13490
OWEN, F. K. ..... N88-13224


## P


PACKMAN, PAUL F. ..... N88-13726
PACOU, C. ..... N88-13222
PADGETT, W. J. ..... N88-13937
PALMBERG, B. ..... N88-13718
PALMERTREE, BILLY ..... N88-13637
PANDOLF, KENT B. ..... N88-13849
PANOSSIAN, H. V. ..... N88-13628
PAPIRNYK, O. ..... N88-13222
PARK, ILL KOO ..... N88-13876
PARKER, JAMES L. ..... N88-13317
PARKISON, C. D. ..... N88-13599
N88-13953
PARZEN, EMANUEL ..... N88-13942
N88-13943
PASCAL, J. ..... N88-13477
PASCUAL, R. ..... N88-13607
PASE, S. ..... N88-14061
PASINI, P. ..... N88-13966
PATEL, P. N. ..... N88-13641
PATIL, S. R. ..... N88-13364
PATZ, G. ..... N88-13545
PAWLEWICZ, W. T. ..... N88-13986
PEDERSEN, A. ..... N88-13826
PEDERSEN, KETILL ..... N88-13654
PEGNEAUX, J. C. ..... N88-13297
PELTIER, JACQUES FRANCOIS ..... N88-13398
PERARNAUD, D. ..... N88-13860
PERRIER, P. ..... N88-13251
PERRIER, PIERRE ..... N88-13321
PERSH, ROBERT I. ..... N88-13612
PETERS, MARY F. ..... N88-13878
PETERSEN, J. D. ..... N88-13425
PETERSEN, RALPH A. ..... N88-13781
PETERSON, A. F. ..... N88-13504
PETERSON, M. B. ..... N88-13456
PETIAU, C. ..... N88-13350
PEZESHKI, CHARLES ..... N88-13644
PFITZNER, MICHAEL ..... N88-13240
PHILLIPS, J. D. ..... N88-13715
PIBULTIP, PITAK ..... N88-13520
PIC, JEAN-MICHEL ..... N88-13886
PIERRE, A. C. ..... N88-14023
PIERSOL, ALLAN G. ..... N88-13610
PIETERS, CARLE M. ..... N88-13766
PIGNIE, G. ..... N88-13901
PILKEY, BARBARA F. ..... N88-13609
PILKEY, W. D. ..... N88-13633
PILKEY, WALTER D. ..... N88-13609
PIN, F. G. ..... N88-13602
PIPERNI, P. ..... N88-13531
PIRE, MICHEL ..... N88-13478
N88-13479
PLAGNE, A. ..... N88-13814
PLANK, VERNON G. ..... N88-13836
PLOTARD ..... N88-13468
PLUMTREE, A. ..... N88-13658
PLUVINAGE, G. ..... N88-13683
PODOBEDOVA, N. V. ..... N88-13437
POGGIO, TOMASO ..... N88-13862
POINSATTE, PHILLIP E. ..... N88-13552
POINTET, ALAIN ..... N88-13336
POLEY, WILLIAM A. ..... N88-13513
PONTAU, A. E. ..... N88-13989
POORAN, FARHAD J. ..... N88-13605
N88-13908
POTEMRA, T. A. ..... N88-13826
POTTER, TERRY W. ..... N88-13897
POTUZNIK, SUZANA ..... N88-13805
POUESSEL, CATHERINE ..... N88-13506
POWELL, B. E. ..... N88-13686
POWELL, D. ..... N88-13860
POWERS, DAVID L. ..... N88-13919
PREMACK, TIMOTHY ..... N88-13605
PRICE, BYRON K. ..... N88-13976
PRICE, CURTIS V. ..... N88-13764
PRITCHARD, A. J. ..... N88-13909
PROGAR, DONALD J. ..... N88-13474
PROGER, S. C. ..... N88-14004
PROSNITZ, D. ..... N88-13589
N88-13953
PRUCZ, JACKY C. ..... N88-13638
PULSIPHER, B. A. ..... N88-13471
PURDY, DARREL W. ..... N88-13875
PURNELL, JOHN HOWARD ..... N88-14022


## Q


QIN, N. ..... N88-13238


## R


RABINOVICH, A. V. ..... N88-13437
RAJAGOPALAN, S. R. ..... N88-13433
N88-13435
RAJU, I. S. ..... N88-13735
RAM, V. S. MOHAN ..... N88-13365
RAMAKER, RUSSELL A. ..... N88-13376
RAMASWAMY, M. A. ..... N88-13364
RAMOND, P. ..... N88-14032
RAMSEY, JOHN K. ..... N88-13753
RAO, DANTAM K. ..... N88-13624
RAO, K. T. VENKATESWARA ..... N88-13671
RASMUSSEN, DARYL ..... N88-13855
RAVEU, BERNARD ..... N88-13507
N88-13508
RE, F. ..... N88-14060
READ, B. J. ..... N88-14038
REBOUCAS, M. J. ..... N88-13950
REDEKER, ARTUR ..... N88-13360
REED, BOBBY E. ..... N88-13637
REED, R. W. ..... N88-13451
REGO, J. ..... N88-13589
REINHARDT, BRUCE A. ..... N88-13462
REISER, C. ..... N88-13590
REISS, H. R. ..... N88-13585
REJ, D. J. ..... N88-13998
REMY, L. ..... N88-13677
N88-13712
RENK, B. ..... N88-13966
REUTER, D. ..... N88-13791
REYNOLDS, G. H. ..... N88-13390
REYNOLDS, R. ..... N88-13347
REYNOLDS, W. C. ..... N88-13536
RHYS-JONES, T. J. ..... N88-13229
RICCARDELLA, P. C. ..... N88-13606
RICHARD, P. ..... N88-13972
RICHARDS, B. E. ..... N88-13238
RICKENBACH, MARK DOUGLAS ..... N88-13311
RIEDELBAUCH, S. ..... N88-13237
RIEGER, H. ..... N88-13235
RIGGS, GEORGE ..... N88-13765
RINALDI, SERGIO ..... N88-13946
RINGLER, THOMAS J. ..... N88-13579
RITCHIE, R. O. ..... N88-13645
N88-13671
N88-13700
RIZK, YEHIA ..... N88-13234
ROBBINS, SUSAN A. ..... N88-13611
ROBERT, M. ..... N88-13688
ROBERTS, D. A. ..... N88-13760
ROBERTSON, DAVID C. ..... N88-13503
ROBIN, C. ..... N88-13683
ROCKWELL, DONALD ..... N88-13307
RODGERS, EDWARD B. ..... N88-13782
RODRIGUEZ, O. ..... N88-13297
N88-13565
ROEDER, H. B. ..... N88-13802
ROEDER, J. L. ..... N88-13969
ROESSNER, H. J. ..... N88-13554
ROGER, MICHEL ..... N88-13959
ROGERS, DAVID L. ..... N88-13913
ROLLBUHLER, R. JAMES ..... N88-13338
ROMERO, L. A. ..... N88-13932
ROSATI, M. ..... N88-13927
ROSEMA, A. ..... N88-13808
ROSSI, J. L. ..... N88-13431
ROUM, CHRISTOPHER J. ..... N88-14034
ROUSTAN, J. ..... N88-13329
N88-13352
ROVEN, H. J. ..... N88-13661
ROWAN, LAWRENCE C. ..... N88-13771
ROWE, J. C. ..... N88-13891
RUAN, JINGHUI ..... N88-14010
RUBENSTEIN, ROBERT ..... N88-13754
RUIZ-ALTABA, M. ..... N88-14032
RULE, WILLIAM K. ..... N88-13634
RUMMEL, JOHN D. ..... N88-13852
RUNNING, STEVEN W. ..... N88-13765
RUNOLFSSON, T. ..... N88-13947
RYON, R. W. ..... N88-13980


## S


SACHER, P. W. ..... N88-13316
N88-13326
SADOWSKI, DENNIS R. ..... N88-14063
SAFREN, H. G. ..... N88-13371
N88-13372
SAGNIER, PH. ..... N88-13222
SAKAGUCHI, S. ..... N88-13716
SAKAMOTO, TOSHIYUKI ..... N88-13278
SALAMON, D. ..... N88-13910
SALMERON, EVA ..... N88-13809
SALOUR, M. M. ..... N88-13982
SALPEKAR, S. A. ..... N88-13735
SAMMS, RICHARD W. ..... N88-13557
SAMORODNITSKY, GENNADY ..... N88-13925
SAMUELSSON, INGEMAR ..... N88-13302
SANDGATHE, SCOTT A. ..... N88-13834
SANDOVAL, W. F. ..... N88-13591
SANZ, JOSE M. ..... N88-13304
SARACENO, P. ..... N88-13985
SARFF, J. S. ..... N88-14004
SASAKI, MIKIO ..... N88-13278
SASTRY, C. V. SRINATH ..... N88-13365
SATO, YUKINORI ..... N88-13265
SATOH, TSUGIHIKO ..... N88-13728
SAUBADE, CH. ..... N88-13945
SAUER, K. ..... N88-14056
SAWADA, KEISUKE ..... N88-13258
SAWAKI, Y. ..... N88-13716
SAWYER, WILLIAM A. ..... N88-13850
SAXENA, A. ..... N88-13724
SCANLON, RANDY J. ..... N88-13833
SCARABOTTOLLO, NELLO ..... N88-13861
SCHADOW, K. C. ..... N88-13232
SCHARLEMANN, E. T. ..... N88-13589
SCHEFFEL, R. ..... N88-13659
SCHEWE, G. ..... N88-13355
SCHIFF, DANIEL ..... N88-13621
SCHMIDINGER, G. ..... N88-13351
SCHMITT, A. J. ..... N88-13992
SCHOCK, HAROLD J. ..... N88-13345
SCHOEBERL, MARK R. ..... N88-13776
N88-13780
SCHRAG, ROBERT L. ..... N88-13310
SCHROEDER, JEFFERY A. ..... N88-13359
SCHUBERT, SIEGFRIED D. ..... N88-13789
SCHUCANY, WILLIAM R. ..... N88-13938
SCHUETZ, W. ..... N88-13690
SCHUFFEL, H. ..... N88-13857
SCHULZ, FREDERICK FAY ..... N88-13957
SCHULZE, CLAUS ..... N88-13741
SCHUSS, Z. ..... N88-13947
SCHWARTZ, ANDERS ..... N88-13480
SCHWARTZKOPF, STEVEN H. ..... N88-13855
SCHWEIGER, J. ..... N88-13355
SCOTT, A. D., JR. ..... N88-13369
SCOTT, PAUL TILDEN ..... N88-13419
SCOTT, R. A. ..... N88-13635
SECHRIST, FRANK S. ..... N88-13781
SEHITOGLU, H. ..... N88-13719
SELLARS, R. J. ..... N88-13325
SELLERS, BACH ..... N88-13564
SELVAGGINI, R. ..... N88-13358
SENSBURG, O. ..... N88-13351
SENTMAN, L. H. ..... N88-13581
N88-13584
SERFOZO, RICHARD F. ..... N88-13921
SEROVY, G. K. ..... N88-13344
SEVRAIN, A. ..... N88-13548
SEYYEDI, J. ..... N88-13717
SHAFFER, IRVING S. ..... N88-13332
SHAING, K. C. ..... N88-14006
SHAMROTH, S. J. ..... N88-13291
SHAPIRO, WILBUR ..... N88-13603
SHARP, MARILYN A. ..... N88-13850
SHARPE, W. E. ..... N88-13349
SHARPE, W. N., JR. ..... N88-13676
SHAVER, CHARLES ..... N88-13367
SHEARER, MICHAEL ..... N88-13538
SHEFFIELD, J. ..... N88-14002

SHEN, H-S. ..... N88-14019
SHENK, WILLIAM E. ..... N88-13801
SHERCLIFF, H. R. ..... N88-13574
SHIDA, YOSHIFUMI ..... N88-13255
SHIGEMI, MASASHI ..... N88-13268
SHIMA, EIJI ..... N88-13259
SHIN, Y. S. ..... N88-13613
SHIOTA, YASUHIRO ..... N88-13261
SHIPMAN, H. M. ..... N88-13760
SHIRAYAMA, SUSUMU ..... N88-13277
N88-13280
N88-13281
N88-13284
SIGNORETTI, F. ..... N88-14060
SIGNORINI, C. ..... N88-13977
N88-14060
SIKKA, V. K. ..... N88-13449
SILVER, L. S. ..... N88-13424
SILVER, R. N. ..... N88-13968
SIMONS, JOHN C. ..... N88-13979
SINGER, J. ..... N88-13385
SINGH, A. K. ..... N88-13434
SINOR, J. E. ..... N88-13475
SKINNER, D. A. ..... N88-14004
SLAUGHTER, E. R. ..... N88-13461
SLETTEN, TIMOTHY N. ..... N88-13829
SLINEY, HAROLD E. ..... N88-13453
SMALLEY, R. E. ..... N88-14018
SMEETS, G. ..... N88-13295
SMEETS, RENE PETER PAUL ..... N88-13529
SMERNOFF, DAVID T. ..... N88-13852
N88-13854
SMIRES, NAJIB ..... N88-13824
SMITH, D. L. ..... N88-14005
SMITH, GREGORY P. ..... N88-13415
SMITH, M. O. ..... N88-13760
SMITH, P. R. ..... N88-13491
SMITH, PAUL G. ..... N88-13674
SNIPES, R. ..... N88-13584
SO, KENNETH T. ..... N88-13369
SOERLEI, ZSUZSA ..... N88-13987
SOHN, D. ..... N88-13307
SOMASUNDAR, H. V. ..... N88-13713
SONIAK, F. ..... N88-13677
SOPOK, SAMUEL ..... N88-13414
SOTTA, J. P. ..... N88-13860
SOWERS, JAMES P. ..... N88-13597
SPADAFORA, STEPHEN J. ..... N88-13454
SPARKS, C. P. ..... N88-13488
SPEAR, R. J. ..... N88-13458
SPECKMAN, D. M. ..... N88-13519
SPIELVOGEL, BERNARD F. ..... N88-13386
SPROTT, J. C. ..... N88-14004
SPYRAKOS, CONSTANTINE ..... N88-13638
SPYRAKOS, CONSTANTINE C. ..... N88-13641
SPYRAKOS, CONSTANTINE CHRIS ..... N88-13632
SREEPATHY, S. ..... N88-13433
N88-13435
SRULIJES, J. ..... N88-13544
ST.CLAIR, TERRY L. ..... N88-13474
STAHL, K. A. ..... N88-13986
STALKER, R. J. ..... N88-13223
STARKE, E. A., JR. ..... N88-13645
N88-13692
N88-13700
STASSINOPOULOS, A. ..... N88-13296
STEFANICK, MICHAEL ..... N88-13778
STEFFEN, ANGELA A. ..... N88-13726
STEGER, JOSEPH ..... N88-13234
STEINKE, R. G. ..... N88-13491
STENBERG, R. ..... N88-13749
STEPHENS, A. B. ..... N88-13923
STEPHENS, R. I. ..... N88-13660
N88-13694
STERZELMEIER, K. ..... N88-13554
STEVENSON, STEVEN M. ..... N88-13515
STEWART, DONALD L., II ..... N88-13439
STINTON, D. P. ..... N88-13408
STOLARSKI, RICHARD S. ..... N88-13775
STOLLERY, J. L. ..... N88-13227
STORINI, M. ..... N88-14061
STOTT, J. H. ..... N88-13494
STROUB, ROBERT H. ..... N88-13290
STUNDER, MARK J. ..... N88-13829
SU, X. ..... N88-13676
SUEMATSU, KAZUYO ..... N88-13276
SUMMERS, DAVID GEORGE ..... N88-13464
SUN, C. T. ..... N88-13639
SUN, CHIEN-EN ..... N88-13864
SUNDER, R. ..... N88-13662
SURI, MANIL ..... N88-13923
SUSSKIND, JOEL ..... N88-13791
N88-13799
SUTO, M. ..... N88-13429
SUZUKI, TAKASHI ..... N88-13275
SVENINGSSON, M. ..... N88-13860
SWANBERG, NANCY A. ..... N88-13761
SWANSSON, N. S. ..... N88-13642
SWEENEY, MICHAEL A. ..... N88-13411
SYKES, ALAN O. ..... N88-13636
SZEKELY, JULIAN ..... N88-13993
SZODRUCH, JOACHIM ..... N88-13243

## T

TAI, K. C. ..... N88-13863
TAKANASHI, SUSUMU ..... N88-13258
N88-13263
N88-13287
N88-13288
N88-13289
TAKAYANAGI, S. ..... N88-13695
TAKEDA, KIICHIROU ..... N88-13284
TAMARELLE, P. J. C. ..... N88-13488
TAMURA, ATSUHIRO ..... N88-13262
N88-13263
TANAKA, K. ..... N88-13678
TANAKA, T. ..... N88-13680
TANAKA, TSUNESHICHI ..... N88-13647
TANENBAUM, A. S. ..... N88-14041
TANGENA, ANTONIUS GERARDUS ..... N88-13601
TAQI, E. A. ..... N88-13702
TARLETON, ROBERT E., JR. ..... N88-13499
TAWARA, H. ..... N88-13988
TAYLOR, E. W. ..... N88-13955
TAYLOR, FRANCIS R. ..... N88-13476
TAYLOR, L. M. ..... N88-13890
TENG, NGAI-HUAT ..... N88-13293
THAPA, KHAGENDRA ..... N88-13803
THEARLING, KURT HENRY ..... N88-13871
THEODOROPOULOS, P. ..... N88-13584
THOMAS, G. A. ..... N88-13496
THOMAS, G. J. ..... N88-13969
THOMAS, GLENN J. ..... N88-13559
THOMAS, J. M. ..... N88-13330
THOMAS, J. S., JR. ..... N88-13687
THOMAS, KENNETH CHARLES ..... N88-13464
THOMASON, P. F. ..... N88-13649
THRESHER, R. W. ..... N88-13815
THWAITES, MICHAEL JOHN ..... N88-14022
TIEMROTH, ERIK CHARLES ..... N88-13534
TIKUISIS, PETER ..... N88-13849
TISCHLER, V. A. ..... N88-13622
TITTEL, F. K. ..... N88-14018
TOBUREN, L. H. ..... N88-13986
TOH, HIDEMI ..... N88-13265
TOKAJI, K. ..... N88-13873
TONG, MICHAEL T. ..... N88-13745
TONNESSEN, A. ..... N88-13646
TORIN, J. ..... N88-13860
TOWE, ELIAS ..... N88-13583
TOWNLEY, S. ..... N88-13909
TOWNSEND, LAWRENCE W. ..... N88-14058
TRAMONTANO, VALENTINO J. ..... N88-13459
TREMOR, JOHN W. ..... N88-13853
TRIANTAFYLLOU, M. S. ..... N88-13747
TRIVEDI, K. S. ..... N88-13870
TROYES, JACQUES ..... N88-13361
TSUWA, YOSHIAKI ..... N88-13270
TUBOI, KAZUHIRO ..... N88-13281
TURENNE, S. ..... N88-13655
TURPIN-INVERNON, CHRISTOPHE ..... N88-13336
TURTON, PHILIP JOHN ..... N88-13393
TYNDEL, M. ..... N88-13966

## U

UCCELLINI, LOUIS ..... N88-13790
UCCELLINI, LOUIS W. ..... N88-13781
UECER, A. S. ..... N88-13344
UEDA, TETSUHIKO ..... N88-13256
UHLMANN, D. R. ..... N88-14023
UMEDA, YOSHIKUNI ..... N88-13274
UNROE, MARILYN R. ..... N88-13462
USTIN, SUSAN L. ..... N88-13763

## V

VAGTS, WAYNE FRANZ ..... N88-13877
VALKERING, THEO P. ..... N88-13928
VANAKEN, JOHANNES M. ..... N88-13290
VANBEEST, C. A. ..... N88-13813
VANDAMME, RUUD ..... N88-13928
VANDERHOEVEN, W. A. G. ..... N88-13882
VANDERLUBBE, J. C. A. ..... N88-13808
VANDERPUT, M. ..... N88-13929
VANDERSLIKKE, J. W. ..... N88-13466
VANE, GREGG ..... N88-13755
N88-13757
VANFOSSEN, G. JAMES ..... N88-13552
VANLIEROP, MARIA LUCIA PETRONELLA . N88-13887
VANMAREN, R. D. ..... N88-13952
VANPUL, CORNELIS LEONARDUS MARIA . N88-13888
VANRENESSE, R. ..... N88-14041
VANRIJ, W. I. ..... N88-14006
VANROESSEL, H. J. ..... N88-13247
VANSICE, J. C. ..... N88-13687
VANSMAALEN, SANDER ..... N88-13740
VANSTAVEREN, H. ..... N88-14041
VARANASI, MURALI R. ..... N88-13595
N88-13596
VAYSSADE, MICHEL ..... N88-13547
VEATCH, PHILLIP A. ..... N88-14045
VEKLEROV, E. ..... N88-13892
VENKAYYA, V. B. ..... N88-13622
VENNE, DAVID E. ..... N88-13832
VERREMAN, Y. ..... N88-13679
VIGNERON, Y. ..... N88-13300
VIGNESOULT, S. ..... N88-13394
VIJAYAN, KALYANI ..... N88-13434
VIJAYARAGHAVAN, S. B. ..... N88-13339
VILLORESI, G. ..... N88-14060
VINCENT, L. ..... N88-13697
VINE, BEN ..... N88-13555
VISCO, M. ..... N88-13528
VITEK, J. M. ..... N88-13451
VITELLO, P. ..... N88-13975
VLIMANT, P. ..... N88-13860
VOGEL, JAMES A. ..... N88-13848
VOUK, MLADEN A. ..... N88-13863
N88-13864
N88-13865
VOYTKO, J. E. ..... N88-13448

## W

WAGNER, JAMES W. ..... N88-13958
WAGNER, TIMOTHY CHARLES ..... N88-13410
WAKE, ALISON J. ..... N88-13252
WAKE, BRIAN ERNEST ..... N88-13533
WAKE, L. V. ..... N88-13328
WALDO, R. ..... N88-13584
WALKER, E. F. ..... N88-13701
WALRAVEN, J. ..... N88-13882
WALSH, J. A. ..... N88-13692
WALTRUP, P. J. ..... N88-13231
WANG, BING ..... N88-13459
WANG, F. W. ..... N88-13391
WANG, SUIFU ..... N88-13525
WANG, XIYOU ..... N88-13483
WARD, L. C. ..... N88-13250
WASEN, J. ..... N88-13657
N88-13727
WATANABE, SHIZUI ..... N88-13272
WATANABE, TADASHI ..... N88-13270
WATKINS, B. J. ..... N88-13822
WEAVER, H. T. ..... N88-14025
WEERTMAN, J. ..... N88-13668
WEI, MAX L. ..... N88-13618
N88-13620
WEI, R. P. ..... N88-13731
WEILAND, CLAUS ..... N88-13240
WEINGARTNER, FRANK J. ..... N88-13831
WEISSMANN, S. ..... N88-13725
WENBERG, A. R. ..... N88-14039
WENDT, J. F. ..... N88-13221
WENSKI, E. G. ..... N88-13722
WERRET, S. T. ..... N88-13486
WERRETT, S. T. ..... N88-13485
WESTMAN, WALTER E. ..... N88-13764
WETZEL, W. ..... N88-13237
WEY, J. ..... N88-13586
WHERRY, D. ..... N88-13980
WHITE, C. ..... N88-13347
WHITE, R. L. ..... N88-13313
WHITTEN, DAVID G. ..... N88-13412
WIEDWALD, J. D. ..... N88-13571
WIESELTHIER, J. E. ..... N88-13500
WIGANT, C. C. ..... N88-13660
WILLIAMS, D. A. ..... N88-13523
WILLIAMS, JAMES H., JR. ..... N88-13920
WILLIAMSON, MICHAEL ..... N88-13367
WILLIS, S. C. ..... N88-13760
WILSON, DAVID CHARLES ..... N88-13464
WILSON, JAMES F. ..... N88-13623
WILSON, JOHN W. ..... N88-14058
WILSON, K. J. ..... N88-13232
WILSON, MAYWOOD L. ..... N88-13388
WITHROW, S. P. ..... N88-14027
WITTLIFF, C. E. ..... N88-13220
WOLD, A. ..... N88-14019
WOLF, G. H. ..... N88-13989
WOLF, M. L. ..... N88-13905
WOODSON, STEVEN W. ..... N88-13521
WOODWARD, R. P. ..... N88-13960

WOODWARD, RICHARD P. ..... N88-13961
WOOLDRIDGE, RICHARD C. ..... N88-13342
WRIGHT, A. D. ..... N88-13815
WRIGHT, JOHN C. ..... N88-13580
WRIGHT, R. N. ..... N88-13450
WROBLEWSKI, MICHAEL RAYMOND ..... N88-13821
WU, M. F. ..... N88-13842
WU, Y. S. ..... N88-13689

## X

XUE, ZHENSHU ..... N88-13483

## Y

YAMAMOTO, SATORU ..... N88-13285
YAMAMURA, Y. ..... N88-13988
YANAGIZAWA, MITSUNORI ..... N88-13267
YANG, JACKSON C. S. ..... N88-13625
N88-13626
YANG, L. ..... N88-13390
YANG, X. ..... N88-14023
YAO, G-Q. ..... N88-14019
YAO, W. P. ..... N88-13685
YATES, E. CARSON, JR. ..... N88-13353
YATES, GEORGE ..... N88-13555
YATSKO, YU. V. ..... N88-13436
YE, C. ..... N88-13429
YE, CHUNTANG ..... N88-14010
YEE, SAMUEL Y. ..... N88-13823
YOROZU, JUNICHI ..... N88-13270
YOSHIDA, MASAHIRO ..... N88-13269
YOSHIHARA, H. ..... N88-13318
YOSHIOKA, S. ..... N88-13695
YOUNG, D. M. ..... N88-13934
YOUSSEF, S. ..... N88-14009
YU, ANSUN ..... N88-14010
YU, W. ..... N88-13671
YURI, T. ..... N88-13695

## Z

ZACKS, S. ..... N88-13914
ZANETTI, L. J. ..... N88-13826
ZANGRILLI, N. L. ..... N88-14060
ZEHNER, EDWIN A. ..... N88-13314
ZHADA, V. T. ..... N88-13436
ZHANG, QIANG ..... N88-13618
N88-13620
ZHANG, RONGSHENG ..... N88-13483
ZHANG, SHIEN ..... N88-13483
ZHENG, XIANGMIAO ..... N88-14010
ZHOU, A. H. ..... N88-13689
ZIMMERMAN, ALBERT H. ..... N88-13519
ZIRIN, HAROLD ..... N88-14055
ZORUMSKI, WILLIAM E. ..... N88-13962
ZOUZIAS, IOANNIS E. ..... N88-13598
ZUKAUSKAS, WALDEMAR ..... N88-13561

## Typical Corporate Source Index Listing

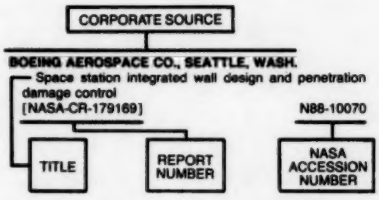


Listings in this index are arranged alphabetically by corporate source. The title of the document provides the user with a brief description of the subject matter. The report number helps to indicate the type of document cited (e.g., NASA report, translation, NASA contractor report). The NASA accession number denotes the number by which the citation is identified. The titles are arranged under each corporate source in ascending accession number order.

## A


**ACADEMIA SINICA, BEIJING (CHINA).**
An experimental study of closure behavior of naturally initiated small cracks N88-13676
Fatigue of 30CrMnSiNi2A notched specimens under spectrum loading N88-13689

**ACADEMY OF SCIENCES, BERLIN (EAST GERMANY).**
A fluid simulation of the AMPTE lithium gas releases in the solar wind
[TRITA-EPP-87-06] N88-14056

**ACOUSTICAL RESEARCH AND APPLICATIONS, VIENNA, VA.**
A passive vibration-cancelling isolation mount N88-13636

**ADVANCED TECHNOLOGY AND RESEARCH, INC., LAUREL, MD.**
Non-linear shipboard shock analysis of the Tomahawk missile shock isolation system N88-13614
A system identification technique based on the random decrement signatures. Part 1: Theory and simulation N88-13625
A system identification technique based on the random decrement signatures. Part 2: Experimental results N88-13626

**ADVISORY GROUP FOR AEROSPACE RESEARCH AND DEVELOPMENT, NEUILLY-SUR-SEINE (FRANCE).**
Aerodynamics of Hypersonic Lifting Vehicles
[AGARD-CP-428] N88-13219
Special Course on Fundamentals of Fighter Aircraft Design
[AGARD-R-740] N88-13315
Workshop on Avionics Corrosion Control
[AGARD-R-733] N88-13331
Application of modified loss and deviation correlations to transonic axial compressors
[AGARD-R-745] N88-13344
Static Aeroelastic Effects on High Performance Aircraft
[AGARD-CP-403] N88-13348
The use of aeroelastic wind tunnel models to prove structural design N88-13355
Calendar of selected aeronautical and space meetings
[AGARD-CAL-87/1] N88-14033
Calendar of selected aeronautical and space meetings
[AGARD-CAL-88/1] N88-14037

**AERONAUTICAL RESEARCH INST. OF SWEDEN, BROMMA.**
Fatigue crack growth: Statistical considerations N88-13718

**AERONAUTICAL RESEARCH INST. OF SWEDEN, STOCKHOLM.**
Computation of rime ice accretion on airfoils
[FFA-TN-1987-08] N88-13301
Low speed wind tunnel investigation of propeller slipstream aerodynamic effects on different nacelle/wing combinations. Part 1: Total forces and moments and pressure distributions on nacelle/wing at different angles of attack and yaw and at different thrust coefficients
[FFA-TN-1987-22] N88-13302
Compressible Euler solution on a multiblock grid around a wing-fuselage configuration
[FFA-TN-1987-46] N88-13303

**AERONAUTICAL RESEARCH LABS., MELBOURNE (AUSTRALIA).**
Environmentally assisted cracking: Overview of evidence for an adsorption-induced localised-slip process
[AD-A185175] N88-13443

**AEROSPACE CORP., EL SEGUNDO, CALIF.**
High energy density rechargeable batteries for aerospace power requirements
[AD-A184883] N88-13519
Restoration of particle pitch angle distribution functions by a maximum entropy algorithm
[ATR-86(7098)-3] N88-13969
A GaAs MESFET balanced mixer with very low intermodulation
[AD-A184848] N88-14015

**AEROSPATIALE USINES DE TOULOUSE (FRANCE).**
Aeroelastic analysis of modern transport aircraft N88-13352

**AIR FORCE GEOPHYSICS LAB., HANSCOM AFB, MASS.**
An analytical soil thermodynamic model for the diurnal variation of ground surface temperature
[AD-A185388] N88-13823
The application of doubly-truncated hydrometeor distributions to numerical cloud models
[AD-A185273] N88-13836

**AIR FORCE INST. OF TECH., WRIGHT-PATTERSON AFB, OHIO.**
Airline safety: A comparative analysis
[AD-A185358] N88-13308
Use of the global positioning system for trajectory determination of SRAM 2 missiles at the Eastern Test Range
[AD-A185266] N88-13314
Dynamics of propellant feedline systems
[AD-A184865] N88-13537
Fiber-optic accelerometer investigation
[AD-A185359] N88-13561
Environmental and convective influence on tropical cyclone development versus non-development
[AD-A185231] N88-13835
Modeling cloudy and clear interval length probabilities using space shuttle imagery
[AD-A185290] N88-13837
Specification of predictors necessary for the determination of over or underestimation of radar derived total rainfall
[AD-A185363] N88-13838

**AIR FORCE MATERIALS LAB., WRIGHT-PATTERSON AFB, OHIO.**
Corrosion of electronic components N88-13333
Significance of fatigue crack closure under spectrum loading N88-13662

**AIR FORCE SYSTEMS COMMAND, WRIGHT-PATTERSON AFB, OHIO.**
New breakthrough in Chinese integrated circuits: Successful development of high-speed CMOS circuits
[AD-A185381] N88-13525
Astrophysics observatory in Byurakan
[AD-A185144] N88-14050

**AIR FORCE WEAPONS LAB., KIRTLAND AFB, N. MEX.**
Extreme ultraviolet beam-foil spectroscopy of highly ionized neon and argon
[AD-A185197] N88-13418
Analytical solution of the equations for a coaxial plasma gun operating in the snowplow mode. 1. Weak coupling limit
[AD-A185370] N88-13994

**AIR FORCE WRIGHT AERONAUTICAL LABS., WRIGHT-PATTERSON AFB, OHIO.**
Lifting bodies: An attractive aerodynamic configuration choice for hypervelocity vehicles N88-13248
Mission requirements and aircraft sizing N88-13317
Thermally stable aromatic structures from acyclic precursors. 1. Para polyphenylene model compounds from 3-Dimethyl amino hex-5-EN-1-YNES
[AD-A185300] N88-13462

**AIR WEATHER SERVICE, SCOTT AFB, ILL.**
Isentropic analysis and interpretation: Operational applications to synoptic and mesoscale forecast problems
[AD-A184814] N88-13830

**AKRON UNIV., OHIO.**
SHARP simulation of discontinuities in highly convective steady flow
[NASA-TM-100240] N88-13931

**ALABAMA A & M UNIV., NORMAL.**
Low thrust viscous nozzle flow fields prediction
[NASA-CR-182334] N88-13551

**ALABAMA UNIV., BIRMINGHAM.**
Displaying three-dimensional data
[AD-A185347] N88-13541

**ALASKA UNIV., FAIRBANKS.**
The polar ionosphere and interplanetary field
[AD-A185386] N88-13822

**ALLIED BENDIX CORP., KANSAS CITY, MO.**
XCUT: A rule-based expert system for the automated process planning of machined parts
[DE87-011638] N88-13905
Using hierarchically structured problem-solving knowledge in a rule-based process planning system
[DE87-011639] N88-13906

**ARIZONA STATE UNIV., TEMPE.**
Studies in Aeolian geology
[NASA-CR-182328] N88-13828
Examining the relative efficiency of Part- versus whole-task practice for multiple-task situations
[AD-A185056] N88-13856

**ARMY ARMAMENT RESEARCH, DEVELOPMENT AND ENGINEERING CENTER, PICATINNY ARSENAL, N.J.**
Performance characteristics of magnesium-sodium nitrate flares in oxygen-nitrogen atmospheres
[AD-A185274] N88-13476

**ARMY ARMAMENT RESEARCH AND DEVELOPMENT COMMAND, WATERVLIET, N. Y.**
The analysis of metal finishing solutions by ion chromatography
[AD-A184812] N88-13414

**ARMY AVIATION RESEARCH AND DEVELOPMENT COMMAND, ST. LOUIS, MO.**
Finite-element grid improvement by minimization of stiffness matrix trace
[NASA-TM-100255] N88-13604

**ARMY ENGINEER WATERWAYS EXPERIMENT STATION, VICKSBURG, MISS.**
Analysis of photopole data reduction models N88-13616
Measurement of suspension and ride characteristics of the M1 main battle tank N88-13637

**ARMY LAB. COMMAND, WATERTOWN, MASS.**
Ion plating for corrosion control
[AD-A185061] N88-13442

**ARMY RESEARCH INST. OF ENVIRONMENTAL MEDICINE, NATICK, MASS.**
Assessment of the reliability of a correction procedure for WGT (Wet Globe Thermometer) (Botsball) measurements of heat stress
[AD-A185193] N88-13559
Cooling electronic equipment at simulated high altitude in hypobaric chambers
[AD-A185196] N88-13560
A plethysmograph for measuring pulmonary ventilation in small animals
[AD-A184978] N88-13846
Physiological determinants of load bearing capacity
[AD-A184977] N88-13848
Human thermoregulatory model for whole body immersion in water at 20 and 28 C
[AD-A185052] N88-13849
A device and methodology for measuring repetitive lifting VO2max (oxygen consumption rate)
[AD-A185195] N88-13850

**ASSURANCE TECHNOLOGY CORP., CARLISLE, MASS.**
Initial dynamic load estimates during configuration design N88-13621
**ASTRON RESEARCH AND ENGINEERING, SANTA MONICA, CALIF.**
The analysis of nonstationary vibration data N88-13610
**ATMOSPHERIC ENVIRONMENT SERVICE, DOWNSVIEW (ONTARIO).**
Dobson-stations performance assessment using TOMS data N88-13792
Comparison of ground based and TOMS measurements of SO2 from volcanic emissions N88-13795
**ATOMIC ENERGY RESEARCH ESTABLISHMENT, HARWELL (ENGLAND).**
the influence of temper embrittlement on fatigue crack growth in hydrogen N88-13709
**AUTOMETRIC CORP., INC., FALLS CHURCH, VA.**
Land cover/use classification of Cairns, Queensland, Australia: A remote sensing study involving the conjunctive use of the airborne imaging spectrometer, the large format camera and the thematic mapper simulator N88-13759
**AVIONS MARCEL DASSAULT-BREGUET AVIATION, SAINT-CLOUD (FRANCE).**
General aerodynamic-aerothermodynamic concepts for Hermes N88-13251
Techniques for performance optimisation in cruise and manoeuverability N88-13321
Trends in aeroelastic analysis of combat aircraft N88-13350

## B

**BALLISTIC RESEARCH LABS., ABERDEEN PROVING GROUND, MD.**
Mechanical property evaluation of a series of commercial tungsten alloys
[AD-A185440] N88-13446
A study of the interaction of laser light with liquid propellant drops
[AD-A185117] N88-13582
Multidimensional least squares fitting of fuzzy models
[AD-A185148] N88-13916
Least squares for fuzzy vector data regression
[AD-A185156] N88-13917
**BIRMINGHAM UNIV. (ENGLAND).**
Fatigue crack growth N88-13734
**BL TECHNOLOGY LTD., WARWICK (ENGLAND).**
The development and evaluation of three-dimensional models of cold flow in internal combustion engines
[DE88-900077] N88-13594
**BOEING MILITARY AIRPLANE DEVELOPMENT, SEATTLE, WASH.**
Design of wings and wing/body configurations for transonic and supersonic speeds N88-13318
**BORDEAUX 1 UNIV., TALENCE (FRANCE).**
Utilization of microwave measuring systems for nondestructive control of composite materials
[SNIAS-872-430-109] N88-13402
**BOSTON UNIV., MASS.**
Atomic beam studies of the interaction of hydrogen with transition metal surfaces
[DE88-000208] N88-13970
**BRITISH AEROSPACE DYNAMICS GROUP, BRISTOL (ENGLAND).**
Evaluation of a cryogenic refrigerator for cooling focal plane instrumentation
[BAE-TP-8095-VOL-1] N88-13485
Evaluation of a cryogenic refrigerator for cooling focal plane instrumentation. Appendix B: Accommodation study
[BAE-TP-8095-VOL-2] N88-13486
**BRITISH AEROSPACE PUBLIC LTD. CO., BRISTOL (ENGLAND).**
Experiences using the Mark IV supersonic hypersonic arbitrary body program N88-13249
**BRITISH AEROSPACE PUBLIC LTD. CO., KINGSTON-UPON-THAMES (ENGLAND).**
Airframe/store compatibility N88-13323
**BRITISH AEROSPACE PUBLIC LTD. CO., PRESTON (ENGLAND).**
Hypersonic aerodynamics: Applications for HOTOL N88-13252
Materials for fighter aircraft N88-13325
Examples of static aeroelastic effects on present combat aircraft projects N88-13349
**BRITISH BROADCASTING CORP., KINGSWOOD (ENGLAND).**
Digital video bit-rate reduction: DPCM for sub-Nyquist PAL
[BBC-RD-1987/16] N88-13494
Improvements to a UHF rebroadcast television link suffering tidal fading: Countisbury UHF relay station
[BBC-RD-1987/14] N88-13495
Television motion measurement for DATV and other applications
[BBC-RD-1987/11] N88-13496
Theoretical and practical aspects of the functional absorber method of arranging sound absorbing panels
[BBC-RD-1987/15] N88-13955
**BRITISH LIBRARY LENDING DIV., BOSTON SPA (ENGLAND).**
A mathematical model of high alloy nickel base high temperature alloys
[BLL-M-37381-(5828.4)] N88-13436
The mechanism by which sigma-phase forms in Fe-Cr-Ni system alloys
[BLL-M-37380-(5828.4)] N88-13437
Corrosion resistance of sintered alloy steels
[BLL-M-37363-(5828.4)] N88-13438
**BRITISH PETROLEUM CO. LTD., SUNBURY-ON-THAMES (ENGLAND).**
Core material
[EP-PATENT-0-196-926-A2] N88-13393
Antistatic coating compositions
[GB-PATENT-2-177-413-A] N88-13463
Flame retardant phenolic foams
[EP-PATENT-0-223-489-A2] N88-13464
Process for the production of a thermoplastic elastomer composition
[EP-PATENT-0-202-782-A2] N88-13485
Optical probe
[EP-PATENT-0-210-869-A1] N88-13984
Preparation of amorphous silicon semiconductors
[GB-PATENT-2-176-054-A] N88-14022
**BRITISH STEEL CORP., ROTHERHAM (ENGLAND).**
A study of corrosion fatigue crack initiation, growth and the threshold condition under variable amplitude loading N88-13701
**BROOKHAVEN NATIONAL LAB., UPTON, N. Y.**
The role of electronic structure calculation in mechanistic analysis of electron transfer reactions in the liquid phase
[DE87-014395] N88-13963
**BROWN UNIV., PROVIDENCE, R. I.**
Computational methods for problems in aerodynamics and large space structure using parallel and vector architectures
[AD-A185401] N88-13294
Plasticity of aluminum and iron at high shear strain rate and high pressure N88-13430
Abundance and distribution of ultramafic microbreccia in Moses Rock Dike: Quantitative application of AIS data N88-13766
Storing and retrieving data in a parallel distributed memory system
[AD-A185177] N88-13897
Preparation and characterization of members of the system (Zn,Se)1-xGaPx
[AD-A185073] N88-14019

## C

**CALCULON CORP., ROCKVILLE, MD.**
Human engineering laboratory grounding analysis (HELGA)-2
[AD-A185367] N88-13524
**CALIFORNIA INST. OF TECH., PASADENA.**
Development of microencapsulation techniques
[AD-A185019] N88-13457
Numerical analysis, computing and fundamental studies in fluid mechanics
[DE88-001912] N88-13550
The appearance and disappearance of magnetic flux on the quiet sun
[AD-A185432] N88-14055
**CALIFORNIA UNIV., BERKELEY.**
The simulation of the viscous flow around a cylinder by the random vortex method N88-13534
Satellite observations of extreme ultraviolet radiation
[AD-A185043] N88-14059
**CALIFORNIA UNIV., BERKELEY. LAWRENCE BERKELEY LAB.**
Pulsed plasma jet igniters: Species measurements in methane combustion
[DE88-001389] N88-13422
Formation and destruction of nitrous oxide in lean, premixed combustion
[DE88-001390] N88-13423
A long electromagnetic wiggler for the paladin free-electron laser experiments
[DE88-000970] N88-13589
The maximum likelihood estimator method of image reconstruction: Its fundamental characteristics and their origin
[DE88-000462] N88-13892
SUSIE reference manual
[DE88-001462] N88-13893
Development of a strong electromagnet wiggler
[DE88-000971] N88-13952
Development of a laced electromagnetic wiggler
[DE88-000972] N88-13953
Heavy-ion accelerator research for inertial fusion
[DE88-000541] N88-14001
**CALIFORNIA UNIV., DAVIS.**
Conditional second order closure for turbulent shear flows
[AD-A185389] N88-13542
**CALIFORNIA UNIV., LOS ANGELES.**
Theoretical and experimental investigation of electron beam acceleration and sub-millimeter wave generation in cyclotron resonant cavities
[AD-A184806] N88-13975
ALT-1 pump limiter experiments
[DE88-000822] N88-13989
**CALIFORNIA UNIV., SAN DIEGO, LA JOLLA.**
Comparing hard and soft prior bounds in geophysical inverse problems
[NASA-CR-181557] N88-13820
Isotropic probability measures in infinite dimensional spaces: Inverse problems/prior information/stochastic inversion
[NASA-CR-181555] N88-13936
**CALSPAN-BUFFALO UNIV. RESEARCH CENTER, N.Y.**
Development of an integrated BEM approach for hot fluid structure interaction
[NASA-CR-181577] N88-13384
**CALSPAN CORP., BUFFALO, N. Y.**
A survey of existing hypersonic ground test facilities: North America N88-13220
**CAMBRIDGE UNIV. (ENGLAND).**
Master plots for predicting the case-depth in laser surface treatments
[PB87-221875] N88-13574
Fatigue crack retardation in aluminium alloys N88-13681
Near-threshold growth of defects in engineering materials N88-13691
**CATHOLIC UNIV. OF AMERICA, WASHINGTON, D.C.**
Optimal control of large space structures via generalized inverse matrix
[NASA-CR-182336] N88-13907
Cartesian path control of a two-degree-of-freedom robot manipulator
[NASA-CR-182331] N88-13908
Ionic transport and electrical relaxation in glass
[DE88-000887] N88-14028
**CENTRE D'ETUDES AERODYNAMIQUES ET THERMIQUES, POITIERS (FRANCE).**
Study of the effect of mass transfer on a transonic boundary layer. Application to flow relaminarization
[ETN-88-91169] N88-13296
**CENTRE NATIONAL D'ETUDES SPATIALES, TOULOUSE (FRANCE).**
The high performance solar array GSR3
[SNIAS-872-422-108] N88-13814
**CENTRE NATIONAL DE LA RECHERCHE SCIENTIFIQUE, MARSEILLES (FRANCE).**
Hot wire and laser velocimeter studies of turbulent flow at supersonic velocities
[ETN-88-91172] N88-13566
**CENTRE NATIONAL DE LA RECHERCHE SCIENTIFIQUE, TOULOUSE (FRANCE).**
Contribution to optimal flow in networks. A experimental multiprocessor for asynchronous iteration implementation
[LAAS-87-269] N88-13510
Digital control of a direct current converter for a hybrid vehicle
[LAAS-87-266] N88-13527
**CENTRO BRASILEIRO DE PESQUISAS FISICAS, RIO DE JANEIRO.**
Non-minimal interaction of gravity with other physical fields: An overview
[DE87-703362] N88-13819
Lagrangian procedures for higher order field equations
[DE87-703365] N88-13911
Computer-aided study of a class of Riemannian space-times
[DE87-703367] N88-13950
Separable orthogonal coordinates and particle creation for an accelerating observer
[DE87-703358] N88-14029
Example of correlation between space and spin coordinates
[DE87-703366] N88-14030
**CENTRO INFORMAZIONI STUDI ESPERIENZE, MILAN (ITALY).**
Low cycle fatigue life predictions of a 1CrMoV steel in terms of a J-controlled short crack growth model N88-13665
**CHALMERS UNIV. OF TECHNOLOGY, GOETEBORG (SWEDEN).**
Crack propagation properties of sintered steel N88-13698

On the geometrical description of fatigue crack surfaces N88-13727
Study of fault tolerant techniques for satellite data handling
[FTT/REP/0001/SAAB] N88-13860

**CHIBA UNIV. (JAPAN).**
Numerical simulation of splash of droplet at unit gravity N88-13275

**CHICAGO UNIV., ILL.**
TOMS as a monitor of the ultraviolet radiation environment: Applications to photobiology N88-13785

**CHINA NUCLEAR INFORMATION CENTRE, BEIJING.**
Development on thin wall tubes of dispersion type
[DE87-703384] N88-13483
Anomalous phonon behavior of superconductor Y-Ba-Cu-O
[DE87-703401] N88-14010

**CHINA SHIP SCIENTIFIC RESEARCH CENTER, WUXI.**
Experimental studies on acoustic emission monitoring of crack propagation in offshore structures: A literature survey N88-13748

**CINCINNATI UNIV., OHIO.**
A spatial marching technique for the inviscid blunt body problem N88-13239
A new method to real-normalize measured complex modes N88-13618
Improvement of modal scaling factors using mass additive technique N88-13620
Simultaneous structural and control optimization via linear quadratic regulator eigenstructure assignment N88-13622

**CLARKSON COLL. OF TECHNOLOGY, POTSDAM, N.Y.**
Extinction by dielectric particles at optical and infrared wavelength
[AD-A184818] N88-13981

**CLARKSON UNIV., POTSDAM, N.Y.**
The matrix exponential in transient structural analysis N88-13619
Eigenvectors of distance-regular graphs
[AD-A185375] N88-13919

**CLEMSON UNIV., S.C.**
Intramolecular energy transfer reactions as a method for metal complex assisted production of hydrogen
[DE88-001621] N88-13425

**COAST GUARD ACADEMY, NEW LONDON, CONN.**
Variable amplitude fatigue crack growth in aluminum alloys 2090-T8E41 and 7075-T651 N88-13687

**COE ENGINEERING, INC., LOS ALTOS, CALIF.**
Predictions of F-111 TACT aircraft buffet response and correlations of fluctuating pressures measured on aluminum and steel models and the aircraft
[NASA-CR-4069] N88-13218

**COLLEGE OF WILLIAM AND MARY, WILLIAMSBURG, VA.**
A requirements specification for a software design support system
[NASA-CR-182333] N88-13896

**COLORADO STATE UNIV., FORT COLLINS.**
Altered and enhanced iodargyrite with bismuth triiodide for use in precipitation enhancement operations
[AD-A185229] N88-13419

**COLORADO UNIV., BOULDER.**
The Portable Instant Display and Analysis Spectrometer (PIDAS) N88-13756
Mapping hydrothermally altered rocks in the Northern Grapevine Mountains, Nevada and California with the airborne imaging spectrometer N88-13772

**COMMANDERS NAVAL AIR FORCES US ATLANTIC AND PACIFIC FLEETS, NORFOLK, VA.**
US Naval Air Force avionic and electrical system corrosion prevention and control maintenance N88-13334

**COMMITTEE ON APPROPRIATIONS (U.S. SENATE).**
National Aeronautics and Space Administration space station proposal, fiscal year 1988
[S-HRG-100-328] N88-14043

**COMMITTEE ON SCIENCE, SPACE AND TECHNOLOGY (U.S. HOUSE).**
The 1988 NASA (National Aeronautics and Space Administration) authorization
[GPO-80-245] N88-14044

**COMMUNICATIONS RESEARCH CENTRE, OTTAWA (ONTARIO).**
Measured characteristics of 800/900 MHz mobile radio channels with high-angle propagation through moderately dense foliage
[CRC-1398] N88-13493

**COMMUNICATIONS SATELLITE CORP., CLARKSBURG, MD.**
Making space nickel/hydrogen batteries lighter and less expensive
[DE88-000168] N88-13530

**COMPLERE, INC., PALO ALTO, CALIF.**
Turbulence measurement in hypersonic flow N88-13224

**CONNECTICUT UNIV., STORRS.**
An overview of fatigue N88-13729

**CONSIGLIO NAZIONALE DELLE RICERCHE, FRASCATI (ITALY).**
Research on Electrodynamic Tether Effects (RETE) experiment Electrical Ground Support Equipment (EGSE)
[IFSI-87-2] N88-13378
Mechanical design of the ac bracket package for the RETE experiment
[IFSI-87-4] N88-13379
RETE experiment Assembly, Integration, and Verification (AIV) activities
[IFSI-87-6] N88-13380
Capacitive resonant transducer for the Frascati gravitational antenna
[IFSI-86-9] N88-13528
The tail lobe ion spectrometer: Theory and observations
[IFSI-86-12] N88-13569
Media calibrations of the Doppler signal for a gravitational wave experiment
[IFSI-86-13] N88-13825
Procedure and program used for data processing in a poll on nuclear energy utilization
[IFSI-87-3] N88-13977
Optical photometer for the Tirgo telescope
[IFSI-87-5] N88-13985
Activities report in interplanetary space physics
[IFSI-86-5] N88-14047
Budget and programs for 1986 research
[IFSI-86-16] N88-14048
Cosmic ray NM-64 neutron monitor data 14, Rome, Italy, January - December 1985
[IFSI-87-8] N88-14060

**CONSIGLIO NAZIONALE DELLE RICERCHE, ROME (ITALY).**
Axial anisotropy of the intensity of the cosmic ray nuclear component
[IFSI-87-7] N88-14061

**CONTROL DATA CORP., MINNEAPOLIS, MINN.**
Application of TOMS data to weather analysis models N88-13787
A single-station weather forecasting expert system
[AD-A184889] N88-13832

**CORNELL UNIV., ITHACA, N.Y.**
Turbulence generation in combustion
[AD-A184810] N88-13413
Cu-2 mechanical properties and microstructural stability of advanced steam cycle materials
[DE88-001519] N88-13452
Illustrative examples of principal component analysis using BMDP/4M
[AD-A185179] N88-13881
Illustrative examples of principal component analysis using SYSTAT/FACTOR
[AD-A184920] N88-13939
Illustrative examples of principal component analysis using GENSTAT/PCP
[AD-A185085] N88-13941

**CRANFIELD INST. OF TECH., BEDFORD (ENGLAND).**
The effects of sweep and bluntness on a glancing shock wave turbulent boundary layer interaction N88-13227

## D

**DANISH METEOROLOGICAL INST., COPENHAGEN.**
The ice conditions in the Greenland waters, 1961
[ISBN-87-7478-276-2] N88-13844

**DAYTON UNIV., OHIO.**
Correlation of air pressure drop and flame arrestor characteristics for explosion suppression materials
[AD-A184960] N88-13340
Asymptotic analysis of a turbulent boundary layer in a strong adverse pressure gradient
[AD-A185406] N88-13543

**DELAWARE UNIV., NEWARK.**
AIS-2 spectra of California wetland vegetation N88-13763

**DEPARTMENT OF AGRICULTURE, BUSHLAND, TEX.**
An overview of the DOE/SANDIA/USDA vertical axis wind turbine Test Bed Project
[DE88-000604] N88-13812

**DEPARTMENT OF DEFENSE, WASHINGTON, D. C.**
University research initiative research program summaries
[AD-A184876] N88-14035

**DEUTSCHE FORSCHUNGS- UND VERSUCHSANSTALT FUER LUFT- UND RAUMFAHRT, COLOGNE (WEST GERMANY).**
Fatigue mechanisms in ARALL, a fatigue resistant hybrid aluminum aramid composite material N88-13711

**DEUTSCHE FORSCHUNGS- UND VERSUCHSANSTALT FUER LUFT- UND RAUMFAHRT, GOETTINGEN (WEST GERMANY).**
Low Reynolds number influence on aerodynamic performance of hypersonic lifting vehicles N88-13230
On the numerical simulation of three-dimensional hypersonic flow N88-13237

**DIRECTION DES RECHERCHES ETUDES ET TECHNIQUES, PARIS (FRANCE).**
Ultrafast intrinsic bistable devices
[PB87-109310] N88-13978

**DORNIER-WERKE G.M.B.H., FRIEDRICHSHAFEN (WEST GERMANY).**
Solution of some 3-D viscous and inviscid supersonic flow problems by finite-volume space-marching schemes N88-13235

**DRAPER (CHARLES STARK) LAB., INC., CAMBRIDGE, MASS.**
Satellite autonomous navigation with SHAD (Stellar Horizon Atmospheric Dispersion)
[AD-A184988] N88-13313

**DREXEL UNIV., PHILADELPHIA, PA.**
A fundamental study of P/M processed elevated temperature aluminum alloys
[AD-A185393] N88-13445

**DUKE UNIV., DURHAM, N. C.**
Studies on syntheses of amine-carboxyboranes (boron analogues of amino acids) and derivatives
[AD-A184838] N88-13386
An examination of chaotic motion for the buckled beam N88-13644
Near-horn prolog
[AD-A185172] N88-13880

**DURHAM UNIV. (ENGLAND).**
Preliminary results from an investigation of AIS-1 data over an area of epithermal alteration: Plateau, Northern Queensland, Australia N88-13768

## E

**ECOLE CENTRALE DE LYON (FRANCE).**
Fretting wear and fretting fatigue damage N88-13697

**ECOLE DES MINES, PARIS (FRANCE).**
Low cycle fatigue behaviour of notched specimens of nickel based superalloy single crystal N88-13712

**ECOLE NATIONALE SUPERIEURE DE LA METALLURGIE ET DE L'INDUSTRIE DES MINES, STE. ETIENNE (FRANCE).**
Coupling effects between the ferrite and austenite phases during corrosion fatigue of a ferrite/austenite duplex stainless steel N88-13706

**ECOLE POLYTECHNIQUE, MONTREAL (QUEBEC).**
The orientations of dipolar walls produced by cyclic deformation N88-13655
Closure and propagation behavior of short fatigue cracks at different R-ratios N88-13679

**EDGERTON, GERMESHAUSEN AND GRIER, INC., IDAHO FALLS, IDAHO.**
Oxygen enriched combustion system performance study
[DE88-001500] N88-13424
Tensile properties of extrusion consolidated Type 304 SS rapidly solidified powders
[DE87-014875] N88-13450
Acoustic emissions at an open crack
[DE88-001504] N88-13751

**EG AND G ENERGY MEASUREMENTS, INC., WOBURN, MASS.**
A focussed MCP (microchannel plate) image intensifier type for high speed gating
[DE88-000480] N88-13555

**ENERGY AND ENVIRONMENTAL RESEARCH CORP., IRVINE, CALIF.**
Oxygen enriched combustion system performance study
[DE88-001500] N88-13424

**ENVIRO-MANAGEMENT AND RESEARCH, INC., SPRINGFIELD, VA.**
Survey state of the art: Electrical load management techniques and equipment
[AD-A184083] N88-13517

**ENVIRONMENTAL PROTECTION AGENCY, RESEARCH TRIANGLE PARK, N.C.**
Short-term in vitro screening studies related to the inhalation toxicology of potentially toxic aerosols
[AD-A184815] N88-13845

**ENVIRONMENTAL PROTECTION AGENCY, WASHINGTON, D.C.**
Innovative and alternative technology projects
[PB87-230165] N88-13818

**EOETVOES LORAND FIZIKAI TARSULAT, BUDAPEST (HUNGARY).**
Proceedings of the 17th International Conference on Phenomena in Ionized Gases held in Budapest, Hungary, July 8-12, 1985: Invited papers
[DE87-703562] N88-13987
**ETA SYSTEMS, INC., SAINT PAUL, MINN.**
Supercomputing at Florida State University (FSU)
[DE87-013900] N88-14009

## F

**FEDERAL COMMUNICATIONS COMMISSION, COLUMBIA, MD.**
Two-signal cross modulation effects, half-IF effects and interference criteria in land mobile sharing with UHF (Ultra High Frequency) television
[PB87-228037] N88-13514
**FENG CHIA UNIV., TAICHUNG (TAIWAN).**
Dynamic response of laminated composite plates using a three-dimensional hybrid-stress finite-element formulation N88-13639
**FIRMA FICHT G.M.B.H., KIRCHSEEON (WEST GERMANY).**
Development, construction and testing of a novel internal combustion engine with conical rotating slide valve
[DE88-900071] N88-13593
**FLORIDA STATE UNIV., TALLAHASSEE.**
Supercomputing at Florida State University (FSU)
[DE87-013900] N88-14009
**FLORIDA UNIV., GAINESVILLE.**
Introduction to string field theory
[DE87-014583] N88-14032
**FORD MOTOR CO., DEARBORN, MICH.**
Applications of fatigue analyses: Transportation N88-13733
**FUJI HEAVY INDUSTRIES LTD., UTSUNOMIYA (JAPAN).**
Computation of nacelle interference using boundary element method N88-13267
**FUJITSU LTD., TOKYO (JAPAN).**
Practical and modern simulation by systematic connection of the LU-ADI code and the solution adaptive grid program N88-13260
Visualization of an aircraft accident based on digital flight data recorder information N88-13278

## G

**GENERAL DYNAMICS CORP., FORT WORTH, TEX.**
Closure behavior under constant effective stress intensity loading conditions N88-13656
**GENERAL ELECTRIC CO., SCHENECTADY, N.Y.**
Modeling the effect of sulfur on the threshold environmental cracking rate of steels in high temperature water N88-13703
**GENERAL MOTORS RESEARCH LABS., WARREN, MICH.**
The growth of persistent slip bands N88-13648
**GEOLOGICAL SURVEY, DENVER, COLO.**
Causes of spurious features in spectral reflectance data N88-13769
Automatic continuum analysis of reflectance spectra N88-13770
**GEOLOGICAL SURVEY, RESTON, VA.**
Analysis of airborne imaging spectrometer data for the Ruby Mountains, Montana, by use of absorption-band-depth images N88-13771
**GEOMET TECHNOLOGIES, INC., GERMANTOWN, MD.**
ZEUS: A knowledge-based expert system that assists in predicting visibility at airbases
[AD-A184197] N88-13829
**GEORGE WASHINGTON UNIV., WASHINGTON, D.C.**
Explicit formulate for the distributions of stopping variables under Wald's truncated SPRT (Sequential Probability Radio Tests) for a poisson process
[AD-A185053] N88-13914
**GEORGETOWN UNIV., WASHINGTON, D.C.**
Study of the properties of a new detector class for liquid chromatography
[DE88-001666] N88-13426
**GEORGIA INST. OF TECH., ATLANTA.**
An investigation of millimeter wave propagation in the atmosphere: Measurement program
[AD-A184837] N88-13498
Solution procedure for the Navier-Stokes equations applied to rotors N88-13533
Coupled elastic rotor/body vibrations with inplane degrees of freedom N88-13643
Telemetric laser extensometry technique for monitoring deflections in small cracks N88-13724
Deformation, fatigue and fracture behavior of two cast anisotropic superalloys N88-13732
**GIFU UNIV. (JAPAN).**
The growth behavior of small fatigue cracks; the effect of microstructure and crack closure N88-13673
**GLASGOW UNIV. (SCOTLAND).**
Numerical experiments with hypersonic flows beneath a cone-delta-wing combination N88-13238
**GRONINGEN RIJKSUNIVERSITEIT (NETHERLANDS).**
Equivalence of input-output stability and exponential stability for infinite dimensional systems
[TW-276] N88-13903
A construction of simple Abelian varieties
[ZW-8702] N88-13929

## H

**HARRY DIAMOND LABS., ADELPHI, MD.**
Resonant level lifetime in GaAs/ AlGaAs double-barrier structures
[AD-A185376] N88-14020
**HELSINKI UNIV. (FINLAND).**
Two low-order mixed methods for the elasticity problem
[PB87-225272] N88-13749
**HONEYWELL, INC., GLENDALE, ARIZ.**
Viscous damped space structure for reduced jitter N88-13623
**HUNGARIAN ACADEMY OF SCIENCES, BUDAPEST.**
Proceedings of the 17th International Conference on Phenomena in Ionized Gases held in Budapest, Hungary, July 8-12, 1985: Invited papers
[DE87-703562] N88-13987

## I

**ILLINOIS UNIV., CHICAGO.**
Approximating multivariate normal orthant probabilities using the Clark algorithm
[AD-A184855] N88-13673
**ILLINOIS UNIV., URBANA.**
Design of low order controllers for robust disturbance rejection in large space structures
[AD-A185202] N88-13376
Eigenvalue projection theory for linear operator equations of electromagnetics
[AD-A185434] N88-13504
Computer simulation of cw HF chemical laser unstable resonator performance
[AD-A185059] N88-13581
An experimental study of CW HF chemical laser amplifier performance and zero power gain
[AD-A185241] N88-13584
Constraint effects in fatigue crack growth N88-13719
Analysis of the breakdown of the Antarctic circumpolar vortex using TOMS ozone data N88-13779
Efficient computation of periodic Green's functions with application to grating structures
[AD-A184853] N88-13912
**ILLINOIS UNIV., URBANA-CHAMPAIGN.**
File usage analysis and resource usage prediction: A measurement-based study
[NASA-CR-181553] N88-13867
Usage analysis of user files in UNIX
[NASA-CR-181561] N88-13868
Predictability of process resource usage: A measurement-based study of UNIX
[NASA-CR-181562] N88-13869
Performability modeling based on real data: A casestudy
[NASA-CR-181563] N88-13870
Diagnostic reasoning in digital systems
[NASA-CR-181564] N88-13871
Error propagation in a digital avionic mini processor
[NASA-CR-181565] N88-13872
**IMPERIAL COLL. OF SCIENCE AND TECHNOLOGY, LONDON (ENGLAND).**
Computation of flow past conical hypersonic wings using a second order Godunov method N88-13241
**INDIAN INST. OF TECH., MADRAS.**
Fatigue characteristics of ion treated surfaces N88-13713
**INDUSTRIAL MARINE PRODUCTS GROUP LTD., DARTMOUTH (NOVA SCOTIA).**
Corrosion in avionics and associated equipment; cause, effect and prevention N88-13335
**INDUSTRIEANLAGEN-BETRIEBSGESELLSCHAFT M.B.H., OTTOBRUNN (WEST GERMANY).**
On the simulation of ballistic shock loads N88-13615
The how and why of variable amplitude testing N88-13690
**INFORMATION AND CONTROL SYSTEMS, INC., HAMPTON, VA.**
Development of response models for the Earth Radiation Budget Experiment (ERBE) sensors. Part 3: ERBE scanner measurement accuracy analysis due to reduced housekeeping data
[NASA-CR-178294] N88-13553
Development of response models for the Earth Radiation Budget Experiment (ERBE) sensors. Part 1: Dynamic models and computer simulations for the ERBE nonscanner, scanner and solar monitor sensors
[NASA-CR-178292] N88-13557
Investigation, development, and application of optimal output feedback theory. Volume 3: The relationship between dynamic compensators and observers and Kalman filters
[NASA-CR-4107] N88-13900
**INSTITUT DE MECANIQUE DES FLUIDES DE LILLE (FRANCE).**
Wakes of two dimensional bluff bodies in subsonic flow. Influence of a separating plate and of a pulsed injection of momentum
[IMFL-4200-86/75] N88-13297
Determination of a flow velocity field using four-exposure laser holography
[IMFL-3114-85/32] N88-13565
**INSTITUT DE MECANIQUE DES FLUIDES DE TOULOUSE (FRANCE).**
Physical analysis and numerical simulation of coherent turbulent structures in mixed layers, jets, and wakes
[ETN-88-91183] N88-13548
**INSTITUT FRANCAIS DU PETROLE, PARIS (FRANCE).**
Design and test of high performance composite tubes for use in deep water drilling and production systems
[SNIAS-872-430-107] N88-13487
**INSTITUT FRANCO-ALLEMAND DE RECHERCHES, ST. LOUIS (FRANCE).**
An ultra-high-speed cinematographic method for the study of wakes in hypersonic ballistic ranges N88-13228
Production of flows for aeroballistic investigation in the shock tubes of the Franco-German Research Institute (ISL), Saint-Louis (France)
[ISL-R-113/86] N88-13295
Trajectory control using laterally ejected jets. Literature review
[ISL-R-117/85] N88-13544
Investigation of the effect of laterally ejected gas jets on flows
[ISL-R-107/86] N88-13545
Optoelectronic measurement methods for ballistic experiments
[PB87-110706] N88-13554
Transient processes in the interaction between pulsed laser radiation and matter
[ISL-R-115/86] N88-13566
**INSTITUT NATIONAL DES SCIENCES APPLIQUEES DE LYON, VILLEURBANNE (FRANCE).**
Dynamic behavior of disymmetric rotor bearings modelled with a periodic coefficient large system N88-13640
**INSTITUTE FOR PERCEPTION RVO-TNO, SOESTERBERG (NETHERLANDS).**
Taskomat, a task battery for information processing
[IZF-1987-2] N88-13851
Sitting posture of helicopter pilots of the Royal Netherlands Air Force; preliminary recommendations
[IZF-1986-16] N88-13857
The use of color in electronic maps. Part 1: Generation and analysis of color on the Gould/DeAnza image processing system
[IZF-1986-32] N88-13882
**INTERNATIONAL BUSINESS MACHINES CORP., POUGHKEEPSIE, N.Y.**
Computer aided modeling and fatigue failure forecast under stochastic loading N88-13720
**IOWA STATE UNIV. OF SCIENCE AND TECHNOLOGY, AMES.**
Effects of free stream turbulence, Reynolds number and incidence angle on axial turbine cascade performance N88-13339
**IOWA UNIV., IOWA CITY.**
Fatigue crack growth behavior of A356-T6 cast aluminum alloy N88-13680
**ISHIKAWAJIMA-HARIMA HEAVY INDUSTRIES CO. LTD., TOKYO (JAPAN).**
Numerical prediction of turbulent flows in dump diffusers N88-13265

## J

**JAYCOR, VIENNA, VA.**
High peak power ka-band gyrotron oscillator experiment
[AD-A185424] N88-13563

**JET PROPULSION LAB., CALIFORNIA INST. OF TECH., PASADENA.**
Proceedings of the Third Airborne Imaging Spectrometer Data Analysis Workshop
[NASA-CR-181552] N88-13755
AIS-2 radiometry and a comparison of methods for the recovery of ground reflectance N88-13757
Guidance for conference rapporteurs
[NASA-CR-182338] N88-14042

**JOHN B. PIERCE FOUNDATION OF CONNECTICUT, NEW HAVEN.**
Microwave challenges to the thermoregulatory system
[AD-A185391] N88-13847

**JOHNS HOPKINS UNIV., BALTIMORE, MD.**
Full field visualization of surface and bulk acoustic waves using heterodyne holographic interferometry
[AD-A185071] N88-13958

**JOHNS HOPKINS UNIV., LAUREL, MD.**
Hypersonic airbreathing propulsion: Evolution and opportunities N88-13231

**JOHNSON CONTROLS, INC., MILWAUKEE, WIS.**
Making space nickel/hydrogen batteries lighter and less expensive
[DE88-000168] N88-13530

## K

**KANSAS STATE UNIV., MANHATTAN.**
Activated metal oxide surfaces as highly basic and reducing environments
[AD-A184958] N88-13417
Atomic physics with highly charged ions
[DE88-000894] N88-13972

**KAWASAKI HEAVY INDUSTRIES LTD., KAGAMIHARA (JAPAN).**
A numerical investigation on wing/nacelle interferences N88-13258
The role of computation fluid dynamics in aeronautical engineering (4). The development and applications of implicit TVD finite volume code N88-13259

**KEIO UNIV., TOKYO (JAPAN).**
Computation of flow around 2-D circular cylinder N88-13284
United States - Japan Workshop on Dielectric and Piezoelectric Ceramics (3rd) held in Toyama, Japan on November 9-12, 1986
[AD-A185113] N88-13460

**KERNFORSCHUNGSANLAGE, JUELICH (WEST GERMANY).**
ALT-1 pump limiter experiments
[DE88-000822] N88-13989

**KEVEX, INC., FOSTER CITY, CALIF.**
X-ray imaging: Status and trends
[DE88-000756] N88-13980

**KYOTO UNIV. (JAPAN).**
Numerical calculations of the flowfield around propellers N88-13261
Numerical analysis of flow characteristics of supersonic free-jets N88-13274
Propagation of small fatigue cracks in 2024-T3 aluminum alloy N88-13678

**KYUSHU UNIV., FUKUOKA (JAPAN).**
Threshold stress for fatigue crack initiation from a small crack N88-13675

## L

**LABORATORIO DE COMPUTACAO CIENTIFICA, RIO DE JANEIRO (BRAZIL).**
Qualification of expansion and joint welding procedures of tube-to-tubesheet joints for heat exchangers in nuclear power plants
[DE87-703526] N88-13592
Welded joint fatigue of a AISI 304 L type stainless steel
[DE87-703530] N88-13607
Finite element model for the stress and flexibility analysis of curved pipes
[DE87-703632] N88-13608

**LAWRENCE LIVERMORE NATIONAL LAB., CALIF.**
Streak camera dynamic range optimization
[DE88-001632] N88-13571
Resolution limitations and optimization of the LLNL streak camera focus
[DE88-001633] N88-13572
Theory of multiphoton ionization of atoms by strong, short pulsed lasers
[DE88-000963] N88-13588
A long electromagnetic wiggler for the paladin free-electron laser experiments
[DE88-000970] N88-13589
Free Lagrange reconnection algorithms for hydrocodes using a quadrilateral mesh
[DE88-001580] N88-13752
Conceptual issues in measuring the behavior of a distributed real-time process-control computer system
[DE87-009748] N88-13898
Conceptual issues in measuring the behavior of a distributed real-time process-control computer system
[DE87-014251] N88-13899
Development of a strong electromagnet wiggler
[DE88-000971] N88-13952
Development of a laced electromagnetic wiggler
[DE88-000972] N88-13953
X-ray imaging: Status and trends
[DE88-000756] N88-13980

**LEHIGH UNIV., BETHLEHEM, PA.**
Vortex interaction with a leading-edge of finite thickness
[NASA-CR-182341] N88-13307
Effect of test temperature and frequency on fatigue crack propagation in PVC N88-13715
Environmentally assisted fatigue crack growth N88-13731

**LISBON UNIV. (PORTUGAL).**
Behavior of short cracks in a 2024 aluminum alloy sheet tested at several stress ratios N88-13669

**LJUBLJANA UNIV. (YUGOSLAVIA).**
Occurance and growth of fatigue cracks in corrosion environment N88-13704

**LOCKHEED-CALIFORNIA CO., BURBANK.**
The off-design performance of hypersonic waveriders N88-13244

**LOS ALAMOS NATIONAL LAB., N. MEX.**
Molecular and supramolecular orientation in conducting polymers
[DE88-000533] N88-13472
Jet initiation of PBX 9502
[DE88-000493] N88-13481
Transient development of stratification in a partially divided enclosure
[DE87-011742] N88-13490
Computer code simulations of explosions in flow networks and comparison with experiments
[DE88-001946] N88-13491
Statistical theory of turbulent incompressible multimaterial flow
[DE88-000435] N88-13535
A focussed MCP (microchannel plate) image intensifier type for high speed gating
[DE88-000480] N88-13555
Chemical analysis for excimer laser systems
[DE88-001941] N88-13591
Mixing Microsoft C and Microsoft FORTRAN program modules on the IBM Personal Computer
[DE88-001947] N88-13895
Chaos: Chto Delat? (What is to be done?)
[DE88-000513] N88-13933
Modeling and generating input processes
[DE87-013162] N88-13948
Theory of neutron scattering experiments on momen tum distributions in quantum fluids
[DE87-01369] N88-13968
Dynamic processes in field-reversed-configuration compact toroids
[DE87-014756] N88-13998
A short introduction to the status and motivation for reversed field pinch and compact toroid research
[DE88-000487] N88-13999
A review of the experimental and theoretical status of the reversed-field pinch
[DE88-000529] N88-14000
Numerical models for high beta magnetohydrodynamic flow
[DE88-001850] N88-14008
An automated supernova search and the design strategy
[DE88-001827] N88-14051
Magnetic field draping about coronal mass ejecta
[DE88-001805] N88-14057

**LOUISIANA STATE UNIV., BATON ROUGE.**
Molecular dynamics studies of aromatic hydrocarbon liquids
[DE88-001473] N88-13973

## M

**MAHARISHI INTERNATIONAL UNIV., FAIRFIELD, IOWA.**
Solitons in stimulated Raman scattering: Generation and control of ultrashort optical pulses
[AD-A185141] N88-13983

**MANCHESTER COLL. OF SCIENCE AND TECHNOLOGY (ENGLAND).**
The influence of crack conditions on hydrogen uptake by steels N88-13702

**MARCONI ELECTRONIC DEVICES LTD., LINCOLN (ENGLAND).**
Optically tuned MM-wave IMPATT source
[AD-A185250] N88-13523

**MARTIN MARIETTA CORP., DENVER, COLO.**
Feasibility study for gas-grain simulation facility
[NASA-CR-177468] N88-13954

**MARYLAND UNIV., COLLEGE PARK.**
Numerical optimization of conical flow waveriders including detailed viscous effects N88-13245
High peak power ka-band gyrotron oscillator experiment
[AD-A185424] N88-13563
Range imagery algorithms for the detection of obstacles by autonomous vehicles
[AD-A185421] N88-14045

**MARYLAND UNIV. BALTIMORE COUNTY, CATONSVILLE.**
Numerical methods for reaction-diffusion problems with non-differentiable kinetics
[AD-A185405] N88-13923

**MASSACHUSETTS INST. OF TECH., CAMBRIDGE.**
Velocity scaled aeroelastic testing of an unducted fan
[GTL-191] N88-13337
Survey on large scale system control methods
[NASA-CR-181556] N88-13374
Effect of rapid solidification on short-range order: A magnetic study
[AD-A185216] N88-13444
Soluble metal chelate polymers of coordination numbers six, seven and eight
[AD-A185094] N88-13459
Time domain electromagnetic waves in multilayered media
[AD-A185055] N88-13502
Model-based motion estimation and its application to restoration and interpolation of motion pictures
[AD-A185054] N88-13558
Phase-locked semiconductor quantum well laser arrays
[AD-A185155] N88-13583
Dynamics of cables and chains N88-13747
Learning a color algorithm from examples
[AD-A184385] N88-13862
The interaction of DC plasma jet with a melting metal: Experimental measurements and mathematical description
[AD-A185173] N88-13993
T.E.M. study of boehmite gels and of their transformation into alpha-alumina
[SNIAS-872-430-121] N88-14023

**MASSACHUSETTS UNIV., AMHERST.**
Molecular-level synthesis and characterization of metal-polymer interfaces
[AD-A184956] N88-13455

**MATERIALS RESEARCH LABS., ASCOT VALE (AUSTRALIA).**
An examination of coating failure on wing pivot fittings of f111 aircraft
[AD-A185028] N88-13328
High explosive moulding powders from RDX and aqueous polyurethane dispersions
[AD-A185026] N88-13458

**MATERIALS RESEARCH LABS., MELBOURNE (AUSTRALIA).**
Application of finite element methods with cyclic elasto-plastic strain analysis to low cycle fatigue analysis of engine components
[AR-004-512] N88-13642

**MAX-PLANCK-INST. FUER METALLFORSCHUNG, STUTTGART (WEST GERMANY).**
Fatigue crack propagation in Al-Zn-Mg bicrystals and its dependence on the environment N88-13707
Deformation mechanisms and crack initiation in fatigue N88-13730

**MCDONNELL-DOUGLAS RESEARCH LABS., ST. LOUIS, MO.**
The influence of slip mechanism on fatigue of Mg and Mg-2.3Li N88-13672

**MECHANICAL TECHNOLOGY, INC., LATHAM, N. Y.**
Seal technology for liquid oxygen (LOX) turbopumps
[NASA-CR-174866] N88-13603
On the glitches in the force transmitted by an electrodynamic exciter to a structure N88-13624

**MESSERSCHMITT-BOELKOW-BLOHM G.M.B.H., HAMBURG (WEST GERMANY).**
Vortex formation over delta, double-delta and wave rider configurations at supersonic speeds N88-13243

**MESSERSCHMITT-BOELKOW-BLOHM G.M.B.H., MUNICH (WEST GERMANY).**
A 3-D Euler solution for hypersonic Mach numbers N88-13240
Fundamentals of fighter aircraft design N88-13316
Aeroelasticity and optimization in fighter aircraft design N88-13324

The role of experimental investigation and computational fluid dynamics during fighter aircraft design N88-13326
Static aeroelastic considerations in the definition of design loads for fighter airplanes N88-13351
Hermes propulsion system
[SNIAS-872-422-109] N88-13383

**METALLURGICAL CONSULTING SERVICES LTD., SASKATOON (SASKATCHEWAN).**
Observations on the effect of overloads on fatigue crack growth N88-13684

**METRAFLU, ECULLY (FRANCE).**
Compressor large bandwidth noise emission mechanisms
[ETN-88-91177] N88-13959

**METZ UNIV. (FRANCE).**
A dislocation model for fatigue crack propagation under variable amplitude loading N88-13683

**MICHIGAN STATE UNIV., EAST LANSING.**
The effect of ion beam mixed Ni-Al surface layers on PSB extrusion morphology in fatigued nickel N88-13652

**MICHIGAN UNIV., ANN ARBOR.**
Shape optimization of damping layers N88-13635
The effects of thin anodic films on the cyclic microstrain/macrostrain behavior of tungsten N88-13650
On linear periodic controllers
[DE87-011174] N88-13904
On the correlation free forms for nonlinear stochastic systems
[DE87-011169] N88-13947

**MICROCOATINGS, WESTFORD, MASS.**
High resolution ultraviolet filter development
[AD-A184183] N88-13979

**MIDWEST RESEARCH INST., GOLDEN, COLO.**
Accurate rotor loads prediction using the FLAP (Force and Loads Analysis Program) dynamics code
[DE88-001109] N88-13815

**MINISTRY OF TRANSPORT AND WATERWAYS, THE HAGUE (NETHERLANDS).**
Civil aeronautics
[ETN-88-90616] N88-13309

**MISSOURI UNIV., KANSAS CITY.**
A comparison of plastic work energy and external input for fatigue crack propagation N88-13722

**MITSUBISHI ELECTRIC CO., AMAGASAKI (JAPAN).**
Fatigue strength of alloy A286 at cryogenic temperature N88-13695

**MITSUBISI ELECTRIC CORP., TOKYO (JAPAN).**
Numerical analysis of supersonic flows using panel method N88-13266

**MITSUBISHI HEAVY-INDUSTRIES LTD., TOKYO (JAPAN).**
Practical application of two-dimensional viscous flow computation N88-13257
Numerical simulation of transonic aircraft in comparison to wind tunnel test N88-13289

**MMR TECHNOLOGIES, INC., MOUNTAIN VIEW, CALIF.**
Development of a low noise 10 K J-T refrigeration system
[AD-A185258] N88-13484

**MONTANA UNIV., MISSOULA.**
Measuring near infrared spectral reflectance changes from water stressed conifer stands with AIS-2 N88-13765

**MSNW, INC., SAN MARCOS, CALIF.**
Plasma joining of metal matrix composites
[AD-A184828] N88-13390

## N

**NAGOYA UNIV. (JAPAN).**
Energy dependence of ion-induced sputtering yields of monatomic solids in the low energy region
[IPPJ-AM-52] N88-13988

**NATIONAL AERONAUTICAL LAB., BANGALORE (INDIA).**
Model helicopter rotor rig and associated strain gauge balance for performance studies
[NAL-TM-AE-8704] N88-13364
Non-linear maximum likelihood estimation of stability derivatives from range data
[NAL-TM-SE-8608] N88-13365
Analysis of nickel sulphamate bath using charging current compensated D.C. polarography
[NAL-TM-MT-8705] N88-13433
X-ray analysis of polycrystalline aluminium subjected to fatigue cycling
[NAL-TM-MT-8706] N88-13434
Analysis of wear metals in engine oils using the atomic absorption spectrophotometric method
[NAL-TM-MT-8704] N88-13435

**NATIONAL AERONAUTICS AND SPACE ADMINISTRATION, WASHINGTON, D.C.**
Space station systems: A bibliography with indexes (Supplement 05)
[NASA-SP-7056(05)] N88-13382
Astronautics and aeronautics, 1978: A chronology
[NASA-SP-4023] N88-14062

**NATIONAL AERONAUTICS AND SPACE ADMINISTRATION. AMES RESEARCH CENTER, MOFFETT FIELD, CALIF.**
Numerical simulation of the hypersonic flow around lifting vehicles N88-13234
Aerothermodynamics research at NASA Ames N88-13242
A perspective of computational fluid dynamics N88-13279
Tip aerodynamics from wind tunnel test of semi-span wing
[NASA-TM-88253] N88-13290
An experimental investigation of the aerodynamics of a NACA 64A010 airfoil-flap combination with and without flap oscillations. Part 1: Steady-state characteristics
[NASA-TM-88217] N88-13305
Interferometric data for a shock-wave/boundary-layer interaction
[NASA-TM-88227] N88-13306
Integrated control and display research for transition and vertical flight on the NASA V/STOL Research Aircraft (VSRA)
[NASA-TM-100029] N88-13359
Full-envelope aerodynamic modeling of the Harrier aircraft
[NASA-TM-88376] N88-13363
Development of an interface for an ultrareliable fault-tolerant control system and an electronic servo-control unit
[NASA-TM-88236] N88-13367
Vortical Flows Research Program of the Fluid Dynamics Research Branch
[NASA-TM-88332] N88-13549
The use of airborne imaging spectrometer data to determine experimentally induced variation in coniferous canopy chemistry N88-13761
Toward detecting California shrubland canopy chemistry with AIS data N88-13764
Controlled Ecological Life Support System. Design, Development, and Use of a Ground-Based Plant Growth Module
[NASA-CP-2479] N88-13852
CELSS Program Meeting N88-13853
Controlled ecological life support systems: Development of a plant growth module N88-13854
Plant Growth Module (PGM) conceptual design N88-13855
A system of three-dimensional complex variables
[NASA-TM-88318] N88-13951

**NATIONAL AERONAUTICS AND SPACE ADMINISTRATION. GODDARD SPACE FLIGHT CENTER, GREENBELT, MD.**
COSPAS-SARSAT satellite orbit predictor, volume 10
[NASA-TM-85015] N88-13370
A computer code to process and plot laser altimetry data interactively on a microcomputer
[NASA-TM-100687] N88-13371
A computer code to calculate line by line atmospheric transmission spectra on a microcomputer
[NASA-TM-100686] N88-13372
Trajectory control of robot manipulators with closed-kinematic chain mechanism
[NASA-TM-89305] N88-13605
In-orbit calibration adjustment of the Nimbus-7 SMMR
[NASA-TM-100678] N88-13773
Scientific and Operational Requirements for TOMS Data
[NASA-CP-2497] N88-13774
TOMS: The Antarctic ozone hole and ozone trends N88-13775
October lower stratospheric Antarctic temperature and total ozone from 1979-1985 N88-13776
Photochemical ozone overburden correction N88-13778
Insights into the general circulation of the lower stratosphere from TOMS N88-13780
Ozone, jet streaks and severe weather N88-13781
Lower-stratospheric/upper-tropospheric exchange processes associated with tropical cyclones as observed by TOMS N88-13782
Northwest Airlines flight experiments N88-13786
Correlations of TOMS total ozone data (Nimbus-7 satellite) with tropopause height N88-13788
An analysis of tropopause pressure and total ozone correlations N88-13789
TOMS ozone data compared at mesoscale resolution to tropopause heights from the AVE radiosonde network and to VAS radiances over the south-central United States N88-13790
The use of TOMS-modified VAS data for large-scale NWP N88-13791
Volcanic eruption detection with TOMS N88-13793
Analysis of SO2 signals in SBUV/TOMS data N88-13794
Determination of total ozone from HIRS2/MSU sounding data N88-13799
Complementary information between UV and IR for remote sensing of total ozone N88-13800
Observation guidelines for a Total Ozone Mapping Spectrometer (TOMS) in geosynchronous orbit N88-13801
A geostationary imaging spectrometer TOMS instrument N88-13802
Global atmospheric circulation statistics: Four year averages
[NASA-TM-100690] N88-13842

**NATIONAL AERONAUTICS AND SPACE ADMINISTRATION. LANGLEY RESEARCH CENTER, HAMPTON, VA.**
Numerical analysis of flow through scramjet engine inlets N88-13233
Nonlinear lift control at high speed and high angle of attack using vortex flow technology N88-13319
Static aeroelastic effects on the flutter of a supercritical wing N88-13353
Prediction of wing aeroelastic effects on aircraft life and pitching moment characteristics N88-13356
Design and assembly sequence analysis of option 3 for CETF reference space station
[NASA-TM-100503] N88-13369
An analytical study of the effects of transverse shear deformation and anisotropy on buckling loads of laminated cylinders
[NASA-TM-100508] N88-13387
Potential for on-orbit manufacture of large space structures using the pultrusion process
[NASA-TM-4016] N88-13388
Flexibilized copolyimide adhesives
[NASA-TM-89303] N88-13474
Strain-energy-release rate analysis of the end-notched flexure specimen using the finite-element method
[NASA-TM-100494] N88-13735
The use of TOMS data for tropospheric ozone studies N88-13784
Effectiveness of back-to-back testing
[TR-87-08] N88-13865
Fluctuating pressure loads under high speed boundary layers
[NASA-TM-100517] N88-13962
Preliminary estimates of galactic cosmic ray exposures for manned interplanetary missions
[NASA-TM-100519] N88-14058

**NATIONAL AERONAUTICS AND SPACE ADMINISTRATION. LEWIS RESEARCH CENTER, CLEVELAND, OHIO.**
Automated design of controlled diffusion blades
[NASA-TM-100251] N88-13304
Combustion characteristics of gas turbine alternative fuels
[NASA-TM-100247] N88-13338
Regressed relations for forced convection heat transfer in a direct injection stratified charge rotary engine
[NASA-TM-100124] N88-13345
Unsteady aerodynamics of an oscillating cascade in a compressible flow field
[NASA-TM-100219] N88-13346
A numerical study of the effects of curvature and convergence on dilution jet mixing
[NASA-TM-89878] N88-13347
Phase purity of NiCo2O4, a catalyst candidate for electrolysis of water
[NASA-TM-100239] N88-13385
Fiber composite structural durability and damage tolerance: Simplified predictive methods
[NASA-TM-100179] N88-13409
Detailed mechanism of toluene oxidation and comparison with benzene
[NASA-TM-100261] N88-13428
Coatings for high-temperature bearings and seals
[NASA-TM-100249] N88-13453
Communications payload concepts for geostationary facilities
[NASA-TM-100154] N88-13513
An evolutionary communications scenario for Mars exploration
[NASA-TM-100263] N88-13515
Measurement of local convective heat transfer coefficients from a smooth and roughened NACA-0012 airfoil: Flight test data
[NASA-TM-100284] N88-13552
Finite-element grid improvement by minimization of stiffness matrix trace
[NASA-TM-100255] N88-13604

Thermal finite-element analysis of space shuttle main engine turbine blade
[NASA-TM-100117] N88-13745
A computer program for calculating unsteady aerodynamic coefficients for cascades in supersonic axial flow
[NASA-TM-100204] N88-13753
STAEBL/general composites with hygrothermal effects (STAEBL/GENCOM)
[NASA-TM-100266] N88-13754
SHARP simulation of discontinuities in highly convective steady flow
[NASA-TM-100240] N88-13931
High speed propeller performance and noise predictions at takeoff/landing conditions
[NASA-TM-100267] N88-13960
Noise of a model counterrotation propeller with reduced aft rotor diameter at simulated takeoff/approach conditions (F7/A3)
[NASA-TM-100254] N88-13961
Progress toward the evolution of a Stirling space engine
[NASA-TM-100221] N88-14046
Small space reactor power systems for unmanned solar system exploration missions
[NASA-TM-100228] N88-14054

**NATIONAL AERONAUTICS AND SPACE ADMINISTRATION. MARSHALL SPACE FLIGHT CENTER, HUNTSVILLE, ALA.**
The 58th Shock and Vibration Symposium, volume 1
[NASA-CP-2488-VOL-1] N88-13609
High frequency data acquisition system for space shuttle main engine testing N88-13630
Space shuttle main engine vibration data base N88-13631

**NATIONAL AEROSPACE LAB., AMSTERDAM (NETHERLANDS).**
Simulated service test behavior of various internal and external coatings applied on CF6-50 first stage turbine blades
[NLR-MP-86018-U] N88-13343
Overlooked potential of systems with Markovian coefficients
[NLR-MP-86049-U] N88-13366
National Point Of Contact (NPOC)-SPOT inquiry 1986
[NLR-MP-86055-U] N88-13807
Study on data compression systems for operational remote sensing
[NLR-TR-86029-L] N88-13808

**NATIONAL AEROSPACE LAB., KAKUDA (JAPAN).**
Development of the computer program for turbulent boundary layers N88-13264

**NATIONAL AEROSPACE LAB., TOKYO (JAPAN).**
Proceedings of the 4th NAL Symposium on Aircraft Computational Aerodynamics
[NAL-SP-7] N88-13253
An analysis of the compressible-viscous flow field around a 3D-oscillating wing N88-13254
Numerica calculation in the Laplace domain for subsonic unsteady aerodynamic forces acting on a finite wing N88-13256
Numerical analysis of cascade flow solving Navier-Stokes equations N88-13262
Inverse design method for two-dimensional transonic cascades N88-13263
Application of discrete vortex method to analysis of separated flow around aerofoils N88-13268
Programming techniques for high-speed processing of large scale numerical simulation on supercomputers N88-13269
Rarefied gas numerical wind tunnel. 2: Two-dimensional and axially symmetric bodies N88-13273
Computer graphics for computational aerodynamics N88-13276
Computations of compressible viscous flows over multiple-bodies N88-13282
Navier-Stokes analysis of laminar flow control of a two-dimensional airfoil N88-13286
Analytical method for generating computational grids about complete aircraft configurations N88-13287
Navier-Stokes simulation of transonic transportation aircraft configurations. 1: Flow-field simulation over wing-fuselage combinations N88-13288

**NATIONAL AIR AND SPACE MUSEUM, WASHINGTON, D.C.**
Environmental processes and spectral reflectance characteristics associated with soil erosion in desert fringe regions
[NASA-CR-182332] N88-13811

**NATIONAL BUREAU OF STANDARDS, GAITHERSBURG, MD.**
In-situ characterization of the interface of glass reinforced composites
[AD-A185136] N88-13391

**NATIONAL OCEANIC AND ATMOSPHERIC ADMINISTRATION, WASHINGTON, D. C.**
TOMS and the NOAA/FAA volcano support plan N88-13796

**NATIONAL RESEARCH COUNCIL OF CANADA, OTTAWA (ONTARIO).**
Aircraft dynamics: Aerodynamic aspects and wind tunnel techniques N88-13320

**NATIONAL TECHNICAL INFORMATION SERVICE, SPRINGFIELD, VA.**
Role of technical information in innovation
[PB87-235388] N88-14039
Role of the technical report in technological innovation
[PB87-232500] N88-14040

**NAVAL AIR DEVELOPMENT CENTER, WARMINSTER, PA.**
Avionic corrosion N88-13332
Water disbondment characterization of organic Coating/metal substrate systems
[AD-A184847] N88-13454

**NAVAL OCEAN SYSTEMS CENTER, SAN DIEGO, CALIF.**
Varifront 3 expedition data report (USNS DE STEIGUER CRUISE 1202-82). Bioluminescence, hydrographic, nutrient, and satellite data from the Gulf of California (November-December 1981)
[AD-A185011] N88-13805

**NAVAL POSTGRADUATE SCHOOL, MONTEREY, CALIF.**
The development of a computer code (U2DIIF) for the numerical solution of unsteady, inviscid and incompressible flow over an airfoil
[AD-A185033] N88-13293
Correction of inertial navigation system drift errors for an autonomous land vehicle using optical radar terrain data
[AD-A184973] N88-13311
Study of electrostatic modulation of fuel sprays to enhance combustion performance in an aviation gas turbine
[AD-A184967] N88-13341
An experimental investigation of the ignition and flammability limits of various hydrocarbon fuels in a two-dimensional solid fuel ramjet
[AD-A184968] N88-13342
Investigation by differential scanning calorimetry of microstructure in a superplastic Al-Mg-Zr alloy
[AD-A184902] N88-13439
The effect of temperature on the tensile properties of HSLA-100 steel
[AD-A184951] N88-13441
The use of coaxial transmission line elements in log-periodic dipole arrays
[AD-A184864] N88-13499
Evaluation of device figure of merit in microwave switching circuit design
[AD-A184896] N88-13520
An investigation of unipolar arcing at atmospheric pressure in aluminum 2024 and aluminum coated glass slides
[AD-A184903] N88-13521
Photocurrent generation from basic metals, utilizing a short pulsed ArF excimer laser
[AD-A184928] N88-13579
Control of a flexible one-link manipulator
[AD-A185035] N88-13598
Experimental studies on the tripping behavior of narrow T-stiffened flat plates subjected to hydrostatic pressure and underwater shock N88-13613
Estimation of marine boundary layer depth and relative humidity with multispectral satellite measurements
[AD-A184881] N88-13804
Development of a data analysis system for the detection of lower level atmospheric turbulence with an acoustic sounder
[AD-A184972] N88-13821
Development of an acoustic echosounder for detection of lower level atmospheric turbulence
[AD-A184877] N88-13831
Mesoscale applications of high resolution imagery
[AD-A185039] N88-13833
Opportunities for tropical cyclone motion research in the Northwest Pacific region
[AD-A185068] N88-13834
Test and evaluation of the transputer in a multi-transputer system
[AD-A184969] N88-13859
A prototype ray tracer
[AD-A184863] N88-13874
Implementation of an FIR band pass filter using a bit-slice processor
[AD-A184895] N88-13875
An adaptive lattice algorithm for spectral line estimation
[AD-A184970] N88-13876
An APL workspace for conducting nonparametric statistical inference
[AD-A184971] N88-13877
An extension to the multilevel logic simulator for microcomputers
[AD-A185032] N88-13879
Cross-correlation of uniform cyclic difference set sequences
[AD-A184879] N88-13913
Development of a new method of measuring the characteristic impedance and complex wave number of a porous acoustic material
[AD-A185038] N88-13957
Cerenkov radiation field analysis due to a passing electron beam
[AD-A184870] N88-13976
Technology upgrade of a silicon compiler
[AD-A184873] N88-14016
A study of the Department of Defense configuration management policies and procedures as applied to the FA-18 Strike/Fighter program
[AD-A184872] N88-14034

**NAVAL RESEARCH LAB., ORLANDO, FLA.**
Damping analysis of flexural waves in fluid-loaded single and constrained plates
[AD-A185116] N88-13739

**NAVAL RESEARCH LAB., WASHINGTON, D.C.**
On-orbit frequency stability analysis of the GPS NAVSTAR 8 rubidium clock and NAVSTARs 9 and 10 cesium clocks
[AD-A184984] N88-13312
An exact analysis and performance of framed ALOHA with capture
[AD-A185006] N88-13500
High peak power ka-band gyrotron oscillator experiment
[AD-A185424] N88-13563
Software design for an airborne gravity measurement system
[AD-A185000] N88-13878
On a boundary data operator and generalized exterior Robin problems for the Helmholtz equation
[AD-A185124] N88-13915
Determining differences in rates corresponding to a given significance level
[AD-A185004] N88-13940
Evolution of mean square magnetic vector potential in compressible, two-dimensional, magnetofluid turbulence
[AD-A184985] N88-13990
Advanced concepts theory annual report 1986
[AD-A184986] N88-13991
Theory of induced spatial incoherence
[AD-A185005] N88-13992

**NAVAL SHIP RESEARCH AND DEVELOPMENT CENTER, BETHESDA, MD.**
An experimental investigation of appendage-flat plate junction flow. Volume 2. Elliptical nose appendage data base
[AD-A184974] N88-13539
BASIC desk-top computer program for the three-dimensional static configuration of an extensible flexible cable in a uniform stream
[AD-A184852] N88-13737
RADSPHERE: A computer program for calculating the steady-state, axially symmetric, forced response and radiation field of a submerged spherical shell
[AD-A185025] N88-13738

**NAVAL SURFACE WEAPONS CENTER, SILVER SPRING, MD.**
Phenomena at a focus in a laser system
[AD-A185442] N88-13585
Scaling the electromagnetically driven explosive shock simulator N88-13612

**NAVAL WEAPONS CENTER, CHINA LAKE, CALIF.**
Combustion related shear-flow dynamics in elliptic supersonic jets N88-13232

**NEVADA UNIV., RENO.**
Effective use of principal component analysis with high resolution remote sensing data to delineate hydrothermal alteration and carbonate rocks N88-13758

**NEW JERSEY MEDICAL SCHOOL, NEWARK.**
Determining differences in rates corresponding to a given significance level
[AD-A185004] N88-13940

**NEW MEXICO INST. OF MINING AND TECHNOLOGY, SOCORRO.**
An automated supernova search and the design strategy
[DE88-001827] N88-14051

**NIPPON ELECTRIC CO. LTD., TOKYO (JAPAN).**
Vectorizing the FFTs on supercomputer SX system N88-13270
Tridiagonal approximate factorization method: A preconditioning technique for solving nonsymmetric linear systems suitable to supercomputers N88-13271

**NISSAN MOTOR CO. LTD., TOKYO (JAPAN).**
Computational study of three-dimensional wake structures
[REPT-2] N88-13281
**NORGES TEKNISKE HOEGSKOLE, TRONDHEIM.**
Cyclic deformation of an extruded AlMgSi alloy N88-13654
Striations and the fatigue growth mechanism in a micro-alloyed steel N88-13661
**NORTH CAROLINA STATE UNIV., RALEIGH.**
Nonlinear hyperbolic conservation laws
[AD-A184963] N88-13538
Experiments in fault tolerant software reliability
[NASA-CR-181554] N88-13863
Reliability of voting in fault-tolerant software systems for small output spaces
[TR-87-16] N88-13864
RSDIMU acceptance testing system: Overview of acceptance software and procedures N88-13866
The numerical and analytic of implicit differential equations and their application to control and circuit problems
[AD-A185404] N88-13922
Fundamental studies in the OM-CVD growth of Ga-In-As-Sb
[AD-A184822] N88-14014
Structural characterization of ion implanted beta-SiC thin films
[DE87-014567] N88-14027
**NORTH CAROLINA UNIV., CHAPEL HILL.**
Point processes
[AD-A185398] N88-13921
Extrema of skewed stable processes
[AD-A185422] N88-13925
Freidlin-Wentzell type estimates and the law of the iterated logarithm for a class of stochastic processes related to symmetric statistics
[AD-A185366] N88-13944
**NORTH DAKOTA UNIV., GRAND FORKS.**
Production of jet fuels from coal derived liquids. Volume 1: Market assessment for liquid by-products from the Great Plains gasification plant
[AD-A184846] N88-13475
**NORTHEASTERN UNIV., BOSTON, MASS.**
Effect of interface on mechanical properties of graphite/201 aluminum composites N88-13717
**NORTHWESTERN UNIV., EVANSTON, ILL.**
The effect of environment on low cycle fatigue properties in HSLA steel N88-13705
**NOTRE DAME UNIV., IND.**
Error control techniques for satellite and space communications
[NASA-CR-181581] N88-13516
**NOTTINGHAM UNIV. (ENGLAND).**
The effect of alpha platelet morphology and beta-grain size on the initiation and growth of short fatigue cracks in Ti6S N88-13667
The effect of microstructure on the surface crack length: Crack depth relationship for short cracks N88-13670

## O

**OAK RIDGE NATIONAL LAB., TENN.**
Fabrication of composites by chemical vapor deposition
[DE87-014565] N88-13408
Advances in processing techniques for nickel aluminides
[DE87-014571] N88-13449
Effect of rapid solidification on stainless steel weld metal microstructures and its implications on the Schaeffler diagram
[DE88-001489] N88-13451
Dealing with unanticipated events in autonomous navigation
[DE88-000590] N88-13602
Economics of fusion reactors
[DE88-000580] N88-14002
Subcommittee for MHD theory
[DE88-000596] N88-14003
Transport scaling in the collisionless-detrapping regime in stellarators
[DE88-001511] N88-14006
Structural characterization of ion implanted beta-SiC thin films
[DE87-014567] N88-14027
**OFFICE NATIONAL D'ETUDES ET DE RECHERCHES AEROSPATIALES, PARIS (FRANCE).**
Preparation of qualification tests of a plasma generator for the feeding of a hypersonic wind tunnel N88-13222
Delta wing in incompressible flow. Experimental study in F2
[ONERA-RT-36/1147-AN-249-G] N88-13296
Fundamentals of fighter aircraft design: Engine intake and afterbody N88-13322
Requirements and recommendations for the development of theoretical codes and experimental facilities in the near future N88-13327
Influence of the static deformation on a wing in the unsteady aerodynamic N88-13357
Measurement of model deformation in wind tunnels N88-13358
Models for the degradation of stratified composite structures
[ONERA-RT-13/3542-RY-061-R] N88-13395
An element of a multilayer shell for the computation of composite structures
[ONERA-RT-14/3542-RY-051-R] N88-13742
**OFFICE NATIONAL D'ETUDES ET DE RECHERCHES AEROSPATIALES, TOULOUSE (FRANCE).**
Hypersonic laminar boundary layer: Parametric study for the representation of real gas effects N88-13236
**OFFICE OF NAVAL RESEARCH, LONDON (ENGLAND).**
Italy's Institute of Research on Electromagnetic Waves--the Istituto di Ricerca sulle Onde Elettromagnetiche
[AD-A185020] N88-13501
AGARD: The NATO Advisory Group for Aerospace Research and Development
[AD-A185062] N88-14063
**OHIO STATE UNIV., COLUMBUS.**
Detection of critical points: The first step to automatic line generalization N88-13803
**OLD DOMINION UNIV., NORFOLK, VA.**
Theoretical studies of solar lasers and converters
[NASA-CR-181569] N88-13577
Guidance and control strategies for aerospace vehicles
[NASA-CR-181579] N88-13935
**OREGON UNIV., EUGENE.**
The production of ultrasmall and superfine holographic diffraction gratings using synchrotron radiation and lithographic techniques
[AD-A185395] N88-13562
**OTTAWA UNIV. (ONTARIO).**
Fracture kinetics of corrosion fatigue N88-13708

## P

**PACIFIC NORTHWEST LABS., RICHLAND, WASH.**
Statistical process control applied to the liquid-fed ceramic melter process
[DE88-000271] N88-13471
Raman microprobe characterization of dielectric films following high-energy pulsed laser irradiation
[DE88-000559] N88-13587
Hanford Meteorological Station computer codes. Volume 5: The TOWER computer code
[DE88-001610] N88-13843
Irradiation preservation of seafood: Literature review
[DE88-001691] N88-13858
Develop techniques for ion implantation of (lead-lanthanum-zirconate-titanate) for adaptive optics
[DE88-000642] N88-13986
**PANAMETRICS, INC., WALTHAM, MASS.**
Fabricate, calibrate and test a dosimeter for integration into the CRRES (Combined Release and Radiation Effects Satellite) satellite
[AD-A185439] N88-13564
**PARIS VI UNIV. (FRANCE).**
Contributions of lidar measurements to the study of long term variations of the middle atmosphere
[ETN-88-91237] N88-13824
**PENNSYLVANIA STATE UNIV., UNIVERSITY PARK.**
The formation and thermochemical properties of multiligand complexes
[AD-A184935] N88-13416
**POLITECNICO DI MILANO (ITALY).**
Arrays for discrete Fourier transform
[REPT-87-019] N88-13861
Behavioral Architecture Robot Control System (BARCS): A new way of building robots
[REPT-87-036] N88-13902
A functional interpretation of the logistic equation
[REPT-87-037] N88-13946
**PORTSMOUTH POLYTECHNIC (ENGLAND).**
Near-threshold short crack growth behavior in Nimonic 105 N88-13663
Crack growth in contrasting titanium alloys under the conjoint action of high and low cycle fatigue N88-13686
**PRAIRIE VIEW AGRICULTURAL AND MECHANICAL COLL., TEX.**
A study of charged particles/radiation damage to VLSI device materials
[NASA-CR-172036] N88-13518
**PRATT AND WHITNEY AIRCRAFT, WEST PALM BEACH, FLA.**
Development of iron aluminides
[AD-A185190] N88-13461
**PRINCETON UNIV. OBSERVATORY, N. J.**
Photon counting image sensor development for astronomical applications
[NASA-CR-181507] N88-14049
**PRINS MAURITS LAB. TNO, RIJSWIJK (NETHERLANDS).**
Resistance of canopy materials against chemicals
[PML-1985-22] N88-13466
Fuel cells
[PML-1986-43] N88-13813
Investigation of the exposure to harmful compounds in the workshop of nondestructive materials testing at Gilze-Rijen (Netherlands)
[PML-1985-42] N88-13816
Investigation of the nature and concentration of vapor and mist during the cleaning of aircraft
[PML-1985-29] N88-13817
**PURDUE UNIV., WEST LAFAYETTE, IND.**
Tensile mean stress effects on uniaxial fatigue behavior of 1045 HR steel N88-13694

## Q

**QUEENSLAND UNIV., BRISBANE (AUSTRALIA).**
Shock tunnels for real gas hypersonics N88-13223

## R

**RADEX, INC., CARLISLE, MASS.**
Analysis of geophysical data bases and models for spacecraft interactions
[AD-A184809] N88-13375
**RENSSELAER POLYTECHNIC INST., TROY, N.Y.**
Improved high modulus fibers
[NASA-CR-181539] N88-13389
Properties of refractory metals processed by enhanced sintering treatments
[AD-A184944] N88-13440
**RESEARCH CENTER GRAZ (AUSTRIA).**
Overview of Austrian Airborne Imaging Spectrometer (AIS) programme and first results N88-13762
**RESEARCH INST. OF NATIONAL DEFENCE, LINKOEPING (SWEDEN).**
Inverse scattering analysis of diffraction limited SAR
[FOA-C-30459-3.2] N88-13512
**RESEARCH INST. OF NATIONAL DEFENCE, STOCKHOLM (SWEDEN).**
Test number 2 of propellant for rocket motor MK52
[PB87-226155] N88-13480
Results from the melting of tungsten composites under microgravity (TEXUS 10 flight)
[FOA-C-20676-2.1] N88-13482
Large bandwidth ground scattering model
[FOA-C-30458-3.2] N88-13511
High resolution satellite imagery simulation
[FOA-C-30462-3.3,9.3] N88-13810
**RICE UNIV., HOUSTON, TEX.**
HF sidebands in the ionosphere N88-13497
Theoretical atomic and molecular physics
[DE88-001625] N88-13974
Supersonic beam observations of semiconductor clusters
[AD-A184991] N88-14018
**RIT RESEARCH CORP., ROCHESTER, N.Y.**
Electromagnetics and electrothermal approach to evaluate failures in microelectronic devices caused by electrostatic discharges: Stochastical aspects of the device reliability
[AD-A184906] N88-13522
**RITSUMEIKAN UNIV., KYOTO (JAPAN).**
Effect of grain orientation on the origination and the initial growth of fatigue cracks in pure iron N88-13647
**ROCHESTER UNIV., N. Y.**
Reactions of porphyrins in surfactant assemblies, microemulsions and in solutions
[AD-A184797] N88-13412
Embrittling effect of the plastic zone N88-13721
**ROCKEFELLER UNIV., NEW YORK.**
Experimental studies of elementary particle interactions at high energies
[DE88-000804] N88-13971
**ROCKWELL INTERNATIONAL CORP., CANOGA PARK, CALIF.**
Fluid mass and thermal loading effects on the modal characteristics of space shuttle main engine liquid oxygen inlet splitter vanes N88-13828
**ROCKWELL INTERNATIONAL CORP., DOWNEY, CALIF.**
Orbital Spacecraft Consumables Resupply System (OSCRS). Volume 1: Executive summary
[NASA-CR-172010] N88-13368

**ROCKWELL INTERNATIONAL CORP., HUNTSVILLE, ALA.**
Incipient failure detection of space shuttle main engine turbopump bearings using vibration envelope detection N88-13629
**ROCKWELL INTERNATIONAL SCIENCE CENTER, ANAHEIM, CALIF.**
Study of solid state photomultiplier [NASA-CR-177465] N88-13556
**ROCKWELL INTERNATIONAL SCIENCE CENTER, THOUSAND OAKS, CALIF.**
The evolution of local mechanical properties of Al 2219-T851 during fatigue N88-13653
The statistics of the shape of small fatigue cracks N88-13666
**ROME UNIV. (ITALY).**
The technical evolution of the Wilson camera: The beginnings (1895-1925) [NOTA-INTERNA-876] N88-13568
Application of the Von Karman equation to the bifurcation theory [NOTA-INTERNA-891] N88-13927
W decays [NOTA-INTERNA-877] N88-13966
The birth of big science: Nuclear physics as advanced technology source [NOTA-INTERNA-881] N88-13967
Procedure and program used for data processing in a poll on nuclear energy utilization [IFSI-87-3] N88-13977
**ROYAL AIRCRAFT ESTABLISHMENT, BEDFORD (ENGLAND).**
The RAE experimental data-base for missiles at high Mach number and its use in assessing CFD methods N88-13250
**ROYAL AIRCRAFT ESTABLISHMENT, FARNBOROUGH (ENGLAND).**
The drag of slender axisymmetric cones in rarefied hypersonic flow N88-13229
Wing divergence of trimmed aircraft N88-13354
**ROYAL INST. OF TECH., STOCKHOLM (SWEDEN).**
Electric field measurements on Viking: First results [TRITA-EPP-87-04] N88-13826
A synthetic plasma source [TRITA-EPP-86-15] N88-13995
Laboratory and near-earth space plasma as a key to the plasma universe [TRITA-EPP-87-09] N88-13996
Observations of propagating double layers in a high current discharge [TRITA-EPP-87-10] N88-13997
Comments on H. Arp The persistent problem of spiral galaxies [TRITA-EPP-87-05] N88-14052
Cosmology in the plasma universe [TRITA-EPP-87-07] N88-14053
**ROYAL NETHERLANDS METEOROLOGICAL INST., DE BILT.**
Active and passive plume distribution models in the convective boundary layer using a large eddy simulation model [KNMI-TR-90] N88-13546
The lengthening and shortening of the day [KNMI-TR-91] N88-13839
Expectations for water level deviations at the delta works: Zierikzee (Netherlands), November 1981-February 1986 [KNMI-TR-93] N88-13840
Inventory of weather stations. Climatological data from Dutch stations, no. 26 [KNMI-150-26] N88-13841
**RUHR UNIV., BOCHUM (WEST GERMANY).**
Interaction of microstructure and fatigue in tool steels N88-13693
**RUTGERS - THE STATE UNIV., PISCATAWAY, N. J.**
Colloidal stability of oxidized silicon particles in ethanolic and aqueous media [DE87-014783] N88-13421
X-ray fatigue failure prediction based on plasticity response to microcracks N88-13725

## S

**SAAB-SPACE A.B., LINKOEPING (SWEDEN).**
Study of fault tolerant techniques for satellite data handling [FTT/REP/0001/SAAB] N88-13860
**SAINT-GOBAIN RECHERCHE, AUBERVILLIERS (FRANCE).**
Composite materials with glass matrix [SGR/PR-4305/86-SV/JC] N88-13394
**SAINT LOUIS UNIV., MO.**
Tropical easterly jet located using TOMS data N88-13783
**SALFORD UNIV. (ENGLAND).**
The mechanics of fatigue-crack nucleation in a low-alloy steel under fretting conditions N88-13649
**SAN DIEGO STATE UNIV., CALIF.**
OH(A-X) fluorescence from photodissociative excitation of HO2 at 157.5 nm [NASA-CR-181580] N88-13429
Varifront 3 expedition data report (USNS DE STEIGUER CRUISE 1202-82). Bioluminescence, hydrographic, nutrient, and satellite data from the Gulf of California (November-December 1981) [AD-A185011] N88-13805
**SANDIA NATIONAL LABS., ALBUQUERQUE, N. MEX.**
New approach to telemetry development will significantly increase productivity of Joint Test Assembly (JTA) teams [DE88-001676] N88-13373
The effect of maximum-allowable payload temperature on the mass of a multimegawatt space-based platform [DE88-001921] N88-13381
Shock compression of solids as a physical-chemical-mechanical process [DE88-001674] N88-13427
Effectiveness of electrodeposited coatings in reducing atmospheric corrosion of copper substrates [DE87-013651] N88-13448
Reactive sticking coefficients of silane on silicon [DE88-000601] N88-13473
Narrow linewidth gain measurements in a KrF excimer amplifier pumped longitudinally by a high-power electron beam [DE88-001365] N88-13575
Low jitter laser-triggered high-voltage vacuum switch using low laser energies [DE88-001922] N88-13576
Anti-Stokes generation of 226 nm light [DE88-001612] N88-13590
Conservatism implications of shock test tailoring for multiple design environments N88-13611
Structural frequency functions for an impulsive, distributed forcing function N88-13627
Analysis of end stresses in glass-metal bimaterial strips [DE87-007848] N88-13750
An overview of the DOE/SANDIA/USDA vertical axis wind turbine Test Bed Project [DE88-000604] N88-13812
Indirect solution of static problems using concurrent vector processing computers [DE87-012105] N88-13889
Structuring data for concurrent vectorized processing in a transient dynamics finite element program [DE87-013082] N88-13890
An Ada graphical tool to support software development [DE87-014854] N88-13891
Sandia software guidelines: Software quality planning [DE88-001931] N88-13894
Tutorial on elementary bifurcation theory [DE87-014849] N88-13932
RIIM two-pulse injector experiments [DE88-000926] N88-14005
MBE growth of InAsSb strained-layer superlattices [DE88-000365] N88-14011
Comparison of 2D memory SEU transport simulation with experiments [ATR-86(8139)-2-REV-A] N88-14025
Novel heterojunction devices [DE87-013716] N88-14026
**SANDIA NATIONAL LABS., LIVERMORE, CALIF.**
ALT-1 pump limiter experiments [DE88-000822] N88-13989
**SANTA CATARINA UNIV., FLORIANOPOLIS (BRAZIL).**
Study of the influence of mechanical - thermal treatments on the creep behavior of a niobium stainless steel [DE87-703506] N88-13431
Microstructure of amorphous and crystalline zirconium alloys rapidly solidified [DE87-703700] N88-13432
**SANTA CLARA UNIV., CALIF.**
Organic molecules on meteoritic solid substrates [NASA-CR-181570] N88-13411
**SASC TECHNOLOGIES, INC., HYATTSVILLE, MD.**
Selection of optimum wavelengths for ozone mapping from satellites N88-13798
**SATEL CONSEIL, PARIS (FRANCE).**
Study of the feasiblity of a satellite communication system for road transportation home office to vehicle communication. Volume 1: Conceptual analysis [SC/87-E/6-VOL-1] N88-13505
Study of the feasibility of a satellite communication system for road transportation home office to vehicle communication. Volume 2: Market study [SC/87-E/6-VOL-2] N88-13506
**SCIENCE APPLICATIONS INTERNATIONAL CORP., MCLEAN, VA.**
High peek power ka-band gyrotron oscillator experiment [AD-A185424] N88-13563
**SCIENCE RESEARCH COUNCIL, CHILTON (ENGLAND).**
Noise modelling in the time domain with the aid of Spice [PB87-221941] N88-13492
Relational data handling system for scientists [PB87-223426] N88-14038
**SCIENTIFIC RESEARCH ASSOCIATES, INC., GLASTONBURY, CONN.**
Calculation of helicopter rotor blade/vortex interaction by Navier-Stokes procedures [NASA-CR-177441] N88-13291
Three-dimensional dynamic labyrinth seal analysis [AD-A185353] N88-13599
**SHEFFIELD UNIV. (ENGLAND).**
Crack initiation studies in hydrogen embrittled spring steel strip N88-13710
**SINOR (J. E.) CONSULTANTS, INC., NIWOT, COLO.**
Production of jet fuels from coal derived liquids. Volume 1: Market assessment for liquid by-products from the Great Plains gasification plant [AD-A184846] N88-13475
**SMITHSONIAN INSTITUTION, WASHINGTON, D. C.**
Use of satellite data in volcano monitoring N88-13797
**SOCIETE D'APPLICATIONS GENERALES D'ELECTRICITE ET DE MECANIQUE, PARIS (FRANCE).**
Avionics and corrosion N88-13336
**SOCIETE NATIONALE INDUSTRIELLE AEROSPATIALE, ISSAC (FRANCE).**
The structures of large wound propulsion shells [SNIAS-872-430-118] N88-13406
**SOCIETE NATIONALE INDUSTRIELLE AEROSPATIALE, LES MUREAUX (FRANCE).**
Determination of the fiber ratio in carbon fiber/resin composites by means of image analysis [SNIAS-872-422-101] N88-13398
Influence of bonding shop moisture on metal-honeycomb junctions bonded with ultra-thin adhesive films [SNIAS-872-422-112] N88-13399
An electric field meter based upon a new principle: A dummy displacement electrode. Application to aerospace vehicles [SNIAS-872-422-106] N88-13567
Matching segments from a map and an aerial image using relaxation techniques [SNIAS-872-422-103] N88-13809
Introduction to local area network design on Ariane 5 and future launchers [SNIAS-872-422-102] N88-13886
Control of an unstable launcher in atmospheric flight using minimax optimal control laws [SNIAS-872-422-107] N88-13901
**SOCIETE NATIONALE INDUSTRIELLE AEROSPATIALE, PARIS (FRANCE).**
A project of an intelligent system to help on-line trouble shooting [SNIAS-872-111-106] N88-13216
Electrical flight commands in transport aircraft [SNIAS-872-111-108] N88-13361
High performance composite tubes for offshore applications [SNIAS-872-430-116] N88-13488
Utilization of dynamic characteristics of materials to optimize military explosive charges. Application to antiship devices [SNIAS-872-320-101] N88-13743
Numerical simulations of impact tests on a rigid wall [SNIAS-872-320-102] N88-13744
**SOCIETE NATIONALE INDUSTRIELLE AEROSPATIALE, SAINT-MEDARD-EN-JALLES (FRANCE).**
Philosophy and practice of nondestructive tests of composite material structures at Aerospatiale Aquitaine [SNIAS-872-430-105] N88-13400
Carbon-carbon composites and Aerospatiale. State of the art and prospects [SNIAS-872-430-108] N88-13401
Measurement and control of damage in composite materials: Nondestructive controls by thermography, holography, and radiography [SNIAS-872-430-110] N88-13403
Mechanics of anisotropic media. Study of the boundary conditions [SNIAS-872-430-112] N88-13404
Micromechanics of the degradation of composite materials [SNIAS-872-430-113] N88-13405
Contribution of acoustic analysis to assess damage in fluid storage tanks under high pressure [SNIAS-872-430-119] N88-13407

Computation of bonded assemblies. Elastoplastic adhesives, first part
[SNIAS-NT-18926/AQET] N88-13467
First International Week of Adhesive Bonding and Assembling
[SNIAS-872-430-106] N88-13468
Study of ceramic-fiber/ceramic sol-gel based matrix composites
[SNIAS-872-430-120] N88-13469
Influence of shock wave and gas pressure on the behavior of a pyrotechnical device
[SNIAS-872-430-111] N88-13477
Advantages of internal thermal protection in a pyrotechnical plunger
[SNIAS-872-430-114] N88-13478
Numerical simulation applied to the development of a pyrotechnical system
[SNIAS-872-430-115] N88-13479
Measurements in an electromagnetic test laboratory
[SNIAS-872-430-102] N88-13507
Electromagnetic tests
[SNIAS-872-430-103] N88-13508
Numerical and analytical study of the equivalent permittivity or permeability of nonhomogeneous materials. Application to the experimental electromagnetic characterization of composites
[SNIAS-872-430-104] N88-13509
Presentation of a computer program permitting the exploitation of tests designed to determine the sensitivity of one shot devices to a parameter. Application to a degenerate one shot sequence
[SNIAS-872-430-117] N88-13945

**SOCIETE NATIONALE INDUSTRIELLE AEROSPATIALE, SURESNES (FRANCE).**
Paints required for aeronautical construction
[SNIAS-872-551-102] N88-13470
Comparison of fire resistance of metallic and nonmetallic structures
[SNIAS-872-551-101] N88-13489

**SOCIETE NATIONALE INDUSTRIELLE AEROSPATIALE, TOULOUSE (FRANCE).**
The A320 Airbus program
[SNIAS-872-111-105] N88-13215
Design and control of repairs of carbon fiber lift augmentation flaps in the ATR42 aircraft
[SNIAS-872-111-112] N88-13217
Validation elements of the computation methods and measurement techniques for high lift aerodynamic systems
[SNIAS-872-111-101] N88-13299
Computation of transonic flows with nacelle simulation
[SNIAS-872-111-117] N88-13300
Aeroelastic analysis of modern transport aircraft
[SNIAS-872-111-102] N88-13329
Damage considerations in sizing aircraft cells. Life predictions
[SNIAS-872-111-116] N88-13330
Reduced order optimal command applied to longitudinal automatic pilots
[SNIAS-872-111-114] N88-13382
A hybrid fibreglass-CFRP cloth for new furnishings
[SNIAS-872-111-109] N88-13396
Surface treatment problems found in new aircraft designed using structural composites
[SNIAS-872-111-113] N88-13397
Overall description of the computer aided design and manufacturing systems associated with the A320 program at Aerospatiale and its partners
[SNIAS-872-111-104] N88-13883
Presentation of SIGMA (Interactive Assisted Geometry System). A computer assisted shape design program developed at the Aerospatiale Aircraft Division
[SNIAS-872-111-110] N88-13884
Structural optimization in the design process
[SNIAS-872-111-115] N88-13885
Operational groups at the Aerospatiale Aircraft Division
[SNIAS-872-111-107] N88-14036

**SOUTH CAROLINA UNIV., COLUMBIA.**
Further studies in estimation of life distribution characteristics from censored data
[AD-A184862] N88-13937

**SOUTHAMPTON UNIV. (ENGLAND).**
Hypersonic static and dynamic stability of axisymmetric shapes: A comparison of prediction methods and experiment N88-13246

**SOUTHERN METHODIST UNIV., DALLAS, TEX.**
An optical interferometry technique to evaluate closure along a crack front N88-13726
Sample reuse in statistical remodeling
[AD-A184916] N88-13938

**SOUTHWEST RESEARCH INST., HOUSTON, TEX.**
Micromechanisms of fatigue crack growth and fracture toughness in metal matrix composites
[AD-A185200] N88-13392

**SOUTHWEST RESEARCH INST., SAN ANTONIO, TEX.**
Literature review of solid lubrication mechanisms
[AD-A185010] N88-13456

**SOUTHWESTERN INST. OF NUCLEAR REACTOR ENGINEERING, SICHUAN (CHINA).**
Development on thin wall tubes of dispersion type
[DE87-703384] N88-13483

**SPECTRAL SCIENCES, INC., BURLINGTON, MASS.**
MODTRAN: A moderate resolution model for LOWTRAN
[AD-A185384] N88-13503

**SRI INTERNATIONAL CORP., MENLO PARK, CALIF.**
Laser probes of propellant combustion chemistry
[AD-A184854] N88-13415

**STANFORD UNIV., CALIF.**
Modeling and control of large flexible vehicles in the atmosphere and space
[AD-A185368] N88-13377
Experimental study of the fluid mechanics of unsteady turbulent boundary layers
[AD-A184856] N88-13536
A note on the use of symmetric line Gauss-Seidel for the steady upwind differenced Euler equations
[AD-A185223] N88-13540
A unified model for fatigue crack initiation, short crack growth, long crack propagation, and closure effects N88-13680
Evaluation of AIS-2 (1986) data over hydrothermally altered granitoid rocks of the Singatse Range (Yerington) Nevada and comparison with 1985 AIS-1 data N88-13767
Computer modeling of complete IC fabrication process
[AD-A184807] N88-14012

**STATE UNIV. OF NEW YORK, BUFFALO.**
Pure dephasing of a vibrational adbond
[AD-A185222] N88-13740

**STATE UNIV. OF NEW YORK AT BUFFALO, AMHERST.**
Dynamical analysis of molecular decay at spherical surfaces
[AD-A184908] N88-13964

**STRUCTURAL DYNAMICS RESEARCH CORP., MILFORD, OHIO.**
An efficient frequency response solution for nonproportionally damped systems N88-13634

**STRUCTURAL DYNAMICS RESEARCH CORP., SAN DIEGO, CALIF.**
Modal survey of the space shuttle solid rocket motor using multiple input methods N88-13617

**STRUCTUREAL INTEGRITY ASSOCIATES, INC., SAN JOSE, CALIF.**
Stress intensity factors for cracking metal structures under rapid thermal loading, phase 1
[AD-A184112] N88-13606

**SVERDRUP TECHNOLOGY, INC., CLEVELAND, OHIO.**
Operating envelopes of particle sizing instrumentation used for icing research
[NASA-CR-180870] N88-13573

**SYSTEMS RESEARCH LABS., INC., DAYTON, OHIO.**
Characterization of the microstructures of various materials
[AD-A184961] N88-14017

## T

**TACAN AEROSPACE CORP., CARLSBAD, CALIF.**
Nonconventional optical techniques for optical wavefront processing
[AD-A185099] N88-13982

**TECHNION RESEARCH AND DEVELOPMENT FOUNDATION LTD., HAIFA (ISRAEL).**
Fatigue crack growth under random overloads N88-13682

**TECHNISCHE HOCHSCHULE, AACHEN (WEST GERMANY).**
Phase diagram and thermochemical properties of the Al-Cu system
[ETN-88-91015] N88-13447

**TECHNISCHE HOCHSCHULE, DARMSTADT (WEST GERMANY).**
Identification of perturbations in turbomachines by the analysis of pressure signals, vibrations and wavelike motions
[ETN-88-90602] N88-13600

**TECHNISCHE HOGESCHOOL, DELFT (NETHERLANDS).**
Precision analysis of regular networks
[B8709808] N88-13806
The estimation of basic matrices using travel intensity theorems
[REPT-87-13] N88-13926
The isotropic rocket: A surveillance evasion game
[REPT-87-21] N88-13949

**TECHNISCHE HOGESCHOOL, EINDHOVEN (NETHERLANDS).**
Coagulation in stirred tanks
[B8711373] N88-13420
Low-current behavior and current chopping of vacuum arcs
[ISBN-90-9001649-X] N88-13529
Tribology of thin film systems
[ETN-88-91365] N88-13601
Digitization functions in computer graphics
[ETN-88-91363] N88-13887
Some distance problems in coding theory
[B8711398] N88-13888
On a numerical method to solve contact problems
[B8711403] N88-13930
The pseudopotential density functional method applied to semiconducting crystals
[ETN-88-91382] N88-14024

**TECHNISCHE HOGESCHOOL TWENTE, ENSCHEDE (NETHERLANDS).**
Simulation of the perpendicular magnetic recording process
[B8713537] N88-13570
Transient periodic behavior related to a saddle-node bifurcation
[ETN-88-91321] N88-13928
A mechanism for symmetry breaking in antiferromagnetic Heisenberg systems
[ETN-88-91320] N88-14031

**TECHNISCHE UNIV., AACHEN (WEST GERMANY).**
Optical deformation measurement on shells following the raster principle
[ETN-88-90608] N88-13741

**TECHNISCHE UNIV., BRUNSWICK (WEST GERMANY).**
Experimental investigations on blunt bodies and corner configurations in hypersonic flow N88-13225
Contribution to the improvement of the guidance accuracy of automatic pilots
[ETN-88-90607] N88-13360

**TECHNISCHE UNIV., MUNICH (WEST GERMANY).**
Establishment of complete minimum test sets for digital circuits with safety engineering significance
[ETN-88-90599] N88-13526

**TEL-AVIV UNIV. (ISRAEL).**
On the correlation free forms for nonlinear stochastic systems
[DE87-011169] N88-13947

**TEXAS A&M UNIV., COLLEGE STATION.**
Quantile based unified distribution of extreme values and order statistics
[AD-A185171] N88-13942
Quantile statistical data analysis
[AD-A185181] N88-13943

**TEXAS UNIV., AUSTIN.**
Driving mechanism of unsteady separation shock motion in hypersonic interactive flow N88-13226
Research and development of finite elements and iterative algorithms for elliptic partial differential equations
[DE88-001381] N88-13934
Application of Vandermonde decomposition to directional and modal analysis of broadband transients
[AD-A185007] N88-13956

**TEXAS UNIV., DALLAS.**
The gamma-ray laser project
[AD-A184824] N88-13578

**TOHOKU UNIV., SENDAI (JAPAN).**
Time-marching finite-difference methods for the three-dimensional Euler equations of contravariant velocity components N88-13285
Environmental fracture toughness and static fatigue crack propagation of silica glass N88-13716

**TOKYO METROPOLITAN UNIV. (JAPAN).**
Numerical analysis of axisymmetric flow with H2-O2 reactions N88-13272

**TOKYO UNIV. (JAPAN).**
Computation of dynamic stall of NACA0012 airfoil by block pentadiagonal matrix scheme N88-13255
Flow visualization in computational fluid dynamics N88-13277
Three-dimensional flow past a two-dimensional body N88-13280
Relaxation method for the compressible Navier-Stokes equations using upwind schemes N88-13283

**TORONTO UNIV. (ONTARIO).**
A complete linearized theory for the analysis and design of two-dimensional hydrofoils near a free surface
[UTIAS-TN-264] N88-13531

**TRW, INC., REDONDO BEACH, CALIF.**
Microwave superheaters for fusion
[DE88-001656] N88-14007

## U

**UNION CARBIDE CORP., TARRYTOWN, N.Y.**
Oxygen enriched combustion system performance study
[DE88-001500] N88-13424

**UNITED KINGDOM ATOMIC ENERGY AUTHORITY, RISLEY (ENGLAND).**
The initiation and growth of fatigue cracks in carburised 9Cr1Mo steel N88-13696
**UNITED TECHNOLOGIES CORP., SAN JOSE, CALIF.**
High energy molecules of high symmetry [AD-A185385] N88-13965
**UNIVERSITE DE TECHNOLOGIE DE COMPIEGNE (FRANCE).**
Utilization of a high rate vector computer in computational fluid mechanics for aeronautics [ETN-88-91171] N88-13547
**UNIVERSITY OF PETROLEUM AND MINERALS, DHAHRAN (SAUDI ARABIA).**
Transient development of stratification in a partially divided enclosure [DE87-011742] N88-13490
**UNIVERSITY OF SOUTH FLORIDA, TAMPA.**
Towards building a team of intelligent robots [NASA-CR-181538] N88-13595
Collision-free motion of two robot arms in a common workspace [CSE-87-00002] N88-13596
A rudimentary database for three-dimensional objects using structural representation [CSE-87-00004] N88-13597
**UNIVERSITY OF SOUTHERN CALIFORNIA, LOS ANGELES.**
Molecular beam epitaxial growth and characterization of 3-5 compound semiconductor single and multiple interface structures [AD-A185400] N88-14021
**UPPSALA IONOSPHERIC OBSERVATORY (SWEDEN).**
Activities report of the Ionospheric Observatory [UIO-SR-87-01] N88-13827
**UTAH UNIV., SALT LAKE CITY.**
The effect of heat treatment on fatigue crack growth in polycarbonate N88-13714

## V

**VIBRATION INST., CLARENDON HILLS, ILL.**
The Shock and Vibration Digest, Volume 19, No. 12 N88-13746
**VIGYAN RESEARCH ASSOCIATES, INC., HAMPTON, VA.**
A swept wing panel in a low speed flexible walled test section [NASA-CR-4106] N88-13292
**VIRGINIA POLYTECHNIC INST. AND STATE UNIV., BLACKSBURG.**
Ignition and flameholding in supersonic flow by injection of dissociated hydrogen N88-13410
A Cartesian finite-volume method for the Euler equations N88-13532
Bending of a bonded beam as a test method for adhesive properties [AD-A184813] N88-13736
**VIRGINIA UNIV., CHARLOTTESVILLE.**
Optimal shock isolation with minimum settling time N88-13633
Fatigue 87, volume 1 [AD-A184045] N88-13645
Cyclic deformation and crack initiation N88-13646
Surface deformation and fatigue crack initiation of alpha-iron N88-13651
Growth of short fatigue cracks in a squeeze formed aluminum alloy N88-13658
Influence of microstructure and aging condition on the fatigue crack propagation in age hardened aluminium alloys N88-13659
Fatigue crack propagation of short and long cracks: Phys. basis, prediction methods and engineering significance N88-13664
The initiation and growth of small fatigue cracks in copper at room and cryogenic temperatures N88-13668
On the role of crack tip shielding in influencing the behavior of long and small fatigue cracks in aluminum-lithium alloy 2090 N88-13671
The influence of microstructure and residual stresses on the initiation and propagation of short surface cracks on AlMgSi1 N88-13674
Behavior of long and short fatigue cracks in a powder metallurgy superalloy at room and at high temperature N88-13677
Crack growth prediction in 3D structures under aeronautical-type spectrum loadings N88-13688
Effects of MN dispersoids on near threshold fatigue crack growth in 2134 type alloys N88-13692
The role of inclusions in corrosion fatigue crack initiation in Q1N N88-13699
Fatigue 87, volume 3 [AD-A184047] N88-13700
Robust prediction operations for stationary processes [AD-A185408] N88-13924
**VOLVO A.B., GOETEBORG (SWEDEN).**
The influence of the topography of fracture surfaces on crack closure N88-13657
**VON KARMAN INST. FOR FLUID DYNAMICS, RHODE-SAINT-GENESE (BELGIUM).**
European hypersonic wind tunnels N88-13221
**VRIJE UNIVERSITEIT, AMSTERDAM (NETHERLANDS).**
Connecting RPC (Remote Procedure Call)-based distributed systems using wide-area networks [PB87-234423] N88-14041

## W

**WARWICK UNIV. COVENTRY (ENGLAND).**
Robustness of linear systems [PB87-220042] N88-13909
Stability properties of spline approximations for retarded systems [PB87-220919] N88-13910
**WASHINGTON UNIV., SEATTLE.**
Calibrating AIS images using the surface as a reference N88-13760
Study of boundary structures [AD-A184808] N88-14013
**WATERLOO UNIV. (ONTARIO).**
Dynamic stability of hypersonic conical lifting vehicles according to Newton-Busemann theory N88-13247
**WEA, CAMBRIDGE, MASS.**
Computation of natural frequencies of planar lattice structure [AD-A185387] N88-13920
**WEAR SCIENCES, INC., ARNOLD, MD.**
Literature review of solid lubrication mechanisms [AD-A185010] N88-13456
**WEST VIRGINIA UNIV., MORGANTOWN.**
Exact finite element method analysis of viscoelastic tapered structures to transient loads N88-13632
Advanced joining concepts for passive vibration control N88-13638
Significance of foundation-soil separation in dynamic soil-structure interaction N88-13641
**WHITAKER COLL., MASS.**
Learning a color algorithm from examples [AD-A184385] N88-13862
**WICHITA STATE UNIV., KANS.**
Theoretical analysis of the electrical aspects of the basic electro-impulse problem in aircraft de-icing applications [NASA-CR-180845] N88-13310
**WISCONSIN UNIV., MADISON.**
Applications of nonlinear hole burning spectroscopy [AD-A184943] N88-13580
Systematic stratospheric-tropospheric exchange viewed from isentropic coordinates N88-13777
Reversed field pinch plasmas with various boundary conditions [DE88-000832] N88-14004
**WYOMING UNIV., LARAMIE.**
Numerical and analytical methods in nonlinear partial differential equations [AD-A185210] N88-13918

## X

**XIAN JIAOTONG UNIV. (CHINA).**
A study of fatigue crack growth life under random stresses N88-13685
Fatigue under nonnormal random stresses using Monte Carlo method N88-13723

## Y

**YOKOHAMA NATIONAL UNIV. (JAPAN).**
Development of research on fatigue of spot-weld in automobile structures in Japan N88-13728

### Typical Contract Number Index Listing

Listings in this index are arranged alphanumerically by contract number. Under each contract number the NASA accession numbers denoting documents that have been produced as a result of research done under that contract are arranged in ascending order. The NASA accession number denotes the number by which the citation is identified.


AF PROJ. 2301 ..... N88-13562
AF PROJ. 2302 ..... N88-13377
AF PROJ. 2304 ..... N88-13294
N88-13541
N88-13922
N88-13923
N88-13924
AF PROJ. 2306 ..... N88-13445
AF PROJ. 2307 ..... N88-13542
AF PROJ. 2310 ..... N88-13822
AF PROJ. 2311 ..... N88-14055
AF PROJ. 2917 ..... N88-14021
AF PROJ. 6670 ..... N88-13836
AF-AFOSR-82-0010 ..... N88-13445
AF-AFOSR-82-0018 ..... N88-14055
AF-AFOSR-82-0062 ..... N88-13377
AF-AFOSR-83-0247 ..... N88-13541
AF-AFOSR-84-0219 ..... N88-13542
AF-AFOSR-84-0240 ..... N88-13922
AF-AFOSR-84-0279 ..... N88-14021
AF-AFOSR-84-0367 ..... N88-13921
AF-AFOSR-85-0258 ..... N88-13822
AF-AFOSR-85-0303 ..... N88-13294
AF-AFOSR-85-0322 ..... N88-13923
AF-AFOSR-85-0326 ..... N88-13562
AF-AFOSR-87-0224 ..... N88-13924
AF-AFOSR-0061-83 ..... N88-13692
AF-AFOSR-0077-82 ..... N88-13686
AF-AFOSR-0112-86 ..... N88-13226
ARPA ORDER 4205 ..... N88-13313
A78/KL/125 ..... N88-13813
A78/KLU/065 ..... N88-13816
N88-13817
A82/KLU/113 ..... N88-13857
A83/K/045 ..... N88-13851
A84/KLU/089 ..... N88-13882
BMVG-T/R-760/F-0001/F-1701 ..... N88-13545
CT/104/D.EN/84 ..... N88-13901
DA PROJ. RR0-4206 ..... N88-13873
DA PROJ. 1L1-61102-BH-57 ..... N88-13523
DA PROJ. 1L1-62716-AH-70 ..... N88-13524
DA PROJ. 1T1-61102-AH-51 ..... N88-13456
DA PROJ. 2480 ..... N88-13475
DAAG29-77-C-0031 ..... N88-14059
DAAG29-79-D-1001 ..... N88-13386
DAAG29-81-K-0173 ..... N88-13498
DAAG29-82-K-0187 ..... N88-13413
DAAG29-83-C-0011 ..... N88-14013
DAAG29-83-K-0022 ..... N88-13993
DAAG29-83-K-0056 ..... N88-13536
DAAG29-83-K-0118 ..... N88-14014
DAAG29-83-K-0125 ..... N88-14012
DAAG29-83-K-0128 ..... N88-13457
DAAG29-84-K-0002 ..... N88-13918
DAAG29-84-K-0011 ..... N88-13412
DAAG29-84-K-0015 ..... N88-13975
DAAG29-84-K-0026 ..... N88-13440
DAAG29-84-K-0051 ..... N88-13417
DAAG29-84-K-0052 ..... N88-13455
DAAG29-84-K-0054 ..... N88-13981
DAAG29-84-K-0056 ..... N88-13444
DAAG29-84-K-0072 ..... N88-13880
DAAG29-84-K-0087 ..... N88-13416
DAAG29-84-K-0092 ..... N88-13415
DAAG29-84-K-0197 ..... N88-13856
DAAG29-84-K-0202 ..... N88-13897
DAAG29-85-C-0018 ..... N88-13881
N88-13939
N88-13941
DAAG29-85-C-0027 ..... N88-13390
DAAG29-85-K-0001 ..... N88-13580
DAAG29-85-K-0029 ..... N88-14018
DAAG29-85-K-0031 ..... N88-13983
DAAG29-85-K-0079 ..... N88-13502
DAAG29-85-K-0166 ..... N88-14013
DAAK11-84-D-0008 ..... N88-13524
DAAK70-85-C-0007 ..... N88-13456
DAAK70-86-C-0035 ..... N88-13517
DAAL03-86-K-0002 ..... N88-13583
DAAL03-86-K-0004 ..... N88-13538
DAAL03-86-K-0167 ..... N88-13983
DAAL03-87-G-0102 ..... N88-13645
N88-13700
DAAL03-87-K-0003 ..... N88-13942
N88-13943
DACA76-84-C-0004 ..... N88-14045
DAJA45-84-C-0045 ..... N88-13523
DE-AC02-76CH-00016 ..... N88-13963
DE-AC02-83CH-10093 ..... N88-13815
DE-AC02-87ER-40325 ..... N88-13971
DE-AC03-76SF-00098 ..... N88-13422
N88-13423
N88-13671
N88-13892
N88-13893
N88-14001
DE-AC04-76DP-00613 ..... N88-13905
N88-13906
DE-AC04-76DP-00789 ..... N88-13373
N88-13381
N88-13427
N88-13448
N88-13473
N88-13530
N88-13575
N88-13576
N88-13590
N88-13750
N88-13812
N88-13889
N88-13890
N88-13891
N88-13894
N88-13932
N88-14005
N88-14011
N88-14026
DE-AC05-84OR-21400 ..... N88-13408
N88-13421
N88-13449
N88-13451
N88-13452
N88-13602
N88-14002
N88-14003
N88-14006
N88-14027
DE-AC06-76RL-01830 ..... N88-13471
N88-13587
N88-13843
N88-13858
N88-13986
DE-AC07-76ID-01570 ..... N88-13424
N88-13450
N88-13751
DE-AI01-85CE-50111 ..... N88-13338
DE-AI01-85CE-50112 ..... N88-13453
DE-AS03-76ER-72012 ..... N88-13550
DE-AS05-78ER-05781 ..... N88-14028
DE-AS05-81ER-10954 ..... N88-13934
DE-AS05-84ER-13168 ..... N88-13974
DE-AS09-80ER-10671 ..... N88-13425
DE-FC05-85ER-25000 ..... N88-14009
DE-FG02-84ER-45109 ..... N88-13729
DE-FG02-84ER-45138 ..... N88-13731
DE-FG02-85ER-13315 ..... N88-13904
N88-13947
DE-FG02-85ER-45201 ..... N88-13721
DE-FG02-85ER-45222 ..... N88-13970
DE-FG02-85ER-53212 ..... N88-14004
DE-FG02-86ER-13491 ..... N88-13972
DE-FG03-84ER-45119 ..... N88-13680
DE-FG03-85ER-51089 ..... N88-13989
DE-FG05-86ER-13487 ..... N88-13426
DE-FG05-86ER-13632 ..... N88-13973
DE-FG05-86ER-40272 ..... N88-14032
DE-FG05-87ER-40319 ..... N88-14009
DRET-83-34-497-00-470-75-01 ..... N88-13959
DRET-83-250 ..... N88-13565
DRET-83-460 ..... N88-13566
DRET-84-163 ..... N88-13467
DRET-84-164 ..... N88-13547
DRET-84-190 ..... N88-13548
DRET-85-34-001-29-8-3-2 ..... N88-13742
DRET-85-003 ..... N88-13297
DRET-85-338 ..... N88-13394
DRET-85-1414 ..... N88-13296
DRET-86-34-001-26 ..... N88-13395
ESA-6023/84-F-RD(SC) ..... N88-13505
N88-13506
ESOC-6141/84-D-IM(SC) ..... N88-13808
ESTEC-5098/82-NL-PB ..... N88-13485
N88-13486
ESTEC-5074/84-NL-PB ..... N88-13860
FMK-F-K-82260-84-254-73-001 ..... N88-13303
F04701-85-C-0086 ..... N88-13519
N88-14015
F19628-82-C-0090 ..... N88-13564
F19628-83-C-0105 ..... N88-13375
F19628-86-C-0030 ..... N88-13832
F19628-86-C-0033 ..... N88-13829
F19628-86-C-0079 ..... N88-13503
F19628-86-C-0173 ..... N88-13979
F29601-85-C-0082 ..... N88-13982
F33615-81-C-5110 ..... N88-13461
F33615-83-C-5073 ..... N88-14017
F33615-84-C-2411 ..... N88-13340
F33615-85-C-4500 ..... N88-13847
F33615-86-C-2665 ..... N88-13599
F33615-86-C-3219 ..... N88-13606
F49420-85-C-0137 ..... N88-13543
F49620-85-C-0034 ..... N88-13666
F49620-85-C-0116 ..... N88-13686
F49620-85-C-0144 ..... N88-13921
N88-13925
N88-13944
F49620-85-C-0148 ..... N88-13920
F049620-85-C-0056 ..... N88-13965
HU-254/2 ..... N88-13225
MIPR-ARO-111-84 ..... N88-13391
MIPR-ARO-113-85 ..... N88-13391
MIPR-ARO-139-85 ..... N88-13937
MIPR-ARO-145-86 ..... N88-13391
MIPR-FY1455-86-N0657 ..... N88-13475
MIPR-86-570 ..... N88-13991
NAGW-661 ..... N88-13429
NAGW-950 ..... N88-13763
NAG1-126 ..... N88-13374
NAG1-461 ..... N88-13307
NAG1-512 ..... N88-13865
NAG1-526 ..... N88-13676
NAG1-802 ..... N88-13872
NAG1-613 ..... N88-13867
N88-13868
N88-13869
N88-13870
N88-13871
NAG1-632 ..... N88-13596
N88-13597
NAG1-647 ..... N88-13896
NAG1-667 ..... N88-13863
N88-13864
N88-13865
NAG1-736 ..... N88-13935
NAG1-757 ..... N88-13577
NAG1-772 ..... N88-13595
NAG3-284 ..... N88-13310

NAG3-503 ..... N88-13732
NAG5-557 ..... N88-13516
NAG5-780 ..... N88-13605
N88-13908
NAG5-818 ..... N88-13820
N88-13936
NAG5-949 ..... N88-13907
NAG7-12 ..... N88-13384
NAG8-064 ..... N88-13551
NASA ORDER W-73289 ..... N88-14062
NAS1-15759 ..... N88-13900
NAS1-16130 ..... N88-13553
N88-13557
NAS1-17705 ..... N88-13865
NAS1-17919 ..... N88-13292
NAS2-11370 ..... N88-13954
NAS2-11420 ..... N88-13218
NAS2-12363 ..... N88-13291
NAS2-12400 ..... N88-13556
NAS3-23260 ..... N88-13803
NAS3-24105 ..... N88-13573
NAS5-28774 ..... N88-13811
NAS7-918 ..... N88-13755
NAS8-36700 ..... N88-13629
NAS8-40000 ..... N88-13628
NAS9-17136 ..... N88-13518
NAS9-17584 ..... N88-13368
NA85RAC-05070 ..... N88-13419
NCC2-27 ..... N88-13852
NCC2-271 ..... N88-13411
NSF AEO-84-20980 ..... N88-13419
NSF ATM-83-13655 ..... N88-13969
NSF DMR-81-04985 ..... N88-13725
NSF DMR-82-16972 ..... N88-13651
N88-13668
NSF DMR-83-03904 ..... N88-13651
NSF DMR-84-12357 ..... N88-13715
NSF DMR-85-0675 ..... N88-13650
NSF DMR-85-20280 ..... N88-13651
NSF EAR-85-21543 ..... N88-13820
N88-13936
NSF ECS-83-05448 ..... N88-13583
NSF ECS-84-07285 ..... N88-13558
NSF MCS-82-10950 ..... N88-13910
NSG-1510 ..... N88-13389
NSG-2284 ..... N88-13828
NSG-7618 ..... N88-14049
N00014-81-C-0803 ..... N88-13313
N00014-81-K-0742 ..... N88-13558
N00014-82-K-0185 ..... N88-13736
N00014-82-K-0335 ..... N88-13540
N00014-82-K-0741 ..... N88-13958
N00014-83-K-0216 ..... N88-13914
N00014-84-C-0149 ..... N88-13376
N88-13504
N88-13912
N00014-84-K-0532 ..... N88-13522
N00014-85-C-0206 ..... N88-13392
N00014-85-K-0124 ..... N88-13662
N00014-85-K-0177 ..... N88-14019
N00014-85-K-0326 ..... N88-13581
N88-13584
N00014-85-K-0340 ..... N88-13938
N00014-85-K-0497 ..... N88-13919
N00014-85-K-0501 ..... N88-13956
N00014-85-K-0586 ..... N88-13873
N00014-86-C-0043 ..... N88-13740
N00014-86-C-0301 ..... N88-13484
N00014-86-C-2488 ..... N88-13578
N00014-86-K-0043 ..... N88-13964
N00014-86-K-0345 ..... N88-13459
N62269-86-C-0261 ..... N88-13653
SCHL-5/82 ..... N88-13225
W-7405-ENG-36 ..... N88-13472
N88-13481
N88-13490
N88-13491
N88-13535
N88-13555
N88-13591
N88-13895
N88-13933
N88-13948
N88-13968
N88-13998
N88-13999
N88-14000
N88-14008
N88-14051
N88-14057
W-7405-ENG-48 ..... N88-13571
N88-13572
N88-13588
N88-13589
N88-13752
N88-13898
N88-13899
N88-13952
N88-13953
N88-13980
N88-14007
199-22-76-01 ..... N88-14058
199-61-12 ..... N88-13852
324-01-08 ..... N88-13291
505-31-90 ..... N88-13305
505-34-01 ..... N88-13367
505-42-11 ..... N88-13290
505-45-58 ..... N88-13754
505-60-01 ..... N88-13951
505-60-31 ..... N88-13549
505-61-01-02 ..... N88-13292
505-61-11-01 ..... N88-13962
505-61-51 ..... N88-13306
505-62-11 ..... N88-13345
505-62-21 ..... N88-13428
N88-13931
505-63-01-05 ..... N88-13735
505-63-01-09 ..... N88-13387
505-63-11 ..... N88-13409
N88-13753
505-63-21 ..... N88-13304
505-63-51 ..... N88-13604
505-66-41 ..... N88-13363
505-66-41-04 ..... N88-13900
505-68-11 ..... N88-13310
N88-13552
N88-13573
506-41-21 ..... N88-13385
506-41-31 ..... N88-14046
N88-14054
506-43-1A ..... N88-13453
506-45-31 ..... N88-13556
506-49-11-01 ..... N88-13388
506-49-31-01 ..... N88-13369
533-02-41 ..... N88-13359
533-04-12 ..... N88-13745
535-03-01 ..... N88-13346
N88-13960
N88-13961
535-05-01 ..... N88-13347
650-60-26 ..... N88-13513
665-45-30-01 ..... N88-13553
N88-13557
666-53-01 ..... N88-13755
778-32-11 ..... N88-13338

# REPORT/ACCESSION NUMBER INDEX



### Typical Report Number Index Listing

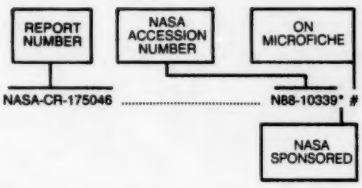


Listings in this index are arranged alphanumerically by report number. The NASA accession number denotes the number by which the citation is identified. An asterisk (*) indicates that the item is a NASA report. A pound sign (#) indicates that the item is available on microfiche.

A-86140 ..... N88-13305* #
A-86158 ..... N88-13306* #
A-86196 ..... N88-13367* #
A-86247 ..... N88-13290* #
A-86302 ..... N88-13951* #
A-86324 ..... N88-13549* #
A-86380 ..... N88-13363* #
A-87255 ..... N88-13852* #
A-87350 ..... N88-13359* #

AAE-TR-87-5 ..... N88-13581 #
AAE-TR-87-6 ..... N88-13584 #

AD-A184045 ..... N88-13645 #
AD-A184047 ..... N88-13700 #
AD-A184083 ..... N88-13517 #
AD-A184112 ..... N88-13606 #
AD-A184183 ..... N88-13979 #
AD-A184197 ..... N88-13829 #
AD-A184385 ..... N88-13862 #
AD-A184797 ..... N88-13412 #
AD-A184806 ..... N88-13975 #
AD-A184807 ..... N88-14012 #
AD-A184808 ..... N88-14013 #
AD-A184809 ..... N88-13375 #
AD-A184810 ..... N88-13413 #
AD-A184812 ..... N88-13414 #
AD-A184813 ..... N88-13736 #
AD-A184814 ..... N88-13830 #
AD-A184815 ..... N88-13845 #
AD-A184818 ..... N88-13981 #
AD-A184822 ..... N88-14014 #
AD-A184824 ..... N88-13578 #
AD-A184828 ..... N88-13390 #
AD-A184837 ..... N88-13498 #
AD-A184838 ..... N88-13386 #
AD-A184846 ..... N88-13475 #
AD-A184847 ..... N88-13454 #
AD-A184848 ..... N88-14015 #
AD-A184852 ..... N88-13737 #
AD-A184853 ..... N88-13912 #
AD-A184854 ..... N88-13415 #
AD-A184855 ..... N88-13873 #
AD-A184856 ..... N88-13536 #
AD-A184862 ..... N88-13937 #
AD-A184863 ..... N88-13874 #
AD-A184864 ..... N88-13499 #
AD-A184865 ..... N88-13537 #
AD-A184870 ..... N88-13976 #
AD-A184872 ..... N88-14034 #
AD-A184873 ..... N88-14016 #
AD-A184876 ..... N88-14035 #
AD-A184877 ..... N88-13831 #
AD-A184879 ..... N88-13913 #
AD-A184881 ..... N88-13804 #
AD-A184883 ..... N88-13519 #
AD-A184889 ..... N88-13832 #
AD-A184895 ..... N88-13875 #
AD-A184896 ..... N88-13520 #
AD-A184902 ..... N88-13439 #
AD-A184903 ..... N88-13521 #
AD-A184906 ..... N88-13522 #
AD-A184908 ..... N88-13964 #
AD-A184916 ..... N88-13938 #
AD-A184920 ..... N88-13939 #
AD-A184928 ..... N88-13579 #
AD-A184935 ..... N88-13416 #
AD-A184943 ..... N88-13580 #
AD-A184944 ..... N88-13440 #
AD-A184951 ..... N88-13441 #
AD-A184956 ..... N88-13455 #
AD-A184958 ..... N88-13417 #
AD-A184960 ..... N88-13340 #
AD-A184961 ..... N88-14017 #
AD-A184963 ..... N88-13538 #
AD-A184967 ..... N88-13341 #
AD-A184968 ..... N88-13342 #
AD-A184969 ..... N88-13859 #
AD-A184970 ..... N88-13876 #
AD-A184971 ..... N88-13877 #
AD-A184972 ..... N88-13821 #
AD-A184973 ..... N88-13311 #
AD-A184974 ..... N88-13539 #
AD-A184977 ..... N88-13848 #
AD-A184978 ..... N88-13846 #
AD-A184984 ..... N88-13312 #
AD-A184985 ..... N88-13990 #
AD-A184986 ..... N88-13991 #
AD-A184988 ..... N88-13313 #
AD-A184991 ..... N88-14018 #
AD-A185000 ..... N88-13878 #
AD-A185004 ..... N88-13940 #
AD-A185005 ..... N88-13992 #
AD-A185006 ..... N88-13500 #
AD-A185007 ..... N88-13956 #
AD-A185010 ..... N88-13456 #
AD-A185011 ..... N88-13805 #
AD-A185019 ..... N88-13457 #
AD-A185020 ..... N88-13501 #
AD-A185025 ..... N88-13738 #
AD-A185026 ..... N88-13458 #
AD-A185028 ..... N88-13328 #
AD-A185032 ..... N88-13879 #
AD-A185033 ..... N88-13293 #
AD-A185035 ..... N88-13598 #
AD-A185038 ..... N88-13957 #
AD-A185039 ..... N88-13833 #
AD-A185043 ..... N88-14059 #
AD-A185052 ..... N88-13849 #
AD-A185053 ..... N88-13914 #
AD-A185054 ..... N88-13558 #
AD-A185055 ..... N88-13502 #
AD-A185056 ..... N88-13856 #
AD-A185059 ..... N88-13581 #
AD-A185061 ..... N88-13442 #
AD-A185062 ..... N88-14063 #
AD-A185068 ..... N88-13834 #
AD-A185071 ..... N88-13958 #
AD-A185073 ..... N88-14019 #
AD-A185085 ..... N88-13941 #
AD-A185094 ..... N88-13459 #
AD-A185099 ..... N88-13982 #
AD-A185113 ..... N88-13460 #
AD-A185116 ..... N88-13739 #
AD-A185117 ..... N88-13582 #
AD-A185124 ..... N88-13915 #
AD-A185136 ..... N88-13391 #
AD-A185141 ..... N88-13983 #
AD-A185144 ..... N88-14050 #
AD-A185148 ..... N88-13916 #
AD-A185155 ..... N88-13583 #
AD-A185156 ..... N88-13917 #
AD-A185171 ..... N88-13942 #
AD-A185172 ..... N88-13880 #
AD-A185173 ..... N88-13993 #
AD-A185175 ..... N88-13443 #
AD-A185177 ..... N88-13897 #
AD-A185179 ..... N88-13881 #
AD-A185181 ..... N88-13943 #
AD-A185190 ..... N88-13461 #
AD-A185193 ..... N88-13559 #
AD-A185195 ..... N88-13850 #
AD-A185196 ..... N88-13560 #
AD-A185197 ..... N88-13418 #
AD-A185200 ..... N88-13392 #
AD-A185202 ..... N88-13376 #
AD-A185210 ..... N88-13918 #
AD-A185216 ..... N88-13444 #
AD-A185222 ..... N88-13740 #
AD-A185223 ..... N88-13540 #
AD-A185229 ..... N88-13419 #
AD-A185231 ..... N88-13835 #
AD-A185241 ..... N88-13584 #
AD-A185250 ..... N88-13523 #
AD-A185258 ..... N88-13484 #
AD-A185266 ..... N88-13314 #
AD-A185273 ..... N88-13836 #
AD-A185274 ..... N88-13476 #
AD-A185290 ..... N88-13837 #
AD-A185300 ..... N88-13482 #
AD-A185347 ..... N88-13541 #
AD-A185353 ..... N88-13599 #
AD-A185358 ..... N88-13308 #
AD-A185359 ..... N88-13561 #
AD-A185363 ..... N88-13838 #
AD-A185366 ..... N88-13944 #
AD-A185367 ..... N88-13524 #
AD-A185368 ..... N88-13377 #
AD-A185369 ..... N88-13542 #
AD-A185370 ..... N88-13994 #
AD-A185375 ..... N88-13919 #
AD-A185376 ..... N88-14020 #
AD-A185381 ..... N88-13525 #
AD-A185384 ..... N88-13503 #
AD-A185385 ..... N88-13965 #
AD-A185386 ..... N88-13822 #
AD-A185387 ..... N88-13920 #
AD-A185388 ..... N88-13823 #
AD-A185391 ..... N88-13847 #
AD-A185393 ..... N88-13445 #
AD-A185395 ..... N88-13562 #
AD-A185396 ..... N88-13921 #
AD-A185400 ..... N88-14021 #
AD-A185401 ..... N88-13294 #
AD-A185404 ..... N88-13922 #
AD-A185405 ..... N88-13923 #
AD-A185406 ..... N88-13543 #
AD-A185408 ..... N88-13924 #
AD-A185421 ..... N88-14045 #
AD-A185422 ..... N88-13925 #
AD-A185424 ..... N88-13563 #
AD-A185432 ..... N88-14055 #
AD-A185434 ..... N88-13504 #
AD-A185439 ..... N88-13564 #
AD-A185440 ..... N88-13446 #
AD-A185442 ..... N88-13585 #

AD-E500888 ..... N88-13919 #
AD-E500888 ..... N88-13994 #
AD-E500888 ..... N88-14020 #

AFGL-ERP-965 ..... N88-13823 #
AFGL-ERP-966 ..... N88-13836 #

AFGL-TR-86-0221 ..... N88-13375 #
AFGL-TR-87-0007 ..... N88-13823 #
AFGL-TR-87-0019 ..... N88-13829 #
AFGL-TR-87-0050 ..... N88-13836 #
AFGL-TR-87-0090 ..... N88-13979 #
AFGL-TR-87-0194 ..... N88-13832 #
AFGL-TR-87-0220 ..... N88-13503 #
AFGL-TR-87-0232 ..... N88-13564 #

AFIT-CI/NR-87-64T ..... N88-13419 #

AFIT/CI/NR-87-36T ..... N88-13837 #
AFIT/CI/NR-87-59T ..... N88-13561 #
AFIT/CI/NR-87-60T ..... N88-13835 #
AFIT/CI/NR-87-63T ..... N88-13838 #
AFIT/CI/NR-87-68T ..... N88-13308 #

AFIT/GA/AA/85D-2 ..... N88-13537 #

AFIT/GSO/ENS-ENG/86D-2 ..... N88-13314 #

AFOSR-87-0962TR ..... N88-13543 #
AFOSR-87-0963TR ..... N88-13562 #

AFOSR-87-0964TR ..... N88-13445 #
AFOSR-87-0992TR ..... N88-13542 #
AFOSR-87-1006TR ..... N88-13920 #
AFOSR-87-1009TR ..... N88-13965 #
AFOSR-87-1036TR ..... N88-13923 #
AFOSR-87-1085TR ..... N88-13924 #
AFOSR-87-1105TR ..... N88-13921 #
AFOSR-87-1106TR ..... N88-13944 #
AFOSR-87-1143TR ..... N88-13925 #
AFOSR-87-1151TR ..... N88-13922 #
AFOSR-87-1171TR ..... N88-13377 #
AFOSR-87-1177TR ..... N88-14021 #
AFOSR-87-1189TR ..... N88-13294 #
AFOSR-87-1190TR ..... N88-13541 #
AFOSR-87-1342TR ..... N88-13822 #
AFOSR-87-1346TR ..... N88-14055 #

AFWAL-TR-86-2087 ..... N88-13340 #
AFWAL-TR-87-2009 ..... N88-13599 #
AFWAL-TR-87-2042-VOL-1 ..... N88-13475 #
AFWAL-TR-87-3022 ..... N88-13606 #
AFWAL-TR-87-4009 ..... N88-13461 #
AFWAL-TR-87-4041 ..... N88-14017 #
AFWAL-TR-87-4065 ..... N88-13462 #

AFWL-TR-86-45 ..... N88-13982 #
AFWL-TR-86-137 ..... N88-13994 #
AFWL-TR-87-26 ..... N88-13418 #

AGARD-CAL-87/1 ..... N88-14033
AGARD-CAL-88/1 ..... N88-14037 #

AGARD-CP-403 ..... N88-13348 #
AGARD-CP-428 ..... N88-13219 #

AGARD-R-733 ..... N88-13331 #
AGARD-R-740 ..... N88-13315 #
AGARD-R-745 ..... N88-13344 #

AI-M-909 ..... N88-13862 #

AIAA-88-0263 ..... N88-13961* #
AIAA-88-0287 ..... N88-13552* #
AIAA-88-0291 ..... N88-13573* #

AR-004-512 ..... N88-13642 #

ARAED-TR-87027 ..... N88-13476 #

ARCCB-TR-87021 ..... N88-13414 #

ARL-AERO-PROP-R-174 ..... N88-13642 #

ARL-TR-87-29 ..... N88-13956 #

ARL/MAT-R-119 ..... N88-13443 #

ARO-13706.5-GS ..... N88-14059 #
ARO-18457.12-GS ..... N88-13498 #
ARO-18738.6-EG ..... N88-13413 #
ARO-19788.10-MS ..... N88-14014 #
ARO-19855.40-MA ..... N88-13918 #
ARO-19904.3-PH ..... N88-14013 #
ARO-19929.3-MS ..... N88-13993 #
ARO-19976.4-EG ..... N88-13536 #
ARO-20030.1-CH ..... N88-13457 #
ARO-20077.11-MS ..... N88-13444 #
ARO-20569.8-EL ..... N88-14012 #
ARO-20766.7-CH ..... N88-13412 #
ARO-20952.10-CH ..... N88-13386 #
ARO-20961.4-MS ..... N88-13455 #
ARO-21020.6-PH ..... N88-13975 #
ARO-21023.4-MS ..... N88-13391 #
ARO-21213.3-MA ..... N88-13880 #
ARO-21245.26-MA ..... N88-13937 #
ARO-21262.6-GS ..... N88-13981 #
ARO-21294.11-MS ..... N88-13440 #
ARO-21367.6-CH ..... N88-13417 #
ARO-21375.2-EL ..... N88-13502 #
ARO-21443.7-CH ..... N88-13415 #
ARO-21724.10-CH ..... N88-14018 #
ARO-21819.11-CH ..... N88-13416 #
ARO-22000.6-LS ..... N88-13897 #
ARO-22256.4-LS ..... N88-13856 #
ARO-22817.6-MS-S ..... N88-13390 #
ARO-23010.1-MA ..... N88-13943 #
ARO-23010.2-MA ..... N88-13942 #
ARO-23188.1-PH ..... N88-14013 #
ARO-23223.26-EL ..... N88-13583 #
ARO-23306.86-MA ..... N88-13881 #
ARO-23306.87-MA ..... N88-13939 #
ARO-23306.93-MA ..... N88-13941 #
ARO-23326.6-MA ..... N88-13536 #
ARO-24134.1-MS-CF-VOL-1 ..... N88-13845 #
ARO-24134.3-MS-CF-VOL-3 ..... N88-13700 #
ARO-24396.1-PH ..... N88-13983 #

ATR-86(7098)-3 ..... N88-13989 #
ATR-86(8139)-2 ..... N88-14025 #
ATR-86(8139)-2-REV-A ..... N88-14025 #

AWS/TN-87/002 ..... N88-13830 #

BAE-RPT/CCE/014 ..... N88-13486 #

BAE-TP-8095-VOL-1 ..... N88-13485 #
BAE-TP-8095-VOL-2 ..... N88-13486 #

BBC-RD-1987/11 ..... N88-13496
BBC-RD-1987/14 ..... N88-13495
BBC-RD-1987/15 ..... N88-13955
BBC-RD-1987/16 ..... N88-13494

BDX-613-3768 ..... N88-13905 #
BDX-6133769 ..... N88-13906 #

BFLRF-213 ..... N88-13456 #

BLL-M-37363-(5828.4) ..... N88-13438 #
BLL-M-37380-(5828.4) ..... N88-13437 #
BLL-M-37381-(5828.4) ..... N88-13436 #

BNL-40183 ..... N88-13963 #

BRL-MR-3579 ..... N88-13582 #
BRL-MR-3606 ..... N88-13446 #

BRL-TR-2803 ..... N88-13916 #
BRL-TR-2817 ..... N88-13917 #

BU-929-M ..... N88-13881 #

B8700739 ..... N88-13546 #
B8700740 ..... N88-13839 #
B8705703 ..... N88-13929 #
B8705873 ..... N88-13903 #
B8707399 ..... N88-13807 #
B8707547 ..... N88-13841 #
B8709747 ..... N88-13840 #
B8709808 ..... N88-13806 #
B8709826 ..... N88-13343 #
B8709829 ..... N88-13366 #
B8711346 ..... N88-13926 #
B8711373 ..... N88-13420
B8711398 ..... N88-13888 #
B8711403 ..... N88-13930 #
B8713114 ..... N88-13949
B8713537 ..... N88-13570

C-47-888 ..... N88-13489 #
C-49-541 ..... N88-13470 #

CAR-TR-309 ..... N88-14045 #

CAS/EMS-87-2 ..... N88-13736 #

CBIP-M-25 ..... N88-13862 #

CBPF-NF-026/86 ..... N88-14029 #
CBPF-NF-033/86 ..... N88-13819 #
CBPF-NF-037/86 ..... N88-13911 #
CBPF-NF-039/86 ..... N88-14030 #
CBPF-NF-041/86 ..... N88-13950 #

CDRL-MA-1023T-VOL-1 ..... N88-13368* #

CLASSIC-87-20 ..... N88-13540 #

CNIC-00014 ..... N88-13483 #
CNIC-00054 ..... N88-14010 #

CONF-850718 ..... N88-13987 #
CONF-861063-9 ..... N88-13450 #
CONF-861299-2 ..... N88-13431 #
CONF-861299-8 ..... N88-13432 #
CONF-870159-5 ..... N88-13933 #
CONF-870249-10 ..... N88-14009 #
CONF-870691-5 ..... N88-13751 #
CONF-870725-13 ..... N88-13587 #
CONF-870753-78 ..... N88-13427 #
CONF-870789-3 ..... N88-13588 #
CONF-870836-1 ..... N88-14000 #
CONF-870901-7 ..... N88-13953 #
CONF-870901-8 ..... N88-13589 #
CONF-870901-9 ..... N88-13952 #
CONF-870908-10 ..... N88-13999 #
CONF-870908-11 ..... N88-14004 #
CONF-870908-12 ..... N88-13998 #
CONF-871007-27 ..... N88-14007 #
CONF-871062-2 ..... N88-13812 #
CONF-871062-5 ..... N88-13815 #
CONF-871118-6 ..... N88-13423 #
CONF-871118-7 ..... N88-13422 #

CONF-871125-6 ..... N88-13473 #
CONF-871207-1 ..... N88-13750 #
CONF-871207-6 ..... N88-13905 #
CONF-871207-8 ..... N88-13490 #
CONF-871207-9 ..... N88-13889 #
CONF-871207-10 ..... N88-13906 #
CONF-871207-12 ..... N88-13890 #
CONF-871207-16 ..... N88-13932 #
CONF-871209-1 ..... N88-13898 #
CONF-871209-1-REV-1 ..... N88-13899 #
CONF-871211-1 ..... N88-13947 #
CONF-871211-2 ..... N88-13904 #
CONF-871211-3 ..... N88-13602 #
CONF-871216-1 ..... N88-13948 #
CONF-871220-1 ..... N88-14026 #
CONF-871225-1 ..... N88-13891 #
CONF-8610317-1-SUMM ..... N88-13592 #
CONF-8610317-5-SUMM ..... N88-13607 #
CONF-8612111-1 ..... N88-14032 #
CONF-8705200-1 ..... N88-13408 #
CONF-8706154-2 ..... N88-14008 #
CONF-8706213-1 ..... N88-13892 #
CONF-8707110-1 ..... N88-13968 #
CONF-8707122-2 ..... N88-13481 #
CONF-8707126-1 ..... N88-14051 #
CONF-8708110-20 ..... N88-13555 #
CONF-8708110-23 ..... N88-13572 #
CONF-8708110-24 ..... N88-13571 #
CONF-8708134-1 ..... N88-13421 #
CONF-8708139-1 ..... N88-13472 #
CONF-8708141-4 ..... N88-14057 #
CONF-8708150-1 ..... N88-13980 #
CONF-8708151-1 ..... N88-14027 #
CONF-8708157-1 ..... N88-13530 #
CONF-8709133-1 ..... N88-14011 #
CONF-8709136-1 ..... N88-13963 #
CONF-8709142-3 ..... N88-14003 #
CONF-8709144-1 ..... N88-13449 #
CONF-8709145-5 ..... N88-14005 #
CONF-8709146-13 ..... N88-13575 #
CONF-8709146-16 ..... N88-13590 #
CONF-8709166-2 ..... N88-13424 #
CONF-8710154-1 ..... N88-13448 #
CONF-8710171-1 ..... N88-13373 #

CRC-1396 ..... N88-13493 #

CS-TR-1888 ..... N88-14045 #

CS-1987-14 ..... N88-13680 #

CSDL-R-1982 ..... N88-13313 #

CSE-87-00002 ..... N88-13596* #
CSE-87-00004 ..... N88-13597* #
CSE-87-00005 ..... N88-13595* #

CSG-74 ..... N88-13872* #
CSG-75 ..... N88-13871* #
CSG-76 ..... N88-13870* #
CSG-77 ..... N88-13869* #
CSG-78 ..... N88-13868* #
CSG-79 ..... N88-13867* #

CSU-ATSP-410 ..... N88-13419 #

CU-REPT-5 ..... N88-13425 #

CUED/C-MATS/TR-134 ..... N88-13574 #

DC-97 ..... N88-13376 #

DE87-01369 ..... N88-13968 #
DE87-007848 ..... N88-13750 #
DE87-009748 ..... N88-13898 #
DE87-011169 ..... N88-13947 #
DE87-011174 ..... N88-13904 #
DE87-011638 ..... N88-13905 #
DE87-011639 ..... N88-13906 #
DE87-011742 ..... N88-13490 #
DE87-012105 ..... N88-13889 #
DE87-013082 ..... N88-13890 #
DE87-013162 ..... N88-13948 #
DE87-013651 ..... N88-13448 #
DE87-013716 ..... N88-14026 #
DE87-013900 ..... N88-14009 #
DE87-014251 ..... N88-13899 #
DE87-014395 ..... N88-13963 #
DE87-014565 ..... N88-13408 #
DE87-014567 ..... N88-14027 #
DE87-014571 ..... N88-13449 #
DE87-014583 ..... N88-14032 #
DE87-014756 ..... N88-13998 #
DE87-014783 ..... N88-13421 #
DE87-014849 ..... N88-13932 #
DE87-014854 ..... N88-13891 #

DE87-014875 ..... N88-13450 #
DE87-703358 ..... N88-14029 #
DE87-703362 ..... N88-13819 #
DE87-703365 ..... N88-13911 #
DE87-703366 ..... N88-14030 #
DE87-703367 ..... N88-13950 #
DE87-703384 ..... N88-13483 #
DE87-703401 ..... N88-14010 #
DE87-703506 ..... N88-13431 #
DE87-703526 ..... N88-13592 #
DE87-703530 ..... N88-13607 #
DE87-703562 ..... N88-13987 #
DE87-703632 ..... N88-13608 #
DE87-703700 ..... N88-13432 #
DE88-000168 ..... N88-13530 #
DE88-000208 ..... N88-13970 #
DE88-000271 ..... N88-13471 #
DE88-000365 ..... N88-14011 #
DE88-000435 ..... N88-13535 #
DE88-000462 ..... N88-13892 #
DE88-000480 ..... N88-13555 #
DE88-000487 ..... N88-13999 #
DE88-000493 ..... N88-13481 #
DE88-000513 ..... N88-13933 #
DE88-000529 ..... N88-14000 #
DE88-000533 ..... N88-13472 #
DE88-000541 ..... N88-14001 #
DE88-000559 ..... N88-13587 #
DE88-000580 ..... N88-14002 #
DE88-000590 ..... N88-13602 #
DE88-000596 ..... N88-14003 #
DE88-000601 ..... N88-13473 #
DE88-000604 ..... N88-13812 #
DE88-000642 ..... N88-13986 #
DE88-000756 ..... N88-13980 #
DE88-000804 ..... N88-13971 #
DE88-000822 ..... N88-13989 #
DE88-000832 ..... N88-14004 #
DE88-000887 ..... N88-14028 #
DE88-000894 ..... N88-13972 #
DE88-000926 ..... N88-14005 #
DE88-000963 ..... N88-13588 #
DE88-000970 ..... N88-13589 #
DE88-000971 ..... N88-13952 #
DE88-000972 ..... N88-13953 #
DE88-001109 ..... N88-13815 #
DE88-001385 ..... N88-13575 #
DE88-001381 ..... N88-13934 #
DE88-001389 ..... N88-13422 #
DE88-001390 ..... N88-13423 #
DE88-001462 ..... N88-13893 #
DE88-001473 ..... N88-13973 #
DE88-001489 ..... N88-13451 #
DE88-001500 ..... N88-13424 #
DE88-001504 ..... N88-13751 #
DE88-001511 ..... N88-14006 #
DE88-001519 ..... N88-13452 #
DE88-001580 ..... N88-13752 #
DE88-001610 ..... N88-13843 #
DE88-001612 ..... N88-13590 #
DE88-001621 ..... N88-13425 #
DE88-001625 ..... N88-13974 #
DE88-001632 ..... N88-13571 #
DE88-001633 ..... N88-13572 #
DE88-001656 ..... N88-14007 #
DE88-001666 ..... N88-13426 #
DE88-001674 ..... N88-13427 #
DE88-001676 ..... N88-13373 #
DE88-001691 ..... N88-13858 #
DE88-001805 ..... N88-14057 #
DE88-001827 ..... N88-14051 #
DE88-001850 ..... N88-14008 #
DE88-001912 ..... N88-13550 #
DE88-001921 ..... N88-13381 #
DE88-001922 ..... N88-13576 #
DE88-001931 ..... N88-13894 #
DE88-001941 ..... N88-13591 #
DE88-001946 ..... N88-13491 #
DE88-001947 ..... N88-13895 #
DE88-900071 ..... N88-13593 #
DE88-900077 ..... N88-13594 #

DOE/ER-05781/1 ..... N88-14028 #
DOE/ER-10671/5 ..... N88-13425 #
DOE/ER-10954/4 ..... N88-13934 #
DOE/ER-13168/3 ..... N88-13974 #
DOE/ER-13487/2 ..... N88-13426 #
DOE/ER-13491/335 ..... N88-13972 #
DOE/ER-13632/1 ..... N88-13973 #
DOE/ER-40272/30 ..... N88-14032 #
DOE/ER-40325/1 ..... N88-13971 #
DOE/ER-45222/05 ..... N88-13970 #
DOE/ER-53212/113 ..... N88-14004 #
DOE/ER-72012/T5 ..... N88-13550 #

DOE/NASA-50112-71 ..... N88-13453* #
DOE/NASA/50111-1 ..... N88-13338* #

DOE/OR-21400/T316 ..... N88-14002 #

DRD-SE-1118T ..... N88-13518* #

DRD-10-VOL-1 ..... N88-13368* #

DRET-84/1376 ..... N88-13978 #

DRL-T-1862 ..... N88-13518* #

DTNSRDC-86/052-VOL-2 ..... N88-13539 #
DTNSRDC-87/031 ..... N88-13738 #

DTNSRSDC-87/029 ..... N88-13737 #

E-3353 ..... N88-13513* #
E-3535 ..... N88-13745* #
E-3548 ..... N88-13347* #
E-3689 ..... N88-13345* #
E-3754 ..... N88-13385* #
E-3755 ..... N88-13409* #
E-3801 ..... N88-13753* #
E-3827 ..... N88-13604* #
E-3830 ..... N88-13346* #
E-3833 ..... N88-14046* #
E-3847 ..... N88-14054* #
E-3863 ..... N88-13931* #
E-3869 ..... N88-13338* #
E-3871 ..... N88-13453* #
E-3877 ..... N88-13304* #
E-3880 ..... N88-13961* #
E-3886 ..... N88-13573* #
E-3889 ..... N88-13428* #
E-3892 ..... N88-13515* #
E-3896 ..... N88-13754* #
E-3898 ..... N88-13960* #
E-3924 ..... N88-13552* #

EEB-86-5 ..... N88-13514 #

EGG-M-08987 ..... N88-13751 #
EGG-M-23387 ..... N88-13424 #
EGG-M-27186 ..... N88-13450 #

EP-PATENT-APPL-SN-86302494.9 ..... N88-13393
EP-PATENT-APPL-SN-86303047.4 ..... N88-13465
EP-PATENT-APPL-SN-86305908.5 ..... N88-13984
EP-PATENT-APPL-SN-86308587.4 ..... N88-13464

EP-PATENT-0-196-926-A2 ..... N88-13393
EP-PATENT-0-202-762-A2 ..... N88-13465
EP-PATENT-0-210-869-A1 ..... N88-13984
EP-PATENT-0-223-489-A2 ..... N88-13464

ESA-CR(P)-2424-VOL-1 ..... N88-13485 #
ESA-CR(P)-2424-VOL-2 ..... N88-13486 #
ESA-CR(P)-2427 ..... N88-13860 #
ESA-CR(P)-2439 ..... N88-13808 #
ESA-CR(P)-2458-VOL-1 ..... N88-13505 #
ESA-CR(P)-2458-VOL-2 ..... N88-13506 #

ETL-0461 ..... N88-14045 #

ETN-88-90517 ..... N88-13463
ETN-88-90599 ..... N88-13526 #
ETN-88-90602 ..... N88-13600 #
ETN-88-90607 ..... N88-13360 #
ETN-88-90608 ..... N88-13741 #
ETN-88-90616 ..... N88-13309 #
ETN-88-90622 ..... N88-13806 #
ETN-88-90633 ..... N88-13544 #
ETN-88-90635 ..... N88-13545 #
ETN-88-90637 ..... N88-13295 #
ETN-88-90638 ..... N88-13586 #
ETN-88-90716 ..... N88-14022
ETN-88-90722 ..... N88-13464
ETN-88-90723 ..... N88-13393
ETN-88-90724 ..... N88-13984
ETN-88-90725 ..... N88-13465
ETN-88-90756 ..... N88-13844 #
ETN-88-90816 ..... N88-13546 #
ETN-88-90817 ..... N88-13839 #
ETN-88-90819 ..... N88-13840 #
ETN-88-90820 ..... N88-13841 #
ETN-88-90830 ..... N88-13807 #
ETN-88-90846 ..... N88-13926 #
ETN-88-90859 ..... N88-13882 #
ETN-88-90860 ..... N88-13851 #
ETN-88-90862 ..... N88-13816
ETN-88-90863 ..... N88-13466
ETN-88-90864 ..... N88-13817
ETN-88-90865 ..... N88-13813
ETN-88-90884 ..... N88-13485 #
ETN-88-90885 ..... N88-13486 #

ETN-88-90886 ..... N88-13860 #
ETN-88-91015 ..... N88-13447 #
ETN-88-91136 ..... N88-13808 #
ETN-88-91152 ..... N88-13505 #
ETN-88-91153 ..... N88-13506 #
ETN-88-91166 ..... N88-13394 #
ETN-88-91169 ..... N88-13296 #
ETN-88-91170 ..... N88-13565 #
ETN-88-91171 ..... N88-13547 #
ETN-88-91172 ..... N88-13566 #
ETN-88-91177 ..... N88-13959 #
ETN-88-91178 ..... N88-13297 #
ETN-88-91179 ..... N88-13395 #
ETN-88-91180 ..... N88-13298 #
ETN-88-91181 ..... N88-13742 #
ETN-88-91182 ..... N88-13467 #
ETN-88-91183 ..... N88-13548 #
ETN-88-91184 ..... N88-13299 #
ETN-88-91185 ..... N88-13329 #
ETN-88-91186 ..... N88-13883 #
ETN-88-91187 ..... N88-13215 #
ETN-88-91188 ..... N88-13216 #
ETN-88-91189 ..... N88-14036 #
ETN-88-91190 ..... N88-13361 #
ETN-88-91191 ..... N88-13396 #
ETN-88-91192 ..... N88-13884 #
ETN-88-91193 ..... N88-13217 #
ETN-88-91194 ..... N88-13397 #
ETN-88-91195 ..... N88-13362 #
ETN-88-91196 ..... N88-13885 #
ETN-88-91197 ..... N88-13330 #
ETN-88-91198 ..... N88-13300 #
ETN-88-91200 ..... N88-13743 #
ETN-88-91201 ..... N88-13744 #
ETN-88-91202 ..... N88-13398 #
ETN-88-91203 ..... N88-13886 #
ETN-88-91204 ..... N88-13809 #
ETN-88-91207 ..... N88-13567 #
ETN-88-91208 ..... N88-13901 #
ETN-88-91209 ..... N88-13814 #
ETN-88-91210 ..... N88-13383 #
ETN-88-91212 ..... N88-13399 #
ETN-88-91213 ..... N88-13507 #
ETN-88-91214 ..... N88-13508 #
ETN-88-91215 ..... N88-13509 #
ETN-88-91216 ..... N88-13400 #
ETN-88-91217 ..... N88-13468 #
ETN-88-91218 ..... N88-13487 #
ETN-88-91219 ..... N88-13401 #
ETN-88-91220 ..... N88-13402 #
ETN-88-91221 ..... N88-13403 #
ETN-88-91222 ..... N88-13477 #
ETN-88-91223 ..... N88-13404 #
ETN-88-91224 ..... N88-13405 #
ETN-88-91225 ..... N88-13478 #
ETN-88-91226 ..... N88-13479 #
ETN-88-91227 ..... N88-13488 #
ETN-88-91228 ..... N88-13945 #
ETN-88-91229 ..... N88-13406 #
ETN-88-91230 ..... N88-13407 #
ETN-88-91231 ..... N88-13469 #
ETN-88-91232 ..... N88-14023 #
ETN-88-91233 ..... N88-13489 #
ETN-88-91234 ..... N88-13470 #
ETN-88-91235 ..... N88-13527 #
ETN-88-91236 ..... N88-13510 #
ETN-88-91237 ..... N88-13824 #
ETN-88-91238 ..... N88-13568 #
ETN-88-91239 ..... N88-13966 #
ETN-88-91242 ..... N88-13967 #
ETN-88-91252 ..... N88-13927 #
ETN-88-91279 ..... N88-14047 #
ETN-88-91281 ..... N88-13528 #
ETN-88-91283 ..... N88-13569 #
ETN-88-91284 ..... N88-13825 #
ETN-88-91287 ..... N88-14048 #
ETN-88-91289 ..... N88-13378 #
ETN-88-91290 ..... N88-13977 #
ETN-88-91291 ..... N88-13379 #
ETN-88-91292 ..... N88-13985 #
ETN-88-91293 ..... N88-13380 #
ETN-88-91294 ..... N88-14060 #
ETN-88-91296 ..... N88-14061 #
ETN-88-91301 ..... N88-13861
ETN-88-91304 ..... N88-13902
ETN-88-91305 ..... N88-13946
ETN-88-91320 ..... N88-14031 #
ETN-88-91321 ..... N88-13928 #
ETN-88-91327 ..... N88-13343 #
ETN-88-91330 ..... N88-13366 #
ETN-88-91341 ..... N88-13949
ETN-88-91345 ..... N88-13929 #
ETN-88-91346 ..... N88-13903 #
ETN-88-91356 ..... N88-13570
ETN-88-91362 ..... N88-14024 #
ETN-88-91363 ..... N88-13887 #

ETN-88-91364 ..... N88-13529 #
ETN-88-91365 ..... N88-13601 #
ETN-88-91367 ..... N88-13930 #
ETN-88-91370 ..... N88-13888 #
ETN-88-91371 ..... N88-13420
ETN-88-91384 ..... N88-13995 #
ETN-88-91385 ..... N88-13826 #
ETN-88-91386 ..... N88-14052 #
ETN-88-91387 ..... N88-14056 #
ETN-88-91388 ..... N88-14053 #
ETN-88-91389 ..... N88-13996 #
ETN-88-91390 ..... N88-13997 #
ETN-88-91391 ..... N88-13827 #
ETN-88-91392 ..... N88-13301 #
ETN-88-91393 ..... N88-13302 #
ETN-88-91394 ..... N88-13303 #
ETN-88-91395 ..... N88-13480 #
ETN-88-91401 ..... N88-13482 #
ETN-88-91405 ..... N88-13511 #
ETN-88-91406 ..... N88-13512 #
ETN-88-91408 ..... N88-13810 #
ETN-88-91716 ..... N88-13857 #

EUR-10733-DE ..... N88-13593 #
EUR-10812-EN ..... N88-13594 #

FFA-TN-1987-08 ..... N88-13301 #
FFA-TN-1987-22 ..... N88-13302 #
FFA-TN-1987-46 ..... N88-13303 #

FOA-C-20660-2.1 ..... N88-13480 #
FOA-C-20676-2.1 ..... N88-13482 #
FOA-C-30458-3.2 ..... N88-13511 #
FOA-C-30459-3.2 ..... N88-13512 #
FOA-C-30462-3.3,9.3 ..... N88-13810 #

FR-687105-PT-3 ..... N88-13553* #

FSU-SCRU-87-08 ..... N88-14009 #

FTD-ID(RS)T-0008-87 ..... N88-13525 #
FTD-ID(RS)T-0627-87 ..... N88-14050 #

FTT/REP/0001/SAAB ..... N88-13860 #

GB-PATENT-APPL-SN-8516168 ..... N88-13463
GB-PATENT-APPL-SN-8613076 ..... N88-14022

GB-PATENT-2-176-054-A ..... N88-14022
GB-PATENT-2-177-413-A ..... N88-13463

GEOMET-EAF-1725 ..... N88-13829 #

GPO-76-948 ..... N88-14043 #
GPO-80-245 ..... N88-14044 #

GTL-191 ..... N88-13337 #

GWU/IMSE/SERIAL-T-516/87 ..... N88-13914 #

HDL-TR-2125 ..... N88-14020 #

HEL-TN-4-87 ..... N88-13524 #

HTKK-MAT-A-247 ..... N88-13749 #

IAE-0016 ..... N88-14010 #

ICOMP-87-9 ..... N88-13931* #

IFSI-88-5 ..... N88-14047 #
IFSI-88-9 ..... N88-13528 #
IFSI-86-12 ..... N88-13569 #
IFSI-86-13 ..... N88-13825 #
IFSI-86-16 ..... N88-14048 #
IFSI-87-2 ..... N88-13378 #
IFSI-87-3 ..... N88-13977 #
IFSI-87-4 ..... N88-13379 #
IFSI-87-5 ..... N88-13985 #
IFSI-87-6 ..... N88-13380 #
IFSI-87-7 ..... N88-14061 #
IFSI-87-8 ..... N88-14060 #

IMFL-3114-85/32 ..... N88-13565 #
IMFL-4200-88/75 ..... N88-13297 #

INIS-BR-756 ..... N88-13431 #
INIS-BR-760 ..... N88-13432 #
INIS-BR-779 ..... N88-13592 #
INIS-BR-784 ..... N88-13607 #

INIS-MF-10971 ..... N88-13987 #

INT-PATENT-CLASS-C08J-9/06 ..... N88-13464
INT-PATENT-CLASS-C08K-5/00 ..... N88-13464
INT-PATENT-CLASS-C08K-5/14 ..... N88-13465

INT-PATENT-CLASS-C08L-9/02 ..... N88-13465
INT-PATENT-CLASS-C08L-23/04 ..... N88-13465
INT-PATENT-CLASS-C08L-61/06 ..... N88-13464
INT-PATENT-CLASS-C09D-3/00 ..... N88-13463
INT-PATENT-CLASS-C09D-5/00 ..... N88-13463
INT-PATENT-CLASS-C23C-16/24 ..... N88-14022

INT-PATENT-CLASS-E04C-2/22 ..... N88-13393
INT-PATENT-CLASS-E04C-5/07 ..... N88-13393

INT-PATENT-CLASS-G01N-21/85 ..... N88-13964

INT-PATENT-CLASS-H01L-21/205 ..... N88-14022

IPPJ-AM-52 ..... N88-13988 #

IR-118 ..... N88-14041 #

ISBN-87-7478-276-2 ..... N88-13844 #
ISBN-90-71382-08-7 ..... N88-13420
ISBN-90-9001649-X ..... N88-13529 #
ISBN-90-9001655-4 ..... N88-13570
ISBN-92-835-0348-4 ..... N88-13344 #
ISBN-92-835-0424-0 ..... N88-13348 #
ISBN-92-835-0427-5 ..... N88-14033
ISBN-92-835-0428-3 ..... N88-13331 #
ISBN-92-835-0435-6 ..... N88-13219 #
ISBN-92-835-0440-2 ..... N88-14037 #
ISBN-92-835-1560-9 ..... N88-13315 #
ISBN-961-754-162-7 ..... N88-13749 #

ISL-CO-207/86 ..... N88-13554 #

ISL-R-107/86 ..... N88-13545 #
ISL-R-113/86 ..... N88-13295 #
ISL-R-115/86 ..... N88-13586 #
ISL-R-117/85 ..... N88-13544 #

ISSN-0082-5263 ..... N88-13531 #
ISSN-0169-1708 ..... N88-13546 #
ISSN-0169-1708 ..... N88-13839 #
ISSN-0169-1708 ..... N88-13840 #
ISSN-0169-3581 ..... N88-13841 #
ISSN-0347-3694 ..... N88-13480 #
ISSN-0347-3694 ..... N88-13482 #
ISSN-0347-3708 ..... N88-13511 #
ISSN-0347-3708 ..... N88-13512 #
ISSN-0347-3708 ..... N88-13810 #
ISSN-0348-7539 ..... N88-13826 #
ISSN-0348-7539 ..... N88-13995 #
ISSN-0348-7539 ..... N88-13996 #
ISSN-0348-7539 ..... N88-13997 #
ISSN-0348-7539 ..... N88-14052 #
ISSN-0348-7539 ..... N88-14053 #
ISSN-0348-7539 ..... N88-14056 #
ISSN-0349-2699 ..... N88-13827 #
ISSN-0452-2982 ..... N88-13253 #
ISSN-0920-2358 ..... N88-13926 #

IZF-1986-16 ..... N88-13857 #
IZF-1986-32 ..... N88-13882 #
IZF-1987-2 ..... N88-13851 #

JPL-D-4956 ..... N88-14042* #

JPL-PUB-87-30 ..... N88-13755* #

KNMI-TR-90 ..... N88-13546 #
KNMI-TR-91 ..... N88-13839 #
KNMI-TR-93 ..... N88-13840 #

KNMI-150-26 ..... N88-13841 #

L-16356 ..... N88-13388* #

LA-UR-87-2135 ..... N88-13490 #
LA-UR-87-2453 ..... N88-13948 #
LA-UR-87-2534 ..... N88-13968 #
LA-UR-87-2854 ..... N88-13998 #
LA-UR-87-2942 ..... N88-13933 #
LA-UR-87-3027 ..... N88-13472 #
LA-UR-87-3042 ..... N88-14000 #
LA-UR-87-3169 ..... N88-13481 #
LA-UR-87-3209 ..... N88-13999 #
LA-UR-87-3305 ..... N88-13555 #
LA-UR-87-3326 ..... N88-14008 #
LA-UR-87-3457 ..... N88-14051 #
LA-UR-87-3643 ..... N88-14057 #

LA-11006-MS ..... N88-13591 #
LA-11086-T ..... N88-13535 #
LA-11089-MS ..... N88-13491 #
LA-11098-MS ..... N88-13895 #

LAAS-87-266 ..... N88-13527 #
LAAS-87-269 ..... N88-13510 #

LBL-PUB-621-8/87 ..... N88-14001 #
LBL-PUB-3061-REV ..... N88-13693 #

LBL-22417 ..... N88-13892 #
LBL-23515 ..... N88-13422 #
LBL-23952 ..... N88-13423 #

LNCC-008/87 ..... N88-13606 #

M-571-VOL-1 ..... N88-13609* #

MRL-R-1060 ..... N88-13328 #
MRL-R-1062 ..... N88-13458 #

MTL-TR-87-41 ..... N88-13442 #

NADC-87114-60 ..... N88-13454 #

NAL-SP-7 ..... N88-13253 #

NAL-TM-AE-8704 ..... N88-13364 #

NAL-TM-MT-8704 ..... N88-13435 #
NAL-TM-MT-8705 ..... N88-13433 #
NAL-TM-MT-8706 ..... N88-13434 #

NAL-TM-SE-8608 ..... N88-13365 #

NAS 1.15:4016 ..... N88-13388* #
NAS 1.15:85015 ..... N88-13370* #
NAS 1.15:88217 ..... N88-13305* #
NAS 1.15:88227 ..... N88-13306* #
NAS 1.15:88236 ..... N88-13367* #
NAS 1.15:88253 ..... N88-13290* #
NAS 1.15:88318 ..... N88-13951* #
NAS 1.15:88332 ..... N88-13549* #
NAS 1.15:88376 ..... N88-13363* #
NAS 1.15:89303 ..... N88-13474* #
NAS 1.15:89305 ..... N88-13605* #
NAS 1.15:89878 ..... N88-13347* #
NAS 1.15:100029 ..... N88-13359* #
NAS 1.15:100117 ..... N88-13745* #
NAS 1.15:100124 ..... N88-13345* #
NAS 1.15:100154 ..... N88-13513* #
NAS 1.15:100179 ..... N88-13409* #
NAS 1.15:100204 ..... N88-13753* #
NAS 1.15:100219 ..... N88-13346* #
NAS 1.15:100221 ..... N88-14046* #
NAS 1.15:100228 ..... N88-14054* #
NAS 1.15:100239 ..... N88-13385* #
NAS 1.15:100240 ..... N88-13931* #
NAS 1.15:100247 ..... N88-13338* #
NAS 1.15:100249 ..... N88-13453* #
NAS 1.15:100251 ..... N88-13304* #
NAS 1.15:100254 ..... N88-13961* #
NAS 1.15:100255 ..... N88-13604* #
NAS 1.15:100261 ..... N88-13428* #
NAS 1.15:100263 ..... N88-13515* #
NAS 1.15:100266 ..... N88-13754* #
NAS 1.15:100267 ..... N88-13960* #
NAS 1.15:100284 ..... N88-13552* #
NAS 1.15:100494 ..... N88-13735* #
NAS 1.15:100503 ..... N88-13369* #
NAS 1.15:100508 ..... N88-13387* #
NAS 1.15:100517 ..... N88-13962* #
NAS 1.15:100519 ..... N88-14058* #
NAS 1.15:100678 ..... N88-13773* #
NAS 1.15:100686 ..... N88-13372* #
NAS 1.15:100687 ..... N88-13371* #
NAS 1.15:100690 ..... N88-13842* #
NAS 1.21:4023 ..... N88-14062*
NAS 1.21:7056(05) ..... N88-13382*
NAS 1.26:4069 ..... N88-13218* #
NAS 1.26:4106 ..... N88-13292* #
NAS 1.26:4107 ..... N88-13900* #
NAS 1.26:172010 ..... N88-13368* #
NAS 1.26:172036 ..... N88-13518* #
NAS 1.26:174866 ..... N88-13803* #
NAS 1.26:177441 ..... N88-13291* #
NAS 1.26:177465 ..... N88-13556* #
NAS 1.26:177468 ..... N88-13954* #
NAS 1.26:178292 ..... N88-13557* #
NAS 1.26:178294 ..... N88-13553* #
NAS 1.26:180845 ..... N88-13310* #
NAS 1.26:180870 ..... N88-13573* #
NAS 1.26:181507 ..... N88-14049* #
NAS 1.26:181538 ..... N88-13595* #
NAS 1.26:181539 ..... N88-13389* #
NAS 1.26:181552 ..... N88-13755* #
NAS 1.26:181553 ..... N88-13867* #
NAS 1.26:181554 ..... N88-13863* #
NAS 1.26:181555 ..... N88-13936* #
NAS 1.26:181556 ..... N88-13374* #
NAS 1.26:181557 ..... N88-13820* #
NAS 1.26:181561 ..... N88-13868* #
NAS 1.26:181562 ..... N88-13869* #

NAS 1.26:181563 ..... N88-13870* #
NAS 1.26:181564 ..... N88-13871* #
NAS 1.26:181565 ..... N88-13872* #
NAS 1.26:181569 ..... N88-13577* #
NAS 1.26:181570 ..... N88-13411* #
NAS 1.26:181577 ..... N88-13384* #
NAS 1.26:181579 ..... N88-13935* #
NAS 1.26:181580 ..... N88-13429* #
NAS 1.26:181581 ..... N88-13516* #
NAS 1.26:182328 ..... N88-13828* #
NAS 1.26:182331 ..... N88-13908* #
NAS 1.26:182332 ..... N88-13811* #
NAS 1.26:182333 ..... N88-13896* #
NAS 1.26:182334 ..... N88-13551* #
NAS 1.26:182336 ..... N88-13907* #
NAS 1.26:182338 ..... N88-14042* #
NAS 1.26:182341 ..... N88-13307* #
NAS 1.55:2479 ..... N88-13852* #
NAS 1.55:2488-VOL-1 ..... N88-13609* #
NAS 1.55:2497 ..... N88-13774* #

NASA-CP-2479 ..... N88-13852* #
NASA-CP-2488-VOL-1 ..... N88-13609* #
NASA-CP-2497 ..... N88-13774* #

NASA-CR-4069 ..... N88-13218* #
NASA-CR-4106 ..... N88-13292* #
NASA-CR-4107 ..... N88-13900* #
NASA-CR-172010 ..... N88-13368* #
NASA-CR-172036 ..... N88-13518* #
NASA-CR-174866 ..... N88-13603* #
NASA-CR-177441 ..... N88-13291* #
NASA-CR-177465 ..... N88-13556* #
NASA-CR-177468 ..... N88-13954* #
NASA-CR-178292 ..... N88-13557* #
NASA-CR-178294 ..... N88-13553* #
NASA-CR-180845 ..... N88-13310* #
NASA-CR-180870 ..... N88-13573* #
NASA-CR-181507 ..... N88-14049* #
NASA-CR-181538 ..... N88-13595* #
NASA-CR-181539 ..... N88-13389* #
NASA-CR-181552 ..... N88-13755* #
NASA-CR-181553 ..... N88-13867* #
NASA-CR-181554 ..... N88-13863* #
NASA-CR-181555 ..... N88-13936* #
NASA-CR-181556 ..... N88-13374* #
NASA-CR-181557 ..... N88-13820* #
NASA-CR-181561 ..... N88-13868* #
NASA-CR-181562 ..... N88-13869* #
NASA-CR-181563 ..... N88-13870* #
NASA-CR-181564 ..... N88-13871* #
NASA-CR-18[illegible]65 ..... N88-13872* #
NASA-CR-18[illegible]69 ..... N88-13577* #
NASA-CR-181[illegible] ..... N88-13411* #
NASA-CR-1815[illegible] ..... N88-13384* #
NASA-CR-181575 ..... N88-13935* #
NASA-CR-181580 ..... N88-13429* #
NASA-CR-181581 ..... N88-13516* #
NASA-CR-182328 ..... N88-13828* #
NASA-CR-182331 ..... N88-13908* #
NASA-CR-182332 ..... N88-13811* #
NASA-CR-182333 ..... N88-13896* #
NASA-CR-182334 ..... N88-13551* #
NASA-CR-182336 ..... N88-13907* #
NASA-CR-182338 ..... N88-14042* #
NASA-CR-182341 ..... N88-13307* #

NASA-SP-4023 ..... N88-14062*
NASA-SP-7056(05) ..... N88-13382*

NASA-TM-4016 ..... N88-13388* #
NASA-TM-85015 ..... N88-13370* #
NASA-TM-86217 ..... N88-13305* #
NASA-TM-86227 ..... N88-13306* #
NASA-TM-86236 ..... N88-13367* #
NASA-TM-86253 ..... N88-13290* #
NASA-TM-88318 ..... N88-13951* #
NASA-TM-88332 ..... N88-13549* #
NASA-TM-88376 ..... N88-13363* #
NASA-TM-89303 ..... N88-13474* #
NASA-TM-89305 ..... N88-13605* #
NASA-TM-89878 ..... N88-13347* #
NASA-TM-100029 ..... N88-13359* #
NASA-TM-100117 ..... N88-13745* #
NASA-TM-100124 ..... N88-13345* #
NASA-TM-100154 ..... N88-13513* #
NASA-TM-100179 ..... N88-13409* #
NASA-TM-100204 ..... N88-13753* #
NASA-TM-100219 ..... N88-13346* #
NASA-TM-100221 ..... N88-14046* #
NASA-TM-100228 ..... N88-14054* #
NASA-TM-100239 ..... N88-13385* #
NASA-TM-100240 ..... N88-13931* #
NASA-TM-100247 ..... N88-13338* #
NASA-TM-100249 ..... N88-13453* #
NASA-TM-100251 ..... N88-13304* #
NASA-TM-100254 ..... N88-13961* #
NASA-TM-100255 ..... N88-13604* #
NASA-TM-100261 ..... N88-13428* #
NASA-TM-100263 ..... N88-13515* #
NASA-TM-100266 ..... N88-13754* #
NASA-TM-100267 ..... N88-13960* #
NASA-TM-100284 ..... N88-13552* #
NASA-TM-100494 ..... N88-13735* #
NASA-TM-100503 ..... N88-13369* #
NASA-TM-100506 ..... N88-13387* #
NASA-TM-100517 ..... N88-13962* #
NASA-TM-100519 ..... N88-14058* #
NASA-TM-100678 ..... N88-13773* #
NASA-TM-100686 ..... N88-13372* #
NASA-TM-100687 ..... N88-13371* #
NASA-TM-100690 ..... N88-13842* #

NBSIR-87-3581 ..... N88-13391 #

NLR-MP-86018-U ..... N88-13343 #
NLR-MP-86049-U ..... N88-13366 #
NLR-MP-86055-U ..... N88-13807 #

NLR-TR-86029-L ..... N88-13808 #

NOSC/TD-992 ..... N88-13805 #

NOTA-INTERNA-876 ..... N88-13568 #
NOTA-INTERNA-877 ..... N88-13966 #
NOTA-INTERNA-881 ..... N88-13967 #
NOTA-INTERNA-891 ..... N88-13927 #

NPS-63-87-006 ..... N88-13834 #

NPS52-87-039 ..... N88-13311 #

NRL-MR-5923 ..... N88-13563 #
NRL-MR-5980 ..... N88-13992 #
NRL-MR-6012 ..... N88-13990 #
NRL-MR-6051 ..... N88-13991 #
NRL-MR-6056 ..... N88-13500 #
NRL-MR-6060 ..... N88-13940 #
NRL-MR-6067 ..... N88-13739 #
NRL-MR-6076 ..... N88-13312 #

NRL-9008 ..... N88-13915 #
NRL-9049 ..... N88-13878 #

NSWC/TR-87-184 ..... N88-13585 #

ONERA-RT-13/3542-RY-061-R ..... N88-13395 #
ONERA-RT-14/3542-RY-051-R ..... N88-13742 #
ONERA-RT-36/1147-AN-249-G ..... N88-13298 #

ONRL-7-021-R ..... N88-13501 #
ONRL-7-025-C ..... N88-14063 #

ORNL/SUB-85-27488/02 ..... N88-13452 #

ORNL/TM-10487 ..... N88-13451 #
ORNL/TM-10574 ..... N88-14006 #

PB87-109310 ..... N88-13978 #
PB87-110706 ..... N88-13554 #
PB87-220042 ..... N88-13909 #
PB87-220919 ..... N88-13910 #
PB87-221875 ..... N88-13574 #
PB87-221941 ..... N88-13492 #
PB87-223426 ..... N88-14038 #
PB87-225272 ..... N88-13749 #
PB87-226155 ..... N88-13480 #
PB87-228037 ..... N88-13514 #
PB87-230165 ..... N88-13818 #
PB87-232500 ..... N88-14040 #
PB87-234423 ..... N88-14041 #
PB87-235388 ..... N88-14039 #

PML-1985-22 ..... N88-13466
PML-1985-29 ..... N88-13817
PML-1985-42 ..... N88-13816
PML-1986-43 ..... N88-13813

PNL-SA-14795 ..... N88-13587 #

PNL-6264 ..... N88-13986 #
PNL-6268 ..... N88-13471 #
PNL-6279-VOL-5 ..... N88-13843 #
PNL-6311 ..... N88-13858 #

PVAMU-EE093087JGO1A ..... N88-13518* #

PW/GRD-FR-18807 ..... N88-13461 #

QTPR-1 ..... N88-13578 #

RAL-86-053 ..... N88-14038 #
RAL-86-104 ..... N88-13492 #

REPT-2 ..... N88-13281 #
REPT-85TR20 ..... N88-13603* #
REPT-86B0201 ..... N88-13372* #
REPT-87-1 ..... N88-13873 #
REPT-87-13 ..... N88-13926 #
REPT-87-21 ..... N88-13949
REPT-87-019 ..... N88-13861
REPT-87-036 ..... N88-13902
REPT-87-037 ..... N88-13946
REPT-87B0206 ..... N88-13774* #
REPT-87B0269 ..... N88-13370* #
REPT-87B0413 ..... N88-13773* #
REPT-87B0437 ..... N88-13842* #
REPT-136 ..... N88-13910 #
REPT-141 ..... N88-13909 #

RITRC-014 ..... N88-13522 #

S-HRG-100-328 ..... N88-14043 #

SAND-85-2344 ..... N88-13894 #
SAND-86-2173C ..... N88-13890 #
SAND-86-2294C ..... N88-13889 #
SAND-87-0432C ..... N88-13750 #
SAND-87-0975C ..... N88-13427 #
SAND-87-1131C ..... N88-13812 #
SAND-87-1239C ..... N88-14011 #
SAND-87-1449 ..... N88-13381 #
SAND-87-1691C ..... N88-14026 #
SAND-87-1718C ..... N88-13448 #
SAND-87-1859C ..... N88-13932 #
SAND-87-1997 ..... N88-13576 #
SAND-87-2009C ..... N88-13891 #
SAND-87-2202C ..... N88-13575 #
SAND-87-2285C ..... N88-13590 #
SAND-87-2321C ..... N88-13473 #
SAND-87-2344C ..... N88-14005 #
SAND-87-2623C ..... N88-13373 #
SAND-87-7153C ..... N88-13530 #

SAWE-PAPER-1783 ..... N88-13388* #

SC/87-E/6-VOL-1 ..... N88-13505 #
SC/87-E/6-VOL-2 ..... N88-13506 #

SC5464.FR ..... N88-13556* #

SD-TR-87-39 ..... N88-14015 #
SD-TR-87-43 ..... N88-13519 #

SERI/TP-217-3223 ..... N88-13815 #

SGR/PR-4305/86-SV/JC ..... N88-13394 #

SINRE-0004 ..... N88-13483 #

SIR-87-005 ..... N88-13606 #

SNIAS-NT-18926/AQET ..... N88-13467 #

SNIAS-872-111-101 ..... N88-13299 #
SNIAS-872-111-102 ..... N88-13329 #
SNIAS-872-111-104 ..... N88-13683 #
SNIAS-872-111-105 ..... N88-13215 #
SNIAS-872-111-106 ..... N88-13216 #
SNIAS-872-111-107 ..... N88-14036 #
SNIAS-872-111-108 ..... N88-13361 #
SNIAS-872-111-109 ..... N88-13396 #
SNIAS-872-111-110 ..... N88-13884 #
SNIAS-872-111-112 ..... N88-13217 #
SNIAS-872-111-113 ..... N88-13397 #
SNIAS-872-111-114 ..... N88-13362 #
SNIAS-872-111-115 ..... N88-13885 #
SNIAS-872-111-116 ..... N88-13330 #
SNIAS-872-111-117 ..... N88-13300 #
SNIAS-872-320-101 ..... N88-13743 #
SNIAS-872-320-102 ..... N88-13744 #
SNIAS-872-422-101 ..... N88-13396 #
SNIAS-872-422-102 ..... N88-13886 #
SNIAS-872-422-103 ..... N88-13809 #
SNIAS-872-422-106 ..... N88-13567 #
SNIAS-872-422-107 ..... N88-13901 #
SNIAS-872-422-108 ..... N88-13814 #
SNIAS-872-422-109 ..... N88-13383 #
SNIAS-872-422-112 ..... N88-13399 #
SNIAS-872-430-102 ..... N88-13507 #
SNIAS-872-430-103 ..... N88-13508 #
SNIAS-872-430-104 ..... N88-13509 #
SNIAS-872-430-105 ..... N88-13400 #
SNIAS-872-430-106 ..... N88-13468 #
SNIAS-872-430-107 ..... N88-13487 #
SNIAS-872-430-108 ..... N88-13401 #
SNIAS-872-430-109 ..... N88-13402 #
SNIAS-872-430-110 ..... N88-13403 #

SNIAS-872-430-111 ..... N88-13477 #
SNIAS-872-430-112 ..... N88-13404 #
SNIAS-872-430-113 ..... N88-13405 #
SNIAS-872-430-114 ..... N88-13478 #
SNIAS-872-430-115 ..... N88-13479 #
SNIAS-872-430-116 ..... N88-13488 #
SNIAS-872-430-117 ..... N88-13945 #
SNIAS-872-430-118 ..... N88-13406 #
SNIAS-872-430-119 ..... N88-13407 #
SNIAS-872-430-120 ..... N88-13469 #
SNIAS-872-430-121 ..... N88-14023 #
SNIAS-872-551-101 ..... N88-13489 #
SNIAS-872-551-102 ..... N88-13470 #

SR-1 ..... N88-13503 #
SR-4 ..... N88-13564 #
SR-12 ..... N88-13550 #

SRA-910017 ..... N88-13599 #

SRL-6810 ..... N88-14017 #

SSI-TR-124 ..... N88-13503 #

STS-86-0302-1A-VOL-1 ..... N88-13368* #

STUDY-2512-A ..... N88-13394 #

SWRI-06-8602 ..... N88-13392 #

TD-86-3428-II ..... N88-13857 #
TD-86-3976 ..... N88-13813
TD-87-0045 ..... N88-13882 #
TD-87-1776 ..... N88-13851 #

TDCK-93458 ..... N88-13466
TDCK-93540 ..... N88-13817
TDCK-93808 ..... N88-13816

TF-29 ..... N88-13536 #

TR-Q-1 ..... N88-13943 #
TR-Q-2 ..... N88-13942 #

TR-4 ..... N88-14019 #
TR-8 ..... N88-13459 #
TR-50 ..... N88-13964 #
TR-87-08 ..... N88-13865* #
TR-87-16 ..... N88-13864* #
TR-87-50 ..... N88-13939 #
TR-87-51 ..... N88-13881 #
TR-184 ..... N88-13944 #
TR-185 ..... N88-13921 #
TR-189 ..... N88-13925 #
TR-526 ..... N88-13583 #
TR-530 ..... N88-13558 #
TR-0086A(2925-02)-3 ..... N88-14015 #
TR-0086A(2945-01)-1 ..... N88-13519 #

TRITA-EPP-86-15 ..... N88-13995 #
TRITA-EPP-87-04 ..... N88-13826 #
TRITA-EPP-87-05 ..... N88-14052 #
TRITA-EPP-87-06 ..... N88-14056 #
TRITA-EPP-87-07 ..... N88-14053 #
TRITA-EPP-87-09 ..... N88-13996 #
TRITA-EPP-87-10 ..... N88-13997 #

TW-276 ..... N88-13903 #

UBUFFALO/DC/87/TR-49 ..... N88-13740 #

UCID-21203 ..... N88-13752 #

UCLA/PPG-1084 ..... N88-13989 #

UCRL-96288 ..... N88-13953 #
UCRL-96289 ..... N88-13952 #
UCRL-96292 ..... N88-13589 #
UCRL-96426 ..... N88-13898 #
UCRL-96426-REV-1 ..... N88-13899 #
UCRL-96517 ..... N88-13980 #
UCRL-96518 ..... N88-13571 #
UCRL-96519 ..... N88-13572 #
UCRL-96631 ..... N88-13588 #
UCRL-96720 ..... N88-14007 #

UDR-TR-86-115 ..... N88-13340 #

UFTP-87-2 ..... N88-14032 #

UILU-ENG-87-0505 ..... N88-13581 #
UILU-ENG-87-0506 ..... N88-13584 #
UILU-ENG-87-2249 ..... N88-13912 #
UILU-ENG-87-2252 ..... N88-13504 #
UILU-ENG-87-2260 ..... N88-13376 #
UILU-ENG-87-2270 ..... N88-13872* #
UILU-ENG-87-2271 ..... N88-13871* #
UILU-ENG-87-2272 ..... N88-13870* #
UILU-ENG-87-2273 ..... N88-13869* #
UILU-ENG-87-2274 ..... N88-13868* #
UILU-ENG-87-2275 ..... N88-13867* #

UIO-SR-87-01 ..... N88-13827 #

UMBC-MRR-86-2 ..... N88-13923 #

US-PATENT-APPL-SN-420451 ..... N88-13836 #

USAAVSCOM-TM-87-B-12 ..... N88-13735* #

USAFSAM-TR-87-7 ..... N88-13847 #

USARIEM-T-17/87 ..... N88-13559 #
USARIEM-T-18-87 ..... N88-13846 #
USARIEM-T-19-87 ..... N88-13848 #
USARIEM-T-23-87 ..... N88-13849 #
USARIEM-T-31/87 ..... N88-13850 #
USARIEM-T-33/87 ..... N88-13560 #

UTD-GRL-8701 ..... N88-13578 #

UTIAS-TN-264 ..... N88-13531 #

UVA/525882/EE88/101 ..... N88-13924 #

VPI-E-87-9 ..... N88-13736 #

ZW-8702 ..... N88-13929 #

86B0419 ..... N88-13371* #

# FEDERAL REGIONAL DEPOSITORY LIBRARIES

## ALABAMA

**AUBURN UNIV. AT MONTGOMERY LIBRARY**
Documents Department
Montgomery, AL 36193
(205) 271-9650

**UNIV. OF ALABAMA LIBRARY**
Documents Dept.-Box S
University, AL 35486
(205) 348-6046

## ARIZONA

**DEPT. OF LIBRARY, ARCHIVES AND PUBLIC RECORDS**
Third Floor—State Cap.
1700 West Washington
Phoenix, AZ 85007
(602) 255-4121

**UNIVERSITY OF ARIZONA LIB.**
Government Documents Dept.
Tucson, AZ 85721
(602) 621-6433

## ARKANSAS

**ARKANSAS STATE LIBRARY**
One Capitol Mall
Little Rock, AR 72201
(501) 371-2326

## CALIFORNIA

**CALIFORNIA STATE LIBRARY**
Govt. Publications Section
P.O. Box 2037
Sacramento, CA 95809
(916) 324-4863

## COLORADO

**UNIV OF COLORADO LIB.**
Government Pub. Division
Campus Box 184
Boulder, CO 80309
(303) 492-8834

**DENVER PUBLIC LIBRARY**
Govt. Pub. Department
1357 Broadway
Denver, CO 80203
(303) 571-2131

## CONNECTICUT

**CONNECTICUT STATE LIBRARY**
Government Documents Unit
231 Capitol Avenue
Hartford, CT 06106
(203) 566-7029

## FLORIDA

**UNIV. OF FLORIDA LIBRARIES**
Library West
Documents Department
Gainesville, FL 32611
(904) 392-0367

## GEORGIA

**UNIV. OF GEORGIA LIBRARIES**
Government Reference Dept.
Athens, GA 30602
(404) 542-8949

## HAWAII

**UNIV. OF HAWAII LIBRARY**
Govt. Documents Collection
2550 The Mall
Honolulu, HI 96822
(808) 948-8230

## IDAHO

**UNIV. OF IDAHO LIBRARY**
Documents Section
Moscow, ID 83843
(208) 885-6344

## ILLINOIS

**ILLINOIS STATE LIBRARY**
Information Services Branch
Centennial Building
Springfield, IL 62756
(217) 782-5185

## INDIANA

**INDIANA STATE LIBRARY**
Serials Documents Section
140 North Senate Avenue
Indianapolis, IN 46204
(317) 232-3686

## IOWA

**UNIV. OF IOWA LIBRARIES**
Govt. Documents Department
Iowa City, IA 52242
(319) 353-3318

## KANSAS

**UNIVERSITY OF KANSAS**
Doc. Collect—Spencer Lib.
Lawrence, KS 66045-2800
(913) 864-4662

## KENTUCKY

**UNIV. OF KENTUCKY LIBRARIES**
Govt. Pub. Department
Lexington, KY 40506-0039
(606) 257-3139

## LOUISIANA

**LOUISIANA STATE UNIVERSITY**
Middleton Library
Govt. Docs. Dept.
Baton Rouge, LA 70803
(504) 388-2570

**LOUISIANA TECHNICAL UNIV. LIBRARY**
Documents Department
Ruston, LA 71272-0046
(318) 257-4962

## MAINE

**UNIVERSITY OF MAINE**
Raymond H. Fogler Library
Tri-State Regional Documents Depository
Orono, ME 04469
(207) 581-1680

## MARYLAND

**UNIVERSITY OF MARYLAND**
McKeldin Lib.—Doc. Div.
College Park, MD 20742
(301) 454-3034

## MASSACHUSETTS

**BOSTON PUBLIC LIBRARY**
Government Docs. Dept.
Boston, MA 02117
(617) 536-5400 ext.226

## MICHIGAN

**DETROIT PUBLIC LIBRARY**
Sociology Department
5201 Woodward Avenue
Detroit, MI 48202-4093
(313) 833-1409

**MICHIGAN STATE LIBRARY**
P.O. Box 30007
Lansing, MI 48909
(517) 373-1593

## MINNESOTA

**UNIVERSITY OF MINNESOTA**
Government Pubs. Division
409 Wilson Library
309 19th Avenue South
Minneapolis, MN 55455
(612) 373-7870

## MISSISSIPPI

**UNIV. OF MISSISSIPPI LIB.**
Documents Department
University, MS 38677
(601) 232-5857

## MONTANA

**UNIV. OF MONTANA**
Mansfield Library
Documents Division
Missoula, MT 59812
(406) 243-6700

## NEBRASKA

**UNIVERSITY OF NEBRASKA - LINCOLN**
Love Library
Documents Department
Lincoln, NE 68588-0410
(402) 472-2562

## NEVADA

**UNIVERSITY OF NEVADA LIB.**
Govt. Pub. Department
Reno, NV 89557-0044
(702) 784-6579

## NEW JERSEY

**NEWARK PUBLIC LIBRARY**
5 Washington Street
Newark, NJ 07101-0630
(201) 733-7812

## NEW MEXICO

**UNIVERSITY OF NEW MEXICO**
Zimmerman Library
Government Pub. Dept.
Albuquerque, NM 87131
(505) 277-5441

**NEW MEXICO STATE LIBRARY**
Reference Department
325 Don Gaspar Avenue
Santa Fe, NM 87503
(505) 827-3826

## NEW YORK

**NEW YORK STATE LIBRARY**
Empire State Plaza
Albany, NY 12230
(518) 474-5563

## NORTH CAROLINA

**UNIVERSITY OF NORTH CAROLINA AT CHAPEL HILL**
Davis Library
BA/SS Documents Division
Chapel Hill, NC 27515
(919) 962-1151

## NORTH DAKOTA

**UNIVERSITY OF NORTH DAKOTA**
Chester Fritz Library
Documents Department
Grand Forks, ND 58202
(701) 777-4629
In cooperation with North Dakota State Univ. Library

## OHIO

**STATE LIBRARY OF OHIO**
Documents Department
65 South Front Street
Columbus, OH 43266-0334
(614) 462-7051

## OKLAHOMA

**OKLAHOMA DEPT. OF LIB.**
Government Documents
200 NE 18th Street
Oklahoma City, OK 73105
(405) 521-2502, ext. 252

**OKLAHOMA STATE UNIV. LIB.**
Documents Department
Stillwater, OK 74078
(405) 624-6546

## OREGON

**PORTLAND STATE UNIV. LIB.**
Documents Department
P.O. Box 1151
Portland, OR 97207
(503) 229-3673

## PENNSYLVANIA

**STATE LIBRARY OF PENN.**
Government Pub. Section
P.O. Box 1601
Harrisburg, PA 17105
(717) 787-3752

## TEXAS

**TEXAS STATE LIBRARY**
Public Services Department
P.O. Box 12927—Cap. Sta.
Austin, TX 78711
(512) 475-2996

**TEXAS TECH. UNIV. LIBRARY**
Govt. Documents Department
Lubbock, TX 79409
(806) 742-2268

## UTAH

**UTAH STATE UNIVERSITY**
Merrill Library, U.M.C. 30
Logan, UT 84322
(801) 750-2682

## VIRGINIA

**UNIVERSITY OF VIRGINIA**
Alderman Lib.—Public Doc.
Charlottesville, VA 22903-2498
(804) 924-3133

## WASHINGTON

**WASHINGTON STATE LIBRARY**
Documents Section
Olympia, WA 98504
(206) 753-4027

## WEST VIRGINIA

**WEST VIRGINIA UNIV. LIB.**
Documents Department
Morgantown, WV 26506-6069
(304) 293-3640

## WISCONSIN

**MILWAUKEE PUBLIC LIBRARY**
814 West Wisconsin Avenue
Milwaukee, WI 53233
(414) 278-3065

**ST. HIST LIB. OF WISCONSIN**
Government Pub. Section
816 State Street
Madison, WI 53706
(608) 262-4347

## WYOMING

**WYOMING STATE LIBRARY**
Supreme Ct. & Library Bld.
Cheyenne, WY 82002
(307) 777-5919

National Aeronautics and
Space Administration
Code NTT-4
Washington, D.C.
20546

Official Business

Penalty for Private Use, $300

SPECIAL FOURTH-CLASS RATE
POSTAGE & FEES PAID
NASA
PERMIT No. G 27

NASA
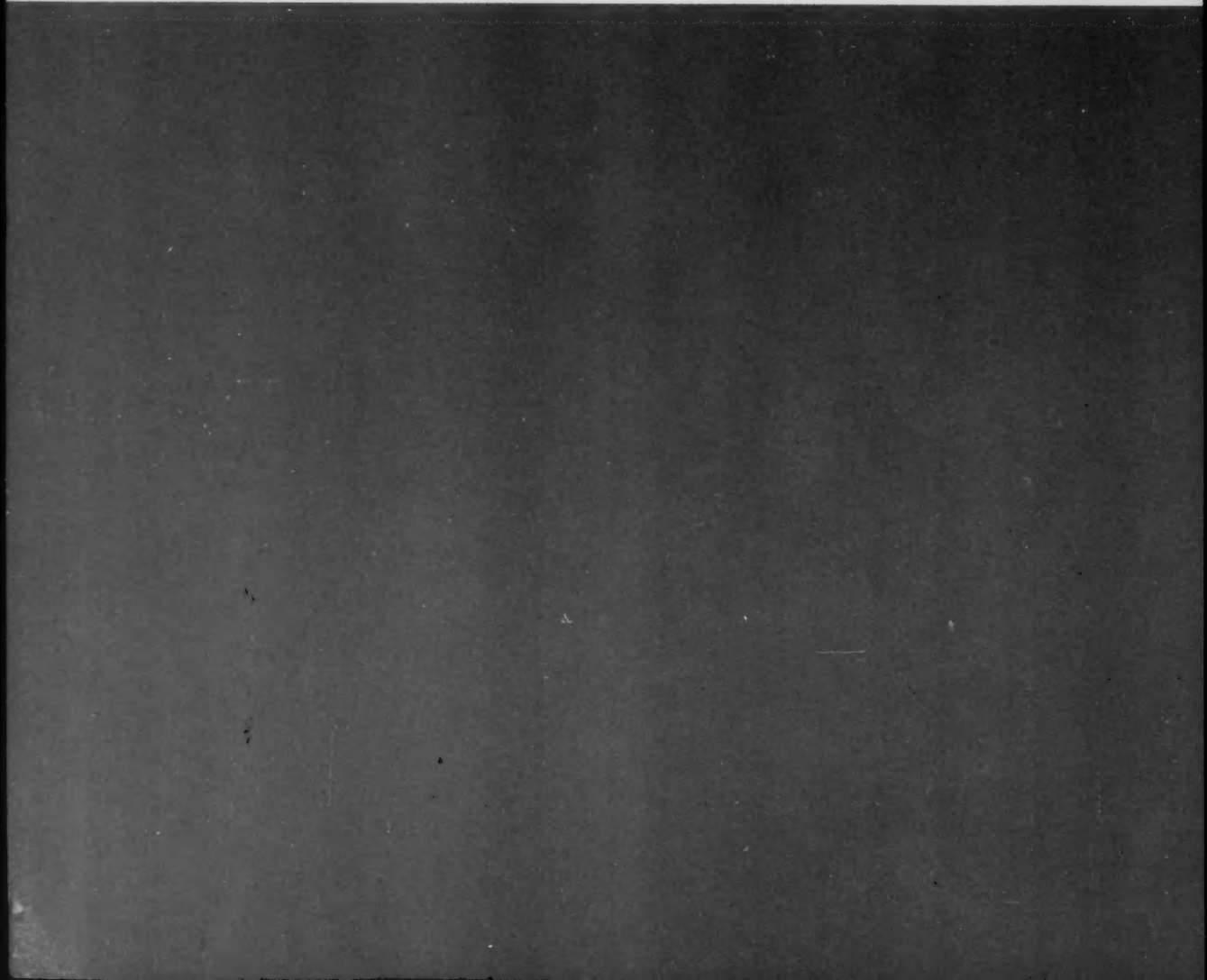
POSTMASTER: If Undeliverable (Section 158
Postal Manual) Do Not Return